Communications and Control Engineering

Bernard Brogliato

Nonsmooth Mechanics

Models, Dynamics and Control

Third Edition

Springer

Communications and Control Engineering

More information about this series at http://www.springer.com/series/61

Bernard Brogliato

Nonsmooth Mechanics

Models, Dynamics and Control

Third Edition

Springer

Bernard Brogliato
INRIA Rhône-Alpes
Saint-Ismier
France

ISSN 0178-5354 ISSN 2197-7119 (electronic)
Communications and Control Engineering
ISBN 978-3-319-28662-4 ISBN 978-3-319-28664-8 (eBook)
DOI 10.1007/978-3-319-28664-8

Library of Congress Control Number: 2015959938

Mathematics Subject Classification: 70Q05, 70E18, 70E50, 70E55, 70E60, 70H30, 70H14, 93C10, 49J53, 93D05

Printed on acid-free paper

This Springer imprint is published by SpringerNature
The registered company is Springer International Publishing AG Switzerland

The original version of the book was revised: For detailed information please see erratum. The erratum to this chapter is available at 10.1007/978-3-319-28664-8_9.

To my son and my wife

Preface

Thank you for opening the third edition of this monograph. The first edition [202] was published in 1996 in the Lecture Notes in Control and Information Sciences series (vol. 220), and the second edition [203] in 1999 in the Communications and Control Engineering series, both at Springer Verlag London. The third edition, written almost 20 years after the first one, is a significantly revised and updated version. Indeed Nonsmooth Mechanics has witnessed intense research during the last two decades, in the fields of Applied Mathematics (existence and uniqueness of solutions, contact complementarity problem well-posedness, numerical analysis, bifurcation analysis), Mechanics (impact modeling, Painlevé paradoxes analysis), Systems and Control (regulation and trajectory tracking), Granular Matter, Robotics, etc. Software packages dedicated to nonsmooth mechanical systems also appeared here and there. It was therefore needed to report about all these novelties.

This book is devoted to the study of a class of nonsmooth dynamical systems of the general form:

$$\begin{cases} \dot{x}(t) \ = \ g(x(t),u) \\ \\ f(x,t) \geq 0, \end{cases} \tag{1}$$

where $x(t) \in \mathbb{R}^n$ is the system's state vector, $u \in \mathbb{R}^{n_u}$ is the vector of inputs, and the function $f(\cdot,\cdot)$ represents a set of m_u unilateral constraints which are imposed on the system. More precisely, the main topic is a subclass of such systems, namely mechanical systems subject to unilateral and bilateral constraints on the position (with or without friction), whose dynamical equations may be in a first instance written as:

$$\begin{cases} M(q(t))\ddot{q}(t) + F(q(t),\dot{q}(t),t,\lambda(t)) \ = \ 0 \\ \\ f(q(t),t) \geq 0, \ \lambda_u(t) \geq 0, \ \lambda_u(t)^T f(q(t),t) \ = \ 0 \\ \\ h(q(t),t) \ = \ 0, \end{cases} \tag{2}$$

where $q(t) \in \mathbb{R}^n$ is the vector of generalized coordinates of the system. The inertia matrix $M(q)$ will be assumed to be always symmetric, but not necessarily full rank (it may be positive semi-definite). The system may be constrained by a set of m_b bilateral constraints $h(q,t) = 0$ (this is the most common case in multibody dynamics). The vector function $f(q,t)$ represents a signed distance between the system and some environment, or more simply a condition for non-penetration between the bodies that constitute the system. The *contact forces* are represented through a *Lagrange multiplier* vector λ, which is split into λ_b for bilateral constraints, and λ_u for unilateral constraints. The multiplier λ_u satisfies a specific set of conditions with the distance function: they have to be both nonnegative (excluding penetrations between the bodies, as well as gluing effects, i.e., only nontensile contact interactions are modeled), and they have to be orthogonal one to each other (excluding distance effects like magnetic forces). These conditions are called *complementarity constraints*, and we will write them more compactly as:

$$0 \leq f(q,t) \perp \lambda_u \geq 0, \tag{3}$$

where inequalities are understood componentwise, so that we may equivalently write $0 \leq f_i(q,t) \perp \lambda_{u,i} \geq 0$ for each i. Complementarity is an ubiquitous concept all through this book. Mechanical systems composed of rigid bodies interacting with each other, fall into this subclass of systems, and may be named *nonsmooth multibody systems*. One particular feature of systems as in (2) is that they are of variable structure, or changing topology, because their dimension may vary due to complementarity constraints (from a certain point of view, this is similar to sliding mode controlled systems where attractive sliding surfaces make the system's dimension decrease or increase, and is met when Coulomb's friction or another tangent forces model imposes sticking modes).

Another feature of systems as in (1) and (2) is that their solutions are nonsmooth (with respect to time): nonsmoothness arises primarily from the occurrence of *impacts* (or *collisions*, or *percussions*) in the dynamical behavior, when the trajectories attain the surface $f(q,t) = 0$. They create velocity discontinuities, and are necessary to keep the trajectories within the subspace $\Phi(t) = \{q \in \mathbb{R}^n | f(q,t) \geq 0\}$ of the system's state space (or configuration space if one adopts a more geometrical point of view). Nonsmoothness may also be due to frictional effects, like when Coulomb's friction model is adopted: then the acceleration may suffer from discontinuities. It is therefore necessary, when dealing with such classes of dynamical systems, to focus on collision dynamics, with or without friction. But this is not sufficient: indeed, another important feature of systems as in (2) is their *hybridness*, where the word hybrid means that both continuous and discrete-event-like dynamics are mixed. Roughly speaking, the continuous dynamics are due to the vector field in (2), whereas the modes correspond to the algebraic constraints ($f(q,t)$ in (2) may be a vector) that may be active or inactive. Without going into further details at this stage (it is the goal of this monograph to provide a complete

tour of such nonsmooth systems), let us already notice that the dynamics will generally be composed of ODEs, DAEs, MDEs[1] and finite automata. The particular feature of nonsmooth systems is that the automaton dynamics is ruled by the complementarity conditions. This renders their analysis so exciting, because it relies on complementarity theory, convex analysis, nonsmooth analysis, and variational inequalities. Actually, notice that nonsmooth models similar as the ones we shall describe here overstep the framework of mechanical systems, since they also apply for instance to electrical circuits [10].

What follows in this paragraph is a not an introduction to the history of nonsmooth phenomena study in mechanics. It only aims at briefly recalling some celebrated names who have been involved one way or another in this topic. The interested (French speaking) readers may have a look at [366, 1050, 1307] for a more complete exposition of history of mechanics. It is worth noting that the problems related to impact dynamics have attracted the interest of physicists for at least three centuries (much more if one includes the studies of ancient Greek engineers and mathematicians like Aristotle and Heron). In the "modern" times, a strong interest about shock phenomena was motivated by the well-known contest organized by the Royal Society of London in 1668. The impact physical laws were in particular discussed, studied, and used initially by scientists like[2] R. Descartes (F, 1596–1650), G. Leibniz (D, 1646–1716), I. Newton (UK, 1642–1727) [246, 925], Jacob Bernoulli [135] (CH, 1654–1705) [519], Jean le Rond d'Alembert (F, 1717–1783) [320] S.D. Poisson (F., 1781–1840) [1008], Ch. Huygens (NL, 1629–1695) [566], G. Coriolis (F., 1792–1843) [301, 302], J. Wallis (UK, 1616–1703), Ch. Wren (UK, 1632–1723), E. Mariotte (F, 1620–1684), L. Carnot (F, 1753–1823), H. Navier (F, 1785–1836) [920], MacLaurin (Scotland, 1698–1746) [920], the well-known Newton's and Poisson's restitution coefficients being still well alive as basic models for rigid bodies collisions. Shock processes were also widely used in the debates between Leibnizians and Newtonians or Cartesians [434, 571, 572], in their controversies about the definition of forces. The first book entirely dedicated to shock theory has been published by Edme Mariotte (F, 1620–1684) intitled *Traité de la Percussion ou Choc des Corps dans Lequel les Principales Règles du Mouvement, Contraires à celles que M. Descartes et quelques Autres Modernes ont Voulu Etablir, sont démontrées par leurs Véritables Causes* in 1673. He was inspired by Wallis, Huygens, and Wren.[3] Huygens wrote in *Projet Inachevé d'un Préface pour un Traité sur le Choc des Corps et la Force Centrifuge (1689)* that he was irritated by Mariotte and accused him of plagiarism:

[1]Measure Differential Equations.

[2]In reality, it seems that the first "published" works on impact dynamics have been those of Thomas Hariot (around 1610–1620) [640] and the Dutch scientist Beeckman (around November–December 1618) who, contrarily to Descartes whose ideas on impact dynamics were almost all false, proposed theories that were not so incoherent when replaced in the early seventeenth century context [640, 1230].

[3]In *Mariotte, savant et philosophe (1684): analyse d'une renommée*, Librairie Philosophique J. Vrin, Paris, 1986.

"Mariotte a tout pris de moy… Je le luy dis un jour et il ne su que respondre." (Mariotte took everything from me… I told him once and he was not able to answer).

Later G. Darboux (F, 1842–1917) [326, 327], E.J. Routh (UK, 1831–1907) [1049], P. Appell (F, 1855–1930) [54], J.W. Gibbs (USA, 1839–1903) [446], A.M. Lyapunov (Ru, 1857–1918) [776], L. Poinsot (F, 1777–1859) [1006, 1007], and others [765, 904, 1265] worked on impact dynamics.[4] Although this fact has been a little forgotten now, rigid body (or more exactly particles) shock dynamics were extensively used in the seventeenth century to study light models [566] and also by artillerists [798] to predict the flight of cannon balls and their impacts. As we pointed out above, much of this scientific excitation was due to the will of the Royal Society of London whose scientists wanted to settle a coherent theory of motion.

Nonsmooth Mechanics belongs to Solid Mechanics. However, several other scientific communities have strong interests in this field. Applied Mathematicians, for problems related to existence and uniqueness of solutions, analysis of complex dynamics of certain impacting systems like billiards,[5] bifurcation analysis, researchers from Mechanical and Civil Engineering, as well as Physicists (the study of granular matter—sandpiles, gravels, planetary rings—has become a very important field that involves these three scientific communities), Robotics (to study the effect of impacts in the joints or the motion of the system after the impact, like in robot manipulators, bipeds, juggling or hopping robots, multifingered hands, $\cdots$), Electromechanics (electromechanical contacts are a major source of failures in many systems like automotives, aircraft, machine tools, consumer electronics, and therefore motivate the study of accurate models for simulation and design purposes), Computer Sciences (graphics, virtual reality) are scientific communities interested in nonsmooth multibody dynamical systems. These models are also used in Chemistry and Biology [285, 647, 1135, 1260, 1273], in Sports Dynamics for the analysis of tennis ball/racket or golf ball/club dynamics [55, 200, 201, 311, 597, 1113], and in Ecology for forest fire modeling [264, 339, 786].

I would like to end this introduction by mentioning two papers that have been, in my opinion, the most important ones in the field of "modern" nonsmooth mechanics:

G. Darboux, 1880 "Etude géométrique sur les percussions et le choc des corps," Bulletin des Sciences Mathématiques et Astronomiques, deuxième série, tome 4, pp. 126–160 and J.J. Moreau, 1988 "Unilateral contact and dry friction in finite freedom dynamics", in J.J. Moreau, P.D. Panagiotopoulos, (Eds.), *Nonsmooth Mechanics and Applications*, CISM Courses and Lectures no 302, International Centre for Mechanical Sciences, Springer-Verlag, pp. 1–82.

---

[4]It is worth recalling that so many great scientists found an interest in impact dynamics. Indeed most of them are not known for their contributions in this field.

[5]In the literature, it seems that the word *vibro-impact systems* is used in the mechanical engineering field to name various types of systems that involve percussions. The word *billiards* refers to theoretical models of particles colliding in a closed domain, and is used mainly in mathematical physics.

The paper by the Mathematician Gaston Darboux (1842–1917) proposes a way to model the shock process and analytical developments that have been, and are still widely used in impact mechanics, more than one century later. The paper by Jean Jacques Moreau (1923–2014), who is one of the foundators of Convex Analysis[6] together with R.T. Rockfellar,[7] settles a general framework for the modeling of mechanical systems with unilateral constraints, based on convex analysis tools. It has motivated subsequent works on both the mathematical (well-posedness) and the numerical simulation sides (in particular concerning granular matter), which have considerable importance in this field.

This choice (both are French…) only reflects my own opinion. Finally, readers who want to learn more about frictionless multiple impact models should have a look at [929], and those who desire to learn about the numerical analysis and simulation of nonsmooth mechanical systems may read [13].

This book deals a lot with *modeling*. Let me quote the following:

Remember that all models are wrong; the practical question is how wrong do they have to be to not be useful. (in G.E.P. Box and N.R. Draper, Empirical Model-Building and Response Surfaces, 1987).

A deep (not superficial) understanding of engineering and physics is required to develop useful mathematical and computational models; the importance of models and their limitations is often given insufficient attention by control researchers. (N.H. McClamroch, IEEE Control Systems Magazine, October 2014).

The way a scientist may describe contact laws depends on his research area, and on the results he desires. [614]

Some authors, arguing that instantaneous forces do not exist, prefer not to use the notion of percussion and subsequent theory that determine their effects. There does not exist neither points nor straight lines in nature. Nevertheless we find such abstract objects useful and interesting. Certainly when passing to applications one has to quantify the errors that one may make by applying theorems derived from pure Science. But this problem is independent of the development of Science itself. [327]

Acknowledgments

This book is the result of more than 20 years of research in the area of nonsmooth mechanical systems. It would not have been possible without fruitful exchanges with the following colleagues and students, whom I warmly thank (hopefully no one is forgotten…): M. Abadie, V. Acary, S. Adly, M. di Bernardo, F. Bertails-Descoubes, A. Blumentals, J.M. Bourgeot, R.M. Brach, C. Georgescu,

[6] *A Mechanician capable of doing Mathematics without any accent*, according to his own words.

[7] R.T. Rockafellar developed Convex Analysis with Mathematical Programming motivations, while J.J. Moreau did it with Nonsmooth Mechanics objectives in mind.

F. Génot, C. Glocker, D. Goeleven, M. Heemels, O. Huber, Y. Hurmuzlu, G. James, R. Kikuuwe, C. Lamarque, B.K. Le, R.I. Leine, C. Liu, M. Mata Jimenez, M. Monteiro-Marques, C.I. Morarescu, N.S. Nguyen, S.I. Niculescu, L. Paoli, C. Prieur, M. Schatzman, A. Tanwani, L. Thibault, A. Vieira, A. Zavala-Rio, H. Zhang, Z. Zhao.

Contents

Notation

- A matrix $M \in \mathbb{R}^{n\times n}$ is positive (semi) definite if $x^T M x > 0$ for all $x \neq 0$ (resp. ≥ 0 for all x): $M \succ 0$ (resp. $M \succeq 0$). M is negative (semi) definite if $-M \succ 0$ (resp. $\succeq 0$): $M \prec 0$ (resp. $\preceq 0$). It is not necessarily symmetric.
- A matrix M is positive (resp. nonnegative) if all its entries M_{ij} are positive (resp. nonnegative).
- Let $f : \mathbb{R}^n \to \mathbb{R}^p$ be a differentiable function. Its Jacobian at x is $\frac{\partial f}{\partial x}(x) \in \mathbb{R}^{p\times n}$, its gradient $\nabla f(x) = \left(\frac{\partial f}{\partial x}(x)\right)^T \in \mathbb{R}^{n\times p}$.
- Let $x \in \mathbb{R}^n$, then $x > 0$ (resp. ≥ 0) means that each component $x_i > 0$ (resp. ≥ 0).
- The kinetic energy of a Lagrange system with generalized coordinate vector q, velocity $\dot{q}$, and inertia matrix $M(q) = M(q)^T \succeq 0$, is denoted $T(q,\dot{q}) = \frac{1}{2}\dot{q}^T M(q)\dot{q}$.
- The $n \times n$ identity matrix is I_n.
- Lexicographical inequalities: $(x_1, x_2, \cdots, x_n) \succcurlyeq 0$ means that if $x_1 = x_2 = \cdots = x_{i-1} = 0$ for $i - 1 < n$, then $x_i \geq 0$ (the first nonzero entry is > 0, or all entries are zero); $(x_1, x_2, \cdots, x_n) \succ 0$ means that not all entries are zero, and the first nonzero entry $x_i > 0$.
- Let $x \in \mathbb{R}^n$, $M = M^T \succeq 0$ a $n \times n$ matrix, and $K \subseteq \mathbb{R}^n$ a nonempty set. The orthogonal projection of x on K in the metric defined by M is denoted as $\text{proj}_M[K; x] \stackrel{\Delta}{=} argmin_{z\in K} \frac{1}{2} z^T M z$. If K is convex and $M \succ 0$ it is unique.
- The boundary of a nonempty set Φ is denoted as $\text{bd}(\Phi)$ (perhaps rarely as $\partial\Phi$ not to confuse with the subdifferential).
- The unit ball is $\mathbb{B} = \{x \in \mathbb{R}^n | \; ||x|| \leq 1\}$ where $||\cdot||$ is a norm.
- Let $u : \mathbb{R} \to \mathbb{R}^n$ be a function which has right and left limits at t. Then $\sigma_u(t) \stackrel{\Delta}{=} u(t^+) - u(t^-)$.
- Subscripts λ_{n} refer to normal direction, λ_{t} to tangential directions, while in λ_n the subscript $n \in \mathbb{N}$ is for a sequence of reals.

- The usual notation A: $\mathbb{R}^n \rightrightarrows \mathbb{R}^m$ is employed for multivalued functions, i.e., functions such that $A(x)$ may be a subset of $\mathbb{R}^m$ for some $x \in \mathbb{R}^n$.
- A function such that $\left(\int_{[a,b]} |f(t)|^p dt\right)^{\frac{1}{p}} < +\infty$, $1 \leq p < +\infty$, is said to belong to the space $L^p([a,b])$ (or sometimes denoted $L_p([a,b])$. When $p = +\infty$, the space $L_\infty([a,b])$ contains functions such that ess $\sup|f(t)| < +\infty$, i.e., functions which are bounded except on a set of measure zero.
- We say that $f \in C^p(I)$ if it is p times differentiable on I, and $f^{(p)}(\cdot)$ is continuous on I.
- $\text{diag}(x_1, x_2, \cdots, x_m)$, is the $m \times m$ diagonal matrix D with diagonal entry $D_{ii} = x_i$.
- Coefficients of restitution (CoRs): e_{n}: Newton (or kinematic) CoR, e_{p} Poisson (or kinetic) CoR, $e_{\star}$ energetic CoR.
- Given a matrix $A \in \mathbb{R}^{n \times n}$, its largest and smallest eigenvalues are denoted $\lambda_{\max}(A)$ and $\lambda_{\min}(A)$, respectively. Let $A \in \mathbb{R}^{n \times m}$, singular values are defined as $\sigma_i = \sqrt{\lambda_i(AA^T)} = \sqrt{\lambda_i(A^TA)}$ for $1 \leq i \leq \min(n,m)$, and the largest singular value is $\sigma_{\max}(A) = \sqrt{\lambda_{\max}(AA^T)}$. One has $\sigma_{\max}(A) = ||A||_2$ where $||\cdot||_2$ is an induced matrix norm, also denoted $||\cdot||_{2,2}$: $||A||_{2,2} = \max_{x \in \mathbb{R}^n \setminus \{0\}} \frac{||Ax||}{||x||}$, where $||\cdot||$ is the Euclidean norm.

Chapter 1
Impulsive Dynamics and Measure Differential Equations

This chapter is devoted to introducing the mathematical basis on which various evolution problems involving impulsive terms rely. Impulsive forces in mechanics are first presented disregarding what they may be produced by. It is shown on simple examples why impulsive mechanics involves only measures (Dirac "functions"), and no distribution of higher degree (derivatives of the Dirac "function"). Various classes of measure differential equations (MDEs), or impulsive systems, are introduced. Then unilaterally constrained dynamical systems are presented, and the differences with the foregoing MDEs are discussed. Variable changes that allow one to transform MDEs into Carathéodory ordinary differential equations (ODEs) or unilaterally constrained mechanical systems into Filippov's differential inclusions, are described in the last section.

1.1 Impulsive Forces

Let us introduce the impacts as purely exogenous actions on a mechanical system, without considering the way by which they may be produced. In other words, we consider impulsive forces (which we may name also exogenous impacts or external percussions). Simply speaking, an impact between two bodies (not necessarily rigid) is a phenomenon of very short duration that implies a sudden change in the bodies dynamics (fast velocity variation). Impacts are treated usually as very large forces acting during an infinitely short time, i.e., if Δt represents the collision duration and $F(\tau)$ represents the force during the collision ($F(\cdot)$ may be viewed as a time function whose support is $K \stackrel{\Delta}{=} [t_k, t_k + \Delta t]$, i.e., $F(\cdot)$ is zero outside K), then the force impulse p_k due to the impact at time t_k is:

$$p_k = \lim_{\Delta t \to 0} \int_{t_k}^{t_k + \Delta t} F(\tau) d\tau. \tag{1.1}$$

B. Brogliato, *Nonsmooth Mechanics*, Communications and Control Engineering,
DOI 10.1007/978-3-319-28664-8_1

In order for the right-hand side of (1.1) to be a nonzero quantity, and as $\Delta t \to 0$, the force $F(\tau)$ must take infinite values, since the integration interval becomes of zero Lebesgue measure. It follows that $F(\cdot)$ cannot be a *function* of time (it is almost everywhere zero and its Lebesgue integral is not zero [1082]) and must be considered as a singular distribution or Dirac measure at time t_k, denoted as δ_{t_k}, with magnitude p_k, i.e., $F = p_k \delta_{t_k}$ which is an equality of measures. It is worth noting that this is not just *one* way to represent the impulsive force which is an equality of measures according to Eq. (1.1), but this is the *only* formulation of such a phenomenon that is mathematically correct: "Analogy between mathematical and physical distributions has not to be shown: *mathematical distributions provide a correct mathematical definition of distributions encountered in physics*," [1081, Chap. 1, p. 84].
One of the main consequences of such an approach is that the impulsive forces imply a discontinuity in the velocity while positions remain continuous. This can be understood from simple examples.

Example 1.1 Assume that a mass m moving on a line, with gravity center coordinate x (the system is depicted in Fig. 1.1), is submitted to an impulsive force of magnitude p_k at the instant t_k. The dynamical equation is given by:

$$m\ddot{x} = p_k \delta_{t_k}, \tag{1.2}$$

which is to be understood as an equality of distributions. Assume now that x and $\dot{x}$ possess (possibly zero) respective jumps $\sigma_x(t_k) \stackrel{\Delta}{=} x(t_k^+) - x(t_k^-)$ and $\sigma_{\dot{x}}(t_k) \stackrel{\Delta}{=} \dot{x}(t_k^+) - \dot{x}(t_k^-)$ at t_k, where $\dot{x}(t_k^+) = \lim_{t \to t_k, t > t_k} x(t)$, $\dot{x}(t_k^-) = \lim_{t \to t_k, t < t_k} x(t)$. In the following we shall prove that $\sigma_x(t_k) = 0$ whereas if p_k is not zero, then neither is $\sigma_{\dot{x}}$. We have:

$$\begin{cases} \dot{x} = \{\dot{x}\} + \sigma_x(t_k)\delta_{t_k} \\ \\ \ddot{x} = \{\ddot{x}\} + \sigma_x(t_k)\dot{\delta}_{t_k} + \sigma_{\{\dot{x}\}}(t_k)\delta_{t_k}, \end{cases} \tag{1.3}$$

where $\{\dot{f}\}$ represents the derivative of $f(\cdot)$ calculated ignoring the points of discontinuity of $f(\cdot)$, and which is not defined at the points of discontinuity [1082, Chap. 2, Sect. 3]. For instance, the distributional derivative of the heavyside function $h(t) \equiv 0$ for $t < t_k$, $h(t) \equiv 1$ for $t \geq t_k$ is $\dot{h} = \{\dot{h}\} + \delta_{t_k} = 0 + \delta_{t_k} = \delta_{t_k}$. The notation Dh instead of $\dot{h}$ is generally used to denote the distributional derivative of a function h [1076], so that $Dh = \delta_{t_k}$. The Eq. (1.2) should be written as the equality of distributions $DX = AX dt + p_k DH$, with $X^T = (x, \dot{x})$, $H^T = (0, h)$, and $A = \begin{pmatrix} 0 & 1 \\ 0 & 0 \end{pmatrix}$. Notice that writing $\sigma_{\dot{x}}(t_k)$ in (1.3) is meaningless since $\dot{x}$ is a priori a singular distri-

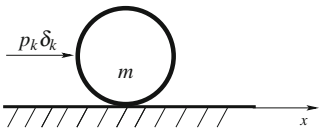

Fig. 1.1 Mass submitted to an impulsive force

bution at $t = t_k$. But $\sigma_{\{\dot{x}\}}(t_k)$ has a meaning since $\{\dot{x}\}$ is a function that might jump. Some basic facts about distributions and measures are recalled in Appendix A.1. The procedure we employ here makes use of the derivative of the Dirac measure, which is not a measure [1082]. This justifies again that we choose Schwartz's distributions as an analytical tool for our study, although the analysis of nonsmooth dynamics for collisions rests only on measures as it involves only signed distributions. We choose here the notation employed in [1082]. Introducing (1.3) into (1.2) we get:

$$m\{\ddot{x}\} = p_k\delta_{t_k} - m\sigma_x(t_k)\dot{\delta}_{t_k} - m\sigma_{\{\dot{x}\}}(t_k)\delta_{t_k}. \tag{1.4}$$

Consider now (1.4). On $[t_0, t_k)$, $t_0 < t_k$, the system has a smooth solution $x(t)$, $\dot{x}(t)$. Thus $m\{\ddot{x}\}$ has support K_1 contained in $[t_0, t_k)$. The right-hand side of (1.4) has support $K_2 = t_k$. Then we conclude that the only way to have (1.4) verified (i.e., $m\{\ddot{x}\} - (p_k - m\sigma_{\{\dot{x}\}}(t_k))\delta_{t_k} + m\sigma_x\dot{\delta}_{t_k} = 0$) is that $m\{\ddot{x}\} = 0$ and $(p_k - m\sigma_{\{\dot{x}\}}(t_k))\delta_{t_k} + m\sigma_x\dot{\delta}_{t_k} = 0$, because these two distributions must take the same value on any function $\varphi \in \mathscr{D}$ whose support does not contain t_k, i.e. zero. Recall that these equalities have to be taken in the sense of distributions, and that the value of the function $\{\ddot{x}\}$ at $t = t_k$ need not to be specified, as almost-everywhere equal functions define the same distribution. Now we are left with $(p_k - m\sigma_{\{\dot{x}\}}(t_k))\delta_{t_k} + m\sigma_x\dot{\delta}_{t_k} = 0$. If these two singular distributions were equal, we should get for any function $\varphi \in \mathscr{D}$ with support K_φ containing t_k: $\langle (p_k - m\sigma_{\{\dot{x}\}})\delta_{t_k} - m\sigma_x\dot{\delta}_{t_k}, \varphi\rangle = (p_k - m\sigma_{\{\dot{x}\}}(t_k))\varphi(t_k) + m\sigma_x\dot{\varphi}(t_k) = 0$.[1] Take $\varphi_{t_k} \equiv \varphi(t - t_k)$ where $\varphi(\cdot)$ is defined in (A.1) (see Appendix A.1), and note that $\frac{d}{dt}\varphi_{t_k}(t_k) = 0$: we obtain $p_k - m\sigma_{\{\dot{x}\}}(t_k) = 0$. Thus $m\sigma_x(t_k) = 0$ as well. Note that we could have also taken two functions $\varphi_1, \varphi_2 \in \mathscr{D}$ such that the matrix $A \stackrel{\Delta}{=} \begin{pmatrix} \varphi_1(t_k) & \dot{\varphi}_1(t_k) \\ \varphi_2(t_k) & \dot{\varphi}_2(t_k) \end{pmatrix}$ is full-rank. Then one gets $A \begin{pmatrix} p_k - m\sigma_{\{\dot{x}\}}(t_k) \\ m\sigma_x(t_k) \end{pmatrix} = 0$, which implies that both components are zero. Hence we get:

$$\begin{cases} m\{\ddot{x}\} = 0 \\ p_k - m\sigma_{\{\dot{x}\}}(t_k) = 0 \\ m\sigma_x(t_k) = 0, \end{cases} \tag{1.5}$$

from which we conclude $\sigma_x(t_k) = 0$ ($x(\cdot)$ is continuous at t_k), $\sigma_{\{\dot{x}\}}(t_k) = \sigma_{\dot{x}}(t_k)\frac{p_k}{m}$ ($\dot{x}(\cdot)$ jumps at t_k and is a function). From (1.5) we deduce that $\dot{x} = \dot{x}(t_k^-) = \dot{x}_0$ for $t < t_k$, $\dot{x} = \dot{x}(t_k^+) = \dot{x}_0 + \frac{p_k}{m}$ for $t \geq t_k$, $\ddot{x}$ is zero almost everywhere and is a Dirac measure of magnitude $\frac{p_k}{m}$ at t_k, $x(t) = \dot{x}_0 t + x_0$ for $t < t_k$, $x(t) = \left(\dot{x}_0 + \frac{p_k}{m}\right)t - \frac{p_k}{m}t_k + x_0$ for $t \geq t_k$. The equalities in (1.5) are therefore necessary for (1.4) to be true. Sufficiency is straightforward. Thus we have proved the following:

[1] Recall that distributions are indefinitely differentiable, and that the derivatives of the Dirac measure are defined as $\langle \delta_{t_k}^{(m)}, \varphi\rangle = (-1)^m\varphi^{(m)}(t_k)$ for $m \geq 0$, [1082].

Proposition 1.1 *Assume the mass is submitted to an impulsive force*[2] *at* $t = t_k$. *Then there is a discontinuity* $\sigma_{\dot{x}}(t_k)$ *in the velocity* $\dot{x}(\cdot)$ *at the time* t_k *while the position* $x(\cdot)$ *remains continuous. Conversely if the velocity is discontinuous at* $t = t_k$ *and the position is continuous, then there is an impulsive force at* $t = t_k$, *and the acceleration is a Dirac measure.*

Let us fix the following definitions [896][3]:

Definition 1.1 A *force* $F(t)$ acting on a system is the density with respect to the Lebesgue measure dt of the *contact impulsion measure* dP, i.e., $P(t) = \int_{t_0}^{t} F(x)dx$.

Definition 1.2 A *contact percussion* is an atom at the impact time t_k of the *contact impulse measure* dP. The *percussion vector* p_k is the density of the atom with respect to the Dirac measure δ_{t_k}, i.e., $dP = F(t)dt + p_k\delta_{t_k}$.

Hence in Proposition 1.1 we should have said contact percussion instead of impulsive percussion. The term impulsive force is also currently used to mean contact percussion. Some basic facts about measures are recalled in Appendix A.2. In particular see Definition A.10. Although the use of such a vocabulary may appear too complex and too mathematical, we shall see in Chaps. 2 and 5, Sect. 5.2, that shock dynamics can be formulated as equalities of measures.

Remark 1.1 The solutions of differential equations with distributions can also be studied by considering sequences of equations whose coefficients are functions that tend towards the distributional coefficients [397]. For instance (1.2) is the limit of $\ddot{x}_n(t) = p_n(t)$, where $\{p_n\}$ is a sequence approximating the Dirac measure, see Appendix A.1. Another point of view is to give the approximating problems an a priori physical meaning by considering state-dependent forces $F_n(x_n)$ that possess certain properties; one has to prove that the limit problem (with respect to a certain notion of convergence) is a dynamical problem involving singular measures. These results are presented in Chaps. 2 and 3.

Example 1.2 Consider a system composed of two masses m_1 and m_2 moving on a horizontal line, with coordinates x_1 and x_2, linked with a spring of stiffness k (see Fig. 1.2). This may represent a simple manipulator with flexible joints. We assume that with a suitable coordinate x_2 transformation, the spring is at rest when $x_1 = x_2$. Also u is the (bounded) force applied on mass 1. The dynamical equations of the system are given by

[2]For the moment, by impulsive force we mean something like $p_k\delta_{t_k}$, for some real p_k and some t_k. More precise definitions are given in Definitions 1.1 and 1.2.

[3]Note that in the following definition, we do not pretend to define the very basic notion of what a force is. We just set what is meant by a "regular" force, in opposition to an "impulsive" force. For a discussion on the basic definition of what forces are, see for instance [1218] and references therein, who argue that in fact, forces in physics should be defined from basic axioms, just like real numbers are in mathematics.

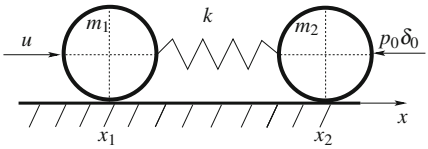

Fig. 1.2 Coupled masses submitted to an impulsive force

$$\begin{cases} m_1\ddot{x}_1 + k(x_1 - x_2) = u \\ \\ m_2\ddot{x}_2 + k(x_2 - x_1) = p_0\delta_0, \end{cases} \tag{1.6}$$

where we assume that the percussion on mass 2 occurs at $t = 0$, and for the moment (1.6) is seen as an equality of distributions. Suppose that x_1, $\dot{x}_1$, x_2, $\dot{x}_2$ possess a discontinuity at $t = 0$; we thus obtain from (1.6):

$$\begin{cases} m_1\{\ddot{x}_1\} + k(x_1 - x_2) = u \\ \\ m_1\sigma_{\dot{x}_1}(0)\delta_0 + m_1\sigma_{x_1}(0)\dot{\delta}_0 = 0 \\ \\ m_2\{\ddot{x}_2\} + k(x_2 - x_1) = 0 \\ \\ m_2\sigma_{x_2}(0)\dot{\delta}_0 + m_2\sigma_{\dot{x}_2}(0)\delta_0 = p_0\delta_0. \end{cases} \tag{1.7}$$

From the analysis done in Example 1.1 we deduce that x_1, $\dot{x}_1$, x_2 are continuous-time functions, whereas $p_0 = m_2\sigma_{\dot{x}_2}(0)$. Let us push this example further by introducing some physics in it. Let us denote $x_c(t) = \frac{m_1x_1 + m_2(x_2 - l)}{m_1 + m_2}$ the position of the center of mass of the system, where l is the spring length. Since $\dot{x}_1$ is continuous, we have:

$$\begin{cases} \dot{x}_c(0^-) = \frac{m_1\dot{x}_1(0) + m_2\dot{x}_2(0^-)}{m_1 + m_2} \\ \\ \dot{x}_c(0^+) = \frac{m_1\dot{x}_1(0) + m_2\dot{x}_2(0^+)}{m_1 + m_2}. \end{cases} \tag{1.8}$$

Thus $m_2\sigma_{\dot{x}_2}(0) = (m_1 + m_2)(\dot{x}_c(0^+) - \dot{x}_c(0^-))$. Also from (1.6) and (1.8) we get:

$$(m_1 + m_2)\{\ddot{x}_c\} = p_0\delta_0 - (m_1 + m_2)\sigma_{\dot{x}_c}(0)\delta_0 + u, \tag{1.9}$$

which governs the system's center of gravity motion. If there is no loss of energy during the impact, the post-impact kinetic energy $T(0^+) = \frac{1}{2}m_1\dot{x}_1(0^+)^2 + m_2\dot{x}_2(0^+)^2 = T(0^-) = \frac{1}{2}m_1\dot{x}_1(0^-)^2 + m_2\dot{x}_2(0^-)^2$, where $T(t)$ denotes the kinetic energy of the system (note that since the potential energy depends on the position only, it does not change at the percussion instant). Thus we get $\dot{x}_2(0^+) = -\dot{x}_2(0^-)$ and $p_0 = 2m_2\dot{x}_2(0^+)$ (the other solution leads to $\dot{x}_2(0^+) = \dot{x}_2(0^-) \Rightarrow p_0 = 0$: there is no impulsive force applied at $t = 0$). When a unilateral constraint is added, we shall see that the second solution yields an unfeasible motion and has to be eliminated.

One sees that whatever u may be at the moment of impact, the motion of mass 2 is independent of u. It can be easily verified that the same result holds (discontinuous $\dot{x}_2$) if a damper is added between the two masses.

Example 1.3 These ideas can be extended to the case of more complicated mechanical systems such as rigid or flexible joint manipulators. For instance, a rigid manipulator with generalized coordinates vector $q \in \mathbb{R}^n$, submitted to a wrench of external forces $\lambda \in \mathbb{R}^m$, $m \leq n$, admits the following state space representation:

$$\begin{cases} \dot{x}_1 = x_2 \\ \dot{x}_2 = -M^{-1}(x_1)\left[C(x_1, x_2)x_2 + g(x_1) - u - J(x_1)^T\lambda\right], \end{cases} \tag{1.10}$$

where $x_1 = q$, $x_2 = \dot{q}$, $M(x_1) \succ 0$ is the symmetric inertia matrix, $C(x_1, x_2)x_2$ contains centrifugal and Coriolis terms, $g(x_1)$ is the generalized gravity vector, $J(x_1)$ is the Jacobian between the joint coordinates q space and the Cartesian space, i.e., if λ works on positions $X \in \mathbb{R}^m$, then $\dot{X} = J(q)\dot{q}$. We assume that $J(x_1) \in \mathbb{R}^{m\times n}$ is full row rank m. The term u is the generalized torque vector applied at the joints, which can be considered as a control input for the robot manipulator, and is assumed to be a bounded function of t, x_1, x_2.
If the system is submitted to an impulsive force $\lambda = p_k\delta_{t_k}$ we can write:

$$\begin{cases} M(x_1)\{\dot{x}_2\} + C(x_1, \{x_2\})\{x_2\} + g(x_1) & = u \\ \\ M(x_1)\left[\sigma_q(t_k)\dot{\delta}_{t_k} + \sigma_{\dot{q}}(t_k)\delta_{t_k}\right] + 2C(x_1, \{x_2\})\sigma_q(t_k)\delta_{t_k} & \\ +C(x_1, \sigma_q(t_k)\delta_{t_k})\sigma_q(t_k)\delta_{t_k} & = J(x_1)^T p_k\delta_{t_k}, \end{cases} \tag{1.11}$$

where we have proceeded as in the foregoing examples to express the distributional derivatives of x_2 and x_1, and we have used the properties of $C(\cdot,\cdot)$, i.e., $C(x, y)z = C(x, z)y$ and $C(x, y + z)w = C(x, y)w + C(x, z)w$: the first equation in (1.11) is an equality of functions, whereas the second one is a relation between distributions. Following the reasoning in Example 1.1, we deduce from (1.11) that $\sigma_q(t_k) = q(t_k^+) - q(t_k^-) = 0$. Moreover note that the last term of the left-hand side of the second equality is not defined, as the product of two distributions does not exist in general: in this particular case obviously $\delta_{t_k}\delta_{t_k}$ has no mathematical meaning [1082, p. 117] [51, §12.5]. Since the position jump is zero, the right-hand side of the second equation in (1.11) is meaningful within the framework of classical distribution and measure differential equations theories, as $J(x_1)^T p_k\delta_{t_k}$ is well defined, $x_1(\cdot)$ being time-continuous. Then it yields

$$M(q)(\dot{q}(t_k^+) - \dot{q}(t_k^-)) = J(q)^T p_k, \tag{1.12}$$

because the acceleration $\ddot{q}$ is the measure $\sigma_{\dot{q}}(t_k)\delta_{t_k} + \{\ddot{q}\}dt$. From (1.12) and from the row full-rank property of $J(q)$, one infers:

$$p_k = \left(J(q)J(q)^T\right)^{-1} J(q)M(q)(\dot{q}(t_k^+) - \dot{q}(t_k^-)). \tag{1.13}$$

Thus Proposition 1.1 is true for Lagrangian systems as well. These systems do not fit within the class of systems studied in Sect. 1.2.1, since the singular measure is premultiplied by a state- dependent term.

Example 1.4 The above analysis may be extended to flexible-joint rigid-link manipulators subject to an impulsive input

$$\begin{cases} M(q_1)\ddot{q}_1 + C(q_1, \dot{q}_1)\dot{q}_1 + g(q_1) = K(q_2 - q_1) \\ J\ddot{q}_2 + K(q_2 - q_1) = \sum_{i=0}^{n} p_k \delta_{t_k}, \end{cases} \tag{1.14}$$

for some $n \in \mathbb{N} \cup \{+\infty\}$, where $q = (q_1^T, q_2^T)^T \in \mathbb{R}^n \times \mathbb{R}^n$, $M(q) = \text{diag}\,(M(q_1), J) \succ 0$, $K \in \mathbb{R}^{n \times n}$ is the joint stiffness matrix. This model is common in control and robotics. One infers that $\dot{q}_2(\cdot)$ is discontinuous at times t_k, $\ddot{q}_2$ is the Dirac measure $\sum_{i=0}^{n} \sigma_{\dot{q}_2}(t_k)\delta_{t_k}$, $q_2(\cdot)$ is continuous piecewise differentiable, $\dot{q}_1(\cdot)$ is continuously differentiable, $q_1(\cdot)$ is continuously twice differentiable, and $\ddot{q}_1(\cdot)$ is continuous piecewise differentiable. It is quite interesting to compare these results with those of Sect. 3.4.2, where unilateral constraints are included. This helps to understand why controlling Lagrangian systems with impulsive control forces (see for instance [605]) and controlling systems with unilateral constraints and impacts, are quite different problems.

This brief analysis shows that in mechanical systems, continuous positions and discontinuous velocities are produced by impulsive forces, and vice versa. *They make a particular case of Measure Differential Equations*,[4] *which are reviewed in the next sections.*

1.2 Measure Differential Equations (MDEs)

Roughly speaking, MDEs are ODEs with impulsive inputs. The state of such systems may jump. Different classes of dynamical systems with state jumps have been studied in applied mathematics and in systems and control literature. We present some of them now. Readers interested in mechanics and not on generalities on other types of impulsive systems, may skip sections on MDEs.

[4]While systems subject to unilateral constraints will be embedded into measure differential **inclusions**

1.2.1 A First Class of MDEs

Until now we have considered simple MDEs modeling mechanical systems subject to exogenous impulsive forces. It is useful to have more insights on MDEs, and which main similarities and discrepancies exist between ODEs and MDEs, as well as between MDEs and dynamics of systems with unilateral constraints. Moreover the MDEs in this section may describe control systems where the control input is impulsive. The material in this section is taken from Schmaedeke [1076]. Let S be a domain in the (t, x) space $\mathbb{R}^{n+1}$, $f(t, x)$ be a real $n-$vector function defined on S. Let $u(t)$ be a real $m-$vector function of bounded variation (or BV, see Appendix A.3), continuous from the right on a time interval I_1, and let $G(t)$ be a time-continuous $n \times m$ matrix defined on I_1. Let (t_0, x_0) be a point in S with $t_0 \in I_1$. Let us denote by $\mathscr{M}$, the differential equation:

$$Dx = f(t, x) + G(t)Du, \quad x(t_0) = x_0. \tag{1.15}$$

As we saw in Sect. 1.1, D denotes the operation of differentiation in the sense of distribution derivatives, with respect to t. It is clear that since $u(\cdot)$ is BV, then Du is a differential measure (see Appendix A.3.2), and so is Dx; so we could use the notation du and dx (we however keep the original notations in [1076]). Therefore $x(\cdot)$ will not be a continuous function of time in general, but it will "copy" the jumps in $u(\cdot)$. A solution $x(t)$ to $\mathscr{M}$ in (1.15) is defined as follows:

Definition 1.3 A solution $x(\cdot)$ of $\mathscr{M}$ is a real bounded variation $n-$vector together with an interval I containing t_0, such that $x(t)$ is continuous from the right on I and

- $(t, x(t)) \in S$ for $t \in I$.
- $x(t_0) = x_0$.
- The distributional derivative of $x(t)$ on I is $f(t, x) + G(t)Du$.

Consider now the integral equation $\mathscr{T}$:

$$x(t) = x_0 + \int_{t_0}^{t} f(s, x(s))ds + \int_{(t_0,t]} G(s)du(s), \tag{1.16}$$

where du denotes the Stieltjes measure determined by $u(t)$. Then we have

Definition 1.4 A solution $x(t)$ of $\mathscr{T}$ is a real bounded variation $n-$vector $x(t)$ together with an interval I such that:

- $(t, x(t)) \in S$ for $t \in I$.
- $x(t)$ satisfies the integral equation.

The following theorem generalizes a well-known result for Carathéodory ODEs [533, 1229], according to which the solution of an ODE $\dot{x}(t) = f(t, x(t))$, $x(t_0) = x_0$ is also a solution of the integral equation $x(t) = x_0 + \int_{t_0}^{t} f(y, x(y))dy$ and *vice versa*.

Theorem 1.1 *[1076] A solution $x(t)$ of $\mathscr{T}$ is a solution $x(t)$ of $\mathscr{M}$ and conversely.*

Remark 1.2 Notice that if $u(t)$ is absolutely continuous, then all these definitions reduce to the classical theory for Carathéodory differential equations. In fact in this case the distributional derivative is just the usual derivative.

Theorem 1.1 is useful to prove local existence and uniqueness results for MDEs as $\mathscr{M}$, using the fixed point property of contraction mappings, see [1076, Theorems 2 and 3] quite similarly as for ODEs [1229]. Following Theorem 1.1, the state $X = (x, \dot{x})^T$ of the simple system in Example 1.1 is a solution of (1.2) if and only if it is a solution of the integral equation

$$X(t) = X(t_0) + \int_{[t_0,t]} AX(\tau)d\tau + \int_{[t_0,t]} \begin{pmatrix} 0 \\ Dh(\tau) \end{pmatrix}, \tag{1.17}$$

and $X(\cdot)$ (hence $\dot{x}(\cdot)$) is necessarily continuous from the right with $h(\cdot)$ defined as above (we could have also defined $h(\cdot)$ as a left-continuous function since Stieltjes measures can indifferently be defined from functions left as well as right-continuous [477, p.133]).
Theorems on existence and uniqueness of solutions are generalized to MDEs. Ordinary Carathéodory differential equations are generalized to Carathéodory measure systems (CMS) defined as follows:

Definition 1.5 [1076] Consider an MDE as in $\mathscr{M}$. Let $f(t, x)$ be defined in a neighborhood of a domain S of $\mathbb{R}^{n+1}$, such that for each point $(t_0, x_0) \in S$ there is a rectangle R_{ab} centered at (t_0, x_0), a constant $K > 0$ and a function $r(t)$ summable on the interval $[t_0 - a, t_0 + a]$ as

- $f(t, x)$ is measurable in t for each fixed x such that $(t, x) \in R_{ab}$.
- $f(t, x)$ is locally Lipschitz continuous with constant K with respect to x, for all $(t, x) \in R_{ab}$.
- $|f(t, x)| \leq r(t)$ in R_{ab}.
- $|| \int_{t_0}^{t} G(s)du||^\star < b$, where the norm is taken on $[t_0 - a, t_0 + a]$.[5]

Then $\mathscr{M}$ is a CMS.

It can be checked that $\mathscr{M}$ with $G(t)$ continuous on an interval I, $u(t)$ right-continuous of bounded variation on I, $[t_0 - a, t_0 + a] \subset I$, is a CMS. What is remarkable in Definition 1.5 is that the initial conditions are taken in a domain S, but one needs to consider the dynamics outside S (indeed the rectangles R_{ab} need not be contained in S). This is not the case for ordinary Carathéodory equations (see Sect. 1.4.1). This is intuitively explained by the fact that for any bounded domain within which the initial conditions may lie, then the jump imposed on the state by $Du(t)$ is likely to take the state outside this domain (instantaneously). This jump $G(t_k)\sigma_{u(t_k)}$ is clearly

[5]The norm $||.||^\star$ is defined as $||f||^\star = \sum_{i=1}^{n} ||f_i||$ with $||f_i|| = \text{var}(f_i, I) + |f_i(a^+)|$ for scalar functions $f_i(\cdot)$ on $I = [a, b]$.

independent of the initial conditions: it is an exogenous variable driven by $u(t)$ and $G(t)$.
The following theorem is an extension of the global existence and uniqueness results for ODEs to MDEs:

Theorem 1.2 *[1076] Consider the MDE in $\mathscr{M}$, satisfying the conditions in Definition 1.5. Then there exists a unique solution $\varphi(t, t_0, x_0)$ of $\mathscr{M}$ for every point $(t_0, x_0) \in S$, where $\varphi(t, t_0, x_0)$ is defined on a maximal open interval $(a, b) \ni t_0$.*

It can be easily checked that the systems we deal with in Examples 1.1 and 1.2 are Carathéodory measure systems as long as we consider exogenous impulsive forces of the form $\sum_{k\geq 0} p_k \delta_{t_k}$ with $\sum_{k\geq 0} |p_k| < +\infty$, and that Theorem 1.2 applies. The classical results for ODEs concerning maximal extension of the solution, global existence when $f(t, x)$ is Lipschitz continuous, also extend to CMS. The result according to which a maximal solution defined on an interval (a, b) with $b < +\infty$ leaves any compact set of the domain of definition of $f(t, x)$ (either it tends to the boundary of that domain, or it escapes, or both [533, §5]) is generalized to CMS [1076, Theorems 5, 6, and Corollaries 1, 2].
Let us note also from [1076, Theorem 9] that the solution of a MDE is generally not continuous with respect to initial time t_0 but of bounded variation in t_0. Example (4.5) in [1076] analyzes the first-order equation $Dx = x + \delta_0$, x scalar, where the solutions $\varphi_1(t; t_1, 1)$ starting at $t_1 < 0$, $x(t_1) = 1$, and $\varphi_2(t; t_2, 1)$ starting at $t_2 > 0$, $x(t_2) = 1$, are given by

- For $t \in [t_1, 0), \varphi(t; t_1, 1) = \exp(t - t_1)$, and for $t \in (0, +\infty), \varphi(t; t_1, 1) = (\exp(-t_1) + 1)\exp(t)$. The jump at $t = 0$ is equal to 1 as expected.
- On $[t_2, +\infty)$, $\varphi(t; t_2, 1) = \exp(t - t_2)$, which is clearly not affected by the Dirac measure.

The solutions are such that:

$$\varphi_1(t_2; t_1, 1) - \varphi_2(t_2; t_2, 1) = \exp(t_2)\{\exp(-t_1) + 1\} - 1, \tag{1.18}$$

that is close to 1 when t_1 and t_2 are close to zero. Clearly $\varphi(0; \cdot, 1)$ is discontinuous at $t_0 = 0$. For $\varphi(0; \cdot, 1)$ to be continuous at $t_0 = 0$ would require that $\varphi(0; t_1, 1) - \varphi(0; t_2, 1) \to 0$ as $t_1 \to 0$ and $t_2 \to 0$. However if $t_1 < 0 < t_2$, and since we specify that solutions are right-continuous, we have $\varphi(0; t_1, 1) = \varphi(0^+; t_1, 1) = \exp(-t_1) + 1$ while $\varphi(0; t_2, 1) = \exp(-t_2)$, so that one gets

$$\varphi(0; t_1, 1) - \varphi(0; t_2, 1) \to 1. \tag{1.19}$$

It is worth remarking the big difference between simple Carathéodory differential equations, for which uniqueness and continuous dependence on initial data (t_0, x_0) are both guaranteed by the local Lipschitz continuity of the vector field [397, Chap. 1] [262, §1.10, Chap. 2] and measure differential equations for which this is not true.
However, continuity with respect to x_0 is true [1076, Theorem 9] and is easily proved following classical arguments for ODEs (see e.g., [1229]). Indeed, let us assume the

existence of solutions of $\mathscr{M}$ in (1.15) on an interval (a, b). Let us consider $x_0 = x(t_0)$ and $y_0 = y(t_0)$, $t_0 \in (a, b)$. Then by (1.16) we have

$$\varphi(t; t_0, x_0) - \varphi(t; t_0, y_0) = x_0 - y_0 + \int_{t_0}^{t} \{f(s, x(s)) - f(s, y(s))\}\, ds, \quad (1.20)$$

where $x(t) = \varphi(t; t_0, x_0)$ and $y(t) = \varphi(t; t_0, y_0)$. Hence from the properties in Definition 1.5, the proof of Theorem 2.4.57 in [1229] applies directly, and the solutions of $\mathscr{M}$ depend continuously on the initial state condition, on any finite-time interval.

Example 1.5 Let $f(t, x) = (x_2, x_3, 0)^T$, $G = (0, 0, 1)^T$ then $\dot{x}_1(t) = x_2(t)$, $\dot{x}_2(t) = x_3(t)$, $Dx_3 = Du$. Since $u \in BV$ then $x_3 \in BV$, $x_2(\cdot)$ is continuous, $x_1(\cdot)$ is continuously differentiable (use Theorem 1.1).

1.2.2 A Second Class of MDEs: ODEs Driven by Measure Inputs

Consider the differential equation:

$$\dot{x}(t) = f(x(t)) + g(x(t))\delta_{t_k}, \quad (1.21)$$

where $x(t) \in \mathbb{R}$, $f(\cdot)$ and $g(\cdot)$ are smooth functions of x. According to the above developments, we should get $\{\dot{x}\} + \sigma_x(t_k)\delta_{t_k} = f(x) + g(x)\delta_{t_k}$, so that

- $\{\dot{x}\} = f(x(t_k))$
- $\sigma_x(t_k) = g(x(t_k))$.

But the second equality is meaningless: indeed the term $g(x)\delta_{t_k}$ represents in fact a distribution, i.e., for any function $\varphi(t)$ with support K_φ containing t_k and continuous at t_k, $\langle g(x)\delta_{t_k}, \varphi\rangle = \int_{K_\varphi} g(x)\delta_{t_k}\varphi(t)dt = g(x(t_k))\varphi(t_k)$. Thus we should write $\sigma_x(t_k) = g(x(t_k))$. But $x(t_k)$ is not well defined and in general, neither is $g(x(t_k))$ (of course if $g(x)$ is replaced by a function of time $g(t)$ then the technique can be employed provided $g(t)$ is continuous at t_k: this is what is described in Sect. 1.2). Intuitively, what happens is that we expect $x(\cdot)$ to copy the jump in the "input" $u(\cdot)$ whose derivative is δ_{t_k}. However, we then obtain that $g(x(t))$ may also jump and the product $g(x(t))\delta_{t_k}$ is not properly defined at $t = t_k$: another path has to be followed to give a meaning to (1.21). Such problems are treated, e.g., in [397, 690]: they do not have in general a unique solution (independently of the choice of the initial data), and the obtained solution strongly depends on the sequence of problems considered to approximate the equation [690, Theorems 5.1 and 5.2] [397, Theorem 4, Chap. 1, §3]. The Czech mathematician, Jaroslav Kurzweil, developed a theoretical framework on a class of differential equations (Kurzweil Differential Equations, KDE) in [690]. Roughly speaking, the underlying idea is to consider ODEs whose right-hand side may not converge to a differentiable function, or even not to a function (like when

delta sequences are considered). Then one rather looks at the associated integral equation (that is a KDE), just forgetting about the differential formulation that might not be defined. Kurzweil provides conditions such that the integral has a meaning, by defining a Kurzweil integral from Kurzweil–Riemann sums. One may construct a KDE from any ODE that satisfies Carthéodory conditions. Then the solution of the KDE and that of the ODE are equal. In this sense KDEs really represent an extension of ODEs. Theorems 5.1 and 5.2 in [690] provide existence results for MDEs as in (1.21), with solutions of bounded variation. It is shown that a solution exists outside the critical point t_k, in the sense that the solutions of an approximating sequence of ODEs (where δ_{t_k} is replaced by a delta sequence) converge uniformly outside t_k.
The MDE in (1.21) belongs to a larger class of impulsive systems that may be written as

$$\dot{x}(t) = f(x(t)) + g(x(t))\dot{u}(t), \quad x(0) = x_0, \tag{1.22}$$

$x(t) \in \mathbb{R}^n$, $u(\cdot)$ is an $m-$input of local bounded variation, $f : \mathbb{R}^n \to \mathbb{R}^n$, $g : \mathbb{R}^n \to \mathbb{R}^m$. It is assumed that the vector fields $f(\cdot), g_1(\cdot), \ldots, g_m(\cdot)$ are continuously differentiable. The input possesses a differential measure du (see Appendix A.3.2) so that the dynamics (1.22) is better rewritten as an equality of measures

$$dx = f(x)dt + g(x)du, \quad x(0) = x_0 \in \mathbb{R}^n. \tag{1.23}$$

The theoretical framework for MDEs as in (1.23) is a bit tricky. It has been settled in [187, 814, 1169]. Let us introduce it briefly now (as done for instance in [1182] where the focus is put on stability). Let $\Phi_G(s; z_0, v)$ denote the Carathéodory solution of the ordinary differential equation $\dot{z}(t) = \sum_{j=1}^m v_j g_j(z(t))$, $z(0) = z_0$ at time $t = s$ with initial condition z_0, i.e., $\Phi_G(0; z_0, v) = z_0$. It also follows that $\Phi_G(s; z_0, 0) = z_0$ for each $s \in \mathbb{R}$. Now let[6] $h_j(z, v) := \int_0^1 g_j(\Phi_G(s; z, v))\, ds$ and to study the solutions to system (1.22), the Cauchy problem we consider is

$$dx = f(x(t))dt + \sum_{j=1}^m h_j(x(t^-), u(t^+) - u(t^-))du, \quad x(t_0) = x_0. \tag{1.24}$$

It is seen that the solution of (1.24) coincides with the solutions of (1.22) whenever $u(\cdot)$ is continuous, since in that case $u(t^+) = u(t^-)$ for all t, $\Phi_G(s; z, v) = z$ and $h_j(x, 0) = g_j(x)$. Formally, the solution to system (1.22) is defined as follows:

Definition 1.6 For a given right-continuous *locally BV* input $u : [t_0, T] \to \mathbb{R}^m$, a right-continuous *locally BV*[7] function $x : [t_0, T] \to \mathbb{R}^n$ is called a solution of (1.22) if it satisfies the following:

[6] The choice of the interval [0, 1] is arbitrary and could be replaced by any other compact interval without changing significantly the developments.

[7] RCLBV in short.

$$\int_{\mathscr{B}} dx = \int_{\mathscr{B}} f(x(t))\,dt + \sum_{j=1}^{m} \int_{\mathscr{B}} h_j(x(t^-), u(t^+) - u(t^-))du,$$

for every Borel measurable set $\mathscr{B} \subset [t_0, T]$.[8]

To study the existence and uniqueness of the Cauchy problem with inputs of bounded variation (1.24), the basic idea is to introduce a graph completion of the input $u(\cdot)$. An auxiliary system is then introduced which is driven by this graph completion, and the solution of this system can be studied in the classical sense. Once the existence of solution is verified in the new coordinates, the solutions of the auxiliary system are mapped back into the original coordinates. Some details of this development are given in [1182], and for detailed proofs, we refer the reader to [814].
It is natural to ask in what sense the solutions of (1.24) generalize the classical solutions of nonlinear ODEs. In particular, when the inputs are continuously differentiable, do we recover the absolutely continuous solutions which are continuous with respect to initial conditions, or inputs? The answer to this question appears in the following result, where the variation is defined in Sect. A.3.1:

Proposition 1.2 *[814, Theorem 4.2] Let $u : [t_0, T] \to \mathbb{R}^m$ be a RCLBV function and consider a sequence $u_j : [t_0, T] \to \mathbb{R}^m$ of RCLBV functions. Assume that*

- *for almost every $t \in I$, $\lim_{j\to\infty} u_j(t) = u(t)$,*
- *$\lim_{j\to\infty} var(u_j; [t_0, t]) = var(u; [t_0, t])$.*

Let $x_j(\cdot)$, $x(\cdot)$ be RCLBV functions obtained as solutions to (1.24) corresponding to $u_j(\cdot)$, and $u(\cdot)$, respectively. Then $\lim_{j\to\infty} x_j(t) = x(t)$ for each $t \in [t_0, T]$, where $u(\cdot)$ is continuous.

As a consequence of this result, it is seen that if $u_j(\cdot)$ is a sequence of continuously differentiable inputs converging to a *locally RCBV* function $u(\cdot)$, so that the solution of (1.22) and (1.24) with inputs $u_j(\cdot)$ could be interpreted in classical sense, then the solution $x(\cdot)$ corresponding to $u(\cdot)$ that we consider is the limit of the solutions $x_j(\cdot)$ obtained from differentiable inputs $u_j(\cdot)$. Let us now specify how the solution of the MDEs behave at discontinuities of $u(\cdot)$. From the system description in (1.24), the solution $x(\cdot)$ at the discontinuities is characterized as follows:

Proposition 1.3 (Jump Characterization) *At the atoms $\{t_k\}$ of du, we have*

$$x(t_k^+) = \Phi_G(1; x(t_k^-), u(t_k^+) - u(t_k^-)). \tag{1.25}$$

To see how we arrive at the formula for $x(t_k^+)$, it follows from the definition of the functions $h_j(\cdot, \cdot)$ that

[8] See Appendix A.2.

$$\sum_{j=1}^{m} v_j h_j(z,v) = \int_0^1 \sum_{j=1}^{m} v_j g_j(\Phi_G(s;z,v))\,ds = \int_0^1 \frac{\partial \Phi_G}{\partial s}(s;z,v)\,ds$$
$$= \Phi_G(1;z,v) - \Phi_G(0;z,v) = \Phi_G(1;z,v) - z.$$

If $u(\cdot)$ is discontinuous at t_k, then (1.24) is interpreted as follows:

$$x(t_k^+) - x(t_k^-) = \sum_{j=1}^{m} h_j(x(t_k^-), u(t_k^+) - u(t_k^-))(u_j(t_k^+) - u_j(t_k^-)) \tag{1.26}$$

and from the above calculations it follows that $x(t_k^+) = \Phi_G(1; x(t_k^-), u(t_k^+) - u(t_k^-))$. Some comments are necessary at this stage of the presentation. The notion of solution introduced in Definition 1.6 is too abstract for engineers. Proposition 1.2 proves that it leads to sound property of continuity of solutions, anyway. The next example taken from [1182] illustrates what it implies in terms of state jump mapping, i.e., it clarifies the meaning of (1.25) and (1.26). Consider a scalar system (1.22) with $f(x) = 0$, $g(x) = x$, and $u(t) = cH(t)$, where $c > 0$, and $H(t) = \begin{cases} 0, & t_0 \le t < t_1 \\ 1, & t_1 \le t < +\infty \end{cases}$. This gives $du = c\delta_{t-t_1}$, where δ_0 is the Dirac measure at time $t = 0$. It is clear that $x(t) = x(t_0)$, for $t_0 \le t < t_1$. For $t \ge t_1$, if we pick $x(t) = (1+c)x(t_0)$, then the equation $\int_{\{t_1\}} dx = x(t_1^-) \int_{\{t_1\}} du$ holds, meaning that this solution corresponds to the MDE:

$$dx = g(x(t_1^-))\delta_{t-t_1}. \tag{1.27}$$

Another candidate solution $x(t) = x(t_0)/(1-c)$ satisfies $\int_{\{t_1\}} dx = x(t_1^+) \int_{\{t_1\}} du$, which results from solving the MDE:

$$dx = g(x(t_1^+))\delta_{t-t_1}. \tag{1.28}$$

A third solution is inspired from Proposition 1.2 by approximating $u(\cdot)$ with a sequence $\{u_k\}_{k=1}^{\infty}$ of continuously differentiable functions. Then for each element of the sequence, the resulting solution is obtained by solving $\frac{\dot{x}_k}{x}(t) = \dot{u}_k(t)$, which leads to $x_k(t) = x_k(t_0)e^{u_k(t)}$. One then takes $x(\cdot)$ to be the limit of the sequence $\{x_k\}_{k=1}^{\infty}$ and let $x(t) = x(t_0)e^{u(t)}$ to be the solution. In terms of the original system description in differential form, this last solution satisfies $\int_{\{t_1\}} dx = \tilde{x} \int_{\{t_1\}} du$, for some $\tilde{x} \in [x(t_1^-), x(t_1^+)]$. To prove the last claim, we introduce the function $\Phi(v) = e^v x_0$, for $v \in [0, c]$. Then by the mean value theorem, there exists $\tilde{v} \in [0, c]$ such that $\frac{\partial \Phi}{\partial v}\big|_{v=\tilde{v}} = \frac{\Phi(c)-\Phi(0)}{c}$, i.e., $e^{\tilde{v}} x_0 = \frac{e^c x_0 - x_0}{c}$ and we note that $\int_{\{t_1\}} dx = e^c x_0 - x_0$, $\int_{\{t_1\}} du = c$, and $\tilde{x} := e^{\tilde{v}} x_0 \in [x(t_1^-), x(t_1^+)]$. This last argument indicates that at the points of discontinuity of $x(\cdot)$ at t_k, we have $\frac{dx}{du}(t_k) = g(\tilde{x})$ and the corresponding MDE is

$$dx = g(\tilde{x})\delta_{t-t_1}, \tag{1.29}$$

where $\tilde{x}$ is some point on the solution curve of the ODE $\dot{z} = (u(t_k^+) - u(t_k^-))g(z)$ solved over the interval [0, 1] with initial condition $z(0) = x(t_k^-)$.

$\rightsquigarrow$ *The MDE in* (1.27) *is in an explicit form, while the MDE in* (1.28) *is in an implicit form. Definition* 1.6 *yields an intermediate form* (1.29).

It is seen from the above that the implicit framework (adopted for instance in [961]) may give rise to unbounded jumps at t (choose $c = 1$). The explicit formulation was chosen in [965] with a specific approximation of the vector field $g(x)$ at jumps, in order to obtain a jump mapping similar to $I(\cdot)$ in (1.31) in the next section.

1.2.3 Further Reading

The study of MDEs as in (1.23) is motivated by optimal control, quantum electronics, economics (see [1182, §1.3]), spiking models for synaptic activity [267]. Their input-to-state stability is deeply investigated in [1182], and summarized in Sect. 7.1.2. Systems for which both the position and the velocity possess discontinuities have been identified and studied by Bressan in [188, 190]. Such systems have been named *hyperimpulsive*. The goal in hyperimpulsive systems is to find out generalized coordinates $\gamma_1, \ldots, \gamma_m$ such that the Hamiltonian system $\dot{q} = Q(q, p, \gamma_i, \dot{\gamma}_i)$, $\dot{p} = P(q, p, \gamma_i, \dot{\gamma}_i)$ can be controlled *via* the γ_i's. Thus choosing a discontinuous γ_i introduces a hyperimpulsive term in the dynamics. In general the $\dot{\gamma}_i$'s appear quadratically in the dynamical equations. Assume that $m = 1$. The general form of the Lagrange dynamical equations is

$$\dot{x}(t) = f(t, x(t), \gamma(t)) + g(t, x(t), \gamma(t))\dot{\gamma}(t) + h(t, x(t), \gamma(t))\dot{\gamma}(t)^2. \quad (1.30)$$

There are two difficulties in the analysis of such systems when $\gamma(t)$ possesses discontinuities: first, the second term on the right-hand side makes it similar to the equation in (1.22). Second, $\dot{\gamma}(t)$ is a Dirac distribution at the discontinuity times, so that its square has no meaning in the theory of distributions, see Appendix A.1. Other works on MDEs similar to the one in (1.15) but with $G = G(x, t)$ can be found in [946, 947]. In [946] the notion of *vibrocorrect* solution is given. Roughly, a solution $x(\cdot)$ is vibrocorrect if the weak$\star$ convergence of a sequence of integrable inputs $v_k = Du_k$ towards $v(\cdot)$, results in the analogous weak$\star$ convergence of the solutions $x_k(\cdot)$ towards $x(\cdot)$, where $x(\cdot)$ is a solution of the MDE when the input is $v(\cdot)$. The conditions for vibrocorrectness are shown to be related to the complete integrability of the system $\frac{d\xi}{dv} = G(\xi, s)$ for any $s \geq 0$ (we recover here the arguments of [814] described in Sect. 1.2.2). The formula allowing the computation of the jump σ_x (in case of an impulsive input Du) is given explicitly. Since this integrability condition is quite stringent (it is not satisfied for mechanical systems), the notion of solution is relaxed in [947]. Differential inclusions with measure inputs and their stability have been tackled in [993].

1.2.4 A Third Class of MDEs: ODEs with State Jump Mappings

Another type of MDEs has been studied extensively in the literature. For instance, Bainov and Simeonov [75, 76] analyze ordinary differential equations with state jumps which are described as

$$\begin{cases} \dot{x}(t) = f(x(t), t), \ \ t \neq t_k(x) \\ \\ \sigma_x(t_k) = I(x(t_k^-)), \ t = t_k(x), \end{cases} \tag{1.31}$$

with $\sigma_x(t_k) = x(t_k^+) - x(t_k^-)$, the vector field $f(\cdot, \cdot)$ is regular enough to guarantee the existence and uniqueness of solutions between state jumps, and $I(\cdot)$ is a continuous mapping. Some assumptions on the discontinuity times t_k are made, the major one being in general that they are separated and in finite number in any compact interval of time, which implies the absence of finite accumulation, i.e., $t_\infty \stackrel{\Delta}{=} \lim_{k \to +\infty} t_k = +\infty$. This is related to what is named the *beating* phenomenon, which occurs when the jump times are calculated from an equation $s(t, x(t)) = 0$: there is beating if this equation has several finite or a countable number of solutions; there is no beating if it has at most one solution. Sufficient conditions to avoid beating are that the functions $t_k(\cdot)$ are differentiable, $\frac{\partial t_k}{\partial x}$ and $f(t, x)$ are bounded, and $\sup_{0 \leq s \leq 1} \frac{\partial t_k}{\partial x}(x + s I_k(x))^T I_k(x) \leq 0$ [75, Corollaries 2.1, 2.2]. As noted in [75], MDEs as in (1.31) do not enjoy the semi-group (autonomy) property, even when the vector field $f(\cdot)$ does not depend explicitly on time. Results on continuous dependence, existence, and uniqueness of solutions (which are supposed to be left-continuous in time: $x(t_k) = x(t_k^-)$) with respect to initial data and parameters can be found in [75, 76]. For the sake of briefness of the exposition we do not reproduce these results here. Let us simply note that such systems are different from the MDEs in (1.15) since the jumps magnitudes are state-dependent. As an illustration, let us consider the system

$$\begin{cases} \dot{x}(t) = 0 \ \text{ for } \ t \neq t_k(x), \ \ x(0) = x_0 \geq 0 \\ \sigma_x(t_k) = 1 \\ t_k(x) = \{t | t = x(t) + 2\}. \end{cases} \tag{1.32}$$

Solutions are initially given by $\varphi(t; \tau_0, x_0) = x_0$, and the first discontinuity occurs at $t_0 = \varphi(t_0; \tau_0, x_0) + 2 = x_0 + 2$. Hence the solution jumps to $x_0 + 1 = \varphi(t_0^+; \tau_0, x_0)$. Then a second jump occurs at $t_1 = \varphi(t_1; t_0^+, x(t_0^+)) + 2$, i.e., $t_1 = x_0 + 3$, with $x(t_1^+) = x_0 + 2$, and so on. Let us consider a second example [546]

$$\begin{cases} \dot{x}(t) = \cos t \ \ \text{ for } \ \ t \neq t_k(x), \ \ x(0) = 0 \\ \sigma_x(t_k) = 1 \\ t_k(x) = \{t | t = -(x + 1) + (2\pi + 1)k\}. \end{cases} \tag{1.33}$$

Then the solutions have jumps at the points of the extended state space $(t, x) = (2k\pi, k-1)$ for $k = 1, 2, \ldots$. The sequence $\{t_k\}_{k\geq 0}$ has no finite left accumulation point. Therefore the solutions are defined globally in time. Actually MDEs as in (1.31), called impulsive ODEs, do not allow for finite accumulation of state jumps if the solutions are to exist globally. This is not the case for MDEs as in (1.22) which naturally incorporate such Zeno phenomena. In some cases it is possible to give closed forms for the solutions of ODEs with state jumps. Let us consider a particular case of (1.31), with inputs and outputs

$$\begin{cases} \dot{x}(t) = Ax(t) + Bu(t) & \text{for } t \neq t_k \\ \sigma_x(t_k) = cx(t_k^-) & \text{for } t = t_k \\ 0 < t_1 < t_2 < \ldots < t_k < t_{k+1} < \ldots, \quad \lim_{k\to+\infty} t_k = +\infty & \\ y = Cx + Du & \\ x(0) = x_0, & \end{cases} \tag{1.34}$$

for some constant c, constant matrices $A \in \mathbb{R}^{n\times n}$, $B \in \mathbb{R}^{n\times m}$, $C \in \mathbb{R}^{p\times n}$, $D \in \mathbb{R}^{p\times m}$. The solutions may be expressed on $t \in (t_{k-1}, t_k]$ as [1283, 1325]:

$$\begin{aligned} x(t) = {} & e^{A(t-t_{k-1})}(1+c)^{k-2}\Pi_{i=k-1}^{1} e^{A(t_i-t_{i-1})}x_0 + \int_{t_{k-1}}^{t_k} e^{A(t-s)}Bu(s)ds \\ & + \sum_{i=1}^{k-1}\left((1+c)^{k-1-i}\int_{t_{i-1}}^{t_i} e^{A(t-t_{k-1})}\Pi_{r=k-1}^{i+1} e^{A(t_r-t_{r-1})}e^{A(t_i-s)}Bu(s)ds\right). \end{aligned} \tag{1.35}$$

The proof for obtaining (1.35) is done by integration over each interval $[0, t_1]$, then $(t_1, t_2]$, etc, and concatenation. It is clear from (1.35) that the impulsive system in (1.34) is linear in x_0 and u. Let us state controllability and observability criteria for (1.34).

Definition 1.7 The system (1.34) is *controllable* on $[0, t_f]$, $t_f > 0$, if given any initial state x_0 there exists a piecewise continuous input $u : [0, t_f] \to \mathbb{R}^m$, such that the corresponding solution satisfies $x(t_f) = 0$. It is *observable* on $[0, t_f]$ if any initial state x_0 is uniquely determined by the corresponding system input $u(\cdot)$ and output $y(\cdot)$ for $t \in [0, t_f]$.

Then we have the following:

Theorem 1.3 (Controllability and observability of (1.34)) *[486] (i) Assume that $c \neq -1$. The system (1.34) is controllable if and only if rank$(B \;\; AB \;\; \ldots \;\; A^{n-1}B) = n$. (ii) Assume that $1+c \geq 0$. The system (1.34) is observable if and only if rank$(S) = n$, where* $S = \begin{pmatrix} C \\ CA \\ \vdots \\ CA^{n-1} \end{pmatrix}$.

One sees that the controllability and observability of (1.34) rely on the rank of the Kalman matrices, as in the non impulsive linear invariant case. The Lyapunov stability of such impulsive ODEs is introduced in Sect. 7.1.

Remark 1.3 Which are the discrepancies between MDEs as in (1.23) and as in (1.31)? Clearly not every mapping $x \mapsto x + I(x)$ in (1.31) satisfies the property of the flow of some vector field (see (1.25)). Thus from the point of view of state jump mappings, (1.31) is more general than (1.23), even if $u(\cdot)$ is chosen as a piecewise constant function. However, (1.23) allows for finite accumulations of discontinuities in $u(\cdot)$, hence in the sequence of state jump times, not hampering existence of solutions on $[0, +\infty)$. On the contrary, impulsive ODEs (1.31) cannot cross a finite accumulation of jump times because they are designed from an event-driven point of view. Also, with a proper choice of $u(\cdot)$, the MDE in (1.22) can represent systems with switching vector field [1182, §4.3].

1.2.5 Further Reading

There is a huge literature on ODEs with state jumps. Many extensions of (1.31) and (1.34) with time-varying matrices $A(t)$, $B(t)$, $C(t)$, $D(t)$, piecewise-constant vector fields $f_k(x, t)$ and mappings $I_k(\cdot)$, retarded and hyperbolic systems, have been studied. Stability, invariance of sets, controllability and observability have been analyzed deeply for all cases, see [125, 192, 281, 486, 1042, 1283, 1325] to cite a few. The above observability criteria are extended to nonlinear vector fields and constant jump times in [1042]. Extensions to infinite dimensional systems, time-delayed systems, have also been the object of many articles. Applications may be found in epidemiology, sampled-data systems, event-triggered control [515, §V.B], cancer therapy [695], species food chain models [269], predator–prey models [73], pest control [612, 1250], management of renewable resources [300], plankton allelopathy [510], diabetic patients [128], etc. Dissipativity of MDEs with separated state-dependent jump times has been investigated in [493]. Roughly speaking, the dissipation inequality and available storage function incorporate the contribution of the state jumps as an infinite discrete sum. Similar extensions of dissipation inequalities are formulated for nonsmooth Lagrangian systems with frictionless unilateral constraints and impacts (see Sect. 7.5.3 and also [218, p. 382]). An extension of impulsive ODEs is proposed in [460], which may be seen as an extension of the impulsive systems studied in [494, Eqs. (2.25) (2.26)], and of the Impulsive Differential Inclusions (IDIs) –where $\dot{x}(t) = f(t, x(t))$ is replaced by $\dot{x}(t) \in F(t, x(t))$ in (1.31) studied in [123]. The generic form of these IDIs (that one may name "hybrid systems") is

$$\begin{cases} \dot{x}(t) \in F(x(t)) & \text{if } x(t) \in C \\ x(t^+) \in G(x(t)) & \text{if } x(t) \in D, \end{cases} \tag{1.36}$$

where C and D are closed sets of $\mathbb{R}^n$, $F(\cdot)$ and $G(\cdot)$ are outer semicontinuous set-valued mappings, respectively locally bounded on C and D[9] $F(x)$ is convex

[9] A multivalued mapping $F : \mathbb{R}^n \rightrightarrows \mathbb{R}^n$ is said outer semicontinuous, if its graph $\{(x, y) | x \in \mathbb{R}^n, y \in F(x)\} \subset \mathbb{R}^{2n}$ is closed. It is locally bounded on C if for each compact set $S \subset C$ one has $F(S)$ bounded.

and nonempty for each $x \in C$, $G(x)$ is nonempty for each $x \in D$. Existence, uniqueness, continuous dependence, and stability of solutions are analyzed in [460]. Similar models of hybrid dynamical systems are considered in [68, 494]. As we shall see later, all these mathematical formalisms are in fact unable to correctly model mechanical systems subject to unilateral constraints and impacts (despite the bouncing ball is always chosen as an illustrative example in most articles). *Indeed they do not encapsulate the fundamental feature of unilaterally constrained systems, which is the possible change of system's dimension along the trajectories*. This particular feature, which is long well-known in mechanics and is also present in sliding mode control, calls for other models involving the contact forces and complementarity conditions, which in turn may be equivalently written with variational inequalities, or specific differential inclusions whose right-hand sides are normal cones to convex (or non-convex) sets. Normal cones cannot be taken into account neither in the sets C or D, not in the locally bounded set-valued maps $F(\cdot)$ or $G(\cdot)$. See also Remark 5.12 for a similar comment and Sect. 7.5.4.

1.3 Systems Subject to Unilateral Constraints

1.3.1 General Considerations

We have for the moment considered the impacts on the system as purely exogenous signals having a particular form, namely a sequence of Dirac measures which we named impulsive forces. This is in fact closely related to *unilateral constraints*. Before going on with the relationships between such constraints and impulses, let us define what is meant by a unilateral constraint.

Definition 1.8 Let a Lagrangian mechanical system be described by a set of generalized coordinates $q \in \mathbb{R}^n$, and let $f_i(q) = 0, i = 1, \ldots, m$, be smooth submanifolds of codimension 1 in the configuration space of the system, such that $\nabla f_i(q) \neq 0$ in the neighborhood of $f_i(q) = 0$. Then the inequality $f(q) \geq 0$ defines a domain of the configuration space $\mathscr{Q}$, namely $\Phi = \{q \in \mathscr{Q} | f(q) \geq 0\} = \cap_{i=1}^{m} \{q \in \mathscr{Q} | f_i(q) \geq 0\}$, where the system is constrained to evolve. The domain Φ is named the *admissible domain*, and is said to be *finitely represented*. The functions $f_i(q)$ are named the *gap functions*. The unilateral constraint $f_i(q) \geq 0$ is said *active* if $f_i(q) = 0$, and *inactive* if $f_i(q) > 0$.

Such unilateral constraints are sometimes called *holonomic* unilateral constraints [466]. Note that there is no reason to have $m < n$: a simple object in a room is usually constrained by several hundreds of surfaces (although in the modeling process one often neglects most of them). For the definition of a submanifold, we refer the reader to [3, 60, 533]. Roughly, if the ambient space is of dimension n, a submanifold of

codimension m[10] is simply a surface of dimension $n - m$ (if $m = 1$ one speaks of a hypersurface) that is embedded into the theoretical setting of manifolds, i.e. is endowed with a special local coordinates structure (a manifold is a set which has locally the structure of a Euclidean space, with linear coordinates). Smooth submanifolds are those that admit a tangent space at each point q. We impose here that the gradient of $f(q)$ be different from zero at each point of the submanifold, hence the normal direction to the surface of constraint is well defined. This is important when we consider the generalized interaction forces acting from the constraint on the system (see Sect. 4.1.3). Note that we can also consider time-varying submanifolds $f(q,t) = 0$, provided $f(q,t)$ is continuous in t. Indeed it is important that at the collision times, continuity with respect to t holds. Otherwise the normal direction to the constraint surface may have a discontinuity at the same instant as bodies strike, and this poses difficulties for the definition of the system's evolution at the impact (see Chap. 6).

Remark 1.4

1. The unilateral constraints can be in general formulated either as $f(q) \geq 0$ or as $g(q) \leq 0$. In the first case the normal vector $\nabla f(q) \in \mathbb{R}^n$ points outwards the constraint surface. In the second case $\nabla g(q)$ points inwards. It is therefore not very important to adopt one or the other convention. However, one should be aware of that fact to compute the admissible normal interaction forces or impulsions.
2. Constraints must be associated with *contact forces*. A *contact model* has to be settled to define these forces. The so-called *complementarity conditions* will be chosen in the sequel. They are introduced in Example 1.6 on a simple system, together with some transformations using convex analysis, which show that the dynamics may be expressed in various ways.

Example 1.6 (*Cable-mass system*) Consider as in Fig. 1.3a the system made of a mass m attached at a point O with coordinate $y(t)$ by a massless inextensible cable of length L. The cable can transmit tensile forces, but negligible compressive forces to the mass. This is a very simple example of a cable network [643], or of a cable-driven system [395], or of a tensegrity structure [1061], or of tethered space systems [551]. For the sake of simplicity, we assume a one-degree-of-freedom system with vertical motion, and the mass coordinate is $x(t)$. The force exerted by the cable on the

[10]The codimension of a submanifold (a surface) is the difference between the dimension of the ambient space and the dimension of the submanifold [60]. Recall that there are three ways of defining a surface S of dimension $n - m$ in an ambient space of dimension n [359]. We make use only of one of them, which consists of defining S through m relationships like $f_i(q_1, \ldots, q_n) = 0$. A *non-singular* point q_0 is such that the Jacobian matrix $\left(\frac{\partial f}{\partial q}(q_0)\right) \in \mathbb{R}^{m \times n}$ has rank m. Then the three definitions are equivalent in a neighborhood of q_0. The codimension of the intersection $S_1 \cap S_2$ is the sum of the codimensions of S_1 and S_2, provided the intersection is transversal, (i.e., the tangent hyperplanes to each one of the surfaces at the intersection span the whole ambient space [487, p. 50]. The reader can think of two planes in $\mathbb{R}^3$ (codimension 1 surfaces): either they are parallel, or they intersect transversally and the intersection is a straight line whose codimension is 2).

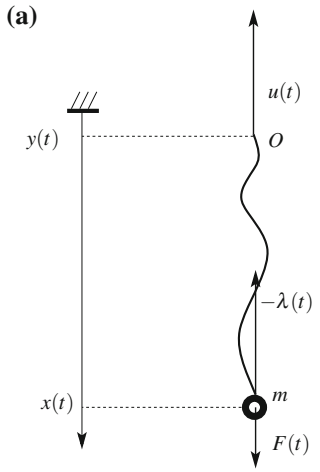

Cable-mass system.

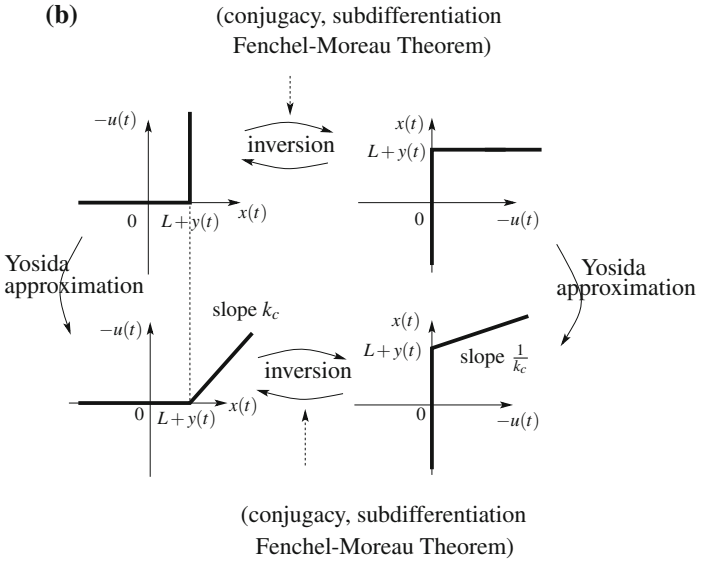

Input-state characteristics (with and without cable stiffness).

Fig. 1.3 Mass suspended to a cable

mass is denoted $\lambda(\cdot)$. When the distance between the mass and O is strictly smaller than L, the cable exerts no force on the mass. This is translated mathematically to: $\lambda(t) = 0$ if $x(t) - y(t) < L$. On the other hand, if $x(t) - y(t) = L$, then the cable may exert a non zero force on the mass, moreover due to the tensile force transmission assumption, this force is signed: $\lambda(t) \geq 0$. The dynamics of the mass is therefore written as:

$$\begin{cases} m\ddot{x}(t) = -\lambda(t) + F(t) \\ \lambda(t) \geq 0,\ \ f(x(t),t) = L - x(t) + y(t) \geq 0,\ \ \lambda(t) f(x(t),t) = 0, \end{cases} \tag{1.37}$$

where $F(t)$ is some bounded external force applied on the mass (could be gravity). The conditions in the second line of (1.37), which we rewrite compactly as

$$0 \leq \lambda(t) \perp f(x(t),t) = L + y(t) - x(t) \geq 0, \tag{1.38}$$

are called *complementarity conditions*. They will be introduced more deeply in other chapters. When the cable passes from the non-elongated state ($x(t) < L$) to the maximum length state ($x(t) - y(t) = L$) an impact may occur. We will come back on this in Sect. 1.3.1.2. Notice that the complementarity conditions (which are some kind of nonsmooth constraints) have been derived from mechanical modeling, and are quite natural if one admits that the above observations are reasonable. Readers who are familiar with optimization know that complementarity conditions may stem from the KKT conditions of optimality. Here no such conditions have been used, only physical observation motivated (1.38). We may use the material in Sect. B.2.1 in order to rewrite (1.37) equivalently as a differential inclusion

$$m\ddot{x}(t) - F(t) \in N_{\mathbb{R}^+}(L + y(t) - x(t)), \tag{1.39}$$

where $\lambda(t) \in -N_{\mathbb{R}^+}(L + y(t) - x(t))$ may be viewed as a selection of the set-valued right-hand side. If there is a force $u(t)$ exerted at O on the cable, and since the string is supposed to be massless, one gets $\lambda(t) = -u(t)$. The two variables $y(t)$ and $u(t)$ can therefore be used to control the system. The inclusion $u(t) \in N_{\mathbb{R}^+}(L + y(t) - x(t)) = -N_{(-\infty, L+y(t)]}(x(t)) \Leftrightarrow L + y(t) - x(t) \in N_{\mathbb{R}^-}(u(t)) \Leftrightarrow x(t) \in \{L + y(t)\} + N_{\mathbb{R}^+}(-u(t)) \Leftrightarrow -u(t) \in N_{(-\infty, L+y(t)]}(x(t))$ represents a particular constraint on the input. The graphs of both set-valued mappings $-u(t) \mapsto x(t)$ and $x(t) \mapsto -u(t)$ are depicted in Fig. 1.3b. This is a simple case of set-valued mapping inversion, using (B.16). Both mappings $x \mapsto -u \in N_{(-\infty, L+y(t)]}(x)$ and $-u \mapsto x \in \{L + y(t)\} + N_{\mathbb{R}^+}(-u)$ are maximal monotone for fixed $y(t)$ (see Definition B.8). It is noteworthy that the dynamics is equivalently rewritten as the differential inclusion

$$m\ddot{x}(t) - F(t) \in -N_{(-\infty, L+y(t)]}(x(t)). \tag{1.40}$$

As alluded to above, one has to complete this model with a suitable impact law. This will further transform (1.40) into a measure differential inclusion, a topic treated in Chaps. 2 and 5.

Remark 1.5 According to the model, the cable attains its maximum length if $u(t) < 0$. If one wants to achieve control without impact or transitions from maximum length to slack state, then necessarily one has to guarantee that $u(t) < 0$ for all times. A good controller may however be designed to be robust with respect to detachment from the constraint and impacts.

Let us now end this example by adding some unilateral linear spring with stiffness $k_c > 0$ in the cable. The force exerted by the cable on the mass is then given by $\lambda(t) = 0$ if $x(t) \leq L + y(t)$ and $\lambda(t) = k_c(x(t) - L - y(t)$ if $x(t) \geq L + y(t)$, which is a piecewise-linear (hence nonlinear!) function of x. Still using $u(t) = -\lambda(t)$, one finds that $-u(t) = \max[0, k_c(x(t) - L - y(t))]$, or equivalently $-u(t)$ is the solution of the linear complementarity problem (LCP)

$$0 \leq -u(t) \perp -u(t) - k_c(x(t) - L - y(t)) \geq 0, \tag{1.41}$$

(this can be checked by simple inspection). This is depicted in Fig. 1.3b. An interesting point is that the case with cable stiffness may be interpreted as the Yosida approximation, or regularization, of the above maximal monotone mappings with infinite rigidity (see Definition B.9 and Figs. B.2, B.4 for examples of Yosida approximations). From the LCP (1.41) and using (B.19) we obtain $-u(t) \in N_{\mathbb{R}^+}(-u(t) - k_c(x(t) - y(t) - L))$ which is equivalent still using (B.19) to $-u(t) \in k_c(x(t) - y(t) - L) - \partial\psi^\star_{\mathbb{R}^+}(-u(t))$, where $\psi^\star_{\mathbb{R}^+}(\cdot)$ is the conjugate function of the indicator of $\mathbb{R}^+$ (see Definition B.11), known as the support function of $\mathbb{R}^+$. Another, equivalent formulation is $-u(t) = \max(0, k_c(x(t) - L - y(t))$, which may also be obtained from (B.21) using the projection. Thus the cable-mass system's dynamics with stiff cable is

$$m\ddot{x}(t) = F(t) - \max(0, k_c(x(t) - L - y(t)), \tag{1.42}$$

which is a piecewise-linear dynamical system with Lipschitz continuous, single-valued right-hand side.[11] In this simple case we have that $\psi^\star_{\mathbb{R}^+}(\cdot) = \psi_{\mathbb{R}^+}(\cdot)$. Therefore $-u(t) \in k_c(x(t) - y(t) - L) - \partial\psi_{\mathbb{R}^+}(-u(t))$, and proceeding similarly $x(t) \in \frac{1}{k_c}(y(t) + L) - \frac{1}{k_c}u(t) - N_{\mathbb{R}^+}(-u(t))$.[12] This last equivalence could also be seen as a consequence of (B.16). Existence of solutions for the cable-mass system may be analyzed with the material of Sect. 2.4, in particular Theorem 2.1. It is also possible to embed its dynamics into the so-called Moreau's sweeping process that is the topic of Sect. 5.2. The yoyo dynamics is similar to the cable-mass system [624, Eq. (2)]. From a control perspective, one has to choose a control input: should it be $y(t)$ in (1.37), or the multiplier λ (the tension in the cable)?[13]

Remark 1.6 (*Nonsmooth Potentials*) It is interesting to interpret the indicator function $U : x \mapsto U(x) = \psi_{(-\infty, L+y(t)]}(x)$ as a nonsmooth potential function associated with the contact force λ, since $\lambda \in \partial U(x) = \partial\psi_{(-\infty, L+y(t)]}(x) = N_{(-\infty, L+y(t)]}(x)$.[14]

[11] It is noteworthy that the system in (1.39) or (1.40) may also be seen as a piecewise-linear system, however not single-valued due to the vertical branch in the graph of the right-hand side set-valued function.

[12] From Definition B.7 we may use either the subdifferential of the indicator function, or the normal cone.

[13] This may be justified for massless or near-massles cables, where the force exerted on one side of the cable equals the tension in it.

[14] Such potentials were introduced by J.J. Moreau who called them *superpotential functions* [879].

Using (B.16) this is equivalently rewritten as $x \in \partial\psi^{\star}_{(-\infty,L+y(t)]}(\lambda)$ with $\psi^{\star}_{(-\infty,L+y(t)]}(\cdot)$ the conjugate function of the indicator function of $(-\infty, L+y(t)]$, that is the support function of this interval. Inverting the potential function one has $x : U \mapsto x(U) = \psi^{\star}_{(-\infty,L+y(t)]}(U) = +\infty$ if $U < 0$, and $(L+y(t))U$ if $U \geq 0$. The Moreau–Yosida approximation of the potential function is $U_\lambda(\cdot)$ which corresponds to the potential associated with the cable with stiffness, choosing $\lambda = \frac{1}{k_c}$ in Definition B.9 (ii). It is equal to $U_\lambda(x) = 0$ if $x \leq L + y(t)$ and $\frac{x^2}{2\lambda}$ if $x > L + y(t)$. This proves that forbidden displacements x which violate the unilateral constraint, create infinite potential $U(x)$. Contact forces for the compliant model are given by the Yosida approximation of the mapping $\partial U(\cdot)$ which is depicted in Fig. 1.3b. The Moreau–Yosida approximation of the inverse potential $x(U)$ is $x_\lambda(U) = (L+y(t))U$ if $U \geq 0$, and $\frac{1}{2\lambda}U^2$ if $U < 0$. This shows that negative potentials create infinite displacements.

Remark 1.7 (*Multivalued Stiffness*) The stiffness may be seen as the gradient of the contact force with respect to the indentation, or displacement. In case of the unilateral linear spring, the characteristic $(x, -u)$ of the Yosida approximation in Fig. 1.3b is not differentiable at $x = L + y$. However, it is subdifferentiable and it admits subgradients everywhere. Using the example of function $f_4(\cdot)$ after Definition B.11 in Appendix B, one finds $\partial\lambda(x) = 0$ if $x < L + y$, $-k_c$ if $x > L + y$, and $[-k_c, 0]$ if $x = L + y$. The stiffness of the unilateral spring is therefore, mathematically speaking, set-valued at the point $(-u, x) = (0, L + y)$ of its graph.

1.3.1.1 Loss of Linearity

One of the main consequences of the addition of unilateral constraints on a system is that even if the unconstrained dynamics is linear, i.e.,

$$\dot{x}(t) = Ax(t) + Bu(t), \tag{1.43}$$

$x(t) \in \mathbb{R}^n$, the complete system with a set of m inequalities (i.e., $C \in \mathbb{R}^{m\times n}$):

$$Cx(t) \geq D, \quad \text{for all } t \geq 0, \tag{1.44}$$

defines a *nonlinear* system. Systems as in (1.43) and (1.44) are sometimes called *convex* systems. If $x(t) = \varphi(t; x_0, u_0)$ and $z(t) = \varphi(t; x_1, u_1)$ are time-continuous solutions of the controlled system in (1.43) and (1.44), then for all $\lambda \in [0, 1]$, $w(t) = \lambda x(t) + (1-\lambda)z(t)$ is a time-continuous solution also [321]. They are called convex *conical* if $D = 0$. The time-continuity is crucial in this definition. Indeed we shall see that the unilateral constraints generally involve state discontinuities. Then if $x(t)$ possesses such a jump, there is no reason for $w(t)$ to be a solution of the system, as the jump will not occur at a contact time for $z(\cdot)$.
It is not difficult to understand where the nonlinearity comes from: indeed the solutions of such systems possess (see Sect. 1.3.1.2) discontinuities at certain times t_k.

In turn, the t_k's are in general nonlinear functions of the initial conditions. Hence the superposition principle for linear systems no longer holds. This may also be seen by noting that if these systems were linear, then $\varphi(t; \lambda x_0, \lambda u_0)$ would be equal to $\lambda\varphi(t; x_0, u_0)$. Now there is no reason why $\lambda\varphi(t; x_0, u_0)$ should be a solution of (1.43) plus (1.44) for any $\lambda \in \mathbb{R}$ (think of the case $C = I$, $D = 0$ and take $\lambda = -1$). We shall retrieve the nonlinearity when we deal with impact Poincaré maps (see Chap. 7). Then the main and fundamental discrepancy between the classical discretization of linear or nonlinear systems, and the calculation of such Poincaré maps lies in the fact that the "sampling" times for the latter are (nonlinear) functions of the system's state. This introduces much difficulty in the dynamical analysis. Even in apparently very simple cases, it is impossible to calculate explicitly the Poincaré map, whose dynamics may display a very complex behavior.

1.3.1.2 The Collisions

Important events in the dynamics of a mechanical system submitted to unilateral constraints are the collisions, which occur at some time instants that we denote generically t_k, $k \in \mathbb{N}$. Those times are defined such that for some $\delta > 0$, $f(q(t)) > 0$ for $t \in [t_k - \delta, t_k)$, and $f(q(t_k)) = 0$ with $\dot{q}(t_k^-)^T \nabla f(q(t_k)) < 0$. Consider Example 1.6. When the string attains its maximum elongation at a time t_k with a positive velocity of the mass $\dot{x}(t_k^-) > 0$, then an impact has to occur which reverses the velocity sign to $\dot{x}(t_k^+) \geq 0$. Otherwise the string would exceed its maximum length, which is not allowed in this model. In the general setting of a Lagrangian system with a frictionless unilateral constraint $f(q) \geq 0$, a necessary and sufficient condition for the interaction force not to be impulsive is that $\dot{q}(t_k^-)^T \nabla f(q)(t_k) = 0$ at the time when contact is established. If the generalized velocity $\dot{q}(\cdot)$ points outwards the admissible domain Φ at $t = t_k$, i.e., $\nabla f(q(t_k))^T \dot{q}(t_k^-) < 0$, then a jump has to occur in $\dot{q}(\cdot)$ at t_k in order to keep the trajectory inside Φ, with $\nabla f(q(t_k))^T \dot{q}(t_k^-) \geq 0$. From the analysis we led in Sect. 1.1, we infer that there must exist an impulsive force in the right-hand side of the dynamics since the acceleration is a Dirac measure. Suppose now that the system has never been in contact with the constraint, so that the first impact time t_0 is implicitly given by the equation:

$$f \circ \varphi_q(t_0; \tau_0, u_0) = 0, \tag{1.45}$$

where $\varphi_q(t; \tau_0, u_0) = q(t)$ is the solution at time t of the dynamical equation before the impact at t_0 with the vector field $G(u)$, starting at $u_0 = (q_0, \dot{q}_0)$ with $q_0 = q(\tau_0)$, $\dot{q}_0 = \dot{q}(\tau_0)$ and with $f(q_0) > 0$. The vector field $G(u)$ between the impacts can be supposed to be smooth, so that all smoothness properties for solutions of ODEs hold. Assume the constraint is of codimension one (hence $f(\cdot)$ is smooth in the region of interest, see Definition 1.8). Assume also that the equation in (1.45) possesses at least one solution $t_0, \tau_0, q_0, \dot{q}_0$: notice that existence of an impact time depends on $G(u)$ and on the constraint. Equation (1.45) provides us with a relationship between t_0, τ_0, q_0 and $\dot{q}_0$, which we can denote as $h(t_0, \tau_0, u_0) = 0$. We

study this relationship and assume that $\frac{\partial h}{\partial t_0}$ exists for all t_0, independently of the fact that the solution φ_q will not be differentiable at t_0, but rather possess a left and a right bounded derivatives. We can use the implicit function theorem [262, 533] to deduce that provided $\frac{\partial h}{\partial t}(t_0) \neq 0$, then there is a smooth enough function $g(\cdot)$ such that $g(\tau_0, u_0) = t_0$, and this relation is valid in a neighborhood of τ_0, u_0. In other words the set $h^{-1}(0) = \{(t, \tau, q, \dot{q}) | h(t, \tau, q, \dot{q}) = 0\}$ is a smooth hypersurface of the $(2n + 2)$-dimensional space of $t, \tau, q, \dot{q}$, in the neighborhood of $t_0, \tau_0, q_0, \dot{q}_0$, defined by the equation $t = g(\tau, q, \dot{q})$. Hence the impact time t_0 clearly depends continuously on the initial data under the stated assumptions.[15] Notice that it makes no sense to let τ_0 tend towards t_0 this time, contrarily to what we did in Sect. 1.2 to show discontinuity of the solution of a simple MDE with respect to the initial time. Given initial state data and the dynamics, necessarily $t_0 \geq \tau_0$, while $t_0 = \tau_0$ if the system is initialized on the constraint $f(q) = 0$.

Example 1.7 Consider the dynamics of a ball falling under the influence of gravity on a rigid ground, i.e., $\ddot{q}(t) = -g$ and the unilateral constraint $q(t) \geq 0$ for all $t \geq 0$. Then $\varphi_q(t; \tau_0, q_0, \dot{q}_0) = -\frac{g}{2}(t - \tau_0)^2 + (t - \tau_0)\dot{q}_0 + q_0$. Equation (1.45) is $h(t_0, \tau_0, q_0, \dot{q}_0) = -\frac{g}{2}(t_0 - \tau_0)^2 + (t_0 - \tau_0)\dot{q}_0 + q_0 = 0$ which possesses two solutions. Only one of them is of interest, such that $t_0 \geq \tau_0$, and is given by $t_0 = \min\left\{2\frac{\dot{q}_0 \pm \sqrt{\dot{q}_0^2 + 2gq_0}}{g}\right\} + \tau_0$. Hence if $q_0 = 0$ one gets $t_0 = \tau_0$. It is easily checked that $\frac{\partial h}{\partial t}(t_0) = -g(t_0 - \tau_0) + \dot{q}_0 \neq 0$, except if $q_0 = \dot{q}_0 = 0$ (then we have a so-called *grazing* trajectory), so that the implicit function theorem applies in a neighborhood of the root of $h(t_0, \tau_0, q_0, \dot{q}_0) = 0$. In this case the function $g(\tau, q, \dot{q})$ is defined globally.

Remark 1.8 One of the differences between systems with unilateral constraints, for which the jump times are defined from an equation as in (1.45), and systems as in (1.31), is that for the former the jump times will often be defined implicitly only in terms of the state (as solutions of unsolvable transcendental equations). Additionally, the state of (1.31) is not a priori restricted to a subset of the state space, and the dynamics is not of the variable structure type. This will be important when dealing with various problems like mathematical analysis, stability, control, and simulation.

1.3.2 Flows with Collisions (Vibro-Impact Systems)

Let us assume that the mechanical systems we deal with have one unilateral constraint and they undergo a series of collisions $\{t_k\}_{k\geq 0}$, $t_\infty \stackrel{\Delta}{=} \lim_{k\to+\infty} t_k$, separated by

[15] In general, the equation in (1.45) possesses several real solutions, and one has to decide which one is the right , e.g., the bouncing ball case in Chap. 7, Eq. (7.7). In the degenerate case, the trajectories in a neighborhood of t_0 are on the manifold $\frac{\partial h}{\partial t}(t_0) = 0, h = 0, f(q) = 0$ and are tangent to the surface $f(q) = 0$ [140]: those orbits are grazing trajectories.

unconstrained phases where $f(q(t)) > 0$. Let $u \stackrel{\Delta}{=} \begin{pmatrix} q \\ \dot{q} \end{pmatrix}$. The dynamical equations can be written as

$$\begin{cases} \dot{u}(t) = G(u(t)) & \text{if } t \neq t_k \\ \sigma_{\dot{q}}(t_k) = J_k\left(\dot{q}(t_k^-)\right) & \text{if } t = t_k \\ f(q(t_k)) = 0, \quad \nabla f(q(t_k))^T \dot{q}(t_k^-) < 0, & \\ \nabla f(q(t_k))^T \dot{q}(t_k^+) \geq 0. & \end{cases} \tag{1.46}$$

for some vector field $G(\cdot)$. This mimics (1.31), however the complete state jump mapping comprises the last three lines of (1.46) and is therefore more complex. It is crucial to see that without any further modeling, the solutions of (1.46) exist for all $t \leq t_\infty$. If $t_\infty < +\infty$, then solutions fail to exist globally in time, in a similar way to (1.31). Persistent contact phases (that correspond to a static equilibrium in case of Example 1.6) are not modeled. In the literature such systems are often called *vibro-impact systems*. From the second line of (1.46) we obtain $\dot{q}(t_k^+) = \dot{q}(t_k^-) + J_k\left(\dot{q}(t_k^-)\right)$: this is a *restitution mapping*.

1.3.2.1 Definition

A natural mathematical interpretation of (1.46) is the concatenation of flows and mappings: the flows represent the dynamics between the impacts,[16] and the mappings are for the relationships between pre and postimpact velocities. We shall study in detail such mappings which are called *restitution rules*, in Chaps. 4 and 6. The terminology *flows with collisions* is from [1274]. In practice they occur in vibro-impact systems, juggling robots or running bipeds when no persistent contact phases occur (thus there is no variation of the state space dimension).

As we shall see in Chap. 2, Sect. 2.4, and in Chap. 5 with the sweeping process formulation, it is possible to define a tangent cone to the constraint, that we denote following [894] as $V(q)$: roughly speaking, this is the half subspace delimited by the hyperplane tangent to the hypersurface $f(q) = 0$, "inside" the admissible domain Φ (see Appendix B for details, Definitions B.2 and B.6). The negative half subspace is denoted as $-V(q)$.

When an impact occurs at t_k, then $\dot{q}(t_k^-) \in -V(q(t_k))$. After the collision, $\dot{q}(t_k^+) \in V(q(t_k))$. Hence the collision mapping $\mathscr{F}_{q(t_k),k}$ at $t = t_k$ is defined as

[16] Recall that given an ODE: $\dot{x}(t) = f(x(t))$, its *flow* is a smooth function of t and $x_0 = x(\tau_0)$, denoted as $\varphi_t(x_0)$, such that $\frac{\partial \varphi_t(x_0)}{\partial t} = f(\varphi_t(x_0))$ and with $\varphi_{\tau_0}(x_0) = x_0$. In other words, a vector field $f(x)$ allows the construction of a flow, and the flow is an integral curve of $f(x)$ (then $f(x)$ is said to *generate* the flow $\varphi_t(x_0)$). A flow may be local or global, and possesses several properties, like invertibilty: $\varphi_t^{-1}(x_0) = \varphi_{-t}(x_0)$, and the autonomy (or semi-group) property: $\varphi_{t+s}(x_0) = \varphi_t(\varphi_s(x_0))$. There is a bijective relation between the set of flows and that of generating vector fields. This means that given a priori a flow, there is one and only one vector field that generates it.

$$\begin{aligned} &\mathscr{F}_{q(t_k),k} : \mathrm{bd}(\Phi) \times \{-V(q(t_k))\} \to \mathrm{bd}(\Phi) \times V(q(t_k)) \\ &\begin{pmatrix} q(t_k) \\ \dot{q}(t_k^-) \end{pmatrix} \mapsto \begin{pmatrix} q(t_k) \\ \dot{q}(t_k^+) \end{pmatrix} = u(t_k^-) + J_k \left(u(t_k^-) \right). \end{aligned} \tag{1.47}$$

We shall assume that the $\mathscr{F}_{q(t_k),k}$'s are continuous and autonomous mappings (i.e., the state postimpact value depends only on the state preimpact value). They will not always be invertible for some sort of collisions (named *purely inelastic*, or *soft*, or *plastic*). They may also be defined implicitly only. Note that they are *local* in nature, because the form of the mapping depends on the system's generalized position at the impact time. In other words, the part of the generalized velocity that jumps at the collision may be modified from one impact to the other, similarly to the tangent cone $V(q)$. We shall also denote $\mathscr{F}_{q(t_k),k}$ as $\mathscr{F}_k$ for simplicity. Let us denote the flow[17] during flight times, defined by $G(u)$, as $\varphi_{\tau-\tau_0}(u_0)$. It can be defined either as a mapping from $\Omega \ni (\tau, u)$ into $\mathbb{R}^{2n}$ [533], or as a mapping from $\mathbb{R}^{2n}$ into $\mathbb{R}^{2n}$ [61]. We adopt the latter definition. φ_0 is the identity map, i.e. $\varphi_0(u_0) = \varphi(\tau_0; \tau_0, u_0) = u_0$. Note that τ in $\varphi(\tau; \tau_0, \cdot)$ may denote either the elapsed time from τ_0, so that the solution is evaluated at the absolute time $t = \tau + \tau_0$, or the absolute time measured from 0. In general (see [262, 533]) one takes $\tau_0 = 0$ so that the absolute value of time and the elapsed time are equal. These are matters of convenience. We shall assume in the following that the first argument in $\varphi(\cdot; \cdot, \cdot)$ is the absolute value of time, so that $u(t) = \varphi(t; \cdot, \cdot)$ for any initial data.
Just after the first shock, the solution is given at $t = t_0^+$ by

$$u(t_0^+) = \begin{pmatrix} q(t_0) \\ \dot{q}(t_0^+) \end{pmatrix} = \mathscr{F}_0 \begin{pmatrix} \varphi_q(t_0; \tau_0, u_0) \\ \varphi_{\dot{q}}(t_0^-; \tau_0, u_0) \end{pmatrix} = \mathscr{F}_0 \circ \varphi_{t_0^- - \tau_0}(u_0). \tag{1.48}$$

Recall that $f \circ \varphi_q(t_0; \tau_0, u_0) = 0$. Notice that the expression $\mathscr{F}_k \circ \varphi_{t-\tau_0}(u)$ is meaningful as soon as t is a collision time. The solution $u(t)$ is obtained by the time-concatenation of the successive values of $\varphi(\cdot; \cdot, \cdot)$ considered as a function of time from τ_0 to t_0^-, t_0^- to t_0^+, t_0^+ to t_1^-,.... In terms of flow we have the composition $\varphi\left(t; \tau, \varphi(\tau_1; \tau_0, u_0)\right) = \varphi_{t-\tau}\left(\varphi_{\tau_1-\tau_0}(u_0)\right) = \varphi_{t-\tau} \circ \varphi_{\tau_1-\tau_0}(u_0)$.
Now during the flight time after the first shock, i.e., on an interval $(t_0, t_0+\delta)$ for some $\delta > 0$, the solution continues to evolve with new initial data $q(t_0)$, $\dot{q}(t_0^+)$ according to the vector field $G(u)$. The solution on this interval is given by $\varphi(t; \tau_0, u_0) = \varphi(t; t_0^+, u(t_0^+)) = \varphi(t; t_0^+, \mathscr{F}_0 \circ \varphi(t_0^-; \tau_0, u_0))$. With the above notation $\varphi^0_{t-\tau_0}(u_0) = \varphi_{t-t_0^+}(u(t_0^+)) = \varphi_{t-t_0^+}\left(\mathscr{F}_0 \circ \varphi_{t_0^- - \tau_0}(u_0)\right) = \varphi_{t-t_0^+} \circ \mathscr{F}_0 \circ \varphi_{t_0^- - \tau_0}(u_0)$. The superscript in $\varphi^0_{t-\tau_0}$ is to indicate for the moment that this denotes the solution after one shock has occurred. Proceeding similarly, after the second shock at t_1, we can write $\varphi^1_{t-\tau_0}(u_0) = \varphi_{t-t_1^+} \circ \mathscr{F}_1 \circ \varphi_{t_1^- - t_0^+} o \mathscr{F}_0 \circ \varphi_{t_0^- - \tau_0}(u_0) = \varphi_{t-t_1^+} \circ \mathscr{F}_1 \circ \varphi^0_{t-\tau_0}(u_0)$. We denote now the solution on (t_k, t_{k+1}) starting at (τ_0, u_0) as $\varphi^c_{t-\tau_0}(u_0) = \varphi^k_{t-\tau_0}(u_0)$. Note that $\varphi^c_0(u_0) = \varphi_0(u_0) = \varphi(\tau_0; \tau_0, u_0) = u_0$ is the identity mapping. The candidate flow

[17] It is justified to speak of the flow between impacts since the dynamics is smooth on those period.

with collisions $\varphi_t^c(u_0)$ is thus defined on (t_k, t_{k+1}) with $\tau_0 = 0$ as

$$\begin{aligned}\varphi_t^c(u_0) &= \varphi_{t-t_k^+} \circ \mathscr{F}_k o \varphi_{t_k^- - t_{k-1}^+} \circ \mathscr{F}_{k-1} \circ \ldots \circ \varphi_{t_2^- - t_1^+} \circ \mathscr{F}_1 o \varphi_{t_1^- - t_0^+} \circ \mathscr{F}_0 \circ \varphi_{t_0^-}(u_0) \\ &= \varphi_{t-t_k^+} \circ \mathscr{F}_k \circ \varphi_{t_k^-}^{k-1}(u_0),\end{aligned} \tag{1.49}$$

that is:

$$\begin{aligned}&\varphi_t^c : \mathbb{R}^{2n} \to \mathrm{bd}(\Phi) \times \{-V(q(t_0))\} \to \mathrm{bd}(\Phi) \times V(q(t_0)) \to \mathrm{bd}(\Phi) \times \{-V(q(t_1))\} \to \ldots \\ &\quad \to \mathrm{bd}(\Phi) \times \{-V(q(t_k))\} \to \mathrm{bd}(\Phi) \times V(q(t_k)) \to \mathbb{R}^{2n} \\ &\quad u_0 \mapsto \varphi(t_0^-; 0, u_0) \mapsto \varphi(t_0^+; 0, u_0) \mapsto \varphi(t_1^-; 0, u_0) \mapsto \ldots \mapsto \varphi(t_k^-; 0, u_0) \\ &\quad \mapsto \varphi(t_k^+; 0, u_0) \mapsto \varphi(t; 0, u_0).\end{aligned} \tag{1.50}$$

1.3.2.2 The Semi-Group Property

Recall that in order to prove that the solution $\varphi(t; \tau_0, u_0)$ defines a flow, we must prove that the autonomy (or semi-group) property [262] is satisfied, i.e., the solution ($\in \mathbb{R}^{2n}$) satisfies $\varphi(t_2+t_1; 0, u_0) = \varphi(t_2; t_1, \varphi(t_1; 0, u_0))$ for all t_2 and t_1: the solution at time $t_2 + t_1$, starting at $t = 0$, with initial condition u_0, and the solution at time t_2 with initial condition $\varphi(t_1; 0, u_0)$, coincide. Equivalently the semi-group property can be stated as $\varphi(t_1; t_0, u_0) = \varphi(t_1 - t_0; 0, u_0)$. The solution at time t_1 starting at time t_0 with initial data u_0, is equal to the solution at time $t_1 - t_0$, starting at $t = 0$ with the same initial state data, for any t_0, t_1. Of course two such solutions are not equal in the extended state space $\ni (x, t)$, but their orbits are equal in the state space (see e.g., [497, Fig. 4.5]). Uniqueness of solutions is the key property (and in turn, uniqueness is implied by continuous dependence on initial conditions). In other words, autonomy means that the absolute value of the initial time is not an important notion. It is rather the elapsed time which has to be considered to compute the solution from a set of initial data[18] [61]. For the sake of simplification of the notations, in the following we shall denote $\varphi(t; 0, u_0)$ as $\varphi(t, u_0)$. Our goal is therefore to show that if $\varphi(t + \tau, u_0)$ and $\varphi(t, \varphi(\tau, u_0))$ are two solutions of the system, they are equal for all $t \geq 0$. The first impact time t_0 is given by $f \circ \varphi_q(t_0, u_0) = 0$. Note that $f \circ \varphi_q(t + \tau, u_0) = 0$ for $t + \tau = t_0$, i.e. $t = \bar{t}_0 = t_0 - \tau$.
If $\tau \leq t_0$, then $\varphi(t, \varphi(\tau, u_0))$ jumps at $\bar{t}_0$ also, and $\varphi(\bar{t}_0^-, \varphi(\tau, u_0)) = \varphi(\bar{t}_0^- + \tau, u_0)$ because the equality is true before any jump occurs. We deduce the equality $\mathscr{F}_0 \circ$

[18] Clearly this property is not true in general for non-autonomous systems, since the initial vector field, i.e., the slope of the curve (the orbit) in the two-dimensional case, changes if the initial time changes. Therefore even if the initial state remains unchanged, there is no reason that after a certain amount of time, both solutions coincide.

$\varphi(\bar{t}_0^-, \varphi(\tau, u_0)) = \mathscr{F}_0 \circ \varphi(\bar{t}_0^- + \tau, u_0)$, i.e. $\varphi^0(\bar{t}_0^+, \varphi(\tau, u_0)) = \varphi^0(\bar{t}_0^+ + \tau, u_0) = \varphi^c_{\bar{t}_0^+ + \tau}(u_0) = \varphi^c_{\bar{t}_0^+} \circ \varphi^c_\tau(u_0)$. We deduce that $\varphi^c_{t+\tau}(u_0) = \varphi^c_t \circ \varphi^c_\tau(u_0)$ for all $t \geq 0$ (until an eventual second impact occurs).

If $\tau > t_0$, the first impact time does not change but $\varphi(\tau, u_0)$ has already jumped. Hence we can attack the proof assuming that the semi-group property is true from $t = 0$ until the second impact at t_1, $t_1 > t_0$ and with $f \circ \varphi_q(t_1, u_0) = 0$. Assume that $\tau < t_1$. Then we can redo the same reasoning as above, replacing t_0 by t_1 and $\mathscr{F}_0$ by $\mathscr{F}_1$.

The reasoning can be extended for any $\tau > 0$. The fact that both functions $\varphi(t+\tau, u_0)$ and $\varphi(t, \varphi(\tau, u_0))$ take the same values for all t and τ relies at each step that there is a unique solution to the dynamical problem considered, for given initial data. As we shall see in Chap. 2, uniqueness for problems with unilateral constraints fails in general if no restrictions are placed on the vector field $G(u)$, on the hypersurface $f(q)$ and on the collision mapping energetical behavior (related to the invertibility of $\mathscr{F}_k$). We have assumed from the beginning that the vector field $G(u)$ is autonomous. This means that the possible external bounded actions on the system are constant on $[\tau_0, +\infty)$. Theorem 5.3 in Chap. 5 allows us to conclude that φ^c_t is a flow. It is noteworthy that the time-independence of both the vector field and the collision mapping is not sufficient to guarantee this result in general, as the conditions of Theorem 5.3 show.

Contrarily to the case of autonomous ODEs, here $\varphi^c_t(\cdot)$ cannot be continuous in t. It can be expected to be $RCLBV$ (or piecewise continuous) in t. Furthermore in order for φ^c_t to be a global flow, it must exist the inverse function $\left(\varphi^c_t\right)^{-1} = \varphi^c_{-t}$ for all $t \geq \tau_0$. Invertibility of the $\mathscr{F}_k$'s is then necessary, since one has

$$\left(\varphi^c_t\right)^{-1} = \varphi^c_{-t} = \varphi_{\tau_0 - t_0^-} \circ \mathscr{F}_0^{-1} \circ \varphi_{t_0^+ - t_1^-} \circ \ldots \circ \varphi_{t_{k-1}^+ - t_k^-} \circ \mathscr{F}_k^{-1} \circ \varphi_{t_k^+ - t}. \quad (1.51)$$

This places the dynamics of so-called *soft* or *inelastic* shocks (in a sense the shock produces a maximal loss of kinetic energy) well apart from those of *hard* or *elastic* shocks (the loss of kinetic energy is zero). For instance, in the case of the bouncing ball, we get $\mathscr{F}(q(t_k), \dot{q}(t_k^-)) = \begin{pmatrix} 1 & 0 \\ 0 & 0 \end{pmatrix} \begin{pmatrix} q(t_k) \\ \dot{q}(t_k^-) \end{pmatrix}$ for the soft case, and $\mathscr{F}(q(t_k), \dot{q}(t_k^-)) = \begin{pmatrix} 1 & 0 \\ 0 & -1 \end{pmatrix} \begin{pmatrix} q(t_k) \\ \dot{q}(t_k^-) \end{pmatrix}$ for the elastic case.

1.3.2.3 Continuity of Solutions in the Initial Data

We have seen in Sect. 1.2 that the solutions of MDEs as defined in (1.15) are not continuous but of bounded variation in the initial time τ_0. They are however continuous in initial state data, and this is easily proved since the jump times are exogenous, hence equal for any trajectory. What about continuity with respect to τ_0, u_0 of the solutions $\varphi(t; \tau_0, u_0)$ of mechanical systems with unilateral constraints? Let us recall that we

assume a codimension one constraint, and that we suppose that solutions exist.[19] Moreover continuity in the initial conditions implies uniqueness of solutions (but the reverse is false: some nonsmooth mechanical systems possess unique solutions, yet continuity in the initial data fails), so that non-uniqueness destroys the continuous dependence.
On $[\tau_0, t_0^-)$ continuity holds. Now at t_0^+, $\varphi(t_0^+; \tau_0, u_0) = \mathscr{F} \circ \varphi(t_0^-; \tau_0, u_0)$. From the continuity of t_0 in τ_0 and u_0, it follows that the last term can be written as $\mathscr{F} \circ m(\tau_0, u_0)$ for some continuous function $m(\cdot, \cdot)$. Now since $\mathscr{F}$ is continuous, it follows that $\varphi(t_0^+; \tau_0, u_0)$ is continuous in τ_0 and u_0. Therefore on (t_0, t_1), the solution $\varphi(t; t_0^+, u(t_0^+))$ is also continuous in the initial data. Now the collision time t_1 is given by $f \circ \varphi(t_1; t_0^+, u(t_0^+)) \stackrel{\Delta}{=} h_1(t_1, t_0, u(t_0^+)) = 0$. Using similar arguments as in Sect. 1.3.1.2 we deduce that t_1 depends continuously on t_0 and on $u(t_0^+)$, hence on τ_0, u_0. Thus on (t_1, t_2), $\varphi(t; \tau_0, u_0) = \varphi\left(t; t_1^+, \mathscr{F} \circ \varphi(t_1^-; \tau_0, u_0)\right)$. Since t_1 depends continuously on τ_0, u_0, the term $\mathscr{F} \circ \varphi(t_1^-; \tau_0, u_0)$ is a continuous function of τ_0, u_0, and so is $\varphi(t; t_1^+, u(t_1^+))$. Reiterating this reasoning, we deduce that the solution depends continuously on τ_0, u_0 on intervals $(t_k, t_{k+1}) \ni t$.

The Jump-Times Mismatch: Let us now examine what happens at the jump times. Let us further suppose first that $t_{k+1} > t_k + \gamma$ for some $\gamma > 0$, i.e., velocities are piecewise time-continuous. In order for the solution to be a continuous function of u at u_0, it must be verified that for all t and for all τ_0, for any $\varepsilon > 0$, there exists a $\delta > 0$ such that for all u_1 with $||u_1 - u_0|| < \delta$, then $||\varphi(t; \tau_0, u_1) - \varphi(t; \tau_0, u_0)|| < \varepsilon$. Let us consider u_0 such that $f(q_0) = 0$ and $\dot{q}_0 \in -V(q_0)$, where the set $V(q)$ is the tangent cone to the admissible domain Φ at q_0). In other words the system is initialized on the constraint and with a velocity pointing outwards Φ: a shock occurs at $t_0 = \tau_0$ and the solution $\varphi(t; \tau_0, u_0)$ jumps at τ_0. Now consider u_1 with $f(q_1) = \mu > 0$ and $\dot{q}_1 = \dot{q}_0$. The solution may or may not jump, but anyway if it does, then it jumps at a time $\bar{t}_0 > t_0$ since the system has to attain the constraint. Hence $\varphi(t; \tau_0, u_1)$ is continuous (in t) at $t = t_0$. The quantity $||\varphi(t_0^+; \tau_0, u_1) - \varphi(t_0^+; \tau_0, u_0)||$ thus cannot be made arbitrarily small even for an arbitrarily small $\mu > 0$. We conclude that for such a u_0, there exist $\varepsilon > 0$ and $t \geq \tau_0$ such that for any τ_0 and for any $\delta > 0$, there exists u_1 with $||u_1 - u_0|| < \delta$ and $||\varphi(t; \tau_0, u_1) - \varphi(t; \tau_0, u_0)|| > \varepsilon$. Another way of seeing this fact is to consider sequences $\{u_n\}$ that converge towards u_0. Then $\varphi(t; \tau_0, u)$ is continuous at u_0 if and only if, for any such sequence $\{u_n\}$, $\varphi(t; \tau_0, u_n)$ converges towards $\varphi(t; \tau_0, u_0)$, for all $t \geq \tau_0$ and for all τ_0. If this is true, then for all $\varepsilon > 0$, there exists $N > 0$, $N \in \mathbb{N}$, such that $n > N$ implies $||\varphi(t; \tau_0, u_n) - \varphi(t; \tau_0, u_0)|| < \varepsilon$, for all t, τ_0. In particular this must hold at $t = t_0^+$ as defined above (the first time of jump for $\varphi(t; \tau_0, u_0)$). Consider for instance q_n such that $f(q_n) = f(q_0) + \frac{1}{n} = \frac{1}{n}$. Then clearly there exists $\varepsilon > 0$ such that for any $N > 0$, there exists $n > N$ such that $||\varphi(t_0^+; \tau_0, u_n) - \varphi(t_0^+; \tau_0, u_0)|| > \varepsilon$.
Notice that if we estimate the solutions at $t \geq t_0 + \alpha$, $\alpha > 0$, then it is always possible to find u_1 so close to u_0 that $\varphi(t; \tau_0, u_1)$ has jumped before such t.

[19] Existence of solutions is a basic property, and we shall come back on existence results in the next chapters (see Theorem 5.3). We take some freedom here with the mathematical logic, since our goal is to highlight the differences between various sorts of measure differential equations.

This is possible since the jump times depend continuously on the initial data. In other words, $||\varphi(t_0+\alpha;\tau_0,u_n)-\varphi(t_0+\alpha;\tau_0,u_0)||$ can be made arbitrarily small by taking n sufficiently large but finite. Indeed the first impact time $t_{0,n}$ associated with the solution initialized at τ_0 (i.e., u_n) can be made arbitrarily close to t_0 by increasing n. We retrieve the fact that if $t \neq t_0$, then the solution is continuous in u_0. This motivates us to define the closeness of two solutions as follows, where t_k denotes the discontinuities of $\varphi(t;\tau_0,u_0)$:

$$\forall\, \varepsilon > 0, \forall\, \alpha > 0, \exists\, \eta > 0 \text{ such that } |t - t_k| > \alpha \text{ and } ||u_0 - u_1|| \leq \eta$$
$$\Rightarrow ||\varphi(t;\tau_0,u_0) - \varphi(t;\tau_0,u_1)|| \leq \varepsilon. \tag{1.52}$$

By letting u_1 tend towards u_0, both solutions become arbitrarily close one to each other, except in a neighborhood of their discontinuities. In conclusion the solutions are continuous in the initial data, in the sense that $\lim_{u_1 \to u_0} \varphi(t;\tau_0,u_1) = \varphi(t;\tau_0,u_0)$ for all times outside the impact times. But the fact that basically the dynamical system consists of flows and diffeomorphisms implies some modifications of the "continuity" definition, taken from the continuous-time point of view only.

Remark 1.9 We shall retrieve in the definition of stability of trajectories (see Definition 7.1) that two solutions cannot be arbitrarily close one to each other in the neighborhood of the discontinuity times. Hence the classical Lyapunov stability definition has to be modified. It is known (see [1229]) that the continuity with respect to initial conditions and the stability are closely related, for solutions of ODEs. Hence it is not surprising that both notions are related also for MDEs representing systems with unilateral constraints. The problem caused by impacts mismatch has been noticed in a Lyapunov stability and trajectory tracking control context in [147, 221, 839] [730, pp. 124–125]. Indeed two trajectories with discontinuities may be close one to each other in a graphical sense,[20] while a mismatch as the above persists in the neighborhood of impact times.

What happens now if the sequence $\{t_k\}$ is infinite and with a finite accumulation point t_∞? Although the above reasoning applies well for $t < t_\infty$, it is not clear how we should study the behavior of the solution at t_∞. Indeed the criterion in (1.52) does not apply well in the limit as $k \to +\infty$, because it is no longer possible to define neighborhoods of the impact times (α is strictly positive in (1.52)). One point of view is to do a sort of time-scaling as follows. Since the sequence is infinite and with $t_\infty < +\infty$, the flight times are bounded and the system's state remains bounded between each impact. Hence the total dynamics define (explicitly or implicitly) an operator (or a mapping) $P : (u(t_k^+), t_k) \mapsto (u(t_{k+1}^+), t_{k+1})$.[21] Let us denote $(u(t_k^+), t_k)$ as x_k. Then $x_k = P^k(x_0)$. We can therefore consider the finite collisions process as an infinite discrete-time system in the k-time scale. From the above developments it is

[20] Consequently closedness of graphs with the Hausdorff distance may be the right notion [888].

[21] Which could as well be defined with preimpact values.

clear that $x_k \stackrel{\Delta}{=} x_k(x_0)$ is continuous in x_0 for all finite k. If it can be proved for instance that the sequence of continuous functions $\{x_k(\cdot)\}$ converges uniformly towards a limit $x(\cdot)$, then $x(\cdot)$ is continuous. Clearly it is not sufficient that continuity holds for any finite k to imply that it holds also at the limit, which might be discontinuous. Another path might be to consider that if a finite accumulation exists in $\{t_k\}$ then the jumps in $\dot{q}(\cdot)$ vanish as $k \to +\infty$ since $\dot{q}(\cdot) \in RCLBV$. Hence the technical difficulties mentioned above due to the discontinuities disappear when approaching the time t_∞.

A Suitable Distance Function: These problems have been overcome for the one-degree-of-freedom case in [1069] by replacing the state $u = (q, \dot{q})$ by its equivalence class $u^\bullet = (q, \dot{q})^\bullet$ defined as follows (we assume that the unilateral constraint is given by $q \geq 0$): $u_1 \mathscr{R} u_2$ if and only if $\{ [u_1 = u_2]$ or $[q_1 = 0$ and $\dot{q}_1 < 0$ and $\dot{q}_2 = -e_{\rm n}\dot{q}_1]$ or $[q_2 = 0$ and $\dot{q}_2 < 0$ and $\dot{q}_2 = -e_{\rm n}\dot{q}_1]\}$. The coefficient $e_{\rm n} \in [0, 1]$ is a restitution coefficient, which we have not yet introduced but is needed at this stage. In other words the pairs $(q(t_k), \dot{q}(t_k^-))$ and $(q(t_k), \dot{q}(t_k^+))$ are identified through the equivalence relation $\mathscr{R}$. Then continuous dependence with respect to the initial data (t_0, u_0) is proved in the sense that if (t_{0n}, u_{0n}) converges towards (t_0, u_0) then the equivalence class $\varphi_n(\cdot; t_{0n}, u_{0n})^\bullet$ converges towards $\varphi(\cdot; t_0, u_0)^\bullet$, uniformly on compact subsets of $[t_0, +\infty)$. The convergence is understood on $\mathbb{R} \times U_e$, where U_e is the quotient space[22] of $U = [0, +\infty) \times \mathbb{R} \ni (q, \dot{q})$ by the equivalence relation $\mathscr{R}$, equipped with a suitable distance

$$d_e(u_1^\bullet, u_2^\bullet) = \min[|q_1 - q_2| + |\dot{q}_1 - \dot{q}_2|, q_1 + q_2 + |\psi(\dot{q}_1) - \psi(\dot{q}_2)|], \qquad (1.53)$$

where $\psi(\dot{q}) = \left\{ \begin{array}{ll} -e_{\rm n}\dot{q} & \text{if } \dot{q} < 0 \\ \dot{q} & \text{if } \dot{q} \geq 0 \end{array} \right\}$. Uniqueness of solutions in U_e is also proved in [1069]. This mathematical framework thus allows one to get rid of the above mentioned problems, at the price of more sophisticated mathematical tools. Interestingly enough, a similar notion of *hybrid distance* ("hybrid" is for hybrid dynamical system) is used in [147] for the design of feedback controllers for systems with state jumps. Continuous dependence problems are more complex when the striked surface has codimension ≥ 2, see Sect. 5.2.3 in Chap. 5.

Remark 1.10 The MDEs formalisms in (1.23) and (1.31) are unable to model systems as in (1.46), except perhaps if one allows for an implicit definition of the velocity jump $t_k(x)$ comprising the last three lines of (1.46). As pointed out in Sect. 1.2.4, the MDE in (1.31) does not satisfy the semi-group property, and it is linear when the vector field and mapping are: both properties are absent in (1.46), which may be sufficient to convince oneself that *"classical" MDEs and impulsive ODEs cannot model mechanical systems with unilateral constraints and impacts, even if they do not undergo variation of the state space dimension*, (i.e., *there are no persistent contact phases with* $\mathrm{bd}(\Phi)$ *but only rebounds on* $\mathrm{bd}(\Phi)$). The formalism in (1.36) has been shown to encapsulate flows with collisions, see [460]. However since contact

[22] i.e., the space that consists of equivalence classes.

forces are absent from all these models,[23] persistent contact with one or several constraints as well as static equilibrium are not modeled, and accumulations of impacts cannot be passed. To be more specific, let us come back to Example 1.6. We can learn at least two things from this simple example (see also Sects. 3.1.2 and (3.11) for another basic example): (1) the complementarity model (1.38) is a quite natural and ubiquitous contact force model, stemming from an extremely simple experimental observation (and it does not prevent the introduction of contact flexibilities, see (1.41)), (2) it yields the dynamics represented by the differential inclusion (1.40), whose right-hand side is a normal cone to a convex set. Suppose that $y(t)$ is constant, and let us rewrite this inclusion in a first-order setting $\dot{x}(t) \in F(x(t))$: the set-valued right-hand side does not satisfy the basic assumptions listed after (1.36), as it is in particular not locally bounded on the admissible domain Φ, being a non-trivial cone on $\mathrm{bd}(\Phi)$. *Thus the set-valued right-hand side in* (1.36) *is not a suitable candidate for selections which are contact forces.*

1.3.3 Unilaterally Constrained Systems: A Geometric Approach

Let us come back to the class of systems as in (1.43) and (1.44), with $m = 1$. In fact we have mainly dealt in the foregoing paragraphs with mechanical systems. They are however, only a subclass of systems as in (1.43) and (1.44) in the sense that only their position is constrained, while any state component may be constrained in (1.44). We deal with linear time-invariant systems in (1.43), the following developments apply as well to nonlinear systems which are affine in the input [322]. It is therefore of interest to investigate some general properties of the state space of such nonlinear unilaterally constrained dynamical systems. The developments that follow essentially aim at understanding the behavior of the system on the set $\{x \in \mathbb{R}^n | Cx = 0\}$ and can be considered as an extension of positive invariance theory for linear systems to this class of restricted linear systems (which are nonlinear).[24] This theory was developed by ten Dam and co-workers in [322, 323].
The basic idea which is ubiquitous in systems with unilateral constraints is to observe the evolution of the derivatives of the "output"

$$\frac{d^i y}{dt^i} = y^{(i)} = Cx^{(i)} = CA^i \varphi(t; \tau_0, x_0, u) + CA^{i-1}Bu + \cdots + CBu^{(i-1)}$$

[23] To be more specific: the set-valued right-hand side in (1.36) is not a suitable set for contact forces that stem from a complementarity modeling.

[24] Positive invariance theory is a field of control theory that deals with the invariance of polyhedral sets under linear- state feedback.

on the set $\{x \in \mathbb{R}^n | y = Cx = 0\} = \text{Ker}(C)$. To this end let us define the mappings:

$$\begin{aligned} h_i &: \text{Ker}(C) \times \mathscr{U}^{\mathbb{N}} \to \mathbb{R} \\ &(x, \underline{u}) \mapsto CA^i \varphi(t; \tau_0, x_0, u) + \textstyle\sum_{j=1}^{i} CA^{j-1} B \underline{u}_{i-j}, \end{aligned} \tag{1.54}$$

where $\underline{u}_i \in \mathscr{U}^{\mathbb{N}}$ are smooth functions of time, (i.e., they are infinitely many times differentiable) or maybe piecewise smooth. The function $\varphi(t; \tau_0, x_0, u)$ denotes the solution of the system with input u, initial data τ_0 and x_0, at time t. If $\underline{u}_i = u^{(i)}(\cdot)$ then clearly $h_i(x(t), \underline{u}(t)) = y^{(i)}(t)$. The objective is to study subsets of $\text{Ker}(C)$ in which there exists a controller such that the trajectories can attain these subsets in a smooth way, or transversally, or if they remain in them, or if they go through the boundary. The study is led by assuming first that the constraints are purely mathematical (or virtual). Then one proceeds to see how collision mappings may be introduced.

Definition 1.9 [323] Let us define the following characteristic numbers:

$$\begin{aligned} r &: \text{Ker}(C) \times \mathscr{U}^{\mathbb{N}} \to \mathbb{N} \cup \{\infty\} \\ &\quad (x, \underline{u}) \mapsto \min[i \in \mathbb{N} | h_i(x, \underline{u}) \neq 0] \\ r_c &: \text{Ker}(C) \to \mathbb{N} \\ &\quad x \mapsto \min[i \in \mathbb{N} | \ \exists \underline{u} \in \mathscr{U}^{\mathbb{N}} : h_i(x, \underline{u}) \neq 0] \\ r_0 &= \min[i \in \mathbb{N} | CA^{i-1}B \neq 0], \end{aligned} \tag{1.55}$$

(when $C \in \mathbb{R}^{1 \times n}$, r_0 is the relative degree of the system with scalar "output" $y = Cx$ and input u).

Example 1.8 As an example let us consider the chain of integrators $\dot{x}_1(t) = x_2(t)$, $\dot{x}_2(t) = x_3(t)$, $\dot{x}_3(t) = u(t)$, $x_1 \geq 0$. Then $r_0 = 3$, and $\text{Ker}(C) = \{x \in \mathbb{R}^3 | x_1 = 0\}$. Since $r(x, \underline{u})$ is defined from $\text{Ker}(C) \times \mathscr{U}^{\mathbb{N}}$, in the following $x_1 = 0$ always; when not mentioned the other state variables are different from 0. Thus $r(x, \underline{u}) = 1$, $r(x_2 = 0, \underline{u}) = 2$, $r(x = 0, \underline{u}) = 3$, $r(x = 0, \underline{u} = 0) = +\infty$, $r(x = 0, u^{(i)} = 0, \ \forall\, 0 \leq i \leq k) = k + 4$, $r_c(x) = 1$, $r_c(x_2 = 0) = 2$, $r_c(x = 0) = 3$.

Let us introduce the following sets, which are subsets of $\text{Ker}(Cx)$:

Definition 1.10 [323] The *contact* set $\mathscr{X}_{con}$ and *release* set $\mathscr{X}_{rel}$ are defined as

- $\mathscr{X}_{con} = \{x \in \text{Ker}(C) | \exists \varphi(\cdot; \tau_0, x_0, u)$ and $\exists\ t^\star$ such that $x_0 = x$ and $Cx(t) = C\varphi(t; \tau_0, x_0, u) > 0, \ \forall\, t : \ t^\star < t < \tau_0\}$.
- $\mathscr{X}_{rel} = \{x \in \text{Ker}(C) | \exists\ \varphi(\cdot; \tau_0, x_0, u)$ and $\exists\ t^\star$ such that $x_0 = x$ and $Cx(t) = C\varphi(\cdot; \tau_0, x_0, u) > 0, \ \forall\, t : \ \tau_0 < t < t^\star\}$.

In words: $\mathscr{X}_{con}$ is the subset of $\text{Ker}(C)$ such that there exist trajectories coming from inside the admissible domain Φ and which attain $\text{Ker}(C)$ at time τ_0; $\mathscr{X}_{rel}$ is the subset of $\text{Ker}(C)$ such that there exist trajectories which leave $\text{Ker}(C) = \text{bd}(\Phi)$ and

reenter Φ. Those subsets are depicted in Fig. 7.4 in Chap. 7 for simple mechanical systems. Consider a one-degree-of-freedom system $\ddot{q}(t) + \lambda_1 \dot{q}(t) + \lambda_2 q(t) = u(t)$, $q \geq 0$, then $\mathscr{X}_{con} = \{(q, \dot{q}) | q = 0, \dot{q} \leq 0\}$, $\mathscr{X}_{rel} = \{(q, \dot{q}) | q = 0, \dot{q} \geq 0\}$: this just translates that the point makes contact with the constraint with a non positive velocity, and leaves the constraint with a non negative velocity. The following is true:

Lemma 1.1 *[323] The contact and release sets are given by*

- $\mathscr{X}_{con} = \{x \in Ker(C) | \exists\ \underline{u} \in \mathscr{U}^{\mathbb{N}}$ *such that* $[r(x, \underline{u}) < +\infty$ *and even, and* $h_{r(x,\underline{u})} > 0]$ *or* $[r(x, \underline{u}) < +\infty$ *and odd, and* $h_{r(x,\underline{u})} < 0]\}$.
- $\mathscr{X}_{rel} = \{x \in Ker(C) | \exists\ \underline{u} \in \mathscr{U}^{\mathbb{N}}$ *such that* $r(x, \underline{u}) < +\infty$ *and* $h_{r(x,\underline{u})} > 0\}$.

Example 1.9 Continuing Example 1.8, one finds that $\mathscr{X}_{con}$ consists of the states x with $x_1 = 0$, and there exists an input such that

- $r(x, \underline{u}) = 2$ and $\ddot{y} > 0$.
- $r(x, \underline{u}) = 1$ and $\dot{y} < 0$.
- $r(x, \underline{u}) = 3$ and $y^{(3)} < 0$.
- $r(x, \underline{u}) = 2k + 4$ and $y^{(2k+4)} = u^{(2k+1)} > 0$, $k \in \mathbb{N}$.
- $r(x, \underline{u}) = 2k + 3$ and $y^{(2k+3)} = u^{(2k+1)} < 0$, $k \in \mathbb{N}$.

In the first item, the system attains the set $x_1 = x_2 = 0$ at $t = 0$, coming from $x_1 > 0$. Necessarily $x_2 < 0$ on $(-\varepsilon, 0)$, for some $\varepsilon > 0$, and necessarily $\dot{x}_2 = x_3 > 0$. In the fourth item, the system attains the set $x = 0$, with $u^{(i)} = 0, 0 \leq i \leq 2k$. Equivalently it attains the set $y^{(i)} = 0, 0 \leq i \leq 2k + 3$. One makes the same reasoning as for the first item, with $y^{(2k+2)}$ and $y^{(2k+3)}$ and one concludes that necessarily $y^{(2k+4)} > 0$ on $(-\varepsilon, 0)$. For item 2, the system attains the set $x_1 = 0$ with $x_1 > 0$ on $(-\varepsilon, 0)$: necessarily $x_2 < 0$ on $(-\varepsilon, 0)$. For items 3 and 5, one makes the same reasoning replacing x_1 and x_2 by x_3 and u, $u^{(2k)}$ and $u^{(2k+1)}$ respectively. Clearly there is an inversion of the sign each time an additional derivative is considered (see Fig. 1.4).

Remark 1.11 As said above, this geometric approach is based on observing the derivatives of the constraint variable $y(t) = Cx(t)$ on $\text{Ker}(C) = \text{bd}(\Phi)$. The numbers introduced in Definition 1.9 are used to define some lexicographical inequalities on

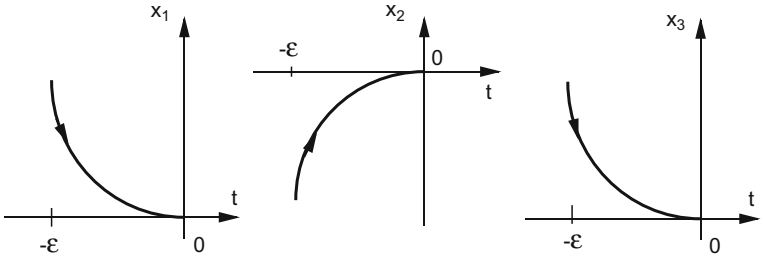

Fig. 1.4 Orbit in $\mathscr{X}_{con}$ attaining $\text{Ker}(Cx)$

the derivatives of $y = Cx$ along the system's dynamics. Observing such derivatives through lexicographical inequalities is ubiquitous in systems with unilateral constraints, and we shall encounter it at several places of this book.

Definition 1.11 [323] Let us introduce the following sets:

- $\mathscr{V}^\star = \{x \in \mathrm{Ker}(C) | \exists\, u \in \mathscr{U}^{\mathbb{N}}$ such that $r(x, \underline{u}) = +\infty\}$.
- $\mathscr{V}_f = \{x \in \mathrm{Ker}(C) | \forall \in \mathscr{U}^{\mathbb{N}}, r_c(x)$ is even, and $h_{r_c(x)}(x, \underline{u}) < 0\}$
- $\mathscr{X}_{con,v} = \{x \in \mathscr{X}_{con} | r_c(x) = 1\}$.
- $\mathscr{X}_{con,h} = \{x \in \mathscr{X}_{con} | \forall\, u \in \mathscr{U}^{\mathbb{N}}, r_c(x) > 1, r_c(x)$ is odd and $h_{r_c(x)}(x, \underline{u}) < 0\}$.

We have also $\mathscr{V}^\star = \{x \in \mathrm{Ker}(C) | r_c(x) = r_0\}$. The set $\mathscr{V}_f$ contains the states in $\mathrm{bd}(\Phi)$ such that all trajectories of the controlled system passing through these states do so coming from outside Φ and remaining outside Φ (one thing that is not possible in mechanics with unilateral constraints, but that is quite possible if the constraints are virtual). The subdivision of $\mathscr{X}_{con}$ is motivated by mechanics: trajectories that make contact in $\mathscr{X}_{con,h}$ attain the boundary $\mathrm{Ker}(C)$ tangentially whereas those that make contact in $\mathscr{X}_{con,v}$ do it transversally. Indeed $r_c(x) = 1$ means that one can find a controller such that $\dot{y} < 0$ in a neighborhood of $\mathrm{Ker}(C)$, hence the contact is made with a nonzero velocity. On the contrary, orbits that make contact in $\mathscr{X}_{con,h}$ attain the boundary with a zero velocity but nonzero higher order derivatives. Trajectories that make contact in $\mathscr{V}^\star$ attain $\mathrm{bd}(\Phi)$ tangentially and there exists at least one of them that remains in $\mathrm{Ker}(C)$ (i.e., there exists one controller in $\mathscr{U}^{\mathbb{N}}$ such that $\varphi(\cdot; \tau_0, x_0, u) \in \mathrm{Ker}(C)$ after contact has been made). For the above one-degree-of-freedom system, $\mathscr{V}^\star = \{(0, 0)\} = \mathscr{X}_{con} \cap \mathscr{X}_{rel}$, the origin of the phase plane. In Sect. 7.4 we shall see that orbits that make contact in the set $\mathscr{V}^\star$ correspond to grazing trajectories which attain $\mathrm{Ker}(C)$ with a zero normal velocity. One notes that all trajectories that make contact in $\mathscr{X}_{con} \backslash \mathscr{V}^\star$ have the tendency to leave $\Phi = \{x \in \mathbb{R}^n | Cx \geq 0\}$: if the constraints are hard and a collision rule is adopted, then a shock occurs at those points of $\mathrm{Ker}(C)$. In [322, 323] collision maps are proposed that relate subsets of $\mathscr{X}_{con} \backslash \mathscr{V}^\star$ with subsets of $\mathscr{X}_{rel} \backslash \mathscr{V}^\star$. In this subset there is no bounded controller that can keep the orbits inside Φ. One has either to apply an impulsive input that modifies instantaneously the vector field, or to introduce a collision mapping in the model. Algorithms that enable one to calculate the various above subspaces are provided in [322].

Remark 1.12 The whole presentation has been made in $\mathrm{Ker}(C) \subset \mathrm{bd}(\Phi)$. It is clear that if the system is to be analyzed on another part of $\mathrm{bd}(\Phi)$ then $\mathrm{Ker}(C)$ may be replaced by $\mathrm{Ker}(\tilde{C})$ where $\tilde{C}$ is a submatrix of C. The case of multiple constraints ($m \geq 2$ in (1.44)) is much more intricate. A discussion on how collision maps may be defined in such a case is made in [322, §VI], highlighting the difficulty which may arise if at the intersection of two boundaries (a codimension-two constraint boundary), one constraint is attained tangentially while the other one is attained transversally: this is exactly the kind of issues raised in multiple impact modelling when some contacts are lasting before a collision occurs at another contact point

(think of a chain of aligned balls like in Newton's cradle). As alluded to above, the theory applies also to a class of nonlinear affine-in-the-input systems, with smooth vector fields. Quite related material is available in [353].

The above geometric approach has been used to analyze quadratic optimal control under inequality state constraints in [208], in order to better understand the qualitative properties of junction states. A notion of controllability, known as the *control holdability*, may be stated for the unilaterally constrained system in (1.43) and (1.44). A subset Φ of the state space is said control holdable if there exists an input $u(\cdot)$ such that the system's solutions $x(t) = x(t; t_0, x_0, u)$ stay in Φ for all $x_0 \in \Phi$.

Proposition 1.4 *[322, Proposition 6.5.1] Let A, B and C in (1.43) and (1.44) be such that (A, B) is a controllable pair, $Im(B) \subseteq Ker(C)$, $C \neq 0$, $\Phi = \{x \in \mathbb{R}^n | Cx \geq 0\} \neq \emptyset$. Consider also bounded inputs, and $m = 1$. Then the admissible domain Φ is a controlled holdable set for the system (1.43) and (1.44) if and only if $\mathscr{X}_{con,v} \cup \mathscr{X}_{con,h} \cup \mathscr{V}_f = \emptyset$.*

Mechanical systems do not satisfy the conditions of this proposition when unilateral conditions on the position q are imposed [322, Corollaries 5.6.1, 6.5.11]. Then the addition of a velocity jump rule (an impact law) is necessary to render Φ invariant.

1.3.4 Bilaterally Constrained Mechanical Systems and Impulsive Dynamics

Let us consider mechanical systems with bilateral (equality) constraints $h(q) = 0$. After tangent linearization these systems may be embedded into descriptor variable systems $E\dot{x}(t) = Ax(t) + Bu(t)$, where the matrix E is singular and u is the control input. The solutions of these differential algebraic equations (DAE) possess a jump in the initial condition, i.e., in general $x(0^-)$ and $x(0^+)$ are not equal, due to nonadmissible initial conditions (which therefore have to jump to become compatible with the constraints). It is possible to decompose descriptor variable systems as [295, 296]

$$\dot{x}_s(t) = E_s x_s(t) + B_s u(t), \tag{1.56}$$

$$E_f \dot{x}_f = x_f + B_f u, \tag{1.57}$$

where E_f is a nilpotent matrix with index of nilpotency $p \geq 2$, i.e. $E_f^p = 0$. Then the solution can be written with some abuse of notation $x = x_s + x_f$, where:

$$x_s(t) = \exp(tE_s)x_{0s} + \exp(tE_s) \star B_s u, \tag{1.58}$$

$$x_f = -\sum_{i=1}^{p-1} \delta_0^{(i-1)} E_f^i x_{0f} - \sum_{i=0}^{p-1} E_f^i B_f u^{(i)}, \tag{1.59}$$

where $\star$ is the convolution product. Notice that $p = 1$ means $E_f = 0$ and $B_f = 0$ so that $x_f = 0$ and $x(\cdot) = x_s(\cdot)$ (see for instance [496, pp. 452–454]). We see that in general, x_f possesses a jump at $t = 0$ and $x_f(0^+) = -\sum_{i=0}^{p-1} E_f^i B_f u^{(i)}(0)$ provided that $u(\cdot)$ is sufficiently smooth. In the case of mechanical systems subject to holonomic constraints $h(q) = 0$, the initial conditions can be chosen in accordance with the constraint so that no impulsive behavior occurs. In fact, the only physically and practically sound initial inconsistency may be due to initial velocity pointing outwards the admissible domain Φ, because one cannot initialize the position outside Φ in practice: thus only Dirac measures may be involved in mechanics with constraints on the position. The point of view of singular systems is used in [850, 851] where a quite interesting and detailed application of the theory in [295, 296] to robotic systems with a linearized model of an n degree-of-freedom manipulator with kinematic constraints is proposed.

Remark 1.13 From (1.59) the solution is a distribution of degree p (derivatives of the Dirac measure), see [1214] for a survey on solution concepts for linear DAEs. It is interesting at this stage to think of system with switching bilateral constraints. At the switching instants, the constraints change, and the pre-switch state may not be compatible with the new constraint after the switch has occurred: a suitable state jump has to be incorporated in the model. This is true if the switches are exogenous [1215], or state-dependent [15]. See Remark 5.23 for more comments on switching DAEs.

1.4 Changes of Coordinates in MDEs

Let us investigate some tools which allow one to eliminate the impulsive effects from MDEs, transforming MDEs into ODEs or (ordinary) differential inclusions. We first consider ODEs with exogenous singular distributions in their right-hand side. Then we investigate the case of mechanical systems subject to a single unilateral constraint and impacts.

1.4.1 From Measure to Carathéodory Systems

Note that we could have proceeded in a different way to solve the dynamics of the system in Example 1.1, Eq. (1.2). Let us write the state space equations for this system

$$\begin{pmatrix} \dot{x}_1(t) \\ \dot{x}_2(t) \end{pmatrix} = \begin{pmatrix} x_2(t) \\ 0 \end{pmatrix} + \begin{pmatrix} 0 \\ \frac{p_k}{m} \dot{h}(t) \end{pmatrix}, \tag{1.60}$$

where $h(t) \equiv 0$ for $0 \leq t < t_k$, $h(t) \equiv 1$ for $t_k \leq t$, $x_1 = x$, $x_2 = \dot{x}$. Following the ideas in [397] on change of variables in differential equations with distributions in

coefficients, let us consider now $y = x_2 - \frac{p_k}{m}h$; then in the (x, y) coordinates (1.60) becomes:

$$\begin{pmatrix} \dot{x}_1(t) \\ \dot{y}(t) \end{pmatrix} = \begin{pmatrix} y(t) \\ 0 \end{pmatrix} + \begin{pmatrix} \frac{p_k}{m}h(t) \\ 0 \end{pmatrix}, \tag{1.61}$$

from which it follows that $y \equiv (t) = y(0) = y_0$ for all $t \geq 0$, $\dot{x}_1(t) = y_0 + \frac{p_k}{m}h(t)$. Thus $x_2(t) = \dot{x}(t) = \frac{p_k}{m}h(t) + y_0$ and we retrieve the preceding results, i.e., the velocity $\dot{x}(\cdot)$ is discontinuous at t_k.
Still following [397] we can proceed as above to draw conclusions about existence and uniqueness of solutions. Notice that we can write (1.10) as follows:

$$\begin{cases} \dot{x}_1(t) = x_2(t) \\ \dot{x}_2(t) = a(x_1(t), x_2(t), t) + b(x_1(t))\dot{h}(t), \end{cases} \tag{1.62}$$

where $a(\cdot, \cdot, \cdot)$ and $b(\cdot)$ have obvious definitions, $h(\cdot)$ is as in (1.60). Now take $y_2 = x_2 - b(x_1)h$, then (1.62) becomes:

$$\begin{cases} \dot{x}_1(t) = y_2(t) + b(x_1(t))h(t) \\ \dot{y}_2(t) = a(x_1(t), y_2(t), t) - \frac{\partial b}{\partial x_1}(x_1(t))\,(y_2(t) + b(x_1(t))h(t))\,h(t). \end{cases} \tag{1.63}$$

The ODE in (1.63) satisfies the Carathéodory conditions on existence and uniqueness of solutions. Recall that considering (1.63) it is possible to assign an initial arbitrary value to y_2 at discontinuities of $h(t)$, but since $x_2(t) = y_2(t) + b(x_1(t))h(t)$, this is not possible for x_2 as $h(t)$ is not defined at those times. Only left and right limits can be assigned to $x_2(t)$. If we write (1.63) compactly as $\dot{z}(t) = g(z(t), t)$ then in a domain S of the (t, x)-space:

- The function $g(z, t)$ is defined and continuous in z for almost all t.
- The function $g(z, t)$ is Lebesgue measurable in t for each z.
- $|g(z, t)| \leq m(t)$ for some measurable function $m(t)$.

Thus there exists a maximal solution $z(t)$ to the system in (1.63) and this solution is a time-continuous function [397, Chap. 1]. Therefore assuming the control input u has been suitably designed, there is no finite escape time in the system, x_1 and y_2 are continuous, and x_2 jumps at the instant of the percussion. Thus clearly such mechanical systems excited by impulses belong to the class of systems with singular distributions in coefficients that can be reduced to a Carathéodory (ordinary) system by a change in the unknown function (see [397] for other examples of such manipulations).

Remark 1.14 The above change of coordinates that allows us to transform a MDE into a Carathéodory ODE is quite similar to generalized state vector transformations in linear systems theory [638], which allow to write a state space representation without derivatives of the input $u(t)$, for systems with polynomial representation $A(D)y(t) = B(D)u(t)$, with $D \stackrel{\Delta}{=} \frac{d}{dt}$, $A(D)$ and $B(D)$ are polynomials of D, with orders n and m, respectively. Such transformations are of the form $z = My_e + M_u u$,

where $y_e = (y, \dot{y}, \ddot{y}, \ldots, y^{(n-1)})^T$, M and M_u are constant matrices of suitable dimensions. It is clear that if a discontinuous control $u(t)$ is applied, then $B(D)u(t)$ contains the Dirac distribution and its derivatives up to order $m-1$. In a suitable state space representation (controllable canonical form for instance) such singular terms are absent.

Let us come back on a simple nonlinear system as in (1.22), with $f(\cdot)$ and $g(\cdot)$ smooth functions of x. Let us prove that there exists a change of coordinates of the form $z = Z(x, u)$ such that at least locally the system becomes in new coordinates $\dot{z}(t) = h(z(t), u(t))$. Indeed one gets (time argument is dropped):

$$\dot{z}(t) = \frac{\partial Z}{\partial x}\dot{x}(t) + \frac{\partial Z}{\partial u}\dot{u}(t) = \frac{\partial Z}{\partial x}[f(x(t)) + g(x(t))\dot{u}(t)] + \frac{\partial Z}{\partial u}\dot{u}(t). \tag{1.64}$$

A sufficient condition for the transformed system to be in the required form is thus that:

$$\frac{\partial Z}{\partial x}g(x) = -\frac{\partial Z}{\partial u}. \tag{1.65}$$

If we can express $x = X(z, u)$, i.e. we can invert the coordinate change, then we get $\frac{\partial Z}{\partial x}f(x) = h(z, u)$. Now let us search for a solution to (1.65) of the form $Z(x, u) = a(x)b(u)$. We obtain:

$$\frac{da}{dx}b(u)g(x) = -a(x)\frac{db}{du}, \tag{1.66}$$

which we can rewrite as:

$$\frac{1}{a(x)}\frac{da}{dx}g(x) = -\frac{1}{b(u)}\frac{db}{du}. \tag{1.67}$$

Now note that since each side of the equality must be verified for all x and u, and since the left-hand side is a function of x while the right-hand side is a function of u, both sides must be equal to the same constant value. Therefore we can search for $a(x)$ and $b(u)$ such that[25]:

$$\frac{da}{dx} = -\frac{a(x)}{g(x)}, \tag{1.68}$$

$$\frac{db}{du} = b(u), \tag{1.69}$$

provided $g(x)$ does not go through zero, which is necessary for the controllability of the system. Suppose that the two ODEs in (1.68) and (1.69) possess solutions $a(x)$ and $b(u)$ for any initial conditions $x(0)$ and $u(0)$. Then $Z(x, u) = a(x)b(u)$ satisfies (1.65) and (1.64) is $\dot{z}(t) = \frac{\partial Z}{\partial x}f(x(t))$. Note however that the resulting system may not be linear in the control input u. As an example, let us consider the system:

[25]The signs in (1.68) and (1.69) can be reversed.

$$\dot{x}(t) = \sin(x(t)) - \cos(x(t))\dot{u}(t), \tag{1.70}$$

(this is inspired from a cart-pendulum system whose complete dynamical equations are of higher order, but with the same nonlinearities). Then the coordinate change $z = |\tan(\frac{x}{2} + \frac{\pi}{4})| \exp(u)$ defined on $\left(-\frac{3\pi}{2}, \frac{\pi}{2}\right)$ transforms the system (1.70) into:

$$\dot{z}(t) = \frac{z(t)^2 \exp(-u(t)) - \exp(u(t))}{2}. \tag{1.71}$$

Notice that the fixed point of (1.70) is given when $u \equiv 0$ by $x^\star = 0$ and corresponds for (1.71) to $z^\star = 1$. However it is possible that other changes of coordinates yield a system linear in the input. Notice that if $Z(x, u)$ is continuous, then since $z(t)$ is continuous the jumps of $u(t)$ must be "compensated" for in $Z(x, u)$. This is therefore a way to compute the jumps of $x(t)$ at times of discontinuities of $u(t)$: $Z(x(t^+), u(t^+)) = Z(x(t^-), u(t^-))$ since $z(t^+) = z(t^-)$.

Remark 1.15 This method does not apply to systems with unilateral constraints and impacts. First, the impact times and hence $h(\cdot)$ are not known in advance. Second, the complementarity conditions cannot be eliminated, rendering the transformed system intrinsically set-valued.

1.4.2 Decoupling of the Impulsive Effects (Commutativity Conditions)

Let us focus on measure driven systems as (1.22) or (1.23). Notions of solutions have been described in Sect. 1.2.2. In some particular cases it is however possible to transform such MDEs into ODEs.

Proposition 1.5 *Consider the MDE*

$$\dot{x}(t) = f(x(t)) + \sum_{i=1}^{m} g_i(x(t))\dot{u}_i(t), \;\; x(0) = x_0, u(0) = u_0, \tag{1.72}$$

with $x \in \mathbb{R}^n$, and $u_i \in RCLBV$, $1 \leq i \leq m$. If the vector fields $g_i(x)$ are continuously differentiable, linearly independent, and if their Lie brackets satisfy $[g_i, g_j] = 0$ for all $i, j \in \{1, \ldots, m\}$ $i \neq j$, then the system in (1.72) can be locally transformed into an MDE as (1.15).

Proof First of all, let us recall that the Lie bracket of two vector fields is given by $[g_i, g_j] = \frac{\partial g_j}{\partial x} g_i - \frac{\partial g_i}{\partial x} g_j$. Now from the conditions of Proposition 1.5 (one says that the vector fields $g_i(x)$ are *commutative*: starting from an initial condition, the flows of

g_i and of g_j may be applied in any order to attain the same state.) and [930 Theorem 2.36], it follows that in suitable coordinates $z \in \mathbb{R}^n$ one has $g_i = \frac{\partial}{\partial z_i}$, $i \in \{1, \ldots, m\}$ (this is a kind of simultaneous rectification of m vector fields *via* a suitable rectifying diffeomorphism [49], see also [497, pp. 186–187] for an accessible proof of existence of this diffeomorphism in the planar case). Notice that continuous differentiability of the g_i's implies that the trajectories of the systems $\dot{x}(t) = g_i(x(t))$ have a well-defined tangent at each $x(t)$, which is an important point for the application of the flow-box (rectification) theorem. Hence locally in the new coordinates one has:

$$\dot{z}(t) = \bar{f}(z(t)) + \sum_{i=1}^{m} \varepsilon_i \dot{u}_i(t), \tag{1.73}$$

where $\varepsilon_i \in \mathbb{R}^m$ is the ith coordinate vector (in fact we could denote ε_i as $\frac{\partial}{\partial z_i}$ or ∂_i). It appears clearly from (1.73) that the coordinate change performs a sort of decoupling so that the problems mentioned in Sect. 1.2.2 disappear since one gets an MDE as in (1.15) with constant $G(t)$. Notice, however, that this result is true locally (in the state) only, and the jumps induced by $u(\cdot)$ should therefore be small enough.

One may go a step further by suppressing $\dot{u}(\cdot)$ in the dynamics. MDEs as in (1.72) with vector fields $g_i(x, u)$) are studied in [189]. The system is first augmented with m integrators $\dot{z}(t) = \dot{u}(t), z(0) = u_0$. The new input vector fields $\tilde{g}_i(x) \stackrel{\Delta}{=} [g_i(x), \varepsilon_i] \in \mathbb{R}^{n+m}$ are assumed to commute. Let us introduce the map $\varphi = (\varphi^1, \cdots, \varphi^n)$ as:

$$\varphi^j(x, u) = \pi_j \circ \exp\left(-\sum_{i=1}^{m} u_i \tilde{g}_i\right)(x, u), \tag{1.74}$$

where $\pi_j(\cdot)$ denotes the jth projection of $\mathbb{R}^{n+m}$ and $\varphi(\cdot, -u) = \varphi^{-1}(\cdot, u)$. Consider the diffeomorphism $\bar{\varphi}(x, u) = (\varphi(x, u), u)$. Then the following is true:

Lemma 1.2 *[189] For each $i = 1, \ldots, m$ and for every $(x, u) \in \mathbb{R}^{n+m}$, one has*

$$\nabla_{(x,u)} \bar{\varphi}^T \tilde{g}_i(x, u) = \varepsilon_{n+i}. \tag{1.75}$$

Thus $\bar{\varphi}(x, u) = (\varphi(x, u), u)$ transforms the augmented vector fields given by $\tilde{f}(x) = (f(x), 0, \ldots, 0)^T$ and $\tilde{g}_i(\cdot)$, $1 \leq i \leq m$, into $(F, 0)$ and ε_{n+i} respectively. Hence there are new coordinates $(\xi, \eta) = \bar{\varphi}(x, u) \in \mathbb{R}^{n+m}$ in which the system in (1.72) takes the form $\dot{\xi}(t) = F(\xi(t), \eta(t)), \dot{\eta}(t) = \dot{u}(t), \xi(0) = \varphi(x_0, u_0)$ [189, Corollary 2.1]. This is further used in [189, Theorem 2.1] to prove the continuous dependence of the solutions on $u(\cdot)$. We see that the measure part of the system is put in $\dot{\eta}(t) = \dot{u}(t)$ while the $\xi-$dynamics is an ODE with a possibly discontinuous "input" $\eta(\cdot)$.

Remark 1.16 (*Mechanical Systems*) In case of a Lagrangian system as in (1.10) subject to exogenous impulsive force inputs, the vector fields $g_i(x)$ possess the

required smoothness and are functions of q only. They have the form $g_i(x) = \begin{pmatrix} 0 \\ ** \end{pmatrix}$, whereas $\frac{\partial g_i}{\partial x} = \left(\frac{\partial g_i}{\partial q}, 0\right)$. Hence the Lie brackets $[g_i, g_j] = 0$. Since the $g_i(x)$ are time-continuous, Proposition 1.5 applies in any neighborhood of $q(t)$ such that $g_i(q(t)) \neq 0$. This does not mean that collisions may be erased from mechanical systems (see the introduction of the next section for an illustration of this fact). Also the rectifying diffeomorphism is a generalized coordinate change, since the vector fields $g_i(q)$ do not depend on $\dot{q}$. It is noteworthy that the above state space change does not stem from a generalized coordinate transformation, and transforms the system in an extended state space with dimension $n + m$.

The commutativity conditions are sufficient conditions for existence and uniqueness of solutions, they are not necessary. Moreover they may not be robust with respect to uncertainties in the vector fields, and thus may not be interesting for control purpose. As we saw in Sect. 1.2.2 we can dispense with them.

1.4.3 *From Unilaterally Constrained Mechanical Systems to Filippov's Differential Inclusions: the Zhuravlev–Ivanov Method*

The transformations of the foregoing sections are not well suited to systems with unilateral constraints and impacts. As an example let us study the one-degree-of-freedom complementarity system $m\ddot{q}(t) = F(t) + \lambda, 0 \leq q(t) \perp \lambda(t) \geq 0, \dot{q}(t_k^+) = -e_n\dot{q}(t_k^-)$, $q(t_k) = 0, \dot{q}(t_k^-) < 0, q(0) = q_0, \dot{q}(0^-) = \dot{q}_0$. This is a particle with a unilateral constraint, and the complementarity condition is introduced in the model for the same reasons as for the cable-mass system of Example 1.6. Let us define $\xi_1(t) = \int_0^t q(s)ds$, $\xi_2(t) = q(t), \xi_2(0) = q_0, \eta(0) = m\dot{q}_0$. Then we can rewrite the dynamics as $\dot{\xi}_1(t) = \xi_2(t), \dot{\xi}_2(t) = \int_0^t \frac{F(s)}{m}ds + \frac{1}{m}\eta(t), \dot{\eta}(t) = \lambda, 0 \leq \lambda \perp \xi_2(t) \geq 0$, $\dot{\xi}_2(t_k^+) = -e_n\dot{\xi}_2(t_k^-), \xi_2(t_k) = 0, \dot{\xi}_2(t_k^-) < 0$. Since the complementarity conditions cannot be eliminated using such an approach, and following the developments made in Example 1.6, we have $\lambda(t) \in -N_{\mathbb{R}^+}(\xi_2(t))$ outside impacts. The complementarity system is thus found equivalent to a specific differential inclusion $\dot{\xi}_1(t) = \xi_2(t)$, $\dot{\xi}_2(t) = \int_0^t \frac{F(s)}{m}ds + \frac{1}{m}\eta(t), \dot{\eta}(t) \in -N_{\mathbb{R}^+}(\xi_2(t))$ outside impacts, and $\dot{\xi}_2(t_k^+) = -e_n\dot{\xi}_2(t_k^-), \xi_2(t_k) = 0, \dot{\xi}_2(t_k^-) < 0$. We retrieve once again the fact that unilaterally constrained systems may live on lower dimensional subspaces, and that impact times are state-dependent.

A quite different approach which allows one to eliminate impulsive forces from the dynamical equations of mechanical systems with unilateral constraints has been proposed in [1336, 1337, 1338, 1339], and extended in [585, 596] for the analytical study of vibro-impact systems. Let us first describe the pioneering work of Zhuravlev [1338]. An n-degree-of-freedom system with generalized coordinates $q = (q_1, \cdots, q_n)^T$, Lagrangian function $L(t, q, \dot{q}) = T(q, \dot{q}) - U(t, q)$ and a

codimension one constraint $f(q) = q_1 \geq 0$ is considered. The Routh's function $R(\cdot)$ is introduced, as[26]:

$$R(p, q, \dot{q}) = L(q, \dot{q}, t) - p^T \dot{y}, \tag{1.76}$$

where $y \stackrel{\Delta}{=} (q_2, \cdots, q_n)^T$, and $p = \frac{\partial L}{\partial \dot{y}}$ is the $(n-1)-$ vector of generalized momenta (the quantities $\frac{\partial L}{\partial \dot{q}_i}$, $2 \leq i \leq n$, are the generalized momenta associated to velocities $\dot{q}_i$). Then the nonsmooth transformation

$$q_1 = |s| \tag{1.77}$$

is introduced. From (1.77) we see that the basic idea is first to consider q_1 as if it was a cyclic variable and apply Routh's method, second to consider the "mirror" system such that on $[t_{2k}, t_{2k+1}]$ the fictitious trajectory $s(t)$ is symmetrical to the actual one $q_1(t)$ with respect to the origin (the first impact occurs at t_0). Notice at once that since $q_1(t_k) = s(t_k) = 0$, we obtain $\dot{q}_1 = \frac{d}{dt}\{s \ \mathrm{sgn}(s)\} + \sum_{k\geq 0} \sigma_s \ \mathrm{sgn}_{(s)}(t_k)\delta_{t_k} = \dot{s} \ \mathrm{sgn}(s)$. The inertia matrix is partitioned as $M(q) = \begin{bmatrix} a(q) & b(q)^T \\ b(q) & A(q)^{-1} \end{bmatrix} \succ 0$, and $R_0 \stackrel{\Delta}{=} \frac{1}{2}\left(a - b^T A b\right)\dot{s}^2 - \frac{1}{2}p^T A p + U(t, q)$, where $a(q) - b(q)^T A(q) b(q) > 0$ by the Schur complement positivity. Then $p = \dot{s} b(q) + A(q)^{-1}\dot{y}$, $\dot{y} = A(q)(p - \dot{s} b(q))$, and the Routh's function is $R(p, q, \dot{q}) = R_0 + \dot{s} p^T A(q) b(q) \mathrm{sgn}(s)$. The dynamical equations are $\frac{d}{dt}\frac{\partial R}{\partial \dot{s}} - \frac{\partial R}{\partial s} = S$, $\dot{y} = -\frac{\partial R}{\partial p}$, $\dot{p} = \frac{\partial R}{\partial y} + Y$, where $S \in \mathbb{R}$ and $Y \in \mathbb{R}^{n-1}$ are the generalized forces performing work on q_1 and y, respectively. The term $\dot{s} p^T A(q) b(q) \mathrm{sgn}(s)$ in $R(p, q, \dot{q})$ is treated as follows: $\frac{\partial}{\partial \dot{s}}(\dot{s} p^T A(q) b(a) \mathrm{sgn}(s)) = p^T A(q) b(a) \mathrm{sgn}(s)$, thus $\frac{d}{dt}\frac{\partial}{\partial \dot{s}}(\dot{s} p^T A(q) b(q) \mathrm{sgn}(s)) = \frac{d}{dt}(p^T A(q) b(q)) \mathrm{sgn}(s) + p^T A(q) b(q) \dot{s} \frac{\partial}{\partial s}(\mathrm{sgn}(s))$. The second term stemming from $-\frac{\partial R}{\partial s}$ is $-\frac{\partial}{\partial s}(\dot{s} p^T A(q) b(q) \mathrm{sgn}(s))$ and after some calculations we find $-\dot{s} p^T \frac{\partial (A(q) b(q))}{\partial s} \mathrm{sgn}(s) - \dot{s} p^T A(q) b(q) \frac{\partial}{\partial s}(\mathrm{sgn}(s))$. Therefore

$$\left(\frac{d}{dt}\frac{\partial}{\partial \dot{s}} - \frac{\partial}{\partial s}\right)(\dot{s} p^T A(q) b(q) \mathrm{sgn}(s)) = \left(\frac{d}{dt}(p^T A(q) b(q)) - \dot{s} p^T \frac{\partial (A(q) b(q))}{\partial s}\right) \mathrm{sgn}(s).$$

From these calculations we deduce that in the coordinates $(s, q_2, \cdots, q_n)$, the dynamics becomes:

[26] The Routh's function is usually introduced for n-degree-of-freedom systems that possess n_c cyclic coordinates [1178] [845, §3.3] (i.e., coordinates $q_1, \cdots, q_{n_c}$ that do not appear in the Lagrangian function L or in the Hamiltonian function H). Every cyclic coordinate yields a first integral of the system since the corresponding momenta $p_1, \cdots, p_{n_c}$ are invariant. Routh's method consists of applying a Legendre transformation only in the coordinates $q_1, \cdots, q_{n_c}$, i.e., the Routh's function is equal to $R = L - \sum_{i=1}^{n_c} p_i \dot{q}_i$. Comparing this formula with (1.76) one sees that the unconstrained coordinates play the role of the cyclic coordinates. The interest of the Routh's function is that it plays the role of a Hamiltonian function for the cyclic coordinates, i.e., $\dot{p}_i = -\frac{\partial R}{\partial q_i}$ and $\dot{q}_i = \frac{\partial R}{\partial p_i}$.

$$\frac{d}{dt}\frac{\partial R_0}{\partial \dot{s}} - \frac{\partial R_0}{\partial s} \in \left[S(t) - \frac{d}{dt}\left(p^T Ab\right) + \dot{s}\, p^T \frac{\partial Ab}{\partial s} \right] \operatorname{sgn}(s), \tag{1.78}$$

$$\begin{cases} \dot{y}(t) \in -\frac{\partial R_0}{\partial p}(t) - \dot{s}(q)A(t)b(q)\ \operatorname{sgn}(s(t)) \\ \\ \dot{p}(t) \in \frac{\partial R_0}{\partial y}(t) + \dot{s}(t)\frac{\partial (p^T Ab)}{\partial y}\ \operatorname{sgn}(s(t)) + Y(t). \end{cases} \tag{1.79}$$

Zhuravlev uses the Routh's function as a descriptive function to write down the dynamics precisely because it allows one to avoid the impulses in the final equations, a goal that could not be reached with Lagrangian or Hamiltonian functions. Note that the dynamics in (1.78) has a Lagrangian form, whereas the one in (1.79) has a Hamiltonian form. From (1.78) and (1.79) the dynamical equations may be embedded into Filippov's differential inclusions, consequently the state of the transformed system is absolutely continuous, which implies that both $s(\cdot)$ and $\dot{s}(\cdot)$ are continuous. However $\ddot{s}(\cdot)$ may have discontinuities. Since $\dot{q}_1 = \dot{s}\operatorname{sgn}(s)$, at a shock instant $\dot{q}_1(t_k^-) = \dot{s}(t_k)$ and $\dot{q}_1(t_k^+) = -\dot{s}(t_k)$, as long as $s(t_k) = 0$ and the trajectories cross the "surface" $s = 0$ at $t = t_k$. Therefore $\dot{q}_1(t_k^+) = -\dot{q}_1(t_k^-)$, $\dot{q}_1(t_k^+)^2 = \dot{q}_1(t_k^-)^2$, and from the fact that the momenta p_i, $2 \le i \le n$, are time-continuous (this is easily proved from the Lagrange dynamics and the form of the gradient $\nabla f(q) = (1, 0, \ldots, 0)^T \in \mathbb{R}^n$), it is possible to show that the total energy is conserved at impacts. The acceleration is a measure $\ddot{q}_1 = \{\ddot{q}_1(t)\}dt + \sum_{k\in\mathbb{N}} \sigma_{\dot{s}\operatorname{sgn}(s)}(t_k)\delta_{t_k}$, where the velocity jumps $\sigma_{\dot{s}\operatorname{sgn}}(s)(t_k) = \sigma_{\dot{q}_1}(t_k)$.

Example 1.10 Let us consider the classical example of a linear oscillator constrained by a rigid obstacle. The dynamical equations are given by

$$\ddot{q}(t) + \lambda_2 q(t) = A\sin(\omega t), \quad f(q(t)) = q(t) \ge 0. \tag{1.80}$$

Applying the proposed method (in this case the variable y does not exist since all the coordinates are unilaterally constrained) we get from (1.78):

$$\ddot{s}(t) + \lambda_2 s(t) \in A\sin(\omega t)\ \operatorname{sgn}(s(t)), \quad s(0) = s_0. \tag{1.81}$$

Indeed in this case $\frac{\partial R_0}{\partial \dot{s}} = \dot{s}$. Existence of solutions for any s_0 follows from [1120, Theorem 4.7], noting in particular that the set-valued right-hand side takes compact convex values for each t.

Example 1.11 As a second example we consider the bouncing ball dynamics: $m\ddot{q}(t) = -mg$, $q(t) \ge 0$, $t \ge 0$, $\dot{q}(t_k^+) = -\dot{q}(t_k^-)$, $q(t_k) = 0$, $\dot{q}(t_k^-) < 0$. The transformation yields $m\ddot{s}(t) \in -mg\operatorname{sgn}(s(t))$. Let $s(0) = s_0 > 0$ and $\dot{s}(0) = \dot{s}_0 = 0$. Then $\dot{s}^2 + 2gs - 2gs_0 = 0$ until the axis $s = 0$ is reached at time $t_0 = \sqrt{\frac{2s_0}{g}}$ with $\dot{s}(t_0) = -\sqrt{2gs_0}$. After t_0 the trajectories enter the left half plane $s < 0$ and $s = \sqrt{2s_0}\frac{\dot{s}-\sqrt{2gs_0}}{\sqrt{g}} + \frac{(\dot{s}-\sqrt{2gs_0})^2}{2g}$. At $t = 2\sqrt{\frac{2s_0}{g}}$ we have $\dot{s}(t) = 0$ and $s(t) = -s_0$ and

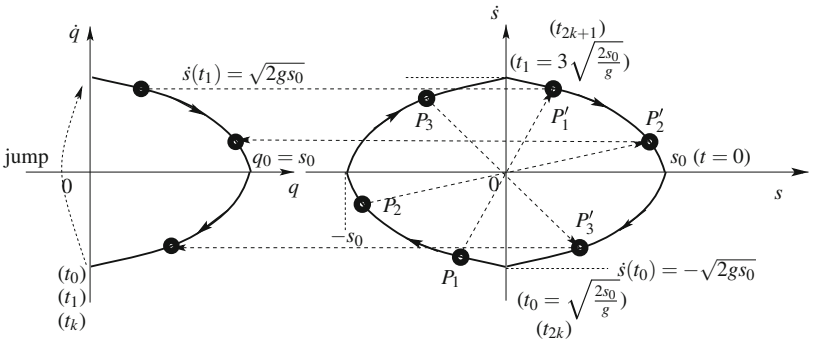

Fig. 1.5 The $(q, \dot{q})$ and the $(s, \dot{s})$ phase portraits

at $t_1 = 3\sqrt{\frac{2s_0}{g}}$ we have $\dot{s}(t_1) = \sqrt{2gs_0}$ and $s(t_1) = 0$. This is depicted in Fig. 1.5 where the correspondance between the transformed and the original trajectories are shown.

Ivanov [585] extends the method to non-purely elastic shocks. He first considers the one-degree-of-freedom system

$$\begin{cases} \ddot{x}(t) = f(t, x(t), \dot{x}(t)) & \text{if } x(t) \geq 0 \\ \ddot{x}(t) = \max(0, f(x(t), \dot{x}(t), t)) & \text{if } \dot{x}(t_k^+) = 0 \text{ and } x(t_k) = 0 \\ \dot{x}(t_k^+) = -e_{\mathrm{n}}\dot{x}(t_k^-) & \text{if } \dot{x}(t_k^-) < 0 \text{ and } x(t_k) = 0, \end{cases} \tag{1.82}$$

where $x(t) \in \mathbb{R}$. As we shall see in Chap. 4, the last algebraic equation in (1.82) is a *restitution law*, and e_{n} is a kinematic restitution coefficient. Getting back to (1.46), this gives $J_k(\dot{x}(t_k^-)) = -(1 + e_{\mathrm{n}})\dot{x}(t_k^-)$. Actually such way of writing the dynamics could be equivalently formulated with a Lagrange multiplier modeling the contact force and complementarity conditions as $0 \leq x(t) \perp \lambda(t) \geq 0$, that we shall decribe in detail in Chaps. 2 and 5. The nonsmooth coordinates change is given by:

$$\begin{cases} x = |s| & \dot{x} = R\nu\mathrm{sgn}(s) \\ R = 1 - k\mathrm{sgn}(s\nu),\ k = \frac{1-e_{\mathrm{n}}}{1+e_{\mathrm{n}}}. \end{cases} \tag{1.83}$$

Using (1.83), it can be shown that (1.82) is transformed into the differential inclusion:

$$\begin{cases} \dot{s}(t) = R\nu(t) \\ \dot{\nu}(t) = R^{-1}\mathrm{sgn}(s(t))\, f(t, |s(t)|, R\nu(t)\ \mathrm{sgn}(s(t))). \end{cases} \tag{1.84}$$

The trajectories of (1.84) may be understood in the sense of Filippov [397], and are absolutely continuous.[27] At the origin $(s, v) = (0, 0)$, the transformed system is defined as $\dot{s} = 0$, $\dot{v} = (1 - k)^{-1} \max(0, f(t, 0, 0))$. From $x = |s| = s\ \mathrm{sgn}(s)$ one deduces that $\dot{x} = \frac{d}{dt}\{s(t)\ \mathrm{sgn}(s(t))\} + \sigma_x(t_j)\delta_{t_j}$, where t_j denotes generically an instant such that the sign of $s(t)$ changes. From the fact that $\sigma_x(t_j) = s(t_j^+)\ \mathrm{sgn}(s(t_j^+)) - s(t_j^-)\ \mathrm{sgn}(s(t_j^-))$ and since $s(t)$ is continuous (because we know that $x(t)$ is), it follows that $\dot{x} = \dot{s}\ \mathrm{sgn}(s) = Rv\ \mathrm{sgn}(s)$ by (1.83). Hence the first equation is as in (1.84). Concerning the acceleration, one gets $\ddot{x} = f(t, x, \dot{x}) + \sigma_{\dot{x}}(t_k)\delta_{t_k} = \frac{d}{dt}\{Rv\ \mathrm{sgn}(s)\} + \sigma_{Rv\,\mathrm{sgn}(s)}(t_j)\delta_{t_j}$, where t_j denotes generically an instant where $\dot{x} = Rv\mathrm{sgn}(s)$ maybe discontinuous: inspection of (1.83) shows that this can occur when $s(t)$ or $v(t)$ crosses zero. If $v(t_j) = 0$, then it is clear that $\sigma_{\dot{x}}(t_j) = 0$. Hence $\ddot{x} = R\dot{v}\ \mathrm{sgn}(s)$ so that $\dot{v}$ is given by the second equation in (1.84). But if the trajectory intersects the v-axis with $v \neq 0$, then the change of sign is due to s and $\sigma_{\dot{x}}(t_j) = 2v(t_j)\ \mathrm{sgn}(s(t_j^+)) = \sigma_{\dot{x}}(t_k)$, where t_k and t_j coincide. Hence starting from the transformed system in (1.84), we retrieve the fact that if the (s, v)-trajectory crosses the s-axis, no impact occurs. If it crosses the v-axis, then this occurs when $s = 0$ (i.e. $x = 0$, the constraint is attained), and an impact takes place since $\sigma_{\dot{x}} \neq 0$ from (1.83).

Remark 1.17 In the case $e_n = 1$, the Zhuravlev–Ivanov coordinate change has also been used in [466] to analyze motions with impacts *via* variational formulations and d'Alembert's principle. It is extended to $e_n \in (0, 1]$, but considering another change of variables: $x = -s$ if $s < 0$ and $x = e_n s$ if $s \geq 0$. Examples are shown on billiards, impacts of a particle against an inclined wall.
From (1.83) one sees that for plastic impacts ($e_n = 0$) the transformation is not well defined, since $R = 0$ when $sv > 0$. Then a trajectory that attains the $s = 0$ axis instantaneously reaches the equilibrium point $(s, v) = (0, 0)$. Whatever the coordinate change may be, this fact is invariant since for a plastic impact, the equilibrium (rest) position is attained immediately after the impact, which corresponds in the (s, v)-plane to intersecting $s = 0$. In addition $(s, v) = (0, 0)$ implies $(x, \dot{x}) = (0, 0)$ and $x = 0$ implies $s = 0$; now note that at $s = x = 0$, $\dot{x}$ is not defined, but the right and left limits when $s \to 0$, $s > 0$ or $s < 0$, respectively, are defined. We retrieve here the discontinuity in the velocity at impact times. Uniqueness of solutions of (1.84) fails if $s(\tau_0) = v(\tau_0) = 0$.

Remark 1.18 It is possible to deduce q_0 from s_0, but not the inverse. Thus the Zhuravlev–Ivanov nonsmooth coordinate change should be seen as a way to design the "standard" differential inclusions (1.79) or (1.84), and then recover the original dynamics.

In fact the basic idea behind the coordinate change in (1.83) is to find out a function $F(s, v)$ such that:

[27] If the function $f(\cdot)$ is nonlinear in its third argument, Filippov's convexification and other frameworks like Utkin's equivalent control method for discontinuous ODEs may not be equivalent, however.

$$\begin{cases} F(0^+, \nu) = -e_{\mathrm{n}} F(0^-, \nu) \text{ for } \nu > 0 \\ \\ F(0^-, \nu) = -e_{\mathrm{n}} F(0^+, \nu) \text{ for } \nu < 0. \end{cases} \tag{1.85}$$

Then the coordinate change is defined as $x = |s|$ and $\dot{x} = F(s, \nu)$. It is possible to define other transformations, discontinuous in $s = 0$ only. Such another possible function $F(s, \nu)$ is given by [585]:

$$F(s, \nu) = \left[1 - 2\frac{R}{\pi} \arctan\left(\frac{\nu}{s}\right) \right] \nu \ \mathrm{sgn}(s). \tag{1.86}$$

Then the transformed system vector field has discontinuities only on the axis $s = 0$.

1.4.3.1 Additional Comments and Studies

Let us note that contrary to the method presented in Sect. 1.4.1 (see (1.63)), the "impact function" $h(t)$ does not appear in this coordinate change, so that no time-dependence is added to the transformed system. This is at the price however of obtaining a state-discontinuous vector field in (1.84), the surface of discontinuity corresponding to the surface of constraint $x = 0$. Therefore the form in (1.84) is much more suited for such analysis: some local stability analyses based on linearization are led in [585]. Smooth [397] or nonsmooth [1106] generalized Lyapunov functions could also be used in this setting. Ivanov [585] studies singular points, stability of equilibria, stability of periodic motions and bifurcations in vibro-impact systems using this setting. The techniques can be extended to n-dimensional systems with a single constraint, and Coulomb's friction can be considered. The work in [467] has been inspired by Zhuravlev [1338] to study the motion of a simple mechanical system with clearance and impacting *via* a nonsmooth coordinate change, and an averaging method to study periodic motions. Analytical, numerical, and experimental results are presented in [467] and are in accordance. The finite-time stabilization of a one-degree-of-freedom mechanical system with a unilateral constraint and impacts, is studied in [950] using the Zhuravlev–Ivanov transformation (see Sect. 7.5.5 for details). The dynamics of ships colliding ice barriers is analyzed in [476] using the Zhuravlev-Ivanov transformation.

The nonsmooth Zhuravlev–Ivanov coordinate change is limited to constraints of codimension one (several constraints may be considered, but then the variable change is valid locally only in the neighborhood of one of the constraints). An important particular case when several constraints may be considered is when the constraints surfaces are mutually orthogonal in the kinetic metric (see Chap. 6).

Chapter 2
Viscoelastic Contact/Impact Rheological Models

The first part of this chapter is dedicated to the analysis of viscoelastic and viscoelasto-plastic rheological contact models (linear and nonlinear parallel spring-dashpot assemblies). The linear spring-dashpot model is studied, and a detailed survey of nonlinear models (like Simon-Hunt-Crossley model and its many variations) as well as other types of assemblies with dry friction elements is made. Emphasis is put on the model's well-posedness, where complementarity systems may be used as a nice mathematical framework. The second part presents some well-posedness results (existence and uniqueness of solutions) of Lagrange dynamics with unilateral constraints and impacts, considering them as the limit of compliant systems when contact stiffness grows unbounded.

Bodies that collide possess a certain compliance and deform during an impact (locally around the contact point, and globally due to vibrations in the bodies). The collision duration is strictly positive.[1] Vibrations may even play in some cases a more important role than the local deformations. Consequently, rigid body dynamics may be considered as a limit case only, which however does not at all preclude its practical as well as theoretical utility. Moreover, the very short collision durations allow one to safely work with two time-scales in many practical cases. Historically, it has very often been difficult for certain scientists to accept the idea of perfect rigidity [1307]. For instance, Leibniz himself [721, 722] (and Bernoulli after him [134]) refused this idea because rigidity yields violation of the "law of continuity" in nature. A strong scientific debate motivated by the London Royal Society in 1668 also concerned the concept of "hardness" (which is to be understood as rigidity in this context): is a hard body able to rebound? Or is it necessary that the bodies possess some "springiness"? Wallis and Mariotte concluded that springs are necessary, while Huygens, Wren, and Malebranche thought that hardness is sufficient [1307]. We know now the difference between a model of nature and nature itself. We also have many more mathematical

[1] However, in many practical cases it is very short: 4.10^{-4} s for a shock between a golf ball and a flat-nosed wooden projectile with a relative speed of 5.334 m/s [196], other authors report values between 7.10^{-4} and 5.10^{-4} s for pre-impact velocities between 10 and 60 m/s [55]; see other values of the same order in Sect. 4.3.10 for slender rods against a massive steel table.

B. Brogliato, *Nonsmooth Mechanics*, Communications and Control Engineering,
DOI 10.1007/978-3-319-28664-8_2

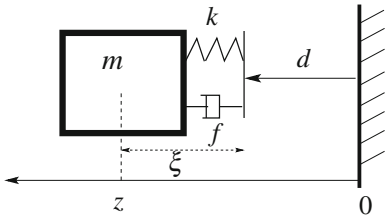

Fig. 2.1 Linear spring/dashpot contact-impact model

tools at our disposal to accept perfect rigidity and to study accurately the relationship between compliant and rigid models.[2]

2.1 Simple Examples

This section is dedicated to the analysis of the simplest compliant contact model: parallel linear spring-dashpot assemblies. Several of their properties are studied: convergence when parameters tend to infinity (rigid body limit), equivalent restitution coefficient, complementarity formalism, well-posedness of simple dynamics incoportating such piecewise-linear models. The considered models possess a mathematical interest where they may be used for existence/uniqueness of solutions proofs, as illustrated in the second part of this chapter. It is noteworthy that the following analysis also holds for two particles moving on a line and colliding, adapting the masses, stiffnesses and damping coefficients to their equivalent (or effective) values. For instance, the effective mass is $m = \frac{m_1 m_2}{m_1+m_2}$, the equivalent stiffness is $k = \frac{k_1 k_2}{k_1+k_2}$, the equivalent damping coefficient is $f = \frac{f_1 f_2}{f_1+f_2}$, for two spring-dashpot systems as on Fig. 2.1 mounted in series.

2.1.1 From Elastic to Hard Impact

Consider that we attach a linear spring with stiffness k to the mass m moving on a horizontal line, and that the mass collides with a wall (infinite mass) through the spring, at time t_0 (take $f = 0$ in Fig. 2.1). The position of the mass is z, and $\xi = l$ corresponds to the spring at rest. Let $k > 0$ be its stiffness, m is the mass. If the spring was a bilateral spring capable of exerting positive and negative forces F on the mass, one would have $F = k(l - \xi)$, so that $F > 0$ if $l - \xi > 0$ (compressed spring, repulsive contact force), and $F < 0$ if $l - \xi < 0$ (stretched spring, attractive contact force). However, in our case the spring is unilateral, which means that it may detach from the "wall". During the contact phases of motion, the spring is compressed, i.e., $l - \xi > 0$, while $z = \xi$, so that $F = k(l - \xi) = k(l - z) > 0$. During non

[2] Although, as we shall see, this still requires advanced mathematical studies.

contact phases one has $F = 0$ and $z > \xi$, while $\xi = l$ since the spring is massless (it has no dynamics by itself). Doing the change of variable $x = z - l$ one obtains $F(x) = 0$ if $x \geq 0$, and $F(x) = -kx$ if $x \leq 0$. The dynamics of the mass is given by $m\ddot{x}(t) = F(x(t))$. Therefore one obtains:

$$\begin{cases} m\ddot{x}(t) = 0 & \text{if } x(t) \geq 0 \\ \\ m\ddot{x}(t) + kx(t) = 0 & \text{if } x(t) \leq 0. \end{cases} \tag{2.1}$$

This model yields a multivalued stiffness, as explained in Example 1.6, Remark 1.7. Assume that the spring remains in contact with the wall on the time interval $[t_0, t_1]$, i.e. t_0 is the instant when the mass/spring system makes contact with the wall, and t_1 the time when it detaches. One has $x(t_1) = x(t_0) = 0$, and $\dot{x}(t_0) = \dot{x}_0 < 0$ while $\dot{x}(t_0) > 0$. Let us set $t_0 = 0$. We obtain during the contact phase $[0, t_1]$: $x(t) = \dot{x}_0\sqrt{\frac{m}{k}}sin(\sqrt{\frac{k}{m}}t)$. The first time instant after the impact such that $x(t_1) = 0$ is the impact duration:

$$t_1 = \sqrt{\frac{m}{k}}\pi. \tag{2.2}$$

(i.e. the spring is being crushed and then restores its potential energy). Note that $\dot{x}(t_1) = -\dot{x}_0 > 0$. Consider now any sequence of stiffness values $\{k_n\}$, $n \in \mathbb{N}$, $k_n < k_{n+1}$, $k_n \to +\infty$ as $n \to +\infty$. Let us denote $F_n(\tau) = -k_n x_n(\tau)$ for $0 \leq \tau \leq t_1$, $F_n(\tau) \equiv 0$ elsewhere. Note that the subscript n in $x_n(t)$ is to emphasize that $x_n(t)$ is the solution of an approximating problem with stiffness k_n. Then, $\int_0^{t_1} F_n(\tau)d\tau = -\int_0^{t_1} k_n x_n(\tau)d\tau = 2|\dot{x}_0|m > 0$ for all $n > 0$. Now notice that $x_n(\tau) \to 0$ on $[0, t_1]$ as $n \to +\infty$ and $t_1 \to 0^+$ as $n \to +\infty$, i.e., if the stiffness is infinite, $x(\cdot)$ remains unchanged during the impact[3] and the impact duration is zero. Moreover, the compliant elastic collision tends towards a hard (i.e., purely elastic and instantaneous) collision. It is easy to verify that the sequence $F_n(\cdot)$ of contact force functions converges to $2|\dot{x}_0|m\delta_0$ as $n \to +\infty$, by checking conditions **i**, **ii** and **iii** for delta-sequences given in Appendix A.1, Sect. A.1.2.

Following the terminology used in most mathematical studies [241, 242, 260, 989, 990] we have chosen a *penalizing function* $F_n(x_n) = -k_n x_n$ if $x_n > 0$, 0 if $x_n \leq 0$, that exactly fits within the conditions imposed by these authors.

2.1.1.1 The Work Performed by Contact Forces

The work effectuated by the contact force during the impact is given by $W_{[0,t_1]} = \int_0^{t_1} \dot{x}_n(t)k_n x_n(t)dt = \frac{m\dot{x}_0^2}{2}[cos^2(\pi) - 1] = 0$ for any $k_n \in \mathbb{R}^+$. Thus, it seems reasonable to consider that the work of the impulsive force at the impact time is zero.

[3] Constant positions is a common assumption in impact mechanics.

This is consistent with the lossless property of this model. The maximum interaction force value is given by:

$$F_{\max} = |\dot{x}_0|\sqrt{km}, \tag{2.3}$$

and therefore tends to infinity as the stiffness k grows unbounded. Thus, the intuitive and widely spread idea of "very large" forces at impacts seems quite justified from this mathematical model. The correct idea is to consider the effect of the interaction force $F(\cdot)$ as a distribution in $\mathscr{D}^\star$. One sees that the action on any function in $\mathscr{D}$ with support containing 0 is finite, for any k, because the support of $F(\cdot)$ tends towards zero so that $F(\cdot)$ becomes atomic. As we have already seen, what is to be considered as the impact magnitude for infinitely large k is the magnitude p of the impulse, which exactly corresponds to the integral of the interaction force over the contact interval (i.e., what is called the impulse of the interaction force during the contact period), and not to the maximum value of this force, that makes no sense when $k = +\infty$. However, for practical purposes one may also argue that the maximum value of the interaction force is important (to be able to prevent possible damage of the materials in contact). Then it is clear that a rigid body model cannot predict such value, and one has to use a suitable compliant approximating model of the contact-impact process.

Remark 2.1 When a constant force F_0 acts on the mass, it is still possible [591] to calculate the solution as $x(t) = \frac{F_0}{k}(1 - \cos(\sqrt{k}t)) + \frac{\dot{x}_0}{\sqrt{k}}\sin(\sqrt{k}t)$, the impact duration as $t_1 = \frac{2}{\sqrt{k}}\arctan\left(-\frac{\sqrt{k}}{F_0}\dot{x}_0\right)$, and the impulsion of the contact force as $P(t_1) = -2\dot{x}_0 + 2\frac{F_0}{\sqrt{k}}\arctan\left(\frac{\sqrt{k}}{F_0}\dot{x}_0\right)$.

2.1.1.2 Complementarity Modelling

Unilaterality is present in the model since the contact force is set to zero when $x > 0$. One says that the contact model is a unilateral linear spring. Let the dynamics be expressed as: $m\ddot{x}(t) - \lambda(x(t)) = 0$, where $\lambda(x)$ is defined as follows:

$$\lambda(x) = \begin{cases} 0 & \text{if } x \geq 0 \\ -kx & \text{if } x \leq 0 \end{cases} \quad \Leftrightarrow \quad \lambda(x) = \max(0, -kx)$$

$$\Leftrightarrow \quad 0 \leq \lambda(x) \perp w(x) = \lambda(x) + kx \geq 0 \quad \Leftrightarrow \quad \lambda(x) = \operatorname{argmin}_{z \geq 0} \tfrac{1}{2}(z + kx)^2, \tag{2.4}$$

where $\perp$ means that the two variables $\lambda(x)$ and $w(x)$ have to be mutually orthogonal: in the scalar case this is simply $\lambda(x)w(x) = 0$. The third formalism in (2.4) is called a *Linear Complementarity Problem* (LCP), a formalism we already met in Example 1.6. The equivalences may be checked by inspection: if $x > 0$, then $-kx < 0$ and the only solution is $\lambda(x) = kx > 0$. If $x < 0$ then $-kx > 0$ and the only solution is $\lambda(x) = 0$. The case $x = 0$ yields $\lambda(0) = 0$. The equivalence with the quadratic program is a consequence of the Karush-Kuhn-Tucker (KKT) conditions which yield

the equivalence between (5.107) and (5.109) in Sect. 5.4.3. The equivalences in (B.19) and (B.20) in the Appendix may also be used. The dynamics of the mass may therefore be written as

$$\begin{cases} m\ddot{x}(t) + \lambda(t) = 0 \\ 0 \leq \lambda(t) \perp w(\lambda(t), x(t)) = \lambda(t) + kx(t) \geq 0, \end{cases} \tag{2.5}$$

which is a simple example of a *Linear Complementarity System*. Obviously the multiplier λ in (2.5) is a function of x, being the solution of the above LCP. It is even a Lipschitz continuous function of x, according to Theorem 5.4. To complete this section, let us notice that the complementarity conditions may be written equivalently as $0 \leq w(t) \perp \lambda(t, x(t)) = w(t) - kx(t) \geq 0$, with $m\ddot{x}(t) = w(t) - kx(t)$ and $\lambda(t) = w(t) - kx(t)$. The distance between the mass + spring-dashpot and the wall is $d(t) \geq 0$, with $d(t) = x(t)$ if $x(t) \geq 0$, and $d(t) = 0$ if $x(t) < 0$. So, we have in fact $w(t) = kd(t)$, so that $0 \leq d(t) \perp d(t) - x(t) \geq 0$. In view of this, since $\lambda(t) = \frac{1}{k}(d(t) - x(t))$, we have that $0 \leq d(t) \perp \lambda(t) \geq 0$, which states the complementarity between the contact force and the distance between the mass and the obstacle: this is a formalism which we will meet all through the book, especially for rigid bodies.

2.1.2 From Damped to Plastic Impact

Let us now assume that only a damper is attached to the mass, with viscous friction coefficient $f > 0$, as shown in Fig. 2.1. The contact force exerted by the viscous friction is $F(\dot{z}) = -f\dot{\xi}$ if $z = \xi$, $F = 0$ if $z > \xi$. Doing the same variable change $x = z - l$ as in Sect. 2.1.1, one obtains

$$\begin{cases} 0 \leq t \leq t_c : m\ddot{x}(t) = 0 \\ \\ t_c \leq t \leq t_1 : m\ddot{x}(t) + f\dot{x}(t) = 0, \end{cases} \tag{2.6}$$

where t_c is the instant when the mass/dashpot system makes contact with the wall. Proceeding as above, we obtain after the impact time $\dot{x}(t) = \dot{x}_0 e^{-\frac{f}{m}t}$, $x(t) = -\frac{m\dot{x}_0}{f}(1 - e^{-\frac{f}{m}t})$. One sees that if $f \to +\infty$, then $x(t) \to x(0) = 0$ and $\dot{x} \to 0$ for all $t > 0$. For any sequence of values of damping coefficient $\{f_n\}$ defined as in the preceding example, let us denote $F_n(\tau) = f_n\dot{x}_n(\tau) + m\dot{x}_0\sqrt{\frac{f_n}{m}}\mathrm{e}^{-\sqrt{\frac{f_n}{m}}}$ for $0 \leq \tau \leq \sqrt{\frac{m}{f_n}}$, $F_n(\tau) \equiv 0$ elsewhere. Then, $\int_0^{\sqrt{\frac{m}{f_n}}} F_n(\tau)d\tau = \int_0^{+\infty} f_n\dot{x}_n(\tau)d\tau$. Note that this time the interaction impulse is calculated on the whole interval $[0, +\infty)$ since the body never detaches from the surface after contact has been established. It is easy to check that $F_n(\cdot)$ satisfies conditions **i**, **ii** and **iii** in Appendix A.1. Hence, we get $F_n(\cdot) \to m\dot{x}_0\delta_0$ as $n \to +\infty$. In the limit, the equation describing the system with one impact at $t = 0$ becomes the MDE $m\ddot{x} = \{\ddot{x}(t)\}dt + m\sigma_{\dot{x}}(0)\delta_0$, with

$\{\ddot{x}(t)\} = 0$ (null acceleration outside the impact time), $\sigma_{\dot{x}}(0) = -\dot{x}(0^-) = -\dot{x}_0$ since $\dot{x}(0^+) = 0$.

2.1.3 The General Case

2.1.3.1 The "Usual" Switching Conditions

Consider now that we attach a spring $k > 0$ and a damper $f > 0$ to the mass as in Fig. 2.1.[4] Proceeding exactly as in the previous two cases, the dynamics during the contact phases of motion is given by

$$\begin{cases} m\ddot{x}(t) + f\dot{x}(t) + kx(t) = 0 \ \text{ if } \ x(t) \leq 0 \\ \\ m\ddot{x}(t) = 0 \ \text{ if } \ x(t) > 0, \end{cases} \tag{2.7}$$

hence, a discontinuous vector field if $\dot{x}(t) \neq 0$ at the transition time. Let us assume that $\Delta \stackrel{\Delta}{=} f^2 - 4km < 0$. Thus, we obtain with the same initial conditions as in the undamped case $x(t) = \frac{\dot{x}_0}{\omega} e^{rt} sin(\omega t)$, $\dot{x}(t) = \dot{x}_0 e^{rt} \left[\frac{r}{\omega} sin(\omega t) + cos(\omega t)\right]$, with $\dot{x}_0 = \dot{x}(0) < 0$, $r = \frac{-f}{2m}$, $\omega = \frac{\sqrt{-\Delta}}{2m}$. The time instant

$$t_1 = \frac{\pi}{\omega} = \pi \left(\frac{k}{m} - \left(\frac{f}{2m} \right)^2 \right)^{-\frac{1}{2}} \tag{2.8}$$

at which $x(t_1) = 0$ and $\dot{x}(t_1) = -\dot{x}_0 e^{\frac{r\pi}{\omega}}$, furnishes the impact duration. Let us choose $0 < \beta \leq 1$, and let us see what happens if[5]:

$$f = 2|ln(\beta)| \left(\frac{km}{\pi^2 + ln^2(\beta)} \right)^{\frac{1}{2}}, \tag{2.9}$$

when $k \to +\infty$ (Such an f guarantees $\Delta < 0$ for $0 < \beta \leq 1$): we get $t_1 \to 0$ and $e^{\frac{r\pi}{\omega}} \to \beta$. Thus, $\dot{x}(t_1) \to -\beta \dot{x}_0$ as $k \to +\infty$ (if $\beta = 1$ then $f \equiv 0$ and we retrieve the above case, and if $0 < \beta < 1$, then $f \to \infty$ as $k \to \infty$). Simple calculations show that $\int_0^{\frac{\pi}{\omega}} F_n(\tau) d\tau \stackrel{\Delta}{=} -\int_0^{\frac{\pi}{\omega}} (f_n \dot{x}_n(\tau) + k_n x_n(\tau))\, d\tau = m|\dot{x}_0|(\beta + 1)$, where $\{k_n\}$ is a sequence of stiffness coefficients defined as previously, and $f_n = 2|ln(\beta)| \left(\frac{k_n m}{\pi^2 + ln^2(\beta)} \right)^{\frac{1}{2}}$. Thus, once again the sequence of force functions $F_n(\cdot)$ during the collision time converges towards a Dirac distribution. Note that to show this, we have considered a sequence of damping coefficients that depend on the mass m. This

[4] This model is often called a *linear spring-dashpot* model, or the Kelvin-Voigt model.

[5] Let us note that the following relationship means that the damping coefficient is taken to be proportional to the square root of the stiffness coefficient.

is at first sight surprizing, as one can expect the nature of collision to be dependent not only on the mass of the bodies that collide, but also on the approach velocity. However, what really matters in this analysis is not how the sequences $\{f_n\}$ and $\{k_n\}$ are defined but rather that they do exist, i.e., we are able to associate a sequence of compliant models to the rigid limiting model.

Remark 2.2 (*Impact duration*) The above calculations show that the impact characteristic time is $\mathcal{O}(\frac{1}{\sqrt{k}})$. As shown in [969] this remains true for a Lagrangian system with a single contact and a linear spring-dashpot model. This is only a crude approximation of experimental data, where it is known that the impact time depends on the pre-impact velocity, see Remark 4.6.

Note that when $\beta \to 0$, $\beta > 0$, then $\Delta \to 0$, $\Delta < 0$, $f \to 2\sqrt{km}$, and as $k \to +\infty$ (the sequence $\{k_n\}$ can be chosen of the form $k_n = k_n^{'} \ln^2(\beta)$, with $k_n^{'} \to +\infty$) then $t_1 \to 0$ and $\dot{x}(t_1) \to 0$ also. More formally, let us define a sequence of positive coefficients β_j, with $\beta_j \to 0$ as $j \to +\infty$. Hence we define the functions $p_{n,j}(t) = -f_{n,j}\dot{x}_{n,j}(t) - k_{n,j}x_{n,j}(t)$. Then, from the above it follows that $F_{n,j}(\cdot) \to m\dot{x}_0(\beta_j + 1)\delta_0 = p_j\delta_0$ and trivially $p_j\delta_0 \to m|\dot{x}_0|\delta_0$ as $j \to +\infty$ (convergence is always understood in the sense of distributions, see Appendix A.1, Sect. A.1.3). Therefore, $F_{n,j}(\cdot) \to m\dot{x}_0\delta_0$ as n and $j \to +\infty$. We have thus found two different sequences of interaction forces, both based on simple mechanical models of contact-impact that both approximate the same limit problem, i.e., a purely inelastic shock.

Remark 2.3 (*Contact Force with Wrong Sign*) The contact force is $F(x, \dot{x}) = -kx - f\dot{x}$ for $x \leq 0$. Normally, we should have $F(x(t), \dot{x}(t)) \geq 0$ during an impact, because no adhesive effects have been modeled with such a linear spring-dashpot assembly. During the compression phase one has $\dot{x}(t) < 0$ so that $-f\dot{x}(t) > 0$ and $F(x(t), \dot{x}(t)) > 0$: the acceleration $\ddot{x}(t)$ is positive, since $\dot{x}(0) < 0$ the velocity increases until it vanishes (maximum compression time) and reverses its sign so that the expansion phase starts. However, during the expansion phase $\dot{x}(t) > 0$ so that the dissipative force $-f\dot{x}(t) < 0$. Close to the detachment position, $x(t)$ is very small and there always exists a position, hence a time, before the detachment occurs, at which the dissipative force dominates the elastic one. Therefore, it is always the case that before detachment, $F(x(t), \dot{x}(t)) < 0$ and this persists until the detachment time occurs, see Fig. 2.4b. Notice anyway that if the contact model guarantees that the impact finishes at some time t_1 with $\dot{x}(t_1) \geq 0$, with an initial velocity $\dot{x}(0) < 0$, then $m(\dot{x}(t_1) - \dot{x}(0)) = \int_{[0,t_1]} F_{\mathrm{n}}(t)dt = p_{\mathrm{n}}(t_1) > 0$, despite possibly negative contact force. This holds for any model satisfying such "collision" assumption.

We have calculated the final collision time as being the first time t_1 when $x(t_1) = 0$. One drawback of this choice is that the force exerted by the spring-dashpot on the mass, may become negative during the impact. This is a nonphysical behavior. This has motivated the choice of another criterion for the end of the impact [239, 274, 474, 475, 1079, 1080], as the first time $t = t_f \neq t_1$ when the contact force vanishes, i.e.,[6]: $f\dot{x}(t_f) + kx(t_f) = 0$. This yields an expression for the ratio $\beta = -\frac{\dot{x}(t_f)}{\dot{x}(t_0)}$ of the

[6] We will see in Sect. 2.1.3.4 that this approach is to be embedded into a complementarity model.

rebound velocity versus the initial one, called the *restitution coefficient*,[7] different from that in (2.9). One finds:

$$\beta = \exp\left(-\frac{\zeta}{\sqrt{1-\zeta^2}}\arccos\left(2\zeta^2-1\right)\right) \tag{2.10}$$

where $\zeta = \frac{f}{2m\omega}$, $\omega = \sqrt{\frac{k}{m}}$, and $0 \leq \zeta < 1$. Further expressions may be calculated for less damped systems with $\zeta \geq 1$ [274]. One obtains for $\zeta > 1$:

$$\beta = \frac{1}{4\zeta\sqrt{\zeta^2-1}}\eta^{-\frac{\zeta}{\sqrt{\zeta^2-1}}}\left(\eta - \frac{1}{\eta}\right), \quad \eta = \sqrt{\frac{2\zeta^2-1+2\zeta\sqrt{\zeta^2-1}}{2\zeta^2-1-2\zeta\sqrt{\zeta^2-1}}}, \tag{2.11}$$

instead of (2.10). Let us come back to the switching conditions in (2.7). Inverting (2.9) the restitution coefficient may be found as:

$$\beta = \exp\left(-\frac{\pi\zeta}{\sqrt{1-\zeta^2}}\right) = \exp\left(-\frac{\pi\mu}{\sqrt{\omega_0^2-\mu^2}}\right), \tag{2.12}$$

where $\zeta = \frac{f}{2\sqrt{km}}$ is supposed to be in $[0, 1]$, $\omega_0 = \sqrt{\frac{k}{m}}$, $\mu = \frac{f}{2m}$ (if the dynamics is equivalently written as $\ddot{x}(t) + 2\mu\dot{x}(t) + \omega_0^2 x(t) = 0$). If $\zeta > 1$ then the restitution coefficient $\beta = 0$ [1080]. It is obvious that β in (2.12) varies from 1 ($\zeta = 0$) to 0 ($\zeta = 1$). It is remarkable that changing the switching surface, changes significantly the equivalent restitution property. As will be seen next, the mathematical analysis differs as well.

Let two one-degree-of-freedom particles collide each other, and one associates a spring-dashpot contact model with each of them. The basic model we used above may be recovered by setting equivalent stiffness $k = \frac{k_1 k_2}{k_1+k_2}$, equivalent damping $f = \frac{f_1 f_2}{f_1+f_2}$, and equivalent mass $m = \frac{m_1 m_2}{m_1+m_2}$, with the coordinate $x = x_1 - x_2$. Newton's third law on action/reaction is used as well.

2.1.3.2 The Work Performed by Contact Forces

The work performed by the contact forces during the impact is given this time by $W_{[0,t_1]} = \int_0^{t_1} \dot{x}_n(t)(f_n\dot{x}_n(t) + k_n x(t))dt = \frac{1}{2}\frac{k\dot{x}_0^2}{\omega^2+r^2}\left[e^{\frac{2r\pi}{\omega}} - 1\right]$ that tends towards $\frac{m\dot{x}(0)^2}{2}(\beta^2 - 1) < 0$ when $k \to +\infty$. We will see later in the book that this quantity is exactly the loss of kinetic energy T_L at impact and can also be deduced from

[7] This restitution coefficient will be denoted as e_n in the rest of the book, where the subscript n is for "normal".

the result in [1192] that states that the work performed by the impact of a particle against a massive barrier is given by an "average" formula $W_{[0,t_1]} = P_{\mathrm{n}}(t_1)\frac{\dot{x}(t_1)+\dot{x}(0)}{2}$ where $P_{\mathrm{n}}(\cdot)$ is the normal impulse of the percussion, i.e., the time integral of the interaction force during the shock interval (thus $P_{\mathrm{n}}(0) = 0$). See Chap. 4 for further developments on the Thomson and Tait formula.

Thus, once again the approximating model allows us to give a meaning to the impulsive work that is consistent with the energetical behavior of the impact (here a loss of energy as long as $\beta < 1$). Note that the distributional formulation permits to calculate easily the loss of kinetic energy but not the impulsive forces work. This is somewhat paradoxical since both quantities are equal and represent the same physical process of energy dissipation. Actually, one needs a generalization of the vis-viva Theorem which states (for smooth motions) that $W_{[t_0,t_1]} = \int_{t_0}^{t_1} F(t)^T \dot{x}(t)dt = T(t_1) - T(t_0)$. The work performed by impulsive forces is sometimes deduced from (1.1) as $W_k = \lim_{\Delta t\to 0}\int_{t_c}^{t_c+\Delta t} p_{\mathrm{n}}(\tau).\dot{x}(\tau)d\tau$: it is clear that without any approximating sequence of impact problems, the integrand is meaningless in the distributional sense. Let us denote the restitution coefficient β as e_{n}. We have proved the following:

Proposition 2.1 *Consider the equation in (1.2) that represents the dynamics of a rigid mass colliding a rigid environment, without any external action. Then, for any energetical behavior of the materials at the impacts (namely for any restitution coefficient* $0 \leq e_{\mathrm{n}} \leq 1$*) we can associate an approximating sequence of compliant models such that the approximating solutions* $x_n(\cdot)$ *converge uniformly towards the solution of (1.2).*

Roughly speaking, as we pointed out in Remark 1.1, we have approximated the limit rigid problem by sequences of differential equations of the form $m\ddot{x}_n(t) = F_n(t)$ for a given sequence of functions $\{F_n(t)\}$, whose limit is a Dirac measure. Results for convergence of this kind may be found for instance in [397, Chap. 1] (see in particular Lemmas 4 and 5 §1, Theorem 1, §2 in that book). Uniform convergence can be proved by using the change of variables indicated in Examples 1.1 and 1.3 since the resulting system is Carathéodory. This holds for $x_n(\cdot)$ only since $\dot{x}_n(\cdot)$ is continuous and cannot thus converge uniformly to a discontinuous $\dot{x}(\cdot)$. The result holds for more general systems like the one in Example 1.3 as long as the "impact function" $h(t)$ is of local bounded variation.[8] We have been able to prove the above because the considered problem is integrable and the exit times can be calculated. As pointed out in the previous section, in the general case the problem is much more involved. A possible work is to find out arguments proving that sequences $\{f_n\}$ and $\{k_n\}$ exist that yield the same results when for instance an external force $u(t)$ acts on the system. As an illustration, consider the classical bouncing ball problem, that corresponds to adding a constant force (gravity) to the mass: then it can be shown that the impulsive force acting on the ball for $0 < e_{\mathrm{n}} < 1$ has the form $F = \sum_{k=0}^{+\infty} p_k\delta_{t_k}$, where $t_\infty < +\infty$ is

[8] Strictly speaking, this fact has to be proved. In the simple examples we have treated, we have been able to integrate the equations and to calculate the functions $F_n(\cdot)$. Obviously, in slightly more complex cases this would not be possible.

an accumulation point of the sequence $\{t_k\}$. A fundamental property of this sequence is that the step function $h(t) \stackrel{\Delta}{=} \sum_{k=0}^{n} p_k$ on $[t_n, t_{n+1}]$, $n \geq 0$ is of bounded variation on $[t_0, t_\infty]$. Hence, from [1082, p. 25, Theorem 2, p. 53] $p = \dot{h}$ can be considered as a Schwartz's distribution since it is a bounded measure. Then, from density of $\mathscr{D}$ in $\mathscr{D}^\star$ [1082, Theorem 15, Chap. 3], we can approximate p and h by sequences of smooth functions $\{p_n\}$ and $\{h_n\}$. From [51, Lemma 2.2.5], $\dot{h}_n = p_n$ since the functions $\dot{h}_n$ are continuous. Are there sequences of damping and stiffness coefficients such that the corresponding compliant model is an approximating sequence for this problem? The work in [969] that we describe later yields a positive answer.

2.1.3.3 Well-Posedness of (2.7)

The system in (2.7) is a switching dynamical system, whose vector field is discontinuous on the switching surface $\Sigma = \{(x, \dot{x}) | x = 0\}$. It is easy to add an external action $F(t)$ to the dynamics (2.7). Let $z_1 = x$ and $z_2 = \dot{x}$, then one may rewrite (2.7) as a first-order switching system $\dot{z}(t) = A_1 z(t) + BF(t)$ if $z_1(t) \leq 0$, $\dot{z}(t) = A_2 z(t) + BF(t)$ if $z_1(t) \geq 0$. On the switching surface Σ, the vector field jumps with a discontinuity equal to $(A_1 - A_2)z(t)$ and $z_1(t) = 0$, so that $(A_1 - A_2)z(t) = (0 \ \frac{-f}{m} z_2(t))^T$. It is possible to embed this system into the general framework of Filippov's differential inclusions, just as the systems of Sect. 1.4.3. Then, one rewrites it as:

$$\dot{z}(t) \begin{cases} = A_1 z(t) + BF(t) \ \text{ if } \ z_1(t) \leq 0 \\ = A_2 z(t) + BF(t) \ \text{ if } \ z_1(t) \geq 0 \\ \\ \in \overline{\text{conv}}(A_1 z(t), A_2 z(t)) \ \text{ if } \ z_1(t) = 0, \end{cases} \tag{2.13}$$

where $\overline{\text{conv}}(A_1 z(t), A_2 z(t))$ is the closure of the convex hull of the two vectors. It is found to be $\text{conv}(A_1 z(t), A_2 z(t)) = \{v \in \mathbb{R}^2 | v = \begin{pmatrix} z_2(t) \\ \frac{-\alpha f}{m} z_2(t) + F(t) \end{pmatrix}, \alpha \in [0, 1]\}$. It is noteworthy that the Filippov's convexification, or regularization method, disregards the value of the vector field on the switching surface Σ. It is therefore not important whether the inequalities defining the switching conditions, are strict or not in (2.7). Due to the way Filippov's right-hand side is constructed, the following holds:

Lemma 2.1 *The differential inclusion in (2.13) possesses for each initial condition* $(z_1(0), z_2(0))$ *an absolutely continuous solution which satisfies the inclusion for almost all* $t \geq 0$.

The simplest example of a Filippov's convexification is the discontinuous system $\dot{z}(t) = 1$ if $z(t) > 0$, $\dot{z}(t) = -1$ if $z(t) < 0$. Then one obtains the differential inclusion $\dot{z}(t) \in \text{sgn}(z(t))$ where $\text{sgn}(\cdot)$ is the set-valued signum function, equal to $\partial|\cdot|$ (see Sect. B.1). There exist other ways to characterize the solutions of (2.7), for instance considering that on Σ one has $\dot{z}(t) \in \{A_1 z(t), A_2 z(t)\}$, i.e., two

values are assigned to the vector field instead of a whole segment. This gives rise to Carathéodory solutions [1197].

What about uniqueness property? The so-called *one-sided Lipschitz* condition for set-valued mappings [13] secures uniqueness of solutions for differential inclusions. However, one may check using [1197, Theorem 2.6] that the mapping in the right-hand side of (2.13) is not one-sided Lipschitz continuous. The criteria in [1197, Theorems 3.1, 3.3, 3.4, Corollary 3.5] may be used to test the uniqueness property. If $F(t) = 0$ [1197 Corollary 3.5] applies and uniqueness of solutions of (2.13) in the sense of Filippov holds. Carathéodory solutions are analyzed in [574].

The Zeno behavior may be characterized through [1197, Theorem 4.2]. Let us remind that the system (2.13) is non-Zeno if the switches, i.e., the time instants when Σ is crossed, are well-separated one from each other. In particular they never accumulate. The criterion in [1197, Theorem 4.2] consists of constructing three equations from "observability" matrices $(C^T\ C^T A_1\ C^T A_1^2)^T$ and $(C^T\ C^T A_2\ C^T A_2^2)^T$, where the switching function $C^T z = (1\ 0)z$ is seen as an output. When applied to (2.13) it yields non-Zenoness provided $F(t) = 0$.

Remark 2.4 The criteria in [1197] rely strongly on observing the derivatives of the switching function, on the switching surface, and characterizing them through lexicographical inequalities. This is an ubiquitous tool for the analysis of switching and unilaterally constrained systems.

2.1.3.4 Complementarity Modelling

The model in Sect. 2.1.1.2 assumes that the switches occur when $x(\cdot)$ crosses the zero value, see (2.7). Let us consider now the other switching condition for the linear spring-dashpot model that yields the restitution coefficient in (2.10). It allows one to eliminate the phases of motion where the contact force may become negative, a phenomenon that is observed with the "usual" swicthing conditions as noted in Remark 2.3 (see also Fig. 2.4b). During the contact phases one still has $z(t) = \xi(t)$ and $F(z, \dot{z}) = -f\dot{z} - k(z - l) = -f\dot{x} - kx$ with $x \stackrel{\Delta}{=} z - l$, and $x(t) \leq 0$. Let us set the following dynamics:

$$\begin{cases} \dot{\eta}(t) = A\eta(t) + B\lambda(t) \\ \\ 0 \leq w(\eta(t)) = C\eta(t) \perp \lambda(t) \geq 0, \end{cases} \tag{2.14}$$

where $\eta^T = (x, \dot{x}, \bar{\xi})$, $\bar{\xi} = \xi - l$, $A = \begin{pmatrix} 0 & 1 & 0 \\ 0 & 0 & 0 \\ 0 & 0 & -\frac{k}{f} \end{pmatrix}$, $B^T = \begin{pmatrix} 0 & \frac{1}{m} & -\frac{1}{f} \end{pmatrix}$, $C = \begin{pmatrix} 1 & 0 & -1 \end{pmatrix}$. The matrix A has two zero eigenvalues and one eigenvalue equal to $-\frac{k}{f}$, and is thus marginally stable. The variable $w(\eta) = z - \xi = x + l - \xi = x - \bar{\xi}$ represents the signed distance between the spring-dashpot system and the constraint,

while ξ is the deformation of the spring and the damper. The contact and noncontact phases correspond to $w(\eta) = 0$ ($\Rightarrow \lambda(\eta) \geq 0$) and $w(\eta) > 0$ ($\Rightarrow \lambda(\eta) = 0$) respectively. During noncontact phases, the spring-dashpot system has the dynamics $\dot{\bar{\xi}}(t) = -\frac{k}{f}\bar{\xi}(t)$, equivalently $f\dot{\xi}(t) = -k(\xi(t) - l)$. Contarily to the undamped case, where $f = 0$ implies $\xi = l$, it has its own dynamics, though it is massless.

The obtained system in (2.14) is a Linear Complementarity System. There is a significant difference between (2.14) and (2.5): in (2.14) the multiplier $\lambda(\eta)$ does not appear in both sides of the complementarity conditions, hence one cannot use straightforwardly the equivalences in (2.4) to compute its value. One has to differentiate once the variable $w(\eta)$ to recover a Linear Complementarity Problem (LCP, see Definition 5.105). If $w(\eta(t)) = C\eta(t) = 0$ on $[t', t'']$, for some $t'' > t'$, then the complementarity condition $0 \leq \dot{w}(t) = C\dot{\eta}(t) \perp \lambda(\eta(t)) \geq 0$ holds on (t', t'').[9] Since $CB = \frac{1}{f} > 0$, $\lambda(\eta(t))$ is at time $t \in [t', t'']$ the unique solution of the LCP:

$$0 \leq \lambda(\eta(t)) \perp \dot{w}(t) = CA\eta(t) + CB\lambda(\eta(t)) \geq 0, \tag{2.15}$$

whose matrix $CB = \frac{1}{f}$ is obviously a P-matrix (see Theorems 5.4 and 5.5). Let $CA\eta(t) = \dot{x}(t) + \frac{k}{f}\bar{\xi}(t) \leq 0$, then the multiplier is given by $\lambda(\eta) = -fCA\eta(t) = -f\dot{x}(t) - kx(t) \geq 0$, noting that during this phase of the motion one has $z(t) = x(t)+l = \xi(t)$. If we have on the contrary $CA\eta(t) \geq 0$ then the multiplier is $\lambda(t) = 0$: there is a detachment from the obstacle at the time instant t_f when $CA\eta(t_f) = 0$, i.e., the force exerted by the obstacle (the spring-dashpot system) on the mass vanishes and then takes negative values.

One may say that the *relative degree* between the "output" $w(\eta)$ and the "input" $\lambda(\eta)$ is equal to zero in (2.5) and equal to one in (2.14).

$\rightsquigarrow$ *It is noteworthy that in both* (2.14) *and* (2.5), *transitions from noncontact to contact occur with a continuous state and a bounded multiplier (contact force)* λ. *There is no state jumps nor Dirac measure.*

To summarize, noncontact phases of motion have the dynamics $\dot{\eta}(t) = A\eta(t)$, while contact phases have the dynamics $\dot{\eta}(t) = \begin{pmatrix} 0 & 1 & 0 \\ \frac{-k}{m} & \frac{-f}{m} & 0 \\ \frac{k}{m} & 1 & \frac{-k}{m} \end{pmatrix} \eta(t)$. Since in the contact phase one has $w(t) = 0 \Leftrightarrow z(t) = \xi(t) = x(t) + l$, the ξ-dynamics reduces to $\dot{\xi}(t) = \dot{z}(t) = \dot{x}(t)$ which trivially holds. The rest of the dynamics is that of a mass with stiffness and damping effects.

Well-Posedness Analysis

Let us refer to Theorem 5.4 in Sect. 5.4.2, which stipulates that $\lambda(x)$ as a solution of the LCP in (2.5), is a Lipschitz continuous function of x. It follows that the system in (2.5) is an Ordinary Differential Equation with Lispchitz continuous vector field (this

[9] Here $\dot{w}(t) = \nabla w(\eta)^T \dot{\eta}(t)$.

continues to hold if an external action $F(t)$ is added, provided $F(t)$ is regular enough). Hence general results about existence, uniqueness and continuous dependence apply to the Linear Complementarity System (2.5), which possesses continuously differentiable solutions. The system (2.5) may also be seen as a piecewise-linear system with continuous vector field. Such straightforward conclusion cannot be drawn for (2.14), which requires more analysis, as in particular its vector field is no longer continuous at the switching surface. Let us first notice that using (B.19) one obtains that (2.14) is equivalent to the differential inclusion:

$$\dot{\eta}(t) - A\eta(t) \in -B\ N_{\mathbb{R}_+}(C\eta(t)). \tag{2.16}$$

A useful relation is that there exists a symmetric, positive definite matrix P such that $PB = C^T$.[10] For instance the matrix:

$$P = \begin{pmatrix} p_{11} & m & 0 \\ m & 1 & \frac{f}{m} \\ 0 & \frac{f}{m} & \frac{f^2}{m^2} + f \end{pmatrix}, \quad p_{11} > f + 1 \tag{2.17}$$

is suitable. The matrix P has a symmetric positive definite square root R, such that $RR = P$. Let $\zeta = R\eta$. The dynamics (2.16) becomes (time argument is dropped):

$$\dot{\zeta} - RAR^{-1}\zeta \in -R^{-1}C^T\ N_{\mathbb{R}_+}(CR^{-1}\zeta) \ \Leftrightarrow \ \begin{cases} \dot{\zeta} = RAR^{-1}z + R^{-1}C^T\lambda \\ \\ 0 \le w = CR^{-1}\zeta \perp \lambda \ge 0. \end{cases} \tag{2.18}$$

Using the symmetry of R (and thus of R^{-1}) one may use Lemma B.1 and Theorem B.2 to deduce that $R^{-1}C^T\ N_{\mathbb{R}_+}(CR^{-1}\zeta) = \partial f(\zeta)$, with $f = \psi_{\mathbb{R}_+} \circ CR^{-1} : \mathbb{R}^3 \to \mathbb{R}$. Consequently the Linear Complementarity System (2.14) is equivalent to the differential inclusion:

$$\dot{\zeta}(t) - RAR^{-1}\zeta(t) \in -\partial f(\zeta(t)). \tag{2.19}$$

Now using Definition B.8, Lemma B.1 and Theorem B.4, one deduces the following:

Lemma 2.2 *The differential inclusion in (2.19) possesses for each initial state $z(0) \in \mathrm{Dom}(\partial f)$ a unique Lipschitz continuous solution, with essentially bounded derivatives.*

[10] This property, which shall be used elsewhere in this book, is implied by the dissipativity of the system, as a consequence of the passivity Linear Matrix Inequality [218, 254].

From the fact that the system (2.5) possesses continuously differentiable solutions, while Lemma 2.2 guarantees only Lipschitz continuous solutions, we may state that:

$\rightsquigarrow$ *The relative degree between the complementarity variables in* (2.5) *and* (2.14) *influences the smoothness of the solution.*

The constraint $\zeta(0) \in \mathrm{Dom}(\partial f)$ that applies to (2.14) means that initially $z(0) \geq \xi(0)$. This implies that the spring-dashpot cannot penetrate into the wall. The last developments have been abundantly used in [22, 205, 213, 214, 215, 217, 226] to analyse various types of nonsmooth systems, relying on dissipativity, maximal monotonicity, and differential inclusions theory. The property $PB = C^T$ states in fact the passivity of the system (2.14), where $\lambda(\eta)$ and $w(\eta)$ are seen as fictitious input and output [218]. Other assemblies of linear springs, dashpots and dry friction elements have been analysed in [100, 103] and shown to yield well-posed differential inclusions whose set-valued part is a maximal monotone mapping. Our short analysis shows that there exist close links between dynamical systems with complementarity conditions, some types of differential inclusions, and some types of piecewise-linear systems. More details on the relationships between these mathematical formalisms of nonsmooth dynamical systems, may be found in [212, 438]. It is noteworthy that the manipulations made to analyze the differential inclusion (2.16) do not easily extend to nonlinear dissipative systems, like Lagrangian systems with a varying mass matrix $M(q)$, see [25] for a detailed analysis of this case.

Remark 2.5 The complementarity system has been put in the equivalent form (2.18). In particular the matrix multiplying the multiplier λ is $R^{-1}C^T$, and the matrix defining w is its transpose CR^{-1}. This allows one to recast this system in the framework of variational inequalities, for which extensions of Lyapunov stability tools exist [463]. This is quite different from systems with unilateral constraints as in (5.1) in Chap. 5. Indeed suppose that the unilateral constraints in (5.1) are of the form $f(q) = Cq \geq 0$. In the state space form of (5.1) with $x \stackrel{\Delta}{=} (q^T, \dot{q}^T)^T$, one has $w = Dx = (C \quad 0)x$. However the contact force multiplier $\lambda_{\mathrm{n},u}$ enters the state space dynamics through the matrix $B = \begin{pmatrix} 0 \\ C^T \end{pmatrix}$. Clearly $B^T \neq D$. This is due to the fact that in (5.1), the relative degree between $w = f(q)$ and λ is, roughly speaking, equal to 2: two differentiations of $w(\cdot)$ are necessary to recover $\lambda(\cdot)$.

Fixed Points of (2.14)

The matrix A is singular, so that the system $\dot{\eta}(t) = A\eta(t)$ possesses an infinity of equilibria. However, the equilibrium points of the differential inclusions (2.14) and (2.18) are given as the solutions of the generalized equations (that take the form of complementarity problems, or of inclusions into normal cones):

$$\begin{cases} A\eta^\star + B\lambda^\star = 0 \\ 0 \le C\eta^\star \perp \lambda^\star \ge 0 \end{cases} \Leftrightarrow \begin{cases} PA\eta^\star + PB\lambda^\star = 0 \\ \lambda^\star \in -N_{\mathbb{R}^+}(C\eta^\star) \end{cases}$$

$$\Leftrightarrow \quad PA\eta^\star \in -C^T N_{\mathbb{R}^+}(C\eta^\star) \quad \Leftrightarrow \quad 0 \in PA\eta^\star + N_\Phi(\eta^\star) \tag{2.20}$$

$$\Leftrightarrow \quad 0 \in -RAR^{-1}\zeta^\star + \partial f(\zeta^\star) \quad \Leftrightarrow \quad \begin{cases} 0 \in RAR^{-1}\zeta^\star + R^{-1}C^T\lambda^\star \\ 0 \le CR^{-1}\zeta^\star \perp \lambda^\star \ge 0, \end{cases}$$

where $\Phi = \{y \in \mathbb{R}^3 | Cy \ge 0\}$, and $\eta^\star = (x^\star, 0, \bar{\xi}^\star)^T$. To get these equivalences we used (B.19), Theorem B.2, Definition B.7, and the fact that P is full rank together with $PB = C^T$. Generally speaking, it could happen that A is singular while the generalized equations in (2.20) possess a unique solution. Obviously in our case there is an infinity of equilibrium points, which correspond to the noncontact phase whose mass dynamics is $\ddot{x}(t) = 0$. All the points $x^\star = z^\star - l > 0$ and $\bar{\xi}^\star = 0$ satisfy the generalized equation (2.20) with $\lambda^\star = 0$. We may modify the dynamics by either adding a constant external force F_{ext} acting on the mass, or with a feedback $u = -k_p x - k_v \dot{x}, k_p > 0, k_v > 0$. The first modification modifies the system in (2.14) as $\dot{\eta}(t) = A\eta(t) + B\lambda(t) + EF_{ext}$, with $E = (0\ \frac{1}{m}\ 0)^T$. Then if $F_{ext} < 0$ one finds that the only equilibrium is $\lambda^\star = -F_{ext}$, $\bar{\xi}^\star = \frac{F_{ext}}{k} = x^\star$ (the equilibrium belongs to the contact phase, the spring being compressed). If $F_{ext} > 0$ there is no equilibrium (the mass moves to the left). The second one modifies A to $\tilde{A} = \begin{pmatrix} 0 & 1 & 0 \\ \frac{-k_p}{m} & \frac{-k_v}{m} & 0 \\ 0 & 0 & -\frac{k}{f} \end{pmatrix}$ which is full rank. One can check that the only equilibrium is given by $x^\star = \bar{\xi}^\star = 0$ and $\lambda^\star = 0$, that corresponds to a degenerate solution of the generalized equations in (2.20).

Dissipativity Properties

It is easy to check that $PA + A^T P$ with P in (2.17) is not definite. Hence the triplet (A, B, C) is not dissipative, though $PB = C^T$.

$\rightsquigarrow$ *It is noteworthy that we are not verifying the dissipativity of a simple double integrator with PD feedback $m\ddot{x} + k_v\dot{x} + k_p x = u$, which is dissipative with supply rate $\langle u, \dot{z}\rangle$. The whole switching, complementarity system is studied.*

Let us assume that (i) $m > 1 + f$, or (ii) $m < 1 - \frac{f}{m}$. Then one can show that there exists (i) large enough k_p for fixed bounded k_v, or (ii) large enough k_v for fixed bounded k_p, such that $P\tilde{A} + \tilde{A}^T P$ is negative definite. Hence under such conditions on the gains, the system $(\tilde{A}, B, C)$ is dissipative with the supply rate $\langle w, \lambda\rangle$, i.e., it is passive. It has the storage function $V(\eta) = \frac{1}{2}\eta^T P\eta$, and due to the negative definiteness of $P\tilde{A} + \tilde{A}^T P$, the equilibrium point $x^\star = \bar{\xi}^\star = 0$ is globally, uniformly

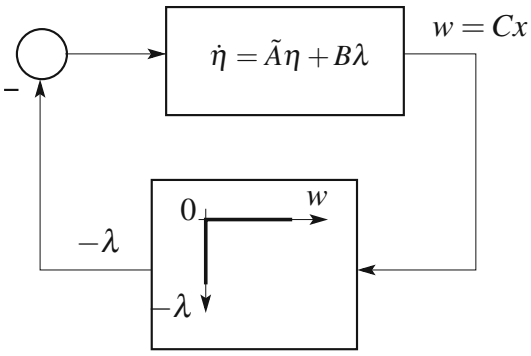

Fig. 2.2 Linear complementarity system: Lur'e set-valued system

asymptotically stable in the sense of Lyapunov. The dissipation equality is satisfied along trajectories

$$\underbrace{V(\eta(t_1))}_{\text{Energy at } t_1} - \underbrace{V(\eta(t_0))}_{\text{Energy at } t_0} = \underbrace{\int_{t_0}^{t_1} w(s)\lambda(s)ds}_{\text{Injected energy on } [t_0,t_1]} + \underbrace{\int_{t_0}^{t_1} \eta(s)^T Q\eta(s)ds}_{\text{Dissipated energy on } [t_0,t_1]}, \tag{2.21}$$

with $Q = P\tilde{A} + \tilde{A}^T P < 0$, and for any $t_0 \leq t_1$. The LCS in (2.14) with the new state matrix $\tilde{A}$ thus has the negative feedback interconnection structure as in Fig. 2.2, and may be interpreted as a Lur'e system with set-valued nonlinearity, where the dynamics is dissipative while the set-valued static nonlinearity is maximal monotone.

2.2 Viscoelastic Contact Models and Restitution Coefficients

2.2.1 Linear Spring-Dashpot

The linear spring-dashpot model has serious flaws: discontinuity in the viscous friction term for nonzero approach velocity [522] producing discontinuous acceleration, possible negative contact force (see Remark 2.3), and an equivalent restitution coefficient $e_n = \beta$ in (2.10), (2.11) or (2.12), that does not depend on the initial impact velocity. All experiments show that the colliding velocity strongly influences the restitution coefficient, that may vary from 0.9 for approach velocities $\approx$ 0.2 m/s, to less than 0.5 for velocities $\approx$ 3–5 m/s (SUJ2 steel[11] sphere/sphere impact [857]), 440c grade 100 wear resistant stainless steel sphere hitting a stainless steel puck with no hardening effects [180]. Figures 165 and 166 in [469] indicate a decrease of the restitution coefficient from 0.9 to 0.2 for lead sphere/sphere impacts, for approach

[11] Steel used for journal bearing, Japanese Industrial Standards.

velocities varyng between 0.1 and 1.6 m/s. In fact the model of Fig. 2.1 is often too simplistic to reproduce experimental results, and has therefore little prediction capabilities.

In [999] the spring-dashpot model as in Sect. 2.1.3 is used to calculate the optimal f and k that minimize the maximum value of the interaction force, given the maximum deformation. Notice that the experimental determination of the contact force represents in itself a topic of research [360, 361, 537, 713, 811]. This is typically an inverse problem in which one knows the output (displacement, velocity, strain) and the structure dynamics (a transfer function for instance [713]) and tries to compute the input (the contact force). A simple experiment allowing one to observe the shape of the curve force versus time is described in [72] for educational purpose. In [150] a nonlinear spring action $k(x)$ is used. The model is validated experimentally for low impact velocities ($\leq$ 8 m/s) of a solid cylindrical mass with blocks of polystyrene aggregate concrete. The maximum force during an impact process between two flexible bodies and using a linear spring-dashpot is calculated in [633]. Comparisons are made with experimental results using various materials. One possibility is to combine the rigid body approach (that provides one with pre and post-impact velocities and percussion) with a suitably chosen compliant model of contact/impact [1]: the compliant model is identified with the supplied data and then used to calculate the force history. Comparisons with calculations of the whole motion with methods using compliant models show good reliability of such procedure. A similar method has been used in [1122] to compare the results obtained from integration with a finite-element code and those of a rigid body approach (namely Darboux-Keller's shock dynamics, see Chap. 4).

The calculation of restitution coefficients has been considered in the mechanical engineering literature for various types of spring-dashpot models. For instance the authors in [1298] calculate e_{n} for a one degree-of-freedom system composed of a mass related to the ground by a spring of stiffness k, and striking in a compliant obstacle composed of a sprink k_1 and a damping coefficient f. Then it is found that $e_{\mathrm{n}} \stackrel{\Delta}{=} \frac{\dot{x}(t_f)}{\dot{x}(t_0)} = \exp\left(\frac{\xi\pi}{\sqrt{1-\xi^2}}\right)$, where $\xi = \frac{f}{\sqrt{(k+k_1)m}}$ (compare with (2.12)). The model of Zener consists of the linear spring-dashpot with stiffness k_1, mounted in series with another spring with stiffness k_2, see Fig. 2.3b. When $\frac{k_1}{k_1+k_2} \ll 1$, this gives the restitution coefficient:

$$e_{\mathrm{n}} = \exp\left(\left(-\frac{\alpha}{\sqrt{1-\alpha^2}} + \eta\ f_1(\alpha)\right)\left(\arctan\left(\frac{2\alpha\sqrt{1-\alpha^2}}{2\alpha^2-1}\right) + \eta\ f_2(\alpha)\right)\right), \tag{2.22}$$

with: $\alpha = \frac{k_2 f}{2(k_1+k_2)m\omega_0}$, $\omega_0 = \sqrt{\frac{k_1 k_2}{m(k_1+k_2)}}$, $\eta = \frac{k_1}{k_1+k_2}$, $f_1(\alpha) = \alpha - \frac{\alpha^3}{2} + \mathscr{O}(\alpha^5)$, $f_2(\alpha) = 2\alpha - 3\alpha^2 + \mathscr{O}(\alpha^5)$. The model of Maxwell consists of a linear spring and a linear damper mounted in series. The contact force and the indentation satisfy $\dot{\xi} = \frac{\dot{F}}{k} + \frac{F}{f}$. This model lacks of physical meaning as far as Solid Mechanics is

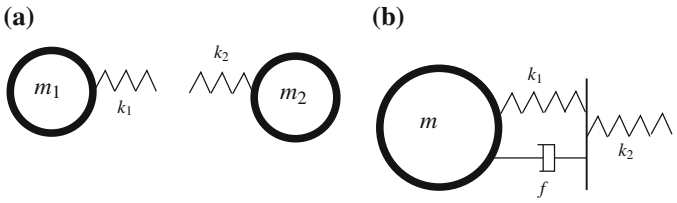

Fig. 2.3 Hodgkinson's and Zener's models

considered, because there is no static equilibrium if a constant force is applied on the system. It seems to be suited more to fluid-like behaviors. Hodgkinson [535] considered the system in Fig. 2.3a, in order to analyse the influence of each body's stiffness on the restitution process. He proposed the formula for composite restitution of coefficient $e_{\mathrm{n},12} = \frac{k_2 e_{\mathrm{n},1} + k_1 e_{\mathrm{n},2}}{k_1 + k_2}$, where $e_{\mathrm{n},1}$ and $e_{\mathrm{n},2}$ are the coefficients obtained for pairs of identical material masses.[12] Though this composite coefficient may be fitted with experiments, it may be energetically inconsistent [313, 1157]. An energetically consistent expression is $e^2_{\mathrm{n},12} = \frac{k_2 e^2_{\mathrm{n},1} + k_1 e^2_{\mathrm{n},2}}{k_1 + k_2}$ [294].

It has been argued [364, 555] that spring-dashpot models for the contacting surfaces are well-suited, because the energy-loss at impacts is associated primarily with damping rather than micro-plastic deformation or permanent strain: this is wrong if the impact velocity is such that plastification occurs. It is pointed out in [1295] after numerical and experimental investigations on impacts of a flexible arm against a rigid obstacle, that although a spring-dashpot and a more sophisticated Hertzian-like model with additional plastic effects provide similar results, the spring-dashpot parameters are more difficult to identify: this is indeed a major drawback of these models.

2.2.2 *Nonlinear Elasticity and Viscous Friction: Simon-Hunt-Crossley and Kuwabara-Kono Dissipations*

Let us remind that Hertz' contact theory yields for sphere/sphere contact an elastic force/indentation relation

$$F = \frac{4}{3} E^\star \sqrt{R} x^{\frac{3}{2}}, \tag{2.23}$$

with $\frac{1}{R} = \frac{1}{R_1} + \frac{1}{R_2}$, $\frac{1}{E^\star} = \frac{1-\nu_1^2}{E_1} + \frac{1-\nu_2^2}{E_2}$, where R_1 and R_2 are the spheres radii, E_1 and E_2 their Young elasticity modulii, ν_1 and ν_2 their Poisson's ratios (see Sect. 4.2.1.1 for more details on Hertz' contact theory). This provides an equivalent stiffness.

[12] In fact, Hodgkinson considered sphere/sphere impacts under Hertz' elasticity, which we simplify here to particle/particle impacts.

Hunt and Crossley [555] proposed a unilateral nonlinear spring-dashpot model of the form:

$$m\ddot{x}(t) = -\gamma x(t)^p \dot{x}(t) - kx(t)^p = -x(t)^p(\gamma \dot{x}(t) + k), \tag{2.24}$$

which we choose to apply during contact phases $x(t) \leq 0$,[13] where γ represents a damping parameter,[14] k is a stiffness parameter, and p is an exponent whose choice is left to the designer ($p = \frac{3}{2}$ is Hertz' elasticity, in which case $k = K_h$ in (2.23)). If we consider bilateral contact then we have to write $\gamma|x(t)|^p\dot{x}(t)$ to guarantee that this term has a meaning for any p. This model is an extension of the model proposed in [1113, Eq. (5)] who wrote it for $p = \frac{3}{2}$ and $\gamma = kf$ for some damping coefficient f, using experimental data in [196]: *The Hunt-Crossley model should thus better be called the Simon-Hunt-Crossley model*, since authors in sports science speak of the Simon's model [492, p. 253]. It has been also proposed in [1228].[15] One sees that the factor x^p in the damping term allows to pass continuously from the free to the contact motion. Let $\gamma = \frac{3}{2}\alpha k$. The model in (2.24) yields $e_\mathrm{n} \approx 1 - \alpha|\dot{x}(t_0)|$ (see [802] for a rigorous proof), with $\alpha \in [0.08, 0.32]$ s/m for steel, bronze or ivory bodies [555].[16] Various viscous friction terms may be assigned to the model by changing γ, hence changing the equivalent coefficient of restitution e_n: $\gamma = \frac{6(1-e_\mathrm{n})}{[(2e_\mathrm{n}-1)^2+3]}\frac{k}{|\dot{x}(t_0)|}$ [522], $\gamma = \frac{3}{4}\alpha k$ [716], $\gamma = \frac{3k(1-e_\mathrm{n}^2)}{4|\dot{x}(t_0)|}$ [704], $\gamma = \frac{3(1-e_\mathrm{n})}{2e_\mathrm{n}|\dot{x}(t_0)|}$ [545], $\gamma = \frac{8(1-e_\mathrm{n})}{5e_\mathrm{n}|\dot{x}(t_0)|}$ [403], $\gamma = \frac{3(1-e_\mathrm{n})}{2|\dot{x}(t_0)|}$ [555], an implicit definition[17]: $k \ln\left(\frac{\gamma|\dot{x}(t_0)|+k}{-\gamma(1-\alpha\dot{x}(t_0))|\dot{x}(t_0)|+k}\right) - 2\gamma|\dot{x}(t_0)| + \alpha\gamma\dot{x}(t_0)^2 = 0$ [470, 1323]. The coefficient α is an empirical parameter that may be obtained by fitting with experiments from the formula $e_\mathrm{n} \approx 1 - \alpha\dot{x}(t_0)$. In practice one estimates e_n via experiments, and deduces γ as in the above expressions, therefore obtaining the right spring-dashpot model. Those nonlinear spring-dashpot models typically have the force/indentation responses shown on Fig. 2.4a [442, 471, 602, 705, 802], while the linear ones typically have the response shown on Fig. 2.4b [12]. The dashed areas represent the dissipated energy during the collision process. A comparative study of all these Simon-Hunt-Crossley models is done in [38]. It follows from [38, Figs. 3, 4, 6, 7, 8, 9] that the contact force/indentation, indentation velocity/indentation displacement, and force/time diagrams show little variations from one model to the other (but the discrepancy with experimental data taken from [1324] increases if the pre-impact velocity increases). All the above models have a dissipation term of the form $D(x, e_\mathrm{n}, \dot{x}(t_0), \gamma, k)\dot{x}$. In [716], the expression

[13] Thus we assume implicitly that $x(t)^p$ exists, or we could just write $|x(t)|^p$.

[14] Often called the *hysteresis factor* [782]. The spring assures the compression/expansion, while the damping creates dissipation and the hysteresis shape.

[15] Notice that contrary to what is written just above [542, Eq. (1)] and could be misleading, the contact model in (2.24) with $p = \frac{3}{2}$ is not at all introduced in [1203].

[16] Such values should be checked and are given here just for the sake of providing an order of magnitude.

[17] It is unclear how the models which include the pre-impact velocity $\dot{x}(t_0)$, may be used in the context of multiple impacts, where some of the contact points are lasting before the collision.

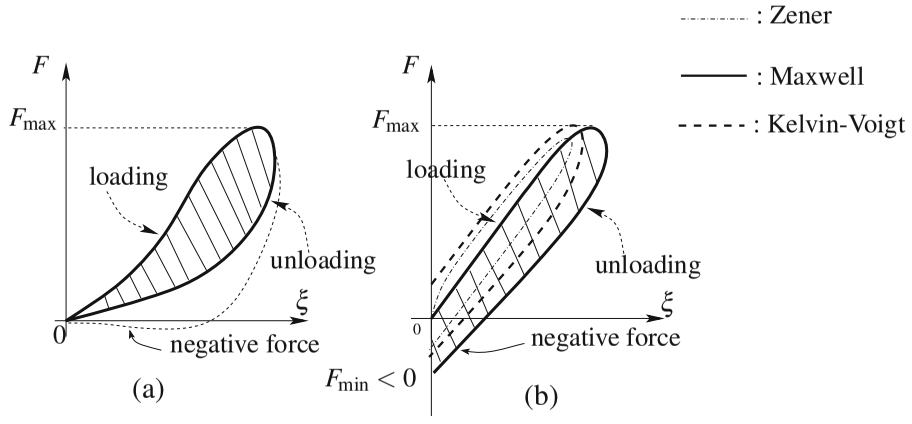

Fig. 2.4 Typical force/indentation responses for nonlinear (**a**) and linear (**b**) spring-dashpots (the abscissa is a generic indentation, or spring deformation, chosen nonnegative)

$D(x, e_\mathrm{n}, \gamma, k) = 2m\sqrt{\frac{k}{m}}\sqrt{\frac{\ln(e_\mathrm{n})^2}{\ln(e_\mathrm{n})^2+\pi^2}}\frac{x+|x|}{2x}\exp\left(\{(x-\varepsilon)-|x-\varepsilon|\}\frac{Q}{\varepsilon}\right)$ is proposed, where Q is a parameter, $0 \leq \varepsilon \leq x_{\max}$, and the contact force $D(x, e_\mathrm{n}, m, k, \varepsilon)\dot{x}+kx^{\frac{3}{2}}$ has to remain nonnegative during the collision process.

Remark 2.6 It is noteworthy that all models with $\dot{x}(t_0)$ in the denominator, yield dynamics which are ODEs of the form $\dot{z}(t) = f(z(t), z(0))$, which is unusual. In fact this corresponds to adding one dimension to the system: $\dot{z}(t) = f(z(t), y(t))$, $\dot{y}(t) = 0$, $y(0) = z(0)$. Moreover since $\dot{x}(t_0)$ is in the denominator of the vector field, some numerical problems may arise if the initial velocity is very small (think of multiple impacts in chains of balls where some balls are at rest initially).

The Simon-Hunt-Crossley model has become popular because it has some nice *ad hoc* mathematical properties, which in fact allow one to derive the above expressions for e_n by varying γ [801, 802, 1157, 1186]. Choosing $\gamma = \frac{3}{2}\alpha k$, the dynamical equation (2.24) is $m\ddot{x}(t) + kx(t)^p(1+\frac{3}{2}\alpha\dot{x}(t)) = 0$ and it is separable as $\int_{\dot{x}(t_0)}^{\dot{x}(t_f)}\frac{\dot{x}}{1+\frac{3}{2}\alpha\dot{x}}d\dot{x} + \frac{k}{m}\int_{x(t_0)}^{x(t_f)}x^p dx = 0$. If the detachment instant is such that $x(t_f) = x(t_0)$ then the second term vanishes. It is possible to show that the maximum compression occurs at $x(t_c)$ such that $x(t_c)^{p+1} = -\frac{(p+1)|\dot{x}(t_0)|}{\gamma} + \frac{k(p+1)}{\gamma^2}\ln\left|1+\frac{\gamma|\dot{x}(t_0)|}{k}\right|$ [602]. This proves that such an assumption renders $\dot{x}(t_f)$ independent of the mass and the stiffness. Introducing the restitution coefficient e_n and integrating the right-hand term, one finds $\frac{3}{2}\alpha|\dot{x}(t_0)| - \ln(1+\frac{3}{2}\alpha|\dot{x}(t_0)|) + e_\mathrm{n}\frac{3}{2}\alpha|\dot{x}(t_0)| + \ln(1-e_\mathrm{n}\frac{3}{2}\alpha|\dot{x}(t_0)|) = 0$, which makes an implicit equation for e_n. In the same vein, Chatterjee [274] computes that for $p = 1$ in (2.24) (a linear spring and a nonlinear dashpot) one obtains $-e_\mathrm{n} - \frac{1}{a}\ln(1-ae_\mathrm{n}) = 1 - \frac{1}{a}\ln(1+a)$, where a is a parameter that depends on m, f, k. The separation property is used in [1186], who noticed that the restitution coefficient does not depend on the elasticity coefficient, in case one takes it equal to kx^n with $n \neq p$ and the viscous friction force is $-\alpha x^n|\dot{x}|^q$ for some q and a parameter α. Then, one obtains the implicit equation for e_n: $\ln\left(\frac{1+\xi}{1-e_\mathrm{n}^q\xi}\right) = \sum_{j=1}^{\frac{2}{q}-1}\left((-1)^{j-1}\frac{\xi^j}{j} + \frac{(e_\mathrm{n}^q\xi)^j}{j}\right)$, with $\xi = \frac{\alpha}{k}|\dot{x}(t_0)|^q$ and $e_\mathrm{n}^q\xi < 1$. The parameters q and α have to be fitted from experiments. In case $q = 1$, the implicit equation reduces to $\ln\left(\frac{1+\xi}{1-e_\mathrm{n}\xi}\right) = (1+e_\mathrm{n})\xi$. This is extended in [373], who consider an elasticity force $f(x)$, $f(0) = 0$, $f(\cdot)$ increasing, a damping force $\gamma f(x)\dot{x}$, and prove that the CoR satisfies the transcendental equation $\gamma\dot{x}(t_0)(1+e_\mathrm{n}) - \ln(1+\gamma|\dot{x}(t_0)|) + \ln(1-e_\mathrm{n}\gamma|\dot{x}(t_0)|) = 0$. For small enough pre-impact velocities, [373] find $e_\mathrm{n} \approx 1 - \frac{2}{3}\gamma|\dot{x}(t_0)|$ which agrees with previous findings.

$\rightsquigarrow$ *These results prove that in the presence of specific damping, the CoR does not depend on the elasticity properties or the material, just as in the undamped (purely elastic) case.*

Experiments with two impacting spheres are reported in [373], showing $q = \frac{1}{5}$ for lead spheres, $q = 1$ for agate, brass, and porcelain spheres. The authors of [602] derive the implicit relationship between displacement and velocity as $\frac{\gamma\dot{x}}{k} -$

$\ln\left|1+\frac{\gamma\dot{x}}{k}\right| = -\frac{\gamma^2(x(t_c)^{p+1}-x^{p+1})}{k(p+1)}$ and approximate the $\ln(\cdot)$ by its Padé approximant. Then, they compute the energetic restitution coefficient (see Sect. 4.3.6) and compare experimental and numerical results. They show that nonlinear damping is necessary to model their experimental setup.

In fact, despite it allows some dependence on the initial impact velocity and avoids tensile contact forces,[18] the Simon-Hunt-Crossley model may lack of physical foundations. It has been experimentally shown to correctly predict the shock process for spheres and plates in [509, 1228], but not for the case of cylinders and plates [317]. In [1324] more precise conclusions have been obtained from experiments with chrome-steel balls impacting steel cylindrical specimens. The measurements concern the impact force response in terms of its peak, slope during compression and expansion phases, times of maximum compression and force peak, and impact duration

- All the above variations of the Simon-Hunt-Crossley model yield the same restitution coefficient when viscous friction is small.
- They are valid for low pre-impact velocities $\dot{x}(t_0)$, for otherwise plastic deformations may occur.
- They yield excellent predictions if $e_n > 0.95$, that is nearly lossless impacts.
- Usually, the peak force for near-elastic impacts is well-predicted, however the contact duration is poorly predicted.
- If plastic deformation occurs, they yield very poor prediction capabilities.

In [442], it is noticed that taking $\gamma = \frac{1}{e_n}\frac{k}{|\dot{x}(t_0)|}$, allows to obtain a model that provides good results for $e_n \leq 0.3$. Similar arguments are used in [403] who proposes $\gamma = k\frac{8(1-e_n)}{5e_n\dot{x}(t_0)}$. As pointed out in [602] there may exist a lag between displacement and force during impacts (detachment occurs while the bodies are still deformed; maximum contact force and maximum deformation do not match in time). The Simon-Hunt-Crossley with classical detachment conditions does not incorporate this lag. Another important issue is whether or not such models may be used in a multibody multicontact framework. As pointed out in [347], the implementation of the Simon-Hunt-Crossley model in a robotic system with unknown environment requires the on-line estimation of k, γ and p. This may not be easy in general, especially if there are many contact points involving various materials with different viscoelastic properties. A survey and comparative analysis of most of these compliant contact models is done in [783], focussing mainly on the impact process.[19]

The power coefficient p in the Simon-Hunt-Crossley model seems to be the result of some empirical idea, fitted with experiments. Starting from the theory of elasticity,

[18] This is true if no external force acts on the body. As shown in [802], when the objects are separated by an external force, then Simon-Hunt-Crossley model may yield sticky contact forces, as illustrated in Fig. 2.4a.

[19] Indeed and most importantly, using such compliant models during persistent contact phases may produce spurious, unphysical oscillations of the contact force and acceleration during numerical simulations. This is visible on many numerical results presented in the literarure, e.g., systems with clearances [403, 489, 679, 941, 1179, 1226]. It may be preferable to switch to other contact models and numerical integrators outside collisions.

and extending it to viscoelastic materials, one finds the so-called Kuwabara-Kono model [197, 198, 199, 525, 691, 902]:

$$m\ddot{x}(t) = -\gamma k|x(t)|^{\frac{1}{2}}\dot{x}(t) - kx(t)^{\frac{3}{2}}, \tag{2.25}$$

for contact phases $x(t) \leq 0$, and which corresponds to choosing $|x|^{p-1}\dot{x}$ instead of $x^p\dot{x}$ in (2.24). This type of nonlinear spring-dashpot model agrees with some experimental results [407]. Unfortunately, it has not been tested in [1324] for experimental validation.

It is clear that the separability property associated with the Simon-Hunt-Crossley models, is lost with the Kuwabara-Kono's approach. Notice that the square root in the right-hand side of (2.25) renders the vector field non-Lipschitz continuous. ODEs with non-Lipschitz vector fields have specific features in general (non uniqueness of solutions, finite-time convergence to equilibria, unbounded jacobians), which should be taken into account for analysis and numerical simulation. It is in fact a little surprizing that a viscoelastic continuum yields a non Lipschtiz continuous contact force. It is also indicated in [199] that the contact force in the right-hand side of (2.25) could be replaced when $x(t) \gg \gamma\dot{x}(t)$ by $-(x(t)+\gamma\dot{x}(t))^{\frac{3}{2}}$, providing equivalently good results when compared to some experiments. The contact force in (2.25) is almost only dissipative for small indentations, since $\gamma k|x|^{\frac{1}{2}}\dot{x} + kx^{\frac{3}{2}} = \sqrt{x}(\gamma\dot{x} + kx^3) \approx \gamma\dot{x}\sqrt{x}$ at the very beginning or at the very end of the collision where velocity is much larger than indentation: *As noticed in [12 §7.1.3], this indicates that contact forces during an impact, in the Kuwabara-Kono model, always become negative during a small period before detachment occurs, while vanishing again at the detachment time (this last property is not shared by the linear spring-dashpot with the naive switching conditions which gives a detachment force with the wrong sign).* Such spurious behavior may be avoided by imposing complementarity conditions between the contact force and the distance function.

Let the dissipative force be written as $-2\frac{\sqrt{R}}{\tilde{D}}\sqrt{x}\dot{x}$, then the Kuwabara-Kono's model for the collinear collision of two spheres gives a normal restitution $e_{\mathrm{n}} \approx 1 - 1.009\frac{5}{2}\tilde{\kappa}\left(\frac{|\dot{x}(t_0)|}{\kappa m^2}\right)^{\frac{1}{5}}$, where m is the effective mass, $\kappa = \frac{4}{5D}\sqrt{R}$, $\frac{1}{R} = \frac{1}{R_1} + \frac{1}{R_2}$, $D = \frac{3}{4}\left(\frac{1-\nu_1}{E_1} + \frac{1-\nu_2}{E_2}\right) = \frac{3}{4}\frac{1}{E^*}$, $\tilde{\kappa} = \frac{4}{5\tilde{D}}\sqrt{R}$, E_i are Young's moduli, ν_i are Poisson's ratios, $\tilde{D}$ is a viscosity parameter to be measured [508]. The impact duration is estimated as $t_f \approx \frac{\pi R}{c}\sqrt{\ln\left(\frac{4c}{|\dot{x}(t_0)|}\right)}$, with $c = \sqrt{\frac{E^*}{\rho}}$ the compressive sound velocity and ρ the density.

The authors in [906, 1027, 1080] consider the shock of two viscoelastic spheres and a Kuwabara-Kono's model $F(x,\dot{x}) = -\rho x^{\frac{3}{2}} - \frac{3}{2}A\rho\sqrt{x}\dot{x}$, where $\rho = \frac{2E\sqrt{R}}{3(1-\nu^2)}$, $A = \frac{1}{3}\frac{(3\eta_2-\eta_1)^2}{3\eta_2+2\eta_1}\left(\frac{(1-\nu^2)(1-2\nu)}{E\nu^2}\right)$, with E the Young modulus, ν the Poisson ratio, $R = \frac{R_1R_2}{R_1+R_2}$ the effective radius of the equivalent system, η_1 and η_2 are viscous material constants relating the dissipative stress and the deformation rate tensors. This yields dynamics as in (2.25). If the end of the impact is supposed to occur at the first

instant t_1 such that $\dot{x}(t_1) = 0$, then one calculates $e_\mathrm{n} = 1 + c_1 v^{\frac{1}{5}} + c_2 |\dot{x}(t_0)|^{\frac{2}{5}} + \ldots$ for some coefficients c_1, c_2 that depend on k. If the end of the collision is the first instant t_f such that $F(t_f) = 0$, then one calculates $e_\mathrm{n} = 1 + \sum_{k=0}^{\infty} h_k v^{\frac{k}{10}}$, where $v = \dot{x}(t_0)^{\frac{4}{5}}$ and for some coefficients h_k that depend on k. The parameter γ is chosen as $\gamma = \frac{\lambda^\star \sqrt{R}}{k}$ in [70], where $\lambda^\star$ is a parameter to be fitted with experimental data. It provides a restitution coefficient that varies linearly with $\ln(|\dot{x}(t_0)|)$ (but not with $\dot{x}(t_0)$). More experimental validations seem to be necessary to confirm the allegations in [70]. The Kuwabara-Kono's model has been generalized in [386] with a damping coefficient equal to $\mu \dot{x} |x|^\alpha$, $\alpha > -1$, and results in $e_n = 1 - \frac{4}{5}\mathscr{B}[\frac{3}{2}, \frac{2}{5}(\alpha+1)]\varphi$, with $\varphi = \frac{\mu}{m}\left(\frac{5m}{4k}\right)^{\frac{2(\alpha+1)}{5}} |\dot{x}(t_0)|^{\frac{(4\alpha-1)}{5}}$, and $\mathscr{B}[\cdot,\cdot]$ is a Beta function.[20] This expression holds for $e_\mathrm{n} \lesssim 1$. Another expression that applies to the nonlinear spring-dahspot with damping term $|x|^\alpha \dot{x}$ and elasticity term x^β is $e_\mathrm{n} \approx 1 - |\dot{x}(t_0)|^{\frac{2\alpha-\beta+1}{\beta+1}}$ for small initial impact velocity $\dot{x}(t_0)$ [771]. Assemblies of spring and fractional order dashpot elements are studied in [908, 1313]: such fractional-elastic rheological models apply to polymer materials. The usual dashpot element with force $f\dot{x}$ is replaced by $f D^\alpha x$, where D^α is the fractional derivative, $\alpha \in (0, 1)$. The linear dashpot is recovered in the limit $\alpha \to 1$. The authors of [197] correct their previous results [906, 1027, 1080] and find that the Kuwabara-Kono dissipative force coefficient in case of two spheres of same viscoelastic material is equal to $\frac{\sqrt{R}}{(1-\nu)^2}[\frac{4}{3}\eta_1(1-\nu+\nu^2) + \eta_2(1-2\nu^2)]$, that is different from the above one. In fact, multibody multicontact applications will in general require some parameter estimation procedure. The form of the dissipative force, (i.e., $-\gamma x^p \dot{x}$ for some p) may be more important than the analytical value of the parameter γ, that will be fitted with experimental data for a particular system.

The Simon-Hunt-Crossley model improves the linear spring-dashpot models since it allows for nonlinear elasticity, it avoids discontinuous contact forces and usually has no spurious contact forces with wrong sign. However the dissipative contact force accounts for an equivalent viscosity of the materials in contact and has to be carefully designed. Kuwabara-Kono's model for the dissipative part of the contact force originates from elasticity theory, and produces contact forces with wrong sign before the end of the collision. It is crucial to apply such models to materials which are known to be viscoelastic in the operating conditions.

Remark 2.7 (*Hamiltonian Interpretation of Simon-Hunt-Crossley and Kuwabara-Kono Model*)] Both dynamics with the Simon-Hunt-Crossley and the Kuwabara-Kono's models, may be expressed in a dissipative Hamiltonian form. Let $\mathbf{p} \stackrel{\Delta}{=} m\dot{q}$ be the linear momentum, and the Hamiltonian is $\mathscr{H}(x, \mathbf{p}) = \frac{1}{2}\frac{\mathbf{p}^2}{m} + \frac{2}{5}kx^{\frac{5}{2}}H(x)$, with

[20] $\mathscr{B}[p, q] = 2\int_0^{\frac{\pi}{2}} \cos^{2p-1}(x)\sin^{2q-1}(x)dx$.

$H(x) = 1$ if $x \leq 0$, $H(x) = 0$ if $x \geq 0$. Both (2.25) and (2.24) with $p = \frac{3}{2}$ are rewritten equivalently as[21]:

$$\begin{pmatrix} \dot{x} \\ \dot{\mathbf{p}} \end{pmatrix} = \left[\begin{pmatrix} 0 & 1 \\ -1 & 0 \end{pmatrix} - R(x) \right] \underbrace{\begin{pmatrix} kx^{\frac{3}{2}} H(x) \\ \frac{\mathbf{p}}{m} \end{pmatrix}}_{= \frac{\partial \mathscr{H}}{\partial (x, \mathbf{p})}}, \tag{2.26}$$

with $R(x) = \begin{pmatrix} 0 & 0 \\ 0 & \gamma \sqrt{|x|} H(x) \end{pmatrix} \geq 0$ for Kuwabara-Kono, and $R(x) = \begin{pmatrix} 0 & 0 \\ 0 & \gamma x^{\frac{3}{2}} H(x) \end{pmatrix} \geq 0$ for Simon-Hunt-Crossley. Adding external force inputs, and defining a proper dissipative output, one finds a so-called *port controlled Hamiltonian system with dissipation* [218, Definition 6.37], which is dissipative in Willem's sense provided the Halmiltonian is bounded from below [218, Lemma 6.38].

A five-parameter viscoelastic model incorporating complementarity conditions has been proposed in [1287]. It is meant to improve the Simon-Hunt-Crossley model, avoiding sticky contact forces, and allowing for non zero remaining indentation. This is particularly important in view of the fact that the Simon-Hunt-Crossley model is known to overestimate the contact time, because the spring has to fully unload to get detachment, if no nonnegativity of the contact force is imposed [602]. The new model is formulated as follows:

$$\begin{cases} a(t) + \left(\frac{1}{\gamma} + \beta_1 + \beta_2 a(t) \right) \dot{a}(t) \in -\partial \psi_{\mathbb{R}^+} (\gamma (a(t) - \delta(t) |\delta(t)|^{\lambda - 1}) + \dot{a}(t)) \\ F(t) = K \left(a(t) + \left(\frac{1}{\gamma} + \beta_1 + \beta_2 a(t) \right) \dot{a}(t) \right), \end{cases} \tag{2.27}$$

with $\lambda \geq 1$, $\beta_1 \geq 0$ and $\beta_2 \geq 0$ are damping parameters, $\gamma > 0$ is a parameter, and $\delta = -x$ is the indentation (i.e., the spring's deformation). The variable $a(t)$ is an internal state. Let us remind that $\partial \psi_{\mathbb{R}^+}(\cdot)$ is the subdifferential in the sense of convex analysis, of the indicator function of $\mathbb{R}^+$ (see Appendix B). One may use the material in Sect. B.2.1 to further develop (2.27). In particular complementarity conditions are present in (2.27), since the first line of (2.27) is equivalent to:

$$0 \leq a(t) + \left(\frac{1}{\gamma} + \beta_1 + \beta_2 a(t) \right) \dot{a}(t) \perp \gamma (a(t) - \delta(t) |\delta(t)|^{\lambda - 1}) + \dot{a}(t) \geq 0, \tag{2.28}$$

[21] For instance, polymers or metals with sufficiently high temperature are known to exhibit viscoelastic behaviors.

letting $\Phi = \mathbb{R}_+$ in (B.19). Let us assume that $\frac{1}{\gamma} + \beta_1 + \beta_2 a(t) > 0$.[22] The first line in (2.27) is equivalent to (time argument is dropped):

$$\begin{aligned} \gamma(a - \delta|\delta|^{\lambda-1}) + \dot{a} + \frac{a - \left(\frac{1}{\gamma} + \beta_1 + \beta_2 a\right)\gamma(a - \delta|\delta|^{\lambda-1})}{\frac{1}{\gamma} + \beta_1 + \beta_2 a} \\ \in -\partial\psi_{\mathbb{R}^+}(\gamma(a - \delta|\delta|^{\lambda-1}) + \dot{a}), \end{aligned} \tag{2.29}$$

Using (B.20) this is equivalently rewritten as:

$$\begin{aligned} \gamma(a - \delta|\delta|^{\lambda-1}) + \dot{a} &= \text{proj}[\mathbb{R}_+; \tfrac{-\gamma a}{1+\gamma(\beta_1+\beta_2 a)} + \gamma(a - \delta|\delta|^{\lambda-1})] \\ &= \max[0; \tfrac{-\gamma a}{1+\gamma(\beta_1+\beta_2 a)} + \gamma(a - \delta|\delta|^{\lambda-1})]. \end{aligned} \tag{2.30}$$

Using the expression of $F(t)$ in (2.27) one obtains:

$$F(t) = k\frac{1 + \gamma(\beta_1 + \beta_2 a(t))}{\gamma}(z(t) + \max[0; -z(t)]), \tag{2.31}$$

with $z(t) = \frac{\gamma a(t)}{1+\gamma(\beta_1+\beta_2 a(t))} - \gamma(a(t) - \delta(t)|\delta(t)|^{\lambda-1})$. Finally one obtains:

$$F(t) = K\max(0; -\delta(t)|\delta(t)|^{\lambda-1} - \gamma(\beta_1 + \beta_2 a(t))(\delta(t)|\delta(t)|^{\lambda-1} - a(t))) \geq 0. \tag{2.32}$$

The expressions in (2.30) and (2.32) may be used to integrate the dynamics, that is a piecewise nonlinear system. The inclusion in (2.27) secures the non negativity of the contact force $F(t)$ in a similar way as (2.15) does. One may rewrite equivalently (2.32) as $F(t) = K\lambda$, with λ the unique solution of the LCP:

$$0 \leq \lambda \perp w(\lambda, \delta, a) = \lambda + \delta(t)|\delta(t)|^{\lambda-1} + \gamma(\beta_1 + \beta_2 a(t))(\delta(t)|\delta(t)|^{\lambda-1} - a(t)) \geq 0. \tag{2.33}$$

The complementarity conditions in (2.5), (2.14) and (2.33) may all be depicted as in Fig. 2.5a.

Setting $\beta_1 = 0$ and $\beta_2 = 0$ and $\lambda = \frac{3}{2}$, it follows that $F(t) = k\max[0; -\delta(t)|\delta(t)|^{\frac{1}{2}}]$, which we may rewrite as $F(t) = 0$ if $x(t) \geq 0$, $F(t) = -kx(t)|x(t)|^{\frac{1}{2}}$ if $x(t) \leq 0$ (in order to recover the conventions adopted above, one just has to set $\delta = -x$). Some comments arise: it seems from the simulations presented in [1287] that the inequality $\frac{1}{\gamma} + \beta_1 + \beta_2 a(t) > 0$ is satisfied when $a(0) = 0$; β_1 determines the residual indentation; β_2 influences the roundedness of the curves $(F(t), x(t))$ and may model the displacement/force lag[23]; while γ influences the overall shape of these curves; the internal state $a(t)$ allows for some dependence of the restitution coefficient

[22] It is not mentioned in [1287] how this condition may be guaranteed.

[23] The shape in Fig. 2.5b for large β_2 presents strong similarities with the experimental curves shown in [602].

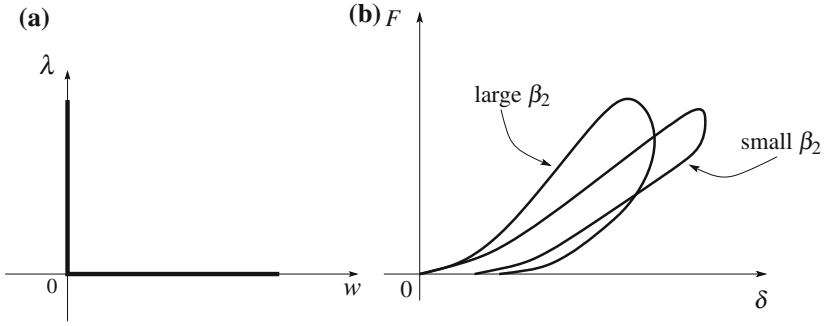

Fig. 2.5 Force/distance and force/indentation *curves*. **a** Complementarity in (2.5), (2.14) and (2.33). **b** For (2.32)

on the pre-impact velocity $\dot{x}(t_0)$. The force/indentation curves typically possess the shape as in Fig. 2.5a. The various force/indentation curves depicted in Figs. 2.4 and 2.5a, have the same global shape as experimental curves shown for instance in [312, Fig. 2], obtained from low-velocity impacts of tennis,[24] golf, baseball, plasticene, steel balls, and superball. In most of the cases, a permanent indentation exists after the shock, indicating some plastification. Vibrations seem to play a role in tennis balls collisions.

Let us end this (non exhaustive) presentation of viscoelastic contact models, by mentioning a sphere/thin plate model using the developments of Zener [1314]. Applications are in harvesting, in order to better understand the dynamics of fruits or potatoes so that clods and stones may be separated from them [426, 430].

2.2.3 Conclusions

⇝ *Most of the above models are of limited practical use in a multibody system context with many contact/impact points, mainly because it is difficult to estimate the contact parameters (even if there is only one contact). Another reason may be related to numerical issues (stability, stiff equations, constraints stabilization). It is also noteworthy that most of them use an empirical, non physical parameter that has to be fitted with experimental data.*

⇝ *Let us remind that all these models assume low velocity impact*, i.e., *local deformations only (this is sometimes called the stereomechanical impacts). Plastification effects are not taken into account. See section 4.2.1 for more details. As a consequence they are valid for very small dissipation collisions only.*

Let us tentatively classify pre-impact velocities, in a kind of "definition".

[24] High-velocity impacts of tennis balls, which are not spheres but shells, involves some buckling effects and cannot be modeled with such simple equations.

Definition 2.1 (*Pre-impact velocities*) *Very low velocity impacts* occur for pre-impact velocities $\in (0 - 100)$ cm/s. *Low-velocity impacts* occur for pre-impact velocities $\in (1 - 10)$ m/s. So-called *hypervelocity impacts* occur for pre-impact velocities $\in [1 - 10]$ km/s [40, 550, 757]. Hypervelocity impacts induce material failure, cracks, craters, debris. *High-velocity impacts* are in-between low-velocity and hypervelocity impacts, with pre-impact velocities ≈ 100 m/s. Body vibrations, temperature rise in the bodies, may not be neglected any longer.

The discrepancy between very low, and low velocities impacts, is that one may observe that $e_{\rm n}$ increases when the pre-impact velocity increases for the former, while $e_{\rm n}$ decreases as the pre-impact velocity increases for the latter. See Sect. 4.2. In nonsmooth mechanics one usually deals with low-velocity impact. However very low velocities and high velocities may be considered as well.

2.3 Viscoelastic Models with Dry Friction Elements: Viscoelasto-Plastic Models

We have focused almost uniquely on very simple assemblies of one spring and one dashpot. Many types of more complex assemblies and patterns have been proposed and analyzed in the Solid Mechanics literature, like generalized Kelvin-Voigt, generalized Maxwell, ladder, Masing models, etc. [100, 103, 104, 1219]. Some of these assemblies are made of springs, dashpots and dry friction elements which aim at modeling plasticity. A "dry friction element", also called a Saint-Venant element, produces a force of the form $F \in -F_c \mathrm{sgn}(v)$, where $\mathrm{sgn}(v) = [-1, 1]$ when $v = 0$, $\mathrm{sgn}(v) = 1$ if $v > 0$ and $\mathrm{sgn}(v) = -1$ if $v < 0$, and $F_c \geq 0$ is known as a Coulomb's force.[25] In the Systems and Control literature this is known as a relay function. Bastien et al. [100, 103, 104] proved that some of these assemblies define maximal monotone mappings. This is a useful step for both mathematical (existence and uniqueness of solutions of the dynamics with set-valued right-hand side) and physical (dissipativity of the contact model) viewpoints. We already tackled this issue in Sect. 2.1.3.4, see Fig. 2.2. Let us focus on the assembly studied in [100], known as Persoz's gephyroidal model,[26] introduced in [997] and depicted in Fig. 2.6. The dry friction elements have the force/velocity set-valued laws $G_i \in -\alpha_i \mathrm{sgn}(\dot{v}_i)$ for $i = 2, 3$ and $G_1 \in -\alpha_1 \mathrm{sgn}(\dot{u}_1)$. The linear springs have the force/displacement laws $F_i = -k_i u_i$, $i = 1, 2, 3$. In order to derive the equations governing this system, we need the following bilateral constraints: $u_0 + v_3 + u_2 = x$, $v_2 + u_3 + u_0 = x$, $u_1 + u_3 = v_3$, plus the force balance equations $G_2 + F_1 + G_1 = F_3$, $G_3 + F_3 = F_0$, $G_3 + G_1 + F_1 = F_2$, and $m\ddot{x}(t) = F_0(t) + F(t)$. There are 14 unknowns and 14 equations. Then the following is true.

[25] Coulomb's friction is introduced in more detail in Sect. 5.3.

[26] The word gephyroidal comes from the Greek "bridge".

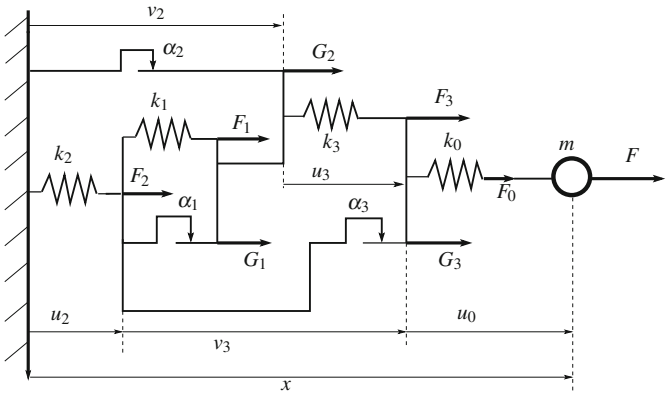

Fig. 2.6 Persoz's rheological (gephyroidal) contact model

Proposition 2.2 *[98, 100] Let* $K = \begin{pmatrix} k_0+k_2 & k_0 & -(k_0+k_2) \\ k_0 & k_0+k_3 & -(k_0+k_3) \\ -(k_0+k_2) & -(k_0+k_3) & k_0+k_1+k_2+k_3 \end{pmatrix}$, $G \triangleq \begin{pmatrix} G_2 \\ G_3 \\ G_1 \end{pmatrix}$, $\phi(G) \triangleq \sum_{i=1}^{3} \psi_{[-\alpha_i,\alpha_i]}(G_i)$, $U = (1\ 1\ -1)^T$, $E = k_0 U^T K^{-1}$, $\delta = k_0(1 - EU)$. *Let also* $k_0 = 0$ *and* $k_i > 0$, *or* $k_0 > 0$ *and at least two among* k_1, k_2, k_3 *are* > 0 ($\Leftrightarrow K = K^T \succ 0$). *Then the Persoz's gephyroidal system dynamics is given by:*

$$\begin{cases} \dot{x}(t) = y(t) \\ \dot{y}(t) = \frac{1}{m}(F(t) - \delta x(t) + EG(t)) \\ \dot{G}(t) + k_0 U y(t) \in -K\ \partial\phi(G(t)), \end{cases} \tag{2.34}$$

which is a differential inclusion of the type $\frac{dz}{dt}(t) - f(t, z(t)) \in -P\ \partial\varphi(z(t))$, $z(0) = z_0$, $P = P^T \succ 0$, *with* $\varphi(\cdot)$ *a proper convex lower semicontinuous function,* $\partial\varphi(\cdot)$ *its subdifferential, and* $P = diag(1, 1, K)$.

Apart from the elimination of some coordinates using the bilateral constraints, the proof uses some tools from convex analysis like the inversion of the dry friction laws (see Appendix B, Fig. B.4), which makes the indicator functions $\psi_{[-\alpha_i,\alpha_i]}(G_i)$ appear (that is, use is made of $x \in \text{sgn}(y) \Leftrightarrow y \in \partial\psi_{[-1,1]}(x) = N_{[-1,1]}(x)$, or the reader may also work with the function $f_4(\cdot)$ defined just above Fig. B.4). The obtained differential inclusion has a maximal monotone set-valued right-hand side, it is similar to the differential inclusion in (2.19) and its well-posedness may be shown using Theorem B.4. For this, one may perform a variable change as $x = R^{-1}z$ with $R = R^T \succ 0$ and $R^2 = P$. Thus, $\dot{x}(t) = R^{-1}\dot{z}(t) \in R^{-1}f(t, Rx(t)) - R\ \partial\varphi(Rx(t))$. Using Theorem B.2 and Lemma B.1, the result follows.

In [1286], similar assemblies called generalized Maxwell-slip friction models are proposed and analyzed for the sake of properly modeling frictional contact. Therein

the Saint-Venant element is not inserted inside the assembly structure, but at the interface between the assembly and the contact point. The Masing model with and without viscosity is depicted in Fig. 2.8a, b. The viscoelasto-plastic model of [1286] is in Fig. 2.8c. The dynamics of the viscous Masing model is given by the differential inclusion [101]:

$$\begin{cases} F(t) = kw(t) + k_0 u(t) + f\dot{u}(t) - k_0 l_0 \\ \dot{w}(t) - \dot{u}(t) \in -\partial\psi_{[-1,1]}\left(\frac{w(t)}{\eta}\right) \\ w(0) = w_0, \end{cases} \tag{2.35}$$

where $w = u_s - l, \eta = \frac{\alpha}{k}, u = u_s + u_t, u_s$ is the spring deflection, u_t is the dry friction element deflection, l and l_0 are the spring-free lengths. Once again the dry friction laws are inversed in this formulation. The existence and uniqueness of solutions for the differential inclusion in (2.35) may be proved using Theorem B.4. When $u(\cdot)$ is periodic, both viscous-free and viscous Masing's model possess a force/indentation (F, u) characteristic with hysteresis stick/slip loop as in Fig. 2.7, which is analyzed in [101]. Parameter identification is performed on a belt tensioner setup in [101].

The dynamics of the model in Fig. 2.8c is given by the differential inclusion:

$$\begin{cases} k_i a_i(t) + f_i \dot{a}_i(t) \in \alpha_i \gamma(t) \mathrm{sgn}(v(t) - \dot{a}_i(t)), \quad 1 \le i \le n \\ \dot{\gamma}(t) = \frac{g(v(t)) - \gamma(t)}{\tau_d} \\ F_c \le \gamma(0) \le F_s, \end{cases} \tag{2.36}$$

where each dry friction element produces the force $\alpha_i \gamma(t)\mathrm{sgn}(v(t) - \dot{a}_i(t))$, $\tau_d > 0$, and $g(v) = F_c + (F_s - F_c)\exp\left(-\left|\frac{v}{v_s}\right|^{\beta}\right)$ models the Stribeck effect during sliding motions, where $0 < F_c < F_s$ so that $g(v) > 0$. This model captures frictional lag with the added state variable $\gamma(\cdot)$. Starting the analysis of (2.36), it is noteworthy that the first line involves $\dot{a}_i(t)$ in both sides of the inclusion.

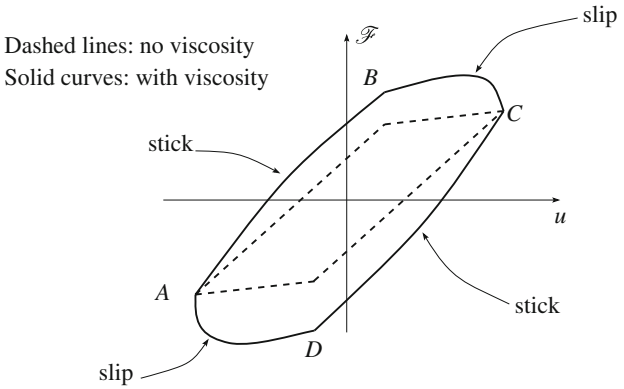

Fig. 2.7 Hysteresis loops in Masing's models with and without viscosity

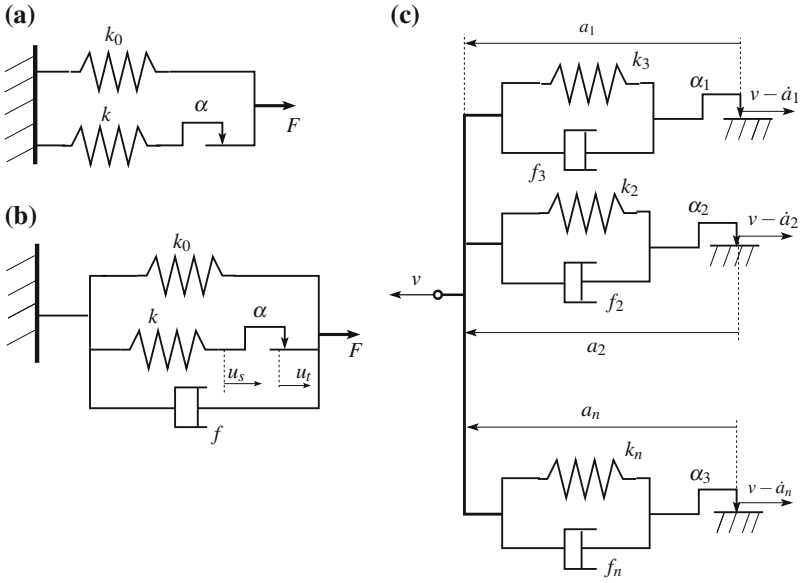

Fig. 2.8 Masing and viscoelasto-plastic contact models

Inverting this inclusion following the tools in Appendix B (see (B.15) and (B.16)) we obtain $-v(t)+\dot{a}_i(t) \in -N_{[-1,1]}\left(\frac{k_i a_i(t)+f_i \dot{a}_i(t)}{\alpha_i \gamma(t)}\right)$. Using (B.20) and the fact that $\gamma(t) > 0$ we infer that $f_i \dot{a}_i(t) + k_i a_{(}t) = \alpha_i \gamma(t)\text{proj}\left([-1,1]; \frac{f_i v(t)+a_i(t)}{\alpha_i \gamma(t)}\right)$. The projection operator is Lipschitz continuous, and one finds by inspection that it may be rewritten using a saturation function sat$(\cdot)$, which is familiar to the Control scientific community. The friction contact force is therefore found to satisfy $F = \sum_{i=1}^{n}(k_i a_i + f_i \dot{a}_i) = \sum_{i=1}^{n} \text{sat}(\alpha_i \gamma(t), k_i a_i(t) + f_i v(t))$. Here sat$(z, x) = 1$ if $x \geq z$, -1 if $x \leq -z$, z if $|x| \leq z$, $z \geq 0$. It is proved in [1286] that this model guarantees that the nonviscous part of the frictional force is bounded, the friction force is time-continuous, and most importantly it is dissipative with storage function $V(a_i) = \sum_{i=1}^{n} \frac{k_i}{2} a_i^2$, and supply rate vF. It is also free of spurious drifting phenomena during sticking modes. Further studies on the same type of assemblies may be found in [1284, 1285]. They are used for energy transfer purpose in two-degree-of-freedom systems in [1077]. All these models, which are encapsulated into differential inclusions with maximal monotone set-valued right-hand side, can be discretized with implicit Euler methods as described in Sect. 5.7.3.4, whose convergence is analyzed in [97, 102].

Remark 2.8 (*Saturation from relay*) As pointed out in [664], the feedback system in Fig. 2.9 realizes a saturation function. This is easily proved using conjugacy, inversion (Definition B.11, (B.16) and Fig. B.4), and (B.20). Let all vari-

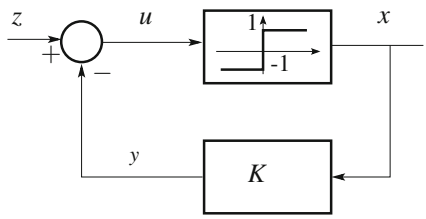

Fig. 2.9 Realization of saturation via set-valued relay

ables be $n-$dimensional, and $\mathrm{sgn}(u) \stackrel{\Delta}{=} (\mathrm{sgn}(u_1), \mathrm{sgn}(u_2), \ldots, \mathrm{sgn}(u_n))^T$.[27] We have $x \in \mathrm{sgn}(u)$ with $u = z - y$ and $y = Kx$, thus $x \in \mathrm{sgn}(z - Kx) \Leftrightarrow Kx - z \in -N_{[-1,1]^n}(x) \stackrel{K=K^T\succ 0}{\Longleftrightarrow} x = \mathrm{proj}_K([-1, 1]^n; K^{-1}z)$, showing that x is a Lipschitz continuous function of z. Let $K = 1$ and $n = 1$, then $x = \mathrm{proj}([-1, 1]; z)$ which is the classical saturation function $\mathrm{sat}(z)$.

2.3.1 Conclusions and Further Reading

The complementarity conditions and associated convex analysis results, prove to be quite powerful tools to enhance the basic spring-dashpot model. It allows the designer to guarantee some fundamental properties of the assemblies like dissipativity, well-posedness, maximal monotonicity using results on complementarity dynamical systems, or differential inclusions with maximal monotone right-hand side (see (2.5), (2.16), (2.27), (2.34), (2.35) and (2.36)). This has important consequences for Mathematical and Numerical Analysis, as well as for Control. Many other assemblies of linear springs and Saint-Venant elements are studied in [103]. Such rheological models are introduced to represent elastoplastic behaviors of materials. The main issue after their dissipativity is to determine whether these assemblies are well-posed, i.e., do they yield a unique contact force and do they define an operator which yields a well-posed dynamical system. The differential inclusion framework adopted in [98, 99, 100, 101, 103] and in [1284, 1285, 1286] is very powerful. A tentative classification of rheological models made of assemblies of linear springs, linear dashpots, and dry friction elements, is made in [103, Table I] from the structure of the convex function $\varphi(\cdot)$ as in Proposition 2.2. It is noteworthy that the analysis that yields Proposition 2.2 as well as the dynamics in (2.35) does not take into account the unilateral feature of the contact: a complementarity condition that rules detachment from the constraint has to be added. It should in particular guarantee $F(t) \geq 0$. Assemblies of spring and fractional order dashpot elements are studied in [908, 1313]: such fractional-elastic rheological models apply to polymer materials. It is noteworthy that various types of assemblies quite similar to the above ones may be used for

[27] Such a definition is logical if one thinks of $\mathrm{sgn}(\cdot)$ as the subdifferential of $f(u) = |u_1| + |u_2| + \ldots + |u_n|$.

vibration absorbers design [545]. The various viscoelastic models reviewed above, show an hysteretic force/indentation law. However the hysteresis phenomenon may be velocity-independent and due only to Coulomb's friction effects, like in felt where the interacting fibers rub each other [817].

2.4 Penalizing Functions in Mathematical Analysis

The goal of the studies summarized below, is to prove that some sequence of second order differential equations $\mathscr{P}_{n,Q}: \ddot{q}_n(t) + F_n(q_n(t), \dot{q}_n(t)) = Q(t, q_n(t), \dot{q}_n(t))$, that is considered to represent the physical model of a body colliding with a compliant constraint, converges towards a limit problem in which the constraints are rigid, i.e., unilateral. By convergence it is meant that solutions $q_n(\cdot)$ converge as $n \to +\infty$. The functions $F_n(\cdot)$ are called penalizing functions and aim at modeling the elasticity and the viscous damping of the body's surface. In all the results that follow, it is assumed a constraint surface of codimension 1, i.e., $f(q) \in \mathbb{R}$, and satisfying the basic requirements of Definition 1.8. The case of multiple unilateral contacts is more tricky, see Chaps. 5 and 6.

Remark 2.9 The dynamical systems that are studied as the limit of a sequence of compliant, or penalized problems, belong to the class of Measure Differential Inclusions: indeed they possess a set-valued right-hand side (due to the unilateral constraints and complementarity conditions), moreover they involve velocity discontinuities at impacts, hence acceleration and contact force are Dirac measures at impact times. Typically, a system like in Example 1.6 with fixed $y(t) = y_0$ can be analyzed with the following tools, showing that the inextensible cable is really a limit of stiff cables.

2.4.1 The Elastic Rebound Case

The basic assumption is that energy is conserved at the impacts. The considered problem is the following and deals with a one-degree-of-freedom system:

Problem 2.1 [260, 261] A locally Lipschitz function $q(\cdot)$ defined on $[0, T]$ is a solution of the one-dimensional rebound problem $\mathscr{P}_Q$ if:

(**a**) $q(t) \leq 0$ on $[0, T]$.
(**b**) $\langle \ddot{q} - Q, \varphi \rangle \leq 0$ for all $\varphi \in \mathscr{D}_{[0,T]}$, $\varphi \geq 0$, $Q \in L_1([0, T])$.
(**c**) If $q < 0$ then $\ddot{q} - Q = 0$ in the distributional sense.
(**d**) $\forall t \in [0, T]$, $\dot{q}(t^+)$ and $\dot{q}(t^-)$ exist, $\dot{q}(0^+)$ and $\dot{q}(0^-)$ exist, $\frac{1}{2}[\dot{q}(t^+)]^2 - \frac{1}{2}[\dot{q}(0^+)]^2 = \int_0^t Q(\tau)\dot{q}(\tau)d\tau$, and the equality holds also for $\dot{q}(t^-)$.

The initial data are naturally assumed to be admissible, in particular if $q(0) = 0$ then $\dot{q}(0^+) \leq 0$, in order not to violate the constraint. (**a**) is the unilateral constraint

condition; (**b**) means that the (impulsive) interaction force at impacts is a negative measure, i.e., there is a measure μ such that $\ddot{q} - Q = \mu$ and $\langle \mu, \varphi \rangle$ is either negative or zero if $q < 0$ as stated by (**c**), which merely means that the smooth dynamical equations are verified (in Example 1.1 we have $\mu = p_k \delta_{t_k}$ and $p_k = -2m\dot{q}(t_k^-) < 0$ when the shock is lossless. Adopting the notations of Chap. 1, we get $\ddot{q} = \{\ddot{q}\} + \sum \sigma_{\dot{q}_k} \delta_{t_k}$, so that (**b**) and (**c**) becomes $\sigma_{\dot{q}}(t_k) < 0$ and $\{\ddot{q}\} = Q$). (**d**) is a dissipation equality which rules the energetical behavior of the system (including at impacts), and the supply rate is the product $Q\dot{q}$, where Q is an external force applied on the system.

One therefore realizes that except for trivial cases ($Q \geq 0$ and $q(0^-) = 0$ or $Q \leq 0$) μ is atomic with atoms the zeros of q. The first aim of these works is to prove the existence of a solution to $\mathscr{P}_Q$. Existence is studied in [260] by choosing in $\mathscr{P}_{n,Q}$ a continuous penalizing function $F_n(q_n(t))$ such that the contact force satisfies $F_n(\zeta) = 0$ if $\zeta \leq 0$, $F_n(\zeta) > 0$ for $\zeta > 0$, $F_n \to +\infty$ on any compact interval of $(0, +\infty)$, and $\lim_{\zeta \to 0^+} \lim_{n \to +\infty} \frac{F_n(\zeta)}{\alpha_n(\zeta)} = +\infty$, with $\alpha_n(\zeta) = \int_0^\zeta F_n(\tau) d\tau$. It is easy to verify that the spring-like environment studied in the preceding part of this chapter fits within this framework (thus clearly such penalizing functions aim at modeling a spring, but other examples with no clear physical meaning may be found, see [260]). Theorem 1 in [260] states that if $q_n(\cdot)$ is a solution to $\mathscr{P}_{n,Q}$ that tends uniformly to a function $q(\cdot)$, then $q(\cdot)$ is a solution of $\mathscr{P}_Q$, and that there exists at least one solution to $\mathscr{P}_Q$ for each initial data, which is the uniform limit of some sequence $\{q_n(\cdot)\}$.

Buttazzo and Percivale [241, 242, 989, 990] considered the same problem $\mathscr{P}$ as Problem 2.1, however for n-degree-of-freedom systems. Similar results as in [260, 261] are obtained in [241] (a paper written between the other two) for the one-dimensional case. Condition (**c**) is stated in [241] (as well as in [242, 989, 990] for the higher-dimensional case) as $\text{supp}(\ddot{q} - Q) \subseteq \{t \in [0, T] | q(t) = 0\}$, *i.e.,* the support of the distribution $\ddot{q} - Q$ is contained in the set of zeros of $q(t)$ when the particle attains the constraint. The results in [242, 989, 990] incorporate a variational formulation of the elastic bounce problem. We shall come back in more details on these articles in Chap. 3, Problem 3.1.

2.4.2 The Case with Dissipation (Linear Viscous Friction)

Let us describe now the work in [969], which considers a rebound problem with possible dissipative collisions. The problem is the following:

Problem 2.2 (*Constant Mass Matrix* [969]) Let $F : [0, T] \times \mathbb{R}^n \times \mathbb{R}^n \to \mathbb{R}^n$ be continuous in t, q, $\dot{q}$ and Lipschitz in q, $\dot{q}$, uniformly with respect to q, Φ be a closed convex domain $\subset \mathbb{R}^n$, with nonempty interior and with smooth boundary $\text{bd}(\Phi)$. Then, $q : [0, T] \to \mathbb{R}^n$ is a solution of the problem $\mathscr{P}_F$: $\ddot{q} + \partial \psi_\Phi(q) \ni F(t, q, \dot{q})$, $\dot{q}_{\text{n}}(t_k^+) = -e_{\text{n}} \dot{q}_{\text{n}}(t_k^-)$ when $q(t_k) \in \text{bd}(\Phi)$, where the subscript $_{\text{n}}$ denotes the component normal to $\text{bd}(\Phi)$, $e_{\text{n}} \in (0, 1]$, if $q(\cdot)$ fulfills the following:

(**a**) $q(\cdot)$ is Lipschitz continuous and $\dot{q}$ is of bounded variation.
(**b**) $q(t) \in \Phi$ for all $t \in [0, T]$.
(**c**) for any continuous function $v : [0, T] \to \Phi$, $\langle v - q, F - \ddot{q} \rangle \leq 0$.
(**d**) the initial data satisfy $\dot{q}_{\mathrm{n}}(0^+) = -e_{\mathrm{n}}\dot{q}_{\mathrm{n}}(0^-)$ when $\dot{q}(0^-)$ points outwards Φ.

Condition **(c)** concerns the reaction on the constraint boundary $\mathrm{bd}(\Phi)$. When $q \in \mathrm{Int}(\Phi)$ then the subdifferential is reduced to $\{0\}$ and the inequality is trivially satisfied. When $q \in \mathrm{bd}(\Phi)$, there is a reaction $\lambda = \ddot{q} - F$ acting on the particle to maintain it inside Φ (mathematically speaking λ is a measure). Hence the inequality in **(c)** can be rewritten as $\langle v - q, \lambda \rangle \geq 0$. Notice that v is a function that takes its values in Φ. This permits to assert that **(c)** implies that $-\sigma_{\dot{q}}(t_k) \in T_{\Phi}(q(t_k))$ (see Definition B.2 for the tangent cone to a closed convex set). The inequality **(c)** means that $(F - \ddot{q})$ is a subgradient of the indicator function $\psi_{\Phi}(\cdot)$, i.e., $\psi_{\Phi}(v) - \psi_{\Phi}(q) \geq (F - \ddot{q})(v - q)$ for all $v \in \mathbb{R}$. Thus $(F - \ddot{q})$ is a vector that belongs to the subdifferential $\partial\psi_{\Phi}(q)$, by definition. See Appendix B for more details.

Example 2.1 Let us consider $q(t) \in \Phi = [a, b]$, $b > a$ real numbers, for all $t \in [0, T]$. Then the following formulations are equivalent (impacts are disregarded):

$$\begin{cases} \ddot{q} = F(t, q, \dot{q}) + \mu \ \text{ in the sense of distributions,} \\ q \in C^0\left([T, T']; \Phi\right), \\ \langle \mu, v - u \rangle \leq 0, \forall\, v \in C^0\left([T, T']; \Phi\right), \ \text{or equivalently :} \ \ \mathrm{supp}(\mu) \subset \{t | u(t) \in \mathrm{bd}(\Phi)\}, \\ \mu \geq 0 \text{ on } \{t | u(t) = a\}, \mu \leq 0 \text{ on } \{t | u(t) = b\}. \end{cases} \tag{2.37}$$

or:

$$\ddot{q}(t) + \partial\psi_{\Phi}(q(t)) \ni F(t, q(t), \dot{q}(t)), \tag{2.38}$$

where (see Appendix B) $\partial\psi_{\Phi}(q) = N_{\Phi}(q) = \begin{cases} \{0\} \text{ if } a < q < b \\ \mathbb{R}^+ \text{ if } q = b \\ \mathbb{R}^- \text{ if } q = a \end{cases}$. This can be seen from the fact that since there are two constraints $f_1(q) = q - a \geq 0$ and $f_2(q) = b - q \geq 0$, one gets $\nabla f_1(a) = 1$, $\nabla f_2(b) = -1$.

A solution $q(\cdot)$ to $\mathscr{P}_F$ is shown to exist by studying the limit of the solutions of a sequence of approximating problems $\mathscr{P}_{n,F}$ with penalizing function $F_n(q_n, \dot{q}_n) = F_{n,1}(q_n, \dot{q}_n) + F_{n,2}(q_n)$ using Yosida's approximants for the elastic term, and a discontinuous function for the viscous friction term (such discontinuity is easily understandable looking at the example above: the total vector field of the system considering both contact and noncontact phases is continuous if only elastic terms are present, but it is not if viscous friction is added). It is worth noting that the viscous friction term contains a coefficient ε that is equal to $\frac{f}{2\sqrt{k}}$ in the preceding section on approximation when $0 < e_{\mathrm{n}} \leq 1$, see (2.9). It is easy to show that $\mathscr{P}_{n,F}$ reduces to our example in the particular one-dimensional case, although the meaning of the approximants in higher dimensions is not obvious. Let us illustrate the theory developed in [969] on this simple one degree-of-freedom case.

Example 2.2 [969] In the case when $n = 1$, $F \equiv 0$ and $\Phi = \mathbb{R}^+$, the system can be written as

$$\begin{cases} \ddot{q}(t) + \partial\psi_{\mathbb{R}^+}(q(t)) \ni 0 \\ \\ \dot{q}(t_k^+) = -e_{\mathrm{n}}\dot{q}(t_k^-) \qquad \text{for all } t_k \text{ such that } \; q(t_k) = 0, \dot{q}(t_k^-) < 0. \end{cases} \tag{2.39}$$

This is the dynamical equations of a point striking an horizontal obstacle, with no external forces. The approximating problem chosen in [969] is

$$\ddot{q}_n(t) + 2\varepsilon\sqrt{k_n}\dot{q}_n(t)\mathrm{sgn}^-(q_n(t)) + k_n q_n(t)\mathrm{sgn}^-(q_n(t)) = 0 \tag{2.40}$$

where $k_n \to +\infty$ as $n \to +\infty$, $\mathrm{sgn}^-(q_n) = \begin{cases} 0 \text{ if } q \geq 0 \\ 1 \text{ otherwise} \end{cases}$, and $\varepsilon = -\frac{\ln(e_{\mathrm{n}})}{\sqrt{\pi^2+\ln^2(e_{\mathrm{n}})}}$.[28] The quantity $e_{\mathrm{n}} \in (0, 1]$ is the restitution coefficient. Note that the function $\mathrm{sgn}^-(q_n)$ allows to write contact and noncontact dynamics in a single equation. The switching conditions are therefore chosen when the position vanishes (as we know this may yield negative reaction forces). The signs are reversed with respect to the examples we have treated above, since free motion occurs now for $q \geq 0$. The initial conditions are chosen as $q_n(0) = a > 0$ and $\dot{q}_n(0) = b < 0$. Hence the mass point starts in the free-motion space with a velocity directed towards the obstacle. Denoting $\tau = -\frac{a}{b}$ and $\tau_n = \tau + \frac{\pi}{\sqrt{k_n(1-\varepsilon^2)}}$, the solutions can be explicitly obtained and are (we recall them for convenience although they have been already obtained above):

$$q_n(t) = \begin{cases} a + bt & \text{for } t \in [0, \tau] \\ e_{\mathrm{n}}^{-\varepsilon(t-\tau)\sqrt{k}} \sin\left[(t-\tau)\sqrt{k(1-\varepsilon^2)}\right] \frac{b}{\sqrt{k(1-\varepsilon^2)}} & \text{for } t \in [\tau, \tau_n] \\ -\exp\left(-\frac{\pi\varepsilon}{\sqrt{1-\varepsilon^2}}\right) b(t-\tau_n) & \text{for } t \in [\tau_n, +\infty[\end{cases} \tag{2.41}$$

Then clearly $q_n(t)$ in (2.41) converges towards

$$q(t) = \begin{cases} a + bt & \text{for } t \in [0, \tau] \\ -e_{\mathrm{n}} b(t-\tau) & \text{for } t \in [\tau, +\infty], \end{cases} \tag{2.42}$$

whose derivative possesses a discontinuity at $t = \tau$.

In case when there is some external force acting on the particle in the Example 2.2, then in general the equations are not integrable. But [969, Theorem 2] guarantees that the solution set of problem $\mathscr{P}_F$ possess an element (not necessarily unique) whose first derivative is of bounded variation. The theorem is stated as follows:

Theorem 2.1 (Constant mass matrix [969]) *Consider the system defined in Problem 2.2. This system admits a solution in the sense defined as in Problem 2.2,* **a**, **b**, **c**, **d**.

[28] Compare the value of the damping in this sequence of approximating problems with the value of the damping in (2.9). It is a common calculation to compute e_{n} for the spring-dashpot model, see [175, Eq. (3.44)].

This solution is obtained as the strong limit in $W^{1,p}([0,T],\mathbb{R}^n)$ *for all* $p \in [1,+\infty)$, *and weak* $\star$ *limit in* $W^{1,\infty}([0,T],\mathbb{R}^n)$,[29] *when* $n \to +\infty$, *of a subsequence of the sequence of solutions of*

$$\ddot{q}_n(t) + 2\varepsilon\sqrt{k_n}G(q_n(t) - P_\Phi(q_n(t)), \dot{q}_n(t)) + k_n(q_n(t) - P_\Phi(q_n(t))) = f(t, q_n(t), \dot{q}_n(t)) \tag{2.43}$$

with $q_n(0) = q_{n,0}$, $\dot{q}_n(0) = \dot{q}_{n,0}$. $P_\Phi(\cdot)$ *denotes the projection on* Φ,[30] *and* $G(v,w) = \begin{cases} \frac{(v^T w)v}{v^T v} & \text{if } v \neq 0 \\ 0 & \text{if } v = 0. \end{cases}$

From the one-degree-of-freedom case in Example 2.2, the different terms of the approximating problems correspond to spring and damper-like actions, with the "usual" switching conditions of Sect. 2.1.3.1. It is clear that due to the chosen switching conditions, the damping term in (2.43) may induce discontinuities in the ODE right-hand side. One may choose to embed (2.43) into Filippov's framework of differential inclusions by convexifying the discontinuous vector field, hence guaranteeing the existence of global absolutely continuous solutions $(q_n(\cdot), \dot{q}_n(\cdot))$ (and, due to the particular structure of a mechanical system, $q_n(\cdot)$ is even continuously differentiable). The proof is redone from scratch in [969].

The proof proceeds in showing that $\mathscr{P}_{n,F}$ possesses L_∞-bounded solutions that converge to q, and that $F_{n,1}(q_n, \dot{q}_n)$ and $F_{n,2}(q_n)$ converge weakly$\star$ towards measures P_1 and P_2 such that $\ddot{q} - F = P_1 + P_2$, and (**c**) is true. The last part of the proof is dedicated to study the rebound conditions. It is clear that since this study encompasses the case of the bouncing ball with $0 < e_n < 1$, finite accumulation points in the impact sequence $\mathscr{P}_F$ are tolerated. This is in contrast with the results in Problems 2.1 and 3.1 that rely on energy preservation at impacts (see [260, Theorems 3 and 4] [989 Lemma 2.1], where it clearly appears that $t_k < t_{k+1}$ for all k is a crucial property for uniqueness). Theorem 2.1 may also be used to study the existence of solutions for the cable system dynamics in Example 1.6 when a restitution impact law is considered.

In Problem 2.2 and Theorem 2.1, the inertia matrix is supposed to be identity, so that the gradient on the configuration manifold is the one in $\mathbb{R}^n$, and the configuration space is Euclidean. On the other hand, the admissible domain Φ defined by the unilateral constraint may not be convex as supposed in Problem 2.2. Actually the convexity of Φ is convenient to assure a unique projection $P_\Phi(q_n)$ in the penalization. Some ideas allowing one to relax the convexity are given in [972, 973]. They are based

---

[29] $W^{1,p}$, $1 \leq p \leq \infty$, denotes Sobolev spaces [191].

Definition 2.2 Let $1 \leq p \leq +\infty$. The Sobolev space $W^{1,p}(I)$, where $I \subset \mathbb{R}$ is an open interval (bounded or not), is the set of functions $f(\cdot)$ such that

(i) $f \in L^p(I)$.

(ii) There exists a function $g \in L^p(I)$ such that $\int_I f\dot{\varphi} = -\int_I g\varphi$ for all $\varphi \in \mathscr{D}$ whose support is contained in I.

Any function $f \in L_p$ possesses a distributional derivative that belongs to $\mathscr{D}^\star$ (see definitions in Appendices A.1 and A.2). Then $f \in W^{1,p}$ if this distributional -or generalized- derivative coincides in $\mathscr{D}^\star$ with a function in L_p. See also Sect. A.1.3 for basic facts about strong and weak$\star$ convergence.

[30] This why Φ is assumed to be convex: this secures a unique projection.

on the use of a discretization of the dynamics, see Sect. 5.7.3. Schatzman relaxed both assumptions in [1070], using the kinetic metric to define the restitution rule in a specific transformed generalized velocity.[31] In [1070] the projection is however applied to positions, in order to enable one to formulate a penalized problem (i.e., a sort of generalized spring-dashpot).

Problem 2.3 (Non-Trivial Mass Matrix [1070]) Let the constrained dynamics be $M(t,q)\ddot{q} = F(t,q,\dot{q}) + \lambda$, where: $M(t,q)$ is twice differentiable, $F(\cdot)$ is continuous in all its arguments, locally Lipschitz continuous in q and $\dot{q}$. The admissible domain $\Phi \subseteq [0,T] \times \mathbb{R}^n$, its boundary $\mathrm{bd}(\Phi(t))$ is a submanifold of class C^3 of $[0,T] \times \mathbb{R}^n$. The vector valued measure λ and the position q satisfy:

- $q(t) \in \Phi$ for all $t \in [0,T]$,
- $\mathrm{supp}(\lambda) \subset \{t \in [0,T] | q(t) \in \mathrm{bd}(\Phi(t))\}$,
- $\lambda = \tilde{\lambda} M(\cdot,q) m(\cdot,q)$, where is the unitary exterior normal vector to $\Phi(t)$.

The vector $m(t,q)$ satisfies $m(t,q)^T M(t,q) m(t,q) = 1$, and when contact is active it is the normal to $\mathrm{bd}(\Phi(t))$ in the kinetic metric (which we shall denote as $\mathbf{n}_q$ in Chap. 6). In case Φ is finitely represented as $\Phi = \{q \in \mathbb{R}^n | f(q) \geq 0\}$, $f : \mathbb{R}^n \to \mathbb{R}$, then it is equal to $\frac{M(q)^1 \nabla f(q)}{\sqrt{\nabla f(q)^T M(q)^{-1} \nabla f(q)}}$ on its boundary. Imposing C^3 regularity on the boundary $\mathrm{bd}(\Phi)$ allows one to locally linearize it. The restitution law is applied to the velocity $\dot{q}_{\mathrm{n}} \stackrel{\Delta}{=} m(\cdot,q) \frac{d}{dt}[m(\cdot,q)^T M(\cdot,q)(q - P_{\mathrm{bd}(\Phi)}(\cdot,q))]$, where $P_{\mathrm{bd}(\Phi)}(\cdot,q)$ is the projection of q on the (time-varying) boundary. A generalized penalization term is introduced and the sequence of solutions of the penalized problems is shown to converge to solutions of the rigid body problem (uniformly for positions, strongly in all spaces L^p with $1 \leq p < +\infty$ for velocities).

Theorem 2.1 might also be considered as a mathematical preliminary study for dynamical analysis of systems like particles bouncing inside a closed[32] curve which are called in mathematical physics *billiards* [137, 683, 1114]. Thus the problem is completely treated from the existence of solutions (but not uniqueness) to the trajectories global behavior. It is noteworthy that the case of nonsmooth $\mathrm{bd}(\Phi)$ is treated also in [966], when the kinetic energy loss satisfies $T_L(t_k) = 0$ at impact times t_k. The shock conditions are then stated simply from the energy conservation equation (see Problems 2.1 and 3.1), which avoids the difficulty encountered with restitution rules at singularities, where the normal to the boundary $\mathrm{bd}(\Phi)$ at q does not reduce to a half-line in $\mathbb{R}^n$, but is the normal cone $N_\Phi(q)$. This proves the existence of a solution in the sense of Problem 2.2, with $\dot{q} \in RCLBV$, for billiards with nonsmooth boundaries and elastic collisions (inside a polygon for instance, see [683, §6.4]).

[31] The use of the kinetic metric to analyze impact dynamics in Lagrangian systems, may be traced back to [581, 589, 683], and in the first edition of this book [202]. It has been deeply used in [209, 210, 228].

[32] Note that closed is to be taken here in the physical or real-world meaning, whereas closed in the Paoli-Schatzman's problem is to be taken in the topological sense, i.e., the whole space itself is in fact closed.

The results of Paoli and Schatzman extend the results in [683, Chap. 1, Theorems 1, 2, 3 and 4] which possess a local-in-time nature only (they are based on singular perturbation like analysis). Schatzman's pioneering work in [1066] treated the same problem, but with an energy conservation equality. It is based on the use of Moreau-Yosida regularization arguments (intuitively, this consists of introducing some penalization into the contact model, see Appendix B).

2.4.3 Uniqueness of Solutions

Since the preceding results deal with the existence of solutions, it is natural to say few words on an other important property: the uniqueness of solutions. We will come back later on this in Chap. 5, in particular Theorem 5.3 states general conditions on the well-posedness of frictionless complementarity Lagrangian systems. In the following we illustrate through an example given by Aldo Bressan in [186], improved later in [80, 1066], how the external action on the system may imply non uniqueness of solutions.

2.4.3.1 Aldo Bressan's Counter-Example

We describe in this section a counter-example invented by Aldo Bressan [186] to prove that the addition of unilateral constraints can, even in very simple cases, yield nonuniqueness of solutions for some initial data, even if smooth (infinitely differentiable) forces are considered. Similar counter-examples have been derived and improved later in [80, 260, 1066]. Let us consider the one degree-of-freedom system:

$$\ddot{q}(t) = Q(t), \quad q(t) \geq 0 \text{ for all } t \geq 0, \quad \dot{q}(t_k^+) = -e_{\mathrm{n}}\dot{q}(t_k^-), \; q(t_k) = 0, \; \dot{q}(t_k^-) < 0, \tag{2.44}$$

and the function:

$$\varphi(t) = \begin{cases} 0 & \text{if } t \leq 0 \text{ or } t = \frac{1}{2^m} \\ \frac{1}{2^{nm}} f\left[2^m f(t - \frac{1}{2^m})\right] = \frac{1}{2^{nm}} f(2^m t - 1) & \text{if } \frac{1}{2^m} < t < \frac{1}{2^{m-1}} \\ g(t) & \text{if } t \geq 1, \end{cases} \tag{2.45}$$

where $m \in \mathbb{N}$, $n \in \mathbb{N}$. The functions $f(\cdot)$ and $g(\cdot)$ satisfy the following conditions:

$$\begin{cases} f : [0,1] \to \mathbb{R} & f(t) > 0, f(0) = f(1) = 0 \\ \frac{df}{dt}(0) = -e_n 2^{1-n} \frac{df}{dt}(1), \; n \geq 3, \; 0 < e_n \leq 1 \\ \frac{d^k f}{dt^k}(0) = \frac{1}{2^{n-k}} \frac{d^k f}{dt^k}(1), & k = 2, \cdots, n-1, \end{cases} \tag{2.46}$$

and:

$$\begin{cases} g(t) > 0 \ \text{ for } \ t \geq 1, \ g(1) = 0, \ \frac{dg}{dt}(1) = \frac{-e_n}{2^{n-1}} \frac{df}{dt}(1) > 0 \\ \\ \frac{d^k g}{dt^k}(1) = \frac{1}{2^{n-k}} \frac{d^k g}{dt^k}(1), \ k = 2, 3, \cdots, n. \end{cases} \tag{2.47}$$

Then the following is true:

Theorem 2.2 *[186] The functions $\varphi(t)$, $\ddot{\varphi}(t)$,$\cdots$, $\varphi^{(n)}(t)$ exist, are continuous and $\varphi(t) \geq 0$ for all $t \in \mathbb{R}$, $\varphi(t) > 0$ for $t > 0$ and $t \neq \frac{1}{2^m}$. The first derivative $\dot{\varphi}(t)$ exists, is continuous for all $t \neq \frac{1}{2^m}$ and*

$$\dot{\varphi}\left[\left(\frac{1}{2^m}\right)^+\right] = -e_n \dot{\varphi}\left[\left(\frac{1}{2^m}\right)^-\right]. \tag{2.48}$$

Hence one has defined a function $\varphi(\cdot)$ which is zero for negative times, then it is composed on $[0, 1]$ of the concatenation of arches whose length tend to zero when t tends to zero (with a sort of reversed accumulation point at $t = 0^+$, that one usually calls a *right-accumulation* because the impacts accumulate on the right of the accumulation time, here $t = 0$: the derivative $\dot{\varphi}(\cdot)$ starts with a reversed accumulation of jumps). Now assume that $\ddot{f}(t) < 0$ and that $\ddot{g}(t) \leq 0$. Then $\ddot{\varphi}(t) \leq 0$ for all $t \in \mathbb{R}$. Roughly, the idea is to get $q(t) \equiv \varphi(t)$ (hence $Q(t) \equiv \ddot{\varphi}(t)$), so that the mass bounces against the constraint (see (2.48)) with a restitution coefficient e_n. This can be obtained as proved in the following:

Theorem 2.3 *[186] Let us choose $Q(t) = \ddot{\varphi}(t)$ in (2.44). Then the functions $Q(t)$, $\dot{Q}(t)$, $\cdots$, $Q^{(n-3)}(t)$ are continuous. The trajectory $q(t) \equiv \varphi(t)$, $t \in \mathbb{R}$, possesses the initial conditions $q(0) = \dot{q}(0) = 0$ and satisfies $\dot{q}(t_m^+) = -e_n \dot{q}(t_m^-)$, $m \in \mathbb{N}$, i.e., it is a trajectory of the dynamical system in (2.44). The trivial trajectory $q(t) = 0$ for all $t \geq 0$ is also a solution of the dynamical equations in (2.44).*

Such a result is surprizing, since the applied force is always negative. Hence, if one initializes the system at rest on the surface $q = 0$, it should logically remain stuck on it. The underlying idea is to consider an external action $Q(t)$ which is negative, but such that its double integral $\varphi(t)$ is positive, is zero at $t = 0$, continuous, and with a first integral $\dot{\varphi}(t)$ that jumps when $\varphi(t)$ attains zero ($t_m = \frac{1}{2^m}$). Clearly such a function is not obvious to construct, but Theorem 2.2 guarantees its existence (an explicit construction of similar functions has been given for instance in [80, 260, 1066]). As shown in [80, 81] in a broader context admitting several frictionless unilateral constraints and a generalized Newton's restitution impact law, analytic data eliminate such right-accumulations of impacts.

2.4.3.2 Sufficient Conditions for Uniqueness

For the sake of completeness of the exposition of the existing mathematical studies on systems with unilateral constraints, we provide now the conditions that have been derived by some authors to prevent such nonuniqueness problems. Using a similar counter-example as [186], [260, 1066] show that uniqueness of solutions to $\mathscr{P}_Q$ may fail even for smooth Q, and give some sufficient conditions for uniqueness to hold:

Theorem 2.4 *[260] Let $Q(\cdot)$ be absolutely continuous in $[0, T]$, $Q \in L^1([0, T])$ and $Q(t) \geq 0$ for all $t \in [0, T]$. Then if $Q(0) > 0$ and $x(0) \neq 0$, $\dot{x}(0^+) \neq 0$, there exists a unique solution to the dynamical problem formulated as in Problem 2.1. If the initial conditions are admissible (i.e., if $x(0) = 0$ then $\dot{x}(0^+) \leq 0$) and if $\dot{x}(0^+)^2 - 2x(0)Q(0) > 0$, then the solution is unique also on $[0, T]$.*

Notice that the signs of the pre and post-impact velocities as well as those of the contact force, are reversed here because the constraint is written as $x \leq 0$ in Problem 2.1 (see Remark 1.4 in Sect. 1.3). The proof is based on several steps. The central fact is that there is a finite number of impact times t_k on $[0, T]$. A sufficient condition for this is that $\dot{x}(t_k^+)^2$ (or equivalently $\dot{x}(t_k^-)^2$) be strictly positive. The conditions of Theorem 2.4 aim at guaranteeing such condition, which can be verified using the conservation of energy equation. In another article [261] the same authors prove the following result:

Theorem 2.5 *[261] The uniqueness of solutions to the Cauchy Problem 2.1 is a generic*[33] *property in $Q \in L_1([0, T], \mathbb{R})$.*

This result shows the prevalence of problems $\mathscr{P}_Q$, i.e., in fact of a particular type of second order differential equations, with unique solutions, as it is the case for ODEs with continuous right-hand sides as Orlicz showed (see [1229]). Note that when the impact is lossless the simple dynamical problem studied in Chap. 1, Example 1.1, is a particular case of problem $\mathscr{P}_Q$ in [261] with a zero external action: thus the results in [261] on uniqueness of the solution trivially hold for that case. In [261] uniqueness is studied as follows: it is shown that for every solution $x(\cdot)$ to $\mathscr{P}_Q$ with force $Q \in L_1$, $Q(\cdot)$ simple[34] there is a sequence $Q_n(\cdot) \to Q(\cdot)$ in L_1 so that $\mathscr{P}_{Q_n}$ has a unique solution $q_n(\cdot) \to q(\cdot)$ uniformly in $[0, T]$. Roughly one then uses density of the set of simple and L_1-bounded functions in the set of L_1-bounded functions to obtain the result in Theorem 2.5.

The first result on uniqueness that applies to n-dimensional System has apparently been given by M. Schatzman in [1066], who established the following result, in addition to existence of solutions in a more general context (external forces are admitted). The problem is that of a system with constant (identity) mass matrix and no external forces, constrained in a convex set.

---

[33] See [533, p. 154]: a property is generic in E if the set G of elements of E which possess it, contains a dense (in E) open set. In a sense, one deduces from the property of density of a set in another one that there are elements of G "almost everywhere" in E.

[34] i.e., $Q([0, T])$ is finite, i.e., it consists of a finite set of numbers $c_1, \cdots, c_n$. In other words, the external action is piecewise-constant, with a finite number of values.

Theorem 2.6 *[1066] Consider the differential inclusion* $\ddot{q}(t) \in -\partial\psi_{\Phi}(q(t))$, $q(0) \in \Phi$, *where* Φ *is a closed convex set. If the boundary* $\mathrm{bd}(\Phi)$ *is of class* C^3 *and has strictly positive Gaussian curvature,*[35] *then the Cauchy problem admits a unique global solution (i.e., on* $[0, +\infty)$*) such that:* $q \in W^{1,\infty}([0, +\infty); \mathbb{R}^n)$, $q(t) \in \Phi$ *for all* $t \geq 0$, *the inclusion is satisfied in the sense of distributions,* $\dot{q}(\cdot)$ *has left and right limits everywhere, the energy is conserved. Moreover, if* $q(0) \in \mathrm{bd}(\Phi)$, *and* $\dot{q}(0^+)$ *is tangent to* $\mathrm{bd}(\Phi)$, *then* $q(\cdot)$ *runs along the geodesic of* $\mathrm{bd}(\Phi)$ *passing through* $q(0)$ *and tangent to* $\dot{q}(0^+)$, *with the speed* $||\dot{q}(0^+)||$. *If the initial data do not satisfy these constraints, then* $q(t)$ *is never tangent to* $\mathrm{bd}(\Phi)$ *and it has a finite number of reflections in a finite time.*

The considered system may be called a billiard. This result is extended in [989, 990] who prove uniqueness of solutions under some analycity conditions.

2.4.4 Further Existence and Uniqueness Results

Let us make a short bibliography of well-posedness results obtained in the literature, which do not necessarily rely on penalizing functions. The uniqueness problem has also been studied for a one degree-of-freedom case in [1069], see Chap. 1, Sect. 1.3.2. It applies to purely elastic as well as nonconservative collisions. A general uniqueness result is proved in [80] who shows that if all the data (including external actions) are piecewise analytical (which is not a restrictive assumption in most applications), then uniqueness of solutions holds and right-accumulations of impacts created by forces like in Bressan's counter-example (see Theorem 2.3) cannot occur: only left-accumulations of impact may exist [81, Proposition 4.11], like in the classical bouncing ball system. Multiple, orthogonal (in the kinetic metric) constraints as well as non conservative impacts are considered in [80]. A general well-posedness theorem is stated in Theorem 5.3 in Chap. 5, which summarizes various existence and uniqueness results obtained after the pioneering results by Schatzman [1066] and Monteiro Marques [866, 867]. Well-posedness problems can be attacked another way, using explicitly the so-called *complementarity conditions*. This is the essence of the studies in [517, 759, 1063, 1064], which essentially focus on Linear Complementarity Systems and are described elsewhere in the book. Other works may be situated in-between differential inclusions and complementarity systems [205, 212, 214, 215, 226, 438].

[35] Let a surface S in $\mathbb{R}^3$ be given by $q_3 = f(q_1, q_2)$, with $\frac{\partial f}{\partial q_1}(q_{10}, q_{20}) = \frac{\partial f}{\partial q_2}(q_{10}, q_{20}) \neq 0$ (these two vectors span the tangent plane to S at P) and the q_3-axis is normal to S at $P = (q_{10}, q_{20}, q_{30})$. Then the Gauss or total curvature of S at P is equal to the determinant of the Hessian of $f(q_1, q_2)$ at P, i.e., the matrix $\frac{\partial^2 f}{\partial q_1 \partial q_2} \in \mathbb{R}^{2\times 2}$. It is for instance easy to verify that a plane given by $q_3 = aq_1 + bq_2$ has zero total curvature at any of its points. The ideas generalize for higher dimensions.

2.5 Some Comments on Compliant Models

As announced in the introduction of this chapter, all the above results and models deal with one contact/impact point. The case of multiple contacts is much more tricky. Analysing the limit as the stiffness diverges, of a compliant contact model when several surfaces are hit at the same time, is a tough mathematical issue tackled in very few articles [973, 975]. As shown in [163] in the case of bilateral (equality) constraints with penalization, very complex phenomena may be found at the limit. A specific feature of unilateral constraints, is that if the boundary $\mathrm{bd}(\Phi)$ of the admissible domain Φ is not smooth (this is the case when multiple constraints are present), then $\mathrm{bd}(\Phi)$ cannot be transformed locally into a hyperplane with a diffeomorphism. However it is locally identifiable with its tangent cone $T_\Phi(q)$ at configuration q. As we shall see later in this book, the geometry of unilaterally constrained Lagrangian systems involves tangent and normal cones.

Penalization may also induce stiff differential equations. Usually, the characteristic time of a spring-dashpot model, is of order $\mathcal{O}(\frac{1}{\sqrt{k}})$. Some authors recommend to compute at least 1000 points during a collision. If k is of order 10^{10} Nm, this represents a collision duration of order 10^{-5} s, hence a time step $h \approx 10^{-8}$ s. Simulation may be quite time-consuming. Moreover the lack of continuity in the initial data, or nonuniqueness of solutions, that is the common situation with multiple rigid contacts, as well as unavoidable round-off numerical errors in contact detection algorithms, may indicate that quite complex and unpredictable behaviors may occur when penalizations are used. The limit solution usually depends significantly on how the limit is reached, as demonstrated by simple chains of aligned balls (see an example in Chap. 6, Sects. 6.1.1.1 and 6.1.3). Mechanically, this is related to the duration of impact (and the maximum compression times at each contact) that varies depending on the stiffness and influences the outcome. Let us end by mentioning a crucial issue related to the stabilization of the normal accelerations and contact forces during persistent contact phases: many numerical simulation results which are shown in the Multibody Systems literature, prove that compliant contact models may yield spurious oscillations which have no Mechanical meaning (as proved by comparisons with experimental data [401, Figs. 5, 6, 8, 11, 12]). The choice of the contact/impact model has to incorporate such drawbacks as well, and the designer (or the Control scientist) should have in mind that a good model is a model with a reliable, robust numerical integration method.

Chapter 3
Variational Principles

This chapter introduces the variational principles of mechanics in the case of unilateral constraints and impacts. We start with virtual displacements and then proceed with variational inequalities formalisms (equivalently inclusions into normal cones to tangent cones and convex sets), Fourier and Jourdain's principles. The second part is dedicated to the Lagrange dynamics. The case with exogenous impulsive forces is obtained from the material of Chap. 1. Hamilton's principle, which is far more involved, is treated in the last part of the chapter. The chapter ends with some comments about the link with optimal control under state inequality constraints.

3.1 Virtual Displacements, Velocities, and Accelerations Principles

3.1.1 The "Classical" Presentation

The principle of virtual displacements is one of the most basic "principles" of classical mechanics. It is well known that in the case of bilateral frictionless holonomic constraints $h(q) = 0$, a mechanical system is in static equilibrium if and only if the total virtual work of the impressed forces is zero. In other words, if $Q \in \mathbb{R}^n$ denotes the vector of generalized forces acting on the system[1] (which are the forces that work on the generalized displacements $\delta q = \dot{q}dt$), and if $q \in \mathbb{R}^n$ is the corresponding vector of generalized coordinates, one has:

$$Q^T \delta_1 q = 0, \tag{3.1}$$

where $\delta_1 q$ represents a virtual displacement compatible with the constraints. The variation considered here is of the δ_1-type, i.e., $\delta_1 t = 0$ (this allows to compare the

[1] Often called the *impressed forces*.

B. Brogliato, *Nonsmooth Mechanics*, Communications and Control Engineering,
DOI 10.1007/978-3-319-28664-8_3

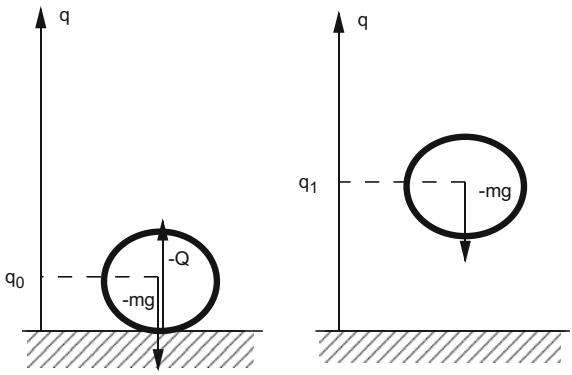

Fig. 3.1 A particle on a plane

state of the system in two fixed different configurations, i.e., this is a *static* equilibrium principle). For frictionless unilateral constraints $f(q) \geq 0$ (hence irreversible displacements on the constraint surface), this principle transforms to

$$Q^T \delta_1 q \leq 0, \tag{3.2}$$

which is known as *Fourier's inequality* [703, p. 87]. The inequality in (3.2) is easily understood as follows: if the system is in free motion ($f(q) > 0$) and in static equilibrium, then (3.1) holds. But if $f(q) = 0$, then the only permitted displacements are in the inward direction inside the admissible domain Φ, i.e., in a direction opposite to that of the impressed forces (i.e., forces applied on the system, but not the interaction forces). Hence a negative virtual work. One may also see this by considering that the interaction force (the Lagrange multiplier) has the same sign as the virtual displacement, and that the impressed forces must have opposite sign (at least in the direction normal to the constraint) to the multiplier to maintain static equlibrium. Consider for instance a ball on a plane in Fig. 3.1. Clearly, if the ball is in static equilibrium ($q = q_0$) then the virtual displacement $\delta_1 q = q_1 - q_0 > 0$ is such that $(q_1 - q_0)Q = (q_1 - q_0)(-mg) < 0$. The $\leq$ in (3.2) is to allow for infinitesimal displacements ($q_1 \to q_0$). In a Lagrangian formalism one has $M(q)\ddot{q} + C(q, \dot{q})\dot{q} = Q + P$, where P represents the contact forces (due to the constraints) and Q includes the forces that derive from a potential (gravity, elastic forces). Since we deal with static equilibrium, we obtain $Q + P = 0$, i.e., $P = -Q$. In terms of the contact forces, (3.1) and (3.2) write $P^T \delta_1 q = 0$ and $P^T \delta_1 q \geq 0$, respectively. The static equilibrium principles generalize dynamic equilibrium and d'Alembert's principle, i.e.,

$$[\underbrace{Q - C(q, \dot{q})\dot{q} - M(q)\ddot{q}}_{=-P}]^T \delta_1 q \leq 0. \tag{3.3}$$

D'Alembert's principle can in turn be transformed into a minimum principle involving the acceleration as the unknown, i.e., Gauss' principle that we shall see in

Sect. 3.3. Gibbs [446] showed that in case of unilateral constraints, d'Alembert's principle generalizes to

$$[\underbrace{Q - C(q,\dot{q})\dot{q} - M(q)\ddot{q}}_{=-P}]^T \delta_2 \ddot{q} \leq 0, \tag{3.4}$$

where the variation is of the δ_2-type, i.e.,

$$\delta_2 q = \delta_2 \dot{q} = 0, \quad \delta_2 t = 0. \tag{3.5}$$

This kind of variation means that one observes the system with a fixed position and velocity at a time $t = \tau_0$, and allows for the acceleration to vary at τ_0^+. This expresses the necessary condition for extremum seeking of $G(\ddot{q})$ in (3.26) below. Gibbs proved that for a system that consists of three particles q_1, q_2, and q_3 one has

$$((3.4) + (3.5) + q_1 \geq 0) \Longleftrightarrow \begin{pmatrix} \ddot{q}_1 = \max\left(0, \frac{Q_1}{m_1}\right) \\ \\ \ddot{q}_2 = \frac{Q_2}{m_2}, \ddot{q}_3 = \frac{Q_3}{m_3} \end{pmatrix}. \tag{3.6}$$

This is to be understood as follows: assume that on an interval $[\tau_0 - \varepsilon, \tau_0)$, $\varepsilon > 0$, contact is permanently established, i.e., $q_1 \equiv 0$. Then at time τ_0 either $Q_1 \leq 0$ and contact does not cease, or $Q_1 > 0$ and contact ceases. Gibbs shows that the δ_2-variation in (3.5) is suitable to establish the equivalence (3.6), whereas (3.3) is not. In other words [(3.4)+(3.5)+($q_1 \geq 0$)] uniquely determines the acceleration at $t = \tau_0^+$, whereas (3.3) instead of (3.4) does not permit this. We retrieve in (3.6) the formulation of (1.82). Gibbs also derived that in case of shocks (although only velocity discontinuities are mentioned in [446], without speaking of collisions), the inequality in (3.4) becomes[2]

$$[\underbrace{Q_{imp} - M(q)\sigma_{\dot{q}}(t_k)}_{\stackrel{\Delta}{=}-R}]^T \delta\left(\sigma_{\dot{q}}(t_k)\right) \leq 0. \tag{3.7}$$

In (3.7) the variation is to be understood on $\dot{q}(t_k^+)$, i.e., the postimpact velocity, and $\sigma_{\dot{q}}(t_k) = \dot{q}(t_k^+) - \dot{q}(t_k^-)$ in the $\delta(\cdot)$ term. If $\dot{q}(t_k^+) = \dot{q}(t_k^-)$ then (3.7) implies $Q_{imp}^T \delta\left(\sigma_{\dot{q}}(t_k)\right) \leq 0$, for all admissible $\dot{q}(t_k^+)$. Since in this case the velocity is continuous (i.e., $q_1 > 0$, or $q \in \mathrm{Int}(\Phi)$), $\delta\left(\sigma_{\dot{q}}(t_k)\right)$ is arbitrary and thus necessarily $Q_{imp} = 0$ and $R = 0$. If $\dot{q}(t_k^+) \neq \dot{q}(t_k^-)$ then $q_1(t_k) = 0$ and necessarily $\dot{q}(t_k^+) \geq 0$ whereas $\dot{q}(t_k^-) < 0$. Then all variations of $\dot{q}(t_k^+)$ are permitted with $\dot{q}(t_k^+) \geq 0$. One has $\sigma_{\dot{q}}(t_k) \geq 0$ and $\delta\left(\sigma_{\dot{q}}(t_k)\right) \geq 0$. Thus (3.7) states $R^T \delta\left(\sigma_{\dot{q}}(t_k)\right) \geq 0$.

[2] According to our notation, $\sigma_f(t) \stackrel{\Delta}{=} f(t^+) - f(t^-)$, and Q_{imp} is a vector of impulsive forces, R is the contact percussion vector (i.e., the density of P considered as a Dirac measure at the impact time).

Besides the two variations δ_1 and δ_2, there is in the literature a third type of variation δ_3 such that

$$\delta_3 t = 0, \quad \delta_3 q = 0. \tag{3.8}$$

In case of bilateral constraints (3.1) is equivalent to

$$Q^T \delta_3 \dot{q} = 0, \tag{3.9}$$

where it is assumed that positions are fixed and satisfy the constraints $h(q) = 0$, while the virtual velocity variation $\delta_3 \dot{q}$ also satisfies the constraints at the velocity level, i.e., $\nabla h(q)^T \delta_3 \dot{q} = 0$. The δ_3-variation is called a Jourdain variation [631] and (3.9) is known as the Jourdain's variational principle (JVP), or the virtual power principle. In its dynamical form, it becomes

$$[Q - C(q, \dot{q})\dot{q} - M(q)\ddot{q}]^T \delta_3 \dot{q} = 0. \tag{3.10}$$

The interest for the δ_3-variation in (3.8) was originally to get a variation intermediate between δ_1 and δ_2. As we shall see this is a very convenient variation for unilaterally constrained systems with impacts. In particular, Moreau's sweeping process is built along Jourdain's variations.

3.1.2 *Using Variational and Quasi-Variational Inequalities Formalisms*

Let us resume the contents of the previous section, from another point of view. To simplify the presentation, let us focus on the so-called bouncing ball system. Using basic mechanical arguments its dynamics is given by

$$\begin{cases} (a) \;\; m\ddot{q}(t) = -mg + Q(t) + \lambda(t) \\ (b) \;\; 0 \le \lambda(t) \perp q(t) \ge 0 \;\; \text{for all} \;\; t \ge 0 \\ (c) \;\; q(0) = q_0 \ge 0, \dot{q}(0^-) = \dot{q}_0, \end{cases} \tag{3.11}$$

where in the above notation $\lambda(t) = P(t)$, m is the ball's mass, g is the gravity acceleration. The complementarity relations in (b) state a particular constitutive contact law which we already introduced in Example 1.6: it says that the contact force exerted by the ground on the ball, is always nonnegative (no adhesive or gluing effects), that the ball cannot penetrate in the ground, that the contact force can be positive only if the ball touches the ground, and that when the ball is not in contact with the ground, then the ground exerts no force on the ball (no distance or magnetic effects). This is therefore a very simple and natural model of contact, which applies in a realistic way to many practical systems. For the moment collisions are disregarded. We assume

that $q(\cdot)$ and $\dot{q}(\cdot)$ are continuous, while $\ddot{q}(\cdot)$ and $\lambda(\cdot)$ may be discontinuous, however they are right-continuous (so $\ddot{q}(t) = \ddot{q}(t^+)$ and $\lambda(t) = \lambda(t^+)$ by definition). Using (B.19), the dynamics (3.11) is equivalently rewritten as the differential inclusion

$$m\ddot{q}(t) + mg = \lambda(t) \in -N_{\mathbb{R}^+}(q(t)), \quad q(t) \in \mathbb{R}^+ \text{ for all } t \geq 0. \tag{3.12}$$

From the normal cone's definition (B.5), this is equivalent to the variational inequality: Find $q(t) \geq 0$ such that

$$\langle \underbrace{m\ddot{q}(t) + mg - Q(t)}_{=\lambda(t)}, q^\star - q(t) \rangle \geq 0, \quad \text{for all } \; q^\star \geq 0. \tag{3.13}$$

Interpreting $q^\star - q(t)$ as a virtual displacement, (3.13) is exactly (3.3) in a particular case. Let $q(t) = 0$, then $\delta q(t) \stackrel{\Delta}{=} q^\star - q(t) = q^\star \geq 0$. Let $q(t) > 0$, then $\delta q(t)$ is unsigned, i.e., $\delta q(t) \in \mathbb{R}$. We infer from this simple example that $\delta q(t) \in T_{\mathbb{R}^+}(q(t))$, the tangent cone to $\mathbb{R}^+$ at $q(t)$. From the fact that $\lambda(t) \in -N_{\mathbb{R}^+}(q(t))$ and $\delta q(t) \in T_{\mathbb{R}^+}(q(t))$, and since the normal and tangent cones are polar one to each other (Definition B.4), we infer that indeed the virtual work produced by $\lambda(t)$ is nonnegative. Let us now replace the normal cone $N_{\mathbb{R}^+}(q(t))$ by the normal cone $N_{T_{\mathbb{R}^+}(q(t))}(\dot{q}(t))$, where the tangent cone $T_{\mathbb{R}^+}(q(t))$ is defined in (B.3). Let us set

$$\lambda(t) \in -N_{T_{\mathbb{R}^+}(q(t))}(\dot{q}(t)). \tag{3.14}$$

If $q(t) > 0$, then $N_{T_{\mathbb{R}^+}(q(t))}(\dot{q}(t)) = N_{\mathbb{R}}(\dot{q}(t)) = \{0\}$ and $\lambda(t) = 0$. If $q(t) = 0$, $N_{T_{\mathbb{R}^+}(q(t))}(\dot{q}(t)) = N_{\mathbb{R}^+}(\dot{q}(t))$. Consequently, if $q(t) = 0$ and $\dot{q}(t) > 0$, one obtains $N_{T_{\mathbb{R}^+}(q(t))}(\dot{q}(t)) = \{0\}$: the ball starts to detach from the constraint, and the constitutive law in velocity implies that the contact force is zero. Now if $q(t) = 0$ and $\dot{q}(t) = 0$, one gets $N_{T_{\mathbb{R}^+}(q(t))}(\dot{q}(t)) = \mathbb{R}^-$: the contact force may take positive values. We have that $0 \leq \lambda(t) \perp \dot{q}(t) \geq 0$. Using this new representation of unilaterality in velocity (instead of the first one that is in position), one obtains the differential inclusion $m\ddot{q}(t) + mg - Q(t) = \lambda(t) \in -N_{T_{\mathbb{R}^+}(q(t))}(\dot{q}(t))$, that is equivalently rewritten as the *quasi-variational inequality* [385, Definition: p. 16]: Given $q(t) \in \mathbb{R}^+$, find $\dot{q}(t) \in T_{\mathbb{R}^+}(q(t))$ such that

$$\langle m\ddot{q}(t) + mg - Q(t), \dot{q}^\star - \dot{q}(t) \rangle \geq 0 \;\; \text{for all } \; \dot{q}^\star \in T_{\mathbb{R}^+}(q(t)). \tag{3.15}$$

The term $\dot{q}^\star - \dot{q}(t)$ may be interpreted as a virtual velocity, and is a Jourdain's variation as in (3.8). Simple calculations yield that when $q(t) = 0$ then $\delta\dot{q}(t) \stackrel{\Delta}{=} \dot{q}^\star - \dot{q}(t) \in T_{\mathbb{R}^+}(\dot{q}(t))$. When $q(t) > 0$ then $\delta\dot{q}(t) \in \mathbb{R}$. When $q(t) = 0$ and $\dot{q}(t) = 0$ then $\delta\dot{q}(t) = \dot{q}^\star \geq 0$. When $q(t) = 0$ and $\dot{q}(t) > 0$ then $\delta\dot{q}(t) = \dot{q}^\star \in \mathbb{R}$. Therefore, $\delta\dot{q}(t) \in T_{T_{\mathbb{R}^+}(q(t))}(\dot{q}(t))$.

Finally, let us investigate a third constitutive law for the contact force, defined as $\lambda(t) \in -N_{T_{T_{\mathbb{R}^+}(q(t))}(\dot{q}(t))}(\ddot{q}(t))$. This time the main variable is the acceleration. If $q(t) > 0$ then the normal cone becomes $N_{T_{\mathbb{R}}(\dot{q}(t))}(\ddot{q}(t)) = N_{\mathbb{R}}(\ddot{q}(t)) = \{0\}$. If $q(t) = 0$ we

obtain $N_{T_{\mathbb{R}^+}(\dot{q}(t))}(\ddot{q}(t))$: if $\dot{q}(t) > 0$ this gives $N_{\mathbb{R}}(\ddot{q}(t)) = \{0\}$, and if $\dot{q}(t) = 0$ this gives $N_{\mathbb{R}^+}(\ddot{q}(t))$. Thus if $q(t) = 0$, $\dot{q}(t) = 0$, and $\ddot{q}(t) > 0$ one gets the right-hand side equal to $N_{\mathbb{R}^+}(\ddot{q}(t)) = \{0\}$, while if $\ddot{q}(t) = 0$ one obtains $N_{\mathbb{R}^+}(\ddot{q}(t)) = \mathbb{R}^-$. The differential inclusion $m\ddot{q}(t) + mg - Q(t) = \lambda(t) \in -N_{T_{\mathbb{R}^+(q(t))}(\dot{q}(t))}(\ddot{q}(t))$ is equivalently rewritten as the quasi-variational inequality: Given $q(t) \in \mathbb{R}^+$ and $\dot{q}(t) \in T_{\mathbb{R}^+}(q(t))$, find $\ddot{q}(t) \in T_{T_{\mathbb{R}^+}(q(t))}(\dot{q}(t))$ such that

$$\langle m\ddot{q}(t^+) + mg - Q(t), \ddot{q}^\star - \ddot{q}(t)\rangle \geq 0 \ \text{ for all } \ \ddot{q}^\star \in T_{T_{\mathbb{R}^+}(q(t))}(\dot{q}(t)). \tag{3.16}$$

The term $\ddot{q}^\star - \ddot{q}(t)$ may be interpreted as a virtual acceleration, close to the δ_2 variation in (3.4). Proceeding as in the two foregoing cases, one finds that $\delta\ddot{q}(t) \stackrel{\Delta}{=} \ddot{q}^\star - \ddot{q}(t) \in T_{T_{\mathbb{R}^+}(q(t))}(\dot{q}(t))}(\ddot{q}(t))$. The different cases can be analyzed similarly to the first two variations. Let us now use (B.19), (B.20) to interpret the inclusion $\ddot{q}(t) + g - \frac{1}{m}Q(t) \in -N_{T_{\mathbb{R}^+}(q(t))}(\dot{q}(t))}(\ddot{q}(t))$. It is equivalent to:

$$\ddot{q}(t) = \text{proj}[T_{T_{\mathbb{R}^+}(q(t))}(\dot{q}(t)); -g + \frac{1}{m}Q(t)]. \tag{3.17}$$

One recognizes Gauss' principle in (3.16). The formulation in (3.16) is therefore the variational inequality form of Gauss' principle.

Remark 3.1 (*Lexicographical Inequalities*) It is noteworthy that the number of tangent cones introduced in the right-hand side of the dynamics, increases with the derivative degree. This is needed to keep the system within the admissible domain Φ. In [15] this idea is extended to systems where derivatives of degree larger than two play a role, within the framework of a higher order Moreau's sweeping process (see Sect. 5.2 for a detailed description of the mechanical case). The underlying idea is to impose lexicographical inequalities on the derivatives of the gap function $f(q)$, which is in our simple example equal to q. Consider the cone $N_{T_{\mathbb{R}^+}(q(t))}(\dot{q}(t))$: if $q(t) > 0$ then $\dot{q}(t)$ may take any value. If $q(t) = 0$ then $\dot{q}(t) \geq 0$. Thus this formulation imposes $(q(t), \dot{q}(t)) \succ 0$.[3] Consider now the cone $N_{T_{\mathbb{R}^+}(q(t))}(\dot{q}(t)}(\ddot{q}(t))$. If $q(t) > 0$, then both $\dot{q}(t)$ and $\ddot{q}(t)$ may take any real value. If $q(t) = 0$, then $\dot{q}(t) \geq 0$ since $T_{\mathbb{R}^+}(q(t)) = \mathbb{R}^+$. If $q(t) = 0$ and $\dot{q}(t) = 0$, then $T^1_{\mathbb{R}^+}(q(t), \dot{q}(t)) \stackrel{\Delta}{=} T_{T_{\mathbb{R}^+}(q(t))}(\dot{q}(t)) = T_{\mathbb{R}^+}(0) = \mathbb{R}^+$, so $\ddot{q}(t) \geq 0$. Thus this normal cone inclusion imposes that $(q(t), \dot{q}(t), \ddot{q}(t)) \succeq 0$. It is proved in [15] that setting the right-hand side as the normal cone to the tangent cone to the tangent cone to the tangent cone... up to the system's relative degree, implies lexicographical inequalities on the gap function derivatives (see [15, Remark 16]). Moreover this allows one to derive a sequence of variational inequalities, see [15, Eq. (62)], which may be interpreted as a virtual displacement, velocity, acceleration, *etc.*, principle if replaced in a physical context. Notice finally that the above process can be continued with higher degree derivatives by defining $T^2_{\mathbb{R}^+}(q(t), \dot{q}(t), \ddot{q}(t)) \stackrel{\Delta}{=} T_{T_{\mathbb{R}^+}(q(t))}(\dot{q}(t)}(\ddot{q}(t))$,

[3] For a vector $x = (x_1, x_2, x_3, \ldots)^T$, $x \succeq 0$ means that the first nonzero element x_i is nonnegative. Thus either all elements are zero, or the first nonzero element is positive.

and $N_{T_{T_{\mathbb{R}^+}(q(t))}(\dot{q}(t))}(\ddot{q}(t))}(q^{(3)}(t))$, and so on with $T^n(q(t), \ldots, q^{(n)}(t))$. As shown in [15, Lemma 3] one has

$$N_{T^n(q(t),\ldots,q^{(n)}(t))}(q^{(n+1)}(t)) \subseteq N_{T^{n-1}(q(t),\ldots,q^{(n-1)}(t))}(q^{(n)}(t)) \ (\subseteq N_{\mathbb{R}^+}(q(t))) \quad (3.18)$$

with $T^0_{\mathbb{R}^+}(q(t)) = T_{\mathbb{R}^+}(q(t))$, and all functions are supposed to be right-continuous, which allow us to consider that these cones may be computed on the right of a possible instant of state jump. Nothing hampers one to write the dynamics as $m\ddot{q}(t) + mg - Q(t) = \lambda(t) \in -N_{T^n(q(t),\ldots,q^{(n)}(t))}(q^{(n+1)}(t))$, which may be useful in an event-driven algorithm to test whether the system detaches from the constraint boundary or not when the first n derivatives of the gap function vanish. The quasi-variational inequality associated with such a differential inclusion is: Find $q(t) \geq 0$, $\dot{q}(t) \in T_{\mathbb{R}^+}(q(t))$, $\ddot{q}(t) \in T_{T_{\mathbb{R}^+}(q(t))}(\dot{q}(t))$,..., $q^{(n+1)}(t) \in T^n(q(t), \ldots, q^{(n)}(t))$ such that

$$\langle m\ddot{q}(t) + mg - Q(t), q^{(n+1),\star} - q^{(n+1)}(t)\rangle \geq 0 \text{ for all } q^{(n+1),\star} \in T^n(q(t), \ldots, q^{(n)}(t)). \quad (3.19)$$

Extending the above three cases of variations, we may infer that $\delta q^{(n+1)}(t) \stackrel{\Delta}{=} q^{(n+1),\star} - q^{(n+1)}(t) \in T_{T^n(q(t),\ldots,q^{(n)}(t))}(q^{(n+1)}(t)) = T^{n+1}(q(t), \ldots, q^{(n+1)}(t))$.

3.1.2.1 Further Reading

Fourier's and Jourdain's principles are discussed within the general setting of systems constrained in closed sets, in [448, 831, 832, 833]. Hemivariational inequalities are used because the sets may not be convex, hence Clarke's subgradient has to be used instead of the subdifferential from convex analysis. A general form of the principle of virtual work for unilaterally constrained systems, using convex analysis tools, is provided in [466]. The virtual displacements are no longer required to be compatible with the constraints nor time-independent: the formulation accomodates for that. The principle of d'Alembert is also analyzed. The example of a unilateral pendulum with a spring whose elastic force $F(x)$ satisfies $-F(x) = \partial U(x)$ for some C^0 function $U(x)$, is given. Glocker [449] gave an exposition of virtual displacement principles in case the boundary $\mathrm{bd}(\Phi)$ of the admissible domain is nonsmooth (or of codimension $\geq$2). The major conclusion in [449] is that this principle can be stated when Φ has a smooth boundary, and in certain nonsmooth cases. Fourier's inequality is used in [964] to characterize the stability of rigid workpieces in contact with fixed rigid bodies, with or without friction, and taking into account the unilaterality of the contacts. The inclusions in Sect. 3.1.2 have been derived by Glocker [448, 452], in the more general setting of right-continuous velocities. It is proved that for a given nonempty set Φ one has

$$N_{\Phi}(q) \supseteq N_{T_{\Phi}(q)}(\dot{q}) \supseteq N_{T_{T_{\Phi}(q)}(\dot{q})}(\ddot{q}), \quad (3.20)$$

velocities and accelerations being assumed right-continuous (the first normal cone inclusion is proved in [894, Proposition 5.1], see also (3.18)). This is quite related to lexicographical inequalities, see Remark 3.1. Here the tangent cone $T_\Phi(q)$ is defined in (B.3), the normal cone is its polar cone in (B.5), and Φ needs not be convex. One may find general formulations of what we presented for the simple system (3.11), in Glocker's monograph [452, Chap. 9]. It is in particular pointed out in [452] that virtual displacements should in general be taken in the contingent cone (which is the tangent cone for tangentially regular sets, which possess no reentrant corners, see Fig. B.1). It has been found in [74] that the JVP is a suitable variational principle because both the time and the position are fixed, whereas the velocity is allowed to vary, this is exactly the case of impulsive dynamics. And it is indeed the case that Jourdain's variations are suitable for unilaterally constrained systems with impacts, see Sect. 5.2.2.2.

3.2 A Coordinate Invariance Principle

As another "principle," let us state the following:

> The power generated by the scalar product of the contact forces with the velocities compatible with the constraints, is the same in any set of coordinates.

Let q and z be two sets of n generalized coordinates of the same Lagrangian system, and let F_q and F_z be the generalized forces associated with q and z, respectively. This "principle" says that $\mathscr{P} = \dot{q}^T F_q = \dot{z}^T F_z$. Thus if $z = Z(q)$ for some diffeomorphism $Z(\cdot)$, so that $\dot{z} = \frac{\partial Z}{\partial q}(q)\dot{q}$ with full rank Jacobian matrix, one obtains $\dot{q}^T F_q = \dot{q}^T \nabla Z(q) F_z$, and consequently the generalized forces are related as follows:

$$F_q = \nabla Z(q) F_z \quad \Leftrightarrow \quad F_z = (\nabla Z(q))^{-1} F_q. \tag{3.21}$$

Let us now assume that we are dealing with a mechanical system that has m contact points. As we shall see in Chap. 4, at each potential contact point i one may associate a local Cartesian frame in which the contact force $F_i \in \mathbb{R}^3$ may be expressed: $F_i = \begin{pmatrix} F_{\mathrm{n},i} \\ F_{\mathrm{t}_1,i} \\ F_{\mathrm{t}_2,i} \end{pmatrix}$. The two vectors $\mathrm{t}_{1,i}$ and $\mathrm{t}_{2,i}$ span the tangent plane that "separates" the bodies in contact at the contact point i, while the vector $\mathrm{n}_i \in \mathbb{R}^3$ (or $\in \mathbb{R}^2$ in the planar case) spans the common normal direction. Similarly, a local relative velocity between the potential contact points is chosen and writen as $v_i = \begin{pmatrix} v_{\mathrm{n},i} \\ v_{\mathrm{t}_1,i} \\ v_{\mathrm{t}_2,i} \end{pmatrix}$ in the same local Cartesian frame. The power performed by F_i is equal to $\mathscr{P}_i = v_i^T F_i = v_{\mathrm{n},i} F_{\mathrm{n},i} + v_{\mathrm{t}_1,i} F_{\mathrm{t}_1,i} + v_{\mathrm{t}_2,i} F_{\mathrm{t}_2,i}$. If the contact i is open this is obviously zero.

Let us assume first that there are no frictional effects, so that $F_{\mathrm{t}_1,i} = F_{\mathrm{t}_2,i} = 0$. Suppose also that, as indicated in Sect. 4.1.3, the unilateral constraints are defined with signed distance functions $f_i(q)$. Hence $v_{\mathrm{n},i} = \nabla f_i(q)^T \dot{q}$. According to the above "principle," one obtains $\mathscr{P}_i = v_{\mathrm{n},i} F_{\mathrm{n}_i} = F_{\mathrm{n},i} \nabla f_i(q)^T \dot{q} = \dot{q}^T F_{q,i}$. One infers that

$$F_{q,i} = \nabla f_i(q) F_{\mathrm{n},i}. \tag{3.22}$$

With this choice of the gap functions $f_i(q)$, the component $F_{\mathrm{n},i}$ acts as the Lagrange multiplier associated with the unilateral constraint $f_i(q) \geq 0$. If there are m constraints, the generalized force that is associated with them is given by

$$F_q = \nabla f(q) F_{\mathrm{n}} = \sum_{i=1}^{m} \nabla f_i(q) F_{\mathrm{n},i}. \tag{3.23}$$

If frictional effects are present, one has in the same manner $v_{\mathrm{t}_{1,i}} = H_{\mathrm{t},1,i}(q)^T \dot{q}$ and $v_{\mathrm{t}_{2,i}} = H_{\mathrm{t},2,i}(q)^T \dot{q}$ for some vectors $H_{\mathrm{t},1,i}(q)$ and $H_{\mathrm{t},2,i}(q)$. Proceeding as above we obtain that the right-hand side of the Lagrange dynamics is

$$F_q = \nabla f(q) F_{\mathrm{n}} + H_{\mathrm{t},1}(q) F_{\mathrm{t}_1} + H_{\mathrm{t},2}(q) F_{\mathrm{t}_2} = \nabla f(q) F_{\mathrm{n}} + H_{\mathrm{t}}(q) F_{\mathrm{t}} \tag{3.24}$$

with $H_{\mathrm{t}}(q) = (H_{\mathrm{t},1}(q) \;\; H_{\mathrm{t},2}(q))$, $F_{\mathrm{t}} = \begin{pmatrix} F_{\mathrm{t}_1} \\ F_{\mathrm{t}_2} \end{pmatrix}$. Usually, one denotes F_{n} as λ_{n} and F_{t} as λ_{t}, to emphasize the fact that these quantities are Lagrange multipliers. These ideas are developed in Sects. 4.1.2 and 4.1.3 for two frictionless bodies with one contact point.

3.2.1 *Perfect Constraints*

(i) Assume that the constraints are holonomic bilateral, given by $h(q) = 0$ for some differentiable function $h : \mathbb{R}^n \to \mathbb{R}^{m_b}$. This means that the system is constrained to evolve in the submanifold $\{(q, \dot{q}) | h(q) = 0, \nabla h(q)^T \dot{q} = 0\}$ of codimension $2m_b$. These equality constraints translate the fact that at m_b contact points i one may associate a local frame such that $v_{\mathrm{n},i} = \nabla h_i(q)^T \dot{q} = 0$. If there are no tangential effects (the joint is said *perfect*), then the power performed by $F_i(t)$ satisfies $\mathscr{P}_i = v_i(t)^T F_i(t) = 0$. One deduces that $F_i = (F_{\mathrm{n},i} \;\; 0 \;\; 0)^T$, since the tangential local velocities are free.
(ii) In case of m_u unilateral constraints, let us assume that the velocities are right-continuous functions of time and that we focus on phases of motion during which there are no impacts, and the unilateral constraint i is active, i.e., $f_i(q(t)) = 0$ on some

open time interval $I \ni t$.[4] Following (3.14) the contact force model is stated at the velocity level as follows: $0 \leq F_{\mathrm{n},i}(t) \perp v_{\mathrm{n},i}(t^+) \geq 0$, for all $1 \leq i \leq m_u$: the normal contact force and local velocity have to satisfy complementarity conditions. More on complementarity will be mentioned in Sect. 5.4. Still using the same "principle," we say that the constraints are perfect if $\mathscr{P}_i = v_i(t^+)^T F_i(t) = 0$. Once again we infer that $F_i = (F_{\mathrm{n},i}\ 0\ 0)^T$. The discrepancy compared to bilateral constraints, is that this time $F_{\mathrm{n},i}(t) \geq 0$, for all $t \geq 0$. See also Remark 5.6 for some thoughts about virtual power and perfect constraints.

(iii) In terms of virtual displacements $\delta_1 q$, perfect unilateral constraints may be defined as follows. Suppose that the system's configuration q is restricted to the set Φ, and that Φ is tangentially regular (see Appendix B for the definition). Then $\delta_1 q \in T_\Phi(q)$: the admissible virtual displacements must belong to the tangent cone to Φ[5], a fact that we proved in Sect. 3.1.2 for the one degree-of-freedom system (3.13). In a more general setting, let Φ be closed nonempty and convex, $q \in \Phi$, $q^\star \in \Phi$, and $\delta_1 q \stackrel{\Delta}{=} q^\star - q$.[6] Then using the first line in Definition B.2 it follows that $\delta_1 q \in T_\Phi(q)$ without any restriction on $\delta_1 q$ (it may not be infinitesimal due to convexity). If Φ is not convex the other definitions of tangent cone in Definition B.2 may be used, and $\delta_1 q$ has to be an infinitesimal variation. One says that unilateral constraints are perfect if the contact force $\lambda(t)$ satisfies $\lambda(t) \in -N_\Phi(q(t))$, for all $t \geq 0$. Then from the fact that the tangent and the normal cones are polar one to each other (see Definitions B.4 and B.5), one obtains $\lambda(t)^T \delta_1 q \geq 0$. This is the generalization of Fourier's inequality in (3.2), that may also be named the principle of d'Alembert–Lagrange in inequality form.

The discrepancy between (ii) (zero contact force power) and (iii) (Fourier's inequality) is that the former stems from (3.14) while the latter is a consequence of $\delta_1 q \in T_\Phi(q)$ and $\lambda(t) \in -N_\Phi(q(t))$, and of the fact that virtual displacements $\delta_1 q$ are considered for fixed (or frozen) time. Since the inclusions (3.20) hold, we deduce that Fourier's inequality is more general than the zero power equality. Bilateral constraints and unconstrained systems may be recovered following the arguments of Remark 3.2 in Sect. 3.5.1.

3.3 Gauss' Principle

Gauss' least action principle is one of the several variational principles of mechanics, within which one can interpret the dynamics of classical mechanical systems (by classical we mean mainly here systems with smooth dynamics). Let us first

[4] It is preferable to take I as an open interval, in order to encompass the right limit at possible impact times.

[5] J.J. Moreau [891] points out that Fourier's inequality in (3.2) is not always equivalent to $Q \in N_\Phi(q)$. One has to assure that $T_\Phi(q) \neq \emptyset$ to secure this.

[6] It is reasonable to define such a virtual displacement vector, since a virtual displacement is an infinitesimal change of coordinates.

recall its formulation for systems subject to holonomic (bilateral) constraints. In fact, Gauss's principle is a reinterpretation of d'Alembert's principle into a minimum principle. For a system of n particles with coordinates $q_i \in \mathbb{R}^3$ and masses m_i, submitted to external forces F_i, Gauss' principle states that the function

$$G(\ddot{q}) \stackrel{\Delta}{=} \sum_{i=1}^{n} \frac{1}{2m_i} (F_i - m_i \ddot{q}_i)^2 \tag{3.25}$$

is minimum for the actual motion. This recasts the research of acceleration at each instant of time into a quadratic programming problem. If the system is free of any constraints, then trivially one retrieves Newton's law of motion, i.e., $m_i \ddot{q}_i(t) = F_i(t)$. In the case of a general n-degree-of-freedom Lagrangian system, the function $G(\ddot{q})$ takes the form

$$G(\ddot{q}) = \frac{1}{2} [M(q)\ddot{q} - C(q, \dot{q})\dot{q} - g(q) + Q]^T M^{-1}(q) [M(q)\ddot{q} - C(q, \dot{q})\dot{q} - g(q) + Q] \tag{3.26}$$

where the different terms are defined in Example 1.3, Eq. (1.10), and Q stands for generalized exogenous forces. The vector $g(q)$ may contain gravity torques and other conservative generalized forces. Let us recall that it is assumed that at the time when (3.26) is considered, all the variables are constant except the acceleration with respect to which the minimization is performed, this is close to a δ_2 variation. It turns out that Gauss' principle is also valid for systems subject to unilateral constraints (when the system performs a constrained motion phase), or to bilateral (holonomic) constraints, or subjected to both. We already saw its extension for perfect unilateral constraints in (3.17), and its extension is possible using (3.20). This will be seen in more detail in Sect. 5.1. Let us mention that Moreau was the first to prove that Gauss' principle applies to frictionless Lagrangian systems with unilateral constraints [877, 878], using convex analysis tools like conjugacy (Definition B.11) and proximality (Definition B.10). Gauss' principle is used in the context of cable-driven robots in [395].

3.3.1 Further Reading

Sinitsyn [1115] studied a system composed of n mass points. He showed that the real acceleration of the system $\ddot{q}_i$, satisfies $\sum_{i=1}^{n} m_i(\ddot{q}_i - \ddot{q}_i^o)^2 \leq \sum_{i=1}^{n} m_i(\ddot{q}_i' - \ddot{q}_i^o)^2$, where $\ddot{q}_i^o$ is the acceleration the system would have with no constraint, and the virtual acceleration $\ddot{q}_i'$ corresponds to virtual displacements δq consistent with the constraints (i.e., $\nabla f_j(q)^T \delta q \leq 0$). Other variational principles, like Maupertuis', can be derived for systems with unilateral constraints. This is investigated in [683] for elastic impacts. Papastavridis [976] shows that the impulsive form of some well-known finite motion equations, like Routh–Voss', Maggi's, Hadamard's,

Boltzmann–Hamel's, Chaplygin–Voronets', and Appell's equations can be derived. Bahar [74] studies the extension of the differential variational principle of Jourdain (JVP) to rigid body shock dynamics, making use of *quasi-velocities*. Starting from a JVP formulation of the shock dynamics (it is assumed that at shock instants the postimpact velocity should be such that this equality is satisfied): $\sigma_{\dot{q}}^T M(q)\delta_3\dot{q} = 0$, and taking into account that preimpact velocities are constants of the problem, this is equivalent to

$$\delta_3 \left\{ \frac{1}{2}\sigma_{\dot{q}}^T M(q)\sigma_{\dot{q}} \right\} = 0. \tag{3.27}$$

The postimpact velocities have to be taken compatible with the constraints, i.e., $\dot{q}(t_k^+)^T \nabla f(q) \geq 0$. The extremum of the function in (3.27) is in fact shown to be a minimum. One recognizes in (3.27) that the term between brackets is Gauss' function in (3.26) expressed in its impulsive form. In fact, and we shall come back on this in Sect. 5.4, other authors [763] calculate the impulsive Lagrangian multiplier λ associated with the active constraints $f(q) = 0$, as

$$\min_{\lambda \geq 0} \frac{1}{2}\lambda^T \nabla f(q)^T M^{-1}(q) \nabla f(q) + \lambda^T \nabla f(q)\dot{q}(t_k^-) \tag{3.28}$$

which is equivalent using impact dynamics and (5.107) to (5.108)

$$\min_{\dot{q}(t_k^+)} \sigma_{\dot{q}}^T M(q)\sigma_{\dot{q}} \tag{3.29}$$

subject to $\nabla f(q)^T \dot{q}(t_k^+) \geq 0$ (a constraint which means that the postimpact velocity must be admissible). Bahar also points out the possible applications of such theoretical results, reconstruction of preimpact velocities from postimpact data (which is very important in studying for instance vehicle accidents, see also Brach [175] for such an application). This is the object of the study in [1272], who proposes to reconstruct preimpact velocities of jack-knifed tractor semitrailers using Gauss' principle and energy balance. An estimation of the lost velocity during the period after the impact must be given, as well as the estimation of lost velocity due to crush, the vehicle geometry after and before the collision, and the brake side distance after sideswipe. Kirgetov [667, 668, 669] studies dynamics of systems of n particles subject to frictionless unilateral constraints. The collisions are assumed to be elastic. It is shown [669] that among all the states consistent with the constraints $f(q) \geq 0$, and satisfying $\nabla f(q)^T \dot{q}(t_k^+) = -\nabla f(q)^T \dot{q}(t_k^-)$, the real state $(q, \dot{q})$ is the one that minimizes the function $\sum_{i=1}^n \frac{m_i}{2} \left(\dot{q}_i(t_k^+) - \dot{q}_i(t_k^-)\right)^2$. This is again quite similar to the above minimization problems and Jourdain's principle.

3.4 Lagrange Dynamics

From a general point of view, a variational problem in mechanics can be formulated as follows [1306]: Given a Lagrangian function $L(\cdot)$, a suitable class of admissible curves $q(\cdot)$ with given endpoints, find the minimum of some quantity called the *action integral*:

$$I(q) = \int_{t_0}^{t_1} L(t, q(t), \dot{q}(t))dt. \tag{3.30}$$

In the unconstrained case, the extremization of $I(q)$ yields the first-order condition called the Euler–Lagrange dynamics: $\frac{d}{dt}\left(\frac{\partial L}{\partial \dot{q}}\right) - \frac{\partial L}{\partial q} = 0$. Actually, in most cases, so-called *least action* principles are not minimum principles, but only *stationary* principles. In this section, we first treat this problem as if there were no difficulties in applying variational techniques to systems subject to impacts, i.e., we simply consider directly the Lagrange equations and we suppose that a generalized *external* impulsive force acts on the system (we have already noted a significant difference between this problem and the problem with unilateral constraints in Chap. 1). Then we discuss about the variational approach to systems with unilateral constraints.

3.4.1 External Impulsive Forces

The Lagrange equations of the system submitted to a generalized force $F_q = F + p_k\delta_{t_k}$, where $F = \{F_q\}$ represents all the generalized forces without taking into account the impulsive ones, are given by $\frac{d}{dt}\left(\frac{\partial L}{\partial \dot{q}}\right) - \frac{\partial L}{\partial q} = F + p_k\delta_{t_k}$. Thus using the notations introduced in Chap. 1 we get

$$\frac{\partial^2 T}{\partial \dot{q}^2}\left(\{\ddot{q}\} + \sigma_{\dot{q}}\delta_{t_k} + \sigma_q\dot{\delta}_{t_k}\right) + \frac{\partial^2 T}{\partial q \partial \dot{q}}\left(\{\dot{q}\} + \sigma_q\delta_{t_k}\right) - \frac{\partial (T-U)}{\partial q} = F + p_k\delta_{t_k}, \tag{3.31}$$

from which we deduce[7]

$$\frac{\partial^2 T}{\partial \dot{q}^2}\sigma_q(t_k) = 0 \text{ and } \frac{\partial^2 T}{\partial q \partial \dot{q}}\sigma_q(t_k) + \frac{\partial^2 T}{\partial \dot{q}^2}\sigma_{\dot{q}}(t_k) = p_k. \tag{3.32}$$

In case the kinetic energy is a quadratic form of the velocity and the problem is not degenerated, $\frac{\partial^2 T}{\partial \dot{q}^2} \succ 0$ is the inertia matrix and we obtain

$$\sigma_q(t_k) = 0 \text{ and } \frac{\partial^2 T}{\partial \dot{q}^2}\sigma_{\dot{q}}(t_k) = \frac{\partial T}{\partial \dot{q}}(t_k^+) - \frac{\partial T}{\partial \dot{q}}(t_k^-), \tag{3.33}$$

[7] The term $\delta_{t_k}\delta_{t_k}$ (see (1.11)) does not appear explicitly in (3.31) but is contained in the second term of the left-hand side.

so that finally the Lagrange equations become in case of external impact

$$\begin{cases} \frac{\partial^2 T}{\partial \dot{q}^2}\{\ddot{q}\} + \frac{\partial^2 T}{\partial q \partial \dot{q}}\dot{q} - \frac{\partial (T-U)}{\partial q} = F \\ \frac{\partial T}{\partial \dot{q}}(t_k^+) - \frac{\partial T}{\partial \dot{q}}(t_k^-) = p_k. \end{cases} \tag{3.34}$$

Note that (1.11) is a particular case of (3.34), and that (3.34) can be extended to the case when the impulsive forces are any distribution in $\mathscr{D}^\star$ (see Appendix A.1 for a definition). The extension of Lagrange dynamics to systems with impulsive forces, has been the object of research since a long time ago [52, 53, 120, 1223].

3.4.2 Example: Flexible Joint Manipulators

Let us illustrate Eq. (3.34) with the case of elastic joint manipulators. These systems have been deeply studied in the robots control literature since they represent a nice example of Lagrangian systems with less inputs than degrees of freedom (the inputs are the torques at the joints) [223]. Two dynamical models have been used to design stabilizing controllers for such systems. The first model has been obtained in [1133]:

$$\begin{cases} M(q_1(t))\ddot{q}_1(t) + C(q_1(t), \dot{q}_1(t))\dot{q}_1(t) + g(q_1(t)) = K(q_2(t) - q_1(t)) \\ J_m \ddot{q}_2(t) + K(q_2(t) - q_1(t)) = u(t), \end{cases} \tag{3.35}$$

where $q_1 \in \mathbb{R}^n$ are the links angles, $q_2 \in \mathbb{R}^n$ are the motorshafts angles, $K \in \mathbb{R}^{n\times n}$ is the joint stiffness matrix, constant and diagonal, J_m is the motor inertia matrix, u is the control input vector. Note at once that the control problem for such systems has been more challenging than for rigid manipulators. Mainly this is due to the fact that the coordinates to be stabilized appear in the first equation in (3.35), and the control appears in the second equation.

Let us now assume that the system is submitted to a unilateral constraint $f(q_1) \geq 0$, with $f(q_1) \in \mathbb{R}$ and smooth. Hence the Euclidean gradient $\nabla f(q_1) = \frac{\partial f}{\partial q}(q_1)^T = \begin{pmatrix} \frac{\partial f}{\partial q_1}(q_1)^T \\ 0 \end{pmatrix}$, and the dynamical equations at the impact time t_k are given by

$$\begin{cases} M(q_1)\sigma_{\dot{q}_1}(t_k) = \frac{\partial f}{\partial q_1}(q_1(t_k)^T p_{\mathrm{n},k} \\ J_m \sigma_{\dot{q}_2}(t_k) = 0, \end{cases} \tag{3.36}$$

where $p_{\mathrm{n},k} \in \mathbb{R}$ is the impulsive Lagrange multiplier corresponding to the normal interaction impulse at the impact (we assume a frictionless surface $\{q \in \mathbb{R}^{2n} | f(q_1) = 0\}$). One concludes that $\dot{q}_2$ remains continuous at the impact. The model in (3.35) is in fact obtained by neglecting the effects of the link velocities $\dot{q}_1$ in the kinetic energy of the motorshafts. When these effects are taken into account, then one obtains a more complex model [1204], given by

$$\begin{cases} M_{11}(q_1)\ddot{q}_1 + M_{21}(q_1)\ddot{q}_2 + C_{11}(q_1,\dot{q}_1)\dot{q}_1 + C_{12}(q_1,\dot{q}_1)\dot{q}_2 + g(q_1) = K(q_2 - q_1) \\ M_{21}(q_1)^T\ddot{q}_1 + M_{22}\ddot{q}_2 + C_{21}(q_1,\dot{q}_1)\dot{q}_1 + K(q_2 - q_1) = u \end{cases} \tag{3.37}$$

where $M_{22} = J_m$. The difference between the two models in (3.35) and (3.37) is that in (3.37) the inertia matrix is no longer block diagonal. Hence there are acceleration cross terms in the dynamical equations. Note that from a control point of view, this drastically complicates the problem. For instance, the model in (3.35) is *static* state feedback linearizable, whereas the one in (3.37) is *dynamic* state feedback linearizable only (see [930] for definitions). Now the impact dynamical equations for (3.37) are given by

$$\begin{cases} M_{11}(q_1)\sigma_{\dot{q}_1}(t_k) + M_{21}(q_1)\sigma_{\dot{q}_2}(t_k) = \frac{\partial f}{\partial q_1}(q_1)^T p_{\mathrm{n},k} \\ M_{21}(q_1)^T\sigma_{\dot{q}_1}(t_k) + M_{22}\sigma_{\dot{q}_2}(t_k) = 0. \end{cases} \tag{3.38}$$

It is obvious from (3.38) that $\dot{q}_2$ may be this time discontinuous at the impact time, contrarily to the previous case where we deduced from (3.36) that it had to remain continuous. This is rather surprizing if we think a little of the mechanical structure of such systems, the impact usually occurs between the last link (the end effector) and the environment. By which dynamical effect could the motorshafts (which are in some sense "protected" by the elasticity) possess a discontinuous velocity? Now let us go a little deeper into the structure of the matrix $M_{21}(q_1)$. It can be shown [1204] that this matrix has the following form:

$$\begin{pmatrix} 0 & M_{21,12} & M_{21,13} & . & . & M_{21,1n} \\ 0 & 0 & M_{21,23} & . & . & M_{21,2n} \\ . & . & . & . & . & \\ . & . & . & . & . & . \\ 0 & 0 & . & . & 0 & M_{21,n-1,n} \\ 0 & 0 & 0 & . & 0 & 0 \end{pmatrix}. \tag{3.39}$$

Let us take the transpose of the matrix in (3.39) and introduce it in the second dynamical equation in (3.38). From the fact that M_{22} is diagonal, it follows that $\sigma_{\dot{q}_{2,1}}(t_k) = 0$. But the rest of the components of $\dot{q}_2$ may possess a discontinuity at the impact time. Indeed, we get $M_{21,12}\sigma_{\dot{q}_{1,1}}(t_k) + J_{22}\sigma_{\dot{q}_{2,2}}(t_k) = 0$, $M_{21,13}\sigma_{\dot{q}_{1,1}}(t_k) + M_{21,23}\sigma_{\dot{q}_{1,2}}(t_k) + M_{22,33}\sigma_{\dot{q}_{2,3}}(t_k) = 0$, and so on. The only component of $\sigma_{\dot{q}_1}$ which does not influence $\dot{q}_2$ is $\dot{q}_{1,n}$. As we shall see in Chap. 4, some collision rules will have to be applied to $\dot{q}_1$. Hence in general some components of $\dot{q}_1$ will be discontinuous. The jumps in $\dot{q}_2$ have then to be computed from the second equation in (3.38), and the percussion is deduced from the first equation in (3.38).

In conclusion, the simplified model in (3.35) always yields continuous motorshaft velocities, whereas the complete model in (3.37) may yield discontinuous motorshaft velocities. This is due to *dynamical coupling* that exists in the robot with elastic joints. This may have some practical consequences, since it means that joint compliance

does not really prevents the impulsive force from acting on the actuators angles (this of course does not mean at all that the actuators suffer from an impulsive force, see the second equation in (3.38)). Note that in certain cases, like *parallel drive manipulators* [1304], where all the actuators are mounted at the fixed base of the robot, then the simplified model is the exact one. In this sense it can be stated that *parallel drive manipulators are less sensitive to impacts*.

3.5 Hamilton's Principle and Unilateral Constraints

We now turn our attention to a much more difficult problem: the variational formulation of unilaterally constrained dynamics.

3.5.1 Hamilton's Principle Without Impacts

Let us start with the case when no impact acts on the system, i.e., the system is either in an unconstrained mode $f(q(t)) > 0$, or some of the constraints are persistently active: $f_i(q(t)) = 0$ for some $1 \leq i \leq m_u$ and $t \in I$, $I = [t_0, t_1]$, $t_1 > t_0$.

Proposition 3.1 *[724] Let us assume that $q(\cdot)$ and $\dot{q}(\cdot)$ are both absolutely continuous while $\ddot{q}(\cdot)$ exists almost everywhere on I. Then $-\delta \int_I L(q(t), \dot{q}(t))dt \geq 0$, for all $\delta q \in T_\Phi(q)$, $q(t_0) = q_0$, $q(t_1) = q_1$, implies that $M(q)\ddot{q}(t) + C(q(t), \dot{q}(t))\dot{q}(t) + g(q(t)) = Q(t)$, with $Q(t) \in -N_\Phi(q(t))$ almost everywhere on I.*

Remind from Definition 1.8 that $\Phi = \{q \in \mathcal{Q} | f(q) \geq 0\}$. As seen previously in this chapter, the generalized contact force takes the generic form $Q = \nabla f(q)\lambda$ for some Lagrange multiplier $\lambda \in \mathbb{R}^{m_u}$, and it satisfies the complementarity conditions $0 \leq f(q(t)) \perp \lambda(t) \geq 0$. Using (B.19) we obtain equivalently $\lambda(t) \in -N_{\mathbb{R}^+_{m_u}}(f(q(t))$. Moreover we have $\nabla f(q) = \partial \psi_{\mathbb{R}^+_{m_u}}(f(q)$. From Theorem B.3 we deduce that $Q \in -N_\Phi(q)$. This may also be written in a variational inequality formalism.

Remark 3.2 Bilateral constraints $h(q) = 0$ can be written as $f_1(q) = h(q) \geq 0$ and $f_2(q) = -h(q) \geq 0$. Let us assume that a suitable constraint qualification is satisfied so that the tangent cone is given as in (B.7). Both unilateral constraints are active, so that we obtain $T_\Phi(q) = \{z \in \mathbb{R}^n | \nabla f_1(q)^T z \geq 0$ and $\nabla f_2(q)^T z \geq 0\} = \ker(\nabla h(q)^T)$. Also $N_\Phi(q) = \ker^\perp(\nabla h(q)^T) = \mathrm{Im}(\nabla h(q))$. Unconstrained systems are recovered with $\Phi = \mathbb{R}^n$ in which case $T_\Phi(q) = \mathbb{R}^n$ and $N_\Phi(q) = \{0\}$, for all q in the configuration space.

3.5.2 Hamilton's Principle With Impacts

Hamilton's principle extension to impacting trajectories may be motivated by the close relationships between Fermat's and Maupertuis' principles [60, p. 252]. The same relationships should hold when reflections are present. Classically, two problems arise in such minimization problems [1306]: (i) Nature of the curves (i.e., in which space have the admissible curves q to be defined?) to ensure existence of an extremum (minimum) of the integral action[8] (ii) Necessary and sufficient conditions to be satisfied by the extremals (Lagrange equations, transversality, and Erdmann–Weierstrass corner conditions).

Roughly, point (i) requires that the nature of the admissible curves be specified as well as the topology associated with the space to which they belong, since existence result can be proved *via* compactness of the level sets and lower semicontinuity of the functional to be minimized, which is known as Tonelli's direct method [813]. The direct method of variational calculus is based on the fact that a function $F(\cdot)$ defined on a compact set C and lower semicontinuous[9] on C, attains its lowerbound on C, i.e., there exists $x_0 \in C$ such that $F(x_0) = \inf_{x \in C} F(x)$. This also applies to functionals $I(q)$, and is known as Tonelli's direct method which allows to prove the *existence* of a minimizing curve q.

Theorem 3.1 (Tonelli [813]) *Assume that* $I : E \to \bar{\mathbb{R}}$[10] *is coercive and lower semicontinuous. Then* $I(\cdot)$ *has a minimum point in* E.

By point it is meant here an element of E, i.e., a curve if I is a functional and E a space of functions. In case E is a metric space, then I is coercive if its level sets , i.e., the sets $\{q \in E | I(q) \leq \alpha\}$, $\alpha \in \mathbb{R}$, have a compact closure [813, Definition 1.12].[11] Also a bilinear form $a(u, y) : L^2 \times L^2 \to \mathbb{R}$ is coercive if $a(u, u) \geq \alpha ||u||_2^2$ for some $\alpha > 0$ [191]. Of course the great difficulty in proving such existence results lies in the choice of suitable spaces of admissible curves E, together with a suitable topology (i.e., a notion of convergence) that allows to prove coercivity and lower semicontinuity of I in E. It is another problem to derive necessary and/or sufficient conditions that an extremal point must satisfy: this is point (ii). A less mathematical formulation of Tonelli's existence theorem is as follows: if the Lagrangian $L(\cdot, \cdot, \cdot)$ is C^2 and satisfies (a) $L(t, q, v) \geq a||v||^{1+b} + c$, for all (t, q, v) and for some constants $a, b > 0$ and $c \in \mathbb{R}$, (b) $\frac{\partial^2 L}{\partial v^2}(t, q, v) \geq 0$, for all (t, q, v), then an absolutely continuous solution that minimizes the action integral $I(q)$ with fixed end points exists. One realizes that these conditions are satisfied in the classical mechanical case where

---

[8] *"Every problem of the calculus of variations has a solution, provided the word "solution" is suitably understood."* (D. Hilbert), so that *... in variational problems the original setting must be modified in accordance with the needs of an existence theory.* [1306, p. 218].

[9] see Definition B.12 in Appendix B.

[10] $\bar{\mathbb{R}} = \mathbb{R} + \{-\infty, +\infty\}$.

[11] Recall that if the level sets are compact, the function is said to be proper [1129, Definition 4.6.1]. Hence properness implies coerciveness.

$L(q,v) = \frac{1}{2} v^T M(q) v + U(q)$, with $M(q) \succ 0$ and provided $U(q) \geq U_{\min} > -\infty$. A natural set for such variational problems is a subset of

$$Q = \{q(\cdot) | q \in AC([t_0, t_1], \mathbb{R}^n), \dot{q} \in RCLBV([t_0, t_1], \mathbb{R}^n), \ddot{q} \in \mathscr{D}^\star\}, \qquad (3.40)$$

endowed with a suitable topology for compactness (in view of the existence results described in Chap. 2, we can even impose $q(\cdot)$ Lipschitz continuous). Note that it is also customary in variational calculus to use as basic spaces of admissible curves Sobolev spaces [191, 813], i.e., $q \in W^{1,p}([t_0, t_1])$, see Appendix A.3 for the definition of such spaces of functions. In some other more general problems [909] that could fit with ours if $q(\cdot)$ was allowed to be discontinuous (thus $L(\cdot)$ would contain singular distributions like in Bressan's hyperimpulsive systems), the basic space is that of equivalent classes of $RCLBV$ functions. In order to get more insight on this point, consider the following one degree-of-freedom simple example, where the dynamics can be integrated at hand. Let a disk with radius $\frac{d}{2}$ move without friction on a horizontal plane between two parallel rigid "walls," situated at a distance $d + 2\varepsilon$ one from each other. This may represent the dynamics of a mechanism with clearance, or with a "bi-unilateral" constraint of the form $c_1 \leq f(x) \leq c_2$, considered for instance in [1003, Chap. 3], or a simplified Fermi accelerator model [540]. There is conservation of energy, and the initial conditions on position and velocity are such that the problem is well-posed. Then the graph of the position of the disk center with respect to time is a "saw-toothed" or "zigzag" diagram. The singular points correspond to the impact times, with $t_k = \frac{(2k+1)\varepsilon}{\dot{x}_0}$ (assuming $x_0 = 0$). By letting ε approach zero, this curve tends toward an infinitesimal zigzag curve, that is not a curve, but a generalized curve [1306, Chap. 6], i.e., an element of the dual space of continuous functions (Young's generalized curves [1306]) or smooth functions (Schwartz's distributions).[12] It is worth noting that in this limit case of zigzag curve with no loss of kinetic energy at impacts, the corresponding velocity $\dot{x}$ is not of bounded variation on any interval of strictly positive measure as $\varepsilon \to 0$, since the percussion magnitude is $2m|\dot{x}_0| > 0$ at each impact and the flight time is $\Delta_k \stackrel{\Delta}{=} \frac{2}{n|\dot{x}_0|}$. Hence by letting $n \to +\infty$, the total variation of the velocity on a bounded interval I grows unbounded. Since anyway the zigzag curve is measurable, it defines a Schwartz' distribution and thus possesses infinitely many distributional (or generalized) derivatives. This may not be of interest for us, since we are rather interested (mainly for stability notions and control purposes) by solutions which are $RCLBV$. It seems that this "pathological" saw-toothed case has not been revealed elsewhere in the literature on impact dynamics. One may be tempted to conjecture

[12] Let us define $n = \frac{1}{\varepsilon}$. The saw-toothed functions $x_n(t)$ converge uniformly toward the function $x \equiv 0$ [397, p. 64], indeed $\sup_{t \in \mathbb{R}} |x_n(t)| = \frac{1}{n} \to 0$ when $n \to +\infty$. However, the sequence $\{\dot{x}_n\}$ does not converge toward $\dot{x} \equiv 0$, not even pointwisely since $|\dot{x}_n(t)| = 1$ for almost all t. Note that this is reassuring for a mechanician: if $\dot{x}_n \to 0$ then $\ddot{x}_n \to 0$ in the distributional sense so that no impacts occur in the limit. Another point of view is that the infinitesimal zigzag curve can be described by assigning the pair of slope $+1$ and -1 at each point with a probability $\frac{1}{2}$ [1306, p. 160]. This makes it clear that the saw-toothed function does not converge to the function $x \equiv \dot{x} \equiv \ddot{x} \equiv ... \equiv 0$ but to something else in a space of "generalized curves".

that problems with unilateral constraints $f(q) \geq 0$ always possess a solution in Q, provided some mild conditions are imposed on the constraint $f(q)$. For instance, this pathological case does not fit with the assumptions of Theorem 5.3 in Chap. 5. Recall that it is difficult in general to assert that the solutions are in Q in (3.40): existence results need deep mathematical investigations, see Chap. 2, and Sect. 5.2. For instance, it is true that for all $I \subset \mathbb{R}$, I compact, then $\int_I T(t)dt < +\infty$, i.e., the kinetic energy is locally integrable. However, this implies that $\dot{q} \in L_2[I]$, which in turn does not imply that $\dot{q}(\cdot)$ is of bounded variation. One could think of the solution as being a measurable function, but then we lose the interpretation of the interaction impulses as being countable. As we shall see, velocities of bounded variation lend themselves very well to some sort of stability results, and are from this point of view quite convenient to work with.

The problem has to be well formulated, this is what we discuss now. Let us illustrate how corners[13] may naturally be contained in a variational problem. For instance, assume that the integrand of $I(x)$ is equal to $L(x, \dot{x}) = (1+x^2)(1+[\dot{x}^2 - 1]^2)$, with endpoint conditions 0, 1, $x(0) = x(1) = 0$. Then the minimizing curve is "naturally" an infinitesimal zigzag [1306, p. 159]. We may say that the integral action "contains" the irregularities. This is not the case for a mechanical problem if a classical Lagrangian is considered as the *Erdmann–Weierstrass corner conditions* [1003] show. These conditions yield

$$\frac{\partial L}{\partial \dot{q}}(t_k^+) = \frac{\partial L}{\partial \dot{q}}(t_k^-) \tag{3.41}$$

and

$$\left(L - \dot{q}^T \frac{\partial L}{\partial \dot{q}}\right)(t_k^+) = \left(L - \dot{q}^T \frac{\partial L}{\partial \dot{q}}\right)(t_k^-). \tag{3.42}$$

Using that $L(q, \dot{q}) = T(q, \dot{q}) - U(q)$, condition (3.41) yields $M(q)\dot{q}(t_k^+) = M(q)\dot{q}(t_k^-)$, while condition (3.42) yields $T(t_k^+) = T(t_k^-)$, where $T(q, \dot{q}) = \frac{1}{2}\dot{q}^T M(q)\dot{q}$. From the first condition, the generalized momentum satisfies $M(q(t_k))\dot{q}(t_k^+) = M(q(t_k))\dot{q}(t_k^-)$ so that the corresponding percussion is zero also, see Example 1.3. Hence $\dot{q}(\cdot)$ is continuous.

Remark 3.3 (Weak and Strong Extrema [724]) The conditions in (3.41) and (3.42) correspond to weak or strong extrema of the action integral in (3.30) [724]: weak extrema fulfill the Euler–Lagrange equations and (3.41), strong extrema fulfill the Euler–Lagrange equations, (3.41) and (3.42). Weak extrema are in the weak norm which roughly is given by $\max_{x\in I} ||f(x)|| + \operatorname{ess\,sup}_{x\in I} ||\dot{f}(x)||$, while the strong norm is $\max_{x\in I} ||f(x)||$.

Consider the bouncing ball (on a fixed table) classical example, whose dynamics is in (3.11). Assume that one wants to search for the extremals of a classical variational

[13] i.e., nondifferentiable points of the curves.

problem $I(q) = \int_{t_0}^{t_1} L(q, \dot{q})dt$, with fixed endpoints and the unilateral condition $q \geq 0$, then for any t_0, t_1, $q(t_0) > 0$, $q(t_1) \geq 0$,[14] the minimization process will always lead to a smooth solution curve, because the endpoint conditions uniquely determine the initial data. Roughly speaking, the solution will always be such that it takes the whole interval $[t_0, t_1]$ to reach the constraint $q = 0$. As a consequence the impacts will always be absent of such a formulation! It is therefore necessary for the solution curve to contain impacts that the endpoint conditions be modified by fixing for instance t_0, t_1, $q(t_0)$, and $\dot{q}(t_0)$, a choice that is also made in [242], see Problem 3.1 below.[15] Notice that this *a priori* fixes $q(t_1)$ if we assume uniqueness of the solutions. Then the constraint $q = 0$ will in general be reached at $t_2 < t_1$ and with a nonzero left velocity $\dot{q}(t_2^-)$. Still this is not sufficient as the corner conditions indicate. The problem thus must be transformed to one of the form in (a) or (b) below. Let us now formulate the variational problem. First, notice that in order for this problem to make sense, either the integral action to be minimized must "contain" the impacts, or the space of admissible curves Q in (3.40) has to be modified. Basically, two paths may be followed:

(a) $m_{\bar{Q}}(I) = \min I(q)$, $q \in \bar{Q} \stackrel{\Delta}{=} \{q \in Q | f(q) \geq 0, \dot{q}_{\mathrm{n}}(t_k^+) = -e_{\mathrm{n}}\dot{q}_{\mathrm{n}}(t_k^-)$ with $f(q(t_k)) = 0, \nabla f(q(t_k))^T \dot{q}(t_k^-) \leq 0$, admissible initial conditions$\}$

(b) $m_Q \bar{I}(q) = \min \bar{I}(q)$, $q \in Q$, with $\bar{I}(q) = \int_{t_0}^{t_1} \bar{L}(q, \dot{q}, \tau)d\tau$, where $\bar{L}(\cdot)$ is a suitably modified Lagrangian function.

In other words, one can *a priori* either modify the set of curves within which the action is to be minimized, without modifying the Lagrangian, or modify the Lagrangian at once.[16] In the sequel we shall describe two solutions that have been proposed by Kozlov and Treshchev [683], Panagiotopoulos and Glocker [960], and Buttazzo and Percivale [242]. The first ones follow path (a), whereas the third ones rather follow path (b). These studies do not aim at showing *existence* of a minimizing curve. The ones in [683, 960] prove that in a modified space of admissible curves, the classical action is extremal for the motion of the system (i.e., for the motion that satisfies Hamilton's principle outside the impacts, and shock conditions at the impact time). The third one [242] proves that the motion of a rigid problem is an extremal of a modified action, which contains the singular measure that corresponds to the impulsive force at impact times.

---

[14] Obviously if the endpoint conditions do not satisfy the constraints, this problem possesses no solution.

[15] Hamilton's principle with fixed t_0, t_1, $q(t_0)$, and $\dot{q}(t_0)$ has been studied in [30]. It is shown that the Lagrangian has to be modified to $K = -\frac{1}{2}\dot{q}^T M(q)\dot{q}(t - t_1) - q^T K q(t - t_1) + 2F^T q(t - t_1)$ in the action integral, where the last two terms account for the potential energy.

[16] In (a) and (b), one may replace min $I(q)$ by extr $I(q)$. Indeed searching for the minimizing curve is very hard even in the nonconstrained case. In general one finds the Euler–Lagrange equations which are only necessary conditions to be satisfied by the extremalizing curve. Whether or not these curves define a minimum point of the action is another problem. Additional assumptions about convexity (i.e., forces derived from a convex potential) permit to derive Hamilton's principle as a minimum principle [958].

3.5.3 Modified Set of Curves

Let us describe the studies proposed in [683, 960]. This way of doing is closer to the usual formulation for smooth motions that one can find in mechanical textbooks, than the mathematical work of [242]. This is the reason why we introduce it first. Let us consider an n degree-of-freedom system, with a unilateral constraint $f(q) \geq 0$. Assume that the shocks are perfectly elastic, i.e., we have $\dot{q}(t_k^+)^T M(q)\dot{q}(t_k^+) = \dot{q}(t_k^-)^T M(q)\dot{q}(t_k^-) \Rightarrow T_L(t_k) = 0$. Let us consider some motion $q_0(t) : [t_1, t_2] \mapsto \mathbb{R}^n$, with $f(q_0(t)) > 0$ for $t \in [t_1, t_2] \setminus \{t_0\}$, $f(q_0(t_0)) = 0$.

Remark 3.4 Note that if kinetic energy is conserved at the impacts, then the impact times satisfy $t_{k+1} > t_k + \delta$, for some $\delta > 0$ depending on initial data $q(t_1), \dot{q}(t_1)$, see Theorem 5.3 in Chap. 5. Hence one can consider without loss of generality only one impact on the interval $[t_1, t_2]$, chosen sufficiently small. If there was some energy loss at t_k, such an assumption would not be possible due to the eventual accumulation point of the impact times sequence $\{t_k\}$ (in that case for any interval $[t_1, t_2]$, there exists initial data at t_1 and external forces such that there is an infinity of rebounds in $[t_1, t_2]$).

Let us now consider the set of varied curves $q_\alpha(t) : [t_1, t_2] \mapsto \mathbb{R}^n$, with $\alpha \in (-\varepsilon, \varepsilon)$ and

- $q_\alpha(t_1) = q_0(t_1), q_\alpha(t_2) = q_0(t_2)$.
- $q_\alpha(t)$ is a smooth function of α and t in $(-\varepsilon, \varepsilon) \times \{[t_1, t_\alpha) \cup (t_\alpha, t_2]\}$.
- $f(q_\alpha(t_\alpha)) = 0$, where $t_\alpha : (-\varepsilon, \varepsilon) \mapsto [t_1, t_2]$ is a smooth function of the parameter α.

Kozlov and Treshchev choose the integral action

$$I(\alpha) = \int_{t_1}^{t_2} L(\dot{q}_\alpha(t), q_\alpha(t))dt, \tag{3.43}$$

where $L(\dot{q}, q)$ is the Lagrangian of the system. It is therefore clear now that the Lagrangian function is not modified, but that the set of varied curves is changed to curves with possible discontinuous derivatives at the times t_α. It is noteworthy that both the curves and the impact times are varied, and that the varied curves attain the constraint. This is illustrated in Fig. 3.2. A first necessary step is to compute the variation of the action. The following is true:

Lemma 3.1 *[683] The variation of the action in (3.43) is given by*

$$\begin{aligned}\delta I(0) = \frac{dI}{d\alpha}(0) = {} & \sigma_{\dot{q}_0}(t_0)^T M(q(t_0)) \frac{d[q_\alpha(t_\alpha)]}{d\alpha}(0) \\ & - \frac{1}{2}\left[\dot{q}_0(t_0^-)^T M(q(t_0))\dot{q}_0(t_0^-) - \dot{q}_0(t_0^+)^T M(q(t_0))\dot{q}_0(t_0^+)\right] \frac{dt_\alpha}{d\alpha}(0) \\ & + \int_{t_1}^{t_2} \left[\frac{\partial L}{\partial q} - \frac{d}{dt}\left(\frac{\partial L}{\partial \dot{q}}\right)\right]_{q=q_0} \frac{\partial q_\alpha(t)}{\partial \alpha}(0)dt.\end{aligned} \tag{3.44}$$

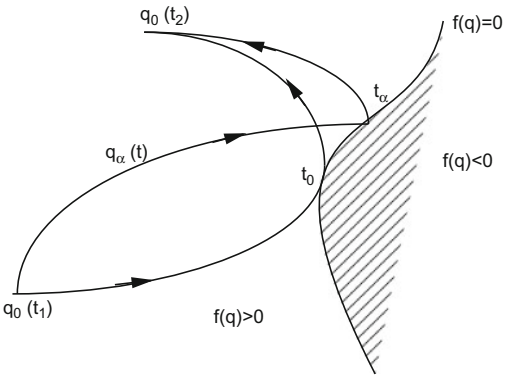

Fig. 3.2 Varied curves

Let us note that $q_\alpha(t_\alpha)$, $q_\alpha(t)$, and t_α are to be considered as functions of α, and their derivatives are calculated at $\alpha = 0$. Note also that the second term in the variation of the action is in fact the kinetic energy loss at impact at time t_0 (if q_0 represents a motion of the system). The proof of Lemma 3.1 can be found in [683, p. 12] and [959]. For the sake of clarity of the exposition, let us investigate it. This is a bit lengthy but is worth following at least once. Since the varied curves q_α are not differentiable at t_α, the first step is to write

$$\frac{dI}{d\alpha}(0) = \frac{d}{d\alpha}\left(\int_{t_1}^{t_\alpha} L(\dot{q}_\alpha(t), q_\alpha(t)) + \int_{t_\alpha}^{t_2} L(\dot{q}_\alpha(t), q_\alpha(t))\right). \tag{3.45}$$

Now consider only the first term between brackets in (3.45), and calculate

$$\begin{aligned}\tfrac{d}{d\alpha}\textstyle\int_{t_1}^{t_\alpha} L(\dot{q}_\alpha(t), q_\alpha(t)) = \lim_{\alpha\to\alpha_0} \tfrac{1}{\alpha_0}\textstyle\int_{t_1}^{t_\alpha} \left[L(\dot{q}_{\alpha+\alpha_0}(t), q_{\alpha+\alpha_0}(t)) - L(\dot{q}_\alpha(t), q_\alpha(t)\right] dt \\ + \lim_{\alpha\to\alpha_0} \tfrac{1}{\alpha_0}\textstyle\int_{t_1}^{t_{\alpha+\alpha_0}} L(\dot{q}_{\alpha+\alpha_0}(t), q_{\alpha+\alpha_0}(t))dt \\ - \textstyle\int_{t_1}^{t_\alpha} L(\dot{q}_{\alpha+\alpha_0}(t), q_{\alpha+\alpha_0})(t)dt.\end{aligned} \tag{3.46}$$

The first term in the right-hand side of (3.46) is found through standard calculations to be equal to

$$\int_{t_1}^{t_\alpha} \left(\frac{\partial L}{\partial \dot{q}_\alpha}\frac{\partial \dot{q}_\alpha}{\partial \alpha} + \frac{\partial L}{\partial q_\alpha}\frac{\partial q_\alpha}{\partial \alpha}\right) dt \tag{3.47}$$

while the second one is

$$\begin{aligned}\lim_{\alpha\to\alpha_0} \tfrac{1}{\alpha_0}\textstyle\int_{t_1}^{t_{\alpha+\alpha_0}-t_\alpha} L(\dot{q}_{\alpha+\alpha_0}(t), q_{\alpha+\alpha_0})(t)dt &= L(\dot{q}_\alpha(t), q_\alpha(t) \lim_{\alpha\to\alpha_0} \tfrac{t_{\alpha+\alpha_0}-t_\alpha}{\alpha_0} \\ &= L(\dot{q}_\alpha(t), q_\alpha(t))\tfrac{dt_\alpha}{d\alpha}.\end{aligned} \tag{3.48}$$

Integrating (3.47) by parts one finds

$$\left[\frac{\partial L}{\partial \dot{q}_\alpha}\frac{\partial q_\alpha}{\partial \alpha}\right]_{t_1}^{t_\alpha} + \int_{t_1}^{t_\alpha}\left\{\frac{\partial L}{\partial q_\alpha}\frac{\partial q_\alpha}{\partial \alpha} - \frac{d}{dt}\left(\frac{\partial L}{\partial \dot{q}_\alpha}\right)\frac{\partial q_\alpha}{\partial \alpha}\right\}dt. \tag{3.49}$$

Now let us rewrite

$$\frac{\partial q_\alpha}{\partial \alpha}(t_\alpha) = \frac{d}{d\alpha}\left(q_\alpha(t_\alpha)\right) - \frac{\partial q_\alpha}{\partial t_\alpha}\frac{dt_\alpha}{d\alpha}, \tag{3.50}$$

and notice that

$$\frac{\partial q_\alpha}{\partial \alpha}(t_1) = 0, \tag{3.51}$$

because $q_\alpha(t_1) = q_0(t_1)$ and is therefore a quantity that does not depend on α. Using (3.50) and (3.51) one gets

$$\frac{\partial L}{\partial \dot{q}_\alpha}\frac{\partial q_\alpha}{\partial \alpha}(t_\alpha) + L(\dot{q}_\alpha, q_\alpha)\frac{dt_\alpha}{d\alpha} = \frac{\partial L}{\partial \dot{q}_\alpha}\frac{d}{d\alpha}(q_\alpha(t_\alpha)) + \left[L(\dot{q}_\alpha, q_\alpha) - \frac{\partial L}{\partial \dot{q}_\alpha}\frac{dq_\alpha}{dt_\alpha}\right]\frac{dt_\alpha}{d\alpha}. \tag{3.52}$$

Introducing (3.50), (3.51), (3.49), (3.52), and (3.48) into (3.46) one obtains

$$\begin{aligned}\tfrac{d}{d\alpha}\textstyle\int_{t_1}^{t_\alpha} L(\dot{q}_\alpha, q_\alpha)dt &= \tfrac{\partial L}{\partial \dot{q}_\alpha}\tfrac{d}{d\alpha}(q_\alpha(t_\alpha)) + \left[L(\dot{q}_\alpha, q_\alpha) - \tfrac{\partial L}{\partial \dot{q}_\alpha}\tfrac{dq_\alpha}{dt_\alpha}\right]\tfrac{dt_\alpha}{d\alpha} \\ &\textstyle\int_{t_1}^{t_\alpha}\left[\tfrac{d}{dt}\left(\tfrac{\partial L}{\partial \dot{q}_\alpha}\right)\tfrac{\partial q_\alpha}{\partial \alpha} + \tfrac{\partial L}{\partial q_\alpha}\tfrac{\partial q_\alpha}{\partial \alpha}\right]dt.\end{aligned} \tag{3.53}$$

Now use the following equalities[17]

$$\begin{cases}\tfrac{\partial L}{\partial \dot{q}_\alpha}\tfrac{dq_\alpha(t_\alpha)}{dt_\alpha}(0) = \dot{q}^T(t_0^-)M(q(t_0))\dot{q}(t_0^-) \\ L[\dot{q}_\alpha(t_\alpha), q_\alpha(t_\alpha)](0) = \frac{1}{2}\dot{q}_0^T(t_0^-)M(q_0(t_0))\dot{q}_0(t_0^-) - U(q_0(t_0)) \\ \tfrac{\partial L}{\partial \dot{q}_\alpha}\tfrac{d}{d\alpha}(q_\alpha(t_\alpha))(0) = \dot{q}^T(t_0^-)M(q(t_0))\tfrac{d}{d\alpha}q_\alpha(t_\alpha)(0).\end{cases} \tag{3.54}$$

We finally obtain

$$\begin{aligned}\tfrac{d}{d\alpha}\left(\textstyle\int_{t_1}^{t_\alpha} L(\dot{q}_\alpha, q_\alpha)dt\right)(0) &= \dot{q}_0^T(t_0^-)M(q(t_0))\tfrac{d}{d\alpha}q_\alpha(t_\alpha)(0) \\ &- \left[\dot{q}_0^T(t_0^-)M(q(t_0))\dot{q}_0(t_0^-) + U(q_0(t_0))\right]\tfrac{dt_\alpha}{d\alpha}(0) \\ &\textstyle\int_{t_1}^{t_\alpha}\left[\tfrac{\partial L}{\partial q} - \tfrac{d}{dt}\left(\tfrac{\partial L}{\partial \dot{q}}\right)\right](\dot{q}_0, q_0)\tfrac{\partial q_\alpha}{\partial \alpha}(0)dt.\end{aligned} \tag{3.55}$$

[17] Notice that the notation $\cdot(0)$ means that the considered function of α is evaluated at $\alpha = 0$. It is clear that since we analyze the action on the interval $[t_1, t_\alpha)$, then $t_\alpha(0) = t_0^-$.

Now one can treat the second term in (3.45) exactly in the same manner, and get the sum of both (in particular the potential energy $U(q)$ vanishes in the sum) to finally obtain (3.44).
The next step is to prove that if q_0 is a motion of the system, then it is an extremal of the action, and *vice versa*. The following result is true.

Lemma 3.2 *[960] Let us consider a time interval (t_1, t_2) incuding one elastic impact, with $\mathrm{bd}(\Phi)$ smooth and Φ a convex set. The curve $q_0(\cdot)$ is a motion of the dynamical system with Lagrangian $L(\dot{q}, q)$, unilateral constraint $f(q) \geq 0$ and elastic collisions, if and only if $\delta I(0) \geq 0$ for any small variation δq such that $q + \delta q \in \Phi$.*

The complete proof can be found in [960]. The variational formulation including an impact time $t_k \in (t_1, t_2)$ can be derived using some manipulations (like Moreau's formula providing the derivative of $f^T g$ when $f(\cdot)$ and $g(\cdot)$ are of bounded variation (hence $f^T g \in BV$), and df is the differential measure, see Appendix A.3.2: $d[f^T g] = df^T g^+ + (f^-)^T dg = df^T g^- + (f^+)^T dg$ [884, 886]). It is then possible to derive a variational formulation providing necessary and sufficient conditions for a function to be a solution of the problem, without variation of the impact time. Let us consider a function in the set Q in (3.40), or with the acceleration being a measure [960]. Then such a function is a solution of the considered mechanical system with unilateral constraints if and only if it satisfies on the required time interval:

$$\begin{aligned} &-[\dot{q}^T M(q)(q^\star - q)](t_2) + [\dot{q}^T M(q)(q^\star - q)](t_1) + \int_{t_1}^{t_k^-} \nabla T^T(\dot{q}^\star - \dot{q})dt \\ &+ \int_{t_k^+}^{t_2} \nabla T^T(\dot{q}^\star - \dot{q})dt + \int_{t_1}^{t_2} F^T(q^\star - q)dt \geq 0 \end{aligned} \tag{3.56}$$

for all functions $q^\star \in \Phi$, where F represents all generalized bounded forces. The inclusion of the impact time variation, that renders the result more general, requires the calculations made above. The longest part of the proof is sufficiency ($\Longleftarrow$). Necessity (the equations of motion imply $\delta I(0) \geq 0$) is easier to check. If the forces derive from a potential, this inequality can in turn be written as $-\int_{t_1}^{t_2} \delta L(q, \dot{q})dt \geq 0$ where the δ is the variation in the sense of the classical calculus of variations, and $\delta q = q^\star - q$ is small enough and satisfies $\delta q = 0$ at the end points t_1 and t_2. These expressions do not yet incorporate a variation of the impact time t_k. The inclusion of this variation can be done as explained above, and enables one to prove that $\delta I(0) \geq 0$. Some facts are important in the proof:

(i) The kinetic energy loss at t_0 is zero (hence the second term in $\delta I(0)$ is zero as well).

(ii) The term $\frac{d[q_\alpha(t_\alpha)]}{d\alpha}(0)$ is orthogonal (in the kinetic metric sense) to $\nabla f(q_0)$, whereas $\sigma_{\dot{q}_0}(t_0)$ is orthogonal to the surface $f(q) = 0$ at q_0. These results can be easily proved using the particular decomposition of the generalized velocity that is described in Chap. 6. Indeed one can show that $\sigma_{\dot{q}_0}(t_0) = \left(\dot{q}_{\mathrm{norm}}(t_0^+) - \dot{q}_{\mathrm{norm}}(t_0^-)\right)\mathbf{n}_q$, with $\mathbf{n}_q$ as in (6.22). Since by assumption $f(q_\alpha(t_\alpha)) = 0$, for all $\alpha \in (-\varepsilon, \varepsilon)$, it follows that $\frac{\partial f}{\partial q}^T \frac{d[q_\alpha(t_\alpha)]}{d\alpha} = 0$, for all α as well, in particular for $\alpha = 0$.

Remark 3.5 A deep analysis of Hamilton's principle is proposed in the seminal article [724]. As alluded to above (see Remark 3.3), it shows that two main forms of variations of the action integral may be considered: weak and strong variations.

3.5.4 Modified Lagrangian Function

Let us choose now path (b). It remains to examine how the integral action whose extremals are the solution of the impact problem can be written. As suggested by the studies presented in Chap. 2, the perfectly rigid case can be regarded as the limit of sequences of continuous dynamics problems $\mathscr{P}_n$. Problems $\mathscr{P}_n$ are typically problems where the integrand of the integral action possesses different values depending on whether a given function $f(q)$ is positive, zero, or negative.
An interesting formulation in direction (b) is the one in [242, 989, 900]. We have already considered such approaches in Chap. 2. These authors consider approximating variational problems $\mathscr{P}_n$ with Lagrangian:

$$L(q_n, \dot{q}_n) = T(q_n, \dot{q}_n) - U(q_n) - \alpha_n(f(q_n)), \tag{3.57}$$

where the last term accounts for the potential elastic energy when there is contact and will be defined below. The limiting or bounce problem $\mathscr{P}$ has Lagrangian $L(q, \dot{q}) = T(q, \dot{q}) - U(q) + f(q)\mu$, where the unilateral constraint is $\mathbb{R} \ni f(q) \geq 0$, and μ is a bounded positive measure that represents the contact force (possibly impulsive). The problem is stated as follows:

Problem 3.1 [242] Let us consider a Lagrangian mechanical system, with $\mathscr{Q}$ the system's configuration space. The vector $q(t) \in \mathscr{Q}$ is the generalized position, subject to the constraint $f(q) \geq 0$, and to a potential $U(q)$. The kinetic metric of the system defines a scalar product on its tangent space at every q. The configuration space $\mathscr{Q}$ is assumed to be be an n-dimensional manifold of class C^3, without boundary. Let $f : \mathscr{Q} \to \mathbb{R}$ be a function of class C^3 such that $\nabla f(q)$ is not zero on the set $\{q \in \mathscr{Q} |\ f(q) = 0\}$. Given $T > 0$, $\mathrm{Lip}(0, T; \mathscr{Q})$ denotes the space of Lipschitz continuous functions from $[0, T]$ into $\mathscr{Q}$. L_1 is the space of $L_1[0, T]$-bounded functions, twice differentiable. Then a pair $(U, q) \in L_1$ x Lip solves the bounce problem $\mathscr{P}$ (or equivalently q is a solution of $\mathscr{P}$ with potential $U(t, q)$) if

(i) $f(q(t)) \geq 0$ for every $t \in [0, T]$.
(ii) There exists a finite positive measure μ on $(0, T)$ such that q is an extremal for the functional

$$\bar{I}(q) = \int_0^T \left[\frac{1}{2}\dot{q}^T M(q(t))\dot{q} - U(q(t))\right] dt + \int_0^T f(q(t))d\mu \tag{3.58}$$

and the support of μ satisfies $\mathrm{supp}\,(\mu) \subseteq \{t \in [0, T] \,|\, f(q(t)) = 0\}$.
(iii) For every $t_1, t_2 \in [0, T]$ the following energy relation holds

$$2\int_{t_1}^{t_2} \nabla U(q(t))^T \dot{q}(t)dt = \dot{q}(t_2^+)^T M(q(t_2))\dot{q}(t_2^+) - \dot{q}(t_1^+)^T M(q(t_1))\dot{q}(t_1^+)$$
$$= \dot{q}(t_2^-)^T M(q(t_2))\dot{q}(t_2^-) - \dot{q}(t_1^-)^T M(q(t_1))\dot{q}(t_1^-). \tag{3.59}$$

Similarly to the Problem 2.1, (i) is the unilateral constraint, (iii) means that the system is conservative (or passive, or lossless in Control Theory language), during smooth motions and at the collisions with $f(q) = 0$: If t_2 is a collision time, then one deduces from (iii) that the kinetic energy loss is $T(t_2^+) = T(t_2^-)$, by taking t_1 during a smooth motion period. In other words, the function $T : t \to \dot{q}(t)^T M(q(t))\dot{q}(t)$ is continuous. From (ii), a solution $q(t)$ must satisfy

$$M(q(t))\ddot{q}(t) + C(q(t), \dot{q}(t))\dot{q}(t) + \frac{\partial U}{\partial q}(q(t)) = \nabla f(q(t))\dot{h}(t). \tag{3.60}$$

Recall that the generalized torque $C(q, \dot{q})\dot{q}$ represents workless gyroscopic inertial forces, not dissipative forces. The last integral term in (3.58) can be written as $\int_0^T f(q(t))\dot{h}$, where using our preceding notations $h(t)$ denotes the "impact" step function such that $dh = \dot{h} = \sigma_h(t_k)\delta_{t_k}$ is a singular distribution. In other words $\sigma_h(t_k)$ is the density of μ with respect to the Dirac measure δ_{t_k}, see Definition 1.2. The notation $d\mu$ $(= dh)$ is a shorthand for $\sigma_h(t_k)\delta_{t_k}$. As we shall see in the sweeping process formulation, the Lagrange equations of the system, which we wrote in (3.60) as an equality between functions, is an equality of measures which has to be written as

$$M(q(t))d\dot{q} + \left[C(q(t), \dot{q}(t))\dot{q}(t) + \frac{\partial U}{\partial q}(q(t))\right]dt = \nabla f(q(t))d\mu, \tag{3.61}$$

where $d\dot{q}$ is the measure[18] defined by the generalized (or distributional) derivative of $\dot{q}$. It is clear that (3.61) can equivalently be rewritten as [1142]

$$\int \varphi^T M(q)du + \int \varphi^T \left[C(q, \dot{q})\dot{q} + \frac{\partial U}{\partial q}(q)\right]dt = \int \varphi^T \nabla f(q)\lambda, \tag{3.62}$$

where du is the measure defined from $u = \frac{d\dot{q}}{dt}$ with $v \in RCLBV$ and λ is the Lagrange multiplier. We modified the notations between (3.61) and (3.62) because the latter are often used in the related literature on Measure Differential Inclusions, see Sect. 5.2. A reader who is not familiar with all those notations might be troubled. Evidently φ in (3.62) is a test function, which can be taken here in the set of continuous functions (one needs not working with Schwartz distributions since as we noted before only signed distributions are involved). From the developments in Chap. 1 this

[18] In Chap. 1 we indicated that distributional derivatives of a function $f(\cdot)$ are sometimes denoted as Df. The notation df is also used in nonsmooth dynamics to denote the measure associated with a function $RCLBV$ [894] and is called the *differential measure* of $f(\cdot)$, see Sect. A.3.2.

is equivalent outside the atoms of μ and of $d\dot{q}$ to the classical Lagrange equations. The formulation as in (3.61) is at the base of nonsmooth dynamics. Similarly as for Problem 2.2, the solutions of the limit problem are such that $\dot{q} \in RCLBV$.

Remark 3.6 Time-dependent potential terms $U(t, q(t))$ can also be considered.

The analysis proceeds to prove that any limit of a sequence of solutions of $\mathscr{P}_n$ converges toward a solution of $\mathscr{P}$, and that any solution of $\mathscr{P}$ is the limit of such an approximating sequence. The approximating sequences are chosen as the pairs $(U, q_n) \in L_1 \times$ Lip such that $q_n(\cdot)$ is the extremal of the functional

$$\bar{I}_n(q_n) = \int_0^T L(q_n(t), \dot{q}_n(t))dt, \tag{3.63}$$

where $L(q_n, \dot{q}_n)$ is defined in (3.57) and the function $\alpha_n(\cdot)$ satisfies

- $\alpha_n(x) = \int_x^0 F_n(y)dy$, $\lim_{n\to+\infty, x\to 0^-} \frac{F_n(x)}{\alpha_n(x)} = +\infty$
- $F_n \to +\infty$ uniformly on any compact subset of $(-\infty, 0)$
- $F_n(\cdot)$ is continuous, $F_n \geq 0$, $F_n(x) = 0$ if $x \geq 0$.

These conditions are similar to those in Problem 2.1: $F_n(x) = -k_n x$ with $k_n > 0$ and $k_n \to +\infty$ as $n \to +\infty$ is suitable. Notice that $\bar{I}_n(q_n)$ in (3.63) and the action I_α in (3.43), Sect. 3.5.3, are of different natures. The first one is a sequence of actions (hence countable set), whereas the second one is a family of actions corresponding to a family of varied curves (α is a real taking values in an open interval).
Convergence of the approximating problems $\mathscr{P}_n$ toward $\mathscr{P}$ is understood in the sense of Γ-convergence [813]. The initial data of the problem are taken as described in Chap. 2. The main result of Buttazzo and Percivale is the following. Let us define the sets

$$\mathscr{A}(\tau_0) = \{(b, U, q) \,|(U, q) \in E, \mathscr{T}(\tau_0, q) = b\} \tag{3.64}$$

and

$$\mathscr{A}_n(\tau_0) = \{(b_n, U_n, q_n) \,|(U_n, q_n) \in E_n, \mathscr{T}_n(\tau_0, q_n) = b_n\} \tag{3.65}$$

where the sets $E, E_n, \mathscr{T}, \mathscr{T}_n$ are defined as follows. Let us define the function (called the *trace* in [990]) $\mathscr{T} : [0, T] \times E \to \mathbb{R}^{3n+2}$ as (we drop the time argument in q and $\dot{q}$ for simplicity)

$$\mathscr{T}(t, q) = \left(\frac{1}{2}\dot{q}^T M(q)\dot{q}, q, \dot{q}_\tau(t), f(q)\dot{q}, 0\right) \tag{3.66}$$

where $\dot{q}_\tau(t) = \nabla f(q)^T M(q) \nabla f(q)\dot{q} - \nabla f(q)^T M(q)\dot{q}\nabla f(q)$. The set E is the set of functions $q(\cdot)$ such that $q(\cdot)$ is Lipschitz continuous on $[0, T]$ and is a solution of Problem 3.1. The interest for defining such initial data for the Cauchy problem is that the usual initial data $q(\tau_0), \dot{q}(\tau_0)$ are not stable when one considers the convergence

of an approximating problem $\mathscr{P}_n$ toward the limit rigid problem $\mathscr{P}$. Indeed, if the function q_n is a solution of $\mathscr{P}_n$, and if the sequence $\{q_n\}$ converges uniformly toward $q(t)$ which is a solution of $\mathscr{P}$, then it is not guaranteed that the initial data of $\mathscr{P}_n$ (i.e., $q_n(\tau_0), \dot{q}_n(\tau_0)$) converge uniformly toward $q(\tau_0), \dot{q}(\tau_0)$, because of possible discontinuities in the velocity. The initial trace in (3.66) allows one to avoid this difficulty. The trace for $\mathscr{P}_n$ is defined as

$$\mathscr{T}_n(t, q_n) = \left(\frac{1}{2} \dot{q}_n^T M(q_n) \dot{q}_n + \alpha_n \left(f(q_n) \right), q_n, \dot{q}_{n,\tau}(t), f(q_n)\dot{q}_n, \frac{1}{n}\dot{q}_n \right) \tag{3.67}$$

The traces $\mathscr{T}$ and $\mathscr{T}_n$ are continuous with respect to t for every $q \in E$ and $q_n \in E_n$, respectively, (E_n is the set of functions $q_n(t)$ such that $q_n(t)$ is Lipschitz continuous on $[0, T]$ and is a solution of the dynamical problem $\mathscr{P}_n$). When $f(q) > 0$, i.e., when the dynamics are smooth, assigning $\mathscr{T}(\tau_0, q(\tau_0))$ is equivalent to assigning the Cauchy data $q(\tau_0), \dot{q}(\tau_0)$ [242]. Then,

Theorem 3.2 *[242] For every $\tau_0 \in [0, T]$, $(b, U, q) \in \mathscr{A}(\tau_0)$ if and only if there exist $b_n \to b$, $U_n \to U$, $q_n \to q$ such that $(b_n, U_n, q_n) \in \mathscr{A}_n(\tau_0)$, for all n large enough.*

In other words, it is proved that if the problems $\mathscr{P}_n$ possess suitable solutions, these solutions converge toward limits which are in turn solution of the limit problem $\mathscr{P}$. *Vice versa*, if a problem $\mathscr{P}$ possesses a solution, then there exists a sequence of approximating problems $\mathscr{P}_n$ whose solutions converge toward that of $\mathscr{P}$.

Remark 3.7 Uniqueness of solutions of Problem 3.1 is proved in [989, 990] under some analycity conditions on the data (analycity, or piecewise analycity of the data is a necessary and sufficient condition to obtain uniqueness of solutions, see Theorem 5.3). The results in [242, 683, 989, 900] are restricted to conservative systems. However, it is known from the inverse problem in dynamics that one can associate a Lagrangian function with dissipative systems. A possible research work is the extension of these studies to dissipative problems $\mathscr{P}_n$, by considering such modified Lagrangians (in the above simple case, we get $L(x_n, \dot{x}_n) = \left(\frac{1}{2} m \dot{x}_n^2 - \frac{1}{2} k_n x_n^2\right) \exp\left(\frac{f_n t}{m}\right)$).

3.5.5 Additional Comments and Studies

A study on variational problems where the integral action has an integrand which varies, can be found, e.g., in [431]: the solution curves (*extremaloids* in the language of [431]) will in general possess *refraction* or *reflection corners* that correspond to jumps in the velocity; Garfinkel [431] proposes a systematic procedure based on necessary and sufficient conditions that the minimizing curves must satisfy to construct explicitly such a curve. However, it is not clear how we should use the work in [431] to study the transition between the compliant and rigid cases. Variational

problems with unilateral constraints are studied in [432, 490] but the solutions possess a continuous first derivative, so that impact dynamics are excluded from these studies. Brief ideas and a sketch of approach are proposed in [1003, §3.8], about the method of penalizing functions (denoted method of elastic stops in [1003]). A pioneering work can also be found in Valentine [1225], where so-called *slack variables* are introduced as time functions $\gamma_i(t)$ such that $f_i(q) - \gamma_i^2(t) = 0$. Tornambé [64, pp. 219–233] [1208] made use of the Valentine's slack variables in a control context. Murray [909] considers a classical Bolza variational problem, i.e., minimization of $I(q) = l(q(t_0), q(t_1)) + \int_{t_0}^{t_1} L(q, \dot{q}, t)dt$, with $L(t, q, v)$ convex in v for each t, q and $l(\cdot, \cdot)$ lower semicontinuous. The trajectories $q(t)$ are allowed to possess discontinuities. Hence the velocity may contain singular distributions. The trajectories considered in [909] are too irregular for an impact problem (where $q(\cdot)$ is absolutely continuous whereas the velocity is of bounded variation). Ivanov and Markeev [596] apply the nonsmooth change of variable described in Sect. 1.4.3 to an n degree-of-freedom system with an ideal constraint $q_0 \geq 0$, and elastic reflections. They prove that in the new coordinates, the curve $q^\star(\cdot) = (q_0^\star(t), q_1(t), \ldots, q_n(t))$, with $q_0(t) = |q_0^\star(t)|$, is an extremal of the action

$$\int_{t_1}^{t_2} L^\star(q^\star(t), \dot{q}^\star(t), t)dt.$$

Hamilton's principle for systems with unilateral constraints has also received attention in the works by Moreau [895] and Panagiotopoulos [959] (extension of Hamilton's principle to the impact problem for deformable bodies). All those studies are restricted to the case $T_L(t_k) = 0$ for all impact times t_k.

3.5.5.1 Optimal Control with Unilateral (Inequality) State Constraints

Hamilton's principle of mechanics and optimal control are known to be closely related problems. The quadratic problem of control, for linear time-invariant systems subjected to linear unilateral constraints, has been analyzed in [208]. The following Bolza problem is of interest

$$\text{minimize}_{u(\cdot)\in\mathbf{U}} \quad I(u) = \frac{1}{2}\int_0^{T_1} [x(t)^T Q x(t) + u(t)^T R u(t)]dt + \frac{1}{2}x(T_1)^T F x(T_1) \tag{3.68}$$

subject to

$$\begin{cases} \dot{x}(t) = Ax(t) + Bu(t), \ x(0) = \bar{x}_0, \ x(T_1) = \bar{x}_1 \\ w(t) = Cx(t) + D \geq 0, \end{cases} \tag{3.69}$$

where A, B, C, and D are constant matrices, (A, B, C) is a minimal state space representation (i.e., (A, B) is controllable and (C, A) is observable), $\bar{x}_0, \bar{x}_1 \in \Phi = \{x \in \mathbb{R}^n | \ Cx + D \geq 0\}$, $\mathbf{U}$ is the set of admissible inputs, $w(t) \in \mathbb{R}^m$, $u(t) \in \mathbb{R}^{n_u}$,

$x(t) \in \mathbb{R}^n$ and $Q = Q^T \geq 0$, $R = R^T > 0$ (the Legendre–Clebsch condition). In (3.69) the constraints are "virtual," and one has to find a control input $u(\cdot)$ such that the trajectories $x(t; u, \bar{x}_0)$ with $x(T_1; u, \bar{x}_0) = \bar{x}_1$ of the controlled system, satisfy $w(x(t; u, \bar{x}_0)) \geq 0$, for all $t \in [0, T_1]$. Intuitively, we see that in general the optimal controller must contain distributions of higher degree, except if restrictions are put on the optimal trajectories at the junction times (i.e., on $w(t)$ and its derivatives at junction times). The first-order necessary conditions for the optimal control problem in (3.68), (3.69) can be formulated as a Boundary Value Linear Complementarity System (BVLCS) [504, 1065]

$$\begin{cases} \begin{pmatrix} \dot{x}(t) \\ \dot{\eta}(t) \end{pmatrix} = \begin{pmatrix} A & BR^{-1}B^T \\ Q & -A^T \end{pmatrix} \begin{pmatrix} x(t) \\ \eta(t) \end{pmatrix} + \begin{pmatrix} 0 \\ -C^T \end{pmatrix} \lambda(t) & (a) \\ x(0) = \bar{x}_0, \eta(T_1) = Fx(T_1) + C^T\gamma + \beta = F\bar{x}_1 + C^T\gamma + \beta = \eta_1 & (b) \\ 0 \leq w(t) = Cx(t) + D \perp \lambda(t) \geq 0, & (c) \end{cases} \tag{3.70}$$

where $\eta(t) \in \mathbb{R}^n$, $0 \leq \gamma \in \mathbb{R}^m$, $\gamma^T(Cx(T_1) + D) = 0$, $\beta \in \mathbb{R}^n$, and the optimal control is given on intervals where $\eta(\cdot)$ is a function by

$$u(t) = \text{argmax}_{u \in \mathbf{U}} \left[-\frac{1}{2} u^T Ru + \eta(t)^T Bu \right] = R^{-1}B^T\eta(t). \tag{3.71}$$

An implicit assumption which allows one to write (3.68), (3.70), and (3.71) is that the multiplier λ is a measure, whose support satisfies $\text{supp}(\lambda) \subset \{t | \; Cx(t) + D = 0\}$. Let us denote $\tilde{x} = (x^T, \eta^T)^T$, $(\tilde{A}, \tilde{B}, \tilde{C})$ the triple associated with the system in (3.70) (a) (c), then the dynamical system in (3.70) (a) (c) may be viewed as the differential inclusion $\dot{\tilde{x}}(t) - \tilde{A}\tilde{x}(t) \in \partial\psi_{\tilde{\Phi}}(\tilde{x}(t))$, with $\tilde{\Phi} = \{\tilde{x} \in \mathbb{R}^{2n} | \; \tilde{C}\tilde{x} + D \geq 0\}$.[19] It is interesting to see that complementarity conditions are present in the necessary conditions, rendering the system (3.70) similar to an LCS as in (5.128). However, this time complementarity is not motivated by the physics but stems from optimality under inequality constraints, thus extending KKT conditions. Moreover, the LCS (3.70) has some particular structural features, see Example 5.20 and Lemma 5.4. We should keep in mind, however, that solutions of an initial value problem and of a boundary value problem may drastically differ, though the dynamics are the same in both problems.

Many studies have been devoted to the problem of optimal control either when some virtual unilateral constraints[20] are imposed on the state and/or the control. The idea is to use the close relationship between variational calculus and optimal control [1306]: instead of minimizing $I(q)$ with Lagrangian $L(q, \dot{q}, t)$, one minimizes $I(u)$, with Lagrangian $L(q, u, t)$, subject to $\dot{q} = u$. Then $q(\cdot)$ is recovered by integration. Let

[19] There is no minus sign before $\partial\psi_{\tilde{\Phi}}(\tilde{x}(t))$ because of the presence of a minus sign in $\begin{pmatrix} 0 \\ -C^T \end{pmatrix}$ in (3.70(a)).

[20] By virtual we mean that the control input has to be such that the state will not escape from a certain given set. However, the system's model itself does not contain unilateral constraints like in mechanics with physical obstacles, or circuits with ideal diodes.

us mention the studies in [129] (restricted to constraints of the form $f(q,u,t) \geq 0$) and in [130] where constraints $f(t,q) \geq 0$ are considered. For the results of the Russian school on the extension of Pontryagin's principle to systems with unilateral state constraints, see, e.g., [62] and references therein. A common fact to all those results is that the solutions possess discontinuities when the boundary of the domain is attained transversally. The existence results in [62] are formulated as a Mayer problem, but apply to integral-type functionals.

Open Problems: The optimal control of complementarity systems has apparently never been tackled. The formulation is the same as in (3.68)–(3.69), except that the dynamical system in (3.69) should be replaced by an LCS as in (5.128). The problem is therefore quite different, because the multiplier λ is designed to keep trajectories intialized inside the admissible domain Φ, inside Φ for all times. The controller $u(\cdot)$ no longer has to do this job, unlike the above problem. One should first start with LCS with continuous solutions, then move to complementarity mechanical systems. A first step in this direction may be found in [193], where differential inclusions with maximal monotonone set-valued right-hand sides are studied. The first-order sweeping process belongs to this class of systems. An optimal control problem is studied and applied to a simple, controlled circuit with an ideal diode inspired from examples in [28], themselves taken from [9, 10, 13, 22, 23, 213, 214, 226], see Sect. 5.4.4 for examples of nonsmooth circuits. It is shown in [193] that the solutions of sequences of approximated problems, converge to the solution of the limit problem.

3.5.5.2 Bilateral Holonomic Constraints

The main part of this chapter was dedicated to unilateral constraints. Bilateral constraints are treated in Remark 3.2. Let a Lagrangian system with Lagrangian function $L(q,\dot{q})$ be subjected to a set of bilateral holonomic constraints $h_i(q) = 0$, $1 \leq i \leq m_b$. One may augment the Lagrangian function to $\bar{L}(q,\dot{q},\lambda) = L(q,\dot{q}) + \lambda^T h(q)$ for some Lagrange multiplier vector $\lambda \in \mathbb{R}^{m_b}$. Then Hamilton's principle applies to the integral action $\bar{I}(q) = \int_{t_0}^{t_1} \bar{L}(q(s),\dot{q}(s),\lambda(s))ds$ and the first-order necessary conditions are $\frac{d}{dt}\left(\frac{\partial \bar{L}}{\partial \dot{q}}\right) - \frac{\partial \bar{L}}{\partial q} = 0$, which is rewritten equivalently $\frac{d}{dt}\left(\frac{\partial L}{\partial \dot{q}}\right) - \frac{\partial L}{\partial q} = \nabla h(q)\lambda$. In this extremization process, λ is considered as an independent variable. One sees that the result of Proposition 3.1 is recovered.

Chapter 4
Two Rigid Bodies Colliding

This chapter starts with the dynamics of two rigid bodies with one contact/impact point, including the local kinematics which allow one to define the unilateral constraint between the two bodies. Rigid body impact laws with or without friction are reviewed in details. Kinematic (Newton), kinetic (Poisson), and energetic (Stronge) coefficients of restitution are analyzed. Several examples are presented in details, as well as the Darboux-Keller's impact dynamics with Coulomb's friction. Models based on Hertz' contact theory and its extension to elastoplastic materials (with or without adhesive or frictional effects) are described, completing the presentation of viscoelastic rheological models made in Chap. 2. A brief introduction to impacts in flexible structures ends the chapter.

4.1 Dynamical Equations of Two Rigid Bodies Colliding

4.1.1 General Considerations

Let each body be represented by a set of generalized coordinates $q_i = \begin{bmatrix} X_i \\ \xi_i \end{bmatrix}$, where $X_i \in \mathbb{R}^3$ represents the gravity center G_i coordinates in some Galilean frame $(O, \mathscr{G})$, and $\xi_i \in \mathbb{R}^3$ is a set of three Euler angles for the bodies orientation. The kinetic energy of each body is given as:

$$T_i(\dot{X}_i, \Omega_i) = \frac{1}{2} m_i \dot{X}_i^T \dot{X}_i + \frac{1}{2} \Omega_i^T \mathscr{I}_i \Omega_i, \tag{4.1}$$

where $\mathscr{I}_i$ is the constant inertia tensor expressed in a suitable body coordinate frame $\mathscr{B}_i$, and $\Omega_i \in \mathbb{R}^3$, $\Omega_i = (\omega_{i1}\ \omega_{i2}\ \omega_{i3})^T$, is the instantaneous angular velocity in the same body frame. The vector Ω_i is related to $\dot{\xi}_i$ by $\Omega_i = J_{\xi_i}(\xi_i)\dot{\xi}_i$, for some locally

B. Brogliato, *Nonsmooth Mechanics*, Communications and Control Engineering,
DOI 10.1007/978-3-319-28664-8_4

nonsingular matrix $J_{\xi_i}(\xi_i)$. It is well-known that $J_{\xi_i}(\xi_i)$ is not in general a Jacobian.[1] When Ω_i is expressed in a coordinate frame attached to the body, and when ξ_i is a set of three z, x, z-Euler angles Φ_i, θ_i, ψ_i, then the so-called Rodrigues[2] formula sets that:

$$J_{\xi_i}(q_i) = \begin{pmatrix} \sin(\psi_i)\sin(\theta_i) & \cos(\psi_i) & 0 \\ \sin(\theta_i)\cos(\psi_i) & -\sin(\psi_i) & 0 \\ \cos(\theta_i) & 0 & 1 \end{pmatrix}, \tag{4.2}$$

whose determinant vanishes at $\theta_i = k\pi, k \in \mathbb{Z}$. From $\Omega_i^T \mathscr{I}_i \Omega_i = \dot{\xi}_i^T J_{\xi_i}^T \mathscr{I}_i J_{\xi_i} \dot{\xi}_i$ and $T_i(\dot{X}_i, \Omega_i) = T_i(q_i, \dot{q}_i) = \frac{1}{2}\dot{q}_i^T M_i(q_i)\dot{q}_i$, we obtain that the inertia matrix of body i is given by:

$$M_i(q_i) = \begin{pmatrix} m_i I_3 & 0 \\ 0 & J_{\xi_i}^T \mathscr{I}_i J_{\xi_i} \end{pmatrix} \in \mathbb{R}^{6\times 6}. \tag{4.3}$$

It is symmetric positive (semi) definite. The body's Lagrangian function is $L_i(q_i, \dot{q}_i) = \frac{1}{2}\dot{q}_i^T M_i(q_i)\dot{q}_i - U(q_i)$, where $U(q_i)$ is the potential energy of body i. The Lagrange equations of bodies 1 and 2 are therefore derived from $\frac{d}{dt}\left(\frac{\partial L_i}{\partial \dot{q}_i}\right) - \frac{\partial L_i}{\partial q_i} = Q_i^{tot}$ as:

$$M_i(q_i)\ddot{q}_i + C_i(q_i, \dot{q}_i)\dot{q}_i + \frac{\partial U_i}{\partial q_i}(q_i) = Q_i^{tot}, \tag{4.4}$$

which is similar to the equation derived in Example 1.3, and $Q_i^{tot} \in \mathbb{R}^6$ denotes the generalized exogenous forces working on $\dot{q}_i$. It gathers external (exogenous) as well as contact forces and torques: $Q_i^{tot} = Q_i^{ext} + Q_i^{con}$. The vector $C_i(q_i, \dot{q}_i)\dot{q}_i = \begin{pmatrix} 0 \\ \frac{d}{dt}(J_{\xi_i}(q_i)^T \mathscr{I}_i J_{\xi}(q_i))\dot{\xi}_i \end{pmatrix}$, represents centrifugal forces. The mass matrix $M_i(q_i)$ becomes singular when $J_{\xi_i}(q_i)$ is not full rank. As, we shall see later in the book (see Chap. 5), some contact problems are less easy to solve in case of singular mass matrix. Rotations can be represented by other parameters than the three Euler angles. For instance, quaternions [863] or the four Euler parameters [1092] may be used. The price to pay is the addition of an equality (perfect bilateral, nonlinear) constraint that relates the parameters, which are indeed no longer independent quantities. Moreover, the obtained dynamics may have singular mass matrix [1092, Eq. (9)].

Remark 4.1 When Ω_i is expressed in a frame fixed $\mathscr{B}_i$ with respect to body i and composed of the principal axes, centered either at the gravity center G_i or at a fixed point of the body, then the so-called Euler equations are given by [60]:

$$\frac{d}{dt}(\mathbf{M}_{a,i}) = \mathbf{M}_{a,i} \times \Omega_i \tag{4.5}$$

[1] That is, there does not exist any function $\zeta_i(\xi_i)$ such that $\frac{\partial \zeta_i}{\partial \xi_i} = J_{\xi_i}(\xi_i)$. However, since $\frac{\partial \Omega_i}{\partial \dot{\xi}_i} = J_{\xi_i}(\xi_i)$, the matrix $J_{\xi_i}(\xi_i)$ is sometimes called a Jacobian [978].

[2] Benjamin-Olinde Rodrigues (1795–1851), French mathematician and mechanician, known as Olinde Rodrigues.

where $\mathbf{M}_{a,i}$ denotes the angular momentum of body i, or, since $\mathbf{M}_{a,i}(t) = \mathscr{I}_i \Omega_i(t)$ in that frame:

$$\mathscr{I}_i \frac{d}{dt}(\Omega_i) = \mathscr{I}_i \Omega_i \times \Omega_i. \tag{4.6}$$

These equations relate the angular momentum variation to the instantaneous velocity. If some torques $\mathscr{C}_i$ act on the body, then we get:

$$\mathscr{I}_i \frac{d}{dt}(\Omega_i) = \mathscr{I}_i \Omega_i \times \Omega_i + \mathscr{C}_i. \tag{4.7}$$

If the torques $\mathscr{C}_i$ are impulsive and equal to $p_k \delta_{t_k}$, we obtain from the analysis of Sect. 1.1 in Chap. 1:

$$\mathscr{I}_i \sigma_{\Omega_i}(t_k) = p_k, \tag{4.8}$$

which provides the instantaneous velocity jump at $t = t_k$. We have also $\sigma_{\xi_i}(t_k) = J_{\xi_i}(\xi_i)^{-1} \sigma_{\Omega_i}(t_k)$.

4.1.2 The Local Kinematics

In Fig. 4.1, two locally convex bodies with smooth boundary are approaching one each other. One defines two points $A_1 \in \mathrm{bd}(S_1)$ and $A_2 \in \mathrm{bd}(S_2)$, such that they minimize the distance between S_1 and S_2; the points A_1 and A_2 are defined from

$$||A_1 A_2|| = \min_{P_1 \in \mathrm{bd}(S_1),\, P_2 \in \mathrm{bd}(S_2)} ||P_1 P_2||. \tag{4.9}$$

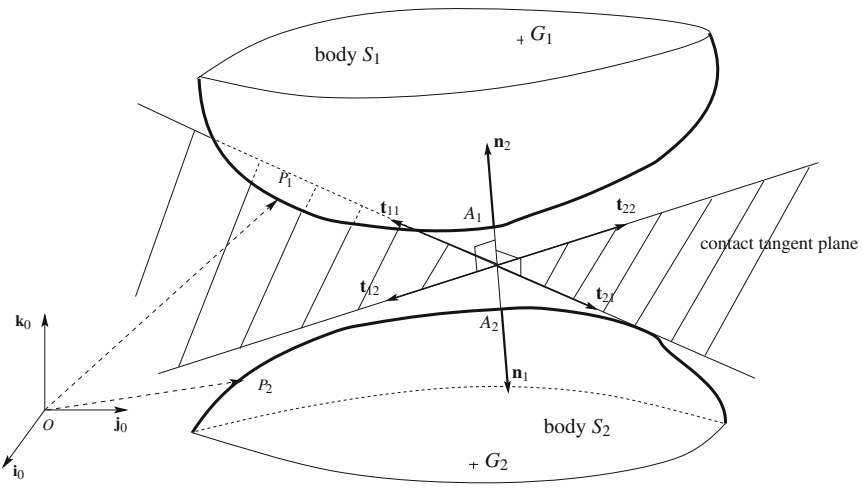

Fig. 4.1 Local frames at the contact point

The minimization may be performed from the knowledge of the vectors OP_1 and OP_2 in a Galilean frame $(O, \mathbf{i}_0, \mathbf{j}_0, \mathbf{k}_0)$, see (4.18) for a simple case. When the two bodies make contact, there is a common point $A = A_1 = A_2$ at which they touch one each other. Let us suppose for the moment that the bodies' surfaces are smooth enough so that a common normal direction $\mathbf{n} \in \mathbb{R}^3$ (or $\mathbb{R}^2$ for the planar case) can be defined. We can define two orthonormal local frames $(A_1, \mathscr{L}_1) = (A_1, \mathbf{n}_1, \mathbf{t}_{11}, \mathbf{t}_{12})$ and $(A_2, \mathscr{L}_2) = (A_2, \mathbf{n}_2, \mathbf{t}_{21}, \mathbf{t}_{22})$, where $\mathbf{n}_1 = -\mathbf{n}_2$ are colinear to $\mathbf{n}$ and point outward the respective bodies, whereas $\mathbf{n}_i \times \mathbf{t}_{i1} = \mathbf{t}_{i2}$, $\mathbf{t}_{i1} \times \mathbf{t}_{i2} = \mathbf{n}_i$, see Fig. 4.1.[3] When one of the bodies is fixed (say S_2), then we set $\mathbf{n}_2 = \mathbf{n}$, $\mathbf{t}_{21} = \mathbf{t}_1$ and $\mathbf{t}_{22} = \mathbf{t}_2$. Now we have:

$$V_{A_i} = V_{G_i} + A_i G_i \times \Omega_i, \tag{4.10}$$

where all the vectors are expressed in the same frame, and the instantaneous angular velocity is written as $\Omega_i = \begin{pmatrix} \omega_{i1} \\ \omega_{i2} \\ \omega_{i3} \end{pmatrix}$. In other words, the twist calculated at G_i is given by $\mathscr{T}_{G_i} = \mathbf{J}(q_i)\dot{q}_i = \begin{bmatrix} \Omega_i \\ V_{G_i} \end{bmatrix} = \begin{bmatrix} \Omega_i \\ \dot{X}_i \end{bmatrix}$, with $\mathbf{J}(q_i) = \begin{bmatrix} 0 & J_{\xi_i}(q_i) \\ I_3 & 0 \end{bmatrix}$, and calculated at A_i using (4.10) by $\mathscr{T}_{A_i} = \begin{bmatrix} \Omega_i \\ V_{A_i} \end{bmatrix}$. These twists can be expressed in the frames $(A_i, \mathscr{L}_i)$ defined above. When dealing with two bodies and contact kinematics and forces to define the gap function, it is preferable to choose either $\mathscr{L}_1$ or $\mathscr{L}_2$ and to express all quantities in a unique frame. In the following, we shall choose without loss of generality the frame $(A_2, \mathscr{L}_2)$, which we denote as $(A, \mathscr{L})$, i.e., we fix $A = A_2$ as the origin of the local contact frame, but the other choice is possible as well. Hence, $v_{r,\mathrm{n}} = v_{1,\mathrm{n}} - v_{2,\mathrm{n}}$ is the component along $\mathbf{n}$ of the relative normal velocity between both bodies, while the relative tangential velocity is $v_{r,\mathrm{t}_1}\mathbf{t}_{21} + v_{r,\mathrm{t}_2}\mathbf{t}_{22}$. We shall write for simplicity in the $(A, \mathscr{L})$ frame $V_{A_i} = v_{i,\mathrm{n}}\mathbf{n} + v_{i,\mathrm{t}_1}\mathbf{t}_1 + v_{i,\mathrm{t}_2}\mathbf{t}_2$. We can now write the transformation between the twists and the generalized velocities as:

$$\mathscr{T}_{A_i} = \begin{bmatrix} \tilde{\Omega}_i \\ V_{A_i} \end{bmatrix} = \mathscr{M}_i(q_i)\dot{q}_i, \tag{4.11}$$

for some (locally) nonsingular transformation matrix $\mathscr{M}_i(q_i) \in \mathbb{R}^{6\times 6}$. If the rotation matrix from $\mathscr{L}$ to $\mathscr{G}$ is $T_i(q_i) \in \mathbb{R}^{3\times 3}$, the rotation matrix from $\mathscr{L}$ to $\mathscr{B}_i$ is $\mathscr{R}_i(q_i) \in \mathbb{R}^{3\times 3}$, and if $A_i G_i = \begin{pmatrix} r_{1i} \\ r_{2i} \\ r_{3i} \end{pmatrix}$,[4] which means that $A_i G_i = r_{1i}\mathbf{n} + r_{2i}\mathbf{t}_1 + r_{3i}\mathbf{t}_2$, then it follows from (4.10) that $\mathscr{M}_i(q_i)$ is given by:

[3] In the following, we shall denote the local normal and tangential vectors $\in \mathbb{R}^2$ or $\in \mathbb{R}^3$ in boldface $\mathbf{n}$ and $\mathbf{t}$ to avoid possible confusion with the number of degrees of freedom n or some other subscripts.

[4] It may, for instance, be assumed that $r_{ji} = r_{ji}(\xi_i)$, $j = 1, 2, 3$, if the bodies' shape lends itself to analytic description.

$$\mathscr{M}_i(q_i) = \begin{bmatrix} 0 & \mathscr{R}_i(q_i)^T J_{\xi_i}(q_i) \\ T_i(q_i)^T & -R_i(q_i)^T \mathscr{R}_i(q_i)^T J_{\xi_i}(q_i) \end{bmatrix} = \frac{\partial \mathscr{T}_{A_i}}{\partial \dot{q}_i}(q_i) \tag{4.12}$$

where $R_i = \begin{pmatrix} 0 & -r_{3i} & r_{2i} \\ r_{3i} & 0 & -r_{1i} \\ -r_{2i} & r_{1i} & 0 \end{pmatrix}$ is the vector product matrix, $\tilde{\Omega}_i = \mathscr{R}_i(q_i)^T J_{\xi_i}(q_i)\dot{\xi}_i$ so that $\Omega_i^T \mathscr{I}_i \Omega_i = \tilde{\Omega}_i \tilde{\mathscr{I}}_i \tilde{\Omega}_i$ with $\tilde{\mathscr{I}}_i = \mathscr{R}_i(q_i)^T \mathscr{I}_i \mathscr{R}_i(q_i)$ is the inertial tensor in $(G_i, \mathscr{L})$. The wrench of all actions acting on body B_i, expressed in the same frame takes the form:

$$\mathscr{W}_{A_i}^{tot} = \begin{bmatrix} F_i^{tot} \\ \mathscr{C}_{A_i}^{tot} \end{bmatrix}, \tag{4.13}$$

where $F_i^{tot} \in \mathbb{R}^3$ is the resulting applied force, and $\mathscr{C}_{A_i}^{tot} \in \mathbb{R}^3$ the resulting torque applied to body i at A_i. Recall that the wrench can be written in its contravariant form as in (4.13) (in which case it is simply a vector of the linear space $\mathbb{R}^6$), or in its covariant form $\mathscr{W}_{A_i}^{tot,\star} = \begin{bmatrix} \mathscr{C}_{A_i}^{tot} \\ F_i^{tot} \end{bmatrix}$, in which case it belongs to the dual space to that linear space (which is the space of the body's twist). Also the scalar product of the twist and the wrench $\mathscr{W}_{A_i}^{tot,\star}$ is an invariant, and represents the power of the forces and torques acting on the body. When this scalar product is zero, then the twist and the wrench are said to be *reciprocal*. This is the case when we consider only contact interactions and the constraints are frictionless and when the velocities are compatible with the constraints (see Sect. 3.2.1). Then the normal (force) subspace and the tangential (velocities) subspace at A are dual subspaces. We can split $\mathscr{W}_{A_i}^{tot} = \mathscr{W}_{A_i}^{ext} + \mathscr{W}_{A_i}^{con}$ as we did for the generalized forces.

Starting from (4.11) and using the invariance principle exposed in Sect. 3.2, the following relationship relates the covariant components of the contact interaction force Q_i^{tot} to the interaction wrench $\mathscr{W}_{A_i}^{tot,\star}$, as:

$$\begin{aligned} Q_i^{tot} &= \mathscr{M}_i(q_i)^T \mathscr{W}_{A_i}^{tot,\star} = \frac{\partial \mathscr{T}_{A_i}}{\partial \dot{q}_i}^T \mathscr{W}_{A_i}^{\star} \\ &= \begin{bmatrix} 0 & T_i(q_i) \\ J_{\xi_i}(q_i)^T \mathscr{R}_i(q_i) & -J_{\xi_i}(q_i)^T \mathscr{R}_i(q_i) R_i(q_i) \end{bmatrix} \begin{bmatrix} \mathscr{C}_{A_i}^{tot} \\ F_i^{tot} \end{bmatrix} \\ &= \begin{bmatrix} \frac{\partial \Omega_i}{\partial \dot{q}_i}^T & \frac{\partial V_{A_i}}{\partial \dot{q}_i}^T \end{bmatrix} \begin{bmatrix} \mathscr{C}_{A_i}^{tot} \\ F_i^{tot} \end{bmatrix}, \end{aligned} \tag{4.14}$$

where use was made of (4.12). The power equality $Q_i^{tot,T} \dot{q}_i = \mathscr{T}_{A_i}^T \mathscr{W}_{A_i}^{tot,\star}$ holds whatever the conditions (perfect, or frictional, or contact point moment-free, or nonmoment-free, constraints). Let us now write down the Lagrange dynamics of the body i. We have $T(q_i, \dot{q}_i) = \frac{1}{2} m_i \dot{X}_i^T \dot{X}_i + \frac{1}{2} \dot{\xi}_i^T J_\xi^T \mathscr{I}_i J_\xi \dot{\xi}_i$, from which we may calculate:

$$M_i(q_i)\ddot{q}_i + \begin{pmatrix} 0 \\ 2J_{\xi_i}^T \mathscr{I}_i \dot{J}_{\xi_i}\dot{\xi} - \frac{1}{2}\frac{\partial}{\partial \xi_i}(\dot{\xi}_i^T J_{\xi_i}^T \mathscr{I}_i J_{\xi_i}\dot{\xi}_i) \end{pmatrix} + \frac{\partial U_i}{\partial q_i}(q_i) = Q_i^{tot}, \quad (4.15)$$

where $Q_i^{tot} = \begin{pmatrix} F_i^{ext} + F_i^{con} \\ J_{\xi_i}^T(\mathscr{C}_i^{ext} + \mathscr{C}_i^{con}) \end{pmatrix}$, the forces (resultant of the wrench) are expressed in $(O, \mathscr{G})$, the torques (moment of the wrench) are expressed in $(G_i, \mathscr{B}_i)$. Let us focus on the contact actions. The moments are transformed as $\mathscr{C}^{con}_{i,(G_i,\mathscr{B}_i)} = \mathscr{R}_i(q_i)\mathscr{C}^{con}_{i,(G_i,\mathscr{L})} = \mathscr{R}_i(q_i)[\mathscr{C}^{con}_{i,(A_i,\mathscr{L})} + G_iA_i \times F^{con}_{i,(A_i,\mathscr{L})}]$. Using the relation $G_iA_i \times F^{con}_{i,(A_i,\mathscr{L})} = -R_i(q_i)F^{con}_{i,(A_i,\mathscr{L})}$ we obtain $\mathscr{C}^{con}_{i,(G_i,\mathscr{B}_i)} = \mathscr{R}_i(q_i)[\mathscr{C}^{con}_{i,(A_i,\mathscr{L})} - R_i(q_i)F^{con}_{i,(A_i,\mathscr{L})}]$, so that $Q_i^{con} = \begin{pmatrix} T_i(q_i)F^{con}_{i,(A_i,\mathscr{L})} \\ J_{\xi_i}(q_i)^T\mathscr{R}_i(q_i)[\mathscr{C}^{con}_{i,(A_i,\mathscr{L})} - R_i(q_i)F^{con}_{i,(A_i,\mathscr{L})}] \end{pmatrix}$. Therefore, we obtain the reciprocal of (4.11):

$$Q_i^{con} = \mathscr{M}_i(q_i)^T \mathscr{W}^{con,\star}_{i,(A_i,\mathscr{L})}. \quad (4.16)$$

The dynamics in (4.15), (4.16) is identical to (4.4). The advantage of the foregoing developments, is that the local contact force components $(F_{i,\mathrm{n}}, F_{i,t_1}, F_{i,t_2})$ explicitly appear in the generalized forces, considering Q_i^{con} and $\mathscr{W}^{con}_{A_i}$ in the right-hand side.

We may use (4.14) to replace the wrench torque by some equivalent expression involving only the instantaneous angular velocity. The last equality in (4.14) is often preferred in the Solid Mechanics literature to link Lagrangian generalized forces to the wrench of interaction forces and torques. This is used in the so-called Kane's equations (see for instance [978, Eqs. (1), (2) (3)]), which are a particular way of writing the dynamical equilibrium of a solid.[5]

4.1.3 The Gap Function

Consider the above local kinematics defined at the potential contact/impact points A_1 and A_2. Let us suppose that a parameterization of $\mathrm{bd}(S_1)$ and $\mathrm{bd}(S_2)$ exists. Let G_i be a point fixed with respect to body S_i (it may be the gravity center). One may write $OP_i = OG_i + G_iP_i$, where $OG_i = f_{i,1}(X_i)$ and $G_iP_i = f_{i,2}(\zeta_i, q_i)$, ζ_i is a parameterization of $\mathrm{bd}(S_i)$, $i = 1, 2$. For given bodies positions and orientations, one can perform the minimization (4.9) over ζ_1 and ζ_2. Then one can define a unilateral constraint which expresses the nonpenetrability of the two bodies from the *signed distance* between them:

$$f(q_1, q_2) = (A_2A_1)^T\mathbf{n} \quad (4.17)$$

[5] There is an incredible number of different ways of writing down the dynamics of rigid bodies, see for instance the survey [523]. Most of them are motivated by computing constraints, or by eliminating constraints from the dynamics. Another one is described in details in Chap. 6, which is well suited to systems with unilateral constraints and impacts. In Chap. 8, we shall use the transformation of McClamroch and Wang [835] which is a coordinate partitioning method that keeps the Lagrangian structure and is therefore well suited for Control purpose.

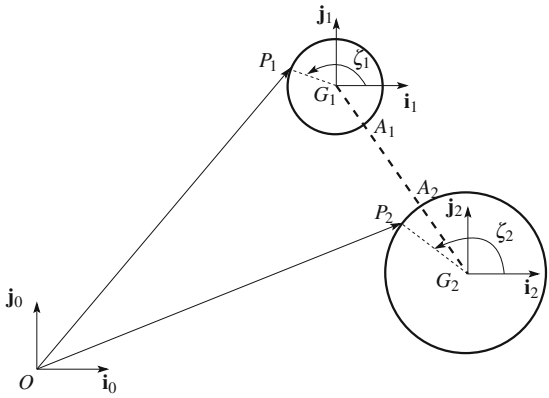

Fig. 4.2 Distance between two balls

for some function $f : \mathbb{R}^{12} \to \mathbb{R}$, assumed to be smooth enough, $q = \begin{pmatrix} q_1 \\ q_2 \end{pmatrix}$. If both vectors are expressed in the Galilean frame, one has to determine A_2A_1 and $\mathbf{n}$ as a function of q_1 and q_2. Then $\frac{d}{dt} f(q) = \nabla f(q)^T \dot{q} = \frac{d}{dt}(A_2A_1(q))^T \mathbf{n} + (A_2A_1(q))^T \frac{d}{dt}(\mathbf{n}(q))$. The velocities V_{A_i} can be expressed in both frames $\mathscr{G} = (O, \mathbf{i}_0, \mathbf{j}_0, \mathbf{k}_0)$ or $(A, \mathbf{n}, \mathbf{t}_1, \mathbf{t}_2)$. In particular, $V_{A_i} = v_{i,\mathrm{n}}\mathbf{n} + v_{i,\mathrm{t}_1}\mathbf{t}_1 + v_{i,\mathrm{t}_2}\mathbf{t}_2$, but $v_{i,\mathrm{n}} \neq V_{A_i}^T \mathbf{n}$ in general, except if $\mathbf{n}$ is fixed in $\mathscr{G}$. The term $(A_2A_1)^T \nabla \mathbf{n}(q)^T \dot{q}$ has to be taken into account. This is incorporated in the matrices $\mathscr{M}_i(q_i)$ which transport local kinematics to generalized coordinates derivatives in (4.11).

A simple example is depicted in Fig. 4.2. The circles with radii R_1 and R_2 are parameterized by the angles ζ_1 and ζ_2, respectively. One has $||P_1P_2|| = ((x_1 - x_2 + R_1\cos(\zeta_1) - R_2\cos(\zeta_2))^2 + (y_1 - y_2 + R_1\sin(\zeta_1) - R_2\sin(\zeta_2))^2)^{\frac{1}{2}}$, and the minimization is performed over $\zeta_1 \in [0, 2\pi]$, $\zeta_2 \in [0, 2\pi]$. From simple geometric arguments A_1 and A_2 must belong to the segment G_1G_2, and on this segment one has $\zeta_1 - \zeta_2 = \pi$. Then the minimization problem in (4.9) reduces to:

$$\min_{\zeta_2 \in [0,2\pi]} \sqrt{(x_1 - x_2 - (R_1 + R_2)\cos(\zeta_2))^2 + (y_1 - y_2 - (R_1 + R_2)\sin(\zeta_2))^2} \tag{4.18}$$

which is a function of $X_1 = (x_1, y_1)^T$ and $X_2 = (x_2, y_2)^T$, the coordinates of G_1 and G_2 in $(O, \mathbf{i}_0, \mathbf{j}_0)$ respectively. Once the value of ζ_2 which minimizes the objective function in (4.18) is known (the so-called argmin value), the coordinates of A_1 and A_2 can be calculated and the signed distance in (4.17) can be obtained as a function of X_1 and X_2.

Remark 4.2 We assume that there is a unique possible contact point between bodies 1 and 2, i.e., the minimization problem in (4.9) has a unique solution (A_1, A_2), so that the surface $f(q_1, q_2) = 0$ is of codimension 1 in $\mathbb{R}^{12}$. As we shall see in the next chapters, this is an important assumption because it means that only *single* impacts are to be considered between the two bodies. If two points were to be reached simultaneously, one would have to treat a *multiple* impact, see Chaps. 5 and 6. The

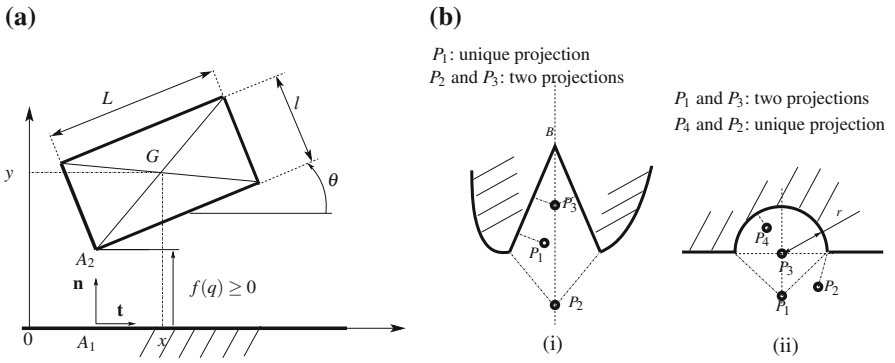

Fig. 4.3 Distances between two bodies. **a** Anvil/block distance. **b** Particle/non-convex body distance

fact that the minimization problem in (4.9) is well-defined and possesses a unique solution pair (A_1, A_2), may be true even if the bodies are not both smooth, see Fig. 4.3a for the case of a planar block and a massive anvil when $\theta \neq 0$ there is a unique pair of closest points A_1 and A_2, however when $\theta = 0$ there is an infinity of such points (a whole segment), and if $\theta < 0$ the distance has to be computed with the other edge of the block, this system has in fact two unilateral constraints. If $\theta > 0$ as in Fig. 4.3a, and if the block has its gravity center G at the geometric center with coordinates x and y, then $f(q) = y - \frac{l}{2}\cos(\theta) - \frac{L}{2}\sin(\theta)$ when $y \leq \frac{\sqrt{l^2+L^2}}{2}$. Also convexity may be relaxed to the so-called r-prox-regularity (see Sect. B.2.3), guaranteeing that if the bodies are close enough one to each other, the solution is still unique. See Fig. 4.3b for the case of a particle and a body in the plane (in this case finding A_1 and A_2 boils down to finding the projection of the particle on the body's boundary): the body in case (i) is not prox-regular, and the particle when in positions P_2 and P_3 on the bissector of the re-entrant corner, has two projections on the body's boundary, however close to the point B it may be. In case (ii) the body is an r-prox-regular set and P_4 has a unique projection on the body's boundary while both P_1 and P_3 have two projections.

Another important issue concerns the gradients of the gap function. Let us consider the system made of two spheres aligned on the $(O, \mathbf{i}_0)$-axis, with gravity centers coordinates x_1 and x_2, respectively. Another choice for the coordinates is $z_1 = x_1 + R_1$, $z_2 = x_2 - R_2$. One may express the inpenetrability between bodies as (i) $f(x) = x_2 - x_1 - (R_1 + R_2) \geq 0$, or (ii) $f(x) = (x_2 - x_1)^2 - (R_1 + R_2)^2 \geq 0$, or (iii) $f(z) = z_2 - z_1 \geq 0$. However, writing $|z_2 - z_1| \geq 0$ is meaningless since such an inequality is always satisfied. It is clear that the mechanical meaning of the multiplier associated with the unilateral constraint, depends on the chosen gap function. If the gap function is defined from the so-called local kinematics (i.e., one defines a local Cartesian frame at each contact point as in Fig. 4.1, and a normal relative velocity $v_{r,\mathrm{n}}$), then the associated multiplier λ_n represents the contact force. Indeed, from the virtual work principle, and denoting $P(q)$ the generalized force due to the contact with generalized coordinates q (here q denotes any generalized

coordinate vector, i.e., in our case $q = (x_1 \ x_2)^T$ or $q = (z_1 \ z_2)^T$), one obtains that the virtual work satisfies $W = P(q)^T \dot{q} dt = \lambda_n^T v_{r,n} dt$, where $\delta q \triangleq \dot{q} dt$ and $v_{r,n} dt$ are virtual displacements. Thus, if $v_{r,n} = \frac{d}{dt}(f(q)) = \nabla f(q)^T \dot{q}$, one obtains $P(q)^T \dot{q} dt = \lambda_n^T \nabla f(q)^T \dot{q} dt$ so that $P(q) = \nabla f(q) \lambda_n$. In the two-sphere system, the relative normal velocity is given by $v_{r,n} = \dot{x}_2 - \dot{x}_1 = \dot{z}_2 - \dot{z}_1$. One has $v_{r,n} = \nabla f(q)^T \dot{q}$ if the gap function is defined as in (i) and (iii), but not in case (ii). In case (ii), one obtains $\nabla f(q)^T \dot{q} = -2(x_2 - x_1)\dot{x}_1 + 2(x_2 - x_1)\dot{x}_2 = 2(x_2 - x_1)v_{r,n}$. When contact is established one has $\nabla f(q)^T \dot{q} = 2(R_1 + R_2)v_{r,n}$, the multiplier associated with this gap function is scaled by $\frac{1}{2(R_1+R_2)}$. The gap function as in (i) and (iii) is a signed distance between the two bodies. This last comment leads us to notice that the gap function $f(q)$ that defines the unilateral constraint, may be scaled by any scalar $\alpha > 0$. Defining $f_\alpha(q) \triangleq \alpha f(q)$, the associated multiplier becomes $\lambda_\alpha = \frac{1}{\alpha}\lambda_n$. Let us end this paragraph with a last observation. Consider now a system made of a sphere with radius $R > 0$, that is constained to evolve above the rigid ground (this is the so-called bouncing ball). Its coordinate is q. The unilateral constraint which describes the inpenetrability of the two bodies (ball and ground) may be (i) $f(q) = q - R \geq 0$, or (ii) $f(q) = q^2 - R^2$. In case (i) one has $\nabla f(q) = 1$, in case (ii) one has $\nabla f(q) = 2q$. Suppose as usual that the coordinate system is chosen such that contact is established at $q = 0$. In case (ii) one has $\nabla f(0) = 0$. If we admit from the above reasoning that the generalized force associated with the contact force between the ball and the ground is given by $P(q) = \nabla f(q)\lambda_n$ for some multiplier λ_n, then at contact $P(0) = 0$; this is not acceptable because it means that the multiplier either takes infinite values, or that the contact force has no influence on the ball's dynamics. This is the reason why it was indicated in Definition 1.8 that the gradients should not vanish in a neighborhood of the boundary of the admissible domain Φ.

> The choice of the gap function that is used to define the unilateral constraints, is a crucial modeling step.

4.1.4 The Two-Body System Dynamics

Let the surfaces be frictionless. This means that the hypersurface defined in the 12-dimensional configuration space $f(q_1, q_2) = 0$ is perfect. By the virtual work principle (see Chap. 3), it must be that when contact is established, all motions compatible with the constraints produce zero work, i.e., $\delta q^T Q^{con} = 0$, where $Q^{con} = \begin{bmatrix} Q_1^{con} \\ Q_2^{con} \end{bmatrix} \in \mathbb{R}^{12}$ and δq is an arbitrary virtual displacement of q, compatible with the constraints. In other words, since such motion is tangential to the surface $f(q_1, q_2) = 0$, one must have $Q^{con} = \lambda_n \nabla f(q_1, q_2)$ for some $\lambda_n \in \mathbb{R}$. Using the coordinate invariance "principle" of Sect. 3.2, as well as (4.15), (4.16) for $i = 1$ and $i = 2$, we may write:

$$\lambda_{\mathrm{n}} \nabla f(q_1, q_2) = \begin{bmatrix} \mathscr{M}_1(q_1)^T \mathscr{W}_{A_1}^{con,\star} \\ \\ \mathscr{M}_2(q_2)^T \mathscr{W}_{A_2}^{con,\star} \end{bmatrix} = \mathscr{M}(q)^T \mathscr{W}^{con,\star} \tag{4.19}$$

with $\mathscr{M}(q)^T = \begin{bmatrix} \mathscr{M}_1(q_1)^T & 0 \\ 0 & \mathscr{M}_2(q_2)^T \end{bmatrix} \in \mathbb{R}^{12\times 12}$, and $\mathscr{W}^{con,\star} = \begin{bmatrix} \mathscr{W}_{A_1}^{con,\star} \\ \mathscr{W}_{A_2}^{con,\star} \end{bmatrix} \in \mathbb{R}^{12\times 1}$. Furthermore, note that the bodies are perfectly rigid and we shall not introduce any moment at the contact point since surfaces are frictionless. Hence $\mathscr{C}_{A_i}^{con} = 0$ and $F_i^{con} = F_{i,\mathrm{n}}\mathbf{n}$ for some $F_{i,\mathrm{n}} \in \mathbb{R}$, i.e., $F_i = \begin{pmatrix} F_{i,\mathrm{n}} \\ 0 \\ 0 \end{pmatrix}$ in the local frame $(A, \mathscr{L})$. From the fact that the constraints are perfect, the following has to be satisfied:

$$\sum_{i=1}^{2} (\mathscr{W}_{A_i}^{con})^T \mathscr{T}_{A_i} = \dot{q}^T Q^{con} = \sum_{i=1}^{2} V_{A_i}^T F_i^{con} = \sum_{i=1}^{2} v_{i,\mathrm{n}} F_{i,\mathrm{n}} = 0. \tag{4.20}$$

From the principle of mutual actions,[6] one has $F_{1,\mathrm{n}} = -F_{2,\mathrm{n}}$, so that from the last equality in (4.20) we infer that $v_{r,\mathrm{n}} F_{2,\mathrm{n}} = 0$. The tangential components v_{i,t_1} and v_{i,t_2} do not play a role in the frictionless case, since $F_{i,\mathrm{t}_1} = F_{i,\mathrm{t}_2} = 0$. However, they will be incorporated later when friction is present at the contact. Let $F_{2,\mathrm{n}} = \lambda_{\mathrm{n}}$, then the equality in (4.19) allows one to link $\nabla f(q_1, q_2)$ with $\mathscr{M}_1(q_1)$ and $\mathscr{M}_2(q_2)$. One obtains $v_{r,\mathrm{n}} F_{2,\mathrm{n}} = \dot{q}^T \nabla f(q_1, q_2) \lambda_{\mathrm{n}}$, which implies that $v_{r,\mathrm{n}} = \nabla f(q_1, q_2)^T \dot{q}$; this is consistent with the way we have calculated the gap function in (4.17). If the contact is broken then $f(q) > 0$ and $F_{i,\mathrm{n}} = 0$, so that (4.20) is still verified despite $A_1 \neq A_2$ and the relative velocity $v_{r,\mathrm{n}}$ may be nonzero. We recover here the *complementarity* between the contact force and the gap function, and between the contact force and the gap function derivative when the contact is closed. If the bodies boundaries are rough, the tangential components F_{i,t_1} and F_{i,t_2} may be nonzero, and produce a non-null work $F_{i,\mathrm{t}_1} v_{i,\mathrm{t}_1} + F_{i,\mathrm{t}_2} v_{i,\mathrm{t}_2}$. We then have to introduce two multipliers $\lambda_{\mathrm{t},1}$ and $\lambda_{\mathrm{t},2}$, as well as a mapping $H_{\mathrm{t}}(q_1, q_2)$ such that the power equality $\dot{q}^T Q_{\mathrm{t}}^{con} = F_{i,\mathrm{t}_1} v_{i,\mathrm{t}_1} + F_{i,\mathrm{t}_2} v_{i,\mathrm{t}_2}$, and $Q_{\mathrm{t}}^{con} = H_{\mathrm{t}}(q_1, q_2)\lambda_{\mathrm{t}}$ while $v_{r,\mathrm{t}} = H_{\mathrm{t}}(q_1, q_2)^T \dot{q}$. Using (4.15), (4.16), let us concatenate the dynamics of the two bodies:

$$\begin{aligned} &\begin{pmatrix} M_1(q_1) & 0 \\ 0 & M_2(q_2) \end{pmatrix} \begin{pmatrix} \ddot{q}_1 \\ \ddot{q}_2 \end{pmatrix} + \begin{pmatrix} C_1(q_1, \dot{q}_1)\dot{q}_1 \\ C_2(q_2, \dot{q}_2)\dot{q}_2 \end{pmatrix} = \\ &= \begin{pmatrix} \mathscr{M}_1(q_1)^T & 0 \\ 0 & \mathscr{M}_2(q_2)^T \end{pmatrix} \begin{pmatrix} \mathscr{W}_{A_1}^{ext,\star} + \mathscr{W}_{A_1}^{con,\star} \\ \mathscr{W}_{A_2}^{ext,\star} + \mathscr{W}_{A_2}^{con,\star} \end{pmatrix} \\ &= \begin{pmatrix} \mathscr{M}_1(q_1)^T & 0 \\ 0 & \mathscr{M}_2(q_2)^T \end{pmatrix} \begin{pmatrix} \mathscr{W}_{A_1}^{ext,\star} \\ \mathscr{W}_{A_2}^{ext,\star} \end{pmatrix} + \nabla f(q_1, q_2)\lambda_{\mathrm{n}} + H_{\mathrm{t}}(q_1, q_2)\lambda_{\mathrm{t}}. \end{aligned} \tag{4.21}$$

[6] This is Newton's third law, which will be supposed later to be true for impulsive interactions also.

The contact wrenches have a specific feature: when contact is not active ($\Leftrightarrow A_1 \neq A_2$), they are zero; this will be reflected formally into complementarity conditions for the normal part $0 \leq f(q_1, q_2) \perp \lambda_n \geq 0$, and friction model for the tangential part which will have to incorporate that $f(q_1, q_2) > 0 \Rightarrow \lambda_t = 0$. They can therefore be expressed at the common point A. We also assumed implicitly that the contact moments $\mathscr{C}_A$ are zero.

Remark 4.3 When there are m_u potential unilateral-contact points A_i^j on body i, $1 \leq j \leq m_u$, then we have $Q^{con} = \sum_{j=1}^{m_u} \lambda_{n,j} \nabla f_j(q_1, q_2) = \nabla f(q_1, q_2)\lambda_n$, with $f : \mathbb{R}^{12} \to \mathbb{R}^{m_u}$ and $\lambda_n \in \mathbb{R}^{m_u}$. The contact forces acting on body i may be denoted as $F_i^{con,j}$, and the contact interaction torques $\mathscr{C}_{A^j}^{con}$, $1 \leq j \leq m_u$. The contact wrenches $\mathscr{W}_{A^j}^{con}$ have to be transported to the contact points A^j as we did above, or the gravity center G_i. Then $\mathscr{W}_A^{con} = \sum_{i=1}^{m_u} \mathscr{W}_{A^j}^{con}$. The local contact forces can be grouped together in a single vector so as to link the generalized and the local kinematics formalisms. The right-hand side of (4.15) is modified accordingly.

Let us now rewrite the Lagrange dynamics in (4.21) compactly as $M(q)\ddot{q} + F(q, \dot{q}, t) = H(q)\lambda$, with $\lambda = (\lambda_n, \lambda_t^T)^T$ and $H(q) = (\nabla f(q), H_t(q))$, $q = (q_1^T, q_2^T)^T$. Let $\mathscr{T}_G = \begin{pmatrix} \mathscr{T}_{G_1} \\ \mathscr{T}_{G_2} \end{pmatrix}$, then $\mathscr{T}_G = T(q)\dot{q}$ for some matrix $T(q)$. From the coordinate invariance virtual power principle, $\dot{q}^T H(q)\lambda = \mathscr{T}_G^T \mathscr{W}_G^{con}$ from which we infer that $T(q)^T \mathscr{W}_G^{con} = H(q)\lambda$. If $T(q)$ is a full rank matrix, we can transform the Lagrange dynamics into:

$$\tilde{M}(q)\frac{d}{dt}(\mathscr{T}_G) + \tilde{F}(q, \dot{q}, t) = \mathscr{W}_G^{con} = T(q)^{-T} H(q)\lambda \tag{4.22}$$

with $\tilde{M}(q) = T(q)^{-T} M(q) T(q)^{-1}$, $\tilde{F}(q, \dot{q}, t) = -T(q)^{-T} M(q) T(q)^{-1} \frac{d}{dt}(T(q))\dot{q} + T(q)^{-T} F(q, \dot{q}, t)$. This kind of manipulation holds in a general context of n bodies with m contact points.

4.1.5 Dynamical Equations and Energy Loss at Collision Times

4.1.5.1 Impact Dynamics

Since we have assumed that the bodies' surfaces are frictionless, the constraints are perfect and interaction at the contact point is along $\mathbf{n} \in \mathbb{R}^3$. We deal with a system with a unilateral constraint, this implies some impulsive behavior when the bodies make contact with nonzero (positive) approach normal relative velocity. Here, we get that each time contact is made at $t = t_k$ with preimpact relative velocity between the two bodies $v_{r,n}(t_k^-) < 0$, a shock occurs between both bodies at A. From (4.15),

(4.16), and (4.11), we obtain the Newton–Euler dynamical equations[7] (arguments are dropped):

$$\bar{\mathbf{M}}_{A_i}\frac{d}{dt}\left(\mathscr{T}_{A_i}\right) - (\mathscr{M}_i\mathscr{M}^T)^{-1}\frac{d}{dt}(\mathscr{M}_i)\dot{q}_i + \mathscr{M}_i^{-T}\left(C(q,\dot{q}_i)\dot{q}_i + \frac{\partial U_i}{\partial q_i}\right) = \mathscr{W}_{A_i}^{tot,\star} \tag{4.23}$$

where Q_i^{tot} contains bounded as well as impulsive contact forces and the last equality comes from (4.14). The matrix $\bar{\mathbf{M}}_{A_i}(q_i)$ is calculated as $\mathscr{M}_i(q_i)^{-T}M_i(q_i)\mathscr{M}_i(q_i)^{-1}$, where $\mathscr{M}_i(q_i)$ is defined in (4.11). The interaction wrench can be split as $\mathscr{W}_{A_i}^{con} = \mathscr{W}_{A_i}^{reg} + \mathscr{W}_{A_i}^{imp}$, where $\mathscr{W}_{A_i}^{reg}$ corresponds to bounded contact forces and moments, while $\mathscr{W}_{A_i}^{imp}$ contains the impulsive torques and forces at impact times t_k. As alluded to above, we have $\mathscr{W}_{A_1}^{imp} = -\mathscr{W}_{A_2}^{imp}$, because Newton's third law holds true at collisions. Hence, following the developments in Chap. 1, one deduces that at a shock instant t_k the following algebraic equations are satisfied:

$$\bar{\mathbf{M}}_{A_i}(q_i(t_k))\begin{bmatrix}\sigma_{\Omega_i}(t_k)\\ \sigma_{V_{A_i}}(t_k)\end{bmatrix} = \begin{bmatrix}0_{3\times 1}\\ \cdots\\ p_{i,\mathrm{n}}(t_k)\\ p_{i,\mathrm{t}_1}(t_k)\\ p_{i,\mathrm{t}_2}(t_k)\end{bmatrix} \quad (= \mathscr{W}_{A_i}^{imp,\star}(t_k)), \tag{4.24}$$

where the quantities are expressed in the local frame $(A, \mathscr{L})$ (at an impact time $A_1 = A_2 = A$), and it is assumed that there is no impulsive moment at the contact point. If there are no tangential effects (like Coulomb's friction), then $p_{i,\mathrm{t}_1} = p_{i,\mathrm{t}_2} = 0$. It is noteworthy that (4.24) is true independently of the fact that the frame $(A, \mathscr{L})$ used to express the dynamics is Galilean or not. In other words, if the used local frame is not Galilean, the velocity of a point M with respect to $\mathscr{G}$ expressed in $\mathscr{G}$ (the *absolute velocity* $V_{M/\mathscr{G},\mathscr{G}}$) is equal to:

$$V_{M/\mathscr{G}} = V(M/\mathscr{L},\mathscr{G}) + V(A/\mathscr{G},\mathscr{G}) + \Omega \times (OM - OA), \tag{4.25}$$

where Ω is the angular velocity of $\mathscr{L}$ with respect to $\mathscr{G}$, and O denotes the origin of $\mathscr{G}$. The first term in the right-hand side of (4.25) is the *relative* velocity, the second term is the velocity of motion of the moving coordinate system in $\mathscr{G}$, the third one is the *transferred* velocity. This is well developed in [60, §26, 27]. Hence, if the motion of the local frame $\mathscr{L}$ with respect to $\mathscr{G}$ is smooth enough,[8] one gets from (4.25)

[7] The expression in (4.23) is certainly not the best way to write the Newton–Euler dynamics, in particular the nonlinearities are not written in a very tractable way. However, we will use (4.23) mainly for collisions, in which case smooth nonlinearities disappear.

[8] Note that this implies in particular that the frame, we have defined above to express the dynamics is not attached to body 1, since the velocity of body 1 undergoes discontinuities at t_k. It is just chosen so that its origin A coincides with the contact point at the shock instant. But it may be mobile, with nonzero acceleration.

that $\sigma_{V_{M/\mathscr{G}}}(t_k) = \sigma_{V(M/\mathscr{L},\mathscr{G})}(t_k)$. In other words, the inertial forces do not play any role in the velocity jump calculation, because such accelerations are merely bounded functions of time, and the jump of the absolute velocity is that of the relative velocity. To avoid getting too cumbersome expressions, let us abusively assume that at the collision time t_k we have $\mathscr{L} = \mathscr{B}_i = \mathscr{G}$, that is $T_i(q_i) = \mathscr{R}_i(q_i) = I_3$ (see anyway (4.35)). Then:

$$\bar{\mathbf{M}}_{A_i}(q_i) = \begin{pmatrix} m_i R_i^T R_i + \mathscr{I}_i & m_i R_i^T \\ m_i R_i & m_i I_3 \end{pmatrix}, \bar{\mathbf{M}}_{A_i}(q_i)^{-1} = \begin{pmatrix} \mathscr{I}_i^{-1} & -\mathscr{I}_i^{-1} R_i \\ -R_i^T \mathscr{I}_i^{-1} & \frac{1}{m_i} I_3 + R_i^T \mathscr{I}_i^{-1} R_i \end{pmatrix}. \tag{4.26}$$

Consequently, using (4.24):

$$\sigma_{V_{A_i}}(t_k) = \left[\frac{1}{m_i} I_3 + R_i^T \mathscr{I}_i^{-1} R_i \right] P_i(t_k) \tag{4.27}$$

$$\sigma_{\Omega_i}(t_k) = -\mathscr{I}_i^{-1} R_i P_i(t_k) \tag{4.28}$$

with $P_i(t_k) = \begin{bmatrix} p_{i,\mathrm{n}}(t_k) \\ p_{i,\mathrm{t}_1}(t_k) \\ p_{i,\mathrm{t}_2}(t_k) \end{bmatrix}$. Notice that $\det(\bar{M}_{A_i}(q_i)) = m_i \mathscr{I}_i > 0$. The inertia center G_i velocity jump is given by:

$$m_i \sigma_{\dot{X}_i}(t_k) = P_i(t_k), \tag{4.29}$$

and the Euler angles derivatives jumps are given by:

$$\sigma_{\dot{\xi}_i}(t_k) = -J_{\xi_i}^{-1} \mathscr{I}_i^{-1} R_i P_i(t_k). \tag{4.30}$$

The relationship in (4.24) relates the jump in the twist of body i to the impulsive wrench at $t = t_k$. Also recall that we have $p_{1,\mathrm{n}}^k = -p_{2,\mathrm{n}}^k$ from the mutual actions principle of Newton. The equality in (4.24) is to be compared with the one in (1.12) in Example 1.3. It is nothing else than the generalization to three-dimensional bodies of the equations of two particles colliding, moving on a line, which gives $m_1 \sigma_{\dot{x}_1}(t_k) = p_{12}(t_k)$ and $m_2 \sigma_{\dot{x}_2}(t_k) = -p_{12}(t_k) = p_{21}(t_k)$ at the impact time. Using $\mathscr{W}_{A_1}^{imp} = -\mathscr{W}_{A_2}^{imp}$, equation $m_1 \sigma_{\dot{x}_1}(t_k) + m_2 \sigma_{\dot{x}_2}(t_k) = 0$ is extended to:

$$\bar{\mathbf{M}}_{A_1}(q_1) \begin{bmatrix} \sigma_{\Omega_1}(t_k) \\ \sigma_{V_{A_1}}(t_k) \end{bmatrix} + \bar{\mathbf{M}}_{A_2}(q_2) \begin{bmatrix} \sigma_{\Omega_2}(t_k) \\ \sigma_{V_{A_2}}(t_k) \end{bmatrix} = 0 \tag{4.31}$$

which is known as the *linear* and *angular momenta conservation equations*. Let us recall that (4.31) contains the conservation of the two-body system's center of mass velocity.

Remark 4.4 The impact equations for two bodies colliding can be written in different ways, one of which is (4.31). In the particular case of two bodies colliding in the plane, the equation in (4.31) can be written as [667]:

$$\sigma_{\dot{x}_1}(t_k) = \sigma_{\dot{x}_2}(t_k) = m_1\sigma_{\dot{y}_1}(t_k) + m_2\sigma_{\dot{y}_2}(t_k) = 0, \tag{4.32}$$

where x_i, y_i are body i gravity center G_i coordinates in the frame $(A, \mathbf{t}, \mathbf{n})$, and:

$$\sigma_{M_{a,i}}(t_k) = 0, \ i = 1, 2, \tag{4.33}$$

where $M_{a,i}$ is body i angular momentum computed at point O_i, where O_i belongs to the axis $(A, \mathbf{n})$, and O_i has coordinates $(0, a_i)$ in the frame $(A, \mathbf{t}, \mathbf{n})$. $M_{a,i} = I_i\Omega_i + m_i AG_i \times V_{G_i} = I_i\Omega_i + m_i[x_i\dot{y}_i - \dot{x}_i(y_i - a_i)]$. This in turn can be rewritten as:

$$I_i\sigma_{\Omega_i}(t_k) + m_i x_i \sigma_{\dot{y}_i}(t_k) = 0, \ i = 1, 2. \tag{4.34}$$

There are 13 unknowns in this dynamical algebraic problem: 12 postimpact velocities (the $\dot{q}_i$'s or equivalently the Ω_i's and the V_{A_i}'s components), and the percussion component $p_{\mathrm{n}} = p_{1,\mathrm{n}} = -p_{2,\mathrm{n}}$. For the moment, we have only 12 equations given by (4.24) for $i = 1, 2$. Clearly, one additional equation is needed to render the impact problem solvable, i.e., calculate the postimpact velocities and the percussion vector. In the following, we discuss the various ways proposed in the literature to model the collisions, i.e., in fact to associate with the dynamical problem suitable relationships that allow to calculate postimpact values. It is noteworthy that linear and angular momenta balance relations cannot be considered as a part of the collision rule; they are just a consequence of the assumption that the mutual action principle holds in the limit of perfectly rigid body impacts, and they may help in calculating the impact outcome.

A Small Aside: If we do not make the simplifying assumption $\mathscr{L} = \mathscr{B} = \mathscr{G}$, then (4.27) and (4.28) are replaced by:

$$\begin{cases} \sigma_{\Omega_i}(t_k) = \mathscr{R}_i\mathscr{I}_i^{-1}\mathscr{R}_i\mathscr{C}_i(t_k) - \mathscr{R}_i\mathscr{I}_i^{-1}\mathscr{R}_i R_i P_i(t_k) \\ \sigma_{V_{A_i}}(t_k) = -R_i\mathscr{I}_i^{-1}\mathscr{C}_i(t_k) + \left(\frac{1}{m_i}T_i^T T_i + R_i^T\mathscr{I}_i^{-1}R_i\right) P_i(t_k) \end{cases} \tag{4.35}$$

where $\mathscr{C}_i(t_k) \in \mathbb{R}^3$ is the vector of impulsive moments at the contact point in the local frame.

4.1.5.2 Kinetic Energy Loss at Impacts

Before going on with restitution laws, let us derive the form of the kinetic energy loss at impacts. We denote the wrench of impulses as $\mathscr{W}^{imp} \triangleq \begin{pmatrix} \mathscr{W}_1^{imp} \\ \mathscr{W}_2^{imp} \end{pmatrix} \in \mathbb{R}^{12}$,

$\bar{\mathbf{M}}(q) \triangleq \text{diag}(\bar{\mathbf{M}}_{A_1}(q_1), \bar{\mathbf{M}}_{A_2}(q_2)) \in \mathbb{R}^{12\times 12}$, the twists $\mathscr{T} = \begin{pmatrix} \mathscr{T}_{A_1} \\ \mathscr{T}_{A_2} \end{pmatrix} \in \mathbb{R}^{12}$. The kinetic energy of the system is given by $T(t) = \frac{1}{2}\sum_{i=1}^{2} \mathscr{T}_{A_i}(t)^T \bar{\mathbf{M}}_{A_i}(q)\mathscr{T}_{A_i}(t)$. From (4.23), we deduce that $\bar{\mathbf{M}}_{A_i}(q_i(t_k))(\mathscr{T}_{A_i}(t_k^+) - \mathscr{T}_{A_i}(t_k^-)) = \mathscr{W}_{A_i}^{imp,\star}(t_k)$ for $i = 1, 2$. Therefore, $\mathscr{T}_{A_i}(t_k^+) = \mathscr{T}_{A_i}(t_k^-) + \bar{\mathbf{M}}_{A_i}(q_i(t_k))^{-1}\mathscr{W}_{A_i}^{imp,\star}(t_k)$, and the kinetic energy loss is calculated as follows:

$$\begin{aligned} T_L(t_k) &= \tfrac{1}{2}\textstyle\sum_{i=1,2}\left[\mathscr{W}_i^{imp,\star}(t_k) + \bar{\mathbf{M}}_{A_i}\mathscr{T}_{A_i}(t_k^-)\right]^T \bar{\mathbf{M}}_{A_i}^{-1}\left[\mathscr{W}_i^{imp,\star}(t_k) + \bar{\mathbf{M}}_{A_i}\mathscr{T}_{A_i}(t_k^-)\right] \\ &= \tfrac{1}{2}\left[\mathscr{W}^{imp,\star}(t_k) + \bar{\mathbf{M}}\mathscr{T}(t_k^-)\right]^T \bar{\mathbf{M}}^{-1}\left[\mathscr{W}^{imp,\star}(t_k) + \bar{\mathbf{M}}\mathscr{T}(t_k^-)\right]. \end{aligned} \tag{4.36}$$

Assume that $T_L(t_k)$ is bounded. Given that the preimpact values are constants of the problems, one sees from (4.36) that the impulsive wrench $\mathscr{W}^{imp,\star}(t_k)$ is constrained to lie in an ellipsoid $\subset \mathbb{R}^{12}$, in fact in $\mathbb{R}^6$ since $\mathscr{W}_1^{imp,\star}(t_k) = -\mathscr{W}_2^{imp,\star}(t_k)$. In case, there is no impulsive torque, this reduces to a three-dimensional ellipsoid in the P-space ($P \triangleq P_1 = -P_2$). Its equation can be derived from (4.36) and using (4.26), (4.27), (4.28). These are straightforward but lengthy calculations. The interest of this manipulation is that one realizes that whatever the shock process may be (frictionless or with friction), the percussion vector has to remain inside a closed domain (whose size evidently depends on preimpact conditions). This can be used to characterize various impact rules that we describe in the next sections, in terms of the set of points that the percussion vector may attain inside the ellipsoid [279]. Another form of $T_L(t_k)$ can be obtained using the equality $\bar{\mathbf{M}}_{A_i}(q_i(t_k))\sigma_{\mathscr{T}_{A_i}}(t_k) = \begin{bmatrix} 0 \\ P_i(t_k) \end{bmatrix}$, as:

$$T_L(t_k) = \sum_{i=1,2} \frac{1}{2}\begin{bmatrix} 0 \\ P_i(t_k) \end{bmatrix}^T \left(\mathscr{T}_{A_i}(t_k^+) + \mathscr{T}_{A_i}(t_k^-)\right), \tag{4.37}$$

which is known as Kelvin's formula. We may derive this expression using directly the above relations for linear and angular velocity jumps. To simplify the presentation, we assume there is a unique body that collides a massive anvil (i.e., body 2 is fixed). We have $V_A = V_G + R\Omega$, from which it follows that:

$$\begin{aligned} T_L(t_k) &= \tfrac{1}{2}m(V_G(t_k^+) - V_G(t_k^-))(V_G(t_k^+) + V_G(t_k^-)) \\ &\quad + \tfrac{1}{2}(\Omega(t_k^+) - \Omega(t_k^-)).\mathscr{I}(\Omega(t_k^+) + \Omega(t_k^-)) \\ &= \tfrac{1}{2}P^T(V_A(t_k^+) + V_A(t_k^-)) - \tfrac{1}{2}P^T R(\Omega(t_k^+) + \Omega(t_k^-)) \\ &\quad + \tfrac{1}{2}(\Omega(t_k^+) + \Omega(t_k^-))R^T P \\ &= \tfrac{1}{2}P^T(V_A(t_k^+) + V_A(t_k^-)), \end{aligned} \tag{4.38}$$

with $P = (p_{\mathrm{n}}\ p_{\mathrm{t}_1}\ p_{\mathrm{t}_2})^T$ and $V_A = (v_{\mathrm{n}}\ v_{\mathrm{t}_1}\ v_{\mathrm{t}_2})^T$. This shows that indeed the kinetic energy loss is due to the (negative) work of the contact forces during the collision, and is closely related to the Thomson and Tait formula (Sect. 4.3.12). Other expressions of energy loss at impacts will be given in Chap. 6.

4.1.6 The Percussion Center

The percussion center [1049, §120], is a notion that is often used in the design of tools that perform colliding tasks, and with a fixed axis (hammers, tennis rackets). Its definition is as follows:

Definition 4.1 Given a rigid body with a fixed axis OO' and gravity center G, mass m, the center of percussion is the point C such that

- There exists a point O'' such that OO' is the principal axis of inertia for O''.
- C lies in a plane containing G and OO', and $\mathrm{proj}(OO'; C) = O''$.
- The radius of inertia ρ with respect to OO'[9] is the geometric mean of the distances from G and C to OO', denoted as d and d_c, respectively.

Let us denote $GO = r_0$, $e = \frac{OO'}{||OO'||}$, $r = GC$. Then the following is true:

Proposition 4.1 *[590] C as in Definition 4.1 exists if and only if*

$$\begin{cases} (\mathscr{I} e \times e)^T r_0 = 0 \\ r^T \mathscr{I} e = 0 \\ d d_c = \rho^2, \end{cases} \tag{4.39}$$

where $\mathscr{I}$ is the body's inertia tensor.

For instance, if the inertia tensor is diagonal with entries satisfying $I_{11} = I_{22} = I_{33}$, then a center of percussion exists for any fixed axis. This supplements a result by Lyapunov [776] according to whom every impact on a spherically symmetric body imparts a revolution motion to the body about a certain axis. The center of percussion also finds more exotic applications, like in tennis dynamics: the so-called *sweet spot* [201] is a special impact point on the racket strings used to prevent jarring of the hand. It is defined either as a vibration node, or as the center of percussion, or as the point where the restitution coefficient (see a definition in the next section) is maximum and vibrations are minimum [201]. The definition as the center of percussion is natural; since the hand more or less corresponds to the rotation axis of the racket, the fact that the impact point coincides with the center of percussion means that this axis is fixed, hence the player does not have to counteract a large torque at the collision instant. Another special impact point is the *dead spot* [311] that corresponds to the point at

[9] ρ is the distance from OO' at which all the mass of the body could be concentrated without modifying the moment of inertia with respect to OO' [1178].

which a rotating racket stops dead on a stationary ball; hence, a tennis player should serve hitting the dead spot, but induced vibrations and large interaction wrench lead most players to strike closer to the center of the strings.

4.2 Restitution Laws

The rules that one may associate to a collision process, and that we shall deal with in the sequel, all aim at making a reasonable prediction of the impact outcome, using a phenomenological model. Since the mechanics of interaction are often simplified or ignored, one cannot expect to get very accurate predictions over a wide range of collisions. However, some basic properties must be satisfied by any restitution rule. Chatterjee [279] provided a tentative listing of such desirable properties:

1. Physical and mechanical constraints (energy loss, frame invariance...).
2. Generality (it should apply to various shapes, mass distribution, velocities, material, surface properties...).
3. Consistency with other physical laws (for instance, it should incorporate dry friction effects and not contradict Coulomb's model).
4. Applicability to simple objects (it should be able to reproduce tangential velocity reversal, like in the superball dynamics,[10] and for certain choices of the parameters).
5. Simplicity (too many parameters are not desirable).
6. Physical interpretation of the parameters.
7. Independently measurable parameters, (i.e., the parameters should be measurable *via* different experiments, and their value should not vary from one experiment to the other).

Such a program is quite ambitious, and it is not an easy task to derive macroscopic rules which satisfy all the above requirements, because restitution laws remain quite simple models aiming at predicting an incredibly complex phenomenon. In the following, we try to give an overview of the existing models for simple impacts between two rigid bodies. The basic and most widely used restitution law for frictionless shocks between rigid bodies is the so-called Newton's rule, which uses a *kinematic* Coefficient of Restitution (CoR). It relates the relative normal velocities after and before the shock as follows:

$$e_{\mathrm{n}} = -\frac{v_{1,\mathrm{n}}(t_k^+) - v_{2,\mathrm{n}}(t_k^+)}{v_{1,\mathrm{n}}(t_k^-) - v_{2,\mathrm{n}}(t_k^-)} = -\frac{v_{r,\mathrm{n}}(t_k^+)}{v_{r,\mathrm{n}}(t_k^-)}. \tag{4.40}$$

The CoR e_{n} is an experimental coefficient, and has a clear energetical meaning. Note that for $e_{\mathrm{n}} = 1$ then $v_{r,\mathrm{n}}$ is reversed. It is important to record that the restitution

[10] The superball-like behavior is observed in some balls made of a special rubber, which rebound in a apparently erratic way on the ground and the walls [433].

coefficient is defined for a set of two bodies; speaking of the restitution coefficient of one body is meaningless. For two frictionless particles with mass m_1 and m_2 colliding, one can show that the kinetic energy loss at impacts is given by:

$$T_L(t_k) \triangleq T(t_k^+) - T(t_k^-) = \frac{1}{2}\frac{m_1 m_2}{m_1 + m_2}(e_{\mathrm{n}}^2 - 1)\left(v_{r,\mathrm{n}}(t_k^-)\right)^2, \tag{4.41}$$

from which it follows that in this particular case $e_{\mathrm{n}} \in [0, 1]$ (negative values produce nonadmissible postimpact velocities). Using the impact dynamic, the postimpact velocities are given by:

$$\begin{cases} v_{1,\mathrm{n}}(t_k^+) = v_{1,\mathrm{n}}(t_k^-) - (1 + e_{\mathrm{n}})\frac{m_2(v_{1,\mathrm{n}}(t_k^-) - v_{2,\mathrm{n}}(t_k^-))}{m_1 + m_2} \\ \\ v_{2,\mathrm{n}}(t_k^+) = v_{2,\mathrm{n}}(t_k^-) + (1 + e_{\mathrm{n}})\frac{m_1(v_{1,\mathrm{n}}(t_k^-) - v_{2,\mathrm{n}}(t_k^-))}{m_1 + m_2}. \end{cases} \tag{4.42}$$

Notice that in this case, the velocities at the contact point are the particles gravity centers velocities, and this also applies to smooth or nonrotating spheres. It is noteworthy that's Gravesand [1090] almost derived (4.41) for $e_{\mathrm{n}} = 0$. The impact problem is always energetically consistent in this case since there cannot be a positive gain of energy at impact. The energetical considerations make it clear why e_{n} is less than unity to insure $T_L(t_k) \leq 0$.[11] Let us note that in general the kinetic energy loss is not an easy expression to obtain, due to the dynamical couplings between the various velocity variables, see (4.24).

Remark 4.5 At some places of this book, we shall say that the notion of restitution coefficients is necessary to render the impact problem solvable. This is not entirely true. More exactly they are sufficient. Indeed one may argue that energy *and* momentum conservation laws[12] may serve as well to solve the shock dynamical equations.[13] It was indeed the underlying basic idea used for instance by Huygens, as well as Wren and Wallis (who both based their developments on momentum conservation) when answering to a suggestion of the Royal Society of London in 1668, about impact dynamics. Huygens' work is recalled in [683]: it relies on both momentum and energetical arguments (clearly, adding an energy constraint like $T_L(t_k) = 0$ provides one more equation to the 12 equations in (4.24)). Most importantly, it is pointed out in [683] that Huygens' arguments are not based on the law of mutual actions, but rather

[11] Some authors [273, 1315] define a restitution coefficient by considering the energy transferred into the "impacted" object as being lost, and by taking into account only the rebound velocity of the "impacting" mass. Hence, an elastic collision without any global kinetic energy loss has a restitution less than 1. See Sect. 4.2.4 for more details.

[12] Most importantly, let us recall that there is no so-called *principle of conservation of momentum*. We saw above that (4.31) is only a consequence of the shock dynamics and of Newton's law on mutual actions. Any other "principle of conservation of momentum" corresponds in fact to an additional assumption on the impact process.

[13] Some authors [308] use the a priori knowledge of the percussion vector to solve the shock process dynamics.

use Galilean principle of relativity together with the assumption that the shocks are purely inelastic. One difference between Huygens and Leibniz or Bernoulli, is that he did not use the conservation of the so-called, *vis-viva* (i.e., twice the kinetic energy) as a principle [565]. On the contrary, Leibniz formulated three basic laws for impacts: the law of the conservation of absolute forces (*vis-viva*), the law of conservation of direction (conservation of momentum), and the law of the conservation of the relative velocity [519]. He was followed by Bernoulli [134]. In order to understand the source of such misconceptions and a priori nonexperimentally motivated "laws," one has to replace those studies in their historical context. A complete description is outside the scope of this book. The interested reader may have a look at [519, 571, 572] for detailed analysis of the Newtonians and Leibnizians controversy. Let us end this short historical parenthesis by insisting on the fact that collisions were at the center of many scientific debates at that time [376, 784, 785, 834, 1089–1091].

The dependence of the restitution upon several parameters has been known and studied for a long time. The restitution coefficient depends mainly on the following physical effects:

- The relative approach velocity $v_{r,\mathrm{n}}(0)$ (which we also denote $v_{r,\mathrm{n}}(t_k^-)$): e_n usually decreases when $v_{r,\mathrm{n}}(0)$ increases, [44]. Experimental studies can be found in [272, 564, 627, 1166, 1175, 1186]. For instance, at moderate contact velocities $v_{r,\mathrm{n}}(0)$ (but high enough so that plastification is attained; for otherwise, the impact is purely elastic), Johnson [627] finds the empirical law $e_\mathrm{n} = |v_{r,\mathrm{n}}(0)|^{-\frac{1}{4}}$, in accordance with some experimental results in [469], confirmed in [194, 469, 691, 1126], but recently authors indicate a dependence as $|v_{r,\mathrm{n}}(0)|^{-\frac{1}{6}}$ [778]. See Sect. 4.2.1 for more details. Hunt and Crossley [555] find the restitution coefficient $e_\mathrm{n} = 1 - \alpha v_{r,\mathrm{n}}(0)$ from the contact/impact model in (2.24) for collisions between nonlinear viscoelastic bodies with low-approach velocities. Ice spheres collision experiments show the same tendency [195, 505, 528, 1168], and fitted empirical power laws show $e_\mathrm{n} = \alpha |v_{r,\mathrm{n}}(0)|^{-\beta}$ with $\beta = 0.19$ or $\beta = 0.15$ [1168], or $e_\mathrm{n} = e_{\mathrm{ne}} \left(\frac{|v_{r,\mathrm{n}}(0)|}{v_c}\right)^{-\ln\left(\frac{|v_{r,\mathrm{n}}(0)|}{v_c}\right)}$, where v_c is a critical velocity separating a quasielastic and an inelastic regimes (an expression of v_c as a function of the sphere radius and temperature is given in [528, Eq. (24)]), e_{ne} fits with e_n in the elastic region. Similar results are given in [1165] for snow particles. Though it is commonly admitted and confirmed experimentally in an impressive number of studies, that e_n decreases with increasing $v_{r,\mathrm{n}}(0)$, this may not be the case at *very low* approach velocities where an increase of e_n may be observed as the approach velocity increases[14] [478, 666]. Other results on rock materials [573], or apple fruit [346] corroborate the general tendency.
- The shapes of the bodies [84, 468, 1033, 1056]. For instance, two spheres may possess a certain restitution. Now a rigid block striking a rigid horizontal surface, both made of the same material as the spheres, will exhibit in general a completely

[14] [666] reports experiments of brass, copper, aluminum, delrin, steel spheres bouncing on granite or steel plates, with $v_{r,\mathrm{n}}(0) \in [0.001, 1]$ m/s. [478] shows experimental data on iron beads with the same preimpact velocities.

different behavior. In particular, Goldsmith [468] studied analytically the effect of the shape on the energy transformed into vibrations,[15] and found that the minimum value occurs for spheres.

- The sizes of the bodies [44, 468, 524, 528]. Experimental results in [63] on steel spheres/steel plates indicate that restitution depends on the spheres radii.[16] Similar conclusions are drawn experimentally in [528] for ice sphere/ice block impacts. The viscoelastic model in (2.12) is used in [342] with $\zeta = \zeta_0(1+\gamma^3)^K(1+\gamma)^{0.2}\left(\frac{r}{2.5}\right)^{-3K-0.2}|v_{r,\mathrm{n}}(0)|^p$, where ζ_0, p, and K are parameters to be fitted from experimental data, r is the sphere radius.
- The masses of the bodies [44, 468, 524], as confirmed by the studies reported in Sect. 4.2.1.
- The elastic modulii of the bodies [44, 468, 524], as confirmed by the studies reported in Sect. 4.2.1.
- The density of the medium in which they collide [338], as confirmed by the studies reported in Sect. 4.2.1.
- The temperature ([196] reported variations between 0.65 and 0.28 for e_n between a golf ball and a flat-nosed wooden projectile, $v_{r,\mathrm{n}}(0^-) = 5.334$ m/s, with temperatures varying between -75 and $+40$°C). [1014] reports experimental results of collisions between a spherical indentor (tungstene carbide) against a PVC target, with varying temperature of the indentor between -20 and $+80$°C, for various preimpact velocities between 1.2 and 0.3 m/s. The restitution coefficient varies from 0.91 to 0.75 for the smallest velocity, and from 0.83 to 0.6 for the largest one. This indicates that the restitution coefficient decreases with increasing temperature of the colliding bodies. This is confirmed in [527, Fig. 6] for ice sphere/ice block collisions.
- The number of repeated impacts for a given preimpact velocity: at the first impacts the restitution coefficient increases, then plastification effects may vanish after several collisions, and the coefficient of restitution becomes constant (for constant approach velocity) [50, 859, 1083, 1084, 1260].
- The external force applied on the system during the collision, see Theorem 4.1.

It is often accepted that the restitution coefficients (Newton's as well as Poisson's) are material dependent; this is clearly only very partially true. Tatara [1185] shows experimentally that when an external force acts on the considered system at the impact time, the period of the shock and the restitution coefficient are different than when no external force is present. In [917], several manners of measuring the kinematic restitution e_n between two spheres were investigated. Depending on the experiment (shock of the spheres in the air, or shock of one sphere on a steel lathe bed), the value of e_n was found to vary of approximately 5 % around an average value. In fact, it may be considered that restitution coefficients are to be considered as "process constants", i.e., for a given process they take a certain value, that may be modified when one of these values changes.

[15] Concerning the importance of vibrations during collisions, see the section below on microcollisions, and Sect. 4.2.4.

[16] However the source of the variations is not clearly identified in [63].

4.2.1 Elastoplastic Impacts and Restitution Coefficients

Viscoelastic rheological models of impacts with the associated restitution coefficients have been reviewed in Chap. 2, Sect. 2.2. As we pointed out, these models possess poor prediction capabilities when plastic deformation is present during the shock, and are restricted to (very) low-impact velocities with $e_{\rm n} \gtrsim 0.95$. Let us make in this section, a short overview of the extension of Hertz' theory for elastoplastic material behaviors.

4.2.1.1 Extension of Hertz' Theory: Plasticity

The fundamentals of these calculations rely on Hertz' elasticity theory and plasticity [469, 627, 826, 1175] in Tribology, where quasistatic equilibrium of the colliding bodies is assumed, see Sect. 4.2.4. The approach thus mixes geometrical and material aspects. Hertz' contact theory relies on several basic assumptions: (i) the contacting bodies can be replaced by elastic half-spaces for small domains of contact, (ii) the contacting surfaces are smooth (frictionless) and non conforming,[17] so that the contact surface can be simplified as a plane, (iii) the contact area is very small compared to the bodies dimensions, stresses, and strains are localized in a neighborhood of the contact point, and the forces applied on the bodies do not influence what happens,[18] (iv) the pressure at contact is normal to the contact surface and there is no tensile stress, (v) the loading phase is quasistatic, and (vi) the materials of the contacting bodies are isotropic and homogeneous, and linearly elastic. A very good introduction of Hertz' theory may be found in [826, §4.4]. Clearly, Hertz' theory relies on drastic assumptions, most of which are never satisfied in practice. However, on one hand it is possible to extend it to cases with viscous friction, Coulomb's friction, plasticity, and adhesion. On the other hand, some assumptions are legitimate in many cases, like (ii): the contact surface curvature may be taken into account, but its influence on the impact duration is negligible [1231].

The next results concern low-velocity colinear impacts[19] between two spheres (with masses m_1 and m_2, radii R_1 and R_2), where the elastic deformation is followed by plastic deformation, then restitution. The relative velocity is denoted as $v_{\rm n}(t_k)$ at the impact time. The frictional effects that may play a role at the contact interface are usually neglected. The onset of yield is therefore a crucial parameter. Let $\frac{1}{E^\star} = \frac{(1-\nu_1^2)}{E_1} + \frac{(1-\nu_2^2)}{E_2}$, E_i and ν_i are the Young modulus and Poisson ratio of each sphere, respectively, $\frac{1}{m} = \frac{1}{m_1} + \frac{1}{m_2}$, $\frac{1}{R} = \frac{1}{R_1} + \frac{1}{R_2}$ (for sphere/flat contact one takes $R_2 = +\infty$, $m_2 = +\infty$). The relative approach velocity is

[17] Typically, sphere/sphere or sphere/plane. The words "conforming" or "conformal" can be used [1251].

[18] For a sphere, all points outside the contact regions have the same velocity as the center.

[19] Let us remind that an impact is said colinear if the contact/impact point belongs to the line passing through the two gravity centers of the bodies. In Fig. 4.1, A belongs to, the line passing through G_1 and G_2.

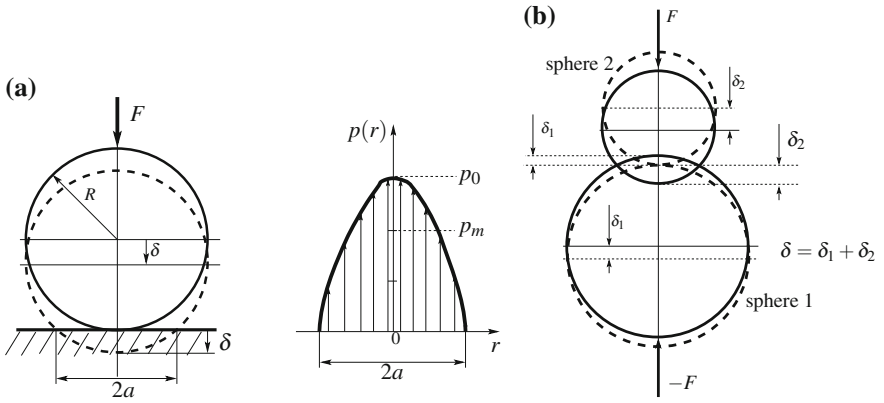

Fig. 4.4 Hertz' contact. **a** Sphere/flat. **b** Sphere/sphere

$v_{\rm n}(t_k^-)(=v_{r,{\rm n}}(t_k^-)) = v_{1,{\rm n}}(t_k^-) - v_{2,{\rm n}}(t_k^-)$, and the relative postimpact velocity is $v_{r,{\rm n}}(t_f) = v_{1,{\rm n}}(t_f) - v_{2,{\rm n}}(t_f)$.[20] Let us recall that the identation δ in Hertz' theory is equal to the relative displacement of the gravity centers of each sphere, which deform around the contact point, see Fig. 4.4a, b. The contact surface is supposed to be a disk whose radius is $a = \left(\frac{3FR}{4E^\star}\right)^{\frac{1}{3}} = \sqrt{R\delta}$ ($\Leftrightarrow \delta = \frac{a^2}{R}$), where F is the contact force and $\delta = \left(\frac{9F^2}{16(E^\star)^2 R}\right)^{\frac{1}{3}}$ is the indentation ($\Leftrightarrow F = \frac{4}{3}E^\star\sqrt{R}\delta^{\frac{3}{2}}$, hence the Hertz' stiffness is equal to $K_h = \frac{4}{3}E^\star\sqrt{R}$). The normal pressure is given at a point of a distance r from the center of the contact area, by $p(r) = p_0\left(1 - \left(\frac{r}{a}\right)^2\right)^{\frac{1}{2}}$, with the maximum pressure $p_0 = \frac{3F}{2\pi a^2} = \frac{3}{2\pi}\left(\frac{4}{3}\right)^{\frac{2}{3}}\left(\frac{F(E^\star)^2}{R^2}\right)^{\frac{1}{3}} = \frac{3}{2}p_m$, where $p_m = \frac{1}{\pi}\left(\frac{4E^\star}{3R}\right)^{\frac{2}{3}}F^{\frac{1}{3}}$ is the mean contact pressure (normal stress), see Fig. 4.4. During an elastic impact one has $p_0 = \frac{3}{2\pi}\left(\frac{4E^\star}{3R^{\frac{3}{4}}}\right)^{\frac{4}{5}}\left(\frac{5}{4}mv_{\rm n}(t_k^-)^2\right)^{\frac{1}{5}}$ [627, Eq. (11.37)]. This serves to determine the contact force, depending on various assumptions to be made on the contact pressure. From Hertz' elasticity theory, the maximum indentation obtained at zero relative velocity (end of the elastic compression phase) is given by:

$$\delta_{\max} = \left(\frac{15mv_{\rm n}(t_k^-)^2}{16\sqrt{R}E^\star}\right)^{\frac{2}{5}} = \left(\frac{15T(t_k^-)}{8\sqrt{R}E^\star}\right)^{\frac{2}{5}} = \left(\frac{5m}{4K_h}\right)^{\frac{2}{5}}(v_{\rm n}(t_k^-))^{\frac{4}{5}}, \qquad (4.43)$$

where $T(t_k^-)$ is the preimpact (initial) kinetic energy. This expression allows one to express the preimpact velocity as a function of the maximum indentation. The minimal velocity such that plastification occurs is deduced as:

[20] Thus the impact occurs on $[t_k, t_f]$ and we keep the notation t_k^- for the preimpact velocity, to be consistent with the rigid body case. As a convention thoughout the book, we have $v_{\rm n}(t_k^-) < 0$.

$$v_y = \sqrt{\frac{16\sqrt{R}E^\star}{15m}\delta_y^{\frac{5}{2}}}. \tag{4.44}$$

The velocity v_y is the so-called yield velocity, i.e., the relative impact velocity below which the interaction behavior is assumed to be elastic. Let δ_y be the normal displacement that initiates yield. To get (4.44), one has set $\delta_y = \delta_{\max}$ in (4.43). It is in fact possible to express (4.44) as:

$$v_y = \left(\frac{16R^3E^\star}{15m}\right)^{\frac{1}{2}}\left(\frac{3\pi}{4}\right)^{\frac{5}{2}}\left(\frac{C_y\sigma_y}{E^\star}\right)^{\frac{5}{2}}, \tag{4.45}$$

where σ_y is the uniaxial yielding stress related to the mean yield pressure[21] (or cutoff pressure, or critical yield pressure) in the contact region by $p_y = C_y\sigma_y$. The value of σ_y is the one of the material that yields first, i.e., $\sigma_y = \min(\sigma_{y,1}, \sigma_{y,2})$, and is a function of the Poisson's ratio ν (from the von Mises criterion, for $\nu = 0.3$ one has $C_y = 1.613$, for $\nu = 0.4$ one has $C_y = 1.738$ [1322]). It is also possible to relate σ_y to the yield normal load F_y as [1322] $F_y = \frac{\pi^3R^2(1-\nu^2)^2}{6(E^\star)^2}(C_y(\nu)\sigma_y)^3$. The dynamic yield stress is a material constant,[22] or it is related to the static yield stress σ_{ys} as $\sigma_y = \beta(\dot{\epsilon})\sigma_{ys}$, where $\beta(\cdot)$ is a coefficient function of the strain rate $\dot{\epsilon}$ [857, Fig. 6] [1084, Fig. 3]. Another expression of v_y is given by [627, Eq. (11.38)]: $v_y \approx \sqrt{\frac{53}{0.5m}R^3\frac{\sigma_y^5}{(E^\star)^4}}$ where $C_y \approx 1.6$. For hard steel sphere impacting a medium hard steel, one has $v_y \approx 0.14$ m/s [627, 1260] (experimental validations may be found in [1175]). Numerical results reported in [181], and validated by careful comparisons with the experimental data in [857] for steel sphere/sphere impacts, indicate that onset of yield occurs at $\delta_y = 0.39\,\mu$m, with penetration depths from $13\,\mu$m for $|v_n(t_k^-)| = 0.25$ m/s, to $244\,\mu$m for $|v_n(t_k^-)| = 5$ m/s. Other numerical figures in [181] concern experiments on aluminum oxide spheres against aluminum alloy [656]. Then $\delta_y = 0.21\mu$m, with penetration depths from $3.40\,\mu$m for $|v_n(t_k^-)| = 0.5$ m/s, to $35.74\,\mu$m for $|v_n(t_k^-)| = 6$ m/s. *These data prove that plastic deformation may be easily reached.* The parameter C_y plays an important role for the collision outcome prediction, and has to be fitted with experiments [858, Fig. 14] [857, 1140, 1279]. It may depend on the contact pressure, which in turn depends on the impact velocity $v_n(t_k^-)$, and hence should not be just a material constant [858]. Based on the von Mises plasticity criterion, one should have $C_y = 1.6$. In [270], a linear approximation $C_y = 1.282 + 1.158\nu$ is obtained for the collision of a sphere with Poisson's ratio ν against a rigid surface. In [600] one finds $C_y = 1.29\exp(0.736\nu)$ for a sphere/sphere impact. Tabor [1174] found that the onset of fully plastic behavior is expected to occur when the stress in the material equals $2.5\sigma_y$. For elastic-perfectly plastic materials, this is confirmed in [154, 503, 714]. The following results assume that an elastic phase is followed by a plastification regime during the loading (sometimes divided

[21] This is the collision maximum contact pressure for the onset of plastic deformation.

[22] Though this is only a very crude approximation, because the dynamic yield stress usually depends on work-hardening of materials; it tends to increase during a collision [1175, p. 121].

into a mixed elastoplastic regime and a fully plastic regime [181]). Then unloading occurs, usually supposed to be elastic with no reverse yielding. Johnson [627, §11.5] assumes three phases with full plasticity, and derives the expression of the restitution coefficient without the elastic loading phase:

$$e_{\mathrm{n}} = -\frac{v_{\mathrm{n}}(t_f)}{v_{\mathrm{n}}(t_k^-)} = \sqrt{\frac{3\sqrt{2}\pi^{\frac{5}{4}}}{5}} \left(\frac{3\sigma_y}{E^\star}\right)^{\frac{1}{2}} \left(\frac{0.5mv_{\mathrm{n}}(t_k^-)^2}{3\sigma_y R^3}\right)^{-\frac{1}{2}}, \tag{4.46}$$

where $C_y = 3$ for nonstrain-hardening material.[23] The work done as plastic energy in producing the remaining indentation after impact has occurred, is given by $W_y = p_y V_r$, where V_r is the volume of the remaining permanent indentation. W_y is the difference between the energy of impact and the energy of rebound. It is assumed in [627] that the maximum average contact pressures during loading and unloading are identical. Johnson's model usually overestimates $v_{\mathrm{n}}(t_f)$ and may yield $e_{\mathrm{n}} > 1$ for too small $v_{\mathrm{n}}(t_k^-)$, this being attributed to a bad choice of the (p_y, σ_y) relation that should be equal to $p_y = 1.24\sigma_y$ [272]. Even for large enough $v_{\mathrm{n}}(t_k^-)$, e_{n} in (4.46) overestimates $v_{\mathrm{n}}(t_f)$. Tabor [1175] derives the expression (implicit in e_{n}):

$$p_y^5 = \frac{e_{\mathrm{n}}^8 v_{\mathrm{n}}(t_k^-)^2}{(1-\frac{3}{8}e_{\mathrm{n}}^2)^3} \frac{m(E^\star)^4}{317.2R^3}. \tag{4.47}$$

Tabor's model (4.47) overestimates $v_{\mathrm{n}}(t_f)$ for too high $v_{\mathrm{n}}(t_k^-)$, and has good prediction capabilities for $|v_n(t_k^-)| \approx v_y$. The kinematic restitution coefficient calculated in Thornton [1194] assumes an elastic stage (with Hertz' law of elasticity) followed by a perfectly plastic stage with linear force/indentation law, followed by elastic unloading. The first assumption is that the onset of yield occurs when the preimpact kinetic energy of a sphere is equal to the work performed during the elasting loading phase, until the yield point is reached. This gives $\delta_y = \left(\frac{\pi C_y \sigma_y}{2E^\star}\right)^2 R = \frac{1}{4}\frac{R}{(E^\star)^2}\pi^2 p_y^2$. The yield force therefore follows from Hertz' contact as $F_y = \frac{4}{3}E^\star\sqrt{R}\delta_y^{\frac{3}{2}}$ (see (2.23)). The next assumption is that the pressure distribution is truncated for all pressures above the yield stress, i.e., $F_p(\delta) = F_y + \pi R C_y \sigma_y(\delta - \delta_y)$ for all $\delta \geq \delta_y$ and $\dot{\delta} \geq 0$ (compression phase). As a consequence, the maximum pressure satisfies $p_{\max} \leq p_y$. The residual values for R and δ are $R_e = R\frac{\frac{4}{3}E^\star\sqrt{R}\delta_y^{\frac{3}{2}}}{F_{\max}}$ and $\delta_e = \delta_{\max} - \left(\frac{3F_{\max}}{4E^\star\sqrt{R_e}}\right)^{\frac{2}{3}}$, where $F_{\max}$ is the maximum contact force during the loading phase. The contact force during the elastic unloading phase is $F_{unl} = \frac{4}{3}E^\star\sqrt{R_e}(\delta - \delta_e)^{\frac{3}{2}}$, with $\dot{\delta} \leq 0$ (restitution phase). See Fig. 4.5a. The yield

[23] The yield stress that enters Equation (11.44) in Johnson's book, is the dynamic yield stress denoted σ_d, and he states that $p_d = 3.0\sigma_d$ where p_d is the mean contact pressure during dynamic loading. It is often assumed that $p_d = C_d\sigma_y$ in (4.46) [272].

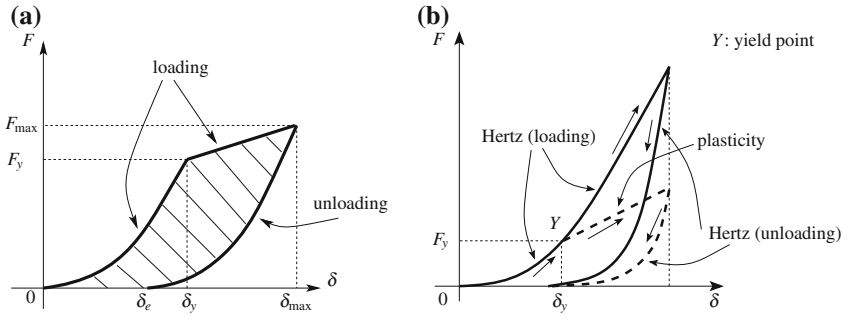

Fig. 4.5 Loading/unloading processes. **a** For Thornton's restitution coefficient. **b** bistiffness versus Thornton's models

velocity is given as $v_y = \left(\frac{\pi}{2E^\star}\right)^2 \left(\frac{8\pi R^3 p_y^5}{15m}\right)^{\frac{1}{2}}$ in [1194]. It is noteworthy that in all the above cases $v_y = C\sqrt{\frac{p_y^5 R^3}{(E^\star)^4 m}}$ for some constant C.

Remark 4.6 (Impact Duration) Neglecting the elastic loading phase, the impact duration according to Thornton's model is estimated as $t_f = 1.118\left(\frac{m^2}{RE^\star v_y}\right)^{\frac{1}{5}}(1+\sqrt{\frac{5}{4}}e_{\rm n})$. If the model is energetically conservative, then $t_f = 2.368\left(\frac{m^2}{R(E^\star)^2|v_{\rm n}(t_k^-)|}\right)^{\frac{1}{5}}$. Compare with $t_1 = \pi\left(\frac{k}{m} - \left(\frac{f}{2m}\right)^2\right)^{-\frac{1}{2}}$ in (2.8) for the linear spring-dashpot model of Sect. 2.1.3. Hertz' model predicts a duration $t_f \approx 2.87\left(\frac{m^2}{R(E^\star)^2}\right)^{\frac{1}{5}}|v_{\rm n}(t_k^-)|^{-\frac{1}{5}} \approx 2.87\left(\frac{m^2}{\frac{9}{16}K_h^2}\right)^{\frac{1}{5}}|v_{r,{\rm n}}(t_k^-)|^{-\frac{1}{5}} \approx 3.21\left(\frac{m^2}{K_h^2}\right)^{\frac{1}{5}}|v_{r,{\rm n}}(t_k^-)|^{-\frac{1}{5}}$ [627, Eq. (11.24)] [469, Eq. (4.27)(4.30)]. We note that Tabor gives the same expression, but with a constant 2.74, and indicates that this holds for Poisson's ratios $\nu_1 = \nu_2 = 0.3$ [1175, Eq. (14)]. Since for most materials $\nu \in [0.3, 0.4]$ and it appears as $(1-\nu^2)$, such terms are often neglected in the calculations. However, a more accurate impact duration of Hertz impact between two elastic spheres is $t_f = 3.29(1-\nu^2)^{\frac{2}{5}}\left(\frac{m^2}{R(E^\star)^2}\right)^{\frac{1}{5}}|v_{\rm n}(t_k^-)|^{-\frac{1}{5}}$ [733, Eq. (25)].

Thornton's restitution coefficient has the value:

$$e_{\rm n} = \left(\frac{6\sqrt{3}}{5}\right)^{\frac{1}{2}}\left[1 - \frac{1}{6}\left(\frac{v_y}{v_{\rm n}(t_k^-)}\right)^2\right]^{\frac{1}{2}}\left[\frac{\left(\frac{v_y}{v_{\rm n}(t_k^-)}\right)}{\frac{v_y}{v_{\rm n}(t_k^-)} + 2\sqrt{\frac{6}{5} - \frac{1}{5}\left(\frac{v_y}{v_{\rm n}(t_k^-)}\right)^2}}\right]^{\frac{1}{4}}. \quad (4.48)$$

This expression provides an analytical form for $e_{\rm n}$ in the range $v_y < v_{\rm n}(t_k^-) < 10v_y$. This is shown to provide good predictions if $C_y = 1.6$ and $v_{\rm n}(t_k^-) \approx v_y$, while

$C_y = 2.8$ and $v_n(t_k^-) > v_y$. It is assumed in [1194] that $e_n = 1$ if there is no plastic deformation, i.e., there is no other dissipation source.[24] Stronge [1154, 1155] calculates:

$$e_n = \frac{v_y}{|v_n(t_k^-)|}\left[\frac{8}{5}\left(\frac{v_n(t_k^-)}{v_y}\right)^2 - \frac{3}{5}\right]^{\frac{3}{8}}. \tag{4.49}$$

It is argued in [1194] that in most cases, this value is less realistic than the one in (4.48) because it leads to $e_n > 1$ for $v_y < |v_n(t_k^-)| < 1.59v_y$, and in many practical problems $v_n(t_k^-)$ is larger than this upperbound. Extensive experiments are reported in [1140] for stainless and hard chrome steel sphere/sphere impacts, with $v_n(t_k^-) \in [0.3, 2.1]$ m/s. Thornton's model is shown to provide good prediction if C_y is fitted to $C_y = 9.14$ instead of 2.8 as recommended in [1279]. In [1246, Fig. 8] Thornton's model is fitted with $C_y = 4.7$ to match with experiments on brass alloy 260, and $C_y = 4.3$ for Al alloy 2017.[25] Thornton's model is improved in [738] by allowing p_y to depend on the contact area radius. In [956], Thornton's CoR is compared with finite element simulations; it significantly underpredicts the contact force during the plastic loading phase. This is attributed in [956] to two factors: the maximum contact pressure does not satisfy $p_{max} \leq p_y$ but can reached 2.31 times that assumed in [1194], and the contact area is about 2.1 times that assumed in [1194].

Another expression is calculated in [796] for elastic, perfectly plastic with strain hardening, impact:

$$e_n = 3\pi\sqrt{\frac{3}{10}}\left(\frac{\sigma_y^2}{E_{ul}^\star}(x+y)^{\frac{3}{2n+4}}\right)^{\frac{1}{2}}\left(\frac{15E_l^\star}{16R^2}(x+y)^{\frac{5}{2n+4}} + \frac{k\pi}{(2+n)R^{n+1}}y\right)^{-\frac{1}{2}}, \tag{4.50}$$

where $x = \left(\frac{9\pi R\sigma_y}{4E_l^\star}\right)^{2n+4}$, $y = \frac{(2n+4)R^{n+1}}{k\pi}\left(\frac{mv_n(t_k^-)^2}{2} - \frac{885735R^3\sigma_y^5}{16394(E_l^\star)^4}\right)$, k, $E_l^\star$, $E_{ul}^\star$, n and k are elasticity material parameters to be fitted with experiments. Johnson's and Tabor's models are improved in [272], where a more general elastoplastic model is used for loading, and a purely elastic model is used for unloading:

$$e_n = 1.704\left(\frac{\sigma_y}{E^\star}\right)^{\frac{1}{2}}\left(\frac{\sigma_y R^3}{0.5mv_n(t_k^-)^2}\right)^{\frac{1}{8}}, \tag{4.51}$$

where it is assumed that $C_y = 1.629$. Other expressions of e_n may be found [469, Eq. (4.54)] and [1260] (see Sect. 4.2.4). Assuming a power law behavior and a viscoplastic phase, Storakers and Larsson derive [1145]:

[24] One has to keep in mind that all the expressions of e_n in elastoplastic impacts, assume a first phase of deformation that is purely elastic, so that $e_n = 1$ for preimpact velocities less than the yield velocity.

[25] These two materials are rate insensitive and thus fit with Thorton's hypothesis. On the contrary stainless steels show a highly strain rate sensitive behavior (stainless steel 302 and 440 C are tested in [1246]).

$$e_{\mathrm{n}} = \frac{4\sqrt{3}}{\pi^{\frac{3}{8}}} \left(\frac{\sigma_y^5 R^3}{m(E^\star)^4 v_{\mathrm{n}}(t_k^-)^2} \right)^{\frac{1}{8}}. \tag{4.52}$$

This coefficient and Johnson's one differ by 20 %, up to a constant [1145]. Finite element results together with Hertz' elastoplasticity are used in [601] to derive a fitted expression as $e_{\mathrm{n}} = 1 - 0.1 \ln\left(\frac{|v_{\mathrm{n}}(t_k^-)|}{v_y}\right)\left(\frac{|v_{\mathrm{n}}(t_k^-)|-v_y}{59v_y}\right)^{0.156}$ if $v_y < |v_{\mathrm{n}}(t_k^-)| \leq 60v_y$, and $e_{\mathrm{n}} = 1 - 0.1\ln(60) - 0.11\ln\left(\frac{|v_{\mathrm{n}}(t_k^-)|}{60v_y}\right)\left(\frac{|v_{\mathrm{n}}(t_k^-)|}{v_y} - 60\right)^{2.36\frac{\sigma_y}{E}}$ if $60v_y \leq |v_{\mathrm{n}}(t_k^-)| \leq 1000v_y$ with $v_y = \sqrt{\frac{2}{m}}\sqrt{\frac{(\pi c_y \sigma_y)^5 R^3}{60(E^\star)^4}}$ and $C_y = 1.295\exp(0.736\nu)$.

Tabor's, Johnson's and Thornton's models have been improved by Brake [180, 181]. In addition to the fully plastic phase, a mixed elastic-plastic phase is added before unloading. The model inputs are the spheres radii, elastic modulus E_i, Poisson's ratios ν_i, yield stresses $\sigma_{y,i}$, densities ρ_i, and (a novelty compared to the above approaches) Brinell's hardness H_i.[26] Tabor defines the hardness as $H = \frac{T(t_k^-)}{V_r} = \frac{1}{2}\frac{m v_{\mathrm{n}}(t_k^-)^2}{V_r}$, where V_r is the residual imprint volume. According to [1175, 1177] the Brinell hardness H of the metals satisfies $\sigma_y = 0.354H$. The constant is a material property (for oxygen-free copper one has $H \approx \sigma_y$ [1171]). Usually one sets $p_y = \theta H_{\min}$ ($H_{\min} = \min(H_1, H_2)$), and fits θ with experiments. Values $\theta = 0.6$ [271], $\theta = 0.4$ [1326], $\theta = 0.577$ [677] may be found in the literature. More on hardness (Brinell, Meier, Vickers) and its relationships with contact mechanics may be found in [627, 855, 856, 1175, 1177]. In [181] it is proposed to take $H = \left(\frac{2}{H_1} + \frac{2}{H_2}\right)^{-1}$. Brake assumes four phases: elastic loading, mixed elastic-plastic regime, fully plastic regime, then unloading with no reverse yielding. Plastification starts at the indentation $\delta_y = \left(\frac{\pi\sigma_y}{2E^\star}\right)^2 \frac{R}{f(\nu)}$, where ν is the Poisson's ratio of the material that yields first, and $f(\nu)$ defines the maximum amplitude of the stress field into the surface. The mixed phase is modeled by interpolating the contact force F and the contact area radius a, with an order 3 polynomial, so as to guarantee some continuity and differentiability properties of the force/indentation function (it may be argued anyway that other fitting functions could be found for the mixed elastoplastic phase, as done, e.g., in [183]). To summarize:

$$\begin{aligned}
&\text{Elastic regime:} && F(\delta) = \tfrac{4}{3}E^\star\sqrt{R}\delta^{\frac{3}{2}},\\
&\text{Mixed elastic-plastic regime:} && F(\delta) = (2F_y - 2F_p + (\delta_p - \delta_y)(\dot{F}_y - \dot{F}_p))\left(\tfrac{\delta-\delta_y}{\delta_p-\delta_y}\right)^3 +\\
&&& \quad (-3F_y + 3F_p + (\delta_p - \delta_y) - 2\dot{F}_y - \dot{F}_p))\left(\tfrac{\delta-\delta_y}{\delta_p-\delta_y}\right)^2\\
&&& \quad +(\delta_p - \delta_y)\dot{F}_y\left(\tfrac{\delta-\delta_y}{\delta_p-\delta_y}\right) + F_y,\\
&\text{Plastic regime:} && F(\delta) = p_0\pi(2R\delta + \xi),\\
&\text{Restitution phase:} && F(\delta) = \tfrac{4}{3}E^\star\sqrt{R_e}(\delta - \delta_e)^{\frac{3}{2}},
\end{aligned} \tag{4.53}$$

[26] Brinell's hardness H is homogenous to a pressure, units Pa.

where $p_0 = Hg10^6$ is the maximum contact pressure (assumed to be uniform over the contact area), $\delta_p = \left(\frac{p_0}{\sigma_y}\right)^2 \delta_y$ is the indentation at the beginning of the plastic regime, $\xi = \left(R\frac{3\pi p_0}{4E^\star}\right)^2 - 2\left(\frac{p_0}{\sigma_y}\right)^2 \delta_p$, $F_y = F(\delta_y) = \frac{4}{3}E^\star\sqrt{R}\delta_y^{\frac{4}{3}}$, $F_p = F(\delta_p) = p_0\pi(2R\delta_p + \xi)$, δ_e is the residual indentation and R_e is the radius of the residual crater. Their values depend on whether the unloading occurs during the elastic, the mixed elastoplastic, or the plastic phases.

A similar approach is proposed in [676], where initiation of yields occurs at $\delta_y = \left(\frac{KH}{2E^\star}\right)^2 R$, K is a hardness coefficient related to Poisson's ratio as $K = 0.454 + 0.41\nu$. The authors take into account three different plastifications zones in the material, define the contact force as $F(\delta) = C\left(\frac{\delta}{\delta_y}\right)^n$, and fit three values of both parameters C and n in each zone, with finite element simulations. The unloading phase is obtained similarly. It is, however, noteworthy that neither Brake's [181] nor Kogut-Etsion's [676] approaches lead to a simple expression of e_n as the ones presented above. They require the time-integration of the dynamics, however the piecewise-continuous law in (4.53) should lend itself to numerical integration. A close Hertzian elastoplastic model with three regimes is proposed in [1296].

Brake's model is validated using experimental data found in [34, 95, 607, 656, 857, 949, 1156] in terms of force/indentation curves, contact area as a function of indentation and contact force, and coefficient of restitution. It is found that the proposed four-phase model provides through simulations, excellent matching with the experimental data. Nine other models are also simulated [271, 363, 598, 600, 676, 1156, 1194, 1322, 1326], and it is shown that they do not possess comparable prediction capabilities. The mixed elastic-plastic phase seems to play a crucial role in central (colinear without body rotation) impacts. Several restitution laws are compared in [180] in terms of their influence on the dynamics of systems (stability, wear, response severity, response frequency range, peaks in the frequency response). It is concluded that different restitution models may yield quite different qualitative and quantitative results. Ma and Liu [778] take into account the elastic, mixed elastic-plastic, fully plastic regimes during loading, and an unloading phase with strain hardening (incorporated in the model *via* a change of the contact radius in Hertz' approach). They impose that the force/indentation curve be continuously differentiable. They derive an expression for the energetic CoR (see Sect. 4.3.6 for a definition):

$$e_\star = \begin{cases} 1 & \text{if } \delta_{\max} \leq \delta_y \\ \sqrt{\frac{\frac{16}{15}E^\star\sqrt{R_e}(\delta_{\max}-\delta_r)^{\frac{5}{2}}}{mv_{r,\mathrm{n}}(t_k^-)^2}} & \text{if } \delta_y < \delta_{\max} < \delta_p \\ \sqrt{\frac{\frac{16}{15}E^\star\sqrt{R_e^p}(\delta_{\max}-\delta_r)^{\frac{5}{2}}}{mv_{r,\mathrm{n}}(t_k^-)^2}} & \text{if } \delta_{\max} \geq \delta_p \end{cases} \tag{4.54}$$

where δ_r is the residual indentation due to plasticity, R_e is the effective radius modified by $F_{\max}$ to account for strain hardening, R_e^p corresponds to the case where the loading phase ends in a fully plastic regime, δ_p is the identation at the onset of fully plastic regime. An interesting point is that they find the closed

expression $e_\star = 0.81(E^\star)^{-\frac{1}{5}}(R_e^p)^{-\frac{1}{6}}k_1^{\frac{5}{12}}m^{-\frac{1}{12}}v_{r,\mathrm{n}}(t_k^-)^{-\frac{1}{6}}$, where k_1 is the slope of the loading force/indentation curve approximated as a straight line. The dependence in the preimpact velocity is therefore different from previous results, in which a dependence $v_{r,\mathrm{n}}(t_k^-)^{-\frac{1}{4}}$ is observed. The results are validated with many comparisons with experimental data found elsewhere in the literature [184, 656, 857, 1276]. Further comparisons between various models in [181, 183, 383, 444, 599–601, 675, 676, 1156, 1194, 1294] and experimental data produced by the authors, are presented in [443] for a stainless steel rod colliding a low-carbon iron flat. The model called MJG in [443], taken from [444] fits the best with experiments. The other models (including Brake's) predict larger values of e_n for small preimpact velocities ($v_{r,\mathrm{n}}(t_k^-)$ varies between 4 and 0.5 m/s). The role of friction during the collision is not analyzed in [443]. It is noteworthy however that the analysis in [180, 443] concern systems with few degrees of freedom. When systems with a large number of contacts and degrees of freedom are considered, other important constraints may appear, like the choice of a suitable numerical method which in turn relies on a suitable model.

$\rightsquigarrow$ *The choice of the right restitution law is a crucial step for the dynamical analysis of a mechanical system. All the above elastoplastic impact models apply to frictionless collisions. Some provide a closed form of the CoR, some require the integration of piecewise-continuous dynamics.*

Remark 4.7 As alluded to above, plasticity effects may no longer play any role in the impact process after a certain number of loading/unloading sequences. The loss of kinetic energy once plastification disappears may be due to body vibrations (steel sphere/aluminum rod impacts in [859, 1083, 1084]), or to a small viscosity for zeolite 13X[27] sphere/sphere impacts [50, Figs. 22, 23 and 26]. It may be clever in that case to use a value of the restitution coefficient that takes this into account: plasticity during the first impacts, small viscosity for the remaining impacts. A similar phenomenon is observed for small ice spheres (radii 2.5 to 5 cm) impacting at low velocities (0.2, 0.3 and 0.8 cm/s) [505]. It is attributed to the presence for small frost particles which become pulverized after few collisions.

4.2.1.2 Bistiffness Models: Crook's Approach

A different class of models, conceptually simpler and empirical, is based on the idea that the permanent residual deformation (due to plasticity, or damage) may be represented by a variation of the contact stiffness between the loading and the unloading phases, as shown in Fig. 4.6a. It seems that this class of continuous, piecewise-smooth models was first introduced by Crook in 1952 [310], who reported experimental results with copper and ebonite cylinders impacting an anvil. Such loading/unloading curves have since then been used and experimentally validated many times [50, 181, 469, 573, 575, 576, 816, 857, 858, 1073, 1084, 1242, 1244, 1247,

[27] Microporous, aluminosilicate minerals.

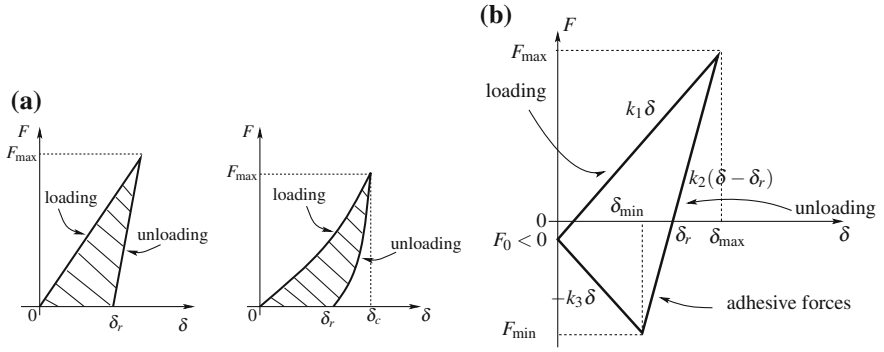

Fig. 4.6 Bistiffness contact/impact models. **a** (i) bilinear, (ii) bi-nonlinear. **b** With adhesive forces

1260, 1279, 1280, 1322]. One however should keep in mind that these models are intended to approximate with two phases, a force/indentation law as in Fig. 4.5a which intrinsically contains three, or four phases. As a consequence, the bistiffness, or two-phase models, are often shown to overestimate the maximum contact force during the loading/unloading process, because they match with Hertz' elasticity only in a small portion of the loading curve, see Fig. 4.5b, and [1322, Fig. 14] [50, Figs. 19 and 21] [857, Fig. 15]. The bistiffness impact laws model dissipation through a variation of the stiffness from the loading to the unloading phases, the rheological models of Sect. 2.2 dissipate through a linear or nonlinear damper, the "contact mechanics" laws of Sect. 4.2.1.1 dissipate with plasticity.

The bilinear model is sometimes called the Walton and Braun model: $F = k_1\delta$ in the compression phase (loading, $\dot{\delta} > 0$), $F = k_2(\delta - \delta_r)$ in the expansion phase (unloading, $\dot{\delta} < 0$). The restitution coefficient is then given by $e_\mathrm{n} = \sqrt{\frac{k_1}{k_2}}$, showing in passing that $k_2 \geq k_1$ to guarantee $e_\mathrm{n} \leq 1$. The same holds in the bi-nonlinear model of Fig. 4.6a (ii) if Hertz' elasticity is adopted. Another expression of Walton and Braun's bistiffness model is obtained setting $F = k_2(\delta - \delta_r)$ in the expansion phase, with $k_2 = k_1 + SF_{max}$ where F_{max} is the maximum force achieved before unloading. Then $e_\mathrm{n} = \sqrt{\frac{\omega}{S\dot{\delta}(t_k^-)+\omega}}$, $\omega = \frac{2\sqrt{k_1}}{m}$ [1243], i.e., the restitution depends on the preimpact velocity, while S is a parameter to be fitted. Another model was proposed in [705] with[28]: $F = k\delta^n$ in compression, $F = \frac{k\delta^n}{(\delta_c-\delta_r)^n}(\delta - \delta_r)^n$ in the expansion phase, for some coefficient n. The restitution coefficient may be obtained from $\delta_r = \frac{(n+1)\dot{\delta}(t_k^-)^2}{2k\delta_c^n} m(1 - e_\mathrm{n}^2)$, where $\dot{\delta}(t_k^-) = v_\mathrm{n}(t_k^-)$ is the indentation velocity at the beginning of the collision. Piano hammer impacts against a rigid stop are modeled with a bistiffness approach in [816] where the contact force during the loading phase is chosen as $F(\delta) = a\delta\exp(b\delta) + c\delta$ for some constants a, b, c, to be fitted with

[28] A quite similar model is presented in [469, §4.3], reporting results from Crook [310] and Barnhart [93].

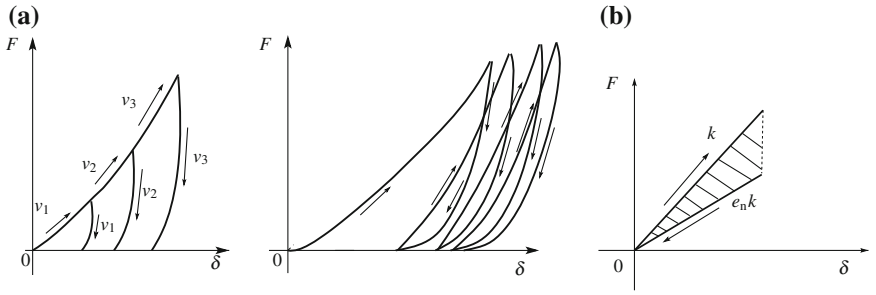

Fig. 4.7 Bistiffness contact/impact models. **a** (a) Different impact velocities $v1 < v2 < v3$, (b) repeated impacts (loading/unloading phases). **b** Bistiffness with force jump

experiments. Comparisons between the models of Hertz, Simon-Hunt-Crossley and [704] (see Sect. 2.2) are made in [782] for knee joint modeling.

Figure 4.7a (a) depicts typical loading/unloading curves for various approach velocities (see, *e.g.,* [1246, Figs. 5 and 6] [50, Fig. 19] [1247, Fig. 5] [1280, Fig. 5] [1279, Fig. 3] [181, Fig. 4] [573, Fig. 2] [1322, Figs. 13 and 14] [445, Fig. 3] [469, Figs. 189, 190] [312, Figs. 2 and 5] [816, Fig. 4] [532, Fig. 4]). Figure 4.7a (b) represents typical repeated loading/unloading force/indentation curves, see, e.g., [50, Fig. 21]. Most of these results are experimental ones. In view of the limitations alluded to above, it is likely that the experimental curves reported in these references, could be only approximated if a two-phase bistiffness model is used.

The above variations of Crook's approach, may be named elastoplastic, as they intend to model some kind of permanent deformation, while the loading and unloading phases are elastic. Ismail and Stronge [575, 576] proposed bistiffness viscoelastic models, using Maxwell's rheological model (a linear spring and a linear dashpot mounted in series), thus mixing viscoelastic models as described in Chap. 2 and bistiffness. The spring stiffness is k during compression, $\frac{k}{\gamma^2}$ during restitution. The damping factor is $\zeta = \frac{m\omega_0}{2f}$, f is the dashpot coefficient, $\omega_0 = \sqrt{\frac{k}{m}}$. The kinetic coefficient of restitution (Poisson's definition in (4.155) below), is calculated as:

$$\bullet\ \zeta < \gamma: \qquad e_{\mathrm{p}} = \gamma \exp\left(\tfrac{\zeta}{\gamma^2}[(1-\gamma^2)\omega_0 t_c - \omega_0 t_f]\right),$$

$$\bullet\ \gamma < \zeta < 1: e_{\mathrm{p}} = \frac{-\gamma^2}{2\zeta\sqrt{1-\frac{\gamma^2}{\zeta^2}}} \exp(-\zeta\omega_0 t_c)\{\exp\left(-\tfrac{\zeta}{\gamma^2}(1+\sqrt{1-\tfrac{\gamma^2}{\zeta^2}})\omega_0(t_f - t_c)\right)$$
$$- \exp\left(-\tfrac{\zeta}{\gamma^2}(1-\sqrt{1-\tfrac{\gamma^2}{\zeta^2}})\omega_0(t_f - t_c)\right)\}, \tag{4.55}$$

with: $t_c = \frac{1}{\omega_0\sqrt{1-\zeta^2}}\left(\pi - \arctan\left(\frac{\sqrt{1-\zeta^2}}{\zeta}\right)\right)$ is the time of transition from compression to expansion, the time of end of the restitution is given by $t_f = -\frac{\gamma\phi}{\omega_0\sqrt{1-\frac{\zeta^2}{\gamma^2}}}$ if $\zeta < \gamma$, $t_f = -\frac{\gamma^2}{2\omega_0\sqrt{1-\frac{\gamma^2}{\zeta^2}}}\ln\left(\frac{1-\sqrt{1-\frac{\gamma^2}{\zeta^2}}}{1+\sqrt{1-\frac{\gamma^2}{\zeta^2}}}\exp\left(-2\frac{\zeta}{\gamma^2}\sqrt{1-\frac{\gamma^2}{\zeta^2}}\omega_0 t_c\right)\right)$ if $\gamma < \zeta < 1$, and $\phi = \arctan\left(-\frac{\gamma}{\zeta}\sqrt{1-\frac{\gamma^2}{\zeta^2}}\right) - \frac{1}{\gamma}\sqrt{1-\frac{\gamma^2}{\zeta^2}}\omega_0 t_c$. The coefficient in (4.55) tends to zero as $\zeta \to 1$ (high damping). If $\zeta = 0$ then $e_\mathrm{p} = \gamma$. Some experimental validations are made in [575], using the data in [312], for low-velocity impacts of golf balls and super ball. The restitution (4.55) does not apply if the compression phase follows Hertz' elasticity. A similar bilinear stiffness rheological model is presented in [1297]. The coefficient γ is however not a priori given as a parameter, but calculated as $\gamma^2 = \frac{2}{3}\frac{k}{K_h}\left(\frac{k}{m\dot{\delta}(t_k^-)^2}\right)^{\frac{1}{4}} = e_\mathrm{n}$ where $K_h = \frac{4}{3}\sqrt{R}E^\star$ is the Hertzian stiffness. We recover here an expression which involves the preimpact velocity in the dynamics denominator, as we already met in Sect. 2.2.2. Hence the linear unloading stiffness depends on the collision initial energy $\frac{1}{2}m\dot{\delta}(t_k^-)^2$, where we remind that according to Hertz' theory, $\dot{\delta}(t) = v_{r,\mathrm{n}}(t)$. Let us finally notice that another type of bistiffness model, with zero residual deformation but a contact force jump as in Fig. 4.7b, is sometimes used [864, 1039]. It is shown in these articles that, given a contact model, the shape, size and geometry of the bodies (the grains) may significantly influence the dynamics of granular matter modeling avalanches.

The bistiffness contact model has been used in the context of multiple impacts in [748–750, 753, 928, 929, 1318–1320, 1327], and this will be presented in Sect. 6.3. A thorough comparison between Thornton's contact model, and various bistiffness models, is made in [1195, 1196] for oblique impacts where friction plays a crucial role. We will come back on friction in Sect. 4.2.5.

$\rightsquigarrow$ *All the models of* Sect. 4.2.1, *how sophisticated they may be, are local: they do not incorporate the possible influence of vibrational effects in the bodies during the shock. It has been known since a long time [556, 1033, 1056] that vibrations can play a significant role in the shock process. Moreover they completely neglect the influence of friction or adhesive effects, which quite often have to be modeled.*

4.2.2 Adhesive Effects

Some of the viscoelastic models of Sects. 2.1.3 and 2.2 may be rejected in most cases because they may create negative contact forces. It is however noteworthy that adhesive forces may exist between colliding bodies [627, 770, 822]. Usually, adhesive contact forces occur at low loads, and one observes that Hertz' theory has to be adapted because its predictions do not match with experimental data (adhesion

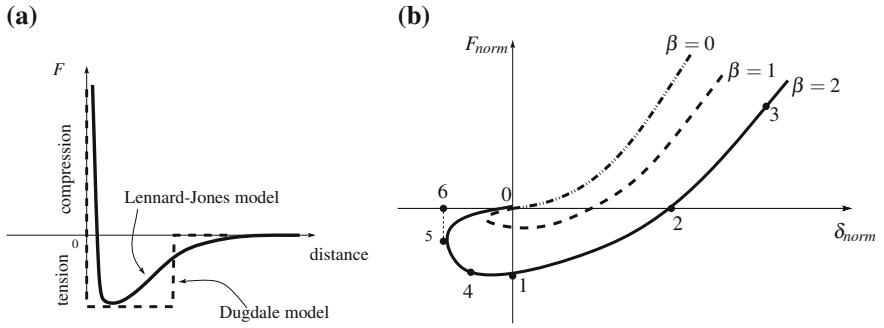

Fig. 4.8 Force/indentation and force/distance curves. **a** Force/distance law with adhesive forces. **b** Force/indentation response for (4.57)

increases the contact area, and modifies the stored elastic energy). Typical curves for adhesive contact forces as function of the "distance" of the solid to the obstacle, are depicted in Fig. 4.8a. They result for instance from the Lennard–Jones potential function, or the Dugdale potential well [628, Fig. 1].

Brach and Dunn [179] study the collisions of microparticles against a rigid obstacle (where adhesion forces play a significant role in the contact-impact process) with the Hertzian model:

$$m\ddot{x}(t) = -\frac{4}{3}E^{\star}\sqrt{R}x(t)^{\frac{3}{2}} - \sqrt{R}kx(t)^{\frac{3}{2}}c_h\dot{x}(t) + 2\pi af_0 + 2\pi af_0c_a\dot{x}(t), \quad (4.56)$$

where f_0 is the magnitude of the adhesion line force, a is the contact area radius, c_h and c_a are dissipation coefficients. In summary, the first term in the right-hand side is the classical Hertzian restoring force, the second is a dissipation term à la Simon-Hunt-Crossley, the third one is an idealized adhesion attraction force term, the fourth one accounts for dissipation due to adhesion. Another approach is in [65], starting from the so-called Johnson–Kendall–Roberts (JKR) theory. Hertz' contact theory is adapted, and it is assumed that the normal contact pressure is given by $p(r) = p_0\left(1 - \left(\frac{r}{a}\right)^2\right)^{\frac{1}{2}} + p_1\left(1 - \left(\frac{r}{a}\right)^2\right)^{-\frac{1}{2}}$, where a is the contact radius [627, §5.5] (see Sect. 4.2.1.1 for more details on Hertz' contact and the expression of $p(r)$ without adhesion). It is assumed that the effect of contact pressure and adhesion occurs only inside the area of contact, but this area differs from that predicted by Hertz: it is bigger as the bodies do not deform in the same way. Said otherwise, the Hertz' contact radius without adhesion a_H is smaller that a. The term p_1 accounts for the adhesion and $p_1 = -\left(\frac{2\gamma E^{\star}}{\pi a}\right)^{\frac{1}{2}}$, where γ is the surface energy (or surface tension[29]) [822], related to the work of adhesion between the two materials as $W_{adh} = \gamma_1 + \gamma_2 - \gamma_{12} = 2\gamma$ if

[29]Quoted from [826, p. 57]: *The dissymetry of interactions at the surface of a solid causes a modification of the lattice parameters of the first atomic planes of the order*1–2 %. *This variation of interatomic distances can occur perpendicularly to the surface (normal relaxation) or parallel*

both spheres are made of the same material and the interfacial energy γ_{12} is zero. The surface energy is a material constant. Also one has $p_0 = \frac{2aE^\star}{\pi R} = \frac{3F}{2\pi a^2}$. The contact force is derived as [627, Eq. (5.49)]:

$$F = -\frac{4a^3E^\star}{3R} + 4\sqrt{\gamma E^\star a^3 \pi}, \tag{4.57}$$

where the first term in the right-hand side is merely a rewriting of the expression giving the contact area radius (see the introduction of Sect. 4.2.1.1). The second term accounts for adhesion (in general this is given by $\sqrt{8\pi a^3 W_{adh}} = \sqrt{8\pi a^3(\gamma_1+\gamma_2-\gamma_{12})}$, which gives the expression in (4.57) if $\gamma_{12} = 0$ and $\gamma_1 = \gamma_2 = \gamma$). The shape of the force/indentation curves depends a lot on a parameter $\beta = b\sqrt{\gamma}$, with $b = \frac{3}{\alpha}\left(\frac{\pi a}{E^\star}\right)^{\frac{1}{2}}$, $\alpha = \frac{1}{R}\left(\frac{3mR^2 v_{\rm n}(t_0^-)^2}{4E^\star}\right)^{\frac{2}{5}}$. Typical shapes are in Fig. 4.8b, where $\delta_{norm} = \frac{\delta}{\alpha}$ is a normalized maximal indentation related to a normalized contact area radius $a_{norm} = \frac{a}{\sqrt{R\alpha}}$ as $\delta_{norm} = a_{norm}^2 - \frac{2}{3}\beta\sqrt{a_{norm}}$. Here $v_{\rm n}(t) = \dot{\delta}(t)$. When $\beta = 0$ (no adhesion) one recovers that $\delta^2 = \frac{a^2}{R}$ (an expression for a given in Sect. 4.2.1.1). It is noteworthy that the indentation may become negative because of adhesion in this model. The curves in Fig. 4.8b are defined parametrically (the parameter being a_{norm}) as $F_{norm}(a_{norm}) = a_{norm}^3 - \beta a_{norm}^{\frac{3}{2}}$, with $F_{norm} = F\frac{1}{mRv_{\rm n}(t_0^-)^2}\left(\frac{3mR^2v_{\rm n}(t_0^-)^2}{4E^\star}\right)^{\frac{2}{5}}$, and the normalized dynamics is $\ddot{\delta}_{norm} = -F_{norm}$ (in a new time scale $\tau = \frac{v_{\rm n}(t_0^-)}{\alpha}t$). They possess the typical shape of force/indentation curves for the adhesive case, see [825, Fig. 7] [94, Fig. 3] [629, Fig. 8]. An impact takes place as follows in Fig. 4.8b: compression is along the path marked by 0-1-2-3; expansion is along 3-2-1-4-5-6. Between 5 and 6 an abrupt pull-off occurs. This model of adhesive impact has been extended to a chain of three aligned balls in [1132]. Several other models have been developed for adhesion, with different assumptions than the JKR model, like the Derjaguin-Muller-Toporov (DMT) model [340] which assumes that the surface of contact satisfies Hertz' theory, and the adhesive forces (like van der Walls' forces) act outside this area, but without deforming the profile which remains Hertzian (while JKR model has a total area of contact that is bigger than Hertz' area [826, §4.5.5 and 4.6]). The main results of the DMT model are that the adherence force $2\pi W_{adh}R$ is attained when the area of contact vanishes, that the adhesion forces around the contact add to the applied load a force which decreases from $2\pi W_{adh}R$ to $\pi W_{adh}R$ when indentation increases, and that the radius of contact under zero load is equal to $a_0 = \left(\frac{\pi W_{adh}R^2}{K}\right)^{\frac{1}{3}}$, $K = \frac{4}{3}E^\star$. Another model relies on the Maugis–Dugdale (MD) theory [825], which unifies both DMT and JKR theories (Tabor's coefficient [1176] also bridges both JKR and DMT models). It uses the Dugdale potential well, whose force/distance law is shown in Fig. 4.8a. In the

to it (tangential relaxation). A form of residual stress is set up at the surface, and leads to surface tension.

MD model it is assumed that the adhesive forces act on a surface with radius $c > a$. Let $K = \frac{4}{3}E^\star$. Following [825] we define the dimensionless parameters:

$$\begin{cases} A = \dfrac{a}{\left(\frac{\pi W_{adh} R^2}{K}\right)^{\frac{1}{3}}}, \ \bar{F} = \dfrac{F}{\pi W_{adh} R}, \ \Delta = \dfrac{\delta}{\left(\frac{\pi^2 W_{adh}^2 R}{K^2}\right)^{\frac{1}{3}}} \\ \lambda = \dfrac{2\sigma_0}{\left(\frac{\pi W_{adh} K^2}{R}\right)^{\frac{1}{3}}}, \end{cases} \tag{4.58}$$

where σ_0 is the constant stress of the Dugdale model outside the area of radius a (and inside the disk of radius c). Hertz theory gives $A^3 = \bar{F}$, $\Delta = A^2 = \bar{F}^{\frac{2}{3}}$, the DMT theory[30] gives $A^3 = \bar{F} + 2$, $\Delta = A^2$, the JKR theory gives $A^3 = \bar{F} + A\sqrt{6A}$, $\Delta = \frac{A^3+2\bar{F}}{3A} = A^2 - \frac{2}{3}\sqrt{6A}$. The MD theory gives:

$$\begin{aligned} &(a)\ \tfrac{\lambda A^2}{2}[\sqrt{m^2-1} + (m^2-2)\arctan(\sqrt{m^2-1})] \\ &\quad + \tfrac{4\lambda^2 A}{3}[\sqrt{m^2-1}\arctan(\sqrt{m^2-1}) - m + 1] = 1 \\ &(b)\ \bar{F} = A^3 - \lambda A^2[\sqrt{m^2-1} + m^2\arctan(\sqrt{m^2-1})] \\ &(c)\ \Delta = A^2 - \tfrac{4}{3}A\lambda\sqrt{m^2-1}, \end{aligned} \tag{4.59}$$

with $m = \frac{c}{a}$. The equation in (4.59) (c) reduces to JKR when $\lambda \to +\infty$, and to DMT when $\lambda \to 0$. These various models yield quite different load/indentation curves, as shown in [629]. Further comparisons between DMT, JKR and MD are in [1108] where it is pointed out that the work of adhesion W_{adh} is more prominent in JKR than in DMT, DMT is more appropriate when $E^\star$ is large (MT theory applies to small, stiff spheres), while JKR is more appropriate when $E^\star$ is small (it applies to large and compliant spheres). Actually the parameter λ in (4.58) is known as the Maugis' parameter. Finally let us mention extensions of the linear bistiffness model that include adhesive effects [770, 979]. The force/indentation characteristic is depicted in Fig. 4.6b for the basic model, but more sophisticated characteristics are studied in [979]. One notices that initially $F_0 < 0$, because of van de Waals attractive forces. Such piecewise-linear models may be simpler to implement in a code when the number of contacts is large (like in granular materials), provided the number of parameters is kept small. They are meant to include elastic, plastic and adhesive effects. Similar approaches were proposed previously by Acary, Monerie and Jean in [5, 18, 616, 865] and implemented in a time-stepping numerical algorithm. See [13, §3.9.4.4] for a detailed description.

[30] JKR and DMT are called "approximations", not theories, in [825], and are said to lack of foundations in the general theory of Contact Mechanics.

4.2.3 Beyond Hertz: Conformal Contact Models

Let us briefly mention some few other contact models that do not fall into the sphere/sphere or sphere/flat class, and for which Hertz' theory does not apply because the shape, the size of the bodies, and the way they are supported have to be taken into account. Contact between cylinders which make contact along a whole long strip parallel to the cylinders axis, of width $2a$ and acted upon by a force F per unit length, is of interest in many applications, like joint clearances. According to the developments in [627, §4.2 (c)], one has $a = 2\left(\frac{FR}{\pi E^\star}\right)^{\frac{1}{2}}$, the Hertz' contact pressure is given by $p(x) = \frac{2F}{\pi a^2}(a^2 - x^2)^{\frac{1}{2}} = p_0\left(1 - \frac{x^2}{a^2}\right)^{\frac{1}{2}}$ (x is the coordinate along an axis perpendicular to the strip of contact, i.e., measuring the strip's width), the maximum contact pressure is $p_0 = \frac{2F}{\pi a} = \left(\frac{FE^\star}{\pi R}\right)^{\frac{1}{2}}$, the mean contact pressure is $p_m = \frac{\pi}{4}p_0$. Johnson considers a cylinder in nonconformal contact with two other surfaces. His theory may be adapted to cylinder/cylinder contact. After some manipulations and assumptions on the stress distribution, one arrives at the indentation/force relation [754, 991, 992]

$$\delta = \frac{F}{\pi E^\star}\left(\ln\left(\frac{4\pi E^\star \Delta R}{F}\right) - 1\right), \tag{4.60}$$

where the radial clearance is $\Delta R = R_2 - R_1$ in case of a pin-in-a-hole (in an infinite plate), R_1 is the pin's radius, R_2 is the hole's radius, while $\Delta R = R_1 + R_2$ in case an external contact geometry is considered. Several severe issues are associated with this model: it is not efficient when inserted in a numerical code, it does not take into account dissipation, it applies only if the contact surfaces are nonconformal (while internal contact surfaces as in a pin-in-a-hole clearance may become conformal). Comparisons between (4.60) and FEM simulations are performed in [754], for internal pin-in-a-hole contacts with $R_2 = 100$ mm. When $\Delta R \leq 0.5$ mm is too small, both solutions drastically differ, while correct matching is obtained for large enough $\Delta R \approx 1$ mm. The discrepancy between both solutions increases with increasing load F. The Hertz' (or Johnson's) model in (4.60) has been improved in [754, 791] (a power law incorporating a Crook's like model with restitution coefficient), and Persson's model as recalled in [754]. Other approaches include Radsimovsky and Goldsmith's models [991].

$\rightsquigarrow$ *All these models are compared through extensive numerical simulations in [991, 992]. The conclusions are not extremely clear, in the sense that the models provide diverging results for most of the values of ΔR (see [992, Fig. 2]).*

In order to highlight the great complexity that is encountered when relaxing the basic Hertz contact assumptions, let us consider the contact problem of a rigid conical frustum indenting a half space [427]. The system is depicted in Fig. 4.9. Let F be the axial force applied on the punch, δ the identation depth of the punch (which does not deform during the process), a the radius of the contact area, a_b the radius of the flat-end area of the punch. Starting from the stress–strain relations in cylindrical

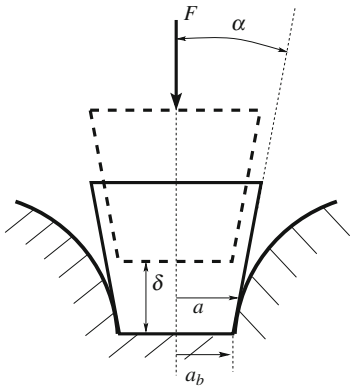

Fig. 4.9 Conical frustum punch with transversally isotropic elastic half-space

coordinates system for a transversally isotropic elastic material, which is an axisymmetric indentation problem, and assuming that $a_b = 0$ (conical indentation with $\delta = \frac{\pi a}{2}\frac{1}{\tan(\alpha)}$), the (F, δ) relation is found to be linear:

$$F = \frac{2Ma}{N}\delta, \tag{4.61}$$

where: $M = \frac{(l_1^{\frac{3}{2}} - l_2^{\frac{3}{2}})d - (\sqrt{l_1} - \sqrt{l_2})md - (l_1\sqrt{l_2} - \sqrt{l_1}l_2)mn + (l_1 l_2^{\frac{3}{2}} - l_1^{\frac{3}{2}} l_2)n}{\sqrt{l_1}(l_1 - m)l_2^{\frac{3}{2}}}$, $m = \frac{s_{13}(s_{11} - s_{12})}{s_{11}s_{33} - s_{13}^2}$, $n = \frac{s_{11}s_{44} + s_{13}(s_{11} - s_{12})}{s_{11}s_{33} - s_{13}^2}$, $l_1, l_2 = \frac{-c_{13}(2c_{44} + c_{13}) + c_{11}c_{33} \pm \sqrt{[c_{13}(2c_{44} + c_{13}) - c_{11}c_{33}]^2 - 4c_{11}c_{33}c_{44}^2}}{2c_{11}c_{44}}$, $c_{11} = \frac{1 - \nu_{TL}\nu_{LT}}{E_T E_L \Delta}$, $c_{12} = \frac{\nu_T + \nu_{LT}\nu_{TL}}{E_T E_L \Delta}$, $c_{13} = \frac{\nu_{LT} + \nu_T \nu_{LT}}{E_T E_L \Delta}$, $c_{33} = \frac{1 - \nu_T^2}{E_T^2 \Delta}$, $c_{44} = \mu_{LT}$, $\Delta = \frac{(1 + \nu_T)(1 - \nu_T - 2\nu_{LT}\nu_{TL})}{E_T^2 E_L}$, $d = \frac{s_{11}^2 - s_{12}^2}{s_{11}s_{33} - s_{13}^2}$, $s_{11} = \frac{1}{E_T}$, $s_{12} = -\frac{\nu_T}{E_T}$, $s_{13} = -\frac{\nu_{LT}}{E_L}$, $s_{33} = \frac{1}{E_L}$, $s_{44} = \frac{1}{\mu_{LT}}$, $N = \frac{e(s_{11} - s_{12})(d - mn)(l_1 - l_2)}{d(l_1 - m)l_2}$, $e = \frac{s_{11} + s_{12}}{s_{11}}$, E_T is the Young's modulus and ν_T is the Poisson ratio of the transverse isotropic plane, E_L is the Young's modulus, ν_{TL} is the Poisson's ratio, μ_{LT} is the shear modulus, in the longitudinal direction, and $\frac{\nu_{LT}}{E_T} = \frac{\nu_{LT}}{E_L}$. When the punch is a cylinder ($\alpha = 0$) then $F = \frac{4Ma}{N}\delta$ which is also linear. The contact between a sphere and a spherical cavity is studied in [388].[31] The boundary of the contact region is a circle, the problem is axisymmetric, the contact area is a curved surface with center the initial contact point. The Hertz' assumption on the contact pressure is generalized to $p(r) = p_0\left(1 - \left(\frac{r}{a}\right)^2\right)^n$, where p_0 is the maximum contact pressure, r is a projective distance from the symmetry axis, a is the projective radius of the boundary of the contact area. Let R_2 be the radius of the spherical cavity. Finite element simulations with fine mesh (between 250.10^3 and 350.10^3 elements) and material parameters for steel/steel and steel/beryllium bronze are used to determine the variation of n by fitting $n = \frac{1}{2} - 0.24\exp(-15.08\left(1 - \frac{a}{R_2}\right))$. If $\frac{a}{R_2}$

[31] Whose title is too enthusiastic, since no model appears to be "universal".

is small one recovers Hertz' coefficient $n = \frac{1}{2}$. The maximum pressure is given by $p_0 = (n+1)\frac{F}{\pi a^2}$, F is the force applied on the sphere. The indentation of points far enough from the symmetry axis is also given.

A more detailed summary on conformal contact and extension of Hertz's theory can be found in [12, §6], with plane/cylinder/plane, cylinder/cantilever beam, contacts. Let us mention contact between hollow spheres (shells) and flat, where the elasticity coefficient is different from 1 (linear elasticity) or $\frac{3}{2}$ (Hertz' elasticity) [926, 983]. A specific feature of such impacts is the possible occurrence of buckling phenomena, (*i.e.*, the creation of a hollow, or concave shape, at the contact area during the collision process). See [1288] for nice photographs of aluminum alloy 6061-T6 circular rings colliding a rigid target, showing the high deformation of the rings at high impact velocities ($\approx$ 90 m/s) (see Definition 2.1). The kinematic restitution coefficient is experimentally shown to decrease linearly from $e_{\rm n} = 0.5$ to 0.05 for the ratio $\frac{|v_{\rm n}(0)|}{v_y} \in [0.9, 4.5]$, with a plateau at $e_{\rm n} = 0.05$ for $\frac{v_{\rm n}(0)}{v_y} \in [4.5, 6]$ at high preimpact velocities $v_{\rm n}(0)$ much larger than the yield velocity, plastic deformation absorbs almost all the kinetic energy of the rings. The restitution seems to be independent of the nondimensional wall thickness of the rings. Values of the elasticity coefficient obtained *via* finite element simulations are reported in [926], and range from 1.222 to 1.504 depending on the ratio between the outer and the inner radii of the spheres.

4.2.4 Conditions for Quasistatic Impacts

In case of sphere/sphere or sphere/anvil impacting at low velocities, body vibrations are negligible, hence the local deformation and dissipation assumption is valid.[32] In fact what one means by *low-velocity impacts*, precisely refers to cases where the vibrations into the colliding bodies can be neglected compared to the other effects due to the collision. Hence the bodies that collide may be assumed to be in a quasistatic equilibrium during the impact (in particular Hertz' theory may be applied if the contacting surfaces are nonconforming). Determining such cases is certainly a hard problem in general. Vibrations play a role in collisions involving rods, beams, thin plates, see Sect. 4.3.10. The importance of body vibrations in shock dynamics was pointed out by G. Coriolis [302] and M. de Saint Venant [1056]. Goldsmith dedicates a whole chapter to vibrational effects in collisions [469, Chap. III], see also [627, Chap. 11]. For a sphere/sphere impact at moderate velocity, one finds [469, p. 23] [1033]

$$\frac{\text{vibrational energy}}{\text{total energy}} = \frac{1}{50}\frac{|v_{\rm n}(t_k^-)|}{c_0}, \quad c_0 = \sqrt{\frac{E^\star}{\rho}}, \tag{4.62}$$

[32] For a sphere/flat impact, it is indicated in [386] that $e_{\rm n}$ may have variations between 0.7 and 2.5 % if vibrations of the sphere and of the flat (calculated from Zener's theory) are taken into account.

where ρ is the mass density, and c_0 is the velocity of the pulse, that may be considered as a characteristic of the material [627, p. 341]. Love [764] proposed an empirical criterion to guarantee quasistaticity of the collision, as:

$$\left(\frac{|v_{\mathrm{n}}(t_k^-)|}{c_0}\right)^{\frac{1}{5}} \ll 1. \tag{4.63}$$

The rationale behind Love's criterion is that there must be sufficient time for the passage of a large number of elastic waves back and forth along the directions involving compression in the contact region, of the two bodies. In other words, the impact duration should be large enough compared to the body vibration period. The total time of impact between two spheres, under Hertz' theory (quasistatic equilibrium, circular frictionless area of contact), is given by $t_f = 2.87\left(\frac{m^2}{R(E^\star)^2|v_{\mathrm{n}}(t_k^-)|}\right)^{\frac{1}{5}}$ [627, p. 354] [556, Eq. (34) (35)], where $R = \frac{R_1R_2}{R_1+R_2}$ and $m = \frac{m_1m_2}{m_1+m_2}$ (the 2.87 is 2.94 in [556]).[33] The time it takes for the wave to travel through the spheres is $\frac{4R}{c_0}$s. Thus $\frac{\frac{4R}{c_0}}{t_f}$ is proportional to $\left(\frac{|v_{\mathrm{n}}(t_k^-)|}{c_0}\right)^{\frac{1}{5}}$ and it is small if Love's criterion holds, showing some consistency between Hertz' assumptions and (4.63). Love's criterion is recovered by Hunter [556, Eq. (37)] for sphere/flat impacts. Hunter supposed an isotropic elastic semi-infinite flat, and calculated that for sphere/flat impacts, the ratio of total vibrational energy W over the initial kinetic energy, is given by

$$\frac{W}{T(t_k^-)} = \frac{2\tau(\frac{4\pi}{3})^{-\frac{1}{5}}\rho_1^{-\frac{1}{5}}(E^\star)^{\frac{6}{5}}|v_{\mathrm{n}}(t_k^-)|^{\frac{3}{5}}}{\rho c_0^3} \tag{4.64}$$

for some material parameters. This gives $\frac{W}{T(t_k^-)} = 1.04\left(\frac{|v_{\mathrm{n}}(t_k^-)|}{c_0}\right)^{\frac{3}{5}}$ for steel sphere/steel flat, $\frac{W}{T(t_k^-)} = 1.27\left(\frac{v_{\mathrm{n}}(t_k^-)}{c_0}\right)^{\frac{3}{5}}$ for hard steel sphere/glass flat. Thus if Love's criterion is satisfied this ratio is very small. All this remains valid if impacts are elastic. Extension when plastic deformation occurs may be found in [563]. As noted by Johnson, *(Love's criterion) clearly leads to logical difficulties when one of the bodies is large so that no reflected waves return to the point of impact!*

If waves inside the bodies are not neglected, the restitution coefficient (more exactly, an apparent CoR) may be < 1 even if bodies are perfectly elastic. Weir and Tallon [1260] take into account loss of energy due to shear waves inside the impacting spheres. The velocity of shear waves is $c_2 = \sqrt{\frac{G}{\rho}}$, where $G = \frac{E^\star}{2(1+\nu)}$ is the elastic shear modulus. Then $e_{\mathrm{n}} \approx \exp\left(-0.6\frac{c_0}{c_2}\left(\frac{|v_{\mathrm{n}}(t_k^-)|}{c_0}\right)^{\frac{3}{5}}\right)$. For low impact velocities $\frac{v_{\mathrm{n}}(t_k^-)}{c_0} \ll 1$ and $e_{\mathrm{n}} \lesssim 1$. Two models of perfectly elastic disks that hit a rigid

[33] For identical spheres the expression $t_f = 5.6R\left(\frac{1}{c_0^4|v_{\mathrm{n}}(t_k^-)|}\right)^{\frac{1}{5}}$ is given in [556, Eq. (37)].

wall are simulated in [507]. The restitution coefficient is shown to vary from 0.98 for $\frac{|v_n(t_k^-)|}{c_0} \approx 0.01$ to 0.93 for $\frac{|v_n(t_k^-)|}{c_0} \approx 0.2$. An estimation of the normal CoR incorporating wave effects in spheres is proposed in [508] as $e_n \approx 0.5827 \frac{\kappa^{\frac{6}{5}}}{\rho m^{\frac{1}{5}} (E^\star)^{\frac{3}{5}}} |v_n(t_k^-)|^{\frac{1}{5}}$ where the constants are defined in Sect. 2.2.2 on Kuwabara-Kono's model, with Poisson's ratio $\nu_i = \frac{1}{4}$; this CoR approximation behaves essentially as the one obtained from a quasistatic assumption and Kuwabara-Kono's model. Collisions between elastic disks are analyzed and simulated in [439]. The restitution coefficient decreases from 1 to 0.65 as the preimpact relative velocity increases, because of potential energy stored in the disks. Experiments of sphere/sphere, steel spring/steel spring, rod/rod collisions have been reported in [316] which demonstrate the role of body vibrations for bodies other than spherical. Related results are in [1184] who shows with statistical physics tools, that the coefficient of restitution of an elastic object made of particles linked by some potential, and striking a rigid elastic wall, both frictionless, satisfies $e_n \leq 1$. Other results may be found in [1058, 1072]. Steel sphere/aluminum rod, half-circular plate, ball, and beam impacts are analyzed numerically and experimentally in [1072]. Elastic linear wave propagation (see Sect. 6.1.1.4), modal approach, finite elements are used for simulations. Wave propagation is negligible in the sphere/ball impact, significant in the sphere/beam impact (80 % of the energy transformed into bulk vibrations). In [1058], simulations with two different models (one-dimensional linear elasticity wave propagation, and finite element method) of two rods impacting axially at a rounded edge, show good agreement with experiments. The impact between aluminum alloy circular rings and a rigid flat, is investigated through finite element simulations in [85]. Three parameters are shown to govern the collision process: the nondimensional thickness $\frac{h}{R}$ (h is the ring width, R is its radius), the yield strain of the material $\frac{\sigma_y}{E}$, and the nondimensional initial velocity $v \triangleq \frac{|v_n(t_k^-)|}{v_y}$ (where v_y is the yield velocity). Four different impact regimes are determined: (i) $v < 0.2$ (elastic deformation), (ii) $0.2 < v < 0.8$ (plastification near the impact point), (iii) $0.8 < v < 2$ (formation of a four-hinge crushing mode), (iv) $v > 2.0$ (five-hinge crushing mode). The translational kinetic energy of the ring after the shock, (i.e., the kinetic energy due to the ring's gravity center velocity), is equal to $\frac{9}{16} T(t_k^-)$ in regime (i), $\frac{1}{16} T(t_k^-)$ in regime (iii), $\frac{1}{100} T(t_k^-)$ in regime (i). The rest of the initial kinetic energy is transferred into vibrations of the ring, and dissipated *via* plastic deformations. Here plastification occurs not only at the contact point, but also in the global deformation of the ring, at the crushing hinges. It is found that even in regime (i), the impact process differs significantly from that of a sphere/flat system: transfer of energy into body vibrations, and asymmetry of the impact force (the compression phase is $\frac{3}{4}$ of the impact duration, while compression and expansion are of equal duration for sphere/sphere or sphere/flat collisions). Due to the predominancy of the bending moment over the axial compression force, the plastic deformation in the circular ring occurs for impact velocities much smaller that v_y, possibly $0.3 v_y$. The restitution coefficient, calculated with the pre- and postimpact velocity of the ring's gravity center, is depicted as a function of v in Fig. 4.10 (this is a summary of [85, Fig. 9a–c]). The most remarkable feature compared to sphere/sphere impacts, is

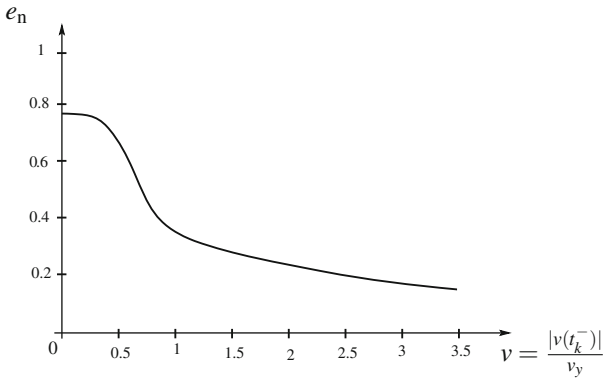

Fig. 4.10 Ring/flat collision: $e_n(v)$ (inspired from [85])

that e_n does not tend to 1 when the preimpact velocity tends to 0 m/s. The collision of a sphere against a thin plate is studied in [1126, 1314] [469, §4.9 and 6.2]. The plate span is supposed to be large enough so that the time required for the flexural wave to travel to the plate boundaries and be reflected back to the loading point, is larger than the contact time. It is concluded that most of the preimpact kinetic energy is converted into plate's vibrations, (i.e., no energy is recovered from the traveling wave). Hertz' theory is used to model the contact between the sphere and the plate. An expression of e_n is given in [469, Eq. (4.179)]. See also Theorem 4.1 in Sect. 4.4. An extension of Zener's model is developed in [426], with applications in fruit collision with an elastic plate. Section 4.3.10 is dedicated to a particular effect of body vibration, called microcollisions, and how these microcollisions produce energy transfer to the bending mode. The collision of an elastic bar with an elastic beam is analyzed and experimentally verified in [918]. The apparent CoR is shown to vary between 0.25 and 1 depending on the position at which the bar collides with the beam. This confirms the study in [557, 1144] summarized in Sect. 4.3.10, that vibrations may play a significant role in impacts of elongated bodies.

Remark 4.8 The fact that body vibrations may be neglected in sphere/sphere impacts for small enough impacting velocity, allows one to consider that impacting spheres may be modeled as point masses with unilateral Hertzian springs (plus plasticity and/or viscosity dissipation if needed). This is crucial for studying multiple impacts in chains of balls and nonlinear wave effects in such systems. It has been validated by careful comparisons between experimental data and numerical simulations [306, 387, 749] for chains of aligned beads falling under the effect of gravity. As alluded to in Sect. 6.1.1.4, these nonlinear waves should not be confused with the linear elasticity bulk waves that create vibration in the bodies during and after impact. Quasistaticity refers to linear elastic waves inside the rigid bodies.

4.2.5 *Incorporating Friction Effects*

One of the fundamental assumptions of Hertz' theory is that the surfaces are smooth enough so that friction can be neglected in the contact/impact process. Obviously friction is often present in real applications. We make in this section a very brief summary of the extension of Hertz' contact to the frictional case.

4.2.5.1 Hertz–Mindlin–Deresiewicz' Approach: Tangential Restitution

Let us consider two identical spheres which collide as in Fig. 4.4b. In addition to the normal compressive force $F_{\rm n}$, one considers now a tangential force $F_{\rm t}$ acting on both spheres. A circular zone of contact with radius a is created. When friction is present at the contact, one may assume following Mindlin–Deresiewicz (MD) [861] that microslip effects exist, and that the contact zone has two parts: an annular microslip zone at the contact perimeter with radius $c \leq r \leq a$, and a central sticking (adherence) disk with radius c. As long as $c > 0$, one has $F_{\rm t} < \mu F_{\rm n}$ and the microslip regime occurs. When $c = 0$ we get $F_{\rm t} = \mu F_{\rm n}$ and the (gross) sliding regime occurs. The MD approach yields $\frac{dF_{\rm t}}{dt}(t) = -K_{\rm t}\frac{d\delta_{\rm t}}{dt}$, where the stiffness $K_{\rm t} = K_{\rm t}(\delta_{\rm n}, \delta_{\rm t}, E^\star, G^\star, R, \mu, \text{path})$, and the equivalent shear modulus $G^\star$ is defined below. Thus the tangential stiffness depends on both normal $\delta_{\rm n}$ and tangential $\delta_{\rm t}$ indentations, and on the path followed by the system during the loading phase. Using the Mindlin–Deresiewicz theory, the tangential displacement relative to the centers of the contacting spheres is given during microslip by [78]:

$$\delta_{\rm t} = \frac{3(2-\nu)\mu F_{\rm n}}{16Ga}\left(1-\frac{c^2}{a^2}\right) = \frac{3(2-\nu)\mu F_{\rm n}}{16Ga}\left(1-\left(1-\frac{F_{\rm n}}{\mu F_{\rm t}}\right)^{\frac{2}{3}}\right) \tag{4.65}$$

where $G = \frac{E}{2(1+\nu)}$. The sliding regime starts when $c = 0$ at $\delta_{{\rm t},s} = \frac{(2-\nu)\mu a^2}{4(1-\nu)R} = \frac{(2-\nu)\mu}{4(1-\nu)}\delta$, where $\delta = \frac{a^2}{R}$. In a collision problem, an important parameter is the impact angle γ^- such that $\tan(\gamma^-) = \frac{v_{\rm t}(t_k^-)}{|v_{\rm n}(t_k^-)|}$. Assuming that the microslip displacement is colinear with the velocity vector, it follows that $\tan(\gamma^-) = \frac{(2-\nu)\mu}{2(1-\nu)}\left(1-\frac{c^2}{a^2}\right)$. Inverting one gets $\frac{c^2}{a^2} = 1 - \frac{2\tan(\gamma^-)(1-\nu)}{\mu(2-\nu)}$. One infers that sliding regime occurs when the impact incidence angle satisfies $\tan(\gamma^-) \geq \frac{(2-\nu)\mu}{2(1-\nu)} \approx \frac{\mu}{4}(2+\nu) \triangleq \tan(\gamma_s^-)$, i.e., the tangential velocity is large enough ("inclined collision"). While the microslip regime occurs for small enough γ^- ("close to normal collision"). The following conclusions are stated in [78]: For $0 \leq \delta_{\rm t} \leq \delta_{{\rm t},s}$ and $\delta_{{\rm t},s} \ll \delta$, the Mindlin–Deresiewicz approach can be applied for the microslip regime; when $\delta_{\rm t} > \delta_{{\rm t},s}$ (or $\gamma^- > \gamma_s^-$), it cannot be applied. The dynamical case is analyzed in [79]. It is assumed that the upper sphere (number 2 in Fig. 4.4b) has a controlled horizontal motion with horizontal (tangential) preimpact velocity $v_{\rm t}(t_k^-)$, while the bottom one is stationary. After a rather complex

analysis, an expression of the tangential restitution coefficient is found as

$$e_{\mathrm{t}} = \pm\left(1 - 2\frac{16\sqrt{2}}{3m(v_{\mathrm{t}}(t_k^-))^2}\mu k_r K_h (2R)^{\frac{5}{2}}\sqrt{1+k_r}((k_r+3)K(k) - 4E(k))\right)^{\frac{1}{2}} \tag{4.66}$$

with $k_r = 1 - \frac{\delta}{R}$, K_h is the Hertz' stiffness, $K(k) = F(1,k)$ and $E(k) = E(1,k)$ are first and second kind complete elliptic integrals, $k = \frac{\sqrt{1-k_r^2}}{1+k_r}$ is the elliptic modulus. The coefficient may be positive or negative to allow for tangential velocity reversal. The critical velocity $v_{\mathrm{t},c}(t_k^-)$ such that the moving (upper) sphere dissipates all the initial kinetic energy at the separating contact point (hence for $v_{\mathrm{t}}(t_k^-) < v_{\mathrm{t},c}(t_k^-)$ the upper sphere stops before separation may occur) is given by $e_{\mathrm{t}} = 0$:

$$v_{\mathrm{t},c}(t_k^-) = \pm\left(2\frac{16\sqrt{2}}{3m}\mu k_r K_h (2R)^{\frac{5}{2}}\sqrt{1+k_r}((k_r+3)K(k) - 4E(k))\right)^{\frac{1}{2}}. \tag{4.67}$$

Figure 7 in [79] shows that $|e_{\mathrm{t}}|$ varies from a small value (≈ 0.12) to 1 as the ratio $\frac{v_{\mathrm{t}}(t_k^-)}{v_{\mathrm{t},c}(t_k^-)}$ varies from 1.01 to 3. Notice that as $v_{\mathrm{t}}(t_k^-) \to 0$ there is no singularity in (4.66) because a zero tangential initial velocity implies a zero indentation δ, hence $k_r = 1$ and $k = 0$, so that $(k_r+3)K(k) - 4E(k) \to 4K(0) - 4E(0) = 0$ since $K(0) = E(0) = \frac{\pi}{2}$.

4.2.5.2 Further Studies

The extension of Hertz contact to the frictional case with improvement of the Mindlin–Deresiewicz theory has received attention in [78, 79, 788, 828, 1036, 1037, 1195, 1196]. Maw et al. [828] improve the Hertz–Mindlin–Deresiewicz (HMD) theory by considering a summation of contribution of several annuli (instead of just two zones in HMD) in the tangential plane area. This gives accurate modeling [657, 1036], but it is very time-consuming in a code, and may be too sophisticated in applications whenever geometry and material parameters are prone to inaccuracies. HMD is in fact an improvement of Mindlin's original results [860] who neglected all slipping effects and considered $F_{\mathrm{t}}(t) = -K_{\mathrm{t},0}(t)\delta_{\mathrm{t}}(t)$ with $K_{\mathrm{t},0}(t) = 8G^\star\sqrt{R\delta_{\mathrm{n}}(t)}$ (thus the stiffness depends on the normal indentation δ_{n}), and $G^\star = \left(\frac{1-\nu_1}{G_1} + \frac{1-\nu_2}{G_2}\right)^{-1}$, G_i is the shear modulus of sphere i, ν_i is its Poisson ratio. Mindlin's stiffness is used in [1220]. Di Renzo and Di Maio [788, 1036, 1037] compare a linear stiffness model, Hertz-Mindlin (HM), HMD and [1220] through numerical simulations and the experimental data of [657]. They conclude that HMD is the more accurate in terms of prediction of the CoR and contact force history but is very complex to insert in a numerical code, the no-slip assumption of HM yields an overestimate of F_{t}, so

that the all-linear model may give better results. In [1037] they propose a variation of the HM model as $F_t(t) = -\frac{2}{3}(8G^\star\sqrt{R\delta_n(t)})\delta_t(t)$ (named HDD in [1037]) and show that it gives results close to the HMD for small or large collision incidence angles, being much simpler to implement in a code. An approximation of the HMD model consists of the so-called *incremental slipping friction* [1036, 1195, 1196]. Let us describe it when the normal indentation δ_n is constant. One starts the loading phase with $F_t(t) = F_t(0) + K_t(t)(\delta_t(t) - \delta_t(0))$, with $K_t(t) = K_{t,0}\left(1 - \frac{\frac{2}{3}K_{t,0}\delta_t}{\mu F_n}\right)^{\frac{1}{2}}$, and then increments this relation at future time steps to get the portion AB. When δ_t starts to decrease, a turning point is attained with a turning force F_t^{TP} and one uses $K_t = K_{t,0}\left(1 - \frac{F_t^{TP} - F_t}{2\mu F_n}\right)^{\frac{1}{3}}$, and similarly for δ_t^{TP}, to get the curve BC. Then a complete unloading curve is calculated, until a reloading phase starts when δ_t starts to increase again, with tangential force F_t^{TTP}. One sets $K_t = K_{t,0}\left(1 - \frac{F_t - F_t^{TTP}}{2\mu F_n}\right)^{\frac{1}{3}}$ and the curve CD. During the whole process it is checked that $||F_t|| \leq F_n$. This gives rise to a loading-unloading-reloading cycle, a typical form of which is depicted in Fig. 4.11a. The HMD model is further simplified in [539] to be inserted in a granular matter code, with complete linearization yielding a path independent force-indentation relation. HMD, HM, linear models typically provide the rebound angle as a function of the incidence angle, as depicted in Fig. 4.11b, however HMD has the best accuracy [1036, Figs. 6, 7]. We will see in Sect. 4.3.1.1 that this can be fairly well approached (except for very small incidence angles) using another type of impact law with Coulomb's friction model.

A very detailed analysis of the gross sliding regime ($\gamma^- > \gamma_s^-$) is made in [78] when the upper sphere displacement is imposed to be horizontal (we refer to Fig. 4.4b while sphere 1 is fixed at its center). Expressions for the contact zone radius, contact tractions, contact geometries are calculated. Detailed analysis of oblique impacts relying on normal and tangential compliances and Poisson's CoR are proposed in [688, 1157]. The three regimes of collision depending on the incidence angle, are

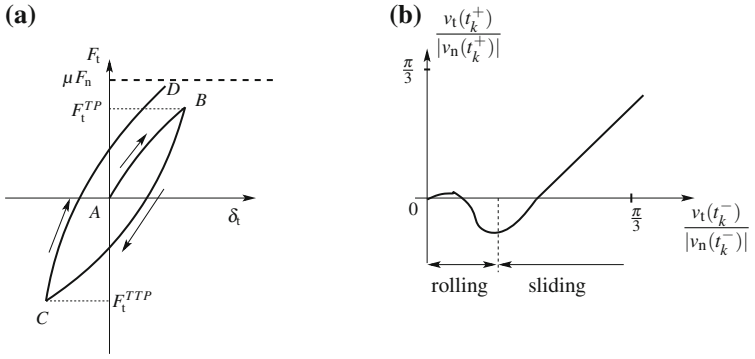

Fig. 4.11 Incremental slipping friction with constant normal indentation

verifiable from material and geometrical parameters as well as the CoR. This is further investigated in [621]: Coulomb friction and tangential compliance are considered for three-dimensional two-body collisions in [621] with a lumped parameter model of contact, where a bistiffness linear compliance is used in both normal and tangential directions, and the energetic CoR rules dissipation. A very detailed analysis of the various contact modes is made. It is pointed out in [526] that the energy dissipated by friction has to be correctly calculated with the true sliding speed for this type of contact model.

4.2.6 Conclusions

We see from Sects. 2.1.3, 2.2, 4.2.1.1, 4.2.1.2, 4.2.4, 4.2.5, Theorem 4.1 in Sect. 4.4, that there is a *proliferation* ("a myriad of models, many of which represent various modifications of the basic theory" according to [20]) of contact models for frictionless and frictional single impacts.[34] Extensive comparisons between numerical and experimental data are available in [180, 1036, 1140], in terms of restitution coefficients, contact force history (duration, maximal force), and evolution of velocities and displacements, for several models. It is sometimes concluded that simple models perform as good as more involved ones in term of postimpact velocity calculation, however more sophisticated models provide better accuracy for the contact force, velocities or displacements (e.g., predicted contact durations may be used to separate models[35]). Comparisons between different contact models have been done in [182, 992]: they show that the dynamical responses of systems may vary a lot if the model is changed. The authors of [996, 1040] conclude that the choice of the damping model depends on the type of external excitation (harmonic or random). The choice of a model has to take into account the nature of the elasticity at the contact/impact points (linear, Hertz, or else), the nature of the dissipation (viscosity, plasticity, vibratory, frictional, or else), and whether or not bulk vibrational effects (linear elasticity) play a role. The fact that the contact model yields an explicit expression of the restitution coefficient, may also be important in some fields like Control, or Robotics, because it enables one to make stability analysis. But piecewise-linear or piecewise-smooth models may be suitable as well, as long as they may be easily incorporated in a multibody systems code. Parameter estimation is a crucial step. One advantage of the models that stem from Contact Mechanics and Hertz' theory is that most of their parameters are material constants, and they require the fitting of none or very few remaining parameters (like the yield constant C_y).

Remark 4.9 What about finite element methods? Let us quote [182]: . . . *single degree of freedom constitutive models . . . enable significantly more efficient simulations of*

[34] Recall that an impact is said to be a *single impact* if there is only one collision occurring in the system at time t_k. If several collisions occur at the same time (or during overlapping periods of time), one speaks of a *multiple impact*.

[35] This is even more true in case of multiple impacts.

Table 4.1 Material parameters values

	E (GPa)	G (GPa)	ν	σ_y (MPa)
Soda-Glass lime	70	28	0.25	
Aluminum oxyde	370–380	154	0.22–0.23	
Brass alloy 260	115		0.3	550
Aluminum Alloy 2017	70	26	0.30–0.35	300–500
Stainless steels	190–210	79	0.3	170–1000
PTFE Liner	52		0.37	
Apple skin	12 MPa		0.35	
Apple Cortex	5 MPa	0.15 MPa	0.35	
Apple Core	7 MPa	0.15 MPa	0.35	
Aluminum-Bronze UNS C61300	115	44	0.312	240–400
Copper (Ultra-Fine-Grained)	110–128	48	0.34	350
E52100 Steel	190–210	80	0.27–0.30	350
Polymer (Polycarbonate)	2.0–2.6		0.38	59–70
Polymer (reinforced ABS)	1.4–3.1		0.35	18.5–51
Gneiss	53–79		0.267	
Ceramic (Al_2O_3)	200–400		0.23	600–5500

impact events than high fidelity finite element simulations as only quantities such as the contact forces and contact areas as functions of penetration depth are calculated. In contrast to the single degree of freedom employed by these models, high-fidelity finite element models of the same phenomena can require up to millions of degrees of freedom to ensure a convergent response.

4.2.7 Material Parameters: Some Values

Since the Contact Mechanics approach relies on the knowledge of material parameters, it may be useful to recall few typical numerical figures, see Table 4.1. It is out of the question to provide an accurate and complete set of data, which can be found in specialized reports for a great number of materials.[36] Our objective is just to easy the life of nonspecialists readers in Control, Robotics, Multibody, who would like to quickly access to realistic data for simulations. Hardness is also often considered as a material parameter, that may be found in materials descriptions. Values for the apple fruits are taken from [346].

[36] http://www-mdp.eng.cam.ac.uk/web/library/enginfo/cueddatabooks/materials.pdf.

4.3 Impacts with Friction

In Sect. 4.2.5 we have seen how Hertz' contact theory may be extended to incorporate frictional effects, using sophisticated contact theories like Mindlin–Deresiewicz. In this part we focus on rigid body models for impacts with Coulomb's friction between two bodies, where the three basic CoRs (kinematic, kinetic, energetic) may be used combined with tangential models. The main discrepancy with respect to compliant contact/impact models, is that we will not integrate second order differential equations during the impact. Of course, the values for restitution coefficient as in (2.10), (2.11), (2.12), (4.46), (4.48), (4.49), (4.50), (4.51), (4.55) or (4.66) may be used in the rigid body context if the required parameters are available. Pioneering results on this topic may be found in [327, 337, 994, 1049], see also [995, Chap. 10] for a thorough treatment of shocks with or without friction, in two- and three-dimensional cases, using graphical tools (some are described in Sect. 4.3.13). It has been the topic of an active research area, after Brach noticed that unrealistic solutions may occur with an improper treatment of the tangential impulse and Kane's example [641, 642] on energetical inconsistencies in some impact problems based on Whittaker's method [1265] and Newton's coefficient, when there is slip reversal at the impact, i.e., the final and initial relative tangential velocity have opposite signs; see for instance [106, 112, 119, 173, 174, 176, 178, 651, 815, 1116, 1121, 1122, 1148, 1149, 1151, 1153, 1254, 1255]. Notice that such energy gains are at first sight surprising since both models (rebound with a kinematic restitution coefficient and Coulomb's friction) are dissipative when considered separately. This phenomenon is actually due to an approximation of the friction law at the impulse level.

4.3.1 Simple Examples

Let us start with some classical examples of impacts of simple bodies with a rough anvil. As usual positions are assumed to be continuous at the impacts, while velocities undergo a jump (see Chap. 1 for the mathematical justification).

4.3.1.1 Two-Dimensional Sphere/Plane Impact

Let us consider a sphere with radius r colliding a rigid rough barrier as in Fig. 4.12a. The Galilean frame and the local frame $(A, \mathbf{n}, \mathbf{t}_1, \mathbf{t}_2)$ are chosen such that $\mathbf{n} = (1, 0, 0)^T, \mathbf{t}_1 = (0, 1, 0)^T, \mathbf{t}_2 = (0, 0, 1)^T$. Since we analyze the system at an impact time and the system is planar, we may choose the local frame so that one tangent unit vector, say $\mathbf{t}_1$, matches with the preimpact tangent velocity orientation, and we denote for simplicity in the plane $(A, \mathbf{n}, \mathbf{t}_1)$: $\mathbf{n} = (1, 0)^T$ and $\mathbf{t}_1 = (0, 1)^T$ the normal and tangential unit vectors at the contact point A. The normal and tangential components of the velocity of the contact point A are denoted as v_n and v_t, the angular velocity

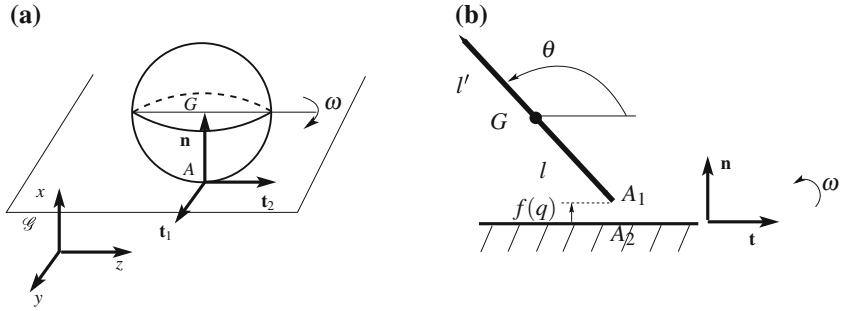

Fig. 4.12 Sphere/plane and rod/plane impacts

component along $\mathbf{t}_2$ as ω, i.e., $\Omega = \omega \mathbf{t}_2$, x and y are the gravity center coordinates, $I = \frac{2}{5}mr^2$ is the sphere moment of inertia along the z axis spanned by $\mathbf{t}_2$. One has $v_\mathrm{t} = \dot{y} - r\omega$[37] and $v_\mathrm{n} = \dot{x}$. We also assume that due to the particular form of the angular velocity Ω the postimpact tangent velocity is colinear to the preimpact one, and we can work in the plane $(A, \mathbf{n}, \mathbf{t}_1)$ (the velocity component $\dot{z}$ remains null). This is not true for general three-dimensional collisions. Let $r > 0$, then the shock dynamical equations are

$$\begin{cases} m\sigma_{\dot{x}}(t_k) = p_\mathrm{n}(t_k) \\ m\sigma_{\dot{y}}(t_k) = p_\mathrm{t}(t_k) \\ I\sigma_\omega(t_k) = -rp_\mathrm{t}(t_k) \end{cases} \iff \begin{cases} m\sigma_{v_\mathrm{n}}(t_k) = p_\mathrm{n}(t_k) \\ m\sigma_{v_\mathrm{t}}(t_k) = \frac{7}{2}p_\mathrm{t}(t_k) \\ \frac{2}{5}mr^2\sigma_\omega(t_k) = -rp_\mathrm{t}(t_k). \end{cases} \tag{4.68}$$

This may be calculated from (4.27) and (4.28). To this we have to add the normal restitution law: $v_\mathrm{n}(t_k^+) = -e_\mathrm{n}v_\mathrm{n}(t_k^-)$ if $v_\mathrm{n}(t_k^-) \leq 0$ and $x(t_k) = r$ (the gap function is equal to $f(q) = x - r \geq 0$), and a tangential contact force model:

$$p_\mathrm{t}(t_k) \in -\mu|p_\mathrm{n}(t_k)|\mathrm{sgn}(\tilde{v}_\mathrm{t}) \tag{4.69}$$

for some $\tilde{v}_\mathrm{t}$ to be chosen, and $\mathrm{sgn}(\cdot)$ is the set-valued signum function (notice that this implies that $P = (p_\mathrm{t}, p_\mathrm{n})^T$ is in the friction cone). Here we assume that $p_\mathrm{n}(t_k) \geq 0$, this may be guaranteed by imposing complementarity conditions at a time of impact: $0 \leq v_\mathrm{n}(t_k^+) + e_\mathrm{n}v_\mathrm{n}(t_k^-) \perp p_\mathrm{n}(t_k) \geq 0$.[38] Using the impact dynamics one finds $0 \leq \frac{1}{m}p_\mathrm{n}(t_k) + (1 + e_\mathrm{n})v_\mathrm{n}(t_k^-) \perp p_\mathrm{n}(t_k) \geq 0$. One may check by inspection that provided $e_\mathrm{n} > 0$, then $v_\mathrm{n}(t_k^-) < 0 \Rightarrow v_\mathrm{n}(t_k^+)) = -e_\mathrm{n}v_\mathrm{n}(t_k^-) > 0$ and $p_\mathrm{n}(t_k) = -m(1 + e_\mathrm{n})v_\mathrm{n}(t_k^-) > 0$, while $v_\mathrm{n}(t_k^-) \geq 0 \Rightarrow p_\mathrm{n}(t_k) = 0$ and $v_\mathrm{n}(t_k^+) = v_\mathrm{n}(t_k^-)$. Inserting this into (4.68), we rewrite the dynamics at an impact time as:

[37] With respect to the notations of Sect. 4.1.2, we set here $r = r_{21}$ in the matrix R_1.

[38] We will see this kind of formulation in a broader context in Sect. 5.2.2.5.

$$\begin{cases} m\sigma_{v_n}(t_k) = -m(1+e_n)v_n(t_k^-) \\ m\sigma_{v_t}(t_k) \in \frac{7}{2}\mu m(1+e_n)v_n(t_k^-)\mathrm{sgn}(\tilde{v}_t) \\ \frac{2}{5}mr^2\sigma_\omega(t_k) \in -r\mu m(1+e_n)v_n(t_k^-)\mathrm{sgn}(\tilde{v}_t). \end{cases} \tag{4.70}$$

Proposition 4.2 *Consider the impact dynamics in (4.70), and assume that* $\tilde{v}_t = \tilde{v}_t(v_t(t_k^+))$ *is a strictly monotone continuous function of* $v_t(t_k^+)$*. Then the postimpact tangential velocity is given as the unique solution of the generalized equation:*

$$0 \in \tilde{v}_t(v_t(t_k^+)) + N_{[v_t(t_k^-)-\beta, v_t(t_k^-)+\beta]}(v_t(t_k^+)), \tag{4.71}$$

where $\beta \triangleq -\frac{7}{2}\mu(1+e_n)v_n(t_k^-) > 0$.

Proof we have $-v_t(t_k^+) + v_t(t_k^-) \in \beta\mathrm{sgn}(\tilde{v}_t(v_t(t_k^+))$, that is equivalent using (B.16) to $\tilde{v}_t(v_t(t_k^+) \in N_{[-\beta,\beta]}(-v_t(t_k^+) + v_t(t_k^-))$. Let $g(v_t(t_k^+)) \triangleq \psi_{[v_t(t_k^-)-\beta, v_t(t_k^-)+\beta]}(v_t(t_k^+))$ one finds $\psi_{[-\beta,\beta]}(-v_t(t_k^+) + v_t(t_k^-)) = g(v_t(t_k^+))$, and from Theorem B.2 we have $\partial g(v_t(t_k^+)) = -N_{[v_t(t_k^-)-\beta, v_t(t_k^+)+\beta]}(v_t(t_k^+))$. The result follows from [385, Theorem 2.3.3, Corollary 2.2.5] since $[v_t(t_k^-) - \beta, v_t(t_k^-) + \beta]$ is compact convex and $\tilde{v}(\cdot)$ is continuous.

We note that the continuity of $\tilde{v}_t(v_t(t_k^+))$ is enough for the existence of a solution. The strict monotonicity assures the uniqueness.

Corollary 4.1 *Let* $\tilde{v}_t(v_t(t_k^+))=v_t(t_k^+)$*, then* $v_t(t_k^+) = v_t(t_k^-) - \mathrm{proj}([-\beta, \beta]; v_t(t_k^-))$.

Proof From (4.71) equivalently $(-v_t(t_k^+) + v_t(t_k^-)) - v_t(t_k^-) \in -N_{[-\beta,\beta]}(-v_t(t_k^+) + v_t(t_k^-))$, using (B.20) the result follows.

We infer that when $\tilde{v}_t(v_t(t_k^+)) = v_t(t_k^+)$ (recall that by assumption $v_n(t_k^-) \le 0$)

1. If $|v_t(t_k^-)| \le -\frac{7}{2}\mu(1+e_n)v_n(t_k^-)$, then $v_t(t_k^+) = 0$ (sticking impact).
2. If $v_t(t_k^-) < \frac{7}{2}\mu(1+e_n)v_n(t_k^-) < 0$, then $v_t(t_k^+) = v_t(t_k^-) - \frac{7}{2}\mu(1+e_n)v_n(t_k^-) < 0$ (negative sliding impact).
3. If $v_t(t_k^-) > -\frac{7}{2}\mu(1+e_n)v_n(t_k^-) > 0$, then $v_t(t_k^+) = v_t(t_k^-) + \frac{7}{2}\mu(1+e_n)v_n(t_k^-) > 0$ (positive sliding impact).

The post- and preimpact tangential velocities have the same sign in the sliding mode, which means that the tangential velocity cannot be reversed in such an impact with this model.

Corollary 4.2 *In the case of sticking, the postimpact angular velocity is given by* $\omega(t_k^+) = \omega^- - \frac{5}{7r}v_t(t_k^-)$.

Proof We have from (4.70) and setting $v_t(t_k^+) = 0$ that the selection $\xi \in \mathrm{sgn}(v_t(t_k^+))$ is equal to $\xi = \frac{2}{7\mu(1+e_n)}\frac{v_t(t_k^-)}{|v_n(t_k^-)|}$. Thus $\omega(t_k^+) = \omega(t_k^-) - \frac{5}{2}\frac{\mu}{r}(1+e_n)v_n(t_k^-)\xi$.

We employ on purpose the word "selection" for the set-valued sign function. Contrarily to what one might think, despite the fact that the right-hand side of the third equation in (4.70) is set-valued at $v_{\mathrm{t}}(t_k^+) = 0$, the selection inside $[-1, 1]$ is unique. Let us now pass to the dissipativity of the impact law. The kinetic energy of the system is $T(\dot{x}, \dot{y}, \omega) = \frac{1}{2}m\dot{x}^2 + \frac{1}{2}m\dot{y}^2 + \frac{1}{2}I\omega^2$, which gives $T(v_{\mathrm{n}}, v_{\mathrm{t}}, \omega) = \frac{1}{2}m(v_{\mathrm{t}} + r\omega)^2 + \frac{1}{2}mv_{\mathrm{n}}^2 + \frac{1}{2}I\omega^2$. After some easy but lengthy calculations, one finds

$$T_L(t_k) = -\frac{1}{2}m(1+e_{\mathrm{n}})(v_{\mathrm{n}}(t_k^-))^2 \left\{(1-e_{\mathrm{n}}) + 2\mu\frac{v_{\mathrm{t}}(t_k^-)}{v_{\mathrm{n}}(t_k^-)}\xi + \frac{7}{2}\mu^2(1+e_{\mathrm{n}})\xi^2\right\} \tag{4.72}$$

with $\xi \in \mathrm{sgn}(\tilde{v}_{\mathrm{t}})$ ($\Rightarrow \xi^2 = 1$ in sliding mode), and we recall that $r > 0$.

Corollary 4.3 *Let* $\tilde{v}_{\mathrm{t}}(v_{\mathrm{t}}(t_k^+)) = v_{\mathrm{t}}(t_k^+)$ *and* $e_{\mathrm{n}} \in [0, 1]$, *then* $T_L(t_k) \leq 0$.

Proof In case of sliding, the conclusion follows since $\mathrm{sgn}(v_{\mathrm{t}}(t_k^+)) = \mathrm{sgn}(v_{\mathrm{t}}(t_k^-))$, hence the term between brackets in (4.72) is always nonnegative. In case of sticking mode, there always exist a selection $\xi \in [-1, 1]$ with the right sign such that the term between brackets is nonnegative as well.

In the sticking mode, the existence of a selection ξ means the existence of an impulse inside the friction cone, see (4.69). Consider items 1, 2, 3 after Corollary 4.1. We may rewrite them as follows:

1. If $\frac{|v_{\mathrm{t}}(t_k^-)|}{|v_{\mathrm{n}}(t_k^-)|} \leq \frac{7}{2}\mu(1+e_{\mathrm{n}})$, then $v_{\mathrm{t}}(t_k^+) = 0$ (sticking impact).
2. If $\frac{v_{\mathrm{t}}(t_k^-)}{|v_{\mathrm{n}}(t_k^-)|} < -\frac{7}{2}\mu(1+e_{\mathrm{n}}) < 0$, then $\frac{v_{\mathrm{t}}(t_k^+)}{|v_{\mathrm{n}}(t_k^+)|} = \frac{1}{e_{\mathrm{n}}}\frac{v_{\mathrm{t}}(t_k^-)}{|v_{\mathrm{n}}(t_k^-)|} + \frac{7}{2}\mu\frac{1+e_{\mathrm{n}}}{e_{\mathrm{n}}}$ (negative sliding impact).
3. If $\frac{v_{\mathrm{t}}(t_k^-)}{|v_{\mathrm{n}}(t_k^-)|} > \frac{7}{2}\mu(1+e_{\mathrm{n}})$, then $\frac{v_{\mathrm{t}}(t_k^+)}{|v_{\mathrm{n}}(t_k^+)|} = \frac{1}{e_{\mathrm{n}}}\frac{v_{\mathrm{t}}(t_k^-)}{|v_{\mathrm{n}}(t_k^-)|} - \frac{7}{2}\mu\frac{1+e_{\mathrm{n}}}{e_{\mathrm{n}}}$ (positive sliding impact).

The interest for this equivalent rewriting, is that it relates the incidence (preimpact) angle defined as $\tan(\gamma^-) \triangleq \frac{v_{\mathrm{t}}(t_k^-)}{|v_{\mathrm{n}}(t_k^-)|}$ to the postimpact angle $\tan(\gamma^+) \triangleq \frac{v_{\mathrm{t}}(t_k^+)}{|v_{\mathrm{n}}(t_k^+)|}$. Examining this relationship proves that the choice $\tilde{v}_{\mathrm{t}} = v_{\mathrm{t}}(t_k^+)$ is to be too simplistic and cannot match experimental data, see a discussion on this point in Sect. 4.3.3.1. Indeed for small incidence angles γ^-, the impact sticks and the graph $(\tan(\gamma^-), \tan(\gamma^+))$ starts with a null slope, while experiments show that it should start with a negative slope. Notice that $\tilde{v}_{\mathrm{t}}(\cdot)$ may be changed to any function of $v_{\mathrm{t}}(t_k^+)$ provided the conditions for existence/uniqueness and dissipativity are still satisfied. However adding parameters with no clear physical may not always be wanted. Let us try $\tilde{v}_{\mathrm{t}} = v_{\mathrm{t}}(t_k^+) + e_{\mathrm{t}}v_{\mathrm{t}}(t_k^-)$ for some tangential restitution coefficient e_{t}. Redoing the above calculations we obtain

$$v_{\mathrm{t}}(t_k^+) = \mathrm{proj}([v_{\mathrm{t}}(t_k^-) - \beta, v_{\mathrm{t}}(t_k^-) + \beta]; -e_{\mathrm{t}}v_{\mathrm{t}}(t_k^-)), \tag{4.73}$$

so that:

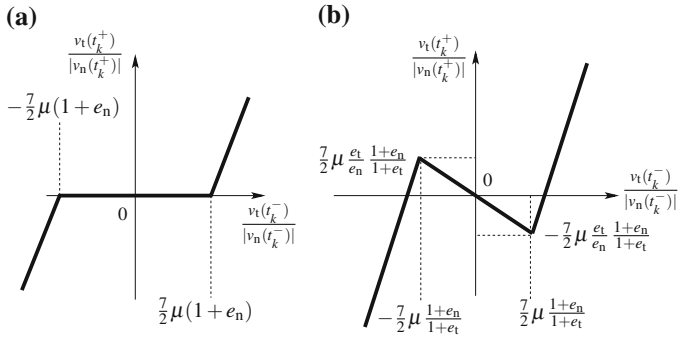

Fig. 4.13 Pre- and postimpact angles relationships: **a** $\tilde{v}_t = v_t(t_k^+)$, **b** $\tilde{v}_t = v_t(t_k^+) + e_t v_t(t_k^-)$

1. If $\frac{|v_t(t_k^-)|}{|v_n(t_k^-)|} \leq \frac{7}{2}\mu\frac{1+e_n}{1+e_t}$, then $v_t(t_k^+) = -e_t v_t(t_k^-)$.
2. $\frac{v_t(t_k^-)}{|v_n(t_k^-)|} < -\frac{7}{2}\mu\frac{1+e_n}{1+e_t}$ (< 0), then $\frac{v_t(t_k^+)}{|v_n(t_k^+)|} = \frac{1}{e_n}\frac{v_t(t_k^-)}{|v_n(t_k^-)|} + \frac{7}{2}\mu\frac{1+e_n}{e_n}$, and $v_t(t_k^+) < 0$.
3. $\frac{v_t(t_k^-)}{|v_n(t_k^-)|} > \frac{7}{2}\mu\frac{1+e_n}{1+e_t}$ (> 0), then $\frac{v_t(t_k^+)}{|v_n(t_k^+)|} = \frac{1}{e_n}\frac{v_t(t_k^-)}{|v_n(t_k^-)|} - \frac{7}{2}\mu\frac{1+e_n}{e_n}$, and $v_t(t_k^+) > 0$.

The two graphs are depicted in Fig. 4.13, with $e_t > 0$. The graph in Fig. 4.13b fits well with the experimental data in [829, Fig. 1], though a finer examination of [828, Fig. 2] reveals that the tangent at the origin should vanish to better model the microslip phase. This is obtained with the more sophisticated but numerically less tractable, models of Sect. 4.2.5. The first case now corresponds to a kind of "average" sticking over the impact with $v_t(t_k^+) + e_t v_t(t_k^-) = 0$. It may also be interpreted as a crude model for a phase of microslip phenomena (see Sect. 4.2.5), before gross slip may occur. The first impact law involves two parameters e_n and μ, the second one involves three parameters e_n, e_t, and μ; since it is "richer," it may model more mechanical effects. It is noteworthy that in modes 2 and 3 there is no tangential velocity reversal.

Remark 4.10 It is sometimes set $v_t(t_k^+) = -e_t v_t(t_k^-)$, see Sect. 4.3.2. In such a case we get from the shock dynamics $p_t(t_k) = -\frac{2}{7}m(1+e_t)v_t(t_k^-)$, while $\frac{v_t(t_k^+)}{v_n(t_k^-)} = -e_t\frac{v_t(t_k^-)}{v_n(t_k^-)} - \frac{7}{2}\mu(1+e_n)$ in sliding regime and $\frac{v_t(t_k^+)}{v_n(t_k^-)} = -(1+e_t)\frac{v_t(t_k^-)}{v_n(t_k^-)}$ in sticking regime [352]. Transitions between stick and slip occur at $\frac{v_t(t_k^-)}{v_n(t_k^-)} = \pm\frac{7}{2}\mu(1+e_n)$. This is different from the above model which takes its roots in Coulomb's friction.

The next step is to check the energetical constraint. In the first mode ("average sticking") we get

$$\begin{aligned} T_L(t_k) = {} & \tfrac{1}{2}m v_n(t_k^-)^2 \left\{ e_n^2 - 1 + (e_t^2 - 1)\left(\frac{v_t(t_k^-)}{v_n(t_k^-)}\right)^2 \right\} \\ & - \tfrac{5}{14}m v_n(t_k^-)^2 - mr\omega(t_k^-)e_t|v_n(t_k^-)|\frac{v_t(t_k^-)}{|v_n(t_k^-)|}. \end{aligned} \tag{4.74}$$

When $e_t = 0$ we are back to the first case and $T_L(t_k) \leq 0$ for all e_n and $e_t \in [-1, 1]$. For the case of a particle $r = 0$ and $T_L(t_k) \leq 0$ for all e_n and $e_t \in [-1, 1]$. If $\omega(t_k^-)v_t(t_k^-) \geq 0$, the last term in (4.74) is always nonpositive. Equivalently, since the tangential restitution reverses the tangential velocity, $\omega(t_k^-)v_t(t_k^+) \leq 0$. This means that if $v_t(t_k^+) > 0$ then the sphere should rotate initially negatively (see the frames in Fig. 4.12a), i.e., the angular velocity contributes positively in $v_t = \dot{y} - r\omega$. And if $v_t(t_k^+) < 0$ the angular velocity should contribute negatively in $v_t = \dot{y} - r\omega$ with $\omega > 0$. It seems therefore relatively easy to find conditions that yield kinetic energy gain, if no restrictions are put on the restitution and friction coefficients. In the mode 2, we obtain:

$$\begin{aligned} T_L(t_k) \leq \tfrac{1}{2}mv_n(t_k^-)^2 \left\{ \tfrac{49}{4} \tfrac{(e_t-1)(1+e_n)^2\mu^2}{e_t+1} + e_n^2 - 1 \right\} \\ -\tfrac{35}{2}m\mu^2(1+e_n)^2 v_n(t_k^-)^2 \tfrac{7+3e_t}{4(1+e_t)}, \end{aligned} \tag{4.75}$$

and a similar expression for mode 3. We see that $T_L(t_k) \leq 0$ for $e_n \in [-1, 1]$ and $e_t \leq 1$ (however, dissipation may hold for other choices of the coefficients: nothing tells us from (4.75) that e_n has to be in this interval). We infer that the choice $\tilde{v}_t = v_t(t_k^+) + e_t v_t(t_k^-)$ is dissipative for a large choice of the restitution coefficients.

Remark 4.11 It is of interest for some applications [314] to investigate whether or not the above choices for $\tilde{v}_t$ allow one to model observed phenomena like sign reversal of $\dot{y}(t_k^-)$ and $\omega(t_k^-)$. For instance, is it possible to get $\dot{y}(t_k^-) > 0$, $\omega(t_k^-) < 0$, and $\dot{y}(t_k^+) < 0$, $\omega(t_k^+) > 0$? We note also that positive as well as negative tangential coefficient restitution are reported in [314]. Let us consider $\tilde{v}_t = v_t(t_k^+)$ and denote $\tan(\beta^+) = \frac{\dot{y}(t_k^+)}{|v_n(t_k^+)|}$ and $\tan(\beta^-) = \frac{\dot{y}(t_k^-)}{|v_n(t_k^-)|}$ the rebound and incidence angles, respectively (see Fig. 4.14a). If $|v_t(t_k^-)| > \frac{7}{2}\mu(1+e_n)|v_n(t_k^-)|$, then $\tan(\beta^+) = \frac{1}{e_n}\tan(\beta^-) - \mu\frac{1+e_n}{e_n}\mathrm{sgn}(v_t(t_k^+))$. If $|v_t(t_k^-)| \leq \frac{7}{2}\mu(1+e_n)|v_n(t_k^-)|$, we are in a sticking

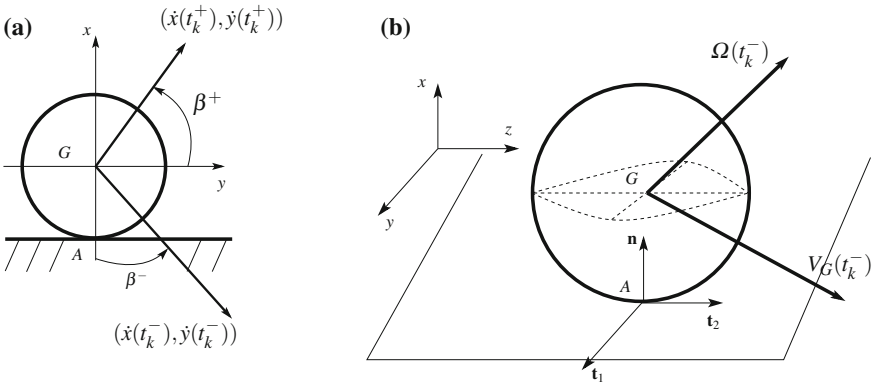

Fig. 4.14 2-D and 3-D spheres

mode and $\tan(\beta^+) = \frac{1}{e_\mathrm{n}}\tan(\beta^-) - \frac{2}{7e_\mathrm{n}}\frac{v_\mathrm{t}(t_k^-)}{|v_\mathrm{n}(t_k^-)|}$, where the selection ξ is calculated from $m\sigma_{v_\mathrm{t}}(t_k) = -mv_\mathrm{t}(t_k^-) = -\frac{7}{2}m\mu(1+e_\mathrm{n})|v_\mathrm{n}(t_k^-)|\xi$. In the latter case, $\tan(\beta^+) \leq \frac{1}{e_\mathrm{n}}\tan(\beta^-) - \mu\frac{1+e_\mathrm{n}}{e_\mathrm{n}}$. Take for instance $\beta^- = \frac{\pi}{4}$, $e_\mathrm{n} = 1$, and $\mu = 0.7$, then $\tan(\beta^+) \leq -0.4$; the sphere rebounds backward.

The three-dimensional sphere/anvil impact with a preimpact angular velocity $\Omega = \omega_\mathrm{n}\mathbf{n} + \omega_{\mathrm{t}_1}\mathbf{t}_1 + \omega_{\mathrm{t}_2}\mathbf{t}_2$ is more involved. In particular the tangential velocity may not only reverse, but change its direction during the shock.

4.3.1.2 Three-Dimensional Sphere/Plane Impact

Let us consider a generalization of the above case, as depicted in Fig. 4.14b. The Galilean frame axis and the local frame axis at the impact time, are chosen equal: $\mathbf{i} = \mathbf{n}$, $\mathbf{j} = \mathbf{t}_1$, $\mathbf{k} = \mathbf{t}_2$. The twist is given by $\mathscr{T}(t_k^-) = \begin{bmatrix} \Omega(t_k^-) \\ V_G(t_k^-) \end{bmatrix}_G = \begin{bmatrix} \Omega(t_k^-) \\ V_G(t_k^-) + AG \times \Omega(t_k^-) \end{bmatrix}_A$, $AG = r\mathbf{n} = r\mathbf{i}$, $\Omega(t_k^-) = \omega_\mathrm{n}(t_k^-)\mathbf{n} + \omega_{\mathrm{t}_1}(t_k^-)\mathbf{t}_1 + \omega_{\mathrm{t}_2}(t_k^-)\mathbf{t}_2$, $V_A = (\dot{x}, \dot{y} - r\omega_{\mathrm{t}_2}, \dot{z} + r\omega_{\mathrm{t}_1})^T = (v_\mathrm{n}, v_{\mathrm{t}_1}, v_{\mathrm{t}_2})^T$. The wrench is $\mathscr{W}(t_k) = \begin{bmatrix} F_A(t_k) \\ 0 \end{bmatrix}_A = \begin{bmatrix} F_A(t_k) \\ GA \times F_A(t_k) \end{bmatrix}_G$, $GA = -r\mathbf{n}$, $GA \times F_A = rF_{\mathrm{t}_2}\mathbf{t}_2 - rF_{\mathrm{t}_1}\mathbf{t}_1$. The inertia tensor is equal to $\mathrm{diag}(I)$, $I = \frac{2}{5}mr^2$. The unilateral constraint is $f(q) = x - r \geq 0$. The shock dynamics is therefore given as:

$$\begin{cases} m\sigma_{\dot{x}}(t_k) = m\sigma_{v_\mathrm{n}}(t_k) = p_\mathrm{n}(t_k) \\ m\sigma_{\dot{y}}(t_k) = p_{\mathrm{t}_1}(t_k) \\ m\sigma_{\dot{z}}(t_k) = p_{\mathrm{t}_2}(t_k) \end{cases} \quad \begin{cases} I\sigma_{\omega_\mathrm{n}}(t_k) = 0 \\ I\sigma_{\omega_{\mathrm{t}_1}}(t_k) = rp_{\mathrm{t}_2}(t_k) \\ I\sigma_{\omega_{\mathrm{t}_2}}(t_k) = -rp_{\mathrm{t}_1}(t_k). \end{cases} \tag{4.76}$$

Using Newton's restitution law and the kinematics, we deduce

$$\begin{cases} \sigma_{v_\mathrm{n}}(t_k) = -(1+e_\mathrm{n})v_\mathrm{n}(t_k^-) \\ \sigma_{v_{\mathrm{t}1}}(t_k) = \frac{I+mr^2}{mI}p_{\mathrm{t}_1}(t_k) \\ \sigma_{v_{\mathrm{t}_2}}(t_k) = \frac{I+mr^2}{mI}p_{\mathrm{t}_2}(t_k) \end{cases} \quad \begin{cases} I\sigma_{\omega_\mathrm{n}}(t_k) = 0 \\ \sigma_{\omega_{\mathrm{t}1}}(t_k) = \frac{r}{I}p_{\mathrm{t}_2}(t_k) \\ \sigma_{\omega_{\mathrm{t}_2}}(t_k) = -\frac{r}{I}p_{\mathrm{t}_1}(t_k). \end{cases} \tag{4.77}$$

The first set of equalities shows that sphere/plane collisions have decoupled normal and tangential effects (in the terminology of [106, 107] they are *balanced collisions*, see Sect. 4.3.5.6).We now have to formulate three-dimensional Coulomb's friction at the impulse level. To this aim we rely on the material of Sect. 5.3, taking some advance. Let us start with De Saxcé's formulation (Sect. 5.3.3) which states that (here we state it at the impulse level):

$$\tilde{v}_{\mathrm{t}_1}\mathbf{t}_1 + \tilde{v}_{\mathrm{t}_2}\mathbf{t}_2 + (\tilde{v}_\mathrm{n} + \mu||\tilde{v}_\mathrm{t}||)\mathbf{n} \in -N_{\mathscr{C}}(P), \tag{4.78}$$

where $\mathscr{C} = \{P = (p_{\mathrm{t}}^T, p_{\mathrm{n}})^T \mid ||p_{\mathrm{t}}|| \leq \mu p_{\mathrm{n}}\}$ is the convex friction cone, and $\tilde{v}_{\mathrm{t}}$ has to be chosen. Recall that $N_{\mathscr{C}}(P)$ is the normal cone to the cone $\mathscr{C}$, computed at P. Using now (B.19), we can rewrite (4.78) equivalently as

$$P \in -N_{\mathscr{C}^\star} \begin{pmatrix} \tilde{v}_{\mathrm{t}_1} \\ \tilde{v}_{\mathrm{t}_2} \\ \tilde{v}_{\mathrm{n}} + \mu ||\tilde{v}_{\mathrm{t}}|| \end{pmatrix} \tag{4.79}$$

and as the cone complementarity problem:

$$\mathscr{C}^\star \ni (\tilde{v}_{\mathrm{t}_1}, \tilde{v}_{\mathrm{t}_2}, \tilde{v}_{\mathrm{n}} + \mu ||\tilde{v}_{\mathrm{t}}||)^T \perp (p_{\mathrm{t}_1}, p_{\mathrm{t}_2}, p_{\mathrm{n}})^T \in \mathscr{C}. \tag{4.80}$$

An important discrepancy compared with the case of sliding motion, is that we can set $\tilde{v}_{\mathrm{n}}(t_k) = v_{\mathrm{n}}(t_k^+) + e_{\mathrm{n}} v_{\mathrm{n}}(t_k^-)$, which is Newton's restitution law. Hence stated, the friction law at the impulse level is equivalent to (we drop the argument t_k):

1. If $\tilde{v}_{\mathrm{t}} = 0$ then $||p_{\mathrm{t}}|| \leq \mu p_{\mathrm{n}}$ ("sticking").
2. If $\tilde{v}_{\mathrm{t}} \neq 0$ then $p_{\mathrm{t}} = -\mu p_{\mathrm{n}} \frac{\tilde{v}_{\mathrm{t}}}{||\tilde{v}_{\mathrm{t}}||}$ ("sliding").
3. $0 \leq p_{\mathrm{n}} \perp \tilde{v}_{\mathrm{n}} \geq 0$.

Recall that the normal complementarity problem can be rewritten using the collision dynamics as the Linear Complementarity Problem $0 \leq v_{\mathrm{n}}(t_k^+) - v_{\mathrm{n}}(t_k^-) \perp v_{\mathrm{n}}(t_k^+) + e_{\mathrm{n}} v_{\mathrm{n}}(t_k^-) \geq 0$, whose solution is $v_{\mathrm{n}}(t_k^+) = v_{\mathrm{n}}(t_k^-)$ if $v_{\mathrm{n}}(t_k^-) \geq 0$, while $v_{\mathrm{n}}(t_k^+) = -e_{\mathrm{n}} v_{\mathrm{n}}(t_k^-)$ if $v_{\mathrm{n}}(t_k^-) < 0$. Taking this into account, $p_{\mathrm{n}}(t_k)$ and $v_{\mathrm{n}}(t_k^+)$ are no longer unknowns of the impact problem.

Now at an impact we can write $p_{\mathrm{t}}(t_k) = \mu m(1 + e_{\mathrm{n}}) v_{\mathrm{n}}(t_k^-) \frac{\tilde{v}_{\mathrm{t}}(t_k)}{||\tilde{v}_{\mathrm{t}}(t_k)||}$, which results in $v_{\mathrm{t}_i}(t_k^+) = v_{\mathrm{t}_i}(t_k^-) + \frac{7}{2m} \mu (1 + e_{\mathrm{n}}) m v_{\mathrm{n}}(t_k^-) \frac{\tilde{v}_{\mathrm{t}_i}(t_k)}{||\tilde{v}_{\mathrm{t}_i}||}$, $i = 1, 2$. If we denote $\tilde{\phi}$ the angle such that $\cos(\tilde{\phi}) = \frac{\tilde{v}_{\mathrm{t}_1}}{||\tilde{v}_{\mathrm{t}_1}||}$ and $\sin(\tilde{\phi}) = \frac{\tilde{v}_{\mathrm{t}_2}}{||\tilde{v}_{\mathrm{t}_2}||}$, then $v_{\mathrm{t}_1}(t_k^+) = v_{\mathrm{t}_1}(t_k^-) + \frac{7}{2} \mu (1 + e_{\mathrm{n}}) m v_{\mathrm{n}}(t_k^-) \cos(\tilde{\phi})$ and $v_{\mathrm{t}_2}(t_k^+) = v_{\mathrm{t}_2}(t_k^-) + \frac{7}{2} \mu (1 + e_{\mathrm{n}}) m v_{\mathrm{n}}(t_k^-) \sin(\tilde{\phi})$. Let us now see how we may derive a generalized equation for the tangential velocity, similar to the one we obtained in the two-dimensional case. Suppose that $\tilde{v}_{\mathrm{t}} = v_{\mathrm{t}}(t_k^+) + \mathscr{E}_{\mathrm{t}} v_{\mathrm{t}}(t_k^-)$. Since $\tilde{v}_{\mathrm{n}} = 0$ we obtain from (4.78):

$$\begin{pmatrix} v_{\mathrm{t}}(t_k^+) + \mathscr{E}_{\mathrm{t}} v_{\mathrm{t}}(t_k^-) \\ \mu ||v_{\mathrm{t}}(t_k^+) + \mathscr{E}_{\mathrm{t}} v_{\mathrm{t}}(t_k^-)|| \end{pmatrix} \in -N_{\mathscr{C}} \begin{pmatrix} \frac{2m}{7}(v_{\mathrm{t}}(t_k^+) - v_{\mathrm{t}}(t_k^-)) \\ -(1 + e_{\mathrm{n}}) m v_{\mathrm{n}}(t_k^-) \end{pmatrix}. \tag{4.81}$$

It is noteworthy that the knowledge of $v_{\mathrm{n}}(t_k^-)$ implies the knowledge *via* Newton's restitution law of $p_{\mathrm{n}}(t_k)$ and hence of Coulomb's disk in Fig. 4.15 (see Sect. 5.3.2). It is therefore convenient to take advantage of this, and to rewrite $-\tilde{v}_{\mathrm{t}} \in \partial \psi_{\mathscr{D}(p_{\mathrm{n}})}(p_{\mathrm{t}}(t_k))$, equivalently $p_{\mathrm{t}}(t_k) \in \partial \psi^\star_{\mathscr{D}(p_{\mathrm{n}})}(-\tilde{v}_{\mathrm{t}})$, where the conjugate function of the indicator function is given by $\psi^\star_{\mathscr{D}(p_{\mathrm{n}})}(\cdot) = \mu p_{\mathrm{n}}(t_k) || \cdot ||$. Here the Coulomb's disk is $\mathscr{D}(p_{\mathrm{n}}(t_k)) = \{p_{\mathrm{t}} \in \mathbb{R}^2 | \sqrt{p_{\mathrm{t}}^T p_{\mathrm{t}}} \leq \mu (1 + e_{\mathrm{n}}) m |v_{\mathrm{n}}(t_k^-)|\}$. We get:

$$v_{\mathrm{t}}(t_k^+) + \mathscr{E}_{\mathrm{t}} v_{\mathrm{t}}(t_k^-) \in -N_{\mathscr{D}(p_{\mathrm{n}}(t_k))} \left(\frac{2}{7}(v_{\mathrm{t}}(t_k^+) - v_{\mathrm{t}}(t_k^-)) \right), \tag{4.82}$$

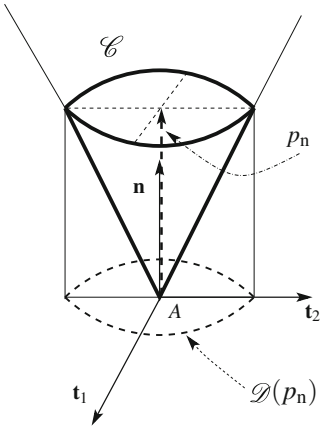

Fig. 4.15 Coulomb's disk

from which we infer that:

$$v_{\mathrm{t}}(t_k^+) = v_{\mathrm{t}}(t_k^-) + \frac{7}{2m}\mathrm{proj}[\mathscr{D}(p_{\mathrm{n}}(t_k)); -\frac{2m}{7}(I_2 + \mathscr{E}_{\mathrm{t}})\, v_{\mathrm{t}}(t_k^-)]. \tag{4.83}$$

This means that the postimpact tangential velocity can be computed by solving a quadratic program with convex constraints, which certainly is a nice feature for numerical simulations. The two-dimensional case can be recovered from (4.83) as a special case. The impulse $p_{\mathrm{t}}(t_k)$ is obtained from the collision dynamics, as well as $\sigma_{\omega_{\mathrm{t}1}}(t_k)$ and $\sigma_{\omega_{\mathrm{t}2}}(t_k)$. Let $\mathscr{E}_{\mathrm{t}} = 0$, then the sticking mode, (i.e., $v_{\mathrm{t}}(t_k^+) = 0$) occurs if and only if $||v_{\mathrm{t}}(t_k^-)|| \leq \frac{7}{2}\mu(1 + e_{\mathrm{n}})|v_{\mathrm{n}}(t_k^-)|$. Let us now pass to the analysis of the kinetic energy loss at the impact time. The kinetic energy is given by $T(V_G, \Omega) = \frac{1}{2}mV_G^T V_G + \frac{1}{2}\Omega^T \mathscr{I}\Omega$, where $\mathscr{I} = \mathrm{diag}(\frac{2}{5}mr^2) \in \mathbb{R}^{3\times 3}$. After some calculations we obtain the following:

$$T_L(t_k) = \frac{1}{2}p_{\mathrm{n}}(t_k)(v_{\mathrm{n}}(t_k^+) + v_{\mathrm{n}}(t_k^-)) + \frac{1}{2}p_{\mathrm{t}}(t_k)^T(v_{\mathrm{t}}(t_k^+) + v_{\mathrm{t}}(t_k^-)) \tag{4.84}$$

with $v_{\mathrm{t}} = v_{\mathrm{t}1}\mathbf{t}_1 + v_{\mathrm{t}2}\mathbf{t}_2$. Notice that if $\mu = 0$ then $p_{\mathrm{t}}(t_k) = 0$ while both $v_{\mathrm{t}}(\cdot)$ and $\Omega(\cdot)$ are continuous at t_k, and $T_L(t_k) = \frac{1}{2}p_{\mathrm{n}}(t_k)(v_{\mathrm{n}}(t_k^+) + v_{\mathrm{n}}(t_k^-))$: we recover the Thomson and Tait formula in (4.184). Starting from (4.84) we state the following:

Proposition 4.3 *Assume that the mappings* $v_{\mathrm{n}}(t_k^+) + v_{\mathrm{n}}(t_k^-) \to -p_{\mathrm{n}}(t_k)$ *and* $v_{\mathrm{t}}(t_k^+) + v_{\mathrm{t}}(t_k^-) \to -p_{\mathrm{t}}(t_k)$ *are monotone. Then* $T_L(t_k) \leq 0$.

Indeed the monotonicity implies that $p_{\mathrm{n}}(t_k)(v_{\mathrm{n}}(t_k^+) + v_{\mathrm{n}}(t_k^-)) \leq 0$ and $p_{\mathrm{t}}(t_k)^T(v_{\mathrm{t}}(t_k^+) + v_{\mathrm{t}}(t_k^-)) \leq 0$. Using Newton's restitution law one gets $p_{\mathrm{n}}(t_k) \geq 0$ and $v_{\mathrm{n}}(t_k^+) + v_{\mathrm{n}}(t_k^-) = (1 - e_{\mathrm{n}})v_{\mathrm{n}}(t_k^-) \leq 0$ for all $e_{\mathrm{n}} \in [0, 1]$, thus Newton's law guarantees the monotonicity of the above mapping. Suppose that $\mathscr{E}_{\mathrm{t}} = I_2$, and that $\tilde{v}_{\mathrm{t}} \neq 0$ (the "sliding" mode), then the monotonicity of the second mapping is guaranteed as

well. It is noteworthy that imposing such conditions yields energy consistency in all tangential modes.

4.3.1.3 Disk/Plane Impact

If the sphere is replaced by a disk with radius $r > 0$, the moment of inertia is changed to $I = \frac{mr^2}{2}$. The impact dynamics in (4.68) becomes:

$$\begin{cases} m\sigma_{v_{\rm n}}(t_k) = p_{\rm n}(t_k) \\ m\sigma_{v_{\rm t}}(t_k) = \left(1 + \frac{mr^2}{I}\right) p_{\rm t}(t_k) = 3p_{\rm t}(t_k) \\ I\sigma_{\omega}(t_k) = -rp_{\rm t}(t_k). \end{cases} \tag{4.85}$$

The kinetic energy loss is given by:

$$T_L(t_k) = \frac{1}{2} m(1+e_{\rm n})(v_{\rm n}(t_k^-))^2 \left\{ e_{\rm n} - 1 - 2\mu \frac{v_{\rm t}(t_k^-)}{v_{\rm n}(t_k^-)} \xi - \frac{I + mr^2}{I} \mu^2 (1+e_{\rm n}) \xi^2 \right\} \tag{4.86}$$

with $\xi \in \text{sgn}(\tilde{v}_{\rm t})$. The constant β in the generalized equation of Proposition 4.2 has also to be adapted accordingly. The conclusions are the same as for the two-dimensional sphere.

4.3.1.4 Particle/Plane Impact

In this case there is no rotational effect, so that the third equation in the left-hand side of (4.68) disappears. The generalized equation of Proposition 4.2 becomes $v_{\rm t}(t_k^+) - v_{\rm t}(t_k^-) \in -\mu(1+e_{\rm n}) v_{\rm n}(t_k^-) \text{sgn}(\tilde{v}_{\rm t}(v_{\rm t}(t_k^+)))$. The kinetic energy loss is:

$$T_L(t_k) = -\frac{1}{2} m(1+e_{\rm n})(v_{\rm n}(t_k^-))^2 \left\{ 1 - e_{\rm n} - \mu^2 (1+e_{\rm n}) \xi - 2\mu \frac{v_{\rm t}(t_k^-)}{v_{\rm n}(t_k^-)} \right\} \tag{4.87}$$

with $\xi \in \text{sgn}(\tilde{v}_{\rm t})$. If $\tilde{v}_{\rm t}(v_{\rm t}(t_k^+)) = v_{\rm t}(t_k^+)$ or $\tilde{v}_{\rm t}(v_{\rm t}(t_k^+)) = v_{\rm t}(t_k^+) + e_{\rm t} v_{\rm t}(t_k^-)$ then the above analysis are led in a similar way.

4.3.1.5 Rigid Rod/Plane Impact

Let us now consider a rigid rod with mass m that collides an anvil as in Fig. 4.12b. The dynamics involves tangential/normal couplings, which render the analysis far more involved (this fact will be encountered again in Sects. 5.5 and 5.6). The objective of this section is to illustrate this fact. The rod's tip has radius zero and its moment of inertia at G is $I = \frac{mL^2}{12}$ with $L = l + l'$, and $q = (x, y, \theta)^T$. The unilateral constraint is $f(q) = y - l\sin(\theta) \geq 0$. The impact dynamics is given by:

$$\begin{cases} m\sigma_{\dot{x}}(t_k) = p_{\mathrm{t}}(t_k) \\ m\sigma_{\dot{y}}(t_k) = p_{\mathrm{n}}(t_k) \\ I\sigma_{\dot{\theta}}(t_k) = -l\cos(\theta(t_k))p_{\mathrm{n}}(t_k) + l\sin(\theta(t_k))p_{\mathrm{t}}(t_k). \end{cases} \tag{4.88}$$

We have $v_{\mathrm{t}} = \dot{x} + l\sin(\theta)\omega$ and $v_{\mathrm{n}} = \dot{y} - l\cos(\theta)\omega$, $\omega = \dot{\theta}$. After some calculations one arrives at

$$\begin{cases} \sigma_{v_{\mathrm{t}}}(t_k) = -\frac{l^2}{I}\sin(\theta(t_k))\cos(\theta(t_k))p_{\mathrm{n}}(t_k) + \left(\frac{1}{m} + \frac{l^2}{I}\sin(\theta(t_k))^2\right)p_{\mathrm{t}}(t_k) \\ \sigma_{v_{\mathrm{n}}}(t_k) = \left(\frac{1}{m} + \frac{l^2}{I}\cos(\theta(t_k))^2\right)p_{\mathrm{n}}(t_k) - \frac{l^2}{I}\sin(\theta(t_k))\cos(\theta(t_k))p_{\mathrm{t}}(t_k) \\ \sigma_{\dot{\theta}}(t_k) = -\frac{l\cos(\theta(t_k))}{I}p_{\mathrm{n}}(t_k) + \frac{l\sin(\theta(t_k))}{I}p_{\mathrm{t}}(t_k). \end{cases} \tag{4.89}$$

The restitution law $v_{\mathrm{n}}(t_k^-) = -e_{\mathrm{n}}v_{\mathrm{n}}(t_k^-)$ and the tangential model in (4.69) yield:

$$p_{\mathrm{n}}(t_k) = \frac{-mI(1+e_{\mathrm{n}})v_{\mathrm{n}}(t_k^-)}{I + ml^2\cos(\theta(t_k))^2 + ml^2\sin(\theta(t_k))\cos(\theta(t_k))\mu\xi} \tag{4.90}$$

with $\xi \in \mathrm{sgn}(\tilde{v}_{\mathrm{t}})$. A novelty appears here, that is a kinetic constraint $p_{\mathrm{n}}(t_k) \geq 0$ which is not automatically guaranteed.

Lemma 4.1 *Let $v_{\mathrm{n}}(t_k^-) < 0$ and (4.69) hold. Let $\theta \in (0, \frac{\pi}{2})$ (resp. $\theta \in (\frac{\pi}{2}, \pi)$). (i) If $\xi > 0$ (resp. $\xi < 0$) then $p_{\mathrm{n}(t_k)}$ in (4.90) is positive for any $\mu \geq 0$. (ii) If $\xi < 0$ (resp. $\xi > 0$), then $p_{\mathrm{n}}(t_k)$ in (4.90) is positive if and only if $\mu < \frac{I+ml^2\cos(\theta(t_k))^2}{-ml^2\sin(\theta(t_k))\cos(\theta(t_k))\xi}$. (iii) If $\xi \in [-1, 1]$, there exists a $\xi^* \in [-1, 1]$ such that $p_{\mathrm{n}}(t_k) \geq 0$. (iv) If $\mu < \mu_{\max}(\theta(t_k)) \stackrel{\Delta}{=} \frac{I+ml^2\cos(\theta(t_k))^2}{ml^2\sin(\theta(t_k))|\cos(\theta(t_k))|}$ then $p_{\mathrm{n}}(t_k) > 0$.*

The fourth condition is sufficient only, hence it may be conservative. Item (iii) means that there exists an impulse inside the friction cone such that the kinetic constraint is satisfied. Obviously when $\theta = \frac{\pi}{2}$ friction plays no role, from (4.89) the normal and tangential effects are decoupled. Suppose that $\tilde{v}_{\mathrm{t}}(v_{\mathrm{t}}(t_k^+)) = v_{\mathrm{t}}(t_k^+)$, then $\xi < 0$ means that $\xi = -1$, so $v_{\mathrm{t}}(t_k^+) < 0$; the rod is pulled toward the left in Fig. 4.12. While $\xi > 0$ means $\xi = 1$, so $v_{\mathrm{t}}(t_k^+) > 0$, the rod is pushed toward the right. Everyday-life experiments show that pulling is easier than pushing. We note that when $l = l'$ and $\theta \in (0, \frac{\pi}{2})$ then $\mu_{\max}(\theta(t_k)) = \frac{1+3\cos(\theta(t_k))^2}{3\sin(\theta(t_k))\cos(\theta(t_k))}$. Proceeding as in Sect. 4.3.1.1, we set the following.

Proposition 4.4 *Let (4.69) hold. Then $v_{\mathrm{t}}(t_k^+)$ is the solution of the generalized equation*[39]*:*

$$A(\theta)v_{\mathrm{t}}(t_k^+) + B(\theta)sgn(\tilde{v}_{\mathrm{t}})v_{\mathrm{t}}(t_k^+) + C(\theta) \in -(1 + D(\theta))sgn(\tilde{v}_{\mathrm{t}}) \tag{4.91}$$

where we have $A(\theta) = \frac{I+ml^2\cos(\theta)^2}{-\mu(I+ml^2\sin(\theta)^2)(1+e_{\mathrm{n}})v_{\mathrm{n}}(t_k^-)}$, $B(\theta) = \frac{-ml^2\sin(\theta)\cos(\theta)}{(I+ml^2\sin(\theta)^2)(1+e_{\mathrm{n}})v_{\mathrm{n}}(t_k^-)}$, $C(\theta) = \frac{(I+ml^2\cos(\theta)^2)v_{\mathrm{t}}(t_k^-)}{\mu(I+ml^2\sin(\theta)^2)(1+e_{\mathrm{n}})v_{\mathrm{n}}(t_k^-)} + \frac{ml^2\sin(\theta)\cos(\theta)}{\mu(I+ml^2\sin(\theta)^2)}$, $D(\theta) = \frac{ml^2\sin(\theta)\cos(\theta)v_{\mathrm{t}}(t_k^-)}{(I+ml^2\sin(\theta)^2)(1+e_{\mathrm{n}})v_{\mathrm{n}}(t_k^-)}$.

[39] The argument t_k is dropped in θ.

We have $A(\theta) > 0$, $B(\theta) > 0$, $C(\theta)$ and $D(\theta)$ depend on the ratio $\frac{v_t(t_k^-)}{v_n(t_k^-)}$. Let $\tilde{v}_t(v_t(t_k^+)) = v_t(t_k^+)$, then we obtain the generalized equation

$$A(\theta(t_k))v_t(t_k^+) + B(\theta(t_k))|v_t(t_k^+)| + C(\theta(t_k)) \in -(1 + D(\theta))\text{sgn}(v_t(t_k^+)) \quad (4.92)$$

whose left-hand side is continuous, single-valued piecewise-linear function of $v_t(t_k^+)$, while the right-hand side is set-valued. The solution is unique if the two graphs have a unique intersection. The analysis of the generalized equation $ax + b|x| + c \in -(1 + d)\text{sgn}(x)$ is necessary. The objective is to calculate the conditions such that the intersection between the graph of the single-valued mapping $x \mapsto ax + b|x| + c$ and the graph of the set-valued mapping $x \mapsto -(1 + d)\text{sgn}(x)$, exists and is unique. This may be done in this simple case by inspection. Let us use however some general tools from variational inequalities, as we did in the proof of Proposition 4.2. Let us first assume that $a + b > 0$, $a - b > 0$, $1 + d > 0$. Let $g(x) \stackrel{\Delta}{=} (1 + d)\text{sgn}(x)$. Then its conjugate function is $g^\star(y) = N_{[-(1+d),1+d]}(y)$. Let us now invert $f(x) = ax + b|x| + c$ as $x = h(y) = \frac{y-c}{a+b}$ if $y \geq c$ and $x = h(y) = \frac{y-c}{a-b}$ if $y \leq c$. Then using (B.16) we obtain the equivalent generalized equation

$$\begin{gathered} 0 \in h(y) + N_{[-(1+d),1+d]}(y) \\ \Updownarrow \\ \text{Find } y \in [-(1 + d), 1 + d] \text{ such that } \langle h(y), z - y\rangle \geq 0 \text{ for all } z \in [-(1 + d), 1 + d] \end{gathered} \quad (4.93)$$

which is a standard form of generalized equations and variational inequalities [385, Definition 1.1.1, Eq. (1.1.3)]. This is depicted in Fig. 4.16 (see Fig.5.22 in Chap. 5 for a similar graphical analysis of another generalized equation). Clearly there is a unique solution y^* whatever the value of c, a conclusion we could get from [385, Theorem 2.3.3] from the fact that the mapping $h(y)$ is continuous and strictly monotone (showing in passing that we could consider more general mappings, relying on [385,

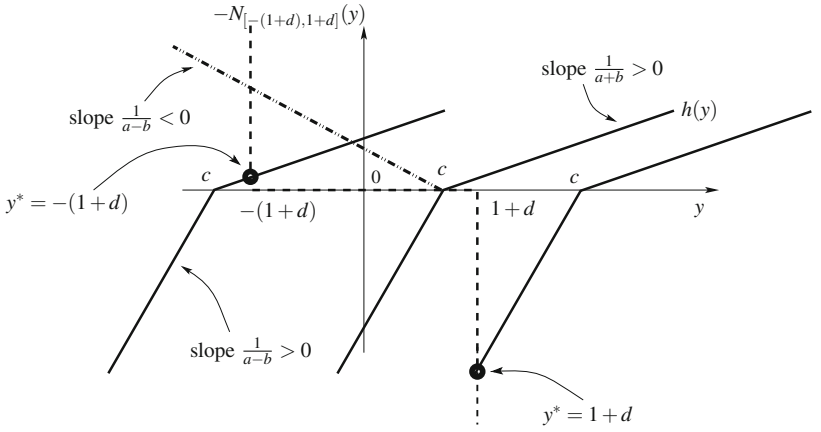

Fig. 4.16 Generalized equation $0 \in h(y) + N_{[-(1+d),1+d]}(y)$

Corollary 2.2.5, Theorem 2.3.3] for existence/uniqueness conditions). If $y^* > c$ then $x^* = \frac{y^*-c}{a+b} > 0$, if $y^* < c$ then $x^* = \frac{y^*-c}{a-b} < 0$. We may treat other cases in a similar way. If for instance $a - b < 0$ instead, then we obtain existence of solutions, but uniqueness is usually lost. Notice that $x^* = 0$ is equivalent to $y^* \in [-1-d, 1+d]$, which is in turn equivalent to $-1 - d < c < 1 + d$. This may be used to calculate conditions for sticking impact: $v_t(t_k^+) = 0$ and $\xi \in [-1, 1]$ (which means that $p = (p_t, p_n)^T$ may lie anywhere inside the friction cone). Now if $c > 1 + d$, we get $y^* = 1 + d$ so $y^* < c$ and $x^* = \frac{y^*-c}{a-b} = \frac{1+d-c}{a-b} < 0$, while if $c < -(1 + d)$, we get $y^* = -(1 + d) < 0$ so $y^* > c$ and $x^* = \frac{y^*-c}{a+b} = \frac{-1-d-c}{a+b} > 0$.

Proposition 4.5 *Let* $\theta \in (0, \frac{\pi}{2})$, $0 \le \mu < \mu_{\max}$, $l = l' (\Rightarrow I = \frac{ml^2}{3})$ *and* $\tilde{v}_t = v_t(t_k^+)$. *Let also* $\frac{v_t(t_k^-)}{|v_n(t_k^-)|} < \mu_{\max}(\theta(t_k))$. *Then*

1. $v_t(t_k^+) = 0$ *if*

$$(1 + e_n)\frac{-3\sin(\theta)\cos(\theta) - \mu(1+3\sin(\theta)^2)}{1+3\cos(\theta)^2+3\mu\cos(\theta)\sin(\theta)} \le \frac{v_t(t_k^-)}{v_n(t_k^-)} \le (1 + e_n)\frac{-3\sin(\theta)\cos(\theta)+\mu(1+3\sin(\theta)^2)}{1+3\cos(\theta)^2-3\mu\cos(\theta)\sin(\theta)}. \tag{4.94}$$

2. $v_t(t_k^+) < 0$ *if* $\frac{v_t(t_k^-)}{v_n(t_k^-)} > (1 + e_n)\frac{-3\sin(\theta)\cos(\theta)+\mu(1+3\sin(\theta)^2)}{1+3\cos(\theta)^2-3\mu\cos(\theta)\sin(\theta)}$.
3. $v_t(t_k^+) > 0$ *if* $\frac{v_t(t_k^-)}{v_n(t_k^-)} < (1 + e_n)\frac{-3\sin(\theta)\cos(\theta)-\mu(1+3\sin(\theta)^2)}{1+3\cos(\theta)^2+3\mu\cos(\theta)\sin(\theta)}$.

Proof The proof follows from applying $1 - D(\theta) \le C(\theta) \le 1 + D(\theta)$, then $C(\theta) > 1 + D(\theta)$, then $C(\theta) < -(1 + D(\theta)$, and noticing that $\mu < \mu_{\max} \Leftrightarrow A(\theta) > B(\theta)$, while $\frac{v_t(t_k^-)}{|v_n(t_k^-)|} < \mu_{\max}(\theta) \Leftrightarrow 1 + D(\theta) > 0$.

This shows logically that a sticking collision occurs in case the preimpact velocity of the tip is not too far from the vertical. Take $\theta = \frac{\pi}{4}$ and denote $\tan(\gamma^-) \stackrel{\Delta}{=} \frac{v_t(t_k^-)}{v_n(t_k^-)}$, then we obtain $(1 + e_n)\frac{-3-5\mu}{5+3\mu} \le \tan(\gamma^-) \le (1 + e_n)\frac{-3+5\mu}{5-3\mu}$, under $0 < \mu < \mu_{\max} = \frac{5}{3}$. For instance for $\mu = \frac{1}{2}$ and $e_n = 0$ we obtain $-1 \le \tan(\gamma^-) \le 1$ (see Fig. 4.17a). On the contrary sliding collisions with $v_t(t_k^+) \ne 0$ occur when the preimpact velocity is "horizontal enough". Here two comments arise: first, we should check whether the various conditions in Proposition 4.5 are compatible (it may be that for some $\theta(t_k)$ and some μ some of the three regimes do not exist); second, we should also analyze the case when the generalized equation (4.92) has more than one solution, because it is possible that the complete problem, including energy constraints, nevertheless has a unique solution. Therefore we propose here only a partial analysis of the whole problem.

Remark 4.12 In the frictionless case $\mu = 0$, one obtains multiplying both sides of (4.92) by μ, or directly from (4.89) and (4.90) that

$$v_t(t_k^+) = v_t(t_k^-) + \frac{ml^2\sin(\theta(t_k))\cos(\theta(t_k))}{I + ml^2\cos(\theta(t_k))^2}(1 + e_n)v_n(t_k^-) \tag{4.95}$$

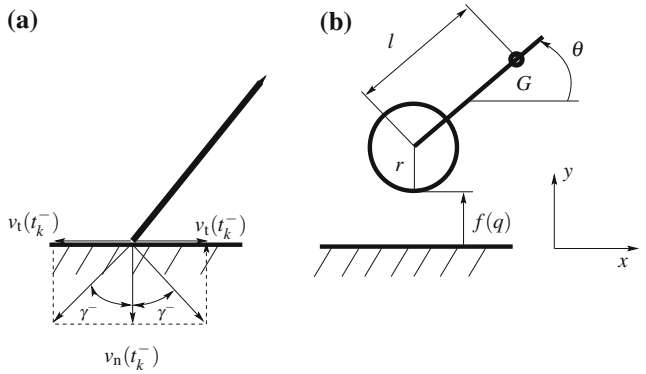

Fig. 4.17 **a** Sticking impact, **b** rod with rounded tip

which shows normal/tangental couplings effects. This is also compatible with (4.94): $v_t(t_k^+) = 0 \Leftrightarrow \frac{v_t(t_k^-)}{v_n(t_k^-)} = -(1+e_n)\frac{3\sin(\theta(t_k))\cos(\theta(t_k))}{1+3\sin(\theta(t_k))^2}$.

Let us now pass to the analysis of the kinetic energy loss $T_L(t_k)$. Let $l = l'$. After calculations we get

$$\begin{aligned} T_L(t_k) &= \tfrac{1}{2}p_t(t_k)[v_t(t_k^+) + v_t(t_k^-)] + \tfrac{1}{2}p_n(t_k)[v_n(t_k^+) + v_n(t_k^-)] \\ &= \tfrac{1}{2}p_n(t_k)\left\{-\mu\xi[v_t(t_k^+) + v_t(t_k^-)] + (1-e_n)v_n(t_k^-)\right\}. \end{aligned} \tag{4.96}$$

This expression is the Thomson and Tait formula (see Sect. 4.3.12) with friction. Developing more

$$\begin{aligned} T_L(t_k) &= p_t(t_k)v_t(t_k^-) + p_n(t_k)v_n(t_k^-) + \tfrac{3}{m}\sin(\theta(t_k))\cos(\theta(t_k))p_t(t_k)p_n(t_k) \\ &\quad + \tfrac{1}{2m}(1+3\sin(\theta(t_k))^2)p_t(t_k)^2 + \tfrac{1}{2m}(1+3\cos(\theta(t_k))^2)p_n(t_k)^2 \\ &= \tfrac{m}{2}(e_n^2-1)(v_n(t_k^-))^2 \\ &\quad + \left(\tfrac{3}{2}\sin(\theta(t_k))\cos(\theta(t_k))p_n(t_k) + (1+3\sin(\theta(t_k))^2)p_t(t_k)\right)(v_t(t_k^+) + v_t(t_k^-)) \\ &\quad + 2l[\cos(\theta(t_k))p_n(t_k) + \sin(\theta(t_k))p_t(t_k)](\dot\theta(t_k^+) + \dot\theta(t_k^-)), \end{aligned} \tag{4.97}$$

with $p_n(t_k) = \frac{-m(1+e_n)v_n(t_k^-)}{1+3\cos(\theta(t_k))^2+3\sin(\theta(t_k))\cos(\theta(t_k))\mu\xi}$, $p_t(t_k) = -\mu p_n\xi$, $v_t(t_k^+) + v_t(t_k^-) = 2v_t(t_k^-) + \frac{3}{m}\sin(\theta(t_k))\cos(\theta(t_k))p_n(t_k) + \frac{1}{m}(1+3\sin(\theta(t_k))^2)p_t(t_k)$, $\dot\theta(t_k^+) + \dot\theta(t_k^-) = 2\dot\theta(t_k^-) + \frac{3}{ml}\cos(\theta(t_k))p_n(t_k) + \frac{3}{ml}\sin(\theta(t_k))p_t(t_k)$, $\xi \in \mathrm{sgn}(v_t(t_k^+))$.

Proposition 4.6 (Sticking impact) *Let the conditions of Proposition 4.5 hold,* $v_n(t_k^-) < 0$ *and* $e_n \in [0,1)$. *Then there exists an impulse* $P = (p_t, p_n)^T$ *inside the friction cone (equivalently there exists* $\xi \in [-1,1]$*) such that* $T_L(t_k) \le 0$.

Proof The proof uses (4.96), which simplifies in the sticking impact case to $T_L(t_k) = \frac{1}{2}p_t(t_k)v_t(t_k^-) + \frac{1}{2}p_n(t_k)(1-e_n)v_n(t_k^-)$, consequently $T_L(t_k) = \frac{1}{2}p_n(t_k)[(e_n -$

$1)|v_{\rm n}(t_k^-)| - \mu v_{\rm t}(t_k^-)\xi]$. For ξ small enough (precisely it has to satisfy $-\mu v_{\rm t}(t_k^-)\xi < (1-e_{\rm n})|v_{\rm n}(t_k^-)|$) , the term between brackets can always be made negative.

If $\mu = 0$ the expression in (4.97) simplifies to

$$T_L(t_k) = \frac{1}{2}\frac{m(e_{\rm n}^2-1)(v_{\rm n}(t_k^-))^2}{1+3\cos(\theta(t_k))^2}, \tag{4.98}$$

which is nonpositive for all $e_{\rm n} \in [0,1]$. The kinetic energy loss is the same as for a particle, however with an equivalent mass $\frac{m}{1+3\cos(\theta(t_k))^2}$. This is different from what shall be exposed in Sect. 4.3.10.2, where it is the CoR that will vary depending on the angle. It may be a rather cumbersome task to analyze the conditions that yield dissipativity with $\mu > 0$, i.e., $T_L(t_k) \leq 0$, when $v_{\rm t}(t_k^+) \neq 0$.[40] Here we may nevertheless use the second expression in (4.96) which helps us to prove the following.

Proposition 4.7 *Let a collision occur at t_k, i.e., $v_{\rm n}(t_k^-) < 0$, $e_{\rm n} \in [0,1]$, and assume that $p_{\rm n}(t_k) > 0$. (i) Let $\tilde{v}_{\rm t} = v_{\rm t}(t_k^+)$. If there is no tangential velocity reversal, then $T_L(t_k) < 0$. (ii) If $\tilde{v}_{\rm t} = v_{\rm t}(t_k^+) + v_{\rm t}(t_k^-)$, then $T_L(t_k) < 0$.*

Proof (i) No velocity reversal means that $v_{\rm t}(t_k^-) > 0 \Rightarrow v_{\rm t}(t_k^+) > 0$ and $v_{\rm t}(t_k^-) < 0 \Rightarrow v_{\rm t}(t_k^+) < 0$. Since $\xi = {\rm sgn}(v_{\rm t}(t_k^+)$, the result follows. (ii) We get $\xi[v_{\rm t}(t_k^+) + v_{\rm t}(t_k^-)] = |v_{\rm t}(t_k^+) + v_{\rm t}(t_k^-)| > 0$, which proves the dissipation.

The slight modification of $\tilde{v}_{\rm t}$ allows to take into account a kind of average impact velocity, which has better dissipativity properties than using only the postimpact velocity (a purely implicit definition). The choice $\tilde{v}_{\rm t}(t_k) = v_{\rm t}(t_k^+) + v_{\rm t}(t_k^-)$ is made in [416, Chap. 4], who treats the falling-rod problem in great details. Case (ii) encompasses both sticking and sliding impacts. We see from Proposition 4.5 that the pre- and postimpact tangential velocities may not always have the same sign, so applying $\tilde{v}_{\rm t}(t_k) = v_{\rm t}(t_k^+)$ may not always be energetically consistent.

$\rightsquigarrow$ *The planar collision of a rigid rod with a rough rigid anvil, yields surprizingly complex postimpact existence and uniqueness, and kinetic energy loss analysis, compared with the foregoing examples. This is due to normal/tangential couplings, which are not met in the foregoing examples.*

To summarize, the rod/plane impact problem boils down to solve the following problem: given $(v_{\rm n}(t_k^-), v_{\rm t}(t_k^-))$, $\mu > 0$, $e_{\rm n}$, find a unique $(v_{\rm n}(t_k^+), v_{\rm t}(t_k^+))$ such that: $p_{\rm n}(t_k) \geq 0$ (kinetic constraint), $T_L(t_k) \leq 0$ (energetic constraint), $v_{\rm n}(t_k^+) \geq 0$ (kinematic constraint, normal restitution), $v_{\rm t}(t_k^+)$ is a solution of the generalized equation (4.91), and $p_{\rm t}(t_k) \in -\mu p_{\rm n}(t_k){\rm sgn}(\tilde{v}_{\rm t})$ (tangential model). But, an impact law that satisfies all these requirements may still need to be improved in order to have good predictability properties; they are just necessary. Such constraints appear to be universal in any collision problem (single or multiple impacts).

[40] This is the reason which motivates the development of general modeling frameworks, which guarantee a priori energetical consistency.

Remark 4.13 The value $\mu_{\max}(\theta(t_k))$ in Lemma 4.1 is usually too large to be of practical importance (for instance let $\theta(t_k) = \frac{\pi}{4}$ and $l = l'$, then $\mu_{\max}(\pi/4) = \frac{5}{3}$). Let us however slightly modify the rod's tip with a rounded tip of radius $r > 0$ (see Fig. 4.17b). The unilateral constraint is now $f(q) = y - r - l\sin(\theta) \geq 0$, and from Varignon's formula one finds $v_{\mathrm{t}} = \dot{x} + (r + l\sin(\theta))\dot{\theta}$, $v_{\mathrm{n}} = \dot{y} - l\dot{\theta}\cos(\theta)$. After some calculations, we obtain

$$\begin{cases} \sigma_{v_{\mathrm{t}}}(t_k) = \frac{I+m(r+l\sin(\theta)^2)}{mI} p_{\mathrm{t}}(t_k) - \frac{l(r+l\sin(\theta))\cos(\theta)}{I} p_{\mathrm{n}}(t_k) \\ \sigma_{v_{\mathrm{n}}}(t_k) = \frac{I+m(r+l\cos(\theta)^2)}{mI} p_{\mathrm{n}}(t_k) - \frac{l(r+l\sin(\theta))\cos(\theta)}{I} p_{\mathrm{t}}(t_k). \end{cases} \tag{4.99}$$

It follows that $p_{\mathrm{n}}(t_k) = \frac{-(1+e_{\mathrm{n}})mI v_{\mathrm{n}}(t_k^-)}{I+ml^2\cos(\theta(t_k))^2+ml\cos(\theta(t_k))(r+l\sin(\theta(t_k)))\mu\xi}$. Therefore $p_{\mathrm{n}}(t_k) \geq 0$ for all ξ is equivalent to $\mu < \mu_{\max} = \frac{I+ml^2\cos(\theta(t_k)^2}{ml\cos(\theta(t_k))(r+l\sin(\theta(t_k)))}$, and simplifying $\mu_{\max} = \frac{(1+3\cos(\theta(t_k))^2)l}{3\cos(\theta(t_k))(r+l\sin(\theta(t_k)))}$. Consider $\theta(t_k) = \frac{\pi}{4}$. Then $\mu_{\max} = \frac{5l}{3\sqrt{2}r+3l}$. For $r = 10l$ we get $\mu_{\max} \approx 0.110$, for $r = 3l$ we get $\mu_{\max} \approx 0.31$.

Such issues are quite similar to what will be described in Sect. 5.6 *on Painlevé paradoxes in sliding motion. The rounded tip case shows that they can occur for arbitrarily small coefficients of friction, and that the contact geometry plays a crucial role. Thus, pretending that these "paradoxes" are of purely theoretical interest, is wrong. The other, important comment, is about the validity of the used contact model that yields such singularities.*

4.3.2 Kinematic CoR: Brach's Method

Brach deals in [173–175, 178] with the planar and three-dimensional cases, and derives T_L as a nonlinear (second order polynomial) function of Newton's coefficient e_{n}, and of an equivalent coefficient of friction or impulse ratio μ. In the two-dimensional case, this ratio is defined as $\mu \triangleq \frac{p_{\mathrm{t}}}{p_{\mathrm{n}}}$, where p_{t} and p_{n} are the tangential and normal impulses respectively at the contact point, i.e., $p_{\mathrm{n}} = p_{i,\mathrm{n}}$ and $p_{\mathrm{t}} = p_{i,\mathrm{t}_1}$, where it is assumed that the axis are chosen such that $p_{i,\mathrm{t}_2} = 0$. Let us denote here the coefficient of friction as f, then $\mu = -f\xi$ where $\xi \in \mathrm{sgn}(\tilde{v}_{\mathrm{t}})$ (notations of the previous sections). In the more general three-dimensional case [174, 175], the impulse on body i is $P_i = p_{i,\mathrm{n}}\mathbf{n} + p_{i,\mathrm{t}_1}\mathbf{t}_1 + p_{i,\mathrm{t}_2}\mathbf{t}_2$. It is then possible to define 2 ratios μ_1 and μ_2 such that $P_i = p_{i,\mathrm{n}}(\mathbf{n} + \mu_1\mathbf{t}_1 + \mu_2\mathbf{t}_2)$ (recall that from the law of mutual actions one has $P_1 = -P_2$, i.e., $p_{1,\mathrm{n}} = -p_{2,\mathrm{n}}$, $p_{1,\mathrm{t}_1} = -p_{2,\mathrm{t}_1}$, $p_{1,\mathrm{t}_2} = -p_{2,\mathrm{t}_2}$). For the case of two particles moving in a plane and colliding with friction, the starting point of the analysis is [173, 469]

$$T_L(t_k) = \frac{1}{2}\frac{m_1 m_2}{m_1 + m_2}\left(v_{r,\mathrm{n}}(t_k^-)\right)^2(1+e_{\mathrm{n}})\left[(e_{\mathrm{n}} - 1) + 2\mu\alpha + (1 + e_{\mathrm{n}})\mu^2\right], \tag{4.100}$$

where $\alpha = \frac{v_{1,\mathrm{t}_1}(t_k^-) - v_{2,\mathrm{t}_1}(t_k^-)}{v_{r,\mathrm{n}}(t_k^-)}$. It is supposed that $v_{i,\mathrm{t}_2}(t_k^-) = 0$, i.e., the initial tangential velocity is along $\mathbf{t}_1$ (more exactly, the local frame at the contact point is chosen such that $\mathbf{t}_2$ is normal to the common plane in which the two particles evolve). The expression in (4.100) is similar to (4.72), using the ratio μ instead of Coulomb's law. More complex collisions are treated like the rod/plane or rod/sphere impacts, with the corresponding expressions of T_L [175, Chaps. 5, 6].

Remark 4.14 (Friction at the impulse level) Pérès [995] stated the following for impacts with dry friction

- If there is a unidirectional sliding velocity during the collision, then $\frac{p_\mathrm{t}}{p_\mathrm{n}} = \mu$. In other words, the impulse vector lies on the boundary $\mathrm{bd}(\mathscr{C})$ of the friction cone.
- If there is a change of the direction of sliding (or tangential velocity reversal), then $||p_\mathrm{t}|| \leq \mu p_\mathrm{n}$, (i.e., the impulse lies inside the friction cone, i.e., in $\mathrm{Int}(\mathscr{C})$)

This is consistent with (4.78), (4.79) and (4.80). Whittaker [1265] states that if $v_\mathrm{t}(t_k^+) = 0$ then the percussion vector $P \in \mathrm{Int}(\mathscr{C})$, whereas if $v_\mathrm{t}(t_k^+) \neq 0$ then $P \in \mathrm{bd}(\mathscr{C})$: in the planar case, this is (4.69) with $\tilde{v}_\mathrm{t} = v_\mathrm{t}(t_k^+)$; as we evidenced from the kinetic energy loss (see (4.38)), such a rule is likely to be energetically inconsistent since the mapping $-p_\mathrm{t} \mapsto v_\mathrm{t}(t_k^+) + v_\mathrm{t}(t_k^-)$ is not monotone with this choice. Kane and Levinson [642] use a similar idea but with a static and a dynamic friction coefficients (see Fig. 5.9b). Smith [1121] proposes another rule to relate tangential and normal components of the percussion vector, see Sect. 4.3.3.

Therefore Pérès' approach treats the coefficient μ similarly as a Coulomb's friction coefficient, and is different from that in [175], according to whom μ is the impulse ratio and is to be determined so that it yields $T_L(e_\mathrm{n}, \mu) \leq 0$. In a practical impact problem, one can use this criteria to check whether the set of coefficients associated a priori or after experiments to the bodies is energetically consistent [175, §5.4]; if it is not, it may signify that the coefficients are wrong, but the work in [173, 174] does not propose any method to a priori compute the value of the coefficient for a given problem [176]. Bounds on the impulse ratio are rather derived, that guarantee energetical consistency of the model; they are called *critical* values [175]. Consider now the energy loss in (4.100). As we pointed out in the introduction of this section, one might think at first sight that since both phenomena (normal process and Coulomb's friction) are dissipative, their combination model will always dissipate energy. As shown in [175, §3.4], such is not the case. For $e_\mathrm{n} \in [0, 1]$, $T_L(t_k)$ decreases when μ increases, but this is true only for $\mu \leq \mu_m = \frac{\alpha}{1+e_\mathrm{n}}$. This is simply found by setting $\frac{\partial T_L}{\partial \mu} = 0$. For two-particle collisions, this value corresponds to the value μ_0 such that the relative tangential velocity is zero at separation, (i.e., at t_k^+), and is clearly a limit value below which unidirectional slip occurs.

The determination of μ is thoroughly covered in [175, §6.3.1], where many different experimental data are analyzed. Experimental results for the determination of the impulse ratio can also be found in [1232] (impacts of steel spheres on plane surfaces made of various alloys-zinc, armco-iron, steel, high-alloyed steel of the austenitic type), [1164] (impacts of hard particles with plastic and rubber specimens), [736]

(impacts of steel spheres against a heavy steel plate, at low speeds -between 0.01 and 0.05 m/s-; the results are confirmed analytically in using a simple approximating model), [564] (impacts of hard steel spheres on mild steel target), [1166] (same experiment as in [564] but with different target materials; both led at high speeds -between 50 and 300 m/s.), [1144] (falling slender rods, but their goal was not to validate the frictional model). All those experiments concluded that the impulse ratio is roughly a constant. In [175, §6.3.1] it is shown that they fit with the model in (4.113) (4.114) below. Note that all the effects that play a role in the determination of μ are specific to the collision process, where in particular high pressure may exist at the contact point. Hence the friction models for shock processes may be quite different from those used when only sliding occurs, see, e.g., [58]. Although it has been often reported from experimental data that $\mu = \frac{p_t}{p_n}$ is constant, this may not always be the case even for very simple bodies. This may be related to the incidence angle (which is constant in [1144], the preimpact velocity being normal to the surface). In [248, 274] results that concern shocks of thin disks with heavy steel plates, and without slip reversal, show that the ratio μ can vary by a factor two. The impulse ratio value depends essentially on the incidence angle, for fairly low approach velocities (between 0.5 and 1.0 m/s), whereas the normal restitution e_n seems constant in all the reported experiments (in agreement with the results in [830, 407]). The transition from sticking to sliding without reversal is responsible for the dependence on the incidence angle. μ becomes equal to the friction coefficient (measured independently) only for grazing incidence impacts. In connection with the experimental results on slender rods in [1144], see Sect. 4.3.10, it is interesting to notice that the conclusions in [1144] are exactly the inverse ones, i.e., μ is independent of the incidence angle, whereas e_n varies with it. Therefore the type of objects that collide may induce very different variations in the shock model parameters.

Remark 4.15 As we shall see in Sect. 4.3.3.1, a natural consequence of the algebraic form of the shock dynamics is that in general the various coefficients that one may define to model the normal and tangential effects are not independent. It is clear for instance that μ and a tangential restitution coefficient e_t must be related, although they relate different quantities (velocities or impulses). See Sect. 4.3.3.1.

In the planar case [173], the value of T_L that corresponds to the sliding case $T_{L,s}$ is used, i.e., when $\alpha \neq 0$ in (4.100). Then it is argued that for $\mu < \mu_m$ (where μ_m minimizes T_L for fixed e_n) there is sliding when the bodies separate, and that $\mu \geq \mu_m$ implies equal final tangential velocities. The reasoning in [173] is the following: for $\mu < \mu_m$, the sliding hypothesis works; for $\mu = \mu_m$ the loss of energy is maximum and this is the first case when final velocities are equal, since an amount of friction tends to "slow down" the bodies; now for any additional amount of friction, the bodies stick before the end of the impact, hence it is incorrect to use $T_{L,s}$ with $\mu > \mu_m$: this last point is supported in [173] by the fact that there cannot be velocity reversal due to passivity of the frictional model, a statement that is true for colinear collisions (hence in particular point mass or particles collisions), as pointed out in [174, 1148], see also [995, Chap. 10 §21]. Recall that colinear collisions between two bodies occur when the vectors G_1A and G_2A are colinear to the common normal

to the tangent plane **n** at the contact point A (which, by the way, does not mean at all that the inertia matrix is diagonal).[41] This work is generalized in [174] to the three-dimensional case. Of particular interest is the slender rod tip impact problem, where the kinematical equations show that tangential velocity reversal occurs for small enough initial value (in general the slip process depends on the values of the coefficients, the initial velocities and the kinematics [1148]). It is assumed in [174] that $0 \leq e_{\mathrm{n}} \leq 1$ but as pointed out in [1121], it is not evident why this should be true in general contrarily to the frictionless or central impact cases where T_L implies it.[42] In fact as we shall see further Brach's method is rather useful to determine lower and upperbounds on restitution coefficients that yield a consistent impact process. In the case of general two-dimensional planar collisions, Brach [174] proposes to choose the sign of μ as the sign of the calculated value $\mu_{\max}$ that maximizes T_L when $e_{\mathrm{n}} = 0$. The impulse ratio should also be upperbounded by a critical value μ_c, i.e.,

$$|\mu| \leq |\mu_c| = \min\left[f, |\mu_0|, |\mu_T|\right], \tag{4.101}$$

where f is the Coulomb friction coefficient,[43] $\mu_0 = \mu_0(e_{\mathrm{n}})$ is the impulse ratio corresponding to zero final relative tangential velocity, and $\mu_T = \mu_T(e_{\mathrm{n}})$ is the impulse ratio such that $T_L = 0$. One has $\mu_T(1) = \mu_0(0) = \mu_{\max}$. For planar collisions between 2 bodies, the value μ_c is the maximum value that any μ may take, without violating the kinetic energy constraint $T_L \leq 0$. The method is extended in [175] to finite contact areas, with an additional moment coefficient of restitution that seems necessary to solve the impact problem (see also [173]). An interesting point in [175] is the consideration of a tangential coefficient of restitution e_{t} to account for tangential compliance when a hard object strikes a compliant surface, see [175, p. 30] (two particle shocks) and [175, pp.132–134] (planar object striking a massive surface). The need for considering such tangential compliance is pointed out for

[41] Central impacts may be defined as colinear impacts for nonrotating bodies. The two terms –central and colinear– are often used to denote the same type of collision. There are in fact three types of impacts: (i) no tangential effects, (ii) decoupled normal and tangential effects, (iii) coupled normal and tangential effects. These notions are gathered into balanced collisions defined later.

[42] This fact has been asserted sometimes: in [196] experiments with a golf ball rebounding on a corrugated inclined plate indicated values of $e_{\mathrm{n}} > 1$ and were automatically rejected. Although the calculations in [196] neglected the postimpact spin of the balls, one cannot assert that $e_{\mathrm{n}} > 1$ is impossible when there is friction. This clearly dissociates collisions with friction from frictionless or central impacts. Similarly, it has been shown [174, 500] that in some cases, T_L increases as e_{n} increases for certain friction coefficient values. It is also pointed out in [1122] an experiment that consists of a superball (a kind of ball made of rubber and that possesses a high restitution coefficient when colliding almost any rigid material, so that it rebounds very high when dropped on the ground) bonded at the end of a slender rod. When collision occurs against a rigid surface, measurements provided values of Newton's coefficient $e_{\mathrm{n}} \in [0.7, 1.4]$ depending on the initial orientation of the rod and on friction. Some experimental results on thin disks colliding a heavy steel plate [248] indicate $e_{\mathrm{n}} = 1.08$ for collisions approaching grazing incidence. It is nevertheless argued in [905] that this may have been due to rounded edges of the disks. Finite element simulations of a disk impacting a wall, with friction, indicate values $e_{\mathrm{n}} \approx 1.3$ for some incidence angles of impact [689]: this is attributed to the local deformation of the wall, while the disk is much harder.

[43] Denoted f here to avoid confusion with the impulse ratio μ.

instance in [773, 775, 1121, 1148], and has been experimentally evidenced in [407, 620, 760, 774, 829, 830], as well as in [603, 604] using sophisticated theories of elastic impacts. From our above discussion on "rigid" slippage (i.e., jumps in the tangential velocity), it seems quite natural to consider such a coefficient. This is introduced in [175, Eq. (2.28)] exactly as Newton's rule, replacing normal velocities by tangential ones. In summary, discontinuities in the tangential velocity may arise from different sources

- Inertial effects (even for frictionless constraints).
- Effects related to Coulomb's friction (or one of its extensions).
- Effects related to tangential compliance, that may be modeled through a tangential restitution.

Further generalizations for the three-dimensional case are presented in [178], not *a priori* assuming $e_{\mathrm{n}} \leq 1$ and incorporating some results in [1148]. To conclude this part, let us summarize Brach's approach [178]:

(a) Use linear and angular momenta theorems (see (4.24) and (4.31)) for rigid bodies collisions, that yield algebraic linear relationships between pre- and postimpact velocities.
(b) Use kinematic and kinetic restitution rules to complete the set of equations so that there are as many equations as unknowns.
(c) These equations provide postimpact velocities and T_L in terms of preimpact ones, inertial properties, initial conditions and coefficients, and can be used to develop bounds on the coefficients using kinematic constraints and/or work and energy conditions. Critical values μ_m, μ_0, μ_T of the impulse ratio, such that $T_L(\mu_T) = 0$, $\frac{\partial T_L}{\partial \mu}(\mu_m) = 0$ and relative tangential velocity zero for μ_0, are at the core of the treatment.
(d) The postimpact velocities and the coefficients bounds are not restricted to point contact (recall there may be rigid surface contacts), are independent of the specific nature of the contact processes, unless a contact process condition is used to establish one of the bounds.
(e) Specific contact process models can be used to relate the above general expressions (the equations, T_L and coefficients bounds) to the physical process and analytically, numerically or experimentally evaluate the coefficients. For instance Hertzian, vibrations or finite element theories [603, 604, 1335] can be used to relate T_L to the dimensions, elastic Young modulus ... and then deduce the coefficients from them.

Concerning step (a), recall that the impulse vector in (4.24) has the form:

$$P_i = (p_{i1}\ p_{i2}\ p_{i3}\ p_{i,\mathrm{n}}\ p_{i,\mathrm{t}_1}\ p_{i,\mathrm{t}_2})^T, \tag{4.102}$$

where p_{i1}, p_{i2} and p_{i3} are impulsive moments. Then from (4.24) it follows that in order to be able to calculate the postimpact velocities and all the components of P_i, (i.e., $12 + 6 = 18$ unknowns to the problem), one must add some relationships

between known values and unknown ones. One solution that comes naturally to one's spirit is to extend Newton's conjecture to all the velocities, i.e., to set:

$$\begin{cases} \omega_{11}(t_k^+) - \omega_{21}(t_k^+) = -e_{\omega,1}(\omega_{11}(t_k^-) - \omega_{21}(t_k^-)) \\ \omega_{12}(t_k^+) - \omega_{22}(t_k^+) = -e_{\omega,2}(\omega_{12}(t_k^-) - \omega_{22}(t_k^-)) \\ \omega_{13}(t_k^+) - \omega_{23}(t_k^+) = -e_{\omega,3}(\omega_{13}(t_k^-) - \omega_{23}(t_k^-)) \\ v_{r,\mathrm{n}}(t_k^+) = -e_{\mathrm{n}} v_{r,\mathrm{n}}(t_k^-) \\ v_{1,\mathrm{t}_1}(t_k^+) - v_{2,\mathrm{t}_1}(t_k^+) = e_{\mathrm{t},1}(v_{1,\mathrm{t}_1}(t_k^-) - v_{2,\mathrm{t}_1}(t_k^-)) \\ v_{1,\mathrm{t}_2}(t_k^+) - v_{2,\mathrm{t}_2}(t_k^+) = e_{\mathrm{t},2}(v_{1,\mathrm{t}_2}(t_k^-) - v_{2,\mathrm{t}_2}(t_k^-)) \end{cases} \tag{4.103}$$

which is step (b). Applying (4.103) corresponds to using a diagonal restitution matrix for the twist in (4.11), see (4.104). For instance torsional restitution is introduced in [175, §6.5] (see also [43]), motivated by experimental results in [541]. It is noteworthy that a diagonal restitution matrix is not always sufficient, see Sect. 6.2 and comments in Sect. 6.2.7 about rockfall modeling. Hence there are 12+6 equations (dynamics and restitution laws). Notice that the first three (kinematic) coefficients in (4.103) are related but not equal to the moment coefficients proposed in [175] (see the paragraph below on equivalence of coefficients). Also the $e_{\omega,i}$'s above do not have to be positive, allowing for nonreversal of the angular velocity. As we will see below the introduction of coefficients $e_{\mathrm{t},i}$ is closely related to friction. Corollary 4.2 shows that $e_{\omega,i}$ and Coulomb's friction are also related.

4.3.3 Additional Comments and Studies

Brach's approach for the treatment of rigid body impact problems has been used in [1301] to study impacts between two free-floating space kinematic chains. The impact occurs between the two end-effectors. Equations similar to (4.23), (4.24) and (4.31) can be derived using the action-reaction law. The author uses a restitution matrix (see (4.103)) to model the shock. From (4.24) and (4.102) one has $\bar{\mathbf{M}}_{A_i}(q_i(t_k))\sigma_{\tau_i}(t_k) = \begin{pmatrix} 0_{3\times 1} \\ P_i(t_k) \end{pmatrix}$, with $P_1(t_k) = -P_2(t_k)$. From (4.103) one has

$$\mathscr{T}_{A_1}(t_k^+) - \mathscr{T}_{A_2}(t_k^+) = \mathscr{E}\left(\mathscr{T}_{A_1}(t_k^-) - \mathscr{T}_{A_2}(t_k^-)\right) \tag{4.104}$$

for some restitution matrix $\mathscr{E} = \mathrm{diag}(-e_{\omega,1}, -e_{\omega,2}, -e_{\omega,3}, -e_{\mathrm{n}}, e_{\mathrm{t},1}, e_{\mathrm{t},2})$. From (4.31) one infers $\bar{\mathbf{M}}_{A_1}(q_1(t_k))\sigma_{\mathscr{T}_{A_1}}(t_k) + \bar{\mathbf{M}}_{A_2}(q_2(t_k))\sigma_{\mathscr{T}_{A_2}}(t_k) = 0$. The following equalities hold $\bar{\mathbf{M}}_{A_1}(q_1(t_k))^{-1}P_1(t_k) = \sigma_{\mathscr{T}_{A_1}}(t_k)$ and $\bar{\mathbf{M}}_{A_2}(q_2(t_k))^{-1}P_1(t_k) = -\sigma_{\mathscr{T}_{A_2}}(t_k)$, from which $\left(\bar{\mathbf{M}}_{A_1}(q_1(t_k))^{-1} + \bar{\mathbf{M}}_{A_2}(q_2(t_k))^{-1}\right)P_1(t_k) = \left(\sigma_{\mathscr{T}_{A_1}}(t_k) - \sigma_{\mathscr{T}_{A_2}}(t_k)\right)$. Hence the impulse magnitude is given by:

$$\left(\bar{\mathbf{M}}_{A_1}(q_1(t_k))^{-1} + \bar{\mathbf{M}}_{A_2}(q_2(t_k))^{-1}\right)P_1(t_k) = (\mathscr{E} - I)\left(\mathscr{T}_{A_1}(t_k^-) - \mathscr{T}_{A_2}(t_k^-)\right), \tag{4.105}$$

which is an expression sometimes used for shock dynamics of free-floating space structures [1301]. Remind from the kinetic energy expression (4.36) that the impulsive wrench has to lie in an ellipsoid $T_L(t_k) \leq 0$. We can again find an expression for $T_L(t_k)$ in which $P_1(t_k)$ appears quadratically, using material similar to that in Sect. 4.1.5.2. Other applications of rigid body shock dynamics in space structures can be found in [399, 735]. Newton's rule is also used in the study of crash phenomena (like when a train hits an obstacle) and the consequence on the motion of a passenger [362]. Experimental results confirm the analysis. Cohen and Mac Sithig [297] also used Brach's philosophy to model shocks between so-called pseudorigid bodies (in which the deformation that occurs inside the bodies is assumed to be represented by a linear field, and is homogeneous). As pointed out above, Kane and Levinson [642] modify Whittaker's method and propose to apply the following rule for impacts with Coulomb's friction

$$||P_{\mathrm{t}}|| \leq \mu_0 |p_{\mathrm{n}}|, \tag{4.106}$$

if and only if $v_{r,\mathrm{t}}(t_k^+) = 0$, and:

$$P_{\mathrm{t}} = -\mu |p_{\mathrm{n}}| \frac{v_{r,\mathrm{t}}(t_k^+)}{||v_{r,\mathrm{t}}(t_k^+)||}, \tag{4.107}$$

in case the inequality in (4.106) is not satisfied. Therefore it is conjectured that the tangential impulse $P_{\mathrm{t}} = p_{\mathrm{t}_1}\mathbf{t}_1 + p_{\mathrm{t}_2}\mathbf{t}_2$ depends only on the normal impulse $P_{\mathrm{n}} = p_{\mathrm{n}}\mathbf{n}$ and on the separation velocity (notice that $||P_{\mathrm{n}}|| = |p_{\mathrm{n}}|$, and if we make the hypothesis that $p_{\mathrm{t}_2} = 0$ from a specific choice of the local frame, then $||P_{\mathrm{t}}|| = |p_{\mathrm{t}_1}|$). Motivated by the fact that during the shock process, the tangential velocity may change its direction, Smith [1121] introduces a new definition of μ that involves an "average" of the final and initial values of $v_{r,\mathrm{t}} = (v_{1,\mathrm{t}_1} - v_{2,\mathrm{t}_1})\mathbf{t}_1 + (v_{1,\mathrm{t}_2} - v_{2,\mathrm{t}_2})\mathbf{t}_2$, i.e., μ is replaced by

$$\mu \frac{||v_{r,\mathrm{t}}(t_k^-)||v_{r,\mathrm{t}}(t_k^-) + ||v_{r,\mathrm{t}}(t_k^+)||v_r(t_k^+)}{||v_r(t_k^-)||^2 + ||v_r(t_k^+)||^2}. \tag{4.108}$$

It is then shown that $T_L(t_k) \leq 0$ for Newton's coefficient $e_{\mathrm{n}} \leq 1$ and with the impulse ratio as in (4.108). It is shown on Kane's example for a particular fixed value of μ that the new definition predicts loss of energy whereas the other one in (4.106), (4.107) predicts a gain. Note that the basic idea in [642] is to choose a definition of μ such that its sign is that of the final value of $v_{r,\mathrm{t}}$, whereas the new definition in [1121] does not neglect what happens initially. It is shown in [279, §5.1.3] that Smith's rule always has at least one solution (percussion vector). Let us denote the mass matrix in the right-hand side of (4.27) as $M_i^{-1} = \frac{1}{m_i} I_3 + R_i^T \mathscr{I}_i R_i$. From (4.27) and the fact that $P_1 = -P_2 = P$, we can write:

$$\sigma_{V_{A,r}}(t_k) = \left(M_1(q_1(t_k))^{-1} + M_2(q_2(t_k))^{-1}\right) P(t_k) \tag{4.109}$$

where $V_{A,r} = V_{A,1} - V_{A,2}$ is the relative velocity between the two bodies, at the contact point. Denoting $M^{-1} \triangleq \left(M_1^{-1} + M_2^{-1}\right)$, and introducing (4.108) into (4.109), one gets

$$p_{\mathrm{n}} \left\{ \begin{array}{c} 1 \\ -\mu \frac{||v_{r,\mathrm{t}}(t_k^-)||v_{r,\mathrm{t}}(t_k^-)+||v_{r,\mathrm{t}}(t_k^+)||v_r(t_k^+)}{||v_r(t_k^-)||^2+||v_r(t_k^+)||^2} \end{array} \right\} - M \left\{ \begin{array}{c} -(1+e_{\mathrm{n}})v_{r,\mathrm{n}}(t_k^-) \\ \sigma_{v_{r,\mathrm{t}}}(t_k) \end{array} \right\} = 0. \quad (4.110)$$

The problem is to study the existence of a solution $(p_{\mathrm{n}}, v_{r,\mathrm{t}}(t_k^+)) \in \mathbb{R}^3$ (recall that $v_{r,\mathrm{t}} = v_{r,\mathrm{t}_1}\mathbf{t}_1 + v_{r,\mathrm{t}_2}\mathbf{t}_2$) to the algebraic nonlinear equation in (4.110). When $\mu = 0$ this reduces to a linear algebraic equation that is easily solved. When μ is small, the implicit function theorem allows one to conclude about existence, in terms of functions $p_{\mathrm{n}}(\mu)$ and $v_{r,\mathrm{t}}(\mu)$. In order to prove existence for any $\mu > 0$, use is made in [279] of the degree theory for differentiable maps.[44] But uniqueness has not been proved (it is said in [1117] that Smith's model may yield several possible outcomes, but no such counterexample is given). The main difficulty is that the law in (4.108) introduces a strong nonlinearity so that solutions can be found numerically only, by iterative methods.

Note that both philosophies in [173, 174, 178, 1121] are different since the first one examines the possible sets of values of e_{n} and μ that yield a consistent solution and can be used in the actual solution (μ being nevertheless by assumption upperbounded by some "critical" values), whereas the second one proposes a more or less *ad hoc* expression of μ that is shown to be always consistent, and thus should fit within the former's framework. The choice of the impulse ratio in (4.108) is shown in [1121] to fit quite well (for the case of two spheres colliding) with the experimental results in [828].

4.3.3.1 Equivalence of Coefficients

In a tangential coordinate direction, one may choose equivalently a kinetic coefficient μ (that may be positive or negative to control velocity sign changes) or a kinematic one e_{t} [175, p. 30]. It may be shown [175, §2] that μ and e_{t} can be related for two particle collisions as[45]

$$\mu = \frac{1+e_{\mathrm{t}}}{1+e_{\mathrm{n}}} \frac{v_{r,\mathrm{t}}(t_k^-)}{v_{r,\mathrm{n}}(t_k^-)}, \quad (4.111)$$

or equivalently:

[44] The development of the degree theory is outside the scope of this monograph. Let us just point out that this is a technique which allows one to prove existence and to explicitly calculate solutions of nonlinear equations, whereas the implicit function theorem, for instance, merely allows one to prove existence.

[45] Most importantly let us recall that for particles the tangential velocity jump cannot be due to inertial effects. It must then be a consequence of another physical phenomenon, like friction or tangential compliance.

$$e_{\mathrm{t}} = -1 + (1 + e_{\mathrm{n}})\mu \frac{v_{r,\mathrm{n}}(t_k^-)}{v_{r,\mathrm{t}}(t_k^-)}. \tag{4.112}$$

Recall velocities and impulses magnitude are algebraically related, see (4.24) and (4.103), although they represent different physical effects, so that in fact the choice of either one coefficient or another is a matter of convenience [176] in the rigid body problems case. In particular e_{t} may take negative values that represent the fact that there may be slip reversal or not (the relative slippage velocity sign changes). Notice that a negative normal restitution is forbidden (this would imply penetration), but in case of tangential motion such negative values must be permitted to allow nonreversal consideration. Actually (4.111) and (4.112) are true for particle collisions only (some experimental data in [773, 828] corroborate such a model). For instance [774, 1242] consider Coulomb's friction and choose to fix $e_{\mathrm{t}} = e_{\mathrm{t},0} \in [0, 1]$ when there is no sliding, whereas $e_{\mathrm{t}} = e_{\mathrm{t}}(f, e_{\mathrm{n}}$, relative velocity, inertia) when there is sliding, where f is the Coulomb friction coefficient. This option is also taken in [274]. These authors thus a priori associate tangential restitution to friction. This is not always the case elsewhere [175, 1148]. More precisely, consider the planar case of a disk with radius r striking a rigid and fixed rough barrier (then $v_{r,\mathrm{t}} = v_{\mathrm{t}}$ and $v_{r,\mathrm{n}} = v_{\mathrm{n}}$). Applying a tangential restitution coefficient, we get

$$v_{\mathrm{t}}(t_k^+) = -e_{\mathrm{t},0} v_{\mathrm{t}}(t_k^-). \tag{4.113}$$

This coefficient may be calculated from Mindlin–Deresiewicz theory as in (4.66), incorporating microslip effects at the contact zone. Now starting from the definition of an impulse ratio μ and using the shock dynamical equations, one gets:

$$v_{\mathrm{t}}(t_k^+) = v_{\mathrm{t}}(t_k^-) - \mu(1 + e_{\mathrm{n}}) \left(1 + \frac{mr^2}{I}\right) v_{\mathrm{n}}(t_k^-). \tag{4.114}$$

For the moment we have not indicated in (4.114) whether there is sliding or sticking at the shock instant. In fact as indicated just above the authors in [774] choose to apply (4.113) when there is sticking, and (4.114) for (gross) sliding. This is in agreement with the conclusions drawn in Sect. 4.2.5. If one assumes that $\mu = -f\,\mathrm{sgn}(v_{\mathrm{t}}(t_k^-))$, then (4.114) becomes:

$$v_{\mathrm{t}}(t_k^+) = -e_{\mathrm{t}} v_{\mathrm{t}}(t_k^-) \tag{4.115}$$

with

$$e_{\mathrm{t}} = -1 + f(1 + e_{\mathrm{n}}) \left(1 + \frac{mr^2}{I}\right) \frac{|v_{\mathrm{n}}(t_k^-)|}{|v_{\mathrm{t}}(t_k^-)|}, \tag{4.116}$$

since $v_{\mathrm{n}}(t_k^-) < 0$. It is shown in [175, Fig. 6.23] that experimental results from [829] validate the existence of tangential restitution as in (4.113) for collisions such that sliding ends before separation (i.e., $v_{\mathrm{t}}(t_k^+) = 0$). Several authors [328, 407, 760, 774, 820] led experiments, showing the validity of the model in (4.113) (4.114) for spheres colliding a fixed wall. The model based on the use of three restitution

coefficients (normal Newton e_{n}, impulse ratio μ and tangential compliance $e_{\mathrm{t},0}$) has been experimentally tested in [407] (3 mm glass and 6 mm cellulose spheres against a plane), [328] (25 mm nylon spheres), [820] (190 and 90 μm spheres in a wind tunnel), [290] (steel disks of mass 4.87 g, radius 1 cm, thickness 2 mm against a massive table), [274] (steel disks of mass 67 g, radius 4.91 cm, thickness 6.4 mm) and found to correctly represent the real process. The experiments were refined in [760] taking into account the surface reflectivity, slight asphericity and surface damage, and still it was concluded about its validity. Other studies on (kinematic) tangential restitution coefficient can be found in [149] : e_{t} is defined as an exponential function of the friction coefficient and the ratio of normal and tangential components of incident velocity. In [910] the above model for Coulomb's friction is taken to study the motion of a sphere colliding a rough inclined plane. In this case sticking occurs if the incidence angle is $\leq \frac{7\mu(1+e_{\mathrm{n}})}{2(1+e_{\mathrm{t},0})}$, otherwise sliding occurs. This is what we obtained in Sect. 4.3.1.1 with $\tilde{v}_{\mathrm{t}} = v_{\mathrm{t}}(t_k^+) + e_{\mathrm{t}} v_{\mathrm{t}}(t_k^-)$. The authors are then able to derive an iterative mapping for the quantity $v_k \stackrel{\Delta}{=} \frac{v_{\mathrm{t}}(t_k^-)}{|v_{\mathrm{n}}(t_k^-)|}$ as $v_{k+1} = -\frac{e_{\mathrm{t},0}}{e_{\mathrm{n}}} v_k + 2\tan(\alpha)$ where α is a parameter. Depending on the value of α with respect to a certain critical value, the collision process may end up in sticking, or sliding, or in a chaotic intermittence between both. In [198, 199] the tangential restitution is also associated with Coulomb's friction, but μ is deduced from a contact model with asperities that may vary in shape and size. The numerical calculations for $e_{\mathrm{t}}(v_{r,\mathrm{n}}(t_k^-), v_{r,\mathrm{t}}(t_k^-))$, agree well with the experimental data of [194] (collisions between ice balls).

In some cases, when the contact process is better known, it may be better to tailor the model, see [175, Chap. 6, Figs. 6.23 and 6.24] for a bilinear model. Let us consider the case of impacts of the edge of a disk with radius r against a flat block of like material (both made of hard steel). It can be shown (see Sect. 4.3.1.1, especially Fig. 4.13, see also [175, 828, 829]) that the curve $y = \tan(\gamma^+) = \frac{v_{\mathrm{t}}(t_k^+)}{v_{\mathrm{n}}(t_k^+)}$ as a function of $x = \tan(\gamma^-) = \frac{v_{\mathrm{t}}(t_k^-)}{|v_{\mathrm{n}}(t_k^-)|}$ consists of two straight lines, one with negative (crossing $(x, y) = (0, 0)$) and the other with positive slopes, where γ^+ and γ^- are the post- and preimpact incidence angles. Consider one of the last two equations in (4.103). It yields after some developments and with the notations of Sect. 4.1 to:

$$v_{\mathrm{t}}(t_k^+) = -e_{\mathrm{t}}(\dot{x}_2(t_k^-) + r\omega_3(t_k^-)), \tag{4.117}$$

which can be rewritten using (4.112) as

$$v_{\mathrm{t}}(t_k^+) = \dot{x}_2(t_k^-) + r\omega_3(t_k^-) - \mu(1+e_{\mathrm{n}})\left(1 + \frac{mr^2}{I}\right) v_{\mathrm{n}}(t_k^-). \tag{4.118}$$

From (4.118) one has $y = x - \mu(1+e_{\mathrm{n}})\left(1 + \frac{mr^2}{I}\right)$ so that a negative slope portion cannot be described by (4.118) (notice also that the application of Whittaker's rule yields a bilinear curve with a portion $y = 0$ and a linear portion with positive slope, see Sect. 4.3.1.1 and Corollary 4.1, therefore it cannot incorporate the negative

slope portion evidenced in [290, 829, 830]). Hence both (4.117) and (4.118) possess their own limited initial velocity x range of applicability; the first one is needed to model low initial tangential velocities effects. The second one models sliding impacts. Let us note that this is a three-parameter law of impact: f or μ, e_{n}, e_{t}. In some other cases where only colinear collisions exist (spheres colliding), tangential reversals are always due to tangential compliance, and not to Coulomb's friction, as we proved in Sect. 4.3.1. Further discussions on modeling of tangential effects can be found in [769] (the intersection of the two linear portions occurs at a critical value of the incidence angle) [1244] (an upperbound on e_{t} is proposed to hamper $T_L(t_k) > 0$), elastic tangential springs have been introduced in [828, 830, 1244]. Maw et al. [828, 830] propose a rather complex modeling approach which enables to avoid the nondifferentiable point on the curve in Fig. 4.13b. The expression for the tangential restitution is rather intricate and requires the knowledge of the compression phase duration.

In summary the three-parameter impact law for shocks of disks or spheres against a massive surface, provides a correct approximation of some complicated local phenomena in the zone of collision, that mainly depend on the angle of approach. It is simple enough to be incorporated in a numerical code, or to be used in a control context.

4.3.4 Kinematic CoR: Frémond's approach

Let us introduce another approach for rigid body collisions, proposed by Frémond [413–415]. It aims at modeling the impact process with one (single impact) or more than two (multiple impact) points of contact. In this section we deal with two-body collisions and single impacts. This approach mainly consists in the derivation of general collision rules taking into account the various physical effects at impacts (normal restitution, tangential effects, influence of geometrical parameters). The proposed rules are implicit in the postimpact velocity, and great care is taken of existence and uniqueness of the impact outcome using maximal monotone operators to guarantee not only energetical consistency, but existence and uniqueness of postimpact velocity. It is assumed that the shock impulse is given by a general rule written as

$$P[v_r(t_k^+), v_r(t_k^-)] \in \partial \Gamma[v_r(t_k^+), v_r(t_k^-)] + P^{\mathrm{reac}}, \tag{4.119}$$

for some $\Gamma(\cdot)$ that may be a function (in the normal direction) or a dissipation pseudopotential (in the tangential direction). P^{reac} corresponds to nondissipative terms in the normal direction of the percussional reaction. The derivation bases on thermodynamical considerations. In the normal direction one may choose:

$$\Gamma_{\mathrm{n}}[(v_{r,\mathrm{n}}(t_k^+), v_{r,\mathrm{n}}(t_k^-)] = \frac{k_{\mathrm{n}}}{p}|v_{r,\mathrm{n}}(t_k^+) + v_{r,\mathrm{n}}(t_k^-)|^p, \tag{4.120}$$

for $p \in \mathbb{R}$, $p > 1$ and $k_\mathrm{n} \geq 0$. Another choice is

$$\Gamma_\mathrm{n}[(v_{r,\mathrm{n}}(t_k^+), v_{r,\mathrm{n}}(t_k^-)] = \frac{k_\mathrm{n}}{p}[\sup\{0, -c - v_{r,\mathrm{n}}(t_k^+) - v_{r,\mathrm{n}}(t_k^-)\}]^p, \tag{4.121}$$

for $p > 1$ and $c \geq 0$. For (4.121) one gets $\partial\Gamma_\mathrm{n}(z) = k_\mathrm{n} \sup(0, -c - z)|c + z|^{p-2}$. In the case $p = 2$ and for the first law, one gets: $p_\mathrm{n} = p_\mathrm{n}(v_{r,\mathrm{n}}(t_k^+), v_{r,\mathrm{n}}(t_k^-)) = -k_\mathrm{n}(v_{r,\mathrm{n}}(t_k^+) + v_{r,\mathrm{n}}(t_k^-)) + \begin{cases} 0 \text{ if } v_{r,\mathrm{n}}(t_k^+) > 0 \\ \mathbb{R}^+ \text{ if } v_{r,n}(t_k^+) = 0 \\ \emptyset \text{ if } v_{r,\mathrm{n}}(t_k^+) < 0 \end{cases}$. In the bouncing ball case with mass m, one finds two possible outcomes after the shock: $v_{r,\mathrm{n}}(t_k^+) = \frac{m-k_\mathrm{n}}{m+k_\mathrm{n}} v_{r,\mathrm{n}}(t_k^-)$ and $P^{\mathrm{reac}} = 0$ if $k_\mathrm{n} \geq m$, or $v_{r,\mathrm{n}}(t_k^+) = 0$ and $P^{\mathrm{reac}} = (m - k_\mathrm{n})v_{r,\mathrm{n}}(t_k^-)$ if $k_\mathrm{n} \leq m$. When rebound is described by the model, then $e_\mathrm{n} = -\frac{m-k_\mathrm{n}}{m+k_\mathrm{n}}$. One sees that this model uses several parameters in the normal direction (p, k_n, c plus the form of $\Gamma(\cdot)$) and thus allows for various types of motion to be described. For $p < 2$, one can model shocks with jamming effect, i.e., rebound for a small approach velocity and plastic impact for high approach velocity. For $p > 2$ the model predicts plastic impacts for low $v_r(t_k^-)$ and rebound for larger $v_r(t_k^-)$.

Tangential viscous friction effects are modeled by choosing a pseudopotential $\Gamma_\mathrm{t}(z) = k_\mathrm{t}[\sup(0, |z| - \rho)]^q$ with $q > 1$ and $\rho \geq 0$. Then the percussion due to those effects in the tangential direction is given by $p_\mathrm{t}^d[(v_{r,\mathrm{t}}(t_k^+), v_{r,\mathrm{t}}(t_k^-)] \in \partial\Gamma_\mathrm{t}^d[v_{r,\mathrm{t}}(t_k^+) + v_{r,\mathrm{t}}(t_k^-)]$. It is shown [290] that the parameter q influences the sign of $v_{r,\mathrm{t}}(t_k^+)$, whereas ρ allows one to describe collisions without reversal of $v_{r,\mathrm{t}}(t_k^+)$ below a critical $v_{r,\mathrm{t}}(t_k^-)$. Coulomb's friction effects at the percussion level are modeled as

$$p_\mathrm{t}(t_k) = \mu|p_\mathrm{n}(t_k)|\Gamma_\mathrm{t}[v_{r,\mathrm{t}}(t_k^+) + v_{r,\mathrm{t}}(t_k^-)], \tag{4.122}$$

which generalizes (4.69). A possible choice is $\Gamma_\mathrm{t}[z] = \min\{k_\mathrm{t}[\sup(0, |z| - \rho)]^{q-1}, 1\}\,\mathrm{sgn}(z)$, with $q > 1$ and $r \geq 0$. Bilinear behaviors as the ones observed in certain experiments (see Sect. 4.3.3.1) are recovered with such a rule, and trilinear models may even be obtained by a proper choice of the coefficient ρ.

Remark 4.16 These rules yield implicit equations for the postimpact velocity. Similarly as for the Smith's model, it is important to study the existence and uniqueness of the solution. This is done in [290] using functional and convex analysis tools. Evidently, the properties of the function Γ in (4.119)—convexity, lower semicontinuity—are quite fundamental: we illustrated this point in Sect. 4.3.1 with various choices of the variable $\tilde{v}_\mathrm{t}(t_k)$. Proofs can be found in [290] for the rocking block and granular material systems.

Experimental validations have been reported in [290]. They concern collisions of disks, triangles and rectangles of small size and weight against a massive steel table. One conclusion is that when there is sticking ($\frac{p_\mathrm{t}}{|p_\mathrm{n}|} < \mu$) then $\frac{p_\mathrm{t}}{|p_\mathrm{n}|}$ depends on $v_r(t_k^+) + v_r(t_k^-)$, which is a choice of $\tilde{v}_\mathrm{t}$ found to be energetically consistent in Sect. 4.3.1.5. The angle between AG and the vertical line is incorporated in the

percussion behavioral laws for the triangle, rectangle and slender rod cases (the experimental data of Stoianovici and Hurmuzlu [1144] are used in the latter case). The friction cone is observed from the experiments, as in [1144].

4.3.5 First Order Impact Dynamics: Darboux-Keller's Shock Equations

4.3.5.1 General Introduction

Let us now pass to another class of models, which are not algebraic but rely on some differential equations and in which the kinetic (Poisson) and energetic CoRs are used. In order to introduce the Darboux-Keller's equations,[46] let us first deal with a one-degree-of-freedom system

$$m\ddot{q}(t) = F(t) + Q(t), \tag{4.123}$$

where $F(t)$ and $Q(t)$ are the forces acting on the particle. Assume that the shock starts at $t = t_k$. Then one makes the assumption that the duration of the shock process is small and that the shock occurs on $[t_k, t_k + t_f]$. Let us do the time scaling $t' = \frac{t-t_k}{t_f}$.[47] Let us further assume that as $t_f \to 0$, then $t_f F(t) \nrightarrow 0$ whereas $t_f Q(t) \to 0$. In other words $F(t)$ is the interaction force that is assumed to be much larger than all other forces $Q(t)$ acting on the particle, and $p = \int_{t_k}^{t_k+t_f} F(\tau)d\tau = \int_0^1 t_f F(t')dt' \neq 0$ whereas $\int_{t_k}^{t_k+t_f} Q(\tau)d\tau = 0$. We can thus write that $\dot{q}(t) = \dot{q}(t_f t' + t_k) = \dot{q} \circ t(t') \stackrel{\Delta}{=} \dot{q}(t')$, and $\frac{d\dot{q}}{dt} = \frac{d\dot{q}}{dt'}\frac{1}{t_f}$. Now since $F > 0$ during the shock, $p(t) = \int_{t_k}^{t} F(\tau)d\tau$ is a strictly increasing function of time, i.e., $p(t) = f(t)$ for some strictly increasing $f(\cdot)$. Hence $f(\cdot)$ in invertible, and $dt = \frac{dp}{df}$. Also $\dot{q}(t) = \dot{q} \circ f^{-1}(p)$ that we may denote simply as $\dot{q}(p)$. We thus obtain

$$m\frac{d\dot{q}(t')}{dt'} = t_f F(t) + t_f Q(t) = t_f \frac{dp}{dt} = \frac{dp}{,}dt' \tag{4.124}$$

where $t_f Q(t)$ is considered to be 0, and the shock process takes place on $t' \in [0, 1]$. Going a step further and noting that $\dot{q}(t') = \dot{q} \circ t'(p)$ so that $\frac{d\dot{q}(t')}{dt'} = \frac{d\dot{q}(p)}{dp}\frac{dp(t')}{dt'}$ yields

$$\frac{d\dot{q}}{dp}(p) = \frac{1}{m}, \tag{4.125}$$

[46] This form of the shock dynamics are also sometimes called *Routh's incremental model* [279] in the planar case. We should perhaps name the model described in this part as the Routh-Darboux-Keller model.

[47] The idea of deriving the Darboux-Keller shock dynamics using this time scaling is due to Keller [651]. Most likely Keller was not aware of Darboux's paper [327] written in French.

where this time the shock process is considered on $p \in [0,\, p(t_k + t_f)] = [0,\, p(t' = 1)]$. One sees at once that the shock duration will be determined provided one knows when the impulsion $p(t')$ attains its final value $p(1)$: Poisson's kinematic CoR e_{p} in (4.155) may be used. If $t'_c = \frac{t_c - t_k}{t_f}$, then it tells us that $p(1) = (1 + e_{\mathrm{p}})p(t'_c)$. One may thus start integrating (4.125): t'_c corresponds to p_c such that $\dot{q}(p_c) = 0$ (termination of the compression phase). Finally notice that the dynamics in (4.125) really possesses the form of shock dynamics (the only variables that change from one impact to another are the initial velocity and the mass, like in pure rigid body algebraic shock equations), but this is an ODE, not an algebraic relationship. Let us state the basic assumptions under which a more general form as in (4.125) will be derived

- The impact forces are so high that all other forces acting on the bodies are negligible.
- The shock process consists of a compression and an expansion phases.
- The positions remain constant during the shock.
- The tangential stiffness is infinite.

As will be seen later, the second assumption may not be satisfied experimentally, even for simple systems like the falling rod. The fourth one neither. This does not call into question the fact that for systems (that certainly exist) for which they are satisfied, then all the conclusions drawn from the use of Darboux-Keller's dynamics are valid and useful.

Let us now deal with the general three-dimensional case. One may start by rewriting (4.29) and (4.28): as

$$\left\{ \begin{array}{l} \frac{d\Omega_i}{dt}(t) = \mathscr{I}_i^{-1} R_i^T(t) F_i(t) \\ \frac{dX_i}{dt}(t) = \frac{1}{m_i} F_i(t), \end{array} \right. \tag{4.126}$$

where i is the body index ($i = 1$ or 2). Let us make the same assumption and the same time scaling as above. Then we obtain since $dt' = \frac{dt}{t_f}$

$$\left[\begin{array}{l} \frac{d\Omega_i}{dt'}(t_f t'') = t_f \mathscr{I}_i^{-1} R_i^T(t_f t'') F_i(t_f t'') \\ \frac{dX_i}{dt'}(t_f t'') = \frac{t_f}{m_i} F_i(t_f t'') \end{array} \right. \tag{4.127}$$

where $t'' = \frac{t_k}{t_f} + t'$. When $t_f \to 0$, $R_i(t') \stackrel{\Delta}{=} R_i(t_f t'') = R_i(t_k + t_f t') \to R_i(t_k) = R_i(t' = 0) = R_i(0)$. Note that $t'(t_k) = 0$, $t'(t_k + t_f) = 1$. Hence, by integrating (4.127) between 0 and 1 one gets:

$$\sigma_{\Omega_i}(t_k) = \Omega_i(t_k + t_f) - \Omega_i(t_k) = -\mathscr{I}_i^{-1} R_i(t_k) P_i(t_k + t_f), \tag{4.128}$$

that we can rewrite in t'-scale as:

$$\sigma_{\Omega_i}(0) = -\mathscr{I}_i^{-1} R_i(0) P_i(1) \tag{4.129}$$

with $P_i(1) = P_i(t = t_k + t_f) = \int_0^1 t_f F_i(t')dt' = P_i(t' = 1)$.[48] Similarly,

$$\sigma_{\dot{X}_i}(t_k) = \frac{1}{m_i} P_i(t_k) \tag{4.130}$$

or equivalently in the t'-scale:

$$\sigma_{\dot{X}_i}(0) = \frac{1}{m_i} P_i(1). \tag{4.131}$$

Let us now focus on the relative velocity of the bodies at the contact point A expressed in the local frame $(A, \mathscr{L})$, *i.e.*,

$$V_{r,A} \triangleq V_{A_1} - V_{A_2} = \begin{pmatrix} v_{1,\mathrm{n}} - v_{2,\mathrm{n}} \\ v_{1,\mathrm{t}_1} - v_{2,\mathrm{t}_1} \\ v_{1,\mathrm{t}_2} - v_{2,\mathrm{t}_2} \end{pmatrix} = \begin{pmatrix} v_{r,\mathrm{n}} \\ v_{r,\mathrm{t}_1} \\ v_{r,\mathrm{t}_2} \end{pmatrix}. \tag{4.132}$$

Supposing a compression–extension shock process, one finds that $v_{1,\mathrm{n}}(t_c) - v_{2,\mathrm{n}}(t_c) = v_{r,\mathrm{n}}(t_c) = 0$, where t_c is when the compression phase ends. Poisson's CoR gives $p_{i,\mathrm{n}}(1) = (1+e_\mathrm{p}) p_{i,\mathrm{n}}(t_c')$, with $t_c' = \frac{t_c - t_k}{t_f}$. From the fact that $p_{i,\mathrm{n}}(t') = \int_0^{t'} F_{i,\mathrm{n}}(u)du$, one has $\frac{dp_{i,\mathrm{n}}}{dt'}(t') = F_{i,\mathrm{n}}(t')$. The interaction force is given by $F_i = \begin{pmatrix} F_{i,\mathrm{n}} \\ F_{i,\mathrm{t}_1} \\ F_{i,\mathrm{t}_2} \end{pmatrix} = F_{i,\mathrm{n}}\mathbf{n} + F_{i,\mathrm{t}_1}\mathbf{t}_1 + F_{i,\mathrm{t}_2}\mathbf{t}_2$. Define the vector $\mathbf{t} = \cos(\zeta)\mathbf{t}_1 + \sin(\zeta)\mathbf{t}_2$ that is colinear to the relative tangential velocity $v_{r,\mathrm{t}}$. Applying Coulomb's friction law we have $||F_{i,\mathrm{t}}|| = \sqrt{F_{i,\mathrm{t}_1}^2 + F_{i,\mathrm{t}_1}^2} = \mu |F_{i,\mathrm{n}}|$, i.e., $\frac{F_{i,\mathrm{t}}}{|F_{i,\mathrm{n}}|} = -\mu\mathbf{t}$ when there is sliding, and F_i lies inside the friction cone when sticking occurs. Hence when sliding occurs one has $F_i(t) = \begin{bmatrix} F_{i,\mathrm{n}} \\ -\mu \frac{v_{r,\mathrm{t}_1}}{||v_{r,\mathrm{t}}||} F_{i,\mathrm{n}} \\ -\mu \frac{v_{r,\mathrm{t}_2}}{||v_{r,\mathrm{t}}||} F_{i,\mathrm{n}} \end{bmatrix} = \begin{bmatrix} 1 \\ -\mu\cos(\zeta) \\ -\mu\sin(\zeta) \end{bmatrix} \frac{dp_{i,\mathrm{n}}}{dt'}$. One finds:

$$P_i(1) = p_{i,\mathrm{n}}(1)\mathbf{n} - \mu \int_0^{p_{i,\mathrm{n}}(1)} \mathbf{t}(p_{i,\mathrm{n}}) dp_{i,\mathrm{n}}, \tag{4.133}$$

where we note that since we are dealing with a differential analysis, $\mathbf{t}$ and ζ are allowed to vary on $[t_k, t_k + t_f]$ (or on $[0, 1]$ in t'-scale), whereas $\mathbf{n}$ is assumed to

[48] Implicitly one supposes that $t_f F_i \nrightarrow 0$ as $t_f \to 0$. This allows to consider all other external actions F_e as negligible during the shock process, since for them $t_f F_e \to 0$ as $t_f \to 0$.

remain constant during the collision.[49] Introducing Poisson's rule into (4.133) it follows that:

$$P_i(1) = (1+e_{\mathrm{p}})\, p_{i,\mathrm{n}}(t_c')\mathbf{n} - \mu \int_0^{(1+e_{\mathrm{p}})p_{i,\mathrm{n}}(t_c')} \mathbf{t}(p_{i,\mathrm{n}})dp_{i,\mathrm{n}} \tag{4.134}$$

One can now introduce (4.134) into (4.129) and (4.131) to obtain the expression relating $\sigma_{\Omega_i}(0)$ and $\sigma_{\dot{X}_i}(0)$ to Poisson's coefficient e_{p}, μ and $p_{i,\mathrm{n}}(t_c')$. Using (4.27) one also finds that

$$\sigma_{V_{A_i}}(0) = \left[\frac{1}{m_i} I_3 + R_i(0)^T \mathscr{I}_i^{-1} R_i(0)\right] P_i(1), \tag{4.135}$$

and we can use (4.132) to relate $\sigma_{v_r}(0)$ to e_{p}, μ and $p_{i,\mathrm{n}}(t_c')$. Now from (4.132) and the time-equivalent of (4.27), *i.e.*,

$$\frac{dV_{A_i}}{dt}(t) = \left[\frac{1}{m_i} I_3 + R_i(t)^T \mathscr{I}_i^{-1} R_i(t)\right] F_i(t), \tag{4.136}$$

one finds by introducing $dt' = \frac{dt}{t_f}$, $dp_{i,\mathrm{n}} = F_{i,\mathrm{n}} dt'$ and Coulomb's friction rule into (4.136):

$$\frac{dV_{A_i}}{dp_{i,\mathrm{n}}}(t') = \left[\frac{1}{m_i} I_3 + R_i(t')^T \mathscr{I}_i^{-1} R_i(t')\right](-\mu\mathbf{t} + \mathbf{n}), \tag{4.137}$$

where it is understood that either one deals with a sliding regime, i.e., the impulse ratio may be identified with Coulomb's coefficient and $F_{\mathrm{t}} = -\mu |F_{\mathrm{n}}|\mathbf{t}$, or one adopts Brach's formulation where μ relates the normal and tangential components and is in general time-varying. Let us denote $\frac{1}{m_i} I_3 + R_i(t')\mathscr{I}_i^{-1} R_i(t')^T \triangleq M_i^{-1}(t')$. Then it follows that $\frac{dV_{A_1}}{dp_{1,\mathrm{n}}} - \frac{dV_{A_2}}{dp_{2,\mathrm{n}}} = M_1^{-1}(-\mu\mathbf{t} + \mathbf{n}) - M_2^{-1}(\mu\mathbf{t} - \mathbf{n})$ (recall that $dp_{1,\mathrm{n}} = -dp_{2,\mathrm{n}}$, $F_{1,\mathrm{t}_1} = -F_{2,\mathrm{t}_1}$ from Newton's principle of mutual actions). One obtains Darboux-Keller's shock equations:

$$\begin{cases} \frac{dv_{r,\mathrm{n}}}{dp_{\mathrm{n}}} = \left[\sum_{i=1}^2 M_i^{-1}(-\mu\mathbf{t} + \mathbf{n})\right]^T \mathbf{n} \\ \frac{dv_{r,\mathrm{t}}}{dp_{\mathrm{n}}} = \left[\sum_{i=1}^2 M_i^{-1}(-\mu\mathbf{t} + \mathbf{n})\right]^T \mathbf{t}, \end{cases} \tag{4.138}$$

[49] Such an assumption is not always realistic, as shown in [907] for granular materials with spherical beads and Kuwabara-Kono viscoelastic model; the normal angle may vary significantly during some collisions.

whith $p_{\rm n} \stackrel{\Delta}{=} p_{1,\rm n}$, $v_{r,\rm t} = v_{r,\rm t_1}\mathbf{t}_1 + v_{r,\rm t_2}\mathbf{t}_2 = ||v_{r,\rm t}||(\cos(\zeta)\mathbf{t}_1 + \sin(\zeta)\mathbf{t}_2)$, $M_i \stackrel{\Delta}{=} M_i(t' = 0)$. The dynamics in (4.138) thus corresponds to a time scaling based on the fact that $p_{\rm n}(\cdot)$ is a monotonic function.[50]

Remark 4.17 According to Darboux [327], Phillips [1002] has been the first to consider the problem of collisions with friction by integrating the differential equations during the shock. Other studies were done in [326, 630, 920, 1038]. Morin [904] conducted experiences that showed that friction during shocks satisfies quite well Coulomb's friction model. In [162] the geometric approach of Darboux has been developed. But Darboux was certainly the first to take into account the fact that the vector $\mathbf{t} = \mathbf{t}(\zeta)$ may vary during the shock, and that this would introduce severe difficulties in the shock process analysis. This is reported in his 1880 seminal paper [327].

Coulomb's friction model applies as $dp_{\rm t} = -\mu|dp_{\rm n}|\frac{v_{\rm t}}{||v_{\rm t}||} = -\mu|dp_{\rm n}|(\cos(\zeta)\mathbf{t}_1 + \sin(\zeta)\mathbf{t}_2)$ for sliding. From (4.138) Darboux [327, Eq. (25)] obtained the shock dynamics under the form:

$$\begin{pmatrix} \frac{dv_{r,\rm n}}{dp_{\rm n}} \\ \frac{dv_{r,\rm t_1}}{dp_{\rm n}} \\ \frac{dv_{r,\rm t_2}}{dp_{\rm n}} \end{pmatrix} = M^{-1} \begin{pmatrix} 1 \\ -\mu\cos(\zeta) \\ -\mu\sin(\zeta) \end{pmatrix}, \tag{4.139}$$

where according to the above notations ζ is the angle made by v_{r,t_1} and v_{r,t_2} in the tangent plane $(\mathbf{t}_1, \mathbf{t}_2)$, i.e., $\zeta = \arctan\left(\frac{v_{r,\rm t_2}}{v_{r,\rm t_1}}\right)$. This is true when there is sliding, for if sticking occurs the right-hand side has to be multivalued with $||dp_{\rm t}|| \leq \mu|dp_{\rm n}|$, that is $dp \in \mathscr{C}$ with $\mathscr{C}$ the Coulomb's cone.

Let us denote the symmetric matrix $M^{-1} \succ 0$ in (4.139) as

$$M^{-1} = \begin{pmatrix} m_{11}^{-1} & m_{12}^{-1} & m_{13}^{-1} \\ m_{12}^{-1} & m_{22}^{-1} & m_{23}^{-1} \\ m_{13}^{-1} & m_{23}^{-1} & m_{33}^{-1} \end{pmatrix} = \begin{pmatrix} M_{\rm nn}^{-1}(q) & M_{\rm nt}^{-1}(q) \\ (M_{\rm nt}^{-1}(q))^T & M_{\rm tt}^{-1}(q) \end{pmatrix}. \tag{4.140}$$

Let us remind that the superscript -1 does not mean that M^{-1} is the inverse of a matrix M, but that it is homogeneous to a mass inverse. The first notation in (4.140) is often used in the literature, while the second one emphasizes the submatrices which correspond to couplings between normal and tangent directions, with dependence on the bodies coordinates $m_{11}^{-1} = M_{\rm nn}^{-1}(q) \in \mathbb{R}$, $M_{\rm tt}^{-1}(q) \in \mathbb{R}^{2\times 2}$.[51] It

[50] Consider an ODE $\dot{x} = f(x,t)$. Assume that $\tau = g(t)$ for some strictly increasing function $g(\cdot)$. Hence $g^{-1}(\cdot)$ exists and is strictly increasing as well. Simple calculations then allow one to write the ODE as $\frac{dx}{d\tau} = \bar{f}(x(\tau),\tau)$ with $\bar{f}(x(\tau),\tau) = \left[\left(\frac{dg}{dt}\circ g^{-1}\right)(\tau)\right]^{-1} f(x\circ g^{-1}(\tau), g^{-1}(\tau))$. Such manipulations can be sometimes useful in the study of ODEs, see, e.g., [1057] and Proposition 5.27 in Chap. 5.

[51] For the readers who wish to look at Darboux's paper, let us mention that the first, second and third rows of M^{-1} are given by a'', b'', c'', a, b, c and a', b', c' in Darboux's notations.

follows from the well-known Schur complement on positive definite matrices that $M_{\rm nn}^{-1}(q) \succ 0$, $M_{\rm tt}^{-1}(q) \succ 0$, $M_{\rm tt}^{-1}(q) - (M_{\rm nt}^{-1}(q))^T (M_{\rm nn}^{-1})^{-1} M_{\rm nt}^{-1}(q) \succ 0$, $M_{\rm nn}^{-1}(q) - M_{\rm nt}^{-1}(q)(M_{\rm tt}^{-1})^{-1}(M_{\rm nt}^{-1}(q))^T > 0$. From (4.138), $M^{-1} = M_1^{-1} + M_2^{-1}$ where M_i^{-1} is defined after (4.137) as $\frac{1}{m_i} I_3 + R_i^T \mathscr{I}_i^{-1} R_i$. It is then possible to give complete expressions for the entries m_{ij}^{-1}. For instance one has $M_{\rm nn}^{-1}(q_1, q_2) = \sum_{i=1,2} r_{3i}^2 j_{22,i} + \overbrace{r_{2i}^2 j_{33,i}}^{=m_{12,i}^{-1}} + \frac{1}{m_i}$, $M_{\rm nt}^{-1}(q_1, q_2) = \sum_{i=1,2} [\overbrace{r_{3i}(-r_{3i} j_{12,i} + r_{2i} j_{13,i}) - r_{1i}(-r_{3i} j_{23,i} + r_{2i} j_{33,i})}^{=m_{13,i}^{-1}}, \overbrace{-r_{2i}(-r_{3i} j_{12,i} + r_{2i} j_{13,i}) + r_{1i}(-r_{3i} j_{22,i} + r_{2i} j_{23,i})}]$, where $j_{kl,i}$ are the entries of $\mathscr{I}_i^{-1}$ (the inverse of the constant inertia tensor $\mathscr{I}_i$ of body i, expressed in a frame fixed w.r.t. the body). For two spheres we get $M_i^{-1} = \frac{1}{m_i} \mathrm{diag}\left(1, \frac{7}{2}, \frac{7}{2}\right)$, $M^{-1} = \frac{m_1+m_2}{m_1 m_2} \mathrm{diag}\left(1, \frac{7}{2}, \frac{7}{2}\right)$, and $\mathscr{I}_i^{-1} R_i^T = \begin{pmatrix} 0 & 0 & 0 \\ 0 & 0 & \frac{5}{2m_i r_i} \\ 0 & \frac{-5}{2m_i r_i} & 0 \end{pmatrix}$, where $r_i = r_{1i}$.

4.3.5.2 The Darboux-Keller's Impact Dynamics

To summarize the two-body collision dynamics with Coulomb's friction is given by the following set of nonlinear equations on $t \in [t_k, t_f]$ (or $p_{\rm n} \in [0, p_{{\rm n},f}]$, with $p_{{\rm n},f} = p_{\rm n}(t_f)$, $p_{\rm n}(t_k) = 0$, and $p_{{\rm n},c} = p_{\rm n}(t_c)$ is the impulse at maximum compression time t_c):

$$
\begin{aligned}
&\begin{pmatrix} \frac{dv_{r,\rm n}}{dp_{\rm n}} \\ \\ \frac{dv_{r,\rm t}}{dp_{\rm n}} \end{pmatrix} = \begin{pmatrix} M_{\rm nn}^{-1}(q(t_k)) & M_{\rm nt}^{-1}(q(t_k)) \\ \\ (M_{\rm nt}^{-1}(q(t_k)))^T & M_{\rm tt}^{-1}(q(t_k)) \end{pmatrix} \begin{pmatrix} 1 \\ \\ \frac{dp_{\rm t}}{dp_{\rm n}} \end{pmatrix} \\
&\frac{d\Omega_i}{dp_{\rm n}} = \mathscr{I}_i^{-1} R_i^T \begin{pmatrix} 1 \\ \frac{dp_{\rm t}}{dp_{\rm n}} \end{pmatrix}, \quad i = 1, 2 \\
&\begin{cases} dp_{\rm t} = -\mu dp_{\rm n} \frac{v_{r,\rm t}}{||v_{r,\rm t}||} & \text{if } v_{r,\rm t} \neq 0 \\ \\ ||dp_{\rm t}|| \leq \mu dp_n & \text{if } v_{r,\rm t} = 0 \end{cases}
\end{aligned}
\tag{4.141}
$$

Restitution law: kinematic $(v_{r,\rm n}(p_{{\rm n},f}) = -e_{\rm n} v_{r,\rm n}(0))$
kinetic $(p_{{\rm n},f} = (1 + e_{\rm p}) p_{{\rm n},c})$,
energetic (see Sect. 4.3.6)

Let us recall that the subscript r in $v_{r,\mathrm{n}}$ and $v_{r,\mathrm{t}}$ is for "relative velocity". If one considers that body 2 is fixed with infinite mass, the r may be dropped for convenience. If we compare this dynamics to restitution mappings like Newton's or Moreau's ones (see Chap. 5.1), and to compliant contact models as in Chap. 2, we see that we have three main types of impact laws: order zero (algebraic impact mappings), order one (Darboux-Keller equations), and order two (compliant models). It is important to notice that (4.141) is not an ordinary differential equation: it is a nonsmooth set-valued system. The equations in (4.141) are integrated with respect to the time scale p_{n}. The parameters are $q(t_k)$, a restitution law, $\mu \geq 0$, and the initial condition is $V_{r,A}(t_k^-)$, with $v_{r,\mathrm{n}}(0) < 0$ for an impact to occur. The first question that comes to any mathematically oriented brain is: is the dynamics in (4.141) well-posed (that is, does there exist solutions over $p_{\mathrm{n}} \in \mathbb{R}^+$, and are solutions unique for given initial conditions)? The first question that comes to any mechanically oriented brain is: how does the contact point status (sticking, sliding, changing direction of sliding) evolve during the impact process, and are all CoRs equivalent? What we describe in the next sections rather deals with the second question.[52] It is noteworthy that $\frac{dv_{r,\mathrm{t}}}{dp_{\mathrm{n}}} \in (M_{\mathrm{nt}}^{-1})^T + M_{\mathrm{tt}}^{-1}\frac{dp_{\mathrm{t}}}{dp_{\mathrm{n}}}$, so that the tangent velocity $v_{\mathrm{t}}(p_{\mathrm{n}})$ evolves in an autonomous way, while the normal velocity does not in general. Let us define $\mathscr{D}_\mu = \{z \in \mathbb{R}^2 | \sqrt{z^T z} \leq \mu\}$. Then the Coulomb's law in (4.141) can be written as $-v_{r,\mathrm{t}} \in N_{\mathscr{D}_\mu}\left(\frac{dp_{\mathrm{t}}}{dp_n}\right)$, equivalently $\frac{dp_{\mathrm{t}}}{dp_n} \in -\partial\psi^\star_{\mathscr{D}_\mu}(v_{r,\mathrm{t}})$, where the conjugate function of the indicator function $\psi_{\mathscr{D}_\mu}$ is $\psi^\star_{\mathscr{D}_\mu}(\cdot) = \mu||\cdot||$ (see the function $f_2(\cdot)$ after Definition B.11 in Appendix B, and (B.16)). We can therefore rewrite the first equations in (4.141) as the differential inclusion:

$$\frac{dV_r}{dp_{\mathrm{n}}} \in M^{-1}\begin{pmatrix} 1 \\ -\partial\psi^\star_{\mathscr{D}_\mu}(v_{r,\mathrm{t}}) \end{pmatrix}. \tag{4.142}$$

The tangent part of the dynamics is $\frac{dv_{r,\mathrm{t}}}{dp_{\mathrm{n}}} \in (M_{\mathrm{nt}}^{-1})^T - M_{\mathrm{tt}}^{-1}\partial\psi^\star_{\mathscr{D}_\mu}(v_{r,\mathrm{t}})$: since $M_{\mathrm{tt}}^{-1} \succ 0$ it can be shown that this differential inclusion satisfies the assumptions for Theorem B.4 to apply, since $\mathscr{D}_\mu$ is a convex set. We infer that the tangential velocity $v_{\mathrm{t}}(p_{\mathrm{n}})$ exists and is unique as a Lipschitz continuous function. Consequently for any initial condition there exists a selection $\xi(p_{\mathrm{n}})$ of the set-valued subdifferential $\partial\psi^\star_{\mathscr{D}_\mu}(v_{r,\mathrm{t}})$ such that $\frac{dv_{r,\mathrm{t}}}{dp_{\mathrm{n}}} = (M_{\mathrm{nt}}^{-1})^T - M_{\mathrm{tt}}^{-1}\xi(p_{\mathrm{n}})$, and then $\frac{dv_{r,\mathrm{n}}}{dp_{\mathrm{n}}} = M_{\mathrm{nn}}^{-1} - M_{\mathrm{nt}}^{-1}\xi(p_{\mathrm{n}})$: $v_{r,\mathrm{n}}(p_{\mathrm{n}})$ exists with uniqueness as a continuously differentiable function. This does not explain how the relative velocity evolves during the shock, but is a good prerequisite for subsequent analysis. The time-discretization of (4.141) will be analyzed in Sect. 5.7.3.4.

[52] The same questions are posed for the Painlevé paradoxes described in Sect. 5.6.

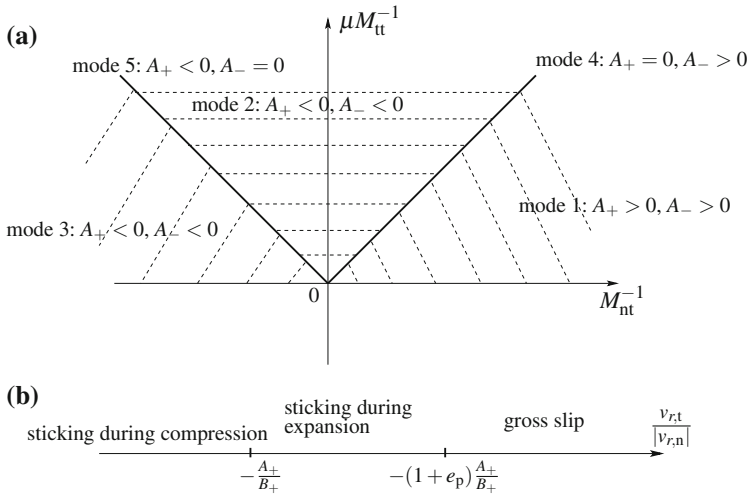

Fig. 4.18 The modes of the $v_{r,\mathrm{t}}-$dynamics

4.3.5.3 Preliminary Results for the Planar Case

Let us restrict ourselves to $v_{r,\mathrm{t}} = v_{r,\mathrm{t}_1}\mathbf{t}_1$, thus $M_{\mathrm{nt}}^{-1} = M_{\mathrm{tn}}^{-1}$ is a scalar and $\frac{dp_{\mathrm{t}}}{dp_{\mathrm{n}}} = -\mu\mathrm{sgn}(v_{r,\mathrm{t}})$, $\mathrm{sgn}(0) = [-1, 1]$. For simplicity we denote also v_{r,t_1} as $v_{r,\mathrm{t}}$. The Darboux-Keller's dynamics reduces to[53] $\frac{dv_{r,\mathrm{n}}}{dp_{\mathrm{n}}} = M_{\mathrm{nn}}^{-1} - \mu M_{\mathrm{nt}}^{-1}\mathrm{sgn}(v_{r,\mathrm{t}})$ and $\frac{dv_{r,\mathrm{t}}}{dp_{\mathrm{n}}} = M_{\mathrm{nt}}^{-1} - \mu M_{\mathrm{tt}}^{-1}\mathrm{sgn}(v_{r,\mathrm{t}})$. Suppose also that $M_{\mathrm{nn}}^{-1} - \mu M_{\mathrm{nt}}^{-1} > 0 \Leftrightarrow \left(\mu < \frac{M_{\mathrm{nn}}^{-1}}{M_{\mathrm{nt}}^{-1}}\right)$ in case $M_{\mathrm{nt}}^{-1} > 0$, or (always true if $M_{\mathrm{nt}}^{-1} < 0$): these conditions allow to avoid jamming, and guarantee a strictly increasing normal velocity. Let us adopt the notations in [1160] and denote $A_+ \triangleq M_{\mathrm{nt}}^{-1} - \mu M_{\mathrm{tt}}^{-1}$, $A_- \triangleq M_{\mathrm{nt}}^{-1} + \mu M_{\mathrm{tt}}^{-1}$, $B_+ \triangleq M_{\mathrm{nn}}^{-1} - \mu M_{\mathrm{nt}}^{-1}$, $B_- \triangleq M_{\mathrm{nn}}^{-1} + \mu M_{\mathrm{nt}}^{-1}$, where the signs $+$ and $-$ just match with the tangential velocity sign. Let us focus on the autonomous differential inclusion satisfied by $v_{r,\mathrm{t}}(p_{\mathrm{n}})$. Its vector field is equal to A_+ for $v_{r,\mathrm{t}} > 0$, and to A_- for $v_{r,\mathrm{t}} < 0$, where the surface $v_{r,\mathrm{t}} = 0$ separates the state space in two parts. We see that the discontinuity in the vector field at $v_{r,\mathrm{t}} = 0$ is $A_+ - A_- = -2\mu M_{\mathrm{tt}}^{-1} < 0$, and the convex hull of the vector fields at the discontinuity is always $[A_+, A_-]$ (hence Filippov's mathematical framework for differential inclusions may be used [397, 398]). This system has five modes which are depicted in Fig. 4.18a:

[53] Here we should once again acknowledge Routh and call the planar Darboux-Keller's dynamics, the Routh's incremental model.

1. **Mode 1** (gross slip or slip reversal): $A_+ > 0$ and $A_- > 0$, equivalently $M_{\mathrm{nt}}^{-1} > 0$ and $0 < \mu < \frac{M_{\mathrm{nt}}^{-1}}{M_{\mathrm{tt}}^{-1}}$. In this mode $\{0\} \notin [A_+, A_-]$. The tangent velocity strictly increases, so if $v_{r,\mathrm{t}}(0) < 0$ there is a time $p_{\mathrm{n},zc}$ such that $v_{\mathrm{t}}(p_{\mathrm{n},zc}) = 0$ and $v_{r,\mathrm{t}}(p_{\mathrm{n}}) > 0$ for $p_{\mathrm{n}} > p_{\mathrm{n},zc}$ provided $p_{\mathrm{n},zc}$ is smaller than the collision termination time $p_{\mathrm{n},f}$.
2. **Mode 2** (gross slip or stable sticking): $A_+ < 0$ and $A_- > 0$, equivalently $\frac{M_{\mathrm{nt}}^{-1}}{M_{\mathrm{tt}}^{-1}} \in (-\mu, \mu)$ and $\mu > 0$. In this mode $\{0\} \in [A_+, A_-]$. If $v_{r,\mathrm{t}}(0) \neq 0$, the tangent velocity strictly decreases until $v_{r,\mathrm{t}}(p_{\mathrm{n},st}) = 0$ provided that $0 < p_{\mathrm{n},st} \leq p_{\mathrm{n},f}$. If $v_{r,\mathrm{t}}(0) = 0$ sticking persists during the whole collision process. In the language of Filippov's differential inclusions, one says that the sticking state is an attractive invariant sliding surface. The $v_{r,\mathrm{t}}-$dynamics at $v_{r,\mathrm{t}} = 0$ is $\frac{dv_{r,\mathrm{t}}}{dp_{\mathrm{n}}} = \xi$, with $\xi \in [A_+, A_-]$ a selection of the set-valued right-hand side.
3. **Mode 3** (gross slip or slip reversal): $A_+ < 0$ and $A_- < 0$, equivalently $M_{\mathrm{nt}}^{-1} < 0$ and $0 < \mu < \frac{-M_{\mathrm{nt}}^{-1}}{M_{\mathrm{tt}}^{-1}}$. In this mode $\{0\} \notin [A_+, A_-]$. The tangent velocity strictly decreases, so if $v_{r,\mathrm{t}}(0) > 0$ there is a time $p_{\mathrm{n},zc}$ such that $v_{r,\mathrm{t}}(p_{\mathrm{n},zc}) = 0$ and $v_{r,\mathrm{t}}(p_{\mathrm{n}}) < 0$ for $p_{\mathrm{n}} > p_{\mathrm{n},zc}$ provided $p_{\mathrm{n},zc}$ is smaller than the collision termination time $p_{\mathrm{n},f}$. In this mode and in mode 1, the switching surface $v_{r,\mathrm{t}} = 0$ is of the crossing type.
4. **Mode 4** (gross slip or semi-sticking): $A_+ = 0$ and $A_- > 0$, equivalently $\mu = \frac{M_{\mathrm{nt}}^{-1}}{M_{\mathrm{tt}}^{-1}}$ and $M_{\mathrm{nt}}^{-1} > 0$. We have $[A_+, A_-] = [0, A_-]$. If $v_{r,\mathrm{t}}(0) \leq 0$ the sticking mode may be attained at $p_{\mathrm{n},st}$, however if $v_{r,\mathrm{t}}(0) > 0$ then $v_{r,\mathrm{t}}(p_{\mathrm{n}}) = v_{r,\mathrm{t}}(0)$ during the whole collision process.
5. **Mode 5** (gross slip or semi-sticking): $A_+ < 0$ and $A_- = 0$, equivalently $\mu = -\frac{M_{\mathrm{nt}}^{-1}}{M_{\mathrm{tt}}^{-1}}$ and $M_{\mathrm{nt}}^{-1} < 0$. We have $[A_+, A_-] = [A_+, 0]$. If $v_{r,\mathrm{t}}(0) \geq 0$ the sticking mode may be attained at $p_{\mathrm{n},st}$, however if $v_{r,\mathrm{t}}(0) < 0$ then $v_{r,\mathrm{t}}(p_{\mathrm{n}}) = v_{r,\mathrm{t}}(0)$ during the whole collision process.

Modes 2, 4 and 5 do not exist if $\mu = 0$. The next step is to analyze the system's dynamics mode by mode. Let us start the analysis with mode 2, which allows for persistent sticking in certain cases. First we notice that nonjamming and mode 2 is a possible mode, since $M^{-1} \succ 0$ which is equivalent to $\frac{M_{\mathrm{nn}}^{-1}}{M_{\mathrm{nt}}^{-1}} > \frac{M_{\mathrm{nt}}^{-1}}{M_{\mathrm{tt}}^{-1}}$. Assume that $v_{r,\mathrm{t}}(0) > 0$, then $\frac{dv_{r,\mathrm{t}}}{dp_{\mathrm{n}}} = A_+ > 0$, hence $v_{r,\mathrm{t}}(p_{\mathrm{n},st}) - v_{r,\mathrm{t}}(0) = A_+ p_{\mathrm{n},st} \Rightarrow p_{\mathrm{n},st} = \frac{-v_{r,\mathrm{t}}(0)}{A_+} > 0$. In the same way if $v_{r,\mathrm{t}}$ keeps its positive sign then the maximum compression occurs at $v_{r,\mathrm{n}}(p_{\mathrm{n},c}) = 0 \Rightarrow p_{\mathrm{n},c} = \frac{-v_{r,\mathrm{n}}(0)}{B_+}$. Thus sticking occurs during the compression phase, i.e., $p_{\mathrm{n},st} < p_{\mathrm{n},c}$, if and only if $\frac{v_{r,\mathrm{t}}(0)}{|v_{r,\mathrm{n}}(0)|} < -\frac{A_+}{B_+} = \frac{M_{\mathrm{tt}}^{-1}}{M_{\mathrm{nn}}^{-1}} \frac{\mu - \frac{M_{\mathrm{nt}}^{-1}}{M_{\mathrm{tt}}^{-1}}}{\frac{M_{\mathrm{nn}}^{-1}}{M_{\mathrm{nt}}^{-1}} - \mu}$. We have $v_{r,\mathrm{n}}(p_{\mathrm{n},st}) = v_{r,\mathrm{n}}(0) - \frac{B_+}{A_+} v_{r,\mathrm{t}}(0) < 0$. Then after $p_{\mathrm{n},st}$ sticking occurs, with $\frac{dv_{r,\mathrm{t}}}{dp_{\mathrm{n}}} = M_{\mathrm{nt}}^{-1} - \mu M_{\mathrm{tt}}^{-1} \xi$ and $\xi = \frac{M_{\mathrm{nt}}^{-1}}{\mu M_{\mathrm{tt}}^{-1}} \in (-1, 1)$. Thus $\frac{dv_{r,\mathrm{n}}}{dp_{\mathrm{n}}} = M_{\mathrm{nn}}^{-1} - \frac{(M_{\mathrm{nt}}^{-1})^2}{M_{\mathrm{tt}}^{-1}} > 0$ (by the Schur complement of $M^{-1} \succ 0$). It follows that $v_{r,\mathrm{n}}(p_{\mathrm{n},c}) - v_{r,\mathrm{n}}(p_{\mathrm{n},st}) = \left(M_{\mathrm{nn}}^{-1} - \frac{(M_{\mathrm{nt}}^{-1})^2}{M_{\mathrm{tt}}^{-1}} \right) (p_{\mathrm{n},c} - p_{\mathrm{n},st})$,

so that after some calculations $p_{\mathrm{n},c} = \frac{M_{\mathrm{nt}}^{-1} v_{r,\mathrm{t}}(0) + M_{\mathrm{tt}}^{-1} |v_{r,\mathrm{n}}(0)|}{M_{\mathrm{nn}}^{-1} M_{\mathrm{tt}}^{-1} - (M_{\mathrm{nt}}^{-1})^2}$. If Poisson's CoR is used, we infer that the collision ends at $p_{\mathrm{n},f} = (1+e_{\mathrm{p}}) \frac{M_{\mathrm{nt}}^{-1} v_{r,\mathrm{t}}(0) + M_{\mathrm{tt}}^{-1} |v_{r,\mathrm{n}}(0)|}{M_{\mathrm{nn}}^{-1} M_{\mathrm{tt}}^{-1} - (M_{\mathrm{nt}}^{-1})^2}$.

Sticking occurs during the expansion phase when $p_{\mathrm{n},st} > p_{\mathrm{n},c} = \frac{-v_{r,\mathrm{n}}(0)}{B_+}$, which occurs only if $\frac{v_{r,\mathrm{t}}(0)}{|v_{r,\mathrm{n}}(0)|} > -\frac{A_+}{B_+} = \frac{M_{\mathrm{tt}}^{-1}}{M_{\mathrm{nn}}^{-1}} \frac{\mu - \frac{M_{\mathrm{nt}}^{-1}}{M_{\mathrm{tt}}^{-1}}}{\frac{M_{\mathrm{nn}}^{-1}}{M_{\mathrm{nt}}^{-1}} - \mu}$. Then $p_{\mathrm{n},f} = (1+e_{\mathrm{p}}) \frac{-v_{r,\mathrm{n}}(0)}{B_+}$. Using $p_{\mathrm{n},st} \leq p_{\mathrm{n},f}$ we infer that sticking occurs during the expansion phase if and only if $-\frac{A_+}{B_+} < \frac{v_{r,\mathrm{t}}(0)}{|v_{r,\mathrm{n}}(0)|} \leq -(1+e_{\mathrm{p}}) \frac{A_+}{B_+}$. We also have $v_{r,\mathrm{n}}(p_{\mathrm{n},st}) = v_{r,\mathrm{n}}(0) - \frac{B_+}{A_+} v_{r,\mathrm{t}}(0)$, and $v_{r,\mathrm{n}}(p_{\mathrm{n},f}) = -\frac{B_+}{A_+} v_{r,\mathrm{t}}(0) + v_{r,\mathrm{n}}(0) + \frac{M_{\mathrm{nn}}^{-1} M_{\mathrm{tt}}^{-1} - (M_{\mathrm{nt}}^{-1})^2}{M_{\mathrm{tt}}^{-1}} \left(-\frac{1+e_{\mathrm{p}}}{B_+} v_{r,\mathrm{n}}(0) + \frac{v_{r,\mathrm{t}}(0)}{A_+} \right)$.

If $\frac{v_{r,\mathrm{t}}(0)}{|v_{r,\mathrm{n}}(0)|} > -(1+e_{\mathrm{p}}) \frac{A_+}{B_+}$ there is unidirectional slip with positive $v_{r,\mathrm{t}}(p_{\mathrm{n}})$ on $[0, p_{\mathrm{n},f}]$. We conclude that if $v_{r,\mathrm{t}}(0)$ is small, sticking occurs during the compression phase, if it increases sticking occurs during the expansion phase, and if it is large enough sticking never occurs during the impact which undergoes a gross slip mode (see Fig. 4.18b).

If one uses Newton's CoR instead, then $v_{r,\mathrm{n}}(p_{\mathrm{n},f}) = -e_{\mathrm{n}} v_{r,\mathrm{n}}(0) = e_{\mathrm{n}} |v_{r,\mathrm{n}}(0)|$. Let sticking occur during the expansion phase. There is sticking on $[p_{\mathrm{n},f}, p_{\mathrm{n},st}]$, thus $v_{r,\mathrm{n}}(p_{\mathrm{n},f}) - v_{r,\mathrm{n}}(p_{\mathrm{n},st}) = \left(M_{\mathrm{nn}}^{-1} - \frac{(M_{\mathrm{nt}}^{-1})^2}{M_{\mathrm{tt}}^{-1}} \right) (p_{\mathrm{n},f} - p_{\mathrm{n},st})$. We deduce the value for $p_{\mathrm{n},f} = \frac{(1+e_{\mathrm{n}}) M_{\mathrm{tt}}^{-1} |v_{r,\mathrm{n}}(0)| + M_{\mathrm{nt}}^{-1} v_{r,\mathrm{t}}(0)}{M_{\mathrm{nn}}^{-1} M_{\mathrm{tt}}^{-1} - (M_{\mathrm{nt}}^{-1})^2}$, which clearly is not equal to the value obtained from Poisson's CoR, in general. The final velocity $v_{r,\mathrm{n}}(p_{\mathrm{n},f})$ obtained with Poisson's CoR, is different from $-e_{\mathrm{n}} v_{r,\mathrm{n}}(0)$. It is anyway noteworthy that if $M_{\mathrm{nt}}^{-1} = 0$ (in this case the collision is said to be *balanced*, see Sect. 4.3.5.6), then the two values are the same and $e_{\mathrm{n}} = e_{\mathrm{p}}$ (when $\mu = 0$ conditions of mode 2 imply $M_{\mathrm{nt}}^{-1} = 0$ so the collision is balanced) . In the same way, in case of unidirectional slip (whatever the mode), one easily finds using the value of $p_{\mathrm{n},c}$ that $v_{r,\mathrm{n}}(p_{\mathrm{n},f}) = e_{\mathrm{p}} |v_{r,\mathrm{n}}(0)|$ so that $e_{\mathrm{p}} = e_{\mathrm{n}}$ as well. Mode 1 may be studied similarly. Let us consider this time that $v_{r,\mathrm{t}}(0) < 0$. The impulse at which the tangential velocity may vanish is $p_{\mathrm{n},zc} = \frac{-v_{r,\mathrm{t}}(0)}{A_-} > 0$. Assume that $p_{\mathrm{n},zc} < p_{\mathrm{n},c}$. Then $\frac{dv_{r,\mathrm{n}}}{dp_{\mathrm{n}}} = B_-$ on $[0, p_{\mathrm{n},zc}]$ and we deduce $v_{r,\mathrm{n}}(p_{\mathrm{n},zc}) = v_{r,\mathrm{n}}(0) - \frac{B_-}{A_-} v_{r,\mathrm{t}}(0)$ and $v_{r,\mathrm{n}}(p_{\mathrm{n},zc}) < 0 \Leftrightarrow \frac{|v_{r,\mathrm{t}}(0)|}{|v_{r,\mathrm{n}}(0)|} < \frac{A_-}{B_-}$. On $[p_{\mathrm{n},zc}, p_{\mathrm{n},c}]$ one has $v_{r,\mathrm{t}}(p_{\mathrm{n}}) - v_{r,\mathrm{t}}(p_{\mathrm{n},zc}) = A_+(p_{\mathrm{n}} - p_{\mathrm{n},zc})$, so $p_{\mathrm{n},c} = p_{\mathrm{n},zc} - \frac{v_{r,\mathrm{n}}(p_{\mathrm{n},zc})}{B_+} = \frac{2\mu M_{\mathrm{nt}}^{-1}}{A_- B_+} v_{r,\mathrm{t}}(0) + \frac{|v_{r,\mathrm{n}}(0)|}{B_+}$. Let now $p_{\mathrm{n},c} < p_{\mathrm{n},zc}$, then $p_{\mathrm{n},c} = \frac{|v_{r,\mathrm{n}}(0)|}{B_-}$. On $[p_{\mathrm{n},c}, p_{\mathrm{n},zc}]$ we have $v_{r,\mathrm{n}}(p_{\mathrm{n}}) = B_-(p_{\mathrm{n},zc} - p_{\mathrm{n},c})$ hence $v_{r,\mathrm{n}}(p_{\mathrm{n},zc}) = v_{r,\mathrm{n}}(0) - \frac{B_-}{A_-} v_{r,\mathrm{t}}(0)$. On $[p_{\mathrm{n},zc}, p_{\mathrm{n},f}]$ we have $\frac{dv_{r,\mathrm{n}}}{dp_{\mathrm{n}}} = B_-$ hence $v_{r,\mathrm{n}}(p_{\mathrm{n},f}) = v_{r,\mathrm{n}}(p_{\mathrm{n},zc}) + B_+(p_{\mathrm{n},f} - p_{\mathrm{n},zc})$. After some calculations we find that if $p_{\mathrm{n},c} < p_{\mathrm{n},zc}$ then $v_{r,\mathrm{n}}(p_{\mathrm{n},f}) = \left(\frac{B_+}{B_-}(1+e_{\mathrm{p}}) - 1 \right) |v_{r,\mathrm{n}}(0)| - \frac{2\mu M_{\mathrm{nt}}^{-1}}{A_-} v_{r,\mathrm{t}}(0)$. If $p_{\mathrm{n},c} > p_{\mathrm{n},zc}$ then $v_{r,\mathrm{n}}(p_{\mathrm{n},f}) = e_{\mathrm{p}} |v_{r,\mathrm{n}}(0)| + \frac{2\mu M_{\mathrm{nt}}^{-1}}{A_-} v_{r,\mathrm{t}}(0)$. Equalling the values obtained for the final velocity using either Poisson or Newton's CoR, we also find that if $v_{r,\mathrm{t}}(0) < 0$ and $p_{\mathrm{n},c} < p_{\mathrm{n},zc}$ then $e_{\mathrm{n}} = e_{\mathrm{p}} \frac{B_+}{B_-} - \frac{2\mu M_{\mathrm{nt}}^{-1}}{B_-} + \frac{2\mu M_{\mathrm{nt}}^{-1}}{A_-} \frac{|v_{r,\mathrm{t}}(0)|}{|v_{r,\mathrm{n}}(0)|}$. If $p_{\mathrm{n},c} > p_{\mathrm{n},zc}$ then $e_{\mathrm{n}} = e_{\mathrm{p}} - \frac{2\mu M_{\mathrm{nt}}^{-1}}{A_-} \frac{|v_{r,\mathrm{t}}(0)|}{|v_{r,\mathrm{n}}(0)|}$: *interestingly enough, we recover here that the CoRs are not independent quantities but have to satisfy some relationships, in a*

way quite similar to what we found in Sect. 4.3.3.1 *between* $e_{\mathrm{n}}, e_{\mathrm{t}}$, *friction coefficient and impulse ratio.* This will be extended to a third CoR in Sect. 4.3.6.

Remark 4.18 Let $M_{\mathrm{nt}}^{-1} > 0$ and $\mu = 0$, which is included in mode 1. Using $v_{r,\mathrm{t}}(p_{\mathrm{n}}) = v_{r,\mathrm{t}}(0) + M_{\mathrm{nt}}^{-1} p_{\mathrm{n}}$ and Poisson's CoR one finds that the tangential velocity may vanish at $p_{\mathrm{n},zc} = -\frac{v_{r,\mathrm{t}}(0)}{M_{\mathrm{nt}}^{-1}}$ which is positive if and only if $v_{r,\mathrm{t}}(0) < 0$. The condition $p_{\mathrm{n},zc} \leq p_{\mathrm{n},f}$ yields that the tangent velocity may cross zero and reverse its sign if and only if $\frac{|v_{r,\mathrm{t}}(0)|}{|v_{r,\mathrm{n}}(0)|} < (1 + e_{\mathrm{p}}) \frac{M_{\mathrm{nt}}^{-1}}{M_{\mathrm{nn}}^{-1}}$.

The other modes can be analyzed similarly. The previous analysis could be led within the framework of Routh's graphical method, introduced in Sect. 4.3.13. However there is more mathematical rigor with the analysis of the differential inclusion. It is surprizing that an apparently simple differential inclusion as in (4.141), yields (just in the planar case) such a variety of behaviors. We have not examined energetical properties. We will summarize some results about this later.

4.3.5.4 Some Results from Darboux

We now consider the three-dimensional case. Let us assume that the impact consists of a compression phase followed by an expansion phase. Results on the Darboux-Keller's dynamics have been obtained in [1116], where it is pointed out following Keller [651] that the equations governing the tangential velocity evolution in (4.138) have the general form:

$$\begin{cases} \frac{d||v_{r,\mathrm{t}}||}{dp_{\mathrm{n}}} = g(\mu, \zeta) \\ ||v_{r,\mathrm{t}}|| \frac{d\zeta}{dp_{\mathrm{n}}} = h(\mu, \zeta), \end{cases} \tag{4.143}$$

where the relative tangential velocity $v_{r,\mathrm{t}} = ||v_{r,\mathrm{t}}||(\cos(\zeta)\mathbf{t}_1 + \sin(\zeta)\mathbf{t}_2)$. The form of $g(\mu, \zeta)$ is given by noting that v_{r,t_1} and v_{r,t_2} can be rewritten as $\frac{\cos(\zeta) d||v_{r,\mathrm{t}}|| - ||v_{r,\mathrm{t}}|| \sin(\zeta) d\zeta}{dp_{\mathrm{n}}}$ and $\frac{\sin(\zeta) d||v_{r,\mathrm{t}}|| + ||v_{r,\mathrm{t}}|| \cos(\zeta) d\zeta}{dp_{\mathrm{n}}}$, respectively. Similarly for $h(\mu, \zeta)$. Darboux analyzed these expressions [327, p. 150]. He noted (see also [651, Eq. (4.17)]) that the normal impulse can be obtained eliminating $||v_{r,\mathrm{t}}||$ from (4.143) as:

$$p_{\mathrm{n}}(\zeta) = ||v_{r,\mathrm{t}}(0)|| \int_{\zeta(0)}^{\zeta} \frac{1}{h(\mu, \zeta')} \exp\left(\int_{\zeta}^{\zeta'} \frac{g(\mu, \zeta'')}{h(\mu, \zeta'')} d\zeta'' \right) d\zeta' \tag{4.144}$$

and

$$||v_{r,\mathrm{t}}|| = ||v_{r,\mathrm{t}}(0)|| \exp\left(\int_{\zeta(0)}^{\zeta} \frac{g(\mu, \zeta')}{h(\mu, \zeta')} d\zeta' \right). \tag{4.145}$$

From (4.145) Darboux stated the following which is true as long as sliding occurs at the contact point A:

Proposition 4.8 (Darboux [327]) *In the tangent plane* $(A, \mathbf{t}_1, \mathbf{t}_2)$*, there exists a curve* (C) *containing the contact point* A *and that gives the shock process law. Its radius represents the tangential percussion due to friction* $p_{\mathrm{t}} = p_{\mathrm{t}_1}\mathbf{t}_1 + p_{\mathrm{t}_2}\mathbf{t}_2$*. Its tangent has the direction of the relative velocity and its curvilinear coordinate* $s(t)$ *is* $s(t) = \mu p_{\mathrm{n}}(t) + s(0)$.

This is illustrated in Fig. 4.19. The next step studied by Darboux is about the determination of the end of the shock process. He points out that if the bodies rebound, then one possibility is to use a Poisson-like rule (but he does not name it explicitly). He concentrates on soft (purely inelastic) shocks for which the condition reduces to $v_{r,\mathrm{n}}(p_{\mathrm{n}}) = 0$ and suffices to determine $p_{\mathrm{n}}(t_f)$. First he notices that $h(\mu, \zeta) = A'\cos(\zeta) - A\sin(\zeta)$, with $A = A(\mu, \zeta)\left(= \frac{dv_{r,\mathrm{t}_1}}{dp_{\mathrm{n}}} = m_{12}^{-1} - m_{22}^{-1}\mu\cos(\zeta) - m_{13}^{-1}\sin(\zeta)\right)$ and $A' = A'(\mu, \zeta)\left(= \frac{dv_{r,\mathrm{t}_2}}{dp_{\mathrm{n}}} = m_{13}^{-1} - m_{23}^{-1}\mu\cos(\zeta) - m_{33}^{-1}\mu\sin(\zeta)\right)$ are obtained from (4.139) and (4.140). From (4.143) one has:

$$dp_{\mathrm{n}} = \frac{||v_{r,\mathrm{t}}||d\zeta}{h(\mu, \zeta)}, \tag{4.146}$$

and we conclude that since $F_{\mathrm{n}} \geq 0$ on $[0, t_f]$, ζ must vary such that $\frac{d\zeta}{h(\mu,\zeta)} \geq 0$. One important parameter of the shock process is therefore the first value of ζ, say ζ_1, such that $h(\mu, \zeta_1) = 0$. Now from (4.139) one has

$$v_{r,\mathrm{n}}(p_{\mathrm{n}}) = v_{r,\mathrm{n}}(0) + \int_{\zeta(0)}^{\zeta(p_{\mathrm{n}})} \frac{A''||v_{r,\mathrm{t}}||d\zeta}{h(\mu, \zeta)} \tag{4.147}$$

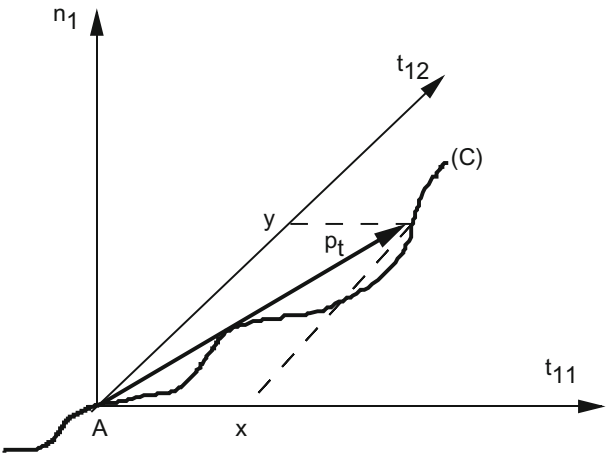

Fig. 4.19 The tangential percussion curve

where $A'' = A''(\mu, \zeta)$ $\left(= \frac{dv_{r,\mathrm{n}}}{dp_{\mathrm{n}}} = m_{11}^{-1} - m_{12}^{-1}\mu\cos(\zeta) - m_{13}^{-1}\mu\sin(\zeta)\right)$. Darboux shows that when $g(\mu, \zeta_1) \geq 0$, the equation in (4.147) possesses a root between 0 and ζ_1. In other words the shock occurs without $h(\mu, \zeta)$ attaining zero. Then the formulas (4.139) can be used to integrate the motion over the whole shock duration. Indeed in that case sliding occurs on the whole time interval $[0, t_f]$. But it may happen also that $g(\mu, \zeta)$ attains 0 at ζ_2 before $\zeta = \zeta_1$[54] and that $g(\mu, \zeta) < 0$ on $[\zeta_2, \zeta_1]$. In this case it is possible that $||v_{r,\mathrm{t}}||$ attains zero before the end of the collision, at $\zeta = \zeta_1$. Then two outcomes are possible: either $v_{r,\mathrm{t}}$ remains zero during the rest of the shock process (which is likely to occur if the initial velocity is small enough and the friction coefficient is large enough), or slip resumes after stopping. Both cases are analyzed by Darboux. Denote the normal impulse such that $||v_{r,\mathrm{t}}||(p_{\mathrm{n}}) = 0$ as $p_{\mathrm{n},e}$; $p_{\mathrm{n},e} > 0$ if $|v_{r,\mathrm{n}}|(0) > 0$. Since $||v_{r,\mathrm{t}}||(p_{\mathrm{n},e}) = 0$ (hence $\zeta(p_{\mathrm{n},e}) = \zeta_1$ from the second equation in (4.143)), it follows that

$$h(\mu, \zeta)d||v_{r,\mathrm{t}}|| = ||v_{r,\mathrm{t}}||g(\mu, \theta)d\zeta. \tag{4.148}$$

The left-hand side of (4.148) is to be interpreted as a function of $||v_{r,\mathrm{t}}||$, whereas the right-hand side is a function of ζ. Hence both sides must be equal to a constant value. Since $||v_{r,\mathrm{t}}||(p_{\mathrm{n},e}) = 0$ (hence $\zeta(p_{\mathrm{n},e}) = \zeta_1$ from the second equation in (4.143)), one deduces that on $[p_{\mathrm{n},e}, p_{\mathrm{n}}(t_f)]$, this constant value must be zero. However $g(\mu, \zeta)$ cannot be identically zero otherwise $||v_{r,\mathrm{t}}||$ would remain zero, a case now excluded. One concludes that necessarily both $d\zeta = 0$ and $h(\mu, \zeta) = 0$ on $[p_{\mathrm{n},e}, p_{\mathrm{n}}(t_f)]$. This means that the slip must occur in a constant direction and orientation in the motion following sliding vanishing. Hence Darboux proved the following:

Proposition 4.9 (Darboux [327]) *If during a soft shock process a sliding phase ends, and if sliding resumes before the end of the collision, then the direction and orientation of the relative tangential velocity on this subsequent period is constant.*

This result is also proved in [1153]. Darboux studies at the end of his seminal article, all possibilities after the sticking instant: in particular can the tangential velocity take nonzero values again ? The proof is too long to be reproduced here, it is based on the analysis of the sign of $g(\mu, \zeta)$ in terms of the roots of $h(\mu, \zeta) = 0$, and shows that in certain cases v_{t} may become zero at $p_{\mathrm{n},st}$ during the shock, while sliding motion restarts after $p_{\mathrm{n},st}$. Finally it is shown in [327] that the problem never contains any indetermination, i.e., those differential equations possess a unique solution for any initial data, a result which we have confirmed in Sect. 4.3.5.2.

4.3.5.5 Further Results

After Darboux several French Mechanicians dealt with collisions with friction [118, 337, 994]. More recently the conditions of slipping during the impact are discussed

[54] This case is precisely the one that had not been studied before [327].

in [1116]. In particular it is pointed out that the three-dimensional case analyzed for instance in [1153] is more complex than the planar case (treated in [1148], see Sect. 4.3.6). Indeed as we saw above, a problem that arises is that if slipping stops during the collision (which may happen if $v_{\mathrm{t}}(t_k^-)$ is small enough), then in a second phase of slip, the tangential velocity may not be directly opposite to the tangential impulse. An interesting work has been proposed [141, 142, 143] to study the possible outcomes of the three-dimensional impact process based on Darboux-Keller's equations as in (4.143), using dynamical systems and bifurcation theory. Their work allows one to determine the regions in parameter space in which typical behaviors occur (sliding, sticking, reversal with or without resume). The various fixed points of those dynamical equations are characterized in [143]. It is noted that the point of sticking corresponds to a singularity in the right-hand side of the differential equation, where $\sqrt{v_{\mathrm{t}_1}^2 + v_{\mathrm{t}_2}^2} \to 0$ (this term appears in the denominator of the sliding direction vector). It is known that one way to cope with such singularities is to perform a time-rescaling of the differential equations as follows. Let us consider the system:

$$\begin{cases} \dot{x}(t) = f(x(t), y(t)) \\ \dot{y}(t) = \frac{g(x(t),y(t))}{h(x(t),y(t))}, \end{cases} \tag{4.149}$$

and assume that $h(x, y) = 0$ is a codimension 1 space of the state space. Then one may study what happens in the neighborhood of this surface by studying (numerically) the associated system:

$$\begin{cases} \frac{dx}{d\tau} = f(x, y)h(x, y) \\ \frac{dy}{d\tau} = g(x, y) \end{cases} \tag{4.150}$$

in the new time scale τ, with $d\tau = \frac{1}{h(x,y)}dt$. Both vector fields in (4.149) and (4.150) are parallel. One thus expects that in the vicinity of singularities, the behavior of the system in (4.150) will bring insight on that of system in (4.149). Concerning Darboux-Keller's equations in the vicinity of sticking, one may perform $d\tau = \frac{\mu}{\sqrt{v_{\mathrm{t}_1}^2 + v_{\mathrm{t}_2}^2}} dp_{\mathrm{n}}$. Such time-rescaling has been used for instance to prove Proposition 5.27 in Chap. 5.

Darboux-Keller's dynamical equations have been investigated in [108], where μ is chosen as the bifurcation parameter. Batlle [112] starts from the Lagrange dynamics to construct (4.140) (we shall see in Sect. 4.3.5.6 how this may be done). The work in [108] concentrates on the sliding velocity flow, that is an autonomous flow (see (4.145)) given by $\frac{dv_{r,\mathrm{t}}}{dp_{\mathrm{n}}} = M_{\mathrm{nt}}^{-1} - \mu M_{\mathrm{tt}}^{-1} \frac{v_{r,\mathrm{t}}}{|v_{r,\mathrm{t}}|}$, whereas $\frac{dv_{r,\mathrm{n}}}{dp_{\mathrm{n}}} = M_{\mathrm{nn}}^{-1} - \mu (M_{\mathrm{nt}}^{-1})^T \frac{v_{r,\mathrm{t}}}{|v_{r,\mathrm{t}}|}$ for sliding and $\frac{dv_{r,\mathrm{n}}}{dp_{\mathrm{n}}} = M_{\mathrm{nn}}^{-1} - (M_{\mathrm{nt}}^{-1})^T (M_{\mathrm{tt}}^{-1})^{-1} M_{\mathrm{nt}}^{-1}$ for sticking. The qualitative behavior of this flow is investigated. The paper [111] rather focuses on the jam phenomenon. In [932] it is supposed that the impact is made of a compression and an expansion phases, then three different mappings relating $V_{A,r}(t_f)$ to initial data and M_{nn}^{-1}, M_{tt}^{-1}, M_{nt}^{-1} are calculated. The regularity of these impact laws (continuous or continuously differentiable) is shown to depend on when sticking occurs.

Let us now briefly discuss the phenomenon called *jam* in a collision process [109–111, 761, 1148].[55] It is in a sense a phenomenon similar to Painlevé paradoxes, because it is created by "too large" friction[56] (or too big normal/tangential couplings) and yields some inconsistent dynamical situations (as we saw above $\mu < \frac{M_{\rm nn}^{-1}}{M_{\rm nt}^{-1}}$ suffices to avoid such cases). Let us consider the Darboux-Keller shock dynamics in (4.141): jam occurs whenever $\frac{dv_{r,\rm n}}{dp_{\rm n}} < 0$, i.e., the tangential force creates a net decrease in $v_{r,\rm n}$. Contrary to the above, one has $M_{\rm nn}^{-1} - \mu M_{\rm nt}^{-1} < 0$, which means that $\frac{dv_{r,\rm n}}{dp_{\rm n}}(0) < 0$. Intuitively speaking, there has to be a tangential velocity mode change during the impact, for otherwise $v_{r,\rm n}(p_{\rm n})$ keeps on decreasing and it is not clear which CoR may be used to determine the collision end. Jam is analyzed for planar systems in [1148]. A detailed analysis of jam conditions in three-dimensional problems is done by Batlle and coauthors in [109–111]. It uses some results on the velocity-flow analysis of the Darboux-Keller's shock dynamics as provided in [108, 112, 141–143]. An important finding is that the collision may not consist of a compression–expansion phase, but that a second compression may start during the expansion phase (a phenomenon which is also met in multiple impacts and is called *repeated impacts*, but is more surprizing in the context of one-point collisions).

Let us analyze jam in the planar case, continuing the analysis of Sect. 4.3.5.3. We take the same initial data $v_{r,\rm n}(0) < 0$ and $v_{r,\rm t}(0) > 0$. However we assume that $M_{\rm nn}^{-1} - \mu M_{\rm nt}^{-1} < 0 \Rightarrow M_{\rm nt}^{-1} > 0$ and then $\mu > \frac{M_{\rm nn}^{-1}}{M_{\rm nt}^{-1}}$, i.e., initially $\frac{dv_{r,\rm n}}{dp_{\rm n}} < 0$. We have $\frac{dv_{r,\rm t}}{dp_{\rm n}} = M_{\rm nt}^{-1} - \mu M_{\rm tt}^{-1} < 0$ (using that $M^{-1} \succ 0$ and the Schur complement), so that $v_{r,\rm t}(p_{\rm n})$ decreases until $p_{{\rm n},st}$ with $v_{r,\rm t}(p_{{\rm n},st}) = 0$. One finds $p_{{\rm n},st} = \frac{-v_{r,\rm t}(0)}{M_{\rm nt}^{-1} - \mu M_{\rm tt}^{-1}} > 0$. On $[0, p_{{\rm n},st})$ the normal velocity decreases strictly to $v_{r,\rm n}(p_{{\rm n},st}) = v_{\rm n}(0) + (M_{\rm nn}^{-1} - \mu M_{\rm nt}^{-1}) p_{{\rm n},st} < v_{\rm n}(0) < 0$. At $p_{{\rm n},st}$ one has $\frac{dv_{r,\rm t}}{dp_{\rm n}} = 0 = M_{\rm nt}^{-1} - \mu M_{\rm tt}^{-1}\xi$ with $\xi = \frac{M_{\rm nt}^{-1}}{\mu M_{\rm tt}^{-1}}$ and $\xi \in [-1, 1]$. Since $M_{\rm nt}^{-1} - \mu M_{\rm tt}^{-1} < 0$ we have that $\mu > \frac{M_{\rm nt}^{-1}}{M_{\rm tt}^{-1}} \Rightarrow \xi \leq 1$. Therefore at $p_{{\rm n},st}$ then tangential dynamics attains its equilibrium and it stays there afterward. We infer that after $p_{{\rm n},st}$ the normal velocity increases because $\frac{dv_{r,\rm n}}{dp_{\rm n}} = M_{\rm nn}^{-1} - \mu M_{\rm nt}^{-1}\xi = M_{\rm nn}^{-1} - \frac{(M_{\rm nt}^{-1})^2}{M_{\rm tt}^{-1}} > 0$ still using the Schur complement of $M^{-1} \succ 0$. Thus there exists a maximum compression at $p_{{\rm n},c}$ and the impact termination may be calculated with Poisson's CoR.

Remark 4.19 When three-dimensional collisions are considered, the matrix $M_{\rm tt} \in \mathbb{R}^{2\times 2}$ may not be diagonal, hence some couplings may exist between the two tangent directions $\frac{dv_{r,\rm t}}{dp_{\rm n}} \in (M_{\rm nt}^{-1})^T - \mu M_{\rm tt}^{-1} \partial ||v_{\rm t}||$, where the subdifferential in that of convex analysis. So it is possible that $v_{r,{\rm t}_1}$ attains zero but not $v_{r,{\rm t}_2}$, and then through the coupling in $M_{\rm tt}^{-1}$, $v_{r,{\rm t}_1}$ takes immediately a nonzero value.

[55] Sometimes also called *dynamic wedging*, or *self-locking*, or *jamb*.

[56] However examples show that the required upperbound for the friction coefficient may not be very large, this is why we put *too large* between quotation marks.

4.3.5.6 Balanced Collisions: Kinematic and Kinetic CoRs Equivalence

Batlle has defined in [106, 107] the so-called *balanced collisions*, an example of which we already met in Sect. 4.3.1. This is a concept which generalizes collinear or central collisions. To properly define balanced collisions in the broad context of Lagrange dynamics, we use the notations in (5.1) at the very beginning of Chap. 5. Since we deal with a single unilateral constraint at a contact point A, we drop the subscript u. Using the results of Sect. 1.1 in Chap.1, we infer that at an impact time t_k we may rewrite (5.1) as:

$$M(q(t_k))[\dot{q}(t_k^+) - \dot{q}(t_k^-)] = \nabla f(q(t_k))\, p_{\mathrm{n}}(t_k) + H_{\mathrm{t}}(q(t_k))\, p_{\mathrm{t}}(t_k), \tag{4.151}$$

where we recall that $H_{\mathrm{t}}(q) \in \mathbb{R}^{n\times p}$ with $p = 1$ (2D friction) or $p = 2$ (3D friction), is obtained from the local kinematics which allows us to compute V_A as a function of the system's generalized coordinates $q \in \mathbb{R}^n$ and their derivatives, so that $v_{\mathrm{t}} = H_{\mathrm{t}}(q)^T \dot{q}$. In addition we have $v_{\mathrm{n}} = \nabla f(q)^T \dot{q}$ still due to the way the gap function is defined. Some easy manipulations then yield (the time argument t_k is dropped inside the matrix):

$$\begin{pmatrix} \sigma_{v_{\mathrm{n}}}(t_k) \\ \\ \sigma_{v_{\mathrm{t}}}(t_k) \end{pmatrix} = \begin{pmatrix} \overbrace{\nabla f(q)^T M(q)^{-1} \nabla f(q)}^{=M_{\mathrm{nn}}^{-1}(q)} & \overbrace{\nabla f(q)^T M(q)^{-1} H_{\mathrm{t}}(q)}^{=M_{\mathrm{nt}}^{-1}(q)} \\ \\ H_{\mathrm{t}}(q)^T M(q)^{-1} \nabla f(q) & \overbrace{H_{\mathrm{t}}(q)^T M(q)^{-1} H_{\mathrm{t}}(q)}^{=M_{\mathrm{tt}}^{-1}(q)} \end{pmatrix} P(t_k) \tag{4.152}$$

where $P = (p_{\mathrm{n}}, p_{\mathrm{t}_1}, p_{\mathrm{t}_2})^T$, and the notations adopted in (4.140) are recalled. If we write (4.152) along Darboux-Keller's shock dynamics, we obtain

$$\begin{pmatrix} \frac{dv_{\mathrm{n}}}{dp_{\mathrm{n}}} \\ \\ \frac{dv_{\mathrm{t}}}{dp_{\mathrm{n}}} \end{pmatrix} = \begin{pmatrix} \nabla f(q)^T M(q)^{-1} \nabla f(q) & \nabla f(q)^T M(q)^{-1} H_{\mathrm{t}}(q) \\ \\ H_{\mathrm{t}}(q)^T M(q)^{-1} \nabla f(q) & H_{\mathrm{t}}(q)^T M(q)^{-1} H_{\mathrm{t}}(q) \end{pmatrix} \begin{pmatrix} 1 \\ \\ \frac{dp_{\mathrm{t}}}{dp_{\mathrm{n}}} \end{pmatrix} \tag{4.153}$$

with constant position $q = q(t_k)$ over the impact period $[t_k, t_f], t_f > t_k$. The collision dynamics in (4.153) is, as far as a two-body impact is considered, equivalent to (4.139), and the collision matrix is equal to the one in (4.140).

Definition 4.2 A collision is said balanced if there are no couplings between the normal and the tangential directions at the impact time, i.e., the diagonal terms $H_{\mathrm{t}}(q(t_k))^T M(q(t_k))^{-1} \nabla f(q(t_k)) = 0$. In other words, the vectors $M(q(t_k)^{-1} \nabla f(q(t_k))$ and $M(q(t_k)^{-1} H_{\mathrm{t}}(q(t_k)$ are orthogonal in the kinetic metric.

Notice that this definition readily extends to the multicontact case,[57] and this is the reason why we chose to present it in a Lagrange dynamics framework.

Corollary 4.4 *Consider the collision of a body against a massive, fixed anvil (that is, take body 2 as a fixed body with infinite mass). Using the notations of Sect. 4.1.5, it follows that a collision is balanced if and only if:*

$$\begin{cases} r_3(-r_3 j_{12} + r_2 j_{13}) = r_1(-r_3 j_{23} + r_2 j_{33}) \\ r_1(-r_3 j_{22} + r_2 j_{23}) = r_2(-r_3 j_{12} + r_2 j_{13}), \end{cases} \tag{4.154}$$

where j_{kl} denote the entries of the inertia tensor of the body $\mathscr{I}^{-1}$, $1 \leq k \leq 3$, $1 \leq l \leq 3$.

Lemma 4.2 *Suppose that the collision is balanced. Then there exists a compression phase during which $v_{\mathrm{n}}(t) < 0$, which ends at a finite time t_c such that $v_{\mathrm{n}}(t_c) = 0$, and an expansion phase during which $v_{\mathrm{n}}(t) > 0$. The end of the expansion phase is determined from a restitution rule.*

The proof uses that $\frac{dv_{\mathrm{n}}}{dp_{\mathrm{n}}} = M_{\mathrm{nn}}^{-1}(q) > 0$ while the preimpact normal velocity satisfies $v_{\mathrm{n}}(t_k) < 0$. The results hold in the time scale p_{n}, and in time t provided $p_{\mathrm{n}}(t)$ is strictly increasing. In case of unbalanced collision, the shock process may be a priori more complex. For the last statement, notice that Poisson's CoR gives $p_{\mathrm{n}}(t_f) = (1 + e_{\mathrm{p}})p_{\mathrm{n}}(t_c)$.

Starting from Coulomb's friction $dp_{\mathrm{t}} \in -\mu dp_{\mathrm{n}} \frac{v_{\mathrm{t}}}{||v_{\mathrm{t}}||}$, there exists in all cases (sliding or sticking) a scalar η such that $dp_{\mathrm{n}} = \eta dv_{\mathrm{n}}$ during the collision [106]. For sliding $\eta^{sl} = \frac{1}{M_{\mathrm{nn}}^{-1} - \mu(M_{\mathrm{nt}}^{-1})^T \frac{v_{\mathrm{t}}}{||v_{\mathrm{t}}||}}$ and for sticking $\eta^{st} = \frac{1}{M_{\mathrm{nn}}^{-1} - (M_{\mathrm{nt}}^{-1})^T (M_{\mathrm{tt}}^{-1})^{-1} M_{\mathrm{nt}}^{-1}}$. During a collision process, the coefficient η keeps a constant value in the following cases: $\mu = 0$, permanent sticking, permanent sliding with constant sliding direction $\frac{v_{\mathrm{t}}}{||v_{\mathrm{t}}||}$, balanced collision. Let us now introduce the so-called Poisson coefficient of restitution. For this we need to assume that the shock is divided into a compression phase on $[t_k, t_c]$ and an expansion phase on $[t_c, t_f]$. The kinetic CoR is defined as the ratio of the contact force impulse during the expansion phase and during the compression phase:

$$e_{\mathrm{p}} = \frac{p_{\mathrm{n}}(t_f) - p_{\mathrm{n}}(t_c)}{p_{\mathrm{n}}(t_c)} \iff \frac{p_{\mathrm{n}}(t_f)}{p_{\mathrm{n}}(t_c)} = 1 + e_{\mathrm{p}} \tag{4.155}$$

It is called a *kinetic* CoR because it relates impulses, not velocities.

Proposition 4.10 *[106] Assume that the coefficient η is constant over the collision process. Then Newton e_{n} and Poisson e_{p} CoRs are equal.*

It appears from Proposition 4.10 that depending on the collision process, various definitions of the CoR may yield the same impact outcome. However this is not always the case, see Sect. 4.3.6.

[57] It is easy to check that the kinetic metric orthogonality is preserved after any diffeomorphic change of generalized coordinates.

Remark 4.20 The superball phenomenon which we briefly describe in Remark 4.23 (tangential velocity reversal in a sphere/anvil impact) cannot be modeled with the Darboux-Keller dynamics because of the assumption of infinite tangential stiffness.

4.3.6 The Energetic Coefficient of Restitution

Newton's CoR is kinematic (it relates velocities), Poisson's CoR is kinetic (it relates impulses). It is natural to think of an energetic CoR relating kinetic energies. The energetic CoR has been introduced by Routh for smooth bodies [1049] and by Boulanger in [164], see also Pérès [995, Chap. 10, pp. 326–328] where it is proved that in the frictionless case, the kinematic and the energetic CoRs are equal. It is clear nevertheless that Stronge is the one who studied it most deeply, so that the energetic CoR is often named *Stronge's coefficient*: Stronge [1148, 1149] studied the two-dimensional dynamics of a lamina striking a massive plane (i.e., body 2 in Fig. 4.1 is fixed and plays the role of a constraint, so that $v_{r,\mathrm{n}} = v_{1,\mathrm{n}} = v_{\mathrm{n}}$ with the notations chosen above). Darboux-Keller's shock dynamics is adopted. The main goal of the work is to prove that the inconsistency of some impact problems comes from neglecting the dependence of e_{n} on the slip process. The impact process is divided in compression $[0, t_c]$ with $v_{\mathrm{n}}(t_c) = 0$, and expansion phases $[t_c, t_f]$. Unidirectional slip is assumed on $[0, t_c]$. In [1148] is introduced the concept of characteristic normal impulse $p_{\mathrm{n},j} = m_j v_{\mathrm{n}}(0)$, $j = \mathrm{sign}(v_{\mathrm{t}}(0))$, and m_j is an equivalent normal mass at the contact point A: $m_j = \frac{m\rho^2}{\rho^2+x^2+j\mu xy}$, where x and y are the mass center coordinates in the local frame, and ρ is the radius of inertia. To clarify how these dynamical equations are obtained, let us recall that the equation of motion applied to the gravity center $F_{\mathrm{n}}dt = m\dot{y}$ can be rewritten as $F_{\mathrm{n}}dt = \frac{m\rho^2}{\rho^2+x^2}dv_{r,\mathrm{n}}$ in the frictionless case, hence the denomination equivalent mass. Note that $p_{\mathrm{n},j}$ corresponds to the normal impulse that terminates the compression phase. Indeed the dynamics of the system leads to $v_{\mathrm{n}}(t) = v_{\mathrm{n}}(0) - \frac{p_{\mathrm{n},j}(t)}{m_j}$ and noting that $v_{\mathrm{n}}(t_c) = 0$ the result follows. Let us note however that $p_{\mathrm{n},j}$ and $p_{\mathrm{n},-j}$ are just normalizing factors which are applied to the dynamical equations during the various phases of variation of v_{t}. It is shown that velocities variations on $[0, t_c]$ are proportional to the relative impulse $\frac{p_{\mathrm{n}}(t)}{p_{\mathrm{n},j}}$, where $p_{\mathrm{n}}(t)$ is the normal impulse at time t (indeed from the above one finds that $\frac{v_{\mathrm{n}}(t)}{v_{\mathrm{n}}(0)} = 1 - \frac{p_{\mathrm{n}}(t)}{p_{\mathrm{n},j}}$). Then two coefficients γ and τ are introduced that quantify the part $\gamma p_{\mathrm{n},j}$ of $p_{\mathrm{n},j}$ that stops slip[58] and the rest of the characteristic impulse $(\tau - \gamma)p_{\mathrm{n},-j}$ on $[t_c, t_f]$. Hence the final impulse is $p_{\mathrm{n}}(t_f) = \gamma p_{\mathrm{n},j} + (\tau - \gamma)p_{\mathrm{n},-j}$, with $\tau \geq 1$ (see Fig. 4.20b for a graphical illustration). If $0 \leq \gamma \leq 1$ slip stops on $[0, t_c]$. If $1 < \gamma$ and $\tau > \gamma$ slip stops during expansion. After the time when $v_{\mathrm{t}} = 0$, either sticking or reverse sliding occur. If the tangential velocity reverses during the shock process this yields for $\gamma p_{\mathrm{n},j} < p_{\mathrm{n}} < p_{\mathrm{n}}(t_f)$:

[58] $\gamma p_{\mathrm{n},j}$ can be calculated from the equations of motion [1153].

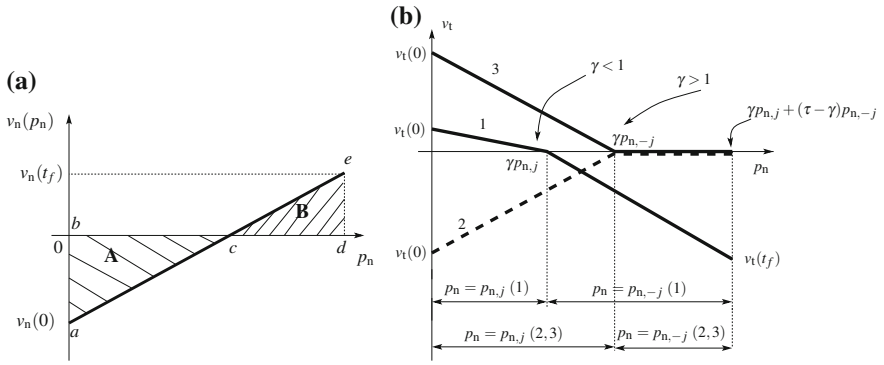

Fig. 4.20 Velocities versus normal impulse. **a** Normal relative velocity versus normal impulse. **b** Tangential velocity vs normal impulse

$$\begin{cases} \frac{v_n}{v_n(0)} = 1 - \gamma - \frac{p_n - \gamma p_{n,j}}{p_{n,-j}} \\ \frac{v_t}{v_n(0)} = j\mu m_{-j} \frac{p_n - \gamma p_{n,j}}{n_{-j} p_{n,-j}}, \end{cases} \tag{4.156}$$

where n_j is the tangential equivalent mass at the contact point: $n_j = \frac{m\rho^2}{\rho^{2+y^2+j\mu^{-1}xy}}$ From (4.156) and the expression of $p_n(t_f)$, one deduces that:

$$\begin{cases} \frac{v_n(t_f)}{v_n(0)} = 1 - \tau \\ \frac{v_t(t_f)}{v_n(0)} = \frac{(\tau - \gamma) j\mu m_{-j}}{n_{-j}}. \end{cases} \tag{4.157}$$

Both reversal and stick cases are encompassed. Then Stronge [1147] calculates the work W_n and W_t performed by the normal and tangential forces in term of P_j, γ, τ, $v_t(0)$, $v_t(t_f)$, $v_n(0)$, $v_n(t_f)$:

$$\begin{cases} W_n = \frac{1}{2} p_{n,j} v_n(0) \gamma (2 - \gamma) + \frac{1}{2} p_{n,-j} v_n(0) \left[(1 - \gamma)^2 - (\tau - 1)^2 \right] \\ W_t = \frac{1}{2} j\mu p_{n,j} v_t(0) \gamma - \frac{1}{2} j\mu p_{n,-j} v_t(t_f)(\tau - \gamma), \end{cases} \tag{4.158}$$

where $T_L = W_n + W_t$. The rest of the study is devoted to compare the three definitions of the coefficient of restitution: Newton's CoR (kinematic), Poisson's CoR (kinetic), and the energetic CoR defined as:

$$e_\star^2 = \frac{\text{elastic energy released on}[t_c, t_f]}{\text{elastic energy absorbed on}[0, t_c]}. \tag{4.159}$$

The coefficient $e_\star$ is found [1148] to be $e_\star^2 = \frac{W_{n,e}}{W_{n,c}}$ when there is no tangential compliance, where $W_{n,e}$ and $W_{n,c}$ are the works performed by the normal contact force during expansion and compression phases respectively. Such result is natural since in the absence of tangential compliance, the elastic effects are normal only.

Another way to express the energetic coefficient is

$$\int_{p_{\mathrm{n}}(t_c)}^{p_{\mathrm{n}}(t_f)} v_{\mathrm{n}}(p_{\mathrm{n}})dp_{\mathrm{n}} = -e_\star^2 \int_0^{p_{\mathrm{n}}(t_c)} v_{\mathrm{n}}(p_{\mathrm{n}})dp_{\mathrm{n}}(t), \tag{4.160}$$

where we have used the fact that the impulsion of the normal force is given by $p_{\mathrm{n}}(t) = \int_0^t F_{\mathrm{n}}(t)dt$, hence $dp_{\mathrm{n}} = F_{\mathrm{n}}(t)dt$ (see also Definition 1.1 in Chap. 1). Thus $F_{\mathrm{n}}(t)v_{\mathrm{n}}(t)dt = v_{\mathrm{n}}(p_{\mathrm{n}})dp_{\mathrm{n}}$.

Remark 4.21 In the case of the system depicted in Fig. 2.1 the impulse during the compression phase is $P_c = \int_0^{t_c} -k(x(t)-x(t_0))dt = -m\dot{x}(0)$ and during the expansion phase $P_e = \int_{t_c}^{t_1} -k(x(t) - x(t_c))dt = m\dot{x}(t_1)$ since $\dot{x}(t_c) = 0$, t_c the time of maximum compression. This suggests that the Poisson's rule may also be given a signification when $k \to +\infty$ by defining $P_c = -m\dot{x}(0^-)$ and $P_e = m\dot{x}(0^+)$. However we have also seen that the distribution theory does not allow to give a meaning to the work at impact times, because it involves the product of a discontinuous function with a Dirac measure. Hence it seems that the energetic coefficient could be given a meaning in the rigid case by replacing the work of the forces by the kinetic energy. One may split the translational velocity kinetic energy into two terms, one for normal velocities and the second for tangential ones. Then Stronge's coefficient is a constraint on the normal kinetic energy loss. Following this reasoning, let us note that the energetic coefficient may be seen as a work-energy constraint saying that $W_{\mathrm{n},e} = e_\star^2 W_{\mathrm{n},c}$. The role of friction is not really clear in these developments since W_{n} is likely to depend on friction when tangential and normal directions are dynamically coupled, although it is claimed in [1149] that $e_\star$ is independent on friction. This point of view has in fact historical roots according to which the normal process is independent of the frictional-tangential effects (this reasoning fails if tangential compliance exists, since in this case the tangential process is no longer a consequence of the normal one). However it is shown in [1154, 1155, 1291], still relying on Darboux-Keller's shock dynamics, that $e_\star$ actually depends on friction. This is obtained by calculating the work done by the normal force during the impact from a Hertz' compliant model and taking plastic deformations into account. The computation of the work done by the normal force hinges on the result presented in [1150], see Sect. 4.3.12 and (4.185) for details. For further informations on the dependence of $e_\star$ on initial conditions see Sect. 4.3.8.

Remark 4.22 It is convenient to visualize the definition of the three restitution coefficients (kinematic, kinetic and energetic) on a diagram as in Fig. 4.20a [247]. Newton's conjecture is that the ratio $\frac{ab}{de}$ is constant, Poisson's conjecture is that the ratio $\frac{dc}{cb}$ is constant, and Stronge's claim is that the ratio $\frac{\mathrm{area}(A)}{\mathrm{area}(B)}$ is constant. Note that such a representation relies on the basic assumption that the positions remain constant during

the shock. Then one has $v_{\rm n} = v_{\rm n}(0) - \frac{1}{m_j} p_{\rm n}$[59] [1148]. This is precisely this type of diagram that is used in [1148] to calculate the three different coefficients depending on the tangential velocity reversal. The simplest case is depicted in Fig. 4.20a, when there is no tangential velocity reversal. Otherwise $v_{\rm n}(p_{\rm n})$ is no longer a straight line, but is made of two segments whose slopes depend on the effective mass m_j and the initial tangential velocity.

Based on the foregoing developments, each value of the restitution coefficient (Newton, Poisson and energetic) is calculated as a function of τ, γ and P_j, depending on whether there is slip reversal or not, and the works $W_{\rm n} = \int_0^{p_{\rm n}} v_{r,{\rm n}}(p_{\rm n}) dp_{\rm n}$ and $W_{\rm t} = \int_0^{p_{\rm n}} v_{r,{\rm t}}(p_{\rm n}) dp_{\rm t}$ are computed in each case. For instance, Newton's coefficient is calculated as $e_{\rm n} = -\frac{v_{r,{\rm n}}(t_f)}{v_{r,{\rm n}}(0)}$ and is found to be $e_{\rm n} = \tau - 1$, see (4.157) above. The kinetic Poisson's coefficient of restitution in (4.155) has a value which depends on the slip process: for example when there is slip reversal and $\gamma < 1$, one finds $e_{\rm p} = \frac{\tau - 1}{(1-\gamma) + \gamma \frac{P_{{\rm n},j}}{P_{{\rm n},-j}}}$. When slip is unidirectional then $e_{\rm p} = \tau - 1$ so that in this case Newton's and Poisson's conjectures are equivalent. However when slip stops or reverses then $e_{\rm p} \neq e_{\rm n}$, which is consistent with the analysis we led in Sect. 4.3.5.3. Finally the same operation is done to compute $e_\star$: for $\gamma < 1$ and slip reversal, one finds $e_\star = \frac{(\tau-1)^2}{(1-\gamma)^2 + \gamma(2-\gamma)\frac{P_{{\rm n},j}}{P_{{\rm n},-j}}}$. For unidirectional slip, then $e_\star = \tau - 1$, which confirms that all three coefficients are the same when there is no tangential velocity reversal (the equality between $e_{\rm n}$ and $e_\star$ is established in [995, Chap. 10 §24] for the frictionless case). In summary, the coefficients are related as follows:

1. When there is slip reversal and slip stops on $[0, t_c]$:

$$e_{\rm p} = \frac{e_{\rm n} p_{{\rm n},-j}}{(1-\gamma) p_{{\rm n},-j} + \gamma p_{{\rm n},j}} \tag{4.161}$$

$$e_\star^2 = \frac{e_{\rm n}^2 p_{{\rm n},-j}}{(1-\gamma)^2 p_{{\rm n},-j} + \gamma(2-\gamma) p_{{\rm n},j}}. \tag{4.162}$$

2. When there is slip reversal and slip stops on $[t_c, t_f]$:

$$e_{\rm p} = \frac{(e_{\rm n} + 1 - \gamma) p_{{\rm n},-j} + (\gamma - 1) p_{{\rm n},j}}{p_{{\rm n},j}} \tag{4.163}$$

$$e_\star^2 = \frac{e_{\rm n}^2 p_{{\rm n},-j} - (\gamma-1)^2 (p_{{\rm n},-j} - p_{{\rm n},j})}{p_{{\rm n},j}}. \tag{4.164}$$

[59] The frames are chosen in [1148] in such a way that $v_{\rm n} > 0$ during the compression and thus initially as well, while $v_{\rm n} > 0$ during expansion. Referring to Fig. 4.1, one chooses $\mathbf{n} = \mathbf{n}_2$ and body 2 is supposed to be fixed. The minus sign in the right-hand side is to keep the non negativity of $p_{\rm n}$.

One sees from (4.157) that $\tau - 1$ equals the ratio of rebound to incident normal relative velocity components, even when sticking or reverse sliding occurs. But in this latter case the values of τ differ from one definition of the coefficient to the other (by considering a coefficient as constant, one may calculate τ in each case and indeed find different values). Since τ is defined as the remaining part of the impulse after slip stops (recall that if there is unidirectional slip and $|v_{\mathrm{t}}(o)| > |v_{\mathrm{t}}(t_f)| > 0$ then $\gamma = \tau$), it can be interpreted as a factor for evaluating the dissipation during the shock process: the larger τ, the smaller the dissipation. It happens that

$$\tau\,(\text{Poisson}) \leq \tau\,(\text{Stronge}) \leq \tau\,(\text{Newton}),$$

which explains why Poisson's conjecture is always dissipative while Newton's one may not be.

The energetic CoR is shown to be the only one that is always energetically consistent: Newton's rule can result in $T_L > 0$ when slip reverses, Poisson's rule always dissipates energy (this is consistent with the conclusions in [584]) but is claimed to be unsatisfactory since nonfrictional dissipation does not vanish when the coefficient equals 1. The above relations between the three CoRs are not very convenient. More explicit relations are calculated in [1160]. Let us recall the notations $A_+ \triangleq M_{\mathrm{nt}}^{-1} - \mu M_{\mathrm{tt}}^{-1}$, $A_- \triangleq M_{\mathrm{nt}}^{-1} + \mu M_{\mathrm{tt}}^{-1}$, $B_+ \triangleq M_{\mathrm{nn}}^{-1} - \mu M_{\mathrm{nt}}^{-1}$, $B_- \triangleq M_{\mathrm{nn}}^{-1} + \mu M_{\mathrm{nt}}^{-1}$, $\Psi_0 \triangleq \frac{B_+}{A_+}\frac{v_{\mathrm{t}}(0)}{v_{\mathrm{n}}(0)}$. Following [1159, 1160], we have:

1. If initial slip stops on $p_{\mathrm{n}} \in [0,\, p_{\mathrm{n},c}]$:
   - $e_{\mathrm{n}} = e_\star \sqrt{\frac{B_-}{B_+} + \left(1 - \frac{B_-}{B_+}\right)(1 - \Psi_0)^2}$,
   - $e_{\mathrm{p}} = e_\star \frac{\sqrt{\frac{B_-}{B_+} + \left(1 - \frac{B_-}{B_+}\right)(1-\Psi_0)^2}}{1 - \Psi_0 + \frac{B_-}{B_+}\Psi_0}$.
2. If initial slip stops on $p_{\mathrm{n}} \in [p_{\mathrm{n},c},\, p_{\mathrm{n},f}]$:
   - $e_{\mathrm{n}} = \sqrt{\left(1 - \frac{B_-}{B_+}\right)(1 - \Psi_0)^2 + \frac{B_-}{B_+} e_\star^2}$,
   - $e_{\mathrm{p}} = \left(\frac{B_+}{B_-} - 1\right)(1 - \Psi_0) + \frac{B_+}{B_-}\sqrt{\left(1 - \frac{B_-}{B_+}\right)(1 - \Psi_0)^2 + \frac{B_-}{B_+} e_\star^2}$.
3. If sliding lasts the whole collision $e_{\mathrm{n}} = e_{\mathrm{p}} = e^\star$.

If $e_\star$ is treated as *the* CoR, then e_{n} and e_{p} vary with μ and system's parameters. We see that in any case, balanced collisions (with $M_{\mathrm{nt}}^{-1} = 0$) also yield $e_{\mathrm{n}} = e_{\mathrm{p}} = e^\star$, completing Proposition 4.10. Again the works performed by the normal and the tangential forces are computed (explicit expressions are given in [1160]) to test the energetic consistency.

4.3.7 Examples

In order to illustrate some of the above developments (which may remain at a too abstract level), let us present in details simple examples.

4.3.7.1 Planar Impact of a Particle on an Anvil

The dynamics is: $\begin{cases} m d\dot{x} = m dv_{\mathrm{t}} = dp_{\mathrm{t}} \\ m d\dot{y} = m dv_{\mathrm{n}} = dp_{\mathrm{n}} \end{cases}$, with $dp_{\mathrm{t}} \in -\mu |dp_{\mathrm{n}}| \mathrm{sgn}(\dot{x})$ and $v_{\mathrm{n}}(0) < 0$. From Lemma 4.2 the shock is made of a compression phase on $[0, t_c]$ and an expansion phase on $[t_c, t_f]$. Since $dp_{\mathrm{n}} > 0$ on $(0, t_f]$ we have $dv_{\mathrm{n}} > 0 \Rightarrow v_{\mathrm{n}}$ strictly increases during the collision with $v_{\mathrm{n}} < 0$ on $[0, t_c)$ and $v_{\mathrm{n}} > 0$ on (t_c, t_f). From $v_{\mathrm{n}}(t_c) = 0$ we deduce that $p_{\mathrm{n}}(t_c)) = -m v_{\mathrm{n}}(0) > 0$ since $v_{\mathrm{n}}(0) < 0$. The expansion lasts until $v_{\mathrm{n}}(t_f) = -e_{\mathrm{n}} v_{\mathrm{n}}(0) \Rightarrow p_{\mathrm{n}}(t_f) = -m(1 + e_{\mathrm{n}}) v_{\mathrm{n}}(0)$ if Newton's CoR is used. If Poisson's CoR is used then $p_{\mathrm{n}}(t_f) = (1 + e_{\mathrm{p}}) p_{\mathrm{n}}(t_c) = -m(1 + e_{\mathrm{p}}) v_{\mathrm{n}}(0)$. If the energetic CoR is used and $\mu = 0$ then $dv_{\mathrm{t}} = 0$ so the kinetic energy is $T(\dot{x}, \dot{y}) = \frac{1}{2} m v_{\mathrm{n}}^2$, and $e_\star^2 = -\frac{T(t_f) - T(t_c)}{T(t_c) - T(0)} = -\frac{v_{\mathrm{n}}(t_f)^2 - v_{\mathrm{n}}(t_c)^2}{v_{\mathrm{n}}(t_c)^2 - v_{\mathrm{n}}(0)^2} =$, thus $v_{\mathrm{n}}(t_f)^2 = (1 + e_\star^2) v_{\mathrm{n}}(t_c)^2 + e_\star^2 v_{\mathrm{n}}(0)^2 = e_\star^2 v_{\mathrm{n}}(0)^2$ since $v_{\mathrm{n}}(t_c) = 0$. Since $v_{\mathrm{n}}(t_f) \geq 0$ (admissible postimpact normal velocity) we have $v_{\mathrm{n}}(t_f) = -e_\star v_{\mathrm{n}}(0)$ and $p_{\mathrm{n}}(t_f) = -m(1 + e_\star) v_{\mathrm{n}}(0)$. From the three expressions for $p_{\mathrm{n}}(t_f)$ we infer that if $\mu = 0$ then $e_{\mathrm{n}} = e_{\mathrm{p}} = e_\star$. This collision is balanced, thus even with friction the equality still holds.

4.3.7.2 Planar Impact of a Compound Pendulum

Consider the dynamics of a planar lamina striking a rigid rough plane, and rotating around a fixed point O, depicted in Fig. 4.21. Let us arbitrarily fix $t_k = 0$ and thus denote the shock interval as $[0, t_f]$, with t_c the time of maximum compression,

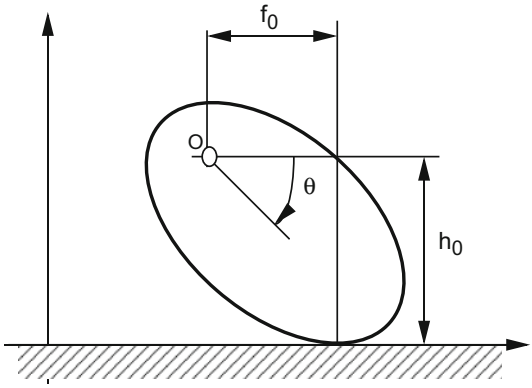

Fig. 4.21 Planar impact of a compound pendulum

(i.e., we *assume* that the collision consists in a compression phase followed by an expansion phase). The kinematics of the contact point A velocities yields:

$$v_{\mathrm{n}}(t) = f_0\dot{\theta}, \tag{4.165}$$

and:

$$v_{\mathrm{t}} = -h_0\dot{\theta}. \tag{4.166}$$

The relationships in (4.165) and (4.166) show in particular that if $f_0 \neq 0$ and $h_0 \neq 0$, $v_{\mathrm{n}}(t_c) = 0$ implies $v_{\mathrm{t}}(t_c) = 0$. Hence the end of the compression phase corresponds to the end of a sliding phase. Notice that this is a one-degree-of-freedom system, with coordinate θ. The kinetic energy loss is given by:

$$T_L = \frac{1}{2}I\left(\dot{\theta}^2(t_f) - \dot{\theta}^2(0)\right) \triangleq -\frac{1}{2}I\delta^2, \tag{4.167}$$

with $0 \leq \delta \leq \dot{\theta}(0)$, and I is the inertia with respect to O. In view of (4.165), we can write Newton's restitution law as

$$\dot{\theta}(t_f) = -e_{\mathrm{n}}\dot{\theta}(0), \tag{4.168}$$

with $e_{\mathrm{n}} = \pm\sqrt{1 - \frac{\delta^2}{\dot{\theta}(0)}}$. It follows that $v_{\mathrm{n}}(t_f) = -e_{\mathrm{n}}v_{\mathrm{n}}(0)$ and $v_{\mathrm{t}}(t_f) = -e_{\mathrm{n}}v_{\mathrm{t}}(0)$. Let us follow Brach's philosophy, i.e., let us express the relationship between the normal and the tangential percussions as $p_{\mathrm{t}} = \mu p_{\mathrm{n}}$, that is, μ is the impulse ratio (different from the friction coefficient). From the shock dynamics expressed at O one has[60]:

$$I\sigma_{\dot{\theta}}(0) = I[\dot{\theta}(t_f) - \dot{\theta}(0)] = (f_0 + \mu h_0)p_{\mathrm{n}}. \tag{4.169}$$

Thus from (4.168) one deduces $p_{\mathrm{n}} = -(1 + e_{\mathrm{n}})\frac{I\dot{\theta}(0)}{f_0+\mu h_0}$. From (4.165) and (4.166) we know that the shock process consists of a compression plus expansion phases, with two unidirectional sliding phases. This allows to apply the Thomson and Tait formula (see Sects. 4.3.12 and (4.185) for details) on each phase separately in order to express $e_\star^2 = \frac{W_{\mathrm{n},e}}{W_{\mathrm{n},c}} = \frac{[p_{\mathrm{n}}(t_f)-p_{\mathrm{n}}(t_c)][v_{\mathrm{n}}(t_f)-v_{\mathrm{n}}(t_c)]}{[p_{\mathrm{n}}(t_c)-p_{\mathrm{n}}(0)][v_{\mathrm{n}}(t_f)+v_{\mathrm{n}}(t_c)]} = \frac{[p_{\mathrm{n}}(t_f)-p_{\mathrm{n}}(t_c)]v_{\mathrm{n}}(t_f)}{p_{\mathrm{n}}(t_c)v_{\mathrm{n}}(t_f)}$. From the dynamics in (4.169) and recalling that positions are assumed to be constant during the shock, one finds also that:

$$p_{\mathrm{n}}(t_f) - p_{\mathrm{n}}(t_c) = \frac{I\dot{\theta}(t_f)}{f_0 + \mu_e h_0}, \tag{4.170}$$

and:

$$p_{\mathrm{n}}(t_c) = -\frac{I\dot{\theta}(0)}{f_0 - \mu_c h_0}. \tag{4.171}$$

[60]The shock is assumed to occur instantaneously so it is logical to denote the jump at time $t = 0$, i.e., the beginning of the collision.

One has $\mu_e = f$ and $\mu_c = -f$, where $f \geq 0$ is the Coulomb friction coefficient (recall that in Brach's approach, the impulse ratio μ may not be constant, which is the case here since there is slip reversal from one phase to the other). One deduces the following formulas relating the three coefficients of restitution[61]:

$$e_{\rm p} = \frac{p_{\rm n}(t_f) - p_{\rm n}(t_c)}{p_{\rm n}(t_c)} = \frac{f_0 + f h_0}{f_0 - f h_0} e_{\rm n}, \tag{4.172}$$

and:

$$e_\star^2 = e_{\rm n}^2 \frac{f_0 + f h_0}{f_0 - f h_0} = e_{\rm p} e_{\rm n}. \tag{4.173}$$

Notice the simplicity of the relationships in (4.172) and (4.173), due to the special kinematics of the problem (the lamina is rotating around a fixed point O), which are not supposed to hold in (4.161) through (4.164). Some bounds can be derived on the CoRs may be found from the above developments [767]. The kinetic energy loss is $T_L = -\frac{1}{2}\dot\theta(0)^2 \left(1 - e_{\rm p}^2 \frac{(f_0 - f h_0)^2}{(f_0 + f h_0)^2}\right)$, from which $e_{\rm p} \leq \frac{f_0 + \mu h_0}{f_0 - f h_0}$. Imposing $e_\star \leq 1$, one finds using the above relations between the CoRs the same upperbound for $e_{\rm p}$. For $f_0 - f h_0 > 0$ one finds $e_{\rm p} \leq \left(1 + \frac{2 f h_0}{f_0 - f h_0}\right)^{\frac{1}{2}}$, and $e_{\rm n} \leq \left(1 - \frac{2 f h_0}{f_0 + f h_0}\right)^{\frac{1}{2}}$. One also has $\frac{p_{\rm n}(t_f)}{p_{\rm n}(t_c)} = 1 + \left(\frac{f_0 + f h_0}{f_0 - f h_0}\right)^{\frac{1}{2}} e_\star$ if $f_0 - f h_0 > 0$. Finally one may relate Brach's impulse ratio $\mu = \frac{\int_0^{t_f} F_{\rm t}(t) dt}{\int_0^{t_f} F_{\rm n}(t) dt}$ to the friction coefficient f as $\mu = \frac{f(1 - e_{\rm p})}{1 + e_{\rm p}}$. It satisfies $-\frac{f_0}{h_0}(1 - \sqrt{1 - \frac{f^2 h_0^2}{f_0^2}}) \leq \mu \leq f$: the lower bound is reached when $e_\star = 1$ and the upper bound when $e_{\rm p} = 0$. It is noteworthy that the lower bound on μ may be negative.

Remark 4.23 (The Superball example) The superball behavior shows that Darboux-Keller's model cannot apply in this case, because it is a balanced collision (sphere on plane) so that no velocity reversal is possible with that model. For instance a superball that is launched diagonally toward the floor with zero spin may bounce off the floor, then strike the underside of a table, then rebound again on the floor and return to the launcher's hand [308]. Such surprizing motions have led some people (essentially physics teachers) to use it as a counterexample to usual models of impacts [308, 433, 626]. The basic assumptions are $T_L(t_k) = 0$ and no slip at the contact point. This, together with the momenta conservation equation and $v_{r,{\rm n}}(t_k^+) = -v_{r,{\rm n}}(t_k^-)$ (which is a consequence of $T_L(t_k) = 0$) is shown [433] to be sufficient to describe a typical superball motion. In fact it allows one to deduce a restitution matrix $\mathscr{E} = \begin{pmatrix} \frac{1-\alpha}{1+\alpha} & \frac{-2\alpha}{1+\alpha} & 0 \\ \frac{-2\alpha}{1+\alpha} & \frac{1-\alpha}{1+\alpha} & 0 \\ 0 & 0 & -1 \end{pmatrix}$, with $V_G(t_k^+) = \mathscr{E} V_G(t_k^-)$, and the moment of inertia $I = \alpha m r^2$. For uniform spheres $\alpha = \frac{2}{5}$, and $\mathscr{E}^2 = I_3$. Hence two bounces

[61] These expressions are valid for the considered particular shock process.

with the floor should restore the initial spin ω and tangential velocity v_t [308]. Such collisions are called *retrodirective* in [308]. Contrarily to [308, 433], use is made in [626] of an impulse ratio μ. It is shown that the rigid body theory does not permit $V_G(t_k^+)^T \mathbf{t} < 0$ and $\omega(t_k^+) < 0$. But resorting to a more sophisticated analysis of the contact/impact process as done in [828, 830] allows one to recover the experimental data. When there is sliding during the whole contact process, then those results provide the same postimpact data as the rigid body theory with $p_t = \mu p_n$. Other studies related to the superball dynamics may be found in [57, 309].

4.3.8 Other Energetical Coefficients

Ivanov [584] introduces the definition of a new restitution coefficient as follows:

$$\eta^2 = \frac{T(t_f) - T_m}{T(0) - T_m} \tag{4.174}$$

where T_m is the lowest value of the kinetic energy during the impact. If there is no friction ($\mu = 0$) then $\eta = e_\star = e_n = e_p$. The coefficient in (4.174) is calculated in [1051] using a different analysis. In [110, 111], Batlle and Cardona have shown that the basic compression–restitution process of the three-dimensional Darboux-Keller's model could be replaced by a more complex sequence of compression and restitution phases, in case of *jam* (see Sect. 4.3.5.3). They introduce the CoR $\nu = \frac{1-e_\star^2}{1+e_\star^2}$.

4.3.9 Additional Comments and Studies

[645] derives conditions under which Newton's and Poisson's coefficients are equal for two bodies colliding, relying on Darboux-Keller's shock equations. Keller's work is extended in [652] to include frictional moments. In [1122] simplifying assumptions on the shock process are made to express the ratios between Newton's e_n, Poisson's e_p and Stronge's $e_\star$ coefficients, which are shown to depend on friction, inertia and initial velocities, i.e., $\frac{e_n}{e_\star} = \frac{e_\star}{e_p} = f(\lambda, \mu, \theta)$, where μ is the Coulomb's coefficient, θ is the rod initial orientation, and λ is an inertial term. A comparison of the theoretical results obtained *via* restitution coefficients and *via* a numerical simulation based on a finite elements method is made. The results in [1122] show a clear discrepancy between the outcomes of Darboux-Keller's model (that neglects tangential compliance) and those of the finite elements code, especially in the tangential percussion. The works in [176, 603, 604, 1122] are steps in this direction. Djerassi [349] leads a complete analysis of two-body impact with the three CoRs and Coulomb's friction, using Routh's graphical method (outlined in Sect. 4.3.13). He concludes that Poisson's CoR supersedes the other two, though this is criticized

in [1158]. The work is extended to three-dimensional two-body collisions in [350], using Darboux-Keller shock dynamics. Stronge [1160] exhibits cases where $T_L > 0$ even when e_{p} is used (while it is generally believed that e_{p} always yields $T_L \leq 0$, contrarily to e_{n}). Najafabadi et al. [914] rediscover ideas in [203, Chap. 6] and [202, Chap. 6] on the use of the kinetic metric to analyze frictionless impacts (see Sect. 6.2 in Chap. 6 for more details). A general expression of the energetic CoR is calculated in [1291] for impacts with planar Coulomb friction, using an expression equivalent to (4.49) involving the normal contact forces work during compression. The CoR $e_\star$ is shown to depend on the incidence angle, as well as on friction.

Brach [176] proposes to compare theoretical predictions with rigid model and simulation results based on an approximation procedure (the Simon-Hunt-Crossley model in (2.24), plus Coulomb friction) of the impulse ratio μ, for a compliant model. The benchmark example of a lamina striking a wall is chosen. Quite interestingly, some simulation results yield $e_\star > 1$. We are tempted to relate this with the fact that in certain cases, increasing the kinematic normal coefficient (i.e., the normal velocity increases during impact) yields a decreasing T_L, because at the same time friction dissipates more energy [174, 500]. The comparative results in [176] show that there is agreement between the compliant and rigid body assumptions in most of the tested cases, although as recognized in [176] much more work is needed: in fact the problem attacked in [176] is that of studying the validity of a limit problem (rigid bodies) by comparing it with a compliant problem to see if both agree. Routh's graphical method is used in [1255] to determine the total impulse. This work is discussed by Stronge (see the same reference in our bibliography), who argues that in case of eccentric collisions or velocity slip reversal, the coefficients as introduced by [1255] depend on initial orientation of the bodies, friction, $v_{r,\mathrm{t}}(0)$ and internal sources of dissipation. Thus Newton's and Poisson's rules cannot be constant and are therefore useless in practice since they depend on too many conditions. These facts are however noted by the authors [1255] not to contradict their results. [1130] makes similar basic hypothesis about rigid dynamics. The impact process is analyzed at 0 and t_f only. T_L is expressed as a function of restitution coefficient, final and initial velocities, and normal impulse $P_{\mathrm{n},c}$ during compression phase (similarly as in [1255] the impulse is split into the two phases); two expressions are given depending on whether $v_{r,\mathrm{t}}(0) \neq 0$ (initial slip) or no slip occurs on $[0, t_f]$. Several examples are given to illustrate the results. In [21] the authors show that the coefficient of restitution for eccentric impacts depend on an "effective" approach velocity (that is the ratio of $v_{\mathrm{n}}(0)$ and a coefficient depending on kinematics and friction, similar to the "effective" masses m_j and n_j in [1148]), thus extending the results in [272, 627, 1175] on dependence of e_{n} on the approach velocity. [580] introduces in the constraints function $f(q)$ a stochastic term $g(q) \ll 1$ that represents the microstructure of the surface. A Kelvin–Voigt (linear spring-dashpot) model is used for the interaction forces. Then a probabilistic restitution rule for $\dot{q}(t_k^+)$ as a function of g and preimpact velocities is deduced, which reduces to Newton's rule for smooth surfaces. The equivalent coefficient of friction μ is also proved to be dependent of the inertia matrix $M(q)$ and preimpact velocities. No mention is made in [580] on the energetical behavior of the proposed model.

4.3.10 *Multiple Microcollisions Phenomenon: Toward a Global Coefficient*

4.3.10.1 The Falling-Rod Benchmark Example Revisited

The vibrations induced by an impact between two bodies do not always play a major role on the collision outcome. This is, for instance, the case of a sphere colliding a massive surface: a very little part of the energy is dissipated in the global deformations [556, 1034], see Sect. 4.2.4 for more details. Such is not always the case, and as guessed by G. Coriolis [302] and M. de Saint Venant [1056], body vibrations have to be taken into account in some collisions analysis. Stoianovici and Hurmuzlu [1144] present experimental results of a slender rod falling on a rigid obstacle. They show that Newton's restitution coefficient varies with the orientation of the rod at the impact time, and hence question the validity of the rigid body assumption for their system. In particular, they point out the importance of the *multiple microcollision* phenomenon that occurs at the impact time: the impact in fact involves successive small collisions between the rod's tip and the obstacle (the phenomenon had also been noticed in [1202]—calculation in closed form of a double microcollision, Chap. 12—[469, 1298] and is due to the flexibility in the bodies: the shock induces vibrations which in turn produce high frequency waves, and subsequent contact instants between the two bodies). This phenomenon is not modeled if perfect rigidity is assumed and if the period during which the microcollisions occur is taken as an instant of time t_k. However, this last assumption can be considered as legitimate due to the very short time of the multiple collisions[62] for instance, a slender rod of length 600 mm typically rebounds in 4×10^{-3} s, and with 15 microcollisions in [1144, Fig. 5e]). A rod of length 100 mm has a shock duration of 13×10^{-5} s, accompanied by two microcollisions. Those values are obtained for an angle of approach $\theta \leq 35$ deg. They are shown to depend a lot on θ. Other experimental results for aluminum bars colliding vertically a flat report shock durations that varies linearly with the bars' lengthes [319, Fig. 6], and vary between 10^{-4} s and 8×10^{-4} s for preimpact velocities between 5 and 30 m/s [319, Fig. 12]. Phenomena close to microcollisions are noticed in [1239] (named therein multiple impact spikes). The problem will therefore be to keep the rigid body assumption while introducing the vibrations in the model. The authors also show that a compliant model of the system, composed of a spring-dashpot obstacle and a rod modeled by several elements related with springs and dampers, provides numerical results close to the experimental ones.[63] We may name such approximating models *global*, in opposition with those that locate the deformations at the contact point only.

[62] Be careful: those multiple collisions are quite distinct from the multiple impact problem that we shall deal with in Chap. 6, which concern shocks with codimension ≥ 2 surfaces, i.e., at several contact/impact points. For the moment, the shocks occur at a single contact point.

[63] An open problem is the optimal choice of the number n of rigid elements that constitute the rod. This might be related to waves travel velocity in the colliding bodies. It is for instance argued in [650] that it is justified to use spring-dashpot like contact/impact models for wave travel velocities between 46 m/s and 5200 m/s, which is the case for most applications [627].

Roughly, the main conclusions from Stoianovici and Hurmuzlu's experiments are that the kinematic restitution coefficient depends on the approach angle of the bar, and that the energy dissipation is not located at the shock, but takes place in the whole rod *via* vibrations: each microcollision excites transversal modes which dissipate energy in the body's bulk. Even more this is the main source of energy dissipation. Do these experimental results tell us that rigid body impact laws should be abandoned? Certainly this is not the case, as recognized by the authors themselves, and despite some controversy [277]. In fact, the lesson is that when noncentral impacts are to occur, then great caution must be taken in applying Newton's restitution law. In the case of the falling slender rod tested in [1144], it may be argued that if the dropping surface was softer, then the restitution coefficient would not have varied as much as reported, mainly because the vibrations would have been reduced. Note, however, that we arrive here at a paradoxical situation: rigid body assumptions work better if the bodies are less rigid!

Other experimental results for the same system have been obtained in [650]. They use a different (*local*) approximating problem as depicted in Fig. 4.22: the tangential compliance is located in the rod's tip, with stiffness k_x, and the contact is modeled by a rigid sledge that slides with Coulomb friction on a rigid ground. It is shown numerically in [650] that the matching between rigid body theories (Poisson, Newton, Stronge) and this compliant contact/impact model, depends a lot on the ratio $\alpha = \frac{k_x}{k_y}$. When $\alpha \to +\infty$ ($\alpha = 100$ in [650]), the energetical coefficient provides results close to those obtained *via* the approximating model (called a *regularized* model in [650]). But Newton and Poisson conjectures do not. However, when α is small ($\alpha = 1$) then the rigid body models results drastically differ from that obtained *via* the regularized one (discrepancy $\geq 40\,\%$). Experimental results are presented in [768]. They concern a bar with length 613 mm, mass 0.0471 kg, endowed with a rubber tip, falling on a glass plane inclined by 45 degrees. The bar slides on the plane and collides a steel gate mounted on the plane. Five different configurations are tested, and the results are compared with the predicted ones. In the central impact case,

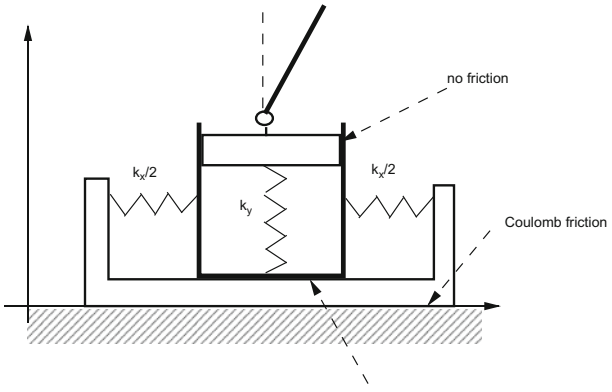

Fig. 4.22 Approximating problem for the slender rod collision

rigid body, regularized prediction and experiments fit quite well. Otherwise, they may differ significantly. Concerning the normal contact velocity, both models seem to provide similar prediction of the postimpact value. For the tangential and angular velocities, the approximating problem provides much better results. Stronge [1152] uses a similar *local* deformation model as in Fig. 4.22 to analyze the contact/impact process (sticking and slipping conditions) for low collision speeds (which allows one to state that $e_\star$ is still given by (4.160)), and colinear shocks. The numerical results are shown to fit with experimental ones in [736] concerning the maximum normal and tangential contact forces. Let us note that the experiments in [736] concern spheres colliding a heavy steel plate. It is, therefore, not surprizing that a local approximating model provides accurate results, since vibrational effects are minimized for colliding spheres [468, 469]. Notice, that vibrations in tennis rackets have been experimentally shown not to perturb the shock process [201] because their frequency is much larger that the impact duration (this contradicts Love's criterion for quasistatic impacts): hence a free racket and a clamped head provide almost the same data in terms of restitution coefficients [200]. Also since modern rackets are so stiff, the soft human hand hardly influences the shock process. Therefore, a simple application of Newton's conjecture proves to provide good predictions. The main facts that influence e_{n} are the place of the collision on the strings (e_{n} decreases at the periphery), the ball speed and the string tension.

4.3.10.2 Restitution Coefficient and Microcollisions

Let us, however, stop this digression on tennis and go back to the slender rod problem. The moral of the tale might be the following: microcollisions play a crucial role in impact phenomena between rigid bodies. They are induced by vibrations in the rod "during" the shock, and may in turn excite vibrational modes. Those vibrations are responsible for loss of energy. At the same time, the shock duration remains so small compared with the overall system's dynamics that it seems quite reasonable to keep the instantaneous feature of the process. The solution to this apparent paradoxical situation is to define a restitution coefficient that incorporates the vibrational loss of energy,, i.e., which does not only represents local phenomena at the contact point, but contains enough informations about the global behavior of the rod. We already saw such modifications of e_{n} in Sect. 4.2.4, see Sect. 4.4 for related material. Motivated by the experimental results in [1144], the authors of [557] introduced a new definition of the energetical restitution. Roughly speaking, the new coefficient is defined as follows: the kinetic energy loss during the shock is the consequence of (i) friction with the ground which produces a loss T_f, (ii) a local loss of energy at the contact point that is modeled through a coefficient $e_\star$ equal to that of Stronge, and produces a loss of kinetic energy T_l, (iii) a coefficient e_G that represents the loss of energy due to vibrations in the bar, and produces a loss of kinetic energy $T_G = e_G T(0)$, where $T(0)$ is the initial kinetic energy.

It is worth remarking that it is postulated that the energy loss due to local deformations can actually be calculated from the work of the normal force, relying on Darboux-Keller's like assumptions (in particular, there exists a time of maximum compression). Let us outline how the coefficient e_G is derived in [557]. First one considers so-called *supercritical* collisions, for which only one bounce occurs. In this case, it is possible to use analytical tools from continuous mechanics to derive an expression of the energy stored internally in the bar, as a function of two parameters $r = \frac{\cos(\theta)}{\cos\theta_c}$ and $\varepsilon^\star$. θ is the initial angle of the bar, θ_c is a so-called *critical* angle (the angle θ at which the internally stored energy is maximum, θ_c exists from experimental and numerical results [1144]), and $\varepsilon^\star$ is a parameter depending on contact properties and the bar geometry. It is noted using a finite element like model that one has:

$$\cos(\theta_c) = 0.25 + 2.61Hr \tag{4.175}$$

and

$$\varepsilon^\star = 0.67 - 2.31Hr, \tag{4.176}$$

for a certain parameter $Hr = (\frac{EI}{kL^3})^{\frac{1}{3}}$, with E the Young modulus, I the moment of inertia, L the length of the bar, and k the ground stiffness. It is clear from (4.175) that this formula is valid only for a certain range of rods, for which $0.25 + 2.61Hr \leq 1$. For such supercritical collisions ($\theta \geq \theta_c$), it is concluded that:

$$e_G = \frac{r^2}{(1-r^2)^2 + \frac{r^2}{\varepsilon^\star}}. \tag{4.177}$$

Given a bar and contact properties, one can thus compute Hr, then θ_c and $\varepsilon^\star$, and r. We recall that for the moment, the expression of e_G in (4.177) is a consequence of an analytical derivation of the stored energy in a static bar under compression, confirmed by numerical and experimental results. Now for *subcritical* collisions ($\theta \leq \theta_c$), microcollisions do exist. They drastically complicate the way one may analytically derive an expression for the stored energy. It is proposed in [557] to simply extend the form in (4.177), with a new critical angle and parameter $\varepsilon^\star$ derived from numerical and experimental curves. Similar to (4.175) and (4.176), but different, formulas for their computation are proposed. This yields a coefficient e_G for $\theta \leq \theta_c$ that completes the one in (4.177). The expression for e_G when $\theta \leq \theta_c$ is given by:

$$e_G = \max\left\{\left[\frac{\frac{1}{\bar{\varepsilon}^\star}}{\left[(1-r^2)^2 + \frac{r^2}{\bar{\varepsilon}^\star}\right]^2}\right]^2, \frac{\frac{\bar{r}^3}{(\bar{\varepsilon}^\star)^{\frac{1}{2}}}}{\left[(1-\bar{r}^2)^2 + \frac{\bar{r}^2}{\bar{\varepsilon}^\star}\right]^{\frac{3}{2}}}\right\}, \tag{4.178}$$

where $\bar{r} = \frac{\cos(\theta)}{\cos(\bar{\theta}_c)}$, $\cos(\bar{\theta}_c) = \min[0.21 + 5.32Hr, 0.38]$, $\bar{\varepsilon}^\star = \min[0.63 - 6.98Hr, 0.41]$. Let us note that due to the way the equation is tailored, the vibrational effects become zero when Hr becomes smaller than a certain value.

In summary, when a slender bar is chosen together with ground parameters, one can compute e_G from Hr, (4.175), (4.176), and (4.177), or (4.178). The total kinetic energy loss is then given by the sum of the three effects enumerated above: $T(t_f) = (1-e_G)T(0) - (1-e_{\star^2}) \int_0^{p_{\rm n}(t_c)} v_{\rm n}(p_{\rm n})dp_{\rm n} - T_f$, where we recall that $v_{\rm n}$ is the normal velocity of the contact point.

Remark 4.24 (Lowerbound for $T_L(t_k)$) It seems that only the upperbound 0 on T_L has been used as a criterion to investigate (or invent) new impact models and analysis tools. However, in a particular impact process there must also exist a lowerbound for the energy loss. For instance, two particles of masses $m_1 = m_2 = 1$ that strike satisfy the dynamical equations $(\dot{x}_1(t_k^+) - \dot{x}_2(t_k^+)) = -e_{\rm n}(\dot{x}_1(t_k^-) - \dot{x}_2(t_k^-))$ and $\dot{x}_1(t_k^+) - \dot{x}_1(t_k^-) = p_{12}$, $\dot{x}_2(t_k^+) - \dot{x}_2^- = -p_{12}$. Assume that $\dot{x}_2^- = 0$, $\dot{x}_1(t_k^-) = 1$. Then one gets $\dot{x}_1(t_k^+) - \dot{x}_2(t_k^+) = -e_{\rm n}$, $\dot{x}_1(t_k^+) = p_{12}$, $\dot{x}_2(t_k^+) = -p_{12}$. If $e_{\rm n} = 0$, $T_L(t_k)$ is maximum (see (4.41)) and we get $\dot{x}_1^+ = \dot{x}_2^+ = \frac{1}{2}$. Hence $T_{L,\max}(t_k) = -\frac{1}{4}$. It is not possible to get more loss of energy at the impact using Newton's restitution rule. In case of a shock of two bodies moving on a line one has $T_{L,\max}(t_k) = T_1(t_k^-)\frac{(1-r)^2}{1+\frac{m_1}{m_2}}$, with $r = \frac{\dot{x}_2(t_k^-)}{\dot{x}_1(t_k^-)}$ that corresponds to an inelastic shock [1028].

4.3.11 Conclusion

It appears clearly from the results in [122, 274, 278, 1001] and in the previous sections, that the tendency is to develop multiparameter (or multicoefficient) collision rules. This permits to describe exhaustively the impact outcomes and to incorporate local physical effects like normal restitution, tangential compliance, Coulomb's friction, as well as global –vibrational– effects (see Sect. 4.3.10). For instance, the need for separating the effects of dissipation due to sliding from those due to normal and tangential compliance was pointed out in [1122] by comparing results obtained from Darboux-Keller's model (no tangential compliance) and from more sophisticated models (finite elements code). As a consequence one has to identify more parameters from experimental data. Also one should keep in mind that it is not sufficient to propose a rule that has enough degrees of freedom so that it spans the whole postimpact outcome space. The parameters have to possess a physical meaning, justified by experiments or by simulations led with sophisticated (e.g., FEM) contact models. The now classical three-parameter law $(\mu, e_{\rm t0}, e_{\rm n})$ has been shown to satisfy these requirements for collisions between spheres.

4.3.12 The Thomson-and-Tait Formula

From (4.136) and Newton's third law, we have:

$$\frac{dV_{A,r}}{dt} = \left(M_1^{-1} + M_2^{-1}\right)\frac{dP}{dt}, \tag{4.179}$$

with $V_{A,r} = V_{A,1} - V_{A,2} \in \mathbb{R}^3$ is the relative spatial velocity at the contact point, and the matrices M^{-1} are defined after (4.137). Hence, the work performed by the interaction force during the collision is:

$$W_{[0,t_f]} = \int_0^{t_f} V_{A,r}(t)^T F(t)dt = \int_0^{t_f} V_{A,r}(t)^T dP(t). \tag{4.180}$$

From (4.179), it follows that:

$$W_{[0,t_f]} = \int_0^{t_f} V_{A,r}(t)^T \left(M_1^{-1} + M_2^{-1}\right)^{-1} \frac{dV_{A,r}}{dt}dt, \tag{4.181}$$

that is:

$$W_{[0,t_f]} = \frac{1}{2}\left[V_{A,r}(t)^T \left(M_1^{-1} + M_2^{-1}\right)^{-1} V_{A,r}(t)\right]_0^{t_f}. \tag{4.182}$$

From the fact that $V_{A,r}(t_f) - V_{A,r}(0) = \left(M_1^{-1} + M_2^{-1}\right)P(t_f)$ (note that $P(0) = 0$), we obtain using the identity $a^2 - b^2 = (a+b)(a-b)$[64]:

$$W_{[0,t_f]} = \frac{1}{2}P(t_f)^T \left(V_{A,r}(t_f) + V_{A,r}(0)\right). \tag{4.183}$$

In case there is no friction at the contact point, the identity in (4.183) reduces to the normal components only, and is known as the *Thomson-and-Tait formula*[65] [1192]:

$$W_{[0,t_f]} = \frac{1}{2}p_{\mathrm{n}}(t_f)[v_{r,\mathrm{n}}(t_f) + v_{r,\mathrm{n}}(0)]. \tag{4.184}$$

Remark 4.25 The formulas in (4.183) and (4.184) are closely related to the thermodynamical Clausius–Duhem inequality for collisions [414, 415], where P should represent the internal percussion (acting for instance at joints) in a system of rigid bodies.

It is pointed out in [1122] that (4.184) does not hold for any collision process when friction exists. Stronge [1150] proved that, in general, the identity in (4.183) can be extended on intervals $[t_1, t_2]$ as

[64] This is indeed the only basic mathematical tool used to derive this result.

[65] Which is also sometimes referred to as the Kelvin-and-Tait formula [592, 653].

$$W_{[t_1,t_2]} = \frac{1}{2}\left[P(t_2 - P(t_1)\right]^T \left[V_{A,r}(t_2) + V_{A,r}(t_1)\right] \tag{4.185}$$

only if slip is unidirectional on $[t_1, t_2]$. But the formula in (4.183) remains valid whatever the shock process may be since it concerns the whole shock interval. Ivanov [592] studied the conditions under which the Thomson-and-Tait's formula can be extended to the case of a body subject to several impulsive forces. Let us assume that a rigid body of mass m and mass center G is submitted to forces $F_k(t)$ on a short time interval $[0, t_f]$, each force acting at a point A_k. The goal is to investigate whether the formula

$$W_{[0,t_f]} = \frac{1}{2}\sum_k P_k(t_f)^T \left(V_{A_k,r}(t_f) + V_{A_k,r}(0)\right) \tag{4.186}$$

is valid or not. The result in [592] is that this is the case when:

- F_k is always parallel to GA_k while F_j, $j \neq k$, satisfy $F_j \perp F_k$. This may be written as
$$F_k(t) \perp \left[F_j(s) + m\left[I^{-1}(GA_j \times F_j(s)) \times GA_j\right]\right] \tag{4.187}$$
for all $s, t \in [0, t_f]$ and all $j \neq k$.
- All F_k's have constant directions and $F_k(t) = \varphi(t)l_k$ for some $\varphi(t) \in \mathbb{R}$ and $l_k \in \mathbb{R}^3$.

Those conditions apply for instance to the case of one body which collides simultaneously with two other rigid bodies at two points A_1 and A_2. Then formula (4.186) applies to represent the work of the shock interaction forces if $G_1A_1 // \mathbf{n}_1$, which in turn implies $\mathbf{n}_1 \perp \mathbf{n}_2$ (the normal directions to the tangent plane at each contact point). The second condition may be used to the case of a lamina colliding a rigid ground with Coulomb's friction. Then formula (4.184) represents the work of the normal interaction force if $GA \perp \mathbf{t}$ or if there is unidirectional sliding on $[0, t_f]$ (hence corroborating the above result by Stronge [1150]).

4.3.13 Graphical Analysis of the Shock Dynamics

4.3.13.1 Routh's Graphical Method

Let us describe a graphical analysis for two-dimensional shock processes between two rigid bodies with friction. This is due to Routh [1049, pp. 154–162] and it solves the impact problem by constructing the total impulse $P(t_f)$, in the $(p_\mathrm{n}, p_\mathrm{t})$ plane, basing on the same assumptions as the Darboux-Keller's dynamics. The arguments that follow are directly taken from Routh's book [1049]. Let us choose notations consistent with those in Sect. 4.1. Let us assume that the Galilean and local frames satisfy $\mathscr{G} = \mathscr{L}$. The gravity centers velocities are $V_{G_i} = \begin{pmatrix} \dot{X}_{i,\mathrm{t}} \\ \dot{X}_{i,\mathrm{n}} \end{pmatrix}$, $i = 1, 2$. For $t \in [0, t_f]$, the dynamics of each body is

$$\begin{cases} m_i \left(\dot{X}_{i,\mathrm{t}}(t) - \dot{X}_{i,\mathrm{t}}(0)\right) = p_{i,\mathrm{t}} \\ m_i \left(\dot{X}_{i,\mathrm{n}}(t) - \dot{X}_{i,\mathrm{n}}(0)\right) = p_{i,\mathrm{n}} \\ m_i \rho_i^2 \left(\omega_i(t) - \omega_i(0)\right) = p_{i,\mathrm{t}} X_{i,\mathrm{n}} - p_{i,\mathrm{n}} X_{i,\mathrm{t}} \end{cases} \tag{4.188}$$

plus Coulomb's friction rule. Recall that $p_{1,\mathrm{t}} = -p_{2,\mathrm{t}}$, $p_{1,\mathrm{n}} = -p_{2,\mathrm{n}}$, ρ_i is the radius of inertia. One also has:

$$\begin{cases} v_{r,\mathrm{t}} = \dot{X}_{1,\mathrm{t}} - \dot{X}_{2,\mathrm{t}} + X_{1,\mathrm{n}}\omega_1 - X_{2,\mathrm{n}}\omega_2 \triangleq S \\ v_{r,\mathrm{n}} = \dot{X}_{1,\mathrm{n}} - \dot{X}_{2,\mathrm{n}} + X_{1,\mathrm{t}}\omega_1 - X_{2,t}\omega_2 \triangleq C. \end{cases} \tag{4.189}$$

Combining both sets of equations, one finds:

$$\begin{cases} S = S_0 + m_{11}^{-1} p_{\mathrm{t}} - m_{12}^{-1} p_{\mathrm{n}} \\ C = C_0 - m_{12}^{-1} p_{\mathrm{t}} + m_{22}^{-1} p_{\mathrm{n}}, \end{cases} \tag{4.190}$$

which is the same dynamics as in (4.139) written in a different way. We chose the same notations to emphasize that the m_{ij}^{-1} are proportional to a mass inverse, and $p_{\mathrm{n}} = p_{1,\mathrm{n}}$, $p_{\mathrm{t}} = p_{1,\mathrm{t}}$. One has [1255]:

$$\begin{cases} m_{11}^{-1} = \frac{1}{m_1} + \frac{1}{m_2} + \frac{X_{1,\mathrm{n}}^2}{m_1\rho_1^2} + \frac{X_{2,\mathrm{n}}^2}{m_2\rho_2^2} \\ m_{22}^{-1} = \frac{1}{m_1} + \frac{1}{m_2} + \frac{X_{1,\mathrm{t}}^2}{m_1\rho_1^2} + \frac{X_{2,\mathrm{t}}^2}{m_2\rho_2^2} \\ m_{12}^{-1} = \frac{X_{1,\mathrm{n}}X_{1,t}}{m_1\rho_1^2} - \frac{X_{2,\mathrm{n}}X_{2,\mathrm{t}}}{m_2\rho_2^2}. \end{cases} \tag{4.191}$$

Routh's method consists of tracing the point $P = \begin{pmatrix} p_{\mathrm{t}} \\ p_{\mathrm{n}} \end{pmatrix}$ in the impulse plane that coincides geometrically with $\mathscr{L}$ (in a more pedantic language one would state that the impulse and velocity spaces are dual but both isomorphic to $\mathbb{R}^2$). Notice that $C = 0$ means that the maximum compression has been attained, while $S = 0$ means that the mode "no sliding" has been entered. The corresponding lines are denoted as MC and NS in Fig. 4.23. Assume that on $[0, \varepsilon)$, for some $\varepsilon > 0$, the bodies slide over each other. Then P moves along a straight line since $p_{\mathrm{t}} = \mu p_{\mathrm{n}}$, until P reaches NS: sliding stops at P_0. If $p_{\mathrm{t}0} < 0$ as in Fig. 4.23 (2) then sticking occurs right at $t = 0$. After P_0 is reached in Fig. 4.23 (1), two cases may occur: if $\alpha < \mathrm{Arctan}\mu$, then along MC one has $p_{\mathrm{t}} < \mu p_{\mathrm{n}}$, hence sticking continues to hold and P moves on MC in the direction of increasing p_{n}, see Fig. 4.23 (1). If $\alpha > \mathrm{Arctan}(\mu)$ then the motion of P along MC is not possible because the condition $|p_{\mathrm{t}}| < \mu p_{\mathrm{n}}$ is not true in this case. Hence there is a sticking point after which sliding continues but with reversed velocity; thus P follows a straight line whose angle β with $\mathbf{n}$ is equal to $(\widehat{AP_0, \mathbf{t}})$, see Fig. 4.23 (3). The compression line MC is actually used only to determine the impact process termination: relying on Poisson's rule, one has $p_{\mathrm{n}}(t_f) = (1 + e_{\mathrm{p}})p_{\mathrm{n}}(t_c)$, where t_c corresponds to the intersection of P with MC, and this provides the value of p_{n} at the end of the collision. One is able to calculate $p_{\mathrm{t}}(t_f)$ and $p_{\mathrm{n}}(t_f)$ for all the possible processes (sliding, sticking during the compression or the restitution phases, reverse

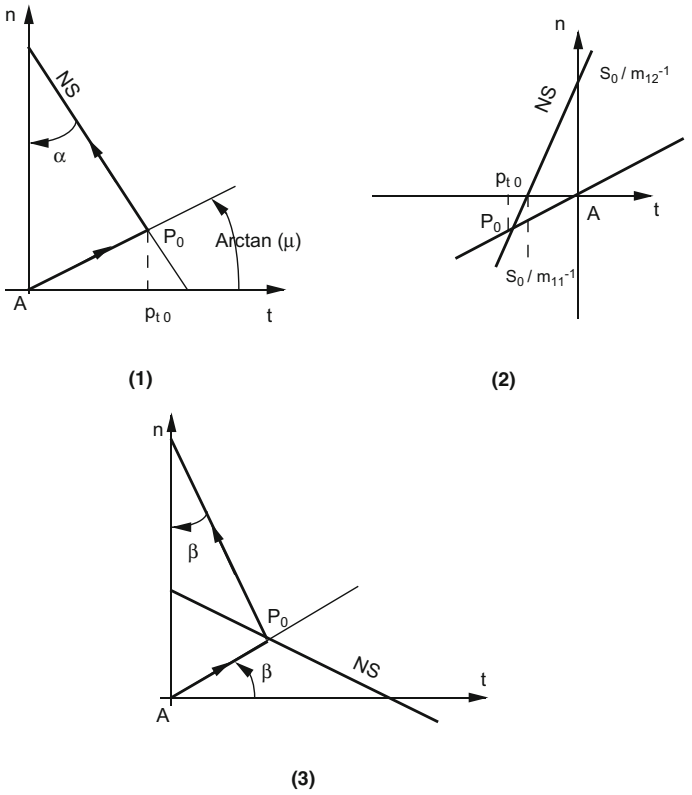

Fig. 4.23 Routh's geometric method

sliding during the compression or the restitution phases—in which cases one also uses MC). If Newton's rule is chosen the shock ends when $v_{r,\mathrm{n}}(t_k^+) = -e_{\mathrm{n}} v_{r,\mathrm{n}}(t_k^-)$ which gives the line of termination T equation: $(1 + e_{\mathrm{n}})S_0 - m_{12}^{-1} p_{\mathrm{t}} + m_{22}^{-1} p_{\mathrm{n}} = 0$. Only three cases (sliding, sticking, reverse sliding) have to be studied, since the line of maximum compression does not have to be used to determine the termination. If the line NS is attained before T, then one has to determine whether NS or the line of reverse sliding RS are followed by P.

Various other cases are described by Routh. Wang and Mason [1255] provide a detailed analysis of the impact process using Routh's method, and show that when $v_{r,\mathrm{n}}(0) = 0$, one has to resort to impulsive forces to prevent penetration. The contact modes of impact (sliding, sticking on $[0, t_c]$ or on $[t_c, t_f]$, reversed sliding on $[0, t_c]$ or on $[t_c, t_f]$) are studied as functions of the system physical and geometrical parameters. Another method is due to Pérès [995] and aims at constructing the contact point relative velocity $(v_{\mathrm{n}}, v_{\mathrm{t}})$ evolution during the shock. It happens that Routh's two-dimensional model is algebraic because the governing differential equations can be solved in closed form. Unfortunately, it cannot be extended to the three-dimensional case because the Darboux-Keller's dynamics are not integrable explicitly.

4.3.13.2 Frictionless Two-Body Collisions

One can also associate diagrams to the frictionless collision process between two rigid bodies. Such diagrams may possess a didactical usefulness since they simplify the algebraic calculations that one needs to perform to solve an impact problem [57, 234, 1005, 1028, 1146]. Basically one combines the kinetic energy constraint $T_L(t_k) \leq 0$ with the conservation of momentum equations. In the velocity space (for the one degree-of-freedom case), the former gives rise to ellipses and the latter to straight lines. The intersections between both represent the initial and final velocities. See Fig. 6.3a for an illustration.

4.4 Impacts in Flexible Structures

4.4.1 Multimodal Modeling Approach

We briefly mentioned at the end of Sect. 4.2.4, that impacts may be modeled between flexible and rigid bodies (like a rigid sphere colliding a thin flat [1314]). A "rigid body" impact model can be used even in this setting. Wagg et al. [1236, 1237] study the impact of linear systems $M\ddot{x}(t) + C\dot{x}(t) + Kx(t) = F_{imp}(t)$ with a rigid obstacle, where $M = mI$, $C = cD$ and $K = kE$ are the constant mass, damping and stiffness matrices, respectively, D is a damping coupling matrix, E is the stiffness coupling matrix, $m > 0$, $c \geq 0$, $k \geq 0$. The impact occurs at the coordinate x_i that is subjected to a unilateral constraint $x_i \geq x_s$. A system as in Fig. 4.24, which may be called an n-degree-of-freedom impact oscillator, possesses such dynamics. This dynamics intends to approximate infinite dimensional systems (like beams), hence the choice of the dimension of x, (i.e., of the number of modes) is a crucial step. A multimodal transformation is applied which puts the dynamics in the form $\ddot{q}(t) + \Xi\dot{q}(t) + \Omega q(t) = \frac{1}{m}\Psi^T F_{imp}(t)$, for some diagonal matrices Ξ and Ω, while Ψ is the orthogonal modal matrix. One has $\Omega = \frac{k}{m}\Gamma$, where Γ is the diagonal eigenvalue matrix. Suppose that the impact occurs over the time interval $[t_0, t_f]$. The energy balance (that is quite close to the so-called dissipation equality of Dissipative Systems Theory [218]) is:

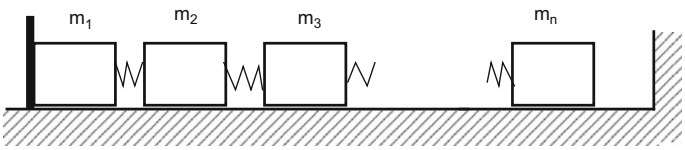

Fig. 4.24 Longitudinal shock in a bar

$$\overbrace{\frac{1}{2}m[\dot{q}(t_f)^T\dot{q}(t_f)-\dot{q}(t_0)^T\dot{q}(t_0)]}^{=T(t_f)-T(t_0)}+\overbrace{\frac{1}{2}k[q^T\Gamma q(t_f)-q^T\Gamma q(t_0)]}^{=\Delta\text{PE}}$$
$$=\underbrace{\int_{t_0}^{t_f}\dot{q}(t)^T\Psi^T F_{imp}(t)dt}_{=\Delta E_{ext}}-\underbrace{m\int_{t_0}^{t_f}\dot{q}(t)^T\Xi\dot{q}(t)dt}_{=DE}, \tag{4.192}$$

where $T(t_f)-T(t_0)$ is the kinetic energy variation during the collision, ΔPE is the elastic potential energy variation, ΔE_{ext} is the energy injected in the system by the contact force (and $\langle\dot{q},\Psi^T F_{imp}\rangle$ is the system's supply rate), DE is the energy dissipated by the system due to its internal damping. It is noteworthy that the Thomson-and-Tait's formula in Sect. 4.3.12, is a particular case of this energy balance. It is postulated that the impact obeys a restitution law of the form $\dot{x}(t_f)=\mathscr{E}\dot{x}(t_0)$, where $\mathscr{E}=\text{diag}(1,1,1\ldots,-e_\text{n},1,1,\ldots,1)$, $e_\text{n}\in[0,1]$ is the ith entry. Therefore $T(t_f)-T(t_0)=-\frac{m}{2}\dot{x}(t_0)^2(1-e_\text{n}^2)$, in a way similar to (4.41). Equalling this expression with the one obtained from (4.192), we get:

$$e_\text{n}=\sqrt{1-\frac{2}{m\dot{x}(t_0)^2}(\Delta\text{PE}+\Delta E_{ext}-\Delta E_{ext})}. \tag{4.193}$$

Vibrational effects are present in (4.193), which however does not provide a closed form of e_n. From (4.193) one sees that even if the body is perfectly elastic, (i.e., there is no internal dissipation: $\Delta E_{ext}=0$), one may have $e_\text{n}<1$ due to the body vibration. The case of a flexible beam impacting transversally a rigid obstacle is treated in [1236, 1238], while longitudinal impacts are experimentally analyzed in [1239]. The instantaneous collision assumption is justified experimentally for longitudinal impact of a cantilever beam against a rigid obstacle in [1239], where it is shown that the system spends less than 2.5 % of the total time in the impact phase. Such multimodal approach of impacts, is applied to cantilever beams colliding transversally a rigid obstacle at $x=b$, with harmonic excitation. Experiments are made in [1238]. The above restitution law approximates $\dot{u}(b,t_k^+)=-e_\text{n}\dot{u}(b,t_k^-)$ and $\dot{u}(s,t_k^+)=-e_\text{n}\dot{u}(s,t_k^-)$, $s\neq b$, when $u(b,t_k)=a$. Contrarily to [870, 1097] who assume that the contact occurs during a sufficiently large time so that the modal properties of the beam are changed during the impact, in [1238] it is assumed that the impact is so short that mode shapes of the beam during collision are not those of a clamped-pinned beam. A Galerkin approach is used to reduce the Euler–Bernoulli beam equation $\frac{EI}{L^4}\frac{\partial^4 u}{\partial s^4}+\eta\frac{\partial u}{\partial t}+\rho A\frac{\partial^2 u}{\partial t^2}=f(s,t)$, $u<a$. Comparisons between experimental and numerical results show good agreement [1238, Fig. 7]. Interestingly enough, the simulations show the existence of accumulation of impacts before the beam sticks on the obstacle, a behavior commonly observed in the bouncing ball system.

4.4.2 *Infinite Dimensional System Approach*

Infinite dimensional models stemming from continuum mechanics and elasticity with unilateral constraints have been investigated, see, e.g., [83, 711, 1067, 1068, 1203]. The usual basic assumptions are that the stress components other than the axial one are negligible, and that the axial stress is uniform across the rod's cross section [1203]. The longitudinal impact of two bars is treated in [1203, §169], as well as the impact of a bar clamped at one end and struck by a mass at the other end. It may be assumed that both bodies are elastic [1058], or that one perfectly rigid body hits an elastic body [1072]. Inspired by [711], Shi [1107] computes the restitution coefficient of an elastic rod acted upon by a force F_{ext} and axially colliding a rigid obstacle.

Theorem 4.1 *[1107] Let $u(x,t)$ be the displacement field of the rod, with the initial data $u(x,0)=0$, $u_t(x,0)=-v_0$. At $x=0$ the Signorini conditions $\sigma(0,t)\leq 0$, $u(0,t)\geq -h$, $\sigma(0,t)[u(0,t)+h]=0$ are imposed, where $\sigma(x,t)$ is the stress field and h is the initial distance between the rod and the obstacle. The rod at rest has total length l. One defines $t^-=\inf\{t|u(0,t)=-h\}$ as the time of the first impact and $t^+=\inf\{t|t\geq t^-, u(0,t)>-h\}$ as the time of first rebound. It is assumed that $t^-=\frac{\sqrt{v_0^2+2F_{ext}h}-v_0}{F_{ext}}<\frac{2l}{c}$, where $c=\sqrt{\frac{E}{\rho}}$, E is the Young's modulus, ρ is the constant density. Then $e_{\mathrm{n}}\overset{\Delta}{=}-\frac{\lim_{t\to t^+,t>t^+}u_t(0,t)}{\lim_{t\to t^-,t<t^-}u_t(0,t)}=\frac{\max[0;c\sqrt{v_0^2+2F_{ext}h}-2F_{ext}l]}{c\sqrt{v_0^2+2F_{ext}h}}$. In case $F_{ext}=0$ (free impact), the impact duration is equal to $\frac{2l}{c}$, and $e_{\mathrm{n}}=1$. If $v_0^2\leq F_{ext}(\frac{4l^2}{c^2}-2h)$ then $e_n=0$.*

It is interesting to notice that for a large enough external force, the bar remains stuck on the obstacle. There exists a variety of cases where the bar rebounds with $e_{\mathrm{n}}<1$: part of the kinetic energy is trapped in the bar through vibrations. Obviously, if the rod is clamped at one end, the results are likely to change.

Remark 4.26 It may be argued that the notion of restitution loses its meaning for the impact of a bar in the longitudinal direction: consider a system with constant total mass as in Fig. 4.24 and let $n\to+\infty$: then $m_n\to 0$ and the dynamical effects of collisions disappear (this is not the case for transversal impacts). Glocker gives a nice interpretation of this effect in [454, §5.7], where he shows that the kinetic angle between the generalized preimpact velocity of the approximated bar in Fig. 4.24 and the unilateral constraint normal, is equal to $\frac{-\dot{q}(t_k^-)^T M(q(t_k))\nabla f(q(t_k))}{\sqrt{\dot{q}(t_k^-)^T M(q(t_k))\dot{q}(t_k^-)}\sqrt{\nabla f(q(t_k))^T M(q(t_k))\nabla f(q(t_k))}}=\frac{1}{\sqrt{n}}$. Hence, as the number of elements $n\to+\infty$, the impact becomes tangential and the contact impulse vanishes.

4.4.3 Further Reading

Narabayashi et al. [918] study the impact of a 1-D (longitudinal) elastic flexible bar with a (transversal) both-ends-supported elastic beam. Using the eigenfunctions of both elastic bodies, which allow one to derive the elastic deformation in the bar and the beam's deflection during collision as infinite series, they derive an expression for the apparent CoR which is defined from the bar's gravity center velocity. Depending on collision parameters, this apparent CoR may range from 0.25 to 1. Multiple microcollisions are analyzed. Bakr et al [77, 660] study the behavior of general multibody systems with both rigid and flexible parts under an impulsive action, using a model based on a finite element procedure. They use a kinematic restitution coefficient to describe the shock process. As an example of possible application, they analyze the dynamics of an aircraft at touch down impact. Other works on the topic and using a restitution coefficient can be found in [544, 659, 661, 1295, 1298]. The theoretical results are validated in [957, 1041]. The so-called Nonlinear Normal Modes approach (which is an extension of the classical Linear Normal Modes [655], as nontrivial periodic solutions of the autonomous dynamical system) is used in [707] to analyze the dynamics of a 1-D rod clamped at one end and hitting a rigid wall at the other end, and of a turbomachinery blade in contact at its tip edge. The applicability of the prediction based on the use of a restitution coefficient is examined in [1298]. These studies show that for the considered systems, experimental and theoretical results fit quite well. Other studies use compliant models of the contact-impact process [273, 662, 1295, 1299]. In [1295], Yigit compares numerically and experimentally three different models (restitution coefficient, spring-dashpot and Hertzian like) and concludes that they provide quite similar results. The Hertzian-like model possesses the advantage that its coefficients are computable from the physical characteristics of the materials. The applications in switches, connectors and electrical contacts are also a strong motivation for contact/impact models study. Indeed contacts provide a major source of failures in automotives, aircraft, machine tools, computers and consumer electronics. Since such electromechanical contacts are often accompanied by large deformations of the bodies, the models used may be deformable slender rods contacting massive tables [800]. Some other electromechanical systems with more complex kinematics motivate the development of specific software packages taking into account their nonsmooth features [1].

4.5 General Comments

All through this chapter as well as Chap. 2, restitution coefficients have been studied and often associated with some constitutive contact/impact models (viscoelastic, elastoplastic, adhesive, with friction, etc.). Nothing hampers that different constitutive models yield the same restitution coefficient for particular parameters tuning. As alluded to before, a restitution coefficient is a parameter that is meant to incor-

porate so many different physical effects occurring during the collision that such a fact should not come as a surprise. Impact models should not be validated only with restitution coefficients, but also with the collision duration, impact force history and maximum value, dependence on initial impacting velocity, etc. In case of a multiple impact, wave effects may also play a crucial role and should be predicted properly. Multiple impacts are the topic of Chap. 6.

Chapter 5
Nonsmooth Lagrangian Systems

This chapter is dedicated to Lagrangian dynamical systems subject to bilateral and unilateral constraints, which we may name *Complementarity Lagrangian Systems*. It starts with the analysis of the contact problem, for perfect bilateral and unilateral constraints. Then Moreau's sweeping process is introduced in detail. Coulomb's model of friction is described, and complementarity problems and systems are presented with examples from Mechanics, Circuits and Optimal Control. The chapter continues with the analysis of the contact problem when friction acts on the system, with a particular emphasis on the so-called Painlevé paradoxes. An introduction to various existing methods for the numerical integration of nonsmooth systems with complementarity relations ends the chapter.

5.1 Lagrange Dynamics with Multiple Constraints

The class of Lagrangian systems that we are going to deal with in the sequel is the following one, with $q(0) = q_0$, $\dot{q}(0^-) = \dot{q}_0$:

$$
\begin{aligned}
&(a)\ \ M(q)\ddot{q} + C(q,\dot{q})\dot{q} + G(q) = \nabla f(q,t)\lambda_{\mathrm{n},u} + \nabla h(q,t)\lambda_{\mathrm{n},b} + H_{\mathrm{t},u}(q,t)\lambda_{\mathrm{t},u} \\
&\qquad\qquad + H_{\mathrm{t},b}(q,t)\lambda_{\mathrm{t},b} + F_{ext} \\
&(b)\ \ 0 \le f(q,t) \perp \lambda_{\mathrm{n},u} \ge 0, \quad f(q_0,0) \ge 0 \\
&(c)\ \ h(q,t) = 0 \\
&(d)\ \ \text{Impact law and friction law}
\end{aligned}
\tag{5.1}
$$

B. Brogliato, *Nonsmooth Mechanics*, Communications and Control Engineering,
DOI 10.1007/978-3-319-28664-8_5

where: q is a vector of n generalized coordinates, $M(q) = M(q)^T \succeq 0$ is the inertia matrix, $C(q, \dot{q})\dot{q}$ contains the Coriolis and centrifugal torques, $G(q)$ contains torques that derive from a potential, i.e., $G(q) = \frac{\partial U}{\partial q}(q)$ for some differentiable potential function $U(q)$, F_{ext} represents external forces as well as possible dissipative terms (like Rayleigh dissipation), $f : \mathbb{R}^n \times \mathbb{R}_+ \to \mathbb{R}^{m_u}$, each unilateral constraint $f_i(\cdot)$ is as in Definition 1.8, $h : \mathbb{R}^n \times \mathbb{R}_+ \to \mathbb{R}^{m_b}$ are bilateral constraints, and the total number of constraints $m = m_u + m_b$. The tangential effects are incorporated through the matrices $H_{\mathrm{t},u}(q, t)$ and $H_{\mathrm{t},b}(q, t)$. It is assumed that the initial data are coherent with the bilateral constraints, i.e., $h(q_0, 0) = 0$ and $\dot{h}(q_0, \dot{q}_0, 0) = 0$. The multipliers $\lambda_{\mathrm{n},u}$, $\lambda_{\mathrm{n},b}$, $\lambda_{\mathrm{t},u}$, and $\lambda_{\mathrm{t},b}$ account for the contact forces in the normal and tangential directions, respectively. Line (b) imposes complementarity conditions between $f(q, t)$ and $\lambda_{\mathrm{n},u}$, hence excluding gluing and magnetic effects. Impact models have already been studied in Chap. 4 for two rigid bodies colliding. Other models that apply to systems with several points colliding at the same time will be analyzed in this chapter and in Chap. 6. Friction will mainly consist of Coulomb's friction model, both for smooth and impacting motions. Let us summarize the general methodology used to obtain the unilateral part of the right-hand side of (5.1) (a) for a multibody system:

- (i) Determine potential contact/impact points using (4.9), providing m_u pairs $(A_{1,i}, A_{2,i})$;
- (ii) Define the local kinematics frames $(A_i, \mathbf{n}_i, \mathbf{t}_{1,i}, \mathbf{t}_{2,i})$ at each contact[1];
- (iii) Calculate the gap functions $f_i(q)$, $1 \le i \le m_u$, using the signed distances (4.17), so that the normal component of the relative velocities is given by $v_{\mathrm{n},u,i} = \nabla f_i(q)^T \dot{q}$;
- (iv) Calculate the matrices $H_{\mathrm{t},u,i}(q)$ from the tangential relative velocities $v_{\mathrm{t},i} = H_{\mathrm{t},u,i}(q)^T \dot{q}$ at each contact.
- (v) Group the normal components $\lambda_{\mathrm{n},u,i}$ $(= F_{\mathrm{n},i})$ of the contact forces in the frames $(A_i, \mathbf{n}_i, \mathbf{t}_{1,i}, \mathbf{t}_{2,i})$ into an m_u-vector $\lambda_{\mathrm{n},u}$, and the tangential components $\lambda_{\mathrm{t},u,i}$ $(= (F_{\mathrm{t}_1,i}, F_{\mathrm{t}_2,i}))$ into a $2m_u$ (three-dimensional) case or an m_u-vector (two-dimensional case) $\lambda_{\mathrm{t},u}$. Therefore, we obtain after suitable renumbering of the components, the following vectors: $\lambda_{\mathrm{t},b} = (F_{1,\mathrm{t}_1}, F_{1,\mathrm{t}_2}, \ldots, F_{m_b,\mathrm{t}_1}, F_{m_b,\mathrm{t}_2})^T$, $\lambda_{\mathrm{t},u} = (F_{m_b+1,\mathrm{t}_1}, F_{m_b+1,\mathrm{t}_2}, \ldots, F_{m,\mathrm{t}_1}, F_{m,\mathrm{t}_2})^T$, $\lambda_{\mathrm{n},b} = (\lambda_{1,\mathrm{n}}, \lambda_{2,\mathrm{n}}, \ldots, \lambda_{m_b,\mathrm{n}})^T$, while finally $\lambda_{\mathrm{n},u} = (\lambda_{m_b+1,\mathrm{n}}, \lambda_{m_b+2,\mathrm{n}}, \ldots, \lambda_{m,\mathrm{n}})^T$.
- (vi) From the invariance principle of Sect. 3.2, the generalized contact force virtual power (outside impact times) $\mathscr{P}^{cont} = \langle F^{cont}, \dot{q} \rangle = \langle v_{\mathrm{n},u}, \lambda_{\mathrm{n},u} \rangle + \langle v_{\mathrm{t},u}, \lambda_{\mathrm{t},u} \rangle = \langle \nabla f(q)^T \dot{q}, \lambda_{\mathrm{n},u} \rangle + \langle H_{\mathrm{t},u}(q)^T \dot{q}, \lambda_{\mathrm{t},u} \rangle = \langle \dot{q}, \nabla f(q) \lambda_{\mathrm{n},u} \rangle + \langle \dot{q}, H_{\mathrm{t},u}(q) \lambda_{\mathrm{t},u} \rangle$. Since this equality has to be satisfied for all $\dot{q}$, one deduces that $F^{cont} = \nabla f(q) \lambda_{\mathrm{n},u} + H_{\mathrm{t},u}(q) \lambda_{\mathrm{t},u}$.

The steps (iii) and (iv) may not be trivial for bodies with a complex geometry, and efficient numerical tools may be necessary for contact detection and gap function calculations.

[1] The index i refers here to the contact number, not to the body 1 or 2 as in Sect. 4.1.2 and Fig. 4.1.

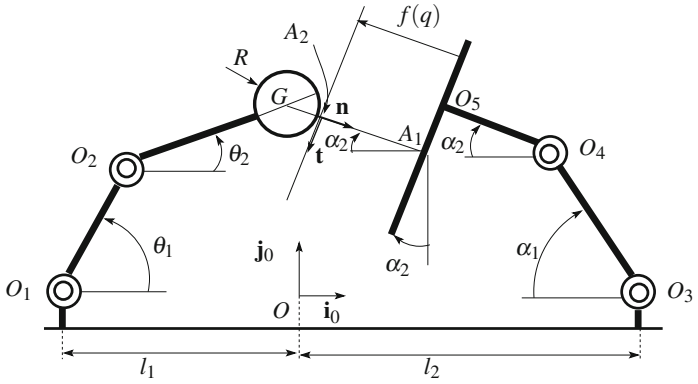

Fig. 5.1 A system with two manipulators

$\rightsquigarrow$ *The Lagrangian dynamics in (5.1) is a very complex nonsmooth dynamical system. It raises problems in Mathematics (existence, uniqueness, continuous dependence), Mechanics (impact and friction modeling), Control (stability, stabilization, trajectory tracking), Numerical Analysis (discrete-time methods convergence, order, precision), Bifurcation Theory, and so on.*

In this section we tackle only the frictionless case. The contact problem when Coulomb's friction is taken into account is treated in Sect. 5.5.

Example 5.1 Let us consider the system in Fig. 5.1. Here $q = (\theta_1, \theta_2, \alpha_1, \alpha_2)^T$. The unilateral constraint is between the sphere held by the left robot, and the plate held by right robot. We have $OG = \begin{pmatrix} -l_1 + l\cos(\theta_1) + (l+R)\cos(\theta_2) \\ l\sin(\theta_1) + (l+R)\sin(\theta_2) \end{pmatrix}$, $GA_2 = \begin{pmatrix} R\cos(\alpha_2) \\ -R\sin(\alpha_2) \end{pmatrix}$, $OO_5 = \begin{pmatrix} l_2 - l\cos(\alpha_1) - l\cos(\alpha_2) \\ l\sin(\alpha_1) + l\sin(\alpha_2) \end{pmatrix}$, in the Galilean frame $(O, \mathbf{i}_0, \mathbf{j}_0)$. The coordinates of A_1 may be obtained from the intersection of the two straight lines $y_{A_1} = -\tan(\alpha_2)x_{A_1} + (y_G + \tan(\alpha_2)x_G)$ and $y_{A_1} = \frac{1}{\tan(\alpha_2)}x_{A_1} + \left(y_{O_5} - \frac{x_{O_5}}{\tan(\alpha_2)}\right)$. We deduce $x_{A_1} = (x_{O_5} + (y_G - y_{O_5})\tan(\alpha_2) + x_G\tan(\alpha_2)^2)\cos(\alpha_2)^2$, and $y_{A_1} = \sin(\alpha_2)\cos(\alpha_2)(-x_{O_5} + (y_{O_5} - y_G)\tan(\alpha_2) - x_G\tan(\alpha_2)^2) + y_G + x_G\tan(\alpha_2)$. This allows us to calculate the vector $A_2A_1 = \begin{pmatrix} x_{A_1} - x_{A_2} \\ y_{A_1} - y_{A_2} \end{pmatrix}$. From the fact that $\mathbf{n} = (\cos(\alpha_2), -\sin(\alpha_2))^T$, we can apply (4.17) to deduce the signed distance $f(q) = (x_{A_1} - x_{A_2})\cos(\alpha_2) - (y_{A_1} - y_{A_2})\sin(\alpha_2) \geq 0$. We can also define the tangent vector in the local frame as $\mathbf{t} = (-\sin(\alpha_2), -\cos(\alpha_2))^T$, and deduce from $(A_2A_1)^T\mathbf{t}$ the tangent relative velocity $\frac{d}{dt}(A_2A_1)^T\mathbf{t} + (A_2A_1)^T\frac{d}{dt}(\mathbf{t}) = H_{\mathrm{t}}(q)^T\dot{q}$, while the normal relative velocity is $\frac{d}{dt}(f(q)) = \nabla f(q)^T\dot{q} = \frac{d}{dt}(A_2A_1)^T\mathbf{n} + (A_2A_1)^T\frac{d}{dt}(\mathbf{n})$, in the Galilean frame. We can therefore deduce the complementarity Lagrange dynamics of this system as $M(q)\ddot{q}(t) + F(q(t), \dot{q}(t)) = F_{ext}(t) + \nabla f(q(t))\lambda_{\mathrm{n},u}(t) + H_{\mathrm{t}}(q(t))\lambda_{\mathrm{t},u}(t)$, where $\lambda_{\mathrm{n},u}$ and $\lambda_{\mathrm{t},u}$ are the components of the contact force in the frame $(A, \mathbf{n}, \mathbf{t})$. Indeed from the contact force power invariance

principle $\langle F^{cont}, \dot{q}\rangle = \langle F_{\rm n}\mathbf{n} + F_{\rm t}\mathbf{t}, v_{\rm n}\mathbf{n} + v_{\rm t}\mathbf{t}\rangle = F_{\rm n}v_{\rm n} + F_{\rm t}v_{\rm t}$. Thus letting $\lambda_{{\rm n},u} = F_{\rm n}$ and $\lambda_{{\rm t},u} = F_{\rm t}$, we obtain $\dot{q}^T\nabla f(q)F_{\rm n} + \dot{q}^T H_{\rm t}(q)F_{\rm t} = F_{\rm n}v_{\rm n} + F_{\rm t}v_{\rm t}$, and since this holds for any velocity and contact force it follows that $v_{\rm n} = \nabla f(q)^T\dot{q}$ and $v_{\rm t} = H_{\rm t}(q)^T\dot{q}$. For such a system it is also possible to do as follows: open the joints at O_2 and O_4, work with redundant coordinates $q \in \mathbb{R}^8$ incorporating the gravity centers coordinates of both end-bodies, add four bilateral constraints to close the two joints and the associated multipliers $\lambda_{{\rm n},b,i}$, and apply the results of Sects. 4.1 and 5.4.1 for the two end-bodies. This provides a systematic way to write the nonsmooth dynamics, with the drawback of adding coordinates and bilateral constraints.[2]

5.1.1 Frictionless Bilateral Constraints: The Contact Problem

Assume first that there are no unilateral constraints (hence no complementarity conditions as in (5.1) (b)), and no friction. Differentiating (5.1) (c) twice one obtains:

$$\frac{d^2}{dt^2}h(q(t),t) = \frac{\partial h}{\partial q}(q,t)\ddot{q} + \underbrace{\frac{d}{dt}\left(\frac{\partial h}{\partial q}(q,t)\right)\dot{q} + \frac{\partial}{\partial q}\left(\frac{\partial h}{\partial t}(q,t)\right)\dot{q} + \frac{\partial^2 h}{\partial t^2}(q,t)}_{\triangleq w_b(q,\dot{q},t)} = 0 \tag{5.2}$$

We remind that $\frac{\partial h}{\partial q}(q,t) = \nabla_q h(q,t)^T$, by definition. For simplicity we denote $\nabla_q h(q,t)$ as $\nabla h(q,t)$. After few manipulations one obtains:

$$\underbrace{\begin{pmatrix} M(q) & -\nabla h(q,t) \\ \nabla h(q,t)^T & 0 \end{pmatrix}}_{\triangleq M_b(q,t)}\begin{pmatrix} \ddot{q} \\ \lambda_{{\rm n},b} \end{pmatrix} = \begin{pmatrix} F_{ext} - F_{iner}(q,\dot{q}) \\ -w_b(q,\dot{q},t) \end{pmatrix} \tag{5.3}$$

where $F_{iner}(q,\dot{q}) = C(q,\dot{q})\dot{q} + G(q)$. The natural question is: does the system in (5.3) possess a unique solution for any value of the right-hand side? Clearly $M(q)$ need not be full rank (think of the system $\begin{pmatrix} 0 & 1 \\ -1 & 0 \end{pmatrix}\begin{pmatrix} x \\ y \end{pmatrix} = z$). The following holds:

Theorem 5.1 *[429] Let F_{ext} and $F_{iner}(q,\dot{q})$ be arbitrary. Assume that* $\ker(M(q)) \cap \ker(\nabla h(q,t)^T) = \{0\}$*, then the solution $\ddot{q}$ and $\nabla h(q,t)\lambda_{{\rm n},b}$ of system (5.3) is unique. If in addition $\nabla h(q,t)$ has full column rank, then $\lambda_{{\rm n},b}$ is unique too.*

This theorem holds true when it is assumed that the system lives on the constraint submanifold $\{(q,\dot{q})|h(q) = 0,\ \nabla h(q)^T\dot{q} = 0\}$, i.e., the initial conditions are chosen

[2] This may render Control or Numerics less easy.

in the submanifold. The matrix $M_b(q,t)$ is called the KKT (Karush–Kuhn–Tucker) matrix of the system. Indeed, consider the optimization problem:

$$\min \frac{1}{2}\ddot{q}^T M(q)\ddot{q} + \ddot{q}^T(F_{iner}(q,\dot{q}) - F_{ext}), \quad \text{subject to: } \nabla h(q,t)^T\ddot{q} + w_b(q,\dot{q},t) = 0. \tag{5.4}$$

The Lagrangian of this problem is $L(\ddot{q},\lambda) = \frac{1}{2}\ddot{q}^T M(q)\ddot{q} + \ddot{q}^T(F_{iner}(q,\dot{q}) - F_{ext}) + \lambda^T(\nabla h(q,t)^T\ddot{q} + w_b(q,\dot{q},t)$. The necessary and sufficient conditions for the existence of a minimizer are $\frac{\partial L}{\partial \ddot{q}} = 0$, $\frac{\partial L}{\partial \lambda} = 0$, $\frac{\partial^2 L}{\partial \ddot{q}^2} \succeq 0$. The third condition is satisfied since $M(q) \succeq 0$. The other two conditions yield (5.3), with $\lambda_{\mathrm{n},b} = \lambda$.

$\rightsquigarrow$ *A Lagrangian system subject to bilateral constraints is a differential algebraic equation (DAE). The above differentiation operations permit to reduce its index from 3 to 1.*

This shows in passing that Gauss' principle applies to Lagrangian systems subject to bilateral constraints in their index 1 formulation. One may recover similar conditions to those of Theorem 5.1 from the optimization problem, applying for instance the conditions for nonsingularity of the KKT matrix in [172, p. 523] (which are anyway stronger than the conditions stated in Theorem 5.1 where it is not assumed that $\nabla h(q,t)$ has full column rank, but that the system evolves on its constraint manifold). Starting from the optimization problem in (5.4) whose KKT system is in (5.3), we may state the following, using [172, p.523].

Proposition 5.1 *Let $\nabla h(q,t)$ have full column rank. Then the KKT matrix $M_b(q,t)$ is nonsingular if and only if $M(q)$ is positive definite on the kernel of $\nabla h(q,t)^T$. Equivalently, $(\nabla h(q,t)^T x = 0,\ x \neq 0) \Rightarrow x^T M(q) x > 0$.*

Assume now that $M(q)$ is invertible and $\nabla h(q,t)$ has full column rank[3]. Then one may calculate $\lambda_{\mathrm{n},b}$ as

$$\begin{aligned}\lambda_{\mathrm{n},b} = {} & (\nabla h(q,t)^T M(q)^{-1}\nabla h(q,t))^{-1}\nabla h(q,t)M(q)^{-1}(F_{iner} - F_{ext}) \\ & -\nabla h(q,t)^T w_b(q,\dot{q},t)\end{aligned} \tag{5.5}$$

Proposition 5.2 *Consider the dynamical system in (5.1) (a) with only frictionless, bilateral constraints. The multiplier $\lambda_{\mathrm{n},b}$ in (5.5) renders the submanifold $\{(q,\dot{q}) \in \mathbb{R}^n \times \mathbb{R}^n | h(q,t) = 0,\ \frac{d}{dt}h(q,t) = 0\}$ invariant.*

Proof Inserting (5.5) into (5.1) (a) with only frictionless, bilateral constraints yields $\nabla h(q,t)^T\ddot{q} + w(q,\dot{q},t) = 0$. Therefore, if the initial data $q(0)$ and $\dot{q}(0)$ satisfy $h(q(0),0) = 0$ and $\nabla h(q(0),0)^T\dot{q}(0) = 0$, the trajectory stays in the submanifold. In other words, let $x_1 = q$ and $x_2 = \dot{q}$, and rewrite the dynamics as a first-order differential equation $\dot{x} = f(x,t,\lambda_{\mathrm{n},b})$. The constraint is given by $g_1(x,t) = h(x_1,t) = 0$ and $g_2(x_1,x_2,t) = \nabla h(x_1,t)^T x_2 + w(x_1,x_2,t) = 0$. Invariance holds if $\frac{\partial g_1}{\partial x} f(x,t) = 0$ and $\frac{\partial g_2}{\partial x} f(x,t) = 0$, which is indeed the case with $\lambda_{\mathrm{n},b}$ in (5.5).

[3] I.e. the vectors $\nabla h_i(q,t)$ are independent in $\mathbb{R}^n$.

The matrix $\nabla h(q,t)^T M(q)^{-1} \nabla h(q,t)$ plays an important role in the above developments. Notice that it is the Schur complement of $M(q)$ in $M_b(q,t)$.[4] Inserting the expression in (5.5) into the dynamics (5.1), therefore, yields a dynamical system which is invariant on the constraint manifold:

$$M(q)\ddot{q} + P(q)(C(q,\dot{q})\dot{q} + G(q)) + \nabla h(q)[\nabla h(q)^T M(q)^{-1} \nabla h(q)]^{-1} \frac{d}{dt}(\nabla h(q)^T)\dot{q} = 0 \tag{5.6}$$

with $P(q) = I + \nabla h(q)[\nabla h(q)^T M(q)^{-1} \nabla h(q)]^{-1} \nabla h(q) M(q)^{-1}$, and we assumed for the sake of simplicity that the constraints do not depend explicitly on time, and $F_{ext} = 0$. Is the dynamics in (5.6) a Lagrange system? The answer is no in general. Consider for instance that $M(q) = M$, so that the "free-motion" Coriolis and centrifugal torques $C(q,\dot{q})\dot{q} = 0$. However, if the constraints are not constant, then the term $\frac{d}{dt}(\nabla h(q)^T)\dot{q}$ brings quadratic terms in $\dot{q}$: this is in contradiction with the structure of Lagrange dynamics.

Further reading: the KKT system (5.3) is ubiquitous in multibody system dynamics. It has raised a quantity of studies for its analysis and numerical solvers, see [113, 160, 409, 429, 706, 803, 1275] to cite a few. In particular, a detailed analysis of existence/uniqueness of solutions is made in [160]. It is noteworthy that a basic assumption that is made implicitly in this section is that the function $h(q,t)$ is smooth enough. More precisely, it should be smooth enough so that the evolution problem obtained by inserting (5.5) into (5.1) (a) with bilateral frictionless contacts is well-posed (existence and uniqueness of solutions) so that Proposition 5.2 is meaningful. Some care has to be taken if the constraints are of class C^1 (continuously differentiable) or less (C^0 constraints). In case of C^1 constraints it may happen that their second derivative is not continuous because $w_b(q,\dot{q},t)$ jumps. Then $\lambda_{\mathrm{n},b}$ jumps as well, and the obtained evolution problem may be embedded into the mathematical formalism of differential inclusions (using for instance Filippov's convexification method). In case of C^0 constraints, there exists some configurations at which the gradient $\nabla h(q,t)$ may jump. The correct way to handle the problem is then to split the constraints into two sufficiently smooth constraints *per* discontinuous constraint: the system is subjected to a switching constraint, or is a switching DAE. When attaining the point of discontinuous gradient, the velocity has to be reinitialized in order for the system to continue its motion along the second constraint. This is an issue quite similar to what is described in Sect. 1.3.4. Glocker proposed to use an extension of Moreau's framework (see Sect. 5.2) to cope with such velocity reinitialization issues in systems subjected to C^0 bilateral constraints [450].

[4] The Schur complement of the invertible matrix A_{11} in the $m \times n$ matrix $A = \begin{pmatrix} A_{11} A_{12} \\ A_{21} A_{22} \end{pmatrix}$ is the matrix $A_{22} - A_{21} A_{11}^{-1} A_{12}$. The Schur complement of the invertible matrix A_{22} in A is the matrix $A_{11} - A_{12} A_{22}^{-1} A_{21}$.

5.1.2 Frictionless Unilateral Constraints: The Contact Problem

5.1.2.1 Construction of the Contact LCP

Let us investigate now the case where there are only frictionless unilateral constraints, i.e., we consider (5.1) (a) and (b). Is it possible to redo the DAE index reduction as in Sect. 5.1.1? The answer is yes, though the context differs. Due to the complementarity conditions in (5.1) (b) it is clear that $f(q,t) > 0 \Rightarrow \lambda_{\mathrm{n},u} = 0$. The two remaining cases occur either (i) at an impact time, or (ii) during persistent contact. Let us focus on case (ii) now. To simplify let us assume that all the constraints are active, i.e., $f_i(q(t),t) = 0$ for all $1 \leq i \leq m_u$ and for all $t \in [t_1, t_2]$, $t_2 > t_1$. Let us assume that the velocity is continuous. One has $\frac{d}{dt} f_i(q(t),t) = \nabla f_i(q,t)\dot{q} + \frac{\partial}{\partial t} f_i(q(t),t) = 0$ for all $1 \leq i \leq m_u$ and for all $t \in [t_1, t_2]$. We however admit that the acceleration may be discontinuous, because a discontinuous external force may be applied to the system (think of a ball at rest on the ground and subject to gravity, and which is suddenly acted upon by an external action that pulls it up, i.e., a discontinuous F_{ext}). Thus one has $\frac{d^2}{dt^2} f_i(q(t),t) = \nabla f_i(q,t)\ddot{q} + w_i(q,\dot{q},t) = 0$ for all $1 \leq i \leq m_u$ and for all $t \in (t_1, t_2)$, and not for all $t \in [t_1, t_2]$: on the left of t_1 an impact may have occurred before the stabilization on the boundary $\mathrm{bd}(\Phi)$, while on the right of t_2 a detachment may occur where the gap function "acceleration" $\frac{d^2}{dt^2} f_i(q(t),t)$ may jump from 0 to a positive value. The objective is to analyze what happens at time t_2.

In an arbitrarily small right neighborhood of t_2, one necessarily has $\frac{d}{dt} f_i(q(t),t) \geq 0$ and $\frac{d^2}{dt^2} f_i(q(t),t) \geq 0$. Indeed, since $f_i(q(t_2,t_2) = 0$, by continuity $\frac{d}{dt} f_i(q(t),t) < 0$ would imply a violation of the nonnegativity $f_i(q(t),t) \geq 0$. Similarly, since $\frac{d}{dt} f_i(q(t_2),t_2) = 0$, having $\frac{d^2}{dt^2} f_i(q(t_2),t_2^+) < 0$ and also in the arbitrarily small neighborhood of t_2, would imply by continuity a violation of the nonnegativity $\frac{d}{dt} f_i(q(t_2),t_2) \geq 0$, and of $f_i(q(t),t) \geq 0$. Therefore, we infer that both $\frac{d}{dt} f_i(q(t),t)$ and $\frac{d^2}{dt^2} f_i(q(t),t)$ are nonnegative in any arbitrarily small neighborhood of t_2. Now let us notice that if $\frac{d^2}{dt^2} f_i(q(t_2),t_2^+) > 0$, then $\frac{d}{dt} f_i(q(t),t) > 0$ and consequently $f_i(q(t),t) > 0$ in any arbitrarily small neighborhood of t_2. Therefore, $\lambda_{\mathrm{n},u,i}(t) = 0$ in the same neighborhood. We conclude that necessarily $0 \leq \frac{d^2}{dt^2} f_i(q(t_2),t_2^+) \perp \lambda_i(t)$, still in the same neighborhood.

We thus have shown that it is legitimate to assert that the following complementarity conditions hold during persistent contact phases, i.e., on $(t_1, t_2]$:

$$0 \leq \frac{d^2}{dt^2} f_i(q(t),t^+) = \nabla f_i(q(t),t)^T \ddot{q} + w_{u,i}(q,\dot{q},t) \perp \lambda_{\mathrm{n},u,i}(t) \geq 0, \quad 1 \leq i \leq m_u \tag{5.7}$$

where $w_u(q,\dot{q},t)$ has the same form as $w(q,\dot{q},t)$ in (5.2). More formally and compactly we may state the following:

Proposition 5.3 *Let $h(\cdot)$ and $\lambda(\cdot)$ be two functions of time, and let $0 \leq h(t) \perp \lambda(t) \geq 0$ for all t. Assume that $h(\cdot)$ is continuous, $\dot{h}(\cdot)$, $\ddot{h}(\cdot)$ and $\lambda(\cdot)$ are*

right-continuous at some time t. (i) Let $h(t) = 0$, then $0 \leq \dot{h}(t) \perp \lambda(t) \geq 0$. (ii) Let $h(t) = 0$ and $\dot{h}(t) = 0$, then $0 \leq \ddot{h}(t) \perp \lambda(t) \geq 0$.

Proof (i) For any $t' \geq t$ one has $h(t') - h(t) = \int_t^{t'} \dot{h}(s)ds$. Suppose that $\dot{h}(t) < 0$. Since $\dot{h}(\cdot)$ is right-continuous, there exists $\varepsilon > 0$ such that $\dot{h}(s) < 0$ for all $s \in [t, t+\varepsilon)$. Thus for any $t' \in [t, t+\varepsilon)$ one has $h(t') < 0$ which is impossible. Thus one has $\dot{h}(t) \geq 0$. Now let $\dot{h}(t) > 0$, by continuity there exists $\varepsilon > 0$ such that for all $t' \in (t, t+\varepsilon)$, one has $\dot{h}(t') > 0$. Consequently, $h(t') > 0$ for all $t' \in (t, t+\varepsilon)$, and $\lambda(t) = 0$. Now suppose that $\lambda(t) > 0$, thus $h(t) = 0$. Assume that $\dot{h}(t) > 0$ so that $h(t') > 0$ for all $t' \in (t, t+\varepsilon)$, so that $\lambda(t') = 0$ for all $t' \in (t, t+\varepsilon)$: this is a contradiction and consequently $\dot{h}(t) \leq 0$. From the nonnegativeness, one infers $\dot{h}(t) = 0$. Hence (i) is proved. Part (ii) is proved in a similar way, noting that $\dot{h}(t') - \dot{h}(t) = \int_t^{t'} \ddot{h}(s)ds$ and $\dot{h}(\cdot)$ is locally continuous in a neighborhood of t.

It is noteworthy that Proposition 5.3 implies the lexicographical inequality

$$(h(t), \dot{h}(t), \ddot{h}(t)) \succcurlyeq 0.$$

The dynamical equation plus the m complementarity conditions in (5.7) form the following mixed linear complementarity problem (mLCP):

$$\begin{cases} M(q)\ddot{q} + F_{iner}(q, \dot{q}) - F_{ext} - \nabla f(q,t)\lambda_{\mathrm{n},u} = 0 \\ 0 \leq \nabla f(q,t)^T \ddot{q} + w_u(q, \dot{q}, t) \perp \lambda_{\mathrm{n},u}(t) \geq 0. \end{cases} \tag{5.8}$$

The mLCP in (5.8) is the counterpart of the linear system (5.3), for unilaterally constrained systems in persistent contact motion. In case $M(q)$ is full rank,[5] $\ddot{q}$ can be eliminated and this mLCP can be transformed into an LCP with unknown $\lambda_{\mathrm{n},u}(t)$:

$$0 \leq \nabla f(q(t),t)^T M(q(t))^{-1} \nabla f(q(t),t)\lambda_{\mathrm{n},u}(t) + b(q, \dot{q}, t) \perp \lambda_{\mathrm{n},u}(t) \geq 0, \tag{5.9}$$

where $b(q, \dot{q}, t) = \nabla f(q(t),t)^T M(q)^{-1}[F_{ext} - F_{iner}(q, \dot{q})] + w_u(q, \dot{q}, t)$. The matrix $D_u(q,t) \triangleq \nabla f(q,t)^T M(q)^{-1} \nabla f(q,t)$, which is at least positive semi-definite, is called the Delassus' matrix.[6] The LCP in (5.9) is named the *contact LCP*.

Some comments arise:

- In order to construct the LCP in (5.9) we had to differentiate the gap function twice: we say that the system has a *relative degree* between the "input" $\lambda_{\mathrm{n},u}$ and the "output" $w(q,t) = f(q,t)$, equal to 2. In fact, rigorously speaking, this is true

[5] This is often assumed, but may not be satisfied in practice, especially for systems with bilateral constraints.

[6] In the honor of Etienne Delassus who was the first to deeply analyze the unilateral contact problem with multiple constraints [333, 335].

only if the Delassus' matrix has full rank. The index of DAE and the relative degree are similar notions.

- According to Theorem 5.4, the LCP in (5.9) is well-posed (it has a unique solution for any $b(q, \dot{q}, t)$) if and only if the Delassus' matrix is a P-matrix, which in this case means that it is positive definite (because it is symmetric), equivalently the gradients $\nabla f_i(q, t)$ are independent vectors of $\mathbb{R}^n$.

Proposition 5.4 *Suppose that the gradients $\nabla f_i(q(t), t)$ are independent vectors of $\mathbb{R}^n$. Then the solution of the LCP in (5.9) is given by*

$$\lambda_{\mathrm{n},u}(t) = \mathrm{proj}_{D_u(q(t),t)}[\mathbb{R}^{m_u}_+; -D_u(q(t), t)^{-1} b(q, \dot{q}, t)]. \tag{5.10}$$

The proof follows from (B.19) and (B.20). The expression in (5.10) is the counterpart of (5.5).

- If the constraints are not independent, then $D_u(q, t) = \nabla f(q, t)^T M(q)^{-1} \nabla f(q, t) \succeq 0$ (it is positive semi-definite). Hence, it is copositive, because a positive semi-definite matrix is copositive. We can therefore apply Theorem 5.6 to analyze the solvability of the contact LCP, following [209, Proposition 3].

Proposition 5.5 *Let n and m_u be arbitrary. Assume that for any v solution of: $0 \leq v \perp D_u(q, t)v \geq 0$ one has $v^T b(q, \dot{q}, t) \geq 0$. Then the contact LCP in (5.9) is solvable.*

In case $\nabla f(q, t)$ has full column rank, then the only solution of the homogenous LCP is $v = 0$, and the implication always holds. Due to the particular structure of the problem (i.e., of the LCP matrix and of $b(q, \dot{q}, t)$), one may formulate necessary and sufficient conditions for solvability, a fact noticed first in [963]. The next result follows from Theorem 5.7, and is proved in [209, Proposition 2].

Proposition 5.6 *Let n and m_u be arbitrary, and let $\lambda_{\mathrm{n},u,1}$ and $\lambda_{\mathrm{n},u,2}$ be two solutions of the LCP in (5.9). Then $\nabla f(q, t)(\lambda_{\mathrm{n},u,1} - \lambda_{\mathrm{n},u,2}) = 0$, and $(\lambda_{\mathrm{n},u,1} - \lambda_{\mathrm{n},u,2})^T b(q, \dot{q}, t) = 0$.*

The first equality says that for any two solutions the force that appears in the dynamics, i.e., $\nabla f(q, t)\lambda_{\mathrm{n},u}$, is unique. Therefore, the acceleration $\ddot{q}$ is unique as well. If in addition $\nabla f(q, t)$ has full column rank, then $\lambda_{\mathrm{n},u}$ is unique. We recover here some results shown by Moreau in [877, 878], see also [762].

$\rightsquigarrow$ *The fundamental discrepancy between bilateral and unilateral constraints is that the former give rise to a linear equation, while the latter give rise to an LCP. In the first case the rank of the system's matrix is the crucial property, while in the second case some "positivity" is required (P-matrix, or positive definite, or copositive).*

5.1.2.2 Gauss' Principle

The projection in (5.10) almost shows that Gauss' principle extends to systems with unilateral constraints. Indeed using (B.20) it follows that (5.10) is equivalent to (we drop the time argument in $q(t)$):

$$\begin{aligned}\lambda_{\mathrm{n},u}(t) &= \operatorname{argmin}_{z\in\mathbb{R}^{m_u}_+} \tfrac{1}{2}(z + D_u(q,t)^{-1}b(q,\dot q,t))^T D_u(q(t),t)(z + D_u(q,t)^{-1}b(q,\dot q,t)) \\ &= \operatorname{argmin}_{z\in\mathbb{R}^{m_u}_+} \tfrac{1}{2}z^T D_u(q,t)z + z^T b(q,\dot q,t).\end{aligned} \tag{5.11}$$

Proposition 5.7 *[209] Let n and m_u be arbitrary. The quadratic program in (5.11) has a solution (is solvable) if (i) $b(q,\dot q,t) \in \mathrm{Im}(D_u(q,t))$, or if (ii) $w_u(q,\dot q,t) = 0$.*

Proof Since $D_u(q,t)$ is positive semi-definite and symmetric, it follows from [307, Exercise 2.10.25 (b)] that condition (i) guarantees the boundedness from below of the quadratic function. The result follows from [307, Theorem 2.8.1] which states that a quadratic function that is bounded from below attains its minimum on a nonempty polyhedron. Condition (ii) implies that $b(q,\dot q,t) = \nabla f(q(t),t)^T M(q)^{-1}[F_{ext} - F_{iner}(q,\dot q)]$. Since $\mathrm{Im}(D_u(q,t)) = \mathrm{Im}(\nabla f(q,t)^T)$,[7] this implies in turn that $b(q,\dot q,t) \in \mathrm{Im}(D_u(q,t))$, so (i) applies.

Let us denote $\ddot f \stackrel{\Delta}{=} \frac{d^2}{dt^2} f(q(t),t)$. Few manipulations (using the dynamical equation in (5.1) (a)) yield that (5.9) is equivalent, when $D_u(q,t)$ is full rank, to

$$0 \le \ddot f \perp D_u(q,t)^{-1}[\ddot f - b(q,\dot q,t)] \ge 0. \tag{5.12}$$

Using (B.20), this is equivalent to

$$\begin{aligned}&\ddot f = \mathrm{proj}_{D_u(q,t)^{-1}}[\mathbb{R}^{m_u}_+; b(q,\dot q,t)] \;\Leftrightarrow\; \ddot f = \operatorname{argmin}_{z\in\mathbb{R}^{m_u}_+} \tfrac{1}{2}z^T D_u(q,t)^{-1}z - z^T b(q,\dot q,t) \\ &\Leftrightarrow\; \ddot f = \operatorname{argmin}_{z\in\mathbb{R}^{m_u}_+} \tfrac{1}{2}(z - b(q,\dot q,t))^T D_u(q,t)^{-1}(z - b(q,\dot q,t)).\end{aligned} \tag{5.13}$$

It is noteworthy that the equivalent of Proposition 5.7 is not possible here, because we assumed that $D_u(q,t)$ is positive definite. Let us now investigate what happens with the acceleration $\ddot q$. From Dorn's duality Theorem (see Theorem 5.10), it follows that the quadratic program in (5.11) has the dual program:

$$\begin{cases} \min \tfrac{1}{2}\lambda_{\mathrm{n},u}^T D_u(q,t)\lambda_{\mathrm{n},u} \\ \\ \text{subject to: } D_u(q,t)\lambda_{\mathrm{n},u} + b(q,\dot q,t) \ge 0. \end{cases} \tag{5.14}$$

Dorn's duality theorem says that if λ_u^{**} solves (5.14) then there exists λ_u^* that solves (5.11) with $D_u(q,t)(\lambda_u^* - \lambda_u^{**}) = 0$. In case $D_u(q,t) \succ 0$ then $\lambda_u^* = \lambda_u^{**}$. Conversely,

[7] This follows using for instance Exercise 6 page 180 and Exercise 7 page 78 in [700].

if λ_u^* solves (5.11) then it solves (5.14) and the two extrema are equal. Using the dynamical equation in (5.1) (a) it follows that the acceleration is the unique solution of the minimization problem:

$$\begin{cases} \min \frac{1}{2}(\ddot{q} + M^{-1}(q)[F_{iner}(q,\dot{q}) - F_{ext}])^T M(q)(\ddot{q} + M^{-1}(q)[F_{iner}(q,\dot{q}) - F_{ext}]) \\ \text{subject to: } \nabla f^T(q,t)\ddot{q} + w_u(q,\dot{q},t) \geq 0. \end{cases} \tag{5.15}$$

The last optimization problem was obtained in [762, 877, 878]. Several other minimization problems for the acceleration have been derived in [209]. Finally, notice that we may use (B.22). Consider the quadratic program:

$$\begin{cases} \min \lambda_{\mathrm{n},u}^T D_u(q,t)\lambda_{\mathrm{n},u} + \lambda_{\mathrm{n},u}^T b(q,\dot{q},t) \\ \text{subject to: } \lambda_{\mathrm{n},u} \geq 0, \quad D_u(q,t)\lambda_{\mathrm{n},u} + b(q,\dot{q},t) \geq 0. \end{cases} \tag{5.16}$$

Since $D_u(q,t) \succeq 0$, it is row sufficient. Thus any solution of the quadratic program (5.16) solves the LCP in (5.9).

Remark 5.1 As we have seen in Sect. 3.1.2, Gauss' principle may be written as in (3.16) and (3.17). In a more general setting, the normal cone in the right-hand side is equal to $N_{T_{\Phi(q)}(\dot{q})}(\ddot{q})$. The dynamics is written as $M(q)\ddot{q} + F_{iner}(q,\dot{q}) - F_{ext} \in -N_{T_{\Phi(q)}(\dot{q})}(\ddot{q})$. Applying (B.20) one finds the extension of (3.17): Given t, $q(t)$ and $\dot{q}(t)$, the acceleration satisfies

$$\ddot{q} = \mathrm{proj}_{M(q)}[T_{T_\Phi(q)}(\dot{q}); -M^{-1}(q)(F_{iner}(q,\dot{q}) - F_{ext})]. \tag{5.17}$$

The discrepancy between (5.15) and (5.17) is that the latter holds for all $q(t) \in \Phi = \{q \in \mathbb{R}^n | f(q) \geq 0\}$ and all $\dot{q}(t) \in T_\Phi(q(t))$, while the developments in this section (and in particular (5.15)) are led for $f(q(t)) = 0 \Leftrightarrow q(t) \in \mathrm{bd}(\Phi)$ and $\nabla f(q(t))^T \dot{q}(t) = 0 \Leftrightarrow (\dot{q}(t) \in \mathrm{bd}(T_\Phi(q(t)))$ and $\mathscr{K}(\dot{q}) = \mathscr{J}(q))$, where the index sets $\mathscr{K}(\dot{q})$ and $\mathscr{J}(q)$ are as in Sect. B.2.2. This allows us to construct the contact LCP. In case $\mathscr{K}(\dot{q}) \subset \mathscr{J}(q)$ the contact LCP has to be constructed with the contacts satisfying $f_i(q) = 0$ and $\nabla f_i(q)^T \dot{q} = 0$ only (for indeed, $f_k(q) = 0$ and $\nabla f_k(q)^T \dot{q} > 0$ imply that $\lambda_{\mathrm{n},u,k} = 0$).

5.1.3 *Mixed Bilateral/Unilateral Frictionless Constraints: The Contact Problem*

5.1.3.1 Construction of the Contact Complementarity Problem

Let us now consider a frictionless Lagrangian system as in (5.1) (a)–(c). The same manipulations as in Sects. 5.1.1 and 5.1.2 will be performed, with index and relative degree reduction from 3 to 1. We therefore assume that the m_u unilateral constraints

are active. The constrained Lagrangian system is rewritten as follows:

$$\begin{cases} (a)\ \ M(q)\ddot{q} + F_{iner}(q,\dot{q}) - F_{ext} - \nabla f(q,t)\lambda_{\mathrm{n},u} - \nabla h(q,t)\lambda_{\mathrm{n},b} = 0 \\ (b)\ \ \nabla h(q,t)^T\ddot{q} + w_b(q,\dot{q},t) = 0 \\ (c)\ \ 0 \le \lambda_{\mathrm{n},u} \perp \nabla f(q,t)^T\ddot{q} + w_u(q,\dot{q},t) \ge 0. \end{cases} \tag{5.18}$$

Let us assume that $M(q)$ has full rank and denote $D_b(q,t) \stackrel{\Delta}{=} \nabla h(q,t)^T M(q)^{-1}\nabla h(q,t)$, and $D_{bu}(q,t) \stackrel{\Delta}{=} \nabla h(q,t)^T M(q)^{-1}\nabla f(q,t)$. One obtains

$$\begin{cases} D_b(q,t)\lambda_{\mathrm{n},b} + D_{bu}(q,t)\lambda_{\mathrm{n},u} + \bar{w}_b(q,\dot{q},t) = 0 \\ 0 \le \lambda_{\mathrm{n},u} \perp D_u(q,t)\lambda_{\mathrm{n},u} + D_{bu}(q,t)^T\lambda_{\mathrm{n},b} + \bar{w}_u(q,\dot{q},t) \ge 0, \end{cases} \tag{5.19}$$

with $\bar{w}_b(q,\dot{q},t) \stackrel{\Delta}{=} \nabla h(q,t)^T M(q)^{-1}(F_{ext} - F_{iner}(q,\dot{q})) + w_b(q,\dot{q},t)$ and $\bar{w}_u(q,\dot{q},t) \stackrel{\Delta}{=} \nabla f(q,t)^T M(q)^{-1}(F_{ext} - F_{iner}(q,\dot{q})) + w_u(q,\dot{q},t)$. The problem in (5.19) is again a mixed LCP as (5.8), but with unknowns the multipliers $\lambda_{\mathrm{n},b}$ and $\lambda_{\mathrm{n},u}$ instead of $\ddot{q}$ and $\lambda_{\mathrm{n},u}$. Let us state a result that assumes that the bilateral constraints are independent.

Proposition 5.8 *Let $M(q)$ and $D_b(q(t),t)$ have full rank. Then the mLCP in (5.19) is equivalent to the LCP:*

$$0 \le \lambda_{\mathrm{n},u} \perp \underbrace{[D_u(q(t),t) - D_{bu}(q(t),t)^T D_b(q(t),t)^{-1} D_{bu}(q(t),t)]}_{\stackrel{\Delta}{=}\tilde{D}_{bu}(q(t),t)}\lambda_{\mathrm{n},u} + \bar{w}_{bu}(q,\dot{q},t) \ge 0 \tag{5.20}$$

where $\bar{w}_{bu}(q,\dot{q},t) = -D_{bu}(q(t),t)^T D_b(q(t),t)^{-1}\bar{w}_b(q,\dot{q},t) + \bar{w}_u(q,\dot{q},t)$.

Some comments [209]:

- The LCP matrix $\tilde{D}_{bu}(q,t)$ is the Schur complement of $D_b(q,t)$ in the matrix $\begin{pmatrix} D_b(q,t) & D_{bu}(q,t) \\ D_{bu}(q,t)^T & D_u(q,t) \end{pmatrix} = \begin{pmatrix} \nabla h(q,t)^T \\ \nabla f(q,t)^T \end{pmatrix} M(q)^{-1}(\nabla h(q,t) \ \ \nabla f(q,t))$.[8]
- The LCP matrix $\tilde{D}_{bu}(q,t)$ can be factorized as $\tilde{D}_{bu}(q,t) = \nabla f(q,t)^T M_c(q)^{-1}\nabla f(q,t)$, with $M_c^{-1}(q) \stackrel{\Delta}{=} M(q)^{-1}[I - G(q)M(q)^{-1}]\nabla f(q,t)$ (this is a non-invertible matrix, the superscript -1 is just to mimic the case without bilateral constraints), and $G(q) = \nabla h(q,t)D_b(q,t)^{-1}\nabla h(q,t)^T$.
- Propositions 5.4 and 5.5 extend to the LCP in (5.20). The interesting point here is to analyze the rank of $\tilde{D}_{bu}(q,t)$.

Proposition 5.9 *[209] Let $D_b(q,t) \succ 0$. Then the following assertions are true:*

- *(i) The matrix $M_c^{-1}(q) \succeq 0$.*

[8] This fact was not noticed in [209], but in [606] in another context.

- *(ii) Let* $\lambda_{\mathrm{n},u,1}$ *and* $\lambda_{\mathrm{n},u,2}$ *be two solutions of the LCP (5.20). Then* $\lambda_{\mathrm{n},u,1} - \lambda_{\mathrm{n},u,2} \in \ker(M_c^{-1}(q))$ *and* $(\lambda_{\mathrm{n},u,1} - \lambda_{\mathrm{n},u,2})^T \bar{w}_{bu}(q, \dot{q}, t) = 0$.
- *(iii) Let* $M_c^{-\frac{1}{2}}(q)$ *be the unique symmetric positive semi-definite square root of* $M_c^{-1}(q)$. *Then* $\tilde{D}_{bu}(q,t) \succ 0$ *if and only if the vectors* $M_c^{-\frac{1}{2}}(q)\nabla f_i(q,t)$, $1 \leq i \leq m_u$ *are independent vectors of* $\mathbb{R}^n$.
- *(iv) The matrix* $\tilde{D}_{bu}(q,t) \succ 0$ *if and only if the matrix* $(\nabla h(q,t) \;\; \nabla f(q,t))$ *has full column rank (i.e., the* $m_u + m_b$ *columns are independent vectors of* $\mathbb{R}^n$*).*

Item (ii) can be proved using Theorem 5.7. Item (iv) follows from the fact that since $D_b(q,t) \succ 0$, the matrix $\begin{pmatrix} D_b(q,t) & D_{bu}(q,t) \\ D_{bu}(q,t)^T & D_u(q,t) \end{pmatrix}$ is positive definite if and only if its Schur complement is positive definite [218, Theorem A.61]. We may state the counterpart of Proposition 5.8. This time the unilateral constraints are supposed to be independent.

Proposition 5.10 *Let* $D_u(q,t) \succ 0$. *Then the mLCP in (5.19) is equivalent to the equation with unknown* $\lambda_{\mathrm{n},b}$*:*

$$D_b(q,t)\lambda_{\mathrm{n},b} + D_{bu}(q,t)\mathrm{proj}_{D_u(q,t)}[\mathbb{R}_+^{m_u}; -D_u(q,t)^{-1}(D_{bu}(q,t)^T\lambda_{\mathrm{n},b} + \bar{w}_u(q,\dot{q},t)] \\ +\bar{w}_b(q,\dot{q},t) = 0. \tag{5.21}$$

The proof uses (B.19), (B.20), and (B.21).

5.1.3.2 The mLCP in (5.18) as an Inclusion

Using (B.19) and Theorem B.2 and (5.18) (c), one may write equivalently that $\nabla f(q,t)\lambda_{\mathrm{n},u} \in -\partial\psi_{K_u}(\ddot{q})$, with $K_u = \{z \in \mathbb{R}^n | \nabla f(q,t)^T z + w_u(q,\dot{q},t) \geq 0\}$, where we assume that K_u is nonempty. Similarly, the generalized force $\nabla h(q,t)\lambda_{\mathrm{n},b} \in \partial\psi_{\{0\}}(\nabla h(q,t)^T\ddot{q} + w_b(q,\dot{q},t))$, which is rewritten equivalently as $\nabla h(q,t)\lambda_{\mathrm{n},b} \in \partial\psi_{K_b}(\ddot{q})$, with $K_b = \{z \in \mathbb{R}^n | \nabla h(q,t)^T z + w_b(q,\dot{q},t) = 0\}$. Let us recall from (B.10) that the sets in both right-hand sides are normal cones. Therefore, the mLCP in (5.18) is rewritten equivalently as

$$M(q)\ddot{q} + F_{iner}(q,\dot{q}) - F_{ext} \in -\partial\psi_{K_u}(\ddot{q}) - \partial\psi_{K_b}(\ddot{q}) = -\partial\psi_{K_u \cap K_b}(\ddot{q}). \tag{5.22}$$

The signum before the bilateral constraints cone is not defined since the multipliers $\lambda_{\mathrm{n},b,i}$ are unsigned. The equality in the right-hand side of (5.22) is obtained from [1045, Theorem 23.8], under the condition that $K_u \cap K_b$ is nonempty. Under the stated assumptions of nonemptyness, it readily follows from (5.22) and (B.21) that if $M(q)$ has full rank then

$$\ddot{q} = \mathrm{proj}_{M(q)}[K_u \cap K_b; -M(q)^{-1}(F_{iner}(q,\dot{q}) - F_{ext})]. \tag{5.23}$$

What about the case when $M(q)$ is only positive semi-definite? To answer this question one may use the material in [216] that is based on results in [23].

Proposition 5.11 *Assume that $K_u \cap K_b$ is nonempty, and that the Mangasarian–Fromowitz constraint qualification holds for the constraints $f_i(q)$, $i \in \mathscr{J}(q)$. Then the inclusion in (5.22) has a solution (solvability) if*

$$T_S(q) \cap \ker(\nabla h(q)^T) \cap \ker(M(q)) = \{0\}, \tag{5.24}$$

where $S = \{q \in \mathbb{R}^n | f_i(q) \geq 0, i \in \mathscr{J}(q)\}$.

It is noteworthy that if the unilateral constraints are transformed into bilateral ones, then $T_s(q) = \ker(\nabla f(q)^T$ and one recovers the conditions of Theorem 5.1. Remind that $T_S(q)$ is the tangent cone to S at q.

5.1.3.3 Gauss' Principle

The basic principle for showing that the acceleration and the multiplier may be calculated as the solution of some quadratic program under constraints is identical to the developments in Sect. 5.1.2.2 starting from the LCP in (5.20) and the assumptions of Proposition 5.8.

5.1.4 Singular Mass Matrix: From Singular Lagrange's to Singular Hamilton's Dynamics

In this section we suppose that $\text{rank}(M(q)) = r \leq n$. The theory of singular Lagrangian and Hamiltonian systems has a long history in Physics, where geometrical, coordinate-free analysis is led. In particular, equivalence between both approaches is shown in [105]. Let us adopt here a different path with generalized (local) coordinates q and quasi-Lagrange dynamics, where basic convex analysis allows us to extend the Legendre transformation to the singular case. It is commonly admitted that Lagrangian and Hamiltonian formalisms are equivalent, and the Fenchel (or Legendre–Fenchel) transformation in Definition B.11 applied to the system's lagrangian function allows one to pass from one formalism to the other, under the condition of strict convexity of the Lagrangian function with respect to $\dot{q}$ [60, §15.A]. When $M(q)$ has full rank n, the Legendre–Fenchel transform of the Lagrangian function $L(q, \dot{q}, \lambda)$, defines the Hamiltonian function $H(q, p, \lambda)$, which is the total mechanical energy of the system. One may write $L(q, \dot{q}, \lambda) = \frac{1}{2}\dot{q}^T M(q)\dot{q} - P(q) + f(q)^T\lambda$ and $H(q, p, \lambda) = \frac{1}{2}p^T M(q)^{-1}p + P(q) - f(q)^T\lambda$ where $P(q)$ is the potential energy. The complementarity Hamiltonian system is given by

$$\begin{cases} \dot{q} = \frac{\partial H}{\partial p} = M(q)^{-1} p \\ \dot{p} = -\frac{\partial H}{\partial q} = -\frac{\partial}{\partial q}\left(\frac{1}{2} p^T M(q)^{-1} p + P(q)\right) + \nabla f(q)\lambda \\ 0 \leq \lambda \perp f(q) \geq 0. \end{cases} \tag{5.25}$$

When $r < n$ the strict convexity is lost, so that the Lagrangian function is a convex degenerate quadratic function of $\dot{q}$. Its Legendre–Fenchel transform $L^\star(q, \dot{q}, \lambda)$ may be calculated following the material in [531, Chap. E, Example 1.1.4]. One obtains

$$\begin{cases} H(q, p, \lambda) = \frac{1}{2} p^T M(q)^\dagger p + P(q) - f(q)^T \lambda \\ p \in \mathrm{Im}(M(q)) \end{cases} \tag{5.26}$$

where $M(q)^\dagger$ is the Moore–Penrose generalized inverse of $M(q)$. Since $M(q)^\dagger$ is symmetric positive semi-definite, the Hamiltonian function $H(q, p, \lambda)$ is convex in p, so its conjugate function is the original Lagrangian function by Theorem B.1, under the constraint $\dot{q} \in \mathrm{Im}(M(q)^\dagger)$. A constraint appears in (5.26), reflecting the loss of rank of $M(q)$ that makes the Lagrangian function degenerate, i.e., $\frac{\partial^2}{\partial \dot{q}^2} L(q, \dot{q}, \lambda)$ is not full rank. Consequently, the Lagrange dynamics is an implicit system. If this constraint is not satisfied then $H(q, p, \lambda) = +\infty$. The basic idea is to use the diagonalization of $M(q)$, so that the kinetic energy (more exactly the kinetic co-energy) expressed in the new variable (a quasi-velocity) has a simple form. There exists a unitary matrix $U(q) \in \mathbb{R}^{n \times n}, U(q)U(q)^T = I_n$, such that $U(q)M(q)U(q)^T = \begin{pmatrix} M_r(q) & 0 \\ 0 & 0 \end{pmatrix}$, where $M_r(q)$ is symmetric positive definite (it is even diagonal) [136, Corollary 5.4.4]. To this end let us introduce the *quasi-velocity* $v = U(q)\dot{q} = \begin{pmatrix} v_r \\ v_{n-r} \end{pmatrix}$. Then the kinetic energy becomes:

$$\begin{aligned} T(q, \dot{q}) = \tfrac{1}{2}\dot{q}^T M(q)\dot{q} &= \tfrac{1}{2}\dot{q}^T U(q)^T U(q) M(q) U(q)^T U(q)\dot{q} \\ &= \tfrac{1}{2}\dot{q}^T U(q)^T \begin{pmatrix} M_r(q) & 0 \\ 0 & 0 \end{pmatrix} U(q)\dot{q} = \tfrac{1}{2} v_r^T M_r(q) v_r = T(q, v_r). \end{aligned} \tag{5.27}$$

One has $M(q)^\dagger = U(q)^T \begin{pmatrix} M_r(q)^{-1} & 0 \\ 0 & 0 \end{pmatrix} U(q)$ [136, Fact 8.15.1 and §6.2]. Thus the kinetic energy is given by

$$\begin{aligned} T(q, p) = \tfrac{1}{2} p^T M(q)^\dagger p &= \tfrac{1}{2} p^T U(q)^T U(q) M(q)^\dagger U(q)^T U p \\ &= \tfrac{1}{2} p^T U(q)^T \begin{pmatrix} M_r(q)^{-1} & 0 \\ 0 & 0 \end{pmatrix} U(q) p. \end{aligned} \tag{5.28}$$

Let $m = U(q)p$. Doing the same partition as for the quasi-velocity, one obtains

$$T(q, p) = \frac{1}{2} m^T \begin{pmatrix} M_r(q)^{-1} & 0 \\ 0 & 0 \end{pmatrix} m = \frac{1}{2} m_r^T M_r(q)^{-1} m_r. \tag{5.29}$$

Equalling the kinetic energy in (5.29) and co-energy in (5.27), one finds that $m_r = M_r(q)v_r$, which extends the relation between the generalized momentum and the generalized velocity for full rank $M(q)$, to quasi-momentum m and quasi-velocity v. The quasi-Lagrange dynamics is obtained as follows:

$$\begin{cases} M_r(q)\dot{v}_r - M_r(q)(\dot{U}(q)U(q)^T v)_r + (U(q)F(q, U(q)^T v, t))_r = (U(q)\nabla f(q))_r \lambda \\ (U(q)F(q, U(q)^T v, t))_{n-r} = (U(q)\nabla f(q))_{n-r}\lambda. \end{cases} \tag{5.30}$$

It is clear that the loss of rank of $M(q)$ imposes an equality constraint in the system, represented by the last $n - r$ lines in (5.30). From the fact that $\dot{q} = \frac{\partial H}{\partial p} = \frac{\partial p}{\partial m}\frac{\partial H}{\partial m}$ and $p = U(q)^T m$, one obtains the quasi-Hamilton dynamics:

$$\begin{cases} \dot{q} = U(q)^T \frac{\partial H}{\partial m} \\ \dot{m} = -U(q)\frac{\partial H}{\partial q} - U(q)\dot{U}(q)m \\ m \in U(q)\mathrm{Im}(M(q)) = \mathrm{Im}(U(q)M(q)) = \mathrm{Im}(U(q)M(q)U(q)^T) \Leftrightarrow m = \begin{pmatrix} m_r \\ 0_{n-r} \end{pmatrix}. \end{cases} \tag{5.31}$$

where the equality constraint appears clearly. More developments may be found in [216].

5.2 Moreau's Sweeping Process

Jean Jacques Moreau introduced the sweeping process at the Convex Analysis Seminar of the university of Montpellier in 1971, 1972, and 1973 [880, 881, 882] and in [887]. We briefly describe the so-called first-order sweeping process (which we shall meet again later in this chapter when we deal with complementarity dynamical systems), and then spend significant time on its second-order version which models nonsmooth multibody systems and was introduced in [890].

5.2.1 First-Order Sweeping Process

Given a convex "moving" (i.e., time-dependent) set $C(t) \subseteq \mathbb{R}^n$, a moving point $x(\cdot)$ is a solution to the first-order sweeping process by $C(t)$ if:

- **(i)** $x(0) \in C(0)$,
- **(ii)** $x(t) \in C(t)$ for all $t > 0$,
- **(iii)** There exists a positive measure μ, relative to which the Stieltjes measure dx possesses a density $\dot{x}(\cdot)$,[9] i.e., $dx = \dot{x}(t)d\mu$, and

$$-\dot{x}(t) \in N_{C(t)}(x(t)). \tag{5.32}$$

[9] See Appendix A.2 for definitions.

Items (**i**) and (**ii**) have an obvious meaning; (**iii**) means that if $x(t)$ is on the boundary of $C(t)$ then its derivative points inward the set $C(t)$; $N_{C(t)}(x)$ denotes the outward normal cone to $C(t)$ at $x(t)$ and can also be denoted as $\partial\psi_{C(t)}(x)$, where $\psi_{C(t)}(\cdot)$ is the indicator function of $C(t)$, see Definitions B.2 and B.7. The name "sweeping process" comes from the fact that if $x(t) \in \text{Int}(C(t))$, then $N_{C(t)}(x(t)) = \{0\} \Rightarrow \dot{x}(t) = 0$: the point does not move. Now if $x(t) \in \text{bd}(C(t))$, there exists an element $\lambda(t)$ in $N_{C(t)}(x(t))$ (which is in this case a convex cone not reduced to the singleton $\{0\}$), such that $-\lambda(t)$ points inward $C(t)$, such that $\dot{x}(t) = -\lambda(t)$: the point $x(t)$ is "swept" by the moving set $C(t)$, and thus cannot escape from it: $x(0) \in C(0) \Rightarrow x(t) \in C(t)$ for all $t \geq 0$. We shall see in Sect. 5.4.4.3 how such a selection $\lambda(t)$ may be calculated, for particular forms of $C(t)$. When $C(t)$ is a nonempty convex cone, then using (B.19) one finds that $\lambda(t) \in N_{C(t)}(x(t)) \Leftrightarrow C(t) \ni x(t) \perp -\lambda(t) \in C^\star(t)$. Then the differential inclusion in (5.32) is equivalently rewritten as a cone complementarity system: $\dot{x}(t) = -\lambda(t)$, $C(t) \ni x(t) \perp -\lambda(t) \in C^\star(t)$.

The sweeping process is therefore a particular first-order differential inclusion. The proof of existence and uniqueness of solutions of the first-order sweeping process has been done when $C(t)$ possesses different properties [867, 887]: using the so-called *Moreau–Yosida's approximants* (which may be seen as a mathematical path to represent contact stiffness, as we saw in Example 1.6 and in Appendix B) and showing convergence in the *filled-in graphs* sense when $C(t)$ is a right-continuous function of bounded variation,[10] using the so-called *catching-up* algorithm $x_{k+1} - x_k \in -N_{C(t_{k+1})}(x_{k+1}) \Leftrightarrow x_{k+1} = \text{proj}[C(t_{k+1}); x_k]$ using (B.20).[11] This allows one to construct uniformly convergent approximants (in the sense of discretization of the solution [891] when $C(t)$ is Hausdorff continuous and has nonempty interior, or when $C(t)$ is right lower semi-continuous with nonempty interior. The first-order sweeping process is extended to its perturbed version as $-\dot{x}(t) + f(x(t), t) \in N_{C(t)}(x(t))$, and to state-dependent moving sets as $-\dot{x}(t) + f(x(t), t) \in N_{C(t,x(t))}(x(t))$ [71]. Applications are in crowd motion [827, 986], problems such as water falling in a cavity [887], plasticity, and the evolution of elastoplastic systems [883, 885] which were the original motivations of the first-order sweeping process, economics [304, 521].

Remark 5.2 Consider (5.32). If initially $x(0^-) \notin C(0)$, then one can apply a jump as $x(0^+) = \text{proj}(C(0); x(0^-))$ so that $x(t) \in C(t)$ for all $t > 0$. Rigorously, one has to allow for the existence of a measure in the system (hence, the differential inclusion (5.32) becomes a measure differential inclusion) and work with the differential measure associated with the function $x(\cdot)$ (supposed to be right-continuous of local bounded variation). One obtains $x(0^+) - x(0^-) \in -N_{C(0)}(x(0^+))$, which from (B.20) gives the projection. We will give more details in (5.144) and (5.145).

[10] See Sect. A.3.1 for definitions.

[11] The name catching-up comes from the fact that the solution has the tendency to catch-up with the moving set, see Fig. 9.6 in [13]. Notice also that the time step h does not appear explicitly since the right-hand side is a cone.

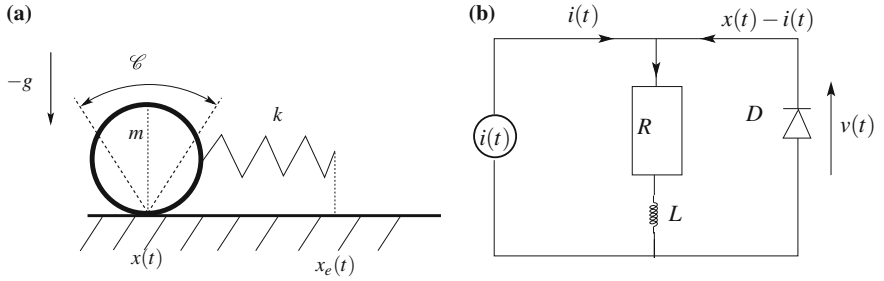

Fig. 5.2 Mechanical and electrical examples. **a**Mass and spring with Coulomb's friction. **b** Circuit with ideal diode and current source

Example 5.2 Consider the circuit in Fig. 5.2b. Its dynamics is given by [10, 226]:

$$\begin{cases} \dot{x}(t) = -\frac{R}{L}x(t) + \frac{v(t)}{L} \\ 0 \le w(t) = x(t) - i(t) \perp v(t) \ge 0. \end{cases} \tag{5.33}$$

The signal $w(t)$ is the current through the diode, $v(t)$ is the voltage across the diode D, $x(t)$ is the current through the inductor/resistor, and $i(t)$ is a current source. The complementarity conditions are similar to those in Example 1.6, (1.37). They form the current/voltage characteristic of an ideal diode, whose graph is depicted in Fig. 5.22. Few manipulations using (B.19) yield an equivalent dynamics: $-\dot{x}(t) - \frac{R}{L}x(t) \in N_{[i(t),+\infty)}(x(t))$.

Example 5.3 Consider the mechanical system depicted in Fig. 5.2a. The linear spring with stiffness $k > 0$ is acted upon by two forces that balance: the elastic force $k(x - x_e(t))$ with $x_e(t)$ a forced displacement, and the friction force $-\mu mg\ \mathrm{sgn}(\dot{x})$, where $\mu > 0$ is the coefficient of friction, g is the gravity acceleration. The equilibrium of the massless spring states that $k(x - x_e(t)) \in -\mu mg\ \mathrm{sgn}(\dot{x})$. Using (B.16) and examples of conjugacy $f_2(\cdot)$ or $f_6(\cdot)$ in the Appendix, this is rewritten equivalently as $\dot{x}(t) \in -N_{[-\frac{\mu mg}{k}+x_e(t),\, \frac{\mu mg}{k}+x_e(t)]}(x(t))$.

5.2.2 *Second-Order Sweeping Process: Frictionless Mechanical Systems*

Following closely [894], we explain how one may construct an evolution problem representing as fairly as possible nonsmooth multibody dynamics, in the setting of the sweeping process. The admissible domain, or *feasible region*, is supposed to be *finitely represented*, i.e., it is given as $\Phi = \{q \in \mathbb{R}^n \,|\, f_i(q) \ge 0,\ 1 \le i \le m\}$, for some functions $f_i(\cdot)$ which satisfy the basic requirements of Definition 1.8. Therefore, the mechanical system is submitted to a set of *frictionless* unilateral constraints $f_i(q) \ge 0$, $i = 1, \ldots, m$, and it is assumed that the gradients $\nabla f_i(q)$ are not zero

in some neighborhood of the surfaces $f_i(q) = 0$. In this section we do not consider bilateral constraints, and thus $m_u = m$.

5.2.2.1 Smooth Motions

It is convenient to consider first the smooth motions of the system. It is also necessary to have in mind some definitions and notations used in the following. The tangent space to the system's configuration space $\mathcal{Q} \supseteq \Phi$ at a point q is denoted as $E(q)$ or $T_q\mathcal{Q}$, to which right velocities $\dot{q}(t^+)$ belong (i.e., right derivatives of $q(t)$). In fact, $E(q)$ can be identified with $\mathbb{R}^n$.

Definition 5.1 (*Tangent cone*) The convex polyhedral tangent cone $V(q)$[12] to the region Φ at point q is given by

$$V(q) = \left\{ v \in E(q) | \ \forall i \in \mathcal{J}(q), v^T \nabla f_i(q) \geq 0 \right\}, \tag{5.34}$$

where

$$\mathcal{J}(q) = \{ i \in \{1, \ldots, m\} \mid f_i(q) \leq 0 \}. \tag{5.35}$$

Note that $V(q) = E(q) = \mathbb{R}^n$ when $\mathcal{J}(q) = \emptyset$, i.e., when $f_i(q) > 0$ for all $1 \leq i \leq m$.[13]

Suppose that the contact index set $\mathcal{J}(q)$ is reduced to one element i. Then $V(q)$ is the half-space $\left\{ v \in \mathbb{R}^n \mid v^T \nabla f_i(q) \geq 0 \right\}$. In this case the hyperplane tangent to $f_i(q) = 0$ is given by

$$T(q) = \left\{ v \in \mathbb{R}^n \mid v^T \nabla f_i(q) = 0 \right\}. \tag{5.36}$$

Note that the cones in Definition 5.1 and in Definition B.6 are not identical: they are if $q(t) \in \Phi$, but not if $q \notin \Phi$: in fact the tangent cone is commonly taken as $\emptyset$ if q is outside Φ, whereas $V(q)$ is not empty in this case (see (5.35) which means that one has to take into account those positions q such that the constraints are violated). As far as impact dynamics are concerned, this distinction is purely formal, because in fact q will be forced to never leave Φ. By doing the assumption that $q(t) \in \Phi$ for all $t \geq \tau_0$,[14] one could therefore define $\mathcal{J}(q)$ in (5.35) writing $f_i(q) = 0$. The definition in (5.35) can be useful in some existence of solutions results where approximating problems will imply some penetration into the constraints, see [867, Chap. 3]. Then one needs to define the tangent cone for points outside Φ. If the unilateral constraints are time-varying, $f(q, t) \geq 0$, then one replaces the above

[12] The notation $V(q)$ is for velocity, since $V(q)$ will appear to be a set of velocities.

[13] In other words, the system is inside the domain Φ and does not touch any constraint hypersurface.

[14] We prefer to denote the initial time as τ_0 instead of t_0, to avoid confusions with the notation for impact times t_k.

tangent cone by $T(q,t) = \left\{v \in E(q) | \ \forall i \in \mathscr{J}(q,t), v^T \nabla f_i(q) + \frac{\partial}{\partial t} f_i(q,t) \geq 0\right\}$, with $\mathscr{J}(q) = \{i \in \{1,\ldots,m\} \mid f_i(q,t) \leq 0\}$.

Polarity is a notion that permits to go from the tangent to the normal cones: it generalizes orthogonality that relates normal and tangent directions. The *polar* cone to $V(q)$ is defined as follows:

Definition 5.2 (*Normal cone*) The closed convex polyhedral cone $N(q)$ is given by

$$N(q) = \left\{r \in E'(q) \mid \forall v \in V(q), v^T r \leq 0\right\} \tag{5.37}$$

where $E'(q)$ denotes the dual space of $E(q)$ (which we can safely take in our setting equal to $\mathbb{R}^n$ since it contains n-dimensional generalized force vectors), to which generalized reaction forces belong. $N(q)$ is the outward normal cone to Φ at q, and is generated by the vectors $\nabla f_i(q)$, $i \in \mathscr{J}(q)$. $N(q) = \{0\}$ if $\mathscr{J}(q) = \emptyset$, i.e., if $q \in \text{Int}(\Phi)$.

The tangent and normal cones as defined above are called the *linearization cones*, see Sect. B.1 and Definition B.6. Under some constraint qualification like the Mangasarian–Fromovitz CQ (see (B.9)), these cones are equal to the usual tangent and normal cones as defined from Definition B.2 (b), (c) and polarity. In the sweeping process formulation, the unknown will not be the position q, but its derivative, i.e., the velocities. More exactly, the unknown will be denoted as a time function u such that

$$q(t) = q(\tau_0) + \int_{\tau_0}^{t} u(\tau) d\tau. \tag{5.38}$$

Such a $u(\cdot)$ is assumed to be Lebesgue integrable, and it will be supposed for the moment locally absolutely continuous. The following propositions are in order:

Proposition 5.12 *[894] If $q(t) \in \Phi$ for every $t \geq \tau_0$, then*

$$u(t^+) \in V(q(t)) \text{ and } u(t^-) \in -V(q(t)). \tag{5.39}$$

Note that if $q(t)$ is in the interior of Φ, this simply reduces to both right and left velocities to be in $\mathbb{R}^n$. Also, for a smooth motion, $u(t)$ is continuous so that its left and right limits are the same; hence, $u(t) \in V(q(t)) \cap -V(q(t))$, which is the linear subspace of $\mathbb{R}^n$ orthogonal to $N(q)$ (hence the whole of $\mathbb{R}^n$ if $q \in \text{Int}(\Phi)$). In case of a single constraint, this set equals $T(q(t))$ in (5.36) if $f(q) = 0$, and otherwise the whole of $\mathbb{R}^n$.

Now if the boundary of Φ is attained at t_k, necessarily $u(t_k^+)^T \nabla f_i(q(t_k)) \geq 0$ and $u(t_k^-)^T \nabla f_i(q(t_k)) \leq 0$ for some i. Roughly, the system must have attained some constraint $f_i(q) = 0$ and must either leave it or remain on it.

Lemma 5.1 (Viability Lemma [894]) *Let $q(t)$ and $u(t)$ be associated as in (5.38). Suppose $q(\tau_0) \in \Phi$, and that $u(t) \in V(q(t))$ Lebesgue-almost everywhere. Then $q(t) \in \Phi$ for all $t \geq \tau_0$.*

Remark 5.3 Notice that we do not care about the possible local existence problems, and we set for simplicity relationships on the whole of $\mathbb{R}^+$. In all the definitions and propositions, one may replace "for all $t \geq \tau_0$" by "for all $t \in I$," for some interval I.

Let us now consider the Lagrange equations of the system. The total reaction $P \in \mathbb{R}^n$ must be along the surface Euclidean normal for the case of one constraint, which generalizes to

$$-P \in N(q) \tag{5.40}$$

for several constraints. It is equivalent (see Definition 5.2 and (B.8)) to write

$$P = \sum_{i \in \mathscr{J}(q)} \lambda_i \nabla f_i(q) \tag{5.41}$$

with $\lambda_i \geq 0$. Hence, the Lagrange equations can be written as

$$-M(q(t))\ddot{q}(t) + Q(t, q(t), \dot{q}(t)) \in N(q(t)), \tag{5.42}$$

that is a second-order *differential inclusion*.[15] We write $Q(t, q, \dot{q})$ to shorten the notations for Coriolis, centrifugal, gravity, and bounded torques, see Example 1.3. The dynamics in (5.42) is for the moment simply a rewriting of classical dynamical equations. Then a smooth motion agrees with the stated mechanical conditions (system inside the domain Φ, reaction in the normal cone to Φ) if an only if (5.42) is satisfied and $q(t) \in \Phi$ for all $t \geq \tau_0$. It is possible to show that every solution of the inclusion (5.42) in fact satisfies a stronger inclusion[16]:

Proposition 5.13 *[894] A smooth motion with initial condition $q(\tau_0) \in \Phi$ is a solution of (5.42) and satisfies $q(t) \in \Phi$ for all $t \geq \tau_0$, if and only if the velocity function associated to q in (5.38) satisfies Lebesgue-almost everywhere the differential inclusion*

$$-M(q(t))\ddot{q}(t) + Q(t, q(t), u(t)) \in \partial\psi_{V(q(t))}(u(t)) \ \ (= N_{V(q(t))}(u(t))), \tag{5.43}$$

where the set in the right-hand side is named Moreau's set.

The subdifferential in the sense of convex analysis is defined in Definition B.7. The sweeping process is therefore an expression of the dynamics in terms of the velocity u. The trick (actually, this is not a trick but a rigorous mathematical setting) is to start from (5.42) and to arrive at (5.43). It is important to notice that $N(q)$ in (5.42),which is the normal cone to Φ (and is closely related to $\partial\psi_\Phi(q)$, see Definitions B.5 and B.7), is replaced by $\partial\psi_{V(q)}(u)$ which is the normal cone in a velocity space (no longer in $\Phi \subset$ the configuration space). In Problem 2.2 we had $\partial\psi_\Phi(q)$, whereas here we

[15] See Corollary B.2 for comments on the right-hand side of (5.42).

[16] As proved in [894, Proposition 5.1] one has $\partial\psi_{V(q)}(u) \subseteq N(q)$, and strict inclusion in general. This can be seen by drawing some planar examples, e.g., when $\mathrm{bd}(\Phi)$ is an angle. See also Sect. B.2.2.

have $\partial\psi_{V(q)}(u)$, because the former is written at the acceleration–force level. Recall that at this stage, u is locally absolutely continuous: jumps are not yet considered. If $m = 1$, then on the boundary of Φ the cone $N_{V(q(t))}(u(t^+))$ is contained in the outward normal half-line spanned by $-\nabla f(q)$. Some examples are depicted in Appendix B.

Remark 5.4 It is crucial to understand that the set-valued right-hand side in (5.43) is a *constitutive model* relating the contact forces and impulses to velocities and positions. As such linear or nonlinear spring-dashpot models, Moreau's set, or complementarity relations, have to be placed on an equal footing: they just are different models. Moreau's set implies some lexicographical inequality on the position and velocity.

It is noteworthy that in view of (B.19) we may equivalently rewrite the dynamics in (5.43) as the cone complementarity system:

$$\begin{cases} M(q(t))\ddot{q}(t) - Q(t, q(t), u(t)) = -P(t) \\ \\ V(q(t)) \ni u(t) \perp P(t) \in N(q(t)). \end{cases} \tag{5.44}$$

5.2.2.2 Sweeping Process and Jourdain's Variations

Let us recall the developments made in Sect. 3.1.2 on the bouncing ball system. It is apparent from (3.15) that the sweeping process corresponds, when expressed in a variational inequality form, to a Jourdain's variation. Indeed from the normal cone definition in (B.6), it follows that (5.43) is equivalently rewritten as follows: Given $q(t) \in \Phi$, find $u(t) \in V(q(t))$ such that

$$\langle M(q(t))\ddot{q}(t) - Q(t, q(t), u(t)), v - u(t)\rangle \geq 0 \text{ for all } v \in V(q(t)). \tag{5.45}$$

The Jourdain's variation is $\delta u = v - u$ and it belongs to $T_{V(q)}(u)$ (noting that $V(q)$ is convex, this can be proved using for instance the first definition of the tangent cone in Definition B.2, hence generalizing the developments made in Sect. 3.1.2 for the dynamics as in (3.15)). The great advantage of Jourdain's variations is that they allow for velocity jumps. More precisely, they allow for an impact mapping calculation as a direct consequence of a simple convex analysis rule. Another advantage of the sweeping process formulation is that given $q \in \Phi$, the mapping $u \mapsto \xi \in N_{V(q)}(u)$ is maximal monotone provided $V(q) \neq \emptyset$, while $q \mapsto \lambda \in N_\Phi(q)$ is maximal monotone only if Φ is closed convex nonempty. Furthermore, $V(q)$ is a polyhedral convex cone. From a computational point of view this is a great advantage because the normal cone $N_{V(q)}(u)$ is easier to calculate as (see Sect. B.2.2):

$$N_{V(q)}(u) = \{w \in \mathbb{R}^n | w = -\sum_{i \in \mathscr{K}(u)} \lambda_i \nabla g_i(u), \lambda_i \geq 0\} \tag{5.46}$$

where $\mathscr{K}(u) = \{i \in \mathscr{J}(q) | g_i(u) = 0\} \subseteq \mathscr{J}(q)$, $g_i(u) = \nabla f_i(q)^T u$, so that $\nabla g_i(u) = \nabla f_i(q)$. Moreover, $0 \leq \lambda_i \perp u^T \nabla f_i(q) \geq 0$ for $i \in \mathscr{J}(q)$: the multipliers

λ_i that correspond to velocities pointing inward $V(q)$ (thus inward Φ) are zero. Those that correspond to velocities tangent to $V(q)$ (hence tangent to Φ) are nonnegative (thus may be positive). It is noteworthy that the multipliers λ_i in (5.46) and in (5.41) are the same. So according to the notation in (5.1), we should write them as $\lambda_{\mathrm{n},u,i}$. Moreau's right-hand side is depicted in simple cases in Figure B.1.

5.2.2.3 Practical Construction of Moreau's Set

The normal cone in (5.46) already provides us with a concrete form of Moreau's set, which allows one to calculate it. In addition, we have $N_{V(q)}(u) = \{0\}$ when $q \in \mathrm{Int}(\Phi)$ ($\Leftrightarrow f(q) > 0$), or when $q \in \mathrm{bd}(\Phi)$ and $u \in \mathrm{Int}(V(q))$. When $q \in \mathrm{bd}(\Phi)$ and $u \in \mathrm{bd}(V(q))$ then (5.46) applies. Notice that the elements w inside $N_{V(q)}(u)$ in (5.46) may be written as $w = -\sum_{i\in\mathscr{J}(u)} \lambda_i \nabla f_i(q), 0 \leq \lambda_i \perp \nabla f_i(q)^T u \geq 0$. While those in the normal cone $N(q)$ are equal to $w = -\sum_{i=1}^m \lambda_i \nabla f_i(q), 0 \leq \lambda_i \perp f_i(q) \geq 0$. It is also noteworthy that

$$P \in -N_{V(q)}(u) \Leftrightarrow V(q) \ni u \perp P \in -N(q),$$

using (B.19), Definition B.4 and polarity of the normal and tangent cones. This implies that the mapping $u \mapsto P$ is maximal monotone, a property that is very useful for stability analysis purpose (see Chap. 7, Sect. 7.5). Notice that from (5.41) we may write that $P = \nabla f(q)\lambda$, keeping in mind that the components of the multiplier λ satisfy complementarity constraints and may therefore vanish depending on the gap functions and on the velocity $u = \dot{q}$.

5.2.2.4 Nonsmooth Motions

To deal with possible collisions, one needs to enlarge the space of functions $u(\cdot)$ to discontinuous functions. The space of functions of local bounded variation functions is quite suitable. Due to velocity jumps, the classical Lagrange equations which are equality of functions will have to be replaced by equality of measures (this should be clear from the developments of Chap. 1). Right-continuous functions of local bounded variation (in short, *RCLBV* functions) possess derivatives which can be identified with Stieltjes measures [1076], and are a natural and convenient setting for the study of measure of differential equations (we already met such functions in MDEs of Sect. 1.2.1). If one associates with such $u(\cdot)$ the measure du (called the *differential measure* of u in [894], and noted as Du in [1076]), then one has that for any compact interval $[t_1, t_2]$ on which $u(\cdot)$ exists, $\int_{[t_1,t_2]} du = u(t_2^+) - u(t_1^-)$, and $\int_{(t_1,t_2)} du = u(t_2^-) - u(t_1^+)$. In particular, if $u(\cdot)$ is discontinuous at $t = t_1 = t_2$, then du possesses an atom at this point, i.e., it is a Dirac distribution (see Sects. A.2 and A.3 in Appendix for more details). Now using (5.38) the Lagrange equations of the system can be written as:

$$M(q)du + Q(t,q,u)dt = Pdt, \tag{5.47}$$

which is an equality of measures, and dt is the Lebesgue measure. All-time functions possess the required smoothness so that the products in (5.47) are well defined. Clearly, the term $M(q(t))du$ in the left-hand side of (5.47) is meaningful only because $q(\cdot)$ is continuous, as we have previously, respectively, noticed and proved, see Example 1.3. This way of writing the dynamics makes sense when $u \in RCLBV$. Also, one can replace the right-hand side of (5.47) by some real measures dP, which represent the total impulse exerted on the system. This allows to encompass impulsive forces and torques. Thus the right-hand side of (5.47) can be written as $dP = F(t,q,u)dt + dR$, where $F(t,q,u)$ are the bounded Lebesgue integrable generalized contact forces, and dR are the contact impulses (see Chap. 1, Sect. 1.1 and Appendix A.2 for the terminology associated to reactions at the contact point). Clearly, in most applications we have:

$$dR = \sum_{k=0}^{+\infty} p_k \delta_{t_k} dt, \tag{5.48}$$

where the times t_k correspond to the instants when $u(\cdot)$ is discontinuous. In other words, we may disregard the nonatomic, non-Lebesgue integrable part of the differential measure representing the acceleration,[17] if a practical point of view is adopted.[18] Since $u \in RCLBV$, the set of velocity-jump times is countable (we shall use this important property of functions of bounded variation when we deal with stability of controlled systems with unilateral constraints in Chap. 8). Hence, the general form of dR in (5.48).

With this material in mind, one easily deduces that the evolution problem at the times of discontinuity in $u(\cdot)$ can be written as

$$M(q)du - Q(t,q,u)dt = dR. \tag{5.49}$$

Consider smooth motions. From Proposition 5.13 it follows that for Lebesgue-almost every t, one has:

$$-P(t) \in \partial\psi_{V(q(t))}(u(t)). \tag{5.50}$$

This secures that $q(t) \in \Phi$ for all $t \geq \tau_0$, see Lemma 5.1 and Proposition 5.13, and Eq. (5.42). One also has that $u(t) \in V(q(t))$ for every t. Now at the discontinuities of $u(\cdot)$ one must choose how to replace $u(t)$ in the right-hand side of (5.50). The following definition is then proposed:

Definition 5.3 (*Soft shocks [894]*) The set of unilateral constraints $f(q) \geq 0$ is said to be *frictionless* and *soft* if the total contact impulsion admits a representation $dR = R'_\mu d\mu$, where μ denotes a nonnegative real measure, and R'_μ is locally integrable

[17] See Appendix A.3, Remark A.4.

[18] Such a point of view is certainly not satisfying for purists and mathematicians.

(with respect to $d\mu$), such that for every t:

$$-R'_\mu(t) \in \partial\psi_{V(q)}(u(t^+)) \quad (= N_{V(q)}(u(t^+))). \tag{5.51}$$

Thus, one replaces $u(\cdot)$ in the right-hand side of (5.50) by its right limit $u(t^+)$, whereas the term $P(t)$ is replaced by the contact percussion $-R'_\mu(t)$, that is, the density of the atom of the contact impulse measure at the impact time t_k (recall that a density of a measure is a *function*, see Appendix A.2, Definition A.10). Furthermore, $R'_\mu(t_k) = p_k$ where p_k is given in (5.48). One feature of the sweeping process formulation is that the way one writes the dynamics is independent of the measure with respect to which the densities of the contact impulse and of the acceleration (i.e., du) are expressed, provided this measure is nonnegative, [894, Proposition 8.2]. Let us recall that the measure μ may encompass singular (Dirac) as well as nonsingular measures (functions of time). This depends on whether the system is in a permanent contact phase, a noncontact mode, or at an impact time t_k.

This type of evolution problem is called a soft shock because it reduces when the surface of constraint has codimension one to the classical inelastic impact, i.e., a coefficient of restitution $e_n = 0$ (see Example 5.4 below). We shall see in the following that the expression in (5.51) is equivalent to some more familiar impact dynamics expressions we have derived before.

Remark 5.5 Notice that (5.51) is stronger than (5.40), because the latter is true for any impact process, whereas (5.51) implies a particular impact process. This is even more noticeable on the equivalent formulations of the sweeping process given below.

From the foregoing developments, the sweeping process problem is mathematically expressed as follows [867, 890]:

Problem 5.1 (*Frictionless sweeping process*) Find a *RCLBV* function $u(\cdot)$ such that $u(\cdot)$ and $q(\cdot)$ defined by (5.38) satisfy the following:

- $q(\tau_0) = q_0$,
- $u(\tau_0) = u_0$,
- $q(t) \in \Phi$ for all $t \geq \tau_0$,
- $u(t) \in V(q(t))$ for all $t \geq \tau_0$,
- $Q(t, q(t), u(t))dt - M(q(t))du \in N_{V(q(t))}(u(t))$,

in the sense of differential measures: there is a (nonunique) positive measure μ with respect to which the Lebesgue measure dt and the Stieltjes measure du both possess densities, respectively, $t'_\mu = \frac{dt}{d\mu}$ and $u'_\mu = \frac{du}{d\mu}$ such that:

$$Q(t, q(t), u(t))t'_\mu - M(q(t))u'_\mu \in N_{V(q(t))}(u(t)) \tag{5.52}$$

μ-almost everywhere.

See Appendix A.2, Definition A.10 for details about the notations for densities. The notation $t'_\mu = \frac{dt}{d\mu}$ is called the Radon–Nikodym derivative of the Lebesgue measure

λ with respect to the measure μ. We do not want to go into mathematical details at this stage, since this is actually not fundamental to understand the sweeping process. Let us notice that the introduction of positive measures μ simply means that since sweeping processes are differential inclusions whose right-hand side is a cone, one may multiply the left-hand side by a positive term without violating the inclusion. In case of an impact at $t = t_k$, then (5.51) holds and Problem 5.1 becomes:

$$-M(q(t_k))\sigma_u(t_k) = -M(q(t_k))[u(t_k^+) - u(t_k^-)] = -R'_\mu(t_k) \in N_{V(q(t_k))}(u(t_k^+)). \tag{5.53}$$

The inclusion in (5.53) can be deduced noticing that the Lebesgue measure has no atoms. Indeed at the times of discontinuities, one has $du = [u(t_k^+) - u(t_k^-)]\delta_{t_k} = \sigma_u(t_k)\delta_{t_k} = \nu_k u'_\mu(t_k)$, and $\nu_k t'_\mu(t_k) = 0$ (in other words the Lebesgue dt and Dirac du measures are mutually singular and one has $dt(\{t_k\}) = 0$). Hence, multiplying both sides of (5.52) by ν_k, one gets (5.53).

From Problem 5.1 and (5.53), one might think that the postimpact velocity must be known to integrate pre-impact motion (i.e., the dynamics is anticipative); however, this is not the case at all:

Proposition 5.14 *[894] For any motion satisfying (5.52), one has*

$$u(t^+) = \mathrm{proj}_{M(q(t))}(V(q(t)); u(t^-)), \tag{5.54}$$

where the projection is understood in the sense of the kinetic metric.

The proof follows from (5.53), using (B.20). We shall find again the same manipulation with time-stepping (event-capturing) methods.

Hence, the velocity after the shock is the vector closest (in the kinetic metric distance sense so that coordinate invariance is guaranteed) to the velocity before the shock, inside $V(q(t))$. If $u(t^-) \in V(q(t))$ then $u(t^+) = u(t^-)$ so that no impact occurs. Some examples are illustrated in Fig. 5.3.[19] From the fact that $u(t^-) \in -V(q(t))$, see Proposition 5.12, $u(t^+)$ lies on the boundary of $V(q(t))$, i.e., *generalized dissipative* impacts are treated that correspond to a restitution coefficient $e_n = 0$ in the one-dimensional case.

Equations (5.51) and (5.53) may also be used to understand where the apparently complex formulation of Problem 5.1 comes from. In case when $M(q)$ is the identity, (5.51) and (5.53) are equivalent to the following conditions:

$$\begin{cases} u(t_k^+) \in V(q(t_k)) \\ -R'_\mu(t_k) \in N(q(t_k)) \\ u(t_k^+)^T R'_\mu(t_k) = 0 \\ \sigma_u(t_k) = R'_\mu(t_k). \end{cases} \tag{5.55}$$

[19] In this figure and others, we draw the cone $q + V(q)$ rather than $V(q)$, and so on for the other cones. This is not a major issue since velocities belong to $V(q)$.

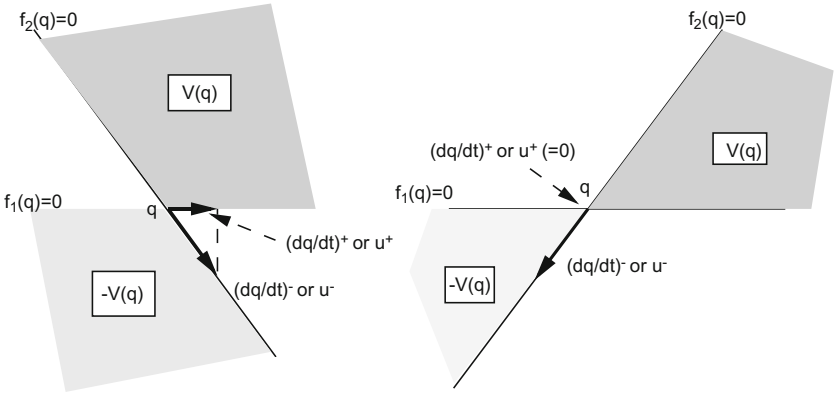

Fig. 5.3 Collision at a singularity (sweeping process)

The equations in (5.55) possess the form of a *Cone Complementarity Problem* (CCP), since they can be rewritten as

$$V(q(t_k)) \ni u(t_k^+) \perp R'_\mu(t_k) \in -N(q(t_k)), \tag{5.56}$$

where the two cones are dual cones. We shall come back in more details on such formulations later in this chapter (see Remark 5.7 below). The equivalence between (5.55) and $-R'_\mu(t) \in \partial\psi_{V(q(t))}(u(t^+)) \Leftrightarrow -u(t^+) \in \partial\psi^\star_{V(q(t))}(R'_\mu(t))$ can be shown using the definitions of the various terms appearing in those formulas, and convex analysis tools. The equations in (5.55) are in turn equivalent to

$$\begin{cases} u(t_k^+) = \text{ proj } (V(q(t_k)), u(t_k^-)) \\ R'_\mu(t_k) = -\text{proj } (N(q(t_k)), u(t_k^-)) \\ u(t_k^+)^T R'_\mu(t_k) = 0. \end{cases} \tag{5.57}$$

The equivalence between (5.55) and (5.57) can be shown via direct application Moreau's Lemma of the two cones, see Lemma B.2, by identifying x with $u(t_k^+)$ and y with $-R'_\mu(t_k)$, recalling that $V(q(t_k))$ and $N(q(t_k))$ are a pair of mutually polar closed convex cones of the Euclidean space $\mathbb{R}^n$ (recall that the inertia matrix is considered to be the identity matrix since we work at fixed $q(t_k)$, so the kinetic metric is the Euclidean one). The sweeping process collision mapping is illustrated in Fig. 5.4 for two different cases.[20]

In case of a nontrivial mass matrix at $t = t_k$, we obtain the following, starting from (5.53) and (5.56). Let us define $N^{M_k}(q) \triangleq M(q(t_k))^{-1}N(q)$, that is, the normal cone in the kinetic metric, and $\bar{R}'_\mu(t_k) \triangleq M(q(t_k))^{-1}R'_\mu(t_k)$. Then we can rewrite (5.56) as $(N^M(q(t_k)))^\circ = V(q(t_k)) \ni u(t_k^+) \perp^{M_k} \bar{R}'_\mu(t_k) \in -N^{M_k}(q(t_k))$, where $x \perp^{M_k} y$

[20] Same comment as for Fig. 5.3.

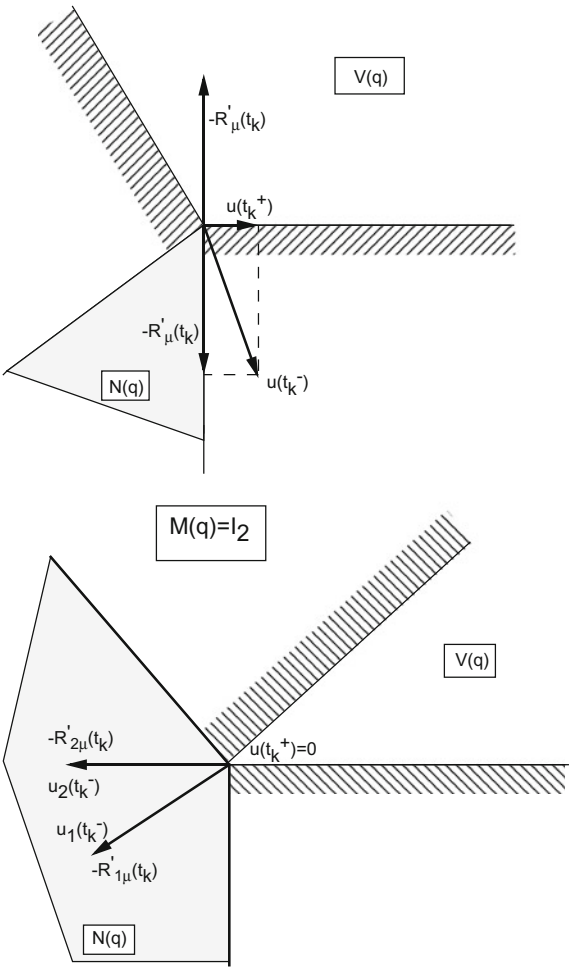

Fig. 5.4 Multiple impacts rule (sweeping process)

means that $\langle x, y\rangle_{M_k} = x^T M_k y = 0$. Notice that $V(q) = \{z \in \mathbb{R}^n |\ z^T y \leq 0,\ y \in N(q)\} = \{z \in \mathbb{R}^n |\ z^T M_k \bar{y} \leq 0,\ \bar{y} \in N^{M_k}(q)\}$, so that indeed $V(q) = (N^{M_k}(q))^\circ$. It follows that $u(t_k^+) - u(t_k^-) \in -N^{M_k}_{V(q(t_k))}(u(t_k^+))$ (from which (5.54) is recovered), equivalently $u(t_k^+) \in -N^{M_k}_{-N^{M_k}(q(t_k))}(u(t_k^+) - u(t_k^-))$, equivalently $\bar{R}'_\mu(t_k) + u(t_k^+) \in -N^{M_k}_{-N^{M_k}(q(t_k))}(\bar{R}'_\mu(t_k))$. We infer that $\bar{R}'_\mu(t_k) = \text{proj}_{M_k}(-N^{M_k}(q(t_k)); -u(t_k^-))$ so that $\bar{R}'_\mu(t_k) = -\text{proj}_{M_k}(N^{M_k}(q(t_k)); u(t_k^-))$, so that finally

$$\begin{aligned} R'_\mu(t_k) &= -M(q(t_k))\text{proj}_{M_k}(N^{M_k}(q(t_k)); u(t_k^-)) \\ &= -M(q(t_k))\ \text{argmin}_{z \in N^{M_k}(q(t_k))}\ \tfrac{1}{2}(z - u(t_k^-))^T M(q(t_k))(z - u(t_k^-)). \end{aligned} \tag{5.58}$$

Of course, we can also obtain $R'_\mu(t_k)$ directly from (5.53) and (5.54).

Remark 5.6 (Virtual powers) The generalized velocities $u(\cdot)$ belong to the tangent space $T_q\mathscr{Q}$ to the configuration space $\mathscr{Q}$ of the system. In case of frictionless (or perfect) bilaterally constrained systems (one considers only the bilateral constraints in (5.1)), the velocities which are compatible with the constraints are in the set $S_q \stackrel{\Delta}{=} \{u \in T_q\mathscr{Q} | \langle \nabla h_i(q), u\rangle = 0, i \in \{1, 2, \ldots, m_b\}\}$. In other words, the admissible virtual velocities are velocities in $T_q\mathscr{Q}$, which are also tangent to the bilateral constraints. In a geometrical context, one may take instead of the Euclidean gradients $\nabla h_i(q)$, the gradients in the Riemannian kinetic metric defined as $x^T M(q) y$ for two vectors x and y, which are given by $dh_i(q) = M(q)^{-1}\nabla h_i(q)$. Then the inner product is defined as $\langle dh_i(q), u\rangle_q = 0$, where $\langle x, y\rangle_q = x^T M(q) y$. The fact that the constraints are supposed perfect means that the contact force R satisfies $\mathscr{P} = \langle R, u\rangle = 0$, for all $u \in S_q$. Equivalently, $R = \sum_i^{m_b} \lambda_i \nabla h_i(q)$ for some (unsigned) multipliers λ_i. If the geometrical path is used, one writes equivalently $\mathscr{P} = \langle R^\star, u\rangle_q = 0$ where $R^\star = M(q)^{-1} R$: vanishing virtual power may be seen as a constitutive law for perfect bilateral constraints. The cone complementarity problem in (5.56) (see also (8.6) in a slightly broader context) generalizes this "virtual power principle" to unilateral constraints.

Example 5.4 Let us consider the dynamics of a ball falling vertically on a soft rigid ground within this framework. We have $\Phi = \{x \in \mathbb{R} | x \geq 0\}$, and the dynamics can be written as

$$-mdu + g \in \partial\psi_{V(x(t))}\left(u(t^+)\right), \tag{5.59}$$

where $x(t)$ is the vertical coordinate of the ball, $u(\cdot)$ equals $\dot{x}(\cdot)$ almost everywhere, and $\partial\psi_{V(x(t))}\left(u(t^+)\right)$ is contained in the outward normal half-line to the contact point when there is contact: if $x(t) = 0$ and $u(t^+) > 0$ then $\partial\psi_{V(x(t))}\left(u(t^+)\right) = N_{\mathbb{R}^+}\left(u(t^+)\right) = \{0\}$, if $x(t) = 0$ and $u(t^+) = 0$ then $\partial\psi_{V(x(t))}\left(u(t^+)\right) = N_{\mathbb{R}^+}(0)) = \mathbb{R}^-$. The cone $\partial\psi_{V(x(t))}\left(u(t^+)\right)$ is the singleton $\{0\}$ when there is no contact $x > 0$. We notice in passing that Moreau's set imposes a lexicographical inequality $(x(t), u(t^+)) \succeq 0$ (see Remark 3.1 for some arguments about lexicographical inequalities). In a more general setting, consider (5.54). If q is in the interior of Φ, then $V(q) = \mathbb{R}^n$ so that $u(t^+)$ can take any value (it is in fact continuous). If $q \in \mathrm{bd}(\Phi)$, then $u(t^+)$ is constrained by (5.54), which may be understood as a kind of nonnegativity condition (in a suitable coordinate frame, the normal components of $u(t^+)$ are nonnegative).

Remark 5.7 The case of non-purely dissipative percussions may be treated by replacing $u(t_k^+)$ by a weighted mean $u_\delta(t_k) = \frac{1+\delta}{2}u(t_k^+) + \frac{1-\delta}{2}u(t_k^-)$ of $u(t_k^+)$ and $u(t_k^-)$ in the right-hand side of (5.51) [894], as $N_{V(q(t))}(u_\delta(t))$. The number δ is called a *dissipation index*. At an impact (5.53) becomes

$$
\begin{aligned}
& M(q(t_k))[u(t_k^+) - u(t_k^-)] \in -N_{V(q(t_k))}(u_\delta(t_k)) \\
& \Leftrightarrow u(t_k^+) - u(t_k^-) \in -M(q(t_k))^{-1} N_{V(q(t_k))}(u_\delta(t_k)) \\
& \Leftrightarrow \tfrac{1+\delta}{2}(u(t_k^+) - u(t_k^-)) \in -M(q(t_k))^{-1} N_{V(q(t_k))}(u_\delta(t_k)) \\
& \Leftrightarrow \tfrac{1+\delta}{2}u(t_k^+) + \tfrac{1-\delta}{2}u(t_k^-) - \tfrac{1-\delta}{2}u(t_k^-) - \tfrac{1+\delta}{2}u(t_k^-) \in -M(q(t_k))^{-1} N_{V(q(t_k))}(u_\delta(t_k)) \\
& \Leftrightarrow u_\delta(t_k) - u(t_k^-) \in -M(q(t_k))^{-1} N_{V(q(t_k))}(u_\delta(t_k)) \\
& \Leftrightarrow u_\delta(t_k) = \mathrm{proj}_{M(q(t_k))}(V(q(t_k)); u(t_k^-)) \\
& \Leftrightarrow u(t_k^+) = \tfrac{\delta-1}{\delta+1}u(t_k^-) + \tfrac{2}{1+\delta}\mathrm{proj}_{M(q(t_k))}(V(q(t_k)); u(t_k^-)) \\
& \Leftrightarrow u(t_k^+) = u(t_k^-) - \tfrac{2}{1+\delta}\mathrm{proj}_{M(q(t_k))}(N(q(t_k)); u(t_k^-)).
\end{aligned}
\tag{5.60}
$$

In these calculations we used the fact that a cone is invariant under multiplication by a positive scalar, and we used also (B.18) which is a corollary of Moreau's Lemma of the two cones. In case of impact $u(t_k^-) \in -V(q(t_k))$, thus $\mathrm{proj}_{M(q(t_k))}(V(q(t_k)); u(t_k^-)) \in \mathrm{bd}(V(q(t_k)))$. In the one degree-of-freedom case of Remark 5.4, $u(t_k^-) \leq 0$ and one gets for the energy conservation case $\frac{1}{2}u(t_k^+) + \frac{1}{2}u(t_k^-) = \mathrm{proj}(\mathbb{R}^+; u(t_k^-)) = 0$. Hence, $u(t_k^+) = -u(t_k^-)$ as expected. In the maximum dissipation case $\delta = 1$ and $u(t_k^+) = \mathrm{proj}(\mathbb{R}^+; u(t_k^-)) = 0$. The relation with the classical restitution coefficient is $\delta = \frac{1-e_\mathrm{n}}{1+e_\mathrm{n}}$, or equivalently $e_\mathrm{n} = \frac{1-\delta}{1+\delta}$, so that $u(t_k^+) = -e_\mathrm{n}u(t_k^-) + (1+e_\mathrm{n})\mathrm{proj}_{M(q(t_k))}(V(q(t_k)); u(t_k^-))$. The following equivalences hold also [780]:

$$
\begin{aligned}
& \tfrac{1}{1+e_\mathrm{n}}\{u(t_k^+) + e_\mathrm{n}u(t_k^-)\} = \mathrm{proj}(V(q(t_k)); u(t_k^-)) \\
& \Leftrightarrow -\tfrac{R'_\mu(t_k)}{1+e_\mathrm{n}} = \mathrm{proj}(N(q(t_k)); u(t_k^-)) \\
& \Leftrightarrow -R'_\mu(t_k) \in N_{V(q(t_k))}(u(t_k^+) + e_\mathrm{n}u(t_k^-)) \\
& \Leftrightarrow \tfrac{R'_\mu(t_k)^T}{1+e_\mathrm{n}}[u(t_k^+) + e_\mathrm{n}u(t_k^-)] = 0 \\
& \Leftrightarrow T(t_k^+) - T(t_k^-) = -\tfrac{1}{2}\tfrac{1-e_\mathrm{n}}{1+e_\mathrm{n}}\sigma_u(t_k)^T M(q(t_k))\sigma_u(t_k).
\end{aligned}
\tag{5.61}
$$

We can redo the same manipulations as above to express these equivalences in the kinetic metric. The first line in (5.61) is just the last-but-one line in (5.60), while the second line in (5.61) is obtained from the last line in (5.60), using the dynamics at impact. The inclusion in the third line in (5.61) uses Moreau's Lemma of the two cones, plus (B.19) noting that $V(q)$ and $N(q)$ are polar cones. The last line is very interesting as it gives the kinetic energy variation induced by Moreau's set at an impact. As an exercise one may check that in case of two particles colliding the expression (4.41) is recovered.

Example 5.5 Consider the 3-ball system with all masses equal to unity so that the inertia matrix is the identity. Let the first ball hit the other two, assumed to be in

contact before the shock: $\dot{q}_1(t_k^-) = 1$ m/s, $\dot{q}_2(t_k^-) = \dot{q}_3(t_k^-) = 0$ m/s. Let us take $\delta = 0 \Leftrightarrow e_n = 1$, i.e., the kinetic energy loss $T_L(t_k) = 0$. Then using (5.60) $\dot{q}(t_k^+)$ is calculated from

$$\frac{1}{2}\left(\dot{q}(t_k^+) + \dot{q}(t_k^-)\right) = \text{proj}\left(V(q(t_k)); \dot{q}(t_k^-)\right), \tag{5.62}$$

where the proximation is in the Euclidean norm since the inertia matrix is the identity 3×3 matrix. We have $\frac{1}{2}\left(\dot{q}(t_k^+) + \dot{q}(t_k^-)\right) = \frac{1}{2}\begin{pmatrix} \dot{q}_1(t_k^+) + 1 \\ \dot{q}_2(t_k^+) \\ \dot{q}_2(t_k^+) \end{pmatrix}$. We can therefore look for a vector $\frac{1}{2}\left(\dot{q}(t_k^+) + \dot{q}(t_k^-)\right)$ that belongs to the boundary of $V(q)$, and such that $||\dot{q}(t_k^+) - \dot{q}(t_k^-)||$ is minimum. This leads us to minimize the last quantity under the constraints $\dot{q}_2(t_k^+) = \dot{q}_1(t_k^+) + 1$, $\dot{q}_3(t_k^+) = \dot{q}_2(t_k^+)$, i.e., minimize the following:

$$\frac{1}{4}\left(\dot{q}_1(t_k^+) - 1\right)^2 + \frac{1}{2}\left(\dot{q}_1(t_k^+) + 1\right)^2 = 3\dot{q}_1^2(t_k^+) + 2\dot{q}_1(t_k^+) + 3. \tag{5.63}$$

This yields finally the outcome $\dot{q}_1(t_k^+) = -\frac{1}{3}$ m/s, $\dot{q}_2(t_k^+) = \dot{q}_3(t_k^+) = \frac{2}{3}$ m/s. This corresponds to the first solution found by the Han and Gilmore algorithm in Chap. 6, Sect. 6.1.2.

Let us now calculate the postimpact velocity with $\delta = 1 \Leftrightarrow e_n = 0$. We have to compute $\dot{q}(t_k^+) = \text{proj}\left(V(q(t_k)), \dot{q}(t_k^-)\right)$. The result is that of minimizing $||\dot{q}(t_k^+) - \dot{q}(t_k^-)||$ under the constraint $\dot{q}(t_k^+) \in V(q(t_k))$. Therefore, it follows that $||\dot{q}(t_k^+) - \dot{q}(t_k^-)||^2 = \left(\dot{q}_1(t_k^+) - 1\right)^2 + \dot{q}_2^2(t_k^+) + \dot{q}_3^2(t_k^+)$, which is equal to $3\dot{q}_1^2(t_k^+) - 2\dot{q}_2(t_k^+) + 1$ on the boundary of $V(q(t_k))$. It follows that $\dot{q}_1(t_k^+) = \dot{q}_2(t_k^+) = \dot{q}_3(t_k^+) = \frac{1}{3}$ m/s. One checks that $T_L(t_k) < 0$.

Remark 5.8 Moreau's set yields an impact mapping which may not fit well with experimental results in many instances, see Example 5.6. However, it clarifies the geometry of unilaterally constrained Lagrangian systems, and settles a general framework which may be enhanced, in particular with better impact mappings. From a more general point of view, it serves as a theoretical basis for the NSCD numerical method (with or without friction) in Sect. 5.7.3.1, which is very efficient for systems which undergo a lot of stick/slip transitions, and few collisions (some granular materials behave like this).

Remark 5.9 As alluded to in Example 5.5, the sweeping process shock rule is equivalent to solving a QP under unilateral constraints. In fact (5.54) is equivalent to

$$u(t_k^+) = \arg\min_{w \in V(q)} \frac{1}{2}[w - u(t_k^-)]^T M(q(t_k))[w - u(t_k^-)]. \tag{5.64}$$

The Kuhn–Tucker's conditions (see Sect. 5.4) tell us that it is then necessary that there exists $\lambda \in \mathbb{R}^{\text{card}(\mathscr{J}(q(t_k)))}$, where $\mathscr{J}(q(t_k))$ is the set of active constraints indices, such that

$$\begin{cases} M(q(t_k))[u(t_k^+) - u(t_k^-)] - \sum_{i \in \mathscr{J}(q(t_k))} \nabla f_i(q(t_k))\lambda_i = 0 \\ \\ \lambda_i \geq 0, \quad \nabla f_i(q(t_k))^T u(t_k^+) \geq 0, \quad \lambda_i \nabla f_i(q(t_k))^T u(t_k^+) = 0, \quad i \in \mathscr{J}(q(t_k)). \end{cases} \tag{5.65}$$

It is clear from the third *complementarity* condition that this rule yields plastic shocks, in the sense that the postimpact generalized velocity is on the boundary of the admissible domain Φ. Notice that λ_i in (5.65) is equal to $R_\mu^{'}(t_k)$, i.e., the density of the atomic contact percussion distribution at $t = t_k$. It is important to understand the relationships between shock rules and complementarity formulations, since this is at the core of many studies, see Sect. 5.4.

5.2.2.5 Further Results on Moreau's Impact Law

Let us consider the following set of relations at an impact time t_k:

$$\begin{array}{ll} (a) & M(q(t_k))(\dot{q}(t_k^+) - \dot{q}(t_k^-)) = p_{\mathrm{n},k} \\ (b) & U_\mathrm{n}(t_k^+) = \nabla f(q(t_k))^T \dot{q}(t_k^+) \\ (c) & U_\mathrm{n}(t_k^-) = \nabla f(q(t_k))^T \dot{q}(t_k^-) \\ (d) & p_{\mathrm{n},k} = \nabla f(q(t_k)) P_{\mathrm{n},k} \\ (e) & 0 \leq U_\mathrm{n}(t_k^+) + \mathscr{E}_{\mathrm{nn}} U_\mathrm{n}(t_k^-) \perp P_{\mathrm{n},k} \geq 0, \end{array} \tag{5.66}$$

where it is assumed that the local velocity vector $U_\mathrm{n}(t_k^-) \leq 0$ (componentwise inequality), i.e., all m contacts collide at the same time. In fact, following the notations adopted in Chap. 4 that stem from the local kinematics at the m contact points, one has $U_\mathrm{n} = (v_{r,\mathrm{n},1}, v_{r,\mathrm{n},2}, \ldots, v_{r,\mathrm{n},m})^T$, where the subscript i refers to the contact point number. What is denoted as p_k in (5.66) is the same as $R'_\mu(t_k)$ in (5.57), while $P_{\mathrm{n},k}$ collects the multipliers λ_i in (5.65) . The reason for different notations of the same mechanical variable comes from the context. The matrix $\mathscr{E}_{\mathrm{nn}} = \mathrm{diag}(e_{\mathrm{n},i})$ is the restitution matrix.[21] The velocity $U_\mathrm{n}(t) \in \mathbb{R}^m$ is the vector collecting the contact points relative normal velocities, which are defined from the gap function (the signed distances) $f(q) \geq 0$. The problem in (5.66) is a mixed LCP (mLCP). Indeed, it can be rewritten as

$$\begin{cases} D_u(q(t_k)) P_{\mathrm{n},k} - U_\mathrm{n}(t_k^+) + U_\mathrm{n}(t_k^-) = 0 \\ \\ 0 \leq U_\mathrm{n}(t_k^+) + \mathscr{E}_{\mathrm{nn}} U_\mathrm{n}(t_k^-) \perp P_{\mathrm{n},k} \geq 0. \end{cases} \tag{5.67}$$

Without loss of generality we suppose in (5.66) that the m constraints are hitted at the same time t_k. If this is not the case one simply has to work with the subset of striked constraints.

[21] The reason for the nn subscript will become clear in Sect. 6.2 when we deal with generalizations of this impact law.

Proposition 5.15 *Let (i) $e_{\mathrm{n},i} = e_{\mathrm{n}}$ for all $1 \leq i \leq m$, and (ii) suppose that there exists z_0 such that $\nabla f(q(t_k))z_0 \in \mathbb{R}^m_+$. The problem in (5.66) is equivalent to Moreau's impact law.*

Proof The proof uses (B.19), (B.20), (B.21), and Theorem B.2. From (5.66) (b) (c) (e) one deduces $p_{\mathrm{n},k} \in -\nabla f(q(t_k))\ N_{\mathbb{R}^m_+}(\nabla f(q(t_k))^T(\dot{q}(t_k^+) + e_{\mathrm{n}}\dot{q}(t_k^-))$, where assumption (i) was used. Using assumption (ii), this is found to be equivalent to $p_{\mathrm{n},k} \in -N_{K(q(t_k))}(\dot{q}(t_k^+) + e_{\mathrm{n}}\dot{q}(t_k^-))$, with $K(q(t_k)) = \{z \in \mathbb{R}^m | \nabla f(q(t_k))^T z \geq 0\}$, which is equal to the tangent cone $V(q(t_k))$ in (5.34). One therefore recovers (5.51) (for the case $e_{\mathrm{n}} = 0$), see Remark 5.7 for the general case.

It is noteworthy that assumption (i) in the proposition could be replaced by the matrices $\mathscr{E}_{\mathrm{nn}}$ and $\nabla f(q(t_k))$ commute. Similar results may also be found, in a geometrical context, in [454]. Now from (5.67) one infers that

$$0 \leq D_u(q(t_k))P_{\mathrm{n},k} + (I + \mathscr{E}_{\mathrm{nn}})U_{\mathrm{n}}(t_k^-) \perp P_{\mathrm{n},k} \geq 0. \tag{5.68}$$

The well-posedness of this LCP depends on whether $D_u(q(t_k))$ is positive definite, or semi-definite. Theorems 5.4, 5.6, and 5.7 may be used.

Lemma 5.2 *Let n and m_u be arbitrary positive integers. Assume that $\mathscr{E}_{\mathrm{nn}}$ and $\nabla f(q(t_k))^T$ commute and let $M(q)$ be full rank. Then the LCP in (5.68) is solvable.*

Proof The proof relies on Theorem 5.6. We drop the time argument in $q(t_k)$. The associated homogenous LCP writes as $0 \leq \nabla f(q)^T M(q)^{-1} \nabla f(q) z \perp z \geq 0$. Its solutions satisfy $z^T \nabla f(q)^T M(q)^{-1} \nabla f(q) z = 0$, so that $z \in \ker(\nabla f(q))$. Thus $z^T (I + \mathscr{E}_{\mathrm{nn}}) U_{\mathrm{n}}(t_k^-) = z^T \nabla f(q)^T (I + \mathscr{E}_{\mathrm{nn}}) \dot{q}(t_k^-) = 0$. Since $\nabla f(q)^T M(q)^{-1} \nabla f(q)$ is (at least) positive semi-definite, hence copositive, from Theorem 5.6 the LCP is solvable.

Lemma 5.2 is important because it proves that a postimpact velocity can always be computed: indeed from (5.66) a value of $P_{\mathrm{n},k}$ yields a value of $p_{\mathrm{n},k}$, thus a value of $\dot{q}(t_k^+)$. Uniqueness also holds for the local velocities:

Corollary 5.1 *Let n and m_u be arbitrary positive integers. Assume that $\mathscr{E}_{\mathrm{nn}}$ and $\nabla f(q(t_k))^T$ commute and $M(q(t_k))$ be full rank. Then $U_{\mathrm{n}}(t_k^+)$ is unique.*

Proof Using Theorem 5.7 (or item (c) of [23, Corollary 4]), one has $P_{\mathrm{n},k,1} - P_{\mathrm{n},k,2} \in \ker(\nabla f(q)^T M(q)^{-1} \nabla f(q))$ for any two solutions $P_{\mathrm{n},k,1}$ and $P_{\mathrm{n},k,2}$ of the LCP (5.68). Using (5.66) one deduces that the corresponding velocities $U_{\mathrm{n},1}(t_k^+)$ and $U_{\mathrm{n},2}(t_k^+)$ satisfy $U_{\mathrm{n},1}(t_k^+) - U_{\mathrm{n},2}(t_k^+) = \nabla f(q)^T M(q)^{-1} \nabla f(q)(P_{\mathrm{n},k,1} - P_{\mathrm{n},k,2}) = 0$.

However, one has that $\nabla f(q)^T(\dot{q}_1(t_k^+) - \dot{q}_2(t_k^+)) = 0$ for the corresponding generalized velocities, which are unique only if dependency restrictions are put on the unilateral constraints. In fact we may do differently, as follows. From (5.66) one infers that:

$$M(q)(\dot{q}(t_k^+) - \dot{q}(t_k^-)) \in -\nabla f(q)\partial\psi_{\mathbb{R}^m_+}(\nabla f(q)^T \dot{q}(t_k^+) + \mathscr{E}_{\rm nn} U_{\rm n}(t_k^-) \\ = -N_{K(q,\dot{q}(t_k^-))}(\dot{q}(t_k^+)), \tag{5.69}$$

where $\psi_{\mathbb{R}^m_+}(\cdot)$ is the indicator function of $\mathbb{R}^m_+$, and $K(q, \dot{q}(t_k^-)) = \{z \in \mathbb{R}^n | \nabla f(q)^T z + \mathscr{E}_{\rm nn} U_{\rm n}(t_k^-) \geq 0\}$. The equality in the right-hand side of (5.69) is obtained under the constraint qualification (CQ): there exists z_0 such that $\nabla f(q)^T z + \mathscr{E}_{\rm nn} U_{\rm n}(t_k^-) \geq 0$. Then Theorem B.2 can be used, as well as Definition B.7. The inclusion in (5.69) has the form as in (B.20), and $K(q, \dot{q}(t_k^-))$ is convex nonempty (due to the CQ) and closed. One infers that if the CQ holds and if $M(q(t_k)$ is full rank, the postimpact velocity is uniquely calculated as a projection on $K(q(t_k), \dot{q}(t_k^-))$ in the metric defined by $M(q(t_k))$.[22] If the mass matrix is singular, one may use [23, Corollary 4] to derive some results. The most immediate one follows from [23, Corollary 4 (c)]: if $\dot{q}_1(t_k^+)$ and $\dot{q}_2(t_k^+)$ are two solutions of (5.69), then $\dot{q}_1(t_k^+) - \dot{q}_2(t_k^+) \in \ker(M(q(t_k))$. A solvability result may also be stated:

Proposition 5.16 *Let n and m be arbitrary, and assume that the above CQ holds. Suppose also that $\{z \in \mathbb{R}^n | \nabla f(q(t_k))^T z \geq 0\} \cap \ker(M(q(t_k)) = \{0\}$. Then the generalized equation in (5.69) has at least a solution $\dot{q}(t_k^+)$.*

Proof The proof relies on [23, Corollary 4 (a)]. The domain of the normal cone in the right-hand side of (5.69) is the closed convex set $K(q, \dot{q}(t_k^-))$, whose recession cone is given by $K_\infty(q, \dot{q}(t_k^-)) = \{z \in \mathbb{R}^n | \nabla f(q)^T z \geq 0\}$. The result follows.

One sees that the set $\{z \in \mathbb{R}^n | \nabla f(q(t_k))^T z \geq 0\}$ is the linearization cone $V(q(t_k))$ of Definition 5.34, which is equal to the tangent cone if the MFCQ in (B.9) holds. Thus the solvability result of Proposition 5.16 means that there is no element of the mass matrix kernel, which produces a motion inside the admissible domain. Said otherwise: a nonzero postimpact velocity that produces motion (hence, a positive kinetic energy) should not be in the mass matrix kernel. This may be seen as a generalization of the results in [429] (see Theorem 5.1) which apply to systems with holonomic, bilateral constraints, and smooth motions (hence the postimpact velocity is replaced by the acceleration). Uniqueness is more stringent, and [23, Corollary 4 (d)] sufficient conditions for uniqueness do not apply to (5.69), because one has $\dot{q}(t_k^-)^T M(q(t_k))z = 0$ for all $z \in \ker(M(q(t_k)))$.

If $D_u(q(t_k))$ is positive definite, then one may write equivalently a well-posed LCP with unknown $w(t_k) = D_u(q(t_k))P_{{\rm n},k} + (I + \mathscr{E}_{\rm nn})U_{\rm n}(t_k^-)$ as

$$0 \leq w(t_k) \perp D_u(q(t_k))^{-1} w(t_k) - D_u(q(t_k))^{-1}(I + \mathscr{E}_{\rm nn})U_{\rm n}(t_k^-) \geq 0. \tag{5.70}$$

$\rightsquigarrow$ *The Proposition 5.15 shows that if all restitution coefficients are equal, then Moreau's impact law and Newton's restitution law applied at each constraint are the same. It also shows how Moreau's impact law may be solved with an LCP, which possesses nice properties.*

[22] Which is the kinetic metric, however, since we deal with a given impact time, the mass matrix is fixed and this is a problem with a Euclidean metric.

In numerical simulations with time-stepping methods, one forms a so-called one-step nonsmooth problem, which is close to the mLCP in (5.67), see [13, Chap. 10].

Remark 5.10 The above results were stated under the collision assumption, i.e., $U_{\mathrm{n},i}(t_k^-) \leq 0$ for all $1 \leq i \leq m$. Equivalently, $\dot{q}(t_k^-) \in -V(q(t_k))$.

Example 5.6 (Example 5.5, continued) The system of three aligned balls (called in the Granular Matter scientific community a monodisperse chain when there is no energy dissipation) may be used to show the limitations of both Moreau and Newton's laws. This is depicted in Fig. 5.5, where $\gamma_1^+ \triangleq \dot{q}_2(t_k^+) - \dot{q}_1(t_k^+)$, $\gamma_2^+ \triangleq \dot{q}_3(t_k^+) - \dot{q}_2(t_k^+)$, $V_s = \dot{q}_1(t_k^-)$, $\dot{q}_3(t_k^-) = \dot{q}_2(t_k^-) = 0$ m/s. In this figure the quantity

$$KER \triangleq \frac{T(q(t_k), \dot{q}(t_k^+))}{T(q(t_k), \dot{q}(t_k^-))} \tag{5.71}$$

characterizes the kinetic energy loss, while the quantity

$$C_{KE} = \frac{1}{\bar{T}^+} \sqrt{\frac{1}{3} \sum_{i=1}^{3} (T_i(t_k^+) - \bar{T}^+)^2}, \tag{5.72}$$

with $\bar{T}^+ = \frac{1}{3} \sum_{i=1}^{3} \frac{1}{2} m_i \dot{q}_i(t_k^+)^2$ characterizes the kinetic energy dispersion in the chain. Moreau's impact law allows to span only the segment denoted as Moreau's line $[O, B]$. In other words, it cannot separate balls 2 and 3 after the collision, for this choice of the initial velocities, which is not observed in many experiments. A "good" impact law should be able to span the whole area that is parameterized by KER and C_{KE}. It is noteworthy that the limitation of Newton's or Moreau's laws has an intrinsic feature, in the sense that it cannot be overcome by choosing nonconstant restitution coefficients. These limitations have been pointed out in [276][23], while Moreau's line is pointed out in the analysis of [454]. Chapter 6 is dedicated to the extension of such kinematic impact laws.

Example 5.7 [Moreau's impact law as a minimization problem] Let us consider a chain made of three aligned balls, with masses m_1, m_2, and m_3, respectively, and the first ball hits at time t_k the other two which are initially in contact. The following is proved in [929, Appendix C], and shows that in some cases Moreau's impact law can be given a meaning in terms of energy dispersion, in addition to energy dissipation.

Proposition 5.17 *Let* $0 < e_{\mathrm{n}} \leq 1$ *and* $m_2 \leq m_3$. *The outcome calculated from Moreau's impact law, i.e.,* $\dot{q}_1(t_k^+) = \frac{m_1 - (m_2+m_3)e_{\mathrm{n}}}{m_1+m_2+m_3} \dot{q}_1(t_k^-)$, $\dot{q}_2(t_k^+) = \frac{m_1(1+e_{\mathrm{n}})}{m_1+m_2+m_3} \dot{q}_1(t_k^-)$, $\dot{q}_3(t_k^+) = \frac{m_1(1+e_{\mathrm{n}})}{m_1+m_2+m_3} \dot{q}_1(t_k^-)$, *is the solution of the minimization problem:*

[23] …complementarity conditions at the velocity level should be viewed as typically inaccurate, but algorithmically convenient, constitutive assumptions.

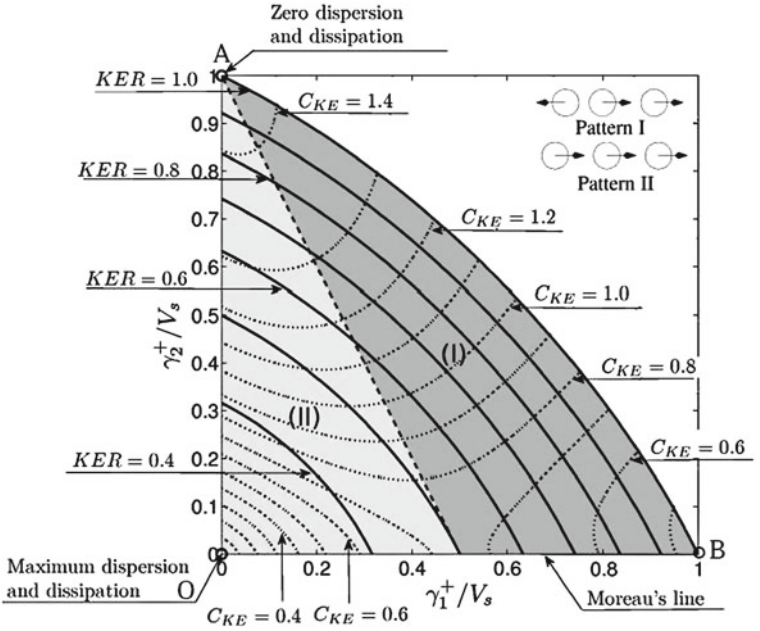

Fig. 5.5 Three-ball chain: Impact geometry (taken from [929, Fig. 2.6])

$$\begin{aligned} &\textit{minimize} \qquad C_{KE}(\dot{q}_1(t_k^+), \dot{q}_2(t_k^+), \dot{q}_2(t_k^+)) \\ &\textit{subjected to:} \ \sum_{i=1}^{3} m_i \dot{q}_i(t_k^+) - m_1 \dot{q}_1(t_k^-) = 0 \\ &\qquad\qquad \sum_{i=1}^{3} m_i \dot{q}_i(t_k^+)^2 - KER\, m_1 \dot{q}_1(t_k^-)^2 = 0 \\ &\qquad\qquad \dot{q}_3(t_k^+) - \dot{q}_2(t_k^+) \geq 0, \ \ \dot{q}_2(t_k^+) - \dot{q}_1(t_k^+) \geq 0 \end{aligned} \tag{5.73}$$

where C_{KE} in (5.72) is the dispersion of energy measure, and KER is in (5.71). If $e_n = 0$ then Moreau's outcome is the unique solution of the minimization problem (5.73).

Remark 5.11 A nice example of a multibody system with unilateral constraints (and friction) is a bipedal robot [560]. Impact laws are used in the control design of such systems. Starting from (5.66) (a) and $U_n(t_k^+) + \mathscr{E} U_n(t_k^-) = 0$ one forms the system [483, Eq. (47)]:

$$\begin{pmatrix} M(q(t_k)) & -\nabla f(q(t_k)) \\ \nabla f(q(t_k)) & 0 \end{pmatrix} \begin{pmatrix} \dot{q}(t_k^+) \\ P_{n,k} \end{pmatrix} = \begin{pmatrix} M(q(t_k))\dot{q}(t_k^-) \\ -\mathscr{E} U_n(t_k^-) \end{pmatrix} \tag{5.74}$$

Usually, one takes $\mathscr{E} = 0$ because the assumption is that impacts are plastic. It is noteworthy that the positivity of $P_{\mathrm{n},k}$ is not at all guaranteed when solving the problem (5.74), which is similar to the problem in (5.3). Thus it is in essence a "bilateral" calculation of impacts.

Let us end this long aside on Moreau's impact law by mentioning that it may be approximated with some kind of over-damped compliant contact model similar to those presented in Sect. 2.4, with convergence to Moreau's law as some stiffness parameter diverges [973, 975].

Moreau's sweeping process is a quite interesting evolution problem, because it settles the correct geometrical framework of Lagrange dynamics with unilateral constraints, despite it yields a weak (in terms of its practical usefulness) collision mapping.

5.2.3 Well-Posedness Results

The first existence of solution proofs for the second-order sweeping process was published by Monteiro Marques in the Convex Analysis Seminar of the Mathematics Department of the University of Montpellier (France) between 1983 and 1987, and can be found in [866, 867].

Theorem 5.2 *[867] Suppose that there is a unique unilateral constraint $m = 1$, $f(\cdot)$ is of class C^1, the vector $Q = Q(t, q)$ in Problem 5.1 is continuous and globally bounded, i.e., $||Q(t, q)|| < M$ for some constant $M > 0$ and all $t \geq \tau_0$ and all $q \in \mathbb{R}^n$. Let us take also $M(q)$ the identity matrix. Let $q(\tau_0) = q_0 \in \Phi$ and $u(\tau_0) = u_0 \in V(q_0)$ be the initial data. Then there exist $\delta > 0$ and $T' > 0$ such that*

$$Int\left(\cap_{||q-q_0||\leq\delta} V(q)\right) \neq \emptyset, \tag{5.75}$$

and $T' = \min\left\{T, \frac{\delta}{M'}\right\}$, $M' = ||u_0|| + 2TM$. On the interval $[\tau_0, T']$, Problem 5.1 has at least one solution $q(t)$ with right-continuous velocity $u(\cdot)$ that satisfies:

$$||u(t)|| \leq ||u_0|| + Mt \tag{5.76}$$

so that:

$$||q(t)|| \leq ||q_0|| + ||u_0||t + \frac{1}{2}Mt^2. \tag{5.77}$$

Theorem 5.2 assures local existence, i.e., for some T' strictly positive. Global existence can also be proved, i.e., a solution exists on $[\tau_0, T]$ for $T \geq \tau_0$, arbitrary. Uniqueness is not discussed in [867], but it is pointed out that nonuniqueness may

occur, see Bressan's counterexample in Chap. 2. This seems to be the only class of counterexamples to nonuniqueness known in the mathematical literature [80, 186, 1066] (that is however to be considered more as a pathological case than as a deep practical problem). Theorem 5.2 has been extended to the partially elastic rebound case $e_{\mathrm{n}} > 0$, and $Q = Q(t, q, \dot{q})$ in [780, 781], with $Q(\cdot, \cdot, \cdot)$ globally Lipschitz in q and $\dot{q}$, and uniformly continuous t. The fact that $e_{\mathrm{n}} > 0$ complicates the analysis and $f(q)$ is required to be $C^{1,\beta}$ with $\beta > \frac{1}{2}$,[24] and this is equivalent to impose some conditions on the curvature of $\mathrm{bd}(\Phi)$ (similarly as in some results for uniqueness conditions, see Chap. 2, Sect. 2.4.3). As we saw in Example 5.4, the sweeping process then reads

$$Q(t, q, u)dt - du \in \partial\psi_{V(q)}(u_e), \tag{5.78}$$

where $u_e = \frac{u^+ + e_{\mathrm{n}}u^-}{1+e_{\mathrm{n}}}$ is named an $e_{\mathrm{n}} - average$ of u (equal to u at continuity points). The proof of existence is divided into four steps, and is based, following [867], on an implicit discretization reminiscent of the catching-up algorithm briefly introduced in Sect. 5.2.1, as

$$\frac{t_{i+1} - t_i}{1 + e_{\mathrm{n}}} Q(t_{i+1}, q(t_{i+1}), u_{i+1}) - \frac{u_{i+1} - u_i}{1 + e_{\mathrm{n}}} \in \partial\psi_{V(q(t_{i+1}))}\left(\frac{u_{i+1} + e_{\mathrm{n}}u_i}{1 + e_{\mathrm{n}}}\right). \tag{5.79}$$

Using (B.20) this is equivalent to

$$\frac{u_{i+1} + e_{\mathrm{n}}u_i}{1 + e_{\mathrm{n}}} = \mathrm{proj}\left(V(q(t_{i+1})), u_i + \frac{t_{i+1} - t_i}{1 + e_{\mathrm{n}}} Q(t_{i+1}, q(t_{i+1}), u_{i+1})\right). \tag{5.80}$$

The time interval $[0, T]$ on which existence is to be shown is divided with a constant step $h = \frac{T}{n}$, and $t_i = ih$. Then one constructs the approximating sequences:

$$\begin{cases} q_{i+1} = q_i + hu_i \\ u_{i+1} = -e_{\mathrm{n}}u_i + (1 + e_{\mathrm{n}})\mathrm{proj}\left(V(q_{i+1}), u_i + \frac{h}{1+e_{\mathrm{n}}} Q(t_{i+1}, q(t_{i+1}), u_{i+1})\right) \end{cases} \tag{5.81}$$

and the approximating step functions:

$$\begin{cases} u_n(t) = u_i \ \text{ if } \ t \in [t_i, t_{i+1}), \ 0 \le i \le n-1 \\ u_n(T) = u_n \\ q_n(t) = q_0 + \int_0^t u_n(\tau)d\tau. \end{cases} \tag{5.82}$$

[24] This means that $f(\cdot)$ is C^1 and $\dot{f}(\cdot)$ is continuous and satisfies $\sup_{x,y} \frac{|\dot{f}(x) - \dot{f}(y)|}{|x-y|^\alpha} < +\infty$, with $0 < \alpha < 1$ [191].

The fist step of the proof consists of showing that the sequences $\{u_n\}$ and $\{q_n\}$ are uniformly bounded. In the second step one calculates a majoration of the measures du_n. This in particular allows one to use a result that guarantees that the sequence $\{u_n\}$ converges everywhere toward a function $u \in RCLBV$, whereas $\{q_n\}$ converges toward a function $q(\cdot)$ that satisfies $f(q(t)) \geq 0$, i.e., $q(t) \in \Phi$. The third step is devoted to prove that the limit $u(\cdot)$ satisfies the sweeping process inclusion almost everywhere, provided $f(\cdot) \in C^{1,\frac{1}{2}}$. The last step is devoted to study the jump conditions in $u(\cdot)$.

Let us end this section on well-posedness issues of frictionless sweeping process, by mentioning the results in [374, 375, 967, 968] which extend the above results to multiple independent constraints (hence a full-rank Delassus' matrix[25]), and/or nontrivial mass matrix $M(q)$. The proofs rely on similar implicit time discretizations as the one we described above. The results in [80, 81] can be used to assert the uniqueness of solutions, under mild assumptions like the piecewise analycity of the data and $e_{\mathrm{n}} \in [0, 1]$ (hence extending the results stated in Sect. 2.4.3 where analycity plays a crucial role). As pointed out in Sect. 2.4.3.1, in such a case right accumulations of impacts cannot exist. Moreover, if $e_{\mathrm{n}} = 1$, then impact instants are isolated and infinite number in any compact interval of time [81, Proposition 4.11]. We may summarize all these results as well as those in Sect. 2.4 in the following, which is the most general well-posedness result on frictionless complementarity Lagrangian systems.

Assumption 5.1 Consider the Lagrangian system in (5.1). Let us denote the impact mapping as $\dot{q}(t_k^-) \mapsto \dot{q}(t_k^+) = \mathscr{F}(q(t_k), \dot{q}(t_k^-))$. Assume further that

- (a) The impact mapping satisfies (i) kinematic, (ii) kinetic, and (iii) energetic constraints:
  - (i) $\mathscr{F}(q(t_k), \dot{q}(t_k^-)) \in V(q(t_k))$,
  - (ii) $\mathscr{F}(q(t_k), \dot{q}(t_k^-)) - \dot{q}(t_k^-) \in -M(q(t_k))^{-1} N_{\Phi}(q(t_k))$,
  - (iii) $\mathscr{F}(q(t_k), \dot{q}(t_k^-))^T M(q(t_k)) \mathscr{F}(q(t_k), \dot{q}(t_k^-)) \leq \dot{q}(t_k^-)^T M(q(t_k)) \dot{q}(t_k^-)$.
- (b) $M(q) = M(q)^T \succ 0$.
- (c) The Delassus' matrix of the active constraints is positive definite (i.e.,, active constraints are functionally independent).
- (d) The data (i.e., $M(q)$, $C(q, \dot{q})$, $G(q)$, $F_{ext}(t)$, $f(q)$) are piecewise analytic.
- (e) The gradients $\nabla f_i(q)$ do not vanish in a neighborhood of $\{q \in \mathbb{R}^n | f_i(q) = 0\}$.

We see that the impact mapping may be different from Moreau's mapping. But Moreau's mapping satisfies the requirements (i)–(iii).

[25] It is important to remind here that only the *active* constraints have to be independent.

Theorem 5.3 (Existence and uniqueness of solutions) *Consider the Lagrangian system in (5.1) without friction and only unilateral constraints. Suppose that Assumption 5.1 holds. Let* $f(q(t_0)) \geq 0$, $\dot{q}(t_0^+) \in T_\Phi(q(t_0))$. *Then the system admits a unique maximal solution* $(q(\cdot), \dot{q}(\cdot))$ *on* $[t_0, T)$ *for some* $T > t_0$, $q(\cdot)$ *is absolutely continuous such that* $\dot{q}(\cdot) = u(\cdot)$ *almost everywhere, where* $u(\cdot)$ *is right-continuous of local bounded variations,* $q(t) = q(t_0) + \int_{t_0}^{t} u(s)ds$ *for all* $t \geq t_0$, *the acceleration is the differential measure of the velocity, i.e.,* $\ddot{q} = du$. *Let* $F(q, \dot{q}, t) \stackrel{\Delta}{=} C(q, \dot{q}) + G(q) - F_{ext}(t)$. *The additional condition* $\sqrt{F(q, \dot{q}, t)^T M(q) F(q, \dot{q}, t)} \leq l(t)(1 + d(q, q(0)) + \sqrt{\dot{q}^T M(q)\dot{q}})$ *for some nonnegative Lebesgue integrable function* $l(\cdot)$ *and where* $d(\cdot, \cdot)$ *is the Riemannian distance guarantees the global existence of solutions.*

Right accumulations of impacts do not occur, and impact times are separated if $e_n = 1$ *(i.e., there is only a finite number of impacts in any compact time interval). Moreover, if (i)* $\nabla f_i(q)^T M(q)^{-1} \nabla f_j(q) \leq 0$ *for all active constraints* i *and* j, $i \neq j$, *when* $e_n = 0$, *or if (ii)* $\nabla f_i(q)^T M(q)^{-1} \nabla f_j(q) = 0$ *for all active constraints* i *and* j, $i \neq j$, *when* $e_n \in [0, 1]$, *then solutions depend continuously on the initial data. Finally, Moreau's sweeping process measure differential inclusion in (5.52) with set-valued right-hand side* $N_{V(q(t))}\left(\frac{u(t^+) + e_n u(t^-)}{1 + e_n}\right)$ *is well-posed for all* $e_n \in [0, 1]$.

An impact may occur initially. The piecewise analycity of the data is imposed if one wants uniqueness, as it prevents right accumulations of impacts to occur as in Bressan's counterexample of Sect. 2.4.3.1. For mere existence (which may be sufficient in many control applications), one may relax analycity to continuity and local Lipschitz continuity of all forces (inertial and external), while $M(q)$ should be at least continuously differentiable (this is a very tiny requirement for practical applications) [968]. Item (a) allows for Moreau's impact law, but opens the door to other, more general laws. This is important since it means that impact laws like those presented in Chap. 6 could be used without altering the systems's well-posedness. The conditions for continuous dependence mean that (i) the active constraints should make acute angles for $e_n = 0$ or (ii) be orthogonal in the kinetic metric. The result guarantees the existence and uniqueness of a maximal solution. If the inertial and external forces satisfy some classical global Lipschitz continuity, global solutions exist on $[t_0, +\infty)$. This is also the case if a Lyapunov function (the total energy) exists for the system (in which case solutions can be continued indefinitely).

Remark 5.12 Second-order sweeping processes of the form $\ddot{x}(t) + F(t, x(t), \dot{x}(t)) \in -N_{K(x(t))}(\dot{x}(t))$ are studied in [165]. It is assumed that $K(x)$ may be nonconvex, but strictly included in some compact convex set. Then Lipschitz continuous solutions $(x(\cdot), \dot{x}(\cdot))$ are proved to exist under some other regularity assumptions on the multivalued mapping $F(t, x(t), \dot{x}(t))$. The major discrepancy with respect to

unilaterally constrained mechanical systems is that the tangent cone $V(q)$ in Moreau's set is not compact. Hence, Lipschitz continuous solutions do not exist.

Example 5.8 Let us state a tricky case in which the assumption (c) is not satisfied at infinity. Let $q = (x, y)^T \in \mathbb{R}^2$, and $f_1(q) = xy + 1 \geq 0$, $f_2(q) = 1 - xy \geq 0$. This is a hyperbolic billiard. The gradients of the constraints satisfy (e), however, when $x \to +\infty$ then the two constraints become active (the particle is jammed in a funnel with both $h_1(q) = h_2(q) = 0$) and since $\nabla h_1(q) = -\nabla h_2(q)$ always, the Delassus's matrix becomes a 2×2 singular matrix at infinity. The same holds asymptotically as $x \to -\infty$, $y \to +\infty$ and $y \to -\infty$. It is noteworthy that such an issue does not exist in a corner with an acute angle, where both constraints always remain independent.

Example 5.9 Moreau [891] gives the following example for a three-degree-of-freedom system: $f_1(q) = q_1 \geq 0$, $f_2(q) = q_2 q_3 - q_1 \geq 0$, $f_3(q) = q_2 + q_3 \geq 0$. At $q(0) = (0, 0, 0)^T$ and with an admissible velocity (i.e., pointing inward Φ) $\dot{q}(0) = (0\ 2\ -1)^T$, no subsequent motion is possible: the system is "pinched" between the boundaries of Φ. Indeed, one has $q_1(t) = \mathcal{O}(t^2)$, $q_2(t) = 2t + \mathcal{O}(t^2)$, $q_3(t) = -t + \mathcal{O}(t^2)$. Thus $f_2(q(t)) = -2t^2 + \mathcal{O}(t^3)$ is violated in any right neighborhood of 0. It is easily checked that condition (c) is not satisfied at the origin because $\nabla f_1(0) = -\nabla f_2(0)$.

Example 5.10 Let us consider the bouncing ball system with continuously differentiable external force $F(t)$ on the ball: $m\ddot{x}(t) = F(t) + \lambda(t)$, $0 \leq \lambda(t) \perp x(t) \geq 0$. Assume that at some time $t = \tau$ one has $x(\tau) = \dot{x}(\tau) = \ddot{x}(\tau) = x^{(3)}(\tau) = 0$. Then $\lambda(\tau) = -F(\tau)$, and $\dot{\lambda}(\tau) = -\dot{F}(\tau)$. Let $\dot{F}(\tau) > 0$ then $\dot{\lambda}(\tau) < 0$: it seems impossible to continue the integration in a right neighborhood of τ, since this would violate the nonnegativity of the contact force. However, notice that $mx^{(3)}(\tau) = \dot{F}(\tau) + \dot{\lambda}(\tau)$. Thus if we admit that $0 \leq \dot{\lambda}(\tau^+) \perp x^{(3)}(\tau^+) \geq 0$ holds, and that we also have $mx^{(3)}(\tau^+) = \dot{F}(\tau) + \dot{\lambda}(\tau^+)$, we obtain from the linear complementarity problem (LCP) $0 \leq \dot{\lambda}(\tau^+) \perp \frac{1}{m}(\dot{F}(\tau) + \dot{\lambda}(\tau^+)) \geq 0$ that the unique solution is $\dot{\lambda}(\tau^+) = 0$ while $x^{(3)}(\tau^+) = \dot{F}(\tau) > 0$: the dynamics becomes coherent by considering right limits and complementarity between derivatives, and tells us that the ball detaches from the constraint in a right neighborhood of τ. The trick here is that (doing proper assumptions on the data as in Proposition 5.3) we should have written $x(\tau) = \dot{x}(\tau^+) = \ddot{x}(\tau^-) = x^{(3)}(\tau^-) = 0$, while $0 \leq \lambda(\tau^+) \perp \ddot{x}(\tau^+) \geq 0$ and $m\ddot{x}(\tau^+) = F(\tau) + \lambda(\tau^+)$ both hold. Then the contact complementarity problem introduced in Sect. 5.1.2 provides the unique solution $\lambda(\tau^+) = 0$. In the right neighborhood of τ, since $\dot{F}(\tau) > 0$, one has $F(\tau + \varepsilon) > 0$ for some arbitrarily small $\varepsilon > 0$ and thus the same complementarity problem yields $\lambda(\tau + \varepsilon) = 0$ while $\ddot{x}(\tau + \varepsilon) > 0$, which in turn implies positivity of $\dot{x}(\tau + \varepsilon)$. During the persistent contact phase of motion, the sweeping process does not help computing explicit values of λ. But its well-posedness guarantees that such a λ exists (as a selection of Moreau's set), uniquely from Assumption 5.1 (c). *Actually, the system's well-posedness as well as its numerical integration (see Sect. 5.7.3) do not need the explicit knowledge of the contact forces.*

Remark 5.13 It is assumed that initial velocities satisfy the right limit condition $\dot{q}(t_0^+) \in T_\Phi(q(t_0))$. This is in agreement with Proposition 5.12 and Lemma 5.1. Note also that $\dot{q}(t_0^-) \in -T_\Phi(q(t_0))$, which is less intuitive to understand. In fact initial velocities such that $\dot{q}(t_0^-) \notin -T_\Phi(q(t_0))$ may be seen as pathological and quite difficult to realize experimentally. For instance, in a chain of three aligned balls, such velocity is obtained if $\dot{q}_2(0^-) < 0, \dot{q}_3(0^-) > 0$, and $\dot{q}_1(0^-) > 0$: the second and third balls tend to separate with positive relative velocity, while the first ball hits the second one at the same time.

We do not enter into details on the mathematical reasons which make it true that analycity implies nonexistence of right accumulations of impacts and uniqueness of solutions. As a hint let us just recall that if an analytic function $f(t) = \sum_{i\geq 0} a_i t^i$ for a sequence of scalars $\{a_i\}_{i\geq 0}$ and $t \geq 0$, then $f(t) = 0$ for all t small enough is equivalent to $a_i = 0$ for all $i \geq 0$. Then all derivatives of any order of $f(\cdot)$ are also zero. Also, $f(t) > 0$ for all t small enough is equivalent to the lexicographic inequality $(a_1\ a_2\ \ldots\ a_n\ a_{n+1}\ \ldots) \succ 0$. In a sense, either the trajectory stays on the constraint, or it leaves it. But it cannot "hesitate" between the two solutions as in Bressan's counterexample.

Remark 5.14 What is very important in Theorem 5.3 is that right accumulations of impacts can be avoided under might conditions on the data. This justifies some assumptions made for control in Chaps. 7 and 8. And this makes a big discrepancy with the MDEs of Sect. 1.2.2. It is noteworthy that in most applications, the piecewise analycity should hold only during small portions of the system's trajectories (when contact is established). This is particularly true for the tasks analyzed in Sects. 8.1.1 and 8.3.1 and decomposed as in (8.4) and (8.37): during free-motion phases, the dynamics is a classical ODE and external actions may just satisfy classical regularity conditions for Caratheodory systems.

Remark 5.15 (Ideal play) The constraints are supposed to be independent in the set of the active constraints $\mathscr{J}(q)$ in [967]. If the system is subject to dependent constraints which cannot be activated at the same time, then the results in [967] hold. This is the case for systems with so-called ideal clearance as in Fig. 5.6a. Its dynamics is

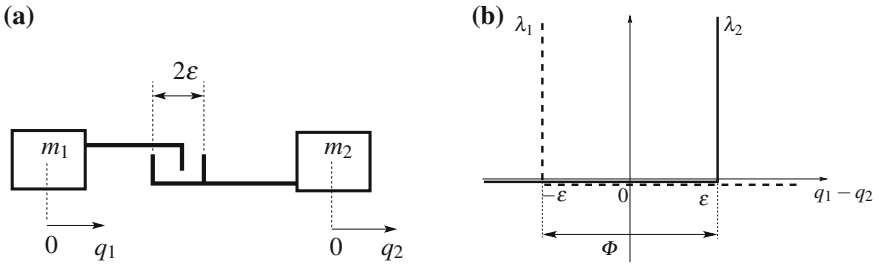

Fig. 5.6 Mechanical clearance

$$\begin{cases} \begin{pmatrix} m_1 & 0 \\ 0 & m_2 \end{pmatrix} \begin{pmatrix} \ddot{q}_1(t) \\ \ddot{q}_2(t) \end{pmatrix} = \begin{pmatrix} 1 & -1 \\ -1 & 1 \end{pmatrix} \begin{pmatrix} \lambda_1(t) \\ \lambda_2(t) \end{pmatrix} \\ 0 \leq \lambda_1 \perp f_1(q) = q_1 - q_2 + \varepsilon \geq 0 \\ 0 \leq \lambda_2 \perp f_2(q) = q_2 - q_1 + \varepsilon \geq 0. \end{cases} \tag{5.83}$$

If one embeds this system into the sweeping process, Moreau's impact law is applied, which boils down to applying Newton's impact law at each constraint with the same CoR e_{n}. One notices that the two constraints are linearly dependent since $\nabla f_1(q) = -\nabla f_2(q)$. However they cannot be active at the same time, because Φ is a strip defined by two parallel lines in the plane. The system is well-posed from Theorem 5.3. The results in [80] may then be applied to conclude about the uniqueness of solutions. Forces $F(q, \dot{q}, t)$ may be considered without altering the conclusions, provided they satisfy some basic regularity properties (piecewise analycity to avoid Bressan's counterexamples of Sect. 2.4.3, and Lipschitz continuity in q and $\dot{q}$). This answers a question raised in [282, 1071] about the well-posedness of systems like (5.83). Notice incidentally that from (5.83) one obtains $\ddot{q}_1(t) - \ddot{q}_2(t) \in -N_{[-\varepsilon,\varepsilon]}(q_1(t) - q_2(t))$. The elements of the normal cone are equal to $\lambda_2(t) - \lambda_1(t)$. This requires the use of (B.19), as well as [1045, Theorem 23.8] applied to the sum of indicator functions. The characteristic of the ideal play is depicted in Fig. 5.6b. Let us write the dynamics in (5.83) into the sweeping process framework. The admissible domain is $\Phi = \{q \in \mathbb{R}^2 | q_1 - q_2 \in [-\varepsilon, \varepsilon]\}$. The tangent cone $V(q)$ to Φ at the configuration q is given by:

$$V(q) = \begin{cases} z \in \mathbb{R}^2 : z_1 - z_2 \geq 0 \text{ if } f_1(q) = 0 \text{ and } f_2(q) > 0 \\ z \in \mathbb{R}^2 : z_2 - z_1 \geq 0 \text{ if } f_2(q) = 0 \text{ and } f_1(q) > 0 \\ \mathbb{R}^2 \qquad\qquad \text{if } f_1(q) > 0 \text{ and } f_2(q) > 0. \end{cases} \tag{5.84}$$

Therefore, Moreau's set (the right-hand side of the sweeping process) is given by:

$$N_{V(q)}(\dot{q}(t^+)) = \begin{cases} \{0\} & \text{if } f_1(q) > 0 \text{ and } f_2(q) > 0 \\ \text{if } f_1(q) = 0 \text{ and } f_2(q) > 0 : \begin{cases} \{0\} & \text{if } \dot{q}_1(t^+) - \dot{q}(t_2^+) > 0 \\ \mathrm{cone} \begin{pmatrix} -1 \\ 1 \end{pmatrix} & \text{if } \dot{q}_1(t^+) - \dot{q}(t_2^+) = 0 \end{cases} \\ \text{if } f_2(q) = 0 \text{ and } f_1(q) > 0 : \begin{cases} \{0\} & \text{if } \dot{q}_2(t^+) - \dot{q}(t_1^+) > 0 \\ \mathrm{cone} \begin{pmatrix} 1 \\ -1 \end{pmatrix} & \text{if } \dot{q}_1(t^+) - \dot{q}(t_2^+) = 0 \end{cases} \end{cases} \tag{5.85}$$

where $\mathrm{cone}(v)$ is the half-line generated by the vector v. Notice from (5.40) and (5.41) that the generalized contact force satisfies $P = \nabla f_1 \lambda_1$ if constraint 1 is active $f_1(q) = 0$ and $P = \nabla f_2 \lambda_2$ if constraint 2 is active $f_2(q) = 0$. Clearly, both constraints cannot be active at the same time. Very few analysis for such ideal play mechanisms have been proposed, see [821] for a specific switching controller which guarantees the

tracking of some trajectories. The state observer design for such systems has been investigated in [843, 844].

5.2.4 Continuous Dependence on Initial Data

The continuous dependence of the solution in the initial conditions fails in general: this is easily understandable from the following example [867, p.129]: imagine in dimension two a convex constraint surface whose boundary is composed of two straight lines that intersect at P, as depicted in Fig. 5.7. Assume that each surface has zero restitution (plastic shock), and that Moreau's impact law is used at the singularity. If the singularity is attained directly along the bissector, then the system remains at rest at $x = y = 0$ for all future times. Now assume that the system is initialized close to the bissector. It first strikes one of the surfaces of the multiple constraint, then it moves along this surface up to the origin, and starts moving along the other surface. This is an example of constraint with nonsmooth boundary. As we shall see in Chap. 6, this kind of singularity occurs also in higher dimension spaces when we consider Lagrangian systems in configuration spaces. As another example of discontinuity with respect to initial data, let us consider the two-cart-with-hook system in Fig. 5.8 [517]. It is assumed that the coordinates have been chosen so that contact occurs with both stops when $q_1 = 0$ and $q_1 = q_2$. In other words, the system is subject to two unilateral constraints $f_1(q) = q_1 \geq 0$ and $f_2(q) = q_1 - q_2 \geq 0$. When both stops are attained at the same time, then $\mathscr{J}(q) = \{1, 2\}$ in Definition 5.1. The initial data $(q_1, q_2, \dot{q}_1, \dot{q}_2) = (\varepsilon, \varepsilon, -2, 1)$ yield for $\varepsilon = 0$ a jump to the equilibrium $(0, 0, 0, 0)$. Now for $\varepsilon > 0$, the constraint $f_2(q)$ (the hook) becomes active first, and the state jumps to $(\varepsilon, 0, -\frac{1}{2}, -\frac{1}{2})$. Then the motion continues in the persistent constrained mode $f_2(q) \equiv 0$, until the surface $f_1(q) = 0$ is attained, with pre-impact state $(0, 0, -\frac{1}{2} + g(\varepsilon), -\frac{1}{2} + g(\varepsilon))$ for some continuous function

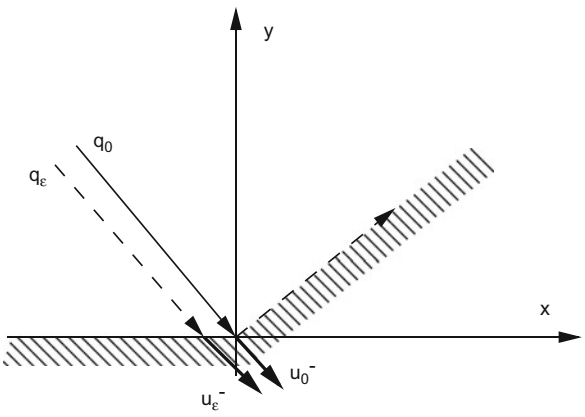

Fig. 5.7 Collision of a particle in an angle ((dis)continuity in the initial data)

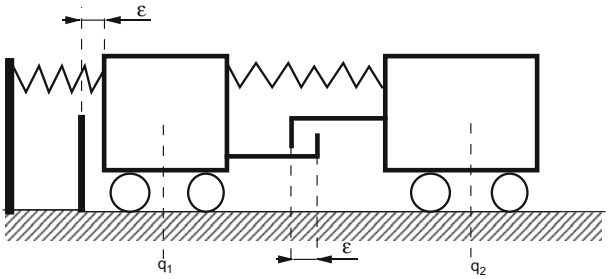

Fig. 5.8 A two-cart system with a hook

$g(\varepsilon)$, $g(0) = 0$. Then a velocity jump occurs to $(0, 0, 0, -\frac{1}{2} + g(\varepsilon))$. If $\varepsilon \to 0^+$, the final state is therefore $(0, 0, 0, -\frac{1}{2})$. Clearly, there is a discontinuity of the flow considered as a function of the initial data at $(0, 0, -2, 1)$. Similar conclusions can be drawn from the initial state $(0, -\varepsilon, -2, 1)$: after two velocity jumps the final state is $(0, 0, \frac{1}{2}, \frac{1}{2})$. It is worth recalling that discontinuity with respect to initial data may not be an obstacle to well-posedness (existence and uniqueness of solutions) as shown in [517]: continuous dependence implies uniqueness, but uniqueness does not imply continuous dependence. For another example, see Sect. 6.1.1.1.

Sufficient conditions for continuous dependence are given in [967]. Let us assume that the conditions in Theorem 5.3 are fulfilled. For all indices i and j in $\mathscr{J}(q)$, $i \neq j$, let $\nabla f_i(q)^T M(q)^{-1} \nabla f_j(q) \geq 0$ if $e_n = 0$, or $\nabla f_i(q)^T M(q)^{-1} \nabla f_j(q) = 0$ if $e_n \in [0, 1]$. Then trajectories are continuous in the initial conditions. The first conditions mean that the constraint boundary makes an acute angle, and the second one that they are orthogonal (in the metric defined by the kinetic energy).

$\rightsquigarrow$ *From an experimental point of view, discontinuity of solutions in the initial data indicates a high sensitivity with respect to the initial position and velocity. This sensitivity may be further studied by choosing a suitable compliant contact model.*

5.3 Coulomb's Friction

The sweeping process may be extended to constraints with friction. First, let us introduce Coulomb's friction model, sometimes also called the Amontons–Coulomb's model, in details.[26]

[26] Guillaume Amontons (1663–1705) and Charles Augustin de Coulomb (1736–1806), both French scientists. What is usually named the Coulomb friction, stemmed from previous analysis by Leonardo Da Vinci (1452–1519), then Amontons after him (and certainly many others at that time). It seems that Coulomb is the one who formulated it in a modern way as $||F_t|| \leq \mu |F_n|$, while Amontons stated that F_t is proportional to F_n and is independent of the contact area. We will adopt the usual way of naming dry friction as Coulomb's friction, though Amontons–Coulomb or Da Vinci–Amontons–Coulomb would be quite suitable.

5.3.1 Coulomb's Friction Model

The local kinematics between two bodies S_1 and S_2 have been investigated in Sect. 4.1.2 (see Fig. 4.1). To lighten the notations, we shall write V_A for the relative velocity (here it is assumed that contact is established, so A_1 and A_2 coincide). Then $V_A = v_{\rm n}\mathbf{n} + v_{\rm t_1}\mathbf{t}_1 + v_{\rm t_2}\mathbf{t}_2$, where $\mathbf{n} \in \mathbb{R}^3$ is the common normal vector at A of S_1 and S_2, while the common tangent plane is spanned by $\mathbf{t}_1$ and $\mathbf{t}_2$. Thus $V_A = (v_{\rm n}, v_{\rm t_1}, v_{\rm t_2})^T = (v_{\rm n}, v_{\rm t}^T)^T$, with $v_{\rm t} = (v_{\rm t_1}, v_{\rm t_2})^T$, all vectors being expressed in the frame $(A, \mathscr{L})$. To simplify further, one may consider that body S_2 is fixed in the Galilean frame, without altering much what follows, and we drop the subscript r in $v_{r,\rm n}$ and $v_{r,\rm t}$. As we have seen in Chap. 4, Sect. 4.1, V_A is a linear function of $\dot{q}_1$ (the generalized velocity of S_1), i.e., $V_A = E_3 \mathscr{M}_1 \dot{q}_1$, $E_3 = [0_{3\times 3} \;\; I_3]$, see (4.11). There is at A an interaction force exerted by S_2 on S_1, denoted as

$$F = F_{\rm t} + F_{\rm n}\mathbf{n} \in \mathbb{R}^3. \tag{5.86}$$

Compared to Sect. 4.1.1, the contact force is not denoted as F_1 to simplify the notations. The vector $F_{\rm t} \in \mathbb{R}^2$ is the component of the interaction force in the tangent plane $\mathscr{T}$ between S_1 and S_2 at A, i.e., $F_{\rm t} = F_{\rm t_1}\mathbf{t}_1 + F_{\rm t_2}\mathbf{t}_2$. From (4.14) one has $Q_1 = \mathscr{M}_1(q_1)^T \mathscr{W}_A^\star = \mathscr{M}_1(q_1)^T \begin{bmatrix} 0 \\ F \end{bmatrix} = \mathscr{M}_1(q_1)^T E_3^T F = \nabla f(q)\lambda_{{\rm n},u} + H_{{\rm t},u}(q)\lambda_{{\rm t},u}$ in the notations of (5.1), $\lambda_{{\rm n},u} = F_{\rm n}$ and $\lambda_{{\rm t},u} = (F_{{\rm t},1}, F_{{\rm t},2})$, where Q_1 is the generalized force on S_1 (see (4.4)). It is assumed that there is no torque at A due to friction or other contact effect (like for instance compliance). The friction cone is a convex cone with apex at A, symmetric with respect to $\mathbf{n}$, defined as $\mathscr{C} = \{F \in \mathbb{R}^3 |\; ||F_{\rm t}|| \le \mu |F_{\rm n}|\}$, where $\mu \ge 0$ is the coefficient of friction. Thus the angle between $\mathbf{n}$ and the cone boundary is $\arctan(\mu)$. The cone is depicted in Fig. 5.10. Coulomb's model of friction reads as follows:

- (sticking) If $v_{\rm t} = 0$ then $F \in \mathscr{C}$.
- (sliding) If $v_{\rm t} \neq 0$, then $||F_{\rm t}|| = \mu |F_{\rm n}|$ and there exists a scalar $\alpha \ge 0$ such that $F_{\rm t} = -\alpha\, v_{\rm t}$.

It is equivalently formulated as [13, §3.9.1.1]:

- $||F_{\rm t}|| \le \mu |F_{\rm n}|$ and
  - (sticking) $||F_{\rm t}|| < \mu |F_{\rm n}| \Rightarrow v_{\rm t} = 0$.
  - (sliding) $||F_{\rm t}|| = \mu |F_{\rm n}| \Rightarrow$ there exists a scalar $\beta \ge 0$ such that $v_{\rm t} = -\beta\, F_{\rm t}$.

In the planar case, $F_{\rm t} = F_{\rm t_1}\mathbf{t}_1$ one may rewrite it equivalently as $F_{{\rm t},1} \in -\mu |F_{\rm n}|\, {\rm sgn}(v_{\rm t})$, where ${\rm sgn}(\cdot)$ is the set-valued signum function. To simplify in the planar case we should denote $F_{\rm t_1}$ as $F_{\rm t}$.

Remark 5.16 A constant friction coefficient may be too restrictive for some applications, and one has to account for various effects [1340].[27] It is quite possible to

[27] I often met colleagues who at the same time would peremptorily reject Coulomb's friction model (arguing that it lacks physical meaning because it does not encapsulate "crucial" effects—some of

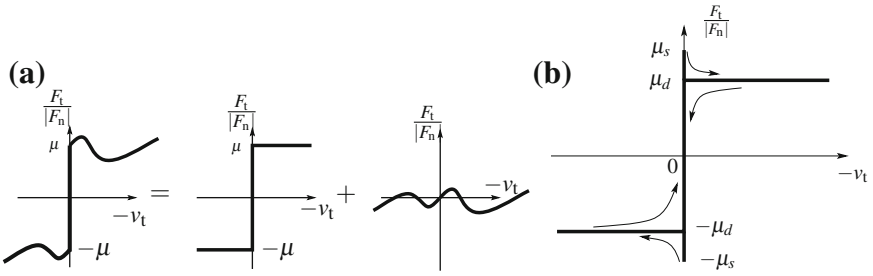

Fig. 5.9 Varying coefficients of friction. **a** Stribeck effect $\mu(v_t)$. **b** Dynamic/static friction

consider a tangential velocity-dependent coefficient $\mu(v_t)$, as for instance depicted in Fig. 5.9a in the two-dimensional case. This does not really change the problem since such a friction law can be written as the sum of the Coulomb's set-valued model, and of a (at least continuous) function of v_t. In many instances (mathematical analysis, time discretization and numerical analysis, stability analysis), such extension does not pose any problem. One well-known model that may be recast in this framework is Stribeck's friction. These models may be considered as being too simple from the tribologist's point of view. However, in the framework of multibody dynamics with possibly large number of contact points, they prove to be extremely useful and with surprisingly good prediction capabilities. Another extension is with a dynamic μ_d (for sliding modes) and a static $\mu_s > \mu_d$ (for stick-to-slip transitions) coefficients of friction, see Fig. 5.9b. A memory has to be added so that the trajectories follow the arrows in the figure for stick/slip and slip/stick transitions. The Coulomb–Contensou friction, which includes a friction torque, is formulated in [726] in a set-valued nonsmooth framework (using extensions of the pseudopotential approach described in Sect. 5.3.2). It is indicated in [726] how to use this model in a multibody, time-stepping method. Other variants of Coulomb's friction are Coulomb–Orowan and Coulomb–Shaw models [1032, §1.4.5]. Finally, the "ice-cream" cone may be extended to cones with sections which are not disks but convex sets (ellipses), for anisotropic friction.

---

which may easily be added to the basic model, like Stribeck effect), and had thoroughly used non-holonomic equality constraints $g(q, \dot{q}) = 0$ for control purpose. These people, themselves lacking of Mechanical culture, could not realize that non-holonomic constraints are obtained assuming a perfect sticking contact, that is, a sub-case of Coulomb's friction, and did not hesitate to use a regularization procedure which suppresses sticking modes …Systems with Coulomb's friction may be seen as an extension of non-holonomic systems, and sticking ($\Leftrightarrow$ set-valuedness at zero tangential velocity) is here to stay in most multibody applications.

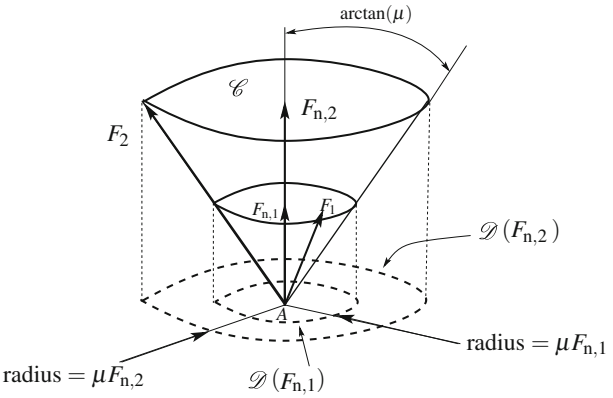

Fig. 5.10 Coulomb–Moreau's disks

5.3.2 Coulomb–Moreau's Disk

Jean Jacques Moreau used convex analysis in [889] to derive an original point of view on Coulomb's model. It relies on what we call next the Coulomb–Moreau's disks. Let us assume that F_n is known. The condition $F \in \mathscr{C}$ is then equivalent to:

$$F_t \in \mathscr{D}(F_n), \tag{5.87}$$

with $F_t = F_{t_1}\mathbf{t}_1 + F_{t_2}\mathbf{t}_2$, and

$$\mathscr{D}(F_n) = \begin{cases} F_n \mathscr{D}_1 & \text{if } F_n \geq 0 \\ \emptyset & \text{otherwise,} \end{cases} \tag{5.88}$$

where $\mathscr{D}_1$ is the orthogonal projection on the tangent plane $\mathscr{T}$ between both bodies at A, of the plane section of $\mathscr{C}$. More clearly, if the Coulomb's law is chosen isotropic, then $\mathscr{D}_1$ is a disk of radius equal to the friction coefficient, centered at A, see Fig. 5.10. Then from (5.86) together with (5.87) Coulomb's friction law can be expressed as the variational inequality [889]: Find $F_t \in \mathscr{D}(F_n)$ such that

$$\forall\ y \in \mathscr{D}(F_n), \quad V_{A,t}^T(y - F_t) \geq 0, \tag{5.89}$$

where $V_{A,t} = v_{t_1}\mathbf{t}_1 + v_{t_2}\mathbf{t}_2$ is the tangential velocity in the tangent contact plane at A, following the notations of Chap. 4.1 (in a broader context one works with the *relative* tangential velocity between two bodies). By drawing little pictures one can convince oneself that the relationships in (5.89) are equivalent to Coulomb's model: if $V_A = 0$ then F_t may lie anywhere in the interior of $\mathscr{D}(F_n)$. If $V_{A,t} \neq 0$, then necessarily $F_t \in \mathrm{bd}(\mathscr{D}(F_n))$ and with opposite direction to $V_{A,t}$. Actually, (5.89) means that given a velocity V_A, the tangential forces that satisfy those relationships

are those where the function $y \mapsto \langle y, V_{A,\mathrm{t}} \rangle$, $y \in \mathscr{D}(F_\mathrm{n})$ attains its infimum relative to $\mathscr{D}$ in (5.88): thus Coulomb's law hinges on a *principle of maximum dissipation*: the (tangential) contact force has to be "as opposite as possible" to the tangential velocity. Notice that $\langle F_\mathrm{t}, V_{A,\mathrm{t}} \rangle \leq 0$, while $\langle F_\mathrm{t}, -V_{A,\mathrm{t}} \rangle \geq 0$ is equal to the mechanical power transformed by friction. Using convex analysis tools, the formulation in (5.89) can in turn be shown to be equivalent to:

$$-V_{A,\mathrm{t}} \in \partial \psi_{\mathscr{D}(F_\mathrm{n})}(F_\mathrm{t}) = N_{\mathscr{D}(F_\mathrm{n})}(F_\mathrm{t}) \tag{5.90}$$

and to:

$$-V_{A,\mathrm{t}} \in \mathrm{proj}_{\mathscr{T}} \partial \psi_{\mathscr{C}}(F) = \mathrm{proj}_{\mathscr{T}} N_{\mathscr{C}}(F) \tag{5.91}$$

(which means that the velocity belongs to the projection on the tangent plane $\mathscr{T}$ of the outward normal cone to $\mathscr{C}$ at F) and to:

$$-F_\mathrm{t} \in \partial \varphi(V_{A,\mathrm{t}}), \tag{5.92}$$

where $\varphi(\cdot) = \mu\, |F_\mathrm{n}|\, ||\cdot||$, with μ the friction coefficient. It is worth noting that the formulation in (5.91) is valid for any reaction λF, $\lambda > 0$: only the direction of F is involved [867, p.79]. If F is in the interior of $\mathscr{C}$, then $N_{\mathscr{C}}(F) = \{0\}$ and $V_{A,\mathrm{t}} = 0$. These features are shown to be essential to formulate the dynamics in terms of differential measures, see Problem 5.2.

The proof of the above developments is given in [892, 894]. For instance, the equivalence between (5.90) and (5.92) can be shown using the fact that the dual function of $||\cdot||$ is the indicator function of the ball $||y|| \leq 1$ (see Appendix B), and that the velocity and the interaction force belong to dual spaces (that can, anyway, both be identified with $\mathbb{R}^3$). In other words, consider the function $\varphi(\cdot)$ in (5.92). Its dual function is given by $\varphi^\star(y) = \psi_{\mu|F_\mathrm{n}|||y||\leq 1}(y)$. The dual function of the indicator function (see Theorem B.1) is given by $\psi^\star_{\mu|F_\mathrm{n}|||y||\leq 1}(u) = \varphi(u)$, so that $\partial\varphi(u) = \partial\psi^\star_{\mu|F_\mathrm{n}|||y||\leq 1}(u)$ is the subdifferential of the support function[28] of the convex set $\mu|F_\mathrm{n}|||y|| \leq 1$.[29] It therefore follows that (5.92) is equivalently rewritten for any $\rho > 0$ as:

$$F_\mathrm{t} \in \partial \psi^\star_{\mathscr{D}(F_\mathrm{n})}(-V_{A,\mathrm{t}}) \;\Leftrightarrow\; F_\mathrm{t} = \mathrm{proj}[\mathscr{D}(F_\mathrm{n}); F_\mathrm{t} - \rho V_{A,\mathrm{t}}] \tag{5.93}$$

where we used (B.20) and the fact that (5.90) is equivalent to (5.93) and to $F_\mathrm{t} - F_\mathrm{t} + \rho V_{A,\mathrm{t}} \in -\partial \psi_{\mathscr{D}(F_\mathrm{n})}(F_\mathrm{t})$. Note that those equivalences hold because $\mathscr{D}(F_\mathrm{n})$ in (5.88)

[28] The support function of a set C is defined as the conjugate function of the indicator of C, i.e., $\psi^\star_C(x) = \sup_{y\in C}\langle y, x\rangle$. The function $\varphi(x)$ in (5.92) is called the *dissipation function* [889], and $\varphi(x) = \psi^\star_C(-x) = -\inf_{y\in C}\langle x, y\rangle$. In Chap. A.1 after Definition B.11, an example is given where $C = [-a, b]$. The name dissipation function is motivated by the fact that Coulomb's law can be formulated as $F_\mathrm{t} \in \mathscr{D}$, $-\langle V_A, F_\mathrm{t}\rangle = \varphi(V_A)$ which represents the dissipated power.

[29] The variables u and y belong to spaces respectively dual one to each other: if u is a velocity then y is a force.

is a convex set. The second expression in (5.93) is implicit in F_t and should be solved with a fixed point algorithm, the projection being a Lipschitz continuous function. Extensions are therefore possible for anisotropic friction replacing the disks by other convex sets.

Remark 5.17 Using the notations of Chap. 4, we may write equivalently $F_\mathrm{t} = \mathrm{argmin}_{||\tilde{F}_\mathrm{t}||\le\mu F_\mathrm{n}} \langle \tilde{F}_{\mathrm{t}_1}\mathbf{t}_1 + \tilde{F}_{\mathrm{t}_2}\mathbf{t}_2, v_{\mathrm{t}_1}\mathbf{t}_1 + v_{\mathrm{t}_2}\mathbf{t}_2\rangle = \mathrm{argmin}_{||\tilde{F}_\mathrm{t}||\le\mu F_\mathrm{n}} \tilde{F}_\mathrm{t}^T v_\mathrm{t}$. If we let $v_\mathrm{t} = H_\mathrm{t}(q)^T\dot{q}$ we obtain $F_\mathrm{t} = \mathrm{argmin}_{||\tilde{F}_\mathrm{t}||\le\mu F_\mathrm{n}} \dot{q}^T H_\mathrm{t}(q)\tilde{F}_\mathrm{t}$, which is again a form of maximum dissipation. See [1163] for the use of (5.93) in a broader context and its numerical analysis.

Remark 5.18 There are similarities between two-dimensional Coulomb's friction with known normal force, sliding mode controllers, and Fuller's phenomenon in optimal control, in the sense that they all involve the set-valued relay function. Their numerical simulation or discrete-time implementation therefore requires similar algorithms. Advanced sliding mode controllers like the so-called twisting controller yield a closed-loop system of the form $m\ddot{q}(t) \in -a\mathrm{sgn}(q(t)) - b\mathrm{sgn}(\dot{q}(t))$ for some gains $a > 0$, $b > 0$. It is proved that under suitable choice of a and b, the origin is finite-time asymptotically stable. This suggests a way to stabilize systems subjected to dry friction.

5.3.3 De Saxcé's Associated Formulation

Coulomb's law together with Signorini-in-velocity conditions cannot be expressed with a convex pseudopotential (i.e., it cannot be formulated as an inclusion in the normal cone to a convex set [534, 1062]: one says it is *nonassociated*; a proof is given below). This has motivated De Saxcé to modify the velocity in order to recover a convex pseudopotential formulation, using the so-called bi-potential function [1062]. Here we adopt the above notation for the relative velocity at a contact point A (as done in Sect. 4.1.1), but we focus on the planar case only and thus simplify it as $V = V_A = v_\mathrm{n}\mathbf{n} + v_\mathrm{t}\mathbf{t}$, while $F = F_\mathrm{n}\mathbf{n} + F_\mathrm{t}\mathbf{t}$. The basic idea is that despite that the velocity $V \notin N_{\mathscr{C}}(F)$, the modified velocity $\hat{V} \triangleq \begin{pmatrix} v_\mathrm{n} + \mu|v_\mathrm{t}| \\ v_\mathrm{t} \end{pmatrix}$ (i.e., $\hat{V} = (v_\mathrm{n} + \mu|v_\mathrm{t}|)\mathbf{n} + v_\mathrm{t}\mathbf{t}$) satisfies $\hat{V} \in -N_{\mathscr{C}}(F)$ as depicted in Fig. 5.11a for $v_\mathrm{n} = 0$. Conversely and using (B.16), one finds $F \in -N_{\mathscr{C}^\star}(\hat{V})$ where $\mathscr{C}^\star$ is the dual cone of $\mathscr{C}$ (its semi-angle is equal to $\arctan\left(\frac{1}{\mu}\right)$ as depicted in Fig. 5.11a while the polar cone $\mathscr{C}^\circ = -\mathscr{C}^\star$. And equivalently $\mathscr{C}^\star \ni \hat{V} \perp F \in \mathscr{C}$ (see (B.19)). The complete friction model taking into account unilateral contact is as follows (see the developments in Sect. 5.1.2.1 and in particular Proposition 5.3), where $R = \begin{pmatrix} F_\mathrm{n} \\ F_\mathrm{t} \end{pmatrix}$ and the contact is active:

$$\begin{cases} 0 \le v_\mathrm{n} \perp F_\mathrm{n} \ge 0 \;\Leftrightarrow\; v_\mathrm{n} \in -N_{\mathbb{R}_+}(F_\mathrm{n}) \\ \\ \mathscr{C}^\star \ni \hat{V} \perp F \in \mathscr{C} \end{cases} \tag{5.94}$$

Clearly, the velocity V does not satisfy the cone complementarity conditions in (5.94), for if it was the case the system could not even slide, with V pointing strictly inward the admissible domain. Let us now analyze (5.94):

- If $F_{\rm n} > 0$, then $v_{\rm n} = 0$ so $\hat{V} = \begin{pmatrix} \mu|v_{\rm t}| \\ v_{\rm t} \end{pmatrix}$.
  - If $v_{\rm t} = 0$, then $\hat{V} = 0$ so that $F \in \mathscr{C}$.
  - If $v_{\rm t} \neq 0$: $\hat{V} \perp F \Rightarrow \mu|v_{\rm t}|F_{\rm n} + v_{\rm t}F_{\rm t} = 0 \Leftrightarrow F_{\rm t} = -\mu F_{\rm n}\frac{|v_{\rm t}|}{v_{\rm t}} = -\mu F_{\rm n}\mathrm{sgn}(v_{\rm t})$.
- If $F_{\rm n} = 0$ ($\Rightarrow F_{\rm t} = 0$), then $v_{\rm n} \geq 0$:
  - If $v_{\rm n} > 0$ then detachment from the constraint occurs with $\hat{V} \in \mathscr{C}^\star$.
  - If $v_{\rm n} = 0$ step 1 may be redone to find $F_{\rm t} = 0$.

One may take it the other way round:

- If $v_{\rm n} > 0$: $\Rightarrow F_{\rm n} = 0$, and detachment occurs with $\hat{V} \in \mathscr{C}^\star$.
- If $v_{\rm n} = 0$: $\Rightarrow F_{\rm n} \geq 0$.
  - If $F_{\rm n} > 0$: $\hat{V} \perp F \Leftrightarrow \mu|v_{\rm t}|F_{\rm n} + v_{\rm t}F_{\rm t} = 0$:
    - If $v_{\rm t} \neq 0$: $F_{\rm t} = -\mu F_{\rm n}\frac{|v_{\rm t}|}{v_{\rm t}}$, so $F \in \mathscr{C}$ (sliding contact).
    - If $v_{\rm t} = 0$: $\hat{V} = 0$ and $F \in \mathscr{C}$ (sticking contact).
  - If $F_{\rm n} = 0$: $\Rightarrow v_{\rm t}F_{\rm t} = 0$.
    - If $v_{\rm t} = 0$: sticking occurs with $F \in \mathscr{C} \Rightarrow F_{\rm t} = 0$ (grazing sticking contact).
    - If $v_{\rm t} \neq 0$: sliding occurs with $F_{\rm t} = 0$ because $F \in \mathscr{C}$ and $F_{\rm n} = 0$ (grazing sliding contact).

This holds also in the three-dimensional case as shown in [1062]. Let us now prove that it is indeed the case that Coulomb's friction cannot be written as a convex pseudopotential. If this was true then the mapping $C_\mu : V \mapsto F$ that incorporates both unilaterality and friction would be monotone. Consider the system in Fig. 5.11b where $v = (\dot{x}\ \dot{y})^T$, and the unilateral constraint is given by $0 \leq y \perp F_{\rm n} \geq 0$. The mapping C_μ is defined by the relations (5.94), i.e.,

$$\begin{cases} F_{\rm n} \in -N_{\mathbb{R}_+}(\dot{y}) \ \Leftrightarrow\ 0 \leq \dot{y} \perp F_{\rm n} \geq 0 \\ \\ F_{\rm t} \in -\mu F_{\rm n}\mathrm{sgn}(\dot{x}) \ \Leftrightarrow\ F \in \mathscr{C}, \end{cases} \tag{5.95}$$

with $\mathrm{sgn}(0) = [-1, 1]$. Monotonicity means that for all V_1 and V_2, all $F_1 \in C_\mu(V_1)$ and all $F_2 \in C_\mu(V_2)$, one has $\langle F_1 - F_2, V_1 - V_2\rangle \geq 0$. Take $V_1 = 0 \Rightarrow F_{\rm n,1} \geq 0$ and $F_{\rm t_1} \in -\mu F_{\rm n,1}[-1, 1]$. Take also $V_2 > 0 \Rightarrow F_{\rm n,2} = 0$ and $F_{\rm t_2} = -\mu F_{\rm n,2} = 0$. Thus we get $\langle F_1, -V_2\rangle = -F_{\rm n,1}\dot{x}_2 - F_{\rm t_1}\dot{y}_2$. The first term of the left-hand side is negative for any $F_{\rm n,1} > 0$. The second term has the sign of $-F_{\rm t,1}$, which may be chosen in the set $-\mu F_{\rm n,1}(0, 1]$. Thus one concludes that there exists two pairs (V_1, F_1) and (V_2, F_2) such that $\langle F_1 - F_2, V_1 - V_2\rangle < 0$. The mapping $C_\mu(\cdot)$ is not monotone, thus cannot be a convex pseudopotential. Other proofs may be found in [1062, §5] and [534, §4].

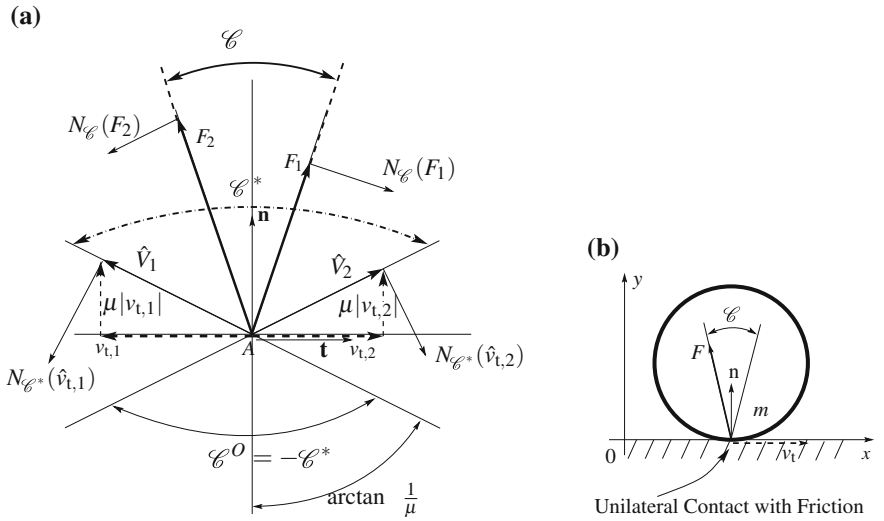

Fig. 5.11 Planar Coulomb's friction. **a** Modified velocity for associated Coulomb's law. **b** A point mass with Coulomb's friction

5.3.4 Coulomb's Friction at the Acceleration Level

An extension of the classical Coulomb's friction has been proposed [452, 963] for sticking contact points, in order to deal with possible stick $\rightarrow$ slip transitions. It writes as follows for a unilateral contact:

- If $v_n > 0$: then $F_n = 0$ from $0 \leq v_n \perp F_n \geq 0$, and detachment occurs.
- If $v_n = 0$, then $F_n \geq 0$ and:
  - (sliding) If $v_t \neq 0$ then $||F_t|| = \mu F_n$ and there exists a scalar $\alpha \geq 0$ such that $F_t = -\alpha v_t$.
  - If $v_t = 0$:
    - (stick $\rightarrow$ slip) If $\dot{v}_t \neq 0$: then $||F_t|| = \mu F_n$ and there exists a scalar $\beta \geq 0$ such that $F_t = -\beta \dot{v}_t$.
    - (sticking) If $\dot{v}_t = 0$: then $F \in \mathscr{C}$.

This model is useful for instance in event-driven numerical schemes, in order to cope with transitions from sticking to sliding modes. In the planar (two-dimensional) case, this becomes for the tangential part [211]:

- (sliding) If $v_t \neq 0$, then $F_t = -\mu F_n \mathrm{sgn}(v_t)$.
- If $v_t = 0$:
  - (stick $\rightarrow$ slip) If $\dot{v}_t \neq 0$, then $F_t = -\mu F_n \mathrm{sgn}(\dot{v}_t)$.
  - (sticking) If $\dot{v}_t = 0$, then $F \in \mathscr{C} \Leftrightarrow |F_t| \leq \mu F_n$.

It is noteworthy that this model, when incorporated in the dynamical equations, makes the acceleration appear on both sides of the dynamics. Hence, it becomes possible to use (B.16) and (B.20) to express the acceleration $\dot{v}_{\mathrm{t}}$ from a quadratic program with constraints. As an illustration, for a two-degree-of-freedom particle we obtain $\ddot{x}(t^+) + F_{ext}(t) \in -\mu|F_{\mathrm{n}}(t)|\mathrm{sgn}(\ddot{x}(t^+)$ when $x(t) = 0$ and $\dot{x}(t) = 0$, where $v_{\mathrm{t}}(t) = \dot{x}(t)$. We find the following:

$$\begin{aligned} \ddot{x}(t^+) &\in N_{[-1,1]}\left(-\tfrac{\ddot{x}(t^+)+F_{ext}(t)}{\mu|F_{\mathrm{n}}(t)|}\right) \\ \Leftrightarrow\ \ddot{x}(t^+) &= -F_{ext} - \mu F_{\mathrm{n}}(t)\mathrm{proj}\left([-1,1]; -\tfrac{F_{ext}(t)}{\mu F_{\mathrm{n}}(t)}\right) \end{aligned} \tag{5.96}$$

It follows that $\frac{F_{ext}}{\mu F_{\mathrm{n}}} \in [-1, 1] \Rightarrow \ddot{x}(t^+) = 0$, and $\left|\frac{F_{ext}}{\mu F_{\mathrm{n}}}\right| < 1 \Rightarrow \ddot{x}(t^+) = -F_{ext}(t) \pm \mu F_{\mathrm{n}}(t)$.

5.3.5 *Further Comments on Friction Models*

As alluded to in Remark 5.16, the basic Coulomb's friction model may be easily modified with varying sliding friction coefficient, while remaining in a set-valued setting to properly model sticking phases. Some viscoelastoplastic models have been presented in Sect. 2.3. In particular, the model in (2.36) is a frictional model that improves Coulomb's model while not calling into question its set-valuedness at zero tangential velocity. Many other friction models have been proposed in the literature (see e.g., [428]), not necessarily stemming from clever motivations. For instance, the Karnopp model has been proposed to cope with the supposedly unsolvable issue related to the impossibility to numerically simulate the set-valued signum function. The idea is therefore to replace the vertical branch of the relay function at zero by some dead zone around zero tangential velocity, or by some regularization procedure,[30] thus avoiding "unsolvable" numerical simulation problems. Doing so, one introduces parameters which may not possess clear physical meaning. It is noteworthy that these numerical issues are exactly the same as those encountered in discrete-time sliding mode control. It is known that an *explicit Euler* discretization of the basic sliding mode controllers yields spurious oscillations around the attractive sliding surface [424, 425, 1308], while an *implicit (or backward Euler)* discretization allows one to avoid such *numerical chattering* [14, 16, 664]. In the context of contact mechanics, it has long been known that a suitable, implicit discretization allows one to properly simulate Coulomb's friction [617, 892]. More details are given in Sect. 5.7.3. Numerical comparisons between friction models as done in [428] would certainly be drastically improved if a correct numerical solver was used. Interesting analysis dealing with such issue (and using backward Euler discretization) is done

[30] This may be done with Moreau–Yosida approximations, see Sect. B.1.

in [663], with both numerical and experimental results on several friction models found suitable for haptic interfaces. See also [1286] for a clever discussion on several frictional models used in friction compensation schemes, and new models improving [663]. A complete survey (though not tackling numerical simulation issues very deeply) on friction models and their domains of application is proposed in [127].

5.3.6 Sweeping Process with Friction

5.3.6.1 General Formulation

A general formulation of the sweeping process with dry friction for an n-degree-of-freedom system with a single unilateral constraint is given as follows:

Problem 5.2 (*Sweeping Process with Friction [867]*) Find an *RCLBV* function $u(\cdot)$ such that $u(\cdot)$ and the function $q(\cdot)$ defined by (5.38) satisfy the following:

- $q(\tau_0) = q_0$, $u(\tau_0) = u_0$,
- $q(t) \in \Phi$ for all $t \geq \tau_0$,
- $u(t) \in V(q(t))$ for all $t \geq \tau_0$,

and the following implications are true μ-almost everywhere:

- $f(q(t)) < 0 \Rightarrow R'_\mu(t) = 0$,
- $f(q(t)) = 0$ and $u(t)^T \nabla f(q(t)) < 0 \Rightarrow R'_\mu(t) = 0$,
- $f(q(t)) = 0$ and $u(t)^T \nabla f(q(t)) = 0 \Rightarrow -u(t) \in \mathrm{proj}_{T(q(t))} N_{\mathscr{C}(q(t))}\left(R'_\mu(t)\right)$
- $Q(t, q, u)dt - M(q(t))du = dR$,

where μ is any positive measure such that R'_μ can be defined with (5.49) and $R'_\mu = \frac{dR}{d\mu}$.

The density function R'_μ denotes as above the interaction force at the contact point, $T(q(t))$ denotes the tangent hyperplane at the contact point, and $\mathscr{C}(q(t))$ is a generalized friction cone. From (5.90), (5.91), and (5.92), the right-hand side of the last implication can be written differently. The first implication means that when the bodies are not in contact, then the interaction force is zero. The second implication means that if there is contact, but the velocity points inward the admissible domain Φ, the interaction force is zero also (this is a kind of grazing point). The third statement means that when the velocity is tangential to the constraint surface, then its opposite belongs to the tangent hypersurface $T(q(t))$ at the contact point $q(t)$, and is in this hypersurface the point the closest to the outward normal cone of $\mathscr{C}(q(t))$ at $R'_\mu(t)$. For instance, consider the two-dimensional case. In particular, when $R'(\mu)(t) \in \mathrm{Int}(\mathscr{C}(q(t)))$, the tangent cone to $\mathscr{C}(q(t))$ at $R'_\mu(t)$ is the whole of $\mathbb{R}^2$, so that the normal cone reduces to the zero 2-vector. Consequently, one gets $-u(t) \in \mathrm{proj}_{T(q(t))}\{0\} = 0$, and one retrieves that when the interaction force lies (strictly) inside the friction cone, the tangential velocity is zero. When the reaction

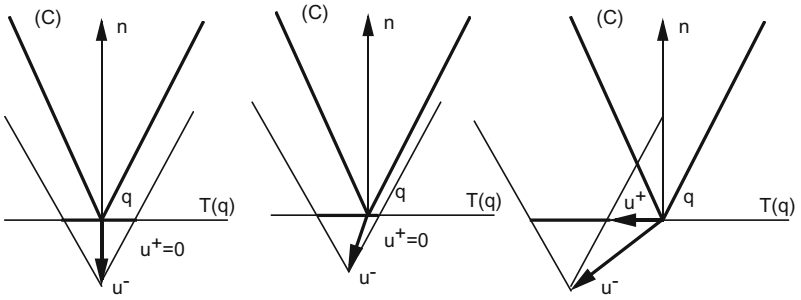

Fig. 5.12 Sweeping process with friction (collision case)

lies on the boundary of the friction cone, indeed (5.91) holds. Notice that this formulation encompasses all possible motions, with or without shocks. When there is a collision, the last condition in Problem 5.2 is equivalent to

$$u(t_k^+) = \text{proj}\left(0, [u(t_k^-) + \mathscr{C}(q(t))] \cap T(q(t))\right). \tag{5.97}$$

Different situations are depicted in Fig. 5.12. The major assumption done in [867] is that the real-world isotropic friction law is transported into a generalized isotropic friction law in the configuration space. In other words, the friction cone $\mathscr{C}(q)$ in the configuration space is revolving about $\nabla f(q)$, with vertex at the contact point.[31] This allows to prove the global existence of a solution to problem 5.2, without facing singularities such as Painlevé paradoxes.

5.3.6.2 Impacts with Friction: Local Kinematics

Let us come back to local kinematics. In order to prepare the dynamical equations, we first have to recall the local kinematics of the problem which allow us to define the m gap functions $f_i(q)$, the vector of normal velocities U_n with $U_{\text{n},i} = v_{r,\text{n},i}$ at contact point i, and the vector of tangential velocities $U_\text{t} = (v_{r,\text{t},1}, v_{r,\text{t},2}, \ldots, v_{r,\text{t},m})^T$ and each $v_{r,\text{t},i}$ is either a scalar (two-dimensional friction) or a two-vector (three-dimensional friction). In turn, we have $v_{r,\text{n},i} = \nabla f_i(q)^T \dot{q}$ and $v_{r,\text{t},i} = H_{\text{t},i}(q)^T \dot{q}$, where $H_\text{t}(q)$ is as in (5.1), and is obtained from the local kinematics and the derivation of velocities V_{A_i} at each contact point i (see Chap. 4, Sects. 4.1.2 and 4.1.3). First, consider the Lagrangian dynamics (5.1) where we write for simplicity $F(q, \dot{q}, t) \stackrel{\Delta}{=} C(q, \dot{q})\dot{q} + G(q) - F_{ext}(t)$ and we do not consider bilateral constraints. We have (the time argument is dropped):

[31] In general, the transportation of the real-world friction cone into the configuration space results in a cone that does not satisfy such assumptions [381, 436, 437]. This result of existence is therefore restricted to material point systems, and does not apply to the Painlevé's example that we shall analyze later.

$$
\begin{aligned}
\ddot{q} \;&= M(q)^{-1}(\nabla f(q), H_{\mathrm{t}}(q))\begin{pmatrix}\lambda_{\mathrm{n}}\\ \lambda_{\mathrm{t}}\end{pmatrix} - M(q)^{-1}F(q,\dot{q},t)\\
\Rightarrow \begin{pmatrix}\nabla f(q)^T\\ H_{\mathrm{t}}(q)^T\end{pmatrix}\ddot{q} &= \begin{pmatrix}\nabla f(q)^T M(q)^{-1}\nabla f(q) & \nabla f(q)^T M(q)^{-1}H_{\mathrm{t}}(q)\\ H_{\mathrm{t}}(q)^T M(q)^{-1}\nabla f(q) & H_{\mathrm{t}}(q)^T M(q)^{-1}H_{\mathrm{t}}(q)\end{pmatrix}\begin{pmatrix}\lambda_{\mathrm{n}}\\ \lambda_{\mathrm{t}}\end{pmatrix}\\
&\quad - \begin{pmatrix}\nabla f(q)^T\\ H_{\mathrm{t}}(q)^T\end{pmatrix} M(q)^{-1}F(q,\dot{q},t)
\end{aligned}
\tag{5.98}
$$

$$
i.e.: \begin{pmatrix}\nabla f(q)^T\\ H_{\mathrm{t}}(q)^T\end{pmatrix}\ddot{q} = \overbrace{\begin{pmatrix}D_{\mathrm{nn}}(q) & D_{\mathrm{nt}}(q)\\ D_{\mathrm{nt}}(q)^T & D_{\mathrm{tt}}(q)\end{pmatrix}}^{\triangleq D(q)}\begin{pmatrix}\lambda_{\mathrm{n}}\\ \lambda_{\mathrm{t}}\end{pmatrix} - \begin{pmatrix}\nabla f(q)^T\\ H_{\mathrm{t}}(q)^T\end{pmatrix} M(q)^{-1}F(q,\dot{q},t)
$$

$$
\Rightarrow \begin{pmatrix}\dot{U}_{\mathrm{n}}\\ \dot{U}_{\mathrm{t}}\end{pmatrix} = D(q)\lambda + G(q,\dot{q},t),
\tag{5.99}
$$

where $G(q,\dot{q})$ collects all the nonlinear terms, including $\frac{d}{dt}\{\begin{pmatrix}\nabla f(q)^T\\ H_{\mathrm{t}}(q)^T\end{pmatrix}\}\dot{q}$ which comes from differentiating $\nabla f(q)^T\dot{q}$ and $H_{\mathrm{t}}(q)^T\dot{q}$. The matrix $D_{\mathrm{nn}}(q)$ is the Delassus' matrix, which we denoted before as $D_u(q)$, and we emphasize here with the nn subscript that it represents only normal/normal couplings. The matrix $D(q)$ may be viewed as an extension of M^{-1} in (4.140) for the case of multibody multicontact systems, see also (4.152). Now we may use the above as well as (4.79) and (4.80) to extend (5.66) as follows, at an impact time $t = t_k$ with m active unilateral constraints such that $U_{\mathrm{n}}(t_k^-) = \nabla f(q(t_k))^T\dot{q}(t_k^-) \le 0$:

$$
\begin{cases}
\begin{pmatrix}U_{\mathrm{n}}(t_k^+) - U_{\mathrm{n}}(t_k^-)\\ U_{\mathrm{t}}(t_k^+) - U_{\mathrm{t}}(t_k^-)\end{pmatrix} = D(q(t_k))\begin{pmatrix}P_{\mathrm{n}}(t_k)\\ P_{\mathrm{t}}(t_k)\end{pmatrix}\\
0 \le U_{\mathrm{n}}(t_k^+) + \mathscr{E}U_{\mathrm{n}}(t_k^-) \perp P_{\mathrm{n}}(t_k) \ge 0\\
\mathscr{C}_i^\star \ni \hat{V}_i(t_k) \perp P_i(t_k) \in \mathscr{C}_i,\ 1 \le i \le m
\end{cases}
\tag{5.100}
$$

with $\hat{V}_i(t_k) = \begin{pmatrix}\tilde{U}_{\mathrm{t},i}(t_k)\\ \tilde{U}_{\mathrm{n},i}(t_k) + \mu||\tilde{U}_{\mathrm{t},i}(t_k)||\end{pmatrix}$, i is the ith contact, $p_{\mathrm{n}}(t_k) = \nabla f(q(t_k))P_{\mathrm{n}}(t_k)$, $p_{\mathrm{t}}(t_k) = H_{\mathrm{t}}(q(t_k))P_{\mathrm{t}}(t_k)$, $\mathscr{C}_i$ is the Coulomb's cone at contact point i, $P_i = \begin{pmatrix}P_{\mathrm{t},i}\\ P_{\mathrm{n},i}\end{pmatrix}$. The velocities $\tilde{U}_{\mathrm{t},i}$ may be chosen following the material in Sect. 4.3.1.2 (where in particular some tangential CoR may be included), and $\tilde{U}_{\mathrm{n},i} = U_{\mathrm{n},i}(t_k^+) + e_{\mathrm{n},i}U_{\mathrm{n}}(t_k^-)$ when $\mathscr{E} = \mathrm{diag}(e_{\mathrm{n},i})$. It is noteworthy that *there is no guarantee that* $T_L(t_k) \le 0$ *with* (5.100) *in the general case.*

Remark 5.19 Depending on the tangential/normal couplings through the matrix $D_{\mathrm{nt}}(q(t_k))$, the tangential components $U_{\mathrm{t}}(t_k)$ may well be discontinuous (in fact, the whole vector $\dot{q}(\cdot)$ may jump at t_k). We retrieve here a comment made for two-body

collisions in Sect. 4.3.2 that tangential velocities may be discontinuous for various reasons, including inertial couplings.

5.3.7 Additional Comments and Studies

Some related existence of solutions problems have been presented in [692, 693, 694]: the system consists of a particle moving on a rigid surface with Coulomb's friction, and acted upon by impulsive forces (i.e., the external force acting on the particle has the general form $F = F_{ac}dt + F_{imp}d\mu$, where $d\mu$ is a series of Dirac measures, whereas dt is the Lebesgue's measure). A solution is shown to exist for sufficiently small friction coefficient. A one-degree-of-freedom system described by a differential inclusion is studied in [868]:

$$M(q(t))\ddot{q}(t) + F(t, q(t), \dot{q}(t)) \in \Gamma(-\dot{q}(t)), \tag{5.101}$$

where q is the system's coordinate, and $\Gamma(u) = -a$ if $u < 0$, $\Gamma(u) = b$ if $u > 0$, $\Gamma(0) = [-a, b]$ represents the friction force. Equivalently, one may write an ODE with discontinuous right-hand side as:

$$M(q(t))\ddot{q}(t) + F(t, q(t), \dot{q}(t)) = \text{proj}_{\Gamma(-\dot{q}(t))}F(t, q(t), \dot{q}(t)), \tag{5.102}$$

It is shown in [868] via a discretization procedure that a *global* solution exists, with $q(\cdot)$ and $\dot{q}(\cdot)$ are continuous, whereas $\ddot{q}(\cdot)$ is of local bounded variation. The results are extended to n-degree-of-freedom systems, with the assumption that the normal component of the interaction force is known and constant.[32] Other well-posedness results making similar assumption on the normal contact force may be found in [27] for linear mechanical systems. Linear mechanical systems with bilateral constraints and Coulomb's friction are analyzed in [82] when the normal contact force is a given Lebesgue integrable function. The only mathematical analysis showing the well-posedness without further assumptions on the normal contact force and on the mass matrix $M(q)$ may be that of Stewart [1141, 1142], which concerns the Painlevé system of Sect. 5.6.

5.4 Complementarity Formulations

At several places of the foregoing chapters, we have met complementarity conditions, which we introduced from mechanical observations about how the contact (interaction) force behaves. Since complementarity conditions and normal cones to finitely

[32] This in particular precludes the application of the result in [868] to the Painlevé's example described in Sect. 5.6.

represented sets are closely related, we also saw that Moreau's sweeping process is a kind of complementarity Lagrangian system (see e.g., (5.44), (5.55), and (5.66)). In this (long) section, we first summarize complementarity conditions, and then expend on complementarity problems, complementarity systems, their well-posedness, dissipativity, controllability.

5.4.1 Two Bodies: Signorini's Conditions

Consider the two-body problem as in Sect. 4.1. The component of the contact force along $\mathbf{n}$ is F_{n}. The so-called *Signorini*'s conditions are complementarity conditions which state that:

$$F_{\mathrm{n}} \geq 0, \quad (A_2A_1)^T\mathbf{n} \geq 0, \quad F_{\mathrm{n}}(A_2A_1)^T\mathbf{n} = 0 \;\Leftrightarrow\; 0 \leq F_{\mathrm{n}} \perp (A_2A_1)^T\mathbf{n} \geq 0. \tag{5.103}$$

The complementarity conditions in (5.103) rely on four fundamental modeling assumptions:

- The contact force exerted by body 1 on body 2 can be positive ($F_{\mathrm{n}} > 0$) only if contact is closed ($(A_2A_1)^T\mathbf{n} = 0 \Leftrightarrow A = A_1 = A_2$).
- If the contact is open ($(A_2A_1)^T\mathbf{n} > 0$), then the contact force exerted by body 1 on body 2 is zero ($F_{\mathrm{n}} = 0$).
- The contact force can take only nonnegative values ($F_{\mathrm{n}} \geq 0$).
- The bodies cannot interpenetrate ($(A_2A_1)^T\mathbf{n} \geq 0$).

This is indeed all what the complementarity condition between the contact force and the gap function means. As we saw in Chap. 2, this does not preclude flexibility since some spring-dashpot models lend themselves to such formalisms. Other possible complementarity formulations equivalent to the one in (5.103) are given by:

$$\begin{cases} F_{\mathrm{n}} \geq 0 \\ \forall p_{\mathrm{n}} \geq 0,\ (p_{\mathrm{n}} - F_{\mathrm{n}})(A_2A_1)^T\mathbf{n} \geq 0 \end{cases} \text{ or } \begin{cases} (A_2A_1)^T\mathbf{n} \geq 0 \\ \forall s_{\mathrm{n}} \geq 0,\ (s_{\mathrm{n}} - (A_2A_1)^T\mathbf{n})F_{\mathrm{n}} \geq 0. \end{cases} \tag{5.104}$$

They can be deduced from convex analysis tools as described in Appendix B.

In case of N contact/impact points in a system of n rigid bodies, one collects all the normal contact forces in a vector $\lambda_{\mathrm{n}} \in \mathbb{R}^N$, and the gap function $f(q)$ is constructed similarly by noting that $x_{2,\mathrm{n}}$ above is a function of the generalized

coordinate vector $q \in \mathbb{R}^{6n}$ of the system.[33] Then the complementarity conditions generalize to $0 \leq \lambda_n \perp f(q) \geq 0$. Due to the nonnegativity, the orthogonality holds componentwise. This is a coordinate invariant property. Indeed, let $q = Q(z)$ for some diffeomorphism $Q : \mathbb{R}^{6n} \to \mathbb{R}^{6n}$. Then $f(q) = f \circ Q(z) \stackrel{\Delta}{=} g(z) \geq 0$. Also $\nabla g(q) = \nabla Q(z) \nabla f(q) = \nabla Q(z) \nabla f(Q(z))$. In the Lagrange dynamics and according to the invariance "principle" of Sect. 3.2, the power equality $\dot{q}^T \nabla f(q) \lambda_n = \dot{z}^T \nabla Q(z) \nabla f(q) \lambda_n = \dot{z}^T \nabla g(z) \lambda_n$ holds. Therefore the vector of multipliers λ_n is unchanged by coordinate change, and one obtains $0 \leq g(z) \perp \lambda_n \geq 0$.

5.4.2 *Linear Complementarity Problem (LCP)*

The complementarity between two variables z and w writes as $0 \leq z \perp w \geq 0$. This becomes an LCP when w is a linear function of z, so that z is the unknown of the problem. Thus an LCP may be seen as a nonsmooth equation, whose well-posedness (existence and uniqueness of solutions) has to be analyzed. The next theorem is a central result of complementarity theory.

Theorem 5.4 *[307] Consider the LCP(r, M) defined as*

$$\begin{cases} z \geq 0 \\ w = r + Mz \geq 0 \\ z^T (r + Mz) = 0 \end{cases} \Leftrightarrow 0 \leq z \perp w = Mz + r \geq 0. \tag{5.105}$$

M is a $n \times n$ P-matrix if and only if the LCP(r, M) has a unique solution for every $r \in \mathbb{R}^n$. This solution z is a piecewise-linear function of r, hence Lipschitz continuous.

The set of relations in (5.105) defines what is named an LCP. The variable w is called a *slack* variable in optimization theory. Notice that since both z and $r + Mz$ are positive, $z^T (r + Mz) = 0$ is equivalent to $z_i (r + Mz)_i = 0$ for each i. The *modes* of the LCP are given by the various combinations $z_i \geq 0$ and $w_i = 0$, or $z_i = 0$ and $w_i \geq 0$, $1 \leq i \leq n$. Thus there are 2^n LCP modes. Let us state the following:

Theorem 5.5 *A matrix is a P-matrix if all its principal minors are positive.*[34]

The inverse of a P-matrix is a P-matrix. The proof is rather simple: let M be a P-matrix, and $0 \leq r \perp w = Mr + q \geq 0$, then $r = M^{-1} w - M^{-1} q$ so we obtain equivalently (since M is square full rank) $0 \leq r = M^{-1} w - M^{-1} q \perp w \geq 0$; since M is a P-matrix there is a unique solution $r^\star$ for any vector q, hence a unique w for any q. Since both LCPs are equivalent, there is also a unique solution $w^\star$ for any $M^{-1} q$ for the second LCP. Thus M^{-1} is a P-matrix. There may exist some couples

[33] Such a calculation may not be trivial, depending on the bodies' shapes.

[34] A positive definite matrix (possibly nonsymmetric) is a P-matrix [307, Theorem 3.1.6], a symmetric matrix is positive definite if and only if it is a P-matrix [307, p.147], but nonsymmetric P-matrices may not be positive definite [307, Example 3.3.2].

(r, M) with M not being a $P-$matrix, such that the LCP possesses a unique solution. However, the LCP has a unique solution for *every* r *if and only if* M is a P-matrix. Actually, another result is also quite powerful. It concerns the *solvability* of an LCP, i.e., the existence of solutions.

Theorem 5.6 *[307, Theorem 3.8.6] Consider the linear complementarity problem* $0 \leq z \perp w = Mz + r \geq 0$. *Suppose that the matrix* M *is copositive, and let* r *be given. If the implication* $0 \leq v \perp Mv \geq 0 \Rightarrow r^T v \geq 0$ *holds, the LCP*(r, M) *has a solution.*

In other words, if the solutions of the homogeneous LCP$(0, M)$ satisfy the required inequality, then the original LCP has a solution. Let us recall the following:

Definition 5.4 A matrix $M \in \mathbb{R}^{n\times n}$ is said *copositive* if $x^T Mx \geq 0$ for all $x \in \mathbb{R}^n_+$.

Thus copositivity is positive semi-definiteness tested on the first orthant. Consequently, a positive semi-definite matrix is automatically copositive. But the inverse is not true: some copositive matrices are not definite. The frictionless contact problem yields an LCP whose matrix M in (5.105) is equal to the Delassus' matrix $D(q) = \nabla f(q)^T M^{-1}(q)\nabla f(q)$. One has to rewrite the complementarity conditions in (5.1) (b) at the acceleration level to get such an LCP whose unknown is the Lagrange multiplier $\lambda_{n,u}$, see Sect. 5.1.2. Another useful result from complementarity theory is the following one:

Theorem 5.7 *[307, Theorem 3.1.7] Consider the LCP*(r, M)*:* $0 \leq z \perp w = Mz + r \geq 0$. *Suppose that the matrix* M *is positive semi-definite, and let* r *be given. Then*

- *If* z_1 *and* z_2 *are two solutions of the LCP*(r, M)*, one has* $z_1^T(r + Mz_2) = z_2^T(r + Mz_1) = 0$.
- *If* M *is symmetric, then* $M(z_1 - z_2) = 0$ *for any two solutions* z_1 *and* z_2.

Many LCPs therefore possess multiple solutions. In some cases, it is useful to focus on a particular solution within the set of all solutions.

Proposition 5.18 *[307, 502] Consider the LCP*(r, M).

- *Suppose that* M *is a Z-matrix*[35] *and that the set of solutions of LCP*(r, M) *is nonempty. Then there is a unique least-element solution* z^* *satisfying* $z^* \leq z$ *for any other solution* z.
- *Suppose that* $M \succeq 0$ *and the set of solutions is nonempty. Then the set of solutions is convex and contains a unique least-norm solution* z^* *satisfying* $||z^*|| \leq ||z||$ *for any other solution* z.
- *Suppose that* $M \succeq 0$ *and there exists* z *such that* $z \geq 0$ *and* $Mz + r \geq 0$ *(the LCP is feasible). Then there exists* λ *such that* $0 \leq \lambda \perp M\lambda + r \geq 0$ *(the LCP is solvable).*

Such results are useful in the context of LCS with a positive semi-definite matrix D (see (5.119)). Indeed, though the multiplier λ may not be unique, the least-norm solution λ is unique and may serve to define some solutions of the LCS.

[35] A square matrix is a Z-matrix if its off-diagonal entries are all nonpositive.

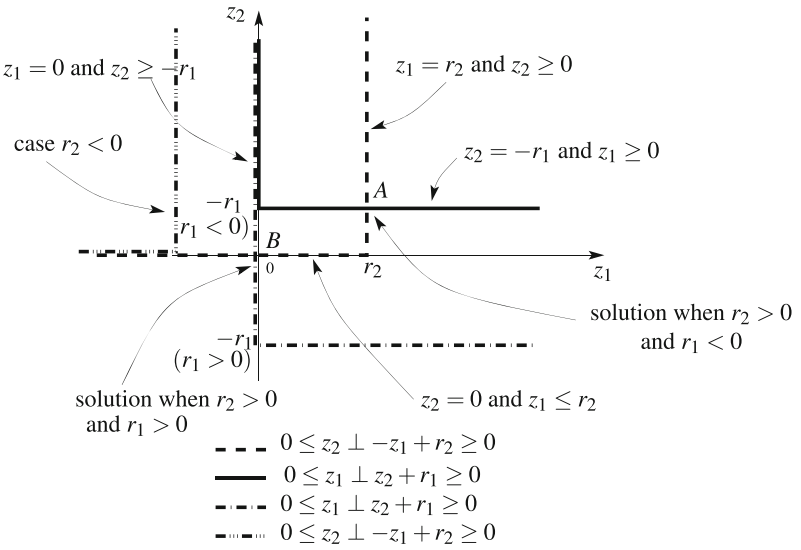

Fig. 5.13 Graphical interpretation of the LCP in Example 5.11

Example 5.11 Consider the two-dimensional LCP with $M = \begin{pmatrix} 0 & 1 \\ -1 & 0 \end{pmatrix} \succeq 0$ and $r = \begin{pmatrix} r_1 \\ r_2 \end{pmatrix}$. The solvability of this LCP holds if and only if $r_2 \geq 0$. Indeed, it is easy to see that if $r_2 < 0$ then one obtains $z_1 = r_2$, which is impossible. Conversely, if $r_2 > 0$ then the unique solution is $z_1 = r_2$ and $z_2 = -r_1$ if $r_1 < 0$ (point A), or $z_1 = 0$ and $z_2 = 0$ if $r_1 > 0$ (point B). If $r_2 = 0$ then the set of solutions is $z_1 = 0$ and $z_2 \geq \max(0, -r_1)$. This is depicted in Fig. 5.13.

Example 5.12 Consider $M = -1$ and $r = -1$: this LCP has no solution since $-z - 1 \geq 0 \Leftrightarrow 0 > -1 \geq z$.

Let us also state the next result which may be useful in the context of dynamical complementarity systems. The Hadamard product of two vectors a and b is denoted as $a \circ b$, that is, a vector with ith component $a_i b_i$.

Proposition 5.19 *[256] Consider the LCP(r, M) and suppose that the set of its solutions SOL$(r, M) \neq \emptyset$. If $z \circ Mz \leq 0 \Rightarrow Bz = 0$ then B SOL(r, M) is a singleton for all r. Equivalently for any two solutions z_1 and z_2 of LCP(r, M), then $Bz_1 = Bz_2 \Leftrightarrow z_1 - z_2 \in \ker(B)$.*

Finally, we end this section with a quite useful result taken from [284], which applies to matrices of the form $N + P$, where $N \succ 0$ or N is a P-matrix, while P is a perturbation. The norm $||\cdot||_2$ is the induced matricial norm such that $||M||_2 = \sigma_{\max}(A) = \sqrt{\lambda_{\max}(AA^T)}$, where $\lambda_{\max}$ is the largest eigenvalue, while $\sigma_{\max}$ is the largest singular value.

Theorem 5.8 *[284] Let $N \in \mathbb{R}^{n\times n}$ be $\succ 0$. Then every matrix*

$$D \in \{D \mid \left|\left|\left(\frac{N+N^T}{2}\right)^{-1}\right|\right|_2 ||N-D||_2 < 1\}$$

satisfies $D \succ 0$. As a consequence let $D = P + N$, where D, P, and N are $n \times n$ real matrices, and $N \succ 0$, not necessarily symmetric. If

$$||P||_2 < \frac{1}{\| \left(\frac{N+N^T}{2}\right)^{-1} \|_2} \tag{5.106}$$

then $D \succ 0$. If N is a P-matrix, then all matrices D such that $\beta_2(N)||N-D||_2 < 1$ are P-matrices, where $\beta_2(N) := \max_{c\in[0,1]^n} ||(I - C + CN)^{-1}C||_2$, $C = diag(c)$. When $N = N^T \succ 0$, $\beta_2(N) = ||N^{-1}||_2$. If $D = P + N$ the condition becomes $||P||_2 < \frac{1}{\beta_2(N)}$.

Corollary 5.2 *Let $M \in \mathbb{R}^{n\times n}$ be a symmetric positive definite matrix. Let $A = BM$ for some matrix B. If*

$$||M^{-1}||_2||M||_2||I - B||_2 < 1,$$

then $A \succ 0$.

Proof Since $M = M^T$ applying Theorem 5.8 gives that $||M^{-1}||_2||M - BM||_2 < 1$ guarantees that $A \succ 0$. Now from [136, Proposition 9.3.5] one has $||M - BM||_2 \leq ||M||_2||I - B||_2$: the result follows.

5.4.3 Relationships with Quadratic Problems

At several places of this book we saw that there are close relationships between complementarity problems and quadratic problems in optimization (the classical monograph [307] starts with such statements). The so-called Karush–Kuhn–Tucker conditions are at the core of the equivalence between LCPs and QPs. The following two QPs can be considered, where $M = M^T \succeq 0$:

$$QP_1 \begin{cases} \min_z \frac{1}{2} z^T M z + z^T r \\ \text{subject to: } z \geq 0, \end{cases} \tag{5.107}$$

and:

$$QP_2 \begin{cases} \min_z \frac{1}{2} z^T M z \\ \text{subject to: } Mz + r \geq 0. \end{cases} \tag{5.108}$$

Consider for instance QP_1 in (5.107). The Lagrangian of this QP is $L_1(z,\lambda) = \frac{1}{2}z^T Mz + z^T r - \lambda^T z$. Then the Karush–Kuhn–Tucker's conditions for z to be a minimizer of the QP are given by:

$$\begin{cases} \frac{\partial L_1}{\partial z} = Mz + r - \lambda = 0 \\ z \geq 0, \quad \lambda \geq 0, \quad z^T\lambda = 0. \end{cases} \tag{5.109}$$

Concerning QP_2, one has $L_2(z,\lambda) = \frac{1}{2}z^T Mz - \lambda^T(Mz + r)$. Kuhn–Tucker's conditions become:

$$\begin{cases} \frac{\partial L_2}{\partial z} = Mz - M^T\lambda = 0 \\ Mz + r \geq 0, \quad \lambda \geq 0, \quad \lambda^T(Mz + r) = 0. \end{cases} \tag{5.110}$$

Note that since M is symmetric, then from the first condition in (5.110) one gets $z = \lambda$, hence, one gets $Mz + r \geq 0$, $z \geq 0$ and $z^T(Mz + r) = 0$ which is an LCP. The QP_2 is named dual to the QP_1 because the multiplier λ of the QP is equal this time to the minimizing value of z, whereas in QP_1 it was equal to $Mz + r$.

Remark 5.20 Let us relate this result to the nonuniqueness of solutions in Problems 2.1 and 3.1. Assuming that one has $q(\tau_0) = 0$ and $\dot{q}(\tau_0) = 0$, i.e., the mass is at rest on the constraint at τ_0, it is evident to write an LCP whose unknown is the interaction force μ, as follows:

$$f + \mu \leq 0,\ \mu \leq 0,\ (f + \mu)\mu = 0. \tag{5.111}$$

Theorem 5.4 guarantees that at each instant, and for any applied force $f \in \mathbb{R}$, there is a unique μ satisfying the set of conditions in (5.111). Trivially, one finds $\mu = -f$. Notice that this does not contradict the fact that depending on f, there may be nonuniqueness of the solution $(q(t), \dot{q}(t))$ whose initial value at τ_0 is $(0, 0)$. This is the case with the external action constructed by Aldo Bressan (see Sect. 2.4.3): two different solutions arise from the same initial state. However, at time τ_0 one has $Q(\tau_0) = \ddot{\varphi}(\tau_0) = 0$ uniquely determined. This shows that solving a force LCP at an instant is just one part of the job in the overall system's well-posedness problem.

The above results extend to nonlinear problems:

$$\min_{h(q)\leq 0} f(q) \tag{5.112}$$

with $h(q) = [h_1(q), \cdots, h_m(q)]^T$. Assume that $\nabla h(q)$ has rank m. Then we have (see for instance [481, p.12]):

Theorem 5.9 *If q_0 is a relative minimum point for (5.112), there is a vector $\lambda \in \mathbb{R}^m$ such that:*

$$\begin{cases} \nabla f(q_0) + \lambda^T \nabla h(q_0) = 0 \\ \lambda \geq 0, \quad \lambda^T h(q_0) = 0. \end{cases} \tag{5.113}$$

The complementarity conditions between λ and $h(q_0)$ clearly appear in (5.113) as $0 \leq \lambda \perp -h(q_0) \geq 0$. If $f(q) = \frac{1}{2} q^T Q q$ for $Q = Q^T \succ 0$ and $h(q) = Aq + B$, then (5.113) yields the LCP: $0 \leq \lambda \perp AQ^{-1}A^T - B \geq 0$. If the m constraints are independent, then $AQ^{-1}A^T \succ 0$ and this LCP has a unique solution by Theorems 5.5 and 5.5.

Let us end this section with a recall on Dorn's duality and converse duality theorems, which we used in Sect. 5.1.2.2.

Theorem 5.10 *[795, Theorems 8.2.4, 8.2.6] Let $Q = Q^T \succeq 0$. Consider the two quadratic programs:*

$$\begin{cases} \min \frac{1}{2} z^T Q z + b^T z \\ \textit{subject to: } Az \geq c, \end{cases} \tag{5.114}$$

and

$$\begin{cases} \min \frac{1}{2} z^T Q z - c^T w \\ \textit{subject to: } A^T w - Qz = b, \ w \geq 0. \end{cases} \tag{5.115}$$

Then:

- *If $\bar{z}$ solves the program (5.114) then there exists $\bar{w}$ such that $(\bar{z}, \bar{w})$ solves the program (5.115). Moreover, the two extrema are equal.*
- *If $(\bar{z}, \bar{w})$ solves the program (5.115) then there exists $\hat{z}$ with $\hat{z} - \bar{z} \in \ker(Q)$ such that $\hat{z}$ solves the program (5.114).*

5.4.4 Linear Complementarity Systems (LCS)

When coupled to a linear invariant system $\dot{x}(t) = Ax(t) + B\lambda(t) + Eu(t)$, complementarity conditions like $0 \leq Cx(t) + D\lambda(t) + Fu(t) \perp \lambda(t) \geq 0$ give rise to LCS. The complementarity conditions are a particular kind of nonsmooth constraint.

5.4.4.1 Introduction

We already met linear complementarity systems in (2.5) and (2.14), for mechanical systems with unilateral springs and dampers. Let us consider the following system [1063]:

$$\begin{cases} \dot{q}_1(t) = q_2(t) \\ \dot{q}_2(t) = q_3(t) \\ \dot{q}_3(t) = -\lambda(t) \\ 0 \leq w(t) = q_1(t) + q_2(t) + q_3(t) \perp \lambda(t) \geq 0, \end{cases} \tag{5.116}$$

where $\lambda(t) \in \mathbb{R}, w \in \mathbb{R}, q_1(t), q_2(t), q_3(t)$ are scalar variables. It has a relative degree 1 between the "input" λ and the "output" w, since $\dot{w} = q_2 + q_3 - \lambda$. Consider now the initial data $[q_1(0), q_2(0), q_3(0), \lambda(0)] = (0, 1, -1, 0)$. Notice that this is typically a configuration for which the constraint is undetermined: it is not possible to know if the system is in an active or inactive constraint mode. Using Proposition 5.3 is therefore possible at time $t = 0$ to express the complementarity condition as:

$$0 \leq \dot{w}(t) \perp \lambda(t) \geq 0. \tag{5.117}$$

Let us check whether the system can remain in the unconstrained mode $\lambda \equiv 0$: at time $t = 0$, one has $\dot{w}(0) = 0$ and, from this assumption, $\ddot{w}(0) = -\lambda(0) + q_3(0) - \dot{\lambda}(0) = q_3(0) = -1$. Hence, the assumption is wrong: the system cannot remain in the mode $\lambda \equiv 0$ ("free-motion" mode). What about the mode $w \equiv 0$? Then one computes that $\dot{\lambda}(0) = q_3(0) - \lambda(0) - \ddot{w}(0) = -q_2(0) = -1$: thus this continuation is also impossible since otherwise $\lambda(t)$ would become negative for $t > 0$. One can consequently think of pulling the system off this "trap" by defining some suitable shock rule: but notice that a collision mapping has to make the state jump when there is a shock, i.e., here if $\dot{w}(0) < 0$, which is not the case. In other words, a "consistent" collision mapping must be one that forces the system to jump from a configuration such that the inequality constraint $w \geq 0$ is going to be violated. Still this is not the case here at $t = 0$. Hence, this configuration constitutes a fixed point of the collision mapping. Notice that the LCP in (5.117) is of the form:

$$0 \leq q_2(t) + q_3(t) - \lambda(t) \perp \lambda(t) \geq 0. \tag{5.118}$$

Hence, the requirements of Theorem 5.4 are not fulfilled. At time $t = 0$ and with the above initial data, there is nevertheless a unique solution given by $\lambda = 0$. Replacing the -1 premultiplying λ in (5.116) by $+1$, then the LCP in (5.118) has a unique solution in terms of the multiplier λ. A stronger result in [1063] assures the existence of a solution to systems like the one in (5.116) if the leading Markov parameter is positive: it is therefore a surprising and nice feature of such that the conditions for existence and uniqueness of a solution λ to the LCP coincide with those for existence and uniqueness of a solution $q(t)$ to the whole dynamical system.[36] Let us summarize the main results in [517, 759, 1063, 1064]. Autonomous linear complementarity systems are governed by the equations:

$$\begin{aligned} &\dot{x}(t) = Ax(t) + B\lambda(t) \\ &0 \leq \lambda(t) \perp w(x(t), \lambda(t)) = Cx(t) + D\lambda(t) \geq 0 \end{aligned} \tag{5.119}$$

[36] Though the system is different, this is consistent with Theorem 5.3, since all the data in (5.116) are analytic.

Notice that linear complementarity Lagrangian systems are a subclass of (5.119), with $D = 0, x = (q^T, \dot{q}^T)^T, C = (I_n, 0)$. The modes of this nonsmooth dynamical system (there are 2^m modes, w and $\lambda \in \mathbb{R}^m$) correspond to $y_i = 0$ for $i \in \mathscr{I} \subseteq \{1, \ldots, m\}$, $\lambda_i = 0$ for $i \in \mathscr{I}^c$, where $\mathscr{I}^c$ is the complement of $\mathscr{I}$ in $\{1, \ldots, m\}$. It is assumed that each mode is autonomous, which means that to every consistent state x_0 there corresponds a unique couple $(x(t), \lambda(t))$, with $\lambda(\cdot)$ smooth (this is a well-posedness condition). The subspace of all consistent states is denoted as $V(A, B, C, D)$. The problem is posed as follows: let us initialize the system in a particular mode i. Then the state evolves as long as the complementarity rules are satisfied. Now if at a given time instant (called an event time) it happens that those rules can no longer be satisfied, the state has to be reinitialized in order to enable one to continue the integration in another mode. The jump rule is based on the decomposition of the state space as $\mathbb{R}^n = V(A, B, C, D) \oplus T(A, B, C, D)$. Roughly speaking, V is the space "tangent" to the constraint, while N is the "normal" space. Such decomposition is closely related to the DAE analysis of Sect. 1.3.4, also used in the framework of switched DAEs (see however Remark 5.23). The state is reinitialized with a jump. Does the continuation in another mode exist and is it unique? Well-posedness means here that after each event time, continuation is possible on a strictly positive measure interval, and with a unique couple (x, λ). This does not preclude finite accumulation of reinitializations, and thus does not guarantee the global existence of solutions on $\mathbb{R}^+$. Moreover, solutions may be discontinuous with respect to initial data, as shown elsewhere in this book for mechanical systems. Let us denote the Markov parameters of the linear system in (5.119) as $H^0 = D, H^i = CA^{i-1}B$ for $i \geq 1$. Their jth column is denoted as $H^i_{\bullet j}$, and their jth row as $H^i_{j\bullet}$. Consider now the column indices $\eta_j = \inf\{i \in \mathbb{N} \,|H^i_{\bullet j} \neq 0\}$, and the row indices $\rho_j = \inf\{i \in \mathbb{N} \,|H^i_{j\bullet} \neq 0\}$. Let us form the matrices $\mathscr{M} = \begin{pmatrix} H^{\rho_1}_{1\bullet} \\ \vdots \\ H^{\rho_m}_{m\bullet} \end{pmatrix}$ and $\mathscr{N} = (H^1_{\bullet 1}, \ldots, H^m_{\bullet m})$. Then the following is true:

Lemma 5.3 *[517] If the matrices $\mathscr{M}$ and $\mathscr{N}$ are P-matrices, then the linear complementarity system in (5.119) is well-posed. Moreover, from each initial condition, smooth continuation is possible after at most one jump.*

This result uses only properties of the "free-motion" system to test the well-posedness of the overall nonsmooth system. The underlying idea for the proof is to consider the Laplace transforms of $w(t)$ and $\lambda(t)$, i.e., $W(s)$ and $\Lambda(s)$ respectively, and to notice that $f(t) \geq 0 \Rightarrow F(s) \geq 0$ for $s \in \mathbb{R}^+$ large enough. Then one can form a so-called *Rational Complementarity Problem* (RCP) as follows: find rational functions $W(s)$, $\Lambda(s)$ such that $W(s) \geq 0$, $\Lambda(s) \geq 0$ for s large enough, and $W(s)^T \Lambda(s) = 0$ for all $s \in \mathbb{R}$. Such a procedure is limited to linear invariant systems, which precludes its application to nonlinear systems like most mechanical systems. It is noteworthy that only the local existence and uniqueness is shown by Lemma 5.3. The global existence may nevertheless be proved [516]. The extension of the above to nonlinear complementarity systems $\dot{x}(t) = f(x(t)) + g(x(t))\lambda(t)), w(t) = h(x(t))$,

$0 \leq \lambda(t) \perp w(t) \geq 0$, $f(\cdot)$, $g(\cdot)$, $h(\cdot)$ analytic functions is tackled in [1064]. Let the system possess a uniform relative degree between λ and w equal to r at x_0, which means that the so-called decoupling matrix $L_g L_f^{r-1} h(x_0)$ is full rank, while $L_g L_f^{i-1} h(x_0) = 0$ for all $1 \leq i < r$ (thus all the successive derivatives of the "outputs" $w_i(t)$ are independent of λ, up to the differentiation degree r where they are all depend on λ). It is shown that well-posedness holds (local existence and uniqueness of an analytic solution in a right neighborhood of a time t_0, with state x_0) provided that the lexicographical inequality $(w(x_0), \dot{w}(x_0), \ldots, w^{(r-1)}(x_0)) \succ 0$ holds, and the matrix $L_g L_f^{r-1} h(x_0)$[37] is a P-matrix. Some comments arise:

- For complementarity systems with uniform relative degree r, it is not worth looking at the derivatives of $w(t)$ of degree larger than r to conclude about well-posedness.
- Systems with several inputs and outputs and with a uniform relative degree are rare. However, frictionless complementarity Lagrangian systems[38] with independent constraints $f_i(q)$ possess a uniform relative degree between $w = f(q)$ and $\lambda_{n,u}$ equal to $r = 2$, for any q. The decoupling matrix $L_g L_f h(q)$ is the Delassus' matrix $\nabla f(q)^T M(q)^{-1} \nabla f(q)$.
- Analycity of the data once again plays a crucial role for uniqueness. External actions (or inputs) are not considered in the above results. Motivated by the case of Mechanics and Theorem 5.3, we conjecture that piecewise-analytic inputs would not alter the existence and uniqueness results.

$\rightsquigarrow$ *This shows that it is not worth looking at derivatives higher than the acceleration, to analyze Lagrangian systems subject to unilateral constraints.*

The well-posedness results summarized in Sect. 2.4 all assume a positive definite Delassus' matrix. As seen in Sect. 5.1.2, the fact that the Delassus' matrix is full rank or positive semi-definite only[39] has a strong influence on the contact problem well-posedness. The condition $PB = C^T$, $P = P^T \succ 0$ also implies in case B has full column rank that the matrix $CB \succ 0$ and the system has uniform relative degree $r = 1$.

Remark 5.21 The reinitialization rule chosen in [517] reduces in the case of linear mechanical systems to Moreau's sweeping process inelastic frictionless shocks. It is also pointed out in [517] that well-posedness may be difficult to prove with other *ad hoc* rules as in [1063], which lack of physical foundations. State jumps in LCS involve solutions which may be measures or Schwarz' distributions. It is noteworthy that a general class of LCS has been embedded into an extension of Moreau's sweeping process named *higher order sweeping process*, but which should better be named *higher relative degree sweeping process* [15]. Describing such *Distribution*

[37] For two smooth vector fields $f(x)$ and $g(x)$, one has $L_f g(x) = \frac{\partial g}{\partial x} f(x)$, and recursively for $L_f^i g(x) = \frac{\partial g(x)}{\partial x} L_f^{i-1} g(x)$, with $L_f^0 g(x) = f(x)$.

[38] With only perfectly rigid contacts, since the presence of unilateral springs may change the conclusion, see Example 5.14.

[39] Recall that the Delassus' matrix is symmetric; hence, if it is not positive definite it cannot be full rank.

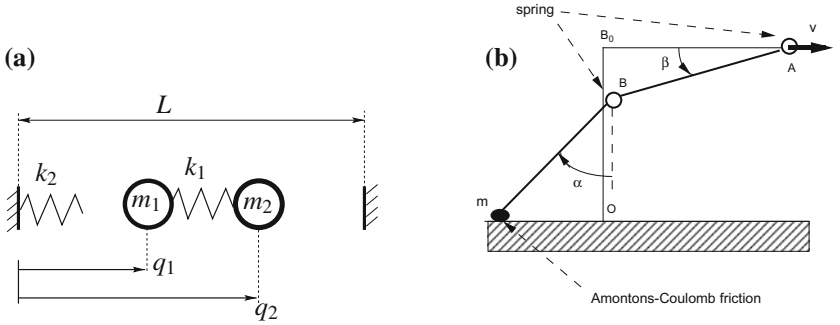

Fig. 5.14 Complementarity mechanical systems. **a** Mixed rigid/compliant contacts. **b** Rigid contacts and friction

Differential Inclusion is outside the scope of this book. We just mention that the functional framework of [15] contains that in [517], and that the basic idea consists of extending Moreau's set in (5.43) to take into account that higher degree derivatives may jump. Well-posedness analysis and a time-stepping discretization are presented in [15]. This framework allows to give a meaning to a problem like $\dot{x}_1(t) = x_2(t)$, $\dot{x}_2(t) = x_3(t)$, $\dot{x}_3(t) = u(t) + \lambda(t)$, $x_1(t) \geq 0$ for all $t \geq 0$.

5.4.4.2 Examples from Mechanics, Electricity, and Optimal Control

Let us illustrate LCS with examples from Mechanics, Circuits and Optimal Control with state constraints.

Example 5.13 (A mechanical complementarity system) Let us consider the example depicted in Fig. 5.14b, analyzed in [371]. It is assumed that the whole mass m is concentrated at the end-point. Also, the system at rest takes the configuration AB_0O. Two torsional springs act at the joints A and B. The length of the bar OB is l_1, and that of the bar AB is l_2. The point A is assumed to have a horizontal motion, with velocity $v(t)$. The goal is therefore to study the motion of this two-degree-of-freedom system, in particular, investigate whether the contact will persist or break. The free-motion dynamics is given by (the time argument is dropped):

$$\begin{cases} ml_1l_2\sin(\beta-\alpha)\ddot{\beta} + ml_1^2\ddot{\alpha} + ml_1l_2\cos(\beta-\alpha)\dot{\beta}^2 + k(\alpha-\beta) + mgl_1\sin(\alpha) \\ \quad = \lambda_t l_1\cos(\alpha) + \lambda_n l_1\sin(\alpha) \\ \\ ml_1l_2\sin(\beta-\alpha)\ddot{\alpha} + ml_2^2\ddot{\beta} - ml_1l_2\cos(\beta-\alpha)\dot{\alpha}^2 + k(2\beta-\alpha) - mgl_2\cos(\beta) \\ \quad = \lambda_t l_2\sin(\beta) - \lambda_n l_2\cos(\beta), \end{cases} \tag{5.120}$$

where λ_t and λ_n are the tangential and normal components of the contact force. It is more convenient to write down those equations in the coordinates of the contact

point (q_1, q_2), where q_1 is the abscissa and q_2 along the normal to the rough rigid ground. One has $q_1 = l_2 - l_2\cos(\beta) + l_1\sin(\alpha)$ and $q_2 = l_1 - l_2\sin(\beta) - l_1\cos(\alpha)$. Linearizing (5.120) around $(\alpha, \beta) = (0, 0)$ and introducing the coordinate change one gets:

$$\begin{cases} ml_1\ddot{q}_1(t) + k\left(\frac{q_1(t)}{l_1} + \frac{q_2(t)}{l_2}\right) = l_1 F_{\mathrm{t}}(t) \\ ml_2\ddot{q}_2(t) + k\left(\frac{q_1(t)}{l_1} + \frac{2q_2(t)}{l_2}\right) = l_2 F_{\mathrm{n}}(t) \\ \\ 0 \le f(q(t)) = q_2(t) \perp F_{\mathrm{n}}(t) \ge 0 \\ \\ F_{\mathrm{t}}(t) \in -\mu F_{\mathrm{n}}(t)\ \mathrm{sgn}(\dot{q}_1(t)), \quad \mu > 0. \end{cases} \tag{5.121}$$

The dynamics in (5.121) fits within the framework in (5.1). If friction is for the moment disregarded (just take $\mu = 0$), it is also an LCS as (5.119). The "$\in$" is important for F_{t} because the sign function is multivalued at $q_1 = 0$: $\mathrm{sgn}(0) = [-1, 1]$. We can also write the Coulomb friction model in a complementarity formalism [13, 249, 671, 1064]. Indeed, using (B.16) the following holds: $x \in -\mathrm{sgn}(y) \Leftrightarrow y \in -N_{[-1,1]}(x)$, and these two inclusions are in turn equivalent to:

$$\begin{cases} x = \frac{\lambda_1 - \lambda_2}{2}, \quad \lambda_1 + \lambda_2 = 2 \\ 0 \le \lambda_1 \perp y + |y| \ge 0 \\ 0 \le \lambda_2 \perp -y + |y| \ge 0 \end{cases} \Leftrightarrow \begin{cases} y = \lambda_1 - \lambda_2 \\ u_1 = 1 + x, \ u_2 = 1 - x \\ 0 \le u_1 \perp \lambda_1 \ge 0 \\ 0 \le u_2 \perp \lambda_2 \ge 0. \end{cases} \tag{5.122}$$

The two formalisms in (5.122) are the inverse of one each other. Let us check this by inspection. Let $y > 0$, then $\lambda_1 = 0$, so $\lambda_2 = 2$, and $x = -1$. Let $y < 0$, then $\lambda_2 = 0$, so $\lambda_1 = 2$, and $x = 1$. Now let $y = 0$, then $\lambda_1 = 2 - \lambda_2$ and $x = 1 - \lambda_2 \le 1$, also $\lambda_2 = 2 - \lambda_1$ and $x = \lambda_1 - 1 \ge -1$. Thus $x \in [-1, 1]$. The second equivalence is proved as follows: let $x = 1$, then $\lambda_1 = 0$ while $\lambda_2 \ge 0$, thus $y \le 0$. Let $x = -1$, then $\lambda_2 = 0$ while $\lambda_1 \ge 0$, thus $y \ge 0$. Let $x \in (-1, 1)$, then $u_1 > 0$, $u_2 > 0$, thus $\lambda_1 = \lambda_2 = y = 0$. In both cases, the complementarity relations allow one to recover the graph of the set-valued sign function. To express Coulomb's friction in a complementarity framework, one just has to set $x = \frac{F_{\mathrm{t}}}{\mu F_{\mathrm{n}}}$ and $y = \dot{q}_1$. The variables λ_1 and λ_2 in (5.122) are multipliers which are just some intermediate variables. It is noteworthy that using (B.16), one also has $x \in -\mathrm{sgn}(y) \Leftrightarrow x \in -\partial|y|$. However, F_{n} in (5.121) has no reason to be constant. Hence, there does not exist, in general, any convex, proper lower semi-continuous function $f(\cdot)$ such that $F_{\mathrm{t}} \in \partial f(\dot{q}_1)$: Coulomb's law coupled with normal conditions is usually nonassociated (see Sect. 5.3.3).

$\rightsquigarrow$ *Coulomb's friction in planar systems—2D friction—lends itself to a representation as linear complementarity conditions. However, in general mechanical systems with unilateral constraints and Coulomb's friction are not LCS.*

The dynamical Eq. (5.121) must be completed by a suitable impact rule. The one chosen in [371] is similar to Moreau's rule (see Sect. 5.6), i.e., an inelastic shock ($e_{\rm n} = 0$) together with Whittaker's rule for relating $p_{\rm t}$ and $p_{\rm n}$. It is shown in [371] that depending on the value of μ with respect to a critical value $\mu_c = \frac{l_1}{l_2}\left(\frac{mg^2 l_2^2}{kv^2-1}\right)$, the motion with $q_1(0) = 0$ and $\dot{q}_1(0) = -v$ starts with sticking, and then evolves in a sliding motion ($\mu < \mu_c$), and detaches ($\mu > \mu_c$). If $\mu = \mu_c$, then $\lambda_{\rm n}$ vanishes but the system grazes the constraint. Detachment conditions are given by the sign of the first nonzero derivative $q_2^{(i)}$, which is found to be $q_2^{(3)}$ when $\mu > \mu_c$, and $q_2^{(4)}$ when $\mu = \mu_c$. Numerical results tend to show that the case of elastic shocks yields a much more complex behavior (finite accumulation of impact times) than the plastic one. Let us notice in relationship with the discussions in Sect. 5.6 that there is no problem of unbounded $\lambda_{\rm n}$ in this system, when the system is in a sliding motion phase (recall however for the sake of comparisons with the slender rod problem analyzed in Sect. 5.6 that the mass is concentrated at the contact point and that the motion of A is constrained to be purely horizontal).

Example 5.14 (A mixed rigid/flexible contacts system) Consider the two degrees of freedom system in Fig. 5.14a. Its dynamics is given by

$$\left\{\begin{array}{l} m_1\ddot{q}_1(t) + k_1(q_1(t) - q_2(t) - l_1) = \lambda_1 \\ m_2\ddot{q}_2(t) + k_2(q_2(t) - q_1(t) + l_1) = \lambda_2 \\ \lambda_1(t) = \max(0, k_2(l_2 - q_1(t))) \;\Leftrightarrow\; 0 \le \lambda_1(t) \perp w_1 = \lambda_1(t) - k_2(l_2 - q_1(t)) \ge 0 \\ 0 \le \lambda_2(t) \perp w_2 = q_2(t) - L \ge 0, \end{array}\right. \tag{5.123}$$

where the bilateral spring with stiffness k_1 is at rest for $q_1(t) - q_2(t) = l_1$, the equivalence for the contact force due to the unilateral spring with stiffness k_2 comes from Sect. 2.1.1.2, i.e., the contact force switches to zero when $q_1 \le l_2$. It is easy to see that $w_1 = \lambda_1(t) - k_2(l_2 - q_1(t))$, while $\ddot{w}_2 = \ddot{q}_2 = \frac{\lambda_2}{m_2} - \frac{k_1}{m_2}(q_2 - q_1 + l_1)$. Thus this complementarity system has a vector relative degree between the "input" $\lambda = (\lambda_1\ \lambda_2)^T$ and the "output" $w = (w_1\ w_2)^T$ equal to $r = (0\ \ 2)^T$. The question which arises is whether or not mechanical systems with mixed rigid/unilateral spring contacts always possess a well-defined relative degree or not. For a specific choice of the generalized coordinates, one obtains the following dynamics (we drop the time argument and disregard impacts):

$$\left\{\begin{array}{l} M(q)\ddot{q} + F(q, \dot{q}, t) = \nabla h_1(q)\lambda_1 + \nabla h_2(q)\lambda_2 \\ \lambda_{1,i} = \max(0, k_i(l_i - q_i)) \;\Leftrightarrow\; 0 \le \lambda_{1,i} \perp w_{1,i} = \lambda_{1,i} - k_i(l_i - q_i) \ge 0,\ 1 \le i \le m_1 \\ 0 \le \lambda_2 \perp w_2 = h_2(q) \ge 0, \end{array}\right. \tag{5.124}$$

where we assumed that the first m_1 contacts are the flexible ones, and the last m_2 ones are the rigid contacts, while $m_1 + m_2 = m$. One calculates that:

$$\begin{pmatrix} w_1 \\ \ddot{w}_2 \end{pmatrix} = \underbrace{\begin{pmatrix} I_{m_1} & 0 \\ \nabla h_2(q)^T M(q)^{-1} \nabla h_1(q) & \nabla h_2(q)^T M(q)^{-1} \nabla h_2(q) \end{pmatrix}}_{\text{Decoupling } m \times m \text{ matrix } D_{12}(q)} \begin{pmatrix} \lambda_1 \\ \lambda_2 \end{pmatrix} + \underbrace{\begin{pmatrix} -K(l - \bar{q}_{m_1}) \\ -\nabla h_2(q)^T M(q)^{-1} F(q, \dot{q}, t) + \frac{d}{dt}(\nabla h_2(q)^T)\dot{q} \end{pmatrix}}_{\stackrel{\Delta}{=} w_{12}(q, \dot{q}, t)} \tag{5.125}$$

where $l = (l_1 \dots l_{m_1})^T$, $\bar{q}_{m_1} = (q_1 \dots . q_{m_1})^T$, $K =$diag(k_i). If the unilateral constraints are independent, the vector relative degree is well defined since the so-called decoupling matrix has full rank m. It is noteworthy that the couplings between the compliant and the rigid contacts play no role in the relative degree well-posedness which involves only rank conditions. However, they may play a role for the contact LCP well-posedness, since the contact LCP matrix is the decoupling matrix. Indeed, the contact LCP is given by:

$$0 \leq \lambda \perp D_{12}(q)\lambda + w_{12}(q, \dot{q}, t) \geq 0. \tag{5.126}$$

We may apply Theorems 5.4, 5.6, and 5.7 to study this contact LCP. It is required that $D_{12}(q)$ be a P-matrix for this LCP to possess a unique solution for any value of $w_{12}(q, \dot{q}, t)$.

Proposition 5.20 *The matrix $D_{12}(q)$ is a P-matrix if and only if the Delassus' matrix $\nabla h_2(q)^T M(q)^{-1} \nabla h_2(q) \succ 0$ (equivalently the constraint functions $h_{2,i}(q)$ are functionally independent).*

Proof The multiplier λ_1 is uniquely determined whatever $-K(l - \bar{q}_{m_1})$. Inserting its value in the second line of the contact LCP, one finds that the multiplier λ_2 is uniquely determined whatever $w_{12}(q, \dot{q}, t)$ if and only if $\nabla h_2(q)^T M(q)^{-1} \nabla h_2(q)$ is a P-matrix, *i.e.,* it is positive definite. The result follows from Theorem 5.4.

Example 5.15 (A first complementarity circuit) The so-called *ideal diodes* possess a voltage/current characteristic that translate a physical observation: when the current through the diode is positive, the voltage is zero. When the voltage is positive, the current is zero. Equivalently, the voltage λ across the diode and the current i through the diode satisfy the complementarity constraint $0 \leq i \perp \lambda \geq 0$. Electrical networks with ideal diodes fit within the class of dynamical systems with unilateral constraints and complementarity conditions, see [10,13,22,226,252,378,720,1063,1064,1227]. Let us consider the circuit with ideal diodes, resistance R, inductance L, and an capacitance C in Fig. 5.15. Its dynamics is given by:

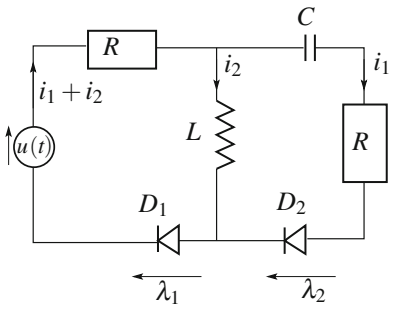

Fig. 5.15 A circuit with two ideal diodes and a voltage source

$$\begin{cases} \dot{x}_1(t) = \frac{-R}{2L}x_1(t) - \frac{1}{2LC}x_2(t) + \frac{1}{2L}u(t) + \frac{1}{2L}(\lambda_1(t) - \lambda_2(t)) \\ \dot{x}_2(t) = -\frac{1}{2}x_1(t) - \frac{1}{2RC}x_2(t) + \frac{1}{2R}u(t) + \frac{1}{2R}(\lambda_1(t) + \lambda_2(t)) \\ \\ 0 \le \lambda_1(t) \perp w_1 = \frac{1}{2}x_1(t) - \frac{1}{2RC}x_2(t) + \frac{1}{2R}u(t) + \frac{1}{2R}(\lambda_1(t) + \lambda_2(t)) \ge 0 \\ 0 \le \lambda_2(t) \perp w_2 = -\frac{1}{2}x_1(t) - \frac{1}{2RC}x_2(t) + \frac{1}{2R}u(t) + \frac{1}{2R}(\lambda_1(t) + \lambda_2(t)) \ge 0 \end{cases} \tag{5.127}$$

where $x_1(t) = i_2(t)$, $x_2(t) = \int_0^t i_1(s)ds$. The two complementarity conditions represent the set-valued current–voltage laws of the diodes. This fits within nonautonomous LCS (one adds exogenous terms in (5.119)):

$$\begin{aligned} &\dot{x}(t) = Ax(t) + B\lambda(t) + Eu(t) \\ &0 \le \lambda(t) \perp w(x(t), \lambda(t), u(t)) = Cx(t) + D\lambda(t) + Fu(t) \ge 0 \end{aligned} \tag{5.128}$$

where $D = \begin{pmatrix} \frac{1}{2R} & \frac{1}{2R} \\ \frac{1}{2R} & \frac{1}{2R} \end{pmatrix}$ is positive semi-definite, $B = \begin{pmatrix} \frac{1}{2L} & -\frac{1}{2L} \\ \frac{1}{2R} & \frac{1}{2R} \end{pmatrix}$, $C = \begin{pmatrix} \frac{1}{2} & \frac{-1}{2RC} \\ \frac{-1}{2} & \frac{-1}{2RC} \end{pmatrix}$. The LCS in (5.128) can be recast into set-valued Lur'e systems with a static feedback nonlinearity of the form $-\lambda(t) \in \partial\psi_{\mathbb{R}^+_m}(w(x(t), \lambda(t), u(t)))$. We shall see later how this static nonlinearity may be further expressed depending on D, see (5.135), (5.140) and (5.146).

Example 5.16 (A second complementarity circuit) The first circuit has a matrix $D \succeq 0$. Let us give an example of a circuit with $D = 0$. Consider the circuit in Fig. 5.16a. Let x_1 be the charge of the capacitor, so that $\dot{x}_1 = x_2 = i$. Its dynamics is

$$\begin{cases} \dot{x}_1(t) = x_2(t) \\ \dot{x}_2(t) = \frac{-1}{LC}x_1(t) - \frac{R}{L}x_2(t) - \frac{1}{L}\lambda(t) + \frac{1}{L}u(t) \\ 0 \le w(x(t)) = -x_2(t) \perp \lambda(t) \ge 0. \end{cases} \tag{5.129}$$

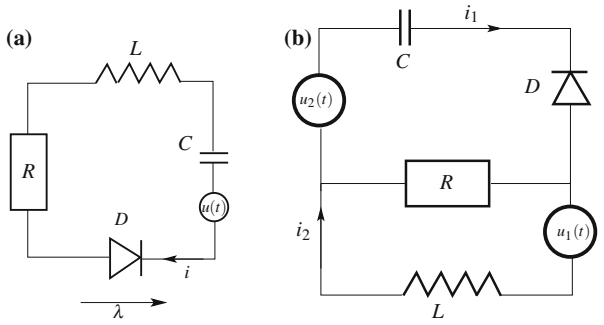

Fig. 5.16 Circuits with an ideal diode and voltage sources

One also has $F = 0$, i.e., the exogenous excitation does not enter the complementarity conditions.

Example 5.17 (A third complementarity circuit) Let us give an example of a circuit with $D \succ 0$. Consider the circuit in Fig. 5.16b. The charge of the capacitor is $\dot{x}_1 = i_1$, and we let $x_2 = i_2$. The dynamics is given by:

$$\begin{cases} \dot{x}_1(t) = \frac{-1}{RC}x_1(t) + x_2(t) - \frac{1}{R}\lambda(t) + \frac{1}{R}(u_2(t) - u_1(t)) \\ \dot{x}_2(t) = \frac{-1}{LC}x_1(t) - \frac{1}{L}\lambda(t) + \frac{1}{L}u_2(t) \\ 0 \leq w(x(t), \lambda(t), t) = \frac{1}{RC}x_1(t) - x_2(t) + \frac{1}{R}\lambda(t) - \frac{1}{R}(u_2(t) - u_1(t)) \perp \lambda(t) \geq 0. \end{cases} \tag{5.130}$$

In (5.130) one has $D \succ 0$, $E \neq 0$, $F \neq 0$.

There are some major discrepancies between these three circuits: (i) the relative degree between λ and w is equal to zero in (5.130), to one in (5.129); the relative degree "à la Isidori" of the bivariable system in (5.127) is not well defined since $D \succeq 0$; however, one may speak of the index of its transfer function $H(s) = C(sI - A)^{-1}B + D, s \in \mathbb{C}$. (ii) The exogenous excitation $u(t)$ does not appear in the complementarity conditions in (5.129), and appears in (5.127) and (5.130). Together with (2.5) and (2.14), the above three circuits show that LCS may embed several classes of mechanical and electrical systems. More on embedding power converters with ideal diodes and switches into complementarity systems can be found in [1088]. Most importantly, the LCS formalism allows one to get rid of the a priori knowledge of the system's sequence of modes and of the switching time instants, both for the analysis (existence of solutions, stability), and for the numerical simulation (see Sect. 5.7.3.5). It is noteworthy that including some feedback law in the model, usually destroys the dissipativity of the overall LCS (see for instance the buck DC–DC converter in [1088, Eq. (48a)–(48h)] that has a nondefinite D matrix).

Example 5.18 (A fourth complementarity circuit) We now deal with ideal Zener diodes and we will generalize (5.122). The ideal Zener diodes of the circuit in Fig. 5.17 (a) have the voltage–current characteristic depicted in Fig. 5.17 (b). This

may be expressed as $i_i(t) \in N_{[-V_i,U_i]}(v_i(t))$, or its inverse $v_i(t) \in \partial\psi^\star_{[-V_i,U_i]}(i_i(t))$, where $\psi^\star_{[-V_i,U_i]}(i_i) = U_i i_i$ if $i_i \geq 0$, $-V_i i_i$ if $i_i \leq 0$ (see Appendix B, Definition B.11 and after). Let us derive the characteristic (v, i) of the two Zener diodes in series. We have $v = v_1 - v_2$, and $i = i_1 = -i_2$. Also, we assume that $U_1 < V_1, U_2 < V_2$ (U_i are leakage voltages, much smaller in practice than the breakdown voltages V_i). Thus $v \in \partial\psi^\star_{[-V_1,U_1]}(i) - \partial\psi^\star_{[-V_2,U_2]}(-i)$. Let us set $f(i) = \partial\psi^\star_{[-V_2,U_2]}(-i)$, then from Theorem B.2 we get $\partial f(i) = -\partial\psi^\star_{[-V_2,U_2]}(-i)$. Therefore, using [1045, Theorem23.8] for the sum of subdifferentials, and defining $g(i) = \psi^\star_{[-V_1,U_1]}(i) + f(i)$ we obtain $v(t) \in \partial g(i(t))$ or equivalently $i(t) \in \partial g^\star(v(t))$, where $g^\star(v) = \psi_{[-V_1-U_2,U_1+V_2]}(v)$ and $\partial g^\star(v) = N_{[-V_1-U_2,U_1+V_2]}(v)$. The graph of the set-valued mapping $i \mapsto v$ is depicted in Fig. 5.17 (c) (it is a relay multifunction). Complementarity formalisms which extend (5.122) of the two mappings $i \mapsto v$ and $v \mapsto i$ are given by:

$$\left\{\begin{array}{l} i = -\lambda_1 + \lambda_2 \\ 0 \leq \lambda_1 \perp v + V_1 + U_2 \geq 0 \\ 0 \leq \lambda_2 \perp U_1 + V_2 - v \geq 0 \end{array}\right. \iff \left\{\begin{array}{l} v = \frac{-V_1-U_2}{\gamma}\lambda_1 + \frac{U_1+V_2}{\gamma}\lambda_2 \\ \lambda_1 + \lambda_2 = \gamma, \quad \gamma > 0 \\ 0 \leq i + |i| \perp \lambda_1 \geq 0 \\ 0 \leq |i| - i \perp \lambda_2 \geq 0. \end{array}\right. \tag{5.131}$$

It is noteworthy that the formalism in the left-hand side of (5.131) can be obtained directly from the expression of the normal cone to the convex set $[-V_1 - U_2, U_1 + V_2)]$ using (B.8). We have $L > 0$, $R > 0$, $C > 0$, and $u(t)$ a voltage source. The circuit dynamics is given by the differential inclusion

$$L\frac{di}{dt}(t) + Ri(t) + \frac{1}{C}\int_0^t i(s)ds + u(t) \in -\partial g(i(t)), \quad i(0) = i_0, \tag{5.132}$$

where $i \mapsto v \in \partial g(i)$ is maximal monotone from Lemma B.1. This may be recast into Lur'e set-valued systems as in Fig. 2.2, with a different static multivalued nonlinearity in the feedback loop. This is quite a similar dynamics as a particle acted upon by dry friction, viscous friction, and linear spring. Letting $x_1(t) = \int_0^t i(s)ds$ be the charge of the capacitor, equilibria of this dynamics are solutions of the generalized equation $\frac{1}{C}x_1^* \in -\partial g(0) = [-U_1 - V_2, U_2 + V_1]$. The voltage $v(t)$ across the two-diode assembly is a selection of the set-valued right-hand side. The well-posedness of such a set-valued circuit may be analyzed from several points of view : complementarity systems if $u(t) = 0$ [745, 759] with piecewise-analytic solutions, differential inclusions with Theorem B.4 (let $x_2(t) = i(t)$, the right-hand side of the circuit dynamics can be written as in (B.24) defining $a(x_1, x_2) = \psi_{\mathbb{R}}(x_1) + g(x_2)$, hence $A(x_1, x_2) = \partial a(x_1, x_2) = \begin{pmatrix} \partial\psi_{\mathbb{R}}(x_1) = \{0\} \\ \partial g(x_2) \end{pmatrix}$), or using Filippov's framework. It is noteworthy that the finite accumulation of events (switching times) is permitted by all these models and mathematical frameworks.

Example 5.19 (A fifth set-valued circuit) Let us continue with Zener diodes. Consider the circuit in Fig. 5.17 (a), with $R = 0$ and $C = \infty$. Its dynamics reads $L\frac{di}{dt}(t) + u(t) \in -\partial g(i(t))$. We now design two circuits $L_i\frac{di_i}{dt}(t) + u_i(t) \in -\partial g_i(i(t))$,

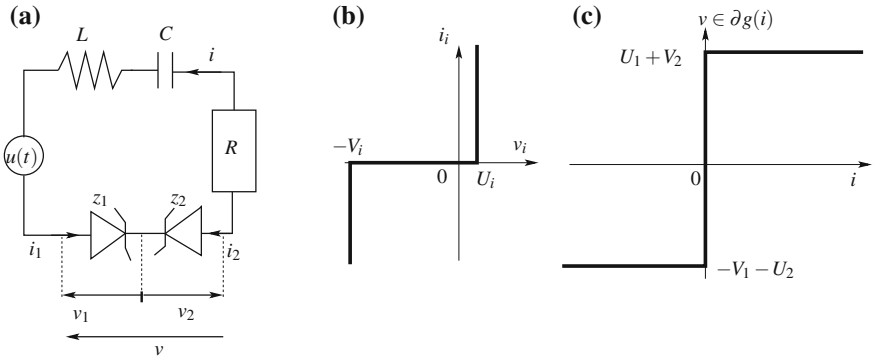

Fig. 5.17 A circuit with two ideal Zener diodes in series (relay multifunction)

$i = 1, 2$, and we set $u_1(t) = -\alpha_1 \bar{v}_2(t)$, $u_2(t) = -\alpha_2 \bar{v}_1(t)$, where $\bar{v}_i = v_{i,1} - v_{i,2}$ is the voltage across the Zener diode assembly of circuit i (i.e., in Fig. 5.17 (a): $\bar{v}$ is v). We therefore obtain the closed-loop dynamics:

$$\begin{cases} L_1 \frac{di_1}{dt}(t) = -\bar{v}_1(t) + \alpha_1 \bar{v}_2(t) \\ L_2 \frac{di_2}{dt}(t) = -\bar{v}_2(t) + \alpha_2 \bar{v}_1(t) \\ \bar{v}_1(t) \in \partial g_1(i_1(t)), \quad \bar{v}_2(t) \in \partial g_2(i_2(t)). \end{cases} \tag{5.133}$$

The dynamics in (5.133) is written compactly as $\dot{x}(t) \in -A\bar{v}(t)$, $\bar{v}(t) \in \partial g(x(t))$, $A = \begin{pmatrix} \frac{1}{L_1} & -\frac{\alpha_1}{L_1} \\ -\frac{\alpha_2}{L_2} & \frac{1}{L_2} \end{pmatrix}$, $g(x) = g_1(x_1) + g_2(x_2)$, $x = (i_1\ i_2)^T$, and can be recast into Lur'e set-valued systems. Depending on the feedback gains α_1 and α_2 such a circuit may possess quite different properties. If $L_1 = L_2 = 1$, $g_1(\cdot) = g_2(\cdot) = \mathrm{sgn}(\cdot)$, $\alpha_1 = 2, \alpha_2 = -2$, the origin $i_1 = i_2 = 0$ is globally finite-time Lyapunov stable and is reached after a finite accumulation of switching times, where trajectories spiral around the origin [397]. The mapping $x \mapsto A\partial g(x)$ may be maximal monotone (if $A = I_2$) but monotonicity is not preserved in general so Theorem B.4 does not apply. However, Filippov's framework for existence of solutions applies. Further applications of the complementarity, differential inclusion, and variational inequality formalisms for more complex circuits may be found in [9, 10, 24, 251, 348, 1227]. The so-called compartmental approach, which consists in splitting a circuit into several blocks, is used in [24] and uses the variational inequality tools of [23] to analyze the well-posedness of equilibria equations. Other circuits with set-valued dynamics are analyzed in [10] and [453], where it is shown that DC–DC buck converters can be cast into linear complementarity Lagrangian systems whose mass matrix is the matrix of inductors [453, Eqs. (32) (33)]. The classical mechanical/electrical analogies mass/inductivity, damping/resistance, and stiffness/capacity are extended to nonsmooth elements sparg clutch/diode and dry friction/spark gaps in [453, Table II].

Example 5.20 (Optimal control with state inequality constraints) The first-order necessary conditions in (3.70) are an LCS (more exactly this is a boundary value LCS). Its feature is that the relative degree between the two complementary variables may be large.

Lemma 5.4 *[208] Consider the optimal control problem in (3.68) and (3.69), with $m = 1$. If $r^{wu} = 1$, then the leading Markov parameter of the triple $(\tilde{A}, \tilde{B}, \tilde{C})$ is $M^{(2)} = -CBB^TC^T < 0$. More generally, if the transfer function of the triple (A, B, C) in (3.69) has a relative degree $r^{wu} \geq 2$, the leading Markov parameter of the triple $(\tilde{A}, \tilde{B}, \tilde{C})$ is $M^{(2r^{wu})} = (-1)^{r^{wu}} CA^{r^{wu}-1}B(CA^{r^{wu}-1}B)^T$ $(= \tilde{C}\tilde{A}^{r-1}\tilde{B})$.*

The fact that the relative degree of the LCS in (3.70) may be ≥ 3 implies that solutions may be distributions of higher degree (derivatives of the Dirac measure). The objective of the analysis in [208] is to take this fact into account by embedding (3.70) into the so-called higher order sweeping process [15], which is a *Distribution Differential Inclusion* (a generalization of measure differential inclusions). The geometrical tools of [322, 323] (see Sect. 1.3.3) are used for a qualitative analysis of junction states and controllers. The link with Mechanics is made in [208]. See also [204, 512] for a survey on LCS.

5.4.4.3 Well-Posedness

A well-posedness analysis is proposed in Sect. 2.1.3.2, which consists of interpreting the LCS as a differential inclusion. Let us present its general version, which bridges the gap between LCS and Moreau's sweeping process. Here we consider the LCS in (5.128). The Lyapunov stability is treated in Sect. 7.7.

Assumption 5.2 The feedthrough matrix $D = 0$, and there exists $P = P^T \succ 0$ such that $PB = C^T$.

This "input/output" constraint is satisfied for dissipative systems for which $D + D^T = 0$, see [218]. It implies that $B^TPB = B^TC^T = (CB)^T$, thus CB is at least positive semi-definite, and positive definite if B has full column rank.[40] In control, the input matrix B is usually considered full column rank to avoid redundant inputs. In nonsmooth set-valued circuits λ is not a real input, and has no reason to have dimension smaller that the state. Thus B is in general not full column rank. The constraint of Assumption 5.2 is therefore a kind of relative degree constraint. Defining R as $R^2 = P$, the symmetric positive definite square root of P, and letting $z = Rx$, one gets from (5.128):

[40] Clearly, Assumption 5.2 implies CB is symmetric and $\succeq 0$. Theorem 2.2 in [547] states necessary and sufficient conditions such that $B^TPB = D$ has a symmetric $\succeq 0$ or $\succ 0$ solution P. Lemma 1 in [258] states that $P = C^T(CB)^\dagger + (I_n - (B^T)^\dagger B^T)U(I_n - (B^T)^\dagger B^T)^T$, with $U = U^T \succeq 0$ arbitrary, and $\dagger$ denotes the generalized inverse.

$$\begin{cases} \dot{z}(t) = R\dot{x}(t) = RAR^{-1}z(t) + REu(t) + RB\lambda(t) \\ 0 \leq \lambda(t) \perp w(z(t), t) = CR^{-1}z(t) + Fu(t) \geq 0. \end{cases} \tag{5.134}$$

Let us assume for the moment that both $\lambda(\cdot)$ and $w(\cdot)$ are functions of time. From (B.21) and (B.7) one may write

$$0 \leq \lambda(t) \perp CR^{-1}z(t) + Fu(t) \geq 0 \Leftrightarrow -\lambda(t) \in \partial\psi_Q(CR^{-1}z(t) + Fu(t)) \tag{5.135}$$

for $Q = \mathbb{R}^m_+$, where $\psi_Q(\cdot)$ denotes the indicator function of the set Q. Consequently, one equivalently rewrites (5.134) as

$$-\dot{z}(t) \in -RAR^{-1}z(t) - REu(t) + RB\ \partial\psi_{\mathbb{R}^m_+}(CR^{-1}z(t) + Fu(t)).$$

The equivalence means here that the two formalisms are strictly the same way of writing a mathematical object like a complementarity problem between two variables, without further consideration on the solutions. Now using $R^2B = C^T$ it follows that

$$-\dot{z}(t) \in -RAR^{-1}z(t) - REu(t) + R^{-1}C^T\ \partial\psi_{\mathbb{R}^m_+}(CR^{-1}z(t) + Fu(t)). \tag{5.136}$$

For each $t \in [0, +\infty[$ the closed set

$$K(t) \stackrel{\Delta}{=} \{x \in \mathbb{R}^n \mid Cx + Fu(t) \geq 0\} \tag{5.137}$$

and $\mathbb{R}^m_+$ are convex polyhedral, and $\psi_{K(t)}(x) = (\psi_{\mathbb{R}^m_+ - Fu(t)} \circ C)(x)$. Therefore, from Theorem B.2, we have

$$C^T\ \partial\psi_{\mathbb{R}^m_+}(Cx + Fu(t)) = \partial\psi_{K(t)}(x),$$

for any $x \in \mathbb{R}^n$. So the inclusion in (5.136) is equivalent to the differential inclusion

$$-\dot{z}(t) + RAR^{-1}z(t) + REu(t) \in R^{-1}\partial\psi_{K(t)}(R^{-1}z(t)). \tag{5.138}$$

Considering the closed convex polyhedral set

$$S(t) \stackrel{\Delta}{=} R(K(t)) = \{Rx \mid x \in K(t)\}, \tag{5.139}$$

it is easy to see that $\psi_{S(t)}(x) = (\psi_{K(t)} \circ R^{-1})(x)$ for all $x \in \mathbb{R}^n$. Since R is invertible and symmetric we have

$$\partial\psi_{S(t)}(x) = R^{-1}(\partial\psi_{K(t)})(R^{-1}x) \quad \text{for all} \quad x \in \mathbb{R}^n,$$

and hence, since $N_{S(t)}(x) = \partial\psi_{S(t)}(x)$ (see (B.7)), the differential inclusion (5.138) may be written in the form

$$-\dot{z}(t) + RAR^{-1}z(t) + REu(t) \in N_{S(t)}(z(t)). \tag{5.140}$$

The inclusion (5.140), which takes the form of a first-order perturbed Moreau's sweeping process, is in turn equivalent to the evolution variational inequality

$$\langle \dot{z}(t) - RAR^{-1}z(t) - REu(t), v - z(t)\rangle \geq 0, \quad \text{for all } v \in S(t), \ \textit{with } z(t) \in S(t).$$

Proposition 5.21 *[226] Assume that the set-valued mapping $K(\cdot)$ is nonempty-valued, i.e., all the sets $S(t)$ are nonempty (which holds in particular whenever the constraint qualification*

$$\mathrm{Rge}\,(C) - \mathbb{R}^m_+ = \mathbb{R}^m \tag{5.141}$$

is fulfilled[41]*). If the component mapping $Fu(\cdot)$ has a local bounded variation (resp. is locally absolutely continuous) on $[0, +\infty[$ (which obviously holds whenever so is the mapping $u(\cdot)$), then the closed convex set-valued mapping $S(\cdot)$ has a local bounded variation (resp. is locally absolutely continuous) too.*[42] *In the same way, $S(\cdot)$ is right-continuous with respect to the Hausdorff distance whenever $Fu(\cdot)$ is right-continuous.*

Theorem 5.11 *[226] Assume that $u(\cdot) \in \mathrm{L}^1_{\mathrm{loc}}([0, +\infty[, dt; \mathbb{R}^p)$, and that the set-valued mapping $S(\cdot) = R(K(\cdot))$ is locally absolutely continuous (resp. locally* RCBV*) with nonempty values. Then the perturbed differential inclusion (5.140) with initial condition $z(0) = z_0 \in R(K(0))$ has one and only one locally absolutely continuous (resp. locally* RCBV*) solution $z(\cdot)$ on $[0, +\infty[$.*

Obviously, the theorem applies equivalently to the LCS in (5.128) with Assumption 5.2. It is noteworthy that we never introduced the initial conditions in the above dynamical systems. The initial state is constrained to be in the initial set in Theorem 5.11. Thus if the set $S(t)$ is locally absolutely continuous, the theorem stipulates that the solutions have no discontinuity. In other words, there is always a element of the normal cone in the right-hand side of (5.140), that is, a function of time, and such that the system can be integrated while always respecting the unilateral constraint (i.e., the state remains in the admissible domain, equivalently $w(z(t), t)$ remains nonnegative). If the initial condition satisfies $z(0^-) \notin R(K(0))$, then an initial jump has to be imposed on z such that $z(0^+) \in R(K(0))$.[43] Consequently, in the locally absolutely continuous case, there is at most one initial jump. At the initial time, the multiplier λ has to be a distribution (a Dirac measure, or a distribution of higher degree). In case of bounded variation, solutions may jump and the dynamics has to be interpreted as a measure differential inclusion, similarly as in Problem 5.1 and (5.52). This is more

[41] The equality in (5.141) means that for all $x \in \mathbb{R}^m$, there exists $y \in \mathrm{Rge}\,(C)$ and $z \in \mathbb{R}^m_+$ such that $z - y = x$. Obviously, it holds whenever the linear mapping associated with C is onto, i.e.,, the matrix C has rank m, but also in many other cases. It is noteworthy that due to Assumption 5.2, the rank of C and the rank of B are not independent quantities.

[42] See Sect. A.3.1 for definitions.

[43] We do not discuss here about the physical realization of such a jump.

involved and we are not going to provide all mathematical details about it. The only thing we may say is that the differential inclusion in (5.140) has to be rewritten as a measure differential inclusion, using the notion of the *differential measure* dz, that is, a generalized derivative associated with right-continuous functions of local bounded variation (see Appendix A.3.2). We already encountered a differential measure in Sect. 5.2.2.4, with the acceleration du. It satisfies:

$$z(t) = z(s) + \int_{]s,t]} dz \quad \text{for all } s, t \in I \text{ with } s \leq t. \tag{5.142}$$

This is a generalization of the fundamental result for absolutely continuous functions with an almost-everywhere derivative (like in (5.38)): the almost-everywhere derivative is replaced with dz. The differential inclusion in (5.140) may be interpreted as the measure differential inclusion:

$$\begin{cases} -dz \in N_{S(t)}(z(t)) + f(t, z(t))\, dt \\ z(0) = z_0 \in S(0), \end{cases} \tag{5.143}$$

where $f(t, y) \stackrel{\Delta}{=} -RAR^{-1}y - REu(t)$ for all $y \in \mathbb{R}^n$. The jump rule may be deduced from (5.143) by noting that state jumps correspond to atoms of the measure dz, so that (5.143) may be rewritten at such atoms as

$$-z(t^+) + z(t^-) \in N_{S(t^+)}(z(t^+)), \tag{5.144}$$

that is equivalent, provided $S(t)$ is a nonempty convex set, to

$$\begin{aligned} & z(t^+) = \text{proj}\,[S(t^+); z(t^-)] \quad \Leftrightarrow \quad z(t^+) = \text{argmin}_{z \in S(t^+)} \tfrac{1}{2}||z - z(t^-)||^2 \\ \Leftrightarrow \quad & x(t^+) = \text{argmin}_{x \in K(t^+)} \tfrac{1}{2}(x - x(t^-))^T P (x - x(t^-)) \\ \Leftrightarrow \quad & K(t^+) \ni x(t^+) \perp P(x(t^+) - x(t^-)) \in K^\star(t^+) \\ \Leftrightarrow \quad & P(x(t^+) - x(t^-)) \in -N_{K(t^+)}(x(t^+)), \end{aligned} \tag{5.145}$$

i.e., $z(t^+)$ $(= z(t))$ is the (unique) closest vector to $z(t^-)$ inside $S(t^+)$ (equivalently, the projection of $z(t^-)$ on $S(t^+)$ in the Euclidean metric). These equivalences may be deduced from (B.19) and (B.20), and remind that $K^\star$ is the dual cone of K. The third line in (5.145) is a cone complementarity problem. It is interesting to notice from (5.145) that the state jump is solved by minimizing an "energy" function defined from the matrix P. In case of a dissipative system, P defines the so-called storage function [218]. One may parallel (5.145) with Moreau's impact law, see for instance (5.64) and (5.53). It is clear that the same interpretation as a Lur'e set-valued system applies for these electrical circuits, as shown in Figs. 2.2 and 7.6.

Notice that in case $u(\cdot)$ is time-continuous, then $S(t^+) = S(t^-) = S(t)$ and $z(t^-) \in S(t)$. It follows from the above that $z(t^+) = z(t^-)$. A state jump may then occur only initially, in case $z(0^-) \notin S(0)$. This is in agreement with Theorem 5.11.

Further Results

The above state jump rule is the same as in Remark 5.2 in Sect. 5.2.1. Existence and uniqueness of solutions is one thing, how to calculate the multiplier $\lambda(t)$ is also of interest. Let us proceed as for the case of Mechanics in Proposition 5.3. To simplify the presentation we assume that the complementarity conditions in (5.134) collect only active constraints $w_i(x) = 0$, for which $\lambda_i(t) \geq 0$. The other multipliers satisfy $\lambda_j(t) = 0$. We also assume that all functions are right-continuous as well as $\dot{u}(\cdot)$. Then we obtain the LCP: $0 \leq \lambda(t) \perp \dot{w}(t) = CAR^{-1}z(t) + CEu(t) + F\dot{u}(t) + CB\lambda(t) \geq 0$, from which $\lambda(t)$ may be computed (at least numerically, see [13] for suitable algorithms). In view of the properties stated above, $CB \succeq 0$ or $CB \succ 0$. One may thus apply one of the results stated in Sect. 5.4.2 for the LCP well-posedness.

Consider the LCS in (5.128) with $D = D^T \succ 0$. Using (B.21), one finds that:

$$\lambda(t) = \mathrm{proj}_D[\mathbb{R}^m_+; -D^{-1}(Cx(t) + Fu(t))]. \tag{5.146}$$

The orthogonal projection is a Lipschitz continuous mapping. Hence, injecting (5.146) into (5.128), one obtains an ordinary differential equation with Lipschitz right-hand side: the well-posedness (existence and uniqueness of a continuously differentiable solution, or of an absolutely continuous solution if the input $u(\cdot)$ is just locally integrable) follows from classical results on ODEs. It is noteworthy that if D is a P-matrix, the same result holds since the multiplier is then a Lipschitz continuous function of the state, see Theorem 5.4 (however, one cannot write (5.146)). In both cases, we also obtain a so-called piecewise-linear system. The case $D \succeq 0$ is somewhat in-between $D \succ 0$ and $D = 0$. It is treated in [214, 215] under an "input-output" constraint $PB = C^T$ for some matrix $P = P^T \succ 0$, $F = 0$, and $D = \mathrm{diag}(D_1, 0)$, $D_1 \succ 0$, and in [252, 258] under a dissipativity condition of the quadruplet (A, B, C, D). The state jump rule in (5.145) is written in a broader context with $D \succeq 0$ in [251, 254, 411, 412, 513] [10, §2.4.3.2]. See also [1227]. A class of nonlinear complementarity systems is analyzed in [214]. LCS are extended to Lur'e set-valued systems in [214], noticing that (5.128) may be embedded into:

$$\begin{cases} \dot{x}(t) - Ax(t) - Eu(t) = B\lambda(t) \\ \\ \lambda(t) \in -(D \cdot + \partial\phi)^{-1}(Cx(t) + Fu(t)), \end{cases} \tag{5.147}$$

where $\phi(\cdot)$ is convex proper lower semi-continuous. In LCS we have $\phi(\cdot) = \psi_{\mathbb{R}^m_+}(\cdot)$. The analysis relies on properties of the operator $B(D \cdot + \partial\phi)^{-1}(C\cdot)$, and various cases are studied in [214, 215]. For instance, if $D \succeq 0$ (not necessarily symmetric),

$\phi(\cdot) = \psi_{\mathbb{R}^p_+}(\cdot)$, $\text{aff}(-D^T\mathbb{R}^p_+ + \text{Int}(\text{Im}(D + D^T) + \mathbb{R}^p_+)) = \text{aff}(\text{Im}(D + N_{\mathbb{R}^p_+}))$,[44] and Assumption 5.2 holds, then $B(D\cdot + \partial\phi)^{-1}(C\cdot)$ is maximal monotone [215, §6.1].

The results of [214, 215] are extended in [258] to general maximal monotone operators (instead of subdifferentials $\partial\phi(\cdot)$) and passive (A, B, C, D), whose matrices necessarily satisfy $\ker(D + D^T) \subseteq \ker(PB - C^T)$ [258, Proposition 3], which is an extension of the condition of Assumption 5.2. See also [1180] for the output regulation problem using such condition. It is noteworthy that (5.147) represents a rather large class of systems, since depending on the D matrix it may range from a nonlinear ODE to a differential inclusion with noncompact set-valued right-hand side.

A general result about the well-posedness of autonomous LCS (i.e., $u(t) \equiv 0$ in (5.128), which yields (5.119)) is stated in [256].

Proposition 5.22 *[256] Consider the LCS in (5.128) with zero input u, and initial condition $x(0) = x_0$. The following statements are equivalent:*

- *For every $x_0 \in \mathbb{R}^n$, the LCS has a unique continuously differentiable solution $x(\cdot, x_0)$ on $[0, +\infty)$.*
- *For every $x_0 \in \mathbb{R}^n$, the set B $SOL(Cx_0, D)$ is a singleton, where $SOL(Cx_0, D)$ denotes the set of solutions of the LCP $0 \le \lambda \perp w_0 = Cx_0 + D\lambda \ge 0$.*

Therefore, a test on the initial LCP is sufficient to infer the global well-posedness of the autonomous LCS. It is clear that if $D \succ 0$ or is a P-matrix, then the conditions of Proposition 5.22 hold. However, these properties may be relaxed if one takes B into account, see Proposition 5.19. Let us finally notice again that similar results as the ones obtained in Sect. 5.1.2 are obtained for passive LCS in [254]. In particular Proposition 5.6 becomes [254, Theorem7] for passive LCS. It says that if λ_1 and λ_2 are two multipliers associated with a solution of the LCS in (5.128), where (A, B, C, D) is a passive system with a positive definite storage function (i.e.,, the above P-matrix is positive definite), then $\lambda_1 - \lambda_2 \in \ker \begin{pmatrix} B \\ D + D^T \end{pmatrix}$. LCS as in (5.119) in an infinite-dimensional setting are studied in [491] as a particular case of differential variational inequalities. When particularized to finite dimension, it shows that approximations (A_n, B_n, C_n, D_n) of the system's matrices which converge to (A, B, C, D) as $n \to +\infty$ yield solutions $(x^n, \lambda^n) \to (x, \lambda)$ solutions of (5.119), provided that $D_n \succeq 0$ for all n. The infinite-dimensional case is also analyzed in [29]. Notice that $K(t)$ and $S(t)$ in (5.137) and (5.139) may be written as $K(u)$ and $S(u)$ where $u(\cdot)$ may be seen as a control input. One therefore obtains in (5.140) a set-valued right-hand side $N_{S(u)}(z(t))$. If u is a feedback $u(x)$, then we obtain a state-dependent sweeping process . If $E = 0$ the system may be controlled only via its moving set which may sweep the state (said otherwise, by the complementarity constraints). In Sect. 5.4.5 the presented LCS are controlled in different ways. As

[44] The set $\text{aff}(K)$ is the affine hull of the set K, i.e., the smallest affine set that contains K: $\text{aff}(K) = \{\sum_{i=1}^n \alpha_i x_i, x_i \in K, \sum_{i=1}^n \alpha_i = 1, \alpha_i \in \mathbb{R}, n \in \mathbb{N}\}$.

alluded to above (see Example 5.20), LCS with higher relative degree between the complementary variables have distributional solutions. This is closely linked with solutions of switching DAEs (see Sect. 1.3.4), excepted that the switching conditions and the state jump mappings are ruled by complementarity conditions in LCS. The well-posedness of higher relative degree LCS is analyzed in [15] and [517]. In [15] LCS are embedded in a generalization of Moreau's sweeping process (which is a distribution differential inclusion), and in [517] rational complementarity problems are used.

5.4.4.4 Zeno Behavior in LCS

In addition to knowing if the solutions are continuous, or of bounded variations (hence with possible discontinuities), it is interesting for control purpose and numerical integration to know if switches between different modes may occur often or not. The modes are defined in LCS with continuous solutions, by the activation/deactivation of the constraints $w_i(x, \lambda, u) = 0$. Intuitively, it is clear that the switching behavior of the LCS will depend on the properties of the complementarity problem $0 \leq \lambda(t) \perp w(x(t), \lambda, u(t)) = Cx(t) + D\lambda(t) + Fu(t) \geq 0$. The Zeno behavior refers to the existence of finite accumulations of events. Such a phenomenon has been known since quite a long time in Mechanics (the impacts accumulation in the bouncing ball of Sect. 7.2.1 is a classical undergraduate exercise). For piecewise-linear systems and LCS, its study is more recent [257, 501, 962, 1102].

Theorem 5.12 *[1102] Consider the LCS in (5.128), with $u(t) \equiv 0$. Assume that D is a P-matrix. Then all the states of (5.128) are strongly non-Zeno.*

As we know, when D is a P-matrix the complementarity conditions in (5.128) make a well-posed LCP whose solution λ is a Lipschitz continuous function of x (see Theorem 5.105). Consider a solution $(x(t), \lambda(t))$ of the LCS, with $x(t_\star) = x_\star$. The state $x_\star$ is said strongly non-Zeno relative to $(x(t), \lambda(t))$ if the system stays in the same mode for all $t \in [t_\star - \varepsilon, t_\star + \varepsilon]$. The modes are defined as the index sets such that $\lambda_i(t) > 0$ and $w_i(t) = 0$, $\lambda_i(t) = 0$ and $w_i(t) > 0$, $\lambda_i(t) = w_i(t) = 0$.

5.4.4.5 Dissipativity of LCS: Generalized Supply Rate

The supply rate of the LCS is the product $\langle w, \lambda \rangle = w^T \lambda$. Suppose that $w = Cx$, and that a jump occurs at time t. Then in the framework of MDIs, λ is a Dirac measure and the product $x^T C^T \lambda$ is not well defined (a similar issue has been met in impulsive ODEs in Sect. 1.2.2). It is, however, possible to give a meaning to the integral term $\int w^T \lambda$ by constructing a measure from a functional [226]. More precisely let $\lambda = \delta_t$, the Dirac measure at time t, and let $w(\cdot)$ be right-continuous at t. The space of functions which are δ_t-integrable contains functions continuous at t, and also all the functions $w(\cdot)$ which are δ_t-almost everywhere equal to an integrable (continuous) function $g(\cdot)$. Since the support of δ_t is $\{t\}$, it is sufficient that $w(t) = g(t)$. Then $\int w d\delta_t = \int g d\delta_t = g(t) = w(t) = w(t^+)$. This may be a path to

properly define the complementary-slackness variables product over any time interval $[0, \tau]$ with $\tau > 0$. However, as shown in [226] this issue can be solved without going into such abstract measure considerations. At atoms of dz (impact times t) one has $dz = \beta(z(t^+) - z(t^-))\delta_t$ for some $\beta > 0$, while the Lebesgue measure dt has no atom. Then (5.143) is equivalent to (5.144) or (5.145). In other words, there is a $\bar{\lambda}(t) \in -N_{S(t)}(z(t^+))$ such that $z(t^+) - z(t^-) = \bar{\lambda}(t)$. The function $\bar{\lambda}(t)$ is the density of λ at the atom t with respect to $d\delta_t$, i.e., the magnitude of the Dirac measure λ. We may consequently write the input–output product associated with the differential inclusion (5.143) as:

$$\begin{aligned} \langle \tfrac{d\lambda}{d\delta_t}(t), w(t) \rangle &= \langle \tfrac{d\lambda}{d\delta_t}(t), \tfrac{1}{2} C R^{-1}(z(t^+) + z(t^-)) + F u(t) \tfrac{dt}{d\delta_t}(t) \rangle \\ &= \langle \tfrac{d\lambda}{d\delta_t}(t), \tfrac{1}{2} C R^{-1}(z(t^+) + z(t^-)) \rangle. \end{aligned} \tag{5.148}$$

Let us place ourselves in the perspective of dissipative systems [218], which satisfy Assumption 5.2 (at the beginning of Sect. 5.4.4.3) for some matrix $P = P^T \succ 0$, and also the Lyapunov equation $PA + A^T P = Q \preceq 0$. Let $V(x) = \frac{1}{2} x^T P x$ be a storage function for the triple (A, B, C). The infinitesimal dissipation equality is equal at the atoms t of dz to:

$$V(t^+) - V(t^-) = \bar{\lambda}^T w(t) = \frac{1}{2} \bar{\lambda}^T C R^{-1}(z(t^+) - z(t^-)). \tag{5.149}$$

Using $C = B^T P = B^T R^2$, where $R \succ 0$ is the symmetric square root of P, and the algebraic form of the dynamics at atoms of dz (i.e., $z(t^+) - z(t^-) = RB\bar{\lambda}(t)$), this can be rewritten as:

$$\begin{aligned} V(t^+) - V(t^-) &= \tfrac{1}{2} z(t^+)^T z(t^+) - \tfrac{1}{2} z(t^-)^T z(t^-) \\ &= \tfrac{1}{2} x(t^+)^T P x(t^+) - \tfrac{1}{2} x(t^-)^T P x(t^-). \end{aligned} \tag{5.150}$$

It is possible to work with densities with respect to some measure μ which encompasses all phases of motion, as done with the sweeping process (see Problem 5.1, see also Sect. 7.5.1). More details may be found in [226]. These ideas are applied to Lagrangian systems in Sect. 7.5.3, where a generalized supply rate is introduced.

Remark 5.22 The passivity of (A, B, C, D) is a strong property, which is omnipresent in the LCS analysis (either directly or through the input–output constraint $PB = C^T$[45]). We saw here and there in this book that the relative degree between the complementarity variables w and λ plays a significant role in the system's behavior, in particular, the nature of the solutions. Passivity is known to constrain the relative degree. In the multivariable case ($w \in \mathbb{R}^m$ and $m \geq 2$ in (5.128)),

[45] The quadruple (A, B, C, D) is passive if and only if there exists $P = P^T \succeq 0$ such that $\begin{pmatrix} A^T P + PA & PB - C^T \\ B^T P - C & -(D + D^T) \end{pmatrix} \preceq 0$. If $D + D^T = 0$ this LMI implies that $PB = C^T$, using [217, Proposition A.63].

the relative degree of (A, B, C, D) may be replaced by the near notion of *index* of the rational transfer matrix $H(s) = C(sI_n - A)^{-1}B + D$, $s \in \mathbb{C}$. $H(s)$ has index r if it is invertible as a rationale matrix and $s^{-r}H(s)^{-1}$ is proper. It is of *total index* r if all its principal submatrices have index r.[46] Passive systems with storage function matrix $P = P^T \succ 0$ and $\begin{pmatrix} B \\ D + D^T \end{pmatrix}$ full column rank have a transfer matrix with total index $r = 1$ [514, Theorem 3.14]. This generalizes the well-known fact that positive real transfer functions have a relative degree 1, 0 or -1 [218]. As shown in [514, Theorem 3.17], LCS as in (5.128) and with a transfer matrix $C(sI_n - A)^{-1}B + D$ of total index 1 possess state jumps only initially and at times when $Fu(\cdot)$ jumps. This is again in agreement with Theorem 5.11 (which nevertheless does not require the same rank condition): if $Fu(\cdot)$ is continuous, then $S(t)$ is continuous and there is no state jump, except possibly initially.

5.4.5 Controllability of LCS

The controllability of LCS as in (5.128) has been tackled in [250, 253] and [206]. Closely related is the analysis in [219] which, however, focuses on the use of impacts in linear complementarity mechanical systems. Let us state the results in [250] and [206], which together with juggling systems controllability highlights the big discrepancies that may exist between various types of LCS. Suppose that there is no unilateral constraint in (5.128), i.e., the admissible domain $\Phi = \mathbb{R}^n$. Classically, one says that the LCS in (5.128) is completely controllable if for any pair of states (x_0, x_f) there exists a locally integrable control $u(\cdot)$ such that the trajectory of the LCS $x(\cdot, t_0, u, x_0)$ satisfies $x(t, t_0, u, x_0) = x_f$ for some $t > 0$.

Theorem 5.13 *[250] Assume that D is a P-matrix, and that the transfer matrix $F + C(sI - A)^{-1}E$ is invertible as a rational matrix ($s \in \mathbb{C}$). Then the LCS in (5.128) is completely controllable if and only if (i) the pair $(A, [E, B])$ is controllable, and (ii) the system of inequalities $\eta \geq 0$, $(\xi^T \ \eta^T)\begin{pmatrix} A - sI & E \\ C & F \end{pmatrix} = 0$, $(\xi^T \ \eta^T)\begin{pmatrix} B \\ D \end{pmatrix} \leq 0$ admits no solution $s \in \mathbb{R}$ and $0 \neq (\xi \ \eta) \in \mathbb{R}^{n+m}$.*

Theorem 5.13 therefore applies to LCS with absolutely continuous state trajectories.[47] We may say that it applies to a particular class of piecewise-linear systems which lend themselves to a complementarity modeling of the nonlinearity. Let us now state a result that is at the same time more restrictive (it applies to planar systems $n = 2$, with $B = C^T$) and more general (it does not need D as a P-matrix). In fact, while Theorem 5.13 considers systems with a constant state dimension, the next

[46] Conjecture (for Control people): if the decoupling matrix is nonsingular, and the vector relative degree is $(r_1, r_2, \ldots, r_m)^T$, then $r_i \leq r$ for all $1 \leq i \leq m$.

[47] Remind that as we saw in Sect. 5.4.4.3, if D is a P-matrix then λ is a Lipschitz continuous function of both x and u, so that the LCS is an ODE $\dot{x}(t) = f(x(t), u(t))$ for a Lipschitz continuous vector field.

result considers lower dimensional regions of the state space. More precisely, let us consider the LCS:

$$\begin{cases} \dot{x}_1(t) = x_2(t) + C_1^T \lambda(t) \\ \dot{x}_2(t) = u(t) + C_2^T \lambda(t) \\ 0 \le \lambda(t) \perp Cx(t) + d \ge 0 \end{cases} \Leftrightarrow \begin{cases} \langle \dot{x}(t) - Ax(t) - Eu(t), v - x(t) \rangle \ge 0, \ \forall v \in \Phi \\ \\ x(t) \in \Phi, \ \forall\, t \ge 0 \end{cases}$$

$$\Leftrightarrow \qquad \dot{x}(t) - Ax(t) - Eu(t) \in -N_{\Phi}(x(t)), \tag{5.151}$$

where $C = (C_1 \ C_2) \in \mathbb{R}^{m \times 2}$, $C_1 \in \mathbb{R}^m$, and $C_2 \in \mathbb{R}^m$ are the two columns of C, $d \in \mathbb{R}^m$, $\lambda \in \mathbb{R}^m$, $x = (x_1, x_2)^T \in \mathbb{R}^2$, $A = \begin{pmatrix} 0 & 1 \\ 0 & 0 \end{pmatrix}$, $E = \begin{pmatrix} 0 \\ 1 \end{pmatrix}$, $\Phi = \{x \in \mathbb{R}^2 |\ Cx + d \ge 0\} = \{(x_1, x_2) \in \mathbb{R}^2 | C_1 x_1 + C_2 x_2 + d \ge 0\}$. We have $B = C^T$ so the well-posedness results of Sect. 5.4.4.3 apply. The equivalence between the three formalisms in (5.151) may be obtained using the material in Sect. B.2.1. The system in (5.151) is said to be $\Phi-$controllable, if any state $x_f \in \Phi$ can be reached from any state $x_0 \in \Phi$, in a finite or infinite time T, $x(t) \in \Phi$ for all $0 \le t \le T$,[48] and with an admissible input $u(\cdot)$.[49] Let $C_1 = (a_1, \ldots, a_m)^T$, $C_2 = (b_1, \ldots, b_m)^T$, $d = (d_1, \ldots, d_m)^T$ and let us denote the faces of the convex set Φ as D^i, such that $D^i \subseteq \{x \in \mathbb{R}^2 | a_i x_1 + b_i x_2 + d_i = 0\}$ and $\bar{D}^i = \{x \in \mathbb{R}^2 | a_i x_1 + b_i x_2 + d_i = 0\}$. In other words, the faces are segments D^i (possibly unbounded, like in the case Φ is a cone, or if Φ is defined as a half-space), and the segments can be extended to straight lines $\bar{D}^i$ whose equations in the plane are $a_i x_1 + b_i x_2 + d_i = 0, 1 \le i \le m$. In Fig. 5.18 and considering the set Φ_1, one has $D^1 = A'A$ whereas $\bar{D}^1$ is the line passing through A' and A and intersecting $\{x \in \mathbb{R}^2 | x_2 = 0\}$ at B.

Proposition 5.23 *[206] The system in (5.151) is $\Phi-$controllable if and only if there is no face of Φ such that*

- *there is a portion of D^i with finite negative slope on the right (resp. left) of the point $\bar{D}^i \cap \{x \in \mathbb{R}^2 | x_1 = 0\}$, when Φ is below (resp. above) D^i.*
- *D^i is vertical and above (resp. below) $\{x \in \mathbb{R}^2 | x_2 = 0\}$ if Φ is on the right (resp. left) of D^i.*
- *D^i is horizontal and in the half-space $\{x \in \mathbb{R}^2 | x_2 < 0\}$ (resp. $\{x \in \mathbb{R}^2 | x_2 > 0\}$) if Φ is below (resp. above) D^i.*
- *$D^i = \{x \in \mathbb{R}^2 | x_2 = 0\}$.*

This result shows that controllability may be obtained because the dynamics changes when the system evolves on $\text{bd}(\Phi)$ of the admissible domain, which may be viewed as a lower dimensional subspace. This is not the case for other types of switching

[48] The dynamics *implies* that the trajectories starting in Φ remain in Φ.

[49] Admissibility means that the system is well-posed.

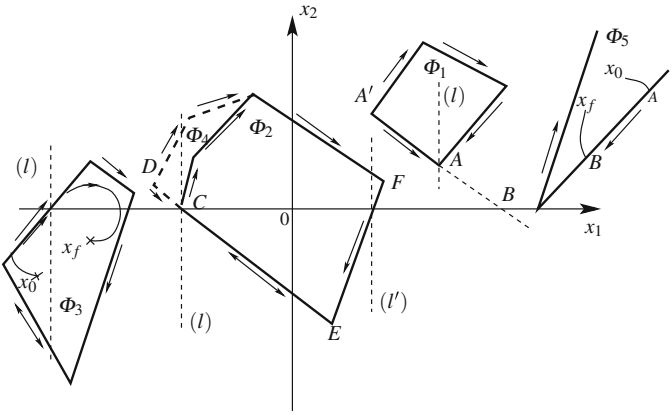

Fig. 5.18 Examples of $\Phi-$controllable and $\Phi-$uncontrollable systems

systems with constant dimension, like $\dot{x}_1(t) = x_2(t)$ if $x_2(t) \leq 0$, $\dot{x}_1(t) = -x_2(t)$ if $x_2(t) \geq 0$, $\dot{x}_2(t) = u(t)$. Here the derivative of $x_1(\cdot)$ is always ≤ 0 (< 0 for $x_2 \neq 0$), so this system cannot be completely controllable. Some examples are depicted in Fig. 5.18. The boundary of the domain Φ_3 in Fig. 5.18 can be tracked clockwise. Consequently, any point x_f on the right of the line (l) can be attained from any point x_0 on the left of (l). There has to be a portion of the trajectory that evolves on $\mathrm{bd}(\Phi_3)$ to reach x_f from x_0. Let us consider the set Φ_1 in Fig. 5.18. The system is not Φ_1-controllable because the only way to attain a point on the left of the vertical line (l) from a point on the right of (l) is to follow the boundary $\mathrm{bd}(\Phi_1)$. However, once the point A has been reached, it is impossible to move on $\mathrm{bd}(\Phi_1)$ toward A'. The system can be steered on the line AA' only in the direction of B. Consequently, all points of Φ_1 which are situated on the left of (l) cannot be attained from points in Φ_1 on the right of (l). It is noteworthy that even local controllability may fail. For instance, two arbitrarily close states x_0 and x_f in Φ_1, with x_0 on the right of (l) and x_f on the left of (l), cannot be joined by a solution of (5.151) with some control $u(\cdot)$. Consider now Φ_2. Then trajectories can be controlled from E to C, though C is reachable in infinite time only. Assume that C is just below the axis $\{x \in \mathbb{R}^2 | x_2 = 0\}$. $\mathrm{bd}(\Phi_2)$ can be tracked clockwise by applying some suitable control input. Thus, the points on the right of the vertical line (l') can be steered to anywhere in Φ_2 by first moving on FE. One may say that the dynamics is suitably modified on the boundary FE so that x_1 can decrease in the first quadrant. In the same way the system is Φ_5-controllable, but it is not Φ_4-controllable (the states on the left of the line (l) cannot be reached from the states in Φ_2). The system is Φ_5-controllable since as illustrated a state x_f that cannot be attained from x_0 via a trajectory which remains in $\Phi_5 \setminus \mathrm{bd}(\Phi_5)$ can be attained via a path $x_0 A B x_f$. The fact that the dynamics changes on the lower dimensional boundary makes it possible to decrease x_1 while being in the first quadrant.

Further Reading

The above two results concern two "extreme" cases: D a P-matrix, and $D = 0$. The cases $D \succeq 0$, or D a P_0-matrix deserve future investigations. Also, E and F have a great importance for controllability. For instance, F nonzero may be interpreted, if some assumptions hold, as a controlled, moving admissible set $\Phi(t)$ in the sweeping process, while E nonzero means that the system can be controlled inside Φ. It is clear that if the sets of Fig. 5.18 are controlled, the overall controllability problem is quite different. The optimal control of first-order Moreau's sweeping process is tackled in [229, 298, 299]. Both the existence of an optimal control [298] and discrete-time approximations [299] in case the control input $u(\cdot)$ appears only in the moving set (equivalently only in the complementarity constraints for an LCS) are treated, while [229] analyzed the case when the control input appears only in the differential equation (and not in the moving set $S(t)$). These results are therefore an important step toward the optimal control of both LCS and Moreau's sweeping processes, though in most applications like circuits, the feedthrough matrix D is not zero but only $\succeq 0$ so that the developments of Sect. 5.4.4.3 which link LCS and sweeping processes do not apply straightforwardly. We may infer that the optimal control of circuits modeled as LCS requires more.

5.4.6 *Observability and Observers for LCS*

The design of state observers for LCS has been tackled in [214, 217, 358, 514] inspired by [205] , with extensions toward set-valued Lur'e systems (as differential inclusions into normal cones to prox-regular time-varying sets) in [1181] and complementarity Lagrangian systems in [1183].[50] All these results make strong use of passivity, and take great care of the observer's well-posedness. The separation principle is shown to hold in [514]. Observability has been studied in [255].

5.4.7 *Complementarity Systems and Hybrid Dynamical Systems*

Hybrid dynamical systems (HDS) consist of any system that combines, one way or another, continuous-time dynamics (differential equations) and some "events" which are seen as discrete-time dynamics. It is therefore a huge class of dynamical systems. They are usually described by modes, switches between modes, possibly state jump rules. Obviously, complementarity conditions coupled to continuous dynamics (linear system, nonlinear system like Lagrangian dynamics), with or without state jumps, can be considered as HDS, whose "modes" or "regimes," as well as

[50] Both [1181, 1183] embed the systems into Moreau's sweeping process.

transitions between them, and are ruled by the complementarity conditions. However, the class of general HDS is too large to constitute an interesting class. Complementarity systems, on the contrary, form a specific class of hybrid (or nonsmooth, or discontinuous) dynamical systems, very rich in terms of its dynamics. It is a compact formalism, with roots in modeling (contact and impact mechanics, circuits with set-valued components), control (optimal control with state inequality constraints), and in optimization (KKT conditions). It relies on mathematical tools from complementarity theory, variational inequalities, differential inclusions, convex and nonsmooth analysis, and maximal monotone operators. This allows one to perform deep analysis for their well-posedness, numerical analysis and simulation, stability and control, and dynamical analysis. It allows also to treat specific phenomena like Zeno behavior, variable structure systems encompassing switches between lower dimensional state subspaces, and large quantities of constraints and switches, which can hardly be taken into account in other, seemingly more general frameworks. Consider for instance a complementarity system with several hundreds, or even several thousands of constraints (a common case in practice, think of a granular system with thousands of grains, unilateral contacts, and Coulomb's friction): on one hand it is impossible to describe such a complementarity system using "if" and "then" conditions (as in a so-called hybrid automaton), since the number of modes increases exponentially with the complementarity variables dimension. On the other hand, such a hybrid point of view would hide the system's structure and properties (to recall a few: the fact that the normal cone to a convex set defines a maximal monotone mapping, or the fact that very efficient numerical solvers exist to compute solutions of complementarity problems and their extensions). *We conclude that it is at best useless to describe complementarity systems within a hybrid system formalism based on hybrid automata.*[51]

Remark 5.23 Switching DAEs of the form $E_\sigma \dot{x}(t) = f_\sigma(x(t))$ as studied in [1215] allow for varying dimensions along system's trajectories, coupled to state reinitialization mappings at the switching times [1215]. This is clearly a nice feature not shared by the various MDEs in (1.15), (1.23), (1.31), and (1.36). Complementarity dynamical systems (CDS), which are equivalently rewritten as measure differential inclusions, or as evolution variational inequalities, may be seen as a particular kind of switching DAEs (though this is not always the case, if for instance the feedthrough matrix $D \succ 0$; and what about the case $D \succeq 0$?). However, on one hand the switching conditions in CDS are ruled by the complementarity conditions which yield complementarity problems (a particularly compact and powerful way of handling the switches); on the other hand, complementarity problems (equivalently inclusions in normal cones to convex sets like Moreau's set) make it possible to get rid of the switching rules to study global properties like dissipativity, maximal

[51] Similar conclusions hold for other fields of control and systems, for example, sliding mode control (SMC). Continuous plants controlled by SMC make hybrid closed-loop systems. However, they possess specific features (set-valuedness of the input, existence of finite-time attractive surfaces) and one would not gain anything by embedding them into a general HDS framework. The same holds for switching systems with continuous vector field.

monotonicity, existence and uniqueness of solutions (both to the switching rules and to the dynamical system), etc.. Moreover, the switching signals σ in [1215] do not allow for accumulations of switching instants (a common situation in CDS), and are not state dependent, while they are in CDS. We conclude that switching DAEs may be a very interesting mathematical framework in applications where the equality constraints change according to some exogenous signal (like in some chemical process dynamics); however, they are not adapted to complementarity systems.

5.5 The Contact Problem with Coulomb's Friction

5.5.1 Introduction

What about Lagrangian systems subject to Coulomb's friction? As we saw in foregoing sections, Coulomb's law may be expressed in a linear complementarity framework. However, this does not mean that Coulomb's friction yields either an LCS or a differential inclusion with maximal monotone right-hand side, when inserted in the dynamics. This is the case in very simple cases, where the normal contact force at the frictional contacts is constant. Consider the terms $H_{\mathrm{t},u}(q,t)\lambda_{\mathrm{t},u}$ and $H_{\mathrm{t},b}(q,t)\lambda_{\mathrm{t},b}$ in (5.1). Suppose that each frictional contact is planar, i.e., we consider two-dimensional friction. The vectors $\lambda_{\mathrm{t},u}$ and $\lambda_{\mathrm{t},b}$ collect the tangential components of the reaction forces $\lambda_{\mathrm{t},u,i}$ and $\lambda_{\mathrm{t},b,i}$, see the introduction of Sect. 5.1. According to Coulomb's law (see Sects. 5.3.1 and 5.3.2),

$$\lambda_{\mathrm{t},u,i} \in -\mu_i \lambda_{\mathrm{n},u,i}\ \mathrm{sgn}(H_{\mathrm{t},u,i}(q,t)^T\dot{q}) = -\mu_i \lambda_{\mathrm{n},u,i}\ \partial|H_{\mathrm{t},u,i}(q,t)^T\dot{q}| \qquad (5.152)$$

and

$$\lambda_{\mathrm{t},b,i} \in -\mu_i|\lambda_{\mathrm{n},b,i}|\ \mathrm{sgn}(H_{\mathrm{t},b,i}(q,t)^T\dot{q}) = -\mu_i|\lambda_{\mathrm{n},b,i}|\ \partial|H_{\mathrm{t},b,i}(q,t)^T\dot{q}|. \qquad (5.153)$$

Use has been made of (5.92), and of the fact that the local tangential velocities can be expressed as $v_{\mathrm{t},i} = H_{\mathrm{t},i}(q)^T\dot{q}$, according to the invariance principle of Sect. 3.2. One has $H_{\mathrm{t},u}(q,t)\lambda_{\mathrm{t},u} = \sum_{i=1}^{m_u} H_{\mathrm{t},u,i}(q,t)\lambda_{\mathrm{t},u,i}$, where $H_{\mathrm{t},u,i}(q,t)$ is the i-th column of $H_{\mathrm{t},u}(q,t)$, and $H_{\mathrm{t},b}(q,t)\lambda_{\mathrm{t},u,b} = \sum_{i=1}^{m_b} H_{\mathrm{t},b,i}(q,t)\lambda_{\mathrm{t},b,i}$. The next step is to examine the terms

$$H_{\mathrm{t},u,i}(q,t)\lambda_{\mathrm{t},u,i} \in -\mu_i \lambda_{\mathrm{t},u,i} H_{\mathrm{t},u,i}(q,t)\ \partial|H_{\mathrm{t},u,i}(q,t)^T\dot{q}|$$

and

$$H_{\mathrm{t},b,i}(q,t)\lambda_{\mathrm{t},b,i} \in -\mu_i|\lambda_{\mathrm{t},b,i}|H_{\mathrm{t},b,i}(q,t)\ \partial|H_{\mathrm{t},b,i}(q,t)^T\dot{q}|.$$

Notice that the subdifferential is calculated with respect to the components of the tangential velocity, i.e., $v_{\mathrm{t},i} = H_{\mathrm{t},i}(q,t)^T\dot{q}$. Suppose that for some reason, the normal contact forces are known, bounded functions of time. Using Theorem B.2, it appears

that $H_{\mathrm{t},u,i}(q,t)\lambda_{\mathrm{t},u,i} \in -\partial g_{u,i}(\dot{q})$ and $H_{\mathrm{t},b,i}(q,t)\lambda_{\mathrm{t},b,i} \in -\partial g_{b,i}(\dot{q})$ where $g_{u,i}(\cdot)$ and $g_{b,i}(\cdot)$ are convex, proper functions. Inserting these expressions in the dynamical equations (5.1), one obtains the set-valued system:

$$M(q)\ddot{q} + C(q,\dot{q})\dot{q} + G(q) = \nabla f(q,t)\lambda_{\mathrm{n},u} + \nabla h(q,t)\lambda_{\mathrm{n},b} + F_{ext} + \partial g(\dot{q}), \tag{5.154}$$

where $g(\dot{q}) = g_{u,1}(\dot{q}) + \ldots + g_{u,m_u}(\dot{q}) + g_{b,1}(\dot{q}) + \ldots + g_{u,m_b}(\dot{q})$.[52] The set-valued part of the right-hand side is a maximal monotone operator, being the subdifferential of a proper convex function, see Lemma B.1. Proving the well-posedness of the differential inclusion in (5.154) may be done, following [25], or [27] in the linear Lagrangian dynamics case. However, the conditions under which (5.154) holds are quite stringent, rarely verified in practice where normal forces usually vary. These developments may be led in the three-dimensional case where $F_{\mathrm{t}} \in \mathbb{R}^2$, using (5.93).

5.5.2 *Dissipativity of the Constrained Lagrange Dynamics*

Coulomb's law is not associated, which means that the relationship satisfied by the contact reaction force and the local frame velocity cannot be written as an inclusion into the subdifferential of the indicator of a convex closed set (or more generally, into the subdifferential of a proper, convex function). Despite of this fact, unilateral contact with Coulomb's friction defines a contact model that dissipates. Consider that contact holds, so that from Proposition 5.3 one has $0 \leq \nabla f(q)^T\dot{q} \perp \lambda_{\mathrm{n},u} \geq 0$ (Signorini-in-velocity conditions). Then using the chain rule theorem B.2 one finds that $\nabla f(q)\lambda_{\mathrm{n},u} \in -N_{T_u(q)}(\dot{q})$ where $T_u(q) = \{z \in \mathbb{R}^n | \nabla f(q)^T z \geq 0\}$. We know that under the Mangasarian–Fromovitz constraint qualification in (B.9), this is the tangent cone to the set $\Phi_u = \{q \in \mathbb{R}^n | f(q) \geq 0\}$. Anyway, the interesting property here is that it is nonempty and convex, so that $\lambda_{\mathrm{n},u}^T \nabla f(q)\dot{q} \leq 0$ since the normal cone mapping $\dot{q} \mapsto -\nabla f(q)\lambda_{\mathrm{n},u}$ is maximal monotone. Using (5.1), (5.152), and (5.153), posing $F_{ext} = u$, and assuming the property that $\dot{q}(t)^T\left[\frac{1}{2}\frac{d}{dt}(M(q(t)) - C(q(t),\dot{q}(t))\right]\dot{q}(t) = 0$ (the matrix between brackets is skew-symmetric provided the Coriolis and centrifugal forces are written with the Christoffel's symbols associated with $M(q)$ [218, §6.1.2]), we find the following dissipation equality including friction, with $E(q,\dot{q}) = T(q,\dot{q}) + U(q)$ the total mechanical energy:

$$E(t_2) - E(t_1) = \int_{t_1}^{t_2} u(t)^T\dot{q}(t)dt - \int_{t_1}^{t_2} \mathscr{D}(q(t),\dot{q}(t))dt, \tag{5.155}$$

[52] The subdifferential of a sum of convex proper functions (which is itself convex proper [1045, Theorem 5.2]) is equal to the sum of their subdifferentials, under some mild conditions [1045, Theorem 23.8] which are satisfied here.

for all $t_2 \geq t_1 \geq 0$, and the dissipation function is

$$\begin{aligned}\mathscr{D}(q,\dot{q}) = -\dot{q}^T \nabla f(q)\lambda_{\mathrm{n},u} + \textstyle\sum_{i=1}^{m_b} |\lambda_{\mathrm{b},i}|\mu_i H_{\mathrm{t},b,i}(q_i)\dot{q}_i \mathrm{sgn}(H_{\mathrm{t},b,i}(q_i)\dot{q}_i) \\ + \textstyle\sum_{i=m_b+1}^{m_b+m_u} |\lambda_{\mathrm{u},i}|\mu_i H_{\mathrm{t},u,i}(q_i)\dot{q}_i \mathrm{sgn}(H_{\mathrm{t},u,i}(q_i)\dot{q}_i) \geq 0.\end{aligned} \tag{5.156}$$

Remark 5.24 In view of the complementarity conditions, we could just write that $\lambda_{\mathrm{n},u}^T \nabla f(q)^T \dot{q} = 0$. We have left here an ambiguity because it is not clear whether $\dot{q}$ means $\dot{q}(t^-)$ or $\dot{q}(t^+)$, and whether $\lambda_{\mathrm{n},u}$ means $\lambda_{\mathrm{n},u}(t^-)$ or $\lambda_{\mathrm{n},u}(t^+)$. This could be important if we want to take impact times into account. If we work with right velocities and right multipliers, then $\lambda_{\mathrm{n},u}(t^+)^T \nabla f(q)^T \dot{q}(t^+) = 0$. Using the material in Sect. 7.5.3, it is possible to extend the dissipation equality to impact times, but taking care of conditions such that the collision rule is indeed dissipative.

$\rightsquigarrow$ *We have not analyzed the problem of existence and uniqueness of the multipliers* λ_{n}, *and we have implicitly assumed that the dynamics is well-posed to get the dissipation equality. This is not guaranteed, even if we look at the system just locally in time during a permanent contact phase. In the next section a partial answer is given.*

5.5.3 Extension of the Results of Sects. 5.1.1, 5.1.2, 5.1.3?

The question mark in the section's title is intentional. In these sections, the well-posedness of the contact problem is tackled. The symmetry and positive definiteness of the LCP matrices are central properties which allow one to infer existence, uniqueness, as well as Gauss' principle extensions. Consider the case with only unilateral constraint and $M(q) \succ 0$. Using (5.1), the contact complementarity problem takes the following form:

$$0 \leq \lambda_{\mathrm{n},u} \perp \ddot{f}(q) = \nabla f(q)^T M(q)^{-1}(\nabla f(q)\lambda_{\mathrm{n},u} + H_{\mathrm{t},u}(q)\lambda_{\mathrm{t},u}) + b(q,\dot{q},t) \geq 0, \tag{5.157}$$

where $b(q,\dot{q},t)$ is as in (5.9). One then has to use the expression for $\lambda_{\mathrm{t},u}$ from Coulomb's law to find the contact LCP. Let us suppose for simplicity that the friction is planar at each contact i, i.e., $\lambda_{\mathrm{t},u,i} \in -\mu_i \lambda_{\mathrm{n},u,i}\mathrm{sgn}(v_{\mathrm{t},u,i})$. Grouping terms we can rewrite more compactly $\lambda_{\mathrm{t},u} \in -[\mu_i \mathrm{sgn}(v_{\mathrm{t},u,i})]\lambda_{\mathrm{n},u}$, where $[a_i]$=diag(a_i). Thus the contact complementarity problem (5.157) is rewritten as

$$0 \leq \lambda_{\mathrm{n},u} \perp \underbrace{\nabla f(q)^T M(q)^{-1}(\nabla f(q)\overbrace{-H_{\mathrm{t},u}(q)[\mu_i \mathrm{sgn}(v_{\mathrm{t},u,i})]}^{\triangleq P^{\mu}(q)})}_{\triangleq D_u^{\mu}(q)} \lambda_{\mathrm{n},u} + b(q,\dot{q},t) \geq 0. \tag{5.158}$$

It is therefore apparent that the contact LCP matrix $D_u^\mu(q)$ is the frictionless Delassus' matrix $D_u(q)$ in (5.9), plus a perturbation $P^\mu(q)$ due to friction. Obviously, both the coefficient of friction and the tangent velocity sign will play a role in the contact LCP well-posedness. Since the Delassus' matrix $D_u(q) = D_u^0(q) \succeq 0$, it is natural to look for perturbations which do not destroy the positive (semi) definiteness, though the symmetry will generally be lost (however, the symmetry is not necessary for the LCP well-posedness). Here we use Theorem 5.8, which has practical interest because it involves maximum singular values of known matrices.

Proposition 5.24 *Assume that the active unilateral constraints are independent* ($\Rightarrow D_u(q) \succ 0$). *Then if* $\sigma_{\max}(P^\mu(q)) < \sigma_{\min}(D_u(q))$, *one has* $D_u^\mu(q) \succ 0$.

The proof follows from Theorem 5.8, noting that $\sigma_{\min}(D_u(q)) = \frac{1}{\sigma_{\max}(D_u(q)^{-1})}$. It is clear that if the coefficients μ_i are small enough, the proposition's inequality is satisfied. An upperbound $\mu_{\max}$ can be calculated from the expression of $P^\mu(q)$ in (5.158). Obviously, such criterion is in general conservative; however, this is the price to pay for generality. Another result is as follows:

Proposition 5.25 *Assume that the active unilateral constraints are independent, and that* q, $v_{\mathrm{t},u} = H_{\mathrm{t},u}(q)^T \dot{q}$ *and* μ_i, $1 \leq i \leq m_u$ *are such that all the entries of* $P^\mu(q)$ *are nonnegative. Suppose further that* $0 \leq z \perp D_u^\mu(q)z \geq 0 \Rightarrow \dot{q}^T b(q, \dot{q}, t) \geq 0$. *Then the contact LCP in (5.158) is solvable.*

The proof uses Theorem 5.6, noting that the conditions of the proposition guarantee that $D_u^\mu(q)$ is copositive. Both Propositions can be used to guarantee that the contact LCP possesses a solution λ_{n} for any $b(q, \dot{q}, t)$ in *sliding regimes*. In sticking regimes the LCP alone cannot yield λ_{n} because the selection of $\mathrm{sgn}(v_{\mathrm{t}}) = \mathrm{sgn}(0)$ remains to be determined.

Remark 5.25 It is noteworthy that $D_u^\mu(q)$ has no reason to be symmetric in general. Thus the equivalence between the LCP and a quadratic program no longer holds (more precisely, the LCP does not represent the necessary conditions of optimality of a quadratic program *via* the Karush–Kuhn–Tucker conditions). This is related to Gauss' principle of Solid Mechanics, which usually does not hold when Coulomb's friction is present (though some relaxation of it may be proposed [160, Sect. 3.3.2]). When Tresca's friction is modeled, then Gauss' principle extends with a specific cost function [1015] (see [595, Eq. (3.6)]).

5.5.4 The Contact Problem for a Planar Particle

Let us analyze the system in Fig. 5.19a, which consists of a particle P subject to a unilateral constraint with Coulomb friction and coefficient $\mu > 0$, Coulomb's cone $\mathscr{C}$, and acted upon by a force $F = (F_x \ F_y)^T$, i.e., $F = F_x\mathbf{i} + F_y\mathbf{j}$. The contact reaction force is $R = \lambda_{\mathrm{n}}\mathbf{n} + \lambda_{\mathrm{t}}\mathbf{t} \in \mathscr{C}$. The objective is to study all the modes of this system: static equilibrium, sliding, detachment, depending on the angles α, and

$\beta = \arctan(\mu)$, as well as the applied force F. The particle is subject to a unilateral constraint $f(q) = y\cos(\alpha) - x\sin(\alpha) \geq 0$, with $\alpha \in (0, \frac{\pi}{2})$. In fact $f(q)$ corresponds to the second coordinate x_{n} of P in the frame $(\mathbf{t}, \mathbf{n})$, which obviously satisfies $x_{\mathrm{n}} \geq 0$. Thus $0 \leq f(q) \perp \lambda_{\mathrm{n}} \geq 0$. One has $\nabla f(q) = (-\sin(\alpha)\ \cos(\alpha))^T$, and $H_{\mathrm{t}} = (\nabla f(q))^{\perp} = (\cos(\alpha)\ \sin(\alpha))^T$. The contact force is also given by $R = (-\lambda_{\mathrm{n}}\sin(\alpha) + \lambda_{\mathrm{t}}\cos(\alpha))\mathbf{i} + (\lambda_{\mathrm{n}}\cos(\alpha) + \lambda_{\mathrm{t}}\sin(\alpha))\mathbf{j}$. We may also introduce the rotation matrix between the two frames: $\begin{pmatrix} R_x \\ R_y \end{pmatrix} = \begin{pmatrix} \cos(\alpha) & -\sin(\alpha) \\ \sin(\alpha) & \cos(\alpha) \end{pmatrix} \begin{pmatrix} \lambda_{\mathrm{t}} \\ \lambda_{\mathrm{n}} \end{pmatrix}$. Therefore, the dynamics of the particle is given by

$$\begin{cases} M\ddot{q} = \begin{pmatrix} -\sin(\alpha) \\ \cos(\alpha) \end{pmatrix} \lambda_{\mathrm{n}} + \begin{pmatrix} \cos(\alpha) \\ \sin(\alpha) \end{pmatrix} \lambda_{\mathrm{t}} + \begin{pmatrix} F_x \\ F_y \end{pmatrix} = \begin{pmatrix} R_x \\ R_y \end{pmatrix} + \begin{pmatrix} F_x \\ F_y \end{pmatrix} \\ 0 \leq f(q) \perp \lambda_{\mathrm{n}} \geq 0 \\ \lambda_{\mathrm{t}} \in -\mu\lambda_{\mathrm{n}}\mathrm{sgn}(H_{\mathrm{t}}^T\dot{q}) \\ q(0) = q_0, \dot{q}(0) = \dot{q}_0, \end{cases} \tag{5.159}$$

with $M = \mathrm{diag}(m)$, and $v_{\mathrm{t}} = H_{\mathrm{t}}^T\dot{q} = \cos(\alpha)\dot{x} + \sin(\alpha)\dot{y}$. Notice that we could equivalently write the dynamics directly in the frame $(\mathbf{t}, \mathbf{n})$: $M \begin{pmatrix} \dot{v}_{\mathrm{t}} \\ \dot{v}_{\mathrm{n}} \end{pmatrix} = \begin{pmatrix} F_{\mathrm{t}} + \lambda_{\mathrm{t}} \\ F_{\mathrm{n}} + \lambda_{\mathrm{n}} \end{pmatrix}$, with $F = F_{\mathrm{t}}\mathbf{t} + F_{\mathrm{n}}\mathbf{n}$, $v_{\mathrm{n}} = \nabla f(q)^T\dot{q}$; however, this does not change the next analysis. As we are going to see through rigorous calculations and analysis, the regimes of the particle depend as expected on whether $F(t)$ is outside or inside the friction cone.

5.5.4.1 The Contact LCP and System's Modes

Few calculations show that the contact LCP is given by

$$0 \leq \lambda_{\mathrm{n}} + \underbrace{\cos(\alpha)F_y - \sin(\alpha)F_x}_{=F_{\mathrm{n}}} \perp \lambda_{\mathrm{n}} \geq 0 \tag{5.160}$$

where the factor $\frac{1}{m}$ has been dropped. The LCP matrix is $D_u = 1$, thus from Theorem 5.4 there is always a unique solution. It is noteworthy that the tangential reaction does not appear in the contact LCP: there is a dynamical normal/tangential decoupling because $H_{\mathrm{t}}^T M^{-1}\nabla f(q) = 0$. We infer that the contact mode is assured provided that $\cos(\alpha)F_y - \sin(\alpha)F_x < 0 \Rightarrow \lambda_{\mathrm{n}} = -\cos(\alpha)F_y + \sin(\alpha)F_x > 0$: in the contact mode the normal multiplier is a function of the applied force F only, and is independent of λ_{t}. It follows that $\lambda_{\mathrm{n}} = -F_{\mathrm{n}}$ in the contact mode, which is merely the particle equilibrium in the normal direction. Thus the contact mode is active in the following cases:

- $F_y < 0$ and $F_x \geq 0$,
- $F_y \geq 0$ and $F_x > 0$ and $\frac{F_y}{F_x} < \tan(\alpha)$,
- $F_y < 0$ and $F_x < 0$ and $\frac{F_y}{F_x} > \tan(\alpha)$.

In case $F_y > 0$ and $F_x \leq 0$ there is detachment from the constraint since $\lambda_n = 0$ and $\ddot{f}(q) > 0$ (recall that we are working with right-continuous accelerations and multipliers). Notice that during contact one has $f(q) = \nabla f(q)^T \dot{q} = 0$, that is $\dot{y}\cos(\alpha) = \dot{x}\sin(\alpha)$. Therefore $v_t = \frac{\dot{x}}{\cos(\alpha)} = \frac{\dot{y}}{\sin(\alpha)}$. Let us now determine whether the contact is in sticking or sliding mode. For this let us calculate using (5.159): $m\dot{v}_t = \frac{\ddot{x}}{\cos(\alpha)} = \sin(\alpha)F_y + \cos(\alpha)F_x + \lambda_t$. If $v_t \neq 0$ the contact is sliding. If $v_t = 0$ and $\dot{v}_t = 0$, the contact is in persistent sticking, if $v_t = 0$ and $\dot{v}_t \neq 0$ the contact is in transition from sticking to sliding.

Let us assume that the particle tangentially sticks, *i.e.,* $v_t = 0 \Leftrightarrow \dot{x} = \dot{y} = 0$. Let us use the Coulomb-in-acceleration model introduced in Sect. 5.3.4 to determine the stick/slip transition conditions. One has $\lambda_t \in -\mu\lambda_n \mathrm{sgn}(\dot{v}_t)$ if $\dot{v}_t \neq 0$. From the above we obtain $\lambda_t \in \mu(\cos(\alpha)F_y - \sin(\alpha)F_x)\mathrm{sgn}(\sin(\alpha)F_y + \cos(\alpha)F_x + \lambda_t)$. This is equivalent, using the material in Appendix B (in particular, the fact that support functions are conjugate of the indicator function, as well as equivalences in Sect. B.2.1), to (recall that $F_t = \sin(\alpha)F_y + \cos(\alpha)F_x$ and $F_n = -\sin(\alpha)F_x + \cos(\alpha)F_y$, so that $m\dot{v}_t = F_t + \lambda_t$)

$$\begin{array}{c} \sin(\alpha)F_y + \cos(\alpha)F_x + \lambda_t \in N_{[-1,1]}\left(\frac{\lambda_t}{\mu(\cos(\alpha)F_y - \sin(\alpha)F_x)}\right) \\ \Updownarrow \\ \lambda_t = \mu(\cos(\alpha)F_y - \sin(\alpha)F_x)\mathrm{proj}\left([-1,1]; -\frac{\sin(\alpha)F_y + \cos(\alpha)F_x}{\mu(\cos(\alpha)F_y - \sin(\alpha)F_x)}\right) \\ \Updownarrow \\ \lambda_t = \mu F_n \mathrm{proj}\left([-1,1]; \frac{-F_t}{\mu F_n}\right). \end{array} \tag{5.161}$$

We can now examine the conditions such that indeed $\dot{v}_t \neq 0$ using (5.161). (i) Suppose that $\left|\frac{\sin(\alpha)F_y + \cos(\alpha)F_x}{\mu(\cos(\alpha)F_y - \sin(\alpha)F_x)}\right| \leq 1$, equivalently $\frac{|F_t|}{|F_n|} \leq \mu \Leftrightarrow F \in \mathscr{C}$, then $\lambda_t = -\sin(\alpha)F_y - \cos(\alpha)F_x = -F_t$, and $\dot{v}_t = 0$. Thus this case does not correspond to a stick/slip transition. (ii) Suppose that $\frac{-F_t}{\mu F_n} < -1 \Leftrightarrow F_t < \mu F_n < 0$, then $m\dot{v}_t = F_t - \mu F_n < 0$. (iii) Suppose that $\frac{-F_t}{\mu F_n} > 1 \Leftrightarrow F_t > -\mu F_n > 0$, then $m\dot{v}_t = F_t + \mu F_n > 0$. We infer that cases (ii) and (iii) correspond to a transition from stick to slip with $v_t = 0$ and $\dot{v}_t \neq 0$, while case (i) corresponds to persistent sticking mode with $v_t = 0, \dot{v}_t = 0$ and tangential equilibrium $F_t + \lambda_t = 0$.

Let us now deal with the sliding regime $v_t \neq 0$. In this case $\lambda_t = -\mu\lambda_n(\pm 1) = \mu(\cos(\alpha)F_y - \sin(\alpha)F_x)(\pm 1)$. If the initial conditions are such that $v_t(0) \neq 0$, then the sliding mode will persist during a certain time, depending on the applied force F.

The transition from sliding to sticking involves the integration of the dynamics. The sticking mode may be attained via *an infinity of trajectories. This is quite similar to the normal stabilization on the constraint boundary* (e.g., *after a sequence of impacts). This is related to the fact that such events render the dynamics irreversible in time.*

Remark 5.26 Let $F(t) \in \mathrm{Int}(\mathscr{C})$ for all $t \geq 0$ and $v_t(0^-) \neq 0$. Is there a contradiction with the above analysis? This analysis says that if $v_t(0) = 0$ and if F is in the friction

cone, then the sticking mode persists because the tangential acceleration $\dot{v}_t = 0$ as well. However, it is quite possible that the system slides on the constraint boundary while all forces balance each other: $F + R = 0$.

5.5.4.2 Well-Posedness of the Contact Dynamics

Proposition 5.26 *Let $f(q(0)) = 0, \nabla f(q(0))^T \dot{q}(0) = 0$, and $F_n(t) < 0 \Leftrightarrow \lambda_n(t) > 0$ for all $t \geq 0$. Let also $F(\cdot)$ be a bounded locally integrable function. Then the system (5.159) has a global solution with absolutely continuous $\dot{q}(\cdot)$ and continuously differentiable $q(\cdot)$ for any initial $v_t(0)$.*

Proof Under the stated assumptions, the particle is in persistent contact with the constraint boundary, and $\lambda_n(t) = -F_n(t)$. Consider the dynamics in the frame $(\mathbf{t}, \mathbf{n})$. The tangential part reads as $m\dot{v}_t \in \{F_t(t)\} - \mu F_n(t)\text{sgn}(v_t)$. This is a differential inclusion of the form $\dot{z}(t) \in F(t, z(t))$. Using the assumption on $F(t)$, the set-valued function $z \mapsto G(t, z)$ is upper semi-continuous for all $t \geq 0$. Moreover, $g(t) \stackrel{\Delta}{=} F_t + \mu F_n(t) \subset G(t, z)$ for any z with $g(\cdot)$ Lebesgue measurable. Third, $|g(t)| \leq b$ for some bounded b. Thus [1120, Theorem 4.7] applies to the tangential part of the dynamics. The normal part reduces to $m\dot{v}_n(t) = 0$.

Here we could prove the proposition because the dynamics is first-order in v_t. In general, it is second order because the position is present in the dynamics. Then the well-posedness is more complex to show, see [82] for a system of the form $\ddot{u}_t(t) + K_t u_t(t) \in \partial\psi^\star_{I(t)}(-\dot{u}_t(t))$, where $\dot{u}_t = v_t$ and $I(t)$ is an interval that depends on $u_t(t)$ and $\lambda_n(t)$.

5.5.5 A Second Simple Mechanism with Friction

We now consider the mechanism depicted in Fig. 5.19b. The objective is to determine the conditions under which the vertical rod's tip P may slide on the horizontally

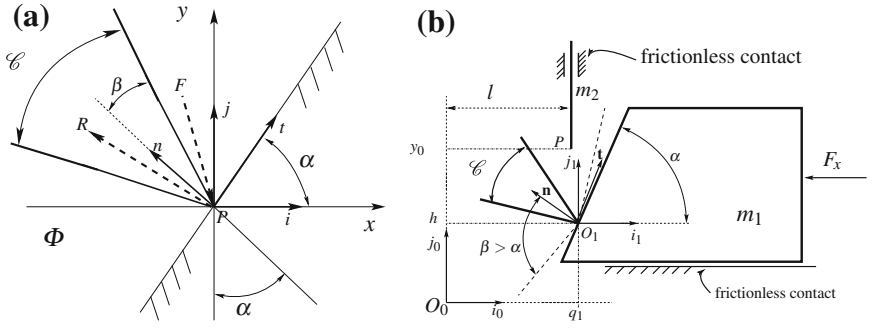

Fig. 5.19 Two simple systems with Coulomb's friction and unilateral contact. **a** Particle P with unilateral contact and Coulomb friction. **b** A 2-degree-of-freedom mechanism

moving workpiece with mass m_1, or may stick on it, when contact is established and a force $F = (F_x, 0)^T$ acts on the workpiece. The rod's mass is m_2, and $\alpha \in [0, \frac{\pi}{2}]$. It is constrained by a frictionless prismatic joint. The coordinates of P in the Galilean frame $(O_0, \mathbf{i}_0, \mathbf{j}_0)$ are $x_0 = l$ and y_0, and in $(O_1, \mathbf{i}_1, \mathbf{j}_1)$ they are $x_1 = l - q_1$ and $y_1 = y_0 - h$, where the coordinates of O_1 in $(O_0, \mathbf{i}_0, \mathbf{j}_0)$ are q_1 and h. Both l and h are arbitrary constants. The system has generalized coordinates $q = (q_1, y_0)^T$. Starting from the coordinates $(x_\mathrm{t}, x_\mathrm{n})$ of P in the frame $(O_1, \mathbf{t}, \mathbf{n})^T$, one obtains from $x_\mathrm{n} = -\sin(\alpha)x_1 + \cos(\alpha)y_1 \geq 0$ the unilateral constraint $f(q) = (q_1 - l)\sin(\alpha) + (y_0 - h)\cos(\alpha) \geq 0$. Thus $\nabla f(q) = (\sin(\alpha)\ \cos(\alpha))^T$. We infer that the dynamics is given by:

$$\begin{cases} \begin{pmatrix} m_1\ddot{q}_1 \\ m_2\ddot{y}_0 \end{pmatrix} = \begin{pmatrix} \sin(\alpha) \\ \cos(\alpha) \end{pmatrix}\lambda_\mathrm{n} + \begin{pmatrix} -\cos(\alpha) \\ \sin(\alpha) \end{pmatrix}\lambda_\mathrm{t} + \begin{pmatrix} F_x \\ 0 \end{pmatrix} \\ 0 \leq f(q) \perp \lambda_\mathrm{n} \geq 0 \\ \lambda_\mathrm{t} \in -\mu\lambda_\mathrm{n}\mathrm{sgn}(H_\mathrm{t}^T\dot{q}) \\ q(0) = q_0, \dot{q}(0) = \dot{q}_0, \end{cases} \tag{5.162}$$

where $v_\mathrm{t} = H_\mathrm{t}^T\dot{q} = -\cos(\alpha)\dot{q}_1 + \sin(\alpha)\dot{y}_0$. From the expression of $\frac{d^2}{dt^2}f(q(t)) = \nabla f(q)^T\ddot{q}$ one obtains the contact LCP:

$$0 \leq \frac{m_1\cos(\alpha)^2 + m_2\sin(\alpha)^2}{m_1m_2}\lambda_\mathrm{n} + \frac{m_1 - m_2}{m_1m_2}\cos(\alpha)\sin(\alpha)\lambda_\mathrm{t} + \frac{\sin(\alpha)}{m_1}F_x \perp \lambda_\mathrm{n} \geq 0 \tag{5.163}$$

Excepted if $m_1 = m_2$, the tangential reaction appears in the contact LCP: there is no decoupling, unlike the foregoing case. Therefore, the LCP matrix may be modified by the tangential effects.

5.5.5.1 Sliding Contact

Let the contact slide, i.e., $v_\mathrm{t} \neq 0$ and $\lambda_\mathrm{t} = -\mathrm{sgn}(v_\mathrm{t})\mu\ \lambda_\mathrm{n}$. The LCP matrix (here a scalar) is calculated to be

$$D_u^\mu(v_\mathrm{t}, m_1, m_2, \alpha) \triangleq \frac{m_1\cos(\alpha)^2 + m_2\sin(\alpha)^2 - \mathrm{sgn}(v_\mathrm{t})\mu(m_1 - m_2)\cos(\alpha)\sin(\alpha)}{m_1m_2} \tag{5.164}$$

Several cases have to be considered:

- **(i)** $D_u^\mu > 0 \Leftrightarrow m_1\cos(\alpha)^2 + m_2\sin(\alpha)^2 > \mathrm{sgn}(v_\mathrm{t})\ \mu\ (m_1 - m_2)\cos(\alpha)\sin(\alpha)$: there is a unique solution λ_n. **(ia)** If $\sin(\alpha)F_x > 0$ then $\lambda_\mathrm{n} = 0$ and there is a transition from contact to noncontact mode. **(ib)** If $\sin(\alpha)F_x < 0$ then $\lambda_\mathrm{n} > 0$ and contact is kept. **(ic)** If $F_x = 0$ then $\lambda_\mathrm{n} = 0$: the system is grazing the constraint boundary. Higher order derivatives have to be examined to determine if contact is kept or not.
- **(ii)** $D_u^\mu < 0 \Leftrightarrow m_1\cos(\alpha)^2 + m_2\sin(\alpha)^2 < \mathrm{sgn}(v_\mathrm{t})\ \mu\ (m_1 - m_2)\cos(\alpha)\sin(\alpha)$: **(iia)** the contact LCP has the solution $\lambda_\mathrm{n} = 0$ if and only if $\sin(\alpha)F_x \geq 0$ (in

this case there is a transition from contact to noncontact mode). **(iib)** Otherwise, there is no solution for the normal multiplier.

- **(iii)** $D_u^\mu = 0 \Leftrightarrow m_1 \cos(\alpha)^2 + m_2 \sin(\alpha)^2 = \text{sgn}(v_\text{t})\ \mu\ (m_1 - m_2)\cos(\alpha)\sin(\alpha)$. The contact LCP is $0 \leq \frac{\sin(\alpha)}{m_1} F_x \perp \lambda_\text{n} \geq 0$. Three cases may be considered **(iiia)** $\sin(\alpha) F_x = 0$, **(iiib)** $\sin(\alpha) F_x > 0$, **(iiic)** $\sin(\alpha) F_x < 0$.

The novelties with respect to the particle system are cases **(iib)** and **(iii)**. Suppose that the system is initialized at time t in a sliding mode such that case **(iib)** occurs. What happens in such an inconsistent case (no solution)? One solution is to augment the model, and to allow the system to jump to a sticking mode with the right velocity $v_\text{t}(t^+) = 0$. Suppose indeed that $D_u^\mu(v_\text{t}(t^-)) < 0$ with $v_\text{t}(t^-) \neq 0$. Without loss of generality let $v_\text{t}(t^-) > 0$ ($\Rightarrow m_1 > m_2$). Then $\text{sgn}(v_\text{t}(t^+)) = \text{sgn}(0) = [-1, 1]$. Thus there is a selection $\xi(t) \in [-1, 1]$ such that $D_u^\mu(v_\text{t}(t^+)) > 0$, since it suffices to choose $\xi(t) < 0$ to get the desired result, with $(\lambda_\text{t}(t^+), \lambda_\text{n}(t^+))^T \in \mathscr{C}$. The same applies if $v_\text{t}(t^-) < 0$ ($\Rightarrow m_2 > m_1$), and $\xi(t) > 0$. The next step is to examine whether or not the contact remains sticking, or if it could slide again after this "tangential impact".[53]

Let $m_1 > 0$ and $m_2 > 0$. Case **(iii)** can occur only if $\text{sgn}(v_\text{t})\ (m_1 - m_2)\cos(\alpha)\sin(\alpha) > 0$, so that $\alpha \in (0, \frac{\pi}{2})$ and either **(a)** ($v_\text{t} > 0$ and $m_2 > m_1$), or **(b)** ($v_\text{t} < 0$ and $m_1 < m_2$). This case **(iiia)** implies $F_x = 0$. Consider case **(a)**. Calculations from $D_u^\mu = 0$ yield $\mu = \tan(\alpha) + \frac{m_1}{m_1 - m_2} \frac{1 + \tan(\alpha)^2}{\tan(\alpha)}$, hence $\tan(\beta) = \mu > \tan(\alpha)$, equivalently $\beta > \alpha$: the cone is as in Fig. 5.19b with the dashed lines. The contact LCP in case **(iiia)** is $0 \leq 0 \perp \lambda_\text{n} \geq 0$. A value $\lambda_\text{n} > 0$ occurs if the system is initialized in a sliding mode with $v_\text{t} > 0$: the contact force lies on the boundary $\partial\mathscr{C}$, and the accelerations $\ddot{q}_1$ and $\ddot{y}_0$ create the inertial forces that dynamically balance the system. The value $\lambda_\text{n} = 0$ is also possible, from the dynamics and Coulomb's law it implies $\ddot{q}_1 = \ddot{y}_0 = 0$ and hence $\dot{v}_\text{t} = 0$ as well. Thus the system just grazes the constraint boundary (the rod's tip grazes the mass m_1) with constant v_t, and $v_\text{n} = 0$ if initially $\nabla f(q)^T \ddot{q} = \dot{v}_\text{n} = 0$ (for otherwise if $\dot{v}_\text{n} > 0$ detachment from the constraint occurs). A similar reasoning applies in case **(b)**. Consider now case **(iiib)**, i.e., $F_x > 0$. Then we obtain $\nabla f(q)^T \ddot{q} = \dot{v}_\text{n} > 0$ and $\lambda_\text{n} = 0$: detachment from the constraint occurs because one pulls the mass m_1 toward the right. Assume now that initially case **(iiic)** occurs for some v_t. The only solution (at least from the mathematical point of view) is to escape from such a situation. Let us try the rule that consists of imposing a jump in v_t so that $v_\text{t}(t^+) = 0$. In fact if the conditions for $D_u^\mu = 0$ hold with say, $v_\text{t}(t^-) > 0$, then there always exists a selection $\xi(t) \in [-1, 1] = \text{sgn}(v_\text{t}(t^+))$ such that they no longer hold on the right of this instant: it suffices that $\xi(t) < 0$. Even better, there always exist such a $\xi(t)$ such that $D_u^\mu > 0$: it suffices to choose it small enough so that $m_1 \cos(\alpha)^2 + m_2 \sin(\alpha)^2 > \xi(t)\ \mu\ (m_1 - m_2)\cos(\alpha)\sin(\alpha)$. It remains to determine $\xi(t)$.

[53] As we shall see later with the Painlevé's paradoxes, such jump in the tangential velocity may be given a physical meaning, using a compliant model in the normal direction and letting the contact stiffness diverge to infinity.

Remark 5.27 It is noteworthy that a small enough $\mu < \mu_{\max}$ can cure all the above diseases by guaranteeing $D_u^\mu > 0$ whenever $v_\mathrm{t} \neq 0$ and for any m_1, m_2 and α, in accordance with Proposition 5.24. Here $\mu_{\max} = \frac{m_1 \cos(\alpha)^2 + m_2 \sin(\alpha)^2}{|m_1 - m_2| \cos(\alpha) \sin(\alpha)}$ (if $m_1 = m_2$ clearly $D_u^\mu = D_u > 0$ whatever μ: in such a case the mass matrix is mI_2 and the normal and tangential directions make a kinetic angle $\frac{\pi}{2}$, hence are dynamically decoupled).

5.5.5.2 Sticking Contact

Let us now assume that the contact is established with $\lambda_\mathrm{n} > 0$ and is in a sticking mode $v_\mathrm{t} = 0$ (and $f(q) = 0$). As for the foregoing system, our objective is to use the acceleration Coulomb's law to determine the conditions for stick/slip transitions with $\dot{v}_\mathrm{t} \neq 0$, or such that sticking persists with $\dot{v}_\mathrm{t} = 0$. Additional conditions are $f(q) = 0$ and $\nabla f(q)^T \dot{q} = v_\mathrm{n} = 0$ (for if $v_\mathrm{n} > 0$ the constraint is deactivated and $\lambda_\mathrm{n}(t^+) = 0$). If one wants to study the conditions under which contact persists then one adds $\nabla f(q)^T \ddot{q} = \dot{v}_\mathrm{n} = 0$, which forces a particular mode of the contact LCP (we call it the normal/tangential stick/stick mode). But if one admits that the system may detach from the constraint then $\dot{v}_\mathrm{n} \geq 0$ and the contact LCP holds.

The normal/tangential stick/stick mode implies that $\ddot{q}_1 = \ddot{y}_0 = 0$, and using the dynamical equation one finds $\lambda_\mathrm{n} = -\sin(\alpha) F_x$, $\lambda_\mathrm{t} = -\cos(\alpha) F_x$. The constraint of the friction cone then implies that $\frac{1}{\tan(\theta)} < \mu = \tan(\beta)$, hence $\beta > \frac{\pi}{2} - \alpha$. In such a case $F = (F_x, 0)^T \in \mathscr{C}$.

One has $\dot{v}_\mathrm{t} = \cos(\alpha)\ddot{q}_1 - \sin(\alpha)\ddot{y}_0 = a\lambda_\mathrm{n} + b\lambda_\mathrm{t} + cF_x$, with $a = \frac{m_1 - m_2}{m_1 m_2} \cos(\alpha) \sin(\alpha)$, $b = \frac{m_2 \cos(\alpha)^2 + m_1 \sin(\alpha)^2}{m_1 m_2}$, $c = \frac{\cos(\alpha)}{m_1}$, where the first equation in (5.162) has been used. When $\dot{v}_\mathrm{t} \neq 0$ Coulomb's law in acceleration states that $\lambda_\mathrm{t} = -\mu\lambda_\mathrm{n}\mathrm{sgn}(\dot{v}_\mathrm{t})$. Therefore, the stick/slip transition may occur if and only if the following generalized equation:

$$\begin{cases} 0 \leq D_u \lambda_\mathrm{n} + a\lambda_\mathrm{t} + \frac{\sin(\alpha)}{m_1} F_x \perp \lambda_\mathrm{n} \geq 0 \\ \lambda_\mathrm{t} \in -\mu\lambda_\mathrm{n}\mathrm{sgn}(a\lambda_\mathrm{n} + b\lambda_\mathrm{t} + cF_x) \\ \dot{v}_\mathrm{t} = a\lambda_\mathrm{n} + b\lambda_\mathrm{t} + cF_x, \end{cases} \tag{5.165}$$

is solvable (recall $D_u = D_u^0$). If it has a solution with $a\lambda_\mathrm{n} + b\lambda_\mathrm{t} + cF_x = 0$ then the normal/tangential stick/stick mode may occur (notice that for the previous particle case, problem (5.165) was greatly simplified since it was possible to choose the external forces such that the contact LCP holds with λ_n explicitly known). If $\dot{v}_\mathrm{t} > 0$ then the LCP matrix in (5.165) is $D_u - a\mu$. If $\dot{v}_\mathrm{t} < 0$ then it is equal to $D_u + a\mu$. One infers that there is always a possible mode where λ_n is unique, provided $\mathrm{sgn}(\dot{v}_\mathrm{t}) = -\mathrm{sgn}(a)$. The LCP matrix is equal to $D_u^\mu(\dot{v}_\mathrm{t}, m_1, m_2, \alpha)$ in (5.164). The situation is, however, different here because the system in (5.162) is an initial value problem

(IVP) for which the initial velocities and positions are arbitrary. Now we are in the process of choosing the acceleration, that is not a priori imposed. This is why we can safely choose a mode in which $D_u^{\mu}(\dot{v}_{\mathrm{t}}, m_1, m_2, \alpha) > 0$, and such a mode always exists.

Using (B.10), the support function definition and the material in Sect. B.2.1, let us rewrite (5.165) equivalently as:

$$\left\{\begin{array}{l} a\lambda_{\mathrm{n}} + b\lambda_{\mathrm{t}} + cF_x \in -\partial\Psi_{[-\mu\lambda_{\mathrm{n}},\mu\lambda_{\mathrm{n}}]}(\lambda_{\mathrm{t}}) \\ \\ D_u\lambda_{\mathrm{n}} + a\lambda_{\mathrm{t}} + \frac{\sin(\alpha)}{m_1}F_x \in -\partial\Psi_{\mathbb{R}^+}(\lambda_{\mathrm{t}}) \end{array}\right. \Leftrightarrow \left\{\begin{array}{l} \lambda_{\mathrm{t}} = \mathrm{proj}\left([-\mu\lambda_{\mathrm{n}}, \mu\lambda_{\mathrm{n}}]; -\frac{a}{b}\lambda_{\mathrm{n}} - \frac{c}{b}F_x\right) \\ \\ \lambda_{\mathrm{n}} = \mathrm{proj}\left(\mathbb{R}^+; -D_u^{-1}(a\lambda_{\mathrm{t}} + \frac{\sin(\alpha)}{m_1}F_x)\right) \end{array}\right. \tag{5.166}$$

It may be checked using (5.166) that $\dot{v}_{\mathrm{t}} > 0 \Leftrightarrow a\lambda_{\mathrm{n}} + cF_x > -b\lambda_{\mathrm{t}} \Rightarrow -\frac{a}{b}\lambda_{\mathrm{n}} - \frac{c}{b}F_x < -\mu\lambda_{\mathrm{n}} \Rightarrow \lambda_{\mathrm{t}} = -\mu\lambda_{\mathrm{n}}$. Similarly for $\dot{v}_{\mathrm{t}} > 0$ and $\dot{v}_{\mathrm{t}} = 0$. Starting from (5.157) an extension of (5.166) may be obtained, which provides a general way to treat the frictional contact problem in sticking mode.

5.5.6 *Non-Uniqueness of the Contact Force*

Let us consider the system depicted in Fig. 5.20. Friction acts at each contact point A_1 and A_2, with coefficients μ_1 and μ_2. The friction cones are depicted with dashed lines. Each friction cone has therefore a half-angle $\theta_i = \arctan(\mu_i)$, or $\tan(\theta_i) = \mu_i$. In Fig. 5.20 (a) we have $\theta_i < \frac{\pi}{2} - \alpha$, while in Fig. 5.20 (b) we have $\theta_i > \frac{\pi}{2} - \alpha$. The question is to know whether there exists none, a unique, or several contact forces which enable to keep the disk in contact with both points, while gravity is present and tends to pull the disk downward. In other words, can we find a

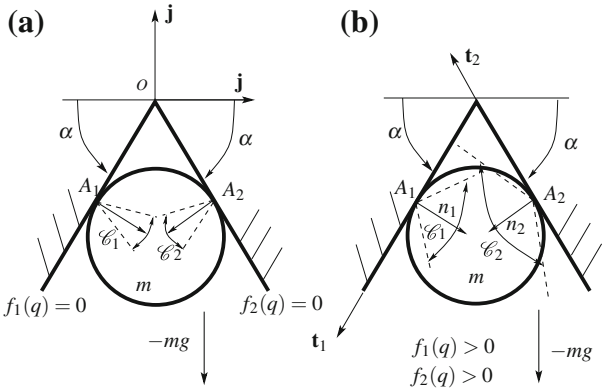

Fig. 5.20 A disk jammed in an angle

contact force inside the friction cones which can compensate for gravity? Clearly in case (a) no contact force inside the cones may compensate for gravity: the disk falls down. In case (b) an infinity of admissible contact forces may compensate for gravity and keep the disk jammed in the angle. Let the coordinates of the disk geometric center be x and y in the frame $(O, \mathbf{i}, \mathbf{j})$, and the disk orientation is θ, i.e., $q = (x, y, \theta)^T$. The local kinematics are defined with the frames $(A_1, \mathbf{t}_1, \mathbf{n}_1)$ and $(A_2, \mathbf{t}_2, \mathbf{n}_2)$. There are two unilateral constraints which express the signed distances at each contact point A_1 and A_2: $f_1(q) = \sin(\alpha)x - \cos(\alpha)y - r \geq 0$ and $f_2(q) = -\sin(\alpha)x - \cos(\alpha)y - r \geq 0$. Thus $\nabla f_1(q) = (\sin(\alpha), -\cos(\alpha))^T$ and $\nabla f_2(q) = (-\sin(\alpha), -\cos(\alpha))^T$. We assume that $\alpha \in [0, \frac{\pi}{2}]$. From Varignon's formula we infer the expression of V_{A_1} which yields $v_{\mathrm{t},1} = H_{\mathrm{t},1}(q)^T\dot{q} = -\cos(\alpha)\dot{x} - \dot{y}\sin(\alpha) + (x\sin(\alpha) - y\cos(\alpha))\dot{\theta}$. Similarly for the other contact with V_{A_2} which yields $v_{\mathrm{t},2} = H_{\mathrm{t},2}(q)^T\dot{q} = -\cos(\alpha)\dot{x} + \dot{y}\sin(\alpha) - (x\sin(\alpha) + y\cos(\alpha))\dot{\theta}$. The dynamics is written as follows:

$$\begin{pmatrix} m\ddot{x}(t) \\ m\ddot{y}(t) \\ I\ddot{\theta}(t) \end{pmatrix} = \begin{pmatrix} \sin(\alpha) & -\cos(\alpha) \\ -\cos(\alpha) & -\sin(\alpha) \\ 0 & x\sin(\alpha) - y\cos(\alpha) \end{pmatrix} \begin{pmatrix} \lambda_{\mathrm{n},1}(t) \\ \lambda_{\mathrm{t},1}(t) \end{pmatrix} + \begin{pmatrix} -\sin(\alpha) & -\cos(\alpha) \\ -\cos(\alpha) & \sin(\alpha) \\ 0 & -x\cos(\alpha) - y\sin(\alpha) \end{pmatrix} \begin{pmatrix} \lambda_{\mathrm{n},2}(t) \\ \lambda_{\mathrm{t},2}(t) \end{pmatrix} + \begin{pmatrix} 0 \\ -mg \\ 0 \end{pmatrix}$$

$$0 \leq \lambda_{\mathrm{n},1}(t) \perp f_1(q(t)) \geq 0, \quad 0 \leq \lambda_{\mathrm{n},2}(t) \perp f_2(q(t)) \geq 0. \tag{5.167}$$

Let us investigate the conditions that yield a static equilibrium with both contacts active. For that it is necessary that the two contact forces compensate for gravity. Taking $\ddot{y}(t) = 0$ this yields the following equation:

$$\begin{gathered} -\cos(\alpha)\lambda_{\mathrm{n},1} - \sin(\alpha)\lambda_{\mathrm{t},1} - \cos(\alpha)\lambda_{\mathrm{n},2} + \sin(\alpha)\lambda_{\mathrm{t},2} = mg \\ \Updownarrow \\ \lambda_{\mathrm{n},1}\cos(\alpha)[\tan(\alpha)\tan(\theta_1)\xi_1 - 1] - \lambda_{\mathrm{n},2}\cos(\alpha)[\tan(\alpha)\tan(\theta_2)\xi_2 + 1] = mg, \end{gathered} \tag{5.168}$$

with $\xi_1 \in \mathrm{sgn}(v_{\mathrm{t},1})$ and $\xi_2 \in \mathrm{sgn}(v_{\mathrm{t},2})$ (here both $v_{\mathrm{t},1} = v_{\mathrm{t},2} = 0$ and there is no reason that $\xi_1 = \xi_2$[54]), and $\lambda_{\mathrm{t},i} = -\mu_i\lambda_{\mathrm{n},i}\xi_i$. The case of Fig. 5.20 (a) corresponds to $\tan(\alpha)\tan(\theta_1) < 1$ and $\tan(\alpha)\tan(\theta_2) < 1$. Then $\tan(\alpha)\tan(\theta_1)\xi_1 - 1 < 0$ and $-\tan(\alpha)\tan(\theta_2)\xi_2 + 1 < 0$ for any $\xi_1, \xi_2 \in [-1, 1]$. Therefore, the Eq. (5.168) has no solution and there are no reaction forces which may compensate for gravity. Now suppose that $\tan(\alpha)\tan(\theta_1) > 1$ and $\tan(\alpha)\tan(\theta_2) > 1$, which is the case in Fig. 5.20 (b). Then there exists $\xi_1 \in [-1, 1]$ and $\xi_2 \in [-1, 1]$ such that $\tan(\alpha)\tan(\theta_1)\xi_1 - 1 > 0$ and $\tan(\alpha)\tan(\theta_2)\xi_2 + 1 < 0$. We can now solve the equation in (5.168) as $\lambda_{\mathrm{n},1} = \frac{mg + \cos(\alpha)[\tan(\alpha)\tan(\theta_2)\xi_2 + 1]\lambda_{\mathrm{n},2}}{\cos(\alpha)[\tan(\alpha)\tan(\theta_1)\xi_1 - 1]}$. Due to the symmetry of the geometry we may take $\lambda_{\mathrm{n},1} = \lambda_{\mathrm{n},2} = \lambda_{\mathrm{n}}$ which leads to $\lambda_{\mathrm{n}} = \frac{1}{\cos(\alpha)} \frac{mg}{\tan(\alpha)\tan(\theta_1)\xi_1 - 1 - \tan(\alpha)\tan(\theta_2)\xi_2 - 1} > 0$. If $\lambda_{\mathrm{n},1} = \lambda_{\mathrm{n},2} = \lambda_{\mathrm{n}}$ the static equilibrium along the $(O, \mathbf{i})$ axis yields the

[54] A common mistake is to state that $\xi_1 = \xi_2$ because they both belong to $\mathrm{sgn}(0)$, which is wrong.

necessary and sufficient condition $\tan(\theta_1)\xi_1 = -\tan(\theta_2)\xi_2 \Leftrightarrow \mu_1\xi_1 = -\mu_2\xi_2$. Therefore, $\lambda_n(t) = \frac{1}{\cos(\alpha)} \frac{mg}{\tan(\alpha)\tan(\theta_1)[\xi_1(t)+\xi_2(t)]-2}$. We see using the above conditions that in case (b) there is an infinity of choices for $\xi_1 + \xi_2$ such that $\lambda_n(t) > 0$.

We may also want to analyze the contact LCP as in (5.158). Certainly, the conditions of Proposition 5.24 will hamper the static equilibrium since they guarantee uniqueness.

5.5.7 Comments

1. The above problem was treated in details (most probably for the first time, when complementarity theory was not yet born) in the frictionless case by Etienne Delassus [333, 335].
2. From the point of view of the dynamics' well-posedness, such contact force nonuniqueness issues may not have serious consequences if the motion is unique. From this point of view this is the same as a hyperstatic system (a chair with four legs in static equilibrium on a rigid ground) for which an infinity of contact forces guarantees the equilibrium. Hyperstaticity is, however, due to dependent constraints yielding a singular contact gradient matrix, while here it is rather the set-valued feature of Coulomb's friction which is the cause of non-uniqueness. Moreover, non-uniqueness issues due to hyperstaticity may be cured by introducing compliance at the contacts. This is not the case for the problem we just studied: *normal compliance at A_1 and A_2 will not imply uniqueness of the contact forces, because Coulomb's friction is the source of the problem. One should also regularize Coulomb's friction law, thereby destroying set-valued sticking modes.*
3. As is known one way to recover uniqueness of contact forces is to introduce some compliance at the contact in the normal direction, or to consider a flexible body. However, first the choice of a good compliant model may not always be obvious; second, this may yield stiff differential equations; third, the estimation of the compliant model parameters may not be straightforward.
4. The behavior of numerical algorithms facing such situations also has to be considered. This is discussed in [899] for time-stepping schemes (see Sect. 5.7.3): the iterative solver used to solve the one-step nonsmooth problem (for instance a Gauss–Seidel algorithm) chooses one particular contact force which depends on the initial guess.
5. A general analysis of three-dimensional sticking unilateral contact with facetized friction cone is made in the seminal article [963] and others [1216, 1217]. Coulomb in acceleration is used for stick-to-slip transition analysis. An LCP $0 \leq \lambda \perp A\lambda + q \geq 0$ (whose unknowns are the contact force multipliers λ) is built and it is proved that under the assumption that $q^T\lambda \geq 0$ for all λ inside the friction cones minus the kernel of the contact matrices, then the all-sticking case is always solvable. In [46], sliding friction is assumed and the notion of *disassemblable* system is introduced, which implies the copositivity of the LCP

matrix and the solvability of the contact LCP for small enough friction coefficient.

5.6 Painlevé's Paradoxes: Sliding Rod Example

The system of Sect. 5.5.4 has no couplings between tangential and normal directions at contact (see the contact LCP in (5.160), while the system in Sect. 5.5.5 has nonzero couplings (see the contact LCP in (5.163) and the LCP matrix in (5.164)). The consequences are a more complex behavior, and some inconsistent configurations. Let us now analyze a system which has couplings also, and in addition the LCP matrix depends on the configuration q, which is not the case of D_u^μ in (5.164).

Inconsistencies and indeterminacies due to Coulomb's friction have been known for a long time [116, 117, 161, 334, 336, 498, 499, 619, 674, 712, 761, 862, 955, 1016]. They may be considered as the dynamical counterpart of the well-known locking phenomenon of statics.[55] Historically, they have been noticed by Jellet [619] and have been made popular by the French scientist Paul Painlevé [954, 955]. The possibility of solutions with velocity discontinuities (which may be thought of as *tangential impacts*) has been first recognized by Lecornu [712], or perhaps more or less at the same time by Bolotov [161]. For this reason Moreau named tangential impacts Lecornu's frictional catastrophes [894]. As we shall see next, the classical sliding rod system has indeterminacies (the contact LCP has several solutions) and inconsistencies (the contact LCP has no solution). There is a peculiarity of this system: if initialized in a well-posed sliding regime where its dynamics is an ODE, it may reach the neighborhood of a point in the $(\theta, \dot{\theta})$ plane (θ is the rod orientation) where the ODE has a singularity. Moreover, this singular ODE cannot be analyzed with the results available in the mathematical literature on singular ODEs. The first detailed results on this particular feature of the Painlevé classical example were published in [436, 437].

5.6.1 The Dynamics of Painlevé's Example

Let us consider the example of a planar slender rod sliding on a rigid surface, with Coulomb's friction at the contact point A, as depicted in Fig. 5.21. We have $||AG|| = l$, the half length of the rod, and we suppose for simplicity that $m = 1$ kg, so that the inertia moment along (G, z) is $I = \frac{l^2}{3}$ kg m^2. We introduce two sets of generalized coordinates: $q = (x, y, \theta)^T$ and $z = (x_a, y_a, \theta)^T$. In q-coordinates, the constraint is given by:

[55] Which is, by the way, extremely useful in some practical instances, where one desires to prevent any relative motion between two bodies.

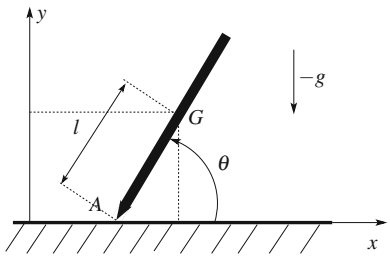

Fig. 5.21 Painlevé's example

$$f(q) = y - l\sin(\theta) \geq 0, \tag{5.169}$$

and by

$$f(z) = y_a \geq 0 \tag{5.170}$$

in z-coordinates.[56] The external actions on the rod are gravity plus the reaction at the contact point A, i.e., $\begin{pmatrix}\lambda_t\\ \lambda_n\end{pmatrix}$, in the Galilean frame.[57] The friction coefficient is $\mu \geq 0$. We assume that contact is established, and that $\dot{x}_a$ is negative (one "pushes" the rod), hence $\lambda_t \in -\mu\lambda_n \text{sgn}(\dot{x}_a) = \mu\lambda_n$. It is also supposed that the orientation satisfies $\theta \in (0, \frac{\pi}{2})$, for otherwise a negative $\dot{x}_a$ would correspond to "pulling" the rod instead of "pushing"). The Jacobian between $\dot{q}$ and $\dot{z}$ is given by $J(\theta) = \begin{pmatrix}1 & 0 & l\sin(\theta)\\ 0 & 1 & -l\cos(\theta)\\ 0 & 0 & 1\end{pmatrix}$, i.e., $\dot{z} = J(\theta)\dot{q}$. Since there is no torque acting on the rod at point A, the dynamical equations in a sliding regime are given by:

$$\begin{cases}\ddot{x}(t) = \mu\lambda_n(t)\\ \ddot{y}(t) = -g + \lambda_n(t)\\ I\ddot{\theta}(t) = (\mu\sin(\theta(t)) - \cos(\theta(t)))\, l\lambda_n(t)\end{cases} \tag{5.171}$$

in q-coordinates, and by (time argument is dropped):

$$\begin{pmatrix}1 & 0 & -l\sin(\theta)\\ 0 & 1 & l\cos(\theta)\\ -l\sin(\theta) & l\cos(\theta) & l^2 + I\end{pmatrix}\begin{pmatrix}\ddot{x}_a\\ \ddot{y}_a\\ \ddot{\theta}\end{pmatrix} = \begin{pmatrix}l\dot{\theta}^2\cos(\theta)\\ l\dot{\theta}^2\sin(\theta)\\ 0\end{pmatrix} + \begin{pmatrix}0\\ -g\\ -gl\cos(\theta)\end{pmatrix} + \begin{pmatrix}\mu\lambda_n\\ \lambda_n\\ 0\end{pmatrix} \tag{5.172}$$

in z-coordinates. The inverse of the inertia matrix in z-coordinates is given by:

[56] With our previous notations, we clearly have $\dot{y}_a = v_n$, and $\dot{x}_a = v_t$.

[57] The subscript u for unilateral is dropped to simplify the notations.

$$M_z^{-1} = \begin{pmatrix} 1 + \frac{l^2}{I}\sin^2(\theta) & -\frac{l^2}{I}\sin(\theta)\cos(\theta) & \frac{l}{I}\sin(\theta) \\ -\frac{l^2}{I}\sin(\theta)\cos(\theta) & 1 + \frac{l^2}{I}\cos^2(\theta) & -\frac{l}{I}\cos(\theta) \\ \frac{l}{I}\sin(\theta) & -\frac{l}{I}\cos(\theta) & \frac{1}{I} \end{pmatrix} \tag{5.173}$$

from which it can be calculated that:

$$\begin{cases} \ddot{x}_a = l\dot{\theta}^2\cos(\theta) + \left(\mu + \mu\frac{l^2}{I}\sin^2(\theta) - \frac{l^2}{I}\sin(\theta)\cos(\theta)\right)\lambda_{\mathrm{n}} \\ \ddot{y}_a = A(\theta)\dot{\theta}^2 + B(\theta,\mu)\lambda_{\mathrm{n}} - g \\ \ddot{\theta} = (\mu\sin(\theta) - \cos(\theta))\frac{l}{I}\lambda_{\mathrm{n}}, \end{cases} \tag{5.174}$$

with:

$$\begin{cases} A(\theta) = l\sin(\theta) \\ B(\theta,\mu) = 1 + \frac{l^2}{I}\cos(\theta)(\cos(\theta) - \mu\sin(\theta)). \end{cases} \tag{5.175}$$

The identification of the various terms in (5.1) (a) is easy from the above, in q or z generalized coordinates.

5.6.2 The Contact LCP

The contact LCP is constructed from the complementarity condition and then using (5.158):

$$0 \le \lambda_{\mathrm{n}} \perp \ddot{y}_a \ge 0 \iff 0 \le \ddot{y}_a = D_u^{\mu}(\theta)\lambda_{\mathrm{n}} - b(\theta,\dot{\theta}) \perp \lambda_{\mathrm{n}} \ge 0, \tag{5.176}$$

where $D_u^{\mu}(\theta) = e_2^T M_z^{-1} e_2 = 1 + \frac{l^2}{I}\cos^2(\theta) = D_u > 0$ if there is no friction, $e_2^T = (0,1,0) = \nabla f(z)$, and $D_u^{\mu}(\theta) = e_2^T M_z^{-1}\begin{pmatrix} \mu \\ 1 \\ 0 \end{pmatrix} = B(\theta,\mu)$ if there is sliding friction with negative $\dot{x}_a$. The term $b(\theta,\dot{\theta}) = g - A(\theta)\dot{\theta}^2$. Provided its matrix is symmetric $\succ 0$, the contact LCP can be phrased as a quadratic program as follows:

$$\text{minimize}_{\lambda_{\mathrm{n}}}\ \lambda_{\mathrm{n}}^2 - b\lambda_{\mathrm{n}},\ \text{subject to}\ \begin{cases} D_u^{\mu}(\theta)\lambda_{\mathrm{n}} \ge b \\ \lambda_{\mathrm{n}} \ge 0. \end{cases} \tag{5.177}$$

The function $D_u^{\mu}(\theta)\lambda_{\mathrm{n}}^2 - b\lambda_{\mathrm{n}}$ is zero for every λ_{n} that satisfies the LCP. The contact LCP is also equivalently rewritten as the generalized equation: $D_u^{\mu}(\theta)\lambda_{\mathrm{n}} - b(\theta,\dot{\theta}) \in -\partial\psi_{\mathbb{R}^+}(\lambda_{\mathrm{n}})$.

The whole problem for the calculation of the interaction force is to find whether the LCP possesses a solution, several solutions, or no solution. One sees that the big discrepancy between the LCP matrix in (5.164) and the one of Painlevé's examples is that the latter depends on the system's coordinate θ. Hence, the properties of $D_u^{\mu}(\theta)$

may change along the trajectories. Several solutions correspond to an *undetermined* problem, something commonly encountered in rigid body dynamics. No solution (in the space of bounded λ_n) corresponds to an *inconsistent* problem: the space of possible solutions has to be modified in order to render the LCP solvable.

5.6.2.1 Indeterminacy

Let us assume that the configuration at time t is such that(we drop the argument t for convenience) $A(\theta)\dot{\theta}^2 - g = 1$, and that $\dot{y}_a = 0$ (*i.e.,* there is no normal relative initial velocity). Let us further assume that $B(\theta, \mu) = -1$ (this is possible with suitable choice of $\mu > 0$). Then the LCP in (5.176) becomes:

$$0 \leq -\lambda_n + 1 \perp \lambda_n \geq 0. \tag{5.178}$$

There are two solutions to (5.178): the first one is $\lambda_n = 0$ (no reaction at the contact point, and the rod is grazing the constraint), and the second one is $\lambda_n = 1$ (the two bodies do not break contact). It is *a priori* impossible to choose among these two solutions: the rigid body model tells us that they are both likely to occur. Let us relate this to the integration of the dynamical system in Fig. 5.21. In a sliding regime $y_a \equiv 0$, as long as $B(\theta, \mu) > 0$ and $A(\theta)\dot{\theta}^2 - g < 0$, then one can compute in a *unique* way $\lambda_n = -\frac{A(\theta)\dot{\theta}^2 - g}{B(\theta,\mu)} > 0$. Now if it happens that both $B(\theta, \mu)$ and $A(\theta)\dot{\theta} - g$ tend to zero simultaneously (or if the numerator tends to zero more rapidly than the denominator), then λ_n remains positive and the system can go through this singularity without any problem. However, if after this time one finds $B(\theta, \mu) < 0$ and $A(\theta)\dot{\theta}^2 - g > 0$, both $\lambda_n = 0$ and $\lambda_n = -\frac{A(\theta)\dot{\theta}^2 - g}{B(\theta,\mu)}$ are solutions to the LCP.

5.6.2.2 Inconsistency

Let us now assume that the configuration is such that $\dot{\theta} = 0$. The rod is sliding horizontally. The LCP in (5.176) hence becomes:

$$0 \leq B(\theta, \mu)\lambda_n - g \perp \lambda_n \geq 0. \tag{5.179}$$

For the first inequality in (5.179) to be verified together with the second one, one must have $B(\theta, \mu) > 0$: this is a *feasibility* condition. If feasibility holds, there exists a bounded $\lambda_n \geq 0$ solution of the LCP. Otherwise, if μ is such that $B(\theta, \mu) < 0$, no bounded positive λ_n can assure that $\ddot{y}_a \geq 0$. In other words, any bounded positive reaction at the contact point will not be sufficient to prevent interpenetration of the two bodies. Intuitively, if one tries to simulate such a configuration using a compliant approximating problem (replacing the surface by a linear spring–damper so that $\lambda_n = -ky_a - f\dot{y}_a$), then (5.174) will become:

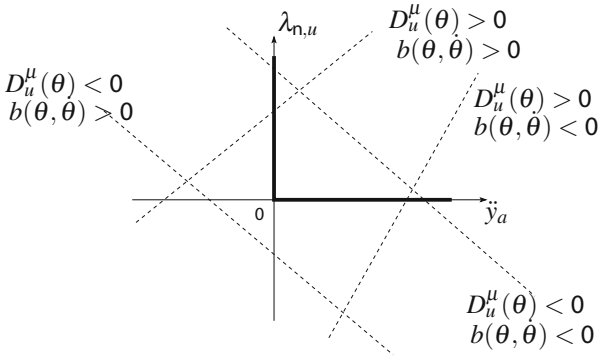

Fig. 5.22 Inconsistencies and indeterminacies for the contact LCP in (5.176)

$$\ddot{y}_a(t) = -B(\theta(t), \mu)(k y_a(t) - f \dot{y}_a(t)) - g, \tag{5.180}$$

which represents an unstable order two system. Hence, y_a may have the tendency to grow without bound, and the interaction force will do as well. If we let k grow without bound, we see that by continuity of $B(\theta, \mu)$ as a function of θ, there will be a nonzero time interval during which the interaction force will grow unbounded as well, since $B(\theta, \mu) < 0$ on this interval so that $y_a(\cdot)$ continues to decrease. A deep analysis of the system's behavior as $k \to +\infty$ is made in [1329]. Anyway, what is interesting and noteworthy is the fact that Coulomb's law of friction creates this sort of positive feedback, which would be impossible without friction, see Remark 5.28.

In summary, given μ and the system's physical parameters, an *indeterminacy* occurs for couples $(\theta, \dot\theta)$ such that the LCP in (5.176) has more than one solution. An *inconsistency* occurs for couples $(\theta, \dot\theta)$ such that the LCP has no solution. Various cases are depicted in Fig. 5.22.

Remark 5.28 (Varying Coefficient of Friction, and Other Models) First of all notice that if $\mu = 0$, then $B(\theta, 0) = \frac{l^2}{I}\cos^2(\theta) + 1 > 0$. Hence, the frictionless case is always consistent and determinate. In fact it may be calculated that the contact LCP matrix $B(\theta, \mu) > 0$ for all $\mu \in [0, \frac{4}{3})$. Hence, if $\mu < \mu_c = \frac{4}{3}$, the contact LCP is always well-posed with a unique solution, whatever the position and velocity. Assume now that the friction model incorporates a varying coefficient $\mu(\dot{x}_a)$ as depicted in Fig. 5.9a. The contact LCP matrix is $B(\theta, \mu(\dot{x}_a)) = 1 + \frac{l^2}{I}\cos(\theta)(\cos(\theta) - \mu(\dot{x}_a)\sin(\theta))$, with $\mu(\dot{x}_a) > 0$ and $\lambda_t(t) = \mu(\dot{x}_a(t))\lambda_n(t)$ for $\dot{x}_a(t) < 0$. Looking at (5.182) we see that the value of $\mathscr{B}(\theta, \mu)$ is affected by the variation of the coefficient of friction, and therefore the critical angles in (5.183) will be affected too. It seems that the extension of Painlevé paradoxes analysis to such case has never been tackled. In the same vein , the Coulomb–Orowan's and Coulomb–Shaw's models could be inserted in the study. These models take the following form. $||F_t|| \le \bar\mu$ with if $||F_t|| < \bar\mu$ then $v_{r,t} = 0$, if $||F_t|| = \bar\mu$ then there exists $\beta \ge 0$ such that $v_{r,t} = -\beta F_t$. In Coulomb–Orowan's law, $\bar\mu = \min(\mu F_n, \kappa)$, where κ is usually

taken as the elastic limit of the material. In Coulomb–Shaw's law, $\bar{\mu} = \alpha\kappa$, where α is related to the contact surface involved in the asperities flattening and depends on the normal pressure at contact. Seen in the planar case, both models modify Coulomb's friction with a saturation of F_{t} after a certain threshold.

5.6.3 *Analysis of the Dynamical Singularities*

Let us introduce the problem another way. Assume the system is initialized in a sliding regime where the LCP and the dynamical system possess unique solutions on an interval $[0, t_0)$ with $t_0 > 0$. In particular on $t \in [0, t_0)$ one has $\lambda_{\mathrm{n}}(t) \geq 0$ and $\ddot{y}_a(t) = 0$. Classically, one calculates λ_{n} from (5.174) to get

$$\lambda_{\mathrm{n}} = \frac{1}{B(\theta, \mu)}(g - A(\theta)\dot{\theta}^2). \tag{5.181}$$

Introducing (5.181) into the dynamics of the sliding regime toward the left ($\dot{x}_a(t) < 0$), one gets [437]:

$$\begin{aligned} \ddot{\theta}(t) &= \tfrac{3}{l}[-\cos(\theta(t)) + \mu\sin(\theta(t))]\tfrac{g - l\dot{\theta}(t)^2\sin(\theta(t))}{1+3\cos(\theta(t))[\cos(\theta(t)) - \mu\sin(\theta(t))]} \\ &\triangleq \mathscr{C}(\theta(t), \mu)\tfrac{\mathscr{A}(\theta(t), \dot{\theta}(t))}{\mathscr{B}(\theta(t), \mu)} \end{aligned} \tag{5.182}$$

This ordinary differential equation (ODE) is central in the study of the Painlevé rod system. It is *singular* since the vector field may diverge to infinity in the vicinity of the critical angle values given by:

$$\theta_{c_1}(\mu) = \arctan\left(\frac{3\mu - \sqrt{9\mu^2 - 16}}{2}\right), \quad \theta_{c_2}(\mu) = \arctan\left(\frac{3\mu + \sqrt{9\mu^2 - 16}}{2}\right). \tag{5.183}$$

We may define the four singular points of the contact LCP as $P_{c_1}^{\pm} = \begin{pmatrix} \theta_{c_1} \\ \dot{\theta}_{c_1} \end{pmatrix}$ and $P_{c_2}^{\pm} = \begin{pmatrix} \theta_{c_2} \\ \dot{\theta}_{c_2} \end{pmatrix}$, $\dot{\theta}_{c_1} = \pm\sqrt{\frac{g}{l\sin(\theta_{c_1})}}$, $\dot{\theta}_{c_2} = \pm\sqrt{\frac{g}{l\sin(\theta_{c_2})}}$, see Fig. 5.23. Singular ODEs have been analyzed in the mathematical literature. However, it is noteworthy that the singular ODE in (5.182) does not satisfy the assumptions usually required in well-posedness analysis [144, Hypotheses4–8]. Figure 5.23 shows the various modes of the LCP that corresponds to this sliding regime. The LCP modes are constructed from (5.174)–(5.176), by studying the signs of $B(\theta, \mu)$ and $b(\theta, \dot{\theta}) = g - l\dot{\theta}^2\sin(\theta)$, see (5.174).

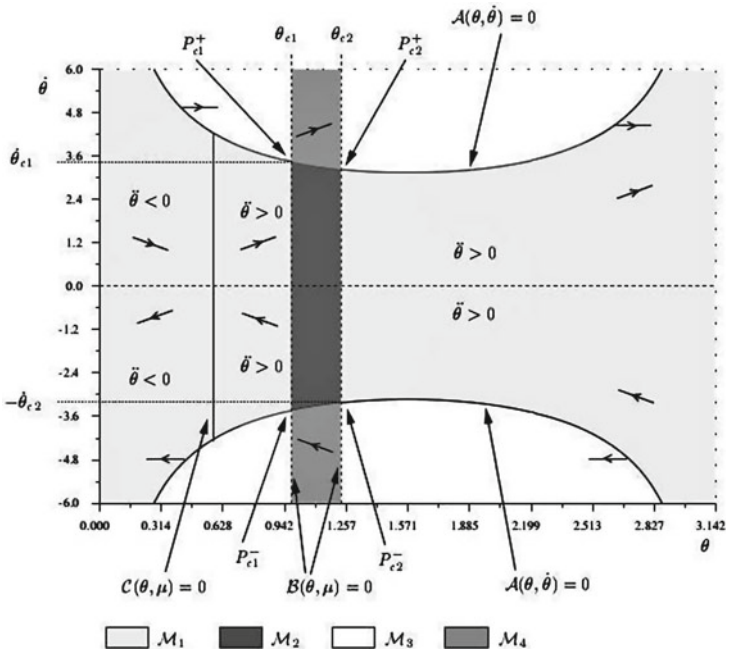

Fig. 5.23 The sliding regime LCP modes

In $\mathscr{M}_1$ and $\mathscr{M}_3$ the LCP has a unique solution λ_n. In $\mathscr{M}_2$ there is no solution at all, and in $\mathscr{M}_4$ there are two solutions. The superscript $+$ is for positive $\dot\theta$, the superscript $-$ is for negative $\dot\theta$. Now our problem is to investigate how the orbits in the $(\theta, \dot\theta)$ plane evolve. Notice that the vector field in (5.182) does not depend on the other state variables. Two main questions arise when looking at Fig. 5.23: what happens when the trajectories start in a mode with a well-posed LCP (like $\mathscr{M}_1$) and evolve toward a neighborhood of the singular points $P_{c_i}^{\pm}$? What can be done if trajectories are initialized in, or enter mode $\mathscr{M}_2$?[58]

The first question is tricky, mainly because in (5.182) both $\mathscr{B}(\theta, \mu)$ and $\mathscr{A}(\theta, \dot\theta)$ tend to zero when orbits approach the critical points $P_{c_i}^{\pm}$. Moreover, below those points, the vector field is tangent to the line $\theta = \theta_{c_1}$. Hence, the results on singular ODEs that based on some transversality conditions in the vicinity of the singular subspace [398] cannot be used here. The following results are proved in [437], and are useful to understand how the system behaves in the neighborhood of the critical points.

Proposition 5.27 *[437] Assume that there exists* $t_1 \geq 0$ *such that* $(q, \dot q) \in \mathscr{M}_1^+ \cup \mathscr{M}_4^-$, *with* $\arctan(\frac{1}{\mu}) < \theta(t_1) < \theta_{c_1}$.

[58] It seems that Painlevé paradoxes are reduced in the relevant literature to the second issue, while the first one remained ignored until [436, 437].

- *If* $\frac{4}{3} \leq \mu < \frac{8}{3\sqrt{3}}$, *then detachment or sticking occurs and the contact force* $\lambda_{\mathrm{n}}(t) = \frac{\mathscr{A}(t)}{\mathscr{B}(t)}$ *always remains bounded.*
- *If* $\mu \geq \frac{8}{3\sqrt{3}}$, *then*
  - *either the orbit passes above the critical line passing through* $P_{c_1}^{\pm}$ *and with slope* $\frac{\dot{\theta}_{c_1} - \dot{\theta}(t_v)}{\theta_{c_1} - \theta(t_v)} = \frac{\alpha_2^{\pm}}{\alpha_1^{\pm} - \alpha_3^{\pm}}$, *and the rod stops sliding or detaches.*
  - *or the orbit passes below the same critical line in the neighborhood of* $P_{c_1}^{\pm}$ *and*
    - *If* $\dot{x}_a(t_v) < \dot{x}_a^{\mathrm{stick}}(t_v)$, *then the rod keeps sliding and the orbit passes through* $P_{c_1}^{\pm}$. *The contact force becomes infinite but its impulse is bounded.*
    - *If* $\dot{x}_a(t_v) \geq \dot{x}_a^{\mathrm{stick}}(t_v)$, *then A sticks before* $P_{c_1}^{\pm}$ *is reached. The contact force remains bounded.*
  - *or the orbit lies on the critical line and reaches* $P_{c_1}^{\pm}$ *at* $t = t_{c_1}$ *with*

$$\lim_{t \to t_{c_1}^-} \lambda_{\mathrm{n}}(t) = \frac{\alpha_1^{\pm}\alpha_2^{\pm}}{\alpha_4^{\pm}\mathscr{C}(\theta_{c_1}, \mu)\left(\alpha_1^{\pm} - \alpha_3^{\pm}\right)} < +\infty. \tag{5.184}$$

where:

$$\begin{cases} \alpha_1^{\pm} = \frac{\partial \mathscr{B}}{\partial \theta}(\theta_{c_1}, \mu)\dot{\theta}_{c_1}^{\pm} = \frac{3\dot{\theta}_{c_1}^{\pm}}{m}[\mu 2\cos\theta_{c_1}(\sin\theta_{c_1} + \mu\cos\theta_{c_1})] \\ \alpha_2^{\pm} = \mathscr{C}(\theta_{c_1}, \mu)\frac{\partial \mathscr{A}}{\partial \theta}(\theta_{c_1}, \dot{\theta}_{c_1}^{\pm}) = -\frac{\dot{\theta}_{c_1}^{\pm 2}}{m} \\ \alpha_3^{\pm} = \mathscr{C}(\theta_{c1}, \mu)\frac{\partial \mathscr{A}}{\partial \dot{\theta}}(\theta_{c_1}, \dot{\theta}_{c1}^{\pm}) = \frac{6}{m}(\cos\theta_{c_1} - \mu\sin\theta_{c1})\dot{\theta}_{c1}^{\pm}\sin\theta_{c1} \\ \alpha_4^{\pm} = \frac{\partial \mathscr{B}}{\partial \theta}(\theta_{c_1}, \mu) = \frac{3}{m}[\mu - 2\cos\theta_{c_1}(\sin\theta_{c_1} + \mu\cos\theta_{c_1})] \\ \dot{x}_a^{\mathrm{stick}}(t_v) \triangleq l(\dot{\theta}(t_v)\sin(\theta(t_v) - \dot{\theta}_{c_1}^{\pm}\sin(\theta_{c_1})) - \frac{\mu}{m}p_{\mathrm{n}}(t_{c_1}). \end{cases} \tag{5.185}$$

The time t_v *is such that the system enters a sufficiently small neighborhood of* $P_{c_1}^{\pm}$, t_{c_1} *is the time when the orbits attain* $P_{c_1}^{+}$, *and the impulse* $p_{\mathrm{n}}(t)$ *is defined in the next Lemma.*

An interesting point here is that the "critical" friction coefficient is bigger than μ_c in Remark 5.28. The analysis allows to refine the friction upperbound. We also have the following.

Lemma 5.5 *[437] Suppose that the trajectory attains* $P_{c_1}^{\pm}$ *at time* t_{c_1}. *There exists* t_v *such that on* $[t_v, t_{c_1}]$ *the nonlinear system (5.186) is equivalent to its tangent linearization. Then*

- *If* $\frac{4}{3} < \mu < \frac{8}{3\sqrt{3}}$, $\lim_{t \to t_{c_1}} \ddot{\theta}^{\pm}(t) = \frac{\alpha_1^{\pm}\alpha_2^{\pm}}{\alpha_4^{\pm}(\alpha_1^{\pm} - \alpha_3^{\pm})} < 0$.
- *If* $\mu > \frac{8}{3\sqrt{3}}$:
  - *If* $\frac{\dot{\theta}_{c_1}^{\pm} - \dot{\theta}(t_v)}{\theta_{c_1} - \theta(t_v)} > \frac{\alpha_2^{\pm}}{\alpha_1^{\pm} - \alpha_3^{\pm}}$, *then* $\lim_{t \to t_{c_1}, t < t_{c_1}} \ddot{\theta}^{\pm}(t) = \pm\infty$.
  - *If* $\frac{\dot{\theta}_{c_1}^{\pm} - \dot{\theta}(t_v)}{\theta_{c_1} - \theta(t_v)} < \frac{\alpha_2^{\pm}}{\alpha_1^{\pm} - \alpha_3^{\pm}}$, *then* $\lim_{t \to t_{c_1}, t < t_{c_1}} \ddot{\theta}^{\pm}(t) = \mp\infty$.
  - *If* $\frac{\dot{\theta}_{c_1}^{\pm} - \dot{\theta}(t_v)}{\theta_{c_1} - \theta(t_v)} = \frac{\alpha_2^{\pm}}{\alpha_1^{\pm} - \alpha_3^{\pm}}$, *then* $\lim_{t \to t_{c_1}, t < t_{c_1}} \ddot{\theta}^{\pm}(t) = \frac{\alpha_1^{\pm}\alpha_2^{\pm}}{\alpha_4^{\pm}(\alpha_1^{\pm} - \alpha_3^{\pm}} > 0$.

- *If* $\mu = \frac{8}{3\sqrt{3}}$ *then* $\lim_{t\to t_{c_1}, t<t_{c_1}} \ddot{\theta}^{\pm}(t) = \mp\infty$.

If it happens that $\lim_{t\to t_{c_1}} \ddot{\theta}^{\pm}(t) = +\infty$, *then* $\lim_{\tau\to t_{c_1}, \tau<t_{c_1}} p_{\mathrm{n}}(\tau) \stackrel{\Delta}{=} \int_{t_v}^{\tau} \lambda_{\mathrm{n}}(t)dt < +\infty$, *and*

- *If* $\dot{x}_a(t_v) < \dot{x}_a^{\mathrm{stick}}(t_v)$, *then the rod keeps sliding and* $P_{c_1}^{\pm}$ *is reached.*
- *If* $\dot{x}_a(t_v) > \ (=)\dot{x}_a^{\mathrm{stick}}(t_v)$, *then the contact point A sticks at* $t = t^* < \ (=)t_{c_1}$, *and*
  - *if the trajectory is in* $\mathscr{M}_1^+$, *then* $y_a(t^{*,+}) = 0$ *and* $\dot{x}_a(t^{*,+}) = 0$,
  - *if the trajectory is in* $\mathscr{M}_4^+$, *then* $y_a(t^{*,+} > 0$ *and the rod detaches at the same time* t^*.

Proposition 5.27 and Lemma 5.5 allow one to determine how the trajectories behave in the vicinity of singular points. Their proofs mainly rely on the study of the following nonlinear system in the neighborhood of the critical points $P_{c1}^{\pm}$:

$$\begin{cases} \frac{dx_1}{ds} = \mathscr{B}(x_1, \mu)x_2 \\ \frac{dx_2}{ds} = \mathscr{C}(x_1, \mu)\mathscr{A}(x_1, x_2) \\ \frac{dt}{ds} = \mathscr{B}(x_1, s). \end{cases} \tag{5.186}$$

This system is obtained from (5.182) after a suitable timescale. Such a procedure is classical for the study of singular ODEs [398]. The time t_v is such that the linearization of the system in (5.186) around the critical point (that now corresponds to a fixed point of the system in (5.186)) is valid. The center manifold theorem is used in the analysis, because the linearization is degenerated (the fixed point is not hyperbolic, some eigenvalues of the Jacobian are always equal to 0). These results are in accordance with the mathematical result in [1142] who uses a quite different way to show that the velocity $\dot{q} \in RCLBV$ (hence, it possesses right and left limits, but this does not hamper $\ddot{q}$ to be unbounded).

Remind that the contact LCP is $0 \le \mathscr{B}(\theta, \mu)\lambda_{\mathrm{n}} - \mathscr{A}(\theta, \dot{\theta}) \perp \lambda_{\mathrm{n}} \ge 0$. Concerning the second question (what if orbits tend to enter the LCP mode $\mathscr{M}_2$, or if the system is initialized therein), notice the following: inconsistency in mode $\mathscr{M}_2$ in the rod example comes from the fact that the configuration is such that $\mathscr{B}(\theta, \mu) < 0$ and $\dot{\theta} = 0$. Now it is clear from (5.174) that there is always a value of $\dot{\theta} \neq 0$ such that even if $\mathscr{B}(\theta, \mu) < 0$, then $\lambda_{\mathrm{n}} \ge 0$ and $\ddot{y}_a \ge 0$ are solutions of the LCP (this is true at least in the first quadrant for θ, since then $\mathscr{A}(\theta, \dot{\theta}) > 0$). This means that if the configuration is inconsistent at time t_0, there exists at least a jump of the velocity $\dot{\theta}$ such that $\dot{\theta}(t_0^+)$ renders the LCP solvable on an interval $(t_0, t_0 + \delta)$, for some $\delta > 0$. But obviously from the developments on MDEs in Chap. 1 such a jump must be accompanied by an impulsive reaction at the contact point: this is an *impact without collision*, or IW/OC. Then $\lambda_{\mathrm{n}} = p_{\mathrm{n}}(t_k)\delta_{t_k}$ and $F_{\mathrm{t}} = p_{\mathrm{t}}(t_k)\delta_{t_k}$ for some time t_k.[59] Some questions arise:

- Should an IW/OC occur only when there is inconsistency?

[59] We adopt here the notation t_k for an eventual time of tangential impact to remain consistent with the rest of the book.

- How can we compute the velocity jump?
- Is it unique?
- If a system is initialized in a sliding regime, will it attain an inconsistent configuration $\mathscr{M}_2$ of its LCP or not?
- If such an IW/OC occurs, where does it originates from? What is the physical phenomenon that produces it?

The fourth question has been examined in [436]. As pointed out above, one should not confuse inconsistencies with configurations at which the contact force may diverge to infinity in finite time: IW/OCs are not be related to finite escape of $\lambda_n(t)$. The fifth question has been analyzed by Le Suan An in [708] and [709, §4.3,4.4] for the case of a bilateral constraint with Coulomb friction (a typical benchmark is depicted in Fig. 5.24). Therein, IW/OCs have been justified as the limit behavior of a sequence of penalized problems. We shall come back on those studies later in this section. Concerning the second question, Baraff [89, §8.1] proposed the following rules, similar to others long before him [161, 954]:

- (a) Since inconsistency is caused by dynamic friction, the impulse must convert at least one of the contact points to static friction.
- (b) The contact impulse must be such that the bodies do not separate after the discontinuity.

The first statement signifies in the sliding rod example that the jump in $\dot{\theta}$ must be such that the rod stops sliding, *i.e.,* $\dot{x}_a(t_k^+) = 0$. It is proven with detailed calculations in [436, Annexe B] that various scenarii can be envisaged from $(\theta(t_k), \dot{\theta}(t_k^-)) \in \mathscr{M}_2$. The sticking case $\dot{x}_a(t_k^+) = 0$ corresponds to the *maximal dissipation* solution which pulls the system out of $\mathscr{M}_2$. The effects of tangential impacts were also connected with stoppage of slipping in [161, 954]. However, other authors [579] argue that in general there is no reason for such sticking to occur after an IW/OC, basing on Darboux–Keller's shock dynamics and analyzing what happens after a shock when the normal approach velocity tends to zero. The second statement (b) means $\dot{y}_a(t_k^+) = 0$. One way to elucidate what may happen is to study an approximate, or regularized problem, where the unilateral constraint is replaced by a linear stiffness, as done in [1329] where a detailed analysis is proposed. It confirms that a slip-to-stick transition occurs, that is, an IW/OC solves the inconsistency issue of mode $\mathscr{M}_2$.

Remark 5.29 The critical values for μ ($\frac{4}{3}$ and $\frac{8}{3\sqrt{3}}$) are not very realistic, since friction coefficients measured between materials usually take much smaller values. However, depending on the contact geometry (for instance a nonzero radius at the edge), inconsistencies and indeterminacies can occur for much smaller values, see [436,725,725,792,894,944]. For instance, the sliding rod with rounded tip with radius $r = l$ has a critical friction coefficient $\mu_c \approx 0.625$ [436, Annexe C]. In [944] critical values $\mu \approx 0.44$ are reported for another system, with a sliding mechanism mounted at the rod's tip. A planar rigid body with point contact A, inertia I, mass m, $||AG|| = l$, has $\mu_c = 2\sqrt{\frac{I}{ml^2}\left(1 + \frac{I}{ml^2}\right)}$ [792, 942]. A planar two-degree-of-freedom robot is also shown to exhibit paradoxes for $\mu \approx 0.9$ in [36]. The Painlevé paradoxes analysis is

therefore not purely academic but can be encountered in practical situations. This is related to the comments in Remark 4.13 about similar phenomena in impact laws.

Remark 5.30 If the friction coefficient is small enough ($\mu < \mu_c$), then there are no indeterminacies nor inconsistencies in the dynamics with sliding friction. Getting the critical value of friction is not straightforward in general, especially when there are multiple bilateral and unilateral constraints with friction. A general analysis is made in [160], relying on the use of Theorem 5.8, where explicit and calculable (but conservative) upperbounds on the coefficients of friction are given, below which the contact LCP is well-posed. Other sufficient conditions for existence of accelerations may be found in [823, 824], but the friction upperbounds are not given explicitly.

5.6.4 Further Reading

A mathematical analysis of the slender rod example, extending well-posedness results which are summarized in Theorem 5.3, has been made in [1141, 1142] who proved that the system has absolutely continuous positions, velocities of local bounded variations, hence admitting measure accelerations. Ivanov [594] constructs the contact mixed LCP and states its well-posedness in terms of the P-property of a matrix. Most importantly the multi-contact case is tackled in [594] and the Painlevé-Klein system (see below) is analyzed. Experimental results have been reported in [1127, 1224, 1331] which prove that Painlevé paradoxes can occur in practice. The classical example of the chalk sliding and bouncing on a black board, drawing dashed lines, [334, 617, 894] is often cited as an illustration of the consequences of Painlevé paradoxes, which produces *chatter* (known as *broutement* or *broutage* in French): the sliding/sticking/detachment cycles when the rod is acted upon by some external action result in chatter. An approximating compliant problem is studied in [370, 1127], using singular perturbations techniques to investigate the contact dynamics when the stiffness and damping tend to infinity. Their analysis permits to eliminate one solution in case the contact LCP is indeterminate. A detailed analysis of the sliding rod example with a compliant (linear spring) normal contact with Coulomb's friction is made in [1329] about states in $\mathscr{M}_2$ (confirming [755, Theorem1]). It shows that the IW/OC is made of three phases of motion: initial slip, a period of stick, and a reverse slip phase, whose durations all vanish as the contact stiffness diverges. A Hertz's compliance is used in [1328] for a three-dimensional sliding slender rod. A study of the so-called Painlevé-Klein systems (i.e., with one bilateral constraint with Coulomb friction) via a penalization is done in [708]. It is shown that the limit velocity as $k \to +\infty$ possesses a jump when the configuration corresponds to undetermined or inconsistent modes, which exactly represents an IW/OC: hence, IW/OCs can be given a physical meaning, and the rigid body case just encapsulates the difficulties one may encounter when simulating numerically a penalized system, with high stiffness's values (which often occur in practice). In [1103] the effect of the flexibilities in the whole body on critical friction coefficients is studied with a

finite-element simulation: critical friction depends on the compliance of the rod. A detailed analysis of a compliant approximation of the sliding rod is made in [933], who show that trajectories cannot enter $\mathscr{M}_2$ coming from $\mathscr{M}_4$. Matrosov and Finogenko [823] analyze n-degree-of-freedom systems subject to unilateral constraints of the form $q_i \geq 0$ and assume that Coulomb's friction law applies directly to these constraints (like in the z-coordinates in (5.172)). The authors derive a condition which asserts that if the friction coefficient is small enough, then the mapping which allows to calculate $\ddot{q}$ from the dynamics is contractive; hence, there is a unique generalized acceleration. These results are hence of the same nature as those in [1216] who establish existence and uniqueness of a solution to NCPs when the friction coefficient is small enough. Jean and Pratt [618] also derived sufficient conditions guaranteeing the local existence of a solution with continuous position and velocity. They show on an example that the considered evolution problem possesses in general a solution only if discontinuous velocities are admitted. Painlevé paradoxes are shown to occur in more complex systems like biped robots [942], or lead screw drives [1224]. The analysis in [436, 437] has been extended in [944] for a rod with a sliding mechanism at the tip, in [792] who proposed a detailed study of regions of possible motions in the $(\theta, \dot{\theta})$ phase plane, in [942] for a simple walking robot, in [1271] who made a very detailed analysis of the Painlevé-Klein and the slender rod systems, and in [1271] for rotating shafts. Bifurcations in the context of Painlevé paradoxes have been studied in [701, 725]. Indeterminacies also appear in granular materials [1023].

Strange behavior of the models with friction can also be given an explanation via the transportation of real-world friction cones into the configuration space [381, 892]. When the configuration space friction cone (i.e., the image of the three- or two-dimensional real-world cone in the configuration space) dips below the tangent space to the constraint boundary at the contact point, the model may possess zero, one, or more solutions.

Consider the system in Fig. 5.24 which is known as the Painlevé-Klein system, and was introduced in [674]. This one-degree-of-freedom system consists of a bar of length $2l$ that slides on two parallel guides. Coulomb friction acts only at one of

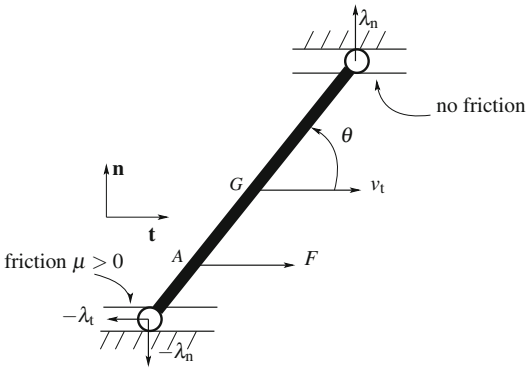

Fig. 5.24 The Painlevé-Klein example

the guides, while the other one is assumed frictionless. The dynamical equations and the bilateral holonomic constraints yield

$$\mu l|\lambda_{\mathrm{n},b}|\mathrm{sgn}(v_{\mathrm{t}}) = \frac{2l-b}{\tan(\theta)}\lambda_{\mathrm{n},b} + bF \tag{5.187}$$

where v_{t} is the tangential velocity of the bottom contact, equal to the horizontal velocity of the bar, F is an exogenous force acting at A with $GA = b$ taken positive as shown in the figure, and G is the gravity center. Also, the static equilibrium yields that $\lambda_{\mathrm{n},b,1} = -\lambda_{\mathrm{n},b,2} = \lambda_{\mathrm{n},b}$. The equality (5.187) is a piecewise-linear equation for λ_{n}. Due to its simplicity it may be analyzed by inspection. In particular, this nonlinear equation has no solution if $\mu > \frac{2}{\tan(\theta}$ and $bF - \frac{b\lambda_{\mathrm{n}}}{\tan(\theta)} = -\mathrm{sgn}(v_{\mathrm{t}})$: this is an inconsistent mode. A very detailed analysis of the Painlevé-Klein system is made in [416, Chap. 4]. It is shown that the system may escape from inconsistent configurations if a suitable velocity jump is applied (which is consistent with the analysis made in [708, 709]). Similar systems have been studied in [240, 416, 419, 708, 922, 1267, 1268, 1269, 1270, 1271]. The monograph [709] is dedicated entirely to systems with bilateral constraints with friction like Painlevé-Klein system. Tangential impacts yielding a slip/stick transition are justified in [709, §4.3,4.4] from the analysis of a system with normal linear elasticity. Let us note that non-existence and non-uniqueness problems also arise in quasistatic problems ($\ddot{q} = 0$) with complementarity conditions and Coulomb friction [673, 741].

Tangential Impacts from Shock Dynamics

Wang and Mason [815, 1255] show that in certain cases, the consideration of an impulsive force is the only possible solution to this dynamical problem, which otherwise possesses no solution at all, thus retrieving a result by Pères in [995, Chap. 10] based on a graphical analysis of a two-dimensional shock process. The three-dimensional case with friction is also treated in [995], using Delassus' Lemma.[60] Other graphical analysis can be found in [369]. The Darboux–Keller impact dynamics is used in [1328] to analyze the three-dimensional slender sliding rod: the sticking phase is proved to exist at paradoxes. A similar study is proposed in [1104]. The study in [1255] is based on Routh's two-dimensional graphical method (see Sect. 4.3.13). Batlle [106] analyzes the same example and assumes that jamb occurs (see paragraph below for a definition of the jamb phenomenon) and that the collision consists of a first phase in which $v_{r,\mathrm{n}}$ evolves from 0 to a negative value until slip stops, a second

[60] Let (S) be a n-dimensional multibody system with generalized coordinate vector q, in contact through its part S_1 with a body S_2 at the point I. Let $\dot{X} = J(q)\dot{q}$ be the velocity of I in a frame centered at I (A task-space frame in robotics language). Then Delassus's lemma states that $\dot{X} = \nabla_{u,v,w}\Phi_q(u, v, w)$ for some quadratic function Φ of the interaction force components u, v, and w in the same frame.

phase in which compression continues and then an expansion phase with sliding. Stronge's energetical coefficient is used to determine the shock termination (from the shock dynamics, one calculates the impulse $p_{\mathrm{n}}(t_f) - p_{\mathrm{n}}(t_c)$, and deduces the value of the final velocity, which provides a termination criterion). Brach [177] used the kinetic energy loss $T_L(t_k)$ to show that in fact, e_{n} does not influence tangential impacts. The two-dimensional analysis in [106, 177, 1255] is not based on an LCP, but on shock dynamics and looking at the outcome when $\dot{y}_a(t_k^-) \to 0$. Chatterjee [274, 278] also studies the behavior of a two-dimensional algebraic collision law based on the calculation of a suitable percussion vector P. This impact rule uses, in addition to the impulse ratio μ, two restitution coefficients, therefore enlarging the space spanned by the possible percussion vectors (recall that Whittaker's, Kane and Levinson's or Smith's models use only one coefficient in addition to μ). It is shown in [278] that given parameters and initial data, the proposed shock rule yields a line of accessible percussions, whereas the others yield a point (i.e., a unique percussion). In [579], Ivanov directly analyzes the contact LCP via tangential collisions with small $v_{r,\mathrm{n}}(0)$. He uses the Darboux–Keller's shock dynamics, and analyzes what happens in the different LCP modes, when a collision occurs with a small approach velocity $v_{r,\mathrm{n}}(0) = -\varepsilon < 0$.

5.6.5 Conclusions

Paul Painlevé wrote in [955]: *On voit que les lois empiriques du frottement sont* logiquement *inadmissibles …dés que le frottement devient assez notable. Il y aurait peut-être quelque intérêt à reprendre à ce point de vue leur étude expérimentale*, which may be translated as *We see that empirical laws of friction are inadmissible from a logical point of view …as soon as friction becomes too large. Consequently, it would be interesting to reconsider their experimental analysis.* Such a point of view was given up soon after him, for instance Delassus admitted in [334] that paradoxes could be solved by sliding/sticking transitions yielding chatter, which have a mechanical meaning. Hopefully, the material in this section is enough to convince the reader that *Painlevé paradoxes are no longer (in fact have never been) paradoxical!* Despite there remains many open issues to be clarified (like the extension of the above to the multicontact case), the results summarized in this section prove that the rigid body model with Coulomb's friction is perfectly sound. It provides a compact way of writing the Lagrange dynamics with contact and impact, which can be used for the mechanical design (reliable numerical methods are available, see the next section), and for the design of control algorithms. Finally, we may comment about two features of rigid body dynamics with Coulomb's friction: nonuniqueness of solutions, and discontinuous dependence of solutions on the initial conditions. Roughly speaking, *nonuniqueness corresponds in stiff compliant approximations to a great instability of solutions, while discontinuous dependence stems from a great sensitivity of solutions.*

5.7 Numerical Simulation

The design of reliable software packages, which rely on robust numerical algorithms, is nowadays crucial for virtual prototyping. This section is dedicated to introduce numerical schemes which are taylored for complementarity Lagrangian systems. We only touch upon this topic (in particular, nothing is said about the iterative algorithms for solving the OSNSP); interested readers may read [13] that is dedicated to the numerical simulation of mechanical systems.

5.7.1 Event-Driven Algorithms

The most basic idea is to integrate the motion between events like impacts or stick/slip transitions, then determine the event time, compute the velocity or acceleration jump, and start again the integration until another event is detected. This is known as *event-driven* algorithms. The main drawbacks of event-driven numerical schemes are on one hand that they are unable to handle accumulations, or large quantities of events, and on the other hand, the thresholds which are necessary for their implementation are not easy to tune. But for simple systems with few events, they may be useful because one may use a very accurate integration method between the event times. The event detection is usually performed with some zero-crossing solver (and it may, in theory, involve an infinity of such zero-crossing detections as well as the construction of an infinity of index sets, see Remark B.2). It has been investigated for instance in [396, 506, 1259, 1281]. The direct extension of Coulomb's law for impacts (see Whittaker's method in Chap. 4, Sect. 4.3.2) is generally adopted. Other methods have been presented in [447, 872, 1253]. In particular, it is emphasized in [1253] that if an explicit form of the impact Poincaré map is available (see Chap. 7), then one can advantageously use this discrete-time system to compute the motion during repeated collisions. A very few convergence and order analysis have been performed for event-driven algorithms. Janin and Lamarque [611] [13, §8.6.5.2] proved on a simple one degree-of-freedom system without accumulations of impacts that the scheme order is related to the order of the method used between impacts and the precision of the interpolation method used to approximate the impact times. A similar work is done in [344] for impulsive ODEs as in (1.31), with separated jump times. Several polynomial extensions are used to locate the state jump times, and a Runge–Kutta method with order p is used to integrate between the jumps. The overall method is proved to be of order p.

5.7.2 Compliant Contact/Impact Models

The second "natural" idea is to replace the constraint by a compliant model (see Chap. 2) like a spring-dashpot model. Then one has to integrate ODEs (except when a right-hand side discontinuous in the state, if damping is nonzero, then the dynamics may be embedded into differential inclusions with continuous solutions[61]). One drawback is that this yields in general stiff ODEs. Therefore, the integration step has to be reduced and the simulation length becomes large, otherwise the simulation is prone to large numerical errors. For instance, it was found in [1144] that suitable stiffness and damping values to model the ground on which a slender rod falls were $k = 5.5 \times 10^7$ N/m and $f = 2.0 \times 10^7$ Ns/m^2 (these values being identified from central collisions of a 200 mm bar). Stiffness and damping values for the contact/impact process in an impact beam system used to model and test shocks in bearings with clearance have been found to be $k = 9.6 \times 10^6$ N/m and $f = 7$ Ns/m for aluminum and $k = 1.5 \times 10^7$ N/m, $f = 20$ Ns/m for steel [331]. Contact stiffness of 10^{10} N/m is usual in gears and pinions [1123]. Similar values are given for a spatial slider crank mechanism.[62] The least requirement to get reliable numerical results is that during a rebound or a collision phases, the algorithm calculates several points. The length Δ of such phases typically satisfies $0 \leq \Delta \leq \alpha\sqrt{\frac{1}{k}}$ for some constant α. Hence, for the above values one finds that a good integration step should be chosen smaller $h = 10^{-5}$ s, for 10 points *per* phase. Some authors [199] suggest to calculate 1000 points to get satisfying numerical accuracy. This clearly hampers one to simulate systems with too many degrees of freedom ($n < 3000$ particles in three dimensions and $n < 10^4$ particles in two dimensions for granular materials [199]—systems for which the free motion between collisions is particularly simple). Easily reproducible numerical results concerning the system in Fig. 2.1 and with a constant force acting on the mass (this is nothing else than a ball subject to gravity and rebounding on an elastic ground) show that for $h = 10^{-3}$ s, a strange behavior of the solution $x(t)$ occurs as soon as $k \geq 7 \times 10^5$ N/m (in theory, the energy is conserved and the motion is periodic: for those values the motion starts to oscillate more or less erratically around the ideal trajectory. For $k = 7 \times 10^6$ N/m, the results totally deteriorate and $x(t)$ has the tendency to converge to zero!). Similar results were found in [1004]. On the other hand, when dealing with complex systems and disregarding such numerical problems, it may not be evident to determine which effects the flexibilities have on the motion of the system, and how they have to be chosen to obtain results close to the real motion. The sensitivity of the impact outcomes with respect to the contact stiffness may be very high: it may then become quite impossible to get reliable simulations. Finally, another major drawback is that the contact parameters may not be easy to estimate, either because they are too many, or they lack of

[61] Recall that in this case the Carathéodory conditions for well-posedness of ODEs no longer apply, and specific analysis is necessary.

[62] Looking at (2.9), one may get an idea of the restitution coefficient that corresponds to such spring-dashpot models. With those numerical values e_n is very close to 1.

mechanical meaning (try to fit parameters of a viscoelastic model with experiments led on an elastoplastic material …), or the experimental data are too noisy.

Remark 5.31 (Systems with Clearance) A constant difficulty in the simulation of systems with constraints (bilateral or unilateral) is the numerical stabilization of the constraints, i.e., the suppression of the drift. This is true for the simulation of rigid-body models and the associated numerical schemes (where suitable projections have to be implemented). This is also true for compliant models as Simon–Hunt–Crossley's and its various modifications (see Sect. 2.2.2), which are widely used for systems with clearance [489]. For instance, the literature on systems with joint clearance is full of simulation results that display spurious unrealistic high-frequency oscillations of the contact normal acceleration and of the contact force, due to the model's flexibility [400, Figs. 4.22, 4.23] [779, Figs.9, 10, 11, 12], [489, Figs.7, 8, 9], see also [679, 941, 1179, 1226] to cite a few. It is not clear at this stage whether the contact/impact model, and/or the numerical methods, has to be changed to suppress such unacceptable numerical simulation results (the experimental data reported in [401, Figs. 5, 6, 8, 11, 12] prove that the oscillations have no mechanical meaning at all). In fact the time-stepping methods associated with a rigid body complementarity model which we describe in the next section have proved to supersede compliant models for systems with mechanical play, and have been shown to possess quite good prediction capabilities, see numerous careful comparisons between numerical and experimental data in [685, 1173, 1198, 1199, 1200, 1201]. It is also noteworthy, as we already pointed out elsewhere in this book, that contrarily to what is sometimes still stated [489], efficient numerical methods exist that do enable designers to model sticking (i.e., multivalued at $v_t = 0$) Coulomb's friction, and adding varying sliding friction coefficient is an easy task. See the next section and [33, 402].

5.7.3 *Time-Stepping (Event-Capturing) Numerical Algorithms*

Let us introduce a class of discretization methods which prove to be in many instances a nice (and close to necessary) alternative to event-driven schemes.

5.7.3.1 The Moreau–Jean Time-Stepping Scheme (Non-Smooth Contact Dynamics Method)

The so-called *time-stepping* or *event-capturing* schemes have been introduced by J.J. Moreau and M. Jean [615, 617, 891, 892, 894, 896, 897] and have been subsequently developed in [6, 7, 8, 47, 232, 283, 1074, 1075, 1143, 1143, 1162]. They have been implemented in engineering software packages for multibody system

simulation like SICONOS and LMGC90[63]: this is what one usually calls the NSCD (Non-Smooth Contact Dynamics) method. Roughly speaking, time-stepping methods approximate the impulse–velocity dynamics on one step of integration. The Moreau–Jean method, originating from Moreau's catching-up algorithm for the discretization of the first-order sweeping process [887], was used in many studies to prove existence of solutions of the continuous-time dynamics, see (5.79), (5.80), (5.81), and (5.82) in Sect. 5.2.3. We now present the NSCD method for systems subjected to unilateral constraints and Coulomb's friction, using De Saxcé's approach (see Sect. 5.3.3). We will just provide the reader in this section with the basic ideas. Interested readers may have a look at [13, Chaps. 10, 12–14] for a very detailed exposition of the NSCD method, in particular, the iterative solvers used to solve the one-step nonsmooth problem (that may take the form of an LCP, or a NCP, or a variational inequality, or an inclusion into a normal cone). The NSCD scheme is similar to the implicit method in (5.79)–(5.81), which is nevertheless rarely used for calculations but preferred for Mathematical Analysis. When formulated for frictionless systems and with a $\theta-$method, the NSCD algorithm is given by [6]

$$
\begin{aligned}
&M(q_{j+\theta})(u_{j+1}-u_j)+hF(t_{j+\theta},q_{j+\theta},u_{j+\theta})=\nabla f(q_{j+\theta})P_{\mathrm{n},j+1},\\
&q_{j+1}=q_j+h\,u_{j+\theta},\\
&U_{\mathrm{n},j+1}=\nabla f(q_{j+\theta})^T u_{j+1},\\
&-P_{\mathrm{n},j+1}\in N_{T_{\mathbb{R}^m_+}(\bar{f}_{j+\gamma})}(U_{\mathrm{n},j+1}+\mathscr{E}_{\mathrm{nn}}U_{\mathrm{n},j}),\\
&\bar{f}_{j+\gamma}=f(q_j)+h\gamma U_{\mathrm{n},j},
\end{aligned}
\tag{5.188}
$$

with $h=t_{j+1}-t_j$, $\theta\in[0,1]$, $\gamma\in[0,1]$, $\mathscr{E}_{\mathrm{nn}}=\mathrm{diag}(e_{\mathrm{n},i})$, $x_{j+\theta}=(1-\theta)x_j+\theta x_{j+1}$, where the following approximations are made: $u_{j+1}\approx u(t_{j+1}^+)$, $U_{\mathrm{n},j+1}\approx U_{\mathrm{n}}(t_{j+1}^+)$, $P_{\mathrm{n},j+1}\approx\lambda_{\mathrm{n}}((t_j,t_{j+1}])$. The nonlinear forces $F(t,q,\dot{q})$ gather $F_{iner}(q,\dot{q})-F_{ext}(t)$ in (5.1). The last approximation is fundamental because it means that the primary variable of the NSCD method is not, at an impact time which is an atom of the measure λ_{n}, the impulsive impact force (which is impossible to approximate with such a scheme), but the measure of the interval $(t_j,t_{j+1}]$ by this impulsive (Dirac) force, a bounded quantity. The constraint $\bar{f}_{j+\gamma}$ is called a fully explicit forecast, and other choices are possible [7].

[63] http://siconos.gforge.inria.fr/ and https://git-xen.lmgc.univ-montp2.fr/lmgc90/lmgc90_user/wikis/git_access.

Remark 5.32 Throughout this section, the discrete times will be denoted t_j. It is clear that they should not be confused with the impact times t_k which concern the continuous-time models.

We also used implicitly a new characterization of Moreau's set (see Sects. 5.2.2.2 and 5.2.2.3), which we more or less already saw in the proof of Proposition 5.15. Let $\mathscr{E}_{\rm nn} = {\rm diag}(e_{\rm n})$, or more generally let $\mathscr{E}_{\rm nn}$ and $\nabla f(q)$ commute. Then $N_{V(q)}(w) = \nabla f(q)\partial\psi_{T_{\mathbb{R}^m_+}(f(q))}(\nabla f(q)w)$, with $w = u(t^+) + e_{\rm n}u(t^-)$. The proof is as follows: $T_{\mathbb{R}^m_+}(f(q)) = \{v \in \mathbb{R}^m_+ | v^T e_i \geq 0, \text{for all } i \in \mathscr{J}(q)\}$, e_i the i-th unit vector of $\mathbb{R}^m_+$, $\mathscr{J}(q) = \{i | f_i(q) = 0\}$. Let $\rho(w) \stackrel{\Delta}{=} \psi_{T_{\mathbb{R}^m_+}(f(q))}(\nabla f(q)^T w)$. From Theorem B.2 and under some constraint qualification, $\partial\rho(w) = \nabla f(q)\partial\psi_{T_{\mathbb{R}^m_+}(f(q))}(\nabla f(q)^T w)$. Now $\nabla f(q)^T w \in T_{\mathbb{R}^m_+}(f(q)) \Rightarrow (\nabla(q)^T w)^T e_i \geq 0$, for all $i \in \mathscr{J}(q) \Leftrightarrow w^T \nabla f(q) e_i \geq 0$, for all $i \in \mathscr{J}(q) \Leftrightarrow w^T \nabla f_i(q) \geq 0$, for all $i \in \mathscr{J}(q) \Rightarrow w \in V(q)$. The converse holds true as well, so the equivalence holds. We infer that $\psi_{T_{\mathbb{R}^m_+}(f(q))}(\nabla f(q)^T w) = \psi_{V(q)}(w)$, and then $\partial\rho(w) = N_{V(q)}(w)$.

Using (B.20), and after few manipulations, we deduce from (5.188) that

$$\begin{aligned} U_{{\rm n},j+1} &= -\mathscr{E}_{\rm nn} U_{{\rm n},j} \\ &+ {\rm proj}_{D_u(q_{j+\theta})^{-1}} \left[T_{\mathbb{R}^m_+}(\bar{f}_{j+\gamma}); \mathscr{E}_{\rm nn} U_{{\rm n},j} - \nabla f(q_{j+\theta})(-u_j + hM(q_{j+\theta})^{-1} F_{j+\theta}) \right] \end{aligned} \tag{5.189}$$

where $D_u(q_{j+\theta}) = \nabla f(q_{j+\theta})^T M(q_{j+\theta})^{-1} \nabla f(q_{j+\theta})$ is the Delassus's matrix, $F_{j+\theta} = F(t_{j+\theta}, q_{j+\theta}, u_{j+\theta})$. Depending on θ this equation may be explicit or implicit, and may necessitate the use of a specific iterative solver. Inverting the inclusion in the fourth line of (5.188), using (B.16) and the polarity between the normal and tangential cones, we find $U_{{\rm n},j+1} + \mathscr{E}_{\rm nn} U_{{\rm n},j} \in N_{N_{\mathbb{R}^m_+}(\bar{f}_{j+\gamma})}(-P_{{\rm n},j+1})$ from which it follows:

$$P_{{\rm n},j+1} = -{\rm proj}_{D_u(q_{j+\theta})}[N_{\mathbb{R}^m_+}(\bar{f}_{j+\theta}); D_u(q_{j+\theta})^{-1}(\mathscr{E}_{\rm nn} U_{{\rm n},j} + u_j - hM(q_{j+\theta})^{-1} F_{j+\theta})] \tag{5.190}$$

When inserted into the first two lines of (5.188), (5.190) allows one to compute u_{j+1} and q_{j+1}, possibly with the help of a suitable iterative solver. In practice, one usually solves (5.190) because (5.189) requires independent constraints.

The inclusion in the fourth line of (5.188) can be rewritten in a more explicit way, allowing for calculations: if $\bar{f}_{i,j+\gamma} \leq 0$ then $0 \leq U_{{\rm n},i,j+1} + e_{{\rm n},i} U_{{\rm n},i,j} \perp P_{{\rm n},i,j+1} \geq 0$, where the index i refers to the constraint $f_i(q)$, $1 \leq i \leq m$, otherwise if $\bar{f}_{i,j+\gamma} > 0$ then $P_{{\rm n},i,j+1} = 0$. We notice the similarity between the time-stepping method equations, and the impact dynamics in (5.66). Solving (5.188) depends on the choice of θ, which in turn may depend on the nonlinear forces (e.g., the system may be stiff). Let us take $\theta = 0$ (explicit case), and let us group the possibly positive components $P_{{\rm n},i,j+1}$ in the vector $P^{act}_{{\rm n},j+1}$, and the corresponding local velocities in the vector $U^{act}_{{\rm n},j}$ (where *act* stands for "active"). Then we obtain $0 \leq U^{act}_{{\rm n},j+1} + \mathscr{E}^{act}_{\rm n} U^{act}_{{\rm n},j} \perp P^{act}_{{\rm n},j+1} \geq 0$. From the first line of (5.188) we deduce that:

$$U^{act}_{\mathrm{n},j+1} = (\nabla f(q_j)^{act})^T u_{j+1} = (\nabla f(q_j)^{act})^T u_j - (\nabla f(q_j)^{act})^T M(q_j)^{-1} hF(t_j, q_j, u_j)$$
$$+ \underbrace{(\nabla f(q_j)^{act})^T M(q_j)^{-1} \nabla f(q_j)^{act}}_{\triangleq D^{act}_u(q_j)} P^{act}_{\mathrm{n},j+1} \tag{5.191}$$

It is clear that we obtain an LCP with unknown $P^{act}_{\mathrm{n},j+1}$. Once this one-step nonsmooth problem (OSNSP) is solved,[64] the value of $P^{act}_{\mathrm{n},j+1}$ can be inserted in the first line of (5.188) to compute u_{j+1} and advance the algorithm to step $j+1$. The convergence of this class of algorithms has been investigated for various cases in [374, 375, 781, 867]. It is noteworthy that the complementarity conditions are not implemented numerically as $0 \le f(q_{j+1}) \perp \lambda_{\mathrm{n},j+1} \ge 0$, as one would expect from a direct discretization of (5.1). Such a scheme does not work, as may be checked on a simple example like the bouncing ball.[65] However, working with velocity introduces problems of drift, well known in the simulation of DAEs. The issue related to the stabilization of the active constraints to avoid the drift phenomenon is tackled in [7], inspired by the Gear–Gupta–Leimkuhler approach of adding an artificial multiplier at the position level as $q_{j+1} = q_j + h\, u_{j+\theta} + \nabla f(q_{j+\theta})\tau_{j+1}$, $\tau_{j+1} \in N_{\mathbb{R}^m_+}(\bar{f}_{j+\gamma}) \Leftrightarrow 0 \le \tau_{j+1} \perp \bar{f}_{j+\gamma} \ge 0$. An analysis of the local orders of consistency is made in [6, Propositions1,2,3] which we roughly summarize as: the scheme is of order 1 in positions, and of order 0 in velocities. A modified time-stepping method is proposed in [6] to get higher order. The energy dissipation properties of the Moreau–Jean scheme are studied in [8].

Proposition 5.28 *[8, Proposition 5.2] Let $F(t, q, \dot{q}) = C\dot{q} + Kq - F_{ext}(t)$ and denote $F_{damp} = C\dot{q}$. The discrete work done by external forces with a step is $W^{ext}_{j+1} = hu^T_{j+\theta} F^{ext}_{j+\theta} \approx \int_{t_j}^{t_{j+1}} F(t)u(t)dt$, and the discrete work done by the damping forces is $W^{damp}_{j+1} = -hu^T_{j+\theta} C u_{j+\theta} \approx -\int_{t_j}^{t_{j+1}} u(t)^T Cu(t)dt$. If $E(q, \dot{q})$ is the total mechanical energy of the system, then the Moreau–Jean method satisfies the discrete-time dissipation inequality: $E(t_{j+1}) - E(t_j) \le W^{ext}_{j+1} + W^{damp}_{j+1}$ if $\frac{1}{2} \le \theta \le \frac{1}{1+\bar{e}_{\mathrm{n}}} \le 1$, $\bar{e}_{\mathrm{n}} = \max_{1\le i\le m} e_{\mathrm{n},i}$. If $\bar{e}_{\mathrm{n}} = 0$ (plastic impacts at all contacts), then the condition becomes $\frac{1}{2} \le \theta \le 1$, and if $\bar{e}_{\mathrm{n}} = 1$ (elastic lossless impacts at all contacts) then $\theta = \frac{1}{2}$.*

Some comments to finish the frictionless part: (1) The Moreau–Jean event-capturing time-stepping method allows to simulate accumulations of impacts (the so-called Zeno phenomenon) without difficulty. More precisely, if there is an accumulation on the left of $t_\infty < +\infty$, then the scheme computes a finite number n_{imp} of impacts before t_∞ (the number of calculated collisions depends on h), and there is one time

[64] This is precisely where we need to use an LCP solver.

[65] Fundamentally, this is due to the fact that the relative degree between q and $\lambda_{\mathrm{n},u}$ is equal to 2. Working with velocities allows to reduce it to 1. Another way to interpret this is that positions and forces are not dual quantities from the point of view of the power, while velocities and forces are reciprocal one to each other: they form a suitable supply rate for dissipation. We retrieve in the discrete-time context the importance of passivity, see Remark 5.22.

step during which an infinity of impacts is neglected before the constraint is activated. One can have a look at [13, Table 14.2] for an example of the variation of n_{imp} with h. (2) The fact that energy is preserved with the midpoint scheme for lossless systems is also found for LCS [408] (discretization of LCS is treated in Sect. 5.7.3.5).

When friction is considered, we may work either in generalized coordinates, or in local coordinates, and express Coulomb's friction using De Saxcé's framework. The resulting one-step nonsmooth problems for the linear or the nonlinear cases are described in detail in the monograph [13, §10.1], and we recall one of them for the sake of completeness. We assume that $F(t,q,\dot{q}) = C\dot{q} + Kq - F_{ext}(t)$, and the inertia matrix is a constant matrix M. Let us define the *iteration matrix* $\widehat{M} = M + h\theta C + h^2\theta^2 K$, and the "free" velocity $u_{free} = u_j + \widehat{M}^{-1}[-hCu_j - hKq_j - h^2\theta K u_j + h(\theta F^{ext}_{j+1} + (1-\theta)F^{ext}_j)]$, which corresponds to the approximated velocity when the reaction forces vanish. Then the following scheme is implemented, which is the discrete-time counterpart of the impact dynamics in (5.100):

$$
\begin{aligned}
&U_{j+1} = \widehat{D}(q_j,\theta)P_{j+1} + U_{free}\\
&U_{free} = \begin{pmatrix} \nabla f(q_j)^T \\ H_{\mathrm{t}}(q_j)^T \end{pmatrix} u_{free} + \textstyle\sum_{i\neq l} \widehat{D}_{il}(q_j,\theta)P_{l,j+1}.\\
&\text{If } f_i(q_j + hu_j) \leq 0 \text{ then:}\\
&\bullet \begin{cases} \mathscr{C}_i^\star \ni \widehat{V}_{i,j+1} \perp \begin{pmatrix} P_{\mathrm{t},i,j+1} \\ P_{\mathrm{n},i,j+1} \end{pmatrix} \in \mathscr{C}_i, \\ \widehat{V}_{i,j+1} = (U^T_{\mathrm{t},i,j+1},\, U_{\mathrm{n},i,j+1} + e_{\mathrm{n},i}U_{\mathrm{n},i,j} + \mu_i||U_{\mathrm{t},i,j+1}||)^T, \quad 1 \leq i \leq m, \end{cases}\\
&\bullet \text{ If } f_i(q_j + hu_j) > 0 \text{ then: } P_{i,j+1} = 0.
\end{aligned}
\tag{5.192}
$$

with $\widehat{D}(q)$ like $D(q)$ in (5.99) with $\widehat{M}^{-1}$ instead of $M(q)^{-1}$. The tools that may be used to solve such a OSNSP are described in detail in [13, Chaps. 12, 13].

Remark 5.33 Just to give some quick insight on the implicit discretization of Coulomb's friction, we consider the simplest case $\dot{x}(t) \in -\mathrm{sgn}(x(t))$, where $x(t)$ may be thought of as a velocity. An Euler implicit discretization yields $x_{j+1} - x_j \in -h\mathrm{sgn}(x_{j+1})$. Let us set $w_{j+1} = -x_{j+1}$. Applying the equivalences in (B.16), (B.20), and (B.21), we see that $w_{j+1} \in -N_{[-h-x_j,h-x_j]}(w_{j+1})$, equivalently $w_{j+1} = \mathrm{proj}([-h-x_j, h-x_j]; 0)$. If $0 \in [-h-x_j, h-x_j]$ then $w_{j+1} = x_{j+1} = 0$. If $h - x_j < 0$, then $w_{j+1} = h - x_j$, and if $-h - x_j > 0$, then $w_{j+1} = -h - x_j$. The generalized equation under the form $0 \in x_{j+1} - x_j + h\mathrm{sgn}(x_{j+1})$ is depicted in Fig. 5.25 (compare Figs. 5.25 and 5.22: two different generalized equations are solved graphically). In case 1, $x_j < -h$ and $x_{j+1} < 0$, in cases 2, 3, 4, $x_j \in [-h,h]$ and

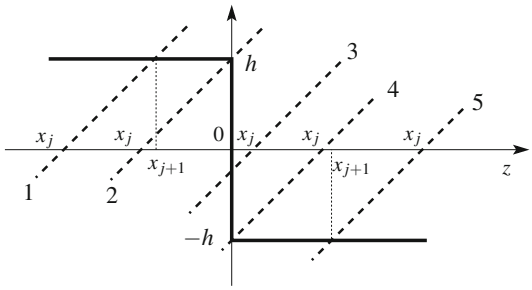

Fig. 5.25 Solving the generalized equation $0 \in x_{j+1} - x_j + h\text{sgn}(x_{j+1})$. *Dashed lines* graph of $z \mapsto z - x_j$, *solid lines* graph of $z \mapsto -h\ \text{sgn}(z)$

$x_{j+1} = 0$, in case 5, $x_j > h$ and $x_{j+1} > 0$. Let $\varphi(x) = |x|$, we also have $x_{j+1} = (I_d + h\partial\varphi)^{-1}(x_j)$, where the resolvent operator $J_h^{\partial\varphi}(\cdot) = (I_d + h\partial\varphi)^{-1}(\cdot)$ is single valued and non-expansive since $\varphi(\cdot)$ is continuous convex proper on $\mathbb{R}$, see Definition B.9. It is then not difficult to prove that the discrete-time system has a globally, finite-time Lyapunov stable fixed point $x^\star = 0$, just as its time-continuous counterpart. An explicit discretization $x_{j+1} - x_j \in -h\text{sgn}(x_j)$ does not share such nice feature [424, 425]. The time discretization of the Darboux–Keller's dynamics in Sect. 5.7.3.4 is quite similar.

Remark 5.34 (Explicit vs. *Implicit Discretization)* Let us consider the simplest case of the first-order sweeping process: $\dot{x}(t) \in -N_{C(t)}(x(t))$. An explicit Euler discretization yields $x_{j+1} - x_j \in -N_{C(t_{j+1})}(x_j)$ (the value given to $C(t)$ is not important here). There is clearly no way, in general, to calculate x_{j+1} from this inclusion (though one may impose a selection criterion like minimum norm solution, or a randomly chosen selection, or a projection on the set-valued right-hand side [355, 356, 649]). Indeed, if it happens that $x_j \notin \text{Int}(C(t_{j+1}))$, then the normal cone is set-valued and one needs a selection procedure to compute a selection $\lambda_j \in N_{C(t_{j+1})}(x_j)$. If we now set $x_{j+1} - x_j \in -N_{C(t_{j+1})}(x_{j+1})$, the equivalences in (B.20) and (B.21) tell us immediately that x_{j+1} can be computed as a projection on $C(t_{j+1})$, which in turn allows us to obtain a selection of the right-hand side. In addition, the implicit discretization yields smooth stabilization on attractive sliding surfaces, while the explicit discretization usually does not, see [356, Figs. 3, 4, 5 and 6] and Fig. 5.26 below.

5.7.3.2 Applications Using the NSCD Method

These time-stepping schemes have been used with success in various applications: Robotics [912, 1212, 1213], Computer Graphics [138], Granular Matter [896, 1023, 1024, 1025], Masonry Structures [5, 616], Circuits with set-valued components [9, 10], Bifurcations analysis [725, 728], Rockfall simulation [729], Gene regulatory networks [17], Grand piano mechanism [66, 1193], Haptics [846], Geosciences [1136, 1137], etc..

Remark 5.35 It is interesting to note that the same system as in [725] is used in [701, 702]. The NSCD method is used in [725], while an event-driven code is

apparently used in [701, 702]. The results of [725] are used in [701, 702] as a benchmark to test the accuracy of their event-driven code (and most probably to tune some numerical parameters like the unavoidable thresholds). Most probably, some kind of hybrid time-stepping/event-driven code could represent the best compromise accuracy/robustness for such nonsmooth systems.

5.7.3.3 Other Time-Stepping Algorithms

• It is worth looking at [459, 1162] for details on the implementation and formulation of the NSCD method.
• Let us describe the general form of the algorithm proposed in [1143], which applies to an n-degree-of-freedom system with a single constraint ($m = 1$, but those schemes work for $m \geq 2$ [1142]) and with Coulomb friction. This method is a Moreau–Jean scheme, where the friction cone (in the three-dimensional case) is facetized along the ideas in [671, 672]:

$$\left\{\begin{array}{lll} \lambda_{\mathrm{n},j+1} \geq 0, & \mathbf{n}(q_j)^T \dot{q}_{j+1} \geq 0, & \lambda_{\mathrm{n},j+1} \mathbf{n}(q_j)^T \dot{q}_{j+1} = 0 \\ \beta_{j+1} \geq 0, & \lambda_{j+1}\mathbf{e} + D(q_j)^T \dot{q}_{j+1} \geq 0, & \beta_{j+1}^T [\lambda_{j+1}\mathbf{e} + D(q_j)^T \dot{q}_{j+1}] = 0 \\ \lambda_{j+1} \geq 0, & \mu\lambda_{n,j+1} - \mathbf{e}^T \beta_{j+1} \geq 0, & \lambda_{j+1}[\mu\lambda_{n,j+1} - \mathbf{e}^T \beta_{j+1}] = 0 \end{array}\right. \tag{5.193}$$

where $\mathbf{n}(q) = \nabla f(q) \in \mathbb{R}^n$, $h > 0$ is the integration step, $\mathbf{e}^T = [1, 1, \ldots, 1] \in \mathbb{R}^l$ where l is the number of edges of the polyhedral approximation of the friction cone. Hence, $\beta \in \mathbb{R}^l$ as well. Notice that $\lambda_{\mathrm{n},j}$ and β_j are to be considered as impulsions since they are proportional to forces times h. Actually, the friction cone is approximated by the polyhedral set $\hat{\mathscr{C}}(q) = \{\lambda_{\mathrm{n}}\mathbf{n} + D(q)\beta, \lambda_{\mathrm{n}} \geq 0, \beta \geq 0, \mathbf{e}^T\beta \leq \mu\lambda_{\mathrm{n}}\}$. The rows D_i^T of the matrix $D(q)$ are vectors that span the tangent subspace at the contact point. It is also assumed that there is always i and l such that $D_i = -D_l$. The last two sets of complementarity conditions represent the frictional effects. The third complementarity relations can be understood as follows [47, 1141]: if $\mu\lambda_{\mathrm{n}} - e^T\beta > 0$ then $\lambda = 0$ and $D(q)^T\dot{q}_{j+1} \geq 0$. Now if $D_i^T\dot{q}_{j+1} > 0$ necessarily there is an l with $D_l^T\dot{q}_{j+1} = -D_i^T\dot{q}_{j+1} < 0$, which contradicts $D(q)^T\dot{q}_{j+1} \geq 0$. Thus $D(q)^T\dot{q}_{j+1} = 0$. Since the vectors D_i span the tangent plane at the contact point (at least for the motion of particles), one deduces that the tangential velocity is zero. Consequently, if the interaction force is inside $\hat{\mathscr{C}}$ (which is the case if $\mu\lambda_{\mathrm{n}} - \mathbf{e}^T\beta > 0$), the relative velocity between the two systems in contact is zero, as expected. Now if there is some relative motion at the contact point, necessarily there is at least one i with $D_i^T\dot{q}_{j+1} > 0$. Thus $\lambda > 0$ since the complementarity relations can be taken componentwise, which forces $\mu\lambda_{\mathrm{n}} = \mathbf{e}^T\beta$, i.e., the contact force lies on $\mathrm{bd}(\mathscr{C})$. One may deduce this form of the Coulomb friction from Kuhn–Tucker conditions, since this law obeys the principle of maximum dissipation, see Sect. 5.3. It can therefore be formulated as the maximization of the quantity $-\mathbf{F}_{\mathrm{t}}v_{r,\mathrm{t}}$ (in one contact case) under the constraint that $\mathbf{F}_{\mathrm{t}}$ belongs to the set in (5.88).

Some comments arise:

1. The variable $\lambda \in \mathbb{R}$ is a slack variable with no real physical meaning.
2. Cone faceting may yield unrealistic behaviors [13, §13.3.7].
3. The unilateral constraint is formulated as $\mathbf{n}(q_j)^T q_j \geq \alpha_0$ in [1143]. Assume also that the inertia matrix M is constant [47]. Then the LCP resulting from (5.193) and with unknowns β, λ_n, and λ always possess a solution that can be computed *via* Lemke's algorithm. Notice also that in (5.193) $M(q)$ is calculated at step $j+1$ using q_{j+1} which is in turn a function of $\dot{q}_{j+1}$. Then one gets from (5.193) a nonlinear complementarity problem [1142]. Instead, in [1141] the inertia matrix is computed with $q_j + h\dot{q}_j$, i.e., with quantities known at step j. Also, [47] use $q_{j+1} = q_j + h\dot{q}_j$ instead of the velocity discretization in (5.193). The work in [1142] uses the scheme in (5.193) to prove existence results. This is an improvement with respect to Problem 5.2 in which the inertia matrix is assumed to be constant. External forces reduce to conservative ones, and the potential energy is assumed to be globally Lipschitz continuous in q.
4. Impact rules have to be chosen in addition to (5.193). In [47] the method in [1001] is taken, whereas [1141, 1142] base on Moreau's inelastic rule. In his pioneering work [763] Lötstedt proposed to extend Gauss' principle to the case of multiple shocks with friction, but his solution lacks of physical meaning.

• Schatzman and Paoli proposed a specific numerical scheme devoted to the integration of systems with unilateral constraints [966, 970]. The nice feature of the proposed discretization is that it is proved that the solution of the approximating problem converges uniformly on any finite time interval toward that of the original system in proportion as the step converges to zero. This numerical scheme applies to particles evolving in a convex set Φ and follows the well-posedness developments of Problem 2.2. It is formulated in a θ-method framework as [7]

$$\begin{cases} M(q_{j+1})(q_{j+1} - 2q_j + q_{j-1}) + h^2 F(t_{j+\theta}, q_{j+\theta}, \dot{q}_{j+\theta}) = p_{j+1}, \\ q_{j+1} = \frac{q_{j+1} - q_{j-1}}{2h}, \\ p_{j+1} \in -N_\Phi \left(\frac{q_{j+1} + e_n q_{j-1}}{2h} \right). \end{cases} \tag{5.194}$$

The mechanical meaning of p_{j+1} is not clear with such a choice of the normal cone argument. One advantage of this scheme may be that for $e_n = 0$ the constraint is satisfied at the position level (in the NSCD method it is satisfied at the velocity level). A weakness is that Φ appears in the normal cone, while $V(q)$ is always convex polyhedral in the sweeping process's right-hand side (consequently in the NSCD method). When the constraint is attained, the discrete-time velocity reverses after two steps. Since this may induce too large numerical errors, some modifications implying a one-step velocity reversal have been proposed [936]. It is noteworthy that extensive numerical testing in [971] on systems ranging from 1 to 29 degrees of freedom has concluded that except in very simple systems, there is no advantage in using a penalization with respect to the numerical scheme in (5.194). A qualitative comparison between the Schatzman–Paoli and the Moreau–Jean schemes is made

in [7]. Extensions have been published in [974] for the one-degree-of-freedom and the n-degree-of-freedom cases with class C^3 boundary $\mathrm{bd}(\Phi)$. The authors of [368] claim that they improve the Schatzman–Paoli's scheme, using a nonstandard finite difference method that renders it unconditionally stable, and it preserves energy between impacts. The nonstandard method mainly consists of replacing h^2 (in the one-degree-of-freedom case or a harmonic oscillator with $F(t,q,\dot{q}) = \omega^2 q$) by $\frac{4}{\omega^2}\sin(\omega\frac{h}{2})^2$.

5.7.3.4 Time-Stepping Algorithm for the Darboux–Keller Impact Dynamics

Let us consider the discretization of (4.141) with an implicit time-stepping scheme. For this let us start from (4.142). We consider the discretization in the p_{n} timescale, on an interval $[0, P]$, $p_{\mathrm{n},j+1} = p_{\mathrm{n},j} + h$, $0 \le j \le N-1$, $p_{\mathrm{n},0} = 0$, $p_{\mathrm{n},N} = P$, $h > 0$. We denote $v_{r,\mathrm{n}}(p_{\mathrm{n},j})$ as $v_{r,\mathrm{n}}^j$, and so on. An implicit Euler discretization is applied:

$$\begin{cases} v_{r,\mathrm{n}}^{j+1} - v_{r,\mathrm{n}}^j \in hM_{\mathrm{nn}}^{-1} - hM_{\mathrm{nt}}^{-1}\partial\psi_{\mathscr{D}_\mu}^{\star}(v_{r,\mathrm{t}}^{j+1}) \\ v_{r,\mathrm{t}}^{j+1} - v_{r,\mathrm{t}}^j \in hM_{\mathrm{nt}}^{-1} - hM_{\mathrm{tt}}^{-1}\partial\psi_{\mathscr{D}_\mu}^{\star}(v_{r,\mathrm{t}}^{j+1}). \end{cases} \tag{5.195}$$

The next proposition shows that the one-step nonsmooth problem for (5.195) is uniquely solvable, where the matrices are assumed to be full rank.

Proposition 5.29 *Given $v_{r,\mathrm{n}}^j$ and $v_{r,\mathrm{t}}^j$, the algorithm in (5.195) gives*

$$v_{r,\mathrm{t}}^{j+1} = v_{r,\mathrm{t}}^j + hM_{\mathrm{nt}}^{-1} - hM_{\mathrm{tt}}^{-1}\mathrm{proj}_{M_{\mathrm{tt}}^{-1}}\left[\mathscr{D}_\mu; \frac{(M_{\mathrm{tt}}^{-1})^{-1}}{h}(v_{r,\mathrm{t}}^j + hM_{\mathrm{nt}}^{-1})\right] \tag{5.196}$$

and

$$v_{r,\mathrm{n}}^{j+1} = v_{r,\mathrm{n}}^j + hM_{\mathrm{nn}}^{-1} - hM_{\mathrm{nt}}^{-1}\mathrm{proj}_{M_{\mathrm{tt}}^{-1}}\left[\mathscr{D}_\mu; \frac{(M_{\mathrm{tt}}^{-1})^{-1}}{h}(v_{r,\mathrm{t}}^j + hM_{\mathrm{nt}}^{-1})\right] \tag{5.197}$$

Proof We have $\frac{(M_{\mathrm{tt}}^{-1})^{-1}}{h}[v_{r,\mathrm{t}}^{j+1} - v_{r,\mathrm{t}}^j - hM_{\mathrm{nt}}^{-1}] \in \partial\psi_{\mathscr{D}_\mu}^{\star}(v_{r,\mathrm{t}}^{j+1})$, which is found using (B.16) to be equivalent to $v_{r,\mathrm{t}}^{j+1} \in N_{\mathscr{D}_\mu}\left(-\frac{(M_{\mathrm{tt}}^{-1})^{-1}}{h}(v_{r,\mathrm{t}}^{j+1} - v_{r,\mathrm{t}}^j - hM_{\mathrm{nt}}^{-1})\right)$. Let $z^{j+1} \triangleq -\frac{(M_{\mathrm{tt}}^{-1})^{-1}}{h}v_{r,\mathrm{t}}^{j+1}$, and $\zeta^j = \frac{(M_{\mathrm{tt}}^{-1})^{-1}}{h}(v_{r,\mathrm{t}}^j + hM_{\mathrm{nt}}^{-1})$. We obtain $M_{\mathrm{tt}}^{-1}(z^{j+1} + \zeta^{j+1}) - M_{\mathrm{tt}}^{-1}\zeta^j \in -N_{\mathscr{D}_\mu}(z^{j+1} + \zeta^j)$. Using (B.20), this gives $z^{j+1} = \zeta^j + \mathrm{proj}_{M_{\mathrm{tt}}^{-1}}[\mathscr{D}_\mu; \zeta^j]$, and thus $z^{j+1} = \frac{(M_{\mathrm{tt}}^{-1})^{-1}}{h}(v_{r,\mathrm{t}}^j + hM_{\mathrm{nt}}^{-1}) + \mathrm{proj}_{M_{\mathrm{tt}}^{-1}}[\mathscr{D}_\mu; \zeta^j]$. This shows (5.196). To prove (5.196), we need to calculate a selection ξ^{j+1} of the set-valued term $\partial\psi_{\mathscr{D}_\mu}^{\star}(v_{r,\mathrm{t}}^{j+1})$. To this aim we can use (5.196) and the second inclusion in (5.195). We find that $\xi^{j+1} = \mathrm{proj}_{M_{\mathrm{tt}}^{-1}}\left[\mathscr{D}_\mu; \frac{(M_{\mathrm{tt}}^{-1})^{-1}}{h}(v_{r,\mathrm{t}}^j + hM_{\mathrm{nt}}^{-1})\right]$, from which (5.197) follows.

It is interesting to see that $v_{r,\mathrm{t}}^{j+1}$ can be obtained at each step by solving a quadratic problem under convex constraints, using the equivalences in (B.20). Notice that if $\frac{(M_{\mathrm{tt}}^{-1})^{-1}}{h}(v_{r,\mathrm{t}}^{j} + hM_{\mathrm{nt}}^{-1}) \in \mathscr{D}_{\mu}$ then $v_{r,\mathrm{t}}^{j+1} = 0$: the sticking mode is attained at $j+1$. The next step is about the convergence of this implicit Euler scheme. For that we first notice that the coordinate change $\tilde{v}_{r,\mathrm{t}} \stackrel{\Delta}{=} R^{-1}v_{r,\mathrm{t}}$, with R the positive definite symmetric square root of M_{tt}^{-1}, allows us to recast the differential inclusion $\frac{dv_{r,\mathrm{t}}}{dp_{\mathrm{n}}} \in M_{\mathrm{nt}}^{-1} - M_{\mathrm{tt}}^{-1}\partial_{\mathscr{D}_{m\mu}}(v_{r,\mathrm{t}})$ into the general framework of (B.24), since $\mathscr{D}_{\mu}$ is closed convex (hence, so is $\psi_{\mathscr{D}_{\mu}}(\cdot)$ and its conjugate function). The implicit algorithm in (5.195) is analyzed in [97, 102]. Then from [102, Proposition 4.4], the algorithm converges and has order $\frac{1}{2}$: there exists a constant c such that for all $h > 0$, we have for all $p_{\mathrm{n}} \in [0, P]$: $||v_{r,\mathrm{t}}(p_{\mathrm{n}}) - v_{r,\mathrm{t}}^{h}(p_{\mathrm{n}})|| \leq c\sqrt{h}$, where $v_{r,\mathrm{t}}^{h}(\cdot)$ is the linear interpolation of the $v_{r,\mathrm{t}}^{k}$'s at times t_k. Moreover, $\lim_{h\to 0, h>0} v_{r,\mathrm{t}}^{h}(\cdot) = v_{r,\mathrm{t}}(\cdot)$ where $v_{r,\mathrm{t}}(\cdot)$ is a solution of the differential inclusion. Moreover, and perhaps most importantly, the sticking phases are simulated without the spurious oscillations around $v_{r,\mathrm{t}} = 0$ which are observed when an explicit Euler scheme is used. This fact has been first observed and proved in [617], see Sect. 5.7.3.7 for similar ideas in discrete-time sliding mode control.

5.7.3.5 Time-Stepping Algorithm for Linear Complementarity Systems

The LCS in (5.128) completed with a state jump rule (5.145) may be discretized with a time-stepping method that is very close to Moreau's catching-up algorithm. Starting from (5.128) we set:

$$\begin{cases} \frac{x_{j+1}-x_j}{h} = Ax_{j+1} + Eu_{j+1} + B\lambda_{j+1} \\ 0 \leq \lambda_{j+1} \perp w_{j+1} = Cx_{j+1} + Fu_{j+1} + D\lambda_{j+1} \geq 0. \end{cases} \tag{5.198}$$

The first equation is rewritten as $(I_n - hA)x_{j+1} = x_j + hEu_{j+1} + B(h\lambda_{j+1})$, thus if $(I_n - hA)$ is invertible, we obtain the LCP:

$$0 \leq \lambda_{j+1} \perp w_{j+1} = \overbrace{[C(I_n - hA)^{-1}hB + D]}^{\stackrel{\Delta}{=}M(h)}\lambda_{j+1} + G(x_j, u_{j+1}) \geq 0, \tag{5.199}$$

with $G(x_j, u_{j+1}) = C(I_n - hA)^{-1}(x_j + hEu_{j+1}) + Fu_{j+1}$. Notice that if the term Ax is discretized explicitly, we obtain instead of (5.199): $0 \leq \lambda_{j+1} \perp w_{j+1} = (hCB + D)\lambda_{j+1} + H(x_j, u_{j+1}) \geq 0$, with $H(x_j, u_{j+1}) = C(I_n + hA)x_j + hCEu_{j+1} + Fu_{j+1}$. The difference between both schemes is that the LCP matrix $M(h)$ is changed to $N(h) = hCB + D$. In both cases from Theorem 5.105, the one-step nonsmooth problem (OSNSP) is solved uniquely for any x_j and u_{j+1}, if and only if $M(h)$ (or $N(h)$) is a P-matrix. Preliminary results on time-stepping discretization of circuits with ideal diodes are in [720] (a brief historical introduction to nonsmooth circuits modeling, analysis, and simulation is in [10, §1.5]). Results

on the convergence of piecewise interpolations $\{\hat{x}^h(\cdot)\} =$ of $\{x_j\}$ and $\{\hat{\lambda}^h(\cdot)\}$ of $\{\lambda_j\}$ are stated in [502], when state trajectories $x(\cdot)$ are continuous and $\lambda(\cdot)$ is Lebesgue integrable. A major conclusion is that if (A, B, C, D) is passive (equivalently it satisfies the passivity linear matrix inequality (LMI)), and $Cx_0 \in LCP - \mathrm{Im}(D)$,[66] then the OSNSP is solvable for h small enough, $\hat{x}^h(\cdot) \to x(\cdot)$ as $h \to 0$ uniformly on the interval of integration $[0, T]$, $\hat{\lambda}^h(\cdot) \to \lambda(\cdot)$ as $h \to 0$ weakly in $L^2(0, T)$, and the limit functions are weak solutions of the continuous-time LCS. This shows once again that passive LCS have continuous solutions, except perhaps initially if $x(0^-)$ does not satisfy $Cx(0^-) \in LCP - \mathrm{Im}(D)$. Then a jump has to be applied so that $Cx(0^+) \in LCP - \mathrm{Im}(D)$. We have seen elsewhere that LCS with a "passivity-like" input–output constraint are quite related to differential inclusions with maximal monotone set-valued right-hand side. In this case, the algorithm in (5.198) is similar to the numerical scheme in [102] where orders $\frac{1}{2}$ or 1 are proved. Remind also that passivity constrains the relative degree between the two complementary variables (or the index in the multivariable case $m \geq 2$).

$\rightsquigarrow$ *Implicit (also called backward Euler) schemes as in (5.198) are well suited to LCS whose transfer matrix* $C(sI_n - A)^{-1}B + D$ *has index* ≤ 1.

The unknown of the LCP in (5.199) is λ_{j+1}, whose interpolation is meant to approximate $\lambda(\cdot)$. If the multiplier is a function this is sound. However, if the LCS has state jumps, λ is a distribution. Consider the material in Sect. 5.4.4.3, which applies when $D = 0$. It shows that under certain conditions an LCS can be transformed into a Moreau's first-order sweeping process (5.140). Then the catching-up algorithm may be applied, in the case of RCLBV solutions (which yield a measure differential inclusion, i.e., λ is a measure). However, the LCP variable, which then becomes a selection of the set-valued right-hand side (a normal cone), is no longer λ_{j+1}, but $\xi_{j+1} \stackrel{\Delta}{=} h\lambda_{j+1}$. The interpretation is that ξ_{j+1} approximates the measure $\lambda([t_j, t_{j+1}))$ of an interval $[t_j, t_{j+1})$ by the measure λ: this is a bounded real number, and it makes sense to calculate it numerically. This is the same issue as we met for Mechanics and impacts. When the LCS are such that λ is a higher degree distributions, we face a distribution differential inclusion, and the framework settled in [15] applies, where a time-stepping scheme extending the catching-up algorithm is proposed.

Remark 5.36 The system in (2.14) is an LCS which models a linear spring-dashpot system with the switching conditions indicated just below Remark 2.2, i.e.,

$$\begin{cases} m\ddot{x}(t) + f\dot{x}(t) + kx(t) = u(t) & \text{if } -f\dot{x}(t) - kx(t) > 0 \\ m\ddot{x}(t) = u(t) & \text{if } -f\dot{x}(t) - kx(t) \leq 0 \end{cases} \tag{5.200}$$

[66] The set $LCP - \mathrm{Im}(D)$ denotes all vectors q such that the LCP $0 \leq \lambda \perp D\lambda + q \geq 0$ is solvable.

where the switching surface is not equal to $\{(x, \dot{x})|x = 0\}$ but $\{(x, \dot{x})|f\dot{x} + kx = 0\}$. With an external action $u(t)$ we have

$$\begin{cases} \dot{\eta}(t) = A\eta(t) + B\lambda(t) + Eu(t) \\ 0 \leq w(\eta(t)) = C\eta(t) \perp \lambda(t) \geq 0 \end{cases} \tag{5.201}$$

with $E = (0, 1, 0)^T$. This perfectly fits with (5.128) with $D = 0$ and $F = 0$. The time discretization of Lagrange dynamics with spring-dashpot normal contact, and Coulomb's friction, has been analyzed in [1128] using complementarity. The limit to the rigid case is studied in [1128, Theorem6], and a condition related to "positive linear independence" of $\nabla f(q)$ and $H_{\mathrm{t}}(q)$ is imposed, which prevents unbounded contact forces in the limit.

One good question is: does there exist a numerical method which preserves the dissipativity properties of the continuous-time LCS? When a $\theta-$method is used instead of the Euler implicit in (5.198), the answer is in [480][67].

5.7.3.6 Time-Stepping Algorithm for Impulsive ODEs

We consider in this section the time discretization of impulsive ODEs as in (1.31). This is a topic that has received very little attention in the related mathematical literature [345, 755, 1029, 1030], which has focused almost uniquely on stability issues. Time-stepping algorithms are studied in [345, 755, 1029], for impulsive ODEs with fixed state jump times t_k. Euler, $\theta-$method, and Runge–Kutta algorithms are analyzed. Since the jump times are known, the discretization grid $\{t_{k,l}\}$ is constructed such that the time step $h = \frac{1}{m}, t_{k,l} = t_k + hl, 0 \leq l \leq m$. Hence, the jump mapping is approximated as $x(t_{k,0}) - x(t_{k-1,m}) = I_k(t_{k-1,m})$. Stability and convergence results are proved in these references.

5.7.3.7 Discrete-Time Sliding Mode Control

The implicit Euler discretization of Coulomb's friction is able to suppress spurious oscillations during the sticking phases of motion which appear when an explicit method is used (see [617] for an early proof of this fact). In sliding mode control, such oscillations are called *chattering* in the neighborhood of the sliding (attractive) surface: they affect the output and the input, which takes the form of a high-frequency bang–bang controller as depicted in Fig. 5.26. The similarity between Coulomb's model and set-valued sliding mode controllers has motivated the analysis of implicit discrete-time sliding mode controllers [14, 16] (see also the close results in [663, 664]), which prove to be quite efficient in practice as they suppress the output and the input chattering phenomena [553, 554, 1245]. The time discretization of set-valued

[67] Which to the best of the author's knowledge is the first article where a rigorous definition of numerical dissipation is given, using Willems' dissipativity in both continuous and discrete-time.

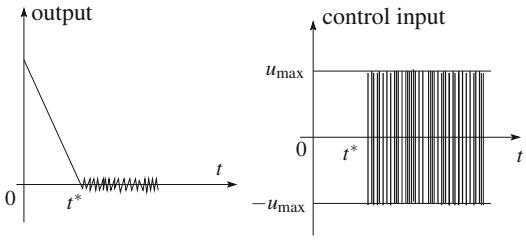

Fig. 5.26 Numerical chattering in the input and the output, with an explicit Euler discretization

controlled Lagrange dynamics is considered in [26], with convergence and order results. Both Euler and zero-order-hold may be considered. Continuing the analogy with Coulomb's friction, the control input in a sliding mode controlled system is a selection of the signum multifunction.

Chapter 6
Generalized Impact Laws and Multiple Impacts

We speak of a *multiple impact* when several collisions occur at the same time in a multibody system. Multiple impacts are complex phenomena which possess particular features, not shared by single impacts. In the first part of this chapter, these specific properties are described. Then, two models of multiple impacts are presented: the first one extends kinematic laws (Newton's and Moreau's impact laws), while the second one extends Darboux-Keller's impact dynamics and uses energetic coefficients of restitution at each contact/impact point. The extension of Poisson's kinetic law is briefly introduced. Chains of balls and the rocking block systems serve as examples.

6.1 Particular Features of Multiple Impacts

A multiple impact occurs each time several contact points of a system may undergo some (local) normal velocity jump ($v_{\mathrm{n},i}(t_k^+) \neq v_{\mathrm{n},i}(t_k^-)$, where i is the contacting points index). This encompasses those contacts with $v_{\mathrm{n},i}(t_k^-) = 0$, i.e. some contacts may be closed (or active) at the impact time, as is the case in the popular Newton's cradle where the balls touch each other at the shock instant (the same occurs for the rocking block system). More rigorously we may state the following. Consider an n-degree-of-freedom system with a configuration space $\mathscr{Q}$, subjected to m unilateral constraints $f(q) \geq 0$. The admissible domain is $\Phi = \{q \in \mathscr{Q} | f(q) \geq 0\}$, impacts occur on its boundary $\mathrm{bd}(\Phi)$. The boundary is made of hypersurfaces $\Sigma_l \stackrel{\Delta}{=} \bigcap_{i=1}^{l} \Sigma_i$, with $\Sigma_i \subseteq \{q \in \mathbb{R}^n | f_i(q) = 0\}$ which is a codimension one hypersurface (with some abuse we will say that Σ_i has also codimension one). Therefore, Σ_l has codimension $l \geq 1$. Physically, this means that l unilateral constraints boundaries are reached at the same time t_k, including situations where some of them become active (i.e. $f_i(q(t)) > 0$ in a left-neighborhood of t_k, and $v_{\mathrm{n},i}(t_k^-) = \nabla f_i(q(t_k))^T \dot{q}(t_k^-) < 0$) while others were already active (i.e. $f_j(q(t)) = 0$ in a left-neighborhood of t_k, and $v_{\mathrm{n},j}(t_k^-) = \nabla f_j(q(t_k))^T \dot{q}(t_k^-) = 0$). The subtlety here is that the previously-lasting

B. Brogliato, *Nonsmooth Mechanics*, Communications and Control Engineering,
DOI 10.1007/978-3-319-28664-8_6

contacts may satisfy $v_{\mathrm{n},j}(t_k^+) = \nabla f_j(q(t_k))^T \dot{q}(t_k^+) > 0$, and this is why they are part of the multiple impact phenomenon. We will see later that such "distance effects" are due to wave transmission through the multibody system.

Definition 6.1 (*Multiple Impact*) We say that an $l-$multiple impact occurs each time the attained boundary hypersurface Σ_l has codimension $l \geq 0$.

Remark 6.1 Physically, and taking into account contact deformations, collisions at different points of a system may be declared to be simultaneous when they overlap and thus may influence each other. In a perfect rigid body model limit, they occur at the same time.

6.1.1 Some Specific Features of Multiple Impacts

A typical case of a multiple impact is the collision of a chain of N aligned identical balls with a rigid ground, as shown in Fig. 6.1. When the impact occurs, the balls are all contacting each other and an $N-1$-impact occurs. The chain is submitted to gravity, and starts at a height h. The mass of a stainless steel bead used in the experiment is $m = 2.05 \times 10^{-3}$ kg. The Young modulus and Poisson ratio for stainless steel are $E = 21 \times 10^{10}$ N/m^2 and $\nu_s = 0.276$, respectively. Thus, the value of the contact stiffness, K_i, $i = 2, \ldots, N$ for sphere/sphere contact is 6.9716×10^9 N/m$^{3/2}$. For the contact between the bead and the wall made of stainless steel, the value of the contact stiffness K_1 for the sphere-plane contact is 9.858×10^9 N/m$^{3/2}$.

It is shown experimentally in [387] and numerically in [749] that the maximum contact force during the impact process, is almost independent of N, i.e. of the total mass of the chain. This is a rather counter-intuitive result. In Fig. 6.2a are depicted the contact forces felt at the ground during the shock, for a column of $N = 1, 2, \ldots, 8$ beads with fall height $h = 3.1$ mm (pre-impact velocity 0.246 m/s). In Fig. 6.2b are depicted the contact forces felt at the ground during the shock, for a column of $N = 5, 6, \ldots, 12$ beads with fall height $h = 5.1$ mm (pre-impact velocity 0.316 m/s). The restitution coefficient between the beads is $e_{\mathrm{n},s} = 0.96$, and the restitution coefficient between the last particle and the ground is $e_{\mathrm{n},p} = 0.92$. The numerical

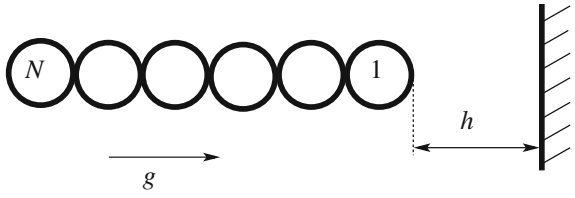

Fig. 6.1 A column of beads colliding against a wall

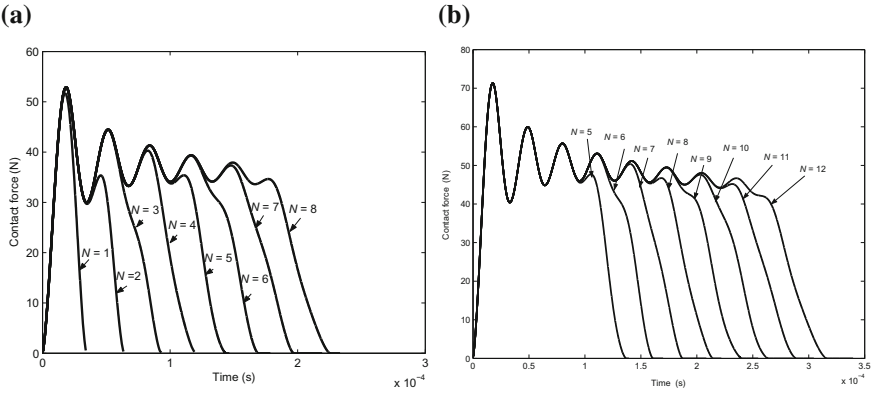

Fig. 6.2 The contact force at the wall during the collision. Taken from [749, Figs. 2, 3]. **a** $N = 1, \ldots, 8$. **b** $N = 5, \ldots, 12$

results are obtained with the LZB model, that is described in Sect. 6.3. Notice that the collisions durations in Fig. 6.2a, b are less than 32 μs, and increase with increasing N. Thus the contact force *impulse* varies with N.

⇝ *The physical phenomenon that is responsible for this observed and simulated behavior, is the presence of nonlinear waves inside the column of beads during the shock. These waves create some energy dispersion inside the chain.*

It is noteworthy that due to the property of sphere/sphere collisions, waves inside the bodies (bulk waves) are negligible (the impacts are quasi-static, see Sect. 4.2.4). Thus an excellent model of the chain, consists of particles interacting with Hertz stiffness (and some damping, the choice of which is crucial and not straightforward). What happens during and after the shock? In a monodisperse chain (all identical, lossless spheres) that is impacted by one of these spheres at one end (this is the "classical" Newton's cradle case study), the waves due to the local deformations of the beads take the form of an almost-perfect solitary wave that travels through the chain (until it arrives at the last "free" bead, which thus takes almost all of the initial kinetic energy). In case of a chain colliding a ground, the wave effects are much less regular.

6.1.1.1 Discontinuity w.r.t. Initial Conditions

The fact that the impact outcome (the postimpact velocities) may depend on the way the system is initialized, has been noticed a long time ago [422]. This is directly related with the order of the pairwise collisions at the various contact points, and to the kinetic angles between the hypersurfaces of constraints. Consider for instance a chain as in Fig. 6.1, with $N = 2$, masses m_1 and m_2, radii R_1 and R_2, coordinates q_1 and q_2, respectively. Its dynamics is given by:

$$\begin{cases} m_1\ddot{q}_1(t) = -m_1 g + \lambda_{12}(t) \\ m_2\ddot{q}_2(t) = -m_2 g - \lambda_{12}(t) + \lambda_2(t) \\ \\ 0 \le \lambda_{12} \perp f_1(q) = q_1 - q_2 - R_1 - R_2 \ge 0 \\ 0 \le \lambda_2 \perp f_2(q) = q_2 - R_2 \ge 0, \end{cases} \tag{6.1}$$

where λ_{12} is the force exerted by ball 1 on ball 2, λ_2 is the force exerted by the wall on ball 2. The impact dynamics is given by:

$$\begin{cases} m_1(\dot{q}_1(t_k^+) - \dot{q}_1(t_k^-)) = p_1(t_k) \\ m_2(\dot{q}_2(t_k^+) - \dot{q}_2(t_k^-)) = -p_1(t_k) + p_2(t_k). \end{cases} \tag{6.2}$$

We associate a Newton's impact law with each contact, with restitution coefficients $e_{\mathrm{n},1}$ and $e_{\mathrm{n},2}$, respectively. The superscript $-$ means pre-impact velocity, whereas $+$ means postimpact velocity. When there are several impacts we indicate it as $++$ or $+++$. The sequence of impacts B_2/wall (Σ_2) and B_1/B_2 (Σ_1) produces the outcome

$$\begin{cases} \dot{q}_1^+ = \frac{m-e_{\mathrm{n},1}}{1+m}\dot{q}_1^- - e_{\mathrm{n},2}\frac{1+e_{\mathrm{n},1}}{1+m}\dot{q}_2^- \\ \\ \dot{q}_2^{++} = \frac{m(1+e_{\mathrm{n},1})}{1+m}\dot{q}_1^- - e_{\mathrm{n},2}\frac{1-e_{\mathrm{n},1}m}{1+m}\dot{q}_2^-, \end{cases} \tag{6.3}$$

with $m \stackrel{\Delta}{=} \frac{m_1}{m_2}$. The sequence of impacts B_1/B_2 (Σ_1) and B_2/wall (Σ_2) and then B_1/B_2 (Σ_1) again, produces the outcome[1]:

$$\begin{cases} \dot{q}_1^{++} = \frac{m-e_{\mathrm{n},1}}{1+m}\left(\frac{m-e_{\mathrm{n},1}}{1+m}\dot{q}_1^- + \frac{1+e_{\mathrm{n},1}}{1+m}\dot{q}_2^-\right) - e_{\mathrm{n},2}\frac{1+e_{\mathrm{n},1}}{1+m}\left(\frac{m(1+e_{\mathrm{n},1})}{1+m}\dot{q}_1^- + \frac{1-e_{\mathrm{n},1}m}{1+m}\dot{q}_2^-\right) \\ \\ \dot{q}_2^{+++} = \frac{m(1+e_{\mathrm{n},1})}{1+m}\left(\frac{m-e_{\mathrm{n},1}}{1+m}\dot{q}_1^- + \frac{1+e_{\mathrm{n},1}}{1+m}\dot{q}_2^-\right) - e_{\mathrm{n},2}\frac{1-e_{\mathrm{n},1}m}{1+m}\left(\frac{m(1+e_{\mathrm{n},1})}{1+m}\dot{q}_1^- + \frac{1-e_{\mathrm{n},1}m}{1+m}\dot{q}_2^-\right). \end{cases} \tag{6.4}$$

Clearly, the final values in (6.3) and (6.4) are not the same. Let us provide a second example on a 3-ball chain as in Fig. 6.4, but where the initial gap between ball 1 and ball 2 is δ_1 and the initial gap between ball 2 and ball 3 is δ_2. Suppose that $\dot{q}_1(t_k^-) = v_s > 0$, $\dot{q}_3(t_k^-) = -v_s < 0$, and $\dot{q}_2(t_k^-) = 0$. Also let us choose $m_1 = m_3 = \frac{m}{4}$ and $m_2 = m$. If $\delta_1 < \delta_2$, one computes the outcome $\dot{q}_1(t_k^+) = -\frac{6v_s}{10}$ m/s, $\dot{q}_2(t_k^+) = -\frac{4v_s}{25}$ m/s, $\dot{q}_3(t_k^+) = \frac{31v_s}{25}$ m/s. Now if $\delta_1 > \delta_2$, one computes the outcome $\dot{q}_1(t_k^+) = -\frac{31v_s}{25}$ m/s, $\dot{q}_2(t_k^+) = \frac{4v_s}{25}$ m/s, $\dot{q}_3(t_k^+) = \frac{3v_s}{5}$ m/s. The problem is perfectly symmetric, and one expects that if $\delta_1 = \delta_2$ the outcome is also symmetric. Energy conservation yields $\dot{q}_1(t_k^+) = -v_s$ m/s, $\dot{q}_3(t_k^+) = v_s$ m/s, $\dot{q}_2(t_k^+) = 0$ m/s. One sees that if the impact occurs as a double impact (i.e. right at the codimension 2 singularity of the admissible domain boundary), it is impossible to deduce it from the limit of the impacts that occur in an arbitarily small neighborhood of this singularity. This

[1] It is implicitly assumed here that there exists initial velocities and positions such that these various sequences of collisions exist, incorporating the kinematic admissibility of the postimpact velocities.

second example shows that continuity in the initial data (see Sect. 1.3.2.3) may not hold for systems with multiple unilateral constraints.

$\rightsquigarrow$ *Multiple surfaces of constraints (equivalently codimension* ≥ 2 *boundaries of the admissible domain* Φ*) may create discontinuity of the solutions with respect to the initial conditions. In this case, it is not possible to deduce the impact law at the singularity (simultaneous impacts) by studying the limit as the initial data approach the singularity.*

This explains why binary collision models have to be used with some care.

6.1.1.2 Momentum Conservation

It is often taken for granted that the conservation of momentum (linear momentum for a chain of aligned balls) is part of an impact law. Such a point of view is absolutely wrong. Indeed, the conservation of linear momentum at an impact time, is a direct consequence of Newton's third law of action/reaction: *When one body exerts a force on a second body, the second body simultaneously exerts a force equal in magnitude and opposite in direction on the first body*. One has to assume that Newton's third law is still valid during collisions, which seems to be a reasonable assumption, though historically subject to some controversy [434]. To illustrate this fact, consider the dynamics of the 3-ball system as in Fig. 6.4, where the balls have radii R. Its dynamics outside impacts is given by:

$$\left\{\begin{array}{l} m_1\ddot{q}_1(t) = -\lambda_{12}(t) \\ m_2\ddot{q}_2(t) = \lambda_{12}(t) - \lambda_{23}(t) \\ m_3\ddot{q}_3(t) = \lambda_{23}(t) \\ \\ f_1(q) = q_2 - q_1 - 2R \geq 0 \\ f_2(q) = q_3 - q_2 - 2R \geq 0. \end{array}\right. \tag{6.5}$$

Let us notice that both (6.1) and (6.5) fit within (5.1). Clearly from (6.5) one has $m_1\ddot{q}_1(t) + m_2\ddot{q}_2(t) + m_3\ddot{q}_3(t) = 0$, from which it follows that the linear momentum satisfies $m_1\dot{q}_1(t)+m_2\dot{q}_2(t)+m_3\dot{q}_3(t) = m_1\dot{q}_1(0)+m_2\dot{q}_2(0)+m_3\dot{q}_3(0)$. This property is kept at the impact time, as shown in (6.9) that yields $m_1\dot{q}_1(t_k^+) + m_2\dot{q}_2(t_k^+) + m_3\dot{q}_3(t_k^+) = m_1\dot{q}_1(t_k^-) + m_2\dot{q}_2(t_k^-) + m_3\dot{q}_3(t_k^-)$. Such is not the case for (6.1), whose impact dynamics is in (6.2).

$\rightsquigarrow$ *The linear momentum may or may not be conserved at an impact. The fact that conservation holds for the 3-ball system, is just an* illustration *of momentum conservation on a specific system. It is not part of any impact law.*

The last point is illustrated in the next section. Historically, Newton's third law has been used for the first time to solve an impact problem, by 'sGravesand in 1721 [1091], who also suspected that plastic deformation could play a role. Leibniz was the first to use kinetic energy conservation together with what we call today Newton's restitution law (with $e_n = 1$) [434].

6.1.1.3 Single Versus Multiple Impacts

Let us make some computations which clarify the major discrepancy between single and multiple impacts. Let us consider the 3-ball system, with initial conditions $\dot{q}_1(t_k^-) = 1$ m/s, $\dot{q}_2(t_k^-) = \dot{q}_3(t_k^-) = 0$ m/s, ball 2 and ball 3 touch each other initially, $m_1 = m_2 = m_3 = 1$ g. The set of equalities and inequalities which have to hold at the impact time t_k are

$$\begin{cases} \dot{q}_1(t_k^+) - 1 = -p_{12}(t_k) \\ \dot{q}_2(t_k^+) = p_{12}(t_k) - p_{23}(t_k) \\ \dot{q}_3(t_k^+) = p_{23}(t_k) \\ \\ p_{23}(t_k) \geq 0,\ p_{12}(t_k) \geq 0 \quad \text{(kinetic constraints)} \\ \\ \nabla f_1(q)^T \dot{q}(t_k^+) = \dot{q}_2(t_k^+) - \dot{q}_1(t_k^+) \geq 0 \\ \nabla f_2(q)^T \dot{q}(t_k^+) = \dot{q}_3(t_k^+) - \dot{q}_2(t_k^+) \geq 0 \quad \text{(kinematic constraints)} \\ \\ \dot{q}_1(t_k^+)^2 + \dot{q}_2(t_k^+)^2 + \dot{q}_3(t_k^+)^2 = 1 \quad \text{(energetic constraint).} \end{cases} \tag{6.6}$$

It follows from the post-velocities admissibility that $\dot{q}_3(t_k^+) \geq \dot{q}_2(t_k^+) \geq \dot{q}_1(t_k^+)$. From the energy constraint $|\dot{q}_1(t_k^+)^2| \leq 1$ so that $p_{12}(t_k) = 1 - \dot{q}_1(t_k^+) \geq 0$. Assume that $\dot{q}_3(t_k^+) \leq 0$, then $\dot{q}_2(t_k^+) \leq 0$ and $\dot{q}_1(t_k^+) \leq 0$: this is impossible from the linear momentum conservation equation $\dot{q}_1(t_k^+) + \dot{q}_2(t_k^+) + \dot{q}_3(t_k^+) = 1$. Thus necessarily $\dot{q}_3(t_k^+) > 0$, hence $p_{23}(t_k) > 0$: the kinetic constraints are automatically satisfied if the other equalities and inequalities hold. We may therefore eliminate the impulses *via* the momentum conservation and solve the problem with velocities only. We are left with the system:

$$\begin{cases} \dot{q}_1(t_k^+) + \dot{q}_2(t_k^+) + \dot{q}_3(t_k^+) = 1 \\ \dot{q}_1(t_k^+)^2 + \dot{q}_2(t_k^+)^2 + \dot{q}_3(t_k^+)^2 = 1 \\ \dot{q}_2(t_k^+) - \dot{q}_1(t_k^+) \geq 0, \quad \dot{q}_3(t_k^+) - \dot{q}_2(t_k^+) \geq 0. \end{cases} \tag{6.7}$$

It happens that the system in (6.7) possesses an infinity of solutions, which are "between" two "extremals": (A) with $(\dot{q}_1(t_k^+), \dot{q}_2(t_k^+), \dot{q}_3(t_k^+)) = (0, 0, 1)$ and (B) with $(\dot{q}_1(t_k^+), \dot{q}_2(t_k^+), \dot{q}_3(t_k^+)) = (-\frac{1}{3}, \frac{2}{3}, \frac{2}{3})$ (see Fig. 6.3b).
Let us consider now the impact between two balls. Doing a similar reasoning it is easy to obtain the system:

$$\begin{cases} \dot{q}_1(t_k^+) + \dot{q}_2(t_k^+) = 1 \\ \dot{q}_1(t_k^+)^2 + \dot{q}_2(t_k^+)^2 = 1 \\ \dot{q}_2(t_k^+) - \dot{q}_1(t_k^+) \geq 0. \end{cases} \tag{6.8}$$

The system in (6.8) has a unique solution $\dot{q}_1(t_k^+) = 0$ m/s, $\dot{q}_2(t_k^+) = 1$ m/s. Imposing Newton's impact law with $e_n = 1$ implies the energy equality, see (4.41). On the other hand, imposing $T_L(t_k) = 0$ and the kinematic constraint implies $e_n = 1$.

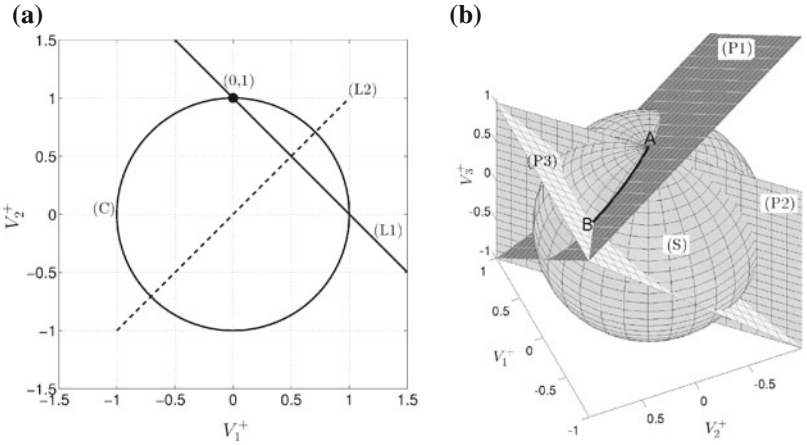

Fig. 6.3 Post-impact velocities domains ($V_i^+ \stackrel{\Delta}{=} \dot{q}_i(t_k^+)$). Taken from [929, Figs. 1.1 and 1.2]. **a** System in (6.8). **b** System in (6.7)

Graphically, the two systems in (6.7) and (6.8) are depicted in Fig. 6.3. In Fig. 6.3b, momentum conservation defines the plane (P_1) is defined from the points $(0, 0, 1)$, $(0, 1, 0)$ and $(1, 0, 0)$. Energy constraint defines the boundary of the sphere. The kinematic constraints impose that the postimpact velocities must be located in front of (P_2) and above (P_3)

$\rightsquigarrow$ *Energy conservation (or a simple impact law) is sufficient to make the impact problem solvable with uniqueness for the central impact of two balls. It is not sufficient to solve with uniqueness the 3-ball system at impact: a multiple impact law is needed. The set of solutions of* (6.7) *corresponds to various dispersions of the kinetic energy in the chain after the collision.*

6.1.1.4 Kinetic Energy Dispersion

The outcome of the central impact between two spheres of masses m_1 and m_2, where friction is neglected (an assumption that we obviously made from the beginning of this section), where $\dot{q}_1(t_k^-) = 1$ m/s and $\dot{q}_2(t_k^-) = 0$ m/s, and energy is conserved, is given using (4.42) by $\dot{q}_1(t_k^+) = \dot{q}_1(t_k^-) - 2\frac{m_2(\dot{q}_1(t_k^-)-\dot{q}_2(t_k^-))}{m_1+m_2} = 1 - \frac{2m_2}{m_1+m_2}$, and $\dot{q}_2(t_k^+) = \dot{q}_2(t_k^-) + 2\frac{m_1(\dot{q}_1(t_k^-)-\dot{q}_2(t_k^-))}{m_1+m_2} = \frac{2m_1}{m_1+m_2}$. Consider now a chain of M aligned identical balls in contact, that impacts a second chain of N identical balls which are also in contact (we may call this an $M : N$-collision). Suppose that $m_1 = Mm$, $m_2 = Nm$, where m is the mass of each ball. If the balls of each sub-chain are glued together (and hence are equivalent to two solid rigid bodies), one obtains the outcome $\dot{q}_1(t_k^+) = \frac{M-N}{M+N}$ and $\dot{q}_2(t_k^+) = \frac{2M}{M+N}$. It is noteworthy that this result holds if a Hertz or linear stiffness is used to model the contact/impact between the two

spheres. Indeed these compliant models yield an equivalent restitution coefficient $e_n = 1$, while energy and momentum (more exaclty, Newton's third law) constraints are unchanged. Thus the kinetic energy of the balls that move forward after the collision, is equal to $\frac{1}{2}Nm\left(\frac{2M}{M+N}\right)^2$ if $N \geq M$ (only ball 2 moves forward), and to $\frac{1}{2}Nm\left(\frac{2M}{M+N}\right)^2 + \frac{1}{2}Mm\left(\frac{M-N}{M+N}\right)^2$ if $N < M$ (both balls move forward). What happens when the balls are not glued, but the contacts are unilateral? Extensive simulations with Hertz unilateral springs[2] are presented in [749, Table II] for $M + N = 10$ balls. They show that as the number of impacting balls M increases, there are $M + 2$ balls that move forward after the shock (with positive velocity), while the remaining balls on the left move backwards with very low negative velocities. Moreover the postimpact kinetic energy of the $M + 2$ "forward" balls is approximately 99 % of the total kinetic energy. Both systems (glued contacts and unilateral contacts) match if and only if $M + 2 = N$ and $N\left(\frac{2M}{N+M}\right)^2 = 0.99M$. This holds if and only if $M = 9$ and $N = 11$. The results are therefore in general quite different one from each other. The reason is that the deformations at the contacts, and the unilaterality, allow the creation of wave phenomena through the chain of $N+M$ balls during the impact. The nonlinear waves are quite irregular ones except if $M = 1$, even if the two sub-chains are monodisperse. They are responsible for the dispersion (or the distribution) of the energy within the chain after the collision. Similar numerical results on $M : N$ collisions with $M + N = 50$ and 100, $N = 1, 2, 3, 4, 5, 6$ are presented in [529, § 5 (c)]. They show that there are M separated solitary waves which are created through the chain, and which are responsible for the balls to fly off after the impact, each solitary wave acting as a "collisional effect" for the last ball. The longer the chain, the more separated the waves. They also show that when $N = 5$ and $M = 1, 2, 3, 4$, then $M + 1$ balls move forward after the collision while the remaining ones move backwards with very small velocities.

$\rightsquigarrow$ *Once again, nonlinear waves make the impacts in chains of balls—and more generally in multibody systems—a quite complex phenomenon. The design of a rigid-body-like model of multiple impacts, that would encapsulate such wave effects, is a hard task.*

Remark 6.2 The dispersion effect, is sometimes named the *distance effect*. Indeed if the collision is assumed to be instantaneous, the impact at one edge of the chain produces an effect at the other edge.

To be complete, we should also consider impacts between two elastic bodies, like sphere/rod or rod/rod collisions, and compare the results with the above. The type of elasticity, and the type of waves (planar displacement linear wave traveling along the rods) is quite different from the nonlinear waves in chains of balls with unilateral Hertz elasticity. Roughly speaking, linear waves in elastic rods follow the 1 dimensional linear wave equation $\frac{\partial^2 u}{\partial t^2} = c^2 \frac{\partial^2 u}{\partial x^2}$, where $u(t, x)$ is the displacement of the rod's thin section, $c = \sqrt{\frac{E}{\rho}}$ is the speed of the uniform planar displacement wave,

[2] Which do represent an excellent, high-fidelity model for impacting spheres [387].

E is the rod's Young modulus and ρ its density. They may be considered as the limit of chains with bilateral, linear springs, when the number of elements tends to infinity (a spatial discretization of the linear wave equation). While nonlinear waves in chains of aligned balls follow nonlinear partial differential equations [609], and there may exist solitary waves in $1 : N$ collisions of monodisperse chains [1087]. These solitons have doubly exponential decay [275], so that they are concentrated on a compact support of five balls in long enough chains.

$\rightsquigarrow$ *The linear waves—bulk vibrational effects—in elastic bodies, and the nonlinear waves in chains of balls with unilateral Hertzian contact, are of quite different nature.*

6.1.1.5 Equivalence of Rheological Compliant Models

When two bodies collide, two contact compliant models (visco-elastic, or elasto-plastic) which provide the same restitution coefficient will give the same postimpact velocity. From this point of view, they are equivalent, despite they may provide quite different impact duration and contact force history. If the same compliant models are used in a chain of balls to model the contact between each pair of balls, the postimpact velocity of the balls may however drastically differ. The reason is that despite they give the same restitution coefficient for pairwise collisions, the contact force history, the impact duration and the maximum compression times that they predict, may differ. These discrepancies may in turn produce quite different impact outcomes, see Sect. 6.1.3 for the lossless case.

6.1.2 Han-Gilmore's and Binary Collisions Models

Let us start with the method proposed by Han and Gilmore [500] that is an analytical computer-oriented method to analyze multiple impacts, including friction. The method in [500] does not apply to closed kinematic-loops, but is rather devoted to granular-like systems. The authors analyze the outcomes in multibody systems when some contacts may break, due to *internal impacts* (see definition below). A computational algorithm is presented, based on a particular topological description of the system: the distance k between contact-impact points is chosen to be the minimum number of bodies that separate a given point and the prespecified reference point. The algorithm uses the impact analysis between two bodies developed in [500] to calculate, for each k (starting at $k = 0$) the postimpact motion. Then an exhaustive procedure that considers all possible outcomes during the impact process is given. Let us note that it is not stated in [500] that the proposed algorithm yields a solution in all cases, and if it does whether it is unique or not. As the simple 3-ball system shows in Sect. 6.1.3, uniqueness cannot be expected in general (the example we treat corresponds to the perfectly elastic case; when the perfectly plastic case is chosen—$e_{\mathrm{n}} = 0$ at both contacts—then Han and Gilmore algorithm converges in an infinite number of iterations [372], see also Sect. 6.1.4 below). A 5-ball system of elastic beads—$e_{\mathrm{n}} = 1$ at all contacts—is analysed in [929, p. 57] with non unique outcome.

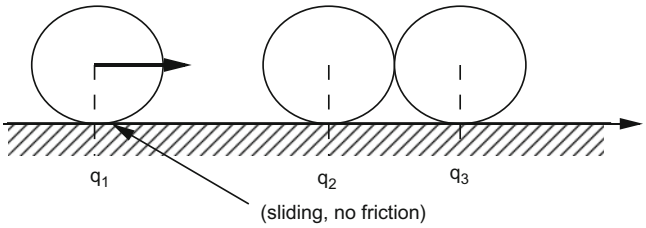

Fig. 6.4 The 3-ball system

Let us consider the system depicted in Fig. 6.4. The three balls (or spheres, or particles) are sliding horizontally. There is no dissipation between the balls and the ground. The notion of *internal* and *sequential* impacts is introduced in [500]: internal impacts are impacts that occur between two bodies previously in contact, i.e. which occur in fact through an internal transmission inside the bodies, and such that they create detachment.[3] The authors also assume the possibility of a certain chronology for the possible impacts occuring in the system, hence sequential impacts. Although such an analysis might appear natural for the treatment of multiple collisions, it will be shown that multiple impact phenomena require deeper analysis because sequential pairwise impacts are not sufficient to model them properly. Let us explain how solutions (i.e. postimpact velocities) can be found. The shock dynamical equations are given at the shock instant t_k by:

$$\left\{\begin{array}{l} \dot{q}_1(t_k^+) - \dot{q}_1(t_k^-) = -p_{12}(t_k) \\ \dot{q}_2(t_k^+) - \dot{q}_2(t_k^-) = p_{12}(t_k) - p_{23}(t_k) \\ \dot{q}_3(t_k^+) - \dot{q}_3(t_k^-) = p_{23}(t_k). \end{array}\right. \tag{6.9}$$

The masses are taken equal to one for simplicity, and the pre-impact velocities are chosen as $\dot{q}_1(t_k^-) = 1, \dot{q}_2(t_k^-) = \dot{q}_3(t_k^-) = 0$. It is supposed no energy loss ($T_L(t_k) = 0$) at impacts. Two postimpact sets of velocities are computed and are given by:

$$\dot{q}_1(t_k^+) = -\tfrac{1}{3},\ \dot{q}_2(t_k^+) = \dot{q}_3(t_k^+) = \tfrac{2}{3}\ \text{m/s}, \tag{6.10}$$

and

$$\dot{q}_1(t_k^+) = \dot{q}_3(t_k^+) = 0,\ \dot{q}_2(t_k^+) = 1\ \text{m/s}. \tag{6.11}$$

The solution in (6.10) can be found by applying Newton's restitution rule with $e_n = 1$ between bodies 1 and 2 (i.e. $\dot{q}_1(t_k^+) = -1 + \dot{q}_2(t_k^+)$), and between bodies 2 and 3 (i.e. $\dot{q}_2(t_k^+) = \dot{q}_3(t_k^+)$), and assuming a nonzero $p_{23}(t_k)$ (i.e. implicitly assuming a nonzero $\dot{q}_3(t_k^+)$). The solution in (6.11) can be found by assuming no shock between bodies 2 and 3, i.e. $p_{23}(t_k) = 0$. Now notice that (6.10) can be set as definitive since postimpact motion is possible: the first body rebounds and the other two remain stuck.

[3] Internal impacts are due to distance effects, created by waves that travel through the multibody system.

But solution 2 is not feasible between bodies 2 and 3: that problem is overcome in [500] by assuming a second impact between bodies 2 and 3. Applying Newton's rule between bodies 1 and 2 and bodies 2 and 3 yields another nonfeasible solution. But assuming there is no impact between 1 and 2 (i.e. $p_{12}(t_k) = 0$) yields a feasible motion. This solution is then given by:

$$\dot{q}_1(t_k^{++}) = \dot{q}_2(t_k^{++}) = 0,\ \dot{q}_3(t_k^{++}) = 1 \text{ m/s}. \tag{6.12}$$

The superscript $^{++}$ is to distinguish the impacts chronologically. This solution is a possible motion: bodies 1 and 2 remain stuck, body 3 moves to the right. In fact the above reasoning relies on three rules:

- (i) The kinetic energy loss at impact is zero (energy constraint).
- (ii) The postimpact velocity must assure a feasible motion, i.e. point inwards the domain inside the constraints (kinematic constraint).
- (iii) Let us denote q_i and q_{i+1} the coordinates of two successive balls. Then if $\dot{q}_i(t_k^-) > \dot{q}_{i+1}(t_k^-)$, the percussion between these two bodies $p_{ij} \neq 0$. If $\dot{q}_i(t_k^-) < \dot{q}_{i+1}(t_k^-)$, $p_{ij} = 0$. If $\dot{q}_i(t_k^-) = \dot{q}_{i+1}(t_k^-)$, then two possibilities must be tested: either $p_{ij}(t_k) = 0$ or $p_{ij}(t_k) > 0$ (kinetic constraint).

It can be shown that due to the particular choice of the initial conditions, (i) implies that the restitution coefficients between the balls is equal to 1. (ii) allows one to decide at each step whether a computed velocity is admissible or not. (iii) is a fundamental rule which permits to decide the form of the percussion vector. It can be shown that in this particular example, the algorithm has a finite number of iterations, and that the only two possible postimpact velocities are the ones in (6.10) and (6.12). When an admissible velocity has been found, it is considered as definitive. But all possible paths have to be tested.

Thus the Han and Gilmore algorithm yields two possible solutions for the postimpact velocities, and it is *a priori* impossible to decide which one is the right one, just relying on rigid body theory. Experimentally, monodisperse 3-ball chains with balls made of very hard material, evolve closely to the solution in (6.12). However the experimental outcome is different: although the third ball detaches quickly from the second one and takes about 98 % of the kinetic energy, the second and the first balls possess nonzero postimpact velocity, and do have a motion after the shock (for instance, values $\dot{q}_1(t_k^+) = -0.0605\dot{q}_1(t_k^-)$ m/s, $\dot{q}_2(t_k^+) = 0.1049\dot{q}_1(t_k^-)$ m/s and $\dot{q}_3(t_k^+) = 0.9978\dot{q}_1(t_k^-)$ m/s are reported from experiments in [985]). This is related to kinetic energy dispersion inside the chain. The balls are commonly made of hard material (iron) so that the rigid body assumption can be considered to be valid in this case. However the small postimpact motion of the first and second balls should not be neglected because it has a great influence on the long-term dynamics of the chain.

Close to the Han and Gilmore algorithm is the so-called *binary collision model*. One starts assuming that the impacts are pairwise and sequential with an *a priori* given order (e.g. for the 3-ball chain, a first impact between ball 1 and ball 2, then a second impact between ball 2 and ball 3). The first collision gives a first postimpact velocity $\dot{q}(t^+)$. One has to check whether $\nabla f(q)^T \dot{q}(t^+) \geq 0$, which implies that the

three balls do not collide again. If this condition is not satisfied, then another impact occurs that gives $\dot{q}(t^{++})$. One then checks if $\nabla f(q)^T \dot{q}(t^{++}) \geq 0$ or not, and so on. Such binary collision approach may yield an accumulation of impacts in a finite time. Moreover it is meant to correctly model the wave effect inside the chain, but does not always provide satisfactory results. Finally, changing the initial sequence of impacts may change the final outcome, because of discontinuity of the trajectories with respect to initial data, as shown in (6.2)–(6.4). For the 3-ball chain, one obtains the following results. Let us assume that $\dot{q}_1(t_0^-) = \dot{q}_1^0 > 0$ m/s, $\dot{q}_2(t_0^-) = \dot{q}_3(t_0^-) = 0$ m/s, and that there is a first impact between balls 1 and 2, then between balls 2 and 3. One obtains [929]:

$$\begin{cases} \dot{q}_1(t_0^{++}) = \dfrac{1-\dfrac{m_2}{m_1}e_{\mathrm{n},1}}{1+\dfrac{m_2}{m_1}}\dot{q}_1^0 \\ \dot{q}_2(T_0^{++}) = \dfrac{(1-\dfrac{m_3}{m_2}e_{\mathrm{n},2})(1+\dfrac{m_2}{m_1}e_{\mathrm{n},1})}{(1+\dfrac{m_2}{m_1})(1+\dfrac{m_3}{m_2})}\dot{q}_1^0 \\ \dot{q}_3(t_0^{++}) = \dfrac{(1+e_{\mathrm{n},1})(1+e_{\mathrm{n},2})}{(1+\dfrac{m_2}{m_1})(1+\dfrac{m_3}{m_2})}\dot{q}_1^0. \end{cases} \tag{6.13}$$

For a monodisperse conservative chain ($e_{\mathrm{n},1} = e_{\mathrm{n},2} = 1$, $m_1 = m_2 = m_3$), the outcome $\dot{q}_1(t_0^{++}) = \dot{q}_2(t_0^{++}) = 0$ and $\dot{q}_3(t_0^{++}) = \dot{q}_1^0$ m/s is found, that corresponds to (6.12). If $e_{\mathrm{n},1} = e_{\mathrm{n},2} = 0$ then $\dot{q}_1(t_0^{++}) = \frac{\dot{q}_1^0}{2}$ m/s, $\dot{q}_2(t_0^{++}) = \dot{q}_3(t_0^{++}) = \frac{\dot{q}_1^0}{4}$ m/s: it does not satisfy the criterion $\nabla f(q)^T \dot{q}(t^{++}) \geq 0$, thus other impacts have to be calculated. It happens that the postimpact velocities outcome domain when both $e_{\mathrm{n},1}$ and $e_{\mathrm{n},2}$ are varied between 0 and 1, does not fill in the whole quarter disk in Fig. 5.5, but just the portion of it denoted (II), see [929, Fig. 3.7]. It is therefore not clear why in general it should be preferred to Moreau's rule, which is much simpler to implement in a code. Experiments on the 2-ball system hitting a wall (take $N = 2$ in Fig. 6.1), are performed in [126] with varying initial gap between the two balls (this is known as the basketball-tennis ball problem[4]). It is shown that as the initial gap becomes very small (the collision approaches a 2-impact), then prediction of binary collision model and experimental results diverge significantly [126, Fig. 3]. It is also striking that the impact duration for positive gap, is quite different from the impact duration for nearly zero gap [126, Fig. 9]. It is shown also in [982] that the binary collision model is valid for certain range of mass and stiffness ratios only: *this proves, if needed, that multiple impacts involve internal mechanisms related to wave effects, which may significantly depart from sequential, binary collisions*. Fundamentally, the fact that the balls' gap is strictly positive, or if it vanishes, drastically modifies

[4] An experiment anyone can do. Put a tennis ball on the top of a basketball, and drop both on a rigid ground. The tennis ball rebounds violently and very high, while the basketball almost does not rebound at all: the whole energy is transferred to the tennis ball during the impact with the ground.

the impact wave that travels through the balls. Further results on the basketball-tennis ball problem, may be found in [315, 906]. It is noteworthy that both balls are shells with internal pressure, and may not obey Hertz' elasticity, nor classical damping (see [751, Sect. 8] and [126]).

Remark 6.3 The analysis of multiple impacts using binary collision models, is closely related to the study of impacts of a particle in a two-dimensional wedge, and to the analysis of billiards. Indeed the 3-ball system is equivalent, after some suitable transformation, to a particle striking a corner, see [929, Appendix A] for a complete analysis. See also Sect. 6.1.4.

6.1.3 Penalization at Contacts (Compliance)

Let us consider the 3-ball system as depicted in Fig. 6.5. The study which follows may be seen as an extension of the contents of Sect. 2.1.1, in a multiple impact context. The dynamical equations are given by:

$$\begin{cases} m_1\ddot{x}_1(t) = k_1(x_2(t) - x_1(t)) \\ m_2\ddot{x}_2(t) = k_1(x_1(t) - x_2(t)) + k_2(x_3(t) - x_2(t)) \\ m_3\ddot{x}_3(t) = k_2(x_2(t) - x_3(t)) \\ x_1(0) = x_2(0) = x_3(0) = 0,\ \dot{x}_1(0) = 1\ m/s, \dot{x}_2(0) = \dot{x}_3(0) = 0\ m/s. \end{cases} \tag{6.14}$$

Let us denote $k_1 = k$, $\frac{k_2}{k_1} = \gamma$, $m_1 = m_2 = m_3 = m$, $\Delta = \sqrt{\gamma^2 - \gamma + 1}$, $\alpha_1 = \sqrt{-\Delta + \gamma + 1}$, $\alpha_2 = \sqrt{\Delta + \gamma + 1}$, $\omega = \sqrt{\frac{k}{m}}$, $\omega_1 = \alpha_1\omega$, $\omega_2 = \alpha_2\omega$. The solution of (6.14) is given by:

$$\begin{cases} x_1(t) = \frac{1}{\omega_1}\left(\frac{1}{3} - \frac{1-2\gamma}{6\Delta}\right)\sin(\omega_1 t) + \frac{1}{\omega_2}\left(\frac{1}{3} + \frac{1-2\gamma}{6\Delta}\right)\sin(\omega_2 t) + \frac{t}{3} \\ x_2(t) = -\frac{1}{\omega_1}\left(\frac{1}{6} - \frac{2-\gamma}{6\Delta}\right)\sin(\omega_1 t) - \frac{1}{\omega_2}\left(\frac{1}{6} + \frac{2-\gamma}{6\Delta}\right)\sin(\omega_2 t) + \frac{t}{3} \\ x_3(t) = -\frac{1}{\omega_1}\left(\frac{1}{6} + \frac{1+\gamma}{6\Delta}\right)\sin(\omega_1 t) - \frac{1}{\omega_2}\left(\frac{1}{6} - \frac{1+\gamma}{6\Delta}\right)\sin(\omega_2 t) + \frac{t}{3}. \end{cases} \tag{6.15}$$

The balls 1 and 2 separate at time t_1 such that $x_1(t_1) = x_2(t_1)$, and the balls 2 and 3 separate at time t_2 such that $x_3(t_2) = x_2(t_2)$, with:

$$\begin{cases} (\Delta - 1 - \gamma)\alpha_2 \sin(\omega_1 t_1) + (\Delta + 1 - \gamma)\alpha_1 \sin(\omega_2 t_1) = 0 \\ \alpha_2 \sin(\omega_1 t_2) - \alpha_1 \sin(\omega_2 t_2) = 0. \end{cases} \tag{6.16}$$

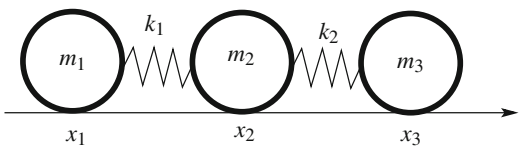

Fig. 6.5 Three-ball system with unilateral elastic contacts

It is noteworthy that the solutions $\omega_1 t_1, \omega_2 t_1, \omega_1 t_2$ and $\omega_2 t_2$ of these two transcendental equations, do not depend on k since their coefficients do not depend on k.

$\rightsquigarrow$ *Thus from* (6.15) *it follows that the velocities at separation times, are independent of* k, *but depend only on the stiffness ratio* γ.

This was already noticed in [202, 203], as well as in [622, 623] for the two-ball system hitting a wall (for which the outcome depends also on the mass ratio only). Let us now study two extreme cases, where $\gamma = 0$ and $\gamma = +\infty$. In the first case $\gamma = 0$, one can show that $\omega_1 = 0$, $\omega_2 = \sqrt{2}\omega$, $\sin(\omega_2 t_1) = 0$ and $t_1 = \frac{\pi}{\sqrt{2}\omega}$ (compare with (2.2)). Consequently, $t_1 < t_2$ and $\dot{x}_1(t_1) = 0$ m/s, $\dot{x}_2(t_1) = 1$ m/s, $\dot{x}_3(t_1) = 0$ m/s. Therefore, balls 2 and 3 continue their collision, and it is easily obtained that at the end of this collision (which is the end of the multiple shock) one has $\dot{x}_1(t_f) = 0$ m/s, $\dot{x}_2(t_f) = 0$ m/s, $\dot{x}_3(t_f) = 1$ m/s. When $\gamma = +\infty$ we find $\omega_1 = \omega$, $\omega_2 = +\infty$, $\sin(\omega_1 t_1) = 0$, $\sin(\omega_1 t_2) = 0$, $t_1 = t_2 = \frac{\pi}{\omega}$ (compare again with (2.2): this time the 2-impact behaves like a single impact!). Then $\dot{x}_1(t_f) = -\frac{1}{3}$ m/s, $\dot{x}_2(t_f) = \dot{x}_3(t_f) = \frac{2}{3}$ m/s. This last outcome is the one obtained applying Moreau's impact law (or Newton's impact law at each contact) with a CoR $e_n = 1$, see Example 5.5. It is important to see that these two extreme cases, can be obtained by letting the stiffnesses k_1 and k_2 both diverge to infinity, but at different rates. This proves that even in the limit of a rigid body model, the outcome of this multiple impact depends strongly on the relative stiffnesses, though they do not depend on the absolute value of the stiffnesses. It is noteworthy that the two extreme cases for the stiffness ratio γ, give the solutions in (6.10) and (6.12).

$\rightsquigarrow$ *The energetical behavior of the system, plus the kinetic and kinematic constraints, are not sufficient to characterize the impact outcome in a multiple impact. The results of the lossless, penalized 3-ball system when the stiffness ratio* γ *varies, confirms the analysis of Sect.* 6.1.1.3: *varying* γ *allows to span the portion of arc* AB *in Fig.* 6.3*b; in Fig.* 5.5, *it allows to span the curve* AB *for* $KER = 1$, *while Moreau's law is "stuck" at* B.

More calculations with different assumptions on the parameters, may be found in [929, Appendix C].

Remark 6.4 (*Zero Dispersion Chains*) We consider the initial velocities in (6.14). Reinsch [1035] has shown that a symmetric chain of $n + 1$ aligned beads, with unilateral linear elastic contacts, is totally *dispersion-free* (that is, the last bead takes exactly all the energy of the impacting one, and the other beads have zero postimpact velocity) if the masses and the stiffnesses are properly chosen [929, Appendix D]. For a 3-ball chain, one finds equal stiffnesses $k_1 = k_2$ and $m_1 = m_3 = m$, $m_2 = \frac{2}{3}m$. Newby [632] investigates a 3-ball chain with equal masses, and whether it is possible to recover γ from the postimpact velocities (this is called in [632] the *inverse scattering* problem): this is not always possible. He finds that all possible postimpact outcomes are described with compliant models such that $\gamma \in (0, \gamma_{\max})$, for some $\gamma_{\max}$. There is therefore a periodicity in γ in the dynamics. In particular the solution $\dot{x}_1(t_f) = -\frac{1}{3}$ m/s, $\dot{x}_2(t_f) = \dot{x}_3(t_f) = \frac{2}{3}$ m/s, occurs for an infinite number of γ's,

not only for $\gamma = \infty$. Newby also finds that balls 1 and 2 separate at the same time as balls 2 and 3 (a sort of symmetrical double collision with $t_1 = t_2$) when $\gamma = \frac{(3n^4-2n^2+3)+\sqrt{9n^8-12n^6-42n^4-12n^2+9}}{8n^2}$, $n = 2, 3, 4 \ldots$.

6.1.4 Multiplicity of Multiple Impacts

When a particle hits an angle in the plane, it may rebound successively on both the surfaces in various ways, depending on the CoRs and the angle value. This is a binary collision model including possible secondary impacts, which gives outcomes for collision that occur near the singularity (a 2-impact in the sense of Definition 6.1). Let us summarize here the results of Towne and Hadlock [1211], who deal with a three-ball chain (that is equivalent to the particle hitting an angle, see [929, Sect. A.1]). The two Newton's CoRs are chosen equal ($e_{\mathrm{n},1} = e_{\mathrm{n},2} = e_{\mathrm{n}}$). The first ball collides the two other balls at rest. The number of collisions and the postimpact velocities depend on the following variable:

$$z = \zeta(e_{\mathrm{n}})\eta(m_{1,2}, m_{3,2}), \tag{6.17}$$

where $\zeta(e_{\mathrm{n}})$ and $\eta(m_{1,2}, m_{3,2})$ are defined as:

$$\begin{cases} \zeta(e_{\mathrm{n}}) = \frac{1}{2}\left(\sqrt{e_{\mathrm{n}}} + \frac{1}{\sqrt{e_{\mathrm{n}}}}\right) \geq 1 & \text{for all } e_{\mathrm{n}} \in (0, 1] \\ \eta(m_{1,2}, m_{3,2}) = \frac{1}{\sqrt{(1+m_{2,1})(1+m_{2,3})}} < 1 & \text{for all } m_{1,2},\ m_{3,2}, \end{cases} \tag{6.18}$$

with $m_{j,i} = m_j/m_i$. We see that $z > 0$ and can diverge to infinity as $e_{\mathrm{n}} \to 0$. The variable z consists of two distinct parts $\zeta(e_{\mathrm{n}})$ and $\eta(m_{1,2}, m_{3,2})$: $\zeta(e_{\mathrm{n}})$ is related to the dissipative behavior of the chain, while $\eta(m_{1,2}, m_{3,2})$ is related to the kinetic angle θ_{12} of the chain defined by $\eta(m_{1,2}, m_{3,2}) = \cos(\theta_{12})$ (this can be calculated from (6.66), see [929, Eq. (A.4)]). The number of binary collisions is given as follows:

- When $0 < z < 1$, the number of collisions N is finite and computed as:

$$N = \left\lfloor \frac{\pi}{\arccos(z)} - 1 \right\rfloor \tag{6.19}$$

- When $z \geq 1$, the number of collisions N is infinite.

The above results show that $N \leq 3$ when $z > 1/2$, i.e. secondary collisions occur when $z > 1/2$. Moreover, the number of collisions N increases as z increases and it becomes infinite when $z \geq 1$. Consider the case when $e_{\mathrm{n}} = 1 \ \Rightarrow \ z = \cos(\theta_{12})$. From (6.19), the number N of collisions is given by:

$$N = \left\lfloor \frac{\pi - \theta_{12}}{\theta_{12}} \right\rfloor. \tag{6.20}$$

The condition for which N is infinite ($z \geq 1$) can be rewritten as:

$$\frac{1}{2}\left(\sqrt{e_{\mathrm{n}}} + \frac{1}{\sqrt{e_{\mathrm{n}}}}\right)\cos(\theta_{12}) \geq 1. \tag{6.21}$$

More on this topic may be found in [683, 936], see also [929, § 3.4, Appendix A]. Extending this type of analysis to $e_{\mathrm{n},1} \neq e_{\mathrm{n},2}$ or to more than three balls (equivalently, to particles in three dimensions hitting a "pyramidal" angle), seems to be at best very difficult.[5] It nevertheless shows that the binary collision model may indeed involve, even in simple systems, an infinity of successive impacts. If this infinity occurs in a finite time, a Zeno phenomenon occurs which may create difficulty for time-integration with an event-driven code.

6.2 Kinematic Multiple-Impact Law (Generalized Newton)

This section is devoted to investigate how we may extend kinematic impact laws like Newton's or Moreau's laws, in order to obtain an impact law which is able to span the whole set of admissible outcomes. To this aim we proceed with a particular transformation of the Lagrange equations in (5.1).

6.2.1 The Quasi-Lagrange Equations

Let us remind that the m_b bilateral constraints are denoted as $h_i(q)$ for $i \in \{1, \ldots, m_b\}$, and the m_u unilateral constraints are $f_i(q) \geq 0$ for $i \in \{m_{b+1}, \ldots, m_u + m_b\}$, and we assume that $m_u + m_b \leq n$. We also assume that $M(q) \succ 0$, and all the constraints $f_i(q)$ and $h_i(q)$ are functionally independent at any $q \in \mathscr{Q}$, that is the $(m_u + m_b) \times n$ gradient matrix $\begin{pmatrix} \nabla f(q) \\ \nabla h(q) \end{pmatrix}$ has full column rank $m_u + m_b$. This in particular precludes that the gradients vanish in the domain of interest on the configuration space $\mathscr{Q}$. The $m_u + m_b$ normal unitary vectors to the codimension 1 constraints manifolds $\Sigma_i = \{q \in \mathscr{Q} | h_i(q) = 0\}$, $1 \leq i \leq m_b$, equipped with the kinetic metric are defined as:

$$\mathbf{n}_{q,i} = \frac{M^{-1}(q)\nabla h_i(q)}{\sqrt{\nabla h_i^T(q) M^{-1}(q) \nabla h_i(q)}}, \quad 1 \leq i \leq m_b, \tag{6.22}$$

and similarly for $\Sigma_i = \{q \in \mathscr{Q} | f_i(q) = 0\}$, $m_b + 1 \leq i \leq m_b + m_u$. Clearly the normal vectors $\mathbf{n}_{q,i} \in \mathbb{R}^n$ are independent. If $m_b + m_u < n$ we have to complete the

[5] It has to the best of the author's knowledge, never been tackled, despite Towne and Hadlock's article was published in 1977.

set $(\mathbf{n}_{q,1}, \ldots, \mathbf{n}_{q,m+p})$ by $n - m_b - m_u$ mutually independent vectors $\mathbf{t}_{q,i}$ in order to make a basis. The $\mathbf{t}_{q,i}$ vectors are chosen such that $\langle \mathbf{t}_{q,i}, \mathbf{n}_{q,j} \rangle_q = \mathbf{t}_{q,i}^T M(q) \mathbf{n}_{q,j} = 0$ for all $i \in \{1, \ldots, n - m_u - m_b\}$, $j \in \{1, \ldots, m_u + m_b\}$. We notice that the vectors $\mathbf{t}_{q,i}^T$ are orthogonal to the kinetic gradients $\mathbf{n}_{q,j}$ in the kinetic metric, and orthogonal to the Euclidean gradients $\nabla h_i(q)$ and $\nabla f_i(q)$ in the Euclidean metric. One may choose unitary vectors $\mathbf{t}_{q,i}$, i.e. $\mathbf{t}_{q,i}^T M(q) \mathbf{t}_{q,i} = 1$. Therefore the vectors $\mathbf{t}_{q,i}$ span $T_q \mathcal{Q}$ whereas the vectors $\mathbf{n}_{q,i}$ span the normal cone $N_\Phi(q)$ to the admissible domain Φ of $\mathcal{Q}$. This admissible domain for q is defined as follows: $\Phi \stackrel{\Delta}{=} \Phi_b \times \Phi_u$ with $\Phi_b = \{q \in \mathcal{Q} | h_i(q) = 0, i \in \{1, \ldots, m_b\}\}$ and $\Phi_u = \{q \in \mathcal{Q} | f_i(q) \geq 0, i \in \{m_b + 1, \ldots, m_b + m_u\}\}$. Thus Φ_b is the bilateral holonomic constraints manifold with codimension m, $\Phi_b = \cap_{i=1}^{m_b} \Sigma_i$, whereas Φ_u is the admissible domain defined by the unilateral constraints, $\Phi_u = \cap_{i=m_b+1}^{m_b+m_u} \Phi_{u,i}$, with $\Phi_{u,i} = \{q \in \mathcal{Q} | f_i(q) \geq 0, i \in \{m_b + 1, \ldots, m_b + m_u\}\}$. For obvious reasons we assume that Φ_u contains a ball of radius > 0. One has $N_\Phi(q) = N_{\Phi_b}(q) \times N_{\Phi_u}(q)$, where $N_{\Phi_b}(q) = \{w \in \mathbb{R}^n | w = \sum_{i=1}^{m_b} \alpha_i \mathbf{n}_{q,i}, \alpha_i \in \mathbb{R}\}$ is the normal cone in the kinetic metric.

6.2.1.1 Frictionless Systems

Let us define the $n \times n$ matrix $\Xi(q) = \begin{pmatrix} \mathbf{n}_q^T \\ \mathbf{t}_q^T \end{pmatrix}$, where $\mathbf{n}_q = (\mathbf{n}_{q,1}, \ldots, \mathbf{n}_{q,m_u+m_b})$ and $\mathbf{t}_q = (\mathbf{t}_{q,1}, \ldots, \mathbf{t}_{q,n-m_u-m_b})$. The *kinetic quasi-velocities* are defined as:

$$v \stackrel{\Delta}{=} \begin{pmatrix} \dot{q}_{\text{norm}} \\ \dot{q}_{\text{tan}} \end{pmatrix} = \Xi(q) M(q) \dot{q} \tag{6.23}$$

where the notation norm and tan come from the fact that v in (6.23) is the Euclidean projection of the generalized momentum $p = M(q)\dot{q}$ on the basis $\mathbf{n}_q$ and $\mathbf{t}_q$ (equivalently the projection of $\dot{q}$ on $\mathbf{n}_q$ and $\mathbf{t}_q$ in the kinetic metric). One could therefore call the kinetic quasi-velocities, the *mass-projected momentum*. From (6.23) $\dot{q}_{\text{norm}} = \mathbf{n}_q^T M(q) \dot{q}$ has dimension $m_u + m_b$ and $\dot{q}_{\text{tan}} = \mathbf{t}_q^T M(q) \dot{q}$ has dimension $n - m_u - m_b$. Notice that the $(m_u + m_b) \times n$ matrix $\mathbf{n}_q^T M(q)$ has rows $\frac{\nabla h_i^T(q)}{||\nabla h_i(q)||_{M^{-1}}}$ and $\frac{\nabla f_i^T(q)}{||\nabla f_i(q)||_{M^{-1}}}$. Thus it follows that $\dot{q}_{\text{norm},i} = \frac{\nabla h_i^T(q) \dot{q}}{||\nabla h_i(q)||_{M^{-1}}}$, and $\mathbf{n}_q = M^{-1}(q)(\nabla h(q), \nabla f(q)) \text{diag}\left(\frac{1}{||\nabla h_i(q)||_{M^{-1}}}, \frac{1}{||\nabla f_i(q)||_{M^{-1}}}\right)$.

Remark 6.5 The developments presented in this section extend the material in the first and second editions of this book [202, 203], and have been investigated in [210, 228]. The use of the kinetic metric for the study of multiple impacts was perhaps first advocated in [581]. It is also implicitly present in Moreau's works [890, 894] where the tangent and normal cones are defined in a generic way, independently of the metric, see also [454, § 4]. The kinetic metrix is also used in mathematical

proofs for convergence of numerical schemes [375]. Notice that far as one analyses the system at a fixed q (like for impacts), then $M(q)$ is constant and the metric is Euclidean.

Example 6.1 For the rocking block system in Sect. 6.3.2.2, we have: $\dot{q}_{\text{norm},1} = \frac{\dot{y}+(\frac{l}{2}\sin(\theta)+\frac{L}{2}\cos(\theta))\dot{\theta}}{\sqrt{\frac{1}{m}+\frac{1}{4I_G}(l\sin(\theta)+L\cos(\theta))^2}}$, $\dot{q}_{\text{norm},2} = \frac{\dot{y}+(\frac{l}{2}\sin(\theta)-\frac{L}{2}\cos(\theta))\dot{\theta}}{\sqrt{\frac{1}{m}+\frac{1}{4I_G}(l\sin(\theta)+L\cos(\theta))^2}}$, $\dot{q}_{\text{tan}} = \sqrt{m}\dot{x}$. For a monodisperse chain of four aligned balls with mass m and radius R, $f_1(q) = q_2 - q_1 - 2R \geq 0$, $f_2(q) = q_3 - q_2 - 2R \geq 0$, $f_3(q) = q_4 - q_3 - 2R \geq 0$. Therefore $\nabla f_1(q) = (-1\ 1\ 0\ 0)^T$, $\nabla f_2(q) = (0\ -1\ 1\ 0)^T$, $\nabla f_3(q) = (0\ 0\ -1\ 1)^T$. After some calculations one finds $\dot{q}_{\text{norm},1} = \frac{1}{\sqrt{2m}}(-\dot{q}_1 + \dot{q}_2)$, $\dot{q}_{\text{norm},2} = \frac{1}{\sqrt{2m}}(-\dot{q}_2 + \dot{q}_3)$, $\dot{q}_{\text{norm},3} = \frac{1}{\sqrt{2m}}(-\dot{q}_3 + \dot{q}_4)$, and $\dot{q}_{\text{tan}} = \frac{\sqrt{m}}{2}(\dot{q}_1 + \dot{q}_2 + \dot{q}_3 + \dot{q}_4)$. It becomes clear from these two examples that in general, $\dot{q}_{\text{tan}}$ does not correspond to the "real-world" tangent velocity at contact points: generalized and local point of views may not match.

Let us denote $F(q, \dot{q}, t) \stackrel{\Delta}{=} C(q, \dot{q})\dot{q} + G(q) - F_{ext}$ in (5.1). Let us now perform the kinetic quasi-velocity transformation of the constrained Lagrange dynamics (5.1) with $H_{\text{t},u}(q, t)\lambda_{\text{t},u} + H_{\text{t},b}(q, t)\lambda_{\text{t},b} = 0$. First notice that:

$$\begin{pmatrix} \ddot{q}_{\text{norm}} \\ \ddot{q}_{\text{tan}} \end{pmatrix} = \Xi(q)M(q)\ddot{q} + \frac{d}{dt}(\Xi(q)M(q))\dot{q} \tag{6.24}$$

Pre-multipyling both sides of (5.1) (a) by $\Xi(q)$ and grouping the normal multipliers as $\lambda_{\text{n}} = \begin{pmatrix} \lambda_{\text{n},b} \\ \lambda_{\text{n},u} \end{pmatrix}$, one obtains:

$$\begin{pmatrix} \ddot{q}_{\text{norm}} \\ \ddot{q}_{\text{tan}} \end{pmatrix} + \Xi(q)F(q, \dot{q}, t) - \frac{d}{dt}(\Xi(q)M(q))\dot{q} = \begin{pmatrix} \mathbf{n}_q^T(\nabla h(q), \nabla f(q))\lambda_{\text{n}} \\ \mathbf{t}_q^T(\nabla h(q), \nabla f(q))\lambda_{\text{n}} \end{pmatrix} \tag{6.25}$$

Let us define $\bar{\lambda}_{\text{n}}$ such that $\bar{\lambda}_{\text{n},b,i} \stackrel{\Delta}{=} ||\nabla h_i(q)||_{M^{-1}}\lambda_{\text{n},b,i}$, $\bar{\lambda}_{\text{n},u,i} \stackrel{\Delta}{=} ||\nabla f_i(q)||_{M^{-1}}\lambda_{\text{n},u,i}$, i.e. $\bar{\lambda}_{\text{n}} = \text{diag}(||\nabla h_i(q)||_{M^{-1}}, ||\nabla f_i(q)||_{M^{-1}})\lambda_{\text{n}}$.[6] From the definition of $\mathbf{t}_{q,i}$ it follows that $\mathbf{t}_q^T(\nabla h(q), \nabla f(q))\lambda_{\text{n}} = 0$, therefore (6.25) becomes:

$$\begin{aligned} &\ddot{q}_{\text{norm}}(t) + F_{\text{norm}}(q(t), \dot{q}_{\text{norm}}(t), \dot{q}_{\text{tan}}(t), t) = [\mathbf{n}_q(t)^T M(q(t))\mathbf{n}_q(t)]\ \bar{\lambda}_{\text{n}}(t) \\ &\ddot{q}_{\text{tan}}(t) + F_{\text{tan}}(q(t), \dot{q}_{\text{norm}}(t), \dot{q}_{\text{tan}}(t), t) = 0 \end{aligned} \tag{6.26}$$

[6] Notice that the assumption that the constraints are functionally independent, guarantees that the norms $||\nabla h_i(q)||_{M^{-1}}$ and $||\nabla f_i(q)||_{M^{-1}}$ never vanish, so $\text{diag}(||\nabla h_i(q)||_{M^{-1}}, ||\nabla f_i(q)||_{M^{-1}})$ is positive definite.

with obvious definitions for $F_{\text{norm}}(q, \dot{q}_{\text{norm}}, \dot{q}_{\text{tan}}, t)$ and $F_{\text{tan}}(q, \dot{q}_{\text{norm}}, \dot{q}_{\text{tan}}, t)$. This canonical form of the dynamics is remarkable because it splits the velocities in a "normal" and a "tangential" parts, similarly to the case of a particle hitting a single frictionless constraint: this is a *generalized particle dynamics*. This is however at the price of introducing additional nonlinearities (stemming from the constraints) in the inertial generalized forces (see the left-hand side in (6.25)). The terms indexed by tan are not affected by the contact force and may be thought of as some kind of tangential dynamics. We may choose to call the first line of (6.26) the *quasi-normal dynamics* and the second line the *quasi-tangential dynamics*. The dynamics in (6.23) (6.26) is consequently a particular case of:

$$\begin{cases} \dot{q}(t) = A(q(t))^{-1} v(t) \\ \bar{M}(q(t))\dot{v}(t) = G(q(t), v(t), t) + A(q(t))^{-T} H(q(t))\lambda \\ v = A(q)\dot{q}, \end{cases} \tag{6.27}$$

where $G(q, v, t)$ gathers inertial forces (centrifugal, Coriolis), forces that derive from the potential energy (gravity, elasticity), external and dissipative forces (control inputs, disturbances, Raileygh dissipation), the mass matrix $\bar{M}(q)$ in (6.27) is not necessarily equal to $M(q)$, v has dimension n, $A(q)$ is invertible but not necessarily integrable, and $H(q)\lambda$ groups all contact forces in the right-hand side of (5.1). In other words, there does not necessarily exist any *quasi-position* $\bar{q} = g(q)$ such that $\frac{d\bar{q}}{dt} = \frac{\partial g}{\partial q}(q)\dot{q}$, so that $A(q)$ is not the Jacobian of any mapping $g(q)$. It is clear that v may correspond to some non-holonomic constraints, hence the name non-holonomic velocities that is sometimes given to quasi-velocities.

It is clear that (6.26) usually is not a Lagrange dynamics since $\bar{M}$ is constant (the identity) whereas nonlinear inertial forces do not vanish (such dynamics are sometimes called Lagrange's equations in quasi-velocities, or Boltzmann-Hamel equations [155], and they may be written in a Lagrangian-like form [367, 417]). Remind that the Delassus' matrix defined when $m_b = 0$ (only unilateral constraints) is equal to $\nabla f(q)^T M(q)^{-1} \nabla f(q)$. The matrix $\mathbf{n}_q^T M(q) \mathbf{n}_q$ may be seen as a normalized Delassus' matrix,[7] whose diagonal entries are equal to 1. It is positive definite if and only if $\mathbf{n}_q$ has full rank $m_u + m_b$. Notice that we can split $\dot{q}_{\text{norm}}$ as $\dot{q}_{\text{norm}} = \begin{pmatrix} \dot{q}^b_{\text{norm}} \\ \dot{q}^u_{\text{norm}} \end{pmatrix}$ with $\dot{q}^b_{\text{norm}} \in \mathbb{R}^{m_b}$ corresponds to bilateral constraints, and $\dot{q}^u_{\text{norm}} \in \mathbb{R}^{m_u}$ corresponds to unilateral constraints. Similarly one has

$$\mathbf{n}_q^T M(q) \mathbf{n}_q = \begin{pmatrix} \mathbf{n}_q^{b,T} M(q) \mathbf{n}_q^b & \mathbf{n}_q^{b,T} M(q) \mathbf{n}_q^u \\ \mathbf{n}_q^{u,T} M(q) \mathbf{n}_q^b & \mathbf{n}_q^{u,T} M(q) \mathbf{n}_q^u \end{pmatrix} \tag{6.28}$$

[7] The Delassus' operator is sometimes called the *fundamental matrix* [185].

Thus the first line in (6.26) can be rewritten as (we drop the time argument in the right-hand side):

$$\begin{cases} \ddot{q}^b_{\text{norm}}(t) + F^b_{\text{norm}}(q(t), \dot{q}_{\text{norm}}(t), \dot{q}_{\text{tan}}(t), t) = \mathbf{n}_q^{b,T} M(q) \mathbf{n}_q^b \bar{\lambda}_{\text{n},b} + \mathbf{n}_q^{b,T} M(q) \mathbf{n}_q^u \bar{\lambda}_{\text{n},u} \\ \ddot{q}^u_{\text{norm}}(t) + F^u_{\text{norm}}(q(t), \dot{q}_{\text{norm}}(t), \dot{q}_{\text{tan}}(t), t) = \mathbf{n}_q^{u,T} M(q) \mathbf{n}_q^b \bar{\lambda}_{\text{n},b} + \mathbf{n}_q^{u,T} M(q) \mathbf{n}_q^u \bar{\lambda}_{\text{n},u} \end{cases} \tag{6.29}$$

Since $\dot{q}^b_{\text{norm}} = 0$ at all times because the system evolves on the codimension $2m_b$ manifold $\{q \in \mathscr{Q} | h_i(q) = 0, \nabla h_i^T(q)\dot{q} = 0, i \in \{1, \ldots, m_b\}\}$, the first equation in (6.29) is equal to $F^b_{\text{norm}}(q, \dot{q}^u_{\text{norm}}, \dot{q}_{\text{tan}}, t) = \mathbf{n}_q^{b,T} M(q) \mathbf{n}_q^b \bar{\lambda}_{\text{n},b} + \mathbf{n}_q^{b,T} M(q) \mathbf{n}_q^u \bar{\lambda}_{\text{n},u}$. If the $m_b \times m_b$ matrix $\mathbf{n}_q^{b,T} M(q) \mathbf{n}_q^b$ is invertible one may obtain λ_n^b from this equation and insert it into the second equation in (6.29) to obtain a dynamics that no longer depends on $\bar{\lambda}_{\text{n},b}$. This modifies the unilateral part of the dynamics (and in particular one obtains a new Delassus' matrix given in (6.35) below). A detailed analysis of the couplings between unilateral and bilateral constraints is made in [209].

6.2.1.2 Systems with Friction

We now incorporate the generalized forces $H_{\text{t}}(q)\lambda_{\text{t}} \stackrel{\Delta}{=} H_{\text{t},u}(q,t)\lambda_{\text{t},u} + H_{\text{t},b}(q,t)$ $\lambda_{\text{t},b} = 0$ in the analysis. Then (6.26) becomes:

$$\begin{aligned} &\ddot{q}_{\text{norm}} - \tfrac{d}{dt}(\mathbf{n}_q^T M(q))\dot{q} + \mathbf{n}_q^T F(q, \dot{q}, t) = \mathbf{n}_q^T M(q) \mathbf{n}_q \ \bar{\lambda}_n + \mathbf{n}_q^T H_{\text{t}}(q) \ \lambda_{\text{t}} \\ &\ddot{q}_{\text{tan}} - \tfrac{d}{dt}(\mathbf{t}_q^T M(q))\dot{q} + \mathbf{t}_q^T F(q, \dot{q}, t) = \mathbf{t}_q^T H_{\text{t}}(q) \ \lambda_{\text{t}} \end{aligned} \tag{6.30}$$

It is remarkable in (6.30) that there is no reason in general that $\mathbf{n}_q^T H_{\text{t}}(q) = 0$, i.e. $\mathbf{n}_q$ is not in general an anihilator of $H_{\text{t}}(q)$. This means that the quasi-tangential dynamics may influence the quasi-normal dynamics, but the reverse never holds since by construction of the basis $(\mathbf{n}_q, \mathbf{t}_q)$ one has $\mathbf{t}_q^T \nabla h(q) = \mathbf{t}_q^T \nabla f(q) = 0$. This is what makes the strong difference between systems with normal/tangential couplings (like the Painlevé example analysed in Sect. 5.6), and systems without normal/tangential couplings. We may say that *generalized particles dynamics usually have normal/tangential inertial couplings, with* $\mathbf{n}_q^T H_{\text{t}}(q) \neq 0$.

6.2.2 The Kinetic Energy

Clearly $\dot{q}^b_{\text{norm}}$ does not play any role in the kinetic energy, being zero. We will see later that the same applies to $\dot{q}_{\text{tan}}$ when one considers the kinetic energy variation at

an impact. Let us assume that $\Xi(q)$ has full rank n. One has:

$$\Xi(q)M(q)\Xi^T(q) = \begin{pmatrix} \mathbf{n}_q^T \\ \mathbf{t}_q^T \end{pmatrix} M(q)(\mathbf{n}_q \ \mathbf{t}_q) = \begin{pmatrix} \mathbf{n}_q^T M(q)\mathbf{n}_q & 0 \\ 0 & \mathbf{t}_q^T M(q)\mathbf{t}_q \end{pmatrix}, \quad (6.31)$$

from which one deduces the inverse matrix:

$$\Xi^{-T}(q)M^{-1}(q)\Xi^{-1}(q) = \begin{pmatrix} (\mathbf{n}_q^T M(q)\mathbf{n}_q)^{-1} & 0 \\ 0 & (\mathbf{t}_q^T M(q)\mathbf{t}_q)^{-1} \end{pmatrix} \quad (6.32)$$

which holds provided the normalized Delassus' matrix has full rank n. Now we have:

$$\begin{aligned} T(q,\dot{q}) &= \tfrac{1}{2}\dot{q}^T M(q)\dot{q} = \tfrac{1}{2}\dot{q}^T M(q)\Xi^T(q)\Xi^{-T}(q)M^{-1}(q)\Xi^{-1}(q)\Xi(q)M(q)\dot{q} \\ &= \tfrac{1}{2}v^T \begin{pmatrix} (\mathbf{n}_q^T M(q)\mathbf{n}_q)^{-1} & 0 \\ 0 & (\mathbf{t}_q^T M(q)\mathbf{t}_q)^{-1} \end{pmatrix} v \\ &= \tfrac{1}{2}\dot{q}_{\text{norm}}^T(\mathbf{n}_q^T M(q)\mathbf{n}_q)^{-1}\dot{q}_{\text{norm}} + \tfrac{1}{2}\dot{q}_{\tan}^T(\mathbf{t}_q^T M(q)\mathbf{t}_q)^{-1}\dot{q}_{\tan} = T(q,v) \end{aligned} \quad (6.33)$$

Now one may use (6.28) and the Schur complement [218, § A.5] to deduce:

$$T(q,\dot{q}) = \tfrac{1}{2}\dot{q}_{\text{norm}}^{u,T} G^{-1}(q)\dot{q}_{\text{norm}}^{u} + \tfrac{1}{2}\dot{q}_{\tan}^T(\mathbf{t}_q^T M(q)\mathbf{t}_q)^{-1}\dot{q}_{\tan} \quad (6.34)$$

with:

$$G(q) = \mathbf{n}_q^{u,T} M(q)\mathbf{n}_q^u - \mathbf{n}_q^{u,T} M(q)\mathbf{n}_q^b(\mathbf{n}_q^{b,T} M(q)\mathbf{n}_q^b)^{-1}\mathbf{n}_q^{b,T} M(q)\mathbf{n}_q^u \quad (6.35)$$

We see that this matrix has the same structure as $\tilde{D}_{bu}(q(t),t)$ in (5.20), and represents the distorsion of the Delassus' matrix due to bilateral constraints. Due to the assumption that the constraints are independent, $G(q)$ has full rank and is even positive definite.[8] If $m_b = 0$ (no bilateral constraints) and $m_u = 1$, then $\dot{q}_{\text{norm}}^u = \dot{q}_{\text{norm}}$ and one recovers the result in [203, Eq. (6.11)] that $T(q,\dot{q}) = \frac{1}{2}\dot{q}_{\text{norm}}^2 + \frac{1}{2}\dot{q}_{\tan}^T(\mathbf{t}_q^T M(q)\mathbf{t}_q)^{-1}\dot{q}_{\tan}$.

It is noteworthy that the basis $(\mathbf{n}_q, \mathbf{t}_q)$ is not orthonormal, because the vectors $\mathbf{n}_{q,i}$, $i \in \{1,\ldots,m_b+m_u\}$, and $\mathbf{t}_{q,i}$, $i \in \{1,\ldots,n-m_b-m_u\}$ are not necessarily orthogonal to one another (except if the constraints are orthogonal). Thus,

[8] Its properties are studied in [209, § 4] without noticing, anyway, that it is a Schur complement.

despite the quasi-mass matrix $\bar{M}(q)$ in (6.26) is the identity, the kinetic energy in (6.34) does not have the simple form $2T(q, v) = v^T v$ as is for instance the case in [155, Eq. (20)].

6.2.3 The Contact Forces Power

6.2.3.1 Normal Contact Forces Power

Let $F_{\mathrm{n}}(q) \stackrel{\Delta}{=} \nabla f(q)\lambda_{\mathrm{n}}$. Let us investigate now the power performed by the generalized contact force: $\mathscr{P}_{\mathrm{n}} = F_{\mathrm{n}}^T(q)\dot{q}$ where $\dot{q}$ is assumed to be compatible with the bilateral and the unilateral constraints (i.e. we consider virtual velocities $\dot{q}$ such that the virtual displacement $\delta q = \dot{q}dt$ is compatible with the constraints and such that the virtual work is $\mathscr{W}_{\mathrm{n}} = \mathscr{P}_{\mathrm{n}}dt$). Then from the above developments we obtain:

$$\begin{aligned}\mathscr{P}_{\mathrm{n}} &= F_{\mathrm{n}}(q)^T\dot{q} = \lambda_{\mathrm{n}}^T\nabla f(q)^T\dot{q} = \lambda_{\mathrm{n}}^T \mathrm{diag}(||\nabla h_i(q)||_{M^{-1}}, ||\nabla f_i(q)||_{M^{-1}})\mathbf{n}_q^T M(q)\dot{q}\\ &= \bar{\lambda}_{\mathrm{n}}^T\mathbf{n}_q^T M(q)\dot{q} = \bar{\lambda}_{\mathrm{n}}^T\dot{q}_{\mathrm{norm}} = \bar{\lambda}_{\mathrm{n},u}^T\dot{q}_{\mathrm{norm}}^u,\end{aligned} \tag{6.36}$$

where we used that $\dot{q}_{\mathrm{norm}}^b = 0$ always. Now, one has $0 \leq \lambda_{\mathrm{n},u} \perp f(q) \geq 0$, therefore if the system lies in the interior of the admissible domain Φ_u one has $\lambda_{\mathrm{n},u} = 0$ and $\mathscr{P}_{\mathrm{n}} = 0$. If the system evolves smoothly on a part of the boundary $\mathrm{bd}(\Phi_u)$ that is finitely represented by the active constraints indexed in $\mathscr{J}(q)$, one has $0 \leq \dot{q}_{\mathrm{norm,i}} \perp \lambda_{\mathrm{n},u,i} \geq 0$ for all $i \in \mathscr{J}(q)$. Consequently in this case also $\mathscr{P}_{\mathrm{n}} = 0$. Since the constraints are all perfect, the power developed by the contact forces outside possible impacts is always zero, as expected. The interest of (6.36) is to highlight the fact that the "forces" that perform work on the quasi-velocities $\dot{q}_{\mathrm{norm}}^u$ are the multipliers $\bar{\lambda}_{\mathrm{n},u}$.

Let us denote $F_{\mathrm{norm}}^{\mathrm{n}}(q) \stackrel{\Delta}{=} \mathbf{n}_q^T M(q)\mathbf{n}_q\bar{\lambda}_{\mathrm{n}}$ and $D_{\mathrm{n}}(q) \stackrel{\Delta}{=} (\mathbf{n}_q^T M(q)\mathbf{n}_q)^{-1}$. Then from (6.36) one gets:

$$\mathscr{P}_{\mathrm{n}} = \bar{\lambda}_{\mathrm{n}}^T\dot{q}_{\mathrm{norm}} = \langle F_{\mathrm{norm}}^{\mathrm{n}}(q), \dot{q}_{\mathrm{norm}}\rangle_{D_{\mathrm{n}}} \tag{6.37}$$

Let us also denote $D_{\mathrm{t}}(q) \stackrel{\Delta}{=} (\mathbf{t}_q^T M(q)\mathbf{t}_q)^{-1}$.[9] As a result, one finds that the frictionless Lagrangian system with a set of holonomic bilateral and unilateral constraints is equivalently represented as a generalized particle with dynamics:

$$\begin{cases}\ddot{q}_{\mathrm{norm}}(t) + F_{\mathrm{norm}}(q, \dot{q}_{\mathrm{norm}}(t), \dot{q}_{\mathrm{tan}}(t), t) = F_{\mathrm{norm}}^{\mathrm{n}}(q(t))\\ \ddot{q}_{\mathrm{tan}}(t) + F_{\mathrm{tan}}(q, \dot{q}_{\mathrm{norm}}(t), \dot{q}_{\mathrm{tan}}(t), t) = 0\end{cases} \tag{6.38}$$

[9] If the vectors $\mathbf{t}_{q,i}$ are chosen mutually orthogonal then $D_{\mathrm{t}}(q) = I$.

and the kinetic metric $D(q) = \text{diag}(D_{\text{n}}(q), D_{\text{t}}(q))$ (see (6.33)), while $\dot{q}_{\text{norm}} dt$ performs work on $F^{\text{n}}_{\text{norm}}(q)$ in the metric of $D_{\text{n}}(q)$.

6.2.3.2 Tangential Contact Forces Power

Let us compute the virtual power developed by the tangential forces. Let $F_{\text{t}}(q) \stackrel{\Delta}{=} \Xi(q) H_{\text{t}}(q) \lambda_{\text{t}} = \begin{pmatrix} F^{\text{t}}_{\text{norm}}(q) \\ F^{\text{t}}_{\text{tan}}(q) \end{pmatrix}$. Then:

$$\begin{aligned} \mathscr{P}_{\text{t}} &= \dot{q}^T H_{\text{t}}(q) \lambda_{\text{t}} = v^T \Xi^{-T}(q) M^{-1}(q) \Xi^{-1}(q) \Xi(q) H_{\text{t}}(q) \lambda_{\text{t}} \\ &= \langle v, F_{\text{t}}(q) \rangle_D = \langle \dot{q}_{\text{norm}}, F^{\text{t}}_{\text{norm}}(q) \rangle_{D_{\text{n}}} + \langle \dot{q}_{\text{tan}}, F^{\text{t}}_{\text{tan}}(q) \rangle_{D_{\text{t}}} \end{aligned} \tag{6.39}$$

Thus, the total virtual power of the contact forces of the dynamics in (6.30) is equal to:

$$\mathscr{P} = \langle F^{\text{n}}_{\text{norm}}(q), \dot{q}_{\text{norm}} \rangle_{D_{\text{n}}} + \langle \dot{q}_{\text{norm}}, F^{\text{t}}_{\text{norm}}(q) \rangle_{D_{\text{n}}} + \langle \dot{q}_{\text{tan}}, F^{\text{t}}_{\text{tan}}(q) \rangle_{D_{\text{t}}} \tag{6.40}$$

The matrices $D_{\text{n}}(q) \succ 0$ and $D_{\text{t}}(q) \succ 0$ define natural metrics for the system analysed in kinetic quasi-velocities. The coupling between normal and tangential directions appears in the second term in (6.40). There is no orthogonality of the quasi-generalized contact forces $\begin{pmatrix} F^{\text{t}}_{\text{norm}}(q) \\ F^{\text{t}}_{\text{tan}}(q) \end{pmatrix}$ and $\begin{pmatrix} F^{c}_{\text{norm}}(q) \\ 0 \end{pmatrix}$ in the inner product defined by the metric $D(q) \succ 0$. This is in contrast with what happens at the local kinematics level at the contact points. Following Sect. 4.1, let us denote the orthonormal local frame at contact point i as $(\mathbf{n}_i, \mathbf{t}_{i,1}, \mathbf{t}_{i,2})$, with $\mathbf{n}_i \in \mathbb{R}^3, \mathbf{t}_{i,j} \in \mathbb{R}^3$. One has $\langle \mathbf{n}_i, \mathbf{t}_{i,j} \rangle = 0$ in the Euclidean metric. Each contact force can be denoted as $F_i = F_{i,\text{n}} + F_{i,\text{t}}$ with $F_{i,\text{n}} = F_{\text{n},i} \mathbf{n}_i$ and $F_{i,\text{t}} = F_{\text{t},1,i} \mathbf{t}_{i,1} + F_{\text{t},2,i} \mathbf{t}_{i,2}$. The Coulomb's cones are denoted as $\mathscr{C}_i$, with $F_i \in \mathscr{C}_i$. Let $U_i \in \mathbb{R}^3$ be the local velocity, decomposed naturally as $U_i = U_{\text{n},i} + U_{\text{t},i} = u_{\text{n},i} \mathbf{n}_i + u_{\text{t},1,i} \mathbf{t}_{i,1} + u_{\text{t},2,i} \mathbf{t}_{i,2}$. We may thus define virtual local velocities that are compatible with the constraints, and the virtual power at contact i is given by $\mathscr{P}_i = \langle U_i, F_i^c \rangle = \langle U_{i,n}, F_{i,\text{n}} \rangle + \langle U_{i,\text{t}}, F_{i,\text{t}} \rangle$, while

$$\mathscr{P} = \sum_{i=1}^{p} \mathscr{P}_{i,\text{n}} + \mathscr{P}_{i,\text{t}} = \mathscr{P}_{\text{n}} + \mathscr{P}_{\text{t}}. \tag{6.41}$$

Thus, in the local kinematics there is a decoupling between tangential and normal virtual powers, which does not transport very well into generalized frameworks, because of the term $\mathbf{n}_q^T H_{\text{t}}(q)$ in (6.30). Notice that if $u_{\text{n},i} = \nabla f_i(q)^T \dot{q}$, then the multiplier vector λ_{n} satisfies $\lambda_{\text{n},i} = F_{\text{n},i}$, and thus $\mathscr{P}_{\text{n}}$ in (6.36) and $\mathscr{P}_{\text{n}}$ in (6.41) are the same.

6.2.4 Restitution Law for Frictionless Systems

Let us assume for simplicity that there are no bilateral constraints (i.e. $m_b = 0$). Thus $G(q) = D_{\rm n}(q)^{-1}$ and in the sequel we shall use both notations equally. We also assume that $\dot{q}_{\rm norm}$ is constructed from the active constraints at the impact time t_k, i.e. with the constraints whose index belongs to $\mathscr{J}(q(t_k)) = \{i \in \{1,\dots,m_u\} | f_i(q(t_k)) = 0\}$. It is noteworthy that we allow for contacts which are active with zero relative pre-impact velocity (like in a chain of balls or a Newton's cradle). We denote $m'_u = \text{card}(\mathscr{J}(q(t_k)))$. The impact dynamics at an instant t_k such that there is at least one $i \in \{1,\dots,m'_u\}$ such that $\dot{q}_{\text{norm,i}}(t_k^-) < 0$ and $f_i(q(t_k)) = 0$[10] is given by (using (6.26)):

$$\begin{cases} \dot{q}_{\rm norm}(t_k^+) - \dot{q}_{\rm norm}(t_k^-) = \mathbf{n}_q^T M(q)\mathbf{n}_q \ \bar{p}_{\rm n}(t_k) \\ \dot{q}_{\rm tan}(t_k^+) - \dot{q}_{\rm tan}(t_k^-) = 0, \end{cases} \tag{6.42}$$

where $\bar{p}_{{\rm n},i} = ||\nabla f_i(q)||_{M^{-1}} p_{{\rm n},i}$, i.e. $\bar{p}_{\rm n} = \text{diag}(||\nabla f_i(q)||_{M^{-1}}) p_{\rm n}$, and $p_{{\rm n},i}(t_k)$ is the impulse of the contact force multiplier $\lambda_{{\rm n},i}$ at the impact instant t_k. More rigorously $\lambda_{{\rm n},i}$ is a measure at t_k and $p_{{\rm n},i}(t)$ is its density with respect to the Dirac measure at the atom t_k. The role played by the projection of the generalized momentum on the basis $\mathbf{t}_q$ clearly appears in (6.42): the quasi-velocities $\dot{q}_{\rm tan}$ are conserved at the impacts when friction is absent (the constraints are said *perfect*). It is important to notice that despite there may be $\dot{q}_{\text{norm,i}}(t_k^-) = 0$ for some $i \in \mathscr{J}(q(t_k))$, all the terms $\dot{q}_{\text{norm,i}}$, $i \in \{1,\dots,m'_u\}$ may undergo a jump because of the inertial couplings between the constraints, as reflected by the normalized Delassus' matrix $\mathbf{n}_q^T M(q)\mathbf{n}_q$ which is not diagonal in general. It readily follows from the impact dynamics in (6.42) and (6.34) that the kinetic energy loss $T_L(t_k) \stackrel{\Delta}{=} T(q(t_k), \dot{q}(t_k^+)) - T(q(t_k), \dot{q}(t_k^-))$ at a time t_k of impact is given by:

$$T_L(t_k) = \frac{1}{2}\dot{q}^u_{\rm norm}(t_k^+)^T G(q)^{-1}\dot{q}^u_{\rm norm}(t_k^+) - \frac{1}{2}\dot{q}^u_{\rm norm}(t_k^-)^T G(q)^{-1}\dot{q}^u_{\rm norm}(t_k^-) \tag{6.43}$$

where q denotes $q(t_k)$. From now on we will drop the superscript u since there are no bilateral constraints. The framework in (6.42) is suitable to formulate a kinematic impact law as:

$$v(t^+) = \begin{pmatrix} \dot{q}_{\rm norm}(t_k^+) \\ \dot{q}_{\rm tan}(t_k^+) \end{pmatrix} = -\mathscr{E} \begin{pmatrix} \dot{q}_{\rm norm}(t_k^-) \\ \dot{q}_{\rm tan}(t_k^-) \end{pmatrix} \tag{6.44}$$

where $\mathscr{E}$ is a generalized $n \times n$ restitution matrix. Its entries will be named the coefficients of restitution. Let us decompose it as:

$$\mathscr{E} = \begin{pmatrix} \mathscr{E}_{\rm nn} & \mathscr{E}_{\rm nt} \\ \mathscr{E}_{\rm tn} & \mathscr{E}_{\rm tt} \end{pmatrix} \tag{6.45}$$

[10] This is equivalently stated as $\dot{q}(t_k^-) \in -T_{\Phi_u}(q(t_k))$.

with obvious dimensions of the four submatrices: $\mathscr{E}_{\rm nn} \in \mathbb{R}^{m'_u \times m'_u}$, $\mathscr{E}_{\rm tt} \in \mathbb{R}^{(n-m'_u)\times(n-m'_u)}$. In the frictionless case one has $\dot{q}_{\rm tan}(t^+) = \dot{q}_{\rm tan}(t^-)$ for any pre-impact velocity $\dot{q}_{\rm norm}(t^-)$, so necessarily $\mathscr{E}_{\rm tn} = 0$ and $\mathscr{E}_{\rm tt} = -I$. The restitution law in (6.44) is very general as the next result shows:

Proposition 6.1 *Suppose that at least one component of $\dot{q}_{\rm norm}(t_k^-)$ or of $\dot{q}_{\rm tan}(t_k^-)$ is nonzero. Then given any postimpact kinetic quasi-velocity, there exists a value of $\mathscr{E}$ such that (6.44) is satisfied. If at least one component of $\dot{q}_{\rm norm}(t_k^-)$ is negative, then there exists a value of $\mathscr{E}_{\rm nn}$ such that $\dot{q}_{\rm norm}(t_k^+) = -\mathscr{E}_{\rm nn}\dot{q}_{\rm norm}(t_k^-)$.*

Proof Without loss of generality suppose that $v_1(t_k^-) \neq 0$ while $v_i(t_k^-) = 0$ for all $i \geq 2$. Then it suffices to choose $\epsilon_{i1} = -\frac{v_i(t_k^+)}{v_1(t_k^-)}$.

As we know there are three types of consistencies that an impact law has to satisfy: kinematic (admissible postimpact velocities), kinetic (non negative impulses), and energetic.

Proposition 6.2 *Let a frictionless impact occur at t_k. It is necessary and sufficient that:*

- *(i) $\mathscr{E}_{\rm nn}$ is nonnegative (kinematic consistency),*
- *(ii) $G^{-1}(q)(I + \mathscr{E}_{\rm nn})$ is nonnegative (kinetic consistency),*

for $\mathscr{E}_{\rm nn}$ to be an admissible restitution matrix for any pre-impact velocity $\dot{q}_{\rm norm}(t_k^-)$.

Proof (i) assures that $\dot{q}_{\rm norm}(t_k^+) = -\mathscr{E}_{\rm nn}\dot{q}_{\rm norm}(t_k^-) \geq 0$ for any $\dot{q}_{\rm norm}(t_k^-) \leq 0$, (ii) guarantees that $\bar{p}_{\rm n}(t_k) = G(q)^{-1}(\dot{q}_{\rm norm}(t_k^+) - \dot{q}_{\rm norm}(t_k^-)) \geq 0$ (kinetic consistency).

We are now going to analyze the energetical consistency, and for that we need equivalent expressions of $T_L(t_k)$:

$$T_L(t_k) = \frac{1}{2}(\dot{q}_{\rm norm}(t_k^+) + \dot{q}_{\rm norm}(t_k^-))^T \bar{p}_{\rm n}(t_k), \tag{6.46}$$

which is the Thomson and Tait formula, or:

$$T_L(t_k) = \frac{1}{2}\dot{q}_{\rm norm}(t_k^-)^T(\mathscr{E}_{\rm nn} - I)^T G(q)^{-1}(\mathscr{E}_{\rm nn} + I)\dot{q}_{\rm norm}(t_k^-), \tag{6.47}$$

or, using the symmetry of $G(q)$[11]:

$$T_L(t_k) = \frac{1}{2}\dot{q}_{\rm norm}(t_k^-)^T(\mathscr{E}_{\rm nn}^T G(q)^{-1}\mathscr{E}_{\rm nn} - G(q)^{-1})\dot{q}_{\rm norm}(t_k^-), \tag{6.48}$$

or, following [455] and with $\xi(t_k) = \dot{q}_{\rm norm}(t_k^+) + \mathscr{E}_{\rm nn}\dot{q}_{\rm norm}(t_k^-)$:

$$T_L(t_k) = \frac{1}{2}\bar{p}_{\rm n}(t_k)^T(2\xi(t_k) - (I - \mathscr{E}_{\rm nn})G(q)\bar{p}_{\rm n}(t_k)). \tag{6.49}$$

[11] $x^T\mathscr{E}_{\rm nn}^T G(q)^{-1}x = x^T(\mathscr{E}_{\rm nn}^T G(q)^{-1})^T x = x^T G(q)^{-1}\mathscr{E}_{\rm nn}x$ for any vector $x \in \mathbb{R}^p$.

We then have several results stating conditions such that the generalized impact law is energetically consistent.

Proposition 6.3 *Suppose that* $-(\mathscr{E}_{\rm nn}-I)^T G(q)^{-1}(\mathscr{E}_{\rm nn}+I)$ *or* $-(\mathscr{E}_{\rm nn}^T G(q)^{-1}\mathscr{E}_{\rm nn}-G(q))^{-1}$ *are copositive matrices. Then* $T_L(t_k)\leq 0$. *If they are strictly copositive then* $T_L(t_k)<0$ *for any nonzero pre-impact velocity.*

Proof Due to the impact conditions one has $\dot{q}_{\rm norm}(t_k^-)\leq 0$, in other words the p dimensional vector $-\dot{q}_{\rm norm}(t^-)$ belongs to $\mathbb{R}^p_+$. From the definition of copositivity the results follow.

Proposition 6.4 *Suppose that* $\mathscr{E}_{\rm nn}=G(q)\mathscr{E}_{\rm nn}^T G(q)^{-1}$ *and* $G(q)$ *is positive definite. Then a necessary and sufficient condition for* $T_L(t)\leq 0$ *for any vector* $\dot{q}_{\rm norm}(t_k^-)$ *is that* $|\lambda_{\max}(\mathscr{E}_{\rm nn})|\leq 1$.

Proof From (6.48) we have $T_L(t_k)\leq 0$ for any $\dot{q}_{\rm norm}(t_k^-)$ if and only if $\mathscr{E}_{\rm nn}^T G(q)^{-1}\mathscr{E}_{\rm nn}\leq G(q)^{-1}$. Let $G^{\frac{1}{2}}(q)$ be the symmetric positive definite square root of $G(q)$. This inequality is equivalent to $G^{\frac{1}{2}}(q)\mathscr{E}_{\rm nn}^T G(q)^{-1}\mathscr{E}_{\rm nn}G^{\frac{1}{2}}(q)\leq I$, using Proposition 8.1.2 xi) and xiii) in [136]. Let us denote $B(q)=G^{\frac{1}{2}}(q)\mathscr{E}_{\rm nn}^T G^{-\frac{1}{2}}(q)$. By the assumption of the proposition we have $G^{-\frac{1}{2}}(q)\mathscr{E}_{\rm nn}G^{\frac{1}{2}}(q)=G^{\frac{1}{2}}(q)\mathscr{E}_{\rm nn}^T G^{-\frac{1}{2}}(q)$ so $B(q)=B^T(q)$, and since $B^T(q)=G^{-\frac{1}{2}}(q)\mathscr{E}_{\rm nn}G^{\frac{1}{2}}(q)$ we obtain $B^2(q)\leq I$. Using [136, Lemma 8.4.1] it follows that equivalently $\lambda_{\max}(B^2(q))\leq 1$, because $B^2(q)=B(q)B^T(q)$ is positive semi definite and symmetric. Now we have that $B^2(q)=G^{\frac{1}{2}}(q)(\mathscr{E}_{\rm nn}^T)^2G^{-\frac{1}{2}}(q)$, and since it is a symmetric matrix one obtains $B^2(q)=G^{-\frac{1}{2}}(q)\mathscr{E}_{\rm nn}^2G^{\frac{1}{2}}(q)$. Therefore $B^2(q)$ and $\mathscr{E}_{\rm nn}^2$ are similar matrices so they have the same eigenvalues [700, Proposition 1, p. 152]. Therefore $\lambda_{\max}(\mathscr{E}_{\rm nn}^2(q))\leq 1$. Since the eigenvalues of $\mathscr{E}_{\rm nn}^2$ are the squares of those of $\mathscr{E}_{\rm nn}$ the result follows.

The condition imposed in Proposition 6.4 holds if for instance $\mathscr{E}_{\rm nn}=\text{diag}(e_{\rm n})$. In fact $\mathscr{E}_{\rm nn}=G(q)\mathscr{E}_{\rm nn}^T G(q)^{-1}$ is equivalent to $G(q)^{-1}\mathscr{E}_{\rm nn}=\mathscr{E}_{\rm nn}^T G(q)^{-1}$, which allows us to rewrite (6.48) as:

$$T_L(t)=\frac{1}{2}\dot{q}_{\rm norm}(t_k^-)^T[(\mathscr{E}_{\rm nn}^T\mathscr{E}_{\rm nn}-I)G(q)^{-1}]\dot{q}_{\rm norm}(t_k^-) \tag{6.50}$$

Proposition 6.5 *Let* $G(q)>0$. *Then* $T_L(t_k)\leq 0$ *if* $\sigma_{\max}(\mathscr{E}_{\rm nn})\leq\frac{1}{\sqrt{\lambda_{\max}(G(q))\lambda_{\max}(G^{-1}(q))}}$, *which implies that* $\sigma_{\max}(\mathscr{E}_{\rm nn})\leq 1$.

Proof The proof begins similarly to the proof of Proposition 6.4, and we obtain that $T_L(t)\leq 0\Leftrightarrow B(q)B^T(q)\leq I$ with $B(q)=G^{\frac{1}{2}}(q)\mathscr{E}_{\rm nn}^T G^{-\frac{1}{2}}(q)$. By [136, Lemma 8.4.1] one has equivalently $\lambda_{\max}(B(q)B^T(q))=\sigma^2_{\max}(B(q))\leq 1$. From [136, Corollary 9.6.5] one has $\sigma_{\max}(B(q))\leq\sigma_{\max}(G^{\frac{1}{2}}(q))\sigma_{\max}(G^{-\frac{1}{2}}(q))\sigma_{\max}(\mathscr{E}_{\rm nn})$. Therefore $\sigma_{\max}(G^{\frac{1}{2}}(q))\sigma_{\max}(G^{-\frac{1}{2}}(q))\sigma_{\max}(\mathscr{E}_{\rm nn})\leq 1$ implies that $\sigma^2_{\max}(B(q))\leq 1$. From the symmetry and positive definiteness of $G(q)$ and of its square root,

one has $\sigma_{\max}(G^{\frac{1}{2}}(q)) = \sqrt{\lambda_{\max}(G(q))}$, so the result follows. For the last statement notice that $I = G^{-\frac{1}{2}}(q)G^{\frac{1}{2}}(q)$ so again from [136, Corollary 9.6.5] $1 \leq \sigma_{\max}(G^{\frac{1}{2}}(q))\sigma_{\max}(G^{-\frac{1}{2}}(q)) = \sqrt{\lambda_{\max}(G(q))\lambda_{\max}(G^{-1}(q))}$.

Remark 6.6 Propositions 6.4 and 6.5 state in a correct way Proposition 1 in [228], which wrongly asserts that $|\lambda_{\max}(\mathscr{E}_{\rm nn})| \leq 1$ is a sufficient condition for $T_L(t) \leq 0$ under symmetry of $\mathscr{E}_{\rm nn}$. The energy consistency of an extended frictionless Moreau's law with $\mathscr{E}_{\rm nn} = \text{diag}(e_{{\rm n},i})$ is analysed in [730, Sect. 7.1] [455], starting from the Thomson and Tait formula (6.46), or from (6.47), or from (6.49). Actually one may use Propositions 7.1 and 7.2 in [730] to analyze (6.50). The condition of Proposition 6.4 is quite close to the commuting conditions of [730, p. 159]. Finally let us remind that in the case Poisson coefficients are used (kinetic impact law) one obtains similar expressions for the loss of kinetic energy (see Eq.(43) in [458]). The quadratic forms in (6.47)–(6.49) therefore possess a general interest for both kinematic and kinetic impact laws. As shown in [210, Sect. 3.1.1], when $\mathscr{E}_{\rm nn} = \text{diag}(e_{\rm n})$ for some CoR $e_{\rm n} \in [0, 1]$, then we recover Moreau's impact law, which is always kinematically and kinetically consistent from Proposition 6.2.

Remark 6.7 From (6.42), the quasi-velocity $\dot{q}_{\rm tan}(\cdot)$ is conserved at frictionless impacts. The physical meaning of $\dot{q}_{\rm tan}(\cdot)$ may change from a system to another one. For a particle hitting a plane, this is the tangent velocity at the contact point $v_{\rm t}$, for a chain of aligned beads this is the velocity of the gravity center of the chain.

Remark 6.8 Starting from (6.42) and (6.44), and assuming kinematic, kinetic and energetic consistencies hold, we can rewrite equivalently the restitution law as:

$$\left\{\begin{array}{c} 0 \leq \dot{q}_{\rm norm}(t_k^+) + \mathscr{E}_{\rm nn}\dot{q}_{\rm norm}(t_k^-) \perp \bar{p}_{\rm n}(t_k) \geq 0 \\ \\ \Longleftrightarrow \ (\text{if } D_{\rm n}(q(t_k)) \succ 0) \\ \\ 0 \leq D_{\rm n}(q(t_k))^{-1}\bar{p}_{\rm n}(t_k) + (I + \mathscr{E}_{\rm nn}\dot{q}_{\rm norm}(t_k^-) \perp \bar{p}_{\rm n}(t_k) \geq 0, \end{array}\right. \tag{6.51}$$

which is quite similar to (5.67) and (5.68), (5.70). Going a step further:

$$D_{\rm n}(q(t_k))[\dot{q}_{\rm norm}(t_k^+) - \dot{q}_{\rm norm}(t_k^-)] \in -N_{\mathbb{R}_+^{m_u}}(\dot{q}_{\rm norm}(t_k^+) + \mathscr{E}_{\rm nn}\dot{q}_{\rm norm}(t_k^-)). \tag{6.52}$$

Let us end this section with Carnot's Theorem:

Theorem 6.1 (Carnot's Theorem) *A frictionless impact after which persistent contact is established, is always accompanied by a kinetic energy loss.*

Proof From (6.42) and (6.46), and taking $\dot{q}_{\rm norm}(t_k^+) = 0$ (i.e. without loss of generality, we suppose that m contacts are established), it follows that $T_L(t_k) = -\frac{1}{2}\dot{q}_{\rm norm}(t_k^-)^T D_{\rm n}(q(t_k))\dot{q}_{\rm norm}(t_k^-) \leq 0$, and this holds even if the constraints are not independent, because $D_{\rm n}(q) \succeq 0$.[12]

[12] Recall however that we assume that $M(q) \succ 0$, for the basic definition of the vectors $\mathbf{n}_{q,i}$.

A geometric interpretation of Carnot's Theorem is given in [569]. It is noteworthy that Theorem 6.1 is stated without chosing any particular restitution mapping.

6.2.5 *Restitution Law with Tangential Effects*

The impact dynamics is in this case equal to:

$$\begin{cases} \dot{q}_{\text{norm}}(t^+) - \dot{q}_{\text{norm}}(t^-) = \mathbf{n}_q^T M(q)\mathbf{n}_q \ \bar{p}_n(t) + \mathbf{n}_q^T H_{\text{T}}(q) \ p_{\text{t}} \\ \dot{q}_{\text{tan}}(t^+) - \dot{q}_{\text{tan}}(t^-) = \mathbf{t}_q^T H_{\text{T}}(q) \ p_{\text{t}}. \end{cases} \tag{6.53}$$

We saw in Sect. 4.3 that tangential effects may be introduced in kinematic restitution laws in three ways: tangential restitution, Coulomb's law at the impulse level, and a mixture of both. Tangential restitution can be readily inserted in (6.45), by defining non null restitution submatrices $\mathscr{E}_{\text{nt}}$, $\mathscr{E}_{\text{tn}}$ and $\mathscr{E}_{\text{tt}}$. For the sake of briefness we present next an extension of the model studied in Sects. 4.3.1.1, 4.3.1.2 and 4.3.1.5, with $\tilde{v}_{\text{t}}(t_k) = v_{\text{t}}(t_k^+) + e_{\text{t}} v_{\text{t}}(t_k^-)$, and $\mathscr{E}_{\text{nt}} = 0$, $\mathscr{E}_{\text{tn}} = 0$ and $\mathscr{E}_{\text{tt}} = 0$ in the restitutiuon matrix $\mathscr{E}$: the tangential restitution submatrix $\mathscr{E}_{\text{tt}}$ is introduced thorugh Coulomb's law. We restrict ourselves to planar friction at each contact point i, and write Coulomb's law at the impulse level as:

$$p_{\text{t},i} \in -\mu_i \, p_{\text{n},i} \ \text{sgn}(v_{\text{t},i}(t_k^+) + e_{\text{t},i} v_{\text{t},i}(t_k^-)) \tag{6.54}$$

for some tangential CoRs $e_{\text{t,i}}$, $1 \leq i \leq m_u'$, which copies (4.69). In the examples studied in Sects. 4.3.1.1, 4.3.1.2 and 4.3.1.5, we proved that it was always possible to compute a unique $v_{\text{t}}(t_k^+)$ when this tangential model is used (see (4.73) and (4.83)). In the general case the mere existence issue if more complex. Inserting (6.54) into (6.42) we find:

$$\begin{cases} -(I + \mathscr{E}_{\text{nn}})\dot{q}_{\text{norm}}(t_k^-) \in G(q)\bar{p}_{\text{n}}(t_k) - \mathbf{n}_q^T H_{\text{t}}(q)[\bar{\mu}][\bar{p}_{\text{n}}(t_k)]\text{Sgn}(v_{\text{t}}(t_k^+) + \mathscr{E}_{\text{tt}} v_{\text{t}}(t_k^-)) \\ \qquad\qquad\qquad\qquad\qquad\qquad \overbrace{\qquad\qquad\qquad\qquad}^{\triangleq \tilde{V}_{\text{t}}(t_k)} \\ \dot{q}_{\text{tan}}(t_k^+) - \dot{q}_{\text{tan}}(t_k^-) \in -\mathbf{t}_q^T H_{\text{t}}(q)[\bar{\mu}][\bar{p}_{\text{n}}(t_k)]\text{Sgn}(\underbrace{v_{\text{t}}(t_k^+) + \mathscr{E}_{\text{tt}} v_{\text{t}}(t_k^-)}) \end{cases} \tag{6.55}$$

with: $[\bar{\mu}] = \text{diag}\left(\frac{\mu_i}{||\nabla f_i(q)||_{M^{-1}}}\right) \in \mathbb{R}^{m_u' \times m_u'}$, $[\bar{p}_n] = \text{diag}(\bar{p}_{\text{n},i})$, $\mathscr{E}_{\text{tt}} = \text{diag}(e_{\text{t},i})$, $v_{\text{t}} = H_{\text{t}}(q)^T \Xi^T(q) v$ (v is in (6.23)), $\text{Sgn}(\tilde{V}_{\text{t}}(t_k)) = (\text{sgn}(\tilde{v}_{\text{t},1}(k), \ldots, \text{sgn}(\tilde{v}_{\text{t},m_u'}(t_k))^T$. The unknowns of the generalized equation (6.55) are the m_u' impulses $\bar{p}_{\text{n},i}$, and the $n - m_u'$ quasi-velocities $\dot{q}_{\text{tan},i}(t_k^+)$, with the constraints $\bar{p}_{\text{n},i} \geq 0$ and $\dot{q}_{\text{norm}}(t_k^+) = -\mathscr{E}_{\text{nn}}\dot{q}_{\text{norm}}(t_k^-)$. The first inclusion in (6.55) may be used to find an extension of (4.90), and we may look for a generalized Lemma 4.1 for the kinetic constraint satisfaction. It may be rewritten equivalently as[13]:

[13] Notice that we recover here a matrix $G^{\mu}(q, v_{\text{t}}(t_k^+))$ which has the same structure as $D^{\mu}(q)$ in (5.158).

$$\overbrace{(G(q)-\mathbf{n}_q^T H_{\mathrm{t}}(q)[\bar{\mu}][\xi_i])}^{\triangleq G^{\mu}(q,v_{\mathrm{t}}(t_k^+))}\bar{p}_{\mathrm{n}}(t_k)\ni -(I+\mathscr{E}_{\mathrm{nn}})\dot{q}_{\mathrm{norm}}(t_k^-) \tag{6.56}$$

with $[\xi_i]=\mathrm{diag}(\xi_i)$ and $\xi_i\in\mathrm{sgn}(\tilde{v}_{\mathrm{t},i}(t_k))$. We can use Theorem 5.8 to guarantee that for small enough friction $\mu_i\leq\mu_{\max}(q)$, $1\leq i\leq m_u$, then $G^{\mu}(q,v_{\mathrm{t}}(t_k^+))\succ 0$ for any frictional mode (i.e. any $\xi_i\in[\text{-}1,1]$), and then insert the found value of $\bar{p}_{\mathrm{n}}(t_k)$ in the second inclusion of (6.55). This gives rise to the program: Given the data $q(t_k)$ and $\dot{q}(t_k^-)$, and the parameters $\mathscr{E}_{\mathrm{nn}}$, $\mathscr{E}_{\mathrm{tt}}$, find $\dot{q}(t_k^+)$ such that:

$$\begin{aligned}&\mathbf{t}_q^T M(q)\dot{q}(t_k^+)=\dot{q}_{\tan}(t_k^-)+\mathbf{t}_q^T H_{\mathrm{t}}(q)[\bar{\mu}](G^{\mu}(q,H_{\mathrm{t}}(q)^T\dot{q}(t_k^+)))^{-1}(I+\mathscr{E}_{\mathrm{nn}})\dot{q}_{\mathrm{norm}}(t_k^-)\xi\\&\text{with: }\nabla f(q)^T\dot{q}(t_k^+)=-\mathscr{E}_{\mathrm{nn}}\dot{q}_{\mathrm{norm}}(t_k^-)\\&\qquad\xi\in\mathrm{Sgn}(H_{\mathrm{t}}(q)^T\dot{q}(t_k^+)+\mathscr{E}_{\mathrm{tt}}v_{\mathrm{t}}(t_k^-))\Leftrightarrow H_{\mathrm{t}}(q)^T\dot{q}(t_k^+)\in-\mathscr{E}_{\mathrm{tt}}v_{\mathrm{t}}(t_k^-)+N_{[-1,1]}(\xi)\end{aligned} \tag{6.57}$$

where we recall that $v_{\mathrm{t}}=H_{\mathrm{t}}(q)^T\dot{q}$ from the local kinematics, and we denoted $q(t_k)$ as q. If this program possesses a solution $\dot{q}(t_k^+)$, then the impact problem with friction is solvable with kinematic and kinetic constraints satisfied. See Sect. 4.3.1.5 for an example, with normal/tangential couplings. The generalized equation is rather tricky since it can hardly be put in a canonical form $0\in F(x)+N_K(x)$, with $F(\cdot)$ continuous and $K=[\text{-}1,1]^{m_u'}$, so that [385, Corollary 2.2.5] may be applied.[14] This fact is not surprizing because the original problem in (6.55) is already nonlinear in its unknowns, due to the products between $\bar{p}_{\mathrm{n}}(t_k)$ and $\mathrm{Sgn}(\tilde{V}_{\mathrm{t}}(t_k))$.

Let us pass now to the energetical behavior of this impact law with friction, assuming that we could find at least one solution to (6.57). Choosing one of these solutions provides us with $\tilde{V}_{\mathrm{t}}(t_k)$ and most importantly with a selection $\xi\in\mathrm{Sgn}(\tilde{V}_{\mathrm{t}}(t_k))$. Extension of (6.46) through (6.49) is:

$$\begin{aligned}T_L(t_k)&=\tfrac{1}{2}\dot{q}_{\mathrm{norm}}(t_k^+)^T D_{\mathrm{n}}(q)\dot{q}_{\mathrm{norm}}(t_k^+)-\tfrac{1}{2}\dot{q}_{\mathrm{norm}}(t_k^-)^T D_{\mathrm{n}}(q)\dot{q}_{\mathrm{norm}}(t^-)\\&+\tfrac{1}{2}\dot{q}_{\tan}(t_k^+)^T D_{\mathrm{t}}(q)\dot{q}_{\tan}(t_k^+)-\tfrac{1}{2}\dot{q}_{\tan}(t_k^-)^T D_{\mathrm{t}}(q)\dot{q}_{\tan}(t_k^-)\\&=\tfrac{1}{2}(\dot{q}_{\mathrm{norm}}(t_k^+)+\dot{q}_{\mathrm{norm}}(t^-))^T D_{\mathrm{n}}(q)(\dot{q}_{\mathrm{norm}}(t_k^+)-\dot{q}_{\mathrm{norm}}(t_k^-))\\&+\tfrac{1}{2}(\dot{q}_{\tan}(t_k^+)+\dot{q}_{\tan}(t_k^-))^T D_{\mathrm{t}}(q)(\dot{q}_{\tan}(t_k^+)-\dot{q}_{\tan}(t_k^-))\\&=\tfrac{1}{2}(\dot{q}_{\mathrm{norm}}(t_k^+)+\dot{q}_{\mathrm{norm}}(t_k^-))^T[\bar{p}_{\mathrm{n}}(t_k)+G(q)\mathbf{n}_q^T H_{\mathrm{t}}(q)p_{\mathrm{t}}(t_k)]\\&+\tfrac{1}{2}(\dot{q}_{\tan}(t_k^+)+\dot{q}_{\tan}(t_k^-))^T D_{\mathrm{t}}(q)\mathbf{t}_q^T H_{\mathrm{t}}(q)p_{\mathrm{t}}(t_k).\end{aligned} \tag{6.58}$$

[14] **Corollary 6.1** *[385, Corollary 2.2.5] Let $K\subseteq\mathbb{R}^n$ be compact convex, and $F:K\to\mathbb{R}^n$ be continuous. Then, the set of solutions to the generalized equation $0\in F(x)+N_K(x)$ is nonempty and compact.*

We assume that the problem (6.55) has been solved for at least one $\bar{p}_{\mathrm{n}}(t_k)$ and one $\dot{q}(t_k^+)$. Then after few manipulations we obtain:

$$\begin{aligned} T_L(t_k) = &-\tfrac{1}{2}\dot{q}_{\mathrm{norm}}(t_k^-)^T \overbrace{(I-\mathscr{E}_{\mathrm{nn}})^T M(q,\mu,v_{\mathrm{t}}(t_k^+))(I+\mathscr{E}_{\mathrm{nn}})}^{\triangleq \bar{M}(q,\mu,v_{\mathrm{t}})} \dot{q}_{\mathrm{norm}}(t_k^-) \\ &+\dot{q}_{\mathrm{tan}}(t_k^-)^T D_{\mathrm{t}}(q)\mathbf{t}_q^T H_{\mathrm{t}}(q)[\bar{\mu}][\xi] G^{\mu}(q,v_{\mathrm{t}}(t_k^+)))^{-1}(I+\mathscr{E}_{\mathrm{nn}})\dot{q}_{\mathrm{norm}}(t_k^-) \\ &+\tfrac{1}{2}\dot{q}_{\mathrm{norm}}(t_k^-)^T K(q,\mu,v_{\mathrm{tt}}(t_k^+))\dot{q}_{\mathrm{norm}}(t_k^-) \end{aligned} \tag{6.59}$$

with $M(q,\mu,v_{\mathrm{t}}) \triangleq G^{\mu}(q,v_{\mathrm{t}})^{-1} - G(q)\mathbf{n}_q^T H_{\mathrm{t}}(q)[\bar{\mu}][\xi] G^{\mu}(q,v_{\mathrm{t}})^{-1}$ and $K(q,\mu,v_{\mathrm{t}}(t_k^+)) \triangleq (I+\mathscr{E}_{\mathrm{nn}})^T G^{\mu}(q,v_{\mathrm{t}}(t_k^+))^{-T}[\bar{\mu}][\xi] H_{\mathrm{t}}(q)^T \mathbf{t}_q D_{\mathrm{t}}(q)\mathbf{t}_q^T H_{\mathrm{t}}(q)[\bar{\mu}][\xi]$ $G^{\mu}(q,v_{\mathrm{t}}(t_k^+))^{-1}(I+\mathscr{E}_{\mathrm{nn}})$. Let us investigate the positive definiteness of the matrix $\bar{M}(M(q,\mu,v_{\mathrm{t}})$.

Proposition 6.6 *[210] Assume that $G(q) \succ 0$. Then:*

1. *If $||G(q)^{-1}||_2||\mathbf{n}_q^T H_{\mathrm{t}}(q)||_2||[\bar{\mu}]||_2 < 1$, one has $G^{\mu}(q,v_{\mathrm{t}}(t_k^+))^{-1} \succ 0$.*
2. *If $||G^{\mu}(q,v_{\mathrm{t}}(t_k^+))||_2||G^{\mu}(q,v_{\mathrm{t}}(t_k^+))^{-1}||_2||G(q)||_2||\mathbf{n}_q^T H_{\mathrm{t}}(q)||_2||[\bar{\mu}]||_2 < 1$ is satisfied, then $M(q,\mu,v_{\mathrm{t}})) \succ 0$.*
3. *If $||\mathscr{E}_{\mathrm{nn}}||_2(1+2||\mathscr{E}_{\mathrm{nn}}||_2) < \frac{1}{||M(q,\mu,v_{\mathrm{t}})||_2} \frac{1}{\left|\left|\left(\frac{M(q,\mu,v_{\mathrm{t}}))+M^T(q,\mu,v_{\mathrm{t}}))}{2}\right)^{-1}\right|\right|_2}$ is satisfied, then $\bar{M}(q,\mu,v_{\mathrm{t}}) \succ 0$.*

Proof (1) $G(q)$ is symmetric positive definite. Applying Theorem 5.8 with $N = G(q)$ and $D = G(q) - \mathbf{n}_q^T H_{\mathrm{T}}(q)[\bar{\mu}][\xi]$ one finds that the inequality in 1 guarantees that $G(q) - \mathbf{n}_q^T H_{\mathrm{T}}(q)[\bar{\mu}][\xi]$ is positive definite. Then this matrix has a positive definite inverse which is $G^{\mu}(q,v_{\mathrm{t}})$. (2) The proof follows from Corollary 5.2, with $M = G^{\mu}(q,v_{\mathrm{t}})^{-1}$, $B = I - G(q)\mathbf{n}_q^T H_{\mathrm{t}}(q)[\bar{\mu}][\xi]$ and $A = M(q,\mu,v_{\mathrm{t}})$. Applying Proposition 9.3.5 in [136] to upper-bound $||G(q)\mathbf{n}_q^T H_{\mathrm{t}}(q)[\bar{\mu}][\xi]||_2$ by the product of norms, the result follows. (3) One has $(I-\mathscr{E}_{\mathrm{nn}})^T M(q,\mu,v_{\mathrm{t}})(I+\mathscr{E}_{\mathrm{nn}}) = M(q,\mu,v_{\mathrm{t}}) + H(q,\mu,e_{\mathrm{n,i}})$, with $H(q,\mu,e_{\mathrm{n,i}}) = -\mathscr{E}_{\mathrm{nn}}^T M(q,\mu,v_{\mathrm{t}})\mathscr{E}_{\mathrm{nn}} - \mathscr{E}_{\mathrm{nn}}^T M(q,\mu,v_{\mathrm{t}}) + M(q,\mu,v_{\mathrm{t}})\mathscr{E}_{\mathrm{nn}}$. Consider Theorem 5.8, with $M = M(q,\mu,v_{\mathrm{t}})$ and $A = M(q,\mu,v_{\mathrm{t}}) + H(q,\mu,e_{\mathrm{n,i}})$. Using Proposition 9.3.5 in [136] and the triangular inequality of norms one finds $||H(q,\mu,e_{\mathrm{n,i}})||_2 \leq ||\mathscr{E}_{\mathrm{nn}}||_2^2||M(q,\mu,v_{\mathrm{t}})||_2 + 2||\mathscr{E}_{\mathrm{nn}}||_2||M(q,\mu,v_{\mathrm{t}})||_2$. Thus it suffices that

$$\left|\left|\left(\frac{M(q,\mu,v_{\mathrm{t}})+M^T(q,\mu,v_{\mathrm{t}})}{2}\right)^{-1}\right|\right|_2 (||\mathscr{E}_{\mathrm{nn}}||_2^2||M(q,\mu,v_{\mathrm{t}})||_2 + 2||\mathscr{E}_{\mathrm{nn}}||_2||M(q,\mu,v_{\mathrm{t}})||_2) < 1$$

and the result follows.

From (6.59) the following holds:

$$T_L(t_k) \leq -\tfrac{1}{2}\lambda_{\min}(\bar{M}(q,\mu,v_{\mathrm{t}}))||\dot{q}_{\mathrm{norm}}(t_k^-)||^2 + \tfrac{1}{2}\lambda_{\max}(K(q,\mu,v_{\mathrm{t}}))||\dot{q}_{\mathrm{norm}}(t_k^-)||^2$$
$$+||D_{\mathrm{t}}(q)\mathbf{t}_q^T H_{\mathrm{t}}(q)||_2||[\bar{\mu}]||_2||I+\mathscr{E}_{\mathrm{nn}}||_2||\dot{q}_{\mathrm{norm}}(t_k^-)||\ ||\dot{q}_{\mathrm{tan}}(t_k^-)|| \tag{6.60}$$

Theorem 6.2 *[210] Provided that*

$$(i)\ \lambda_{\min}(\bar{M}(q,\mu,v_{\mathrm{t}}(t_k^+))) > \lambda_{\max}(K(q,\mu_i,v_{\mathrm{t}}(t_k^+)))$$
$$(ii)\ \frac{||\dot{q}_{\mathrm{norm}}(t_k^-)||}{||\dot{q}_{\mathrm{tan}}(t_k^-)||} \geq 2\frac{||D_{\mathrm{t}}(q)\mathbf{t}_q^T H_{\mathrm{t}}(q)||_2||[\bar{\mu}]||_2||I+\mathscr{E}_{\mathrm{nn}}||_2}{\lambda_{\min}(\bar{M}(q,\mu,v_{\mathrm{t}}(t_k^+)))-\lambda_{\max}(K(q,\mu,v_{\mathrm{t}}(t_k^+)))}, \tag{6.61}$$

one has $T_L(t_k) \leq 0$.

Proof Follows directly from (6.60).

Example 6.2 Let us illustrate the above developments on the simplest case of a planar particle hitting a line. The horizontal position is x, the vertical one (normal to the line) is y. One has $\dot{q}_{\mathrm{norm}} = \sqrt{m}\dot{y}$, $\dot{q}_{\mathrm{tan}} = \sqrt{m}\dot{x}$, $\bar{p}_{\mathrm{n}} = \frac{1}{\sqrt{m}}p_{\mathrm{n}}$, $G^{\mu}(q,v_{\mathrm{t}}) = 1$, $M(q,\mu) = 1, \bar{M}(q,\mu) = 1-e_{\mathrm{n}}^2, K(q,\mu_i,x(t_k^+)) = \mu^2(1+e_{\mathrm{n}})^2, D_{\mathrm{t}} = 1, \mathbf{t}_q^T D_{\mathrm{t}}\mathbf{t}_q = \frac{1}{m}, \mathbf{t}_q^T H_{\mathrm{t}}(q) = \frac{1}{\sqrt{m}}, G(q) = 1, \bar{p}_{\mathrm{n}} = -(1+e_{\mathrm{n}})\dot{q}_{\mathrm{norm}}(t_k^-), \ddot{q}_{\mathrm{norm}} = \bar{p}_{\mathrm{n}}, \ddot{q}_{\mathrm{tan}} = \frac{1}{\sqrt{m}}p_{\mathrm{t}}$, $\dot{q}_{\mathrm{tan}}(t^+) - \dot{q}_{\mathrm{tan}}(t_k^-) = \frac{1}{\sqrt{m}}(1+e_{\mathrm{n}})\dot{q}_{\mathrm{norm}}(t_k^-)\bar{\mu}\xi$, with $\xi \in \mathrm{sgn}(\dot{x}(t_k^+) + e_{\mathrm{t}}\dot{x}(t^-))$. The conditions of the Theorems imply that $e_{\mathrm{n}} \leq 1$, while the kinematic admissibility implies that $e_{\mathrm{n}} \geq 0$. The direct application of Theorem 6.2 gives:

$$(i)\ 1-e_{\mathrm{n}} > \mu^2(1+e_{\mathrm{n}})$$
$$(ii)\ \frac{|\dot{y}(t_k^-)|}{|\dot{x}(t_k^-)|} \geq \frac{2\mu}{1-e_{\mathrm{n}}-\mu^2(1+e_{\mathrm{n}})}. \tag{6.62}$$

Notice that condition (i) implies that $e_{\mathrm{n}} < 1$. If $e_{\mathrm{n}} = 0$ then $\mu < 1$ and $\frac{|\dot{y}(t_k^-)|}{|\dot{x}(t_k^-)|} \geq \frac{2\mu}{1-\mu^2}$. If $e_{\mathrm{n}} = 1$ only the frictionless case is admitted, because in that case $\bar{M}(q,\mu,v_{\mathrm{t}}) = 0$, and we have excluded this case from the beginning.

Remark 6.9 The major drawback of the generalized kinematic impact law, is that in most cases one has to identify the parameters for a given collision, i.e. for a given set of initial data and mechanical parameters: this is mainly due to the lack of information on contact flexibility in the model, which hampers to predict wave effects inside the multibody system. The LZB law introduced in Sect. 6.3 is from this point of view, much better. A possible way to enhance the generalized kinematic law, could be to use the information about the postimpact pattern, which is sometimes available (see Fig. 5.5 where two general patterns appear, see also [621, Fig. 1] for a two-ball system hitting a wall). Another drawback is related with its insertion in a

time-stepping algorithm for simulation: does it have to be used only in event-driven integrators?

6.2.6 Tangential Restitution

Motivated by the models described in Sects. 4.3.1, 4.3.2 and 4.3.3, where a tangential restitution coefficient is discussed *vs.* Coulomb's friction at the impulse level, we may introduce a generalized restitution as follows. We may impose $\bar{p}_{\rm n} \in -N_{V_{\rm n}(q)}(\Gamma_{\rm n}(\dot{q}_{\rm norm}(t^+) + \Lambda_{\rm n}\dot{q}_{\rm norm}(t^-)))$ and $p_{\rm t} \in -N_{V_{\rm t(q)}}(\Gamma_{\rm t}(\dot{q}_{\rm tan}(t^+) + \Lambda_{\rm t}\dot{q}_{\rm tan}(t^-)))$, for some matrices $\Lambda_{\rm n}$, $\Lambda_{\rm t}$, $\Gamma_{\rm n}$, $\Gamma_{\rm t}$, and convex sets $V_{\rm n}(q)$ and $V_{\rm t}(q)$. Inserting this into (6.53) one obtains the generalized equation:

$$v(t^+) - v(t^-) \in -\bar{G}(q) \begin{pmatrix} N_{V_{\rm n}(q)}(\Gamma_{\rm n}(\dot{q}_{\rm norm}(t^+) + \Lambda_{\rm n}\dot{q}_{\rm norm}(t^-))) \\ N_{V_{\rm t(q)}}(\Gamma_{\rm t}(\dot{q}_{\rm tan}(t^+) + \Lambda_{\rm t}\dot{q}_{\rm tan}(t^-))) \end{pmatrix}. \tag{6.63}$$

Defining the convex set $W(q) \stackrel{\Delta}{=} V_{\rm n}(q) \times V_{\rm t}(q)$ and Λ =diag$(\Lambda_{\rm n}, \Lambda_{\rm t})$, Γ =diag $(\Gamma_{\rm n}, \Gamma_{\rm t})$, we get :

$$v(t^+) - v(t^-) \in -\bar{G}(q)\, N_{W(q)}(\Gamma(v(t^+) + \Lambda v(t^-))), \tag{6.64}$$

with $\bar{G}(q) = \begin{pmatrix} G(q) & \mathbf{n}_q^T H_{\rm T}(q) \\ 0 & \mathbf{t}_q^T H_{\rm T}(q) \end{pmatrix}$. Existence and uniqueness of a solution $v(t^+)$ to the generalized equation in (6.64) depend on the matrices $\bar{G}(q)$, Γ, Λ, and on the convex sets $V_{\rm n}(q)$ and $V_{\rm t}(q)$. Suppose that there exists a symmetric positive definite matrix P such that $P\bar{G}(q) = \Gamma^T$, and let us denote R its symmetric square root $R^2 = P$. Then, using Convex Analysis tools (which we already used a lot throughout this book) we get:

$$v(t^+) = -\Lambda v(t^-) + R^{-1}\text{proj}[\bar{W}(q);\, R(\Lambda + I)v(t^-)] \tag{6.65}$$

with $\bar{W}(q) = \{x | \bar{G}^T Rx \in W(q)\}$ a convex set.

6.2.7 Comments

The generalized restitution law (6.44) and (6.45) has been studied in detail when applied on the planar rocking block and chains of aligned balls, in [228] (see Sect. 6.3.2.2). The domains where the entries of $\mathscr{E}_{\rm nn}$ have to lie in order for kinematic, kinetic and energetic consistencies to hold, are summarized in [228, Table 1]

in several cases: free rocking with or without sliding, half-rocking. It is also shown that the three consistency constraints plus the pre-impact velocity, do not define a unique set of CoRs (entries of $\mathscr{E}_{\rm nn}$) in general, or that some of the CoRs are admissible while >1. As noted by Moreau [900], adding a tangential CoR within a generalized framework, is more a trick than the result of deep modeling. The normalized Delassus's matrix is the matrix of *kinetic angles* between the constraints. More precisely, the kinetic angle between two constraints is defined as

$$\theta_{ij}(q) = \pi - \arccos \frac{\nabla f_i(q)^T M^{-1}(q) \nabla f_j(q)}{\sqrt{\nabla f_i(q)^T M^{-1}(q) \nabla f_i(q)} \sqrt{\nabla f_j(q)^T M^{-1}(q) \nabla f_j(q)}}. \quad (6.66)$$

Kinetic angles are quantities that reflect the couplings between the inertial and the geometrical properties of the system with unilateral constraints. It readily follows that $\mathbf{n}_q^T M(q) \mathbf{n}_q = [\cos(\pi - \theta_{ij})] = -[\cos(\theta_{ij})]$. In particular $\theta_{ii} = \pi$ and the diagonal entries are $-\cos(\theta_{ii}) = 1$. Kinetic angles play a major role in continuity of solutions w.r.t. initial data (see Sect. 5.2.4). Obviously they also play a major role in multiple impacts, for if constraints are pairwise orthogonal, then the Delassus's matrix is diagonal and collisions are decoupled. We based the definition of the generalized impact law in (6.44) and (6.45) on geometrical arguments, starting from the normal vectors $\mathbf{n}_{q,i}$ in (6.22), which have the interpretation of normals to the constraint boundary where $f_i(q) = 0$ in the kinetic metric. This is the only little piece of differential geometry in this book. For readers who like to swim in geometrical waters, let us refer to [305, 568, 980, 981]. The tangential restitution operator in Sect. 6.2.6 is strongly inspired from Frémond [414, 415] and close results have also been stated in [455, 730]. Sufficient conditions about energetic consistency may be found in [228, Sect. 3.2]. The most general restitution matrix (with tangential $\mathscr{E}_{\rm tt}$ and normal/tangential couplings $\mathscr{E}_{\rm nt}$ and $\mathscr{E}_{\rm tn}$) may be seen as an extension of Brach's approach in (4.103), formulated in a Lagrange dynamics context instead of Newton-Euler's dynamics. Interestingly enough, it happens in some applications like rockfalls [169] that a diagonal restitution matrix like in (4.103) is not sufficient: couplings have to be considered [169, Eq. (4)], and stochastic model of the CoRs is needed [168, 169, 170].

6.3 Energetic-CoR Multiple-Impact Law

We describe in this section an extension of the Darboux-Keller's shock dynamics, which applies to multiple impacts. Like for the Darboux-Keller's approach, the positions are assumed to be constant during the impact, and the dynamics is integrated with respect to the contact force impulse. This was introduced in [749, 750, 753, 1327], and is named the LZB impact dynamics.

6.3.1 Presentation of the LZB Impact Dynamics

The LZB approach yields an extension of the Darboux-Keller's impact dynamics, in case of multiple contacts/impacts. Thus basic assumptions are constant position q, and negligible forces (other than the impact forces) during the shock. It uses a bistiffness model as in Fig. 4.6a. We recall that this model is a crude approximation of the force/indentation law for elasto-plastic rate-independent materials, because it does not limit the contact force, and it dissipates energy even for very low pre-impact velocity (hence, for very low impact velocities which are below the minimum plastification velocity, a monostiffness model should be used). Moreover, it models dissipation during the expansion phase, while plasticification occurs during the compression phase (loading), see Sect. 4.2.1. An improvement is proposed in [929, Sect. 4.2.7] which we do not describe here.

Let F_j be the contact force at contact point j, and δ_j the normal indentation (whence $\dot{\delta}_j = \nabla f_j(q)^T \dot{q}$). During the compression (loading) phase, $F_{c,j} = k_j (\delta_{c,j})^{\eta_j}$, and during the expansion (unloading) phase, $F_{e,j} = F_{\max,j} \left(\frac{\delta_{e,j} - \delta_{r,j}}{\delta_{c,j} - \delta_{r,j}} \right)^{\eta_j}$. The corresponding works are given by $W_{c,j} = \int_0^{\delta_{c,j}} F_{c,j}(\delta_{c,j}) d\delta_{c,j} = \frac{1}{1+\eta_j} k_j (\delta_{c,j})^{\eta_j+1}$, and $W_{e,j} = \int_{\delta_{c,j}}^{\delta_{r,j}} F_{e,j}(\delta_{e,j}) d\delta_{e,j} = -\frac{1}{1+\eta_j} k (\delta_{c,j})^{\eta_j} (\delta_{c,j} - \delta_{r,j})$. Using the energetical CoR $e_{\star,j}$ as defined in (4.159), we infer that $\delta_{r,j} = \delta_{c,j}(1 - e_{\star,j}^2)$, which relates the CoR and the residual indentation. Notice that $\delta_{c,j}$ is the maximum compression indentation, so it is not a parameter of the impact dynamics, it is computed by integration of the collision dynamics. Few manipulations show that we also have $e_{\star,j}^2 = \frac{\delta_{c,j} - \delta_{r,j}}{\delta_{c,j}} = \left(\frac{k_{c,j}}{k_{e,j}} \right)^{\frac{1}{\eta_j}}$,[15] where $k_{c,j} = k_j$ is the stiffness during compression, $k_{e,j} = k_{c,j} \left(\frac{\delta_{c,j}}{\delta_{c,j} - \delta_{r,j}} \right)^{\eta_j}$ is the stiffness during expansion. According to the bistiffness model, the work done by the contact force during compression, is entirely converted into elastic potential energy stored in the bodies. Thus, the potential energy at the "instant" p_j during compression is $E_j(p_j) = \int_0^{p_j} \dot{\delta}_j(p_j) dp_j$, $0 \le p_j \le p_{c,j}$, where $p_{c,j}$ corresponds to maximal compression.[16] Then the residual potential energy during the expansion phase, is $E_j(p_j) = \int_0^{p_{c,j}} \dot{\delta}_j(p_j) dp_j + \frac{1}{e_{\star,j}^2} \int_{p_{c,j}}^{p_i} \dot{\delta}_j(p_j) dp_j = W_{c,j} + \frac{1}{e_{\star,j}^2} \int_{p_{c,j}}^{p_i} \dot{\delta}_j(p_j) dp_j$, $p_{c,j} \le p_j \le p_{f,j}$, where $p_{f,j}$ is the normal contact force impulse at the end of the expansion phase. The proof of this is given in [750, Sect. 3 (b)].

The normal contact force satisfies during the compression phase $\frac{dF_j}{dt} = \frac{dF_j}{dp_j} \frac{dp_j}{dt} = F_j \frac{dF_j}{dp_j}$, hence using that $\frac{dF_j}{dt} = \eta_j k_j (\delta_j)^{\eta_j - 1} \nabla f_j(q)^T \dot{q}$, we deduce that $F_j^{\frac{1}{\eta_j}} dF_j = \eta_j k_j^{\frac{1}{\eta_j}} \nabla f_j(q)^T \dot{q} \, dp_j$. We finally obtain $F_j(p_j) = \left((\eta_j + 1) \int_0^{p_j} k_j^{\frac{1}{\eta_j}} \nabla f_j(q)^T \dot{q} \, dp_j \right)^{\frac{\eta_j}{1+\eta_j}}$. We remind that these calculations are possible because it is assumed that the position

[15] This is consistent with what is stated in Sect. 4.2.1.2.

[16] We should denote $p_{\mathrm{n},j}$ to be consistent with the notations adopted elsewhere in the book.

q is constant, $q = q(0)$. One can then deduce that the ratio of two normal impulses at contact points j and i is given by $\frac{dp_j}{dp_i} = \frac{(\eta_j+1)^{\frac{\eta_j}{\eta_j+1}} k_j^{\frac{1}{\eta_j+1}} \left(\int_0^{p_j} \nabla f_j(q)^T \dot{q}\, dp_j\right)^{\frac{\eta_j}{\eta_j+1}}}{(\eta_i+1)^{\frac{\eta_i}{\eta_i+1}} k_i^{\frac{1}{\eta_i+1}} \left(\int_0^{p_i} \nabla f_i(q)^T \dot{q}\, dp_i)\right)^{\frac{\eta_i}{\eta_i+1}}}$. Noting that the potential energy $E_j(p_j)$ at contact point j equals $\int_0^{p_j} \nabla f_j(q)^T \dot{q}\, dp_j$, we can rewrite the impulse ratio as $\frac{dp_j}{dp_i} = \frac{(\eta_j+1)^{\frac{\eta_j}{\eta_j+1}} k_j^{\frac{1}{\eta_j+1}} (E_j(p_j))^{\frac{\eta_j}{\eta_j+1}}}{(\eta_i+1)^{\frac{\eta_i}{\eta_i+1}} k_i^{\frac{1}{\eta_i+1}} (E_i(p_i))^{\frac{\eta_i}{\eta_i+1}}}$. The next question is whether this continues to hold during the whole compression/expansion cycle. The answer is yes, as shown in [750, Sect. 3(d)].

In general there may be either a precompression at the contact point j, or a *repeated collision*: a first collision starts (compression, then expansion), but a second compression phase starts again before the expansion phase terminates (i.e., before the contact j opens), followed by an expansion phase. Suppose that the force/indentation relationship remains unchanged during repeated impacts, as depicted in Fig. 6.6. It is possible to prove the following, during a repeated impact at contact j:

$$E_j(p) = \begin{cases} E_0 + \int_0^{p_j} \dot{\delta}_j(p_j)\, dp_j & \text{if } Q \in \widehat{OM_{c,1}} \\ E_{M_{c,1}} + \frac{1}{e_{\star,j}^2} \int_{p_{M_{c,1}}}^{p_j} \dot{\delta}_j(p_j)\, dp_j & \text{if } Q \in \widehat{M_{c,1}R} \\ E_R + \int_{p_R}^{p_j} \dot{\delta}_j(p_j)\, dp_j & \text{if } Q \in \widehat{RM_{c,2}} \\ E_{M_{c,2}} + \frac{1}{e_{\star,j}^2} \int_{p_{M_{c,2}}}^{p_j} \dot{\delta}_j(p_j)\, dp_j & \text{if } Q \in \widehat{M_{c,2}B}, \end{cases} \tag{6.67}$$

where the cycle is as in Fig. 6.6 and Q is a generic point on the force/indentation curve corresponding to time p_j. The quantities E_0, $E_{M_{c,1}}$, E_R and $E_{M_{c,2}}$ are the residual potential energies at the points O, $M_{c,1}$, R and $M_{c,2}$, respectively. If the initial contact force at contact j is $F_{0,j}$ with indentation $\delta_{0,j}$, then, the initial potential energy is $E_{0,j} = \int_0^{\delta_{0,j}} \lambda_{c,j}(\delta_j) d\delta_j = \frac{(F_{0,j})^{\frac{\eta_j+1}{\eta_j}}}{(\eta_j+1) k_j^{\frac{1}{\eta_j+1}}}$. From the above expression of $F_j(p_j)$, we infer that $F_j(p_j) = (1+\eta_j)^{\frac{\eta_j}{\eta_j+1}} k_j^{\frac{1}{\eta_j+1}} \left(\frac{(F_{0,j})^{\frac{\eta_j+1}{\eta_j}}}{(\eta_j+1) k_j^{\frac{1}{\eta_j+1}}} + \int_0^{p_j} \dot{\delta}_j(p_j) dp_j \right)^{\frac{\eta_j}{\eta_j+1}}$, where one sees from (6.67) that the term between brackets is the potential enery $E_j(p_j)$. After some calculations the contact force during the expansion phase satisfies $F_{e,j} dF_{e,j} = \eta_j F_{\max,j} \left(\frac{\delta_j - \delta_{r,j}}{\delta_{c,j} - \delta_{r,j}}\right)^{\eta_j - 1} \frac{\dot{\delta}_j}{\delta_{c,j} - \delta_{r,j}} dp_j$, and using that $\delta_{c,j} - \delta_{r,j} = e_{\star,j}^2 \delta_{c,j}$, one finds $(F_{e,j})^{\frac{1}{\eta_j}} dF_{e,j} = \eta_j (F_{e,j})^{\frac{1}{\eta_j}} \frac{\dot{\delta}_j}{e_{\star,j}^2 \delta_{c,j}} dp_j$. At the end of the compression phase we have $F_{c,j} = k_j (\delta_{c,j})^{\eta^j}$, hence $(F_{e,j})^{\frac{1}{\eta_j}} dF_{e,j} = \frac{1}{e_{\star,j}^2} \eta_j (k_j)^{\frac{1}{\eta_j}} \dot{\delta}_j dp_j$. At the beginning of the expansion phase, we have $p_j = p_{c,j}$ and $\dot{\delta}_j = 0$, and $F_j(p_{c,j}) = (1+\eta_j)^{\frac{\eta_j}{1+\eta_j}} k_j^{\frac{1}{\eta_j}+1} (E_j(p_{c,j}))^{\frac{\eta_j}{\eta_j+1}}$. Integrating one obtains $(F_{e,j}(p_j))^{\frac{\eta_j+1}{\eta_j}} = (\eta_j + 1) k_j^{\frac{1}{\eta_j+1}} E_j(p_j)$. Thus the contact force during expansion at the impulse instant p_j is

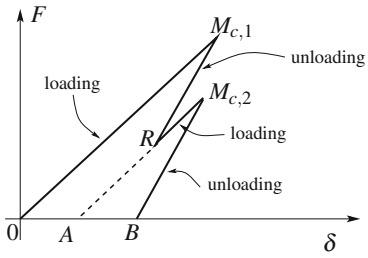

Fig. 6.6 A repeated impact (linear elasticity: $\eta = 1$)

given by $F_{e,j} = (1+\eta_j)^{\frac{\eta_j}{1+\eta_j}} k_j^{\frac{1}{1+\eta_j}} (E_j(p_j))^{\frac{\eta_j}{1+\eta_j}}$. This is the same expression as for the compression phase.
We therefore deduce that the ratios of the normal contact forces impulses at contact points j and i, are given generically by the *distributing rule*:

$$\Gamma_{ji} = \frac{dp_j}{dp_i} = \frac{(1+\eta_j)^{\frac{\eta_j}{\eta_j+1}} k_j^{\frac{1}{1+\eta_j}} E_j^{\frac{\eta_j}{1+\eta_j}}}{(1+\eta_i)^{\frac{\eta_i}{\eta_i+1}} k_i^{\frac{1}{1+\eta_i}} E_i^{\frac{\eta_i}{1+\eta_i}}}. \tag{6.68}$$

It follows that if the elasticity constants $\eta_j = \eta - i = \eta$, then Γ_{ij} does depend only on the stiffness ratio $\gamma_{ji} = \frac{k_j}{k_i}$, not on the absolute values of the stiffnesses. This is coherent with what we already noticed in Sect. 6.1.3 on a particular case. It is interesting to see now that this is not true if the elasticity coefficients are not identical. The multiple impact terminates when all the potential energy that has been stored during the compression phases, is entirely released or dissipated and all contacts open, that is $E_j(p_{f,j}) = 0$ and $\dot{\delta}_j(p_{f,j}) \geq 0$ for all j that participate into the collision. The LZB impact dynamics is summarized as follows:

- Contact parameters $e_{\star,j}$, η_j, $1 \leq j \leq m$, γ_{ij}, precompression potential energies $E_{0,j}$ and indentations $\delta_{0,j}$.
- Darboux-Keller's dynamics:

$$\boldsymbol{M}(q)\frac{d\dot{\boldsymbol{q}}}{dp_i} = \nabla f(q)\boldsymbol{\Gamma}, \tag{6.69}$$

  with contact i being the primary contact.
- Ratio $\Gamma_{ji} = \dfrac{dp_j}{dp_i}$ of the normal impulse increment at contact j to that at the primary contact i:

$$\Gamma_{ji} = \frac{(1+\eta_j)^{\eta_j/(\eta_j+1)}}{(1+\eta_i)^{\eta_i/(\eta_i+1)}} \frac{k_j^{1/(1+\eta_j)}}{k_i^{1/(1+\eta_i)}} \frac{E_j^{\eta_j/(\eta_j+1)}}{E_i^{\eta_i/(\eta_i+1)}}. \tag{6.70}$$

and $\Gamma = (\Gamma_{1i}, \Gamma_{2i}, .., \Gamma_{i-1,i}, 1, \Gamma_{i+1,i}, \ldots, \Gamma_{mi})^T$.

- Potential energy E_j:

$$E_j(p_j) = \int_0^{p_j} \dot{\delta}_j(p_j) dp_j, \text{ if } 0 \leq p_j \leq p_{c,j}, \tag{6.71}$$

$$E_j(p_j) = W_{c,j} + \frac{1}{e_{\star,j}^2} \int_{p_{c,j}}^{p_j} \dot{\delta}_j(p_j) dp_j, \text{ if } p_j^c \leq p_j \leq p_{f,j}, \tag{6.72}$$

with $\dot{\delta}_j = \nabla f_j(q)^T \dot{q}$, $p_{c,j}$ is the impulse at the end of the compression phase ($\dot{\delta}_j(p_{c,j}) = 0$), and $p_{f,j}$ is the terminal impulse.

- Impact termination condition:

$$E_j = 0, \ \dot{\delta}_j \leq 0, \text{ for all } j = 1, 2, \ldots, m. \tag{6.73}$$

where m is the number of impacting points.

The primary impulse p_i has to be chosen properly, for in particular it should not vanish, and may be changed during the collision integration. Its choice for the numerical integration of the LZB impact dynamics, is explained in [753], and in [929, Algorithm 3, page 90]. A numerical algorithm is detailed in [753] which explains how the LZB impact dynamics may be integrated. See also [929, Sects. 4.2, 4.3] for a very detailed presentation of the LZB dynamics integration and its insertion in an event-driven algorithm. The case with friction is detailed in [752]. Possible numerical instability due to the elasticity coefficients η_j that make the LZB dynamics stiff, is studied in [929, § 4.2.9].

6.3.2 Applications and Validations

The LZB model has been validated through numerous comparisons with experimental data.

6.3.2.1 Chains of Aligned Beads

Probably the most fundamental microscopic property of granular materials is irreversible energy dissipation in the course of interaction (collision) between particles [56]. A correct modeling of the dissipation at impacts (and also outside impacts during persistent contact phases of motion), and a correct numerical algorithm for simulation, are therefore of utmost importance in granular matter. Chains of balls are a first, simple instance of granular mechanical systems. Numerical results with the LZB model have been compared to experimental results obtained on various types of chains of aligned balls [387, 625, 838, 915, 1059], in [749, 753, 928, 929, 1331]. Some of them have been presented in Figs. 6.1 and 6.2a, b. The comparisons concern

not only the postimpact velocities and kinetic energy, but also and most importantly the waves that travel through the chains, maximum impact force and force pulse amplitude for monodisperse as well as tapered and stepped chains [753, 928, 929]. They prove that the LZB model encapsulates the main phenomena (nonlinear waves) which are responsible for the multiple impact. As we said above, this is due to the fact that the LZB model contains the information on stiffness ratios between the contact points. A complete exposition of the event-driven codes used to simulate the chains, is made in [929]. *The LZB model for multiple impacts may be the very first instance where it is proved experimentally that the energetic CoR supersedes the kinematic and the kinetic CoRs*.

Further Reading: Newton's cradle and chains of balls are apparently simple, almost toy-systems, however thet have received a lot of attention since a long time, especially in the Physics teachers literature. Since the appearance of Granular Matter as a scientific field, and the discoveries of their great complexity from the point of view of nonlinear waves transmission, they serve as an example of one-dimensional granular material. We do not survey all the results about chains of aligned beads in this book. Let us mention that the discovery of nonlinear solitary waves in monodisperse chains (identical balls) is due to Nesterenko [924], and justified experimentally in [306]. Since then nonlinear waves have been studied in several types of chains, varying the radii (hence the masses) of the balls, the contact interaction potentials, and the curve of the chain [145, 245, 529, 608, 609, 610, 613, 772, 956, 1012, 1086] to cite a few.

6.3.2.2 Rocking Block

We consider the system in Fig. 6.7a, which has two unilateral constraints (provided the base line is assumed to be concave) when $y \leq \frac{\sqrt{l^2+L^2}}{2}$: $f_1(q) = y - \frac{l}{2}\cos(\theta) + \frac{L}{2}\sin(\theta) \geq 0$, and $f_2(q) = y - \frac{l}{2}\cos(\theta) - \frac{L}{2}\sin(\theta) \geq 0$. It is interesting to notice that the admissible domain Φ which depicted in Fig. 6.7b, is not convex. Assuming that the dynamical effects of the block on the base are negligible, the dynamics of the block with Coulomb friction is given by

$$\left\{\begin{array}{l} m\ddot{x}(t) = \lambda_{\mathrm{t},1}(t) + \lambda_{\mathrm{t},2}(t) \\ m\ddot{y}(t) = \lambda_{\mathrm{n},1}(t) + \lambda_{\mathrm{n},2}(t) - mg \\ I_G\ddot{\theta}(t) = \lambda_{\mathrm{n},1}(t)\left(\frac{l}{2}\sin(\theta(t)) + \frac{L}{2}\cos(\theta(t))\right) + \lambda_{\mathrm{n},2}(t)\left(\frac{l}{2}\sin(\theta(t)) - \frac{L}{2}\cos(\theta(t))\right) \\ \qquad + \left(\frac{l}{2}\cos(\theta(t)) - \frac{L}{2}\sin(\theta(t))\right)\lambda_{\mathrm{t},1} + \left(\frac{l}{2}\cos(\theta(t)) + \frac{L}{2}\sin(\theta(t))\right)\lambda_{\mathrm{t},2} \\ \\ \qquad 0 \leq \lambda_{\mathrm{n}}(t) \perp f(q(t)) \geq 0 \\ \qquad \lambda_{\mathrm{t},i}(t) \in -\mu_i\lambda_{\mathrm{n},i}(t)\ \mathrm{sgn}(v_{\mathrm{t},i}(t) - v_b(t)), i = 1, 2, \end{array}\right. \tag{6.74}$$

where $v_b(t) = \dot{x}_b(t)$ is the base horizontal velocity, $\mu_i > 0$ is the friction coefficient at contact i, and $v_{\mathrm{t},i}$ is the tangential velocity at the point i, i.e. $v_{\mathrm{t},1} = \dot{x} + \left(\frac{l}{2}\cos(\theta) - \frac{L}{2}\sin(\theta)\right)\dot{\theta}$ at B and $v_{\mathrm{t},2} = \dot{x} + \left(\frac{l}{2}\cos(\theta) + \frac{L}{2}\sin(\theta)\right)\dot{\theta}$ at A (from which $v_{\mathrm{t},1} = v_{\mathrm{t},2}$ when $\theta = 0$). With $q = (x, y, \theta)^T$, one can identify M, F_{ext}, $\nabla f(q)$ and $H_{\mathrm{t}}(q)$ in (5.1) from (6.74).

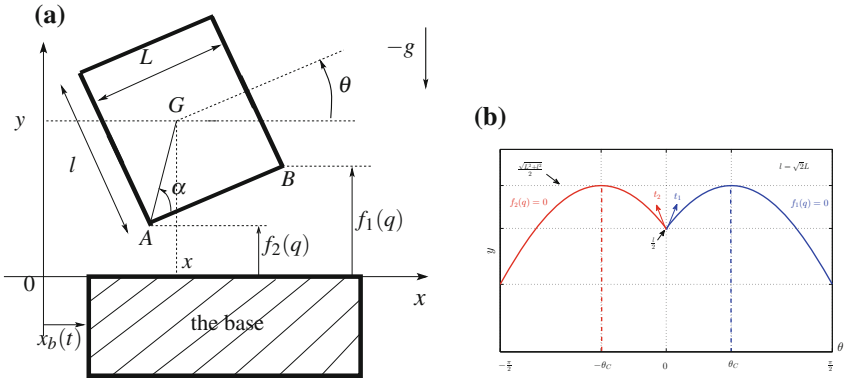

Fig. 6.7 The rocking block. **a** The system. **b** Admissible domain (taken from [1318])

The contact LCP is $0 \leq \lambda_{\mathrm{n}} \perp D_{\mathrm{nn}}(\theta)\lambda_{\mathrm{n}} + \nabla f(\theta)^T M^{-1} H_{\mathrm{t}}(\theta)\lambda_{\mathrm{t}} + B(\theta, \dot{\theta}) \geq 0$ with $D_{\mathrm{nn}}(\theta) = \begin{pmatrix} \frac{1}{m} + \frac{1}{4I_G}(l\sin(\theta) + L\cos(\theta))^2 & \frac{1}{m} + \frac{1}{4I_G}(l^2\sin^2(\theta) - L^2\cos^2(\theta)) \\ \frac{1}{m} + \frac{1}{4I_G}(l^2\sin^2(\theta) - L^2\cos^2(\theta)) & \frac{1}{m} + \frac{1}{4I_G}(l\sin(\theta) - L\cos(\theta))^2 \end{pmatrix}$ and $B(\theta, \dot{\theta}) = \begin{pmatrix} -g + \frac{1}{2}\dot{\theta}^2(l\cos(\theta) - L\sin(\theta)) \\ -g + \frac{1}{2}\dot{\theta}^2(l\cos(\theta) + L\sin(\theta)) \end{pmatrix}$. The Delassus' matrix $D_{\mathrm{nn}}(\theta) \succ 0$ except at $\theta = \pm\frac{\pi}{2}$.

Remark 6.10 (Kinetic Angles) The kinetic angle θ_{12} between the two constraints is given by:

$$\theta_{12} = \pi - \arccos\left(\frac{l^2 - 2L^2}{l^2 + 4L^2}\right) \tag{6.75}$$

at $\theta = 0$. Denoting the aspect ratio as $a \stackrel{\Delta}{=} l/L$ we may rewrite it as $\theta_{12} = \pi - \arccos\left((a^2 - 2)/(a^2 + 4)\right)$: there is a one-to-one correspondence between a and θ_{12}. It satisfies $\theta_{12} = \pi/2$ if $l = \sqrt{2}L$, $0 < \theta_{12} < \pi/2$ if $0 < l < \sqrt{2}L$ (flat block), and $\pi > \theta_{12} > \pi/2$ if $l > \sqrt{2}L$ (slender block). When a varies from 0 (infinitely flat block with infinite width L) to $+\infty$ (infinitely slender block with infinite height l) then θ_{12} varies from $\pi/4$ to π. The fact that $\theta_{12} \in [\pi/4, \pi]$ means that one expects that the block/ground system possesses a rich dynamics, and may serve as a nice example of multiple impact with friction. The interest of studying the block dynamics as a function of the kinetic angle between the two boundaries at $\theta = 0$, is that it allows us to determine that a block is not of the slender type just if $l > L$. As shown in [1318] using the LZB model with friction, the dispersion factor $d \stackrel{\Delta}{=} \frac{\dot{y}_A(t_k^+)}{\dot{y}_B(t_k^-)}$ displays a particular $V-$shaped as a function of θ_{12} (equivalently of a) and for varying friction [1318, Figs. 6, 7, 12], and there exists a critical kinetic angle at which d is minimum, which is independent of the CoR [1318, Fig. 10], see Fig. 6.8b.

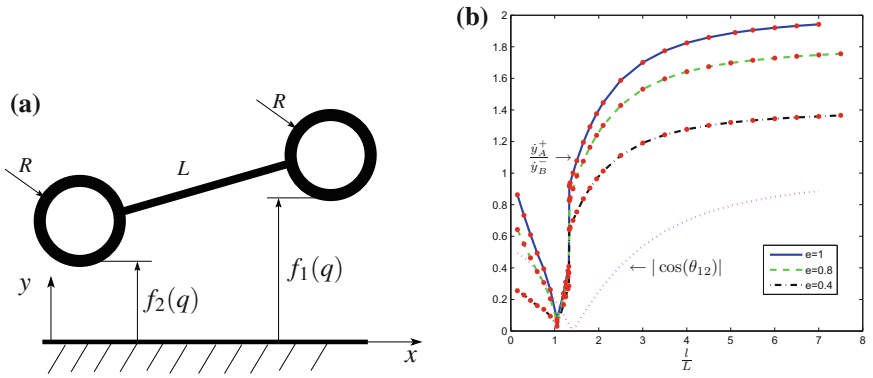

Fig. 6.8 The dimer, and rocking block's critical aspect ratio. **a** The bouncing dimer. **b** Critical kinetic angle for the rocking block's energy dispersion (taken from [1318])

Remark 6.11 (Kinetic Angles (continued)) A system that is close to the classical rocking block, is the bouncing dimer studied in [357, 1327] and depicted in Fig. 6.8a. The dimer is made of two identical spheres with radius R connected by a rigid rod with length L. Using the same notations as for the block, the two unilateral constraints for the dimer are $f_1(q) = y + (L/2 + R)\sin(\theta) - R \geq 0$ and $f_2(q) = y - (L/2 + R)\sin(\theta) - R \geq 0$. Some calculations yield that the kinetic angle between the two constraints at $\theta = 0$ (double impact) and with all masses equal to 1 for simplicity, is given by $\theta_{12} = \pi - \arccos\left((1/3 - \alpha)/(1/3 + \alpha)\right)$ with $\alpha = (1+2a)^2/(16a^2/5 + 1/3 + 2(1+2a)^2)$, $a = R/L$. The flatest dimer has $L = +\infty$, and the less flat one has $L = 0$ (the two balls are stuck together). The two kinetic angle values that correspond to these extreme cases are $\theta_{12} = \pi - \arccos(-1/8) \approx 1.445$ rad and $\theta_{12} = \pi - \arccos(-1/29) \approx 1.536$ rad, which are both slightly smaller than $\pi/2 \approx 1.571$ rad. This means that the dimer and the block, despite their apparent similarity, possess different dynamical behaviors in the sense that the dimer kinetic angle varies little and never exceeds $\pi/2$ (the dimer is always flat), while the block kinetic angle may vary much more.

The LZB model applied to the block/anvil system for rocking, onset of rocking, with harmonic base excitations, is validated in [1319] with thorough comparisons between numerical simulations and the experimental data obtained on blue granite stone blocks reported in [987, 988].[17] The masses of the blocks are estimated from their dimensions and density, and are given by 503, 228, 120, 245 kg, demonstrating the scope of the experiments. The overturning phenomenon is also analysed in [1319].

[17] All the experimental data used for the comparisons with numerical data presented in [1319] have been made available to the authors by Dr F. Pena from Instituto di Ingenieria, UNAM, Mexico.

It is noteworthy that the parameters (equivalent width and length, CoRs) have been fitted from the free-rocking experimental data, and then used without modification for the other comparisons with an excited base (onset of rocking).

Further Reading, Comments and Perspectives: The rocking block dynamics has been studied since a long time in the Earthquake Engineering literature, because of its interest in better understanding buildings dynamics under seismic excitation, see e.g. [19, 41, 42, 379, 543, 747, 1010, 1017, 1131]. The restitution law that is widely used is $\dot{\theta}(t_k^+) = e_\theta \dot{\theta}(t_k^-)$ for some CoR e_θ. This seems to be an *ad hoc* restitution law, however this is not quite the case. The link between $\mathscr{E}$ in (6.44) and (6.45) and e_θ as well as local tangential restitution is made in [228]. It is found that in case of rocking motion (the block rotates around A, hits the ground at B without rebound, then rotates around B, hits the ground at A without rebound, etc), we have $\mathscr{E} = \begin{pmatrix} 0 & -e_\theta & 0 \\ -e_\theta & 0 & 0 \\ 0 & 0 & e_\theta \end{pmatrix}$. Therefore, *the angular velocity CoR is interpreted via the generalized restitution law, as a tangential CoR for* $\dot{q}_{\tan}$. Moreover, let $v_{\mathrm{t},i}(t_k^+) = e_{\mathrm{t}} v_{\mathrm{t},i}(t_k^+)$, $i = 1, 2$ at A and B, where e_{t} is the local tangential CoR. Then it can be shown that $e_{\mathrm{t}} = -e_{\mathrm{t},3} = -e_{\mathrm{n},1} + e_{\mathrm{n},21}$ [228, Sect. 6]. It follows that if one imposes in addition that there is no slip at the impacting point, then $e_{\mathrm{t}} = 0$, while no rebound at the impacting point implies $e_{\mathrm{n},1} = 0$. We infer that necessarily $\mathscr{E} = 0$. It is also proved in [228, Sect. 3.6] that Coulomb's friction (at the impulse level) with $\tilde{v}_{\mathrm{t}}(t_k) = v_{\mathrm{t}}(t_k^+)$ in (4.69) and a diagonal $\mathscr{E}_{\mathrm{nn}}$, cannot model rocking motion: off-diagonal terms in $\mathscr{E}_{\mathrm{nn}}$ and tangential restitution CoR are needed. It is nevertheless noteworthy that such impact law cannot model very finely the real block motion. In practice, one observes usually rebounds at both A and B even during a rocking global motion, and slip/stick phases.

Some experiments in [987, 988] show the existence of non-negligible three-dimensional effects, due to body vibrations and torsion. This proves the need to go beyond planar systems. The study of three-dimensional rocking blocks with flexibilities is an interesting topic for future investigations. The rocking block system involves *line/line impact* (or *plane/plane impact* in the thee-dimensional case), for which the two-point contact model is a crude approximation (implying in particular the estimation of an equivalent width which does not necessarily match with the geometrical width). Line/line impacts modeling is investigated in [1330].

6.3.2.3 Other Experimental Validations of the LZB Model

The LZB model has been further validated with careful comparisons between experimental and numerical data, in [1248, 1249] (three-dimensional bouncing dimer), [1327] (two-dimensional bouncing dimer), a disk-ball system [748, 1321].

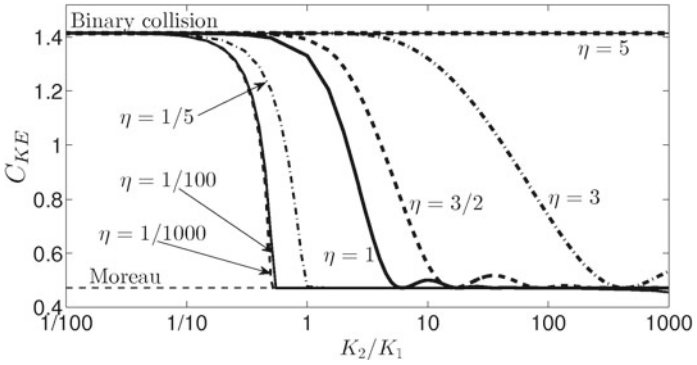

Fig. 6.9 Relation C_{KE} - k_2/k_1 for different values of η: Moreau, binary collisions, LZB (taken from [929, Fig. 6.12])

6.3.3 Comparison of Different Multiple Impact Mappings

A thorough comparison between Moreau's law, the binary collision model, and the LZB approach, is made on the monodisperse three-ball chain in [929, Chap. 6]. The comparisons are made by varying elasticity coefficients, masses, and stiffnesses ratio, with the "usual" initial conditions (the first bead hits the other two, in contact and at rest). We present in Fig. 6.9 the kinetic energy dispersion variable C_{KE} defined in (5.72) in Chap. 5, as a function of the stiffness ratio $\frac{k_2}{k_1}$ and the elasticity coefficient η ($\eta = 1$ for linear elasticity, $\eta = \frac{3}{2}$ for Hertz' elasticity, etc). This figure shows that the energy dispersion varies significantly with η and $\frac{k_2}{k_1}$, and that Moreau's law applies for low C_{KE} index[18] (i.e. high dispersion, "large" $\frac{k_2}{k_1}$ and "small" η), while the binary collision applies to high C_{KE} index (i.e. low dispersion, "small" $\frac{k_2}{k_1}$ and "large" η). Such analysis would deserve an extension to more general chains, in order to determine validity areas for Moreau/Newton, binary collision, Pfeiffer-Glocker/Poisson approaches. Once again it is clear that the great advantage of the LZB approach is that it encapsulates information on the stiffness ratio. The domains of validity of the Moreau's or binary collisions laws, depend in turn on the form of the waves created by the collision between the first and the second balls, which varies depending on η_j [529, 1086]. Let us mention an interesting comparative analysis between visco-elastic models (see Chap. 2), binary collisions approach, bistiffness model and elasto-plastic approaches (see Sect. 4.2.1), when applied on the three-ball system in [354].

[18] In agreement with Proposition 5.17 which states that Moreau's law minimizes C_{KE}.

6.4 Further Reading

6.4.1 Kinetic Restitution (Poisson)

Pfeiffer and Glocker introduced a generalization of Poisson's impact law in [1001]. It consists of solving a two-stage LCP at each contact point. Let us illustrate it on a simple case of two aligned balls hitting a wall. A crucial assumption is that the maximum compression times at each contact/impact point, are equal (see [929, Sect. 3.1.2] for detailed calculations on a 3-ball chain, showing the necessity of this assumption). This may be the main and less realistic hypothesis of this approach, because in most cases maximum compression times do not match, and there may even exist repeated impacts. Let us apply the method to the case of a chain of two balls, that strikes a rigid wall (i.e., take $N = 2$ in Fig. 6.1). Roughly, the problem is solved by constructing two LCPs, one for the end of the compression phase ($t = t_c$), the second one for the end of the expansion phase ($t = t_f$). Coefficients $e_{\mathrm{p},1}$ and $e_{\mathrm{p},2}$ are associated with each contact. The LCPs at each contact, $i = 1, 2$, are as follows:

- At $t = t_c$:

$$\left\{\begin{array}{l} p_i(t)\,\dot{f}_i(q(t)) = 0 \\ \dot{f}_i(q(t)) \geq 0 \\ p_i(t) \geq 0 \end{array}\right. \tag{6.76}$$

- At $t = t_f$:

$$\left\{\begin{array}{l} p_i(t_f) - p_i(t_c) - e_{\mathrm{p},i}\,p_i(t_c) \geq 0 \\ \dot{f}_i(q(t_f)) \geq 0 \\ \{p_i(t_f) - p_i(t_c) - e_{\mathrm{p},i}\,p_i(t_c)\}\,\dot{f}_i(q(t_f)) = 0 \end{array}\right. \tag{6.77}$$

where $f_1(q) = q_1 - q_2$ and $f_2(q) = q_2$ are the two unilateral constraints. Introducing the impact dynamics (we use the same initial data and masses as above) $\dot{q}_1(t_c) + 1 = p_1(t_c), \dot{q}_2(t_c) = -p_1(t_c) + p_2(t_c), \dot{q}_1(t_f) - \dot{q}_1(t_c) = p_1(t_f) - p_1(t_c), \dot{q}_2(t_f) - \dot{q}_2(t_c) = -p_1(t_f) + p_1(t_c) + p_2(t_f) - p_2(t_c)$, one therefore gets four LCPs (two for each contact)

$$\left\{\begin{array}{l} p_1(t_c)(\dot{q}_1 - \dot{q}_2)(t_c) = 0 \\ (\dot{q}_1 - \dot{q}_2)(t_c) \geq 0 \\ p_1(t_c) \geq 0 \end{array}\right. , \left\{\begin{array}{l} p_2(t_c)\dot{q}_2(t_c) = 0 \\ \dot{q}_2(t_c) \geq 0 \\ p_2(t_c) \geq 0 \end{array}\right. \tag{6.78}$$

$$\begin{array}{l} \left\{\begin{array}{l} p_1(t_f) - p_1(t_c) - e_{\mathrm{p},1}\,p_1(t_c) \geq 0 \\ (\dot{q}_1 - \dot{q}_2)(t_f) \geq 0 \\ \{p_1(t_f) - p_1(t_c) - e_{\mathrm{p},1}\,p_1(t_c)\}(\dot{q}_1 - \dot{q}_2)(t_c) = 0 \end{array}\right. \\ \left\{\begin{array}{l} p_2(t_f) - p_2(t_c) - e_{\mathrm{p},2}\,p_2(t_c) \geq 0 \\ \dot{q}_2(t_f) \geq 0 \\ (p_2(t_f) - p_2(t_c) - e_{\mathrm{p},2}\,p_2(t_c))(\dot{q}_1 - \dot{q}_2)(t_f) = 0. \end{array}\right. \end{array} \tag{6.79}$$

If both CoR's are equal to 1, it is easily checked that there is a unique solution given by $(\dot{q}_1 - \dot{q}_2)(t_f) = 1$, $\dot{q}_2(t_f) = 0$, so that $\dot{q}_1(t_f) = 1$ and $\dot{q}_2(t_f) = 0$. The case with friction is discussed in [1000]. It is shown in [929, Fig. 3.1] that in order to fill in the whole admissible postimpact velocity domain of Fig. 5.5, it is necessary to consider CoRs $e_{\mathrm{p},i} > 1$, which may lack of physical meaning. Pfeiffer-Glocker's approach with a two-stage LCP is used in [47, 48] in a three-dimensional setting and Coulomb friction with facetized cone. A thorough analysis of the energetic consistency of Pfeiffer-Glocker's law with or without friction, is made in [456]. It has also been implemented in [1022] for ice floes simulation with an event-driven code.

6.4.2 Kinematic Restitution (Newton and Moreau)

Inspired by Frémond whose framework introduced in Sect. 4.3.4 extends to multiple shocks [266, 290, 836] [415, Chap. 8] [416, Chapitre 5], Glocker has introduced in [451, 454, 985] a restitution matrix similar to $\mathscr{E}_{\mathrm{nn}}$ in (6.45), and makes a thorough geometrical analysis of Moreau's impact law, he also extends it to re-entrant corners [454, Sect. 5.4], which are excluded from Moreau's framework which is based on finitely represented admissible domains Φ. Leine and van de Wouw [730, 732] extend Moreau's framework by formulating impact laws with friction as inclusions in normal cones to convex sets (or the reverse inclusions in subdifferentials of support functions) [730, Chap. 5]. Restitution matrices are allowed, and conditions for dissipativity are given [730, pp.159–160] which are used for stability purpose [730, Theorem 7.6]. In [1026], a kinematic restitution matrix is introduced (in a way similar to our $\mathscr{E}_{\mathrm{nn}}$ above, or to Glocker's matrix in [451, 454, 985], see also the formulations in [730] which accomodate for restitution matrices and also friction), while friction is modeled at the impulse level with a friction cone faceting procedure.

6.4.3 Other Approaches

Bowling and Rodriguez [1048] use Routh's incremental approach and energetical CoRs at each contact in a chain of aligned balls to solve the multiple impact: energy dispersion is modeled. The same authors formulate in [171, 1047] the multiple impact with friction as an optimization problem which includes kinetic and energetic constraints, starting from the maximum dissipation principle of friction, and a diagonal restitution matrix with kinematic CoRs (this may be seen as a rewriting of Moreau's rule with friction). Barjau et al. [90, 91] use a stiff unilateral compliant normal contact model, combined with a modal analysis, for frictionless redundant contacts. Bistiffness-like models are used in [91] to account for energy loss. Jia [622, 623] presents a very detailed analysis close to the one in Sect. 6.3.1, with a state-transition diagram to describe the multiple impact. Their approach is close to the one in Sect. 6.3.1: a linear bistiffness law is chosen, repeated impacts are taken

into account, and the distributing law is derived in a particular case [623, Eq. (15)]. Hurmuzlu and co-authors introduced in [268, 441, 558, 1187, 1300] a method which consists of using Routh's incremental two-dimensional approach, with so-called impulse correlation ratios (ICR), which are constants relating the impact forces impulses (the percussion $p_{\mathrm{n},i}$ at each contact i, in the sense of Definition 1.2). The ICRs permit to introduce some distance effects (or energy dispersion) in the impact dynamics. However as shown on numerical simulations in [11] and in the above distributing rule (6.68), impulse ratios are not be constant in general but could vary a lot depending on the initial data and parameters, and should therefore be fitted with experiments. Hurmuzlu and Marghitu [561] deal with planar kinematic chains with multiple contact/impact points (see also [559] for a preliminary result). Collisions are treated with Routh' incremental method (two-dimensional Darboux-Keller's dynamics), and an event-driven-like algorithm is proposed to calculate the postimpact velocity, testing all possible cases (stick-slip transitions in both directions, constraint deactivation).

Chapter 7
Stability of Nonsmooth Dynamical Systems

This chapter starts with stability of various systems with state jumps: Lyapunov stability of Measure Differential Equations, vibro-impact systems, and impact oscillators. Then the so-called grazing bifurcations are introduced. The Lyapunov stability of complementarity Lagrangian mechanical systems is analyzed in detail, and it is shown how the Zhuravlev-Ivanov nonsmooth transformation introduced in Chap. 1 may be used for finite-time stabilization with a sliding-mode controller. The chapter ends with the analysis of Lyapunov stability of a simple system hitting a unilateral spring-like environment, and the use of copositive matrices for studying the stability of linear complementarity systems.

7.1 Stability of Measure Differential Equations

In this section we briefly review some stability concepts for the MDEs we introduced in Chap. 1.

7.1.1 Stability of Impulsive ODEs

Let us consider the following class of MDEs, which we introduced in Sect. 1.2.4:

$$\begin{cases} \dot{x}(t) = f(x(t), t), & t \neq t_k(x) \\ \sigma_x(t_k) = I_k(x(t_k^-)), & t = t_k(x), \end{cases} \tag{7.1}$$

and $x(0^-) = x_0$. Let the following conditions be satisfied:

- The function $f(x, t)$ satisfies the basic conditions for existence, uniqueness, and continuous dependence of the ODE $\dot{x}(t) = f(x(t), t)$, $f(t, 0) = 0$.
- The functions $I_k(\cdot)$ are continuous and $I_k(0) = 0$ for $k \in \mathbb{N}$.

B. Brogliato, *Nonsmooth Mechanics*, Communications and Control Engineering,
DOI 10.1007/978-3-319-28664-8_7

- There exists a constant $h < +\infty$ such that if $||x|| \leq h$, then $x + I_k(x) < +\infty$.
- The discontinuity times of any solution $x(t)$ satisfy $0 = t_0 < t_1(x) < t_2(x) < \ldots$, $\lim_{k\to+\infty} t_k(x) = +\infty$. The functions $t_k(\cdot)$ are continuous. Moreover, in the extended state space (t, x), there is no beating, i.e. trajectories do not meet infinitely often the same hypersurface where state jumps occur, i.e. surfaces $S_k = \{(t, x)|t = t_k(x)\}$.

One has to analyze the system during continuous motion on intervals (t_k, t_{k+1}) and at discontinuity instants t_k. Derivatives of Lyapunov functions $V(\cdot)$ have to be understood as $\dot{V}_{rd}(t) = \lim_{h\to 0^+} \sup \frac{V(t+h)-V(t)}{h}$ (the upper right Dini derivative of $V(\cdot)$) almost everywhere, and $\dot{V}(t_k) = \sigma_V(t_k)\delta_{t_k}$.[1] Lyapunov's second method extends by stating $\dot{V}_{rd}(t) \leq 0$ and $\sigma_V(t_k) \leq 0$.

Definition 7.1 [76] The solution $x(t)$ of system (7.1) is stable if for all $\varepsilon > 0$, for all $\eta > 0$, for all $\tau_0 \geq 0$ such that $|\tau_0 - t_k| > \eta$, there exists a $\delta > 0$ such that for all $x_0 \in \mathbb{R}^n$ with $|x_0 - x(\tau_0)| < \delta$, for all $t \in J^+(\tau_0, x_0)$ with $|t - t_k| > \eta$, then $|\varphi(t; \tau_0, x_0) - x(t)| < \varepsilon$.

The set $J^+(\tau_0, x_0)$ denotes the maximal interval of existence of the solution $\varphi(t; \tau_0, x_0)$ with initial conditions (τ_0, x_0). Similar definitions can be adapted to uniform, asymptotic stability, as in the classical non-impulsive case. Note that in general (when the t_k's are not fixed but depend on the state), two different solutions $x(t)$ and $\varphi(t)$ will possess discontinuities at different times: this is the mismatch issue described in Sect. 1.3.2.3. For the case when we study the stabilty of a fixed point $x(t) = x^\star$ (note that $x^\star = 0$ is a fixed point of the system (7.1)), one can define Lyapunov stability in the classical way. This is also the case if the t_k's are fixed, since then all solutions have discontinuities simultaneously. Let us recall some classical definitions: a function $\alpha : [0, \infty) \to [0, \infty)$ belongs to class $\mathscr{K}$ if it is continuous, strictly increasing, and $\alpha(0) = 0$. If, in addition, $\alpha(\cdot)$ is unbounded then $\alpha(\cdot)$ belongs to class $\mathscr{K}_\infty$. A function $\beta : [0, \infty) \times [0, \infty) \to [0, \infty)$ belongs to class $\mathscr{K}\mathscr{L}$ if $\beta(\cdot, t) \in \mathscr{K}$ for each $t \geq 0$, $\beta(r, \cdot)$ is strictly decreasing for each $r \geq 0$ and $\beta(r, t) \to 0$ as $t \to \infty$.

The Lyapunov second method extends to such systems.

Theorem 7.1 (Lyapunov second method [76, Theorem 13.1]) *Let the above conditions be satisfied, and let functions $V(t, x)$ and $\alpha(\cdot)$ of class $\mathscr{K}$ exist, with $V(t, 0) = 0$ for all $t \geq \tau_0$, such that along the system's trajectories we have:*

$$\begin{cases} \alpha(||x(t)||) \leq V(t, x(t)) & \text{for all } t \geq \tau_0 \text{ and } x \in \mathbb{R}^n, \\ \dot{V}_{rd}(t, x(t)), \leq 0 & \text{for all } t \neq t_k(x) \\ \sigma_V(t_k) \leq 0 & \text{for } t = t_k(x). \end{cases} \tag{7.2}$$

[1] Notice that in general we do not have $\dot{V} = \frac{\partial V}{\partial x}\left(\{\dot{x}\} + \sigma_x \delta_{t_k}\right)$, but we do have $\dot{V} = \{\dot{V}\} + \sigma_V(t_k)\delta_{t_k}$. If $V(\cdot)$ is quadratic in x and $x \in RCLBV$, then Moreau's rule can be applied to get $dV = d(x^T Px) = (x^+ + x^-)^T P dx$ [867]. Outside jumps $dV = 2x^T P dx$ and at discontinuity instants $dV = (x^+ + x^-)^T P(x^+ - x^-)\delta_t = [(x^+)^T Px^+ - (x^-)^T Px^-]\delta_t = \sigma_V \delta_t$. dV and dx are called differential measures or Stieltjes measures of $V(\cdot)$ and $x \in RCLBV$.

Then the trivial solution $x^\star = 0$ of the system (7.1) is stable in the sense of Definition 7.1.

Theorem 7.1 can be extended to guarantee uniform, asymptotic, exponential stability, see [76, Theorems 13.2–13.5].

7.1.2 Stability of Measure Driven ODEs (MDEs)

Let us focus on the MDEs introduced in Sect. 1.2.2, in particular (1.22). The following notion of stability is considered.

Definition 7.2 [1182] We call the system (1.23) *uniformly asymptotically stable* over a set of inputs $\mathscr{U}$ if there exists a class $\mathscr{KL}$ function $\beta(\cdot,\cdot)$ such that every state trajectory $x(\cdot)$ resulting from the input $u \in \mathscr{U}$ as a solution of (1.23) satisfies $|x(t)| \leq \beta(|x(t_0)|, t - t_0)$.

We recall that $u(\cdot)$ is an $m-$input of local bounded variation. The following holds:

Theorem 7.2 (Asymptotic Stability [1182]) *Assume that there exist a continuously differentiable function $V : \mathbb{R}^n \to \mathbb{R}_+$, some class $\mathscr{K}_\infty$ functions $\alpha_1(\cdot)$, $\alpha_2(\cdot)$, and some constants $a, \underline{b}, \bar{b} \in \mathbb{R}$ such that the following holds for each $x \in \mathbb{R}^n$:*

$$\begin{cases} \alpha_1(|x|) \leq V(x) \leq \alpha_2(|x|), \\ \langle \nabla V(x), f(x) \rangle \leq a V(x), \\ \underline{b}_j \, V(x) \leq \left\langle \nabla V(x), g_j(x) \right\rangle \leq \bar{b}_j \, V(x), \quad j = 1, \ldots, m. \end{cases} \tag{7.3}$$

For some $c \in \mathbb{R}$ and $\theta(\cdot) \in \mathscr{K}_\infty$, let $\mathscr{U}_{c,\theta}$ denote the class of inputs satisfying:

$$a(t - t_0) + \sum_{j=1}^{m} \bar{b}_j \mu_j^+([t_0, t]) - \sum_{j=1}^{m} \underline{b}_j \mu_j^-([t_0, t]) \leq c - \theta(t - t_0), \tag{7.4}$$

for every $t \geq t_0$, $t_0 \in \mathbb{R}$. Then, system (1.23) is uniformly asymptotically stable over $\mathscr{U}_{c,\theta}$. Let $\mathscr{U}_M$ denote the class of inputs for which the total variation of the inputs is bounded by some constant $M > 0$. Suppose the above hypotheses hold with $a < 0$ in (7.3). Then system (1.23) is uniformly asymptotically stable over $\mathscr{U}_M$.

In the Theorem, μ_j^+ (resp. μ_j^-) is the differential measure associated with the function $u_j^+(\cdot)$ (resp. $u^-(\cdot)$), which is the increasing (resp. the decreasing) part of the entry $u_j(\cdot)$ of $u(\cdot)$. The proof of Theorem 7.2 is too long to be given here. Roughly speaking, the solution of system (1.23) could be seen as flows along the vector fields $f(\cdot)$ and $g_j(\cdot)$. Condition (7.4) in Theorem 7.2 basically assigns the weight on how long each of these vector fields should be active for the system to be asymptotically stable. For this, neither $f(\cdot)$ nor any of the control vector fields $g_j(\cdot)$ need to be stable in the classical sense. However, an appropriate choice of $u(\cdot)$ may render the system

asymptotically stable depending on the signs of the scalars $a, \underline{b}_j, \bar{b}_j$ appearing in (7.4). Corollaries of Theorem 7.2 show how to characterize the stability of switched and impulsive systems.

Another notion of stability, important in Control, is that of input-to-state stability (ISS). In the following, du is the differential measure associated with $u(\cdot)$ and $|du|$ is its total variation, i.e. $|du|([t_0, t]) = \text{var}(u, [t_0, t])$ (see Sect. A.3.1). The motivation is to consider systems that are not necessarily asymptotically stable but the maximum value of the state trajectories depends on some norm of the driving input. This may be interesting when $u(\cdot)$ models additive noise or there are undesired impulsive perturbations in the state trajectory.

Definition 7.3 [1182] System (1.23) is called input-to-state stable (ISS) with respect to variation of the input $u(\cdot)$ if there exist a class $\mathscr{KL}$ function $\beta(\cdot, \cdot)$ and a class $\mathscr{K}_\infty$ function $\gamma(\cdot)$ such that

$$|x(t)| \leq \beta(|x(t_0)|, t - t_0) + \gamma(|du|_{[t_0,t]}) \quad t \geq t_0. \tag{7.5}$$

Since we are dealing with inputs that have finite variation on every compact interval, it means that the state trajectories satisfying the estimate (7.5) belong to some compact set in the state space at each time in the interval over which they are defined.

Theorem 7.3 (ISS with Variation [1182]) *Suppose there exist a continuously differentiable function $V : \mathbb{R}^n \to \mathbb{R}_+$, some class $\mathscr{K}_\infty$ functions $\alpha_1(\cdot), \alpha_2(\cdot)$, and some positive constants $a, b, c > 0$ such that for each $x \in \mathbb{R}^n$:*

$$\begin{cases} \alpha_1(|x|) \leq V(x) \leq \alpha_2(|x|) \\ \langle \nabla V(x), f(x) \rangle \leq -aV(x) \\ -bV(x) - c \leq \langle \nabla V(x), g_i(x) \rangle \leq bV(x) + c, \qquad i = 1, \ldots, m, \end{cases} \tag{7.6}$$

then the system (1.23) is ISS with respect to the variation of $u(\cdot)$.

7.1.3 Additional Comments and Studies

Liu [696, 756] extends the definition of stability of impulsive ODEs in the spirit of [76], and considers stability in terms of two *measures* (here the word measure has not the common meaning of a measure as a function from a set of subsets into $[0, +\infty)$ [477]: it refers to functions $h(t, x)$ having certain properties). Roughly, the fixed point of the system (still given by the smooth part of the dynamics) is (h_0, h)-stable if for any $\varepsilon > 0$, there exists a $\delta(\varepsilon) > 0$ such that $h_0(t_0, x_0) < \delta$ implies $h(t, x(t)) < \varepsilon$, for any solution $x(t)$ of the system. By considering different sorts of functions $h_0(\cdot)$ and $h(\cdot)$, one can encompass various types of stability (in particular classical Lyapunov stability if $h(\cdot)$ and $h_0(\cdot)$ are the Euclidean norms). [756] gives sufficient conditions that guarantee stability (see e.g. [76, Corollary 3.6]). Interestingly, [76, Theorem 13.3] and [756] consider the situations in which $\dot{V}_{rd}(\cdot)$ is only *semi-negative*

definite and one wants to prove asymptotic stability, extending Matrosov's result for non-autonomous continuous vector fields. Other stability criteria have been proposed in Michel et al. [847, 1293], for systems as in (7.1). It is shown that the existence of a positive definite function $V(t,x)$, $\gamma_1(||x||) \leq V(t,x) \leq \gamma_2(||x||)$, $\gamma_i(\cdot)$ class-$\mathscr{K}$ functions, such that (i) $V(t,x) \leq h(V(t_k^+, x(t_k^+))$ on $(t_k, t_{k+1}]$, (ii) $V(t_k^+) \leq V(t_{k-1}^+)$, where $h(\cdot)$ is a continuous function, $h(0) = 0$, ensures stability of the fixed point $x^\star = 0$. The additional condition (iii) $V(t_k^+) - V(t_{k-1}^+) \leq -\Delta_{k+1}\gamma_3(||x(t_k^-)||)$, with $\gamma_3(\cdot)$ a class-$\mathscr{K}$ function, ensures the asymptotic stability. Results close in spirit to these can be found in [739]. They aim at relaxing the requirements previous results by allowing the function $V(t,x)$ to increase between two jumps. Note that the jump times are not assumed to be fixed but may be state-dependent [847, 1293]. In this case it is important to study conditions under which the beating phenomenon does not occur. For instance the system in (1.33) has no beating, i.e. its solutions have no finite-accumulations of jumps. Sufficient conditions for no-beating are given in [75, Theorem 2.1,Corollaries 2.1, 2.2] and [696]. Maximum and minimum dwell times which guarantee global asymptotic stability are characterized in [192] for linear impulsive ODEs with fixed state-jump times, using Lyapunov equations and non-monotonic Lyapunov functions.[2] The articles [719, 1031] consider the impulses Du as a perturbation of a Lyapunov stable smooth system with u an exogenous function in *RCLBV*, and study conditions on Du (see hypothesis (H_4) through (H_8) in [719], Definition 2.1 in [1031]) such that stability is preserved (roughly the jumps in $u(\cdot)$ must converge sufficiently fast to zero; notice that similarly the conditons $I_k(0) = 0$ and $I_k(\cdot)$ continuous in (7.1) imply that as the state approaches the fixed point, the autonomous jumps vanish). Lyapunov functions are defined for measure systems, and can be used to prove asymptotic-self-invariance (ASI) [718] of the equilibrium point $x^\star = 0$ of the smooth dynamics. (ASI is a stability concept adapted to perturbed systems with asymptotically vanishing disturbances: for instance, the set $\{x \in \mathbb{R}^n | x = 0\}$ is ASI relative to $\dot{x} = -x + e^{-t}$ [718]).

7.2 Stability of the Discrete Dynamic Equations

One way to characterize the stability of impacting systems is to study the discrete-time system associated to the overall dynamics. More precisely, by integrating the smooth vector field and incorporating the impact conditions, one is theoretically able to derive the *impact Poincaré map* of the system.[3] This is usually only one part only of the stability analysis of the mechanical complementarity system, where one focuses solely on the "vibro-impact" behavior. In other words, only the rebounding phases are considered.

[2] Nonmonotonic Lyapunov functions are often met in systems with state jumps, see Chap. 8. This is because possible strict decrease at state-jump times may compensate for (not too big) increase between the jumps.

[3] Such maps are also called first-return mapping, monodromy operator, successor mapping.

7.2.1 The Bouncing-Ball with Fixed Obstacle

To illustrate this in a simple case, let us consider the bouncing-ball dynamics, when the flat is motionless and has infinite mass. We may write it as follows:

$$\begin{cases} mdv = -mgdt + \sum_{k=0}^{+\infty} p_k \delta_{t_k} + \lambda(t)dt \\ x(0) = x_0 \geq 0, \dot{x}(0^-) = \dot{x}_0 \\ m[\dot{x}(t_k^+) - \dot{x}(t_k^-)] = p_k, \quad x(t_k) = 0, \dot{x}(t_k^-) < 0 \\ \dot{x}(t_k^+) = -e_{\mathrm{n}} \dot{x}(t_k^-) \\ 0 \leq \lambda(t) \perp x(t) \geq 0, \end{cases} \tag{7.7}$$

where $\lambda(t)$ is the function part of the contact force, and $dv = \ddot{x}(t)dt + \sum_{k\geq 0}[\dot{x}(t_k^+) - \dot{x}(t_k^-)]\delta_{t_k}$ is the differential measure of the velocity, i.e. the acceleration is seen as a measure, and δ_{t_k} is the Dirac measure with atom $t = t_k$.[4] The contact force impulse has magnitude $p_k = p_{\mathrm{n}}(t_k)$ with our previous notations. The initial data and the collision rule in (7.7) secure that $x(t) \geq 0$ for all $t \geq 0$ (even without stating the non negativeness in the complementarity conditions). It may be deduced from (7.7) that the total time of rebounding is bounded. In other words, the impact times sequence $\{t_k\}_{k\in\mathbb{N}}$ possesses a finite accumulation time $t_\infty < +\infty$, and an infinity of impacts occurs within a finite time interval: this is a *left-accumulation* of impacts (and of velocity jumps). Let $\Delta_{k+1} = t_{k+1} - t_k$, $k \geq 0$, be the time elapsed between two impacts. Integrating the motion from the post-impact motion at t_k until the pre-impact motion at t_{k+1}, using $x(t_k) = x(t_{k+1}) = 0$ and Newton's impact law, one finds $\Delta_{k+1} = \frac{2}{g}\dot{x}(t_k^+) = -\frac{2}{g}e_{\mathrm{n}}\dot{x}(t_k^-)$, and $\dot{x}(t_{k+1}^-) = -\dot{x}(t_k^-)$ (the flight motion is lossless, so the kinetic energy is conserved). Thus $\Delta_{k+1} = -\frac{2}{g}e_{\mathrm{n}}^m \dot{x}(t_{k-m+1}^-)$. Letting $m = k+1$ one gets $\Delta_{k+1} = -\frac{2}{g}e_{\mathrm{n}}^{k+1}\dot{x}(t_0^-) = \frac{2}{g}e_{\mathrm{n}}^k \dot{x}(t_0^+)$. One then infers that the total time of rebounds $[t_0, t_\infty]$ is given by $t_\infty - t_0 = \sum_{k\geq 0}\Delta_{k+1} = \frac{2}{g}\dot{x}(t_0^+)\frac{1+e_{\mathrm{n}}}{1-e_{\mathrm{n}}}$. If the ball falls from a height h, then one obtains $\Delta_{k+1} = e_{\mathrm{n}}^{k+1}\sqrt{\frac{8h}{g}}$ and $t_\infty - t_0 = \frac{1+e_{\mathrm{n}}}{1-e_{\mathrm{n}}}\sqrt{\frac{8h}{g}}$.

When the restitution coefficient varies from one shock to the next, in which case we shall denote it as $e_{\mathrm{n},k}$, then the ball comes to rest after a period $\Delta = \sum_{k=1}^{+\infty} = \sqrt{\frac{8h}{g}}\left(\frac{1}{2} + \sum_{k=1}^{+\infty}\prod_{j=1}^{k} e_{\mathrm{n},j}\right)$ [479]. Finite accumulations of impacts have been studied in more general settings in [243, 727, 1253]. In [286] it is shown that a finite accumulation of impacts still exists if $e_{\mathrm{n}} = 1 - \alpha\dot{x}(t_k^-)^{\frac{1}{5}}$.

7.2.1.1 Lyapunov Stability

Let us analyze the Lyapunov stability of the bouncing ball. Here two paths may be followed. The first path is to study the stability of the fixed point $(x^\star, \dot{x}^\star) = (0, 0)$

[4] Due to its simplicity, the bouncing-ball dynamics velocity is of special bounded variation, which allows one to get rid of the third term of its derivative as a measure, denoted μ_{na} in Remark A.4.

of the complete nonsmooth mechanical system, including all phases of motion (free, contact, impact): this will be done in Sect. 7.5 in a general framework. The second path is to consider only the rebounding phase, i.e. the interval $[t_0, t_\infty)$.

Let us consider the system's total energy $V(x, \dot{x}) = \frac{1}{2}m\dot{x}^2 + mgx$. Obviously, this function is not positive definite over $\mathbb{R} \times \mathbb{R}$, because of the gravity potential energy. We may however circumvent this obstacle as follows. Consider the impact Poincaré surface $\Sigma^+ = \{(x, \dot{x}) | x(t_k) = 0, \dot{x}(t_k^+) > 0\}$, i.e. one looks at the system on the right of each impact. We easily calculate that $V(t_{k+1}^+) - V(t_k^+) = V(t_{k+1}^+) - V(t_{k+1}^-) + V(t_{k+1}^-) - V(t_k^+)$,[5] hence $V(t_{k+1}^+) - V(t_k^+) = \frac{1}{2}m\dot{x}(t_{k+1}^-)^2 + \underbrace{\int_{(t_k, t_{k+1})} \dot{V}(t)\, dt}_{=0}$, hence $V(t_{k+1}^+) - V(t_k^+) = \frac{1}{2}m(e_n^2 - 1)\dot{x}(t_{k+1}^-)^2 < 0$ for any $\dot{x}(t_{k+1}^-) \neq 0$ and $e_n \in (0, 1)$. Notice that the restriction of $V(\cdot)$ to Σ^+ satisfies the same inequality and equals $V_\Sigma(x(t_k), \dot{x}(t_k^+)) = V_\Sigma(0, \dot{x}(t_k^+)) = V_\Sigma(\dot{x}(t_k^+)) = \frac{1}{2}m\dot{x}(t_k^+)^2$. Hence, the impact Poincaré map of the bouncing ball, considered as a mapping $\dot{x}(t_k^+) \to \dot{x}(t_{k+1}^+)$, defined on the sequence of impact times $\{t_k\}_{k\geq 0}$, has a globally asymptoticaly stable equilibrium $\dot{x}^\star = 0$ in the sense of Lyapunov.

What about the complete system's equilibrium stability? From the above analysis one has $\dot{V}(t) = 0$ during flight phases $t \in (t_k, t_{k+1})$, and $V(t_k^+) - V(t_k^-) \leq 0$ at impact times. During persistent contact motion, the dynamics is given by $m\ddot{x}(t) = -mg + \lambda(t) = 0$, where $\lambda(t) \geq 0$ from the complementarity conditions, and is in this simple case explicitly calculable as $\lambda = mg > 0$. On persistent contact phases of motion, one finds $\dot{V}(t) = \dot{x}(t^+)\lambda = mg\dot{x}(t^+) = 0$ since $\dot{x}(t^+) = 0$ (here we have to consider the right-velocity, because we want to encapsulate the velocities after an impact time). In a more general setting, complementarity $0 \leq \dot{x}(t^+) \perp \lambda(t^+) \geq 0$ holds on persistent contact phases (see Sect. 5.1.2.1), and implies that $\lambda(t^+) > 0 \Rightarrow \dot{x}(t^+) = 0$. This will be used more systematically in Sect. 7.5. Therefore $V(\cdot)$ is a nonincreasing function. If we restrict its analysis in the domain $\Phi = \{x \in \mathbb{R} | x \geq 0\}$, then $V(x, \dot{x}) \geq 0$. This is equivalent to modifying it to the nonsmooth function $V(x, \dot{x}) = \frac{1}{2}m\dot{x}^2 + mgx + \psi_{\mathbb{R}^+}(x)$, where $\psi_{\mathbb{R}_+}(\cdot)$ is the indicator function of $\mathbb{R}_+$. We can then conclude about the Lyapunov stability of the fixed point $(x^\star, \dot{x}^\star) = (0, 0)$.

It is noteworthy that the stability analysis of the impact Poincaré map, may be interpreted as the analysis of the system over a discrete time space made of the infinite number of impact times. This is the approach taken in [462, 943, 945]. They propose the Lyapunov function candidate $V(x, \dot{x}) = \dot{x} + k\sqrt{\frac{1}{2}\dot{x}^2 + gx}, k > \sqrt{2}\frac{1+e_n}{1-e_n}$. This function is positive definite in Φ, satisfies $\dot{V}(t) < 0$ for all x and $\dot{x}$ outside impact times, and $V(t_k^+) - V(t_k^-) \leq 0$ at impact times. The system's equilibrium is said uniformly Zeno asymptotically stable. A kind of robustness stability analysis is proposed in [945], where the constant force (the gravity) is assumed to be in a given interval. It is a priori not surprising that the magnitude of this force, does not modify the stability of the bouncing ball's fixed point. It is noteworthy that the analysis in

[5] To simplify the presentation, we denote $V(x(t), \dot{x}(t))$ as $V(t)$, and its derivative along the system's trajectories as $\dot{V}(t)$.

[462, 945] relies on a partial model that does incorporates neither the contact forces outside impacts, nor the complementarity conditions. The notion of Zenon equilibria is introduced in [943] as fixed points of the impact Poincaré map, together with the notion of bounded-time local stability, which is shown to depend on the signum of $\ddot{h}(q^\star, \dot{q}^\star)$.

7.2.1.2 Dissipativity

The above developments strongly suggest a dissipativity interpretation of the ball's dynamics, where the mechanical energy plays the role of a storage function (see [218] for a complete exposition of dissipativity theory). Let us consider two time-instants $T_1 \geq T_0 \geq 0$, and the total mechanical energy as the Lyapunov function, then:

$$\underbrace{V(T_1) - V(T_0)}_{\text{energy variation on } [T_0, T_1]} = \underbrace{\int_{[T_0,T_1]\setminus\{t_k\}_{k\in[k_0,k_1]}} \dot{V}(t)dt}_{\text{energy dissipated outside impacts}} + \underbrace{\sum_{k\in[k_0,k_1]} \sigma_V(t_k)}_{\text{energy dissipated at impact times}} + \underbrace{\int_{[T_0,T_1]\setminus\{t_k\}_{k\in[k_0,k_1]}} \dot{x}(t)\lambda(t)dt}_{\text{energy ``injected'' in the ball outside impacts:=0}} \tag{7.8}$$

where t_{k_0}, t_{k_0+1}, …, t_{k_1} are impact times in $[T_0, T_1]$. One may use the developments in Sects. 5.4.4.5 and 7.5.3 to group the last two terms on the right-hand side, with a generalized supply rate as in (5.148) or (7.60).

Remark 7.1 Real systems do not show an infinity of impacts in a finite time, because they possess some flexibility and plastic deformation at the contact area. Thus any experiment of a ball bouncing on a flat would demonstrate a finite number of collisions before the ball rests on the flat [386]. The rigid body model is an approximation of the real process, and its Zeno behavior is to be considered as a model artifact. However, one one hand it does represent the fact that if the ball and the flat are made of very hard materials with some dissipation, there will nevertheless exist many collisions with increasing frequency. On the other hand, such models are widely used for mathematical and numerical analysis, feedback control, simulation, and one has to incorporate in the analysis the existence of finite accumulations. Finally, it is noteworthy that time-stepping numerical methods (Sect. 5.7.3) compute only a finite number of collisions even in the presence of an accumulation of impact times, and therefore reproduce the physics of the real system: in a sense the discretization corrects the model's behavior. A "flexible" bouncing ball is studied in [286], which consists of two particles linked with a linear spring, moving vertically, one of them colliding with the ground. A restitution coefficient models the impacts. For almost all initial conditions, the system reaches its static equilibrium asymptotically only. This proves that considering body flexibilities may influence significantly the system's behavior.

7.2.2 Lyapunov Stability of Discrete-Time Systems

The stability of systems with impulses can therefore be attacked *via* the discrete system (or impact map, or Poincaré impact map) associated to the total system. Notice that this map is different from the discrete map considered in Definition 7.1, which was simply the jump map of the system: the integration of the trajectories between the jumps is needed to get the Poincaré impact map. Stability definitions and criteria for such maps are given in [421]. Let it be given as:

$$x_{n+1} = f(x_n). \tag{7.9}$$

Assume that $f(x^\star) = x^\star$ for some fixed point $x^\star$ of the map. Then we have:

Definition 7.4 [421] The fixed point $x^\star$ of the map in (7.9) is stable in the sense of Lyapunov if and only if for all $n_0 \in \mathbb{N}$, for all $\varepsilon > 0$, there exists $\delta > 0$ such that if $||x_0 - x^\star|| < \delta$, then for all $n \geq n_0$, $||x_n(x_0, n_0) - x^\star|| < \varepsilon$.

Here, x_0 denotes x_{n_0}, and $x_n(x_0, n_0)$ denotes the n-th iterated value starting with initial conditions x_0, n_0. Then Lyapunov's second method provides the following result:

Theorem 7.4 *[421] The fixed point $x^\star$ of the map in (7.9) is Lyapunov stable if and only if there exist a continuous function $V(\cdot)$ and a class $\mathscr{K}$ function $\alpha(\cdot)$, a ball $B_r(x^\star)$ with radius r, centered at $x^\star$, such that for all $x_n \in B_r(x^\star)$*

- $V(x_n) \geq \alpha||x_n - x^\star||$
- $V(x_{n+1}) - V(x_n) \leq 0$
- $V(x^\star) = 0$

Let us reiterate that both stability Definitions 7.4 and 7.1 are not equivalent. First of all, the stability in Definition 7.1 concerns the whole system with state vector $x \in \mathbb{R}^n$. On the contrary, the second stability definition concerns a reduced order system (this is indeed the aim of Poincaré maps to reduce the dimension of the system by analyzing it only in one Poincaré section of the state space. For the bouncing ball the section we chose is $x = 0$). Furthermore, the bouncing ball example shows that in certain cases, the impact Poincaré map is easily derived, and Lyapunov stability as in Theorem 7.4 can be proved. Notice that the state variables for the discrete-time associated system may be chosen as $\dot{x}(t_k^+)$ and Δ_k [639]. The discrete mapping fixed point is given for the times t_k as t_∞ or as 0 for the flight-times Δ_{k+1}. This is equivalent to studying the trajectories through the section $x = 0$ of the extended state space $(t, x, \dot{x})$. It is apparent from (7.7) that the bouncing ball problem includes a finite accumulation point of rebounds, i.e. the sequence $\{t_k\}$ is infinite and has a finite limit $t_\infty < +\infty$. This is really created by the discrete (or impulsive) dynamics themselves. It is a general fact that the impulsive dynamics may drastically modify the total dynamics. Let us consider as an additional proof of this fact the following:

Example 7.1 Let us consider the following system [756]:

$$\begin{cases} \dot{x}(t) = 1 + x(t)^2, \ x(0) = 0, t \neq t_k \\ \sigma_x(t_k) = -1, \qquad t_k = \frac{k\pi}{4}, k = 1, 2, \ldots \end{cases} \tag{7.10}$$

Then the solution of the smooth dynamics, without any impulse, is given by $x(t) = \tan(t)$, and therefore escapes in finite time. On the contrary, the solution of the whole system is given as

$$x(t) = \tan\left(t - \tfrac{k\pi}{4}\right), \ \tfrac{k\pi}{4} < t < \tfrac{(k+1)\pi}{4} \ k = 1, 2, \ldots \tag{7.11}$$

The solution in (7.11) is periodic with period $\frac{\pi}{4}$, and jumps from 1 to 0 at t_k. We have $x(t_k^+) = 0$ and $x(t_{k+1}^-) = 1$. By choosing either the post or the pre-impulse values, it is easily visualized that the corresponding discrete map has a unique value at 0 or at 1.

7.3 Impact Oscillators

The study of the dynamical behavior of impact oscillators is an important application of shock dynamics. Let us start with a tentative definition of what is meant by impact oscillators in the literature:

Definition 7.5 (*Impact oscillators [151]*) An *impact oscillator* is a system which is driven in some way and which also undergoes intermittent or a continuous sequence of contacts with motion limiting constraints.

As we shall see in the sequel, many simple mechanical systems fall into this definition. Impact oscillators are also often called *vibro-impact* systems. One of the goals is prediction of the possible different regimes that may occur in a real system, in order to "capture" part or all of the vibrational energy which is unwanted in the main structure. We mention many applications later. We focus mainly on the following in the research of periodic trajectories in impact oscillators.

7.3.1 Existence of Periodic Trajectories

A logical method to prove the existence of periodic trajectories in an impacting system is the following: assume that one seeks for trajectories with period T and two impacts *per* period. First, calculate the solution $\varphi(\cdot)$ of the system on (t_k, t_{k+1}) and on (t_{k+1}, t_{k+2}), with $t_{k+1} = t_k + \frac{T}{2}$ for all $k \geq 0$. Then search which conditions the system's parameters have to satisfy so that $\varphi(t_{k+2}^+; t_k, u_k) = \varphi(t_k^+; t_k, u_k)$ with u_k the solution at t_k^-. This provides a set of initial data u_k and of parameters such that there exists such periodic trajectory (or there does not exist!).

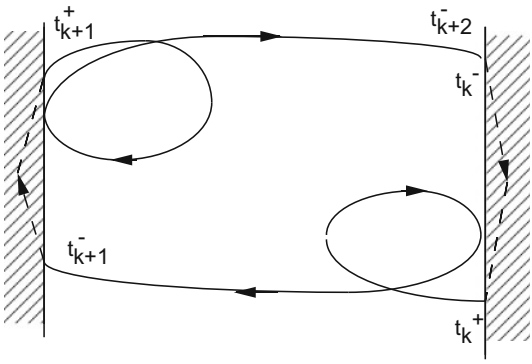

Fig. 7.1 The viability conditions and grazing orbits

Remark 7.2 (*Viability of Trajectories*) If there are several constraints, say two, and if one looks for trajectories that collide one surface Σ_1 at t_k and then the other Σ_2 at t_{k+1} before a third impact with Σ_1 at t_{k+2}, one must take care of the fact that the existence conditions have to incorporate that there is no impact with Σ_1 on (t_k, t_{k+1}), and not only the fact that there exists a strictly positive $\Delta_{k+1} = t_{k+1} - t_k$ such that the trajectory attains Σ_2 at t_{k+1}. In other words, certain existence results may include the possibility of trajectories which indeed attain Σ_2 after a strictly positive flight-time Δ_{k+1}, but which have to cross Σ_1 on (t_k, t_{k+1}), see Fig. 7.1. It seems that the works described in this section did not take into account such a constraint on the trajectory between the collisions. The conditions that guarantee no such accidental collisions may be called *viability conditions* [518], a term that is quite consistent with the language of differential inclusions theory [67]. In case of a codimension one constraint, the shock necessarily occurs with the same surface. However, the viability conditions also have to be checked before stating any necessary and sufficient existence condition.

This classical technique has been employed in many studies to prove the existence of periodic trajectories, and mainly relies on the ability to calculate the solution between the shocks. Note that one implicitly chooses one constraint surface (there may be several) as the Poincaré section, and with velocities pointing inwards the admissible domain Φ. Let us now describe in some detail pioneering work in the field, by Masri and Caughey [819].[6] The system is depicted in Fig. 7.2, and consists of a free mass m, sliding without friction on a block of mass M. The free mass is constrained by two limiting rigid stops (a mechanical play). Notice that Theorem 5.3 applies to this impact damper, as noted in Remark 5.15. The absolute coordinates are denoted as y_a and x for the free mass and the block respectively. The relative coordinate of the free mass in a frame fixed with respect to the block is denoted as $y_r = y_a - x$. Hence, $-\frac{d}{2} \leq y_r \leq \frac{d}{2}$ define the two unilateral constraints on y_r. We denote $q = (x, y_a)^T$ the vector of generalized coordinates, the two unilateral constraints are $f_1(q) = -y_r + \frac{d}{2} \geq 0$, $f_2(q) = y_r + \frac{d}{2} \geq 0$. Finally, we employ

[6] A similar study was also published at the same time by Feigin [390].

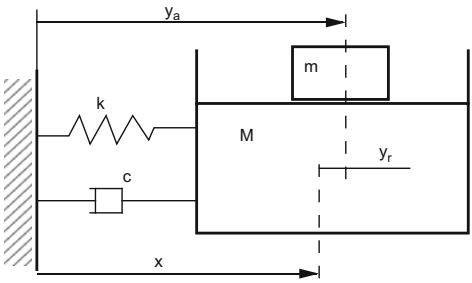

Fig. 7.2 The impact-damper

the notation t_k^1 for impacts with $f_1(q) = 0$, and t_k^2 for impacts with $f_2(q) = 0$. The dynamical equations of the system can be written as

$$\begin{cases} M\ddot{x}(t) + c\dot{x}(t) + kx(t) = A_0 \sin(\Omega t + \alpha) & \text{when } |y_r(t)| > \frac{d}{2} \\ m\ddot{y}_a(t) = 0 & \text{when } |y_r(t)| > \frac{d}{2} \\ \dot{q}(t_k^{i,+})^T \nabla f_i(q) = -e_n \dot{q}(t_k^{i,-})^T \nabla f_i(q) & \text{where } f_i(q(t_k^i)) = 0, \dot{q}(t_k^{i,-})^T \nabla f_i(q) < 0. \end{cases} \tag{7.12}$$

The block motion between impacts is given as

$$x(t) = \exp(-\delta\omega t)\,(B_1 \sin(\eta\omega t) + B_2 \cos(\eta\omega t)) + A \sin(\Omega t + \tau), \tag{7.13}$$

where B_1 and B_2 depend on initial data, and $\delta = \frac{c}{2\sqrt{kM}}$, $\omega = \sqrt{kM}$, $\eta = \sqrt{1-\delta^2}$, $r = \frac{\Omega}{\omega}$, $A = \frac{A_0}{k\sqrt{(1-r^2)^2+4\delta^2 r^2}}$, $\tau = \alpha - \Psi$, $\tan(\Psi) = \frac{2\delta r}{1-r^2}$, $0 < \Psi < \pi$. The goal is to find out conditions on the system's parameters (physical parameters, initial data, external excitation) such that there exists a trajectory with two impacts *per* period, i.e. $t_{k+1}^i = t_k^j + \frac{\pi}{\Omega}$, $i, j = 1, 2$, $i \neq j$. Such a trajectory will exist if one is able to show the existence of B_1, B_2 and τ which determine the block motion. The analysis proceeds first by fixing the following objectives:

$$\begin{cases} \dot{y}_a(t_k^{1,+}) = -v, \ \dot{y}_a(t_k^{1,-}) = v, \ \dot{y}_a(t_k^{2,-}) = -v, \\ \dot{y}_a(t) = (d + 2x(t_k^1))\frac{\Omega}{\pi} = v \ \text{ for } \ t_k^1 < t < t_k^2. \end{cases} \tag{7.14}$$

The third condition comes from the assumption that the mass m evolves freely between collisions, with velocity magnitude v, and has to slide on a distance equal to $d + 2x(t_k^1)$ (in the absolute coordinate frame). These conditions impose some symmetry restrictions on the type of periodic trajectories one is looking for.[7] Indeed one fixes not only the number of impacts *per* period, but also the pre- and post-impact

[7]Notice that it is not possible in this case to have a periodic trajectory with collisions occuring repeatedly on the same constraint, since the mass m is horizontally free between impacts. This however is possible with other systems, like the inverted pendulum in a box.

absolute velocities of the ball.[8] Using the shock dynamical equations, one can compute the postimpact velocities of the ball and of the block. Then using the conditions in (7.14), it is possible to derive expressions relating $x(t_k^1)$ to $\dot{x}(t_k^{1,-})$ or to $\dot{x}(t_k^{1,+})$, as

$$\begin{cases} x(t_k^1) = -\frac{\pi}{2\Omega}\left(\frac{1+e_n}{1-e_n+2\kappa}\right)\dot{x}(t_k^{1,-}) - \frac{d}{2} \\ x(t_k^1) = -\frac{\pi}{2\Omega}\left(\frac{1+e_n}{1-e_n+2\kappa e_n}\right)\dot{x}(t_k^{1,-}) - \frac{d}{2}, \end{cases} \tag{7.15}$$

where $\kappa = \frac{m}{M}$. The next step is to use the block equation of motion obtained from (7.12): if we replace the block position and velocity in (7.15) by the calculated ones from the first equation in (7.12), we find a complex set of equations which relate all the system's parameters with the clearance size $\frac{d}{2}$, of the form:

$$\mathscr{P}(\delta, \omega, \Omega, r, \tau, \eta, \kappa, e)\zeta = \bar{d}, \tag{7.16}$$

where: $\zeta = \left(x(t_k^1), \dot{x}(t_k^{1,-}), \dot{x}(t_k^{1,+}), B_1, B_2, A\right)^T$ and $\bar{d} = \left(0, 0, 0, 0, -\frac{d}{2}, -\frac{d}{2}\right)^T$. $\mathscr{P}$ is a 6×6 matrix. The aim is to determine whether this system admits a solution, or not. For the sake of brevity, we do not recall here the explicit form of the matrix $\mathscr{P}$ (see Masri and Caughey [819] for details). We simply mention that this system of algebraic equations can be solved, and one obtains:

$$\begin{cases} A = \frac{d}{2\Delta}\left[h_1(\sigma_1\theta_2) - (\sigma_1\theta_1 + \eta\sigma_2\omega)(1+h_2)\right] \\ B_1 = \frac{d}{2}(1+h_2)(\sigma_2 - \sigma_1)C \\ B_2 = \frac{d}{2}h_1(\sigma_1 - \sigma_2)C, \end{cases} \tag{7.17}$$

with:

$$\begin{cases} \Delta = h_1\left[C(\sigma_1 - \sigma_2) - (S + C\sigma_2)\sigma_1\theta_1 + (S + C\sigma_1)\delta\omega\sigma_2\right] \\ +(1+h_2)\left[(S + C\sigma_2)\sigma_1\theta_1 + (S + C\sigma_1 - \eta\omega\sigma_2\right], \\ S = \sin(\tau),\ C = \Omega\cos(\tau), \\ h_1 = \exp\left(-\frac{\delta\pi}{r}\right)\sin\left(\eta\frac{\pi}{r}\right),\ h_2 = \exp\left(-\frac{\delta\pi}{r}\right)\cos\left(\eta\frac{\pi}{r}\right), \\ \sigma_1 = \frac{\pi}{2\Omega}\frac{1+e}{1-e+2\kappa},\ \sigma_2 = \frac{\pi}{2\Omega}\frac{1+e}{1-e-2\kappa e}, \\ \theta_1 = \omega\exp\left(-\frac{\delta\pi}{r}\right)\left[-\delta\sin\left(\eta\frac{\pi}{r}\right) + \eta\cos\left(\eta\frac{\pi}{r}\right)\right], \\ \theta_2 = \omega\exp\left(-\frac{\delta\pi}{r}\right)\left[-\delta\cos\left(\eta\frac{\pi}{r}\right) - \eta\sin\left(\eta\frac{\pi}{r}\right)\right]. \end{cases} \tag{7.18}$$

[8] In relationship with the fact that the calculated jump in the velocity, is independent of the fact that the used frame is Galilean or not (see Chap. 4, Sect. 4.1.5), it is clear here that the frame fixed with respect to the block is not Galilean, and does not satisfy the smoothness requirements discussed in Sect. 4.1.5, Eq. (4.25), since $\dot{x}$ is discontinuous at impacts. In other words, the jump of the absolute velocity $\dot{y}_a(\cdot)$ is clearly different from that of the relative velocity $\dot{y}_r(\cdot)$.

It can be seen that the last two equations in (7.17) directly define the set of initial data which are needed to obtain a periodic trajectory with two impacts *per* period. The first equation in (7.17) is put in [819] under the form:

$$2\sin(\tau) + H\cos(\tau) = -\frac{d}{A}, \tag{7.19}$$

for some $H(\sigma_1, \sigma_2, \delta, \omega, h_1, h_2, \theta_1, \theta_2, \Omega)$. For the searched trajectories to exist, one must be able to compute $\sin(\tau)$ and $\cos(\tau)$. This implies conditions on the coefficients of the equation in (7.19). In particular one finds the condition $\left(\frac{d}{A}\right)^2 \leq H^2 + 4$, which means that the clearance d should not be too large. Then the motion of the block is entirely known (since B_1, B_2, A and τ are known), and that of the mass also. It is therefore shown that periodic *symmetric* trajectories with two impacts *per* period and period $\frac{2\pi}{\Omega}$ exist only if the parameters satisfy the suitable conditions.

Remark 7.3 The technique that consists of verifying the existence of $T-$periodic trajectories checking that $\varphi(t+T;\tau_0,u_0) = \varphi(t;\tau_0,u_0)$ has also been employed in the context of impulsive ODEs as in (7.1), see [76, Example 10.3] for the case of a species-food system.

Remark 7.4 (*Passive Nonlinear Energy Pumping*) It is noteworthy that a complete dynamical analysis has to include not only the dynamics of the impact damper, but also the dynamics of the system whose vibrations are to be damped out, and on which the impact damper is mounted: this is the problem of *passive nonlinear energy pumping*. The dynamical couplings between both subsystems have to be analyzed carefully, so that the vibrational energy transfer from the system to the impact damper is guaranteed. The objective may be summarized as follows [938]: *Design a set of Nonlinear Energy Sinks (NESs) that are locally attached to a main structure, with the purpose of passively absorbing a significant part of the applied seismic energy, locally confining it and then dissipating it in the smallest possible time* . This is the object of the studies in [435, 697, 717, 938, 1077]. A typical example [938] of a two-degree-of-freedom system coupled to two NESs is depicted in Fig. 7.3. Here the NESs take the form of impact ocillators.

7.3.2 Further Reading

We have reproduced in some detail the results in [819] to illustrate once again the gap between the simplicity of the reasoning used to search for periodic trajectories, the (apparent) simplicity of the dynamical equations, and the complexity of the calculations. The system as in [819] that consists of a loose auxiliary mass m which impacts against the ends of a container fixed to the primary mass M is called an *impact damper*, because its practical usefulness is often to damp vibrations. When there are several loose masses m_i, this is a *multi-unit* impact damper (see [159] for a classification of one and two-degree-of-freedom impact oscillators). Due to collisions, an

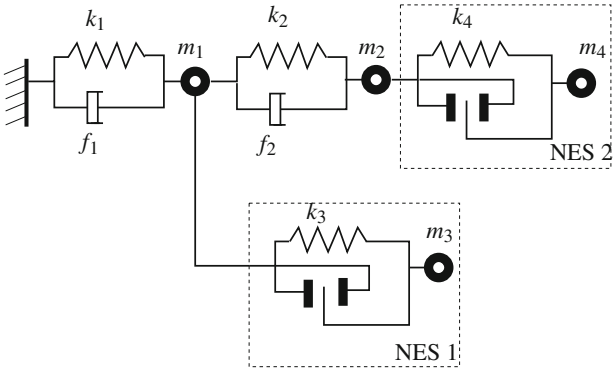

Fig. 7.3 Passive control *via* coupling with two NESs

attenuation of the amplitude of vibration of the principal mass M may be achieved within a certain range of the forcing term frequency. For instance, it is shown in [280] that an autonomous van der Pol oscillator (i.e. a second order oscillator with a specific nonlinear damping) can have its natural limit cycle amplitude decreased by a suitable choice of impact damper parameters. In other words, replace the damping coefficient c in Fig. 7.2 by a nonlinear coefficient $\varepsilon\dot{x}(x^2 - 1)$. The autonomous system hence obtained possesses, in the absence of the loose mass m, a limit cycle whose amplitude A does not depend on the parameter ε. The goal may be to reduce A by properly choosing the impact damper. It is concluded in [280] that for fixed restitution $e_n = 0.2$, and for fixed ratio $\frac{m}{M}$, the plot A versus d (the value of the clearance) presents a jump: a good design should therefore be outside this jump zone, and this may not be obvious in practice due to uncertainties on the system parameters. The potential applications of such devices are to reduce vibrations in switching relays, turbine buckets, antennas, lathe tools, airplane ailerons, helicopter tension rods, machines used in pile driving, compacting, crushing, rivetting, rock drilling, impact printing $\cdots$, and also the study of dynamics of systems with clearance, of the effects of snubbers and baffle plates which limit deflection of piping, tubes in power, chemical and nuclear industries, and marine structures $\cdots$. Impact dampers can also be used in an effective manner to limit disturbance amplitudes in some space applications [230, 1054]. Models as in Fig. 7.2 can be used to represent sloshing of liquid in containers [570]. Other references to the impact damper are [390] (numerical study to show resonance behavior) [391] (conditions of existence and stability of periodic trajectories with two impacts *per* period, where the impacts are represented by instantaneous coupling between the two masses, corresponding to plastic impact as in [648]) [518] (basically use the Poincaré map Jacobian DP_Σ to study the stability of two impacts *per* period motions, and derives numerically a bifurcation analysis) [87, 1011] (derive closed-form solutions as Masri and Caughey, but for other kinds of periodic trajectories, and present numerical and experimental results) [86] (considers a two-stops one degree-of-freedom oscillator, and develops exact

closed form expressions for one and two equispaced and non-equispaced impact *per* cycle motions) and also [472] (present a more accurate way than simple integration to investigate bifurcations, and finds a cascade of subharmonic bifurcations leading to chaos) [418] (study of the dynamics of a percussive rock-drilling machine), [1167] (show the existence of various types of local -pitchfork, saddle-node, Hopf...- and global bifurcations, and a period-doubling sequence leading to chaos in the impact damper), [279] (investigate thoroughly the dynamics of the impact damper, and show the existence of various periodic regimes, separated by complex motions, in function of physical parameters; these are confirmed experimentally in [158, 797] (multi-unit dampers with Coulomb friction effects between the loose mass and the principal mass) [1055, 1118, 1222] (application to printing machines). In [1139] similar calculations are made for the existence problem, but with a slightly different impact damper. The main motivation therein is about robotic manipulators and possible clearance in the joint. Other systems that may be submitted to impacts are vibration hammers, machinery for driving, compacting, milling and forming, vibratory conveyers, platforms and shaking grizzlies, heat exchangers, and fuel elements of nuclear reactors. In all these systems collisions play a significant role. This may be a positive action (as for a juggling robot: one uses the impacts to create motion), or a negative action (impacts as disturbances that create wear and fatigue, failures, noise, and shorter service life $\cdots$).

7.3.3 *Comments on the Poincaré Impact Map Stability Analysis*

The global transformation of the dynamics into recurrence equations relies on strong properties of the trajectories (e.g. boundedness, periodicity) and on the ability of explicitly obtaining the solutions between impacts. This is a hard task except in very simple cases. In slightly more complex cases, the recurrence equations may still be obtained in an implicit form (because the flight-times durations cannot be obtained explicitly), see e.g. [1252]. This may be illustrated as follows: we have seen in Chap. 1 that a vibro-impact system with a unilateral constraint can be considered as a flow with collisions, see Sect. 1.3:

$$\begin{aligned}
&\varphi_t^c : \mathbb{R}^{2n} \to \mathrm{bd}(\Phi) \times \{-V(q(t_0))\} \to \mathrm{bd}(\Phi) \times V(q(t_0)) \to \mathrm{bd}(\Phi) \times \{-V(q(t_1))\} \to \dots \\
&\quad \to \mathrm{bd}(\Phi) \times \{-V(q(t_k))\} \to \mathrm{bd}(\Phi) \times V(q(t_k)) \to \mathbb{R}^{2n}, \\
&u_0 \mapsto \varphi(t_0^-; 0, u_0) \overset{\mathscr{F}_0}{\mapsto} \varphi(t_0^+; 0, u_0) \mapsto \varphi(t_1^-; 0, u_0) \overset{\mathscr{F}_1}{\mapsto} \dots \mapsto \varphi(t_k^-; 0, u_0) \\
&\overset{\mathscr{F}_k}{\mapsto} \varphi(t_k^+; 0, u_0) \mapsto \varphi(t; 0, u_0).
\end{aligned} \tag{7.20}$$

To go from the flow with collisions $\varphi_t^c(\cdot)$ to the impact Poincaré map $P_\Sigma(\cdot)$ one may consider the following steps:

- Let us denote

$$\begin{aligned} P : \mathrm{bd}(\Phi) \times V(q(t_k)) &\to \mathrm{bd}(\Phi) \times V(q(t_{k+1})) \\ u(t_{k+1}^+) &= P(u(t_k^+)) \end{aligned} \tag{7.21}$$

  the mapping such that $P(u(t_k^+)) = \varphi^c_{t_k^+}(u_0)$, u_0 the initial data. Notice that u_0 need not belong to $\mathrm{bd}(\Phi) \times V(q)$. This equality merely means that the value of P at t_k^+ is given by the value of the flow with collisions with an admissible initial data u_0, considered at t_k^+. $P(\cdot)$ may be called the *section map* of the flow φ_t^c. Clearly, $u(t_{k+1}^+) = P(u(t_k^+)) = \mathscr{F}_{k+1} \circ \varphi^c_{t_{k+1}^- - \tau_0}(u_0) = \mathscr{F}_{k+1} \circ \varphi^c_{t_{k+1}^- - t_k^+}(u(t_k^+))$, where τ_0 is the initial time, i.e. $u_0 = u(\tau_0)$. If we want to consider the Poincaré map from t_k to t_{k+2} (two impacts *per* period for instance, which could be named the second return map instead of the first return map) then we have to compute $u(t_{k+2}^+) = P(u(t_k^+)) = \mathscr{F}_{k+2} \circ \varphi_{t_{k+2}^- - t_{k+1}^+} \circ \mathscr{F}_{k+1} \circ \varphi_{t_{k+1}^- - t_k^+}(u(t_k^+))$. Then by the chain rule one gets:

$$DP(u(t_k^+)) = D\mathscr{F}_{k+2} D\varphi_{t_{k+2}^- - t_{k+1}^+} D\mathscr{F}_{k+1} D\varphi_{t_{k+1}^- - t_k^+}(u(t_k^+)), \tag{7.22}$$

  where $DP(u_0)$ denotes the linear differential operator of $P(\cdot)$ calculated at u_0, such that $DP(u_0) = \frac{\partial P}{\partial u}(u_0)^T$. Notice that $\mathscr{F}_k(\cdot)$ may not be constant but may in general depend on q.
- To compute the impact Poincaré map $P_\Sigma(\cdot)$ one has to first clarify the definition of its state vector which we denote as $\bar{u}_\Sigma$.[9] The section is $\Sigma = \{u | f(q) = 0\}$ (with a codimension one constraint $f(q) \in \mathbb{R}$, but one may imagine to define a codimension ≥ 2 section if the system is assured to strike it repeatedly). The most natural way to proceed is to introduce the quasi-coordinate $\bar{q}_1 \stackrel{\Delta}{=} f(q)$ and to assume that the transformation:

$$\begin{aligned} \bar{G} : \mathbb{R}^{2n} &\to \mathbb{R}^{2n} \\ u &\mapsto \bar{u}^T = (\bar{q}_1, q_2, \ldots, q_n, \dot{\bar{q}}_1, \dot{q}_2, \ldots, \dot{q}_n) \end{aligned} \tag{7.23}$$

  is a global diffeomorphism.[10] Hence, $\bar{u} = \bar{G}(u)$ and $u = \bar{G}^{-1}(\bar{u})$. Therefore, $P(u(t_k^+)) = P \mathrm{o} \bar{G}^{-1}(\bar{u}(t_k^+))$. Now notice that:

$$\bar{u}(t_k^+)^T = (0, q_2, \ldots, q_n, \dot{\bar{q}}_1(t_k^+), \dot{q}_2(t_k^+), \ldots, \dot{q}_n(t_k^+)), \tag{7.24}$$

[9] The reason for this apparently complicated notation is that we shall need several steps to go from u to $\bar{u}_\Sigma$.

[10] In most cases it is clear that this will imply a reordering of the generalized coordinates. For instance if $f(q) = q_2$, then evidently one will not define $G(\cdot)$ as above, but rather first exchange q_1 and q_2 in q, or simply define $G(\cdot)$ with $\bar{q}_1$ as the second component of $\bar{u}$.

and define:

$$\bar{u}^T_{\Sigma,k} = (q_2(t_k), \ldots, q_n(t_k), \dot{\bar{q}}_1(t_k^+), \dot{q}_2(t_k^+), \ldots, \dot{q}_n(t_k^+)). \tag{7.25}$$

Then the impact Poincaré map value at $\bar{u}_{\Sigma,k}$ is given as:

$$P_\Sigma(\bar{u}_{\Sigma,k}) = P \circ \bar{G}^{-1}(\bar{u}(t_k^+)), \tag{7.26}$$

i.e. $P_\Sigma(\cdot)$ is the restriction of $P \circ \bar{G}^{-1}(\cdot)$ to $\Sigma = \left\{\bar{u} | \bar{q}_1 = 0, \dot{\bar{q}}_1 > 0\right\} = \mathrm{bd}(\Phi) \times V(q(t_k))$, and $P_\Sigma : \Sigma \to \Sigma$.

- Finally, although the value taken by $P_\Sigma(\cdot)$ at $\bar{u}_{\Sigma,k}$ is given by (7.26), its explicit calculation requires to be able to express $\bar{u}_{\Sigma,k+1}$ as a function of $\bar{u}_{\Sigma,k}$, i.e. $\bar{u}_{\Sigma,k+1} = P_\Sigma(\bar{u}_{\Sigma,k})$. This is in general impossible, because this hinges on the explicit calculation of the impact times t_k, which usually cannot be obtained. However as we shall see below, in certain cases the Jacobian of $P_\Sigma(\cdot)$ can be explicitly calculated.

Remark 7.5 A nice property of the impact map is that contrary to the flow with collisions, it does not depend explicitly on the collision times. Hence its Jacobian can be calculated.

Thus in order to explicitly obtain the impact Poincaré map $P_\Sigma(\cdot)$, one must be able to calculate the impact times $t_0, t_1, \cdots$ When this is not possible, these times can be obtained in an implicit form, see (1.45). In a more general setting, the impact section map and the impact Poincaré map are implicitly expressed from (1.46) as:

$$\begin{cases} f \circ \varphi_q(t_{k+1}; t_k, u_k) = 0 & \text{with } u_k = u(t_k^+) \\ u_{k+1} = I_{k+1}(u(t_{k+1}^-)) \\ u(t_{k+1}^-) = u_k + \int_{(t_k, t_{k+1})} G(u(t))dt. \end{cases} \tag{7.27}$$

It is also possible to make the flight-times $\Delta_{k+1} = t_{k+1} - t_k$ explicitly appear in this formulation by simply replacing t_{k+1} by $t_k + \Delta_{k+1}$.[11] Now notice that $P_\Sigma(\cdot)$ can be expressed as $P_\Sigma = P_{r,k} \circ P_{f,k}$, where $P_{r,k}(\cdot)$ corresponds to the restitution mapping $\mathscr{F}_k$, whereas $P_{f,k}(\cdot)$ corresponds to the flow between impacts. For instance, assume that $f(q) = \bar{q}_1$ as above. Then $P_{f,k} : \bar{u}_{\Sigma,k} \mapsto \bar{u}_\Sigma(t_k^-)$ and $P_{r,k} : \bar{u}_\Sigma(t_k^-) \mapsto \bar{u}_{\Sigma,k+1}$. Clearly $P_{r,k}(\cdot)$ can be simply expressed from the restitution mapping $\mathscr{F}_k(\cdot)$. The problem is to calculate t_{k+1} to get the explicit form of $P_{f,k}(\cdot)$. This may be done *via* an implicit equation of the form:

$$h(t_{k+1}, t_k, u_k) = 0, \tag{7.28}$$

[11] Apart from the examples presented here, the interested reader may have a look at [911] Eq. (1.3), [1252] Eq. (1.3), [1252] Eqs. (24)–(29), [998] Eq. (4), [1100] Eq. (2), [1095] equations (4) (5) for examples of implicit Poincaré maps as in (7.27).

similar to (1.45). Notice that the Jacobian of $P_\Sigma(\cdot)$ at a point $\bar{u}_{\Sigma,0}$ is given from the chain rule by[12] $DP_\Sigma \stackrel{\Delta}{=} \frac{\partial P_\Sigma}{\partial \bar{u}_\Sigma}^T(\bar{u}_{\Sigma,0}) = \frac{\partial P_{r,k}}{\partial \bar{u}_\Sigma}^T(y)\frac{\partial P_{f,k}}{\partial \bar{u}_\Sigma}^T(\bar{u}_{\Sigma,0}) = DP_{r,k}(y)\, DP_{f,k}(\bar{u}_{\Sigma,0})$, with $y = P_{f,k}(\bar{u}_{\Sigma,0})$. Obviously, we have not made a big advance if these Jacobians are not known explicitly. It is noteworthy that in certain cases, t_{k+1} may be known only implicitly, while DP_Σ is known explicitly. For instance, an example is treated in [869] where the equation in (7.28) cannot be solved to yield t_{k+1} as a function of t_k and u_k. But one is able to derive conditions on the system's parameters such that a periodic motion, with specified period T, exists (similarly as for the Masri and Caughey example above). Hence, one is able to express DP_Σ as a function of T and t_k, $\bar{u}_{\Sigma,k}$ and calculate its eigenvalues (to apply Floquet's theory to check the stability of the fixed point of P, or to investigate the type of bifurcation that occurs when parameters are varied). It happens that the bifurcation condition on the excitation magnitude is independent of t_k [737, 1100]. The eigenvalues of the Floquet's matrix can thus be investigated in function of the system's parameters (input magnitude and period, dissipation coefficient, restitution coefficient), and the type of local bifurcation can be deduced. A multiple degree-of-freedom impact oscillator is studied in [1209], using the eigenbase of the linear free-motion structure to compute an analytical form of the response to harmonic and impulsive periodic inputs. The determination of κ-impact q-periodic motions then amounts to solving an algebraic equation $F(\mu, \{p_k\}, \{t_k\}) = P_\Sigma^\kappa(\mu, x_\Sigma) - x_\Sigma = 0$, where $\{p_k\}, \{t_k\}$ denote the percussions and impact times sequences, $1 \leq k \leq \kappa$, μ denotes the varied parameters (restitution coefficient, excitation magnitude and frequency, equilibrium position of the structure without obstacle). Various bifurcations are investigated in [1209]. It is pointed out that Hopf bifurcations in impacting motions can be encountered in the multiple degree-of-freedom case, whereas they cannot in the one degree-of-freedom case: indeed in that case the Jacobian is a 2×2 matrix whose determinant is $e_{\mathrm{n}}^{2\kappa} < 1$ for a (κ, q) orbit. Hence the two eigenvalues cannot have modulus 1 at the same time. The central tools for the numerical investigations in [472, 1209] are continuation methods to solve $F(\mu, \{p_k\}, \{t_k\}) = 0$: one starts with an initial solution and then proceeds to generate a curve in the phase-parameter space by finding a neighboring solution and iterating the process. It is argued in [472, 1209] that the proposed method yields much better numerical accuracy than the classical ones. In [1210] the authors focus on sticking periodic motions (i.e. motions that consist of a succession of free-motion and permanently constrained-motion phases, possibly separated by a sequence of infinite impacts). They identify a new type of bifurcation called *rising bifurcation*: when a sticking periodic orbit with transition through an infinite sequence of impacts is settled, it may happen by varying some parameter that the contact force during the constrained-motion phase goes to zero. This may give rise to a new periodic orbit with two or three sticking phases *per* period. These bifurcations are similar in nature to the grazing ones (see Sect. 7.4). The determinant of the Jacobian of the impact

[12] If $g = f \circ h$ with $h : \mathbb{R}^n \to \mathbb{R}^p$, $f : \mathbb{R}^p \to \mathbb{R}^k$, then $\nabla g(x_0) = \nabla h(x_0)\nabla f(y_0)$ and $Dg(x_0) = Df(y_0)Dh(x_0)$, where $y_0 = h(x_0)$.

Poincaré map around a (locally) stable periodic trajectory is equal to e_{n}^{2p}, where p denotes the number of impacts *per* period. The trace of the Jacobian is equal to the sum of the eigenvalues [472]. This in particular means that some types of bifurcations cannot occur in certain impacting systems. To see this, let us consider a two-degree-of-freedom nonautonomous system $\ddot{q}(t) + q(t) = A\sin(\omega t)$, $q \geq 1$. The Poincaré application has two eigenvalues, whose product equals $\det(DP_\Sigma)$. The characteristic polynomial of DP_Σ can therefore be written as $\lambda^2 - \mathrm{tr}(DP_\Sigma)\lambda + \det(DP_\Sigma)$. When a local bifurcation occurs, which means that at least one of the eigenvalues passes through a value with magnitude 1, the eigenvalues cannot be complex conjugate as long as $e_{\mathrm{n}} < 1$: otherwise, they would have same magnitude equal to 1, hence a contradiction. This in particular hampers the occurence of a Hopf bifurcation, but saddle-node or flip bifurcations can exist [472].

7.3.4 Other Studies on Stability

Wang [1253] deals with a lamina submitted to a time-varying unilateral constraint, in relation with catching tasks in robotics. The flight-times are given implicitly only in general, from the first equation in (7.27). He linearizes $P_\Sigma(\cdot)$ and assumes that conclusions about the linearized map can be carried to the nonlinear system in the degenerate case when there is a continuum of fixed points. The global analysis that takes into account the nonlinearities effects will generally require a numerical procedure [1253]. Wang's analysis is extended in [243]. Many other studies contain a stability analysis of periodic trajectories, see e.g. [391] (stability analysis of an impact damper), Markeev [804, 806–808] (stability of periodic motions of an ellipsoid of revolution colliding with a fixed smooth plane, using Poincaré map analysis) [583] (studies trajectories which attain the constraint tangentially, i.e. collision free trajectories, and their stability) [585] (uses the Zhuravlev-Ivanov nonsmooth coordinate change to study the local stability *via* tangent linearization, of fixed point and periodic trajectories) [582, 596] (orbital stability of periodic motions of n degree-of-freedom systems with $T_L(t_k) = 0$ and a codimension one unilateral constraint; use of Lyapunov's holomorphic integral theorem[13] to prove *via* local arguments the existence of periodic trajectories), see also [683]. Impulsive ODEs, with jump times defined as $x(t_k^-) \in S$ for some hypersurface S of the state space, are used in [482] to model biped robots. Impact Poincaré maps are used to analyze the stability of feedback controllers.

[13] In the case of Hamiltonian (i.e. conservative) systems with an analytic Hamiltonian function, Lyapunov's holomorphic integral theorem states that for every pair of pure imaginary roots $\pm j\lambda$ of the system's characteristic equation, and when there are no other roots, a family of periodic solutions exists whose period tend to $\frac{2\pi}{\lambda}$ as their amplitude tends to zero.

7.3.5 Bouncing-Ball with Moving Base

The benchmark example of the bouncing ball has been thoroughly studied. The model of the bouncing ball when the table is moving is often simplified in order to explicitly get a two-dimensional Poincaré map from (7.27). In fact, all the external effects acting on the table are neglected to consider the table's motion, so that it simply appears in the model as a time-dependent unilateral constraint (such assumption has also been made in some studies on juggling robots [237, 238, 1043, 1044]). Let the table motion be given as $x_2(t) = -A\sin(\omega t)$, while $x_1(\cdot)$ denotes the ball's position. Here one does not care about how such motion may be created, by which control. The assumption that the mass of the table is infinite (equivalently the mass of the ball is close to zero) allows to disregard the effects of the shocks on its velocity. Assume further that $t_{k+1} - t_k = \frac{2\dot{x}_1(t_k^+)}{g}$, and that $\dot{x}_1(t_{k+1}^-) = -\dot{x}_1(t_k^+)$. These assumptions are satisfied if it is supposed that the ball strikes the table at the same height at each impact,[14] and that the displacements of the table are negligible compared to those of the table. In other words although the true dynamics cannot be explicitly solved, such hypotheses allow one to approximate (7.27). Then it is possible to derive the following impact map:

$$\begin{cases} \Phi_{k+1} = \Phi_k + \dot{x}_k \\ \dot{x}_{k+1} = e_{\mathrm{n}}\dot{x}_k - \gamma\cos(\Phi_k + \dot{x}_k), \end{cases} \tag{7.29}$$

where $\dot{x}_k = \frac{2\omega\dot{x}_1(t_k^+)}{g}$, $\Phi_k = \omega t_k$, and $\gamma = \frac{2\omega^2(1+e_{\mathrm{n}})A}{g}$. It is noteworthy that since the system is nonautonomous, the Poincaré impact map must explicitly contain the time: indeed the flight-times a priori depend on the exogenous excitation of the table, and are not only a function of the postimpact state values. Such a map can be shown to possess a complex dynamical behavior, and has been the object of many publications [88, 384, 410, 487, 538, 681, 684, 837, 871, 1019, 1020, 1095, 1191, 1221, 1266, 1277]. If $e_{\mathrm{n}} < 1$, the velocity remains bounded and there exists a trapping region in the plane $(\Phi, \dot{x})$ [487], which hampers unboundedness results as in the following ($f(t) = f(t+T)$ is a periodic analytic function representing the table position):

Theorem 7.5 *[1019] Assume that $e_{\mathrm{n}} = 1$ and that there is an integer $N > 0$ and a time t_0 such that $\dot{f}(t_0) = \frac{TgN}{2}$, $-g < \ddot{f}(t_0) < 0$. Assume also that $\dddot{f}(t_0) \neq -\frac{g}{2} + \frac{g}{2}\cos\left(2\pi\frac{m}{n}\right)$, $m = 0, \pm1, \ldots, \pm n$, $n = 1, 2, \ldots, 262$, and that there exist two functions $a_0(\cdot)$ and $a_1(\cdot)$ such that $a_0(\ddot{f}(t_0))\frac{d^4 f}{dt^4}(t_0) + a_1(\ddot{f}(t_0))\frac{d^3 f}{dt^3}(t_0) \neq 0$, with $a_0(\ddot{f}(t_0)) \neq 0$. Then there exists in the plane $(t, \dot{x})$ a set of positive measure of initial data such that the post-impact velocity tends to infinity.*[15]

[14] This, in case of feedback control of a juggling robot, should be guaranteed by the controller, but not a priori supposed.

[15] In other words, the trajectories of the impact Poincaré map increase in velocity to infinity.

This result is true for purely elastic impacts, hence it may lack in practical importance.[16] However, it completes the dynamics study of the bouncing ball. Notice that these studies prove that the time-dependence of the unilateral constraints $f(q,t) \geq 0$ has great influence on the system's dynamics (which is not so apparent by comparing (7.7)–(7.29), but it is a property of certain apparently simple systems to have a complex "hidden" behavior). The bouncing-ball dynamical system may be seen as a simplified version of the Fermi accelerator model: a ball bounces between a fixed and a sinusoidally moving walls [540, 742].

7.3.6 Additional Comments and Studies

The major difficulty in studying impacting systems is that in general, not only are the impact Poincaré maps difficult to obtain explicitly (but this is not specific to those systems), but they are of dimension ≥ 2. Hence all the tools that apply to one-dimensional systems, like the celebrated Sarkovskii's ordering theorem [487], do not apply. Pioneering works on the dynamics of simple impacting systems can be found in [59, 365, 382, 484, 485, 743, 744, 819, 1256]. Among the first papers containing a study on existence of periodic trajectories and their stability, see the works by Masri and Caughey [819], which we described above, and Feigin [390]. More recently, the dynamical analysis of simple impacting devices (impacting oscillator, damper $\cdots$) has received attention in numerous works, see e.g. [115, 121,157, 291, 329, 472, 518, 530, 577, 578, 582, 583, 586, 587, 639, 644, 680, 787, 805–809, 818, 927, 934, 998, 1094, 1096, 1098–1101, 1209, 1210, 1228, 1241, 1257, 1263, 1339]. For instance, it is concluded in [157] that the bifurcation diagram of the impact damper, with dry friction between the two masses, seems independent of the chosen friction model (Coulomb or a more sophisticated model). But the qualitative behavior of the system is highly sensitive to the value of the physical parameters (like the restitution coefficient, and the friction model parameters): the authors conclude that for such impacting systems with friction, *it is almost impossible to build mathematical models that can qualitatively describe experimental results for all possible values of system parameters*. Experimental results are presented in [869, 871, 1138], and in [158] for simple impact dampers. The dynamics of a shaft rotating inside an annular guard, both being supported from the base by spring-dashpot systems, is studied in [1290]. In [121] the numerical study of a one-degree-of-freedom oscillator with two elastic compliant stops with Coulomb friction is proposed, and experimental results show good accordance with theory (the stops are made of rubber which explains the need

[16] Note anyway that as pointed out in [92], if the case $e_n = 1$ did not exist in nature, then all molecular motion would long since have ceased. But we leave here engineering. Such problems were discussed by Huygens and Leibniz at a time when scientists were trying to discover whether springiness or hardness (to be understood here as non-penetrability) is the real physical phenomenon that produces rebound [1050].

for taking compliance into account in the model). Contrary to [157], it is concluded in [1138] that the model allows the designer to predict motion with good accuracy even if uncertainties are present in the parameters. A numerical study showed that for the values of the experiment, the system's behavior is not very sensitive to forcing amplitude, damping of CoRs values. Also, the numerical and experimental results in [1138] clearly show the existence of C-bifurcations (see Sect. 7.4). The form of the attractors correspond to that found in other studies, using different models [1097, 1191].

The research on dynamics of impacting simple systems was motivated by applications: mechanisms with clearance, see [156, 289, 495, 634, 637] like gearboxes [540, 635, 636, 646, 1060] and references therein (let us also mention the work of A.E. Kobrinskii cited in [87] on dynamics of systems with clearance),[17] the use of pin joints in space truss structures and chaotic dynamics of these systems [737, 869], drilling machines [457], motion of fluid tanks [919], motion in print hammers [520], rotor systems [921], vibrations in high speed machinery [330, 377], heat exchangers tubes subject to aerodynamic excitation [953, 1263], doorbells [31], and have been verified experimentally, see e.g. among others [681, 871]. In [1172] the motion of a two degree-of-freedom gyropendulum that strikes a rough rigid wall through the rim of its wheel is studied numerically. This may represent the dynamics of a Kaplan-turbine which rubs along its labyrinth seals, or when a magnetically suspended rotor touches upon its emergency bearing. Preliminary experimental results are presented. Applications can also be found in practical devices used to generate aerosol streams: the model is a particle bouncing between two charged diverging plates, see [175, §9.1] and [940]. The French company Electricité de France (EDF) conducted research on the dynamics of assembly devices where impacts play an important role [966, Chap. 2] [1209, 1210], and also in nuclear plants [45]. The study of impact oscillators has also been motivated by dynamics of offshore environment impacting as a result of wave forcing [1189, 1190]: oil is transferred from an offshore platform to a tanker, *via* an articulated column maintained by a tether, which becomes infinitely stiff when stretched, hence impacts (see Example 1.6 in Chap. 1). Other examples exist in marine technology [710]: rattling resonances often occur between the leg of the platform and pre-drilled piles during docking procedures, when new offshore platforms are constructed [151]. Chaos in impacting systems is apparently not restricted to values of e_{n} close to 1, but can appear for inelastic impacts ($e_{\mathrm{n}} = 0.6$ in [998]). Let us finally mention the study in [678] about the dynamical behavior of n degree-of-freedom systems with smooth unilateral constraints, $T_L(t_k) = 0$, and acted upon by external forces of stochastic nature.

[17] The study of rattling-noise in gearboxes is fundamental to reduce the noise level and the vibrations in engines.

7.4 Grazing or *C*-Bifurcations

The stroboscopic Poincaré map can have a singular Jacobian at certain points. This is related to so-called C-bifurcations (or grazing bifurcations), which occur when the system evolves from a free regime of motion to an impacting regime, through a *grazing trajectory*. More precisely, in a one-degree-of-freedom case with unilateral constraint $q \geq 0$, a C-bifurcation occurs in a configuration such that $q_0 = 0, \dot{q}_0 = 0$ and the normal component of the force points inwards the admissible domain Φ, i.e. $\ddot{q}_0 \geq 0$. In this case the system may evolve from an impact-free periodic motion, to a low-velocity-impacting motion, and a bifurcation corresponds to this particular evolution.

Before going into the calculations needed to show that the section map $P(\cdot)$ (or the stroboscopic Poincaré map) can possess a discontinuity at such a point, let us investigate the difficulties in properly defining a Poincaré map close to grazing trajectories, considering a system in the plane. To this end it is useful to split the section $\Sigma \stackrel{\Delta}{=} \{(q, \dot{q}) | q = c\}$ into three parts (see Fig. 7.4): $\Sigma = \mathscr{X}_{con} \cup \mathscr{X}_{rel} \cup \mathscr{V}^\star$, see Sect. 1.3.3 for the definition of the various subspaces. In Fig. 7.4 $x_1 = q$ and $x_2 = \dot{q}$. Also $\mathscr{X}_{rel} = \{x \in \mathbb{R}^2 | x_1 = c, x_2 \leq 0\}$, $\mathscr{X}_{con} = \{x \in \mathbb{R}^2 | x_1 = c, x_2 \geq 0\}$, $\mathscr{V}^\star = \{x \in \mathbb{R}^2 | x_1 = x_2 = 0\}$. Orbits that make contact in $\mathscr{V}^\star$ have a local extremum at this point (disregarding collisions for the moment). In [1262] the set $\mathscr{V}^\star$ is subsequently divided into $A^+ = \{x \in \mathscr{V}^\star \mid \dot{x}_2(t_k^-) > 0\}$, $A^- = \{x \in \mathscr{V}^\star \mid \dot{x}_2(t_k^-) < 0\}$ and $A^0 = \{x \in \mathscr{V}^\star \mid \dot{x}_2(t_k^-) = 0\}$ (A is for Acceleration). Orbits that make contact in A^0 correspond to degenerate impacts (contact with zero velocity) which are a point of inflexion for the trajectory. They remain in $\mathrm{bd}(\Phi)$ for a non zero time interval, i.e. these degenerate impacts yield trapping, until the acceleration $\dot{x}_2$ next

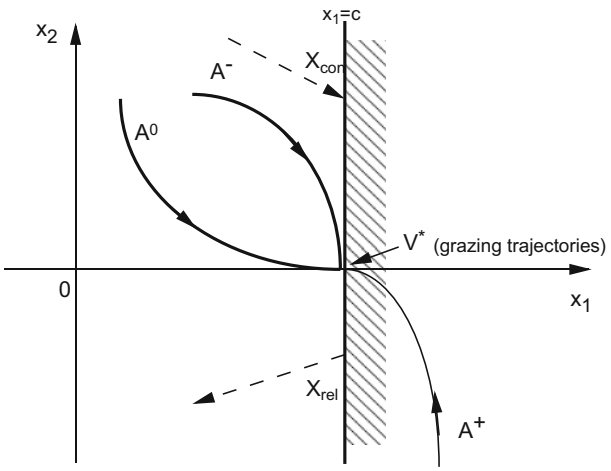

Fig. 7.4 The phase space around grazing orbits

passes through 0. Whiston [1262] introduces a mapping $P : \mathscr{X}_{rel}\backslash\mathscr{V}^\star \to \mathscr{X}_{con}$ and the pre-images sets $P^{-1}(A^+)$, $P^{-1}(A^-)$, $P^{-1}(A^0)$. Roughly, $P(\cdot)$ maps post-impact velocities at t_k to pre-impact ones at t_{k+1}. One has $P^{-1}(A^+) = \emptyset$: there is no state in Φ whose image is in A^+. $P^{-1}(A^-)$ is the set of initial conditions in $\mathscr{X}_{rel}\backslash\mathscr{V}^\star$ that yield a grazing orbit. $P^{-1}(A^0)$ is the set of initial conditions in $\mathscr{X}_{rel}\backslash\mathscr{V}^\star$ that drive the system at rest on the constraint, in $\mathscr{V}^\star$. $P(x)$ is grazing if $\dot{x}_2(t_k^-) < 0$, and has an inflexion point for $x_1(t)$ at $t = t_k$ if $x_2(t_k) = \dot{x}_2(t_k^-) = 0$ (in which case the trajectory that emerges from such x attains Σ in A^0). Hence, if $\ddot{x}_2(t_k^-) > 0$ the impacts are trapped and the system remains stuck on $\mathrm{bd}(\Phi)$: this is called α-points. If $\ddot{x}_2(t_k^-) < 0$: impacts are released and there is detachment: this is ω-points. The sets A^+, A^- and A^0 are calculated in [1262] for the simple system $\dot{x}_2(t) + x_1(t) = \beta\cos(\omega t)$, $x_1 \leq c$, $x_2(t_k^+) = -e_{\mathrm{n}}x_2(t_k^-)$, $e_{\mathrm{n}} \in (0, 1)$. Let $N_c \subset \mathscr{X}_{rel}$ denote those states that do not eventualy collide: it is proved in [1262] that $\mathscr{X}_{rel} \cup N_c = \emptyset$, i.e. all initial data in $\mathscr{X}_{rel}$ with $x_2 < 0$ (i.e. initial data in $\mathscr{X}_{rel}\backslash\mathscr{V}^\star$) yield impacts: this is indeed crucial to assure that the map P well-defined.

Proposition 7.1 *[1262] For the above one-degree-of-freedom system, one has (the value of the positions is given between parentheses):*

- *If* $0 \leq c < \beta$*:* $A^- = \left(\frac{\pi}{\omega} - \tau, \frac{\pi}{\omega} + \tau\right)$*, with* τ *increasing monotically from* $\frac{\pi}{2\omega}$ *to* $\frac{\pi}{\omega}$ *as* c *varies from* 0 *to* β*;* $A^0 = \left(\frac{\pi}{\omega} - \tau, \frac{\pi}{\omega} + \tau\right)$*;* $\frac{\pi}{\omega} + \tau$ *is an* $\alpha-$*point,* $\frac{\pi}{\omega} - \tau$ *is an* ω*-point.*
- *If* $c = \beta$*:* $A^- = (0, 2\pi)$*;* $A^0 = \{0\}$ *is both an* α*- and an* ω*-point.*
- *If* $c > \beta$*:* $A^- = \mathscr{V}^\star$*,* $A^0 = \emptyset$*.*

There is a problem in extending the mapping $P(\cdot)$ to the whole of $\mathscr{X}_{rel}$ because in $\mathscr{V}^\star$ the velocity is zero, hence injectivity and invertibility are lost (several states may be mapped to $\mathscr{V}^\star$). Denote all times (for states in $\mathscr{V}^\star$) such that the velocity is zero as τ_z. Let τ_0 denote the next zero-crossing time of the acceleration ($\dot{x}_2(\tau_0) = 0$), i.e. $P(x_1, x_2, t) = P(c, 0, \tau_z) = P(c, 0, \tau_0)$ for all trapped τ_z (the image of all the points when the system is constrained is the same). Such a case occurs when the system remains stuck on the constraint for a while (i.e. in $\mathscr{V}^\star$): during this interval of time all the states $(x_1, x_2, \tau_z) = (0, 0, \tau_z)$ will be mapped *via* $P(\cdot)$ to some other state. Obviously P is no longer injective in this case. In other words τ_0 is the time when detachment conditions are fulfilled. The conclusion of this is that in general, for such unilaterally constrained systems, the Poincaré map will be difficult to construct properly, since its definition involves that of $P(\cdot)$ (corresponding to flight-times). Whiston proposes to extend $P(\cdot)$ to an injective map as follows:

- – If $\mathscr{V}^\star$ contains α- and ω-points, define $\Sigma_c^- = \mathscr{X}_{rel}\backslash A^+$, i.e. substract all states in $\mathscr{X}_{rel} \supset \mathscr{V}^\star$ with positive acceleration $\ddot{x}_2$.
  – If $x \in A^-$ or $x = \omega$-point, $P_2(x)$ is the succeeding impact and $P_2(\alpha - \text{point}) = \omega$-point.
- $\Sigma_c^- = \mathscr{X}_{rel}$ if $A^- = \mathscr{V}^\star$ or if an $\alpha - \omega$-point exists. Then $P(x)$ is the succeeding impact state if $x \in A^-$ or $x = \alpha$-point.

- Σ_c^+ is constructed similarly (as $\mathscr{X}_{con}\backslash A^+$ or $\mathscr{X}_{con}$) and $P : \Sigma_c^- \to \Sigma_c^+$ is bijective and differentiable almost everywhere.
- Now let $P_2 : \mathscr{X}_{con} \to \mathscr{X}_{rel}$ be the impact rule and restrict it to $\Sigma_c^+ \to \Sigma_c^-$ in order to give a meaning to the Poincaré map $P_\Sigma = P \circ P_2$ which is singular at grazing orbits. The restriction of P_2 leaves $A^- \cup A^0$ invariant because one does not want that states in $\mathscr{V}^\star$ and with zero or negative acceleration jump, from obvious physical arguments.

In summary, [1262] clarifies the definition of the different sets of the extended phase-space which are useful in understanding the difficulties for constructing a nice Poincaré mapping for systems with possible grazing orbits. He shows how to construct a bijective Poincaré mapping despite "singularities" due to grazing trajectories. In the following we shall rather concentrate on the study of the singularities of the mapping $P(\cdot)$ and on its explicit form.

7.4.1 The Stroboscopic Poincaré Map Discontinuities

In order to show how a singularity appears in the Jacobian of a stroboscopic Poincaré map $P_{\Sigma_i}(\cdot)$, let us consider the simplest example of a one degree-of-freedom system as in (7.43) below [934, 937]. In particular we assume that the constraint is written as $f(q) = q - q_0 \geq 0$. Recall that the only difference between the stroboscopic and the impact Poincaré maps, is of the order of concatenation of the continuous flow and the restitution map. If $P_f(\cdot)$ generically denotes a map associated to the flow between impacts whereas $P_r(\cdot)$ denotes the restitution map (or collision mapping), then one roughly has in general $P_{\Sigma_i} = P_{f,1} \circ P_r \circ P_{f,2}$. The mappings $P_{f,1}(\cdot)$ and $P_{f,2}(\cdot)$ map respectively $\mathscr{X}_{rel} \times S^1 \to \Sigma_0$ and $\Sigma_1 \to \mathscr{X}_{con} \times S^1$, where S^1 is the 2π-unit circle (the space of the phase $\Omega = \omega t$), whereas Σ_i denotes generically a constant phase plane. The impact Poincaré map has the general form $P_\Sigma = P_f \circ P_r$ (this evidently holds only when such maps are defined). Let us note that despite the fact that the impact Poincaré map $P_\Sigma(\cdot)$ does not exist for non-impacting motions, its Jacobian for low pre-impact velocities can be computed. The following calculations show once again the fundamental difference between systems as in (7.1) (namely ODEs with impulsive perturbations) and systems with unilateral constraints.

Let us consider (1.45) with $f(q) = q - q_0$, and for simplicity we take $\tau_0 = 0$. Thus we have:

$$\varphi_q(t_0; 0, u_0) - q_0 = 0, \tag{7.30}$$

from which it follows that:

$$D_{u_0}\varphi_q(t_0; 0, u_0) = \frac{\partial \varphi_q}{\partial t_0}(t_0^-)\frac{dt_0}{du_0}(u_0) + \frac{\partial \varphi_q}{\partial u_0}(u_0) + \begin{pmatrix} 1 \\ 0 \end{pmatrix} = 0. \tag{7.31}$$

Noting that $\frac{\partial \varphi_q}{\partial t_0}(t_0^-) = \dot{q}(t_0^-)$ one obtains:

$$\frac{dt_0}{du_0}(u_0) = -\frac{1}{\dot{q}(t_0^-)}\left\{\frac{\partial \varphi_q}{\partial u_0}(u_0) - \begin{pmatrix}1\\0\end{pmatrix}\right\}. \tag{7.32}$$

It is therefore clear from (7.32) that the impact-time gradient with respect to the initial state diverges as soon as the pre-impact velocity tends to zero. Let us now compute the Jacobian of the flow with collisions $\varphi^c_{t_k^- - t_{k-1}^+}(u(t_{k-1}^+)) = \varphi(t_k^-; t_{k-1}^+, u(t_{k-1}^+)) = \varphi(t_k^-; 0, u_0) = \varphi^c_{t_k^-}(u_0) = u(t_k^-) = P(u(t_{k-1}^+))$, see Sect. 1.3.2 and (7.21) and (7.22) (the following calculation corresponds to computing the last term in (7.22)). We get:

$$\begin{aligned} D_u\varphi^c_{t_k^- - t_{k-1}^+}(u(t_{k-1}^+)) &= D_u\varphi(t_k^-; t_{k-1}^+, u(t_{k-1}^+)) \\ &= \frac{\partial \varphi}{\partial t}^T(t_k^-)\frac{dt_k}{du}^T(u(t_{k-1}^+)) + \frac{\partial \varphi}{\partial u}^T(u(t_{k-1}^+)). \end{aligned} \tag{7.33}$$

Introducing (7.32) into (7.33) we obtain:

$$\begin{aligned} D_u\varphi^c_{t_k^- - t_{k-1}^+}(u(t_{k-1}^+)) = -\frac{\partial \varphi}{\partial t}^T(t_k^-)\frac{1}{\dot{q}(t_k^-)}\left[\frac{\partial \varphi_q}{\partial u}^T(u(t_{k-1}^+)) + \begin{pmatrix}-1\\0\end{pmatrix}\right] \\ + \frac{\partial \varphi}{\partial u}^T(u(t_{k-1}^+)) \in \mathbb{R}^{2\times 2}, \end{aligned} \tag{7.34}$$

where $\varphi(\cdot)$ and $\varphi_q(\cdot)$ denote $\varphi(t_k^-; t_{k-1}^+, u(t_{k-1}^+))$ and $\varphi_q(t_k^-; t_{k-1}^+, u(t_{k-1}^+))$, respectively, and the gradient $\frac{\partial \varphi}{\partial t} \in \mathbb{R}^{2\times 1}$, whereas its transpose is the Jacobian $D_t\varphi \in \mathbb{R}^{2\times 1}$. In practice, one integrates the system from t_{k-1}^+ to t_k^- and then computes the corresponding gradients. It appears from (7.34) that whatever manner one uses to calculate the Poincaré map, a singular term will always be present in its Jacobian, because of the gradient of the impact times in (7.32).

Notice from (7.34) that we can continue the calculations further to obtain the Jacobian of the flow with collisions from t_{k-1}^+ to t_k^+, incorporating the restitution matrix $\mathscr{E} = \begin{pmatrix}1 & 0\\ 0 & -e_n\end{pmatrix}$. We obtain

$$D_u\varphi^c_{t_k^+ - t_{k-1}^+}(u(t_{k-1}^+)) = \mathscr{E}\begin{pmatrix} -\frac{\partial \varphi_q}{\partial q} + \frac{\partial \varphi_q}{\partial q} + 1 & -\frac{\partial \varphi_q}{\partial \dot{q}} + \frac{\partial \varphi_q}{\partial \dot{q}} \\ -\frac{g(t_k^-)}{\dot{q}(t_k^-)}\frac{\partial \varphi_q}{\partial q} + \frac{\partial \varphi_{\dot{q}}}{\partial q} + \frac{g(t_k^-)}{\dot{q}(t_k^-)} & -\frac{g(t_k^-)}{\dot{q}(t_k^-)}\frac{\partial \varphi_q}{\partial \dot{q}} + \frac{\partial \varphi_{\dot{q}}}{\partial \dot{q}} \end{pmatrix} \tag{7.35}$$

i.e.:

$$D_u\varphi^c_{t_k^+ - t_{k-1}^+}(u(t_{k-1}^+)) = \begin{pmatrix} 1 & 0 \\ e_n\left(\frac{g(t_k^-)}{\dot{q}(t_k^-)}\frac{\partial \varphi_q}{\partial q} - \frac{\partial \varphi_{\dot{q}}}{\partial q} + \frac{g(t_k^-)}{\dot{q}(t_k^-)}\right) & e_n\left(\frac{g(t_k^-)}{\dot{q}(t_k^-)}\frac{\partial \varphi_q}{\partial \dot{q}} - \frac{\partial \varphi_{\dot{q}}}{\partial \dot{q}}\right) \end{pmatrix} \tag{7.36}$$

where we have dropped the arguments for convenience. In (7.35) and (7.36), $g(t_k^-)$ denotes the second component of the vector field $G(u(t_k^-))$ in (1.46). Therefore, one eigenvalue of the Jacobian is always equal to 1, whereas the other eigenvalue is $-e_{\rm n}\left(\frac{g(t_k^-)}{\dot q(t_k^-)}\frac{\partial \varphi_q}{\partial \dot q}(t_{k-1}^+)+\frac{\partial \varphi_{\dot q}}{\partial \dot q}(t_{k-1}^+)\right)$. This indicates that the flow is computed between two instants at which the position $\varphi_q(\cdot)$ takes the same value. If we had chosen a constant phase section, hence a stroboscopic map, we would have had to compute the Jacobian of $\varphi^c_{\tau_1-\tau_0}(u_0)=\varphi_{\tau_1-t_k^+}\circ\mathscr{F}_k\circ\varphi_{t_k^--\tau_0}(u_0)$, where $\tau_0<t_k<\tau_1$ and τ_0, τ_1 are the times of first return of the phase Ω to the Poincaré section Σ_i. For instance if the external excitation has period $T=\frac{2\pi}{\omega}$, then $\tau_1=\tau_0+T$ and $\Omega(\tau_1)=\Omega(\tau_0)\bmod 2\pi$. The conclusions would not have been modified since the gradient in (7.32) necessarily appears in the Jacobian calculated on the impacting side Σ_i^-. Let us also add that these conclusions are independent of the fact that the vector field $G(u)$ be autonomous or nonautonomous. In the second case one has to incorporate the time t_k in the Poincaré mapping state, but one row of the section map Jacobian remains equal to $(1,0\ldots,0)$ (the one that corresponds to the coordinate transversal to the section).

Example 7.2 Let us consider as an example the bouncing ball with damping during flight-times. Calculations yield:

$$\frac{dt_k}{du}(u(t_{k-1}^+))=-\frac{1}{\dot q(t_k^-)}\begin{pmatrix}0\\ \\ \frac{m}{\lambda+c}\left[\exp\left(-\frac{\lambda+c}{m}(t_{k+1}-t_k)\right)-1\right]\end{pmatrix} \tag{7.37}$$

When $\lambda+c\to 0$, one retrieves that $\frac{\partial t_k}{\partial \dot q(t_k^+)}=\frac{t_k-t_{k-1}}{\dot q(t_k^-)}=\frac{2m}{F_d}$. It also follows that $e_{\rm n}\frac{g(t_k^-)}{\dot q(t_k^-)}\frac{\partial \varphi_q}{\partial \dot q}(t_{k-1}^+)-e_{\rm n}\frac{\partial \varphi_{\dot q}}{\partial \dot q}(t_{k-1}^+)=-e_{\rm n}\frac{F_d}{m\dot q(t_k^-)}\frac{m}{\lambda+c}\left[\exp\left(-\frac{\lambda+c}{m}(t_k-t_{k-1})\right)-1\right]+e_{\rm n}$. When $\lambda+c\to 0$ one finds that this term is equal to $-e_{\rm n}\frac{F_d}{m\dot q(t_k^-)}(t_k-t_{k-1})+e_{\rm n}=-e_{\rm n}$, hence the second eigenvalue is equal to $e_{\rm n}\le 1$.

Example 7.3 Following [591], let us consider a one degree-of-freedom system $\ddot q(t)=f(t,q(t),\dot q(t))$, $q\ge 0$, with Newton's impact rule. Assume that there exists a periodic solution $q_0(\cdot)$ with period $T=2n\pi$ and k shocks *per* period. Between impacts it is easy to calculate the flow of the linearized perturbed system as $(\dot{\delta x})=A(\tau_0,t)\delta x$, with $\delta x=\begin{pmatrix}q-q_0\\ \dot q-\dot q_0\end{pmatrix}$, A is the fundamental solution matrix of the linearized system satisfying $\dot A=B(t)A$, $B(t)=\begin{pmatrix}0 & 1\\ \frac{\partial f}{\partial q}(q_0,\dot q_0) & \frac{\partial f}{\partial \dot q}(q_0,\dot q_0)\end{pmatrix}$, $B(\tau_0,\tau_0)=I_2$. The impact instants over one period are denoted as $t_0,t_1,\ldots,t_{k-1}$. The perturbed motion will not collide at t_0 but at $t_0+\Delta t_0$ for some Δt_0. One can show using a Taylor expansion and neglecting higher order terms that $q(t_0+\Delta t_0)=q(t_0)+\dot q_0(t_0^-)\Delta t_0=0$. Also from the dynamics and the expression of $\Delta t_0=-\frac{q(t_0)}{\dot q(t_0^-)}$, it follows that $\dot q[(t_0+\Delta t_0)^-]=\dot q(t_0^-)-\Delta t_0 f(t_0,0,\dot q_0(t_0^-))$. Using the impact rule one can now calculate $\dot q[(t_0+\Delta t_0)^+]$, i.e. the value of the velocity of the perturbed

periodic orbit after its collision with $q = 0$. There follows an expression of the form $(\dot{\delta x}) = B_0 \delta x$, with $B_0 = \begin{pmatrix} -e_n & 0 \\ \frac{1}{\dot{q}(t_0^-)} f(t_0, 0, -e_n \dot{q}_0(t_0^-)) + e_n f(t_0, 0, \dot{q}(t_0^-)) & -e_n \end{pmatrix}$. Similar expressions may be computed for the other jumps. Then the Floquet multipliers of the periodic motion $q_0(\cdot)$ are the eigenvalues of the matrix $A(t_{k-1}, \tau_0 + 2n\pi) B_{k-1} A(t_{k-2}, t_{k-3}) \cdots B_0 A(\tau_0, t_0)$. We recover that the linearized system (around $q_0(\cdot)$) defines a flow with collisions with an alternation of matrices calculated from the continuous phases of motion and matrices corresponding to the discontinuities. These calculations were already made in (7.22) and (7.33). Once again it is apparent that stability and bifurcation analysis can be done for periodic motions using the Floquet theory as long as the matrices B_j are bounded. When the approach velocity tends to zero, these matrices grow unbounded.

In conclusion, although the determinant of the Jacobian always remains ≤ 1 since the system is dissipative and contracts volumes in state space, see [742, pp. 459–460],[18] there is an entry of the Jacobian that depends inversely on the velocity at impact: for low velocities, this entry tends to infinity. The result is a large stretching and compression of areas in phase space due to the mappings $P_{f,1}(\cdot)$ and $P_{f,2}(\cdot)$ which define the stroboscopic Poincaré map $P_{\Sigma_i}(\cdot)$ [934].

To finish this section, notice that a particular feature of grazing bifurcations is that, contrary to bifurcations in smooth vector fields or mappings, they cannot be predicted from the observation of the Jacobian, i.e. by looking at the local properties of the orbit (say periodic) just before the bifurcation [935].

7.4.2 *The Stroboscopic Poincaré Map Around Grazing-Motions*

The above singularity concerns the Jacobian of the mapping on the impacting side. It results in important stretching and compression of areas in a constant-phase section region, under the action of the Poincaré mapping. Let us now investigate the form of a stroboscopic Poincaré mapping in the vicinity of grazing trajectories [406, 934], for a two-dimensional impact oscillator, with $f(q) = q - q_0 \leq 0$. To this end, let us consider a low-velocity contacting point $P_0 = (q, \dot{q}, t) = (q_0, \dot{q}(t_k^-), t_k)$, and two points of the trajectory: $P_1 = (q(t_1), \dot{q}(t_1), t_1)$ and $P_2 = (q(t_2), \dot{q}(t_2), t_2)$ which are arbitrarily close to $(q_0, \dot{q}(t_k^-), t_k)$, i.e. $\Delta t_1 \stackrel{\Delta}{=} t_k - t_1 > 0$ and $\Delta t_2 \stackrel{\Delta}{=} t_2 - t_k > 0$ are very small quantities (in other words, the surfaces Σ_0 and Σ_1 needed to define the mappings $P_{f,1}(\cdot)$ and $P_{f,2}(\cdot)$ above are chosen very close to the impacting surface C_j).

[18] Dissipativity holds between the harmonic force input and the velocity, i.e. with supply rate $w(u, y) = F(t)\dot{q}(t)$. Dissipative systems with no input define Lyapunov stable systems [218]. Hence the eigenvalues of the system's matrix A must have magnitude ≤ 1.

The first point thus belongs to the trajectory before the shock, and the second point is after the shock. Expanding in Taylor series around t_k one finds:

$$\begin{cases} q(t_1) = q_0 - \dot{q}(t_k^-)\Delta t_1 + \frac{1}{2}\ddot{q}(t_k^-)\Delta t_1^2 + \mathscr{O}(\Delta t_1^3) \\ \dot{q}(t_1) = \dot{q}(t_k^-) - \ddot{q}(t_k^-)\Delta t_1 + \mathscr{O}(\Delta t_1^2), \end{cases} \tag{7.38}$$

and:

$$\begin{cases} q(t_2) = q_0 - e_{\mathrm{n}}\dot{q}(t_k^-)\Delta t_2 + \frac{1}{2}\ddot{q}(t_k^+)\Delta t_2^2 + \mathscr{O}(\Delta t_2^3) \\ \dot{q}(t_2) = -e_{\mathrm{n}}\dot{q}(t_k^-) - \ddot{q}(t_k^+)\Delta t_2 + \mathscr{O}(\Delta t_2^2). \end{cases} \tag{7.39}$$

We assume that the trajectory we are studying possesses only one grazing impact on (t_1, t_2). Since our goal is to obtain a local form of a stroboscopic Poincaré mapping around a grazing trajectory, we can combine the expressions in (7.38) and (7.39), take $\Delta t_1 = \Delta t_2$ and neglect high-order terms to get the following [406]:

$$\begin{cases} q(t_2) = (q_0 - q(t_1))\left(2e_{\mathrm{n}} + \frac{\ddot{q}(t_k^-)}{\ddot{q}(t_k^+)}\right) + q_0 - e_{\mathrm{n}}\dot{q}(t_1) \\ \dot{q}(t_2) = -\sqrt{\dot{q}^2(t_1) - 2\ddot{q}(t_k^-)(q(t_1) - q_0)}\left(\frac{\ddot{q}(t_k^+)}{\ddot{q}(t_k^-)} + e_{\mathrm{n}}\right) + \dot{q}(t_1)\frac{\ddot{q}(t_k^+)}{\ddot{q}(t_k^-)}. \end{cases} \tag{7.40}$$

We note that the vector field between Σ_1 and Σ_0 is linear and thus will not modify the characteristics of the mapping. Combining the two equations in (7.38) it is also possible to calculate that:

$$\dot{q}^2(t_k^-) = \dot{q}^2(t_1) - 2\ddot{q}(t_k^-)(q(t_1) - q_0) + \ldots \tag{7.41}$$

where ... $= \frac{\Delta t}{\ddot{q}(t_k^-)}$. Note from (7.41) that the term on the right-hand side must be positive for the expression of $\dot{q}(t_2)$ in (7.40) to make sense. Also $\dot{q}(t_k^-) \geq 0$, which is deduced from the fact that $q \leq q_0$ is the unilateral constraint, see Remark 1.4. From (7.41) one also deduces that if $\dot{q}(t_k^-) \to 0$, then the right-hand side expression does the same. From (7.40) and the fact that we have assumed that the trajectory returns after one period to the constant phase section $t_1 \pmod{2\pi}$, one therefore realizes that for low-velocity impacts, the derivative of the Poincaré mapping takes very large values, and possesses a *square-root type* singularity. Indeed, $\frac{\partial \dot{q}(t_2)}{\partial \dot{q}(t_1)}$ and $\frac{\partial \dot{q}(t_2)}{\partial q(t_1)}$ both contain $\dot{q}(t_k^-)$ in their denominator. One therefore retrieves the above derivation and singularity of the Jacobian. The interest for deriving a formal expression for the Poincaré mapping in the neighborhood of grazing trajectories evidently lies in the ability of studying whether the system can cross a C-bifurcation without losing its stability, see for instance [934].

Let us summarize: assume that the system evolves around an impactless periodic trajectory. Then a parameter that guides the magnitude of the periodic orbit is varied such that the trajectory (the iterates of the Poincaré mapping) approaches a grazing trajectory. At the grazing time, the form of the Poincaré mapping suddenly jumps from a linear form to the nonlinear form in (7.40). Introducing a suitable state transformation into local normal/tangential coordinates $(x_{\Sigma_i,\mathrm{n}}, x_{\Sigma_i,\mathrm{t}})$, the Poincaré

mapping takes the form [287, 934]:

$$\begin{cases} x_{\Sigma_i,\mathrm{n}}(k+1) = -\gamma e_{\mathrm{n}}^2 x_{\Sigma_i,\mathrm{t}}(k) \\ x_{\Sigma_i,\mathrm{t}}(k+1) = b\sqrt{-x_{\Sigma_i,\mathrm{t}}(k)} + x_{\Sigma_i,\mathrm{n}}(k). \end{cases} \tag{7.42}$$

7.4.3 Further Comments and Studies

Major references about bifurcations and chaos in nonsmooth dynamical systems are [69, 132, 728], which interested readers have to read. The survey article [789] as well as the Special Issue [790] are also worth reading. Perhaps one of the first study on bifurcations in nonsmooth systems goes back to [233], in which the authors investigated the transition from a periodic orbit to another one, or merging of both, or disappearance. More recently the study of grazing-bifurcations, mainly related to impact oscillators, has received attention in [152, 235, 236, 265, 287, 392–394, 404–406, 585, 587, 699, 934, 939, 1262, 1264]. When the parameters of the system are varied (for instance the forcing term magnitude or frequency), the trajectories' behavior can change suddenly at the grazing trajectory. A periodic trajectory can be changed into chaotic motion, followed by a period adding cascade, or the creation of a large number of periodic trajectories. In the literature, researches have been mainly focused on one-degree-of-freedom systems with one limiting stop (or two stops [404]), i.e. whose dynamics can be reduced to:

$$\ddot{q}(t) + c\dot{q}(t) + kq(t) = A\cos(\omega t),\ q(t) \geq 0 \text{ for all } t \geq 0,\ e_{\mathrm{n}} \in [0, 1]. \tag{7.43}$$

Let us mention that the study of grazing orbits for another class of dynamical systems of higher dimension and with a scalar unilateral constraint and a specific structure can be found in [473]. Ivanov [587] studies this problem using an approximating problem $\mathscr{P}_n$ and results on convergence of solutions of $\mathscr{P}_n$ [682, 683]. The same philosophy is adopted in [405], who compare the results obtained when the rigid body assumption is replaced by a compliant Hertz model. The numerical results in [405] show that when the stiffness is high enough, $k = 2000$ N/m, then the respective behaviors of both models are quite similar in terms of bifurcations. The authors conclude that the observed C-bifurcation must be, in some sense, the limit of the bifurcation for the compliant model. Notice that this is not surprising, since these systems belong to the class of systems studied by Paoli and Schatzman, see Problem 2.2: the trajectories of the compliant model converge towards those of the rigid one when $k \to +\infty$. Hence C-bifurcations are indeed the limit of more conventional types of bifurcations. In [591] Ivanov presents an analysis of grazing impacts of periodic orbits using a general form of compliant contact model. Various bifurcations are discovered: disappearance, survival with or without stability. The results are not related to those in [934], although once again convergence of solutions should bridge the gap between compliance and rigidity. In [588] the nonsmooth coordinate change of Sect. 1.4.3 is used to investigate C-bifurcations. Chin et al. [287] consider the

Nordmark map given as:

$$\begin{cases} x_{n+1} = \alpha x_n + y_n + \rho \\ y_{n+1} = -\gamma x_n \end{cases} \quad \text{for } x_n \leq 0, \qquad \begin{cases} x_{n+1} = -\sqrt{x_n} + y_n + \rho \\ y_{n+1} = -\gamma e_{\mathrm{n}}^2 x_n \end{cases} \quad \text{for } x_n > 0, \tag{7.44}$$

and observe three major types of C-bifurcations in a simple impact oscillator: from stable period-1 orbits to a reversed infinite period adding cascade, or to attracting chaos occupying a full interval of the bifurcation parameter, and collision of an unstable maximal periodic orbit and a period-1 orbit. They all are unconventional, in the sense that they do not occur in smooth systems. The Nordmark map is also studied in [265]. In [404] two distinct types of C-bifurcations are observed: in the first one, the stable orbit disappears and the system stabilizes onto an already existing stable trajectory. In the second one, there is an immediate jump to a chaotic motion. In both cases the subsequent motion has a large amplitude. An experimental validation has been presented in [153]. Budd et al. [235, 699], Foale and Bishop [405], Nusse et al. [287, 939] propose to refine the study of C-bifurcations by using one-dimensional mappings with the same square-root type singularity as that of grazing-bifurcations, given as:

$$F_\varepsilon(\chi) = \begin{cases} \alpha\chi + \varepsilon & \text{if } \chi \leq 0 \\ \beta\chi^d + \varepsilon & \text{if } \chi > 0, \end{cases} \tag{7.45}$$

with $0 < \alpha < 1$, $\beta < -1$ and $0 < d < 1$, whereas ε is the parameter that is to be varied and gives rise to a bifurcation. Near-grazing dynamics in frictionless impact oscillators are controlled by feedack strategies in [324, 325]. A one-degree-of-freedom mass acted upon by Coulomb friction and a linear spring, and impacted by a controlled mass, is studied in [1170]. Feedback control of the Poincaré map at grazing impacts is designed by controlling the distance between the two masses, to regulate the grazing-induced bifurcation scenario. We end this short survey by mentioning application in the modeling of forest fire regimes [264, 339, 786]. It is shown that impact mechanics can very well reproduce the qualitative features of the periodic fire regimes of savannas and boreal forests, as well as the chaotic fire dynamics of Meditarranean forest.

7.5 Complementarity Lagrangian Systems: Stability of Fixed Points

In this section we study the stability of the second-order sweeping process, that was presented in Sect. 5.2.2. Although it implies a restitution law with quite limited scope, it does represent an interesting class of nonsmooth Lagrangian systems, because it

settles the global geometrical framework of complementarity Lagrangian systems (moreover, see Remark 7.6 below).

7.5.1 The Dynamical System

Let us consider the following subclass of nonsmooth mechanical systems in (5.1), with no friction and no bilateral holonomic constraints:

$$\begin{cases} M(q)\ddot{q}(t) + F(q(t), \dot{q}(t)) = \nabla f(q(t))\lambda_{\mathrm{n},u}(t), \\ q(0) = q_0, \dot{q}(0^-) = \dot{q}_0, \\ 0 \leq f(q(t)) \perp \lambda_{\mathrm{n},u}(t) \geq 0 \text{ for all } t \geq 0, \\ \dot{q}(t_k^+) = -e_{\mathrm{n}}\dot{q}(t_k^-) + (1 + e_{\mathrm{n}})\mathrm{proj}_{M(q(t_k))}[V(q(t_k)); \dot{q}(t_k^-)], \end{cases} \tag{7.46}$$

with $F(q, \dot{q}) = C(q, \dot{q})\dot{q} + \frac{\partial U}{\partial q}(q)$, $C(q, \dot{q})\dot{q}$ collects Coriolis and centrifugal forces, $U(q)$ is a smooth potential energy from which conservative forces derive, $f : \mathbb{R}^n \mapsto \mathbb{R}^m$. We assume that $f(q_0) \geq 0$. The impact times are denoted as usual as t_k, the left-limit $\dot{q}(t_k^-) \in -V(q(t_k))$ whereas the right-limit $\dot{q}(t_k^+) \in V(q(t_k))$. The third line in (7.46) is Moreau's collision mapping, see Sect. 5.2.2.

Remark 7.6 Instead of Moreau's law, we could use the generalized impact law in (6.44) and (6.45) with $\mathscr{E}_{\mathrm{nt}} = 0$, $\mathscr{E}_{\mathrm{tn}} = 0$, $\mathscr{E}_{\mathrm{tt}} = 0$, together with the restrictions on $\mathscr{E}_{\mathrm{nn}}$ which guarantee energetic, kinetic, and kinematic consistencies (Propositions 6.2, 6.3, 6.4 and 6.5). This does not change the analysis much since (7.55) below it is satisfied while the Lagrangian system is well-posed according to Theorem 5.3. The MDI would not change outside impacts, anyway.

The impact law in (7.46) implies that the kinetic energy loss at time t_k satisfies:

$$T_L(t_k) = -\frac{1}{2}\frac{1 - e_{\mathrm{n}}}{1 + e_{\mathrm{n}}}\left(\dot{q}(t_k^+) - \dot{q}(t_k^-)\right)^T M(q(t_k))\left(\dot{q}(t_k^+) - \dot{q}(t_k^-)\right) \leq 0 \tag{7.47}$$

Note that the tangent cone $V(q(t))$ is assumed to have its origin at $q(t)$ so that $0 \in V(q(t))$ to allow for post-impact velocities tangential to the admissible set boundary $\mathrm{bd}(\Phi)$. We first need to guarantee the well-posedness of the dynamics. To this aim we may rely on Theorem 5.3 and we are thus led to make the next assumption.

Assumption 7.3 The gradients $\nabla f_i(q)$ are not zero and are independent at the active contacts $f_i(q) = 0$. Furthermore the functions $f(\cdot)$, $F(q, \dot{q})$, $M(q)$ and the system's configuration manifold are real analytic, and $||F(q, \dot{q})||_q \leq d(q, q(0)) + ||\dot{q}||_q$, where $d(\cdot, \cdot)$ is the Riemannian distance and $||\cdot||_q$ is the norm induced by the kinetic metric.

It is then reasonable to assume that the next properties hold:

(i) Solutions of (7.46) exist on $[0, +\infty)$ such that $q(\cdot)$ is absolutely continuous (AC), whereas $\dot{q}(\cdot)$ is right-continuous of local bounded variation (RCLBV). In particular, the left and right-limits of these functions exist everywhere.

(ii) The function $q(\cdot)$ cannot be supposed to be everywhere differentiable. One has $q(t) = q(0) + \int_0^t u(s)ds$ for some function $u(\cdot) \overset{\text{a.e.}}{=} \dot{q}(\cdot)$. Moreover $\dot{q}(t^+) = u(t^+)$ and $\dot{q}(t^-) = u(t^-)$.

(iii) Solutions are unique (however, in general they do not depend continuously on the initial conditions).

(iv) The acceleration $\ddot{q}$ is a *measure* du, which is the sum of two measures: an atomic measure $d\mu_a$, and a Lebesgue integrable function which we denote $\ddot{q}(\cdot)$, i.e. $du = d\mu_a + \ddot{q}(t)dt$. The atoms correspond to the impact times.

(v) The set of impact times is countable. In many applications one has $d\mu_a = \sum_{k\geq 0}[\dot{q}(t_k^+) - \dot{q}(t_k^-)]\delta_{t_k}$, where δ_t is the Dirac measure at t and the sequence $\{t_k\}_{k\geq 0}$ can be ordered, i.e. $t_{k+1} > t_k$. However, phenomena like accumulations of left-accumulations of impacts may exist (at least bounded variation does not preclude them). This is a sort of complex Zeno behavior.[19] In the case of elastic impacts ($e_n = 1$) it follows from [80, Proposition 4.11] that impact times are in finite number in any compact time interval: there exists $\rho(q(0), \dot{q}(0)) > 0$ such that $t_{k+1} - t_k \geq \rho(q(0), \dot{q}(0))$. This is some kind of piecewise-continuity of the solutions, though the constant $\rho(q(0), \dot{q}(0))$ may be arbitrarily small.

We remind that any quadratic function $W(\cdot)$ of $\dot{q}$ is itself RCLBV, hence its derivative is a measure dW. Consequently, $dW \leq 0$ has a meaning and implies that the function $W(\cdot)$ does not increase. As we know from Sect. 5.2.2, the Lagrangian dynamics in (7.46) can be written as the following Measure Differential Inclusion (MDI), which is the second order sweeping process:

$$-M(q(t))du - F(q(t), u(t^+))dt \in \partial\psi_{V(q(t))}(w(t)) \subseteq \partial\psi_{\Phi}(q(t)), \qquad (7.48)$$

where $w(t) = \frac{u(t^+)+eu(t^-)}{1+e_n}$ from (7.46). If $e_n = 0$ then $w(t) = u(t^+)$, if $e_n = 1$ then $w(t) = \frac{u(t^+)+u(t^-)}{2}$. Moreover, when $u(\cdot)$ is continuous then $w(t) = u(t)$. When $\dot{q}(t)$ is discontinuous, (7.48) implies that Moreau's collision rule is satisfied. The term $\psi_{V(q(t))}(w(t))$ can be interpreted as a velocity potential and its subdifferential $\partial\psi_{V(q(t))}(w(t))$. Let us recall some facts from Sect. 5.2.2. The MDI in (7.48), whose left-hand side is a measure and whose right-hand side is a cone, has the following meaning: there exists a positive measure $d\mu$ such that both dt and du possess densities with respect to $d\mu$, denoted respectively as $\frac{dt}{d\mu}(\cdot)$ and $\frac{du}{d\mu}(\cdot)$. One has $\frac{dt}{d\mu}(t) = \lim_{\varepsilon\to 0,\varepsilon>0} \frac{dt([t,t+\varepsilon])}{d\mu([t,t+\varepsilon])}$, which shows the link with the usual notion of a derivative. The choice of $d\mu$ is not unique because the right-hand side is a cone. However, by the Lebesgue-Radon-Nikodym Theorem [1053], the densities $\frac{dt}{d\mu}(\cdot)$ and $\frac{du}{d\mu}(\cdot)$ are unique functions for a given $d\mu$. To shed some light on this, let us consider

[19] i.e. all phenomena involving an infinity of events in a finite time interval.

for instance $d\mu = dt + \Sigma_{k\geq 0}\delta_{t_k}$, which corresponds to applications where the system is subject to impacts at times t_k and otherwise evolves freely. Then $\frac{dt}{d\mu}(t_k) = 0$ (the Lebesgue measure dt and the Dirac measure δ_t are mutually singular), whereas $\frac{du}{d\mu}(t_k) = u(t_k^+) - u(t_k^-)$ (t_k is an atom of the measure du). When $t \neq t_k$ then $\frac{dt}{d\mu}(t) = 1$ and $\frac{du}{d\mu}(t) = \dot{v}(t)$. Therefore, the meaning of (7.48) is that there exists a positive measure $d\mu$ with respect to which both dt and du possess densities, and

$$-M(q(t))\frac{du}{d\mu}(t) - F(q(t), u(t^+))\frac{dt}{d\mu}(t) \in \partial\psi_{V(q(t))}(w(t)) \tag{7.49}$$

holds $d\mu-$almost everywhere. In a sense, densities replace derivatives, for measures. When dealing with measure differential equations or inclusions, it is then natural to manipulate densities instead of derivatives. In general one can choose $d\mu = |du|+dt$ [867, p.90], where $|du|$ is the absolute value of du, or $d\mu = ||u(t)||dt + d\mu_a$, or $d\mu = dt + d\mu_a$. It is fundamental to recall at this stage that the solution of (7.49) does not depend on this choice. For instance, if $d\mu = ||u(t)||dt + d\mu_a$ then for all $t \neq t_k$, $\frac{dt}{d\mu}(t) = \frac{1}{||u(t)||}$ and $\frac{du}{d\mu}(t) = \frac{\ddot{q}(t)}{||u(t)||}$. Whereas if $d\mu = dt + d\mu_a$ then for all $t \neq t_k$, $\frac{dt}{d\mu}(t) = 1$ and $\frac{du}{d\mu}(t) = \ddot{q}(t)$.

Remark 7.7 It is fundamental to keep in mind that the contact force multipliers $\lambda_{n,u}$ are still present in the inclusion in (7.49): the terms $\nabla f(q)\lambda_{n,u}$ represent *selections* of the set-valued right-hand side $\partial\psi_{V(q(t))}(w(t)) \subseteq \partial\psi_{\Phi}(q(t))$. The right-hand side is in turn constructed in such a way that these selections satisfy complementarity relations with the gap function $f(q)$, see Sect. 5.2.2.3. Therefore, the stability analysis holds for all phases of motion: unconstrained ($f(q) > 0$), constrained ($f(q) = 0$), and at impact times.

7.5.2 The Stability Analysis

In the case of unconstrained Lagrangian mechanical systems, the Lagrange-Dirichlet (or Lejeune-Dirichlet) Theorem states that the equilibrium point $(q, \dot{q}) = (q^*, 0)$ is locally stable if the potential energy $U(q)$ has a strict minimum at $q^\star$. First notice that since $F(q, 0) = \frac{\partial U}{\partial q}(q)$ and $0 \in V(q)$, fixed points of (7.48) satisfy the generalized equation

$$0 \in \partial\psi_{\Phi}(q^\star) + \frac{\partial U}{\partial q}(q^\star), \tag{7.50}$$

which in particular implies $q^\star \in \Phi$. Equivalently starting from (7.46) the equilibrium pair $(q^\star, \lambda^\star_{n,u})$ is the solution of

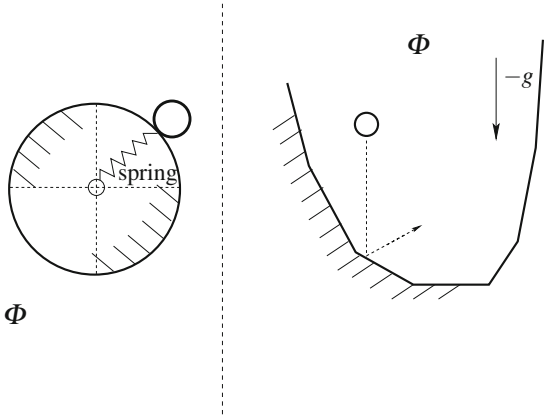

Fig. 7.5 Nonconvex (prox-regular) and convex admissible sets

$$\begin{cases} F(q^\star, 0) = \nabla f(q^\star)\lambda^\star_{\mathrm{n},u} \\ 0 \le f(q^\star \perp \lambda^\star_{\mathrm{n},u} \ge 0. \end{cases} \tag{7.51}$$

It follows from the material in Sect. B.2.1 that both (7.50) and (7.51) are in turn equivalent to the optimization problem:

$$q^\star = \underset{q\in\mathbb{R}^n}{\operatorname{argmin}}\, \psi_\Phi(q) + U(q) = \underset{q\in\Phi}{\operatorname{argmin}}\, U(q). \tag{7.52}$$

In the following we shall assume for simplicity that the equilibria are isolated, or even that the two equations in (7.50) and (7.51) have a unique solution $q^\star$. The second characterization suggests that one should better speak of the equilibrium as the triple $(q, \dot{q}, \lambda_{\mathrm{n},u}) = (q^\star, 0, \lambda^\star_{\mathrm{n},u})$. The generalized equations in (7.51) are quite similar to the ones in (2.20), which characterize the fixed points of mechanical systems with compliant unilateral contact.

Lemma 7.1 *Consider a mechanical system as in (7.46). Suppose that* $U(q) \ge \gamma(||q||)$ *for some class* $\mathscr{K}$ *function* $\gamma(\cdot)$ *and all* $q \in \Phi$. *Then if* $\psi_\Phi(q) + U(q)$ *has a strict minimum at* $q^\star$, *the equilibrium point* $(q^\star, 0)$ *is Lyapunov stable.*[20]

Let us note that Φ need not be convex in general. The equilibrium may exist in $\mathrm{Int}(\Phi)$, or it may belong to $\mathrm{bd}(\Phi)$ but be forced by the continuous dynamics; see Fig. 7.5 for planar examples with both convex and nonconvex Φ. It is obvious that in the depicted nonconvex case all points $(q^\star, 0)$ with $q^\star \in \mathrm{bd}(\Phi)$ are fixed points of the dynamics. The nonconvex domain is described by $\Phi = \{(q_1, q_2) | f(q) = q_1^2 + q_2^2 - r^2 \ge 0\}$ for some $r > 0$. This is an $r-$prox-regular domain, see Sect. B.2.3, for which the Mangasarian-Fromovitz CQ in (B.9) is satisfied: one has $\nabla f(q) = (2q_1 \quad 2q_2)^T$. Since q_1 and q_2 cannot vanish simultaneously on the disk boundary, the gradient is nonzero and a vector v as in (B.9) can always be found. For such a domain Φ,

[20] The *asymptotic* Lyapunov stability is not shown.

Definition B.6 applies and the normal and tangent cones are equal to their respective linearization cones (see Remark B.1).

Proof The proof of Lemma 7.1 may be led as follows. Let us consider the nonsmooth Lyapunov candidate function:

$$W(q,\dot{q}) = \frac{1}{2}\dot{q}^T M(q)\dot{q} + \psi_\Phi(q) + U(q) - U(q^\star). \tag{7.53}$$

Since the potential $\psi_\Phi(q) + U(q)$ has a strict minimum at $q^\star$ equal to $U(q^\star)$, $W(\cdot)$ is positive definite on the whole state space. Also $\alpha(||q||, ||\dot{q}||) \leq W(q,\dot{q}) \leq \beta(||q||, ||\dot{q}||)$ for some class $\mathscr{K}$ functions $\alpha(\cdot)$ and $\beta(\cdot)$, is satisfied on Φ ($\ni q(t)$ for all $t \geq 0$). The potential function $\psi_\Phi(q) + U(q)$ is continuous on Φ. Thus $W(q,\dot{q})$ in (7.53) satisfies the requirements of a Lyapunov function candidate on Φ, despite the indicator function has a discontinuity on $\mathrm{bd}(\Phi)$, but is continuous on the closed set Φ. Moreover, since (7.48) secures that $q(t) \in \Phi$ for all $t \geq 0$, it follows that $\psi_\Phi(q(t)) = 0$ for all $t \geq 0$. In view of this one can safely discard the indicator function in the subsequent stability analysis. Let us examine the variation of $W(q,\dot{q})$ along trajectories of (7.49). In view of the above discussion, one can characterize the measure dW by its density with respect to $d\mu$ and the function $W(\cdot)$ decreases if its density $\frac{dW}{d\mu}(t) \leq 0$ for all $t \geq 0$. We recall Moreau's rule for differentiation of quadratic functions of RCLVB functions [867, p.8-9]: let $u(\cdot)$ be RCLBV, then $d(u^2) = (u^+ + u^-)du$ where u^+ and u^- are the right-limit and left-limit functions of $u(\cdot)$. Let us now compute the density of the measure dW with respect to $d\mu$:

$$\begin{aligned}\frac{dW}{d\mu}(t) = \frac{1}{2}\left[\dot{q}(t^+) + \dot{q}(t^-)\right]^T M(q(t))\frac{dv}{d\mu}(t) + \frac{\partial U}{\partial q}\frac{dq}{d\mu}(t)\\ + \frac{1}{2}\frac{\partial}{\partial q}\left(\dot{q}(t^+)^T M(q(t))\dot{q}(t^+)\right)\frac{dq}{d\mu}(t),\end{aligned} \tag{7.54}$$

where $dq = u(t)dt$ since the function $u(\cdot)$ is Lebesgue integrable. Let us now choose $d\mu = dt + d\mu_a$. Since $\frac{dt}{d\mu}(t_k) = 0$ and $\frac{dq}{d\mu}(t_k) = 0$, whereas $\frac{dv}{d\mu}(t_k) = u(t_k^+) - u(t_k^-) = \dot{q}(t_k^+) - \dot{q}(t_k^-)$, it follows from (7.54) that at impact times one gets:

$$\frac{dW}{d\mu}(t_k) = \frac{1}{2}\left[\dot{q}(t_k^+) + \dot{q}(t_k^-)\right]^T M(q(t))\left[\dot{q}(t_k^+) - \dot{q}(t_k^-)\right] = T_L(t_k) \leq 0, \tag{7.55}$$

where $T_L(t_k)$ is in (7.47). Let the matrix function $\dot{M}(q,\dot{q})$ be defined by $\dot{M}(q(t), \dot{q}(t)) = \frac{d}{dt}M(q(t))$. Let us use the expression of $F(q,\dot{q})$ given after (7.46), and let us assume that Christoffel's symbols of the first kind are used to express the vector $C(q,\dot{q})\dot{q} = \dot{M}(q,\dot{q}) - \frac{1}{2}\left[\frac{\partial}{\partial q}\left(\dot{q}^T M(q(t))\dot{q}\right)\right]^T$. Then the matrix $\dot{M}(q,\dot{q}) - 2C(q,\dot{q})$ is skew-symmetric [218]. Now if $t \neq t_k$, one gets $\frac{du}{d\mu}(t) = \dot{u}(t) = \ddot{q}(t)$ and $\frac{dt}{d\mu}(t) = 1$ [867, p.76] and one can calculate from (7.54), using the dynamics and the skew-symmetry property:

$$\frac{dW}{d\mu}(t) = \frac{dW}{dt}(t) = -\dot{q}(t)^T C(q(t), \dot{q}(t))\dot{q}(t) + \frac{1}{2}\dot{q}(t)^T \dot{M}(q(t), \dot{q}(t))\dot{q}(t) - \dot{q}(t)^T z_1(t)$$
$$= -\dot{q}(t)^T z_1(t), \tag{7.56}$$

where $z_1(t) \in -\partial\psi_{V(q(t))}(w(t))$ and $W(\cdot)$ is defined in (7.53). Notice that $\dot{q}$ is to be understood as $\dot{q}(t) = \dot{q}(t^+)$ since $t \neq t_k$. Now since for all $t \geq 0$ $\dot{q}(t^+) \in V(q(t))$ which is polar to $\partial\psi_\Phi(q(t))$, and from the inclusion in Appendix B.2.2 it follows that $z_1(t)^T\dot{q}(t^+) \geq 0$. Therefore, the *measure* dW is non-positive. Consequently, the *function* $W(\cdot)$ is nonincreasing [341, p.101], and Lemma 7.1 is proved.

Remark 7.8

- The inclusion of the indicator function $\psi_\Phi(q(t))$ in the Lyapunov function not only guarantees its positive definiteness (which anyway is assured along solutions of (7.49) which remain in Φ), but it also allows one to consider cases where the smooth potential has a minimum that is outside Φ. Saying "$\psi_\Phi(q) + U(q)$ has a strict minimum at $q^\star$" is the same as saying "$U(q)$ has a strict minimum at $q^\star$ inside Φ." Since the indicator function has originally been introduced by Moreau as a potential associated to unilateral constraints, it finds here its natural use. In fact we could have kept the indicator function in the stability analysis. This would just add a null term $\dot{q}(t^+)^T z_2(t)\frac{dt}{d\mu}(t)$ in the right-hand side of (7.54), with $z_2(t) \in \partial\psi_\Phi(q(t))$.
- As alluded to above, taking $e_n = 1$ in (7.46) assures that there is no accumulation of impacts, thus the sequence of impact times $\{t_k\}_{k\geq 0}$ can be ordered, $d\mu_a = \sum_{k\geq 0}\delta_{t_k}$, and velocities are piecewise continuous. Then a much simpler formulation can be adopted by separating continuous motion phases occurring on intervals (t_k, t_{k+1}) from impact times. The system is therefore non-Zeno for $e_n = 1$ and if Assumption 7.3 holds.
- One does not need to make further assumptions on the measure $d\mu_a$ to conclude, and we see that this conclusion is obtained directly applying general differentiation rules of RCLBV functions. The dynamics might even contain dense sets of velocity discontinuities, (7.54) and (7.55) would continue to hold. This shows that using the MDI formalism in (7.48) or (7.49) places the stability analysis in a much more general perspective than, say, restricting $\dot{q}(\cdot)$ to be piecewise continuous.
- The continuity with respect to initial data is used nowhere in the stability proof.

7.5.3 Dissipativity Properties

The dynamics in (7.48) has the interpretation in Fig. 7.6 with $\xi \in \partial\psi_{V(q(t))}(w(t))$. Since $\partial\psi_{V(q(t))}(w(t)) \subseteq N_\Phi(q(t)) = V^\circ(q(t))$ (the cone polar to $V(q(t))$), the feedback loop in Fig. 7.6 contains the cone complementarity problem

$$N_\Phi(q(t)) \supseteq \partial\psi_{V(q(t))}(w(t)) \ni \xi \perp w(t) \in V(q(t)). \tag{7.57}$$

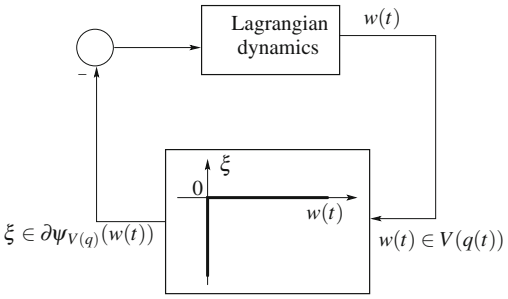

Fig. 7.6 Unilaterally constrained Lagrangian system: Passive interconnection as a set-valued nonsmooth Lur'e system

When $m = 1$ and $q \in \mathrm{bd}(\Phi)$, one has $V(q) = \mathbb{R}^+$ and $N_\Phi(q) = \mathbb{R}^-$ in a suitable frame attached to q, and the graph of the multivalued mapping is the so-called corner law. In general, this is an example of an m-dimensional monotone multivalued mapping $w(t) \mapsto \xi$. Thus Lemma 7.1 extends the absolute stability problem and (7.48) (or (7.49)) is interpreted as a Lur'e set-valued dynamical system. It is noteworthy that the feedback loop in Fig. 7.6 contains both the complementarity conditions and the collision mapping in (7.46). It is natural then to write a dissipation equality, following the developments of Sect. 5.4.4.5. To that end let us take advantage of the compact formalism (7.49). We consider a Lebesgue measurable input $\tau(\cdot)$ so that (7.49) becomes:

$$-M(q(t))\frac{du}{d\mu}(t) - F(q(t), u(t^+))\frac{dt}{d\mu}(t) - \tau(t)\frac{dt}{d\mu} \in \partial\psi_{V(q(t))}(w(t)). \quad (7.58)$$

Let ξ denote a measure that belongs to the normal cone to the tangent cone $\partial\psi_{V(q(t))}(w(t))$, and let us denote $\frac{dR}{d\mu}(\cdot)$ its density with respect to μ. The system in (7.58) is dissipative with respect to the generalized supply rate:

$$\langle \frac{1}{2}(u(t^+) + u(t^-)), \tau(t)\frac{dt}{d\mu} + \frac{dR}{d\mu}(t)\rangle, \quad (7.59)$$

where $\langle \cdot, \cdot, \cdot \rangle$ denotes the scalar product. Noting that $\xi = \nabla f(q(t))\lambda_{\mathrm{n},u}$ for some measure $\lambda_{\mathrm{n},u}$ we obtain

$$\langle \frac{1}{2}(u(t^+) + u(t^-)), \tau(t)\frac{dt}{d\mu} + \nabla f(q(t))\frac{d\lambda_{\mathrm{n},u}}{d\mu}(t)\rangle, \quad (7.60)$$

where we recall that outside impacts (i.e. outside atoms of the measure dR) one has $\frac{dt}{d\mu} = 0$ because the Lebesgue measure has no atom. It is noteworthy that (7.60) is a generalization of the Thomson-Tait's Formula, which expresses the work performed by the contact forces during an impact. The supply rate in (7.60) may be split into two parts: a function part and a measure part. The function part describes what happens outside impacts, and one has $\frac{1}{2}(u(t^+) + u(t^-) = u(t) = \dot{q}(t)$. The measure part describes what happens at impacts t_k. Then one gets:

$$\begin{aligned}&\langle (u(t_k^+)+u(t_k^-)), \nabla f(q(t))\tfrac{d\lambda_{\mathrm{n},u}}{d\mu}(t_k)\rangle = \langle (u(t_k^+)+u(t_k^-)), M(q(t_k)(u(t_k^+)-u(t_k^-))\rangle\\ &= u(t_k^+)^T M(q(t_k))u(t_k^+) - u(t_k^-)^T M(q(t_k))u(t_k^-) = 2T_L(t_k) \le 0,\end{aligned} \tag{7.61}$$

where we used the fact that the dynamics at an impact time is algebraic:

$$M(q(t_k))(u(t_k^+)-u(t_k^-)) = \nabla f(q(t))\frac{d\lambda_{\mathrm{n},u}}{d\mu}(t_k),$$

with a suitable choice of the basis measure μ. The storage function of the system is nothing else but its total energy. It may be viewed as the usual smooth energy $\frac{1}{2}\dot{q}^T M(q)\dot{q} + U(q)$, or as the *unilateral energy* $\frac{1}{2}\dot{q}^T M(q)\dot{q} + U(q) + \psi_\Phi(q)$, which is nonsmooth on $\mathbb{R}^n \times \mathbb{R}^n$. It is worth remarking, however, that the nonsmoothness of the storage function is not a consequence of the impacts, but of the complementarity condition $0 \le f(q) \perp \lambda \ge 0$. Using the generalized supply rate in (7.59), and using the calculations made in the proof of Lemma 7.1 (in particular the skew-symmetry property used to get (7.56)), one can write down the dissipation equality: for any time instants $T_1 \ge T_0 \ge 0$:

$$\begin{aligned}W(T_1) - W(T_0) &= \langle \tfrac{1}{2}(u(t^+)+u(t^-)), \tau(t)\tfrac{dt}{d\mu} + \tfrac{dR}{d\mu}(t)\rangle\\ &= \langle \tfrac{1}{2}(u(t^+)+u(t^-)), \tfrac{dR}{d\mu}(t)\rangle + \langle u(t), \tau(t)\tfrac{dt}{d\mu}\rangle\\ &= \textstyle\sum_{k\in\{k_0,k_1\}}\langle (u(t_k^+)+u(t_k^-)), \nabla f(q)\tfrac{d\lambda}{d\mu}(t_k)\rangle + \langle u(t), \tau(t)\tfrac{dt}{d\mu}\rangle\\ &= \textstyle\sum_{k\in\{k_0,k_1\}} T_L(t_k) + \langle u(t), \tau(t)\tfrac{dt}{d\mu}\rangle,\end{aligned} \tag{7.62}$$

where $t_{k_0}, t_{k_0+1}, \ldots, t_{k_1}$ are impact times in $[T_0, T_1]$.

Remark 7.9 The difference between LCS as in (5.128) and Lagrangian complementarity systems is that the external input $u(t)$ and the multiplier $\lambda_{\mathrm{n},u}(t)$ in (5.128) do not enter the dynamics through the same matrix (in general $B \neq E$). Thus the dissipativity may hold with the supply rate $\langle \lambda_{\mathrm{n},u}, w\rangle$ while it does not with $\langle u, w\rangle$. In Lagrangian systems both the control input $\tau(t)$ and the generalized contact force R enter the dynamics similarly. This is why they both appear in the generalized supply rate in (7.59). Let us finally note that if the Lagrangian dynamics contains a dissipative force like a Rayleigh dissipation, then this has to be added in (7.62). Energy balance equalities similar to the dissipation equality (7.62) have been derived in [80, Proposition 7] and [243, Proposition 2.3], see also [218, Sect. 7.2].

Example 7.4 Let us consider the system in Fig. 7.7 whose dynamics is given as

$$\begin{cases} m\ddot{x}(t) = -f\dot{x}(t) - kx(t)\\ m\ddot{y}(t) = -mg + \lambda(t), \quad 0 \le y(t) \perp \lambda(t) \ge 0\\ \dot{y}(t_k^+) = -e_{\mathrm{n}}\dot{y}(t_k^-) \text{ when } y(t_k) = 0,\ \dot{y}(t_k^-) < 0, \end{cases} \tag{7.63}$$

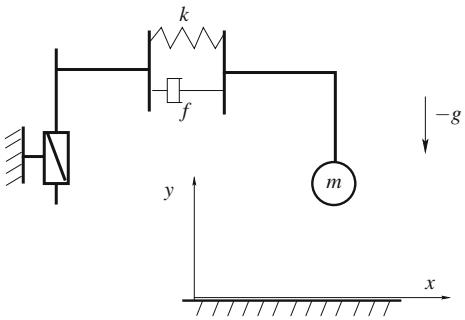

Fig. 7.7 A simple two-dof system

where $f > 0$ is the damping, $k > 0$ is the stiffness of the spring-dashpot apparatus. Obviously $(q, \dot{q}) = (0, 0)$ is the unique fixed point of (7.63) and one can check that the same dynamics with $y \leq 0$ no longer possesses any fixed point. For any $y(0) > 0$ and $e_n \in (0, 1)$ the sequence of impact times has a finite accumulation t_∞. The function in (7.53) is equal to:

$$W(q, \dot{q}) = \frac{1}{2} m \dot{x}^2 + \frac{1}{2} m \dot{y}^2 + \psi_{\mathbb{R}^+}(y) + mgy + \frac{1}{2} k x^2. \tag{7.64}$$

One may check that this function has the properties required in the proof of Lemma 7.1.

7.5.4 Further Reading and Comments

A complete exposition of Lyapunov stability, invariance principle for measure differential inclusions, and their application to nonsmooth Lagrangian systems, is made by Leine and van de Wouw in [730]. See in particular [730, Sects. 7.2 and 7.3] for further extensions of Lemma 7.1. For instance [730, Theorem 7.6] may be used to prove the asymptotic stability under certain conditions (like $e_n \in [0, 1)$, and continuous dependence of solutions with respect to initial data).[21] Tangential effects like Coulomb's friction are taken into account in [730]. In this case one should not expect

[21] Basically, this is a sufficient condition for the Krasovskii-LaSalle invariance principle to hold, because it implies that positive limit sets of solutions are positively invariant [730, Proposition 6.12]. The autonomy property is central in the proof of [730, Proposition 6.12], and recall from Sect. 1.3.2 that it is implied by the uniqueness of solutions which is itself assured by the continuous dependence on initial data.

the uniqueness of fixed points, but rather the existence of *equilibrium sets* (and in fact, the mere issue of the existence and uniqueness of an equilibrium, which is a static equilibrium of the system, requires investigations [595, 964], see Sect. 5.5). The attractivity of equilibrium sets for unilateral constraints and Coulomb's friction is tackled in [730, §7.3.1]. See also [96] for a complete stability analysis of a simple planar system with one unilateral contact with friction, and [593], who shows that the uniqueness of $\ddot{q}$ and $\nabla f(q)\lambda$ at the equilibrium $(q^\star, 0)$[22] is necessary for its stability. Further results are in [595]. The uniform, global asymptotic Lyapunov stability of the Hill's equation with unilateral constraints and impacts, is studied in [723] (Hill's equation is a system with varying parameter: $\ddot{x}(t) + g(t)x(t) = 0$, $g(t) = g(t+\pi)$). It is found [723, Theorem 2] that the restitution coefficient should be small enough (i.e. impacts have to dissipate enough energy), depending on some characteristics of the unconstrained Hill's equation. Another analysis on a similar system may be found in [1021]. Section 7.3.5 summarizes results on the dynamical behavior of the bouncing ball with an excited base. Results of the Lyapunov stability of the bouncing-ball have been published in [462, 727, 945]. The study in [727] concerns a bouncing-ball with excited base. It is made in the framework of Moreau's sweeping process, hence the dynamics encapsulates all phases of motion, including persistent contact phases and accumulations of impacts (Zeno pheomenon): $mdv + mgdt + m\ddot{e}(t)dt \in -N_{T_{\mathbb{R}^+}(q(t))}(w(t))$, $a_{\min} \leq \ddot{e}(t) \leq a_{\max}$ for all t, and w is as in (7.48). The authors introduce the terminology of *symptotic stability* to denote that the system's fixed point is not only attractive but the trajectories converge to it in finite time. They use nonmonotonic (or almost decreasing) Lyapunov functions, but the requirements on the variation of the Lyapunov functions differ from those in Propositions 8.1 and 8.5: it has to be upperbounded by a step function (the steps being defined from the impact times) which decreases.

Proposition 7.2 *[727] Suppose that* $0 \leq e_{\mathrm{n}} \leq \bar{e}_{\mathrm{n}} < 1$. *Let* $\frac{g+a_{\max}}{g+a_{\min}}\bar{e}_{\mathrm{n}}^2 < 1$, *then the fixed point* $q^\star = 0$, $\dot{q}^\star = 0$ *of the excited bouncing-ball system is globally uniformly symptotically attractively stable.*

Related results are in [460, 462, 916, 943, 945], who nevertheless do not consider a complete mechanical model, because the contact forces are not taken into account (see comments in Remark 1.10). Thus only some kind of vibro-impact model is studied (or flows with collisions, see Sect. 1.3.2), and in case of finite accumulation of impacts, the stability analysis "stops" when the accumulation is attained. This is named Zeno stability. The analysis in [146, 147] also use this hybrid dynamical systems framework.

[22] See Sects. 5.1.1, 5.1.2, 5.1.3, 5.5, 5.5.6, for results in this direction.

When considering mechanical systems, the main issue with the approaches based on impulsive ODEs, impulsive Differential Inclusions or measure-driven differential equations (see Chap. 1), is either the absence of contact forces, or a set-valued right-hand side which is not a suitable set for contact forces. Indeed the equilibrium is a static mechanical equilibrium of the ball on the ground, stating that the gravity force and the contact force balance each other (by Newton's third law of action/reaction). Such an equilibrium cannot exist without suitably chosen contact forces in the model. Introducing contact force multiplier $\lambda_{\mathrm{n},u}$ implies, however, the consideration of the complementarity conditions $0 \leq \lambda_{\mathrm{n},u} \perp q \geq 0$ (equivalently the inclusion into normal cones like Moreau's set). This is the same, in fact, for all complementarity dynamical systems.

Similar problems are met in [777], see [207]. As alluded to in Remark 7.7, the MDI in (7.49) does not share such drawback. This is clear if one follows the developments of Sect. 5.2.2. Roughly speaking, the fundamental meaning of a differential inclusion like $\dot{x}(t) \in G(x(t))$, disregarding any property to be assigned to the set $G(x)$ for securing the well-posedness, is that there exists an element of $G(x(t))$, say $\lambda(t)$, such that $\dot{x}(t) = \lambda(t)$ for all $t \geq 0$. Such an element $\lambda(t)$ is called a *selection* of the inclusion's right-hand side. Consider for instance the differential inclusion (DI) in (5.42), which models only smooth phases of motion. The meaning of this DI is that there exists a selection P satisfying (5.40). Due to the particular structure of the normal cone, this selection satisfies complementarity conditions with the gap function $f(q)$. Introducing the contact force and the complementarity conditions, allows one to trivially answer the question: "is there a life after Zeno?" [39], since the switch to a holonomically constrained system is automatically handled by the complementarity conditions. One should however not disregard the fact that once this switch has occurred, the contact is handled by a complementarity problem, see Sect. 5.1.2, and that the constraints, even if closed, are not bilateral constraints.

$\rightsquigarrow$ *The same remark applies to the electrical circuits with ideal diodes in* Sect. 5.4.4.

A Lyapunov function is derived in [462, 945] for the excited-base bouncing-ball as $V(q,\dot{q}) = \frac{1}{g} + k\sqrt{\frac{1}{2}\dot{q}^2 + gq}$, where $k > \sqrt{2}\frac{1+e_{\mathrm{n}}}{1-e_{\mathrm{n}}}$. Roughly speaking, it is required to strictly decrease outside impacts and not to increase at impact times [945, Proposition 1]. An interesting question is whether or not such Lyapunov function could be used in the trajectory tracking framework described in Sect. 8.1, during the transition phases. One would obtain what was called the *strong stability* in [220].

$\rightsquigarrow$ *It is noteworthy that contrary to some other results which do not take into account contact forces and complementarity conditions (hence which basically deal with vibro-impact systems that involve ODEs and velocity jumps), the stability results*

in [727, 730], in Sects. 7.5, 8.1 and 8.3, do *incorporate all phases of motion and a correct modelling of the contact forces.*

Most of these results nevertheless show asymptotic stability only, while one would expect in many instances finite-time stabilization on the constraint boundary, as is the case for the "basic" bouncing-ball. Apart from the already cited work [727], results in this direction may be found in [243, 1252, 1253].

7.5.5 *Global Finite-Time Stability* via *the Zhuravlev-Ivanov Transformation*

Let us illustrate how the nonsmooth Zhuravlev-Ivanov transformation of Sect. 1.4.3 may be used to design a finite-time stable controller for a double integrator subjected to a unilateral constraint, as done by Oza, Orlov, and Spurgeon in [950]. The plant dynamics is given as:

$$\begin{cases} \dot{x}_1(t) = x_2(t) \\ \dot{x}_2(t) = u(x_1(t), x_2(t)) + \omega(x_1(t), x_2(t), t) \\ x_1(t) \geq 0 \text{ for all } t \geq 0 \\ x_2(t_k^+) = -e_{\mathrm{n}} x_2(t_k^-), x_1(t_k) = 0, x_2(t_k^-) < 0, e_{\mathrm{n}} \in (0, 1), \end{cases} \tag{7.65}$$

where $\omega(\cdot)$ is a piecewise continuous disturbance, $|\omega(x_1, x_2, t)| \leq M$. The proposed controller is a twisting sliding-mode input[23] of the form:

$$u(x_1, x_2) = -\mu_1 \mathrm{sgn}(x_2) - \mu_2 \mathrm{sgn}(x_1), \tag{7.66}$$

with $\mu_2 > \mu_1 > M > 0$. The Zhuravlev-Ivanov change of state space in (1.83) is used to transform (7.65) and (7.66) into:

$$\begin{cases} \dot{s}(t) = Rv(t) \\ \dot{v}(t) \in R^{-1}\mathrm{sgn}(s(t))[u(|s(t)|, Rv(t)\mathrm{sgn}(s(t))) + \omega(|s(t)|, Rv(t)\mathrm{sgn}(s(t)), t)] \\ u(s, v) = -\mu_1 \mathrm{sgn}(sv) - \mu_2, \end{cases} \tag{7.67}$$

which we rewrite as the differential inclusion:

$$\begin{cases} \dot{s}(t) = Rv(t) \\ \dot{v}(t) \in -\mu_1 R^{-1}\mathrm{sgn}(v(t)) - \mu_2 R^{-1}\mathrm{sgn}(s(t)) + R^{-1}\mathrm{sgn}(s(t))\omega(s(t), v(t), t). \end{cases} \tag{7.68}$$

We see that $(s, v) = (0, 0)$ is the unique fixed point of the closed-loop system (7.68), since the conditions on the gains and the disturbance guarantee that the generalized equation $0 = -\mu_1 \xi_2(t) - \mu_2 \xi_1(t) + \xi_1(t)\omega(0, 0, t)$, $\xi_1(t) \in \mathrm{sgn}(v = 0) = [-1, 1]$,

[23] This type of set-valued controller is quite popular in the Sliding Mode Control scientific community, was introduced in [734] and its finite-time stability studied in [948].

$\xi_2(t) \in \text{sgn}(s = 0) = [-1, 1]$, has the solution $\xi_1 = \xi_2 = 0$. Moreover, $(s, v) = 0 \Rightarrow (x_1, x_2) = (0, 0)$. Therefore, if the controller drives the trajectories of (7.68) to the origin in finite-time, the origin of (7.65) and (7.66) is also attained in finite time. If in addition the Lyapunov function used for the proof is a Lyapunov function in the original coordinates, stability holds for both systems. The next result shows finite-time stability and is inspired by [948].

Theorem 7.6 *[950] Let $e_n \in (0, 1)$. (i) Let $M = 0$ (no disturbance), then both systems (7.68) and (7.65), (7.66) are globally finite-time stable, and (7.68) is uniformly globally finite-time stable. (ii) Let $M < \mu_1 < \mu_2 - M$, then both systems (7.68) and (7.65), (7.66) are globally finite-time stable.*

Proof (i) The Lyapunov function candidate $V(s, v) = \mu_2|s| + \frac{1}{2}v^2$ is chosen. After some calculations one obtains $\dot{V}(s, v) \leq -\mu_2|v||R - R^{-1}| - \mu_1 R^{-1} v$ along the trajectories of (7.68). The invariance principle for differential inclusions [37, 1106] applied on the manifold $v = 0$ allows one to conclude the global uniform asymptotic stability of (7.68). Homogeneity arguments for the differential inclusion (7.68) allow one to use [948, Theorem 3.1] to conclude the finite-time stability. (ii) The global stability is proved similarly as in (i), using the same Lyapunov function.[24] The rest of the proof proceeds in three steps. (a) One starts with the function $\tilde{V}(s, v) = V(s, v) + \kappa s v$, with $\kappa < \min\left\{1, \frac{2\mu_2^2}{\tilde{R}}, \frac{\mu_2|R_1 - R_1^{-1}| + R_1^{-1}(\mu_1 - M)}{R_1\sqrt{2\tilde{R}}}\right\}$, $R_1 = \frac{2}{1+e_n}$ if $\text{sgn}(sv) = -1$. It is possible to show that $\tilde{V}(s, v)$ is positive definite on the compact sets $D = \{(s, v) | V(s, v) \leq \tilde{R}\}$, and inside D one has $|s| \leq \frac{\tilde{R}}{\mu_2}$, $|v| \leq \sqrt{2\tilde{R}}$. Moreover we have $\dot{\tilde{V}}(s, v) \leq -K\tilde{V}(s, v)$ on the sets D, with $K(\mu_1, \mu_2) = c\left[\max\left\{\frac{2\mu_2^2 + \kappa\tilde{R}}{2\mu_2}, \sqrt{\frac{\tilde{R}}{\cdot}}2(1 + \kappa)\right\}\right]^{-1} > 0$ and $c = \min(\kappa R_1^{-1}(\mu_2 - \mu_1 - M), \mu_2|R_1 - R_1^{-1}| + (\mu_1 - M)R_1^{-1} - \kappa R_1\sqrt{2\tilde{R}})$. (b) We infer that $V(s, v)$ decreases exponentially fast: $\tilde{V}(s(t), v(t)) \leq \tilde{V}(s(0), v(0)) \exp(-K(\mu_1\mu_2)t)$ where the initial time has been taken zero. On the compact sets D the following holds: $LV(s, v) \leq \tilde{V}(s, v) \leq MV(s, v)$, with $0 < L < \min\left\{\frac{2\mu_2^2 - \tilde{R}\kappa}{2\mu_2^2}, 1 - \kappa\right\}$, $M > \max\left\{\frac{2\mu_2^2 + \tilde{R}\kappa}{2\mu_2^2}, 1 + \kappa\right\} > 0$. Thus we get $V(s(t), v(t)) \leq L^{-1}M\tilde{R}\exp(-K(\mu_1\mu_2)t)$ along the trajectories of (7.68). Thus since all the above holds for arbitrary $\tilde{R} > 0$, the origin of the system with disturbance is globally uniformy asymptotically stable. (c) Homogeneity is used again to prove the finite-time stability with [948, Theorem 3.2].

The origin of (7.68) is also shown to be reached after trajectories make an infinite number of revolutions around it, which corresponds to a finite accumulation of impacts in (7.65) and (7.66), and an estimate of the settling time is computed.

[24] At this step, one may also invoke LaSalle's invariance principle, though the differential inclusion is time-dependent, transforming the perturbed time-varying differential inclusion in an equivalent autonomous differential equation with rectangular uncertainties [948, §2].

Remark 7.10 A one-degree-of-freedom system consisting of a mass moving on a flat plane, with Coulomb's friction is considered in [1278]. The controller is an impulsive force which creates a finite accumulation of tangential velocity discontinuities. Therefore the closed-loop system is quite similar to (7.65) and (7.66), in that it mixes set-valued terms like sign function and impulsive terms. The MDEs described in Chap. 1 do not encapsulate such nonsmooth dynamics.

7.6 Stabilization of Impacting Systems: From Compliant to Rigid Models

The goal of the study in this section is to point out some problems related with stabilization of motion-controlled manipulators that come in contact with a compliant environment (in particular, the sufficient conditions guaranteeing asymptotic convergence of the solutions towards the steady-state solution), and to propose a particular stability analysis that applies to both the compliant and the rigid cases. The motivations for doing this are clear: since one is able to prove that the trajectories of compliant models converge towards those of rigid models, stability properties and analysis should apply to both cases. We restrict ourselves to a simple continuous PD motion controller, and to the case of a purely elastic environment (that corresponds to the limit case when the impact itself does not dissipate energy). The material in this section is consequently close to the one in Sect. 2.1.

7.6.1 System's Dynamics

The system depicted in Fig. 7.8 consists of a simple mass moving horizontally without friction, whose position is given by $x(t)$, and a compliant environment at $x = 0$ whose model is a massless spring with stiffness $k > 0$. This is the model that was used in Sect. 2.1.1. The control law is given by $u(x, \dot{x}, x_d) = -\lambda_2 \dot{x} - \lambda_1 (x - x_d)$, $x_d \geq 0$, $\lambda_1 > 0$, $\lambda_2 > 0$. The equations that govern our system are

$$\begin{cases} m\ddot{x}(t) + \lambda_2 \dot{x}(t) + \lambda_1 x(t) = \lambda_1 x_d & \text{if } x(t) < 0 \\ m\ddot{x}(t) + \lambda_2 \dot{x}(t) + (\lambda_1 + k) x(t) = \lambda_1 x_d & \text{if } x(t) \geq 0, \end{cases} \tag{7.69}$$

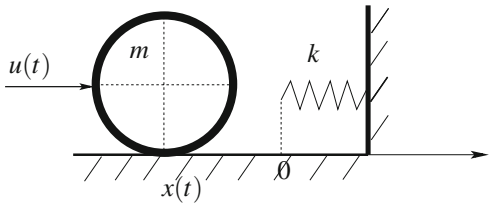

Fig. 7.8 Controlled mass colliding an elastic wall

which according to the material of Sect. 2.1.1.2, can be rewritten equivalently as a linear complementarity system: $m\ddot{x}(t) + \lambda_2\dot{x}(t) + \lambda_1 x(t) - \lambda_1 x_d = -\lambda(t)$, $0 \leq \lambda(t) \perp \lambda(t) - kx(t) \geq 0$. Although this system consists of two switching vector fields, the transition between both is continuous: this is called a *continuous switching system*. If damping is added in the environment model, then the system is a discontinuous switching system that may be embedded into Filippov's differential inclusions, see Sect. 2.1.3. Convergence of the state $(x, \dot{x})$ towards the fixed point $(x^\star, 0)$ of the second equation in (7.69) may be investigated by considering the associated equivalent total energy of the closed-loop system in (7.69). If one assumes that contact persists, then a Lyapunov function of the form $V(x, \dot{x}) = T(x, \dot{x}) + U(x) - U(x^\star)$, where $U(x)$ is the elastic potential energy, can be used to show *via* the Lagrange-Dirichlet [60, §22B] and Krasovskii-LaSalle's Lemma [1229] that the fixed point $(x^\star, 0)$ is asymptotically stable. But in the unilateral case it happens that the equivalent closed-loop energy is not so simple since $U(x)$ possesses a discontinuity at $x = 0$. One therefore has to explicitly calculate a storage function of the complete system. To this aim let us choose the input $u = -\lambda_2\dot{x} - \lambda_1(x - x_d) + v$. The so-called available storage function is then defined as $V_a(x_0, \dot{x}_0) = \sup_{t,v} -\int_{t_0}^{t} v(r)\dot{x}(r)dr$. In our case the available storage is given by [218]:

$$V_a(x_0, \dot{x}_0) = \begin{cases} \frac{\dot{x}_0^2}{2} + \frac{\lambda_1 x_0^2}{2} - \lambda_1 x_d x_0 + \frac{\lambda_1^2 x_d^2}{2(\lambda_1 + k)} & \text{if } x_0 \leq 0 \\ \frac{\dot{x}_0^2}{2} + \frac{(\lambda_1 + k)}{2}\left(x_0 - \frac{\lambda_1 x_d}{\lambda_1 + k}\right)^2 & \text{if } x_0 > 0. \end{cases} \tag{7.70}$$

This function is a Lyapunov function for the system in (7.69), and it can be used to prove the global asymptotic stability of the systems fixed point. However in the sequel we focus on a particular stability property of this equilibrium point. The motivation for studying this type of stability is evident if one thinks of more complicated tasks as considered for instance in [852], where tracking is considered and hence hampers the direct application of invariance principles. Also, the equivalence with a mechanical system may no longer be possible in certain cases, e.g. when the feedback loop contains time-delays. From the mathematical results presented in Chap. 2, see Theorem 2.1, it follows that as $k \to +\infty$, the solutions of the dynamical system in (7.69) converge towards the solution of the system:

$$\begin{cases} m\ddot{x}(t) + \lambda_2\dot{x}(t) + \lambda_1 x(t) = \lambda_1 x_d \\ \ddot{x}(t_k) = \min(0, -\lambda_2\dot{x}(t_k) - \lambda_1 x(t_k) + \lambda_1 x_d) & \text{if } \dot{x}(t_k^+) = 0, x(t_k) = 0 \\ x(t) \leq 0 \text{ for all } t \geq 0 \\ \dot{x}(t_k^+) = -\dot{x}(t_k^-) & \text{if } x(t_k) = 0, \dot{x}(t_k^-) > 0. \end{cases} \tag{7.71}$$

Note that this convergence remains true even if damping is added, introducing a suitable restitution coefficient. Our main goal is therefore to look for a stability analysis that is able to encompass both systems in (7.69) and (7.71). Since the solutions $x_n(t)$, $\dot{x}_n(t)$ of (7.69) (with $k = k_n$, $\{k_n\}$ a strictly increasing sequence) tend as $n \to +\infty$

towards a solution of (7.71), there should logically exist a way to analyze their stability within a common framework.

7.6.2 Lyapunov Stability Analysis

In the following we analyze the stability of system (7.69) using a single Lyapunov function. To begin with, we show how the stability analysis of the closed-loop system in (7.69) can be led with a particular Lyapunov function candidate. Let us consider:

$$V(x,\dot{x}) = \frac{1}{2}m\dot{x}^2 + \frac{1}{2}\lambda\tilde{x}^2 + c\tilde{x}\dot{x}, \tag{7.72}$$

with $\lambda = \lambda_1 + k + \frac{\lambda_2 c}{m}$, $c > 0$ is such that $c^2 - \lambda_2 c - m(\lambda_1 + k) < 0$ (since $\Delta = \lambda_2^2 + 4m(\lambda_1 + k) > 0$, and $\sqrt{\Delta} - \lambda_2 > 0$, such a c can always be chosen arbitrarily small), and $\tilde{x} = x - \frac{\lambda_1 x_d}{\lambda_1 + k}$. λ and c guarantee that $V(x,\dot{x})$ is positive definite. We obtain:

• $x < 0$ (noncontact phase)

$$\dot{V}(t) \leq (-\lambda_2 + c + \frac{1}{2}k^2 + \frac{1}{2})\dot{x}^2 + (-\frac{c\lambda_1}{m} + 1)\tilde{x}^2 + \overbrace{\frac{1}{2}\left(\frac{\lambda_1 k}{\lambda_1 + k}x_d\right)^2 + \frac{1}{2}\left(\frac{c\lambda_1 k}{(\lambda_1 + k)m}x_d\right)^2}^{\triangleq R(\lambda_1,k,x_d)} \tag{7.73}$$

or in compact form:

$$\dot{V}(t) = -a_{nc}(k,\lambda_2)\dot{x}(t)^2 - b_{nc}(\lambda_1)\tilde{x}(t)^2 + R(\lambda_1,k,x_d). \tag{7.74}$$

• $x > 0$ (contact phase)

$$\dot{V}(t) = (-\lambda_2 + c)\dot{x}(t)^2 - \frac{\lambda_1 + k}{m}c\tilde{x}(t)^2 = -a_c(\lambda_2)\dot{x}(t)^2 - b_c(k,\lambda_1)\tilde{x}(t)^2. \tag{7.75}$$

We denote $z = (\tilde{x},\dot{x})^T$.

Proposition 7.3 (Quadratic Stability) *[222] For any stiffness $0 < k < +\infty$ there exist $P = P^T > 0$, $Q = Q^T > 0$, $\lambda_1^\star < +\infty$, $\lambda_2^\star < +\infty$ such that $\lambda_1 > \lambda_1^\star$, $\lambda_2 > \lambda_2^\star$ implies that for all $t \geq 0$, $V(z) = z^T Pz$, and $\dot{V}(z) \leq -z^T Qz$ along the trajectories of (7.69). Thus the equilibrium point $z = 0$ is globally asymptotically stable in the sense of Lyapunov and the system in (7.69) is quadratically stable.*

Proof The control gains λ_1 and λ_2 can be chosen such that $a_{nc} > 0$ and $b_{nc} > 0$. Thus we conclude that for all x: $\dot{V}(t) \leq -\alpha\dot{x}(t)^2 - \beta\tilde{x}(t)^2 + R$, with $\alpha = \min(a_{nc}, a_c)$, $\beta = \min(b_{nc}, b_c)$. Following the arguments in [303], we deduce that the state $(\tilde{x},\dot{x})$ converges in finite time in a ball with radius r, with $r \to 0$ as λ_1 and λ_2 tend

to $+\infty$. Therefore for all $t \geq \bar{t}$, $\bar{t} < +\infty$, we get $|\tilde{x}| < r$. Now notice (see (7.73)) that $R \to \frac{1}{2}k^2 x_d^2(1 + \frac{c^2}{m^2})$ as $\lambda_1 \to +\infty$. Since by taking λ_1 and λ_2 large enough r can be made arbitrarily small and since $\frac{\lambda_1 x_d}{\lambda_1 + k} \to x_d$ when $\lambda_1 \to +\infty$, it follows that for λ_1 and λ_2 large enough, $|\tilde{x}(t)| < r$ for $t \geq \bar{t}$ implies $x(t) > 0$ for $t \geq \bar{t}$. Then (7.75) implies that both $\dot{x}$ and $\tilde{x}$ converge asymptotically to zero. Notice that outside some ball $B_{\bar{R}}$ we have for some $Q = Q^T > 0$: $\dot{V}(t) \leq -z^T Q z$. This can be easily deduced by spliting α and β into α_1 and α_2, β_1 and β_2: then $\dot{V}(t) \leq -\alpha_1 \dot{x}(t)^2 - \beta_1 \tilde{x}(t)^2 - \alpha_2 \dot{x}(t)^2 - \beta_2 \tilde{x}(t)^2 + R$, so that outside the ball $B_{\bar{R}}$ with $\bar{R} = \frac{R}{\min(\alpha_2, \beta_2)}$, we get $\dot{V}(t) \leq -\alpha_1 \dot{x}(t)^2 - \beta_1 \tilde{x}(t)^2$. Still λ_1 and λ_2 can be chosen large enough so that $\bar{R}$ is as small as desired. Thus we deduce that for $0 \leq t \leq \bar{t}$, $\| z(t) \| \leq \sqrt{\frac{V(0)}{\lambda_{\min} P}} \exp(-\frac{\lambda_{\min} Q}{\lambda_{\max} P} t)$, i.e. the ball $B_{\bar{R}}$ is reached exponentially fast.

7.6.3 *Analysis of Quadratic Stability Conditions for Large Stiffness Values*

We shall be content with the existence results on the feedback gains in Proposition 7.3. However, note that if one takes the sufficient conditions for stability deduced from this analysis, then λ_1 and $\lambda_2 \to +\infty$ as $k \to +\infty$. In other words, the sufficient conditions imply feedback gains growing without bound as $k \to +\infty$. This suggests that in order to obtain quadratic Lyapunov stability of (7.69) one has to choose feedback gains proportional to the stiffness k as k becomes large. The aim of this section is to prove that this is true. Notice that such a result is not satisfying, because the solutions of (7.71) are bounded and in a sense are Lyapunov stable. This can be shown by taking $k = +\infty$ for $V(\cdot)$ in (7.72), so that $\tilde{x} = x$: then one computes that $V(t_{k+1}^-) - V(t_k^+) \leq 0$ and that $\sigma_V(t_k) = 0$, using the fact that $x(t_k) = 0$, $x(t) < 0$ on (t_k, t_{k+1}) and that the sequence $\{t_k\}$ exists.[25] Then one notes that the restriction of $V(\cdot)$ to Σ, i.e. $V_\Sigma(\cdot)$, satisfies these inequalities also since $V_\Sigma(t_k) = V(t_k)$, hence Lyapunov stability of the fixed point $\dot{x}(t_k) = 0$ of P_Σ (although P_Σ is not calculable explicitly). Since this stability is obtained for bounded feedback gains, one logically expects to be able to find out a stability criterion that works "uniformly" with respect to k, including $k = +\infty$. Let us rewrite (7.69) in state space form as

$$\begin{cases} z \in (\mathscr{NC}) \stackrel{\Delta}{=} \{x \ | x < 0\} : \dot{z}(t) = A_c z(t) + \begin{pmatrix} 0 \\ \frac{k}{m} x(t) \end{pmatrix} \\ z \in (\mathscr{C}) \stackrel{\Delta}{=} \{x \ | x \geq 0\} : \quad \dot{z}(t) = A_c z(t), \end{cases} \tag{7.76}$$

[25] This last point will be important to assure *via* a suitable controller when one wants to stabilize a system on a surface.

where $z = \left(x - \frac{\lambda_1 x_d}{\lambda_1 + k}, \dot{x}\right)^T$, $A_c = \begin{pmatrix} 0 & 1 \\ \frac{-1}{m}(\lambda_1 + k) & \frac{-\lambda_2}{m} \end{pmatrix}$. Clearly, the choice of the first component of z stems from the fact that we want to stabilize the system in contact with the environment. Moreover, from (7.69) one sees that the equilibrium point of the first equation belongs to $(\mathscr{C})$, which means that the system in (7.76) possesses in fact only one equilibrium point, i.e. $z^T = (0, 0)$ (the uniqueness holds for any value of x_d; when $x_d = 0$ both equations in (7.69) have the same equilibrium point $(x, \dot{x}) = (0, 0)$). Stability of A_c is independent of k since its eigenvalues are either real strictly negative or with real part equal to $\frac{-\lambda_2}{2m}$. In this way, for any $Q_c = Q_c^T > 0$ there always exists $P = P^T > 0$ such that $A_c^T P + P A_c = -Q_c$. Since we want to stabilize the equilibrium point $z = 0$, we choose a Lyapunov function candidate as $V(z) = z^T P z$. Along trajectories in $(\mathscr{NC})$ we get $\dot{V}(t) = -z(t)^T Q_c z(t) + z(t)^T P \begin{pmatrix} 0 \\ \frac{2k}{m} x(t) \end{pmatrix}$. For simplicity of the analysis, let us choose $x_d = 0$. Then we can write $\dot{V}(t) = -z(t)^T Q_c z(t) + z(t)^T P K z(t) \stackrel{\Delta}{=} -z(t)^T \bar{Q}_c z(t)$, with $K \stackrel{\Delta}{=} \begin{pmatrix} 0 & 0 \\ \frac{2k}{m} & 0 \end{pmatrix}$. Simple calculations yield:

$$Q_c = \begin{bmatrix} 2\frac{\lambda_1 + k}{m} p_{12} & \frac{\lambda_2}{m} p_{12} + \frac{\lambda_1 + k}{m} p_{22} - p_{11} \\ \frac{\lambda_2}{m} p_{12} + \frac{\lambda_1 + k}{m} p_{22} - p_{11} & 2\left(\frac{\lambda_2}{m} p_{22} - p_{12}\right) \end{bmatrix} \tag{7.77}$$

$$Q_{nc} = \begin{bmatrix} \frac{2\lambda_1}{m} p_{12} & \frac{\lambda_2}{m} p_{12} + \frac{\lambda_1}{m} p_{22} - p_{11} \\ \frac{\lambda_2}{m} p_{12} + \frac{\lambda_1}{m} p_{22} - p_{11} & 2\left(\frac{\lambda_2}{m} p_{22} - p_{12}\right) \end{bmatrix}, \tag{7.78}$$

where Q_{nc} is the symmetric part of the matrix $\bar{Q}_c$, that is independent of k. It is worth noting that only the skew-symmetric part of $\bar{Q}_c$ depends on k. Thus a necessary condition for Q_c to be positive definite is that:

- $\frac{\lambda_1 + k}{m} p_{12} > 0$
- $\det(Q_c) = 4\frac{\lambda_1 + k}{m} p_{12}\left(\frac{\lambda_2}{m} p_{22} - p_{12}\right) - \left(\frac{\lambda_2}{m} p_{12} + \frac{\lambda_1 + k}{m} p_{22} - p_{11}\right)^2 > 0.$

For Q_{nc} the necessary conditions are the following:

- $\frac{2\lambda_1}{m} p_{12} > 0$
- $\det(Q_{nc}) = 4\frac{\lambda_1}{m} p_{12}\left(\frac{\lambda_2}{m} p_{22} - p_{12}\right) - \left(\frac{\lambda_2}{m} p_{12} + \frac{\lambda_1}{m} p_{22} - p_{11}\right)^2 > 0.$

Our aim in this section is to examine the conditions such that the simple system (7.69) is Lyapunov quadratically stable, and in particular to find out which kind of conditions this implies on the feedback gains. As shown below, the following result is true ($\lambda_{\min}(P)$ denotes the minimum eigenvalue of the matrix P):

Proposition 7.4 *[222] Consider the one degree-of-freedom closed-loop equations in (7.69) with $x_d = 0$. Then quadratic stability of the system implies conditions such that when the environment's stiffness k grows unbounded, then the feedback*

gains λ_1 and/or λ_2 have to be chosen of order $\geq k^\beta$, $\beta \geq \frac{1}{2}$ to guarantee that the solution P of the Lyapunov equation remains bounded away from singularities (i.e., $\lambda_{\min}(P) \geq \delta > 0$ for some δ) and that the matrices Q_c and Q_{nc} remain positive definite.

Remark 7.11 Clearly when $x_d = 0$ the system in (7.69) can be analyzed considering the first equation only provided the initial condition $x(0)$ is negative (which is the only possible choice when $k = +\infty$). Then a simple choice of feedback gains implies that the mass never collides with the environment. The above conclusions come from the fact that the analysis is led considering *both* equations in (7.69), i.e. we require the derivative of a Lyapunov function to be negative definite along two vector fields at the same time.

Proof (of Proposition 7.4) Starting from the Lyapunov equation, one may first fix Q_c as a positive definite matrix and then try to calculate the unique corresponding positive definite P [1229, Lemma 42, Chap. 5] . A second way to attack the problem is to pick a $P > 0$ and study the properties of the resulting Q_c [1229, p.198]. In fact, instead of choosing a $Q_c > 0$ and solving the Lyapunov equation for P, we rather consider a matrix P and find conditions such that the corresponding Q_c is positive definite, together with Q_{nc}. Thus we prove that the only way for P not to tend towards a singular matrix while keeping $Q_c > 0$ and $Q_{nc} > 0$ when k increases is to take the gain λ_1 of order k^2. The above determinants can be written in the following way:

$$\det(Q_{nc}) = 4\frac{\lambda_1}{m}(p_{11}p_{22} - p_{12}^2) - (\frac{\lambda_1}{m}p_{22} + p_{11} - \frac{\lambda_2}{m}p_{12})^2$$

$$\begin{aligned}\det(Q_c) &= 4\frac{\lambda_1 + k}{m}(p_{11}p_{22} - p_{12}^2) - (\frac{\lambda_1 + k}{m}p_{22} + p_{11} - \frac{\lambda_2}{m}p_{12})^2 \\ &= -\frac{1}{m^2}(\lambda_1 p_{22} + mp_{11} - \lambda_2 p_{12})^2 - 2\frac{kp_{22}}{m^2}(\lambda_1 p_{22} + mp_{11} - \lambda_2 p_{12}) \\ &\quad + 4\frac{\lambda_1 + k}{m}(p_{11}p_{22} - p_{12}^2) - \left(\frac{kp_{22}}{m}\right)^2.\end{aligned}$$

Let us denote $Y \stackrel{\Delta}{=} \lambda_1 p_{22} + mp_{11} - \lambda_2 p_{12}$ and $|P| = p_{11}p_{22} - p_{12}^2$ then :

- $\det(Q_{nc}) > 0 \iff 4\lambda_1 m|P| - Y^2 > 0$
- $\det(Q_c) > 0 \iff Y^2 + 2kp_{22}Y - 4(\lambda_1 + k)m|P| + (kp_{22})^2 < 0.$

We deduce that Y has to satisfy the following inequalities:

$$\begin{cases} -2\sqrt{m\lambda_1|P|} < Y < 2\sqrt{m\lambda_1|P|} \\ -k\,p_{22} - 2\sqrt{m(\lambda_1 + k)|P|} < Y < -k\,p_{22} + 2\sqrt{m(\lambda_1 + k)|P|}. \end{cases} \tag{7.79}$$

Since $-k\,p_{22} - 2\sqrt{m(\lambda_1 + k)|P|} < -2\sqrt{m\lambda_1|P|}$ there exists a solution for Y if and only if $-2\sqrt{m\lambda_1|P|} < -k\,p_{22} + 2\sqrt{m(\lambda_1 + k)|P|}$, which is found after some

manipulations to be equivalent to the following conditions:

$$\begin{cases} 2\Lambda_k^2\, p_{11} - 2\sqrt{\Lambda_k^2(\Lambda_k^2\, p_{11}^2 - p_{12}^2)} < p_{22} < 2\Lambda_k^2\, p_{11} + 2\sqrt{\Lambda_k^2(\Lambda_k^2\, p_{11}^2 - p_{12}^2)} \\ p_{12} < \Lambda_k\, p_{11}. \end{cases} \tag{7.80}$$

with $\Lambda_k = \frac{\sqrt{m(\lambda_1+k)}+\sqrt{m\lambda_1}}{k}$. Notice that by choosing $p_{22} = 2\Lambda_k^2 p_{11}$ we can find P that satisfies (7.80) and that is positive-definite. From (7.79), Y satisfies the following inequalities:

$$-2\sqrt{m\lambda_1|P|} < Y < \min(-k\, p_{22} + 2\sqrt{m(\lambda_1+k)|P|}, 2\sqrt{m\lambda_1|P|}). \tag{7.81}$$

We can prove that $\lambda_{\min}(P) \leq p_{22}$ and $\lambda_{\max}(P) \geq p_{11}$ from which we deduce that:

$$\frac{\lambda_{\max}(P)}{\lambda_{\min}(P)} \geq \frac{p_{11}}{p_{22}}. \tag{7.82}$$

From (7.80), we can write $p_{22} < 4\Lambda_k^2\, p_{11}$, thus P has bounded entries when p_{11} is bounded and the above conditions are fulfilled. Then if p_{11} is a finite real number the conditions of existence of Y imply that the coefficients p_{12} and p_{22} tend to zero when the stiffness of the environment becomes infinite, rendering the matrix P singular. Let us note that the stability analysis then becomes asymptotically (i.e. when $k \to +\infty$) meaningless since Q_{nc} in (7.78) has bounded entries. The only way to avoid this problem is to increase the gain λ_1 such that the coefficient Λ_k does not tend towards zero when the stiffness increases, i.e. λ_1 has to be chosen of order $\geq k^2$. Assume that this is done so that P is well conditioned, and let us examine how λ_2 has to be chosen. λ_2 may be found by using (7.81):

$$\frac{mp_{11} + \lambda_1 p_{22} - Y_{\max}}{p_{12}} < \lambda_2 < \frac{mp_{11} + \lambda_1 p_{22} + 2\sqrt{m\lambda_1|P|}}{p_{12}}, \tag{7.83}$$

where $Y_{\max} = \min(-k\, p_{22} + 2\sqrt{m(\lambda_1+k)|P|}, 2\sqrt{m\lambda_1|P|})$. This implies that when λ_1 is of order k^2 and k grows unbounded, the gain λ_2 becomes infinite too. Let us examine what happens if we allow p_{11} to be proportional to k^α, $\alpha > 1$. Then p_{22} may be chosen of order $\leq k^{\alpha-1}$ from (7.80). Also, p_{12} will be of order $\leq k^{\alpha-\frac{1}{2}}$ from the second condition in (7.80). Now from (7.83) we have the following: if $Y_{\max} \leq 0$ then obviously λ_2 is of order $k^{\frac{1}{2}}$ as $k \to +\infty$. If $Y_{\max} > 0$, let us analyze the case when $Y_{\max} = 2\sqrt{m\lambda_1|P|}$: this value is maximum when p_{12} is minimum, hence bounded, and when both p_{11} and p_{22} are maximum, i.e. respectively, of orders k^α and $k^{\alpha-1}$; then $Y_{\max}$ is of order $k^{\alpha-\frac{1}{2}}$ so that λ_2 grows as $k^{\frac{1}{2}}$. Now if $Y_{\max} \stackrel{\Delta}{=} A = -k\, p_{22} + 2\sqrt{m(\lambda_1+k)|P|}$ that we assume > 0: then necessarily since $p_{22} \geq 0$, the second term in A is at least of the same order as kp_{22} in k as k grows unbounded. Thus at most the order of $Y_{\max}$ will be that of the second term $2\sqrt{m(\lambda_1+k)|P|}$, which is found to be at most k^α. But if this is the case then this

term dominates $2\sqrt{m\lambda_1|P|}$ and asymptotically (in k) $Y_{\max}$ will necessarily be equal to this last term, hence we are back to the previous case. Now if the order of A is k^γ with $\gamma < \alpha$ then p_{11} will asymptotically dominate $Y_{\max}$ and the left-hand side of (7.83) is asymptotically of order $k^{\frac{1}{2}}$. Thus λ_1 may be chosen bounded but λ_2 will grow unbounded to guarantee $\lambda_{\min} P \geq \delta > 0$ for any arbitrarily small but fixed δ and $Q_c > 0$, $Q_{nc} > 0$.

7.6.4 A Stiffness-Independent Convergence Analysis

First, let us consider the system in (7.71). Let us take the Poincaré section $\Sigma^+ = \left\{(x, \dot{x})|x = 0, \dot{x}(t_k^+)\right\}$. Notice that if $x(0) > 0$, then the sequence of impact times $\{t_k\}$ is infinite (this can be easily shown by studying the vector field between the impacts, which forces the system to attain in finite time the constraint surface $x = 0$ whatever bounded initial conditions one may choose). The impact Poincaré map $P_\Sigma : \dot{x}(t_k^+) \to \dot{x}(t_{k+1}^+)$ is thus well defined. However it is not explicitly calculable, despite the simplicity of the dynamics. This is due to the nonzero dissipation during flight-times. Let us choose $V_\Sigma(k) = \frac{1}{2}m\dot{x}^2(t_k^+)$. We prove that $P_\Sigma(\cdot)$ is Lyapunov stable with $V_\Sigma(\cdot)$ as a Lyapunov function as follows. Consider the function $V(x - x_d, \dot{x}) = \frac{1}{2}m\dot{x}^2 + \frac{1}{2}\lambda_1(x - x_d)^2$. Along free-motion trajectories of (7.71) one obtains $\dot{V}(t) = -\lambda_2\dot{x}(t)^2$ and at the impact times the jump $\sigma_V(t_k) = \frac{1}{2}\left[\dot{x}^2(t_k^+) - \dot{x}^2(t_k^-)\right] = 0$. Hence we obtain:

$$V(t_{k+1}^+) - V(t_k^+) = -\lambda_2 \int_{(t_k, t_{k+1})} \dot{x}(\tau)^2 d\tau \leq 0. \tag{7.84}$$

Now from the fact that $V(t_{k+1}^+) - V(t_k^+) = V_\Sigma(k+1) - V_\Sigma(k) \leq 0$, we conclude the proof. This stability result suggests[26] that one should be able to analyze the stability of the system in (7.69) for any $k \geq 0$, without the drawbacks encountered in the previous section.

7.6.4.1 Asymptotic Convergence Analysis

Let us propose now a convergence analysis different from the one in Sect. 7.6.3 to prove that the equilibrium point of (7.69) is asymptotically reached for any initial condition and any value of the feedback gains, independently of the value of k. The particular feature of the analysis is that it extends naturally to the rigid environment case (i.e. $k = +\infty$), contrary to the foregoing one. Roughly speaking, we consider a particular section of the phase-plane: $x = 0$. Then we analyze the mass velocity

[26] Notice that we have not proved the *asymptotic* stability of P_Σ.

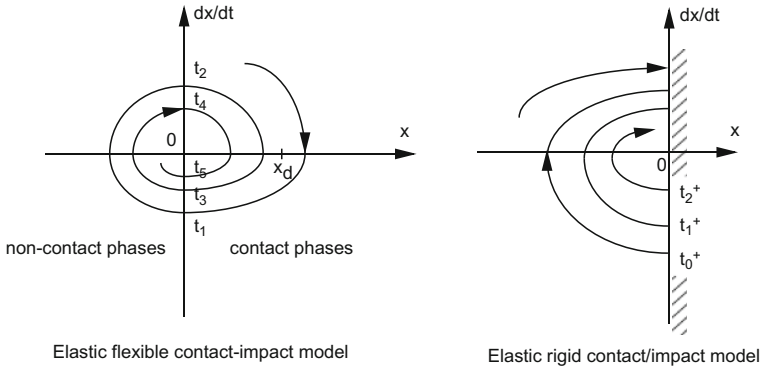

Fig. 7.9 Times t_i and t_k^+

at the instants t_i when the trajectories cross this section.[27] We use the fact that these times define a sequence along which the kinetic energy is nonincreasing. It follows that if $\{t_i\}$ is an infinite sequence, the velocity must converge to zero when $i \to +\infty$. This leads to a contradiction and there is a finite number of bounces, so that both $\tilde{x}$ and $\dot{x}$ converge to zero. To clarify the notations the instants t_i and t_k are depicted in Fig. 7.9. We assume that the mass makes contact with the environment at $t = t_i$, loses contact at $t = t_{i+1}, i \in \mathbb{N}$, and that contact occurs at $x = 0$. Thus contact occurs on intervals $[t_{2i}, t_{2i+1}]$, and free motion on intervals $[t_{2i+1}, t_{2i+2}]$. Let us consider the positive definite functions:

$$V_c(x, \dot{x}) = \frac{1}{2}m\dot{x}^2 + \frac{1}{2}(\lambda_1 + k)\left(x - \frac{\lambda_1 x_d}{\lambda_1 + k}\right)^2 \tag{7.85}$$

and:

$$V_{nc}(x, \dot{x}) = \frac{1}{2}m\dot{x}^2 + \frac{1}{2}\lambda_1(x - x_d)^2. \tag{7.86}$$

On intervals $[t_{2i}, t_{2i+1}]$, $\dot{V}_c(t) = -\lambda_2\dot{x}(t)^2$. On intervals $[t_{2i+1}, t_{2i+2}]$, $\dot{V}_{nc}(t) = -\lambda_2\dot{x}(t)^2$. Let $T(t)$ denote the system's kinetic energy. From the fact that $V_c(t_{2i+1}) - V_c(t_{2i}) = T(t_{2i+1}) - T(t_{2i})$ and $V_{nc}(t_{2i+2}) - V_{nc}(t_{2i+1}) = T(t_{2i+2}) - T(t_{2i+1})$, we deduce that for all i, $T(t_{i+1}) - T(t_i) < 0$, hence $|\dot{x}(t_{i+1})| < |\dot{x}(t_i)|$. The same inequalities hold for V_c and V_{nc}. Now notice that there are two situations: either the sequence of instants t_i is finite (the bounces stop after a finite time t_{2N}, $N < +\infty$, and since $x_d > 0, x(t) > 0$ for all $t > t_{2N}$), or this sequence is infinite i.e. $N = +\infty$.

• If $N < +\infty$, then for $t > t_{2N}$ the system is governed by the second equation in (7.69) (indeed each time the mass is "outside" the environment, it necessarily collides

[27] We do not use the notation t_k because the t_i's may correspond to detachment. In fact if contact is made at t_{2i} and lost at t_{2i+1}, then $t_k = t_{2i}$.

again after a finite time) and we conclude that $x \to \frac{\lambda_1 x_d}{\lambda_1 + k}, \dot{x} \to 0$ asymptotically, globally, and uniformly.

• Assume that $N = +\infty$. Since the kinetic energy is a positive definite function of the velocity that is nonincreasing at times t_i, $T(t_i)$ converges as $i \to +\infty$, and so does $\dot{x}(t_i)$. Suppose that $|\dot{x}(t_i)| \to |\dot{x}_{ss}|$ with $|\dot{x}_{ss}| \geq \delta > 0$ (the ss subscript is for steady-state value). Now $\delta > 0$ and since $\text{sgn}(\dot{x}(t_i)) = -\text{sgn}(\dot{x}(t_{i+1}))$, $x(t_i) = x(t_{i+1}) = 0$, the length of the orbit between t_i and t_{i+1} is strictly positive. Since the flow of both equations in (7.69) is exponential and bounded for bounded feedback gains and stiffness k, clearly $\lambda[t_i, t_{i+1}] \stackrel{\Delta}{=} \mu_{i+1} > 0$ and $T(t_i) - T(t_{i+1}) \stackrel{\Delta}{=} \beta_{i+1} = \lambda_2 \int_{t_i}^{t_{i+1}} \dot{x}^2 dt > 0$. Note that for fixed and bounded coefficients in (7.69) μ_i and β_i depend only on δ (the other "initial" condition on the position remaining fixed at the times t_i) so that in particular $\beta_i \geq \beta(\delta) > 0$ for all $i \geq 0$ and $\delta > 0$. Since $T(t_i)$ is nonincreasing, its limit value is its minimum value and for all $i \geq 0$, $|\dot{x}(t_i)| \geq |\dot{x}_{ss}| > \delta$. From the strictly positive variation of the kinetic energy we deduce that $\dot{x}^2(t_{i+1}) = \dot{x}^2(t_i) - \frac{2\beta_i}{m}$, so that $\dot{x}_i^2 = \dot{x}_0^2 - \sum_{j=0}^{j=i-1} \beta_j$. Therefore, from the fact that the β_i's are strictly positive, we deduce that $|\dot{x}(t_i)|$ cannot converge towards a strictly positive $|\dot{x}_{ss}|$. Since however $T(t_i)$ and thus $\dot{x}(t_i)$ converge, we deduce that the only possible limit value for the velocity is $\dot{x}_{ss} = 0$. Notice that if $\delta = 0$, then both μ_i and β_i may asymptotically take arbitrarily small values and $\dot{x}_i^2 = \dot{x}_0^2 - \sum_{j=0}^{j=i-1} \beta_j$ no longer leads to a contradiction. Thus we have shown that if there is an infinite number of bounces, the value of the velocity when contact is established or lost ($x(t_i) = 0$) is bounded and tends to zero.

Let us now consider an arbitrarily large integer i such that $|\dot{x}(t_i)|$ is arbitrarily small, or in other words, for any $\varepsilon > 0$, there exists $N(\varepsilon) > 0$ such that $i > N$ implies $|\dot{x}(t_i)| < \varepsilon$. We shall denote $\Delta_{i+1} \stackrel{\Delta}{=} t_{i+1} - t_i$. First note that from any of the two dynamic equations in (7.69) we get $\Delta_i \leq \Delta_{\max} < +\infty$ for some $\Delta_{\max}$ since the "initial" velocities at times t_i are bounded and tend towards zero. Now we use the fact that both vector fields in (7.69) are explicitly integrable; assume that we place ourselves at t_{2i} such that $\dot{x}(t_{2i}) = \varepsilon > 0$, hence the system is in a contact phase for some time since $\ddot{x}(t_i) = \lambda_1 x_d - \lambda_2 \varepsilon > 0$ for some $\varepsilon > 0$. We thus consider the second equation in (7.69); If the negative roots r_1 and r_2 of the characteristic equation are real and separated, $r_1 < r_2$, then the solution can be expressed as (recall that $x(t_i) = 0$ for all i): $x(t) = \gamma_1 e^{r_1(t-t_{2i})} + \gamma_2 e^{r_2(t-t_{2i})} + \bar{x}_d$, with $\bar{x}_d = \frac{\lambda_1 x_d}{\lambda_1 + k}$, and $\gamma_1 = -\gamma_2 - \bar{x}_d$, $\gamma_1 r_1 = -\gamma_2 r_2 + \varepsilon$. Since we assume *a priori* that the sequence $\{t_i\}$ is infinite, t_{2i+1} exists and we get:

$$\dot{x}(t_{2i+1}) = \gamma_1 r_1 (e^{r_1 \Delta_{2i+1}} - (1 - \varepsilon) e^{r_2 \Delta_{2i+1}}). \tag{7.87}$$

From the monotonicity of $\{|\dot{x}(t_i)|\}$ and its convergence, we deduce that $|\dot{x}(t_{2i+1})| \leq \varepsilon$. Assume now that the sequence $\{\Delta_{2i+1}\}$ does not converge towards zero, i.e. there exists $\Delta > 0$ such that $\Delta_{2i+1} \geq \Delta$ for all i. Then we get for any $\varepsilon > 0$:

$$|(1 - \frac{\varepsilon}{\gamma_1 r_1}) e^{(r_2 - r_1)\Delta_{2i+1}} - 1| \geq \eta(r_1, r_2, \Delta) > 0, \tag{7.88}$$

and $e^{r_1 \Delta_{2i+1}} \geq \kappa(\Delta_{\max}, r_1) > 0$. From (7.87) we get $|\gamma_1 r_1 \kappa(\Delta_{\max}, r_1)\eta(r_1, r_2, \Delta)| < \varepsilon$, which cannot be true for ε small enough (note that the roots as well as Δ and $\Delta_{\max}$ do not depend on ε). Since ε is arbitrarily small, we deduce that $\Delta_{2i+1} \to 0$ as $i \to +\infty$. A similar reasoning may be done for the case when $r_1 = r_2$. When the roots are complex conjugate $r_1 = r + j\omega$, $r_2 = r - j\omega$, the solution is given by $x(t) = \gamma e^{r(t-t_{2i})} \cos(\omega(t - t_{2i}) + \varphi) + \bar{x}_d$, with $\gamma = -\frac{\bar{x}_d}{\cos\varphi}$ and $\tan\varphi = \frac{\varepsilon + \bar{x}_d r}{\bar{x}_d \omega}$. Now we obtain:

$$\dot{x}(t_{2i+1}) = \gamma e^{r\Delta_{2i+1}} \sqrt{r^2 + \omega^2} \cos(\omega \Delta_{2i+1} + \varphi + \Phi), \tag{7.89}$$

with $\tan\Phi = \frac{\omega}{r}$. Using the same arguments as in the real roots case, one sees that for $\dot{x}(t_{2i+1})$ to be arbitrarily small, we must have $\cos(\omega\Delta_{2i+1} + \varphi + \Phi)$ arbitrarily small, from which we deduce that $\omega\Delta_{2i+1} + \varphi + \Phi$ is arbitrarily close to $\frac{\pi}{2}$. Now for ε arbitrarily small, $\tan\varphi \to \frac{r}{\omega}$, and $\tan(\varphi + \Phi) \to +\infty$. But since Δ_{2i+1} is assumed to be bounded away from zero (and strictly positive by definition), $\tan(\frac{\pi}{2} - \omega\Delta_{2i+1})$ is clearly bounded. Thus by contradiction we deduce that $\{\Delta_{2i+1}\}$ converges to zero. Now exactly the same reasoning may be done for the case of noncontact phases. It follows that if the velocities at times t_i converge towards zero, so do the intervals Δ_i. Since again the sequence $\{t_i\}$ is infinite, if its limit is infinite also then $(0, 0)$ is an equilibrium point of the system in (7.69). Clearly this is not the case, except if $x_d = 0$ (for the sake of brevity this case is not analyzed here; the analysis can be done using similar arguments). In conclusion, we have proved that the sequence $\{t_i\}$ is either finite, or possesses a finite accumulation point. In both cases, we deduce that the equilibrium point of the system in (7.69) is asymptotically attained.

7.6.4.2 Relationship with the Case of a Rigid Environment

In Sects. 7.6.2 and 7.6.3, we have seen that some stability analysis may not be suitable in the sense that the conditions deduced on the feedback gains are obviously useless in practice as soon as the stiffness becomes too large. However, the analysis in Sect. 7.6.4.1 proves that the equilibrium point of the system in (7.69) will be attained for any (strictly positive) value of the feedback gains, and any (bounded but arbitrarily large) value of the stiffness k. In the rigid limit case, the system is described by the equations in (7.71). Note that by considering the elastic dynamical problem in (7.71) we get as long as contact is maintained $x \equiv \dot{x} \equiv 0$, so that $V_c(x, \dot{x}) = \frac{1}{2}kx^2 = 0$ since the elastic potential energy vanishes. The only things that are modified in the rigid case are that since the intervals $[t_{2i}, t_{2i+1}] \to \{t_{2i}\}$, the distinction between instants t_{2i} and t_{2i+1} becomes worthless (we can take the notation $t_{2i} = t_k$). Consequently, $\mu_{2i+1} = \beta_{2i+1} = 0$ while $\mu_{2i} > 0$ and $\beta_{2i} > 0$. Basing on the analytical tools we have outlined one can easily adapt the above analysis when $k = +\infty$. If $N < +\infty$, then necessarily after a finite time $x \equiv \dot{x} \equiv 0$. Notice that as long as the restitution coefficient $e_n > 0$, then $\{t_k\}$ is an infinite sequence except if $\dot{x}(0^-) = 0$ and $x(0) = 0$. If $N = +\infty$, $T(t_k)$ converges as $i \to +\infty$, hence $\dot{x}(t_k) \to 0$. Note that only the flow of the first equation in (7.69) has to be considered in the reasoning. The remaining

arguments are the same. One sees that the stability analysis is simpler in the rigid case, due to the fact that the contact equations are algebraic, no longer dynamical. This enables us to study the variation of $V_{nc}(\cdot)$ not only on smooth dynamics but also "during" contact, i.e. at impact times, i.e. in fact for all $t \geq 0$.[28] Hence only $V_{nc}(\cdot)$ is needed to study the limit rigid case, since the contact phases reduce to instants t_k and with $\sigma_{V_c}(t_k) = 0$. It is finally noteworthy that since $\dot{V}_{nc}(t) \leq 0$ on (t_k, t_{k+1}) and $\sigma_{V_{nc}}(t_k) = T_L(t_k) = 0$, one gets $V_{nc}(t_{k+1}^+) \leq V_{nc}(t_k^+)$ for all $k \geq 0$. Now since the restriction of $V_{nc}(\cdot)$ to the surface $\Sigma = \{(x, \dot{x}) | x = 0\}$, is such that $V_{nc,\Sigma}(t_k) = V_{nc}(t_k)$, one deduces that $V_{nc,\Sigma}(\cdot)$ is a Lyapunov function for the impact Poincaré map P_Σ. Therefore, the stability analysis made in Sect. 7.6.4 yields in the limit as $k \to +\infty$ Lyapunov stability of the map P_Σ. We thus have proved the following:

Proposition 7.5 *[222] Consider the closed-loop equations in (7.69). Then for any* $\lambda_1 > 0$, $\lambda_2 > 0$, $k \in [0, +\infty]$, *and for all initial conditions* $x(0)$, $\dot{x}(0)$, $x \to \frac{\lambda_1 x_d}{\lambda_1 + k}$ *and* $\dot{x} \to 0$ *as* $t \to +\infty$.

A distinction has to be made between two different cases of analysis: we may consider (i) either an arbitrarily large but bounded k, (ii) a k that tends to infinity (that is implicitly a sequence of stiffnesses k_n with unbounded limit together with the corresponding dynamics). Clearly Proposition 7.5 can be concluded from the analysis in Sects. 7.6.2 and 7.6.3 in case (i), but not in case (ii). The utility of the analysis proposed in Sect. 7.6.4 is to enable us to draw conclusions in both the compliant and the rigid environment cases within a unique framework.

7.7 Stability of Linear Complementarity Systems

Sections 7.5 and 7.6 deal with mechanical systems with unilateral constraints and impacts. Let us focus on LCS as introduced in Sect. 5.4.4, where their well-posedness and controllability have been analysed. The Lyapunov stability of equilibria for various kinds of LCS has been tackled in [213–215, 252, 256, 463]. Consider the dynamical system in (5.128) with zero input $u(t)$. Some of these results assume that the feedthrough matrix D is a P-matrix [256], some others that $D = 0$ [463], or that the quadruple (A, B, C, D) is dissipative [252], which allows for $D \succeq 0$. First of all recall that the fixed points of the autonomous LCS in (5.128) are the solutions of the generalized equation (given here as a mixed LCP):

$$\begin{cases} 0 = Ax^\star + B\lambda^\star \\ 0 \leq \lambda^\star \perp w^\star = Cx^\star + D\lambda^\star \geq 0. \end{cases} \tag{7.90}$$

[28] This is not the case for the compliant model since $\dot{V}_{nc}(t) = -\lambda_2 \dot{x}(t)^2 - k\dot{x}(t)x(t)$ during contact phases and $\dot{V}_c(t) = -\lambda_2 \dot{x}(t)^2 + k\dot{x}(t)x(t)$ during free-motion phases.

Let us summarize results from [256] on one hand, and from [463] on the other hand. D being a P-matrix implies that the complementarity conditions of the LCS form a uniquely solvable LCP, whose solution is a piecewise linear function of the state. $D = 0$ means that the LCS is a differential inclusion of the generic form $\dot{x}(t) + f(x(t), t) \in -N_K(x(t))$, with K a closed convex set. In both cases we deal with continuous solutions, see Theorem 5.11. The first result which we will state, needs few definitions which extend the classical, unconstrained, Lyapunov's second method. They apply to a general convex closed set $K \subset \mathbb{R}^n$ and nonlinear single-valued vector fields $f(\cdot, \cdot)$; however, we choose here a particular case where $K = \{z \in \mathbb{R}^n | Cz + d \geq 0\}$ for some $d \in \mathbb{R}^n$, i.e. K is not necessarily a cone, and the vector field is linear invariant. First, we extend the notion of copositive matrices of Definition 5.4. A matrix $P \in \mathbb{R}^{n\times n}$ is said to be copositive on K if $x^T Px \geq 0$, for all $x \in K$. It is said to be strictly copositive on K if $x^T Px > 0$ for all $x \in K\backslash\{0\}$. Let us denote by $\mathscr{P}_K$ (resp. $\mathscr{P}_K^+$) the set of copositive (resp. strictly copositive) matrices on K. Let us also denote by $\mathscr{P}_K^{++}$ the set of matrices satisfying $\mathscr{P}_K^{++} = \left\{B \in \mathbb{R}^{n\times n} \mid \inf_{x\in K\backslash\{0\}} \frac{x^T Bx}{\|x\|^2} > 0\right\}$. It is clear that $\mathscr{P}_K^{++} \subset \mathscr{P}_K^+ \subset \mathscr{P}_K$, and $K_1 \subset K_2 \Rightarrow \mathscr{P}_{K_2}^{++} \subset \mathscr{P}_{K_1}^{++}$. If K is a cone then $\mathscr{P}_K^{++} = \mathscr{P}_K^+$ [463, Proposition 1]. Let us now denote by $\mathscr{L}_K$ the set of Lyapunov positive stable matrices on K and by $\mathscr{L}_K^{++}$ the set of Lyapunov positive strictly-stable matrices on K. They are defined as

$$\begin{aligned}
\mathscr{L}_K &= \left\{A \in I\!R^{n\times n} | \exists P \in \mathscr{P}_K^{++} \text{ such that } (I - [P + P^T])(\partial K) \subset K \right. \\
&\qquad \left. \text{and } PA + A^T P \in \mathscr{P}_K\right\}. \\
\mathscr{L}_K^{++} &= \left\{A \in I\!R^{n\times n} | \exists P \in \mathscr{P}_K^{++} \text{ such that } (I - [P + P^T])(\partial K) \subset K \right. \\
&\qquad \left. \text{and } PA + A^T P \in \mathscr{P}_K^{++}\right\}.
\end{aligned} \tag{7.91}$$

We have $(I - [P + P^T])(\partial K) = \{z \in \mathbb{R}^n | z = (I - [P + P^T])y \text{ for } y \in \partial K\}$. Let $V(x) = \frac{1}{2}x^T(P + P^T)x$. The condition $(I - [P + P^T])(\partial K) \subset K$ implies that $-\nabla V(x) \in T_K(x)$[29] on ∂K: it characterizes the orientation of the level sets of $V(x)$ on the boundary ∂K. If K satisfies the requirements (B.7) may be used to rewrite this condition. Let us note that P needs not be symmetric.

Theorem 7.7 (463, Theorems 1 and 5) *Consider the multivalued complementarity system $\dot{x}(t) = Ax(t) + B\lambda(t)$, $0 \leq \lambda(t) \perp w(x(t)) = Cx(t) + d \geq 0$, $x(0) = x_0$. Suppose that $0 \in K$, $x_0 \in K$, and $B = C^T$. The system has unique continuous solutions with right-continuous derivatives. If $A \in \mathscr{L}_K$ the trivial solution $x^* = 0$ is Lyapunov stable. If $A \in \mathscr{L}_K^{++}$ it is asymptotically Lyapunov stable.*

The systems we consider in Theorem 7.7 are as in (5.134) and can therefore be obtained from LCS doing Assumption 2. They are differential inclusions. As alluded to above, Theorem 7.7 also applies to systems with nonlinear vector field [463, Theorem 7] and with general closed convex set K (not necessarily polyhedral). Jumps are not included in the stability analysis, they should be with state jump rules as in (5.144) and (5.145).

[29] The tangent cone to K at x.

The next result assumes the feedthrough matrix D is a P-matrix. This secures that the multiplier $\lambda(\cdot)$ is a Lipschitz continuous function of the state x, see Theorem 5.4. Thus $\lambda(x)$ has a directional derivative $\lambda'(x;d) \stackrel{\Delta}{=} \lim_{\tau\to 0,\tau>0} \frac{\lambda(x+\tau d)-\lambda(x)}{\tau}$. The LCS map is defined as $\mathrm{SOL}'_{LCS}(x) = \begin{pmatrix} \lambda(x) \\ \lambda'(x;dx) \end{pmatrix}$, with the direction $dx \stackrel{\Delta}{=} Ax + B\lambda(x)$. Its graph is denoted $\mathrm{GrSOL}'_{LCS}(x)$. The Lyapunov function is designed as $V(x) = (x^T, \lambda(x)^T) M \begin{pmatrix} x \\ \lambda(x) \end{pmatrix}$, $M = \begin{pmatrix} P & Q \\ Q^T & R \end{pmatrix}$, $P = P^T$, $R = R^T$. Let also $N = \begin{pmatrix} A^TP + PA & PB + A^TQ & Q \\ B^TP + Q^TA & Q^TB + B^TQ & R \\ Q^T & R & 0 \end{pmatrix}$. One also needs to define $\mathrm{GrSOL}_{CD} = \{(x, \lambda(x)) | 0 \le \lambda(x) \perp Cx + D\lambda(x) \ge 0\}$.

Theorem 7.8 *[256] Consider the autonomous LCS in (5.119), $x(0) = x_0$. Let D be a P-matrix. Assume that M is strictly copositive on GrSOL_{CD}. If $-N$ is copositive on $\mathrm{GrSOL}'_{LCS}(x)$, the fixed point $x^* = 0$ is Lyapunov stable. If $-N$ is strictly copositive on $\mathrm{GrSOL}'_{LCS}(x)$, the fixed point $x^* = 0$ is exponentially stable.*

It is interesting to see that both Theorems use copositive matrices, instead of the usual positive (semi) definite matrices of the Lyapunov equation.

7.8 Further Reading

It is shown in [147], using a similar "hybrid distance" as the one defined in (1.53) that a switching PD controller applied to the bouncing ball allows to asymptotically locally track some reference trajectory $(x_r(t), \dot{x}_r(t))$, which is itself a bouncing ball trajectory. The switching times are defined from the comparison of two quadratic functions of $(x - x_r, \dot{x} - \dot{x}_r)$ and $(x + x_r, \dot{x} + \dot{x}_r)$, respectively. Preliminary studies on rotorcrafts and aerial robots that may interact with compliant environments (unilateral spring) or rigid environment (complementarity conditions and kinematic restitution coefficient) may be found in [35, 420, 562, 799]. The same system as in Sect. 7.6 is considered in [511], with a linear spring-dashpot and discontinuous contact force (see Sect. 2.1.3.1). A switching contact/noncontact controller is designed for trajectory tracking, and the piecewise-linear closed-loop system is shown to be globally uniformly asymptotically stable under certain conditions relating the feedback gains and the contact parameters (stiffness and damping coefficients). Mills and co-workers studied the stability of manipulators colliding compliant environments in [758, 849, 852–854]. A Maxwell model in parallel with a linear spring is used in [852], and is augmented with a spring/daspot mounted in series with it and connected with a mass in [853]. This may be very rare instances in Control where authors consider compliant contact models which are not the basic spring-dahspot model with naive switching conditions (see Sect. 2.1.3). A linear dynamic model of the environment is also chosen in [849]. We note that the analysis made in Sect. 7.6.3

was originally motivated by the (sufficient) conditions of stability in [852], which indeed imply that the control gains diverge as the contact stiffness goes to infinity. Similar issues exist in [740].

$\rightsquigarrow$ *In view of the different rheological models presented in* Sects. 2.1, 2.2, 2.3 *and* 4.2.1, 4.2.2, *it could be useful to derive controllers which guarantee the stability of general tasks, for larger classes of contact/impact models.*

Further results on Lyapunov stability and LaSalle invariance of LCS and differential inclusions into normal cones to convex sets, may be found in [213–215, 252, 256, 463]. Some necessary conditions for stability known for smooth systems, are extended to a class of LCS in [464]. In particular the case where $D \succeq 0$ may be treated using dissipativity [214, 252]. The results in [214, 215] hold for larger classes of Lur'e set-valued systems. Closely related to complementarity systems and their stability, are *projected dynamical systems* [1316], see [212] for a complete analysis of the equivalences between these formalisms. An interesting topic concerns the use of the LCS formalism of the mass-spring-dashpot system we derived in Chap. 2, and the results on observability, observer design and closed-loop stability in [217, 514]. More generally, we try to take advantage of the maximal monotonicity of some compliant viscoelastoplastic models (see Sect. 2.3 for an introduction) for the sake of stabilization of contact–noncontact robotic tasks.

Chapter 8
Trajectory Tracking Feedback Control

This chapter is dedicated to the trajectory tracking control of a large class of frictionless Lagrangian systems with multiple unilateral constraints, complementarity conditions and impacts: rigid-joint rigid-body systems and flexible-joint rigid-body systems. The proposed controllers originate from [166, 220, 221], and aim at settling a general framework for the stability analysis of tracking control of complementarity Lagrangian systems. The complete stability analysis was achieved in [873, 874]. They may be considered as the extension of the fixed parameters, passivity-based controllers designed in [1119] and [223, 766] for Lagrangian systems without constraints. Juggling systems dynamics and observability issues are briefly reviewed at the end of the chapter.

8.1 Trajectory Tracking: Rigid-Joint Rigid-Body Systems

This section focuses on the problem of tracking control of complementarity Lagrangian systems subject to frictionless unilateral constraints whose dynamics are expressed as:

$$\begin{cases} M(X)\ddot{X} + C(X,\dot{X})\dot{X} + G(X) = U + \nabla f(X)\lambda_X, \\ 0 \leq \lambda_X \perp F(X) \geq 0, \\ \text{Collision rule}, \end{cases} \tag{8.1}$$

where $X(t) \in \mathbb{R}^n$ is the vector of generalized coordinates, $M(X) = M^T(X) \in \mathbb{R}^{n\times n}$ is the positive definite inertia matrix, $f(X) \in \mathbb{R}^m$ represents the signed distances to the constraints, $C(X, \dot{X})$ is the matrix containing Coriolis and centripetal forces, $G(X)$ contains conservative forces which derive from a potential, $\lambda_X \in \mathbb{R}^m$ is the vector of the Lagrangian multipliers associated with the constraints,[1] and $U \in \mathbb{R}^n$

[1] We denoted it $\lambda_{n,u}$ in (5.1). In this chapter we adopt a new notation because we will make a generalized coordinate change.

B. Brogliato, *Nonsmooth Mechanics*, Communications and Control Engineering,
DOI 10.1007/978-3-319-28664-8_8

is the vector of generalized torque inputs. For the sake of completeness we precise that ∇ denotes the Euclidean gradient $\nabla f(X) = (\nabla f_1(X), \ldots, \nabla f_m(X)) \in \mathbb{R}^{n\times m}$ where $\nabla f_i(X) \in \mathbb{R}^n$ represents the vector of partial derivatives of $f_i(\cdot)$ w.r.t. the components of X. We assume that the functions $f_i(\cdot)$ are continuously differentiable and that $\nabla f_i(X) \neq 0$ for all X with $f_i(X) = 0$, according to Definition 1.8. For any function $f(\cdot)$ the limit to the right at the instant t will be denoted by $g(t^+)$ and the limit to the left will be denoted by $g(t^-)$. A simple jump of the function $g(\cdot)$ at the moment $t = t_\ell$ is denoted as usual as: $\sigma_g(t_\ell) = g(t_\ell^+) - g(t_\ell^-)$. The Dirac measure at time t is δ_t. The admissible domain associated with the system (8.1) is the closed set Φ where the system can evolve and it is described as the finitely represented set:

$$\Phi = \{X \in \mathbb{R}^n \mid f(X) \geq 0\} = \bigcap_{1\leq i\leq m} \Phi_i,$$

where $\Phi_i = \{X \in \mathbb{R}^n \mid f_i(X) \geq 0\}$ considering that a vector is nonnegative if and only if all its components are nonnegative. In order to have a well-posed problem with a physical meaning we consider that Φ contains at least a closed ball of positive radius.

Definition 8.1 A singularity of the boundary $\mathrm{bd}(\Phi)$ of Φ is the intersection of two or more codimension one surfaces $\Sigma_i \subseteq \{X \in \mathbb{R}^n \mid f_i(X) = 0\}$.

It is obvious that $m > 1$ allows both simple impacts (when one constraint is involved) and multiple impacts (when singularities or surfaces of codimension larger than 1 are involved). Let us introduce the following notion of p_ε-impact, which will be useful for stability analysis.

Definition 8.2 Let $\varepsilon \geq 0$ be a fixed real number. We say that a p_ε-impact occurs at the instant t if

$$||f_I(X(t))|| \leq \varepsilon, \quad \prod_{i\in I} f_i(X(t)) = 0$$

where $I = \{i_1, i_2, \ldots, i_p\} \subset 1, \ldots, m$, $f_I(X) = (f_{i_1}(X), f_{i_2}(X), ..., f_{i_p}(X))^T$.

If $\varepsilon = 0$ the p surfaces Σ_i, $i \in I$ are stroked simultaneously and a $p-$impact occurs. When $\varepsilon > 0$ the system collides $\mathrm{bd}(\Phi)$ in a neighborhood of the intersection $\bigcap_{i\in I} \Sigma_i$.

Let us briefly recall that in Moreau's sweeping process framework, the tangent cone to $\Phi = \{X \in \mathbb{R}^n \mid f_i(X) \geq 0, \forall i = 1, \ldots, m\}$ at $X \in \mathbb{R}^n$ is defined as:

$$T_\Phi(X) = \{z \in \mathbb{R}^n \mid z^T \nabla f_i(X) \geq 0, \forall i = J(X)\}$$

where $J(X) \triangleq \{i \in \{1, \ldots, m\} \mid f_i(X) \leq 0\}$ is the index set of active constraints. When $X \in \Phi \setminus \mathrm{bd}(\Phi)$ one has $J(X) = \emptyset$ and $T_\Phi(X) = \mathbb{R}^n$. The normal cone to Φ at X is defined as the polar cone to $T_\Phi(X)$:

$$N_\Phi(X) = \{y \in \mathbb{R}^n \mid \forall z \in T_\Phi(X), y^T z \leq 0\} = (T_\Phi(X))^\circ.$$

Contrarily to Sect. 5.2, we do not use the notation $V(X)$ for the tangent cone, in order to avoid confusion with Lyapunov functions. Throughout this section the collision rule will be defined by Moreau's relation (see Sect. 5.2, Remark 5.7):

$$\dot{X}(t_\ell^+) = -e_{\mathrm{n}}\dot{X}(t_\ell^-) + \underset{z\in T_\Phi(X(t_\ell))}{\arg\min} \frac{(1+e_{\mathrm{n}})}{2}[z-\dot{X}(t_\ell^-)]^T M(X(t_\ell))[z-\dot{X}(t_\ell^-)] \quad (8.2)$$

where $\dot{X}(t_\ell^+)$ is the postimpact velocity, $\dot{X}(t_\ell^-)$ is the pre-impact velocity and $e_{\mathrm{n}} \in [0,1]$ is the restitution coefficient. Denoting by $T(X,\dot{X})$ the kinetic energy of the system, we can compute the kinetic energy loss at the impact time t_ℓ as[2]:

$$\begin{aligned} T_L(t_\ell) &= T(X(t_\ell^+),\dot{X}(t_\ell^+)) - T(X(t_\ell^-),\dot{X}(t_\ell^-)) \\ &= -\tfrac{1-e_{\mathrm{n}}}{2(1+e_{\mathrm{n}})}\Big[[\dot{X}(t_\ell^+)-\dot{X}(t_\ell^-)]^T M(X(t_\ell))[\dot{X}(t_\ell^+)-\dot{X}(t_\ell^-)]\Big] \le 0. \end{aligned} \quad (8.3)$$

However as noted in Remark 7.6 for the case of stability, we could enlarge the analysis and use the generalized impact law in (6.44) and (6.45).

8.1.1 Basic Concepts

The following notations will be adopted: $b_p \in \mathbb{R}^p$ and $b_{n-p} \in \mathbb{R}^{n-p}$ are the vectors formed with the first p and the last $n-p$ components of $b \in \mathbb{R}^n$, respectively, $\lambda_{min}(\cdot)$ and $\lambda_{max}(\cdot)$ represent the smallest and the largest eigenvalues of a symmetric positive definite matrix, respectively.

8.1.1.1 Typical Task

The time axis can be split into intervals Ω_k and I_k corresponding to specific phases of motion. Due to the singularities of $\mathrm{bd}(\Phi)$, the constrained motion phases need to be decomposed in subphases where some specific constraints are active. Between two such subphases a transition phase occurs only when the number of active constraints increases. This means that a typical task can be represented in the time domain as:

$$\begin{gathered} t \in \mathbb{R}^+ = \Omega_0^\emptyset \cup \left[\bigcup_{k\ge 1}\left(I_k \cup \left(\bigcup_{i=1}^{m_k} \Omega_k^{J_{k,i}}\right)\right)\right] \\ J_{k,m_k} \subset J_{k+1,1},\ J_{k,m_k} \subset J_{k,m_k-1}, \subset \ldots \subset J_{k,1} \end{gathered} \quad (8.4)$$

[2] In this section and the next one, impact times are denoted as t_l instead of t_k, since the subscript k is kept for the cycles in (8.4).

where the superscript $J_{k,i} = \{j \in \{1,\ldots,m\} \mid f_j(X) = 0\}$ represents the set of active constraints during the corresponding motion phase, and I_k denotes the transient between two Ω_k phases when the number of active constraints increases. Inside $\bigcup_{i=1}^{m_k} \Omega_k^{J_{k,i}}$, the number of active constraints decreases. Thus there is no need for transition phases between $\Omega_k^{J_{k,i}}$ and $\Omega_k^{J_{k,i+1}}$. Without loss of generality we suppose that the system is initialized in the interior of Φ at a free-motion phase. The impacts during I_k involve $p = |J_{k,1}|$ constraints (p_ε-impacts). Furthermore we shall prove that the first impact of I_k is a p_ε-impact with ε bounded by a parameter chosen by the designer. When the number of active constraints decreases there is no impact, thus no other transition phases are needed. We note that $J_{k,i} = \emptyset$ corresponds to free-motion ($f(X) > 0$). It is assumed in (8.4) that the system is initialized in a free-motion mode.

Since the tracking control problem involves no difficulty during the Ω_k phases, *the central issue is the study of the passages between them (the design of transition phases I_k and detachment conditions), and the stability of the trajectories evolving along (8.4)* (i.e., an infinity of cycles). As alluded to above, the passage $\Omega_k^{J_{k,i}} \to \Omega_k^{J_{k,i+1}}$ consists of detachments from some constraints. In Sect. 8.1.5 we consider that p constraints are active and we give the conditions to smoothly take off from r of them. It is clear that once we know how to do that, we can manage all the transitions mentioned above. Throughout this section, the sequence $I_k \cup \left(\bigcup_{i=1}^{m_k} \Omega_k^{J_{k,i}}\right)$ will be referred to as the cycle C_k of the system's evolution, hence $\mathbb{R}^+ = \Omega_0^{\emptyset} \bigcup_{k\geq 1} C_k$. From cycle k to cycle $k+1$, the number of active constraints increases: a transition phase is needed. For robustness reasons during transition phases I_k we impose a closed-loop dynamics (containing impacts) that mimics somehow the bouncing ball dynamics (thus avoiding the precise knowledge of the constraint position and of the coefficient of restitution).

8.1.1.2 Exogenous Signals Entering the Dynamics

In this section we introduce the trajectories playing a role in the dynamics and the design of the controller. Some instants that will be used further are also defined.

- $X^{nc}(\cdot)$ denotes the desired trajectory of the unconstrained system (i.e., the trajectory that the system should track if there were no constraints). We suppose that $f(X^{nc}(t) < 0$ for some t, otherwise the problem reduces to the tracking control of a system with no constraints.
- $X_d^*(\cdot)$ denotes the signal entering the control input and playing the role of the desired trajectory during some parts of the motion.
- $X_d(\cdot)$ represents the signal entering the Lyapunov function. This signal is set on $\mathrm{bd}(\Phi)$ after the first impact of each cycle.

The signals $X_d^*(\cdot)$ and $X_d(\cdot)$ coincide on the Ω_k phases while $X^{nc}(\cdot)$ is used to define everywhere $X_d^*(\cdot)$ and $X_d(\cdot)$. These three functions coincide only on the $\Omega_k^{\emptyset}$ phases.

Throughout the section we consider $I_k = [\tau_0^k, t_f^k]$, where τ_0^k is chosen by the designer as the start of the transition phase I_k and t_f^k is the end of I_k. We note that all superscripts $(\cdot)^k$ will refer to the cycle k of the system motion. We also use the following notations:

- t_0^k is the first impact during the cycle k,
- t_∞^k is the accumulation point of the sequence $\{t_\ell^k\}_{\ell \geq 0}$ of the impact instants during the cycle k ($t_f^k \geq t_\infty^k$),
- τ_1^k will be explicitly defined later and represents the instant when the signal $X_d^*(\cdot)$ reaches a given value chosen by the designer in order to impose a closed-loop dynamics with impacts during the transition phases,
- $t_d^{k,i}$ is the desired detachment instant at the end of the phase $\Omega_k^{J_{k,i}}$.

It is noteworthy that t_0^k, t_∞^k are state dependent, whereas τ_0^k, τ_1^k and $t_d^{k,i}$ are exogenous and imposed by the designer. To better understand the definition of these specific instants, in Fig. 8.1 we represent the exogenous signals $X^{nc}(\cdot)$, $X_d(\cdot)$, $X_d^*(\cdot)$ during a sequence $\Omega_{k-1}^{J_{k-1}} \cup I_k \cup \Omega_k^{J_{k,1}} \cup \Omega_k^{J_{k,2}}$ when the motion is simplified as follows:

- during the transition phase we take into account only the constraints that must be activated $J_{k,1} \setminus J_{k-1,m_{k-1}}$.
- at the end of the phase $\Omega_k^{J_{k,1}}$ we take into account only the constraints that must be deactivated $J_{k,1} \setminus J_{k,2}$.

The points A, A', A'' and C in Fig. 8.1 correspond to the moments τ_0^k, t_0^k, t_f^k and $t_d^{k,1}$ respectively. We have seen that the choice of τ_0^k plays an important role in the stability criterion given by Proposition 8.1. On the other hand in Fig. 8.1 we see that starting from A the desired trajectory $X_d(\cdot) = X_d^*(\cdot)$ is deformed compared to $X^{nc}(\cdot)$.

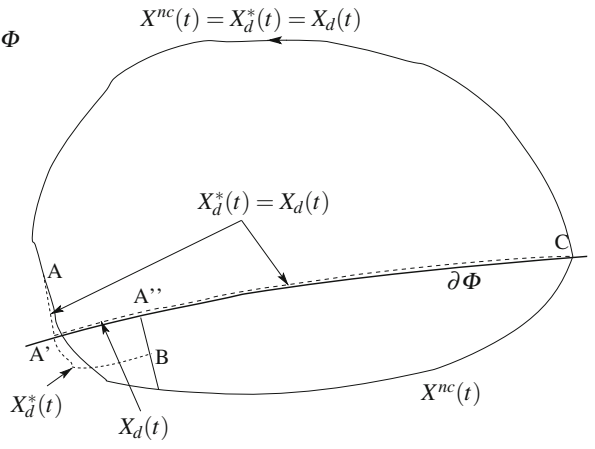

Fig. 8.1 The closed-loop desired trajectory and control signals ($\partial\Phi = \mathrm{bd}(\Phi)$)

In order to reduce this deformation, the time τ_0^k and implicitly the point A must be close to bd(Φ) (see also Fig. 8.4). Further details on the choice of τ_0^k will be given later. Taking into account just the constraints $J_{k,1} \setminus J_{k,2}$ we can identify $t_d^{k,1}$ with the moment when $X_d(\cdot)$ and $X^{nc}(\cdot)$ rejoin at C. See also Fig. 8.4 for an illustration on an example.

8.1.1.3 Stability Analysis Criteria

The system (8.1) is a complex nonsmooth and nonlinear dynamical system which involves continuous and discrete time phases. A stability framework for this type of systems has been proposed in [220] and extended in [166]. This is an extension of the Lyapunov second method adapted to closed-loop mechanical systems with unilateral constraints. Since we use this criterion in the following tracking control strategy it is worth to clarify the framework and to introduce some definitions.

Let us define Ω as the complement in $\mathbb{R}^+$ of $I = \bigcup_{k\geq 1} I_k$ and assume that the Lebesgue measure of Ω, denoted $\eta[\Omega]$, equals infinity. Consider $x(\cdot)$ the state of the closed-loop system in (8.1) with some feedback controller $U(X, \dot{X}, X_d^*, \dot{X}_d^*, \ddot{X}_d^*)$.

Definition 8.3 (*Weakly Stable System* [166]) The closed-loop system is called weakly stable if for each $\varepsilon > 0$ there exists $\delta(\varepsilon) > 0$ such that $||x(0)|| \leq \delta(\varepsilon) \Rightarrow ||x(t)|| \leq \varepsilon$ for all $t \geq 0$, $t \in \Omega$. The system is asymptotically weakly stable if it is weakly stable and $\lim_{t\in\Omega,\, t\to\infty} x(t) = 0$. Finally, the practical weak stability holds if there exists $0 < R < +\infty$ and $t^* < +\infty$ such that $||x(t)|| < R$ for all $t > t^*$, $t \in \Omega$.

Weak stability is therefore Lyapunov stability without looking at the transition phases. Consider $V(\cdot)$ such that there exists class $\mathcal{K}$ functions $\alpha(\cdot)$ and $\beta(\cdot)$ such that $\alpha(||x||) \leq V(x,t) \leq \beta(||x||)$.

Definition 8.4 A transition phase I_k is called finite if it involves a sequence of impact times $(t_\ell^k)_{0\leq\ell\leq N}$, $N \leq \infty$ with the accumulation point $t_N^k < \infty$ (for the sake of simplicity we shall denote the accumulation point by t_∞^k even if $N < \infty$).

In the sequel all the transition phases are supposed finite, which implies that $e_n < 1$ (in [81] it is shown that $e = 1$ implies that $t_\infty^k = +\infty$). The following criterion will be used to study the stability of the closed-loop system (8.1), with U given in Sect. 8.1.2.

Proposition 8.1 (Weak Stability) *Assume that the task admits the representation (8.4) and that*

(a) $\eta[I_k] < +\infty, \quad \forall k \in \mathbb{N}$,
(b) *outside the impact accumulation phases* $[t_0^k, t_\infty^k]$ *one has* $\dot{V}(x(t), t) \leq -\gamma V(x(t), t)$ *for some constant* $\gamma > 0$,
(c) $\sum_{\ell \geq 0} \left[V(t_{\ell+1}^{k-}) - V(t_\ell^{k+}) \right] \leq K_1 V^{p_1}(\tau_0^k), \ \forall k \in \mathbb{N}$ *for some* $p_1 \geq 0, \ K_1 \geq 0$,
(d) *the system is initialized on* Ω_0 *such that* $V(\tau_0^1) \leq 1$,
(e) $\sum_{\ell \geq 0} \sigma_V(t_\ell^k) \leq K_2 V^{p_2}(\tau_0^k) + \xi, \ \forall k \in \mathbb{N}$ *for some* $p_2 \geq 0, \ K_2 \geq 0$ *and* $\xi \geq 0$.

If $p = \min\{p_1, p_2\} < 1$ *then* $V(\tau_0^k) \leq \delta(\gamma, \xi), \ \forall k \geq 2$, *where* $\delta(\gamma, \xi)$ *is a function that can be made arbitrarily small by increasing the value of* γ. *The system is practically weakly stable with* $R = \alpha^{-1}(\delta(\gamma, \xi))$.

Proof From assumption (b) one has

$$V(t_f^k) \leq V(t_\infty^k) e^{-\gamma (t_f^k - t_\infty^k)}.$$

It is clear that condition (c) combined with (e) leads to

$$V(t_\infty^k) \leq V(\tau_0^k) + K_1 V^{p_1}(\tau_0^k) + K_2 V^{p_2}(\tau_0^k) + \xi.$$

Considering $p < 1$, the assumption (d) guarantees that $\max\{V(\tau_0^k), V^{p_1}(\tau_0^k), V^{p_2}(\tau_0^k)\} \leq V^p(\tau_0^k) \leq 1$ and we get:

$$V(t_f^k) \leq e^{-\gamma (t_f^k - t_\infty^k)} [1 + K_1 + K_2 + \xi] \triangleq \delta(\gamma, \xi).$$

From assumption (b) one has $V(\tau_0^{k+1}) \leq V(t_f^k)$ and thus $V(\tau_0^k) \leq \delta(\gamma, \xi), \ \forall k \geq 2$. The term $\delta(\gamma, \xi)$ can be made as small as desired increasing either γ or the length of the interval $[t_\infty^k, t_f^k]$. The proof is completed by the relation $\alpha(||x||) \leq V(x, t), \ \forall x, \ t$.

Remark 8.1 Since the Lyapunov function is exponentially decreasing on the Ω_k phases, assumption (d) in Proposition 8.1 means that the system is initialized on Ω_0 sufficiently far from the moment when the trajectory $X^{nc}(\cdot)$ leaves the admissible domain.

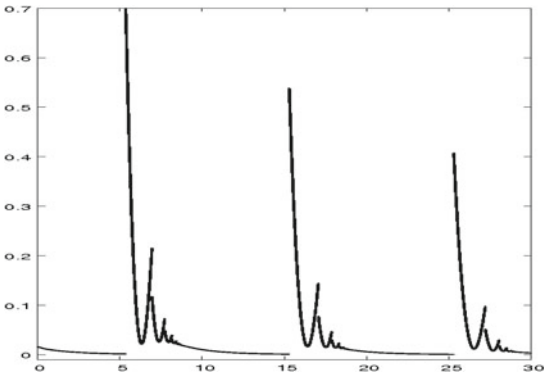

Fig. 8.2 Typical evolution of the Lyapunov function of weakly stable systems

Precisely, the weak stability is characterized by an "almost decreasing" Lyapunov function $V(x(\cdot).\cdot)$ as illustrated in Fig. 8.2.

Remark 8.2 It is worth to point out the local character of the stability criterion proposed by Proposition 8.1. This character is first given by condition (d) of the statement and second by the synchronization constraints of the control law and the motion phase of the system (see (8.4) and (8.7) below).

The practical stability is very useful because attaining asymptotic stability is not an easy task for the unilaterally constrained systems described by (8.1) especially when $n \geq 2$ and $M(q)$ is not a diagonal matrix (i.e., there are inertial couplings, which is the general case).

8.1.1.4 Dissipativity and Tracking Versus Stabilization

Let us make a parenthesis to highlight the major discrepancy between the trajectory tracking problem and the stabilization problem treated in Sect. 7.5. To this aim let us first recall that the dynamics in (8.1) and (8.2) can be equivalently rewritten as the *sweeping process Measure Differential Inclusion* (see Sect. 5.2 for details):

$$\begin{cases} -M(q(t))dv - [C(X(t), v(t^+))v(t^+) - G(X(t)) + U(t)]dt \in N_{T_\Phi(X(t))}(w(t)) \\ w(t) = \frac{v(t^+)+e_n v(t^-)}{1+e_n}, \end{cases} \tag{8.5}$$

where dv is the differential measure associated with the velocity $v(\cdot)$ that is a right-continuous function of local bounded variation, $v(\cdot)$ is equal almost everywhere to $\dot{X}(\cdot)$, $X(\cdot)$ is absolutely continuous and $X(t) - X(0) = \int_{[0,t]} v(s)ds$. The right-hand side is the normal cone to the tangent cone, also named Moreau's set

(see (5.43)). As shown in Sect. 7.5, a crucial property for stabilization is that the *Cone Complementarity Problem*:

$$N_{T_\Phi(X(t))}(w(t)) \ni \xi \perp w(t) \in T_\Phi(X(t)) \tag{8.6}$$

defines a maximal monotone mapping $\xi \mapsto w$, because the two cones $T_\Phi(\cdot)$ and $N_\Phi(\cdot)$ are polar cones, and $N_{T_\Phi(X(t))}(\cdot) \subseteq N_\Phi(\cdot)$ (see section B.2.2 for a proof). This maximal monotonicity property allows one to use dissipativity arguments in an absolute stability framework to derive a Lyapunov function, as illustrated in Figure 7.6. Let us consider now the tracking control problem. The new closed-loop state vector is $(\tilde{X}, \dot{\tilde{X}})$. Therefore the right-hand side of the closed-loop measure differential inclusion becomes the normal cone $N_{T_\Phi(\tilde{X}(t)+X_d(t))}(\tilde{w}(t) + w_d(t))$, with $w_d(t) = \frac{v_d(t^+)+e_n v_d(t^-)}{1+e_n}$. The sets $T_{\Phi_t}(\cdot) \stackrel{\Delta}{=} T_\Phi(\cdot + X_d(t))$ and $N_{T^t_{\Phi_t}}(\cdot) \stackrel{\Delta}{=} N_{T_{\Phi_t}}(\cdot + w_d(t))$ are now time varying, and the monotonicity property is generally lost. *This explains why the trajectory tracking problem is much more intricate than its stabilization counterpart.*

8.1.2 Controller Design

In order to overcome some difficulties that can appear in the controller definition, the dynamical equations (8.1) will be expressed in the generalized coordinates introduced by McClamroch and Wang [835], which allow one to split the generalized coordinates into "normal" and "tangential" parts, with a suitable diffeomorphic transformation $q = Q(X)$. This is a coordinate partitioning method, however, preserving the Lagrangian structure of the dynamical equations since it uses a diffeomorphic generalized coordinate transformation.[3] We suppose that the generalized coordinates transformation holds globally in Φ, which may obviously not be the case in general.

Let us consider $D = [I_m \vdots O] \in \mathbb{R}^{m\times n}$, $I_m \in \mathbb{R}^{m\times m}$ the identity matrix. The new coordinates will be $q = Q(X) \in \mathbb{R}^n$, with $q = \begin{bmatrix} q_1 \\ q_2 \end{bmatrix}$, $q_1 = \begin{bmatrix} q_1^1 \\ \vdots \\ q_1^m \end{bmatrix}$ such that $\Phi = \{q \mid Dq \geq 0\}$.[4] The tangent cone $T_\Phi(q_1 = 0) = \{v \in \mathbb{R}^n | Dv \geq 0\}$ is the space of admissible velocities on $\mathrm{bd}(\Phi)$ at $q_1 = 0$. More generally, if only p components of q_1 satisfy $q_1^i = 0$, then $T_\Phi(q_1) = \{v \in \mathbb{R}^n | D_p v \geq 0\}$ for the corresponding submatrix $D_p \in \mathbb{R}^{p\times n}$.

[3] The Lagrangian dynamics is preserved by diffeomorphic generalized coordinates transformations.

[4] In particular it is implicitly assumed that the functions $f_i(\cdot)$ in (8.1) are linearly independent, i.e., the gradients $\nabla f_i(X)$ are independent vectors, $1 \leq i \leq m$.

The controller used here consists of different low-level control laws for each phase of the system. More precisely, the switching controller can be expressed as

$$W(q)U = \begin{cases} U_{nc} \text{ for } t \in \Omega_k^{\emptyset} \\ U_t^J \text{ for } t \in I_k \\ U_c^J \text{ for } t \in \Omega_k^J, \end{cases} \tag{8.7}$$

where $W(q) = \begin{pmatrix} W_1(q) \\ W_2(q) \end{pmatrix} \in \mathbb{R}^{n \times n}$ is fullrank under some basic assumptions like independency of the constraints [835]. The subscript nc is for non-contact, t is for transition, and c is for contact. The dynamics becomes:

$$\begin{cases} M_{11}(q)\ddot{q}_1 + M_{12}(q)\ddot{q}_2 + C_1(q,\dot{q})\dot{q} + g_1(q) = W_1(q)U + \lambda \\ M_{21}(q)\ddot{q}_1 + M_{22}(q)\ddot{q}_2 + C_2(q,\dot{q})\dot{q} + g_2(q) = W_2(q)U \\ q_1^i \geq 0,\ q_1^i \lambda_i = 0,\ \lambda_i \geq 0,\ 1 \leq i \leq m \\ \text{Collision rule,} \end{cases} \tag{8.8}$$

where the set of complementary relations can be written more compactly as $0 \leq \lambda \perp Dq \geq 0$. One sees that the proposed coordinate change allows one to simplify the form of the unilateral constraints. It is noteworthy that this is not a quasi-coordinate change: the dynamics in (8.8) is a complementarity Lagrangian system. Again one may write (8.8) as a Moreau's sweeping process in the q-coordinates. For control design purpose, it is however more convenient to work within the complementarity framework, because LCPs can be analyzed.

Remark 8.3 The McClamroch and Wang [835] transformation was introduced originaly for bilateral holonomic frictionless constraints $h(q) = 0$. Then the dynamics is reduced since $q_1(\cdot)$ is identically null along the constraint manifold.

In the sequel U_{nc} coincides with the fixed-parameter controller proposed in [1119] and the closed-loop stability analysis of the system is based on Proposition 8.1. First, let us introduce some notations: $\tilde{q} = q - q_d$, $\bar{q} = q - q_d^*$, $s = \dot{\tilde{q}} + \gamma_2 \tilde{q}$, $\bar{s} = \dot{\bar{q}} + \gamma_2 \bar{q}$, $\dot{q}_e = \dot{q}_d - \gamma_2 \tilde{q}$ where $\gamma_2 > 0$ is a scalar gain and $q_d(\cdot)$, $q_d^*(\cdot)$ represent the desired trajectories defined in the previous section in the X-coordinates. Using the above notations the controller is given by:

$$W(q)U \triangleq \begin{cases} U_{nc} = M(q)\ddot{q}_e + C(q,\dot{q})\dot{q}_e + G(q) - \gamma_1 s \\ U_t^J = U_{nc},\ t \leq t_0^k \\ U_t^J = M(q)\ddot{q}_e + C(q,\dot{q})\dot{q}_e + G(q) - \gamma_1 \bar{s},\ t > t_0^k \\ U_c^J = U_{nc} - P_d + K_f(P_q - P_d), \end{cases} \tag{8.9}$$

where $\gamma_1 > 0$ is a scalar gain, $K_f \succ 0$, $P_q = D^T\lambda$ and $P_d = D^T\lambda_d$ is the desired contact force during persistently constrained motion. It is clear that during Ω_k^J not all the constraints are active and, therefore, some components of λ and λ_d are zero.

In order to prove the stability of the closed-loop system (8.7)–(8.9) we will use the following positive definite function:

$$V(t, s, \tilde{q}) = \frac{1}{2} s^T M(q) s + \gamma_1 \gamma_2 \tilde{q}^T \tilde{q}. \tag{8.10}$$

8.1.3 Tracking Control Framework

8.1.3.1 Design of the Desired Trajectories

The tracking control problem for the closed-loop dynamical system (8.7)–(8.9) is analyzed with the complete desired path, a priori taking into account the complementarity conditions and the impacts. In order to define the desired trajectory let us consider the motion of a virtual and unconstrained particle perfectly following a trajectory (represented by $X^{nc}(\cdot)$ in Fig. 8.1) with an orbit that leaves the admissible domain for a given period. Therefore, the orbit of the virtual particle can be split into two parts, one of them belonging to the admissible domain (inner part) and the other one outside the admissible domain (outer part). In the sequel we deal with the tracking control strategy when the desired trajectory is constructed such that:

(i) when no activated constraints, it coincides with the trajectory of the virtual particle (the desired path and velocity are defined by the path and velocity of the virtual particle, respectively),
(ii) when $p \leq m$ constraints are active, its orbit coincides with the projection of the outer part of the virtual particle's orbit on the surface of codimension p defined by the activated constraints (X_d between A'' and C in Fig. 8.1),
(iii) the desired detachment moment and the moment when the virtual particle re-enters the admissible domain (with respect to $p \leq m$ constraints) are synchronized.

Therefore we have not only to track a desired path but also to impose a desired velocity allowing the motion synchronization on the admissible domain. The main difficulties here consist of:

- stabilizing the system on $\mathrm{bd}(\Phi)$ during the transition phases I_k and incorporating the velocity jumps in the overall stability analysis;
- deactivating some constraints at the moment when the unconstrained trajectory re-enters the admissible domain with respect to them;
- maintaining a persistently constrained motion between the moment when the system was stabilized on $\mathrm{bd}(\Phi)$ and the detachment moment.

Remark 8.4 The problem can be relaxed considering that we want to track only a desired path like $X^{nc}(\cdot)$ (without imposing a desired velocity on the inner part of

the desired trajectory and/or a given period to complete a cycle). In this way the synchronization problem (iii) disappears and we can assume there exists a twice differentiable desired trajectory outside $[t_0^k, t_f^k]$ that assures the detachment when the force control is dropped. In other words, in this case we have to design the desired trajectory only during I_k phases.

8.1.3.2 Design of $q_d^*(\cdot)$ and $q_d(\cdot)$ on the Phases I_k

During the transition phases the system must be stabilized on $\mathrm{bd}(\Phi)$. Obviously, this does not mean that all the constraints have to be activated (i.e., $q_1^i(t) = 0$, $\forall i = 1, \ldots, m$). Let us consider that only the first p constraints (eventually reordering the coordinates) define the boundary of Φ where the system must be stabilized. The following methodology will be used to define $q_d^*(\cdot)$:

(1) During a small period $\delta > 0$ chosen by the designer the desired velocity becomes zero preserving the twice differentiability of $q_d^*(\cdot)$. For instance we can use the following definition:

$$q_d^*(t) = q^{nc}\left(\tau_0^k + \frac{(t-\tau_0^k-\delta)^2(t-\tau_0^k)}{\delta^2}\right), \quad t \in [\tau_0^k, \tau_0^k + \delta],$$

which means $q_d^*(\tau_0^k + \delta) = q_d^*(\tau_0^k) = q^{nc}(\tau_0^k)$, $\dot{q}_d^*(\tau_0^k + \delta) = 0$ and $\dot{q}_d^*(\tau_0^k) = \dot{q}^{nc}(\tau_0^k)$.

(2) The last $n - p$ components of $q_d^*(\cdot)$ are frozen:

$$\left(q_d^*\right)_{n-p}(t) = q_{n-p}^{nc}(\tau_0^k), \quad t \in (\tau_0^k + \delta, t_f^k]. \tag{8.11}$$

(3) For a fixed $\varphi > 0$ the moment τ_1^k is chosen by the designer as the instant when the limit conditions $\left(q_d^i\right)^*(\tau_1^k) = -\nu V^{1/3}(\tau_0^k)$, $\left(\dot{q}_d^i\right)^*(\tau_1^k) = 0$, $\forall i = 1, \ldots, p$, hold. On $[\tau_0^k + \delta, \tau_1^k)$ we define $q_d^*(\cdot)$ as a twice differentiable decreasing signal. Precisely, denoting $t' = \frac{t-(\tau_0^k+\delta)}{\tau_1^k-(\tau_0^k+\delta)}$, the components $\left(q_d^i\right)^*(\cdot)$, $i = 1, \ldots, p$ of $\left(q_d^*\right)_p(\cdot)$ are defined as:

$$\left(q_d^i\right)^*(t) = \begin{cases} a_3^i(t')^3 + a_2^i(t')^2 + a_0^i, & t \in [\tau_0^k + \delta, \min\{\tau_1^k; t_0^k\}] \\ -\varphi V^{1/3}(\tau_0^k), & t \in (\min\{\tau_1^k; t_0^k\}, t_f^k], \end{cases} \tag{8.12}$$

where $V(\cdot)$ is defined in (8.10) and the coefficients are:

$$\begin{cases} a_3^i = 2[\left(q^i\right)^{nc}(\tau_0^k) + \varphi V^{1/3}(\tau_0^k)] \\ a_2^i = -3[\left(q^i\right)^{nc}(\tau_0^k) + \varphi V^{1/3}(\tau_0^k)] \\ a_0^i = \left(q^i\right)^{nc}(\tau_0^k) \end{cases} \tag{8.13}$$

The rationale behind the choice of $q_d^*(\cdot)$ is on one hand to assure a robust stabilization on $\mathrm{bd}(\Phi)$, mimicking the bouncing ball dynamics; on the other hand to enable one to compute suitable upper bounds that will help using Proposition 8.1, hence the $V^{1/3}(\cdot)$ terms in (8.12) with $V(\cdot)$ in (8.10).

$\rightsquigarrow$ *The idea of inserting the Lyapunov function $V(\cdot)$ in the definition of the desired trajectory was first introduced in [221]. In case the closed-loop system is asymptotically weakly stable, this implies that collisions vanish asymptotically (i.e., as $k \to \infty$ where k is the cycles index). The rationale behind this choice is that impacts necessarily imply positive jumps in the Lyapunov function if $V = 0$, thus preventing asymptotic stability.*

Remark 8.5 Two different situations are possible. The first one is given by $t_0^k > \tau_1^k$ (see Fig. 8.3) and we shall prove that in this situation all the jumps of the Lyapunov function in (8.10) are negative. The second situation was pointed out in [166] and is given by $t_0^k < \tau_1^k$. In this situation the first jump at t_0^k in the Lyapunov function may be positive. It is noteworthy that $q_d^*(\cdot)$ will then have a jump at the time t_0^k since $(q_d^i)^*(t_0^{k+}) = -\varphi V^{1/3}(\tau_0^k)$, $\forall i = 1, \ldots, p$ (see (8.12)).

In order to limit the deformation of the desired trajectory $q_d^*(\cdot)$ w.r.t. the unconstrained trajectory $q^{nc}(\cdot)$ during the I_k phases (see Figs. 8.1 and 8.3), we impose in the sequel

$$||q_p^{nc}(\tau_0^k)|| \leq \psi, \tag{8.14}$$

where $\psi > 0$ is chosen by the designer. It is obvious that a smaller ψ leads to smaller deformation of the desired trajectory and to smaller deformation of the real trajectory as we shall see in Sect. 8.1.7. Nevertheless, due to the tracking error, ψ cannot be chosen zero. We also note that $||q_p^{nc}(\tau_0^k)|| \leq \psi$ is a practical way to choose τ_0^k. During the transition phases I_k we define $(q_d)_{n-p}(t) = \left(q_d^*\right)_{n-p}(t)$. Assuming

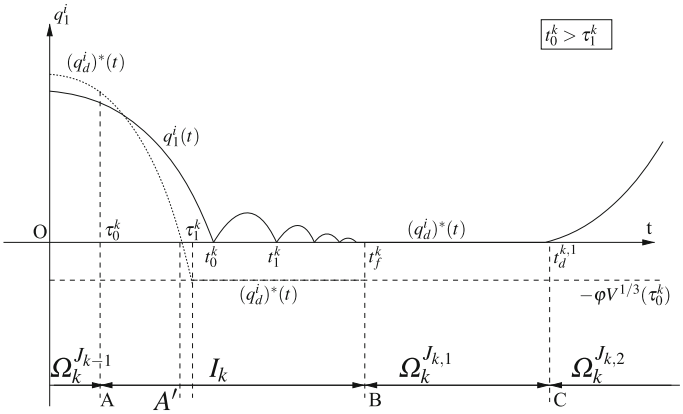

Fig. 8.3 The design of q_{1d}^* on the transition phases I_k

a finite accumulation of impact times, the impact process can be considered in some way equivalent to a plastic impact. Therefore, $(q_d)_p(\cdot)$ and $(\dot{q}_d)_p(\cdot)$ are set to zero on the right of t_0^k.

8.1.4 Design of the Desired Contact Force During Constraint Phases

For the sake of simplicity we consider the case of the constraint phase Ω_k^J, $J \neq \emptyset$ with $J = \{1, \ldots, p\}$. Obviously, a sufficiently large desired contact force P_d assures a constrained movement on Ω_k^J. Nevertheless at the end of the Ω_k^J phases a detachment from some surfaces Σ_i has to take place. It is clear that a takeoff implies not only a well-defined desired trajectory but also some small values of the corresponding contact force components. On the other hand, if the components of the desired contact force decrease too much a detachment can take place before the end of the Ω_k^J phases which can generate other impacts. Therefore we need a lower bound of the desired force which assures the contact during the Ω_k^J phases. Dropping the time argument, the dynamics of the system on Ω_k^J can be written as the complementarity Lagrangian system:

$$\begin{cases} M(q)\ddot{q} + F(q,\dot{q}) = U_c + D_p^T \lambda_p \\ 0 \leq q_p \perp \lambda_p \geq 0, \end{cases} \tag{8.15}$$

where $F(q,\dot{q}) = C(q,\dot{q})\dot{q} + G(q)$ and $D_p = [I_p \vdots O] \in \mathbb{R}^{p\times n}$. The mass matrix $M(q)$ is given in (8.8). On Ω_k^J the system is permanently constrained which implies $q_p(\cdot) = 0$ and $\dot{q}_p(\cdot) = 0$. In order to assure these conditions it is sufficient to have $\lambda_p > 0$.

In the following let us denote $M(q)^{-1} = \begin{pmatrix} [M(q)^{-1}]_{p,p} & [M(q)^{-1}]_{p,n-p} \\ [M(q)^{-1}]_{n-p,p} & [M(q)^{-1}]_{n-p,n-p} \end{pmatrix}$ and

$C(q,\dot{q}) = \begin{pmatrix} C(q,\dot{q})_{p,p} & C(q,\dot{q})_{p,n-p} \\ C(q,\dot{q})_{n-p,p} & C(q,\dot{q})_{n-p,n-p} \end{pmatrix}$ where the meaning of each component is obvious.

Proposition 8.2 *On Ω_k^J the constraint motion of the closed-loop system (8.15), (8.7), and (8.9) is assured if the desired contact force is defined by*

$$\begin{aligned} (\lambda_d)_p \triangleq \beta - \frac{\bar{M}_{p,p}(q)}{1+K_f} \big(& [M(q)^{-1}]_{p,p} C_{p,n-p}(q,\dot{q}) + \\ & + [M(q)^{-1}]_{p,n-p} C_{n-p,n-p}(q,\dot{q}) + \gamma_1 [M(q)^{-1}]_{p,n-p} \big) s_{n-p}, \end{aligned} \tag{8.16}$$

where $\bar{M}_{p,p}(q) = \left([M(q)^{-1}]_{p,p}\right)^{-1} = \left(D_p M(q)^{-1} D_p^T\right)^{-1}$ is the inverse of the Delassus' matrix and $\beta \in \mathbb{R}^p$, $\beta > 0$.

Proof First, we notice that the second relation in (8.15) implies on Ω_k^J complementarity at the acceleration level:

$$0 \leq \ddot{q}_p \perp \lambda_p \geq 0 \Leftrightarrow 0 \leq D_p \ddot{q} \perp \lambda_p \geq 0. \tag{8.17}$$

From (8.15) and (8.9) one easily gets:

$$\ddot{q} = M(q)^{-1}\big[- F(q,\dot{q}) + U_{nc} + (1+K_f) D_p^T (\lambda - \lambda_d)_p \big].$$

Combining the last two equations we obtain the following LCP with unknown λ_p:

$$\begin{aligned} 0 \leq D_p M(q)^{-1}\big[- F(q,\dot{q}) + U_{nc} - (1+K_f) D_p^T \, (\lambda_d)_p \, \big] \\ + (1+K_f) D_p M(q)^{-1} D_p^T \lambda_p \perp \lambda_p \geq 0. \end{aligned} \tag{8.18}$$

Since $(1+K_f) D_p M(q)^{-1} D_p^T \succ 0$ and hence is a P-matrix, the LCP (8.18) has a unique solution and one deduces that $\lambda_p > 0$ if and only if:

$$\begin{aligned} & \tfrac{\bar{M}_{p,p}(q)}{1+K_f} D_p M(q)^{-1}\big[U_{nc} - F(q,\dot{q}) - (1+K_f) D_p^T \, (\lambda_d)_p \, \big] < 0 \\ & \Leftrightarrow (\lambda_d)_p > \tfrac{\bar{M}_{p,p}(q)}{1+K_f} D_p M(q)^{-1}\big[U_{nc} - F(q,\dot{q})\big] \\ & \Leftrightarrow (\lambda_d)_p = \beta + \tfrac{\bar{M}_{p,p}(q)}{1+K_f} D_p M(q)^{-1}\big[U_{nc} - F(q,\dot{q})\big], \end{aligned} \tag{8.19}$$

with $\beta \in \mathbb{R}^p$, $\beta > 0$. Indeed the LCP $0 \leq x \perp Ax + b \geq 0$ has a solution $x > 0$ (componentwise) only if $Ax + b = 0$. If A is a P-matrix, uniqueness of the solution guarantees the "if". Since $U_{nc} - F(q,\dot{q}) = M(q)\ddot{q}_e - C(q,\dot{q})s - \gamma_1 s$, $(\ddot{q}_e)_p = 0$ and $s_p = 0$, (8.19) rewrites as (8.16) and the proof is finished. It is noteworthy that:

$$\begin{aligned} \lambda_p &= -\frac{\bar{M}_{p,p}(q)}{1+K_f} D_p M(q)^{-1}\big[U_{nc} - F(q,\dot{q}) \\ &\qquad\qquad - (1+K_f) D_p^T \, (\lambda_d)_p \, \big] \\ &= (\lambda_d)_p - \frac{\bar{M}_{p,p}(q)}{1+K_f} D_p M(q)^{-1}\big[U_{nc} - F(q,\dot{q})\big] = \beta. \end{aligned}$$

Remark 8.6 The control law used in this section with the design of λ_d described above leads to the following closed-loop dynamics on Ω_k^J.

$$\begin{cases} M_{p,n-p}(q)\dot{s}_{n-p} + C_{p,n-p}(q,\dot{q}) s_{n-p} = (1+K_f)(\lambda - \lambda_d)_p \\ M_{n-p,n-p}(q)\dot{s}_{n-p} + C_{n-p,n-p}(q,\dot{q}) s_{n-p} + \gamma_1 s_{n-p} = 0 \\ q_p = 0, \quad \lambda_p = \beta. \end{cases}$$

It is noteworthy that the closed-loop dynamics is nonlinear and therefore the feedback stabilization proposed in [835] is not used.

8.1.5 Strategy for Takeoff at the End of Constraint Phases Ω_k^J

We have discussed in the previous sections the necessity of a trajectory with impacts in order to assure the robust stabilization on $\mathrm{bd}(\Phi)$ in finite time, and the design of the desired trajectory to stabilize the system on $\mathrm{bd}(\Phi)$. Now, we are interested in finding the conditions on the control signal U_c^J that assure the takeoff at the end of the constrained phases Ω_k^J. We consider the phase Ω_k^J expressed as the time interval $[t_f^k, t_d^k)$. The dynamics on $[t_f^k, t_d^k)$ is given by (8.15) and the system is permanently constrained, which implies $q_p(\cdot) = 0$ and $\dot{q_p}(\cdot) = 0$. Let us also consider that the first r constraints ($r < p$) have to be deactivated. Thus, the detachment takes place at t_d^k if $\ddot{q}_r(t_d^{k+}) > 0$ which requires $\lambda_r(t_d^{k-}) = 0$. The last $p - r$ constraints remain active which means $\lambda_{p-r}(t_d^{k-}) > 0$. To simplify the notation we drop the arguments t and q in many equations of this section. We decompose the LCP matrix (which is the Delassus' matrix $D_p M(q)^{-1} D_p^T$ multiplied by $(1 + K_f)$) as:

$$(1 + K_f) D_p M(q)^{-1} D_p^T = \begin{pmatrix} A_1(q) & A_2(q) \\ A_2(q)^T & A_3(q) \end{pmatrix},$$

with $A_1 \in \mathbb{R}^{r \times r}$, $A_2 \in \mathbb{R}^{r \times (p-r)}$ and $A_3 \in \mathbb{R}^{(p-r) \times (p-r)}$.

Proposition 8.3 *For the closed-loop system (8.15), (8.7), and (8.9) the decrease of the active constraints number from p to $p - r$ (with $r < p$), is possible if*

$$\begin{pmatrix} (\lambda_d)_r\,(t_d^k) \\ (\lambda_d)_{p-r}\,(t_d^k) \end{pmatrix} = \begin{pmatrix} \left(A_1 - A_2 A_3^{-1} A_2^T\right)^{-1} \left(b_r - A_2 A_3^{-1} b_{p-r}\right) - C_1 \\ C_2 + A_3^{-1} \left(b_{p-r} - A_2^T\,(\lambda_d)_r\right) \end{pmatrix} \tag{8.20}$$

where

$$b_p \triangleq b(q, \dot{q}, U_{nc}) \triangleq D_p M^{-1}(q)[U_{nc} - F(q, \dot{q})] \geq 0,$$

and $C_1 \in \mathbb{R}^r$, $C_2 \in \mathbb{R}^{p-r}$ such that $C_1 \geq 0$, $C_2 > 0$.

Proof From (8.9) and (8.15) one gets

$$\ddot{q}_p(t) = b_p + (1 + K_f) D_p M(q)^{-1} D_p^T (\lambda - \lambda_d).$$

Therefore the LCP (8.17) rewrites as:

$$0 \leq \begin{pmatrix} \lambda_r \\ \lambda_{p-r} \end{pmatrix} \perp \begin{pmatrix} b_r + A_1(\lambda - \lambda_d)_r + A_2(\lambda - \lambda_d)_{p-r} \\ b_{p-r} + A_2^T(\lambda - \lambda_d)_r + A_3(\lambda - \lambda_d)_{p-r} \end{pmatrix} \geq 0. \tag{8.21}$$

Under the conditions $\lambda_r = 0$ and $\lambda_{p-r} > 0$ one has

$$0 \leq \lambda_{p-r} \perp b_{p-r} - A_2^T(\lambda_d)_r + A_3(\lambda - \lambda_d)_{p-r} \geq 0.$$

with the solution

$$\lambda_{p-r} = -A_3^{-1}\left(b_{p-r} - A_2^T(\lambda_d)_r - A_3(\lambda_d)_{p-r}\right). \tag{8.22}$$

Thus $\lambda_{p-r} > 0$ is equivalent to

$$(\lambda_d)_{p-r} > A_3^{-1}\left(b_{p-r} - A_2^T(\lambda_d)_r\right),$$

which leads to the second part of definition (8.20). Furthermore, replacing $(\lambda_d)_{p-r}$ in (8.22) we get $\lambda_{p-r} = C_2$ and $b_r + A_1(\lambda - \lambda_d)_r + A_2(\lambda - \lambda_d)_{p-r} \geq 0$ yields the first part of definition (8.20). To conclude, the solution of the LCP (8.21) is $\lambda_p = \begin{pmatrix} 0 \\ C_2 \end{pmatrix} \in \mathbb{R}^p$ and $(\lambda_d)_p$ is defined by (8.20).

Proposition 8.4 *The closed-loop system (8.15), (8.7), and (8.9) is permanently constrained on $[t_f^k, t_d^k)$ and a smooth detachment is guaranteed on $[t_d^k, t_d^k + \bar{\varepsilon})$ ($\bar{\varepsilon}$ is a small positive real number chosen by the designer) if*

(i) $(\lambda_d)_p(\cdot)$ *is defined on $[t_f^k, t_d^k)$ by (8.20) where C_1 is replaced by $C_1(t - t_d^k)$.*

(ii) On $[t_d^k, t_d^k + \bar{\varepsilon})$

$$q_d^*(t) = q_d(t) = \begin{pmatrix} q_r^*(t) \\ q_{n-r}^{nc}(t) \end{pmatrix},$$

where $q_r^*(\cdot)$ is a twice differentiable function such that

$$\begin{cases} q_r^*(t_d^k) = 0,\ q_r^*(t_d^k + \bar{\varepsilon}) = q_r^{nc}(t_d^k + \bar{\varepsilon}), \\ \dot{q}_r^*(t_d^k) = 0,\ \dot{q}_r^*(t_d^k + \bar{\varepsilon}) = \dot{q}_r^{nc}(t_d^k + \bar{\varepsilon}), \end{cases} \tag{8.23}$$

and $\ddot{q}_r^*(t_d^{k+}) = a > \max\left(0,\ -A_1(q)\,(\lambda_d)_r\,(t_d^{k-})\right)$.

Proof (i) The uniqueness of solution of the LCP (8.17) guarantees that (8.16) and (8.20) agree if $C_1 < 0$. In other words, replacing C_1 by $C_1(t - t_d^k)$ in (8.20) we assure a constrained motion on $[t_f^k, t_d^k)$ and the necessary conditions for detachment on $[t_d^k, t_d^k + \bar{\varepsilon})$.
(ii) Obviously (8.23) is imposed in order to assure the twice differentiability of the desired trajectory. Finally, straightforward computations show that

$$\sigma_{\ddot{q}_r(t_d^k)} = \ddot{q}_r^*(t_d^{k+}) + A_1(q)\,(\lambda_d)_r\,(t_d^{k-}),$$

which means that the detachment is guaranteed and no other impacts occur when the desired acceleration satisfies $\ddot{q}_r^*(t_d^{k+}) > \max\left(0,\ -A_1(q)\,(\lambda_d)_r\,(t_d^{k-})\right)$.

8.1.6 Closed-Loop Stability Analysis

In the case $\Phi = \mathbb{R}^n$, the function $V(t, s, \tilde{q})$ in (8.10) can be used in order to prove the closed-loop stability of the system (8.8) and (8.9), as shown in [1134]. In the case studied here ($\Phi \subset \mathbb{R}^n$) the analysis becomes more complex.

To simplify the notation $V(t, s(t), \tilde{q}(t))$ is denoted as $V(t)$. In order to introduce the main result of this section we make the next assumption, which is verified in practice for dissipative systems.

Assumption 4 The controller U_t in (8.9) assures that all the transition phases are finite (see Definition 8.4) and the accumulation point t_∞^k is smaller than $t_d^{k,1}$ for all $k \in \mathbb{N}$.

Assumption 5 The Christoffel's symbols asociated with the inertia matrix $M(q)$ are used to write (8.8), so that the matrix $\frac{d}{dt}(M(q)) - 2C(q, \dot{q})$ is skew symmetric.

Since outside $[t_0^k, t_f^k]$ we will show that the Lyapunov function exponentially decreases, we may presume that all the impacts take place during I_k.

Lemma 8.1 *Consider the closed-loop system (8.7)–(8.9) with $(q_d^*)_p(\cdot)$ defined on the interval $[\tau_0^k, t_0^k]$ as in (8.12)–(8.11). Let us also suppose that condition (b) of Proposition 8.1 is satisfied. The following inequalities hold:*

$$\begin{cases} ||\tilde{q}(t_0^{k-})|| \leq \sqrt{\frac{V(\tau_0^k)}{\gamma_1\gamma_2}},\ ||s(t_0^{k-})|| \leq \sqrt{\frac{2V(\tau_0^k)}{\lambda_{min}(M(q))}} \\ ||\dot{\tilde{q}}(t_0^{k-})|| \leq \left(\sqrt{\frac{2}{\lambda_{min}(M(q))}} + \sqrt{\frac{\gamma_2}{\gamma_1}}\right) V^{1/2}(\tau_0^k). \end{cases} \tag{8.24}$$

Furthermore, if $t_0^k \leq \tau_1^k$ and t_0^k is a p_{ε_k}-impact one has:

$$||(q_d)_p(t_0^{k-})|| \leq \varepsilon_k + \sqrt{\frac{V(\tau_0^k)}{\gamma_1\gamma_2}},\quad \text{and}\quad ||(\dot{q}_d)_p(t_0^{k-})|| \leq K + K' V^{1/3}(\tau_0^k), \tag{8.25}$$

where $\varepsilon_k \leq \max\{\psi, \sqrt{p}\varphi V^{1/3}(\tau_0^k)\} + \sqrt{\frac{V(\tau_0^k)}{\gamma_1\gamma_2}}\}$, and $K,\ K' > 0$ are some constant real numbers that will be defined in the proof.

Proof See Sect. 8.1.8.

The main result of this section can be stated as follows.

Theorem 8.1 *Let Assumptions 4 and 5 hold,* $e_{\mathrm{n}} \in [0, 1)$ *and* $(q_d^*)_p(\cdot)$ *defined as in (8.12)–(8.11). The closed-loop system (8.7)–(8.9) initialized on* Ω_0 *such that* $V(\tau_0^0) \leq 1$*, satisfies the requirements of Proposition 8.1 and is therefore practically weakly stable with the closed-loop state* $x(\cdot) = [s(\cdot), \tilde{q}(\cdot)]$ *and* $R = \sqrt{e^{-\gamma(t_f^k - t_\infty^k)}(1 + K_1 + K_2 + \xi)/\rho}$ *where* $\rho = \min\{\lambda_{min}(M(q))/2; \gamma_1\gamma_2\}$ *and* K_1, K_2 *are defined in the proof.*

Proof See Sect. 8.1.9.

Since the closed-loop system (8.7)–(8.9) satisfies the requirements of Proposition 8.1 one also deduces $V(\tau_0^k) \leq \delta(\gamma, \xi)$, so $\varepsilon_k \leq \max\{\psi, \sqrt{p}\varphi\delta(\gamma, \xi)^{1/3}\} + \sqrt{\frac{\delta(\gamma,\xi)}{\gamma_1\gamma_2}}\}$, for all $k \geq 1$. In other words the sequence $\{\varepsilon_k\}_k$ is uniformly upperbounded and the upperbound can be decreased by adjusting the parameters ψ and γ.

8.1.7 Illustrative Examples

8.1.7.1 A Planar Two-Link Rigid-Joint Manipulator with One Constraint

The main issues of the control scheme proposed in this section are first emphasized simulating the behavior of a planar two-link rigid-joint manipulator in the presence of one unilateral constraint. The lengths l_1, l_2 of the manipulator's links are set to $0.5m$, and their masses m_1, m_2 are set to $1\,kg$, g is the gravity acceleration. Denoting by θ_i the joint angle of the link i and I_i the moment of inertia of link i about the axis that passes through the center of mass and is parallel to the OZ axis, the dynamics of the two-link manipulator is given by (8.1) with $M = \begin{bmatrix} M_{11} & M_{12} \\ M_{21} & M_{22} \end{bmatrix}$, $C = \begin{bmatrix} C_{11} & C_{12} \\ C_{21} & C_{22} \end{bmatrix}$, $G = \begin{bmatrix} G_1 \\ G_1 \end{bmatrix}$ and:

$$\begin{cases} M_{11} = \dfrac{m_1 l_1^2}{4} + m_2\left(l_1^2 + \dfrac{l_2^2}{4} l_1 l_2 \cos\theta_2\right) + I_1 + I_2 \\ M_{12} = M_{21} = \dfrac{m_2 l_2^2}{4} + \dfrac{m_2 l_1 l_2}{2}\cos\theta_2 + I_2, \quad M_{22} = \dfrac{m_2 l_2^2}{4} + I_2 \end{cases}$$

$$\begin{cases} C_{11} = -m_2 l_1 l_2 \dot{\theta}_2 \sin\theta_2, \quad C_{12} = -\dfrac{m_2 l_1 l_2}{2}\dot{\theta}_2 \sin\theta_2 \\ C_{21} = \dfrac{m_2 l_1 l_2}{2}\dot{\theta}_1 \sin\theta_2, \quad C_{22} = 0 \end{cases}$$

$$\begin{cases} G_1 = \dfrac{g}{2}[l_1(2m_1 + m_2)\cos\theta_1 + m_2 l_2 \cos(\theta_1 + \theta_2)] \\ G_2 = \dfrac{m_2 g l_2}{2}\cos(\theta_1 + \theta_2). \end{cases}$$

The dynamics can be rewritten in the cartesian coordinates using the change of variables:

$$q = \begin{pmatrix} y \\ x \end{pmatrix} = \begin{pmatrix} l_1 \sin(\theta_1) + l_2 \sin(\theta_1 + \theta_2) \\ l_1 \cos(\theta_1) + l_2 \cos(\theta_1 + \theta_2) \end{pmatrix} = Q(X). \tag{8.26}$$

The admissible domain is the upper half plane $y \geq 0$ (here $m = 1$ and $q_1 = y$) and the unconstrained desired trajectory $q^{nc}(\cdot)$ is given by a circle that violates the constraint. Precisely, the end effector must follow a half-circle, stabilize on the constraint ($y = 0$) and move on the constraint until the point where the circle $q^{nc}(\cdot)$ re-enters the admissible domain. Thus (8.4) writes as

$$\mathbb{R}^+ = \Omega_0^{\emptyset} \cup I_1 \cup \Omega_1^{\{1\}} \cup \Omega_1^{\emptyset} \cup I_2 \cup \Omega_2^{\{1\}} \cup \Omega_2^{\emptyset} \cup \ldots$$

with $m_k = 2$ for all $k \geq 0$, $J_{k,1} = \{1\}$, $J_{k,2} = \emptyset$. Using the $q-$coordinates x_d^* is frozen during the transition phases I_k while y_d^* is defined by (8.12)–(8.13). Furthermore, the controller $W(q)U$ is computed by (8.9) where K_f is set to 0.5 and $(\lambda_d)_y$ (i.e., the desired contact force corresponding to the constraint $y = 0$) is given by (8.16) where β has a decreasing profile like in item (i) of Proposition 8.4). The impacts are imposed using the parameter $\varphi = 100$ in (8.12)–(8.13). The numerical simulations are done with the Moreau's time-stepping algorithm of the SICONOS software platform (http://siconos.gforge.inria.fr). The choice of a time-stepping algorithm was mainly dictated by the presence of accumulations of impacts which render the use of event-driven methods difficult, as we discussed in Sect. 5.7.1. A further reason to choose the SICONOS software platform for the simulation of the complementarity systems is its capability to solve LCPs.[5]

Let us set $e_n = 0.7$, $\gamma_1 = 8$, $\gamma_2 = 7$, 10 seconds the period of each cycle and 30 seconds the final simulation time. First, let us point out (Fig. 8.4 (left)) the influence of ψ (i.e., the choice of τ_0^k) on the deformation of the real trajectory w.r.t. the desired unconstrained one. As we have pointed out in Sect. 8.1.3 the deformation gets smaller when $\psi > 0$ decreases. It is noteworthy that the tangential approach corresponding to $\psi = 0$ lacks of robustness and is unreliable due to the nonzero initial tracking errors.

In Fig. 8.4 (right) one sees that since $q_d(\cdot) = q_d^*(\cdot)$ before the first impact t_0^k of each cycle and $t_0^k < \tau_1^k$, there exists a jump at the moment $t_0^k \approx 6$s in $q_d(\cdot)$, $q_d^*(\cdot)$,

[5]The control scheme proposed in this section may require to solve an LCP of dimension $\bar{p} \approx 10$ (reasonable in some control applications). But this requires a specific solver since the usual "hybrid" methods must treat $2^{\bar{p}}$ cases and quickly become inefficient [13].

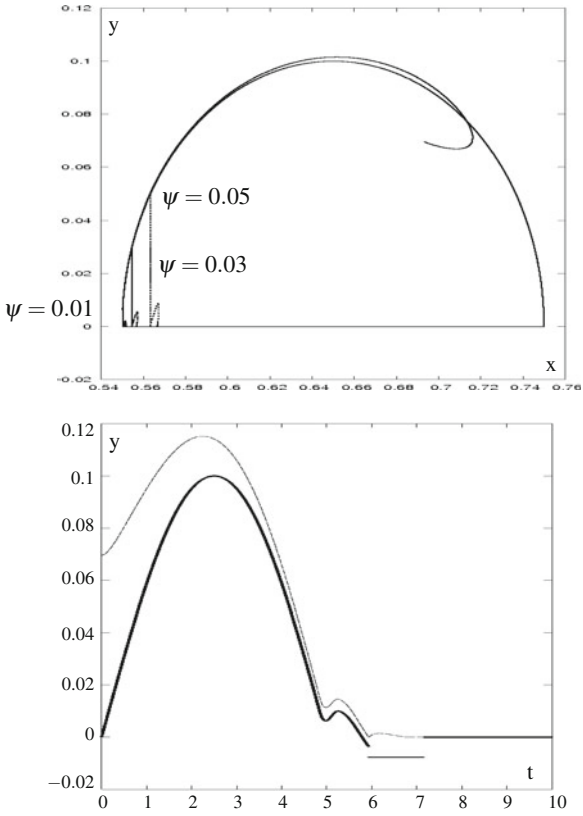

Fig. 8.4 *Up* The influence of ψ on the real trajectory's deformation for controller's gains set to $\gamma_1 = 8,\ \gamma_2 = 7$. *Down* $y(t) = q^1(t)$ (*dashed*) and $y_d^*(t) = (q_d^1)^*(t)$ (*solid*) during the first cycle ($\psi = 0.01$)

respectively, and both signals are set to zero at $t \approx 7.2$s. The jump of $q_d(\cdot)$ induces a positive jump in the variation of $V(\cdot)$ (details are in Sect. 8.1.9). The switches of the controller during the first 10 seconds are depicted in Fig. 8.5 (left). Clearly since the velocity jumps, the controller jumps as well.

The Fig. 8.5 (right) presents the variation of the contact force λ. One sees that λ remains 0 during the free-motion phases. The contact force λ is designed as a decreasing linear function during constrained motion phases $\Omega_k^{\{1\}}$ in order to allow a smooth detachment at the end of these phases. It is worth to mention that the magnitude of λ depends indirectly on $V(\tau_0^k)$. Precisely, when $V(\tau_0^k)$ approaches zero the system tends to a tangential stabilization on the boundary $\mathrm{bd}(\Phi)$, which implies larger values of t_0^k and consequently smaller length of $[t_f^k, t_d^{k,1}]$ and smaller magnitude of the contact force measured by λ (see Proposition 8.4).

Figure 8.6 shows that the tracking error described by the Lyapunov function rapidly decreases and remains close to 0. In other words the practical weak stability of Proposition 8.1 is guaranteed. On the zoom made in Fig. 8.6 one can also observe the behavior of $V(\cdot)$ during the stabilization on $\mathrm{bd}(\Phi)$, that is an almost decreasing function.

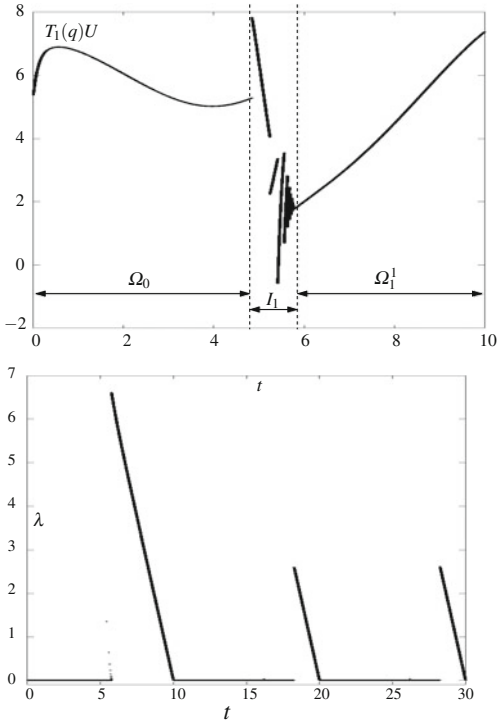

Fig. 8.5 *Up* The switching controller during the first 10 seconds; *Down* Variation of the contact force λ

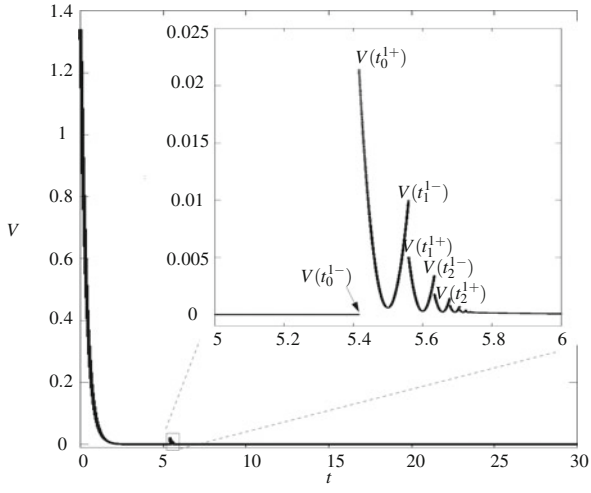

Fig. 8.6 Variation of the Lyapunov function for $\gamma_1 = 8$, $\gamma_2 = 7$; Zoom: Variation of the Lyapunov function during the phase I_0

8.1.7.2 A Planar Two-Link Rigid-Joint Manipulator with Two Constraints

In the sequel we introduce another constraint into the previous dynamics. Precisely, we impose an admissible domain $\Phi = \{(x, y) \mid y \geq 0,\ 0.7 - x \geq 0\}$. Let us also consider an unconstrained desired trajectory given by the circle $\{(x, y) \mid (x - 0.7)^2 + y^2 = 0.5\}$ that violates both constraints. In other words, the two-link planar manipulator must track a quarter-circle; stabilize on and then follow the line $\Sigma_1 = \{(x, y) \mid y = 0\}$; stabilize on the intersection of Σ_1 and $\Sigma_2 = \{(x, y) \mid x = 0.7\}$; detach from Σ_1 and follow Σ_2 until the unconstrained circle re-enters Φ and finally takeoff from Σ_2 in order to repeat the previous steps. Therefore, we have:

$$\mathbb{R}^+ = \Omega_0^{\emptyset} \cup I_1 \cup \Omega_1^{J_{1,1}} \cup I_2 \cup \Omega_2^{J_{2,1}} \cup \Omega_2^{J_{2,2}} \cup \Omega_2^{J_{2,3}} \cup I_3 \cup \Omega_2^{J_{3,1}} \cup I_4 \cup \ldots$$

with $J_{1,1} = \{1\}$, $J_{2,1} = \{1, 2\}$, $J_{2,2} = \{2\}$, $J_{2,3} = \emptyset$, etc. We note that during I_{2k+1} the system is stabilized on Σ_1 (1-impacts) while during I_{2k} the system is stabilized on $\Sigma_1 \cap \Sigma_2$ (2_{ε_k}−impacts).

The numerical values used for the dynamical model are again $l_1 = l_2 = 0.5\text{m}$, $I_1 = I_2 = 1\,\text{kg}\,\text{m}^2$, $m_1 = m_2 = 1\,\text{kg}$ and the restitution coefficient $e_\text{n} = 0.7$. The impacts are imposed by $\varphi = 100$ in (8.12) and (8.13) and the beginning of transition phases are defined using $\psi = 0.05$ in (8.14). We impose a period of 10 seconds for two consecutive cycles and we simulate the dynamics during 60 seconds. Setting the controller gains $\gamma_1 = 15$, $\gamma_2 = 15$ we see in Fig. 8.7 (left) that the desired trajectory is accurately followed. The jumps in the variation of the Lyapunov function are pointed out in Fig. 8.7 (right).

In this case we have imposed a constant contactforce λ_1 during the motion on the surface Σ_1 (see Fig. 8.8 (left)) and a decreasing contactforce, that allows a smooth detachment, during the motion on Σ_2 (see Fig. 8.8 (right)). In Fig. 8.9 the values of the multipliers λ_1 and λ_2 during the transition phase I_2 (stabilization in the corner) are depicted.

8.1.8 *Proof of Lemma 8.1*

From (8.10) we can deduce on one hand that

$$V(t_0^{k-}) \geq \gamma_1 \gamma_2 ||\tilde{q}(t_0^{k-})||^2,$$

and on the other hand

$$V(t_0^{k-}) \geq \frac{1}{2} s(t_0^{k-})^T M(q(t_0^{k-})) s(t_0^{k-}).$$

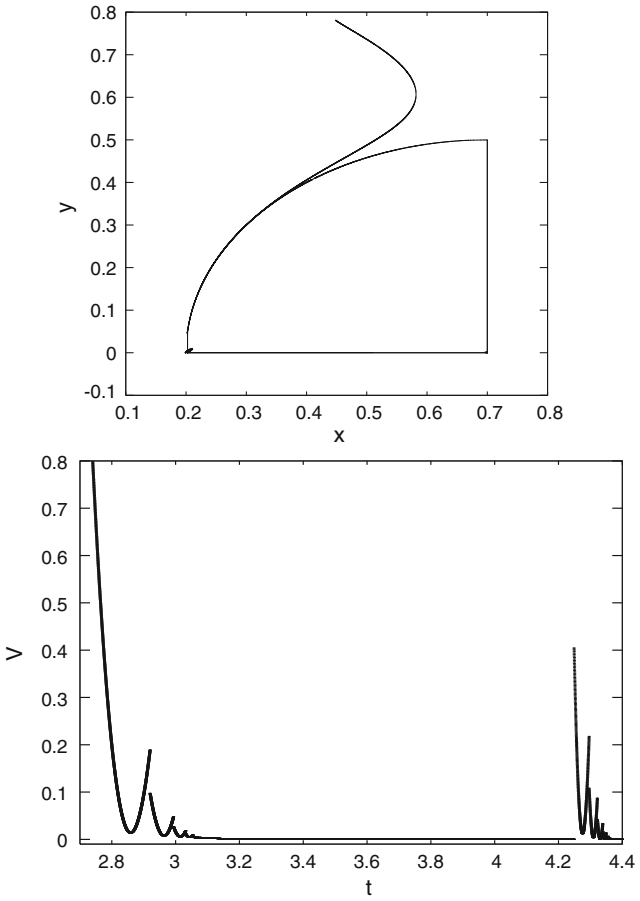

Fig. 8.7 *Up* The trajectory of the system during 6 cycles; *Down* Zoom on the variation of the Lyapunov function on the first two transition phases

Since condition (b) of Proposition 8.1 is satisfied one has $V(\tau_0^k) \geq V(t_0^{k-})$ and the first two inequalities in (8.24) become trivial. Let us recall that $s(t) = \dot{\tilde{q}}(t) + \gamma_2 \tilde{q}(t)$ which implies $||\dot{\tilde{q}}(t_0^{k-})|| \leq ||s(t_0^{k-})|| + \gamma_2 ||\tilde{q}(t_0^{k-})||$. Combining this with the first two inequalities in (8.24) we derive the third inequality in (8.24).

For the rest of the proof we assume that $t_0^k \leq \tau_1^k$. Therefore $(q_d)_p(t_0^{k-}) = (q_d^*)_p(t_0^k)$. Since $(q_d)_p(\cdot)$ is a continuous function with all the components $q_d^i(\cdot)$ defined as decreasing functions on $[\tau_0^k + \delta, \tau_1^k]$, it is obvious that $||(q_d)_p(t_0^{k-})|| \leq \max\{||(q_d)_p(\tau_0^k + \delta)||, ||(q_d)_p(\tau_1^k)||\} = \max\{\psi, \sqrt{p}\varphi V^{1/3}(\tau_0^k)\}$. Furthermore:

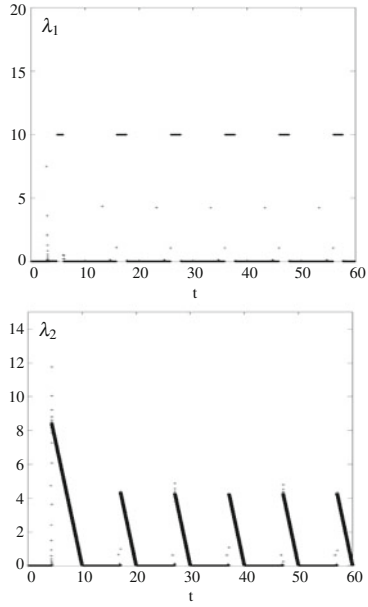

Fig. 8.8 *Up* Variation of the contact force during the motion on Σ_1; *Down* Variation of the contact force during the motion on Σ_2

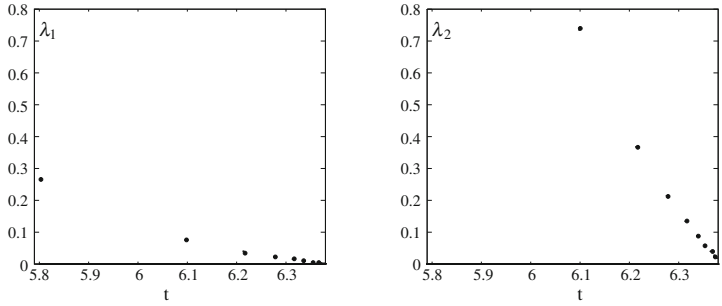

Fig. 8.9 Zoom on the transition phase I_2 with $2_\varepsilon-$impacts (*dots* are the impulsive force magnitude at impacts)

$$
\begin{aligned}
||q_p(t_0^k)|| &\leq ||\tilde{q}_p(t_0^{k-})|| + ||(q_d)_p(t_0^{k-})|| \\
&\leq \sqrt{\frac{V(\tau_0^k)}{\gamma_1\gamma_2}} + \max\{\psi, \sqrt{p}\varphi V^{1/3}(\tau_0^k)\}.
\end{aligned}
$$

Thus t_0^k is a p_{ε_k}-impact with $\varepsilon_k \leq \max\{\psi, \sqrt{p}\varphi V^{1/3}(\tau_0^k)\} + \sqrt{\frac{V(\tau_0^k)}{\gamma_1\gamma_2}}\}$. From Definition 8.2 one has $||q_p(t_0^k)|| \leq \varepsilon_k$ and using:

$$||(q_d)_p(t_0^{k-})|| \leq ||\tilde{q}_p(t_0^{k-})|| + ||q_p(t_0^k)||,$$

one obtains the first inequality (8.25). Let us denote $t_k' = \frac{t_0^k - \tau_0^k - \delta}{\tau_1^k - \tau_0^k - \delta} \in [0, 1]$. We recall here that τ_0^k was chosen such that $||q_p^{nc}(\tau_0^k)|| \leq \psi$. From (8.12) and (8.13) and the first inequality in (8.25), for $i = 1, \ldots, p$ one has:

$$\begin{aligned} q_d^i(t_0^{k-}) &= \left[(q^i)^{nc}(\tau_0^k) + \varphi V^{1/3}(\tau_0^k)\right]\left(2(t_k')^3 - 3(t_k')^2\right) + (q^i)^{nc}(\tau_0^k) \\ &\leq \varepsilon_k + \sqrt{\frac{V(\tau_0^k)}{\gamma_1\gamma_2}}. \end{aligned}$$

It follows that:

$$3(t_k')^2 - 2(t_k')^3 \geq \frac{(q^i)^{nc}(\tau_0^k) - \varepsilon_k - \sqrt{\frac{V(\tau_0^k)}{\gamma_1\gamma_2}}}{(q^i)^{nc}(\tau_0^k) + \varphi V^{1/3}(\tau_0^k)}.$$

For $t > 0$ one has $2t - t^2 \geq 3t^2 - 2t^3$, therefore:

$$2t_k' - (t_k')^2 \geq \frac{(q^i)^{nc}(\tau_0^k) - \varepsilon_k - \sqrt{\frac{V(\tau_0^k)}{\gamma_1\gamma_2}}}{(q^i)^{nc}(\tau_0^k) + \varphi V^{1/3}(\tau_0^k)},$$

which means that

$$(1 - t_k')^2 \leq \frac{\sqrt{\frac{V(\tau_0^k)}{\gamma_1\gamma_2}} + \varphi V^{1/3}(\tau_0^k) + \varepsilon_k}{(q^i)^{nc}(\tau_0^k) + \varphi V^{1/3}(\tau_0^k)}.$$

Straightforward computations lead to

$$|\dot{q}_d^i(t_0^{k-})| = \frac{6((q^i)^{nc}(\tau_0^k) + \varphi V^{1/3}(\tau_0^k))}{\tau_1^k - \tau_0^k - \delta}\left(t_k' - (t_k')^2\right).$$

Since $t_k' - (t_k')^2 \leq 1 - t_k'$ and from (8.14) one has $(q^i)^{nc}(\tau_0^k) \leq \psi$, one arrives at:

$$\begin{aligned} |\dot{q}_d^i(t_0^{k-})| &\leq \frac{6((q^i)^{nc}(\tau_0^k) + \varphi V^{1/3}(\tau_0^k))}{\tau_1^k - \tau_0^k - \delta}(1 - t_k') \\ &\leq \frac{6\sqrt{(\psi + \varphi V^{1/3}(\tau_0^k))\left(\sqrt{\frac{V(\tau_0^k)}{\gamma_1\gamma_2}} + \varphi V^{1/3}(\tau_0^k) + \varepsilon_k\right)}}{\tau_1^k - \tau_0^k - \delta} \\ &= \frac{6}{\tau_1^k - \tau_0^k - \delta}\sqrt{\left\{\psi\varepsilon_k + (\psi\varphi + \varepsilon_k\varphi)V^{1/3}(\tau_0^k) + \right.} \\ &\qquad \left. \overline{\varphi^2 V^{2/3}(\tau_0^k) + \frac{\varphi V^{5/6}(\tau_0^k) + \psi V^{1/2}(\tau_0^k)}{\sqrt{\gamma_1\gamma_2}}}\right\}. \end{aligned}$$

Since $V(\tau_0^k) < 1$ (thus $V^{p_1}(\tau_0^k) > V^{p_2}(\tau_0^k)$ for $p_1 < p_2$) we obtain:

$$|\dot{q}_d^i(t_0^{k-})| \leq \frac{6\sqrt{\psi\varepsilon_k + \left[\left(\frac{1}{\sqrt{\gamma_1\gamma_2}} + \varphi\right)(\varphi+\psi) + \varepsilon_k\varphi\right] V^{1/3}(\tau_0^k)}}{\tau_1^k - \tau_0^k - \delta}.$$

Furthermore $\varepsilon_k \leq \psi + \sqrt{p}\varphi V^{1/3}(\tau_0^k) + \sqrt{\frac{V(\tau_0^k)}{\gamma_1\gamma_2}}$ and

$$|\dot{q}_d^i(t_0^{k-})| \leq \frac{6\psi}{\tau_1^k - \tau_0^k - \delta} + \frac{6\sqrt{\left(\frac{2}{\sqrt{\gamma_1\gamma_2}} + (1+\sqrt{p})\varphi\right)(\varphi+\psi) + \psi\varphi}}{\tau_1^k - \tau_0^k - \delta} V^{1/3}(\tau_0^k).$$

Consequently, the second inequality in (8.25) holds with

$$\begin{cases} K = \dfrac{6p\psi}{\tau_1^k - \tau_0^k - \delta}, \\ K' = \dfrac{6\sqrt{p}}{\tau_1^k - \tau_0^k - \delta}\sqrt{\left(\dfrac{2}{\sqrt{\gamma_1\gamma_2}} + (1+\sqrt{p})\varphi\right)(\varphi+\psi) + \psi\varphi}. \end{cases}$$

8.1.9 *Proof of Theorem 8.1*

First we observe that conditions (a) and (d) of Proposition 8.1 hold when the hypothesis of the Theorem are verified. Thus in order to prove Theorem 8.1 it is sufficient to verify the conditions (b), (c) and (e) of Proposition 8.1. To this aim we shall also use the function $V_1(t,s) = \frac{1}{2}s(t)^T M(q)s(t)$.
(b) Using that $\dot{M}(q) - 2C(q,\dot{q}))$ is a skew-symmetric matrix from Assumption 5, straightforward computations show that on $\mathbb{R}_+ \setminus \bigcup_{k\geq 1}[t_0^k, t_f^k]$ the time derivative of the Lyapunov function is given by

$$\dot{V}(t) = -\gamma_1 s^T s + 2\gamma_1\gamma_2\tilde{q}^T\dot{\tilde{q}} = -\gamma_1||\dot{\tilde{q}}||^2 - \gamma_1\gamma_2^2||\tilde{q}||^2.$$

On the other hand

$$V(t) \leq \frac{\lambda_{max}(M(q))}{2}||s||^2 + \gamma_1\gamma_2||\tilde{q}||^2 \leq \gamma^{-1}[\gamma_1||\dot{\tilde{q}}||^2 + \gamma_1\gamma_2^2||\tilde{q}||^2],$$

where $\gamma^{-1} = \max\left\{\lambda_{max}(M(q))\frac{1+2\gamma_2}{2\gamma_1}; \frac{\lambda_{max}(M(q))(\gamma_2+2)+2\gamma_1}{2\gamma_1\gamma_2}\right\} > 0$. Therefore $\dot{V}(t) \leq -\gamma^{-1}V(t)$ on $\mathbb{R}_+ \setminus \bigcup_{k\geq 1}[t_0^k, t_f^k]$.

(c) By definition

$$V(t_{\ell+1}^{k-}) - V(t_\ell^{k+}) = V_1(t_{\ell+1}^{k-}) - V_1(t_\ell^{k+}) + \gamma_1\gamma_2[\tilde{q}(t_{\ell+1}^{k-})^T\tilde{q}(t_{\ell+1}^{k-}) - \tilde{q}(t_\ell^{k+})^T\tilde{q}(t_\ell^{k+})]. \tag{8.27}$$

On the other hand, straightforward computations show that

$$\begin{aligned} V_1(t_{\ell+1}^{k-}) - V_1(t_\ell^{k+}) &= \int_{(t_\ell^k, t_{\ell+1}^k)} \dot{V}_1(t)\mathrm{d}t \\ &= \gamma_1\gamma_2 \int_{(t_\ell^k, t_{\ell+1}^k)} s_p(t)^T (q_d^*)_p(t)\mathrm{d}t - \gamma_1 \int_{(t_\ell^k, t_{\ell+1}^k)} s(t)^T s(t)\mathrm{d}t \end{aligned} \tag{8.28}$$

Furthermore,

$$\begin{aligned} \int_{(t_\ell^k, t_{\ell+1}^k)} s(t)^T s(t)\mathrm{d}t = &\int_{(t_\ell^k, t_{\ell+1}^k)} ||\dot{\tilde{q}}(t)||^2 + \gamma_2^2||\tilde{q}(t)||^2\mathrm{d}t \\ &+\gamma_2[\tilde{q}(t_{\ell+1}^{k-})^T\tilde{q}(t_{\ell+1}^{k-}) - \tilde{q}(t_\ell^{k+})^T\tilde{q}(t_\ell^{k+})]. \end{aligned} \tag{8.29}$$

Therefore, inserting successively (8.29) in (8.28) and (8.28) in (8.27) we arrive at:

$$V(t_{\ell+1}^{k-}) - V(t_\ell^{k+}) \leq \gamma_1\gamma_2 \int_{(t_\ell^k, t_{\ell+1}^k)} s_p(t)^T (q_d^*)_p(t)\mathrm{d}t. \tag{8.30}$$

In the sequel let us denote by $S(v)$ the sum of all the components of a vector v. Taking into account the definition (8.12) and the fact that $(q_d)_p$ and $(\dot{q}_d)_p$ are set to zero at t_0^{k+} one obtains:

$$\int_{(t_\ell^k, t_{\ell+1}^k)} s_p(t)^T (q_d^*)_p(t)\mathrm{d}t = -\varphi V^{1/3}(\tau_0^k)\left(\int_{(t_\ell^k, t_{\ell+1}^k)} S(\dot{q}_p(t))\mathrm{d}t + \gamma_2 \int_{(t_\ell^k, t_{\ell+1}^k)} S(q_p(t))\mathrm{d}t\right).$$

Since $\varphi\gamma_2 V^{1/3}(\tau_0^k) \geq 0$ and $S(q_p(t)) \geq 0$ it follows that

$$\int_{t_\ell^k}^{t_{\ell+1}^k} s_p(t)^T (q_d^*)_p(t)\mathrm{d}t \leq \varphi V^{1/3}(\tau_0^k)[S(q_p(t_\ell^k)) - S(q_p(t_{\ell+1}^k))].$$

Thus:

$$\begin{aligned} \sum_{\ell\geq 0}\left[V(t_{\ell+1}^{k-}) - V(t_\ell^{k+})\right] &\leq \gamma_1\gamma_2\varphi V^{1/3}(\tau_0^k)S(q_p(t_0^k)) \\ &\leq \gamma_1\gamma_2\varphi V^{1/3}(\tau_0^k)\sqrt{3}||q_p(t_0^k)||. \end{aligned}$$

Since t_0^k is a p_{ε_k}-impact and $\varepsilon_k \leq \psi + \sqrt{p}\varphi V^{1/3}(\tau_0^k) + \sqrt{\frac{V(\tau_0^k)}{\gamma_1\gamma_2}}$ one gets

$$\sum_{\ell\geq 0}\left[V(t_{\ell+1}^{k-}) - V(t_\ell^{k+})\right] \leq K_1 V^{p_1}(\tau_0^k),$$

where $K_1 = \sqrt{3}\gamma_1\gamma_2\varphi(\psi + \sqrt{p}\varphi + \frac{1}{\sqrt{\gamma_1\gamma_2}}) > 0$ and $p_1 = \frac{2}{3}$.

(e) First, let us compute the Lyapunov function's jumps at the instants t_ℓ^k, $\ell \geq 1$. Using the continuity of the position $q(\cdot)$ and the definition of the desired trajectory $q_d(\cdot)$ on the I_k phases (i.e. $q_d(t_\ell^{k+}) = q_d(t_\ell^{k-})$, $\dot{q}_d(t_\ell^{k+}) = 0 = \dot{q}_d(t_\ell^{k-})$) we obtain:

$$\begin{aligned}\sigma_V(t_\ell^k) &= V(t_\ell^{k+}) - V(t_\ell^{k-}) \\ &= \gamma_1\gamma_2\sigma_{||\tilde{q}||^2}(t_\ell^k) + + \frac{s(t_\ell^{k+})^T M_\ell^k s(t_\ell^{k+}) - s(t_\ell^{k-})^T M_\ell^k s(t_\ell^{k-})}{2} \\ &= T_L(t_\ell^k) + \gamma_2\tilde{q}(t_\ell^k)^T M_\ell^k \sigma_{\dot{q}}(t_\ell^k),\end{aligned} \tag{8.31}$$

where M_ℓ^k denotes the inertia matrix $M(q(t_\ell^k))$ and $T_L(t_\ell^k)$ is the kinetic energy loss at the impact time t_ℓ^k. From Eq. (8.3) we have $T_L(t_\ell^k) \leq 0$ and Eq. (8.31) becomes $\sigma_V(t_\ell^k) \leq \gamma_2\tilde{q}(t_\ell^k)^T M_\ell^k \sigma_{\dot{q}}(t_\ell^k)$. Let us recall that $M_\ell^k\sigma_{\dot{q}}(t_\ell^k)$ is the magnitude of the impulsive contact force (or its impulse), denoted here as $\mathscr{P}$ (see Chap. 1). In the generalized coordinates introduced in Sect. 8.1.2 one obtains $M_\ell^k\sigma_{\dot{q}}(t_\ell^k) = D^T\mathscr{P}$ with $\lambda = \mathscr{P}\delta_{t_\ell^k}$. The vector $\dot{q}_{\tan}$ (see Chap. 6) is equal to $\dot{q}_{n-m}$ (i.e. $\sigma_{\dot{q}}(t_\ell^k) = \begin{pmatrix}\sigma_{\dot{q}_m}(t_\ell^k) \\ \mathbf{0}_{n-m}\end{pmatrix}$ where $\mathbf{0}_{n-m}$ denotes the $n-m$ vector with all its components equal zero). Therefore:

$$\sigma_V(t_\ell^k) \leq \gamma_2\tilde{q}(t_\ell^k)^T M_\ell^k\sigma_{\dot{q}}(t_\ell^k) = \gamma_2 q_p(t_\ell^k)^T\mathscr{P} = 0, \tag{8.32}$$

where we have used $(q_d)_p(t_\ell^{k+}) = 0 = (q_d)_p(t_\ell^{k-})$ and the last equality is stated using the complementarity relation entering the dynamics, which impose that $\mathscr{P}$ is orthogonal to $\mathrm{bd}(\Phi)$.

The Lyapunov function's jump corresponding to the first impact of each cycle can be computed as:

$$\begin{aligned}\sigma_V(t_0^k) &= V(t_0^{k+}) - V(t_0^{k-}) \\ &= \gamma_1\gamma_2\sigma_{||\tilde{q}||^2}(t_0^k) + + \frac{s(t_0^{k+})^T M_0 s(t_0^{k+}) - s(t_0^{k-})^T M_0 s(t_0^{k-})}{2}.\end{aligned} \tag{8.33}$$

- It is clear that $t_0^k > \tau_1^k$ implies $q_d(t_0^{k+}) = q_d(t_0^{k-})$ and $\dot{q}_d(t_0^{k+}) = 0 = \dot{q}_d(t_0^{k-})$. Thus, the computations for t_ℓ^k, $\ell \geq 1$ hold also for t_0^k.
- If $t_0^k \leq \tau_1^k$ one has $(q_d)_p(t_0^{k-}) \neq (q_d)_p(t_0^{k+}) = 0$ and $(\dot{q}_d)_p(t_0^{k-}) \neq (\dot{q}_d)_p(t_0^{k+}) = 0$. Then the initial jump of each cycle is given by:

$$\begin{aligned}\sigma_V(t_0^k) &= T_L(t_0^k) + \dot{q}_d(t_0^{k-})^T M_0\dot{q}(t_0^{k-}) \\ &\quad + \frac{\gamma_2^2}{2}\left(\tilde{q}(t_0^{k+})^T M_0\tilde{q}(t_0^{k+}) - \tilde{q}(t_0^{k-})^T M_0\tilde{q}(t_0^{k-})\right) \\ &\quad + \gamma_2\left(\dot{q}(t_0^{k+})^T M_0\tilde{q}(t_0^{k+}) - \dot{\tilde{q}}(t_0^{k-})^T M_0\tilde{q}(t_0^{k-})\right) \\ &\quad - \frac{1}{2}\dot{q}_d(t_0^{k-})^T M_0\dot{q}_d(t_0^{k-}).\end{aligned} \tag{8.34}$$

Since $T_L(t_0^k) \leq 0$ the Eq. (8.34) rewrites as:

$$\begin{aligned}\sigma_V(t_0^k) \leq \lambda_{max}(M(q))\Big[&\gamma_2\big(||(\dot{q}_d)_p(t_0^{k-})|| \cdot ||\tilde{q}(t_0^{k-})|| \\ &+ ||\dot{q}(t_0^{k-})|| \cdot ||(q_d)_p(t_0^{k-})||\big) + \frac{1}{2}||(\dot{q}_d)_p(t_0^{k-})||^2 \\ &+ \frac{\gamma_2^2}{2}\big(||q_p(t_0^k)||^2 + ||\tilde{q}_p(t_0^{k-})||^2 \\ &+ 2||(q_d)_p(t_0^{k-})|| \cdot ||\tilde{q}_{n-p}(t_0^{k-})||\big) + ||(\dot{q}_d)_p(t_0^{k-})|| \cdot ||\dot{q}(t_0^{k-})||.\Big]\end{aligned} \tag{8.35}$$

Obviously $||\dot{q}(t_0^{k-})|| = ||\dot{\tilde{q}}(t_0^{k-}) + (\dot{q}_d)_p(t_0^{k-})||$ and Lemma 8.1 combined with $V(\tau_0^k) < 1$ yields:

$$||\dot{q}(t_0^{k-})|| \leq K + \left(\sqrt{\frac{2}{\lambda_{min}(M)}} + \sqrt{\frac{\gamma_2}{\gamma_1}} + K'\right) V^{1/3}(\tau_0^k).$$

Therefore

$$\sigma_V(t_0^k) \leq K_2 V^{p_2}(\tau_0^k) + \xi,$$

where $p_2 = \frac{1}{3}$, $\xi = \frac{3}{2}K^2 + \gamma_2 \psi K + \frac{\gamma_2^2 \psi^2}{2}$ and

$$\begin{aligned}K_2 = \lambda_{max}(M(q))\Big[&3KK' + \tfrac{3}{2}(K')^2 + \gamma_2 \psi K + \sqrt{\tfrac{2\gamma_2}{\lambda_{min}(M(q))\gamma_1}} \\ &+ (K' + K)\left(\gamma_2\sqrt{p}\varphi + 3\sqrt{\tfrac{\gamma_2}{\gamma_1}} + \sqrt{\tfrac{2}{\lambda_{min}(M(q))}}\right) \\ &+ \gamma_2\left(\sqrt{\tfrac{2}{\lambda_{min}(M(q))}} + 3\sqrt{\tfrac{\gamma_2}{\gamma_1}}\right)(\psi + \sqrt{p}\varphi) + \gamma_2^2\psi\varphi\sqrt{p} + \tfrac{\gamma_2^2\varphi^2 p}{2} + \tfrac{4\gamma_2}{\gamma_1} \\ &+ \psi\gamma_2\left(2\sqrt{\tfrac{\gamma_2}{\gamma_1}} + \sqrt{\tfrac{2}{\lambda_{min}(M(q))}} + K'\right)\Big].\end{aligned}$$

Defining $\alpha : \mathbb{R}_+ \mapsto \mathbb{R}_+$, $\alpha(\omega) = \rho\omega^2$ we get $\alpha(0) = 0$ and $\alpha(|||[s(t), \tilde{q}(t)]|||) \leq V(t, s, \tilde{q})$. Thus, Proposition 8.1 also yields

$$R = \alpha^{-1}(e^{-\gamma(t_f^k - t_\infty^k)}(1 + K_1 + K_2 + \xi)) = \sqrt{e^{-\gamma(t_f^k - t_\infty^k)}(1 + K_1 + K_2 + \xi)/\rho},$$

which ends the proof.

8.2 Short Bibliography

The control of mechanical systems subject to unilateral constraints has been the object of many studies. Theoretical aspects of their Lyapunov stability and the related stabilization issues have been studied in [205, 730, 731, 1208]. The specific, yet important

task of the stabilization of impacting transition phases was analyzed and experimentally tested in [715, 952, 1085, 1233, 1234, 1289], see also Sect. 8.5.1. From the point of view of tracking control of complementarity Lagrangian systems along general constrained/unconstrained paths, such studies focus on a module of the overall control problem. The problem of robust impact detection with only position measurement received attention in [167]. One of the first results formulating the control of complete robotic tasks via unilateral constraints and complementarity conditions was presented in [548, 549]. In that work the impacts were considered inelastic and the control problem was solved using a time optimal problem. Other results can be found in [244, 351, 793, 794, 810, 849, 853, 854, 984, 1205, 1206, 1207, 1282, 1332, 1333]. The tracking control problem under consideration, involving systems that undergo transitions from free to constrained motions, and *vice versa*, along an infinity of cycles, was formulated and studied in [220, 221] for the one-degree-of-freedom case and in [166] for the n-degree-of-freedom case. These articles consider systems with only one unilateral frictionless constraint, and the stability framework is more stringent than those used above. The results presented in this section not only consider the multiconstraint case, but the results in Sect. 8.1.6 relax some very hard to verify conditions imposed in [166] to assure the stability. Moreover the accurate design of the control law that guarantees the detachment from the constraints is formulated and incorporated in the stability analysis for the first time. Considering multiple constraints may be quite important in applications like virtual reality and haptic systems, where typical tasks involve manipulating objects modeled as rigid bodies [389] in complex environments with many unilateral constraints. We note that in the case of a single nonsmooth impact the exponential stability and bounded-input bounded-state (BIBS) stability was studied in [841] using a state feedback control law. A study for a multiple-degree-of-freedom linear systems subject to nonsmooth impacts can be found in [840]. That approach proposes a proportional-derivative control law in order to study BIBS stability via Lyapunov techniques. State observers for systems without finite accumulations of impacts have been studied in [843, 844]. Other approaches for the tracking control of nonsmooth mechanical systems in a more restricted context than the one above can be found in [147, 148, 408, 423, 839, 916, 951] and in [732]. Most of these articles focus on vibro-impact systems, i.e., they disregard contact phases and/or contact forces (hence the crucial complementarity conditions), and assume that impact times are separated (no finite accumulations). The underlying stability concept may anyway be different from the one we chose above, see for instance [147] where a hybrid distance function as in (1.53) is used. An interesting direction of research could be to use the ideas in [147] for the transition phase control. The analysis and control of systems subject to unilateral constraints also received attention in [124]. Almost decreasing Lyapunov functions (also called *nonmonotonic*) seem to have been introduced first in [220, 1292, 1293], later in [192, 263, 848, 1112]. Interesting results have been obtained in [243, 1253], which extend the bouncing ball dynamics with finite accumulation of impact times, toward more general systems. Such asymptotic analysis could be used to prove that the transition controller U_t guarantees that Assumption 4 holds. Lyapunov functions for the impacting phase of bouncing ball dynamics, are proposed in [461, 462, 727, 945],

see more detailed comments in Sect. 7.5.4. Results in the same vein are in [1188] (it is noteworthy that the hybrid systems dynamical framework in [461, 1188] *does not* encapsulates complementarity Lagrangian systems). See also the material in Sect. 7.6.4.2.

8.3 Trajectory Tracking: Flexible-Joint Rigid-Link Systems

Impacts may excite vibrational modes in structures, due to the system's flexibilities. It is therefore important to compensate for flexibilities effects *via* the feedback controller, as shown experimentally in [224, 225] for free-motion tasks. Let us deal with a class of Lagrangian systems with lumped flexibilities (encompassing flexible-joint rigid-link manipulators) subject to frictionless unilateral constraints, whose dynamics is supposed to be expressed as:

$$\begin{cases} M(q)\ddot{q} + C(q,\dot{q})\dot{q} + G(q) + K(q-\theta) = D^T\lambda \\ J\ddot{\theta} + K(\theta - q) - \mathscr{K}(q,\theta) = U \\ q^1 \geq 0,\ (q^1)^T\lambda = 0,\ \lambda \geq 0 \\ \text{Collision rule,} \end{cases} \tag{8.36}$$

where $q \in \mathbb{R}^n$ is the vector of rigid links angles, $\theta \in \mathbb{R}^n$ is the vector of motor shaft angles, $M(q) = M(q)^T \in \mathbb{R}^{n\times n}$ is the positive definite inertia matrix, $C(q,\dot{q})$ is the matrix containing Coriolis and centripetal forces, $G(q)$ contains conservative forces, $\lambda \in \mathbb{R}^m$ is the vector of Lagrangian multipliers associated with the constraints, $J \in \mathbb{R}^{n\times n}$ is the diagonal and constant matrix of actuator inertia, $K = K^T > 0$, $K \in \mathbb{R}^{n\times n}$ represents the stiffness matrix, $U \in \mathbb{R}^n$ is the vector of generalized torque inputs, and $q^1 = Dq \in \mathbb{R}^m$ with $D = [I_m\ 0_{m\times(n-m)}]$. As usual constraint i is said to be *active* if $q_i^1 = 0$, and *inactive* if $q_i^1 > 0$. The dynamics in (8.36) is a simplified dynamics obtained from more general Lagrangian systems using the generalized coordinate transformation which allowed us to transform (8.1) into (8.8). The system's mass matrix is now given by $\bar{M}(q) = \text{diag}(M(q), J) \in \mathbb{R}^{2n\times 2n}$. It is supposed to hold globally in the configuration space. Notice that a nonlinear stiffness $\mathscr{K}(q,\theta)$ may appear due to the transformation, see [875, §3] for details about this. The same impact law as in (8.2) is used, however, one has to adapt the tangent cones calculations [875, Definition 4]. In particular we have a continuous $\dot{\theta}(\cdot)$ at impacts, in agreement with the results of Sect. 3.4.2. The dynamical system in (8.36) is underactuated.

The following notations will be adopted in this section: for a real-valued function $f{:}\mathbb{R}^+ \mapsto \mathbb{R}$ one denotes by $S(f)$ the set of all real-valued function $g{:}\mathbb{R}^+ \mapsto \mathbb{R}$ such that there exists a positive real constant $0 < c < \infty$ satisfying $g(t) \leq cf(t)$, for all $t \geq 0$. One writes $g \in S(1) \equiv L^\infty$ if $f(t) = 1$, for all $t \geq 0$. 0_n is the n-vector with entries 0, and $0_{n\times m}$ is the $n \times m$-zero matrix. I_m is the $m \times m$ identity matrix.

The admissible domain associated to the system (8.36) is the finitely represented closed subset of $\mathbb{R}^{2n}$: $\Phi \triangleq \{(q,\theta) \in \mathbb{R}^{2n} \mid q^1 \geq 0\} = \left(\bigcap_{1\leq i\leq m} \Phi_i\right) \times \mathbb{R}^n$ where

$\Phi_i = \{q \in \mathbb{R}^n \mid q_i^1 \geq 0\}$. In the sequel $\left(\bigcap_{1\leq i\leq m} \Phi_i\right)$ will be denoted by $\Phi \subset \mathbb{R}^n$. Mimicking the rigid link–rigid joint case, let us introduce the following notion of p_ε-impact, that is similar to Definition 8.2.

Definition 8.5 Let $\varepsilon \geq 0$ be a fixed real number. We say that a p_ε-impact occurs at the instant t if

$$||\left(q_i^1\right)_{i\in I}(t)|| \leq \varepsilon, \quad \prod_{i\in I} q_i^1(t) = 0$$

where $I \subset \{1, \ldots, m\}$, $card(I) = p$.

If $\varepsilon = 0$ all p surfaces $\Sigma_i \subseteq \text{bd}(\Phi_i) = \{q \in \mathbb{R}^n \mid q_i^1 = 0\}$, $i \in I$ are struck simultaneously and we get a $p-$impact in the sense of Definition 6.1. When $\varepsilon > 0$ the system collides bd(Φ) in a neighborhood of the intersection $\bigcap_{i\in I} \Sigma_i$.

8.3.1 Basic Concepts

8.3.1.1 Typical Task

Since the system's dynamics does not change when the number of active constraints decreases one gets the following typical task representation:

$$\begin{gathered}\mathbb{R}^+ = \bigcup_{k\geq 0}\left(\Omega_{2k}^{B_k} \cup I_k^{B_k} \cup \left(\bigcup_{i=1}^{m_k} \Omega_{2k+1}^{B_{k,i}}\right)\right) \\ B_k \subset B_{k,1};\ B_{k+1} \subset B_{k,m_k} \subset B_{k,m_k-1} \subset \ldots B_{k,1}\end{gathered} \tag{8.37}$$

where the superscript B_k represents the set of active constraints during the corresponding motion phase, and $I_k^{B_k}$ denotes the transient between two Ω_k phases when the number of active constraints increases. We note that $B_k = \emptyset$ corresponds to free motion. When the number of active constraints decreases no transition phases are needed, thus, for the sake of simplicity we replace $\bigcup_{i=1}^{m_k} \Omega_{2k+1}^{B_{k,i}}$ by $\Omega_{2k+1}^{B'_k}$ and the typical task representation simplifies as follows:

$$\begin{gathered}\mathbb{R}^+ = \bigcup_{k\geq 0}\left(\Omega_{2k}^{B_k} \cup I_k^{B_k} \cup \Omega_{2k+1}^{B'_k}\right) \\ B_k \subset B'_k, \quad B_{k+1} \subset B'_k\end{gathered} \tag{8.38}$$

Similarly to what we stated in Sect. 8.1.1.3, since the tracking control problem involves no difficulty during the Ω_k-phases, *the central issue is once again the study of the passages between them (the design of transition phases I_k and detachment conditions), and the stability of the trajectories evolving along (8.38)* (i.e., an infinity of cycles). Throughout the section, the sequence $\Omega_{2k}^{B_k} \cup I_k^{B_k} \cup \Omega_{2k+1}^{B'_k}$ will be referred to

as the cycle C_k of the system's evolution: $\mathbb{R}^+ = \bigcup_{k\geq 0} C_k$. It is noteworthy that the descriptions in (8.4) and (8.37) are the same, but the cycles are defined differently. More precisely, one has respectively:

$$\mathbb{R}^+ = \Omega_0^{\emptyset} \cup \overbrace{I_1 \bigcup_{1}^{m_1} \Omega_1^{J_{1,i}}}^{C_1} \cup \overbrace{I_2 \bigcup_{1}^{m_2} \Omega_2^{J_{2,i}}}^{C_2} \cup \overbrace{I_3 \bigcup_{1}^{m_3} \Omega_3^{J_{3,i}}}^{C_3} \cup ... \tag{8.39}$$

and

$$\mathbb{R}^+ = \overbrace{\Omega_0^{B_0} \cup I_0^{B_0} \bigcup_{i=1}^{m_0} \Omega_1^{B_{0,i}}}^{C_0} \cup \overbrace{\Omega_2^{B_1} \cup I_1^{B_1} \bigcup_{i=1}^{m_1} \Omega_3^{B_{1,i}}}^{C_1} \cup \overbrace{\Omega_4^{B_2} \cup I_2^{B_2} \bigcup_{i=1}^{m_2} \Omega_1^{B_{2,i}}}^{C_2} \cup ... \tag{8.40}$$

with $B_0 \subset B_{0,1}$, $B_1 \subset B_{0,m_0} \subset B_{0,m_0-1} \subset ... \subset B_{0,1}$, $J_{1,m_1} \subset J_{2,1}$, $J_{1,m_1} \subset J_{1,m_1-1} \subset ... \subset J_{1,1}$. There is therefore a certain freedom in the choice of the task framework.

8.3.1.2 System Properties

For kinematic chains with prismatic or revolute joints the following properties hold, if Christoffel's symbols associated with the mass matrix are used to write $C(q, \dot{q})$.

Property 8.1 The matrix $\frac{d}{dt}M(q) - 2C(q, \dot{q})$ is skew symmetric, equivalently $\dot{M}(q) \triangleq \frac{d}{dt}M(q) = C(q, \dot{q}) + C(q, \dot{q})^T$. Furthermore the matrix $C(q, \dot{q})$ is a smooth function of q and $\dot{q}$ with the well-known properties $||C(q, \dot{q})|| \in S(||\dot{q}||)$ and $C(q, y)z = C(q, z)y$, for all $q, y, z \in \mathbb{R}^n$.

Property 8.2 The conservative forces vector $G(q)$ is such that $\left|\left|\frac{\partial G(q)}{\partial q}\right|\right| \in S(1)$ which implies by the mean value theorem $||G(q_1) - G(q_2)|| \in S(||q_1 - q_2||)$, for all $q_1, q_2 \in \mathbb{R}^n$.

Property 8.3 The matrix $C(q, \dot{q})$ is such that $\left|\left|\frac{\partial C(q,\dot{q})}{\partial q}\right|\right| \in S(||\dot{q}||)$ and $\left|\left|\frac{\partial C(q,\dot{q})}{\partial \dot{q}}\right|\right| \in S(1)$.

8.3.1.3 Stability Analysis Criteria

The system (8.36) is a complex nonsmooth and nonlinear dynamical system. Let us introduce the framework the stability analysis framework as well as some definitions. Let us define Ω as the complement in $\mathbb{R}_+$ of $I = \bigcup_{k\geq 0} I_k^{B_k}$ and assume that the Lebesgue

measure $\eta[\Omega]$, equals infinity. Let $x(\cdot)$ be the state of the closed-loop system in (8.36) with some feedback controller $U(q, \dot{q}, \theta, \dot{\theta}, t)$.

Consider $I_k^{B_k} \triangleq [\tau_0^k, t_f^k]$ and $V(\cdot)$ such that there exists class $\mathscr{K}$ functions $\alpha(\cdot)$ and $\beta(\cdot)$ such that $\alpha(||x||) \leq V(x,t) \leq \beta(||x||)$. In the sequel, we consider that for each cycle the sequence of impact instants $\{t_\ell^k\}_{\ell \geq 0}$ has an accumulation point t_∞^k. Stability in the sense of Definition 8.3 is guaranteed by the following proposition, which slightly differs from Proposition 8.1.

Proposition 8.5 (Weak Stability) *Assume that the task admits the representation (8.38) and that*

(a) $\eta[I_k^{B_k}] < +\infty, \quad \forall k \in \mathbb{N}$,
(b) *outside the impact accumulation phases* $[t_0^k, t_\infty^k]$ *one has* $\dot{V}(x(t), t) \leq -\gamma V(x(t), t)$ *for some constant* $\gamma > 0$,
(c) *the system is initialized on* Ω_0 *such that* $V(\tau_0^0) \leq 1$,
(d) $V(t_\infty^k) \leq \rho^* V(\tau_0^k) + \xi$ *where* $\rho^*, \ \xi \in \mathbb{R}_+$.

Then $V(\tau_0^k) \leq \delta(\gamma, \xi)$, $\forall k \geq 1$ *where* $\delta(\gamma, \xi)$ *is a function that can be made arbitrarily small by increasing either the value of* γ *or the length of the time interval* $[t_\infty, t_f]$. *Thus, the system is practically weakly stable with* $R = \alpha^{-1}(\delta(\gamma, \xi))$.

Proof From assumption (b) one has

$$V(t_f^k) \leq V(t_\infty^k) e^{-\gamma(t_f^k - t_\infty^k)},$$

and using condition (d) and (c) we arrive at

$$V(t_f^k) \leq e^{-\gamma(t_f^k - t_\infty^k)}(\rho^* + \xi) \triangleq \delta(\gamma, \xi).$$

Assumption (b) also guarantees that $V(\tau_0^{k+1}) \leq V(t_f^k)$ and thus $V(\tau_0^{k+1}) \leq \delta(\gamma, \xi)$, for all $k \geq 1$. The term $\delta(\gamma, \xi)$ can be made as small as desired increasing either γ or the length of the interval $[t_\infty^k, t_f^k]$. The proof is completed by the relation $\alpha(||x||) \leq V(x,t)$, for all $x, \ t$.

It is worth to point out the local character of the stability criterion in Proposition 8.5. This is first due to condition (c) and second by the synchronization constraints of the control law and the motion phase of the system (see (8.38) and (8.7)–(8.42) below). Once again the weak stability relies on *almost decreasing functions*. Condition (d) means that the impacts may be considered as a kind of disturbance that can be suitably upper bounded. This is certainly the most crucial point in Proposition 8.5.

8.3.2 Tracking Control Framework

Similarly as in Sect. 8.1.1.2, the following trajectories will play a role in the closed-loop dynamics:

- $q^{nc}(\cdot)$ denotes the desired trajectory that the system should track if there were no constraints. We suppose that $q^{1,nc}(t) < 0$ for some t, otherwise the problem reduces to the tracking control of a system with no constraints.
- $q_d^*(\cdot)$ denotes the signal entering the control input and playing the role of the desired trajectory during some parts of the motion.
- $q_d(\cdot)$ represents the signal entering the Lyapunov function $V(\cdot)$. This signal is set on the boundary $\mathrm{bd}(\Phi)$ after the first impact of each cycle.

These signals may coincide on some time intervals as we shall see later. Let us remind that $\tilde{\psi} = \begin{pmatrix} \tilde{q} \\ \tilde{\theta} \end{pmatrix} = \psi - \psi_d$ and introduce the following tracking control variables, which are classically used in passivity-based control algorithms: $s_1 = \dot{\tilde{q}} + \gamma_2 \tilde{q}$, $s_2 = \dot{\tilde{\theta}} + \gamma_2 \tilde{\theta}$, $s = \begin{pmatrix} s_1 \\ s_2 \end{pmatrix}$, $\dot{q}_r = \dot{q}_d - \gamma_2 \tilde{q}$, $\overline{q} = q - q_d^*$ and $\overline{s}_1 = \dot{\overline{q}} + \gamma_2 \overline{q}$, where $\gamma_2 > 0$ is a scalar gain and $\psi_d = \begin{pmatrix} q_d \\ \theta_d \end{pmatrix}$.

8.3.2.1 Controller Design

The tracking problem is solved using a generalization of the backstepping passivity-based controller proposed in [223, Eq. (28)] and the closed-loop stability analysis of the system is based on Proposition 8.5. the controller is defined by

$$\begin{cases} U = J\ddot{\theta}_r + K(\theta_d - q_d) - \gamma_1 s_2 - \mathscr{K}(\psi) \\ \theta_d = q_d + K^{-1} U_r, \end{cases} \tag{8.41}$$

i.e. the nonlinear flexible term is supposed to be exactly known and compensated for, where U_r is given by:

$$U_r = \begin{cases} U_c^{\emptyset} \triangleq U_{nc} = M(q)\ddot{q}_r + C(q,\dot{q})\dot{q}_r + G(q) - \gamma_1 s_1 \ \text{ for } t \in \Omega_{2k}^{\emptyset}, \\ U_c^{B_k} = U_{nc} - P_d + K_f(P_q - P_d) \text{ for } t \in \Omega_k^{B_k}, \\ U_c^{B_k} \ \text{ for } t \in I_k^{B_k} \text{ before the first impact}, \\ U_t^{B_k} = M(q)\ddot{q}_r + C(q,\dot{q})\dot{q}_r + G(q) - \gamma_1 \overline{s}_1 \text{ for } I_k^{B_k} \ni t > \text{first impact time}, \end{cases} \tag{8.42}$$

where $\gamma_1 > 0$ is a scalar gain, $K_f \succ 0$, $P_q = D^T \lambda$ and $P_d = D^T \lambda_d$ is the desired contact force during the persistently constrained motion. It is clear that during $\Omega_k^{B_k}$ not all the constraints are active and, therefore, some components of λ and λ_d are zero. Notice that on impacting phases no force feedback is applied. Also U is a function

of $q, \theta, \dot{q}, \dot{\theta}$ only (no acceleration feedback). The closed-loop error dynamics on $\Omega_{2k}^{\emptyset}$ is given by:

$$\begin{cases} M(q)\dot{s}_1 + C(q,\dot{q})s_1 + \gamma_1 s_1 + K(\tilde{q} - \tilde{\theta}) = 0 \\ J\dot{s}_2 + \gamma_1 s_2 + K(\tilde{\theta} - \tilde{q}) = 0. \end{cases}$$

The rationale behind the change of structure of U_r after the first impact, is that it facilitates the calculation of some upper bounds which are necessary to recast the closed-loop stability analysis into Proposition 8.5.

In order to prove the stability of the closed-loop system (8.36), (8.41) and (8.42) we will use the following positive definite function:

$$\begin{aligned} V(t, s, \tilde{\psi}) = \frac{1}{2} s_1^T M(q) s_1 + \frac{1}{2} s_2^T J s_2 + \gamma_1 \gamma_2 \tilde{q}^T \tilde{q} \\ + \gamma_1 \gamma_2 \tilde{\theta}^T \tilde{\theta} + \frac{1}{2} (\tilde{q} - \tilde{\theta})^T K (\tilde{q} - \tilde{\theta}). \end{aligned} \tag{8.43}$$

One of the difficulties of the flexible-joint case, compared with the rigid case, is that the jumps in the function $V(\cdot)$ in (8.43) are less easy to characterize. Indeed the terms $\theta_d(\cdot)$ and $\dot{\theta}_d(\cdot)$ are designed from a backstepping procedure and cannot be given arbitrary values, contrarily to other desired trajectories. The calculations of various upper bounds are consequently intricate.

8.3.2.2 Design of the Exogenous Trajectory

Globally the same framework as depicted in Fig. 8.1 holds. We consider that the unconstrained desired trajectory $q^{nc}(\cdot)$ can be split into two parts, one of them belonging to the admissible domain (inner part) and the other one outside the admissible domain (outer part). Throughout the analysis we consider $I_k^{B_k} = [\tau_0^k, t_f^k]$ where τ_0^k is chosen by the designer as the start of the transition phase $I_k^{B_k}$ and t_f^k is the end of this phase. During the transition phases the system must be stabilized on the intersection of some surfaces Σ_i. This will be done by mimicking the behavior of a ball falling on the ground under gravity. Therefore all the components except the ones that are normal to the constraints belonging to B_k will be frozen. Moreover for robustness reasons one avoids a tangential approach and imposes some impacts defining a exogenous signal q_d^* that violates the constraints. In the sequel we deal with the tracking control strategy when the trajectory $q_d(\cdot)$ is constructed such that:

(i) when no activated constraint the orbit of $q_d(\cdot)$ coincides with the orbit of $q^{nc}(\cdot)$ and $\dot{q}_d(\tau_0^k) = 0$,
(ii) when $p \leq m$ constraints are active, its orbit coincides with the projection of the outer part of $q^{nc}(\cdot)$ on the surface of codimension p defined by the activated constraints.

In order to simplify the presentation we introduce the following notations (where all superscripts $(\cdot)^k$ will refer to the cycle k of the system motion):

- t_0^k is the first impact during the cycle k,
- t_∞^k is the accumulation point of the sequence $\{t_\ell^k\}_{\ell\geq 0}$ of the impact instants during the cycle k ($t_f^k \geq t_\infty^k$),
- τ_1^k will be explicitly defined later and represents the instant when the exogenous signal q_d^* reaches a given value chosen by the designer in order to impose a closed-loop dynamics with impacts during the transition phases,
- t_d^k is the desired detachment instant.

It is noteworthy that $t_0^k,\ t_\infty^k,\ t_d^k$ are state dependent, whereas τ_1^k and τ_0^k are exogenous and imposed by the designer.

8.3.2.3 Design of $q_d^*(\cdot)$ and $q_d(\cdot)$ During the Phases $I_k^{B_k}$

During the impacting transition phases the system must be stabilized on the boundary $\mathrm{bd}(\Phi)$. Obviously, this does not mean that all the constraints have to be activated (i.e., $q_i^1(t) = 0$, for all $i = 1, \ldots, m$). Let us consider that only the first p constraints (eventually reordering the coordinates) define the border of Φ where the system must be stabilized. The signal $q_d^*(\cdot)$ will be then defined as follows:

- choosing $\nu > 0$ and denoting $t' = \frac{t-\tau_0^k}{\tau_1^k-\tau_0^k}$, the components $\left(q_d^i\right)^*,\ i = 1, \ldots, p$ of $\left(q_d^*\right)_p$ are defined as:

$$\left(q_d^i\right)^*(t) = \begin{cases} a_3(t')^3 + a_2(t')^2 + a_0, & t \in [\tau_0^k, \min\{\tau_1^k; t_0^k\}] \\ -\nu V^{1/3}(\tau_0^k), & t \in (\min\{\tau_1^k; t_0^k\}, t_f^k], \end{cases} \tag{8.44}$$

  where $V(\cdot)$ is defined in (8.43) and τ_1^k is chosen by the designer such that the limit conditions $\left(q_d^i\right)^*(\tau_1^k) = -\nu V^{1/3}(\tau_0^k),\ \left(\dot{q}_d^i\right)^*(\tau_1^k) = 0$ hold, which allows the computation of the previous coefficients as:

$$\begin{cases} a_3 = 2[\left(q^i\right)^{nc}(\tau_0^k) + \nu V^{1/2}(\tau_0^k)] \\ a_2 = -3[\left(q^i\right)^{nc}(\tau_0^k) + \nu V^{1/2}(\tau_0^k)] \\ a_0 = \left(q^i\right)^{nc}(\tau_0^k). \end{cases} \tag{8.45}$$

- all the other components of $q_d^*(\cdot)$ are frozen:

$$\left(q_d^*\right)_{n-p}(t) = q_{n-p}^{nc}(\tau_0^k), \quad t \in (\tau_0^k, t_f^k]. \tag{8.46}$$

As we said before, behind the choice of $q_d^*(\cdot)$ is the strategy to assure a robust stabilization on $\mathrm{bd}(\Phi)$ by mimicking the bouncing ball dynamics. On the other hand this enables one to compute suitable upper bounds that will help using Proposition 8.5.

In order to limit the deformation of the desired trajectory $q_d^*(\cdot)$ w.r.t. $q^{nc}(\cdot)$ during the I_k phases, we impose in the sequel

$$||q_p^{nc}(\tau_0^k)|| \leq \nu_1, \tag{8.47}$$

where $\nu_1 > 0$ is chosen by the designer. It is obvious that a smaller ν_1 leads to smaller deformation of the desired trajectory and to smaller deformation of the real trajectory as we shall see in Sect. 8.1.7. Nevertheless, due to the tracking error, ν_1 cannot be chosen zero. We also note that (8.47) is a practical way to choose τ_0^k.

During the transition phases I_k we define $(q_d)_{n-p}(t) = \left(q_d^*\right)_{n-p}(t)$. Assuming a finite accumulation period, the impact process can be considered in some way equivalent to a plastic impact. Therefore, $(q_d)_p(\cdot)$ and $(\dot{q}_d)_p(\cdot)$ are set to zero on the right of t_0^k. It is worth to recall that the first impact time t_0^k of each cycle k, is unknown.

8.3.3 Desired Contact Force During Constraint Phases

The desired contact force $P_d = D^T \lambda_d$ must be designed such that it is large enough to assure the constraint motion on the $\Omega_{2k+1}^{B_k}$-phases. Some contact force components have also to be decreased at the end of the $\Omega_{2k+1}^{B_k}$-phases in order to allow the detachment. Therefore we need a lower bound of the desired force which assures both the contact (without any undesired detachment which can generate other impacts) during the $\Omega_{2k+1}^{B_k}$ phases and a smooth detachment at the end of $\Omega_{2k+1}^{B_k}$. Dropping the time argument, the dynamics of the system on $\Omega_{2k+1}^{B_k}$ can be written as the complementarity system:

$$\begin{cases} M(q)\ddot{q} + F(q, \dot{q}, \tilde{q}, \dot{\tilde{q}}, \tilde{\theta}) = (1 + K_f) D_p^T (\lambda - \lambda_d) \\ J\dot{s}_2 + \gamma_1 s_2 + K(\tilde{\theta} - \tilde{q}) = 0 \\ 0 \leq q_p \perp \lambda_p \geq 0, \end{cases} \tag{8.48}$$

with $F(q, \dot{q}, \tilde{q}, \dot{\tilde{q}}, \tilde{\theta}) = -M(q)\ddot{q}_r + C(q, \dot{q})s_1 + \gamma_1 s_1 + K(\tilde{q} - \tilde{\theta})$, $D_p = [I_p \vdots O_{p\times(n-p)}] \in \mathbb{R}^{p\times n}$. On $\Omega_{2k+1}^{B_k}$ the system has to be permanently constrained which is equivalent to $q_p(\cdot) = 0$ and $\dot{q}_p(\cdot) = 0$. In order to assure these conditions it is sufficient to have $\lambda_p > 0$. We denote $M(q)^{-1} = \begin{pmatrix} [M^{-1}(q)]_{p,p} & [M^{-1}(q)]_{p,n-p} \\ [M^{-1}(q)]_{n-p,p} & [M^{-1}(q)]_{n-p,n-p} \end{pmatrix}$ and $C(q, \dot{q}) = \begin{pmatrix} C(q, \dot{q})_{p,p} & C(q, \dot{q})_{p,n-p} \\ C(q, \dot{q})_{n-p,p} & C(q, \dot{q})_{n-p,n-p} \end{pmatrix}$ where the meaning of each component is obvious. Let us also denote by K_p the matrix made of the first p rows and p columns of K.

Proposition 8.6 *On $\Omega_k^{B_k}$ the constraint motion of the closed-loop system (8.48), (8.7) and (8.42) is assured if the desired contact force is defined by:*

$$\begin{aligned}(\lambda_d)_p \triangleq & \nu_p + \frac{K_p\tilde{\theta}_p}{1+K_f} - \frac{\bar{M}_{p,p}(q)}{1+K_f}\Big([M(q)^{-1}]_{p,p}C_{p,n-p}(q,\dot{q}) \\ & + [M(q)^{-1}]_{p,n-p}(C_{n-p,n-p}(q,\dot{q}) + \gamma_1 I_{n-p})\Big)(s_1)_{n-p},\end{aligned} \tag{8.49}$$

where $\bar{M}_{p,p}(q) = \left([M(q)^{-1}]_{p,p}\right)^{-1} = \left(D_p M(q)^T D_p^T\right)^{-1}$ is the inverse of the so-called Delassus' matrix and $\nu_p \in \mathbb{R}^p,\ \nu_p > 0$.

Proof It is noteworthy that the third relation in (8.48) implies on $\Omega_{2k+1}^{B_k}$ that complementarity holds at the acceleration level:

$$0 \le \ddot{q}_p \perp \lambda_p \ge 0 \Leftrightarrow 0 \le D_p\ddot{q} \perp \lambda_p \ge 0. \tag{8.50}$$

From (8.48) one easily gets:

$$\ddot{q} = M(q)^{-1}\big[-F + (1+K_f)D_p^T(\lambda - \lambda_d)_p\big].$$

Combining the last two equations we obtain the following LCP with unknown λ:

$$0 \le D_p M(q)^{-1}\big[-F - (1+K_f)D_p^T(\lambda_d)_p\big] + (1+K_f)D_p M(q)^{-1}D_p^T\lambda_p \perp \lambda_p \ge 0 \tag{8.51}$$

Since $(1+K_f)D_pM(q)^{-1}D_p^T \succ 0$ and hence is a P-matrix, the LCP (8.51) has a unique solution and one deduces that $\lambda_p > 0$ if and only if

$$\begin{aligned}&\frac{\bar{M}_{p,p}(q)}{1+K_f}D_pM^{-1}(q)\big[-F-(1+K_f)D_p^T(\lambda_d)_p\big] < 0 \Leftrightarrow \\ &(\lambda_d)_p > -\frac{\bar{M}_{p,p}(q)}{1+K_f}D_pM(q)^{-1}F \Leftrightarrow (\lambda_d)_p = \nu_p - \frac{\bar{M}_{p,p}(q)}{1+K_f}D_pM^{-1}(q)F,\end{aligned}$$

with $\nu_p \in \mathbb{R}^p,\ \nu_p > 0$. Since $F = -M(q)\ddot{q}_r + C(q,\dot{q})s_1 + \gamma_1 s_1 + K(\tilde{q} - \tilde{\theta}),\ (\ddot{q}_r)_p = 0$ and $(s_1)_p = 0$, (8.19) rewrites as (8.16) and the proof is finished. It is noteworthy that the unique solution of the LCP (8.18) is:

$$\begin{aligned}\lambda_p &= \frac{\bar{M}_{p,p}(q)}{1+K_f}D_pM(q)^{-1}\big[F + (1+K_f)D_p^T(\lambda_d)_p\big] \\ &= (\lambda_d)_p + \frac{\bar{M}_{p,p}(q)}{1+K_f}D_pM(q)^{-1}F = \nu_p,\end{aligned} \tag{8.52}$$

where (8.49) has been used.

8.3.4 Strategy for Takeoff at the End of Constraint Phases $\Omega_{2k+1}^{B_k}$

In this section we are interested in finding the conditions on the control signal $U_c^{B_k}$ that assures the takeoff at the end of constraint phases $\Omega_{2k+1}^{B_k}$. As we have already seen before, the phase $\Omega_{2k+1}^{B_k}$ corresponds to the time interval $[t_f^k, t_d^k)$. The dynamics on $[t_f^k, t_d^k)$ is given by (8.15) and the system is permanently constrained, which implies $q_p(\cdot) = 0$ and $\dot{q_p}(\cdot) = 0$. Let us also consider that the first h constraints $(h < p)$ have to be deactivated. Thus, the detachment takes place at t_d^k if $\ddot{q}_h(t_d^{k+}) > 0$ which requires $\lambda_h(t_d^{k-}) = 0$. The last $p - h$ constraints remain active which means $\lambda_{p-h}(t_d^{k-}) > 0$.

To simplify the notation we drop the time argument in many equations of this section. We decompose the LCP matrix (which is the Delassus' matrix multiplied by $1 + K_f$) as:

$$(1 + K_f) D_p M(q)^{-1} D_p^T = \begin{pmatrix} A_1(q) & A_2(q) \\ A_2(q)^T & A_3(q) \end{pmatrix}, \tag{8.53}$$

with $A_1 \in \mathbb{R}^{h \times h}$, $A_2 \in \mathbb{R}^{h \times (p-h)}$ and $A_3 \in \mathbb{R}^{(p-h) \times (p-h)}$

Proposition 8.7 *The closed-loop system (8.15), (8.7) and (8.42) is permanently constrained on $[t_f^k, t_d^k)$ and a smooth detachment is guaranteed on $[t_d^k, t_d^k + \varepsilon)$ (ε is a small positive real number chosen by the designer) if*

(i)

$$\begin{pmatrix} (\lambda_d)_h\,(t_d^k) \\ (\lambda_d)_{p-h}\,(t_d^k) \end{pmatrix} = \begin{pmatrix} \left(A_1 - A_2 A_3^{-1} A_2^T\right)^{-1} \left(b_h - A_2 A_3^{-1} b_{p-h}\right) - C_1 (t - t_d^k) \\ C_2 + A_3^{-1} \left(b_{p-h} - A_2^T\,(\lambda_d)_h\right) \end{pmatrix} \tag{8.54}$$

where

$$b_p \triangleq b(q, \dot{q}, U_c^{\emptyset}) \triangleq -D_p M(q)^{-1} F \geq 0,$$

and $C_1 \in \mathbb{R}^h$, $C_2 \in \mathbb{R}^{p-h}$ such that $C_1 \geq 0$, $C_2 > 0$.

(ii) *On $[t_d^k, t_d^k + \varepsilon) q_d^*(t) = q_d(t) = \begin{pmatrix} q_h^*(t) \\ q_{n-h}^{nc}(t) \end{pmatrix}$, where $q_h^*(\cdot)$ is a twice differentiable function such that*

$$\begin{cases} q_h^*(t_d^k) = 0,\ q_h^*(t_d^k + \varepsilon) = q_h^{nc}(t_d^k + \varepsilon), \\ \dot{q}_h^*(t_d^k) = 0,\ \dot{q}_h^*(t_d^k + \varepsilon) = \dot{q}_h^{nc}(t_d^k + \varepsilon), \end{cases} \tag{8.55}$$

and $\ddot{q}_h^*(t_d^{k+}) = a > \max\left(0,\ -A_1(q)(\lambda_d)_h(t_d^{k-})\right)$.

Proof See Sect. 8.3.7.

8.3.5 Closed-Loop Stability Analysis

To simplify the notation $V(t, s(t), \tilde{\psi}(t))$ is denoted as $V(t)$. In order to introduce the main result of this section we make the next assumption, which is verified in practice for dissipative systems with $e_{\mathrm{n}} \in [0, 1)$.

Assumption 6 The controller U in (8.7) and (8.42) assures that all the transition phases are finite.

Lemma 8.2 *Consider the closed-loop system (8.36), (8.41) and (8.42) with $(q_d^*)_p(\cdot)$ defined on the interval $[\tau_0^k, t_0^k]$ as in (8.12)–(8.11). Let us also suppose that condition (b) of Proposition 8.5 is satisfied. The following inequalities hold:*

$$\begin{cases} ||\tilde{q}(t_0^{k-})|| \leq \sqrt{\dfrac{V(\tau_0^k)}{\gamma_1\gamma_2}}, & ||s_1(t_0^{k-})|| \leq \sqrt{\dfrac{2V(\tau_0^k)}{\lambda_{min}(M(q))}}, \\ ||\tilde{\theta}(t_0^{k-})|| \leq \sqrt{\dfrac{V(\tau_0^k)}{\gamma_1\gamma_2}}, & ||s_2(t_0^{k-})|| \leq \sqrt{\dfrac{2V(\tau_0^k)}{\lambda_{min}(J)}}, \end{cases} \tag{8.56}$$

and

$$\begin{cases} ||\dot{\tilde{q}}(t_0^{k-})|| \leq \left(\sqrt{\dfrac{2}{\lambda_{min}(M(q))}} + \sqrt{\dfrac{\gamma_2}{\gamma_1}}\right) V^{1/2}(\tau_0^k) \\ ||\dot{\tilde{\theta}}(t_0^{k-})|| \leq \left(\sqrt{\dfrac{2}{\lambda_{min}(J)}} + \sqrt{\dfrac{\gamma_2}{\gamma_1}}\right) V^{1/2}(\tau_0^k) \end{cases} \tag{8.57}$$

Furthermore, if $t_0^k \leq \tau_1^k$ one has

$$\begin{cases} ||(q_d)_p(t_0^{k-})|| \leq \varepsilon + \sqrt{\frac{V(\tau_0^k)}{\gamma_1\gamma_2}} \\ ||(\dot{q}_d)_p(t_0^{k-})|| \leq \bar{k} + k^* V^{1/6}(\tau_0^k) \\ ||(\ddot{q}_d)_p(t_0^{k-})|| \leq 6\sqrt{2}\left(||q_p^{nc}(\tau_0^k)|| + \sqrt{p}\nu V^{1/2}(\tau_0^k)\right) \\ ||(q_d^{(3)})_p(t_0^{k-})|| \leq 6\sqrt{2}\left(||q_p^{nc}(\tau_0^k)|| + \sqrt{p}\nu V^{1/2}(\tau_0^k)\right), \end{cases}$$

where ε is the real constant fixed in Definition 8.2 and $\bar{k}$, $k^* > 0$ are some constant real numbers that will be defined in the proof.

Proof See Sect. 8.3.8.

It is noteworthy that $q(\cdot)$ is a continuous signal. Nevertheless the velocity $\dot{q}(\cdot)$ presents discontinuities of the first kind at the impact times. From (8.42) one deduces that the controller U_r jumps also at the impact times generating a jump in the desired signal $\theta_d(\cdot)$ in (8.41). Therefore, in order to study the evolution of the Lyapunov function candidate (8.10) one has to analyze the jumps $\sigma_{\tilde{\theta}}(\cdot)$ and $\sigma_{\dot{\tilde{\theta}}}(\cdot)$.

$\rightsquigarrow$ *The backstepping passivity-based method requires particular care about the behavior of the "fictitious" controller $\theta_d(\cdot)$ at the impact times. Though $\dot{\theta}(\cdot)$ is continuous at impact times, $\theta_d(\cdot)$ and $\dot{\theta}_d(\cdot)$ may not be.*

Lemma 8.3 *The controller U in (8.7) and (8.42) guarantees that $||\sigma_{\tilde{\theta}}(\cdot)||$, $||\sigma_{\dot{\tilde{\theta}}}(\cdot)|| \in S(1) \equiv L^\infty$.*

Proof See Sect. 8.3.9.

We now state the main result of this section.

Theorem 8.2 *Let Assumption 1 hold, $e_n = 0$ and $q_d^*(\cdot)$ defined as in (8.12)–(8.11). The closed-loop system (8.36), (8.41) and (8.42) initialized on Ω_0 such that $V(\tau_0^0) \leq 1$, satisfies the requirements of Proposition 8.1 and is therefore practically weakly stable with the closed-loop state $x(\cdot) = [\tilde{\psi}(\cdot), s(\cdot)]$ and $R = \sqrt{e^{-\gamma(t_f^k - t_\infty^k)}(\rho^* + \xi)/\bar{\rho}}$ where ρ^*, $\bar{\rho}$ and ξ are defined in the proof.*

Proof See Sect. 8.3.10.

8.3.6 Illustrative Example

Some experimental results are obtained by simulating the behavior of a planar two-link flexible-joint manipulator in the presence of two constraints. As in Sect. 8.1.7, we impose an admissible domain $\Phi = \{(x, y) \mid y \geq 0,\ 0.7 - x \geq 0\}$. Let us also consider an unconstrained desired trajectory $q^{nc}(\cdot)$ whose orbit is given by the circle $\{(x, y) \mid (x - 0.7)^2 + y^2 = 0.5\}$. It violates both constraints. In other words, the two-link planar manipulator must track a quarter-circle; stabilize on and then follow the line $\Sigma_1 = \{(x, y) \mid y = 0\}$; stabilize on the intersection of Σ_1 and $\Sigma_2 = \{(x, y) \mid x = 0.7\}$; detach from Σ_1 and follow Σ_2 until the unconstrained circle reenters Φ and finally takeoff from Σ_2 in order to repeat the previous steps.

The task representation here is given by (see (8.4)) $B_{2k} = \emptyset, m_{2k} = 1,\ B_{2k,1} = \{1\}, B_{2k+1} = \{1\},\ m_{2k+1} = 2,\ B_{2k+1,1} = \{1, 2\},\ B_{2k+1,2} = \{2\}$. The numerical values used for the dynamical model are $l_1 = l_2 = 0.5\,\text{m}$, $m_1 = m_2 = 1\,\text{kg}$, $I_1 = I_2 = 0.5\,\text{kg}\,\text{m}^2$, $J_1 = J_2 = 0.1\,\text{kg}\,\text{m}^2$ and the impacts are imposed by $\nu = 10$ in (8.12) and (8.13). The stiffness matrix is defined by $K = \text{diag}(2000\,\text{N/m}, 2000\,\text{N/m})$. Let us say that the quarter-circle is completely tracked in one round. We set the period of each round to 10 seconds and we simulate the dynamics during 6 rounds using the Moreau's time-stepping algorithm of the SICONOS software platform. We set the controller gains $\gamma_1 = 10,\ \gamma_2 = 1$ and we choose $\nu_1 = 0.1$ (like this we implicitly set τ_0^k see (8.14)) in order to better point out the deformation of $q_d(\cdot)$ on the transition phases (Figs. 8.7 (left) and 8.10). In Fig. 8.11 we have shifted backward the desired

trajectory on $I_2^{B_2}$ to highlight that the Lyapunov function at the instant τ_0^k is smaller when k increases.

The behavior of the system during one round is emphasized in Fig. 8.10 (right) and the shape of the control law is depicted in Fig. 8.12.

Compensation of Flexibilities

As noticed in [224, 225] the control laws designed for rigid systems behave well for manipulators with large joint stiffness (see also Fig. 8.13 for the multi-constraint case).

In order to highlight the importance of flexibilities' compensation we keep the numerical values used in the previous Subsection with one exception, the stiffness matrix is defined by $K = \text{diag}(200\,\text{N/m}, 200\,\text{N/m})$. Using the control with no flexibility compensation (named the "rigid controller") one obtains a completely deteriorated behavior (see Fig. 8.14). Furthermore, the control signal oscillates very much after the first impact (Fig. 8.15).

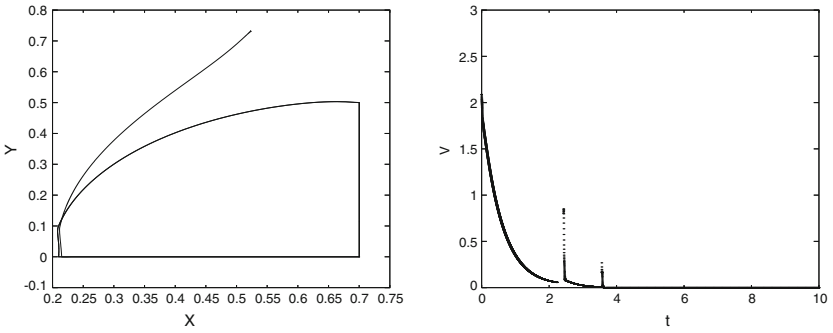

Fig. 8.10 *Left* The trajectory of the system during 6 rounds; *Right* The variation of the almost nonincreasing Lyapunov function during the first round

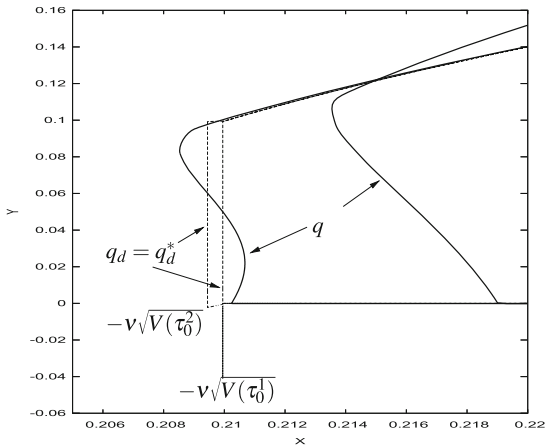

Fig. 8.11 Zoom on the transition phases $I_{2k}^{B_{2k}}$

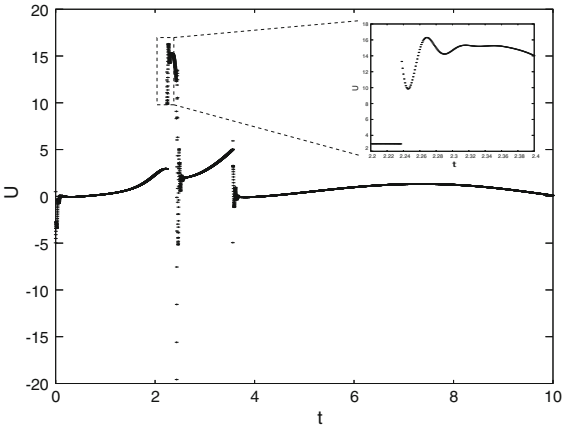

Fig. 8.12 The control law applied to θ_1 during the first round

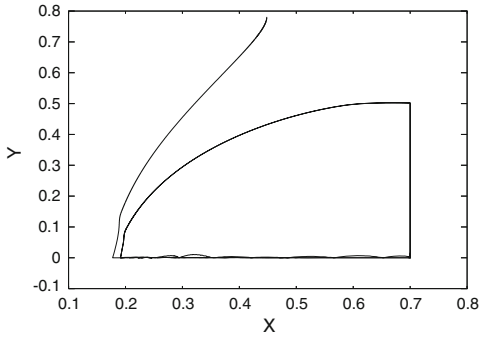

Fig. 8.13 The variation of the end-effector coordinates using the rigid controller when the stiffness matrix is defined by $K = \text{diag}(5000\,\text{N/m}, 5000\,\text{N/m})$

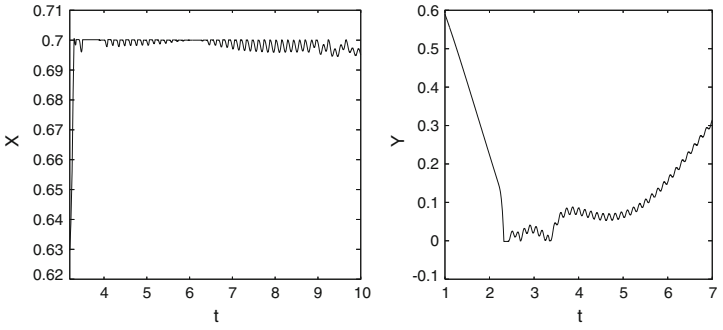

Fig. 8.14 The variation of the end-effector coordinates using the rigid controller

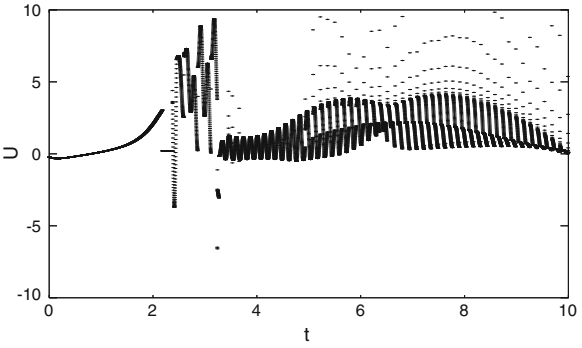

Fig. 8.15 The rigid control applied to θ_1 during the first round

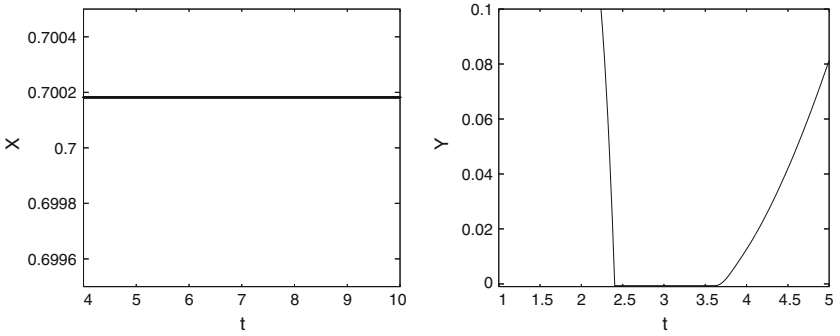

Fig. 8.16 The variation of the end-effector coordinates using the controller (8.41) and (8.42)

On the other hand using the controller designed in this section the desired trajectory is well tracked (see Fig. 8.16) and the control signal is quickly stabilized during the I_k phases (see Fig. 8.17). More numerical results can be found in [875].

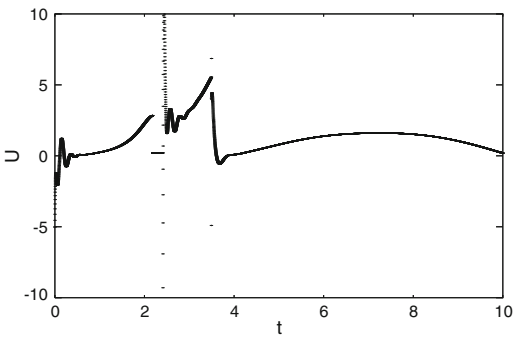

Fig. 8.17 The control law applied to θ_1 during the first round

8.3.7 *Proof of Proposition 8.7*

The necessary condition for takeoff after the instant t_d^k is given by $\lambda_h(t_d^{k-}) = 0$ and $\lambda_{p-h}(t_d^{k-}) > 0$. Precisely, we impose a positive contact force on $[t_f^k, t_d^k)$ with the first h components approaching 0 when t approaches t_d^k. From (8.53) and (8.15) it is straightforward that the LCP (8.17) rewrites as:

$$0 \leq \begin{pmatrix} \lambda_h \\ \lambda_{p-h} \end{pmatrix} \perp \begin{pmatrix} b_h + A_1(\lambda - \lambda_d)_h + A_2(\lambda - \lambda_d)_{p-h} \\ b_{p-h} + A_2^T(\lambda - \lambda_d)_h + A_3(\lambda - \lambda_d)_{p-h} \end{pmatrix} \geq 0. \tag{8.58}$$

Since $(1 + K_f)D_p M(q)^{-1} D_p^T \succ 0$, the LCP (8.50) (or the equivalent one (8.58)) has a unique solution. Imposing $\lambda_h = 0$ one gets:

$$0 \leq \lambda_{p-h} \perp b_{p-h} - A_2^T(\lambda_d)_r + A_3(\lambda - \lambda_d)_{p-h} \geq 0,$$

with the solution

$$\lambda_{p-h} = -A_3^{-1}\left(b_{p-h} - A_2^T(\lambda_d)_h - A_3(\lambda_d)_{p-h}\right). \tag{8.59}$$

Thus $\lambda_{p-h} > 0$ is equivalent to:

$$(\lambda_d)_{p-h} > A_3^{-1}\left(b_{p-h} - A_2^T(\lambda_d)_h\right),$$

which leads to the second part of the definition in (8.54). Furthermore, replacing $(\lambda_d)_{p-h}$ in (8.59) we get $\lambda_{p-h} = C_2$ and $b_h + A_1(\lambda - \lambda_d)_h + A_2(\lambda - \lambda_d)_{p-h} \geq 0$ yields the first part of the definition in (8.54). Consequently the solution of the LCP (8.58) is $\lambda_p = \begin{pmatrix} 0 \\ C_2 \end{pmatrix} \in \mathbb{R}^p$ when $(\lambda_d)_p$ is defined by (8.54).

The jumps in the Lyapunov function are avoided during the detachment phase using a twice differentiable desired trajectory $q_d(\cdot)$ defined as in item (ii) of Proposition 8.7. In order to assure a smooth detachment (without impacts) on $[t_d^k, t_d^k + \varepsilon)$ we need a large enough positive desired acceleration $(\ddot{q}_d)_h$. At t_d^{k-} one has

$$\ddot{q}_h(t_d^{k-}) = -D_h M(q)^{-1}\left[F + (1 + K_f)D_h^T(\lambda_d)_h\right],$$

while at t_d^{k+} one has $\ddot{q}_{p-h}(t_d^{k+}) = D_h M(q)^{-1} F$. Since $(\ddot{q}_d)_h(t_d^{k-}) = 0$ we arrive at

$$\sigma_{\ddot{q}_h(t_d^k)} = (\ddot{q}_d)_h(t_d^{k+}) + A_1(q)(\lambda_d)_h(t_d^{k-}).$$

Therefore $\ddot{q}_{1d}(t_d^{k+})$ has to be positive and large enough in order to compensate for $-A_1(q)(\lambda_d)_h(t_d^{k-})$ at the instant t_d^k. Consequently one defines $\ddot{q}_1^*(t_d^{k+}) = a > \max\left(0, -A_1(q)(\lambda_d)_h(t_d^{k-})\right)$ and the detachment is assured.

8.3.8 *Proof of Lemma 8.2*

From (8.43) one deduces $V(t_0^{k-}) \geq \gamma_1\gamma_2||\tilde{q}(t_0^{k-})||^2$, $V(t_0^{k-}) \geq \frac{1}{2}s_1(t_0^{k-})^T M(q(t_0^{k-}))$ $s_1(t_0^{k-})$ and

$$V(t_0^{k-}) \geq \gamma_1\gamma_2||\tilde{\theta}(t_0^{k-})||^2, \quad V(t_0^{k-}) \geq \frac{1}{2}s_2(t_0^{k-})^T J s_2(t_0^{k-}).$$

Since condition (b) of Proposition 8.5 is satisfied one has $V(\tau_0^k) \geq V(t_0^{k-})$ and (8.56) becomes trivial. Let us recall that $s_1(t) = \dot{\tilde{q}}(t) + \gamma_2\tilde{q}(t)$ and $s_2(t) = \dot{\tilde{\theta}}(t) + \gamma_2\tilde{\theta}(t)$ which implies $||\dot{\tilde{q}}(t_0^{k-})|| \leq ||s_1(t_0^{k-})|| + \gamma_2||\tilde{q}(t_0^{k-})||$ and $||\dot{\tilde{\theta}}(t_0^{k-})|| \leq ||s_2(t_0^{k-})|| + \gamma_2||\tilde{\theta}(t_0^{k-})||$ respectively. Combining this with (8.56) we derive (8.57).

The proof of (8.2) follows the ideas presented in Sect. 8.1. Roughly the first inequality in (8.2) is based on the definition of p_ε-impacts (see Definition 8.5). The remaining inequalities in (8.2) are based on the particular definition of $(q_d^*)_p(\cdot)$ (see (8.44), (8.45)). The upper bound of $||(\dot{q}_d)_p(t_0^{k-})||$ was derived in Sect. 8.1 (see Sect. 8.1.8) with $\bar{k} = \dfrac{6\sqrt{p\nu_1\varepsilon}}{\tau_1^k - \tau_0^k}$ and:

$$k^* = \frac{6\sqrt{p}}{\tau_1^k - \tau_0^k}\sqrt{\left(\frac{1}{\sqrt{\gamma_1\gamma_2}} + \nu\right)(\nu + \nu_1) + \varepsilon\nu}.$$

Finally, differentiating (8.44) two and three times respectively one obtains:

$$\begin{cases} \ddot{q}_d^i(t_0^{k-}) & = \lim_{t\to t_0^k, t<t_0^k} 6((q^i)^{\mathrm{nc}}(\tau_0^k) + \nu V^{1/2}(\tau_0^k))(2t' - 1) \\ & \leq \lim_{t\to t_0^k, t<t_0^k} 6((q^i)^{\mathrm{nc}}(\tau_0^k) + \nu V^{1/2}(\tau_0^k)), \\ (q_d^i)^{(3)}(t_0^{k-}) & = \lim_{t\to t_0^k, t<t_0^k} 6((q^i)^{\mathrm{nc}}(\tau_0^k) + \nu V^{1/2}(\tau_0^k)), \end{cases} \tag{8.60}$$

which leads to the upper bounds of $||(\ddot{q}_d)_p(t_0^{k-})||$ and $||(q_d^{(3)})_p(t_0^{k-})||$ respectively.

8.3.9 *Proof of Lemma 8.3*

Since $\theta(\cdot)$, $\dot{\theta}(\cdot)$ are continuous on $\mathbb{R}_+$ and $\theta_d(\cdot)$, $\dot{\theta}_d(\cdot)$ are continuous on $\mathbb{R}_+ \setminus \{t_0^k \mid k \in \mathbb{Z}\}$ one deduces that $\sigma_{\tilde{\theta}}(t) = 0 = \sigma_{\dot{\tilde{\theta}}}(t)$, $\forall t \neq t_0^k$. Therefore Lemma 8.3 holds if there exist some real constants that upper bound $||\sigma_{\tilde{\theta}}(t_0^k)||$, $||\sigma_{\dot{\tilde{\theta}}}(t_0^k)||$, for all $k \in \mathbb{Z}$. The definition of $\theta_d(\cdot)$ (see (8.41)) allows us to write:

$$\begin{aligned}\sigma_{\tilde{\theta}}(t_0^k) &= -\sigma_{\theta_d}(t_0^k) = -\sigma_{q_d}(t_0^k) - K^{-1}\sigma_{U_r}(t_0^k)\\ &= \begin{pmatrix}(q_d)_p(t_0^{k-})\\ 0\end{pmatrix} - K^{-1}\sigma_{U_r}(t_0^k)\\ \sigma_{\dot{\tilde{\theta}}}(t_0^k) &= -\sigma_{\dot{\theta}_d}(t_0^k) = -\sigma_{\dot{q}_d}(t_0^k) - K^{-1}\sigma_{\dot{U}_r}(t_0^k)\\ &= \begin{pmatrix}(\dot{q}_d)_p(t_0^{k-})\\ 0\end{pmatrix} - K^{-1}\sigma_{\dot{U}_r}(t_0^k).\end{aligned} \tag{8.61}$$

Therefore:

$$\begin{aligned}||\sigma_{\tilde{\theta}}(t_0^k)|| &\le ||(q_d)_p(t_0^{k-})|| + \lambda_{max}(K^{-1})||\sigma_{U_r}(t_0^k)||\\ ||\sigma_{\dot{\tilde{\theta}}}(t_0^k)|| &\le ||(\dot{q}_d)_p(t_0^{k-})|| + \lambda_{max}(K^{-1})||\sigma_{\dot{U}_r}(t_0^k)||.\end{aligned}$$

Using (8.42) one obtains:

$$\sigma_{U_r}(t_0^k) = M(q)\sigma_{\ddot{q}_r}(t_0^k) + \sigma_{C(q,\dot{q})\dot{q}_r}(t_0^k) - \gamma_1\sigma_{s_1}(t_0^k).$$

From (8.46) one has $(\dot{q}_d)_{n-p}(t) = 0$, $(\ddot{q}_d)_{n-p}(t) = 0$, for all $t \in [\tau_0^k, t_f^k]$. Moreover, as we have mentioned at the end of Sect. 8.3.2, $(q_d)_p(\cdot)$, $(\dot{q}_d)_p(\cdot)$ and implicitly $(\ddot{q}_d)_p(\cdot)$ are set to zero on $(t_0^k, t_f^k]$. Thus taking into account the relation $||\dot{q}(t_0^{k+})|| \le \mathbf{w}||\dot{q}(t_0^{k-})||$ (where $\mathbf{w} = \sqrt{\frac{\lambda_{max}(M)}{\lambda_{min}(M)}}$) and Property 8.1 one arrives at

$$\begin{aligned}||\sigma_{\ddot{q}_r}(t_0^k)|| \le& ||(\ddot{q}_d)_p(t_0^{k-})|| + \gamma_2||(\dot{q}_d)_p(t_0^{k-})|| + \gamma_2(1+\mathbf{w})||\dot{q}(t_0^{k-})||\\ ||\sigma_{C(q,\dot{q})\dot{q}_r}(t_0^k)|| \le& ||\sigma_{C(q,\dot{q})}\dot{q}_r(t_0^{k-})|| + ||C(q,\dot{q}(t_0^{k+}))\sigma_{\dot{q}_r}(t_0^k)||\\ \in& S\big(2(1+\gamma_2)||\dot{q}(t_0^{k-})||\,||(\dot{q}_d)_p(t_0^{k-})|| + \gamma_2||(q_d)_p(t_0^{k-})||\big)\\ ||\sigma_{s_1}(t_0^k)|| \le& (1+\mathbf{w})||\dot{q}(t_0^{k-})|| + ||(\dot{q}_d)_p(t_0^{k-})||\\ &+ \gamma_2||(q_d)_p(t_0^{k-})||.\end{aligned} \tag{8.62}$$

When $V(\tau_0^k) \le 1$, Lemma 8.2 states that $||(\dot{q}_d)_p(t_0^{k-})||$, $||(q_d)_p(t_0^{k-})||$ and $||\dot{q}(t_0^{k-})||$ are bounded by some constants. Thus all the quantities in (8.62) are bounded by some constants independent of the cycle index k. This means that $||\sigma_{U_r}(t_0^k)||$ is bounded by a constant independent of the cycle index, which implies the same for $||\sigma_{\tilde{\theta}}(t_0^k)||$. In other words $||\sigma_{\tilde{\theta}}(t)|| \in S(1)$. Differentiating (8.42) we obtain:

$$\begin{aligned}\dot{U}_r(t) =& M(q)q_r^{(3)}(t) + \dot{M}(q)\ddot{q}_r(t) + C(q,\dot{q})\ddot{q}_r(t)\\ &+ \dot{C}(q,\dot{q})\dot{q}_r(t) + \frac{\partial G}{\partial q}\dot{q}(t) - \gamma_1\dot{s}_1(t),\end{aligned} \tag{8.63}$$

where $\dot{M}$, $\dot{C}$ stand for $\frac{dM}{dt}$ and $\frac{dC}{dt}$ respectively. It is clear that

$$\dot{C}(q,\dot{q})(t) = \frac{\partial C}{\partial q}(q,\dot{q})\dot{q}(t) + \frac{\partial C}{\partial \dot{q}}(q,\dot{q})\ddot{q}(t),$$

and using Properties 8.1 and 8.3 one derives:

$$||\dot{C}(q,\dot{q})(t)|| \in S(||\dot{q}(t)||^2 + ||\ddot{q}(t)||).$$

Furthermore, Lemma 8.2 and the first equation in (8.36) assure that $||\dot{q}(t)||^2$, $||\ddot{q}(t)|| \in S(1)$. Thus $||\dot{C}(q,\dot{q})(\cdot)||$, $||\sigma_{\dot{C}(q,\dot{q})}(\cdot)|| \in S(1)$ and one derives that

$$\begin{aligned} ||\sigma_{\dot{C}(q,\dot{q})}(t_0^k)\dot{q}_r(t_0^k)|| \leq\ & ||\sigma_{\dot{C}(q,\dot{q})}(t_0^k)||\ ||\dot{q}_r(t_0^{k+})|| \\ & + ||\dot{C}(q,\dot{q})(t_0^{k-})||\ ||\sigma_{\dot{q}_r}(t_0^k)|| \in S(1). \end{aligned} \tag{8.64}$$

Property 8.1 allows us to replace $\dot{M}(q)$ by $C(q,\dot{q}) + C(q,\dot{q})^T$ which leads to:

$$\begin{aligned} &\dot{M}(q)\ddot{q}_r(t) + C(q,\dot{q})\ddot{q}_r(t) = (2C(q,\dot{q}) + C(q,\dot{q}))^T\ddot{q}_r(t) \Rightarrow \\ &||\dot{M}(q)\ddot{q}_r(t) + C(q,\dot{q})\ddot{q}_r(t)|| \leq 3||C(q,\dot{q})||.||\ddot{q}_r(t)|| \Rightarrow \\ &||\dot{M}(q)\ddot{q}_r(t) + C(q,\dot{q})\ddot{q}_r(t)|| \in S(||\dot{q}||.||\ddot{q}_r(t))||). \end{aligned}$$

Since $||\ddot{q}_r(t))|| \leq ||\ddot{q}_d(t)|| + \gamma_2||\dddot{\tilde{q}}(t)||$, using Lemma 8.2 one gets:

$$||\dot{M}(q)\ddot{q}_r(t) + C(q,\dot{q})\ddot{q}_r(t)|| \in S(1). \tag{8.65}$$

The definitions (8.44)–(8.46) and the first equation in (8.36) assure that $||q_r^{(3)}(t)|| \in S(1)$. Therefore:

$$||M(q)q_r^{(3)}(t)|| \leq \lambda_{max}(M)||q_r^{(3)}(t)|| \in S(1). \tag{8.66}$$

Property 8.2 states that $||\frac{\partial G}{\partial q}|| \in S(1)$, which implies

$$\left.\begin{array}{l} \left|\left|\frac{\partial G}{\partial q}\dot{q}(t)\right|\right| \in S(||\dot{q}(t)||) \\ ||\dot{q}(t)|| \in S(1) \end{array}\right\} \Rightarrow \left|\left|\frac{\partial G}{\partial q}\dot{q}(t)\right|\right| \in S(1). \tag{8.67}$$

Introducing (8.64)–(8.67) in (8.63) and taking into account the last inequality in (8.62) we arrive at $||\sigma_{\dot{U}_r}(t)|| \in S(1)$ and thus $||\sigma_{\dot{\tilde{\theta}}}(t)|| \in S(1)$.

8.3.10 *Proof of Theorem 8.2*

First we observe that conditions (a) and (c) of Proposition 8.5 hold when the hypothesis of the Theorem are verified. Thus Theorem 8.2 holds if the conditions (b), (d) of Proposition 8.5 are verified.

(b) Using that $\dot{M}(q) - 2C(q,\dot{q})$ is a skew-symmetric matrix (see Property 8.1), straightforward computations show that on $\mathbb{R}_+ \setminus \bigcup_{k\geq 0}[t_0^k, t_f^k]$ the time derivative of the Lyapunov function is given by:

$$\begin{aligned}\dot{V}(t) =& -\gamma_1||\dot{\tilde{q}}||^2 - \gamma_1\gamma_2^2||\tilde{q}||^2 - \gamma_1||\dot{\tilde{\theta}}||^2 - \gamma_1\gamma_2^2||\tilde{\theta}||^2 \\ & - \gamma_2(\tilde{q}-\tilde{\theta})^T K(\tilde{q}-\tilde{\theta}) + (1+K_f)s_1^T D_p^T(\lambda-\lambda_d)_p \\ =& -\gamma_1||\dot{\tilde{q}}||^2 - \gamma_1\gamma_2^2||\tilde{q}||^2 - \gamma_1||\dot{\tilde{\theta}}||^2 - \gamma_1\gamma_2^2||\tilde{\theta}||^2 \\ & - \gamma_2(\tilde{q}-\tilde{\theta})^T K(\tilde{q}-\tilde{\theta}) \leq 0,\end{aligned}$$

where we have used the fact that $(q_d)_p \equiv 0$, $(\dot{q}_d)_p \equiv 0$, $q_p \equiv 0$, $\dot{q}_p \equiv 0$, thus $(s_1)_p \equiv 0$ on constraint phases and $\lambda_p \equiv 0$, $(\lambda_d)_p \equiv 0$ on free-motion phases. On the other hand

$$\begin{aligned}V(t) \leq & \frac{\lambda_{max}(M(q))}{2}||s_1||^2 + \frac{\lambda_{max}(J)}{2}||s_2||^2 + \gamma_1\gamma_2||\tilde{q}||^2 \\ & + \gamma_1\gamma_2||\tilde{\theta}||^2 + \frac{1}{2}(\tilde{q}-\tilde{\theta})^T K(\tilde{q}-\tilde{\theta}) \\ & \leq \gamma^{-1}[\gamma_1||\dot{\tilde{q}}||^2 + \gamma_1\gamma_2^2||\tilde{q}||^2 + \gamma_1||\dot{\tilde{\theta}}||^2 + \gamma_1\gamma_2^2||\tilde{\theta}||^2 \\ & + \gamma_2(\tilde{q}-\tilde{\theta})^T K(\tilde{q}-\tilde{\theta})],\end{aligned}$$

where

$$\gamma^{-1} = \max\left\{\lambda_{max}(\mathbf{M}(q))\frac{1+2\gamma_2}{2\gamma_1}; \frac{\lambda_{max}(\mathbf{M}(q))(\gamma_2+2)+2\gamma_1}{2\gamma_1\gamma_2}; \frac{1}{2\gamma_2}\right\} > 0,$$

with $\mathbf{M}(q) = \begin{pmatrix} M(q) & 0_{n\times n} \\ 0_{n\times n} & J \end{pmatrix}$. Therefore $\dot{V}(t) \leq -\gamma^{-1}V(t)$ on $\mathbb{R}_+ \setminus \bigcup_{k\geq 0}[t_0^k, t_f^k]$.

(d) There is only one impact during each transition phase since $e_n = 0$ and with the choice of U_t^B in (8.42). Therefore $V(t_\infty^k) = V(t_0^{k-}) + \sigma_V(t_0^k) \leq V(\tau_0^k) + \sigma_V(t_0^k)$. We compute now the jump of the Lyapunov function at the impact time t_0^k. Let $\mathscr{K} = \begin{pmatrix} K & -K \\ -K & K \end{pmatrix}$ and $\psi = (q^T, \theta^T)^T$.

$$\begin{aligned}V(t_0^{k+}) - V(t_0^{k-}) =& \gamma_1\gamma_2\sigma_{\tilde{\psi}^T\tilde{\psi}}(t_0^k) \\ & + \tfrac{1}{2}\left(s(t_0^{k+})^T\mathbf{M}(q)s(t_0^{k+}) - s(t_0^{k-})^T\mathbf{M}(q)s(t_0^{k-})\right) \\ & + \tfrac{1}{2}\left(\tilde{\psi}(t_0^{k+})^T\mathscr{K}\tilde{\psi}(t_0^{k+}) - \tilde{\psi}(t_0^{k-})^T\mathscr{K}\tilde{\psi}(t_0^{k-})\right).\end{aligned} \tag{8.68}$$

Replacing $\tilde{\psi}(t_0^{k+})$ by $\tilde{\psi}(t_0^{k-}) + \sigma_{\tilde{\psi}}(t_0^k)$, the second term of the right-hand side of (8.68) becomes

$$\frac{1}{2}\left(2\tilde{\psi}(t_0^{k-})^T\mathscr{K}\sigma_{\tilde{\psi}}(t_0^k) + \sigma_{\tilde{\psi}}(t_0^k)^T\mathscr{K}\sigma_{\tilde{\psi}}(t_0^k)\right)$$

which is upperbounded by:

$$\lambda_{max}(\mathscr{K})(||\tilde{\psi}(t_0^{k-})||\ ||\sigma_{\tilde{\psi}}(t_0^k)|| + \frac{1}{2}||\sigma_{\tilde{\psi}}(t_0^k)||^2).$$

Therefore Lemmas 8.1 and 8.3 imply that there exists a real positive constant c_1 such that

$$\frac{1}{2}\left(\tilde{\psi}(t_0^{k+})^T\mathscr{K}\tilde{\psi}(t_0^{k+}) - \tilde{\psi}(t_0^{k-})^T\mathscr{K}\tilde{\psi}(t_0^{k-})\right) \leq c_1, \text{ for all } k \geq 0. \tag{8.69}$$

On the other hand

$$s(t_0^{k+})^T\mathbf{M}(q)s(t_0^{k+}) - s(t_0^{k-})^T\mathbf{M}(q)s(t_0^{k-}) = \sigma_{s_1^T M(q)s_1}(t_0^k) + \sigma_{s_2^T J s_2}(t_0^k).$$

It is easy to see that

$$\sigma_{s_2^T J s_2}(t_0^k) = 2s_2(t_0^{k-})^T J\sigma_{s_2}(t_0^k) + \sigma_{s_2}(t_0^k)^T J\sigma_{s_2}(t_0^k),$$

and using Lemmas 8.2 and 8.3 and the relation $\sigma_{s_2}(t_0^k) = \sigma_{\dot{\tilde{\theta}}}(t_0^k) + \gamma_2\sigma_{\tilde{\theta}}(t_0^k)$, one deduces that there exist a real positive constant c_2 such that:

$$\sigma_{s_2^T J s_2}(t_0^k) \leq c_2, \quad \text{for all } k \geq 0. \tag{8.70}$$

As proved in Sect. 8.1, there exists a real positive constant c_3 such that:

$$\sigma_{s_1^T M(q)s_1}(t_0^k) + \gamma_1\gamma_2\sigma_{\tilde{q}^T\tilde{q}}(t_0^k) \leq c_3, \quad \text{for all } k \geq 0 \tag{8.71}$$

Finally, Lemma 8.3 assures the existence of $c_4 \in \mathbb{R}_+$ such that:

$$\gamma_1\gamma_2\sigma_{\tilde{\theta}^T\tilde{\theta}}(t_0^k) \leq c_4, \quad \text{for all } k \geq 0. \tag{8.72}$$

In conclusion, inserting (8.69), (8.70), (8.71) and (8.72) in (8.68) one gets

$$V(t_0^{k+}) - V(t_0^{k-}) \leq c_1 + c_2 + c_3 + c_4, \quad \text{for all } k \geq 0 \tag{8.73}$$

Thus condition (d) of Proposition 8.5 is verified for $\rho^* = 1,\ \xi = c_1 + c_2 + c_3 + c_4$ and the closed-loop system (8.36), (8.41) and (8.42) is practically weakly stable with $R = \alpha^{-1}\left(e^{-\gamma(t_f^k - t_\infty^k)}(1+\xi)\right)$.

Let us consider $\bar{\rho} = \min\{\lambda_{min}(\mathbf{M}(q))/2; \gamma_1\gamma_2\}$. Defining $\alpha : \mathbb{R}_+ \mapsto \mathbb{R}_+,\ \alpha(\omega) = \bar{\rho}\omega^2$ we get $\alpha(0) = 0,\ \alpha(||[s(t), \tilde{q}(t)]||) \leq V(t, s, \tilde{q})$ and the proof is finished.

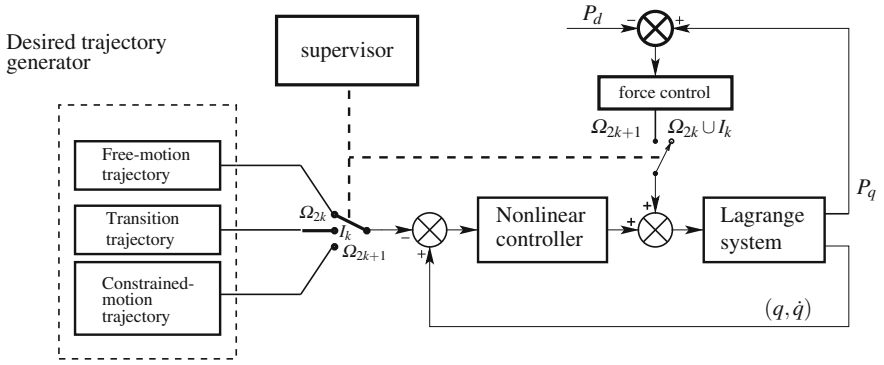

Fig. 8.18 Structure of the controller

8.4 A Unified Point of View

The block-diagram structure of the switching feedback controllers in (8.9) and (8.42) is depicted in Fig. 8.18. The block "Nonlinear controller" is for U_{nc} in (8.9) and (8.42). The block "Lagrangian System" is for (8.1) and (8.36), respectively.

A complete analysis would include frictional effects, including at impacts (a step in this direction may be found in [1013]), and bilateral constraints $h(q) = 0$. Hopefully, the framework proposed in this chapter, paves the way toward such extensions.

8.5 Further Results

8.5.1 Experimental Control of the Transition Phase

In [536] an experimental evaluation of impedance control during a contact task is presented; the strategy proves to behave stably during the transition phase, even if the environment is very rigid. The main drawback of the method is that as the same feedback gains are used during the whole task, the position tracking performances are poor. In [1305], experiments on a one-degree-of-freedom robot are reported. An integral force controller that acts as a low-pass filter for high-frequency components of impact transients plus velocity feedback that damps the system is shown to perform well during the transition phase. These results are contradicted in [1234] who show that integral force control behaves at best with oscillations during the transition phase: due to the integrator wind-up, the second impact has larger magnitude than the first one. Moreover too large integral gains lead to instability. The discrepancy between the results in [1305, 1234] mainly comes from the fact that the environment is either rigid [1305] or compliant [1234]. The work in [1305] contains simulations based on a rigid impact model and compared with experiences. In [1234], several control

strategies are tested. In particular, it appears that integral force control leads to a poorly behaved transition phase, whereas proportional gain force feedback behaves correctly (notice that it is shown in [380] that for flexible-joint one-degree-of-freedom robots, proportional force feedback *always* yields limit cycles when the gain is high enough). However, integral action is needed when contact is established to get good force regulation. The main conclusion in [1234] is that three distinct controllers have to be used: position control, impact control and proportional gain force feedback. No general stability analysis is given to corroborate these experimental results. In [1334] the effects of impacts in the joints of a rigid manipulator are studied, using a Netwon–Euler recursive algorithm to describe the dynamics. The authors of [4] also investigated the collisions effects in n-degree-of-freedom manipulators. They studied the distribution of kinetic energy after the impact in the robot links. In [658], the authors propose to increase damping (velocity feedback) during a transitory stage after the first impact has occurred. This so-called *impact transition control stage* [658] aims at dissipating the impact energy to avoid excessive bouncing, and minimizes force overshoot at the moment of impact. Experimental results on a one axis impact testbed are presented in [567]: several control strategies available in the literature are implemented and shown to improve the transition phase behavior. In [670], a simple switching strategy which consists of a proportional force-velocity feedback (contact mode) and a velocity feedback (non-contact mode) is tested. Experimental results are presented. Unfortunately, the value of the contact stiffness is not provided: it seems indeed that if the shocks have a small duration (typically of the order of 1 ms, see [1144]), the impacts will act as a disturbance for the force sensor, and incorporating its response in the controller will necessarily decrease the performance. Other related studies can be found in [288, 1111] (use of stochastic methods to derive controllers robust with respect to collisions) [903, 1078, 1093, 1261] (methods to reduce impact forces after one collision has been detected) [1124, 1125] (impact detection *via* acceleration measurement and high-level control in insertion tasks). Experiments have also been led in [1109, 1110] in the framework of multifingered hands. Collisions of fingers of different nature (plastic, rubber, gel, paste, powder, sponge) with a rigid obstacle are tested. Newton's kinematic restitution coefficient e_{n} was measured in each case. Apparently the influence of the pre-impact velocity value on e_{n} was not investigated. The results show how the peak impact forces vary with the materials in contact. Similar investigations were led in [32, 654]. Some results in [1110] show that large force peaks may exist at the collisions. The specific yet important task of the stabilization of impacting transition phases was analyzed and experimentally tested in [715, 952, 1085, 1233, 1289].

Purely kinematic solutions to reduce impact effects are studied in [292, 440, 665, 746, 1240, 1333], mainly using the relationship between the impulsive force and the generalized velocities jump, see Example 1.3. Possible redundancy of the manipulator provides more freedom to reduce the impact magnitude [292, 746, 1240]. The impacts effects in space manipulators have been investigated [2, 318, 343, 552, 755, 913, 923, 1258, 1301, 1302, 1303], see Sect. 4.3.3. Application in landing aircrafts are in [1309]. Impact devices have been built to estimate the collision effects. They are composed of piezoelectric sensor to measure the impact force and encoder to

measure pre- and postimpact velocities. The improvement of the impact control *via* the addition of compliance at the contact has been studied in [977]. Flexible-joint manipulators subject to collision are studied in [1317] using Denavit–Hartenberg coordinate frames.

Let us summarize the main conclusions that can be drawn from the experimental works that have been conducted in impact control, and which are in agreement with the controllers presented in Sects. 8.1 and 8.3:

- The approach velocity plays a crucial role and should be decreased. This may be done *via* the control (damping during the approach) or *via* kinematic solutions (manipulator configuration). Impacts may be destabilizing and have to be taken into account in the control design.
- When the contact stiffness is small enough (i.e., the impact duration is large enough), force plus velocity feedback control during the transition phase provides good results (shocks attenuation). However in many cases where the contact duration during the bouncing phase is very small (of the order of 1 ms), measuring and using the force during the impact in the controller, is meaningless (the contact force peak is too high to be compensated for by the control, and the sensor plus motor bandwidth is too low to avoid delays in the compensation).
- Three different controllers have to be used in general that correspond to the three phases of motion (free motion, constrained motion and transition phase). In particular integral force feedback seems to be suitable for constrained motion phases, whereas proportional force feedback is more suitable for bouncing phases (although non-colocated modes may introduce limit cycles – bouncing phases – for high enough gains).

8.5.2 *Juggling Robots Analysis and Control*

Juggling mechanical systems form a particular class of complementarity Lagrangian systems, whose dynamics is a subclass of (5.1). Juggling systems dynamics can be split into two subparts:

$$\begin{cases} M_1(q_1(t))\ddot{q}_1(t) + F_1(q_1(t), \dot{q}_1(t)) = \frac{\partial f}{\partial q_1}(q_1(t), q_2(t))^T \lambda_{\mathrm{n},u} \\ M_2(q_2(t))\ddot{q}_2(t) + F_2(q_1(t), \dot{q}_1(t), q_2(t), \dot{q}_2(t) = \frac{\partial f}{\partial q_2}(q_1(t), q_2(t))^T \lambda_{\mathrm{n},u} + E(q)u(t) \\ 0 \le \lambda_{\mathrm{n},u}(t) \perp f(q_1(t), q_2(t)) \ge 0 \\ \text{Contact law.} \end{cases} \tag{8.74}$$

The $(q_1, \dot{q}_1)$ may be named the *object* dynamics (which may be a real object as a in real juggling system, or the gravity center of a jumping robot, etc.), and the $(q_2, \dot{q}_2)$ is the controlled *robot* dynamics. The only way to control the object is through the multiplier $\lambda_{\mathrm{n},u}$, either at impacts or during persistent contact phases. The control, the controllability and the state observation of juggling systems have been analyzed in [219, 227, 843, 1310, 1311, 1312].

Remark 8.7 It is interesting here to make the link with the cable-mass system of Example 1.6, where the control appears in the complementarity conditions (should it be λ, or $y(t)$, or $\ddot{y}(t)$). From the point of view of Control, we therefore face two quite different subclasses of nonsmooth Lagrangian systems: jugglers and cable-driven systems (whose control is of interest in the Robotics scientific community [139, 259, 395], [231, Parts VII and VIII]), as well as biped robots which may nevertheless involve additional constraints [1105]. This motivates us to propose a general *control* framework for complementarity Lagrangian systems, which mimics that of LCS (compare (8.75) and (5.128)):

$$\left\{\begin{array}{l} M(q)\ddot{q} + F(q,\dot{q}) = E(q)\tau + \nabla h(q)\lambda_{\mathrm{n},b} + \nabla f^{cont}(q,v)\lambda_{\mathrm{n},u} + \nabla f^{free}(q)w \\ 0 \le \lambda_{\mathrm{n},u} \perp f^{cont}(q,v) \ge 0 \\ 0 \le w \perp f^{free}(q) \ge 0 \\ h(q) = 0,\ q(0) \in \Phi,\ \dot{q}(0^+) \in T_\Phi(q(0)), \\ \text{Collision and friction model} \end{array}\right. \tag{8.75}$$

where τ, v and w are control inputs, and we recall that gradients are calculated with respect to q, while Assumption 1 in Sect. 5.2.3 has to be satisfied for Theorem 5.3 to apply.

8.5.3 Mechanisms with Joint Clearance

Joint clearances are a major issue in the design and the control of mechanisms. Indeed they not only introduce nonsmooth phenomena like collisions, but they add degrees of freedom in the system. For instance, a four-bar planar mechanism has one degree of freedom (DOF) in the perfect case. If one joint has mechanical play, it has three DOFs, if two joints have play, it has five DOFs: each clearance adds two DOFs. Both the modeling and the numerical simulation of systems with clearances, are tough issues, especially in the three-dimensional case where cylinder/bore conformal contacts may occur if the clearances are not large enough. The slider-crank mechanism has been widely studied as a benchmark example in the Mechanical Engineering literature, see [400] and references therein, and the various contact/impact models described in Chap. 4 have been tried (some of these with the drawbacks alluded to in Remark 5.31, Sect. 5.7.2, for the numerical simulation). The control of such mechanisms is limited in most of the Systems and Control literature, to very simple systems with oversimplifying contact modeling assumption, which neglects all dynamical effects (in short, clearances are supposed to be static hysteresis or dead zone). A switching control strategy taking into account dynamical effects of impacts, has been proposed in [821] to control a system as in Fig. 5.6a. See also [33] for a numerical analysis of the robustness of various collocated and non-collocated feedback controllers (PD, feedback linearization, passivity-based control) applied on a planar four-bar mechanism with joint clearance. The NSCD method described in

Sect. 5.7.3.1 and implemented in the INRIA SICONOS software,[6] is used in [33], with Coulomb's friction, and constraint stabilization [7]. Other control strategies to compensate for mechanical play in parallel mechanisms consist in redundant actuation, which however requires some care because of "mutual fighting" of the actuators [1018].

8.5.4 Observability and State Observers

Let us quote an interesting example form [843], which shows how impacts may render a system observable. We consider a system with mechanical play:

$$\begin{cases} m_1\ddot{q}_1(t) = \lambda_1(t) - \lambda_2(t) \\ m_2\ddot{q}_2(t) = \lambda_2(t) - \lambda_1(t) + u(t) \\ y(t) = q_2(t) \\ 0 \le f(q_1(t), q_2(t)) \perp \lambda(t) \ge 0 \\ \dot{q}(t_k^+) = \mathscr{E}\dot{q}(t_k^-), \end{cases} \tag{8.76}$$

where $q = (q_1, q_2)^T$, $f(q_1, q_2) = \begin{pmatrix} q_2 - q_1 \\ q_2 - q_1 - 1 \end{pmatrix}$. Suppose that $u(t) = 1$ for all $t \ge 0$, with $q_1(0) = q_2(0) = 1$, $0 < \dot{q}_1(0^+) - \dot{q}_2(0^+) < \sqrt{2}$. Assume that both constraints have a CoR $e_n = 1$, i.e. $\mathscr{E} = \begin{pmatrix} 0 & 1 \\ 1 & 0 \end{pmatrix}$. From these conditions it follows that $t_{k+1} - t_k = 2(\dot{q}_1(0^+) - \dot{q}_2(0^+))$, and that all impacts occur with the constraint boundary $f_2(q) = 0$. Then the following impact Poincaré map can be derived:

$$\begin{cases} z(t_{k+1}^+) = A_1(A_2 z(t_k^+) + B_2) + B_1 \\ y(t_k^+) = Cz(t_k^+) \end{cases} \tag{8.77}$$

where $z = (q_1, \dot{q}_1, q_2, \dot{q}_2)^T$, A_1 and B_1 take into account the impact conditions, A_2 and B_2 come from the continuous, unconstrained part of the dynamics. It happens that the pair (C, A_2) is not observable, but the pair (C, A_1A_2) is observable: impacts may provide the system with some observability property.

The design of state observers for complementarity Lagrangian systems, taking into account all phases of motion (unconstrained, constrained) as well as topology changes (switches between spaces of lower dimensions than n), has been tackled in [1183] and [114] in a general dynamical setting, relying on Measure Differential Inclusions similar to Moreau's second-order sweeping process. The state observers designed in [1183] are a particular, new type of first order perturbed sweeping processes whose well-posedness, inspired by the results in [375] which use an implicit algorithm as in (5.81) and (5.82), is carefully checked by studying the limit of discretized solutions. Accumulations of impacts (Zeno phenomenon) are allowed in the plant velocity.

[6] http://siconos.gforge.inria.fr/.

Specifically and very briefly, the state observers in [1183] take the form:

$$\begin{cases} \dot{z}_1(t) = F_1(t, q(t), z(t)) \\ \\ M(q(t))dz_2 + F_2(t, q(t), z(t))dt \in -N_{V(q(t))}(\hat{v}_e(t)), \end{cases} \tag{8.78}$$

where $\hat{v}_e(t) = \frac{\hat{v}(t^+)+e_n\hat{v}(t^-)}{1+e_n}$, and the state estimate is defined as $\hat{q}(t) = f_1(z_1(t), q(t))$, $\hat{v}(t) = z_2(t) + f_2(z_1(t), q(t))$. The functions $F_1(\cdot)$, $F_2(\cdot)$, $f_1(\cdot)$, $f_2(\cdot)$, are part of the design procedure. It also possible to rewrite the observer (8.78) in the $(\hat{q}, \hat{v})$ coordinates. The second line in (8.78) is a Measure Differential Inclusion (state jumps are allowed in both the plant and the observer dynamics), and $q(t)$ is seen as an external input to the observer dynamics. See also [812, 842, 843, 844] for other state observers design.

Erratum to: Nonsmooth Mechanics

Erratum to: B. Brogliato, *Nonsmooth Mechanics*, Communications and Control Engineering,

DOI 10.1007/978-3-319-28664-8

The original version of the book was inadvertently published with incorrect text, figures and equations. The incorrect text, figures and equations were corrected. The erratum chapters and the book have been updated with the changes.

- Page 21: Figure 1.3 (b) has a severe shortcut in the right curved arrow indicating "Yosida approximation". A better view of the transformations is depicted in Figure 1 below. In the same vein it is worth reading [1].
- Page 49, Section 1.4.3.1: other studies using the Zhuravlev-Ivanov nonsmooth transformation may be found in [3–6].
- Pages 71-72: A first comment is that the damping coefficients that incorporate e_{n} (as those listed page 71), may be seen as extensions to the nonlinear spring-dashpot model, of (2.9) page 56 which also involves the CoR. We note that in reference 1220, the coefficient p in (2.24) is found heuristically to be $p = \frac{1}{4}$. Thus their model has a dissipative force equal to $\alpha\sqrt{mK_h}x^{\frac{1}{4}}\dot{x}$ if x is the normal indentation, with $\alpha = -\ln(e_{\mathrm{n}})\sqrt{\frac{5}{\pi^2+\ln(e_{\mathrm{n}}^2)}}$ (compare with the expression in (2.9) dropping km outside the parantheses). In [7] it is proposed to enlarge the right-hand side of (2.24) to $-\gamma x(t)^p\dot{x}(t) - kx(t)^w$, and γ is chosen as $\alpha m\dot{x}(t_0)\left(\frac{k}{m\dot{x}(t_0)^2}\right)^{\frac{1+p}{1+w}}$. They find that $p = \frac{1-w}{2}$ yields $\alpha = -\ln(e_{\mathrm{n}})\sqrt{\frac{2(1+w)}{\pi^2+\ln(e_{\mathrm{n}})^2}}$. According to [7, Figure 2], their model has a loading-unloading curve similar to Figure 2.4 (a) page 70, with no negative contact force near zero indentation. Several nonlinear spring-dashpot models (Kuwabara-Kono, Hu et al, Tsuji et al) are further compared in [8] in terms of variation of e_{n} with respect to the damping coefficient, acceleration histories, acceleration/identation loading/unloading curves, *etc*, for the case of two spheres colliding. Then

The updated original online version for this book can be found at 10.1007/978-3-319-28664-8

B. Brogliato, *Nonsmooth Mechanics*, Communications and Control Engineering,
DOI 10.1007/978-3-319-28664-8_9

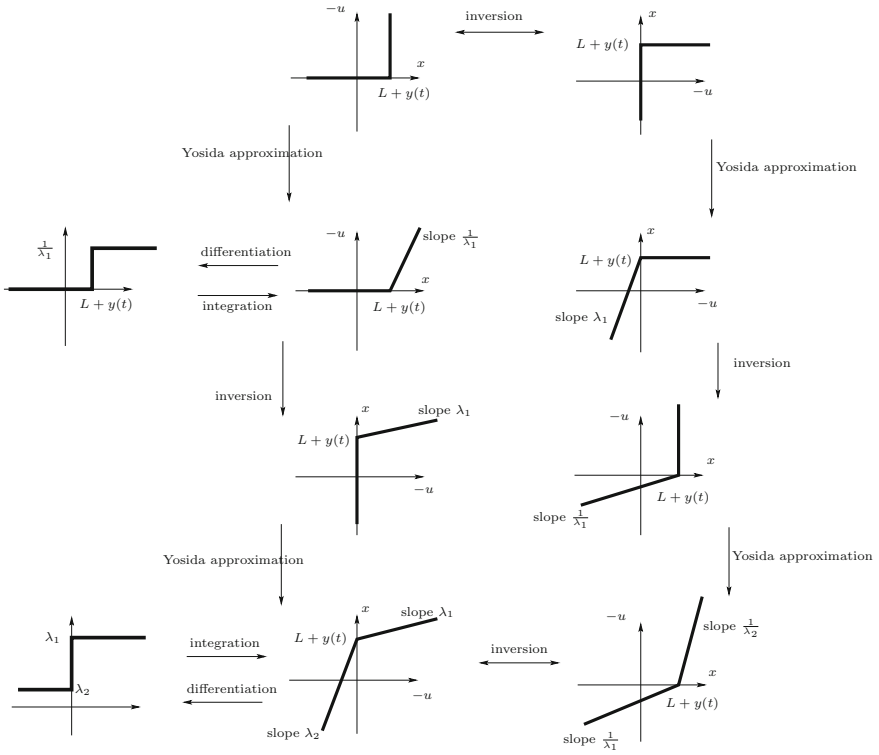

Fig. 1 Enhanced Fig. 1.3 (b)

[8] investigates the influence of the spring-dashpot models on a multiple impact process in a chain of aligned balls. To this aim they rely on the experimental data in reference 625. In particular [8, Figure 11] is exactly Figure 20 in [9] (reference 928) and Figure 29 in [10] (reference 629), where the numerical results are obtained with the LZB model (section 6.3). More work is necessary to determine the domains of validity (in terms of applications, ease of numerical simulation, *etc*) of these models.

- Page 75: footnote 21 should be on page 74, at the end of the framed paragraph.
- Page 99, line 5: replace (B.5) by (B.6). The calculations after (3.13) are in fact the proof in this particular case, that the normal cone can also be written as in (B.5) page 549.
- Page 102, line -5: replace $\mathrm{n}_i \in I\!R^3$ by $\mathrm{n} \in I\!R^3$ (the subscript i in $F_{\mathrm{n},i}$ refers to the contact point number).
- Page 103, line 4: $\mathcal{P}_i = v_{\mathrm{n},i} F_{\mathrm{n},i} = \ldots$
- Page 113: Equation (3.41) is obtained assuming that at an impact instant all virtual displacements and velocities are allowed. This indeed results in zero impact because $M(q(t_k))(\dot{q}(t_k^+) - \dot{q}(t_k^-)) = 0 \Rightarrow \dot{q}(t_k^+) - \dot{q}(t_k^-) = 0$ (the mass matrix is assumed to be full rank). In reference 724 it is *supposed* that the generalized momentum satisfies $p(t_k^+) - p(t_k^-) \in -N_\Phi(q(t_k))$, as a *modelling assumption* since constraints are perfect during impacts (see (iii) page 104). It is shown in reference 724 that this inclusion is equivalent to the variational inequality $\langle p(t_k^+) - p(t_k^-), \bar{\delta}_q \rangle \geq 0$ for all $\bar{\delta}_q \in T_\Phi(q(t_k))$,

where the virtual displacements $\bar{\delta}_q$ are continuous (we can therefore see these developments as the extension of the material in (3.13) and below, to the case with elastic impacts). This equivalence is not surprizing when we consider the normal cone definition in (B.5), recalling that this definition remains true even for nonconvex sets, see Remark B.1 page 550. Using that $p(t) = M(q(t))\dot{q}(t)$ and Moreau's set inclusion in Section B.2.2, we may impose the stricter inclusion $M(q(t_k))(\dot{q}(t_k^+) - \dot{q}(t_k^-)) \in -N_{T_{\Phi(q(t_k))}}(\dot{q}(t_k^+))$ which is equivalently rewritten as the variational inequality: find $\dot{q}(t_k^+) \in T_\Phi(q(t_k))$ such that $\langle M(q(t_k))(\dot{q}(t_k^+) - \dot{q}(t_k^-)), v - \dot{q}(t_k^+)\rangle \geq 0$ for all $v \in T_\Phi(q(t_k))$ (see (5.53) and (5.60) in Section 5.2). Thus we obtain this time the extension of (3.7) where virtual velocities are considered, and the extension of (5.45) for the case of impacting motions. We note in passing that the arguments that yield [13, Equation (1a)] (which is the same as $p(t_k^+) - p(t_k^-) \in -N_\Phi(q(tk))$ with missing mass matrix and minus sign in the right-hand side) are spurious: there is a shortcoming in the reasoning in [13] because of the use of the condition $\delta_q(t_k) + \dot{q}(t_k)\delta t_k \in T_{q(t_k)}$ bd(Φ), while $\dot{q}(\cdot)$ jumps at t_k, and $T_{q(t_k)}$ bd(Φ) denotes the tangent plane at $q(t_k)$ (and not the tangent *cone*) to the boundary of the admissible domain (the correct way to derive the material page 385 in [13], is in Section 6 of reference 724 by Leine et al).

The above basic assumption yields Theorem 3 in reference 724 which is a Hamilton principle in strong norm, or strong Hamilton principle. There exists a weak norm for a weak Hamilton's principle which somewhat relaxes the assumption on the generalized momenta at impact times, see Theorem 4 and condition (99) in reference 724.

- Page 130, about the calculation of the normal and tangential vectors at the contact point A (local kinematics): the starting point is that if a 3D surface is defined by two parameters u and v and a differentiable function $r(u, v), r : I\!R^2 \to I\!R^3$, then $\frac{\partial r}{\partial u}(u_1, v_1) \in I\!R^3$ and $\frac{\partial r}{\partial v}(u_1, v_1) \in I\!R^3$ span the tangent plane at the point A_1 parameterized by u_1 and v_1, and one can then define the normal vector as the cross product $\mathbf{n}_1 = \frac{\partial r}{\partial u}^T(u_1, v_1) \times \frac{\partial r}{\partial v}^T(u_1, v_1)$ (one should take care of the correct order to get the right orientation of the normal).
- Page 133, about the time-derivative of the right-hand side of (4.17): Let us denote the Galilean frame as $\mathcal{L}_0 = \mathcal{G}$ and the local frame as $\mathcal{L}$. The angular velocity vector between both frames is denoted as $\Omega_{\mathcal{L}/\mathcal{L}_0}$. We obtain $\frac{d}{dt}[(A_2A_1)^T\mathbf{n}] = \frac{d}{dt}[(A_2A_1)^T]\mathbf{n} + (A_2A_1)^T\frac{d}{dt}\mathbf{n} = \frac{d}{dt}[(A_2A_1)^T]\mathbf{n} + (A_2A_1)^T\frac{d}{dt}\mathbf{n}$. Assume that the vectors are expressed in $\mathcal{L}_0$. Then basic kinematics say that $\frac{d}{dt}\mathbf{n} = \frac{d}{dt}\mathbf{n}|_\mathcal{L} + \Omega_{\mathcal{L}/\mathcal{L}_0} \times \mathbf{n} = \Omega_{\mathcal{L}/\mathcal{L}_0} \times \mathbf{n}$ since $\mathbf{n}$ is constant in $\mathcal{L}$. Thus $(A_2A_1)^T\frac{d}{dt}\mathbf{n} = (A_2A_1)^T(\Omega_{\mathcal{L}/\mathcal{L}_0} \times \mathbf{n}) = 0$ since the vector product is orthogonal to $\mathbf{n}$ and the vector (A_2A_1) is along $\mathbf{n}$. Therefore $\frac{d}{dt}[(A_2A_1)^T\mathbf{n}] = \frac{d}{dt}[(A_2A_1)^T]\mathbf{n}$. The vector $\frac{d}{dt}[(A_2A_1)^T]$ is the time derivative of (A_2A_1) in L_0 and may be named the relative velocity between both bodies. The sentence "In particular..., except if $\mathbf{n}$ is fixed in $\mathcal{G}$" is meaningless and should be deleted. It becomes true if stated in terms of the acceleration $\frac{d}{dt}V_{A_i}$ and $\dot{v}_{i,\mathrm{n}}$.
- Page 162, Section 4.2.3 (also page 169, section 4.2.5.2): [25] study the force/identation relation $f(\delta) = k\delta^n$ for an elastic body with a rough surface in contact with a rigid flat surface. A three-dimensional rough surface is constructed using a modified two-variable Weierstrass-Mandelbrot fractal function. Results in [25, Table 2] show that n can vary between 2.11 and 1.19 depending on some parameters (like fractal dimension, fractal roughness, root-mean-square roughness and arithmetic average height R_a). Thus the elasticity is found to be superlinear and even sometimes super-Hertz. Compared with the study described in Section 4.2.3 where $n = 1$ in (4.61), it seems that surface roughness increases n. The interest of

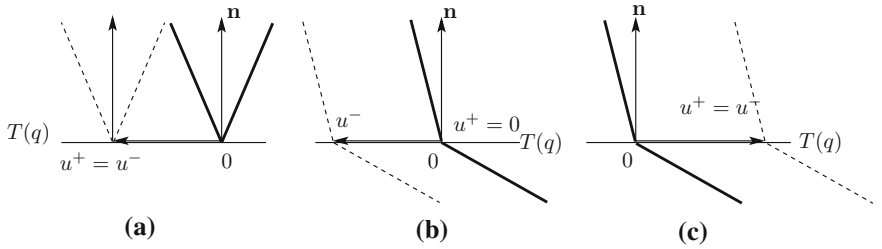

Fig. 2 Sweeping process with friction

such study is to show that Hertz' fundamental assumption (ii) page 147 (introduction of Section 4.2.1.1) on smooth contacting surfaces, may play a role in the elasticity coefficient. However we should also note that the surfaces in contact considered in [25] are conforming in addition to be rough, and that contrary to (4.61) the flat is considered non-deformable.

- Page 164, Section 4.2.4: see a comment below (page 384).
- Page 165: Hurmuzlu's analysis of the micro-impact phenomenon (Section 4.3.10.2) seems to contradict Love's criterion, because micro-collisions excite transversal modes in the beam (page 228) and these vibrations dissipate energy.
- Pages 165-166: estimations of the CoR for harmonic chains of aligned beads colliding a wall, and taking into account sequences of repeated impacts as well as the vibrational energy trapped in the chain, are given in [28, 29].
- Page 200, Equation (4.124): the last term is $\frac{dp}{dt'}$,.
- Page 245, line 6: $\ldots + w_b(q, \dot{q}, t)$.
- Pages 247-248, Proposition 5.3: The equality $h(t') - h(t) = \int_t^{t'} \dot{h}(s)ds$ used in the proof means that $h(\cdot)$ is absolutely continuous (not just continuous) and that what is denoted as $\dot{h}(\cdot)$ is its almost-everywhere derivative. The same holds for (ii), where $\dot{h}(\cdot)$ has to be absolutely continuous as well.
- Page 270, line above (5.61): [780, 781].
- Page 280, in Theorem 5.3, line 3: replace $T_\Phi(q(t_0))$ by $V(q(t_0))$, as it is not guaranteed in general that both tangent cones are equal. Same page 282 in Remark 5.13.
- Page 286, about Coulomb's friction: notice that in the sliding mode one has $\|F_t\| = \alpha\|v_t\| = \mu\|F_n\| \Leftrightarrow \alpha = \frac{\mu\|F_n\|}{\|v_t\|}$. Hence we recover the equivalent classical way of expressing sliding Coulomb's friction as $F_t = -\mu\|F_n\|\frac{v_t}{\|v_t\|}$.
- Page 293, line 5: $\ldots$ sgn $(\ddot{x}(t^+))$ when $\dot{x}(t) = 0, \ldots$
- Page 295: in case of non trivial mass matrix, Equation (5.97) becomes $u(t_k^+) = \text{proj}(0, [u(t_k^-) + M(q(t))^{-1}\mathcal{C}(q(t))] \cap T(q(t))$ [15]. Proposition 3.3 in [16] extends (5.97), and Figure 5.12 which depicts the algorithm in case of a trivial mass matrix. Additional figures which complete Fig. 5.12 page 295, are in Figure 2. Case (a) shows that if the mass matrix is trivial (the identity matrix) then when $u(t^-)$ is tangent to the constraint boundary, there is no velocity jump (no impact without collision). Case (b) shows that when the mass matrix is not trivial and the generalized friction cone dips below the tangent hyperplane, then the velocity may jump. But case (c) shows that depending on the tangent velocity signum, the velocity may remain continuous. It is noteworthy that the zero vector in (5.97) refers to velocities, not positions.
- Page 298, last line: replace $x_{2,n}$ by $(A_2A_1)^T\mathbf{n}$.

- Page 299, more details about P-matrices and the difference with positive definite matrices. *Principal minors* are the determinants of the principal submatrices, they are sometimes also called *principal subdeterminants. Principal submatrices* of a matrix $M \in I\!R^{n\times n}$ are constructed as follows: let the index set $\mathcal{I} = \{1, 2, \ldots, n\}$, and consider any subset $\mathcal{J} \subseteq \mathcal{I}$. Let us denote $\mathcal{J} = \{i_1, i_2, \ldots, i_m\}$, with $m \leq n$, and $i_k \in \mathcal{I}$ for all $1 \leq k \leq m$. Delete all rows and columns of M which are indexed by i with $i \notin \mathcal{J}$. The obtained matrix $M_{\mathcal{J}} \in I\!R^{m\times m}$ is a principal submatrix of M. A *leading* principal submatrix of M is obtained by considering $i_k = k, k = 1, 2, \ldots, m$. The determinant of a leading principal submatrix is a *leading principal minor*.
  Theorem 5.5 states that a P-matrix has to have all its principal submatrices with positive determinant, *i.e.* all positive principal minors. A (real) matrix M (nor necessarily symmetric) is positive definite if and only if $M^T + M$ has all its leading principal minors positive (and also its leading principal submatrices are positive definite matrices). If in addition $M = M^T$, then $M \succ 0$ if and only if all its principal minors are positive (and another characterization is: if and only if all its leading principal minors are positive, showing in passing that a positive definite matrix is a P-matrix). A (real) matrix M (nor necessarily symmetric) is positive semidefinite if and only if $M^T + M$ has all its principal minors non negative. Thus for positive definiteness it is sufficient to check the leading principal submatrices, while for positive semi definiteness all principal submatrices have to be checked.
  Another characterization of P-matrices is as follows [2, Lemma 16, Theorem 59]: if M is a P- matrix, the inequalities $Mx \leq 0$ and $x \geq 0$ have only the trivial solution $x = 0$. Also there exists $x > 0$ such that $Ax > 0$.

- Section 5.4.2: I said nothing on *cone linear complementarity problems* of the form $K \ni z \perp w = Mz + r \in K^*$ where K is a closed convex cone. See Theorem 8 and Corollary 5 in reference 23 for the existence of solutions to CLCP.
- Section 5.4.2. Another result that completes this section concerns the number of solutions to LCPs for which uniqueness fails. This is tackled in [14]. A matrix is said to be an $\mathcal{N}$-matrix if its all principal minors are negative. For such matrices, the LCP (5.105) has either 0, 1, 2 or 3 solutions. A solution z^* is degenerate if $z^*_i = 0$ and $w_i = (Mz^*)_i + r_i = 0$ for some i.

Lemma 1 *[14, Lemma 2.4, Theorem 3.2, Theorem 3.3, Theorem 3.4] (i) Let M be an $\mathcal{N}$-matrix and $M \prec 0$. Then for each $r \geq 0$, the LCP in (5.105) has a solution, and has no solution for $r \ngeq 0$ (componentwise inequality). The LCP has exactly two solutions for $r > 0$. (ii) Let M be an $\mathcal{N}$-matrix and $r \in I\!R^n$. Then if M is not negative definite and $r \ngeq 0$, the LCP (5.105) has a unique solution. (iii) Let M be an $\mathcal{N}$-matrix, non negative definite, and $r > 0$. Then if all solutions of the LCP (5.105) are non degenerate, the LCP has exactly three solutions. Otherwise it has exactly two solutions. (iv) Let M be an $\mathcal{N}$-matrix, non negative definite, and $0 \neq r \geq 0$, with $r_i = 0$ for some i. Then the LCP (5.105) has exactly two solutions, with one solution degenerate.*

- Page 313: replace $u_2(t)$ — $u_1(t)$ by $u_2(t)$, and replace $u_2(t)$ by $u_2(t)$ — $u_1(t)$, in the dynamical equations (5.130).
- Pages 320–321: further studies on the stability of nonsmooth circuits (characterization of equilibria, Lyapunov stability) may be found in [20, 21].
- Page 322: in the paragraph after Theorem 5.12: $\mathcal{E} > 0$.
- Page 323: in (5.150) it happens that $V(t^+) - V(t^-) \leq 0$ provided that $0 \in S(t)$, with $S(t)$ in (5.139). See reference 480, Lemma 3.
- Page 328, line 1: delete the "and".

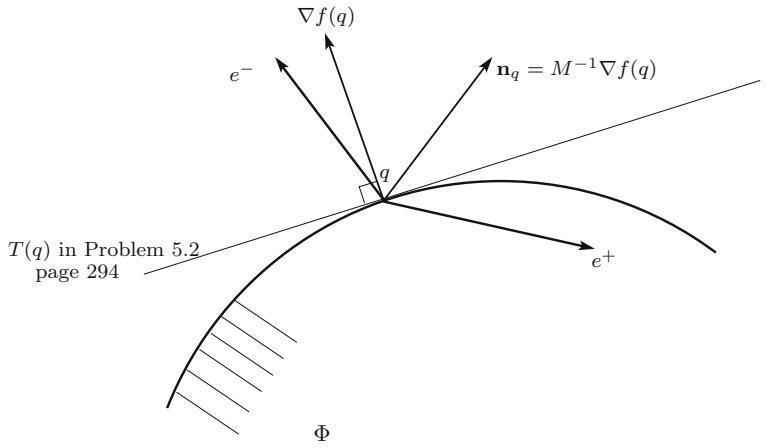

Fig. 3 Painlevé paradox and generalized friction cone

- Page 332, Proposition 5.24 and Equation (5.158): the matrix $P^{\mu}(q)$ is defined as

$$-\nabla f(q)^T M(q)^{-1} H_{\mathrm{t},u}(q)[\mu_i \mathrm{sgn}(\nu_{\mathrm{t},u,i})].$$

- Page 352, Section 5.6.4. Mathematical results on the existence of solutions (velocity $u(.)$ of local bounded variation, $q(t) = q(0) + \int_0^t u(s)ds$) which extend results in both references 867 and 1141, 1142, can be found in [15, 16]. It incorporates Painlevé paradoxes, in the sense that the generalized friction cone may dip below the tangent cone boundary at the considered contact point (as pointed out in footnote 31 page 295, and in a paragraph above Figure 5.24 page 353). An example of calculation of the generalized friction cone for the Painlevé sliding rod system, may be found in [17, Section 2.2] . Using the notation of Equation (5.1) and of Section 6.2, the Painlevé sliding rod example of Section 5.6.1 may be written as $\ddot{q} = \mathbf{n}_q \lambda_{\mathrm{n}} + M^{-1} H_{\mathrm{t}}(q)\lambda_{\mathrm{t}}$. The generalized friction cone is the cone generated by $\mathbf{n}_q = \frac{1}{m}(0, 1, -\frac{3}{l}\cos(\theta))^T$ and $\pm\mu M^{-1} H_t(q)$, $H_t(q) = M(1, 0, \frac{3}{l}\sin(0))^T$, $M = \mathrm{diag}(m, m, I)$, with the edges $e^{\pm} = \mathbf{n}_q \pm \mu M^{-1} H_{\mathrm{t}}(q)$. It is not symmetric around $\mathbf{n}_q$, and $\mathbf{n}_q^T M e^+ = \nabla f(q)^T e^+ = B(\theta, \mu)$ in (5.175) so that the generalized cone may dip below the tangent hyperplane $T(q)$, this reflects normal/tangential couplings as in Equation (6.30). This is depicted in Figure 3.

- Page 352, Section 5.6.4, line 18: replace [755, Theorem 1] by [1328, Theorem 1].
- Page 352, Section 5.6.4: the article [11] is worth reading.
- Pages 367 and 430 (Sections 5.7.3.5 and 7.3.2): a (θ, γ) time stepping scheme is used in [12] to calculate periodic solutions of set-valued Lur'e systems (as in Figure 2.2 but with a feedback setvalued nonlinearity of the more general form $(w, \lambda) \in \mathcal{R}$). After discretization a mixed quadratic complementarity problem (MQCP) is constructed. State jumps are incorporated in the problem (remind that LCS may have state discontinuities, see Section 5.4.4.3). The period, the state and the multiplier λ are unknowns of the MQCP. A MQCP is a complementarity problem of the form: Find z, w, v such that

$$\varphi(z) + Mz + q = w - v$$
$$l \leq z \leq u, (z-l)^T w = 0, (u-z)^T v = 0 \quad (1)$$

where $\varphi(\cdot)$ is a vector of quadratic forms in z. The solver PATH is used to solve the discretized MQCP.

- Page 363, Section 5.7.3.2: an interesting application of the NSCD method is in [24] that deals with collapse mechanism of ancient stone arches. Though the NSCD method (the Moreau-Jean algorithm in Section 5.7.3.1) has several shortcomings (like a simplistic impact law as explained in Example 5.6 page 275, see also Section 6.3.3 and the comments page 411), it is interesting for complex systems with many degrees of freedom and unilateral contacts and seems to encapsulate essential modeling features in this case. For a finer analysis of stacked blocks dynamics under base excitation, one should certainly use more sophisticated models like LZB.
- Page 384: it is shown that varying the stiffness ratio γ in the 3-ball system, changes a lot the impact outcome, and this is also true when the mass ratios are varied (the kinetic angle between the two constraints surfaces). This is also true for the 2-ball system hitting a rigid wall (take $m_3 = +\infty$ in Figure 6.5 page 383). The analysis in [27] shows that the mass ratio and the stiffness ratio have a great influence on the kinematic CoR, which varies between 0.2 and 1 (the possibility of several impacts before definitive separation -a kind of micro-collisions effect-between the first ball and the wall is taken into account[1]). For the 2-ball system hitting a wall, the kinematic CoR is defined as $-\frac{v(t_f)}{v(t_0)}$ where $v = \frac{m1v1+m2v2}{m1+m2}$ is the center of mass velocity, t_0 is the time of the first impact, t_f is the time of the last impact before complete separation of the 2-ball system and the wall. Thus depending on these ratios, the system made of the two beads (which we can see as an approximation of the flexibilities in a rigid body like a rod) will rebound with a low or a high velocity. The apparently loss kinetic energy is in fact transformed into potential energy stored in the system's spring under the form of vibrations that persist after the impact is ended. This is therefore also quite related to Sections 4.2.4 and 4.4 material. It is also interesting to compare this result to Theorem 4.1 page 238, which stipulates that an elastic rod that collides a wall with zero external force, has $e_n = 1$. Thus the 2-ball system is not in general a good approximation of the infinite dimensional model. However the results in [27, Figure 2a] show that with equal masses and equal stiffnesses, then $e_n \approx 1$. This is extended to N-ball systems (see also [28, 29]). One assumption that is made in these studies, and might make the analysed chains behaviour different from an elastic rod impacting axially a wall, is that it is assumed that the first (colliding) ball reverses its velocity instantaneously [29].
- Page 394 *(relations between Moreau's impact law in (5.60) (5.61), and the restitution mapping in (6.44) (6.45))*. Here I also refer to the reference [210, Section 3.1.1], with some inaccuracies in Equation (44). Let $\mathcal{I}(q(t))$ be the index set of active constraints at position $q(t)$. Moreau's law states that $\dot{q}(t^+) = \dot{q}(t^-) - (1+e_n)\text{proj}_{M(q(t))}[N(q(t)); \dot{q}(t^-)]$, see (5.60). Clearly if $\dot{q}(t^-)$ is in the interior of $N(q(t))$ then $\dot{q}(t^+) = -e_n\dot{q}(t^-)$. If this is not the case, one has to project $\dot{q}(t^-)$ onto the normal cone, which is a polyhedral cone generated by the normals $\mathbf{n}_{q,i}, i \in \mathcal{I}(q(t))$. In case $N(q(t))$ is a so-called *latticial* cone, then the material in [210, Section 3.1.1] is correct. We recall that $N(q(t))$ is a latticial cone if $\dim(q(t)) = \text{card}(\mathcal{I}(q(t))$, in other words the number of active constraints is equal

[1] In [27] this is called multiple impacts, however in our terminology multiple impacts are simultaneous collisions, not a sequence of separated collisions.

to the dimension of $q(t)$) (the configuration space), and the active constraints (hence the vectors $\mathbf{n}_{q,i}$, $i \in \mathcal{I}(q(t))$) are independent (see Németh and Németh, How to project onto an isotone projection cone, Linear Algebra and its Applications, vol.433, 41-51, 2010). In this case the projection of $\dot{q}(t^-)$ onto $N^M_{\Phi_u}(q)$ in [210, Section 3.1.1, line 8 after (43)], is correct according to Theorem 2 in Németh and Németh.
One difference between the impact law in (6.44) (6.45), and Moreau's impact rule, is first on the choice of the vectors $\dot{q}_{\text{norm}}$ and $\dot{q}_{\text{tan}}$. This explains some discrepancies between both models, as demonstrated for instance on the rocking block problem, see [228, Section 3.4] which shows that with a specific choice of $\dot{q}_{\text{norm},1}$ and $\dot{q}_{\text{norm},2}$, rocking motion is possible only if off-diagonal terms in the restitution matrix in (6.45) are introduced, whatever the kinetic angle value. On the contrary Moreau's law allows for rocking in some situations when the kinetic angle between the two active constraints, is larger than $\pi/2$, see [31].
In practice one uses the equivalent form of Moreau's law in (5.66) and solves a LCP or a mLCP. Using (5.67) and assuming that $D_u(q(t_k)) \succ 0$, it is easy to construct a LCP with unknown $W(tk) \triangleq U_{\text{n}}(t_k^+) + \mathcal{E}_{\text{nn}} U_{\text{n}}(t_k^-)$:

$$0 \leq W(t_k) \perp D_u(q(t_k))^{-1} W(t_k) - D_u(q(t_k))^{-1}(I_m + \mathcal{E}_{\text{nn}}) U_{\text{n}}(t_k^-) \geq 0. \qquad (2)$$

This LCP always has a unique solution. If $D_u(q(t_k))^{-1}(I_m + \mathcal{E}_{\text{nn}}) U_{\text{n}}(t^-) < 0$, then $U_{\text{n}}(t_k^+) + \mathcal{E}_{\text{nn}} U_{\text{n}}(t_k^-) = 0$ which gives Newton's law at each contact with CoR e_{n} if $\mathcal{E}_{\text{nn}} = \text{diag}(e_{\text{n}})$ (see Proposition 5.15 for the link between Moreau's impact law and Newton's law at each contact with complementarity, see also the seminal reference [454]). The next step is to write down Moreau's law when $\dot{q}(t^-)$ is not in the interior of $N(q(t))$, but has to be projected on it. When the constraints are not independent, one can still use a numerical solver that computes a solution for LCPs with positive semi-deifnite matrices (like Lemke's algorithm).

- Page 398, line 2: choosing
- Page 400, line just above Proposition 6.6: replace $\bar{M}(M(q, \mu, v_{\text{t}})$ by $\bar{M}(q, \mu, v_{\text{t}})$.
- Page 406, line 7 after (6.68): $\dot{\delta}_j(p_{f,j}) \leq 0$ (here we assume that compression occurs with positive identation velocity $\dot{\delta}_j > 0$ and expansion occurs with negative identation velocity $\dot{\delta}_j < 0$), in agreement with Figure 6.6. Thus indentation increases during compression and decreases during expansion (or restitution).
- Page 407: Notice that Equations (6.71) (6.72) can be rewritten in a differential form $\frac{dE_j}{dp_j}(p_j) = \dot{\delta}_j(p_j) dp_j$ and similarly for (6.72), so that the whole LZB dynamics is a first-order dynamics with augmented state variable (the potential energy becomes a state variable). Thus the calculation of the positions (assumed to be constant in the LZB approach) is not at all needed to integrate the system (see reference 929 Equations (4.42) and (4.43) where a midpoint rule is used to approximate the potential energies). Notice further that (6.72) indeed stipulates that according to the energetic constraint $W_{e,j} = -e^2_{*,j} W_{c,j}$ (using (4.159)), then at the end of the impact $E_j(p_{f,j}) = 0$.
- Page 407 Section 6.3.2: another interesting application of the LZB model is in [26].
- Page 415, line 8: drop the "be".
- Page 429, Equation (7.18): replace e in σ_1 and σ_2 by e_{n}.
- Page 452, Equation (7.51): $0 \leq f(q^*) \perp \lambda^*_{\text{n},u} \geq 0$.
- Page 456, Equation (7.62), last two lines: $\Sigma_{k\in[k_0,k_1]}$ instead of $\Sigma_{k\in[k_0,k_1]}$ which might let one think that only the two values k_0 and k_1 are taken into account.

- Pages 457-458: The stability (finite-time convergence to a fixed point, plus Lyapunov stability) of simple systems with set-valued terms encompassing Coulomb's friction with constant normal force, is analysed in [22]. The discretisation of the same dynamics is studied in [23], where it is shown that the sequence of discrete solutions converges in a finite number of steps to its limit. This is quite similar to the results mentioned in Section 5.7.3.7 about implicit discretetime sliding mode control (though control has its own peculiarities like the fact that one wants to study robustness with respect to parameter uncertainties, unmatched disturbances, more complex attractive surfaces, *etc*). It may also be seen as a generalization of the case treated in Remark 5.33 pages 362-363.
- Pages 457-458: it is clear that the fixed points of a system with unilateral contact and Coulomb friction are also solutions of a generalized equation, extending (7.51). As said page 458, in general uniqueness of the equilibrium is lost. Consider for instance (5.162) page 336. For this system the equilibria $(q, \dot{q}) = (q^*, 0)$ satisfy the generalized equation:

$$\begin{cases} \begin{pmatrix} 0 \\ 0 \end{pmatrix} = \begin{pmatrix} \sin(\alpha) \\ \cos(\alpha) \end{pmatrix} \lambda_{\mathrm{n}}^* + \begin{pmatrix} -\cos(\alpha) \\ \sin(\alpha) \end{pmatrix} \lambda_{\mathrm{t}}^* + \begin{pmatrix} F_x \\ 0 \end{pmatrix} \\ 0 \leq f(q^*) \perp \lambda_{\mathrm{n}}^* \geq 0 \\ \lambda_{\mathrm{t}}^* \in -\mu \lambda_{\mathrm{n}}^* \mathrm{sgn}(0) \end{cases} \tag{3}$$

  with sgn(0) = [-1, 1]. It is noteworthy that usually the generalized equation for equilibria and the generalized equation for sticking contacts, are not the same (in this example they are the same because sticking contact implies that the system does not move, and conversely). Also this is different from the generalized equation in (5.165) which is obtained from the acceleration Coulomb's friction model.

- Page 462: Chapter 7 could ne nicely completed with the study in [32] which analyzes the contact stability of a simple system, with a force feedback controller, and subject to delay in the force feedback. These theoretical results were experimentally validated by Tornambé in [33].
- Page 531, Section 8.5.2: controllability of juggling systems (with the important assumption that the robot dynamics in (8.74) has much bigger mass than the object, so that $\dot{q}_2$ is continuous at impacts) as well as their stabilization, is studied in [30].
- Page 551, Lemma B.1: it is more appropriate to write $f : \mathrm{dom}(f) \subseteq I\!R^n \to I\!R \cup \{+\infty\}$ (though one might understand that $I\!R$ contains the infinity).
- Page 552, figure B.2: in the first figure on the left, replace $f_\lambda(x)$ by $-f_\lambda(x)$. The Moreau-Yosida approximation is a convex function. It becomes obvious also from this figure, that the function $-f_\lambda(\cdot)$ represents the potential energy function of a unilateral spring, and has to be compared with the indicator function which represents the potential energy associated with complementarity conditions (which are a particular contact model).
- Page 553: For better clarity replace the set Φ in the paragraph after (B.12), by $\mathcal{C}$.
- Page 560, Section B.2.2: line 3: replace (5.35) by (5.35), line 6: replace Definition 5.34 by (5.34).
- Pages 561-562, about prox-regular sets. Characterizations of finitely represented sets which are prox-regular are given in [18, Theorems 3.1, 4.1] , in addition to Theorem B.5. An interesting result about the preservation of prox-regularity under an inverse linear transformation $S' = H^{-1}(S) = \{z | Hz \in S\}$, is in [19, Lemma 2.7] (reference 1181 in the book's bibliography). If $S \subset I\!R^l$ is r—prox-regular, and if S is in the range space of $H : I\!R^n \to I\!R^l$,

then S' is r'—prox-regular with $r' = \frac{r\sigma_H^+}{\|H\|^2}$, where σ_H^+ is the least positive singular value of H and $\|H\|$ is an induced matrix norm. An extension is in [18, Corollary 6.5].

- Page 622, index for G, add for Gauss's principle: systems with friction, 332.

References

1. A. Curnier, Unilateral Contact: Mechanical Modelling. In: New Developments in Contact Problems, P. Wriggers and P.D. Panagiotopoulos (Eds.), CISM Courses and Lectures no 384, Springer Wien New York, pp.1-54, 1999
2. P. Moylan, Dissipative Systems and Stability, Newcastle, NSW, Australia, http://www.pmoylan.org
3. Li, C., Xu, W., Feng, J., Wang, L.: Response probability density functions of Duffing-Van der Pol vibro-impact system under correlated Gaussian white noise excitation. Physica A **392**, 1269–1279 (2013)
4. Rong, H., Wang, X., Xu, W., Fang, T.: Subharmonic response of a single-degree-of-freedom nonlinear vibroimpact system to a ramdomly disordered periodic excitation. Journal of Sound and Vibration **327**, 173–182 (2009)
5. Feng, J., Xu, W., Rong, H., Wang, R.: Stochastic responses of Duffing-Van der Pol vibro-impact system under additive and multiplicative random excitations. Int. J. of Non-Linear Mechanics **44**, 51–57 (2009)
6. Feng, J., Xu, W., Wang, R.: Stochastic responses of vibro-impact Duffing oscillator excited by additive Gaussian noise. Journal of Sound and Vibration **309**, 730–738 (2009)
7. G. Hu, Z. Hu, B. Jian, L. Liu, H. Wan, On the determination of the damping coefficient of nonlinear spring-dashpot system to model Hertz contact for simulation by discrete element method, Information Engineering (ICIE), 2010 WASE International Conference on, vol.3, pp.295-298, 14, 15 August 2010
8. Kacianauskas, R., Kruggel-Emden, H., Zdancevicius, E., Markauskas, D.: Comparative evaluation of normal viscoelastic contact force models in low velocity impact situations. Advanced Powder Technology (2016). doi:10.1016/j.apt.2016.04.031
9. Nguyen, N.S., Brogliato, B.: Shock dynamics in granular chains: numerical simulations and comparisons with experimental tests. Granular Matter **14**(3), 341–362 (2012)
10. N.S. Nguyen, B. Brogliato, *Multiple Impacts in Dissipative Granular Chains,* Springer Verlag, Lecture Notes in Applied and Computational Mechanics vol.72, 2014
11. Champneys, A., Varkonyi, P.: The Painlevé paradox in contact mechanics. IMA Journal of Applied Mathematics **81**, 538–588 (2016)
12. V. Sessa, L. Iannelli, F. Vasca, V. Acary, A complementarity approach for the computation of periodic oscillations in piecewise linear systems, Nonlinear Dynamics, DOI: 10.1007/s11071-016- 2758-5
13. Fetecau, R.C., Mardsen, J.E., Ortiz, M., West, M.: Nonsmooth Lagrangian mechanics and variational collision integrators. SIAM J. Applied Dynamical Systems **2**(3), 381–416 (2003)
14. Kojima, M., Saigal, R.: On the number of solutions to a class of linear complementarity problems. Mathematical Programming **17**, 136–139 (1979)
15. Paoli, L.: Vibro-impact problems with dry friction-Part I: Existence result. SIAM J. Math. Anal. **47**(5), 3285–3313 (2015)
16. Paoli, L.: Vibro-impact problems with dry friction-Part II: Tangential contacts and frictional catastrophes. SIAM J. Math. Anal. **48**(2), 1272–1296 (2016)
17. F. Génot, B. Brogliato, New results on Painlevé paradoxes, INRIA Research Report 3366, February 1998, https://hal.inria.fr/inria-00073323
18. Adly, S., Nacry, F., Thibault, L.: Preservation of prox-regularity of sets with applications to constrained optimization. SIAM J. Optim. **26**(1), 448–473 (2016)

19. Tanwani, A., Brogliato, B., Prieur, C.: Stability and observer design for Lur'e systems with multivalued, non-monotone, time-varying nonlinearities and state jumps. SIAM J. Control and Optimization **56**(2), 3639–3672 (2014)
20. Adly, S., Goeleven, D., Le, B.K.: Stability analysis and attractivity results of a DC-DC Buck converter. Set-Valued Var. Anal. **20**, 331–353 (2012)
21. Adly, S., Cibulka, R., Massias, H.: Variational analysis and generalized equations in electronics. Set-Valued Var. Anal. **21**, 333–358 (2013)
22. S. Adly, H. Attouch, A. Cabot, Finite time stabilisation of nonlinear oscillators subject to dry friction, in Nonsmooth Mechanics and Analysis, P. Alart, O. Maisonneuve, R.T. Rockafellar (Eds.), Springer, Chapter 24, pp.289-304, 2006
23. Baji, B., Cabot, A.: An inertial proximal algorithm with dry friction: finite convergence results. Set-Valued Analysis **9**, 1–23 (2006)
24. Lancioni, G., Gentilucci, D., Quagliarini, E., Lenci, S.: Seismic vulnerability of ancient stone arches by using a numerical model based on the Non-Smooth Contact Dynamics method. Engineering Structures **119**, 110–121 (2016)
25. Xiao, H., Shao, Y., Brennan, M.J.: On the contact stiffness and nonlinear vibration of an elastic body with a rough surface in contact with a rigid flat surface. European Journal of Mechanics A/Solids **49**, 321–328 (2015)
26. Z. Zhao, C. Liu, T. Chen, Docking dynamics between two spacecrafts with APDSes, Multibody System Dynamics, 2016
27. Ruan, H.H., Yu, T.X.: The unexpectedly small coefficient of restitution of a two-degree-of-freedom mass-spring system and its implications. International Journal of Impact Engineering **88**, 1–11 (2016)
28. Basile, A.G., Dumont, R.S.: Coefficient of restitution for one-dimensional harmonic solids. Phys. Rev. E **61**(2), 2015–2023 (2000)
29. Nagahiro, S.I., Hayakawa, Y.: Collision of one-dimensional nonlinear chains. Physical Review A **67**, 036609 (2003)
30. Lynch, K.M., Black, C.K.: Recurrence, controllability, and stabilization of juggling. IEEE Transactions on Robotics and Automation **17**(2), 113–124 (2001)
31. A.I. Giouvanidis, E.G. Dimitrakopoulos, Modelling contact in rocking structures with a non-smooth dynamics approach, ECCOMAS Congress 2016, VVII European Congress on Computational Methods in Applied Sciences and Engineering, M. Papadrakakis, V. Papadopoulos, G. Stefanou, V. Plevris (eds.), Crete Island, Greece, 5-10 June 2016
32. Niculescu, S.I., Brogliato, B.: Force measurement time-delays and contact instability phenomenon. European Journal of Control **5**, 279–289 (1999)
33. Tornambé, A.: Discussion on "Force measurement time-delays and contact instability phenomenon". European Journal of Control **5**, 290–292 (1999)

Appendix A
Distributions, Measures, Functions of Bounded Variations

Sections A.1 and A.2 are given for the sake of completeness because some notions are used in Chaps. 1 and 2, but may be safely skipped since their implication on understanding Nonsmooth Mechanics is weak. By contrast, Sects. A.3 and B survey useful mathematical tools that cannot be ignored.

A.1 Schwartz' Distributions

A.1.1 The Functional Approach

In this section we first briefly introduce the *functional* notion of a distribution as defined in [1082].

Definition A.1 $\mathscr{D}$ is the subspace of smooth[1] functions $\varphi : \mathbb{R}^n \to \mathbf{C}$, with bounded support.

Thus a function $\varphi(\cdot)$ on $\mathbb{R}^n$ belongs to $\mathscr{D}$, if and only if $\varphi(\cdot)$ is smooth, and there exists a bounded set K_φ of $\mathbb{R}^n$ outside of which $\varphi \equiv 0$. As an example, L. Schwartz gives the following function [1082, Chap. 1,§2], with $n = 1$, $K_\varphi = [-1, 1]$:

$$\varphi(t) = \begin{cases} 0 & \text{if} \quad |t| \geq 1 \\ e^{\frac{-1}{1-t^2}} & \text{if} \quad |t| < 1 \end{cases} \tag{A.1}$$

Definition A.2 A distribution D is a continuous linear form defined on the vector space $\mathscr{D}$.

This means that to any $\varphi \in \mathscr{D}$, D associates a complex number $D(\varphi)$, noted $\langle D, \varphi \rangle$. The space of distributions on $\mathscr{D}$ is the dual space of $\mathscr{D}$ and is noted $\mathscr{D}^\star$. The functions in $\mathscr{D}$ are sometimes called *test-functions*.

[1] i.e., indefinitely differentiable.

B. Brogliato, *Nonsmooth Mechanics*, Communications and Control Engineering,
DOI 10.1007/978-3-319-28664-8

Two distributions D_1, D_2 are equal on an open interval Δ if $D_1 - D_2 = 0$ on Δ, i.e., if for any $\varphi \in \mathscr{D}$ whose support K_φ is contained in Δ, then $\langle D_1 - D_2, \varphi\rangle = 0$. In fact, one can generate a distribution from any locally integrable function f, via the integral $\int_{K_\varphi} f(x)\varphi(x)dx$. However, some distributions cannot be generated by locally integrable functions, like for instance, the Dirac distribution and its derivatives. They are called *singular* distributions (or sometimes *generalized functions*).

Contrarily to functions, all distributions (i.e., elements of $\mathscr{D}^\star$) are infinitely differentiable. The mth derivative of $T \in \mathscr{D}^\star$ is given by $\langle T^{(m)}, \varphi\rangle = (-1)^m\langle T, \varphi^{(m)}\rangle$, for all $m \in \mathbb{N}$. An important feature of distributions is that, in general, the product of two distributions does not define a distribution.

A.1.2 The Sequential Approach

Schwartz' distributions can be defined via the sequential approach [51, §4.3]. Roughly, one starts by defining *fundamental* sequences of continuous functions on a fixed interval (a, b), and then a relation of equivalence between fundamental sequences. Distributions can thus be defined as limits of sequences of continuous functions, but there are sequences of continuous functions that do not converge toward a function, as it is well known for the Dirac distribution. This shows that the space of functions has to be completed by other mathematical objects, which one calls distributions.

Definition A.3 A sequence $\{f_n(\cdot)\}$ of continuous functions defined on (a, b) is *fundamental* if there exist a sequence of functions $\{F_n(\cdot)\}$ and an integer $k \in \mathbb{N}$ such that

- $F_n^{(k)}(x) = f_n(x)$ for all $x \in (a, b)$.
- $\{F_n(\cdot)\}$ converges almost uniformly

A sequence of functions converges *almost uniformly* (a.u.) on (a, b) if it converges uniformly on any interval $[c, d] \subset (a, b)$ (for instance, $\{\frac{x}{n}\}$ converges a.u. toward 0 on $(-\infty, +\infty)$. Before defining distributions, one needs to define equivalent fundamental sequences:

Definition A.4 Two fundamental sequences $\{f_n(\cdot)\}$, $\{g_n(\cdot)\}$ are *equivalent* if there exist $\{F_n(\cdot)\}$, $\{G_n(\cdot)\}$ and $k \in \mathbb{N}$ such that

- $F_n^{(k)}(x) = f_n(x)$ and $G_n^{(k)}(x) = g_n(x)$.
- $\{F_n(\cdot)\}$ and $\{G_n(\cdot)\}$ converge a.u. toward the same limit.

One denotes $\{f_n(\cdot)\} \sim \{g_n(\cdot)\}$. A distribution on (a, b) is an equivalent class in the set of all fundamental sequences on (a, b).

For instance, the Dirac distribution has to be seen as the limit of a sequence of continuous functions $\delta_n(\cdot)$ with support $K_n = [t_c, t_c + \Delta t_n]$, $\Delta t_n \to 0$ as $n \to +\infty$, and:

- **(i)** $\delta_n(\cdot) \geq 0$
- **(ii)** for all $n \in \mathbb{N}$, $\int_{-\infty}^{+\infty} \delta_n(\tau)d\tau = 1$
- **(iii)** for all $a > 0$, $\lim_{n\to+\infty} \int_{|\tau|>a+t_c} \delta_n(\tau)d\tau = 0$

Then $\delta_n(\cdot) \to \delta_{t_c}$ as $n \to +\infty$, and we know that there exists a sequence of continuous functions $P_n(t)$ and k such that $P_n^{(k)} = \delta_n$, and $\{P_n\}$ converges uniformly. Note that such a fundamental sequence (called a *delta-sequence*) that determines the Dirac measure is by far not unique. Examples of functions δ_n that belong to this equivalent class are given in [51, Chaps. 1,2]: $\delta_{t=0} = \left[\sqrt{\frac{n}{2\pi}} \exp\left(-n\frac{x^2}{2}\right)\right] = \left[\frac{\sin(nx)}{\pi x}\right] = \left[\frac{n}{2} \exp(-n|x|)\right] = \left[\frac{1}{\pi} \frac{n}{\exp(nx)+\exp(-nx)}\right]$.

Distributions have derivatives of any order:

Definition A.5 If a fundamental sequence $\{f_n(\cdot)\}$ consists of functions with continuous mth derivatives (i.e., $f_n \in C^m(a, b)$) then the distribution $[f_n^{(m)}(\cdot)]$ is the mth derivative of the distribution $[f_n(\cdot)]$.

Each distribution has derivatives of all orders as one can always choose a fundamental sequence of functions which are differentiable up to an arbitrary order. For instance, if $f_n(x) = \sqrt{\frac{n}{2\pi}} \exp\left(-n\frac{x^2}{2}\right)$, $[f_n^{(m)}(\cdot)] = \delta_{t=0}^{(m)}$. From [51, Theorem 2.2.5], the mth derivative of the Dirac distribution δ_0 is given by $[\delta_n^{(m)}]$ where $\{\delta_n\}$ is a delta sequence with continuous first m derivatives.

A.1.3 Notions of Convergence

Some existence of solution results presented in Chap. 2 use the notion of strong and weak$\star$ convergence. Let us explain here what this means. For simplicity, we restrict ourselves to the spaces $\mathscr{D}$ and $\mathscr{D}^\star$. The definitions also exist for other spaces of functions and their dual spaces like Sobolev spaces, see [191].

Definition A.6 A sequence of functions $\varphi_n \in \mathscr{D}$ is *weakly convergent* to $\varphi \in \mathscr{D}$ if for each $T \in \mathscr{D}^\star$ one has

$$\lim_{n\to+\infty} \langle T, \varphi_n\rangle = \langle T, \varphi\rangle \tag{A.2}$$

The sequence $\varphi_n \in \mathscr{D}$ is convergent to $\varphi(\cdot)$ in the topology of $\mathscr{D}$ if their supports are contained in a fixed compact set, $\varphi_n \to \varphi$ uniformly and all derivatives $\varphi_n^{(k)} \to \varphi^{(k)}$ uniformly, for all $k \geq 1$.

Definition A.7 A sequence of functionals $T_n \in \mathscr{D}^\star$ is *weakly$\star$ convergent* to $T \in \mathscr{D}^\star$ if for each $\varphi \in \mathscr{D}$ one has

$$\lim_{n\to+\infty} \langle T_n, \varphi\rangle = \langle T, \varphi\rangle \tag{A.3}$$

It is also possible to define a strong convergence in $\mathscr{D}^\star$. However, in $\mathscr{D}$ and $\mathscr{D}^\star$, strong and weak convergences coincide [1082] [488, §6.3,Theorem 2].

The notation weak$\star$ is to recall that this applies to elements of $\mathscr{D}^\star$. As an example, consider the sequence of functions $f_n(x) = n\cos(nx)$. Clearly, $\sup_{x\in\mathbb{R}} |f_n(x)| = n$ so that this sequence does not converge uniformly. However, $-\frac{1}{n}\langle \cos(nx), \ddot{\varphi}\rangle = \langle \sin(nx), \dot{\varphi}\rangle = \langle n\cos(nx), \varphi\rangle = \langle f_n, \varphi\rangle \to 0$ as $n \to +\infty$. Hence $\{f_n\} \to 0$ in a weak$\star$ sense. One says that f_n converges strongly to f in L^p if $||f_n - f||_{L^p} \to 0$ as $n \to +\infty$. One says that f_n converges weakly$\star$ in L^p to f if $\int f_n\varphi \to \int f\varphi$ as $n \to +\infty$, for $\varphi \in L^q$, $\frac{1}{p} + \frac{1}{q} = 1$, $p < +\infty$. For $1 < p < +\infty$, weak$\star$ and strong convergences are the same.

Consider the proofs of existence of solutions based on discretization of the measure differential inclusions, like those in [867] or [1142]. The constructed discrete-time solutions are such that the acceleration is a function. Now, a sequence of functions converges strongly in the sense of measures toward a limit that is also a function. Hence, the only way to get a limit that is a singular measure (thus not identifiable with a function) is to consider its weak$\star$ convergence, because weak$\star$ convergence permits functions (considered as measures) to tend to singular measures. Without this notion of convergence it would be hopeless to get a limit with discontinuous velocity.

A.2 Measures and Integrals

We have seen that a proper statement of nonsmooth shock dynamics involves to consider bounded forces as *density* with respect to the Lebesgue measure dx of the *contact impulse measure*, whereas *contact percussions* are *atoms* of the contact impulse measure, and the impulse magnitude is the density of these atoms with respect to the Dirac measure at the impact time δ_{t_k}. The aim of this appendix is to introduce all these notions.

Let us start by defining abruptly what is meant by a measure [477]:

Definition A.8 Let $(X, \mathscr{R})$ be a measurable space. A positive measure (or simply measure) on $(X, \mathscr{R})$ is a *mapping* $\mu : \mathscr{R} \to [0, +\infty]$ with the following properties:

- $\mu(\emptyset) = 0$.
- $\mu\left(\cup_{n\geq 1} A_n\right) = \sum_{n\geq 1} \mu(A_n)$ for any sequence $\{A_n\}$ of subsets of $\mathscr{R}$, with $A_n \cap A_m = \emptyset$ for $n \neq m$.

Such a mapping that satisfies the second property is called *countably additive*.

Engineers should recall that a measure is defined as a function of sets of X that belong to a family of sets $\mathscr{R}$, i.e., it assigns to a set a positive real number.

Remark A.1 In fact it would be preferable to denote $(X, \mathscr{R}, \mu)$ a measurable space, to emphasize that it is attached to a measure μ.

An example of measurable space is $(\mathbb{N}, \mathscr{R})$ where $\mathscr{R}$ is a σ-ring of subsets of $\mathbb{N}$, and the measure is defined as $\mu(A) =$(the number of elements of A), with $A \subset \mathscr{R}$. One has for any A and $B \in \mathscr{R}$ [477, p.78]:

$$\begin{aligned}\mu(A)+\mu(B)&=\mu(A\cup B)+\mu(A\cap B)\\ \mu(A-B)&=\mu(A)-\mu(A\cap B)\end{aligned}\tag{A.4}$$

Now we are ready to introduce what is called the Lebesgue measure:

Theorem A.1 *[477] There exists a unique measure λ on the measurable space $(\mathbb{R},\mathscr{B})$ such that $\lambda[[a,b)]=b-a$ for all couples (a,b) of real numbers, with $a\leq b$.*

Before introducing the Lebesgue's integral, let us recall what is meant by a measurable function.

Definition A.9 Let $(X,\mathscr{R})$ be a measurable space, and Y a topological space. Then $f:X\to Y$ is *measurable* if for all open subsets $B\subset Y$, the set $f^{-1}(B)$ belongs to $\mathscr{R}$.

Recall that a set that belongs to $\mathscr{R}$ is called measurable. Hence a function is measurable if its inverse sends any open set into a measurable set. It is important to note that measurability is characterized by starting from the image space Y. This we shall retrieve in the definition of Lebesgue's sums below. This allows to treat functions that seem very complex when considered from the source space, but rather simple when considered from the image space.

Example A.1 For instance, let us consider the following well-known example $f:[0,1]\to[0,1]$, $f(x)=0$ if x is rational, $f(x)=1$ otherwise. It seems that $f(\cdot)$ is very irregular, since it is everywhere discontinuous, hence not Riemann integrable (or not Riemann measurable) [477, p.4]. But $f(\cdot)$ is a very simple measurable function. Indeed, consider for instance the set $f^{-1}\left((-\frac{1}{2},\frac{1}{2})\right)$: this is the set of rational numbers on $[0,1]$. Such a set is negligible (it is countable[2]), so it is measurable. One can take other examples and check measurability in all cases. It is a simple matter to prove that this function is not Riemann integrable [477]: indeed for any subdivision of $[0,1]$, as fine as desired, the difference between the Riemann's sums is always 1, due to density of rationals in $\mathbb{R}$.

Remark A.2 Since this function $f(\cdot)$ is measurable, it defines a distribution. Thus it admits a *generalized* derivative,[3] or a derivative in the sense of distributions, defined as $\langle\dot{f}(x),\varphi(x)\rangle=-\int_{K_\varphi}f(x)\dot{\varphi}(x)dx$. Apparently, it is not easy to visualize what such a $\dot{f}$ is: recall that this is not a function. However since $f\equiv 1$ (except on a countable, negligible set), one has $\langle\dot{f},\varphi\rangle=-\int_{K_\varphi}\dot{\varphi}(x)dx=0$ because $\varphi(\cdot)$ is zero outside K_φ. Thus $\dot{f}(\cdot)$ is the zero distribution.

As a matter of fact, and to stress that all these notions have a purely theoretical interest, one can only prove that there *exists* nonmeasurable functions [1081]. But

[2]Recall that a set is said to be *countable* when there is a bijection between the set and $\mathbb{N}$.

[3]Some authors [931, 1235] introduce the notion of distributions through so-called generalized derivatives.

it is not possible to explicitly construct them. Lebesgue's integration theory relies on measure theory. Let us introduce the relationship between measures, which are notions attached to sets, and integrals which are notions attached to functions. To begin with, let us consider a bounded and positive simple function $u : X \to [0, +\infty]$, $u = \sum_{i=1}^{n} c_i \chi_{C_i}$, where $\{c_1, \cdots, c_n\}$ is the (finite) set of values taken by u, $C_i = u^{-1}(c_i)$, $\chi_{C_i}(\cdot)$ is the indicator function of the set C_i: $\chi_{C_i}(x) = 1$ if $x \in C_i$, $\chi_{C_i}(x) = 0$ if $x \notin C_i$. The integral of u is defined as the number:

$$\int u \triangleq \sum_{i=1}^{n} c_i \mu(C_i) \tag{A.5}$$

where μ is a measure. Note that this definition *a priori* attaches the integral to a particular measure. Consider now a positive function $f : X \to [0, +\infty]$. Then the integral of $f(\cdot)$ is given by

$$\int f \triangleq \sup_{u \in \mathscr{U}} \left(\int u \right) \tag{A.6}$$

where $\mathscr{U}$ is the set of simple functions $u : X \to [0, +\infty]$ with $u \leq f$. One generally denotes the integral of f as $\int f d\mu$ when μ is not the Lebesgue measure. One generally denotes the Lebesgue measure as $\lambda[\cdot]$, or as dx, and the Lebesgue integral of a measurable function f on $[a, b]$ as $\int_{[a,b]} f d\lambda$ or as $\int_a^b f(x)dx$. All these notations denote the same object. Also, the Lebesgue measure (or the length) of an interval $[a, b)$ is the number $\lambda[[a, b)] = \int_{\mathbb{R}} \chi_{[a,b]} d\lambda = \int_a^b dx$, where $\chi_{[a,b]}$ is the indicator function of the interval $[a, b)$ (that is measurable if the interval is, since $\chi_{[a,b]}^{-1}(I)$ is either $\emptyset$, $[a, b)$ or $\mathbb{R}$ depending on I[4]).

It could seem at first sight that the consideration of positive functions is restrictive. It is not, because every function can be decomposed into its positive and negative parts f^+ and f^-, with $f = f^+ - f^-$. Then f is integrable if and only if f^+ and f^- are. In other words, f is μ-integrable if the number $\int |f| d\mu$ is finite. In Example A.1, $\int_{[0,1]} f(x)dx = 1$.

The density of a measure is defined as follows [477, p.145]:

Definition A.10 Let μ be a measure, and let $g(\cdot)$ be μ-integrable function. Let μ be defined as $\mu(E) = \int_E f(x)dx$ for any measurable set E, and for some Lebesgue measurable function $f : \mathbb{R} \to [0, +\infty] = \bar{\mathbb{R}}^+$. Then $f(\cdot)$ is called the density of μ and

$$\int g d\mu = \int g(x) f(x) dx \tag{A.7}$$

If $f(\cdot)$ is continuous, then the function $F : x \mapsto \int_0^x f(t)dt$ is differentiable and $\frac{dF}{dx} = f(x)$. One denotes the measure μ as dF or as μ_f. Notice that $F(\cdot)$ is nondecreasing which is necessary for dF to be a measure.

[4]Recall that $f^{-1}(I) = \{x \mid f(x) \in I\}$.

For instance in Chap. 5, Sect. 5.2, we saw that the sweeping process can be formulated with respect to any measure. It was then necessary to define the densities of the Lebesgue and the Stieltjes measures dt and du with respect to a measure μ. These densities are denoted as t'_μ and u'_μ respectively. In view of Definition A.10, these notations mean that for some function f as in Definition A.10, $d\mu = f dt$ so that $t'_\mu(t) = \frac{dt}{d\mu} = \frac{1}{f(t)}$, whereas $u'_\mu = \frac{du}{d\mu} = \frac{\dot{u}(t)}{f(t)}$ for $t \neq t_k$, and $u'_\mu(t_k) = \frac{1}{f(t_k)}\sigma_u(t_k)$. In relationship with the formulation of the sweeping process in Problem 5.1 where terms like $u'_\mu = \frac{du}{d\mu}$ appear, let us **roughly** define the meaning of such a ratio. If one considers two measures μ and ν such that μ satisfies: $\mu(\Gamma) = 0$ each time $\nu(\Gamma) = 0$ for all measurable sets Γ (in which case μ is said to be absolutely continuous with respect to ν), then there exists a function $f(\cdot) \geq 0$ such that $\mu(\Gamma) = \int_\Gamma f d\nu$ –so $f(\cdot)$ is the density of μ–. The notation $f = \frac{d\mu}{d\nu}$ which denotes the Radon–Nikodym derivative of μ with respect to ν, is also motivated by the fact that $f(t) = \lim_{\varepsilon \to 0} \frac{\mu([t,t+\varepsilon])}{\nu([t,t+\varepsilon])}$.

Let us consider some examples of measures:

- If $f(x) = 1$, then $dF = dx (= \lambda)$, dF is the Lebesgue measure.
- If $f(x)$ is a continuous function, dF is a Lebesgue–Stieltjes measure. The length of an interval $[a, b]$ is equal to $\int_{[a,b]} dx$ (i.e., the Lebesgue integral of its indicator function). The Lebesgue–Stieltjes integral generalizes the notion of length to $\int_{[a,b]} dF = \int_{[a,b]} f(x)dx = F(b) - F(a) = \mu_f [[a, b)] \geq 0$ (this is assured because f takes nonnegative values, see Definition A.10).
- The Dirac measure δ_0 is the distributional derivative and Stieltjes measure of the Heaviside function $h(\cdot)$, i.e., $\delta_0 = dh = \dot{h}$. In fact if $\varphi \in \mathscr{D}$, then $\langle \delta_0, \varphi \rangle = \varphi(0)$ (by definition) and:

$$\langle \dot{h}, \varphi \rangle = -\int h(t)\dot{\varphi}(t)dt = -\int_0^{+\infty} h(t)\dot{\varphi}(t)dt = \varphi(0) \tag{A.8}$$

Looking at the equation from another angle, we know that

$$\delta_0([a, b)) = \begin{cases} 0 \text{ if } \{0\} \notin [a, b) \\ \\ 1 \text{ if } \{0\} \in [a, b) \end{cases} \tag{A.9}$$

To find the integral of a continuous function f with respect to δ_0, we approximate it by a sequence $\{u_n\}$ of step functions such that $u_n \to f$ pointwise. From [1052, Theorem 11.30], if $u_n(x) = c_{n,i}$ on $[c_{n,i}, c_{n,i+1})$, one gets $\int u_n d\delta_0 = \sum_{i=0}^m c_{n,i}\delta_0([c_{n,i}, c_{n,i+1})) = c_{n,k}$, where $0 \in [c_{n,k}, c_{n,k+1})$. Since $u_n(0) = c_{n,k} \to f(0)$ we conclude that:

$$\int f d\delta_0 = \lim_{n \to +\infty} \int u_n d\delta_0 = \lim_{n \to +\infty} c_{n,k} = f(0) \tag{A.10}$$

as expected. This is one of the ways in which Dirac measures can be introduced, besides the distributional interpretation as the limit of fundamental sequences of continuous functions, see Sect. A.1.2.

Remark A.3 A measure μ possesses an *atom* at $x \in X$ if $\mu(A) > 0$ for any set $A \subset \mathscr{B}$ which contains x. If outside the atoms $\mu = 0$ (i.e., for any set A containing no atoms, $\mu(A) = 0$), then μ is said to be *purely atomic*. In other words, a measure is purely atomic if it is concentrated on a countable set. For instance, the Dirac measure or any sum of Dirac measures are atomic measures. A measure with no atoms is said *non-atomic*, i.e., $\mu(\{x\}) = 0$ for all point $x \in X$. An atomic μ_a and a non-atomic μ_{na} measures are always *mutually singular*, *i.e.,* there exists a set $B \in \mathscr{B}$ with complement C_B such that $\mu_a(B) = \mu_{na}(C_B) = 0$. As another example of a measure, let us consider the mass of a body B defined as $m(B) = \int_B dm$. When B reduces to a material point, then the measure m is atomic since B has zero Lebesgue measure while the mass is positive.

In relationship with Definition A.10, notice that if $F(\cdot)$ is a bounded, right-continuous and nondecreasing function, then dF (or μ_f) is nonatomic if and only if $F(\cdot)$ is continuous. This is easily seen as follows: consider a point $x \in (X, \mathscr{R}, \mu)$:

$$\begin{aligned} dF(\{x\}) &= \lim_{\varepsilon \to 0, \varepsilon > 0} dF\left((x - \varepsilon, x]\right) = \lim_{\varepsilon \to 0, \varepsilon > 0} \left(F(x) - F(x - \varepsilon)\right) \\ &= F(x) - F(x^-) \end{aligned} \tag{A.11}$$

Hence $dF(\{x\}) > 0 \iff \sigma_F(x) > 0$. In this latter case dF has a density with respect to the Dirac measure at x, equal to $\sigma_F(x)$. Thus dF has an atom at x, or x is an atom of dF.

A.2.1 Zero-Measure, Almost-Everywhere

There is a notion that is often used and that deserves to be defined: when one says that some property is true *almost everywhere* (a.e.). A set A is of zero-measure (or μ-negligible, or of μ-measure 0) if it is contained in a measurable set B with μ-measure 0 (i.e., $\int \chi_B d\mu = 0$). A property is true μ-a.e. if the set for which the property fails has μ-measure 0. A function is a.e. zero if the set $f^{-1}(0)$ is the complement of a zero-measure set, and two functions $f(\cdot)$ and $g(\cdot)$ are μ-a.e. equal if $\int |f - g| d\mu = 0$. Note that a countable set has Lebesgue measure zero: for instance the set of rational numbers in $\mathbb{R}$. Sets of measure zero may be different for different measures.

A necessary and sufficient condition for a bounded function on a bounded interval to be Riemann integrable, is that its set of discontinuity points be of zero Lebesgue measure. Note that although the set of rational numbers is countable, the function in Example A.1 is not Riemann integrable, because it is discontinuous everywhere.

A.3 Functions of Bounded Variation in Time

A.3.1 Definition and Generalities

Roughly speaking, a function of *local bounded variation* (LBV) is a function that does not vary too much on any bounded interval of its domain of definition. More rigorously, let $f(\cdot)$ be a single-valued function $I \subseteq \mathbb{R} \to \mathbb{R}^n$. Let $x_0 < x_1 < \cdots < x_n$ be any subdivision S_n of I. Then $f(\cdot)$ has bounded variation on I if

$$\text{var}(S_n, f, I) \stackrel{\Delta}{=} \sum_{i=0}^{n} ||f(x_{i+1}) - f(x_i)|| \leq C \tag{A.12}$$

for some bounded constant C. The number $\text{var}(f, I) \stackrel{\Delta}{=} \sup_{S_n} \text{var}(S_n, f, I)$ is called the *total variation* of $f(\cdot)$ on I. If $f(\cdot)$ has bounded total variation on any compact subinterval of I, it is said of *local bounded variation* ($f \in LBV$). If it is in addition right-continuous, we denote it as $f \in RCLBV$.

Let us provide some intuitive thoughts on such functions, before introducing other equivalent definitions. When $f(\cdot)$ is simple (i.e., $f(I)$ consists of a finite set of real numbers, or in other words $f(\cdot)$ is piecewise constant with finite number of values), then one easily sees that $f(\cdot)$ is LBV means that the jumps of $f(\cdot)$ are bounded. On the other hand, if this same $f(\cdot)$ possesses very large number of discontinuities, one intuitively deduces that the jumps magnitudes necessarily have to become very small. If the number of jumps becomes infinite, most of them have to be almost zero, otherwise a constant C as in (A.12) cannot be found. Obviously, it is necessary to be more accurate on what is meant by an infinite number of jumps. In fact, a function that satisfies (A.12) can be shown to possess at most a *countable set* of discontinuity points. This means that one is able to associate an integer $n \in \mathbb{N}$ to each $x \in I$ at which $f(\cdot)$ jumps. In other words, the discontinuity points constitute a sequence $\{x_n\}$, $n \in \mathbb{N}$, possibly infinite. It follows that in the case of functions of one variable only, bounded variation implies that the function has only points of continuity or jump points. No other sort of point can be encountered. The property in (A.12) is equivalent to anyone of the following statements:

(i) There exists a constant $C < +\infty$ such that for all $\varphi \in \mathscr{D}$, one has $|\langle f, \dot{\varphi}\rangle| = |\int_{K_\varphi} f(t)\dot{\varphi}(t)dt| \leq C \sup_{t \in K_\varphi} ||\varphi(t)||$,

(ii) $f \in L^1(I)$ and the generalized derivative of $f(\cdot)$ (or equivalently its distributional derivative) is a bounded measure.

(iii) There exist two nondecreasing functions f_1 and f_2 such that $f = f_2 - f_1$.

(iv) There exist a continuous function $g(\cdot)$ of bounded variation and a piecewise constant function $s(\cdot)$ (called the *jump* function) such that $f = g + s$.

Let $I = [a, b]$. A function $f(\cdot)$ of bounded variation in I has right-limits on $[a, b)$, left-limits on $(a, b]$ and is bounded on I. Moreover:

(v) Every function $\varphi \in C^0(I)$ is Riemann integrable with respect to f and one has $|\int_I \varphi(x)df(x)| \leq K \sup_{x\in I} ||\varphi(x)||$ for some $K < +\infty$. Moreover, $\text{var}(f, I)$ is the smallest K such that the inequality is satisfied.

The number $\int_I \varphi(x)df(x)$ is called the Riemann–Stieltjes integral of φ on I with respect to df. Roughly speaking, the Riemann–Stieltjes integral of a function is defined similarly as the Riemann integral. Riemann's sums are defined as $R(\varphi, I) = \sum_{i=1}^n \varphi(\xi_i)(x_i - x_{i-1})$, where the x_i's form a subdivision of I and $\xi_i \in [x_i, x_{i-1})$. Riemann–Stieltjes' sums are defined as $RS(\varphi, I) = \sum_{i=1}^n \varphi(\xi_i)\,(f(x_i) - f(x_{i-1}))$. Under certain conditions on the functions $\varphi(\cdot)$ and $f(\cdot)$, it can be proved that by taking the supremum of these sums over all possible subdivisions of I, one obtains a unique number called the integral of $f(\cdot)$ on I.

Remark A.4 The distributional derivative of $f(\cdot)$ is the sum of three terms: an atomic measure μ_a which is the derivative of the jump function s, a Lebesgue integrable function $\dot{f}$ and a singular (with respect to the Lebesgue measure) nonatomic measure μ_{na}. The sum of μ_{na} with $\dot{f}dt$ is the derivative of $g(\cdot)$.

The above extends to set-valued mappings as follows. Consider a set-valued mapping $S : I \to \mathbb{R}^n$ and replace the expression in (A.12) $\|f(x_{i+1}) - f(x_i)\|$ by the Hausdorff distance $\text{haus}\,(S(t_{i+1}), S(t_i))$. One obtains the concept of set-valued mappings with *bounded variation* on I. The Hausdorff distance between two subsets Q_1 and Q_2 in $\mathbb{R}^n$ is given as usual by

$$\text{haus}\,(Q_1, Q_2) \stackrel{\Delta}{=} \max\{\sup_{x\in Q_1} d(x, Q_2),\ \sup_{x\in Q_2} d(x, Q_1)\},$$

where $d(x, Q) = \inf\{\|x - y\|\ y \in Q\}$. Denote by $\text{var}_S(t)$ the variation of $S(\cdot)$ over $[0, t]$. When the variation function $\text{var}_S(\cdot)$ is locally absolutely continuous on $[0, +\infty[$, the set-valued mapping $S(\cdot)$ is said to be *locally absolutely continuous* on $[0, +\infty)$. As usual the local absolute continuity of the function $v(\cdot) \stackrel{\Delta}{=} \text{var}_S(\cdot)$ means that for each $T \in [0, +\infty)$ and for any positive number ε there exists some positive number η such that $\sum_{i=1}^k |v(t_i) - v(s_i)| < \varepsilon$ whenever $\sum_{i=1}^k (t_i - s_i) < \eta$ with $s_i < t_i < s_{i+1}$ in $[0, T]$.

A.3.2 Differential Measures

Let $x : I \to \mathbb{R}^n$ be a function with bounded variation, $I \neq \emptyset$, $I \subseteq \mathbb{R}$. With $x(\cdot)$ is associated its differential measure dx. If $x(\cdot)$ is constant, $dx = 0$. If $dx = 0$ and $x(\cdot)$ is right continuous in the interior of I, then $x(\cdot)$ is constant. If $x(\cdot)$ is a step function, then dx is the sum of a finite collection of Dirac measures with atoms at the discontinuity points of $x(\cdot)$. For $a \leq b$, $a, b \in I$:

$$\begin{array}{l} dx([a, b]) = x(b^+) - x(a^-),\ dx([a, b)) = x(b^-) - x(a^-) \\ dx((a, b]) = x(b^+) - x(a^+),\ dx((a, b)) = x(b^-) - x(a^+) \end{array} \tag{A.13}$$

In particular, we have

$$dx(\{a\}) = x(a^+) - x(a^-)$$

$\rightsquigarrow$ *In most of the applications we deal with in this book, one may think of the differential measure associated with a right-continuous LBV function, as the sum of an absolutely continuous function and a sum of Dirac measures. This may be sufficient for most engineering problems.*

Remark A.5 Notice that not all continuous functions are LBV. For instance, the function $f : [0, 1] \to \mathbb{R}$, $f(0) = 0$, $f(x) = x \sin(\frac{\pi}{x})$ is continuous on $[0, 1]$, but it is not of bounded variation. This is easy to see intuitively since as x approaches zero, $f(\cdot)$ oscillates infinitely often between -1 and $+1$.

More details on functions of bounded variation may be found in [893, 1161, 1235].

Appendix B
Elements of Convex Analysis

As we have seen throughout the book, an important class of studies devoted to mechanical systems with unilateral constraints uses mathematical tools from convex analysis. This is the case, for example, for the Moreau's sweeping process and the results in [969, 1066]. We recall here some basic definitions used in this setting. Roughly speaking, convex analysis is that part of nonlinear and variational analysis, dealing with convex sets and functions [898]. As we noticed in Sect. 5.2, all those mathematical tools aim at generalizing to nonsmooth functions the simple well-known notions of tangent space, normal direction, in order to get a powerful framework to study evolution problems, one of which is the dynamics of systems subject to unilateral constraints. But there are other applications, see the book [901]. Nonsmooth analysis is also used in the framework of nonsmooth Lyapunov functions, with Clarke's generalized derivative. One important tool is the so-called *subdifferential* of a function. Roughly, the goal is to replace the notion of the slope at a point by introducing a set of vectors. It is known that if $f : \mathbb{R}^n \to \mathbb{R}$ is convex and smooth at x_0, then $f(x) - f(x_0) \geq \nabla f^T(x_0)[x - x_0]$, for all x. If $f(\cdot)$ is not differentiable at x_0, one introduces a vector γ, that is called a *subgradient* if it satisfies the subgradient inequality:

$$f(x) - f(x_0) \geq \gamma^T (x - x_0) \tag{B.1}$$

for all x. The set of all such subgradients forms the subdifferential at x_0: $\partial f(x_0) = \{\gamma \in \mathbb{R}^n | f(x) - f(x_0) \geq \gamma^T (x - x_0)$, for all $x \in \mathbb{R}^n\}$. This generalization also applies to nonconvex functions, see [293]. The material that follows is mainly taken from the classical references [385, 465, 531, 1045].

B.1 Definitions and Examples

Let us now introduce the tools which we need in mechanics with unilateral constraints.

B. Brogliato, *Nonsmooth Mechanics*, Communications and Control Engineering,
DOI 10.1007/978-3-319-28664-8

Definition B.1 (*Indicator Function*) Let $\Phi \subset \mathbb{R}^n$. Then the indicator function of Φ is given by:

$$\psi_\Phi(q) = \begin{cases} 0 & \text{if } q \in \Phi \\ +\infty & \text{otherwise.} \end{cases} \tag{B.2}$$

The indicator function $\psi_\Phi(q)$ is convex if and only if Φ is a convex set [898, p.11]. J.J. Moreau introduced the indicator function in order to mathematically represent the potential associated with unilateral constraints. Such potential is sometimes named *hard wall potential* in the literature [822, p.138], or superpotential.

Definition B.2 (*Tangent Cone*) Let Φ be convex, closed nonempty subset of $\mathbb{R}^n$. The tangent cone to Φ at a point $q \in \Phi$ is defined as:

$$\begin{aligned} T_\Phi(q) &= \text{cl}\{d \in \mathbb{R}^n | d = \lambda(y-q),\, y \in \Phi,\, \lambda \geq 0\} && (a) \\ &= \{y \in \mathbb{R}^n | \exists \{q_n\} \subset \Phi, \{\lambda_n\} \subset \mathbb{R}_+, \lambda_n \searrow 0, q_n \to q, \tfrac{q_n - q}{\lambda_n} \to y\} && (b) \\ &= \{y \in \mathbb{R}^n | \text{ for } \mu_n \searrow 0 \text{ and } q_n \to q, \{q_n\} \subset \Phi,\ \exists\, y_n \to y \\ &\quad \text{with } q_n + \mu_n y_n \in \Phi\}. && (c) \end{aligned} \tag{B.3}$$

When $q \notin \Phi$, one normally defines $T_\Phi(q) = \emptyset$.

The tangent cone is a closed convex cone. The cl denotes the closure: tangent cones are closed. The elements of the tangent cone, are the tangent vectors to Φ at q. Let us give a simple example. Let $\Phi = [a, b]$, $a < b$. Then $T_\Phi(a) = \mathbb{R}^+$, $T_\Phi(b) = \mathbb{R}^-$, and $T_\Phi(x) = \mathbb{R}$ if $a < x < b$. As pointed out in Sect. 3.1.2.1, the following may also be useful in the virtual displacements method:

Definition B.3 (*Contingent Cone*) The *contingent* or *Bouligand* cone to a subset $\Phi \subset \mathbb{R}^n$ (not necessarily convex) at q is defined as the closed cone:

$$K_\Phi(q) = \{y \in \mathbb{R}^n | \text{ for } \mu_n \searrow 0\ \exists\ y_n \to y \text{ with } q + \mu_n y_n \in \Phi\}. \tag{B.4}$$

One has $K_\Phi(q) = \emptyset$ if $q \notin \Phi$, and $T_\Phi(q) \subseteq K_\Phi(q)$.

Other formulations of the definitions of the tangent and contingent cones exist, using the notion of distance from a point to a set, and which may be more tractable when one wants to draw simple figures, see [293] for details. When $T_\Phi(q) = K_\Phi(q)$ for all $q \in \Phi$, the set Φ is called *tangentially regular*. This is the case of convex sets. If Φ is nonconvex, one usually has $T_\Phi \subset K_\Phi$. For instance sets with re-entrant corner points are not tangentially regular, see Fig. B.1. Virtual displacements for unilaterally constrained mechanical systems have generally to be taken in K_Φ [449].

Another important class of nonconvex sets which have no re-entrant corners, and are tangentially regular, are prox-regular sets, see Sect. B.2.3.

Definition B.4 (*Polarity and Duality*) Let Φ be a convex, closed nonempty cone of $\mathbb{R}^n$. Its polar cone is defined by $\Phi^\circ = \{s \in \mathbb{R}^n | s^T y \leq 0 \ \ \forall \ \ y \in \Phi\}$, and $(\Phi^\circ)^\circ = \Phi$. Its dual cone is $\Phi^\star = -\Phi^\circ$.

Polarity and duality extend to convex closed sets containing the origin. The polar of a closed convex set containing 0, is another closed convex set containing 0. The polar of the polar is the set itself. One has $\Phi_1 \subset \Phi_2 \Leftrightarrow \Phi_2^\star \subset \Phi_1^\star \Leftrightarrow \Phi_2^\circ \subset \Phi_1^\circ$.

Definition B.5 (*Normal Cone*) Let Φ be a convex, closed and nonempty set of $\mathbb{R}^n$. The normal cone to Φ at q is defined as the polar cone to the tangent cone, i.e.:

$$N_\Phi(q) = \left\{y \in \mathbb{R}^n |\ y^T z \leq 0 \text{ for all } z \in T_\Phi(q)\right\}. \tag{B.5}$$

Equivalently:

$$N_\Phi(q) = \left\{y \in \mathbb{R}^n | y^T (s - q) \leq 0, \ \forall\, s \in \Phi\right\}. \tag{B.6}$$

The normal cone is closed convex.

Let $\Phi = [a, b]$, $a < b$. Then $N_\Phi(a) = \mathbb{R}^-$, $N_\Phi(b) = \mathbb{R}^+$, and $N_\Phi(x) = \{0\}$ if $a < x < b$. The tangent cone in definition B.2 can be equivalently defined as the polar cone to the normal cone defined as in (B.6), as long as the set Φ is nonempty closed convex. One has $N_{\Phi_1}(q) \subset N_{\Phi_2}(q) \Leftrightarrow T_{\Phi_2}(q) \subset T_{\Phi_1}(q)$ as a consequence of polarity. For finitely represented sets as $\Phi = \{z \in \mathbb{R}^n | f(z) \geq 0\}$ for some continuously differentiable function $f : \mathbb{R}^n \mapsto \mathbb{R}^m$, the notion of *linearization cones* of $N_\Phi(q)$ and $T_\Phi(q)$ are defined as follows:

Definition B.6 (*Tangent and Normal Cones Linearization*) Let $\Phi = \{z \in \mathbb{R}^n | f(z) \geq 0\}$ be a finitely represented set of $\mathbb{R}^n$ for some continuously differentiable function $f : \mathbb{R}^n \mapsto \mathbb{R}^m$, Φ not necessarily convex. Let $\mathscr{J}(z) = \{i \in \{1, 2, \ldots, m\} | f_i(z) = 0\}$ be the set of active constraints indices. The tangent cone linearization cone at $z \in \Phi$ is:

$$T_\Phi^h(z) = \{y \in \mathbb{R}^n | \nabla f_i(z)^T y \geq 0, \text{ for all } i \in \mathscr{J}(z)\}. \tag{B.7}$$

The normal cone linearization cone at $z \in \Phi$ is:

$$N_\Phi^h(z) = (T_\Phi^h(z))^\circ = \{y \in \mathbb{R}^n | y = -\sum_{i \in \mathscr{J}(z)} \lambda_i \nabla f_i(z), \ i \in \mathscr{J}(z), \lambda_i \geq 0\}. \tag{B.8}$$

Both are convex polyhedral cones. One always has $T_\Phi(z) \subseteq T_\Phi^h(z)$, *i.e.,* the linearization tangent cone is a "bigger" cone. On the contrary by polarity $N_\Phi^h(z) \subseteq N_\Phi(q)$: the linearization normal cone is a "smaller" cone.

Then tangent and normal cones are equal to their respective linearization cones, if some *constraint qualifications* are satisfied. One of these is the so-called Mangasarian-Fromovitz CQ (the MFCQ). The MFCQ holds at a point z if:

$$(MFCQ) \quad \text{There exists a vector } v \in \mathbb{R}^n \text{ such that } \nabla f_i(z)^T v > 0 \text{ for all } i \in \mathscr{J}(z) \tag{B.9}$$

Thus, one observes the gradients at z for constraints such that $f_i(z) = 0$. If the gradients are lineary independent at z, then the MFCQ is satisfied. If the set Φ is represented by both equality (bilateral) and inequality (unilateral) constraints, the MFCQ requires in addition that the equality constraints gradients be linearly independent. Relaxation of the MFCQ exist [686], however, the MFCQ has the advantage of being verifiable while some other constraint qualification conditions may not.

Remark B.1 (*Nonconvex sets*) In fact the tangent cone definitions in (B.3) (b) and (c), which is the set of all tangent vectors to Φ at q, do not require that Φ be convex, but are applicable to any set Φ [686]. It still holds that it is closed convex even if Φ is not convex and, if not empty, it contains $\{0\}$. The normal cone may also be defined for a nonconvex set as in (B.5), it is still closed convex and, if not empty, it contains $\{0\}$. The same holds for the linearization cones in Definition B.6. However, there is equivalence between (B.5) and (B.6) only if Φ is convex. The tangent and normal cones in Definitions 5.1 and 5.2, are linearization cones.

The following definition states that the subdifferential of indicator functions of convex sets, is in fact the normal cone.

Definition B.7 Let Φ be closed and convex. The subdifferential of $\psi_\Phi(\cdot)$, denoted as $\partial\psi_\Phi(\cdot)$, is defined as:

$$\partial\psi_\Phi(q) = \begin{cases} \{0\} & \text{if } q \in \text{Int}\,(\Phi) \\ \\ N_\Phi(q) & \text{if } q \in (\Phi). \end{cases} \tag{B.10}$$

One may also directly define $N_\Phi(q) = \{0\}$ if $q \in \text{Int}(\Phi)$. In case of a smooth codimension one constraint, the normal cone reduces to the classical normal direction to the considered surface $\text{bd}(\Phi)$ at the considered point q. The tangent, contingent, and normal cones are illustrated on simple cases in Fig. B.1, together with Moreau's right-hand side, where the expression in (5.46) is illustrated.

The notion of a maximal monotone operator is important in the theory of differential inclusions.

Definition B.8 (*Maximal Monotone Mapping*) Let $A : \mathbb{R}^n \rightrightarrows \mathbb{R}^m$ be a multivalued operator, with domain $\text{Dom}(A) = \{x \in \mathbb{R}^n | A(x) \neq \emptyset\}$. Let $y_1 \in A(x_1)$, $y_2 \in A(x_2)$ for arbitrary x_1 and $x_2 \in \text{Dom}(A)$. Then $A(\cdot)$ is said *monotone* if:

$$\langle x_1 - x_2, y_1 - y_2 \rangle \geq 0. \tag{B.11}$$

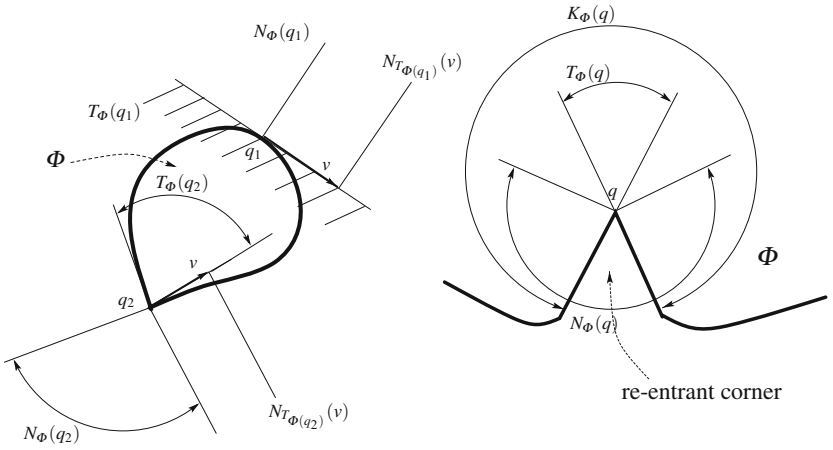

Fig. B.1 Tangent, contingent, normal cones, and Moreau's cone

It is said *maximal* (monotone) if there is no monotone operator that properly contains the graph of A. It is said ξ-monotone if $\langle x_1 - x_2, y_1 - y_2\rangle \geq c||x_1 - x_2||^\xi$ for some $c > 0$ and some $\xi > 1$, and strictly monotone if $\langle x_1 - x_2, y_1 - y_2\rangle > 0$ for all $x_1 \neq x_2$.

For instance, the sign multifunction $\text{sgn}(x) = \begin{cases} +1 & \text{if } x > 0 \\ -1 & \text{if } x < 0 \\ [-1, 1] & \text{if } x = 0 \end{cases}$, is monotone. Its graph cannot be extended without losing the monotonicity, so it is maximal monotone. The subdifferential of a convex function has an interesting property:

Lemma B.1 *Let $f : \text{dom}(f) \subseteq \mathbb{R}^n \to \mathbb{R}$ be a convex, proper, lower semicontinuous function. Then $\partial f : \text{Dom}(\partial f) \subseteq \mathbb{R}^n \rightrightarrows \mathbb{R}^n$ is a maximal monotone operator.*

In fact it is even true that if an operator A is maximal monotone, then it is a subgradient if and only if it is cyclically monotone: for all $y_i \in A(x_i)$, $\langle y_1, x_2 - x_1\rangle + \cdots + \langle y_{n-1}, x_n - x_{n-1}\rangle + \langle y_n, x_1 - x_n\rangle \geq 0$. One has $\text{sgn}(x) = \partial|x|$, and the absolute value function satisfies the requirements of the lemma. The same hold for the indicator function of a closed convex set and its subdifferential in Definitions B.1 and B.7. Usually the closedness of the function is required, however closedness is implied by proper lower semicontinuity. Let us remind that a nonlinearity $\phi(x)$ is said to belong to the sector $[a, b]$ if $\phi(0) = 0$ and $(\phi(x) - ax)^T(bx - \phi(x)) \geq 0$ for all $x \in \mathbb{R}^n$.

Corollary B.1 *Let $A : \mathbb{R}^n \rightrightarrows \mathbb{R}^m$ be a multivalued operator, with domain $\text{Dom}(A) = \{x \in \mathbb{R}^n | A(x) \neq \emptyset\}$. Assume that $0 \in A(0)$ (equivalently $(0, 0)$ belongs to the graph of $A(\cdot)$). Then $A(\cdot)$ lies in the sector $[0, +\infty]$.*

The proof follows from (B.11) with $x_2 = y_2 = 0$. It is noteworthy that the allowed sectors include infinite values, which correspond to vertical segments of the graph at the origin (hence including indicator functions or relay functions).

An important tool of convex analysis is the so-called Yosida approximation of maximal monotone mappings. For a multivaluyed mapping $A : \mathbb{R}^n \rightrightarrows \mathbb{R}^m$, the graph $\mathrm{Gr}(A) = \{(x, y) \in \mathbb{R}^n \times \mathbb{R}^m | y \in A(x)\}$. The inverse mapping is $A^{-1} : \mathbb{R}^m \rightrightarrows \mathbb{R}^n$ such that $y \in A(x) \Leftrightarrow x \in A^{-1}(y)$, or equivalently $(x, y) \in \mathrm{Gr}(A) \Leftrightarrow (y, x) \in \mathrm{Gr}(A^{-1})$.

Definition B.9 (*Yosida and Moreau–Yosida Approximations*) **(i)** Let $A : \mathbb{R}^n \rightrightarrows \mathbb{R}^m$ be a maximal monotone multivalued operator, with domain $\mathrm{Dom}(A)$, and $\lambda > 0$. The resolvent of A is the non-expansive and single-valued mapping $J_\lambda^A(\cdot) \triangleq (I + \lambda A)^{-1}(\cdot)$. The Yosida approximation of A is $A_\lambda(\cdot) \triangleq \frac{1}{\lambda}(I - J_\lambda^A)(\cdot) = (\lambda I + A^{-1})^{-1}(\cdot)$. It is Lipschitz continuous with constant $\frac{1}{\lambda}$ and it is maximal monotone. **(ii)** Let $f : \mathrm{dom}(f) \subseteq \mathbb{R}^n \to \mathbb{R}$ be a convex proper function. For each $\lambda > 0$, its Moreau–Yosida approximation is the function $f_\lambda(\cdot) = \inf_{z \in \mathbb{R}^n} \left\{ f(z) + \frac{1}{2\lambda} ||z - \cdot||^2 \right\}$.

As Example 1.6 shows, Yosida approximations correspond to some regularization of set-valued characteristics. Let $f : x \mapsto y = \psi_{\mathbb{R}^+}(x)$, and $A = \partial f : x \mapsto y \in \partial \psi_{\mathbb{R}^+}(x) = N_{\mathbb{R}^+}(x)$. Then $A^{-1} : y \mapsto x \in \partial \psi_{\mathbb{R}^-}(x)$, $A_\lambda(x) = (\lambda + \partial \psi_{\mathbb{R}^-})^{-1}(x) = 0$ if $x \geq 0$, $\frac{x}{\lambda}$ if $x < 0$, $f_\lambda(x) = 0$ if $x \geq 0$, $\frac{x^2}{2\lambda}$ if $x < 0$. This is depicted in Fig. B.2. Let $f(x) = |x|$, then $A(x) = \partial f(x) = 1$ if $x > 0$, -1 if $x < 0$ and $[-1, 1]$ if $x = 0$, $A_\lambda(x) = \frac{x}{\lambda}$ if $|x| \leq \lambda$, 1 if $x > \lambda$, -1 if $x < -\lambda$, and $f_\lambda(x) = \frac{x^2}{2\lambda}$ if $|x| \leq \lambda$, $|x| - \frac{\lambda}{2}$ if $|x| > \lambda$. This is depicted in Fig. B.4. If $f(x) = \psi_{[-1,1]}(x)$, then $f_\lambda(x) = 0$ if $|x| \leq \lambda$, $\frac{x^2}{2\lambda}$ if $|x| > \lambda$. It subdifferential denoted $B(\cdot)$ is depicted in Fig. B.4, and its Yosida approximation is denoted $B_\lambda(\cdot)$.

In relationship with some equivalences needed in the sweeping process formulation, let us introduce the following definitions and lemma:

Definition B.10 (*Proximal points* [878]) Given a linear space $E \ni x$ and a convex, lower semicontinuous, nonidentically infinite function $f(\cdot)$, the *proximal point* of z with respect to f, denoted as prox $_f(z)$, is the point where the function

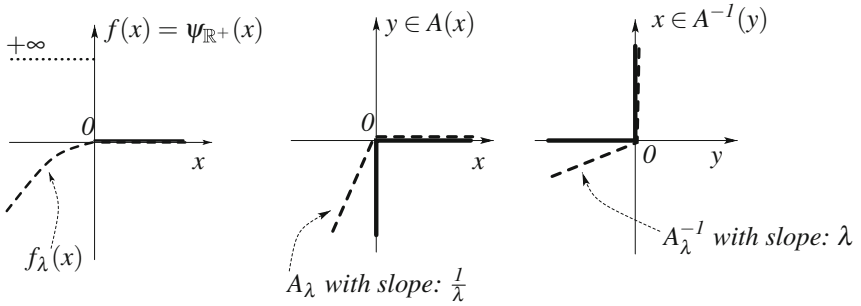

Fig. B.2 Yosida and Moreau–Yosida approximations (*dashed lines*: Yosida approximations)

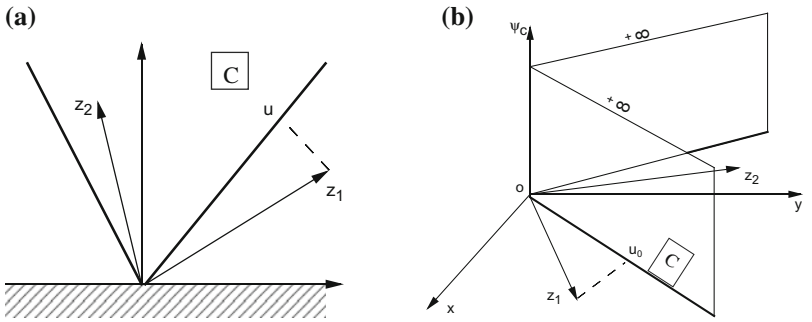

Fig. B.3 Proximal points and indicator function of a cone. **a** Proximal points. **b** The cone and its indicator function

$$u \mapsto \frac{1}{2}||z-u||^2 + f(u) \tag{B.12}$$

attains its minimum, i.e., $\text{prox}_f(z) = \text{argmin}(f(\cdot) + \frac{1}{2}||z-\cdot||^2)$.

If $f(\cdot)$ is the indicator function of a closed convex set $\mathscr{C}$, i.e., $f(\cdot) = \psi_{\mathscr{C}}(\cdot)$, then prox $_f z$ is the nearest point from z that belongs to $\mathscr{C}$, denoted as $\text{proj}(\mathscr{C}; z)$. Also, for a convex set Φ one has $-x \in \partial\psi_\Phi(u) \Leftrightarrow u = \text{proj}(\Phi; (u-\rho x)) \Leftrightarrow u = \text{prox}_{\psi_\Phi}(u-\rho x)$ for all $\rho > 0$.[5] As an illustration let us consider the case when $\mathscr{C}$ is a cone as in Fig. B.3a.

Let $z_1 \notin \mathscr{C}$ and $z_2 \in \mathscr{C}$. The calculations yield:

$$\begin{aligned} \min_u \tfrac{1}{2}||z_1-u||^2 + \psi_{\mathscr{C}}(u) &= \min_{u\in\mathscr{C}} \tfrac{1}{2}||z_1-u||^2 + \psi_{\mathscr{C}}(u) \\ &= \min_{u\in\mathscr{C}} \tfrac{1}{2}||z_1-u||^2 \\ \Longrightarrow u = \text{prox}_{\psi_{\mathscr{C}}} z_1 &= \text{proj}(\mathscr{C}; z_1) = u_0 \end{aligned} \tag{B.13}$$

Similarly:

$$\begin{aligned} \min_u \tfrac{1}{2}||z_2-u||^2 + \psi_{\mathscr{C}}(u) = \min_{u\in\mathscr{C}} \tfrac{1}{2}||z_2-u||^2 = 0 \\ \Longrightarrow z_2 = u_0 \end{aligned} \tag{B.14}$$

In Fig. B.3b the indicator function of the cone $\mathscr{C}$ is depicted. The following definition may be found in [191, 878, 898].

Definition B.11 (*Conjugate Function, Fenchel Transformation*) Let E be a linear space equipped with a scalar product $\langle\cdot,\cdot\rangle$. To any convex, lower semicontinuous function $f(x)$ not identically infinite (i.e., proper), one associates its *conjugate* function

$$f^\star(y) \stackrel{\Delta}{=} \sup_{x\in E} [\langle x, y\rangle - f(x)]$$

[5] Such formulation are used when one deals with complementarity formulations of normal and frictional directions, see Chap. 5, Sects. 5.3 and 5.4.

which is closed convex proper. The function $f^\star(\cdot)$ is thus the smallest function for which $f(x) + f^\star(y) \geq \langle x, y\rangle$. The mapping $f \mapsto f^\star$ is called the Fenchel transformation, or the Fenchel–Legendre transformation.

The inequality $f(x) + f^\star(y) \geq \langle x, y\rangle$ when $f(\cdot)$ and $f^\star(\cdot)$ are dual functions, is called the *Young's inequality* [60, p.64], or more classically in convex analysis the *Fenchel inequality*. Notice that it is sufficient that $f(\cdot)$ in Definition B.11 be nonidentically $+\infty$ to define its conjugate [191, p.9]. If $f(\cdot)$ is convex and lower semicontinuous, then Fenchel–Moreau Theorem (see below) applies. As an illustration of such dual functions, let us consider the following examples:

- If $f_1(x) = x^2$, one finds that $f_1^\star(y) = \frac{y^2}{4}$
- If $f_2(x) = ||x||$, then $f_2^\star(y) = \begin{cases} 0 & \text{if } ||y|| \leq 1 \\ +\infty & \text{if } ||y|| > 1 \end{cases}$. Note that this function $f_2^\star(\cdot)$ is the indicator function of the ball $||y|| \leq 1$, *i.e.*, $\psi_{||y||\leq 1}(\cdot)$.
- If $f_3(x) = \frac{x^\alpha}{\alpha}$, then $f_3^\star(y) = \frac{y^\beta}{\beta}$, with $\frac{1}{\alpha} + \frac{1}{\beta} = 1$, $\alpha > 1$, $\beta > 1$.
- Consider the function $f_4(x) = \begin{cases} -a & \text{if } x < 0 \\ b & \text{if } x > 0 \\ [-a, b] & \text{if } x = 0 \end{cases}$. Consider also the indicator function $\psi_{[-a,b]}(y)$ of the interval $[-a, b]$. Its conjugate function is the *support function* of the set $[-a, b]$ and is given by $\psi^\star_{[-a,b]}(x) = \sup_{y\in[-a,b]}\langle x, y\rangle = \begin{cases} -ax & \text{if } x < 0 \\ bx & \text{if } x \geq 0 \end{cases}$ [898, Example 6.c]. Then $f_4(x) = \partial\psi^\star_{[-a,b]}(x)$, the subdifferential (or Clarke's gradient) of $\psi^\star_{[-a,b]}(\cdot)$ at x. One recognizes the expression of a simplified Coulomb's friction law in the definition of the function $f_4(x)$. If x is the velocity then the tangential force F_t satisfies $F_\mathrm{t} \in \partial\psi^\star_{[-a,b]}(-x)$ which is equivalent to $-x \in \partial\psi_{[-a,b]}(F_t)$, with $a = b = |F_\mathrm{n}(t)|\mu$, and the normal reaction is supposed to be known.
- Let $f_5(x) = \psi_{(-\infty,a]}(x)$, then $f_5^\star(y) = \psi^\star_{(-\infty,a]}(y) = ay$ if $y \geq 0$, and $+\infty$ if $y < 0$. This case can be applied to Example 1.6 (see Remark 1.6) where $f_5(\cdot)$ plays the role of the potential function associated with the unilateral constraint contact force.
- Let $f_6(x) = |x_1| + |x_2| + \ldots + |x_n|$. Then:

$$\begin{cases} \partial f_6(x) = (\mathrm{sgn}(x_1)\ \mathrm{sgn}(x_2)\ \ldots\ \mathrm{sgn}(x_n))^T \\ f_6^\star(x) = \psi_{[-1,1]}(x_1) + \psi_{[-1,1]}(x_2) + \ldots + \psi_{[-1,1]}(x_n) \\ \partial f_6^\star(x) = (N_{[-1,1]}(x_1)\ N_{[-1,1]}(x_2)\ \ldots\ N_{[-1,1]}(x_n))^T \end{cases} \tag{B.15}$$

Subdifferentiation, conjugacy, inversion, support function, Moreau–Yosida and Yosida approximations, are illustrated in Fig. B.4. The absolute value function is taken as an example, and from the above one has $f(x) = |x| = \psi^\star_{[-1,1]}(x)$.

It is a general result [898] that if $f(\cdot)$ and $f^\star(\cdot)$ are 2 dual functions, then for any x and y in their respective domains, one has:

$$y \in \partial f(x) \Leftrightarrow x \in \partial f^\star(y) \Leftrightarrow f(x) + f^\star(y) = \langle x, y\rangle \tag{B.16}$$

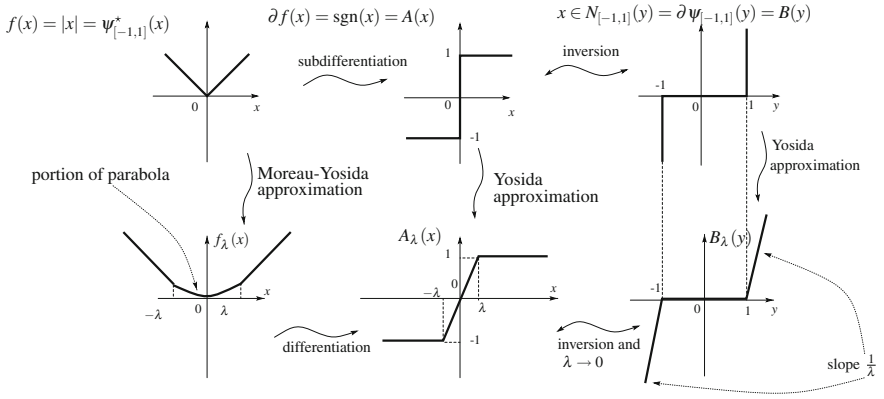

Fig. B.4 Subdifferentiation, conjugacy, inversion, Moreau–Yosida, and Yosida approximations

In other words, the subdifferential of $f(\cdot)$ at x is the set $\partial f = \{y | f(x) + f^{\star}(y) = \langle x, y\rangle\}$. These equivalencies may be used to express the same law of motion in various manners, either using a function or its conjugate. Getting back to the sweeping process formulation, one has $y \in \partial\psi_{V(q)}(x) = \{y | \psi_{V(q)}(x) + \psi^{\star}_{V(q)}(y) - \langle x, y\rangle\}$ that is equivalent to $x = \mathrm{proj}[V(q); x + y]$. If $p_k = M(q(t_k))[\dot{q}(t_k^+) - \dot{q}(t_k^-)]$, then $\dot{q}(t_k^+) = \mathrm{proj}_{M(q)}[V(q); \dot{q}(t_k^-)] = \mathrm{proj}_{M(q)}[V(q); -M(q)^{-1}p_k + \dot{q}(t_k^+)]$ so that $M(q)[-M(q)^{-1}p_k] = -p_k \in \partial\psi_{V(q)}(\dot{q}(t_k^+))$, and $\psi_{V(q)}(\dot{q}(t_k^+)) + \psi^{\star}_{V(q)}(-M(q)^{-1}p_k) = \dot{q}^T(t_k^+)M(q)[-M(q)^{-1}p_k]$. We dropped some arguments, but all quantities are calculated at $t = t_k$. This is why considering the kinetic metric as $M(q) = I_n$ does not influence much the formulation. Also, one deduces that if a function $f(x)$ possesses a minimum at x_0, then one has:

$$0 \in \partial f(x_0) \Leftrightarrow x_0 \in \partial f^{\star}(0) \Leftrightarrow f(x_0) + f^{\star}(0) = 0 \tag{B.17}$$

which means that $f^{\star}(\cdot)$ must be subdifferentiable at $y = 0$ for x_0 to be a minimum point of f, and *vice versa* [898, p.60]. The equivalences in (B.17) are a particular case of the so-called *conjugate subgradient theorem* of convex analysis. As an example consider $f(x) = x^2$ and $f^{\star}(y) = \frac{y^2}{4}$ as above. Then $y \in \partial f(x) = 2x$ and $x \in \partial f^{\star}(y) = \frac{y}{2}$, $f(x) + f^{\star}(y) = \frac{y^2}{2} = 2x^2 = \langle x, y\rangle$, where $\langle x, y\rangle = xy$. The proof that x_0 minimizes $f(\cdot)$ if and only if $0 \in \partial f(x_0)$ is simple using the definition of the subdifferential as a set of vectors γ satisfying: $\gamma \in \partial f(x_0)$ if by definition $f(x) \geq f(x_0) + \gamma^T(x - x_0)$, $\forall x \in \mathbb{R}^n$. Actually, such an x_0 must satisfy $f(x) \geq f(x_0)$, $\forall x \in \mathbb{R}^n$. Note that $0 \in \partial f(x_0) \Longleftrightarrow f(x) \geq f(x_0) + 0^T(x - x_0)$, which ends the proof.

• Let K be a closed convex cone, and $N_K(\cdot)$ its normal cone mapping. Then for all $x \in K$, $(N_K(x))^{\star} = -(N_K(x))^{\circ} = -T_K(x)$. On the other hand, let $f(x) = \psi_K(x)$, then $f^{\star}(y) = \psi^{\star}_K(y) = \psi_{K^{\circ}}(y)$, and thus $\partial f^{\star}(y) = \partial\psi^{\star}_K(y) = N_{K^{\circ}}(y)$. The function $f^{\star}(\cdot)$ is the support function of the set K.

• In Mechanics, the dual function is obtained through the so-called Legendre transformation [60, §14], which allows one to construct the Hamiltonian function from the Lagrangian, where the Lagrangian is seen as a function of $\dot{q}$, whereas the Hamiltonian is seen as a function of generalized momentum p. If $L(q,\dot{q}) = \frac{1}{2}\dot{q}^T M(q)\dot{q} - U(q)$ and $M(q) \succ 0$, then $H(p,q) = \frac{1}{2}p^T M^{-1} p + U(q)$. It is known that the Legendre transformation is involutive (*i.e.,* when applied twice, it is the identity) [60, §14,C]. Extensions when $M(q) \succeq 0$ may be found in [216]. In fact, the following is true.

Theorem B.1 (Fenchel–Moreau [191]) *Assume that $f(\cdot)$ is convex, lower semicontinuous, and $f \not\equiv +\infty$. Then $f^{\star\star} = f$, i.e., the dual function of the dual function of f, is f itself.*

Hence from the example above, one deduces that $||x|| = \sup_{y\in E^\star, ||y||\leq 1} |\langle y, x\rangle|$, which is in fact the definition of the norm of $x \in E$ [191]. In classical mechanics, one obtains that the Legendre transformation of the Hamiltonian is the Lagrangian. It is clear in this context why the function $f^\star(y)$ is called the dual function of $f(x)$, since the Hamiltonian formulation of dynamics involves generalized momenta p, which belong to the dual space $T_q^\star Q$ of the tangent space $T_q Q \ni \dot{q}$ of the system's configuration space Q at the point q. $T_q^\star Q$ is also called the cotangent space to Q at q [60, p.202].

Recall that given a cone $V(q)$, it *polar* cone $N(q)$ is defined as $N(q) = \{u | \forall v \in V(q), \langle v, u\rangle \leq 0\}$, where it is understood that u belongs to the space dual of that of v [891]. The normal cone in Definition B.5 is the polar cone of the tangent cone in Definition B.2. Polarity may be seen as a generalization of orthogonality. One has $\psi^\star_{V(q)}(\cdot) = \psi_{N(q)}(\cdot)$, i.e., the indicator function of the tangent cone is the dual of the indicator of the normal cone, because they are polar one to each other. The following lemma is a fundamental result of convex analysis, and it is useful to write down the different formulations of the sweeping process:

Lemma B.2 (Moreau's Lemma of the Two Cones [876]) *If V and N denote a pair of mutually polar closed convex cones of a Euclidean linear space E, and if x, y, z are three points of E, the following assertions are equivalent:*

- $x = \text{proj}\,(V; z)$, $y = \text{proj}\,(N; z)$
- $z = x + y$, $x \in V$, $y \in N$, $x^T y = 0$

One notices that x and y satisfy a cone complementarity relation, and may be identified with $u(t_k^+)$ and $-R'_\mu(t_k)$ in (5.57), whereas z plays the role of $u(t_k^-)$. It also follows as a corollary that:

$$x = \text{proj}\,(V; z) \Leftrightarrow z - x = \text{proj}\,(N; z) \tag{B.18}$$

Lower semicontinuous functions are used in several places of this book.

Definition B.12 A function $f : E \to (-\infty, +\infty]$ is *lower semicontinuous* (lsc) if the set $\text{epi}(f) \stackrel{\Delta}{=} \{(x,\alpha) \in E \times \mathbb{R} | f(x) \leq \alpha\}$ is closed. In other words, f is lsc at

x_0 if for all $b \in \bar{\mathbb{R}}$ such that $b < f(x_0)$, there exists a neighborhood V of x_0 such that for all $x \in V$, $b < f(x)$. $f(\cdot)$ is lsc on E if it is lsc for all $x_0 \in E$.

For instance, the characteristic function χ_I of an open interval $I = (a, b)$ is lsc. Indeed since I is open, for any $x \in I$ there exists a ball $B(x, r)$ centered at x, of radius $r > 0$, such that for all $y \in B(x, r)$, then$y \in I$ (i.e., $B(x, r) \subset I$). Hence take $b < 1$: clearly for any $x \in I$, it suffices to take $V = B(x, r)$ as a neighborhood of x. And if $x \notin I$, and $b < 0 = \chi_I$, it suffices to take $V = \mathbb{R}$. Also, the indicator function of a closed convex nonempty domain is lsc [191].

B.2 Further Useful Results

B.2.1 From Convex Analysis

Let us state the following equivalences. Let $\Phi \subseteq \mathbb{R}^n$ be a closed, convex cone.

$$\Phi \ni x \perp y \in \Phi^\star \;\Leftrightarrow\; x \in -N_{\Phi^\star}(y) \;\Leftrightarrow\; y \in -N_\Phi(x), \tag{B.19}$$

where $\Phi^\star$ is the dual cone. In many practical cases $\Phi = \Phi^\star = \mathbb{R}^n_+$. Let now $y = Mx + q$, for some matrix $M = M^T \succ 0$ and a vector q, both with appropriate dimensions. Let also Φ be a convex, closed nonempty set (not necessarily a cone).

$$\begin{aligned} & Mx + q \in -N_\Phi(x) \;\Leftrightarrow\; x = \text{proj}_M[\Phi; -M^{-1}q] \\ & \Leftrightarrow\; x = \text{argmin}_{z \in \Phi} \tfrac{1}{2}(z + M^{-1}q)^T M(z + M^{-1}q) \\ & \Leftrightarrow \langle Mx + q, v - x\rangle + \psi_\Phi(v) - \psi_\Phi(x) \geq 0 \;\text{ for all }\; v \in \mathbb{R}^n, \end{aligned} \tag{B.20}$$

where $\text{proj}_M[\Phi; z]$ is the orthogonal projection of z on Φ. Such a projection is unique since Φ is convex. The last line of (B.20) is a variational inequality, which comes from the definition of a subgradient. From the definition of the indicator function, it is equivalent to: find $x \in \Phi$ such that $\langle Mx + q, v - x\rangle \geq 0$ for all $v \in \Phi$. When $\Phi = \mathbb{R}^m_+ = \{z \in \mathbb{R}^m | z_i \geq 0 \text{ for all } 1 \leq i \leq m\} = \Phi^\star$, then:

$$\begin{aligned} & \min_{x \geq 0} \tfrac{1}{2}x^T Mx + q^T x \quad \overset{M = M^T \succeq 0}{\Leftrightarrow} \quad 0 \leq Mx + q \perp x \geq 0 \\ & Mx + q \in -N_{\mathbb{R}^m_+}(x) \quad \overset{M = M^T \succ 0}{\Leftrightarrow} \quad x = \text{proj}_M[\mathbb{R}^m_+; -M^{-1}q] \\ & \Leftrightarrow \quad x = \text{argmin}_{z \geq 0} \tfrac{1}{2}(z + M^{-1}q)^T M(z + M^{-1}q). \end{aligned} \tag{B.21}$$

Some positive definiteness and symmetry is imposed on M in these equivalences, that is, the quadratic functions are convex. In fact one has also the following that re-

laxes convexity of the objective function. Consider the quadratic programme (Notice that the quadratic function in (B.22) is not equal to the one in the first equivalence in (B.21)):

$$\begin{aligned} &\min x^T Mx + x^T q \\ &\text{subject to: } x \geq 0 \text{ and } Mx + q \geq 0. \end{aligned} \tag{B.22}$$

Then for every q such that the programme (B.22) is feasible, every stationary point of (B.22) solves the LCP $0 \leq Mx + q \perp x \geq 0$. Equivalently, M is a row-sufficient matrix, i.e., $[x_i(M^T x)_i \leq 0 \text{ for all } i] \Rightarrow [x_i(M^T x)_i = 0 \text{ for all } i]$. A row-sufficient matrix may not be positive semi-definite (e.g., $M = \begin{pmatrix} 0 & 0 \\ 1 & 1 \end{pmatrix}$). Since a positive semi-definite matrix is row sufficient, this applies if $M \succeq 0$. If $M \succ 0$ then the LCP has always a unique solution (see Theorem 5.4) so the programme (B.22) and the LCP(q, M) are equivalent.

To finish with equivalences, let us state the following: let $M = M^T$ be positive semi-definite and $\phi : \mathbb{R}^n \to \mathbb{R} \cup \{+\infty\}$ be a proper, convex, lower semicontinuous function with closed domain. Then:

$$\begin{aligned} \min_{x \in \mathbb{R}^n} \tfrac{1}{2} x^T Mx + q^T x + \phi(x) \Leftrightarrow \quad & Mx + q \in -\partial\phi(x) \\ \Leftrightarrow \quad & \langle Mx + q, v - x \rangle + \phi(v) - \phi(x) \geq 0 \text{ for all } v \in \mathbb{R}^n \end{aligned} \tag{B.23}$$

in the sense that if $x^\star$ solves one of these problems, it solves the other ones.

The next result is an extension of the chain rule, for convex functions.

Theorem B.2 *Let $f(x) = h(Ax)$, where $h(\cdot)$ is a proper convex function on $\mathbb{R}^m$ and A is a linear transformation from $\mathbb{R}^n$ to $\mathbb{R}^m$. If the image of A contains a point in the relative interior of dom(h), of if $h(\cdot)$ is polyhedral and the image of A contains a point of dom(h), then $\partial f(x) = A^T \partial f(Ax)$ for all x.*

Recall that $\text{dom}(h) = \{x \in \mathbb{R}^m | h(x) < +\infty\}$, and that a function is polyhedral if its epigraph is polyhedral. We usually work with polyhedral functions (like indicator functions of polyhedral sets), or with functions with domain equal to the whole of $\mathbb{R}^m$. Thus the first assertion of the theorem is not really useful to us, in general. Let us just mention that the relative interior of a convex set, is its interior for the topology relative to its affine hull. For instance, consider a two-dimensional disk with radius $R > 0$, lying in $\mathbb{R}^3$: its interior in $\mathbb{R}^3$ is clearly empty. However if we consider that the disk belongs to a plane of $\mathbb{R}^3$, and view it as a domain of this plane, its interior is the usual interior of a disk with area (Lebesgue measure) equal to πR^2: this is its relative interior. Extension of Theorem B.2 to the nonconvex case exists.

Theorem B.3 *Let $g(q) = \psi_{\mathbb{R}^m_+} \circ f(q)$ for a mapping $f : \mathbb{R}^n \mapsto \mathbb{R}^m$ that is continuously differentiable at a point q such that $f(q) \geq 0$. Then $\partial g(q) = \nabla f(q)^T \partial \psi_{\mathbb{R}^m_+}(f(q))$.*

The proof follows from [1046, Theorem 10.6], noting that the conditions stated therein hold since $\psi_{\mathbb{R}^m_+}(\cdot)$ is convex and the range of the mapping $q \to f(q) +$

$\nabla f(q)w$ cannot be separated from $\mathbb{R}^m_+$ for $f(q) \geq 0$. Moreover, $\psi_{\mathbb{R}^m_+}(\cdot)$ being convex Clarke regularity [1046, Definition 6.3] holds.

Corollary B.2 *The right-hand side of frictionless unilaterally constrained Lagrange equations as in (5.1), i.e., $\nabla f(q)^T \lambda_{n,u}$, and with continuously differentiable constraint functions $f_i(q)$, can be equivalently rewritten as $-N_\Phi(q)$.*

Notice that since $g(q) = \psi_\Phi(q)$ with $\Phi = \{q \in \mathbb{R}^n | f(q) \geq 0\}$, then $\partial g(q) = N_\Phi(q)$. Now one has $0 \leq \lambda_{n,u} \perp f(q) \geq 0 \Leftrightarrow \lambda_{n,u} \in -\partial\psi_{\mathbb{R}^m_+}(f(q))$, which proves the result. Let us consider now (5.42), where the normal cone is the linearization normal cone $N^h(q)$. Since $N^h(q) \subseteq N_\Phi(q)$ it follows that the differential inclusion in (5.42) has a smaller set-valued right-hand side than (5.1) (when considering only perfect unilateral constraints). If some constraint qualification is imposed (like the MFCQ) then both right-hand sides are identical.

Let us state a result used for instance to show the energetic consistency of some impact laws [455], or Fourier's inequality with unilateral constraints.

Proposition B.1 *Let K be a closed, nonempty, and convex set, with $0 \in K$. If $x \in -N_K(\lambda)$, then $x^T\lambda \leq 0$.*

Proof By the monotonicity of the mapping $\lambda \rightarrow N_K(\lambda)$, one has for all λ_1, λ_2, $y_1 \in N_K(\lambda_1)$, $y_2 \in N_K(\lambda_2)$: $\langle \lambda_1 - \lambda_2, y_1 - y_2 \rangle \geq 0$. Since $0 \in K$ we may take $\lambda_1 = 0$, and also $y_1 = 0$. Then $\langle \lambda_2, y_2 \rangle \geq 0$. Take $x_2 = -\lambda_2$ to infer that for all λ_2 and x_2 with $x_2 \in -N_K(\lambda_2)$, one has $x_2^T\lambda_2 \leq 0$.

The next theorem states the well-posedness of a class of differential inclusions:

$$\begin{cases} \dot{x}(t) \in -A(x(t)) + f(t, x(t)), & \text{a.e. on } (0, T) \\ x(0) = x_0. \end{cases} \tag{B.24}$$

The following assumption is made:

Assumption 7 The following items hold:

- **(i)** $A(\cdot)$ is a multivalued maximal monotone operator from $\mathbb{R}^n$ into $\mathbb{R}^n$, with domain $\mathrm{dom}(A)$.
- **(ii)** There exists $L \geq 0$ such that for all $t \in [0, T]$, for all $x_1, x_2 \in \mathbb{R}^n$, one has $||f(t, x_1) - f(t, x_2)|| \leq L||x_1 - x_2||$.
- **(iii)** There exists a function $\varphi(\cdot)$ such that for all $R \geq 0$:

$$\varphi(R) = \sup \left\{ \| \frac{\partial f}{\partial t}(\cdot, v) \|_{L^2((0,T);\mathbb{R}^n)} \mid \| v \|_{L^2((0,T);\mathbb{R}^n)} \leq R \right\} < +\infty$$

.

The following is proved in [104].

Theorem B.4 *Let Assumption 7 hold, and let $x_0 \in \mathrm{dom}(A)$. Then the differential inclusion (B.24) has a unique solution $x : (0, T) \rightarrow \mathbb{R}^n$ that is Lipschitz continuous.*

This does not straighforwardly extend when the set-valued right-hand side depends explicitly on time: $A(t,x)$, even if it is maximal monotone for each t. Corollary 9.2 and Theorem 10.5 in [332] may be used. Sufficient conditions for existence of absolutely continuous solutions in of $\dot{x}(t) \in -A(t,x(t))$ on an interval I, $x(0) \in \text{dom}(A)$, are:

- (i) $A(\cdot,x)$ has a strongly measurable selection, $A(t,\cdot)$ is upper semicontinuous.
- One of the following holds:
  - (ii-1) For all $y_1 \in A(t,x_1)$ and all $y_2 \in A(t,x_2)$: $\langle y_1 - y_2, x_1 - x_2\rangle \geq -k(t)||x_1 - x_2||^2$, $k \in L^1(I)$.
  - (ii-2) $A(t,x)$ has closed convex values.
- (iii) $||f(t,x)|| \leq c(t)(1+||x||)$ for all $f(t,x) \in A(t,x)$, $t \in I$.

In addition (ii-1) guarantees the uniqueness of solutions. We recalls that a selection is any function $f(t,x) \in -A(t,x)$ for all $t \in I$ and x. A set-valued mapping $F(\cdot)$ is upper semicontinuous if $F^{-1}(S) = \{x \in \text{dom}(F) | F(x) \in S\}$ is closed for any closed set S. If $F(\cdot)$ is single-valued, then this definition of upper semicontinuity implies the usual continuity. The set-valued map $x \mapsto \alpha(t)\text{sgn}(x)$ for a non negative bounded function $\alpha(t)$, satisfies all the above properties (if $\alpha(t)$ is unsigned, then (ii-1) does not hold and only existence without uniqueness can be assured, think of $\dot{x}(t) \in \text{sgn}(x(t))$). Moreover, if $\alpha(t) \geq \delta > 0$ for some δ and all t, then the differential inclusion $\dot{x}(t) \in -\alpha(t)\text{sgn}(x(t))$ has a global, finite-time Lyapunov stable fixed point $x^* = 0$. Indeed let $V(x) = \frac{1}{2}x^2$, then along trajectories of the DI we have $\dot{V}(x(t)) = -\alpha(t)x(t)\text{sgn}(x(t)) = -\alpha(t)|x(t)| \leq -\delta|x(t)| = -\delta\sqrt{\frac{V(x(t))}{2}}$. It follows that $|x(t)| \leq -2\delta t + |x(0)|$. Thus there exists $t^* < \frac{|x(0)|}{2\delta}$ such that $x(t^*) = 0$. After t^* the state stays at the origin which is an attractive point.

B.2.2 Moreau's Set Inclusion

The inclusion $N_{V(q)}(w) \subseteq N_\Phi(q)$ is proved in [894, Proposition 5.1] for finitely represented sets Φ as in Sect. 5.2.2. It uses the definition of the (linearized) tangent cone in (5.35) to a finitely represented set, which is a convex polyhedral set (however this time Φ itself needs not be convex). Let us assume that Φ is finitely represented by inequalities $f(q) \geq 0$, and that the MFCQ holds. One has $V(q) = \{v \in \mathbb{R}^n | v^T \nabla f_i(q) \geq 0, i \in \mathscr{J}(q)\}$ (see Definition 5.34), so denoting $g_i(v) \stackrel{\Delta}{=} v^T \nabla f_i(q)$ we obtain $V(q) = \{v \in \mathbb{R}^n | g_i(v) \geq 0, i \in \mathscr{J}(q)\}$. Therefore, for all $v \in \text{bd}(V(q))$ one has (using (B.8) and replacing Φ by $V(q)$ that is a velocity set): $\partial\psi_{V(q)}(v) = N_{V(q)}(v) = \{w \in \mathbb{R}^n | w = -\sum_{i\in\mathscr{K}(v)} \lambda_i \nabla g_i(v), \lambda_i \geq 0\}$, where $\mathscr{K}(v) = \{i \in \mathscr{J}(q) | g_i(v) = v^T \nabla f_i(q) = 0\}$ is the set of active constraints at the velocity level (thus both $\mathscr{K}(v)$ and $\mathscr{J}(q)$ are indices sets, and $\mathscr{K}(v) \subseteq \mathscr{J}(q)$, the equality being true if and only if all velocities at the active contact points, are tangent to the admissible domain Φ). Noting that $\nabla g_i(v) = \nabla f_i(q)$ and using (B.8)

the inclusion is proved. Thus, for $q \in \text{bd}(\Phi)$ and $w \in \text{bd}(V(q))$, the equality $N_{V(q)}(w) = N_\Phi(q)$ holds if and only if $\nabla f_i(q)^T v = 0$ for all $i \in \mathscr{J}(q)$ (i.e., $\mathscr{K}(v) = \mathscr{J}(q)$). Notice that if $q \in \text{Int}(\Phi)$ then both cones are equal to $\{0\}$.

The inclusions in (3.20) could be proved in a similar way, introducing the set of indices $\mathscr{L}(w) = \{k \in \mathscr{K}(v) | h_k(w) = \nabla f_k(q)^T w + \frac{d}{dt}(\nabla f_k(q)^T)v = 0\} \subseteq \mathscr{K}(v) \subseteq \mathscr{J}(q)$. First notice that $T_{V(q)}(v) = \{w \in \mathbb{R}^n | h_k(w) \geq 0, k \in \mathscr{K}(v)\}$. Then $N_{T_{V(q)}(v)}(w) = \{z \in \mathbb{R}^n | z = -\sum_{k \in \mathscr{L}(w)} \nabla h_k(w)\lambda_k, \lambda_k \geq 0\}$. Noting that $\nabla h_k(w) = \nabla g_k(v) = \nabla f_k(q)$ the result follows.

Such type of inclusions have also been shown in the broader context of distribution differential inclusions in [15], see in particular [15, Lemma3] and (3.18) in Chap. 3.

Remark B.2 As alluded to in Remark 3.1, the normal cones inclusions could be used in an event-driven scheme to detect detachment from $\text{bd}(\Phi)$ when the first derivatives vanish. It is clear from the above developments that this implies the construction of various index sets (in theory, the process should be continued as long as the derivatives of the gap function are zero).

B.2.3 Prox-Regular Sets

Tangent and normal cones in (B.3) and (B.5) are defined for general sets (convex or non convex, see Remark B.1). For the particular case of finitely represented sets, one may also define the linearization tangent and normal cones in (B.7) and (B.8). Under the MFCQ the linearization cones and the normal and tangent cones, are equal. Let us now briefly introduce the so-called $r-$prox-regular sets. Roughly speaking, a set Φ is convex if and only if any point y has a unique projection on it: a set Φ is $r-$prox-regular if the same holds, for all points y close enough to Φ, where the closeness is measured by r. To start with let us define Fréchet normals. For a closed set $\Phi \subset \mathbb{R}^n$, and $x \in \Phi$, the vector $w \in \mathbb{R}^n$ is called a Fréchet normal to Φ at x if, for every $\varepsilon > 0$, there exists $\delta > 0$ such that $\langle w, x' - x\rangle \leq \varepsilon ||x' - x||$ for all $x' \in \Phi$, $||x' - x|| < \delta$. The set of all Fréchet normals at $x \in \Phi$ make a cone which we denote as usual $N_\Phi(x)$.

Definition B.13 (*r-prox-regular set* [1009]) The closed set Φ is $r-$prox-regular if and only if for any $x_i \in \Phi$ $(i = 1, 2)$, the inequality

$$\langle v_1 - v_2, x_1 - x_2\rangle \geq -||x_1 - x_2||^2 \tag{B.25}$$

holds whenever $v_i \in N_\Phi(x_i)$ with $||v_i|| < r$. Equivalently, for each $w \in N_\Phi(x)$:

$$\langle \frac{w}{||w||}, x - x'\rangle \geq -\frac{1}{2r}||x - x'||^2, \text{ for all } x' \in \Phi. \tag{B.26}$$

Any closed convex set Φ is $r-$prox-regular with $r = +\infty$, and w in (B.26) becomes a subgradient of the indicator function ψ_Φ at x in the sense of convex analysis. The set represented by the dashed area in Fig. 4.3b (ii) is r-prox-regular, see also Fig. B.5. Let $P_\Phi(x)$ denote the set of all nearest points of Φ to x. If x belongs to the open r-tube around Φ, given by $\{z \in \mathbb{R}^n | 0 < d_\Phi(z) < r\}$ where $d_\Phi(z) = \inf\{||z - y||, y \in \Phi\}$ is the distance from x to Φ, then $P_\Phi(x)$ is unique (and is the projection of x on Φ) [131, Theorem 6.2]. The normal cone $N_\Phi(x)$ can also be, under some constraint qualifications, written in its linearization form (B.8), see [1046, Theorem 6.14]. In particular, this holds since a prox-regular set is also Clarke regular [1046, Definition 6.3].

Remark B.3 The tangent cone to an $r-$prox-regular set can be defined as in (B.3). From [1046, Corollary 6.29] the normal and tangent cones are mutually polar.[6] There are many different notions of a normal cone to a set. For prox-regular sets they all coincide (Clarke, Mordukovich, Fréchet cones are the same [226, §A.1]). Since one can always define the tangent cone as the polar cone to the normal cone, one infers that there is also a unique definition of tangent cones to prox-regular sets. In particular the contingent and the tangent cones in (B.3) and (B.2) respectively, are equal: prox-regular sets are tangentially regular and have no re-entrant corners.

The relationships between finitely represented sets, and prox-regular sets are not so well-known. A result in this direction is given in [133, Theorem 4.1].

Theorem B.5 *[133] Let $C_i = \{q \in \mathbb{R}^n | f_i(x) \geq 0\}$ and $C = \cap_{1 \leq m} C_i$. Assume that for all $x \in C_i + \kappa\mathbb{B}$ one has $\alpha \leq ||\nabla f_i(x)|| \leq \beta$ and $||D^2 f_i(x)|| \leq M$, for some positive constants α, β, M and κ. Let $I_\rho(x) = \{i \in [1, m] | f_i(x) \leq \rho\}$, for some positive constant ρ. Assume there exists $\gamma > 0$ and nonnegative reals λ_i such that $\sum_{i \in I_\rho(x)} \lambda_i ||\nabla f_i(x)|| \leq \gamma || \sum_{i \in I_\rho(x)} \lambda_i \nabla f_i(x)||$. Then there exists $\eta(\alpha, M, \gamma)$ such that the set C is $\eta-$prox-regular.*

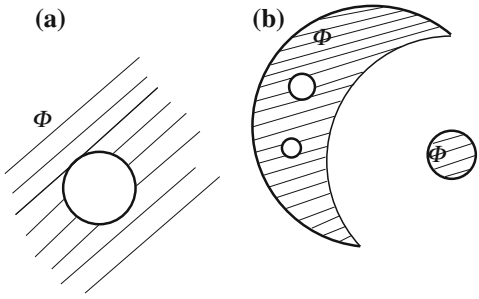

Fig. B.5 Two prox-regular sets Φ (*dashed areas*)

[6] Here the normal cone is to be understood as the proximal normal cone.

References

1. Abadie, M.: Dynamic simulation of rigid bodies: modelling of frictional contacts. In: Brogliato, B. (ed.) Impacts in Mechanical Systems. Analysis and Modelling, Lecture Notes in Physics, vol. 551, pp. 61–144. Springer, New York (2000)
2. Abiko, S., Lampariello, R., Hirzinger, G.: Impedance control for a free-floating robot in the grasping of a tumbling target with parameter uncertainty. In: Proceedings of IEEE/RSJ International Conference on Intelligent Robots and Systems, pp. 1020–1025. Beijing, China (2006)
3. Abraham, R., Mardsen, J.E.: Foundations of Mechanics. 2nd edn. Addison-Wesley (1978)
4. Acaccia, G.M., Cagetti, P.C., Callegari, M., Michelini, R.C., Molfino, R.M.: Modeling the impact dynamics of robotic manipulators. In: IFAC Symposium on Robot Control, pp. 559–564. Capri, Italy (1994)
5. Acary, V.: Contribution to the numerical and mechanical modelling of masonry buildings. Ph.D. thesis, University of Aix-Marseille, Marseille, France (2001). https://tel.archives-ouvertes.fr/tel-00163767
6. Acary, V.: Higher order event capturing time-stepping schemes for nonsmooth multibody systems with unilateral constraints and impacts. Appl. Numer. Math. **62**, 1259–1275 (2012)
7. Acary, V.: Projected event-capturing time-stepping schemes for nonsmooth mechanical systems with unilateral contact and Coulomb's friction. Comput. Methods Appl. Mech. Eng. **256**, 224–250 (2013)
8. Acary, V.: Energy conservation and dissipation properties of time-integration methods for nonsmooth elastodynamics with contact. ZAMM-J. Appl. Math. Mech./Z. Angew. Math. Mechanik **95**(12) (2015). doi:10.1002/zamm.201400231
9. Acary, V., Bonnefon, O., Brogliato, B.: Time-stepping numerical simulation of switched circuits with the nonsmooth dynamical systems approach. IEEE Trans. Comput. Aided Des. Integr. Circ. Syst. **29**(7), 1042–1055 (2010)
10. Acary, V., Bonnefon, O., Brogliato, B.: Nonsmooth modeling and simulation for switched circuits. Lecture Notes in Electrical Engineering, vol. 69. Springer (2011)
11. Acary, V., Brogliato, B.: Concurrent multiple impacts modelling: case study of a 3-ball chain. In: Bath, K. (ed.) Proceedings of Second MIT Conference on Computational Fluid and Solid Mechanics, pp. 1842–1847. Cambridge, USA (2003)
12. Acary, V., Brogliato, B.: Coefficients de restitution et efforts aux impacts. Revue et comparaison des estimations analytiques. Tech. Rep. 5401, INRIA (2004). ISSN 0249–6399. https://hal.inria.fr/inria-00070602

B. Brogliato, *Nonsmooth Mechanics*, Communications and Control Engineering,
DOI 10.1007/978-3-319-28664-8

13. Acary, V., Brogliato, B.: Numerical methods for nonsmooth dynamical systems. Applications in Mechanics and Electronics. Lecture Notes in Applied and Computational Mechanics, vol. 35. Springer, Berlin (2008)
14. Acary, V., Brogliato, B.: Implicit Euler numerical scheme and chattering-free implementation of sliding mode systems. Syst. Control Lett. **59**, 284–293 (2010)
15. Acary, V., Brogliato, B., Goeleven, D.: Higher order Moreau's sweeping process: mathematical formulation and numerical simulation. Math. Prog. A **113**(1), 133–217 (2008). doi:10.1007/s10107-006-0041-0
16. Acary, V., Brogliato, B., Orlov, Y.: Chattering-free digital sliding-mode control with state observer and disturbance rejection. IEEE Trans. Autom. Control **57**(5), 1087–1101 (2012)
17. Acary, V., de Jong, H., Brogliato, B.: Numerical simulation of piecewise-linear models of gene regulatory networks using complementarity systems. Phys. D Nonlinear Phenom **269**, 103–119 (2014)
18. Acary, V., Monerie, Y.: Nonsmooth fracture dynamics using a cohesive zone approach. INRIA Research Report 6032 (2006). https://hal.inria.fr/inria-00110560
19. Acikgoz, S., DeJong, M.: The interaction of elasticity and rocking in flexible structures allowed to uplift. Earthquake Eng. Struct. Dynam. **41**(15), 2177–2194 (2012)
20. Adams, G.G., Nosonovsky, M.: Contact modeling-forces. Tribol. Int. **33**, 431–442 (2000)
21. Adams, G.G., Tran, D.N.: The coefficients of restitution of a planar 2-body eccentric impact. ASME J. Appl. Mech. **60**(4), 1058–1060 (1993)
22. Addi, K., Adly, S., Brogliato, B., Goeleven, D.: A method using the appproach of Moreau and Panagiotopoulos for the mathematical formulation of non-regular circuits in electronics. Nonlinear Anal. Hybrid Syst. **1**(1), 30–43 (2007)
23. Addi, K., Brogliato, B., Goeleven, D.: A qualitative mathematical analysis of a class of linear variational inequalities via semi-complementarity problems: applications in electronics. Math. Program. Ser. A **126**, 31–67 (2011)
24. Addi, K., Despotovic, Z., Goeleven, D., Rodic, A.: Modelling and analysis of a non-regular electronic circuit via a variational inequality formulation. Appl. Math. Model. **35**, 2172–2184 (2011)
25. Adly, S., Brogliato, B., Le, B.K.: Well-posedness, robustness and stability analysis of a set-valued controller for lagrangian systems. SIAM J. Control Optim. **51**(2), 1592–1614 (2013). http://dx.doi.org/10.1137/120872450
26. Adly, S., Brogliato, B., Le, B.K.: Implicit Euler time-discretization of a class of Lagrangian systems with set-valued robust controller. J. Convex Anal. **23**(1-2-3) (2016). Dedicated to the memory of Jean Jacques Moreau, 1923–2014
27. Adly, S., Goeleven, D.: A stability theory for second-order nonsmooth dynamical systems with application to friction problems. J. de Mathématiques Pures et Appliquées **83**(1), 17–51 (2004)
28. Adly, S., Haddad, T., Thibault, L.: Convex sweeping process in the framework of measure differential inclusions and evolution variational inequalities. Math. Program. Ser. B **148**, 5–47 (2014)
29. Adly, S., Hantoute, A., Le, B.K.: Nonsmooth Lur'e dynamical systems in Hilbert spaces. Set-Valued and Variational Analysis (2015). doi:10.1007/s11228-015-0334-7
30. Ainola, L.I.: Integral variational principle of mechanics. J. Appl. Math. Mech. **30**(5), 1124–1128 (1966)
31. Akashi, H.: The motion of an electric bell. Am. Math. Monthly **65**, 255–258 (1958)
32. Akella, P., Siegwart, R., Cutkosky, M.R.: Manipulating with soft fingers: contact force control. In: IEEE International Conference on Robotics and Automation, pp. 652–657. Sacramento, CA (1991)
33. Akhadkar, N., Acary, V., Brogliato, B.: Analysis of collocated feedback controllers for four-bar planar mechanisms with joint clearances (2015). INRIA Report, https://hal.inria.fr/hal-01218531
34. Alcala, J., Giannakopoulos, A.E., Suresh, S.: Continuous measurements of load penetration curves with spherical microindenters and the estimation of mechanical properties. J. Mater. Res. **13**, 1390–1400 (1998)

35. Alexis, K., Huerzeler, C., Siegwart, R.: Hybrid predictive control of a coaxial aerial robot for physical interaction through contact. Control Eng. Pract. **32**, 96–112 (2014)
36. Alkomy, A.M., Elkaranshawy, H.E., Ashour, A.S., Mohamed, K.T.: Effect of robot configur ation parameters, masses and friction on Painlevé paradox for a sliding two- link (p-r) robot. Int. J. Mech., Aerosp., Ind., Mechatron. Manuf. Eng. **9**(10), 1540–1545 (2015)
37. Alvarez, J., Orlov, Y., Acho, L.: An invariance principle for discontinuous dynamic systems with applications to a Coulomb friction oscillator. ASME J. Dyn. Syst., Meas. Control **74**, 190–198 (2000)
38. Alves, J., Peixinnho, N., da Silva, M.T., Flores, P., Lankarani, H.M.: A comparative study of the viscoelastic constitutive models for frictionless contact interfaces in solids. Mech. Mach. Theory **85**, 172–188 (2015)
39. Ames, A.D., Haiyang, Z., Gregg, R.D., Sastry, S.: Is there life after Zeno? Taking executions past the breaking (Zeno) point. In: Proceedings of American Control Conference, pp. 2652–2657. Minneapolis, MN, USA (2006)
40. Anderson, C.E., Holmquist, T.J.: Application of a computational glass model to compute propagation of failure from ballistic impact of borosilicate glass targets. Int. J. Impact Eng. **56**, 2–11 (2013)
41. Andreaus, U., Casini, P.: Dynamics of three-block assemblies with unilateral deformable contacts. part 1: contact modelling. Earthquake Eng. Struct. Dyn. **28**, 1621–1636 (1999)
42. Andreaus, U., Casini, P.: On the rocking-uplifting motion of a rigid block in free and forced motion: influence of sliding and bouncing. Acta Mech. **138**, 219–241 (1999)
43. Andrews, J.G.: A mechanical analysis of a special class of rebound phenomena. Med. Sci. Sports Exerc. **15**(3), 256–266 (1983)
44. Andrews, J.P.: Theory of collision of spheres of soft metals. Philos. Mag. Ser. **7**(9), 593–610 (1930)
45. Anglès, J.: Etude qualitative des vibrations en présence d'obstacle d'un système mécanique. Ph.D. thesis, DER Electricté de France, Paris (1996)
46. Anitescu, M., Cremer, J.F., Potra, F.A.: On the existence of solutions to complementarity formulations of contact problems with friction. In: Pang, J., Ferris, M. (eds.) Complemenarity and Variational Problems: State of the Art, pp. 12–21. SIAM (1997)
47. Anitescu, M., Potra, F.A.: Formulating dynamic multi-rigid-body contact problems with friction as solvable linear complementarity problems. Nonlinear Dyn. **14**(3), 231–247 (1997)
48. Anitescu, M., Potra, F.A., Stewart, D.: Time-stepping for three-dimensional rigid body dynamics. Comput. Methods Appl. Mech. Eng. **177**, 183–197 (1999)
49. Anosov, D.V., Aranson, S.K., Arnold, V.I., Bronshtein, I.U., Grines, V.Z., Ilyashenko, Y.S.: Ordinary Differential Equations and Smooth Dynamical Systems. Springer (1997). 3rd printing
50. Antonyuk, S., Heinrich, S., Tomas, J., Deen, N.G., van Buijtenen, M.S., Kuipers, J.A.M.: Energy absorption during compression and impact of dry elastic-plastic spherical granules. Granular Matter **12**, 15–47 (2010)
51. Antosik, P., Mikusinski, J., Sikorski, R.: Theory of Distributions-The Sequential Approach. Elsevier Scientific Publishing Company, Polish Scientific Publishers, Amsterdam, Warszawa (1973)
52. Appel, P.: Sur l'emploi des équations de Lagrange dans la théorie du choc et des percussions. J. Mathématiques Pures et Appliquées 5ème série Tome II, 5–20 (1896)
53. Appel, P.: Remarques sur les systèmes non holonomes. J. de Mathématiques Tome IX (Fasc. I), 27–28 (1903)
54. Appel, P.: Traité de Mécanique Rationnelle, vol. 2. Gauthiers-Villars, Paris (1911). 3 ème édition
55. Arakawa, K., Mada, T., Komatsu, H., Shimizu, T., Satou, M., Takehara, K., Etoh, G.: Dynamic contact behaviour of a golf ball during an oblique impact. Exp. Mech. **46**, 691–697 (2006)
56. Aranson, I.S., Tsimring, L.S.: Patterns and collective behavior in granular material: theoretical concepts. Rev. Mod. Phys. **78**, 641–692 (2006)

57. Armstrong, H.L.: On elastic and inelastic collisions of bodies. Am. J. Phys. **32**, 964–965 (1964)
58. Armstrong-Hélouvry, B., Dupont, P., de Wit, C.C.: A survey of models, analysis tools and compensation methods for the control of machines with friction. Automatica **30**(7), 1083–1138 (1994)
59. Arnold, R.N.: Response of an impact vibration absorber to forced vibration. In: 9th International Congress of Applied Mechanics. Brussels (1957)
60. Arnold, V.: Mathematical Methods of Classical Mechanics, Graduate Texts in Mathematics, 2nd Edn., vol. 60. Springer (1978)
61. Arnold, V.: Equations Différentielle Ordinaires. Editions MIR, Moscou (1988). 4ème édition
62. Arutyunov, A.V., Aseev, S.M.: State constraints in optimal control. The degeneracy phenomenon. Syst. Control Lett. **26**, 267–273 (1995)
63. Aryaei, A., Hashemnia, K., Jafarpur, K.: Experimental and numerical study of ball size effect on restitution coefficient in low velocity impacts. Int. J. Impact Eng. **37**, 1037–1044 (2010)
64. Astolfi, A., Limebeer, D.J.N., Melchiorri, C., Tornambé, A., Vinter, R.B. (eds.): Modelling and Control of Mechanical Systems. Imperial College Press, World Scientific Publishers (1997)
65. Atanackovic, T.M., Spasic, D.T.: On the imapct of elastic bodies with adhesive forces. Meccanica **34**, 367–377 (1999)
66. Thorin, A.: Non-smooth model of the grand piano action. Ph.D. thesis, Ecole Polytechnique (2013). https://pastel.archives-ouvertes.fr/pastel-00939493
67. Aubin, J.P.: A survey of viability theory. SIAM J. Control Optim. **28**(4), 749–788 (1990)
68. Aubin, J.P., Quincampoix, M., Sastry, S., Seube, N.: Impulse differential inclusions: a viability approach to hybrid systems. IEEE Trans. Autom. Control **47**(1), 2–20 (2002)
69. Awrejcewicz, J., Lamarque, C.H.: Bifurcation and Chaos in Nonsmooth Mechanical Systems, Nonlinear Science, vol. 45. World Scientific Publishing (2003)
70. Azad, M., Featherstone, R.: A new nonlinear model of contact normal force. IEEE Trans. Robot. **30**(3), 736–739 (2014). doi:10.1109/TRO.2013.2293833
71. Azzam-Laouir, D., Izza, S., Thibault, L.: Mixed semicontinuous perturbation of nonconvex state-dependent sweeping process. Set-Valued Variational Anal. **22**(1), 271–283 (2014)
72. Bacon, M.E., Stevenson, B., Baines, C.G.S.: Impulse and momentum experiments using piezo disks. Am. J. Phys. **66**(5), 445–448 (1998)
73. Baek, H.K.: Qualitative analysis of Beddington-DeAngelis type impulsive predator-prey models. Nonlinear Analysis: Real World Applications **11**, 1312–1322 (2010)
74. Bahar, L.Y.: On the use of quasi-velocities in impulsive motion. Int. J. Eng. Sci. **32**(11), 1669–1686 (1994)
75. Bainov, D., Simeonov, P.: Impulsive Differential Equations: periodic Solutions and Applications. Pitman Monographs and Surveys in Pure and Applied Mathematics, Longman Group UK Limited (1993)
76. Bainov, D.D., Simeonov, P.S.: Systems with Impulse Effects; Stability. Wiley, Theory and Applications. Ellis Horwood series in Mathematics and its applications (1989)
77. Bakr, E.M., Shabana, A.A.: Effect of geometric elastic non-linearities on the impact response of flexible multi-body system. J. Sound Vib. **112**(3), 415–432 (1987)
78. Balevicius, R., Mroz, Z.: A finite sliding model of two identical spheres under displacement and force control-Part I: static analysis. Acta Mech. **224**(8), 1659–1684 (2013)
79. Balevicius, R., Mroz, Z.: A finite sliding model of two identical spheres under displacement and force control-Part II: dynamic analysis. Acta Mech. **225**(6), 1735–1759 (2014)
80. Ballard, P.: The dynamics of discrete mechanical systems with perfect unilateral constraints. Arch. Ration. Mech. Anal. **154**(3), 199–274 (2000)
81. Ballard, P.: Formulation and well-posedness of the dynamics of rigid body systems with perfect unilateral constraints. Phil. Trans. R. Soc. Lond. A **359**(1789), 2327–2346 (2001)
82. Ballard, P., Basseville, S.: Existence and uniqueness for frictional unilateral contact with Coulomb friction: a model problem. ESAIM: M2AN. Math. Model. Numer. Anal. **39**, 59–75 (2005)

83. Bamberger, A., Schatzman, M.: New results on the vibrating string with a continuous obstacle. SIAM J. Math. Anal. **14**(3), 560–595 (1983)
84. Banerji, S.: On aerial waves generated by impact. Philos. Mag. Ser. **6–32**(187), 96–111 (1916)
85. Bao, R.H., Yu, T.X.: Impact and rebound of an elastic-plastic ring on a rigid target. Int. J. Mech. Sci. (2014). doi:10.1016/j.ijmecsci.2014.03.031
86. Bapat, C.N.: Periodic motions of an impact oscillator. J. Sound Vib. **209**(1), 43–60 (1998)
87. Bapat, C.N., Popplewell, N., MacLachlan, K.: Stable periodic motion of an impact pair. J. Sound Vib. **87**, 19–47 (1983)
88. Bapat, C.N., Sankar, S., Popplewell, N.: Repeated impacts on a sinusoidally vibrating table reappraised. J. Sound Vib. **108**(1), 99–115 (1986)
89. Baraff, D.: Issues in computing contact forces for non-penetrating rigid bodies. Algorithmica **10**, 292–352 (1993)
90. Barjau, A., Batlle, J.A., Font-Lagunes, J.M.: Combining vibrational linear-by-part dynamics and kinetic-based decoupling of the dynamics for multiple smooth impacts with redundancy. Multibody Sys. Dyn. **31**(4), 497–517 (2014)
91. Barjau, A., Batlle, J.A., Font-Lagunes, J.M.: Combining vibrational linear-by-part dynamics and kinetic-based decoupling of the dynamics for multiple elastoplastic smooth impacts. Multibody Syst. Dyn. **35**(3), 233–256 (2015). doi:10.1007/s11044-015-9454-y
92. Barmes, G.: Study of collisions, part 1: Survey of the periodical literature. part 2: survey of the textbooks. Am. J. Phys. **26**, 5–12 (1958)
93. Barnhart, K.E.: Transverse impact on elastically supported beams. Ph.D. thesis, The University of California, Berkeley, USA (1955)
94. Barthel, E.: On the description of the adhesive contact of spheres with arbitrary interaction potentials. J. Colloid Interface Sci. **200**, 7–18 (1998)
95. Bartier, O., Hernot, X., Mauvoisin, G.: Theoretical and experimental analysis of contact radius for spherical indentation. Mech. Mater. **42**, 640–656 (2010)
96. Basseville, S., Leger, A.: Stability of equilibrium states in a simple system with unilateral contact and Coulomb friction. Arch. Appl. Mech. **76**, 403–428 (2006)
97. Bastien, J.: Convergence order of implicit Euler numerical scheme for maximal monotone differential inclusions. Z. Angew. Math. Phys. **64**, 955–966 (2013). doi:10.1007/s00033-012-0276-y
98. Bastien, J., Bernardin, F., Lamarque, C.H.: Systèmes Dynamiques Discrets Non Réguliers Déterministes ou Stochastiques. Lavoisier, Paris, France (2012)
99. Bastien, J., Bernardin, F., Lamarque, C.H.: Non Smooth Deterministic or Stochastic Discrete Dynamical Systems. ISTE Ltd and Wiley, London and Hoboken (2013)
100. Bastien, J., Lamarque, C.: Persoz's gephyroidal model described by a maximal monotone differential inclusion. Arch. Appl. Mech. **78**(5), 393–407 (2008)
101. Bastien, J., Michon, G., Manin, L., Dufour, R.: An analysis of the modified Dahl and Masing models: application to a belt tensioner. J. Sound Vib. **302**, 841–864 (2007)
102. Bastien, J., Schatzman, M.: Numerical precision for differential inclusions with uniqueness. Math. Model. Numer. Anal., ESAIM: M2AN **36**(3), 427–460 (2002)
103. Bastien, J., Schatzman, M., Lamarque, C.: Study of some rheological models with a finite number of degrees of freedom. Eur. J. Mech./A Solids **19**(2), 277–307 (2000)
104. Bastien, J., Schatzman, M., Lamarque, C.H.: Study of an elastoplastic model with an infinite number of internal degrees of freedom. Eur. J. Mech. A/Solids **21**, 199–222 (2002)
105. Batlle, C., Gomis, J., Pons, J.M., Roman-Roy, N.: Equivalence between the Lagrangian and Hamiltonian formalism for constrained systems. J. Math. Phys. **27**(12), 2953–2962 (1986)
106. Batlle, J.A.: On Newton's and Poisson's rules of percussive dynamics. ASME J. Appl. Mech. **60**, 376–381 (1993)
107. Batlle, J.A.: Rough balanced collisions. ASME J. Appl. Mech. **63**(1), 168–172 (1996)
108. Batlle, J.A.: The sliding velocity flow of rough collisions in multibody systems. ASME J. Appl. Dyn. **63**(3), 804–809 (1996)

109. Batlle, J.A.: Conditions for dual compression in perfectly elastic three-dimensional collisions. ASME J. Appl. Mech. **66**(3), 607–611 (1999)
110. Batlle, J.A.: Termination conditions for three-dimensional inelastic collisions in multibody systems. Int. J. Impact Eng. **25**, 615–629 (2001)
111. Batlle, J.A., Cardona, S.: The jamb (self-locking) process in three-dimensional rough collisions. ASME J. Appl. Mech. **65** (1998)
112. Batlle, J.A., Condomines, A.B.: Rough collisions in multibody systems. Mech. Mach. Theory **26**(6), 565–577 (1991)
113. Bauchau, O.A., Laulusa, A.: Review of contemporary approaches for constraint enforcement in multibody systems. ASME J. Comput. Nonlinear Dyn. **3**(1), 011,005 (2008)
114. Baumann, M., Leine, R.I.: A synchronization-based state observer for impact oscillators using only collision time information. Int. J, Robust Nonlinear Control (2015)
115. Bayly, P.V., Virgin, L.N.: An experimental study of an impacting oscillator. J. Sound Vib. **164**(2), 364–374 (1993)
116. Beghin, H.: Sur certains problèmes de frottement. Nouvelles Annales de Math., série 2–5, 305–312 (1923–1924)
117. Beghin, H.: Sur l'indétermination de certains problèmes de frottement. Nouvelles Ann. Math **3**, 343–347 (1924–1925)
118. Beghin, H.: Sur le choc de deux solides entenant compte du frottement. Bulletin de la Société Mathématique de France, tome **57**, 111–117 (1929)
119. Beghin, H.: Cours de Mécanique Théorique et Appliquée, pp. 457–483. Gauthier-Villars, Paris (1967)
120. Beghin, H., Rousseau, M.: Sur les percussions dans les systèmes non holonomes. J. Math., 5ème série, pp. 21–28 1903. Tome IX, fasc. I
121. Begley, C.J., Virgin, L.N.: Impact response and the influence of friction. J. Sound Vib. **211**(5), 808–818 (1998)
122. Beitelschmidt, M., Pfeiffer, F.: Impacts with friction and normal and tangential reversibility in multibody systems. ZAMM Z. angew. Math. Mech. **77**, 29–30 (1997)
123. Benchohra, M., Henderson, J., Ntouyas, S.: Impulsive Differential Equations and Inclusions, Contemporary Mathematics and Its Applications, vol. 2. Hindawi Publishing Corporation (2006)
124. Bentsman, J., Miller, B.M.: Dynamical systems with active singularities of elastic type: a modeling and controller synthesis framework. IEEE Trans. Autom. Control **52**(1), 39–55 (2007)
125. Benzaid, Z., Sznaier, M.: Constrained controllability of linear impulse differential systems. IEEE Trans. Autom. Control **39**(5), 1064–1066 (1994)
126. Berdeni, Y., Champneys, A., Szalai, R.: The two-ball bounce problem. Proc. Royal Soc. London A: Math., Phys. Eng. Sci. **471**(2179) (2015). doi:10.1098/rspa.2015.0286
127. Berger, E.J.: Friction modeling for dynamic system simulation. ASME Appl. Mech. Rev. **55**(6), 535–577 (2002)
128. Bergman, R., Philips, L., Cobelli, C.: Physiologic evaluation of factors controlling glucose tolerance in man: measurement of insulin sensitivity and beta-cell glucose sensitivity from the response to intravenous glucose. J. Clin. Invest. **68**(6), 1456–1467 (1981)
129. Berkovitz, L.D.: Variational methods in problems of control and programming. J. Math. Anal. Appl. **3**, 145–169 (1961)
130. Berkovitz, L.D.: On control problems with bounded state variables. J. Math. Anal. Appl. **5**, 488–498 (1962)
131. Bernard, F., Thibault, L., Zlateva, N.: Characterizations of prox-regular sets in uniformly convex banach spaces. J. Convex Anal. **13**(3), 525–559 (2006)
132. di Bernardo, M., Budd, C.J., Champneys, A.R., Kowalczyk, P.: Piecewise-smooth Dynamical Systems. Theory and Applications, Applied Mathematical Sciences, vol. 163. Springer (2008)
133. Bernicot, F., Venel, J.: Existence of solutions for second-order differential inclusions involving proximal normal cones. J. Math. Pures Appl. **98**, 257–294 (2012)

134. Bernoulli, J.: Discours sur le Mouvement, vol. III. Opera Omnia. pp. 9f. (1724)
135. Bernoulli, J.: Die werke von Jacob Bernoulli. Birkhauser (1969–1993)
136. Bernstein, D.S.: Matrix, Mathematics. Theory, Facts, and Formulas with Application to Linear Systems Theory. Princeton University Press (2005)
137. Berry, M.V.: Regularity and chaos in classical mechanics, illustrated by three deformations of a circular 'billiard'. Eur. J. Phys. **2**, 91–102 (1981)
138. Bertails-Descoubes, F., Cadoux, F., Daviet, G., Acary, V.: A nonsmooth Newton solver for capturing exact Coulomb friction in fiber assemblies. ACM Trans. Graph. **30**(1), 1–14 (2011)
139. Berti, A., Merlet, J.P., Carricato, M.: Solving the direct geometrico-static problem of underconstrained cable-driven parallel robots by interval analysis. Int. J. Robot. Res. (2015). doi:10.1177/0278364915595277
140. Bespalova, L.V., Neimark, I.I., Feigin, M.I.: Dynamic systems with shock interactions and the theory of nonlinear oscillators. Inzhenernaya Zhurnal, Mekhanika tverdogo tela (1966)
141. Bhatt, V., Koechling, J.: Classifying dynamic behaviour during three dimensional frictional rigid body impact. In: Proceedings of the IEEE International Conference on Robotics and Automation, pp. 2342–2348. San Diego, USA (1994)
142. Bhatt, V., Koechling, J.: Partitioning the parameter space according to different behaviours during three-dimensional impacts. ASME J. Appl. Mech. **62**, 740–746 (1995)
143. Bhatt, V., Koechling, J.: Three-dimensional frictional rigid-body impact. ASME J. Appl. Mech. **62**, 893–898 (1995)
144. Bianchini, S., Spinolo, L.V.: Invariant manifolds for a singular ordinary differential equation. J. Differ. Equ. **250**, 1788–1827 (2011)
145. Bidgaray-Fesqueta, B., Dumas, E., James, G.: From Newton's cradle to the discrete p-Schrödinger equation. SIAM J. Math. Anal. **45**, 3404–3430 (2013)
146. Biemond, J., Heemels, M., Sanfelice, R.G., van de Wouw, N.: Distance function design and Lyapunov techniques for the stability of hybrid trajectories (2015). arxiv.org/abs/1501.00161v1
147. Biemond, J., van de Wouw, N., Heemels, W., Nijmeijer, H.: Tracking control for hybrid systems with state-triggered jumps. IEEE Trans. Autom. Control **58**(4), 876–890 (2013)
148. Biemond, J., van de Wouw, N., Heemels, W., Sanfelice, R., Nijmeijer, H.: Tracking control of mechanical systems with a unilateral position constraint inducing dissipative impacts. In: Proceedings of the IEEE Conference on Decision and Control, pp. 4223–4228 (2012)
149. Bilbao, A., Campos, J., Bastero, C.: On the planar impact of an elastic body with a rough surface. Int. J. Mech. Eng. Educ. **17**, 205–210 (1989)
150. Bischoff, P.H., Perry, S.H., Eibl, J.: Contact force calculations with a simple spring-mass model for hard impacts: A case study using polystyrene aggregate concrete. Int. J. Impact Eng. **9**(3), 317–325 (1990)
151. Bishop, S.R.: Impact oscillators. Phil. Trans. R. Soc. Lond. A **347**, 347–351 (1994)
152. Bishop, S.R., Thompson, M., Foale, S.: Prediction of period-1 impacts in a driven beam. Proc. R. Soc. Lond. A **452**, 2579–2592 (1996)
153. Bishop, S.R., Thompson, M.G., Foale, S.: An experimental study of low velocity impacts. Mach. Vib. **3**, 10–17 (1994)
154. Biwa, S., Storakers, B.: An analysis of fully plastic Brinell indentation. J. Mech. Phys. Solids **43**, 1303–1333 (1995)
155. Blajer, W.: A geometrical interpretation and uniform matrix formulation of multibody system dynamics. ZAMM Z. Angew. Math. Mech. **81**(4), 247–259 (2001)
156. Blakenship, G.W., Kahraman, A.: Steady-state forced response of a mechanical oscillator with combined parametric excitation and clearance type non-linearity. J. Sound Vib. **185**, 743–765 (1995)
157. Blazejczyk, B., Kapitaniak, T.: Dynamics of impact oscillators with dry friction. Chaos, Solitons Fractals **7**(9), 1455–1459 (1996)
158. Blazejczyk, B., Kapitaniak, T., Wojewoda, J., Barron, R.: Experimental observation of intermittent chaos in a mechanical system with impacts. J. Sound Vib. **178**, 272–275 (1994)

159. Blazejczyk-Okolewska, B., Czolczynski, K., Kapitaniak, T.: Calssification principles of types of mechanical systems with impacts-fundamental assumption and rules. Eur. J. Mech. A/Solids **23**, 517–537 (2004)
160. Blumentals, A., Brogliato, B., Bertails-Descoubes, F.: The contact problem in Lagrangian systems subject to bilateral and unilateral constraints, with or without sliding Coulomb's friction: A tutorial (2015). https://hal.archives-ouvertes.fr/hal-01096394
161. Bolotov, E.A.: On the motion of a material plane figure constrained by links with friction. Universitetskaya Tip, Moscow (1906)
162. Bolotov, E.A.: On the impact of two rigid bodies under the action of friction. Izv. Mosk. inzh. uchilishcha (paper written in old Russian) **2**(2) (1908)
163. Bornemann, F.: Homogenization in Time of Singularly Perturbed Mechanical Systems. Lecture Notes in Mathematics, vol. 1687. Springer, Berlin (1998)
164. Boulanger, G.: Sur le choc avec frottement des corps non parfaitement élastiques. Revue Sci. **77**, 325–327 (1939)
165. Bounkhel, M.: General existence results for second order nonconvex sweeping process with unbounded perturbations. Portugaliae Math. **60**(3) (2003). Nova Série
166. Bourgeot, J.M., Brogliato, B.: Tracking control of lagrangian complementarity systems. Int. J. Bifurcation Chaos **15**(6), 1839–1866 (2005). Special issue on Nonsmooth Dynamical Systems
167. Bourgeot, J.M., Delaleau, E.: Fast algebraic impact times estimation for a linear system subject to unilateral constraint. In: Proceedings of the 46th IEEE Conference on Decision and Control, pp. 2701–2706. New Orleans, LA, USA (2007)
168. Bourrier, F., Bellot, N.E.H., Heymann, A., Nicot, F., Darve, F.: Numerical modelling of physical processes involved during the impact of a rock on a coarse soil. In: Proceedings of 3rd Euro- Mediterranean Symposium on Advances in Geomaterial and Structures, pp. 501–506. Hermes Science Publishing, Paris, France (2008)
169. Bourrier, F., Dorren, L., Nicot, F., Berger, F., Darve, F.: Toward objective rockfall trajectory simulation using a stochastic impact model. Geomorphology **110**, 68–79 (2009)
170. Bourrier, F., Nicot, F., Darve, F.: Rockfall modelling: numerical simulation of the impact of a particle on a coarse granular medium. In: Proceedings of 10th International Congress on Numerical Model in Geomechanics, pp. 699–705. Balkema, Rotterdam, NL (2007)
171. Bowling, A., Flickinger, D.M., Harmeyer, S.: Energetically consistent simulation of simultaneous impacts and contacts in multibody systems with friction. Multibody Syst. Dyn. **22**(1), 27–45 (2009)
172. Boyd, S.P., Vandenberghe, L.: Convex Optimization. Cambridge University Press (2004)
173. Brach, R.M.: Friction, restitution and energy loss in planar collisions. ASME J. Appl. Mech. **51**, 164–170 (1984)
174. Brach, R.M.: Rigid body collisions. ASME J. Appl. Mech. **56**, 133–138 (1989)
175. Brach, R.M.: Mechanical Impact Dynamics. Wiley, New York (1991)
176. Brach, R.M.: Classical planar impact theory and the tip impact of a slender rod. Int. J. Impact Eng. **13**(1), 21–33 (1993)
177. Brach, R.M.: Impact coefficients and tangential impacts. ASME J. Appl. Mech. **64**, 1014–1017 (1997)
178. Brach, R.M.: Formulation of rigid body impact problems using generalized coefficients. Int. J. Eng. Sci. **36**(1), 61–72 (1998)
179. Brach, R.M., Dunn, P.F.: Macrodynamics of microparticles. J. Aerosol Sci. Technol. **33**(1), 51–71 (1995)
180. Brake, M.: The effect of the contact model on the impact-vibration response of continuous and discrete systems. J. Sound Vib. **332**, 3849–3878 (2013)
181. Brake, M.R.: An analytical elastic-perfectly plastic contact model. Int. J. Solids Struct. **49**, 3129–3141 (2012)
182. Brake, M.R.: The role of epistemic uncertainty of contact models in the design and optimization of mechanical systems with aleatoric uncertainty. Nonlinear Dyn. (2014). doi:10.1007/s11071-014-1350-0

183. Brake, M.R.: An analyticval elastic-plastic contact model with strain hardening and frictional effects for normal and oblique impacts. Int. J. Solids Struct. **62**, 104–123 (2015)
184. Brake, M.R., Reu, P., Vangoethem, D.J., Bejarano, M.V., Sumali, A.: Experimental validation of an elastic-plastic contact model. Tech. rep. (2011). ASME paper no IMECE2011-65736
185. Brauchli, H.: Mass-orthogonal formulation of equations of motion for multibody systems. J. Appl. Math. Phys. (ZAMP) **42**, 169–182 (1991)
186. Bressan, A.: Incompatibilità dei teoremi di esistenza e di unicità del moto per un tipo molto comune e regolare di sistemi meccanici. Rend. Scu. Norm. di Pisa 333–348 (1959)
187. Bressan, A.: On differential systems with impulsive controls. Rend. Sem. Mat. Univ. Padova **78**, 227–236 (1987)
188. Bressan, A.: On the application of control theory to certain problems for lagrangian systems, and hyper-impulsive motion for these. i. some general mathematical considerations on controllizable parameters; ii. some purely mathematical considerations for hyper-impulsive motions. application to lagrangian systems. Atti. Accad. Naz. Lincei, Rend. Fisica Matematica **8**(LXXXII), 91–118 (1988)
189. Bressan, A., Rampazzo, F.: Impulsive control systems with commutative vector fields. J. Optim. Theory Appl. **71**(1), 67–83 (1991)
190. Bressan, A., Rampazzo, F.: On differential systems with quadratic impulses and their application to lagrangian mechanics. SIAM J. Control Optim. **31**(5), 1205–1220 (1993)
191. Brezis, H.: Analyse Fonctionnelle. Théorie et applications. Masson, Paris (1993)
192. Briat, C., Seuret, A.: Convex dwell-time characterizations for uncertain linear impulsive systems. IEEE Trans. Autom. Control **57**(12), 3241–3246 (2012)
193. Briceno-Arias, L.M., Hoang, N.D., Peypouquet, J.: Existence, stability and optimality for optimal control problems governed by maximal monotone operators. J. Differ, Equ (2015)
194. Bridges, F.G., Hatzes, A., Lin, D.N.C.: Structure, stability and evolution of saturn's rings. Nature **309**, 333–335 (1984)
195. Bridges, F.G., Supulver, K.D., Lin, D.N.C., Knight, R., Zafra, M.: Energy loss and sticking mechanisms in particle aggregation in planetesimal formation. Icarus **123**, 422–435 (1996)
196. Briggs, L.J.: Methods for measuring the coefficient of restitution and the spin of a ball. J. Res. National Bureau Stand. **34**, 1–23 (1945)
197. Brilliantov, N.V., Pimenova, A.V., Goldbin, D.S.: A dissipative force between colliding viscoelastic bodies: Rigorous approach. EPL **109**, 14,005 (2015). doi:10.1209/0295-5075/109/14005
198. Brilliantov, N.V., Spahn, F., Hertzsch, J.M., Pöschel, T.: The collision of particles in granular systems. Phys. A **231**, 417–424 (1996)
199. Brilliantov, N.V., Spahn, F., Hertzsch, J.M., Pöschel, T.: Model for collisions in granular gases. Phys. Rev. E **53**(5), 5382–5392 (1996)
200. Brody, H.: Tennis Science for Tennis Players. University of Pennsylvania Press (1987)
201. Brody, H.: The physics of tennis iii. the ball-racket interaction. Am. J. Phys. **65**(10), 981–987 (1997)
202. Brogliato, B.: Nonsmooth Impact Mechanics. Models, Dynamics and Control, Lecture Notes in Control and Information Sciences, vol. 220, first edn. Springer, London (1996)
203. Brogliato, B.: Nonsmooth Mechanics. Dynamics and Control, second edn. Communications and Control Engineering. Springer, London, Models (1999)
204. Brogliato, B.: Some perspectives on the analysis and control of complementarity systems. IEEE Trans. Autom. Control **48**(6), 918–935 (2003)
205. Brogliato, B.: Absolute stability and the Lagrange-Dirichlet theorem with monotone multivalued mappings. Syst. Control Lett. **51**(5), 343–353 (2004)
206. Brogliato, B.: Some results on the controllability of planar evolution variational inequalities. Syst. Control Lett. **54**(1), 65–71 (2005)
207. Brogliato, B.: Comments on "Dynamical properties of hybrid automata". IEEE Trans. Autom. Control **48**, 2–14, 2003 (2006). INRIA Research Report RR-4839, http://hal.inria.fr/inria-00071746, ISSN 0249–6399

208. Brogliato, B.: Some results on the optimal control with unilateral state constraints. Nonlinear Anal.: Theory, Methods Appl. **70**(15), 3626–3657 (2009)
209. Brogliato, B.: Inertial couplings between unilateral and bilateral holonomic constraints in frictionless Lagrangian systems. Multibody Syst. Dyn. **29**(3), 289–325 (2013)
210. Brogliato, B.: Kinetic quasi-velocities in unilaterally constrained Lagrangian mechanics with impacts and friction. Multibody Syst. Dyn. **32**(2), 175–216 (2014). doi:10.1007/s11044-013-9392-5
211. Brogliato, B., ten Dam, A.A., Paoli, L., Génot, F., Abadie, M.: Numerical simulation of finite dimensional multibody nonsmooth mechanical systems. ASME Appl. Mech. Rev. **55**(2), 107–150 (2002)
212. Brogliato, B., Daniilidis, A., Lemaréchal, C., Acary, V.: On the equivalence between complementarity systems, projected systems and differential inclusions. Syst. Control Lett. **55**(1), 45–51 (2006)
213. Brogliato, B., Goeleven, D.: The Krazovskii-LaSalle invariance principle for a class of unilateral dynamical systems. Math. Control, Signals Syst. **17**, 57–76 (2005)
214. Brogliato, B., Goeleven, D.: Well-posedness, stability and invariance results for a class of multivalued Lur'e dynamical systems. Nonlinear Anal.: Theory, Methods Appl. **74**, 195–212 (2011)
215. Brogliato, B., Goeleven, D.: Existence, uniqueness of solutions and stability of nonsmooth multivalued Lur'e dynamical systems. J. Convex Anal. **20**(3), 881–900 (2013)
216. Brogliato, B., Goeleven, D.: Singular mass matrix and redundant constraints in unilaterally constrained Lagrangian and Hamiltonian systems. Multibody Syst. Dyn. **35**(1), 39–61 (2015). doi:10.1007/s11044-014-9437-4
217. Brogliato, B., Heemels, W.P.M.H.: Observer design for Lur'e systems with multivalued mappings: a passivity approach. IEEE Trans. Autom. Control **54**(8), 1996–2001 (2009)
218. Brogliato, B., Lozano, R., Maschke, B., Egeland, O.: Dissipative Systems Analysis and Control, 2nd edn. Communications and Control Engineering. Springer, London (2007)
219. Brogliato, B., Mabrouk, M., Rio, A.Z.: On the controllability of linear juggling mechanical systems. Syst. Control Lett. **55**(4), 350–367 (2006)
220. Brogliato, B., Niculescu, S., Orhant, P.: On the control of finite dimensional mechanical systems with unilateral constraints. IEEE Trans. Autom. Control **42**(2), 200–215 (1997)
221. Brogliato, B., Niculescu, S.I., Monteiro-Marques, M.: On tracking control of a class of complementary-slackness hybrid mechanical systems. Syst. Control Lett. **39**(4), 255–266 (2000)
222. Brogliato, B., Orhant, P.: Contact stability analysis of one degree-of-freedom robot. Dyn. Control **8**(1), 37–53 (1998)
223. Brogliato, B., Ortega, R., Lozano, R.: Global tracking controllers for flexible joint manipulators: a comparative study. Automatica **31**(7), 941–956 (1995)
224. Brogliato, B., Pastore, A., Rey, D., Barnier, J.: Experimental comparison of nonlinear controllers for flexible joint manipulators. Int. J. Robot. Res. **17**(3), 260–281 (1998)
225. Brogliato, B., Rey, D.: Further experimental results on nonlinear control of flexible joint manipulators. In: Proceedings of the American Control Conference, vol. 4, pp. 2209–2211. Philadelphia, USA (1998)
226. Brogliato, B., Thibault, L.: Existence and uniqueness of solutions for non-autonomous complementarity dynamical systems. J. Convex Anal. **17**(3–4), 961–990 (2010)
227. Brogliato, B., Zavala-Rio, A.: On the control of complementary-slackness mechanical juggling systems. IEEE Trans. Autom. Control **45**(2), 235–246 (2000)
228. Brogliato, B., Zhang, H., Liu, C.: Analysis of a generalized kinematic impact law for multibody-multicontact systems, with application to the planar rocking block and chains of balls. Multibody Syst. Dyn. **27**(3), 351–382 (2012)
229. Brokate, M., Krejci, P.: Optimal control of ODE systems involving a rate independent variational inequality. Discret. Contin. Dyn. Syst. Ser. B **18**, 331–348 (2013)
230. Brown, G.V., North, C.M.: The impact damped harmonic oscillator in free decay. In: 11th Biennal Conference on Mechanical Vibrations and Noise. ASME, Boston (1987)

231. Bruckmann, T., Pott, A. (eds.): Cable-Driven Parallel Robots. Springer, Berlin (2013). doi:10.1007/978-3-642-31988-4
232. Brüls, O., Acary, V., Cardona, A.: Simultaneous enforcement of constraints at position and velocity levels in the nonsmooth generalized$-\alpha$ scheme. Comput. Methods Appl. Eng. **281**, 131–161 (2014)
233. Brusin, V.A., Neimark, I.I., Feigin, M.I.: On certain cases of dependence of the periodic motions of a relay system on parameters. Izv. Vysshikh Ucheb. Zaved, Radiofizika **4** (1963)
234. Bucher, M.: Diagram for head-on collisions. Am. J. Phys. **55**, 1042–1043 (1987)
235. Budd, C., Dux, F.: Chattering and related behaviour in impact oscillators. Proc. Phil. Trans. Roy. Soc. London A **347**(1683), 365–389 (1994)
236. Budd, C., Dux, F.: Intermittency in impact oscillators close to resonance. Nonlinearity **7**(4), 1191–1224 (1994). doi:10.1088/0951-7715/7/4/007
237. Bühler, M., Koditshek, D.E., Kindlmann, P.J.: A family of robot control strategies for intermittent dynamical environments. IEEE Control Syst. Mag. **10**(2), 16–22 (1990)
238. Bühler, M., Koditshek, D.E., Kindlmann, P.J.: Planning and control of robotic juggling and catching tasks. Int. J. Robot. Res. **13**(2), 101–118 (1994)
239. Butcher, E.A., Segalman, D.J.: Characterizing damping and restitution in compliant impacts via modified KV and higher-order linear viscoelastic models. ASME J. Appl. Mech. **67**(4), 831–834 (2000)
240. Butenin, N.V.: Examination of degenerate systems using the discontinuity hypothesis. Prikl. Math. Mekh. **12**(1), 3–22 (1948)
241. Buttazzo, G., Percivale, D.: Sull' approssimazione del problema del rimbalzo unidimensionale. Ricerche Mat. **30**, 217–231 (1981)
242. Buttazzo, G., Percivale, D.: On the approximation of the elastic bounce problem on riemannian manifolds. J. Differ. Equ. **47**, 227–275 (1983)
243. Cabot, A., Paoli, L.: Asymptotics for some vibro-impact problem with linear dissipation term. J. Mathématiques Pures et Appliquées **87**(3), 291–323 (2007)
244. Cai, L., Goldenberg, A.A.: Robust control of position and force for robot manipulators involving both free and constrained motion. In: Proceedings of the IEEE Conference on Decision and Control, pp. 1943–1948. Honolulu (1990)
245. Cai, L., Yang, J., Rizzo, P., Ni, X., Daraio, C.: Propagation of highly nonlinear solitary waves in a curved granular chain. Granular Matter **15**(3), 357–366 (2013). doi:10.1007/s10035-013-0414-z
246. Cajori, F.: Newton's Principia-A Revision of Mott's Translation. University of California Press, Berkeley (1934)
247. Calladine, C.R.: The teaching of some aspects of the theory of inelastic collision. Int. J. Mech. Eng. Edu. **18**(4), 301–310 (1990)
248. Calsamiglia, J., Kennedy, S.W., Chatterjee, A., Ruina, A.L., Jenkins, J.T.: Anomalous frictional behaviour in collisions of thin disks. ASME J. Appl. Mech. **66**, 146–152 (1999)
249. Camlibel, M.K.: Complementarity methods in the analysis of piecewise linear dynamical systems. Ph.D. thesis, Katholieke Universiteit Brabant, The Netherlands (2001). ISBN 90 5668 073X
250. Camlibel, M.K.: Popov-Belevitch-Hautus type controllability tests for linear complementarity systems. Syst. Control Lett. **56**(5), 381–387 (2007)
251. Camlibel, M.K., Heemels, W.P.M.H., van der Schaft, A.J., Schumacher, H.: Switched networks and complementarity. IEEE Trans. Circuits Syst. I: Fundam. Theory Appl. **50**(8), 1036–1046 (2003)
252. Camlibel, M.K., Heemels, W.P.M.H., Schumacher, J.M.: On linear passive complementarity systems. Eur. J. Control **8**, 220–237 (2002)
253. Camlibel, M.K., Heemels, W.P.M.H., Schumacher, J.M.: Algebraic necessary and sufficient conditions for the controllability of conewise linear systems. IEEE Trans. Autom. Control **53**(3), 762–774 (2008)
254. Camlibel, M.K., Iannelli, L., Vasca, F.: Passivity and complementarity. Math. Prog. Ser. A **145**, 531–563 (2014)

255. Camlibel, M.K., Pang, J.S., Shen, J.: Conewise linear systems: non-zenoness and observability. SIAM J. Control Optim. **45**(5), 1769–1800 (2006)
256. Camlibel, M.K., Pang, J.S., Shen, J.: Lyapunov stability of complementarity and extended systems. SIAM J. Optim. **17**(4), 1056–1101 (2006)
257. Camlibel, M.K., Schumacher, J.M.: On the Zeno behaviour of linear complementarity systems. In: Proceedings of the IEEE Conference on Decision and Control, pp. 346–351 (2001)
258. Camlibel, M.K., Schumacher, J.M.: Linear passive systems and maximal monotone mappings. Math. Prog. Ser. B (2016). doi:10.1007/s10107-015-0945-7
259. Carricato, M., Merlet, J.P.: Stability analysis of underconstrained cable-driven parallel robots. IEEE Trans. Robot. **29**(1), 288–296 (2013)
260. Carriero, M., Pascali, E.: Il problema del rimbalzo unidimensionale e sue approssimazioni con penalizzazioni non convess. Rendiconti di Matematica **13**, 541–553 (1980). Ser.VI, fasc.1
261. Carriero, M., Pascali, E.: Uniqueness of the one-dimensional bounce problem as a generic property in $l_1([0, t], r)$. Bolletino U.M.I. 6(1-A), 87–91 (1982)
262. Cartan, H.: Cours de Calcul Différentiel. Hermann, Paris (1967)
263. Casagrande, D., Astolfi, A., Parisini, T.: Global asymptotic stabilization of the attitude and the angular rates of an underactuated non-symmetric rigid body. Automatica **44**(7), 1781–1789 (2008)
264. Casagrandi, R., Rinaldi, S.: A minimal model for forest fire regimes. Am. Nat. **153**, 527–539 (1999)
265. Casas, F., Chin, W., Grebogi, C., Ott, E.: Universal grazing bifurcations in impact oscillators. Phys. Rev. E **53**, 134–139 (1996)
266. Caselli, F., Frémond, M.: Collision of three balls on a plane. Comput. Mech. **43**, 743–754 (2009)
267. Catlla, A.J., Schaeffer, D.G., Witelski, T.P., Monson, E.E., Lin, A.L.: On spiking models for synaptic activity and impulsive differential equations. SIAM Rev. **50**(3), 553–569 (2008)
268. Ceanga, V., Hurmuzlu, Y.: A new look at an old problem: Newton's cradle. ASME J. Appl. Mech. **68**, 575–583 (2001)
269. Chakraborty, K., Das, K., Yu, H.: Modeling and analysis of a modified Leslie-Gower type three species food chain model with an impulsive control strategy. Nonlinear Anal.: Hybrid Syst. **15**, 171–184 (2015)
270. Chang, W.R.: Contact, adhesion and static friction of metallic rough surfaces. Ph.D. thesis, University of California, Berkeley, USA (1986)
271. Chang, W.R., Etsion, I., Bogy, D.B.: An elastic-plastic model for the contact of rough surfaces. ASME J. Tribol. **109**, 257–263 (1987)
272. Chang, W.R., Ling, F.F.: Normal impact model of rough surfaces. ASME J. Tribol. **114**, 439–447 (1992)
273. Chapnik, B.V., Heppler, G.R., Aplevich, J.D.: Modeling impact on a one-link flexible robotic arm. IEEE Trans. Robot. Autom. **7**, 479–488 (1991)
274. Chatterjee, A.: Rigid body collisions: Some general considerations, new collision laws, and some experimental data. Ph.D. thesis, Cornell University, Ithaca, NY, USA (1997)
275. Chatterjee, A.: Asymptotic solutions for solitary waves in a chain of elastic spheres. Phys. Rev. E **59**, 5912–5918 (1999)
276. Chatterjee, A.: On the realism of complementarity conditions in rigid body collisions. Nonlinear Dyn. **20**, 159–168 (1999)
277. Chatterjee, A., Ruina, A.: A critical study of the applicability of rigid-body collision theory-discussion. ASME J. Appl. Mech. **64**, 247–248 (1997)
278. Chatterjee, A., Ruina, A.: A new algebraic rigid body collision law based on impulse space considerations. ASME J. Appl. Mech. **65**, 939–951 (1998)
279. Chatterjee, S., Mallik, A.K.: Bifurcations and chaos in autonomous self-excited oscillators with impact damping. J. Sound Vib. **191**(4), 539–562 (1996)
280. Chatterjee, S., Mallik, A.K., Ghosh, A.: Impact dampers for controlling self-excited oscillators. J. Sound Vib. **193**(5), 1003–1014 (1996)

281. Chellaboina, V., Bhat, S.P., Haddad, W.M.: An invariance principle for nonlinear hybrid impulsive dynamical systems. Nonlinear Anal. **53**, 527–550 (2003)
282. Chen, M.Z.Q., Papageorgiou, C., Scheibe, F., Wang, F.C., Smith, M.C.: The missing mechanical circuit element. IEEE Circ. Syst. Mag. 10–26 (2009)
283. Chen, Q.Z., Acary, V., Virlez, G., Brüls, O.: A nonsmooth generalized-α scheme for flexible multibody systems with unilateral constraints. Int. J. Numer. Methods Eng. **96**(8), 487–511 (2013)
284. Chen, X., Xiang, S.: Perturbation bounds of P-matrix linear complementarity problems. SIAM J. Optim. **18**(4), 1250–1265 (2007)
285. Chernov, N.I., Sinai, Y.: Entropy of the gas of hard spheres with respect to the group of time space translations. In: Proceedings of the I.G. Petrovsky seminar, vol. 8, pp. 218–238 (1982)
286. Cherubini, A.M., Metafune, G., Paparella, F.: On the stopping time of a bouncing ball. Discrete Continuous Dyn. Syst. Ser. B **10**, 43–72 (2008)
287. Chin, W., Ott, E., Nusse, H.E., Grebogi, C.: Grazing bifurcations in impact oscillators. Phys. Rev. E **50**(6), 4427–4444 (1994)
288. Chiu, D., Lee, S.: Design and experimentation of jump impact controller. In: Proceedings of the IEEE International Conference on Robotics and Automation, pp. 1903–1908. Minneapolis, USA. (1996)
289. Choi, Y.S., Noah, S.T.: Forced periodic vibration of unsymmetric piecewise-linear systems. J. Sound Vib. **121**, 117–126 (1988)
290. Cholet, C.: Chocs de solides rigides. Ph.D. thesis, Laboratoire d'Analyse Numérique-Université Paris 6 and Laboratoire des Matériaux et des Structures du Génie Civil- LCPC-CNRS, Paris, France (1998)
291. Chow, S.N., Shaw, S.W.: Bifurcations in subharmonics. J. Differ. Equ. **65**, 304–320 (1986)
292. Chung, W.J., Kim, I.H., Joh, J.: Null-space dynamics-based control of redundant manipulators in reducing impact. Control Eng. Practice **5**(9), 1273–1282 (1997)
293. Clarke, F.H., Ledyaev, Y.S., Stern, R.J., Wolenski, P.R.: Nonsmooth Analysis and Control Theory. Springer, Graduate texts in Mathematics (1998)
294. Coaplen, J., Stronge, W.J., Ravani, B.: Work equivalent composite coefficient of restitution. Int. J. Impact Eng. **30**(6), 581–591 (2004)
295. Cobb, D.: On the solution of linear differential equations with singular coefficients. J. Differ. Equ. **46**, 310–323 (1982)
296. Cobb, D.: Descriptor variable systems and optimal state regulation. IEEE Trans. Autom. Control **28**(5), 601–611 (1983)
297. Cohen, H., Sithig, G.P.M.: Collisions of pseudo-rigid bodies: A Brach-type treatment. Int. J. Eng. Sci. **34**(3), 249–256 (1996)
298. Colombo, G., Henrion, R., Hoang, N.D., Mordukovich, B.S.: Optimal control of the sweeping process. Dyn. Contin. Discret. Impuls. Syst. Ser. B **19**, 117–159 (2012)
299. Colombo, G., Henrion, R., Hoang, N.D., Mordukovich, B.S.: Discrete approximations of a controlled sweeping process. Set-Valued Var, Anal (2015)
300. Cordova-Lepe, F., Pinto, M., Gonzalez-Olivares, E.: A new class of differential equations with impulses at instants dependent on preceding pulses. Applications to management of renewable resources. Nonlinear Analysis: Real World Applications **13**, 2313–2322 (2012)
301. Coriolis, G.: Théorie Mathématique du Jeu de Billard. Corilian Goeuvy, Paris (1835)
302. Coriolis, G.: Traité de la Mécanique des Corps Solides et du Calcul de l'Effet des Machines, seconde edn. Carilian-Goeury (1844)
303. Corless, M., Leitmann, G.: Continuous state feedback guaranteeing uniform ultimate boundedness for uncertain dynamical systems. IEEE Trans. Autom. Control **26**(5), 1139–1144 (1981)
304. Cornet, B.: Existence of slow solutions for a class of differential inclusions. J. Math. Anal. Appl. **96**(1), 130–147 (1983)
305. Cortes, J., Vinogradov, A.M.: Hamiltonian theory of constrained impulsive motion. J. Math. Phys. **47**, 042,905 (2006)

306. Coste, C., Falcon, E., Fauve, S.: Solitary waves in a chain of beads under Hertz contact. Phys. Rev. E **56**, 6104–6117 (1997). doi:10.1103/PhysRevE.56.6104
307. Cottle, R.W., Pang, J.S., Stone, R.E.: The Linear Complementarity Problem. Academic Press (1992)
308. Crawford, F.S.: A theorem on elastic collisions between ideal rigid bodies. Am. J. Phys. **57**(2), 121–125 (1989)
309. Crawford, F.S.: Time-reversal invariance in multiple collisions between coupled masses. Am. J. Phys. 57, 333 (1989). http://dx.doi.org/10.1119/1.16042
310. Crook, A.W.: A study of some impacts between metal bodies by a piezoelectric method. Proc. Roy. Soc. A, Math., Phys. Eng. Sci. **212**(1110), 377–390 (1952)
311. Cross, R.: The dead spot of a tennis racket. Am. J. Phys. **65**(8), 754–764 (1997)
312. Cross, R.: The bounce of a ball. Am. J. Phys. **67**(3), 222–227 (1999)
313. Cross, R.: The coefficient of restitution for collisions of happy balls, unhappy balls, and tennis balls. Am. J. Phys. **68**(11), 1025–1031 (2000)
314. Cross, R.: Measurements of the horizontal coefficient of restitution for a superball and a tennis ball. Am. J. Phys. **70**(5), 482–489 (2002)
315. Cross, R.: Vertical bounce of two vertically aligned balls. Am. J. Phys. **75**(11) (2007)
316. Cross, R.: Differences between bouncing balls, springs and rods. Am. J. Phys. **76**(10), 908–915 (2008)
317. Crossley, F.R.E., Oledzki, A., Szydlowski, W.: On modelling impacts of two bodies having flat and cylindrical surfaces with application to cam mechanisms. In: Proceedings of the 5th World Congres, pp. 1090–1092. IFToMM, Montreal, Canada (1979)
318. Cyril, X., Jaar, G.J., Misra, A.K.: The effect of a payload impact on the dynamics of a space robot. In: IEEE/RSJ International Conference on Intelligent Robots and Systems, pp. 2070–2075. Yokohama, Japan (1993)
319. Daimaruya, M., Naitoh, M., Kobayashi, H., Tanimura, S.: A sensing-plate method for measuring force and duration of impact in elastic-plastic impact of bodies. Experimental Mechanics September, 268–273 (1989)
320. d'Alembert, J.L.R.: Traité de Dynamique. David, Paris (1743)
321. ten Dam, A.A.: Representations of dynamical systems described by behavioral inequalities. In: Proceedings of European Control Conference, pp. 1780–1783. Groningen, NL (1993)
322. ten Dam, A.A.: Unilaterally constrained dynamical systems. Ph.D. thesis, Rijksuniversiteit Groningen, NL (1997). http://dissertations.ub.rug.nl/FILES/faculties/science/1997/a.a.ten.dam/thesis.pdf
323. ten Dam, A.A., Dwarshuis, E., Willems, J.: The contact problem for linear continuous-time dynamical systems: a geometric approach. IEEE Trans. Autom. Control **42**(4), 458–472 (1997)
324. Dankowicz, H., Jerrelind, J.: Control of near-grazing dynamics in impact oscillator. Proc. Roy. Soc. London A: Math., Phys. Eng. Sci. **461**, 3365–3380 (2005)
325. Dankowicz, H., Svahn, F.: On the stabilizability of near-grazing dynamics in impact oscillators. Int. J. Robust Nonlinear Control **17**, 1405–1429 (2007)
326. Darboux, G.: Sur le choc des corps. Comptes Rendus de l'Académie des Sciences **LXXVIII**, 1421–1425 (1874). Also page 1645 with friction; additions pages 1767
327. Darboux, G.: Etude géométrique sur les percussions et le choc des corps. Bulletin des Sciences Mathématiques et Astronomiques, deuxième série **4**(1), 126–160 (1880)
328. Dave, R., Yu, J., Rosato, A.D.: Measurements of collisional properties of spheres using high-speed video analysis. In: ASME Winter Annual Meeting, Symposium on Mechatronics, pp. 217–222 (1993)
329. Davies, H.G.: Random vibration of a beam impacting stops. J. Sound Vib. **68**(4), 479–487 (1980)
330. Deck, J.F., Dubowsky, S.: On the limitations of predictions of the dynamic response of machines with clearance connections. Flexible Mech., Dyn. Anal., ASME **47**, 461–469 (1992)

331. Deck, J.F., Dubowsky, S.: On the limitations of predictions of the dynamic response of machines with clearance connections. ASME J. Mech. Design **116**, 833–841 (1994)
332. Deimling, K.: Multivalued Differential Equations. Nonlinar Analysis and Applications. De Gruyter, New York (1992)
333. Delassus, E.: Mémoire sur la théorie des liaisons finies unilatérales. Annales Scientifiques del' Ecole Normale Supèrieure **34**, 95–179 (1917)
334. Delassus, E.: Considérations sur le frottement de glissement. Nouvelles Annales de Math., 4ème série **20**, 485–496 (1920)
335. Delassus, E.: Exposé élémentaire d'une théorie rigoureuse des liaisons finies unilatérales. Nouvelles Annales de Mathématiques, 4ème série, tome **20** pp. 1–12 (1920). Second part pp. 81–93
336. Delassus, E.: Sur les lois du frottement de glissement. Bull. Soc. Math. France **51**, 22–33 (1923)
337. Delassus, E., Pérès, J.: Note sur le choc en tenant compte du frottement de glissement. Nouvelles Annales de Mathématiques, 5ème série **2**, 383–391 (1923)
338. Deodhar, D.B.: Phil. Mag. **48**, 89 (1924)
339. Dercole, F., Maggi, S.: Detection and continuation of a border collision bifurcation in a forest fire model. Appl. Math. Comput. **168**, 623–635 (2005)
340. Derjaguin, B.V., Muller, V.M., Toporov, Y.P.: Effect of contact deformations on the adhesion of particles. J. Colloid Interf. Sci. **53**(2), 314–326 (1977)
341. Dieudonné, J.: Eléments d'Analyse, tome 2. Gauthier-Villars, Paris (1969)
342. Dilley, J.P.: Energy loss in collisions of icy spheres: Loss mechanism and size-mass dependence. Icarus **105**, 225–234 (1993)
343. Dimitrov, D.N., Yoshida, K.: Momentum distribution in a space manipulator for facilitating the post-impact control. In: Proceedings of IEEE/RSJ International Conference on Intelligent Robots and Systems, pp. 3345–3350. Sendai, Japan (2004)
344. Din, Q., Donchev, T., Nosheen, A., Rafaqat, M.: Runge-Kutta methods for differential equations with variable time of impulses. Numer. Funct. Anal. Optim. **36**, 777–791 (2015)
345. Ding, X., Wu, K., Liu, M.: The Euler scheme and its convergence for impulsive delay differential equations. Appl. Math. Comput. **216**, 1566–1570 (2010)
346. Dintwa, E., van Zeebroeck, M., Ramon, H., Tijskens, E.: Finite element analysis of the dynamic collision of apple fruit. Postharvest Biology and Technology **49**, 260–276 (2008)
347. Diolaiti, N., Melchiorri, C., Stramigioli, S.: Contact impedance estimation for robotic systems. IEEE Trans. Robot. **21**(5), 925–935 (2005)
348. Dizqah, A.M., Maheri, A., Busawon, K., Fritzson, P.: Standalone DC microgrids as complementarity dynamical systems: Modeling and applications. Control Eng. Pract. **35**, 102–112 (2015)
349. Djerassi, S.: Collision with friction; part A: Newtons hypothesis. Part B: Poisson and Stornge's hypothesis. Multibody Syst. Dyn. **21**(1), 37–70 (2009)
350. Djerassi, S.: Three-dimensional, one-point collision with friction. Multibody Syst. Dyn. **27**(2), 173–195 (2012)
351. Djerassi, S., Faibish, S., Prinz, M.: Three phase motion control of robotic arms. In: Proceedings of IEEE International Conference on Robotics and Automation, pp. 3695–3700. Minneapolis, USA (1996)
352. Domenech-Carbo, A.: On the tangential restitution problem: independent friction-restitution modeling. Granular Matter **16**(4), 573–582 (2014)
353. Dona, J.A.D., Lévine, J.: On barriers in state and input constrained nonlinear systems. SIAM J. Control Optim. **51**(4), 3208–3234 (2013)
354. Donahue, C.M., Hrenya, C.M., Zelinskaya, A.P., Nakagawa, K.J.: Newton's cradle undone: experiments and collision models for the normal collision of three solid spheres. Physi. Fluids **20**, 113,301 (2008)
355. Donchev, T., Farkhi, E., Mordukhovich, B.S.: Discrete approximations, relaxation, and optimization of one-sided Lipschitzian differential inclusions in Hilbert spaces. J. Differ. Equ. **243**, 301–328 (2007)

356. Dontchev, A., Lempio, F.: Difference methods for differential inclusions: a survey. SIAM Rev. **34**(2), 263–294 (1992)
357. Dorbolo, S., Volfson, D., Tsimring, L., Krudolli, A.: Dynamics of a bouncing dimer. Phys. Rev. Lett. **95**(4), 1–4 (2005)
358. Doris, A., Juloski, A.L., Mihajlovic, N., Heemels, W.P.M.H., van de Wouw, N.: Observer design for experimental non-smooth and discontinuous systems. IEEE Trans. Control Syst. Technol. **16**(6), 1323–1332 (2008)
359. Doubrovine, B., Novikov, S., Fomenko, A.: Géométrie contemporaine, Méthodes et applications, 1ère partie: Géométrie des surfaces, des groupes de transformations et des champs. MIR, Moscou (1982)
360. Doyle, J.F.: Further developments in determining the dynamic contact law. Exp. Mech. **24**, 265–270 (1984)
361. Doyle, J.F.: A wavelet deconvolution method for impact force identification. Exp. Mech. **37**(4), 403–408 (1997)
362. Drazetic, P., Level, P., Canaple, B., Mongenie, P.: Impact on planar kinematic chains of rigid bodies: Application to movements of anthropomorphic dummy in a crash. Int. J. Impact Eng. **18**(5), 505–516 (1996)
363. Du, Y., Wang, S.: Energy dissipation innormal elastoplastic impact between two spheres. ASME J. Appl. Mech. **76**(6), 061,010 (2009)
364. Dubowsky, S., Young, S.C.: An experimental and analytical study of connection forces in high-speed mechanisms. ASME J. Eng. Ind. **87**, 1166–1174 (1975)
365. Duckwald, C.S.: Impact damping for turbine buckets. Report R55GL108, General engineering laboratory, General Electric (1955)
366. Dugas, R.: Histoire de la Mécanique. Dunod et éditions du Griffon, Paris, France and Neuchatel, Suisse (1950)
367. Duindam, V., Stramigioli, S.: Singularity-free dynamic equations of open-chain mechanisms with general holonomic and nonholonomic joints. IEEE Trans. Robot. **24**(3), 517–526 (2008)
368. Dumont, Y., Lubuma, J.M.S.: Non-standard finite-difference methods for vibro-impact problems. Proc. Roy. Soc. London A: Math., Phys. Eng. Sci. **461**(2058), 1927–1950 (2005). doi:10.1098/rspa.2004.1425
369. Dupont, P.E.: The effect of Coulomb friction on the existence and uniqueness of the forward dynamics problem. In: Proceedings of the IEEE International Conference on Robotics and Automation, pp. 1442–1447. Nice, France (1992)
370. Dupont, P.E., Yamajako, S.P.: Stability of rigid body dynamics with sliding frictional contacts. IEEE Trans. Robot. Autom. **13**(2), 230–236 (1997)
371. Durand, S.: Contact Mechanics, chap. Unilateral contact with bounces. Plenum Press, New York (1995)
372. Durand, S.: Dynamique des systèmes à liaisons unilatérales avec frottement sec. Ph.D. thesis, Ecole Nationale des Ponts et Chaussées, Paris, France (1996)
373. Dyagel, R.V., Lapshin, V.V.: On a nonlinear viscoelastic model of Hunt-Crossley impact. Mech. Solids **46**(5), 798–806 (2011)
374. Dzonou, R., Marques, M.D.P.M.: A sweeping process approach to inelastic contact problems with general inertia operators. Eur. J. Mech. A/Solids **26**(3), 474–490 (2007)
375. Dzonou, R., Marques, M.D.P.M., Paoli, L.: A convergence result for a vibro-impact problem with a general inertia operator. Nonlinear Dyn. **58**(1–2), 361–384 (2009)
376. Eames, J.: A remark upon the new opinion relating to the forces of moving bodies, in the case of the collision of non-elastic bodies. Philos. Trans. **xxxiv**, 183–187 (1726)
377. Earles, S.W.E., Seneviratne, L.D.: Design guidelines for predicting contact loss in revolute joints of planar linkage mechanisms. Proc. Instn. Mech. Engrs. **204**, 9–18 (1990)
378. van Eijndhoven, J.: Solving the linear complementarity problem in circuit simulation. SIAM J. Control Optim. **24**, 1050–1062 (1986)
379. ElGawady, M.A., Ma, Q., Butterworth, J.W., Ingham, J.: Effects of interface material on the performance of free rocking blocks. Earthquake Eng. Struc. Dyn. **40**(4), 375–392 (2011)

380. Eppinger, S.D., Seering, W.P.: Understanding bandwidth limitations robot force contro. In: IEEE International Conference on Robotics and Automation, pp. 904–909. Raleigh, USA (1987)
381. Erdmann, M.: On a representation of friction in configuration space. Int. J. Robot. Res. **13**(3), 240–271 (1994)
382. Estabrook, L.H., Plunkett, R.: Design parameters for impact dampers. Report R55GL250, General Engineering laboratory, General Electric (1955)
383. Etsion, I., Klingerman, Y., Kadin, Y.: Unlaoding of an elastic-plastic loaded spherical contact. Int. J. Solids Struct. **42**(13), 3716–3729 (2005)
384. Everson, R.M.: Chaotic dynamics of a bouncing ball. Phys. D **19**(3), 355–383 (1986)
385. Facchinei, F., Pang, J.S.: Finite-Dimensional Variational Inequalities and Complementarity Problems, vol. I. Springer, Springer Series in Operations Research (2003)
386. Falcon, E., Laroche, C., Fauve, S., Coste, C.: Behaviour of one inelastic ball bouncing repeatedly off the ground. Eur. Phys. J. B **3**(1), 45–57 (1998)
387. Falcon, E., Laroche, C., Fauve, S., Coste, C.: Collision of a 1-D column of beads with a wall. Eur. Phys. J. B **5**(1), 111–131 (1998)
388. Fang, X., Zhang, C., Chen, X., Wang, Y., Tan, Y.: A new universal approximate model for conformal contact and non-conformal contact of spherical surfaces. Acta Mech. (2015). doi:10.1007/s00707-014-1277-z
389. Faulring, E.L., Lynch, K.M., Colgate, J.E., Peshkin, M.A.: Haptic display of constrained dynamic systems via admittance displays. IEEE Trans. Robot. **23**(1), 101–111 (2007)
390. Feigin, M.I.: Resonance behaviour of a dynamical system with collisions. J. Appl. Math. Mech. **30**(5), 1118–1123 (1966)
391. Feigin, M.I.: Dynamic theory of a controlled vibration damping model. J. Appl. Math. Mech. **31**(1), 166–171 (1967)
392. Feigin, M.I.: Doubling the oscillation period with c-bifurcations in piecewise continuous systems. J. Appl. Math. Mech. **34**(5), 822–830 (1970)
393. Feigin, M.I.: On the generation of sets of subharmonic modes in a piecewise continuous system. J. Appl. Math. Mech. **38**(5), 759–767 (1974)
394. Feigin, M.I.: On the behaviour of dynamic systems in the vicinity of existence boundaries of periodic motions. J. Appl. Math. Mech. **41**(4), 642–650 (1977)
395. Feng, Q., Tu, J.: Modeling and algorithm on a class of mechanical systems with unilateral constraints. Arch. Appl. Mech. **76**(1–2), 103–116 (2006). doi:10.1007/s00419-006-0008-x
396. Ferretti, G., Maffezzoni, C., Magnani, G., Rocco, P.: Simulating discontinuous phenomana affecting robot motion. J. Intell. Robot. Syst. **15**, 53–65 (1996)
397. Filippov, A.F.: Differential Equations with Discontinuous Right Hand Sides. Kluwer Academic Publishers, Dordrecht (1988)
398. Filippov, A.F.: Application of the axiomatic method for the investigation of differential equations with singularities. Differ. Equ. **32**(2), 208–218 (1996)
399. Fitz-Coy, N.G., Cochran, J.E.: Space station/shuttle orbiter dynamics during docking. In: Structural Dynamics and Control Interaction of Flexible Structure conference, pp. 133–174. NASA Conference publication 2467, Huntsville, AL (1986)
400. Flores, P., Ambrosio, J., Claro, J.C.P., Lankarani, H.M.: Kinematics and Dynamics of Multibody Systems with Imperfect Joints. Lecture Notes in Applied and Computational Mechanics, vol. 34. Springer, Heidelberg (2008)
401. Flores, P., Koshy, C.S., Lankarani, H.M., Ambrosio, J., Claro, J.C.P.: Numerical and experimental investigation on multibody systems with revolute clearance joints. Nonlinear Dyn. **65**, 383–398 (2011)
402. Flores, P., Leine, R.I., Glocker, C.: Modeling and analysis of planar rigid multibody systems with translational clearance joints based on the non-smooth dynamics approach. Multibody Syst. Dyn. **23**, 165–190 (2010). doi:10.1007/s11044-009-9178-y
403. Flores, P., Machado, M., Silva, M.T., Martins, J.M.: On the continuous contact force models for soft materials in multibody dynamics. Multibody Syst. Dyn. **25**, 357–375 (2011)

404. Foale, S., Bishop, S.R.: Dynamical complexities of forced impacting systems. Phil. Trans. R. Soc. Lond. **338**, 547–556 (1992)
405. Foale, S., Bishop, S.R.: Bifurcations in impact oscillations. Nonlinear Dyn. **6**(3), 285–299 (1994)
406. Foale, S., Bishop, S.R.: Nonlinearity and Chaos in Engineering Dynamics, j.m.t. thompson and s.r. bishop edn., chap. Bifurcations in impact oscillators: theory and experiments. Wiley, Australia (1994)
407. Foerster, S., Louge, M., Chang, H., Allia, K.: Measurements of the collision properties of small spheres. Phys. Fluids **6**(3), 1108–1115 (1994). http://dx.doi.org/10.1063/1.868282
408. Forni, F., Teel, A.R., Zaccarian, L.: Follow the bouncing ball: Global results on tracking and state estimation with impacts. IEEE Trans. Autom. Control **58**(6), 1470–1485 (2013)
409. Fraczek, J., Wojtyra, M.: On the unique solvability of a direct dynamics problem for mechanisms with redundant constraints and Coulomb friction in joints. Mech. Mach. Theory **46**(3), 312–334 (2011)
410. Franaszek, M., Isomaki, H.M.: Anomalous chaotic transients and repellers of the bouncing ball dynamics. Phys. Rev. A **43**(8), 4231–4237 (1991)
411. Frasca, R., Camlibel, M.K., Goknar, I.C., Iannelli, L.: Linear passive networks with ideal switches: Consistent initial conditions and state discontinuities. IEEE Trans. Circ. Syst. I: Regul. Pap. **57**(12), 3138–3151 (2010)
412. Frasca, R., Camlibel, M.K., Goknar, I.C., Iannelli, L., Vasca, F.: State discontinuity analysis of linear switched systems via energy function optimization. In: Proceedings of IEEE Symposium on Circuits and Systems ISCAS2008, pp. 540–543. Seattle, USA (2008)
413. Frémond, M.: Contact mechanics international symposium, chap. In: Raous, M., Jean, M., Moreau, J.J. (eds.) Chocs d'un solide rigide avec un plan. Plenum Press, Carry-le-Rouet, France (1994)
414. Frémond, M.: Rigid bodies collisions. Phys. Lett. A **204**(1), 33–41 (1995)
415. Frémond, M.: Non-Smooth Thermo-mechanics. Springer, Berlin (2002)
416. Frémond, M.: Collisions. Facolta di Ingegneria di Roma Tor Vergata, Roma (2007). (In French)
417. From, P.J.: An explicit formulation of singularity-free dynamic equations of mechanical systems in lagrangian form-part one: Single rigid bodies. Part two: Multibody systems. Modeling, Identification and Control **33**(2), 45–68 (2012)
418. Fu, C.C., Paul, B.: Dynamic stability of an impact system connected with rock drilling. ASME J. Appl. Mech. **91**(4), 743–749 (1969)
419. Fufaev, N.A.: Dynamics of the system in the Painlevé-Klein example: the Painlevé paradoxes. Izv. AN SSSR MTT (Mech. Solids) **26**(4), 45–50 (1991)
420. Fumagalli, M., Naldi, R., Macchelli, A., Forte, F., Keemink, A.Q.L., Stramigioli, S., Carloni, R., Marconi, L.: Developping and aerial manipulator prototype. IEEE Robot. Autom. Mag. 41–50 (2014)
421. Gajewski, K., Radziszewski, B.: On the stability of impact systems. Bull. Polish Acad. Sci., Tech. Sci., Appl. Mech. **35**(3–4), 183–189 (1987)
422. Gale, D.: An indeterminate problem in classical mechanics. Am. Math. Mon. **59**(5), 291–295 (1952)
423. Galeani, S., Menini, L., Potini, A.: A., Tornambé: Trajectory tracking for a particle in elliptical billiards. Int. J. Control **81**(2), 189–213 (2008)
424. Galias, Z., Yu, X.: Complex discretization behaviours of a simple sliding-mode control system. IEEE Trans. Circuits Syst.-II: Express. Briefs **53**(8), 652–656 (2006)
425. Galias, Z., Yu, X.: Analysis of zero-order holder discretization of two-dimensional sliding-mode control systems. IEEE Trans. Circ. Syst.-II: Express. Briefs **55**(12), 1269–1273 (2008)
426. Gan-Mor, S., Galili, N.: Rheological model of fruit collision with an elastic plate. J. Agric. Eng. Res. **75**, 139–147 (2000)
427. Gao, X.L., Mao, C.L.: Solution of the contact problemof a rigid conical frustum indenting a transversally isotropic elastic half-space. ASME J. Appl. Mech. **81**, 041,007 (2014)

428. Garcia, C.: Comparison of friction models applied to a control valve. Control Eng. Pract. **16**, 1231–1243 (2008)
429. de Jalon, G.: J., Gutierrez-Lopez, M.D.: Multibody dynamics with redundant constraints and singular mass matrix: existence, uniqueness, and determination of solutions for accelerations and constraints forces. Multibody Syst. Dyn. **30**(3), 311–341 (2013). doi:10.1007/s11044-013-9358-7
430. Garcia-Ramos, F.J., Valero, C., Homer, I., Ortiz-Canavate, J., Ruiz-Altisent, M.: Non-destructive fruit firmless sensors: a review. Span. J. Agric. Res. **3**(1), 61–73 (2005)
431. Garfinkel, B.: Topics in optimization, Math. Sci. Eng., vol. 31, chap. Discontinuities in a variational problem. Academic Press, New York (1967)
432. Garfinkel, B.: Topics in Optimization, chap. In: Leitmann, G. (ed.) Inequalities in a variational problem. Academic Press, New York (1967)
433. Garwin, R.L.: Kinematics of an ultraelastic rough ball. Am. J. Phys. **37**(1), 88–92 (1969)
434. Gauld, C.: Solutions to the problem of impact in the 17th and 18th centuries and teaching Newton's third law today. Sci. Edu. **7**, 49–67 (1998)
435. Gendelman, O.V.: Targeted energy transfer in systems with non-polynomial nonlinearity. J. Sound Vib. **315**, 732–745 (2008)
436. Génot, F.: Contributions à la modèlisation et à la commande des systèmes mécaniques de corps rigides avec contraintes unilatérales. Ph.D. thesis, Grenoble National Institute of Technology (INPG), Computer Science Doctoral School, Grenoble (1998)
437. Génot, F., Brogliato, B.: New results on Painlevé paradoxes. Eur. J. Mech. A/Solids **18**(4), 653–677 (1999). https://hal.inria.fr/inria-00073323 (See also INRIA Research Report RR-3366)
438. Georgescu, C., Brogliato, B., Acary, V.: Switching, relay and complementarity systems: a tutorial on their well-posedness and relationships. Phys. D: Nonlinear Phenom. **241**(22), 1985–2002 (2012)
439. Gerl, F., Zippelius, A.: Coefficient of restitution for elastic disks. Phys. Rev. E **59**(2), 2361–2372 (1999)
440. Gertz, M.W., Kim, J.O., Khosla, P.: Exploiting redundancy to reduce impact force. In: IEEE/RSJ International Conference Intellegent Robotic Systems, vol. 1, pp. 179–184. Osaka, Japan (1991)
441. Gharib, M., Celik, A., Hurmuzlu, Y.: Shock absorption using linear particle chains with multiple impacts. ASME J. Appl. Mech. **73**, 031,005 (2011)
442. Gharib, M., Hurmuzlu, Y.: A new contact force model for low coefficient of restitution impact. ASME J. Appl. Mech. **79**(6), 064,506 (2012)
443. Gheadnia, H., Cermik, O., Marghitu, D.B.: Experimental and theoretical analysis of the elasto-plastic oblique impact of a rod with a flat. Int. J. Impact Eng. **86**, 307–317 (2015)
444. Gheadnia, H., Marghitu, D.B., Jackson, R.L.: Predicting the permanent deformation after the impact of a rod with a flat surface. J. Tribol. **137**(1), 011,403 (2014)
445. Giannakopoulos, A.E., Suresh, S.: Determination of elastoplastic properties by instrumented sharp indentation. Scripta Materialia **40**(10), 1191–1198 (1999)
446. Gibbs, J.W.: On the fundamental formulae of dynamics. Am. J. Math. **2**, 49–64 (1879)
447. Gilmore, B.J., Cipra, R.J.: Simulation of planar dynamic mechanical systems with changing topologies: Part 1: Characterization and prediction of the kinematic constraint; part 2: Implementation strategy and simulation resuls for example dynamic systems. In: Rao, S. (ed.) Advances in Design Automation, pp. 369–388. ASME (1987)
448. Glocker, C.: The principles of d'Alembert, Jourdain and Gauss in nonsmooth dynamics. part I: Scleronomic multibody systems. ZAMM Z. Angew. Math. Mech. **78**, 21–37 (1998)
449. Glocker, C.: Discussion of d'Alembert's principle for nonsmooth unilateral constraints. ZAMM J. Appl. Math. Mech. **79**(S1), 91–94 (1999). doi:10.1002/zamm.19990791324
450. Glocker, C.: Velocity jumps induced by C^0-constraints. In: Proceedings of the ASME 1999 Design Engineering Technical Conferences. Las Vegas (1999). DETC99/VIB-8344
451. Glocker, C.: On frictionless impact models in rigid-body systems. Philos. Trans. Roy. Soc. London **359**(1789), 2385–2404 (2001)

452. Glocker, C.: Set-Valued Force Laws: Dynamics of Non-Smooth Systems. Lecture Notes in Applied Mechanics, vol. 1. Springer, Heidelberg (2001)
453. Glocker, C.: Models of non-smooth switches in electrical systems. Int. J. Circ. Theory Appl. **33**, 205–234 (2005)
454. Glocker, C.: An introduction to impacts. In: Haslinger, J., Stavroulakis, G. (eds.) Nonsmooth Mechanics of Solids, CISM Courses and Lectures, vol. 485. Springer, Wien (2006)
455. Glocker, C.: Energetic consistency conditions for standard impacts. Part I: Newton-type inequality impact laws and Kanes example. Multibody Syst. Dyn. (2013). doi:10.1007/s11044-012-9316-9
456. Glocker, C.: Energetic consistency conditions for standard impacts. Part II: Poisson-type inequality impact laws. Multibody Syst. Dyn. **32**, 445–509 (2014). doi:10.1007/s11044-013-9387-2
457. Glocker, C., Pfeiffer, F.: Dynamical systems with unilateral contacts. Nonlinear Dyn. **3**(4), 245–259 (1992)
458. Glocker, C., Pfeiffer, F.: Multiple impacts with friction in rigid multibody systems. Nonlinear Dyn. **7**(4), 471–497 (1995). doi:10.1007/BF00121109
459. Glocker, C., Studer, C.: Formulation and preparation for numerical evaluation of linear complementarity systems in dynamics. Multibody Syst. Dyn. **13**(4), 447–463 (2005). doi:10.1007/s11044-005-2519-6
460. Goebel, R., Sanfelice, R.G., Teel, A.R.: Hybrid dynamical systems. **29**(2), 28–93 (2009)
461. Goebel, R., Sanfelice, R.G., Teel, A.R.: Hybrid Dynamical Systems: Modeling, Stability, and Robustness. Princeton University Press (2012)
462. Goebel, R., Teel, A.R.: Lyapunov characterization of Zeno behavior in hybrid systems. In: Proceedings of 47th IEEE Conference on Decision and Control, pp. 2752–2757. Cancun, Mexico (2008)
463. Goeleven, D., Brogliato, B.: Stability and instability matrices for linear evolution variational inequalities. IEEE Trans. Autom. Control **49**(4), 521–534 (2004)
464. Goeleven, D., Brogliato, B.: Necessary conditions of asymptotic stability for unilateral dynamical systems. Nonlinear Anal.: Theory, Methods Appl. **61**(6), 961–1004 (2005)
465. Goeleven, D., Motreanu, D., Dumont, Y., Rochdi, M.: Variational and Hemivariational Inequalities: Theory, Methods and Applications, Nonconvex Optimization and its Applications, vol. I: Unilateral Analysis and Unilateral Mechanics. Springer Science+Business Media, New York (2003)
466. Goeleven, D., Panagiotopoulos, P.D., Lebeau, C., Plotnikova, G.: Inequality forms of d'Alembert's principle in mechanics of systems with holonomic unilateral constraints. ZAMM-J. Appl. Math. Mech. **77**(7), 483–501 (1997)
467. Goldman, P., Muszynska, A.: Dynamic effects in mechanical structures with gaps and impacting: Order and chaos. ASME J. Vib. Acoust. **116**(4), 541–547 (1994)
468. Goldsmith, W.: The coefficient of restitution. Bull. Appl. Mech. Div., Am. Soc. Engrs. Educ. **2**, 10 (1952)
469. Goldsmith, W.: Impact : The Theory and physical Behaviour of Colliding Solids. Edward Arnold Publishers, London (1960). Dover edition published in 2001
470. Gonthier, Y., McPhee, J., Lange, C., Piedboeuf, J.: A regularized contact model with asymmetric damping and dwell-time dependent friction. In: Forum 2002, SCGM Queen's University. Kingston, ON, Canada (2002)
471. Gonthier, Y., McPhee, J., Lange, C., Piedboeuf, J.: A regularized contact model with asymmetric damping and dwell-time dependent friction. Multibody Syst. Dyn. **11**(3), 209–233 (2004)
472. Gontier, C., Toulemonde, C.: Approach to the periodic and chaotic behaviour of the impact oscillator by a continuation method. Eur. J. Mech. A/Solids **16**(1), 141–163 (1997)
473. Gorbikov, S.P.: Differential equations determined by dynamical systems with shock interactions on the boundary of the domain where infinite-shock motions exist. Differ. Equ. **34**(1), 16–21 (1998)

474. Goyal, S., Pinson, E.N., Sinden, F.W.: Simulation of dynamics of interactiong rigid bodies including friction I: General problem and contact mode. Eng. Comput. **10**(3), 162–174 (1994). doi:10.1007/BF01198742
475. Goyal, S., Pinson, E.N., Sinden, F.W.: Simulation of dynamics of interactiong rigid bodies including friction II: Software system design and implementation. Eng. Comput. **10**(3), 175–195 (1994). doi:10.1007/BF01198743
476. Grace, I.M., Ibrahim, R.A., Pilipchuk, V.N.: Inelastic impact dynamics of ships with one-sided barriers. Part I: analytical and numerical investigations. Part II: experimental validation. Nonlinear Dyn. **66**, 589–623 (2011)
477. Gramain, A.: Intégration. Hermann, Paris (1988)
478. Grasselli, Y., Bossis, G., Goutallier, G.: Velocity-dependent restitution coefficient and granular cooling in microgravity. EPL **86**, 60,007 (2009). doi:10.1209/0295-5075/86/60007
479. Greenberg, L.H.: Discoveries in Physics for Scientists and Engineers. Saunders, Philadelphia, USA (1975)
480. Greenhalgh, S., Acary, V., Brogliato, B.: On preserving dissipativity properties of linear complementarity dynamical systems with the θ-method. Numerische Mathematik **125**, 601–637 (2013). doi:10.1007/s00211-013-0553-5
481. Gregory, J., Lin, C.: Constrained Optimization in the Calculus of Variations and Optimal Control Theory. Chapman and Hall, London (1992)
482. Grizzle, J.W., Abba, G., Plestan, F.: Asymptotically stable walking for biped robots: Analysis via systems with impulse effects. IEEE Trans. Autom. Control **46**(1), 51–64 (2001)
483. Grizzle, J.W., Chevallereau, C., Sinnet, R.W., Ames, A.D.: Models, feedback control, and open problems of 3D bipedal robotic walking. Automatica (2014). http://dx.doi.org/10.1016/j.automatica.2014.04.021
484. Grubin, C.: On the theory of the acceleration damper. ASME J. Appl. Mech. pp. 373–378 (1956)
485. Grubin, C., Lieber, P.: Further considerations on the theory of the acceleration damper. Report TR AE54021, Rensselaer Polytechnic Institute Aeronautical Laboratory (1954)
486. Guan, Z.H., Qian, T.H., Yu, X.: On controllability and observability for a class of impulsive systems. Syst. Control Lett. **47**, 247–257 (2002)
487. Guckenheimer, J., Holmes, P.: Nonlinear Oscillations, Dynamical Systems, and Bifurcations of Vector Fields, Applied Mathematical Sciences, vol. 42. Springer, New York (1983)
488. Guelfand, I.M., Chilov, G.E.: Les Distributions. Tome 2. Espaces Fondamentaux. Dunod, Paris (1964)
489. Gummer, A., Sauer, B.: Modeling planar slider-crank mechanisms with clearance joints in RecurDyn. Multibody Syst. Dyn. **31**, 127–145 (2014)
490. Gumowski, I., Mira, C.: L'Optimisation- La Théorie et ses Problèmes. Dunod, Paris (1970)
491. Gwinner, J.: On a new class of differential variational inequalities and a stability result. Math. Program. Ser. B **139**, 205–221 (2013)
492. Haake, S. (ed.): The Engineering of Sport. A.A. Balkema, Rotterdam (1996) Proceedings of 1st International Conference on Engineerng of Sport, Sheffield, UK, 1996
493. Haddad, W.M., Chellaboina, V., Hui, Q., Nersesov, S.: Vector dissipativity theory for large-scale impulsive dynamical systems. Math. Probl. Eng. (3), 225–262 (2004). http://dx.doi.org/10.1155/S1024123X04310021
494. Haddad, W.M., Chellaboina, V., Nersesov, S.G.: Impulsive and Hybrid Dynamical Systems. Princeton University Press, Applied Mathematics (2006)
495. Haines, R.S.: Survey: 2-dimensional motion and impact at revolute joints. Mech. Mach. Theory **15**(5), 361–370 (1980)
496. Hairer, E., Wanner, G.: Solving Ordinary Differential Equations II. Stiff and Differential-Algebraic Problems. Springer Series in Computational Mathematics. Springer (2002). Second revised edition
497. Hale, J.K., Koçak, H.: Dynamics and Bifurcations, Texts in Applied Mathematics, vol. 3. Springer (1991)

498. Hamel, G.: Bemerkungen zu den vorstehenden aufsätzen der herren F. Klein und R. v. Mises. Zeitsch. Math. Phys. **58**, 195–196 (1910)
499. Hamel, G.: Theoretische Mechanik. Springer, Berlin (1949). Pp.393-402, pp. 543–549
500. Han, I., Gilmore, B.J.: Multi-body impact motion with friction-analysis, simulation, and experimental validation. ASME J. Mech. Design **115**(3), 412–422 (1993). doi:10.1115/1.2919206
501. Han, L., Pang, J.S.: Non-Zenoness of a class of differential quasi-variational inequalities. Math. Program. Ser. A **121**, 171–199 (2010)
502. Han, L., Tiwari, A., Camlibel, M.K., Pang, J.S.: Convergence of time-stepping schemes for passive and extended linear complementarity systems. SIAM J. Numer. Anal. **47**(5), 3768–3796 (2009)
503. Hardy, C., Baronet, C.N., Tordion, G.V.: The elasto-plastic indentation of a half-space by a rigid sphere. Int. J. Numer, Methods Eng **3**(4), 451–462 (1971)
504. Hartl, R.F., Sethi, S.P., Vickson, R.G.: A survey of the maximum principles for optimal control problems with state constraints. SIAM Rev. **37**(2), 181–212 (1995)
505. Hatzes, A.P., Bridges, F.G., Lin, D.N.C.: Collisional properties of ice spheres at low impact velocities. Mon. not. R. Astr. Soc. **231**, 1091–1115 (1988)
506. Haug, E.J., Wu, S.C., Yan, S.M.: Dynamics and mechanical systems with Coulomb friction, stiction, impact and constraint addition-deletion-i. Mech. Mach. Theory **21**(5), 401–416 (1986)
507. Hayakawa, H., Kuninaka, H.: Simulation and theory of the impact of two-dimensional elastic disks. Chem. Eng. Sci. **57**(2), 239–252 (2002)
508. Hayakawa, H., Kuninaka, H.: Theory of inelastic impact of elastic materials. Phase Transitions: A Multinational J. **77**(8–10), 889–909 (2004)
509. Hayashi, T., Crossley, F.R.E., Larionescu, D.: Analog simulations of repetitive impacts. In: Proceedings 4th World Congress, pp. 1073–1077. IFToMM, Newcastle upon Tyne, England (1975)
510. He, M., Chen, F., Li, Z.: Almost periodic solution of an impulsive differential equation model of plankton allelopathy. Nonlinear Anal.: Real World Appl. **11**, 2296–2301 (2010)
511. Heck, D., Saccon, A., van de Wouw, N., Nijmeijer, H.: Guaranteeing stable tracking of hybrid position-force trajectories for a robot manipulator interacting with a stiff environment. Automatica **63**, 235–247 (2016)
512. Heemels, W.P.M.H., Brogliato, B.: The complementarity class of hybrid dynamical systems. Eur. J. Control **9**(2–3), 322–360 (2003)
513. Heemels, W.P.M.H., Camlibel, M.K., van der Schaft, A.J., Schumacher, H.: Modelling, well-posedness, and stability of switched electrical networks. In: Maler, O., Pnueli, A. (eds.) Proceedings of 6th International Workshop Hybrid Systems: Computation and Control. Lecture Notes in Computer Science, vol. 2623, pp. 249–266. Springer, Prague, Czech Republic (2003)
514. Heemels, W.P.M.H., Camlibel, M.K., Schumacher, J.M., Brogliato, B.: Observer-based control of linear complementarity systems. Int. J. Robust Nonlinear Control **21**(10), 1193–1218 (2010)
515. Heemels, W.P.M.H., Johansson, K.H., Tabuada, P.: An introduction to event-triggered and self-triggered control. In: Proceedings of the 51st IEEE Conference on Decision and Control, pp. 3270–3285. Hawaii, USA (2012)
516. Heemels, W.P.M.H., Schumacher, J.M., Weiland, S.: Well-posedness of linear complementarity systems. In: Proceedings of the 38th IEEE International Conference on Decision and Control, pp. 3037–3042. Phoenix, Arizona, USA (1999)
517. Heemels, W.P.M.H., Schumacher, J.M., Weiland, S.: Linear complementarity systems. SIAM J. Appl. Math. **60**(4), 1234–1269 (2000)
518. Heiman, M.S., Sherman, P.J., Bajaj, A.K.: On the dynamics and stability of an inclined impact pair. J. Sound Vib. **114**(3), 535–547 (1987)
519. Heimann, P.M.: Geometry and nature: Leibniz and Johann Bernoulli's theory of motion. Centaurus **21**(1), 1–26 (1977)

520. Hendricks, F.: Bounce and chaotic motion in impact print hammers. IBM J. Res. Dev. **27**(3), 24–31 (1983)
521. Henry, C.: An existence theorem for a class of differential equations with multivalued right-hand side. J. Math. Anal. Appl. **41**, 179–186 (1973)
522. Herbert, R.G., McWhannel, D.C.: Shape and frequency composition of pulses from an impact pair. ASME J. Eng. Ind. **99**(3), 513–518 (1977). doi:10.1115/1.3439270
523. Herman, P., Kozlowski, K.: A survey of equations of motion in terms of inertial quasi-velocities for serial manipulators. Arch. Appl. Mech. **76**, 579–614 (2006)
524. Hertz, H.: On the contact of elastic solids. Z. Angew. Math. und Phys. **92**, 155 (1881)
525. Hertzsch, J.M., Spahn, F., Brilliantov, N.V.: On low-velocity collisions of viscoelastic particles. J. Phys. I **I**(5), 1725–1738 (1995)
526. Hien, T.: A correction on the calculation of frictional dissipation in planar impact of rough compliant bodies by W.J. Stronge. Int. J. Impact Eng. **37**, 995–998 (2010)
527. Higa, M., Arakawa, M., Maeno, M.: Measurements of restitution coefficients of ice at low temperature. Planet. Space Sci. **44**(9), 917–925 (1996)
528. Higa, M., Arakawa, M., Maeno, N.: Size dependence of restitution coefficients of ice in relation to collision strength. Icarus **133**, 310–320 (1998)
529. Hinch, E.J., Saint-Jean, S.: The fragmentation of a line of balls by an impact. Pro. Roy. Soc. London A **455**, 3201–3220 (1999)
530. Hindmarsh, M.B., Jefferies, D.J.: On the motions of the offset impact oscillator. J. Phys. A: Math. Gen. **17**(9), 1791–1803 (1984). doi:10.1088/0305-4470/17/9/015
531. Hiriart-Urruty, J.B., Lemaréchal, C.: Fundamentals of Convex Analysis. Springer, Grundlehren Text Editions (2001)
532. Hirschkorn, M., McPhee, J., Birkett, S.H.: Dynamic modeling and experimental testing of a piano action mechanism. ASME J. Comput. Nonlinear Dyn. **1**(1), 47–55 (2006)
533. Hirsh, M.W., Smale, S.: Differential Equations. Dynamical Systems and Linear Algebra. Academic Press, New York (1974)
534. Hjiaj, M., de Saxcé, G., Mroz, Z.: A variational inequality-based formulation of the frictional contact law with non-associated sliding rule. Eur. J. Mech. A/Solids **21**, 49–59 (2002)
535. Hodgkinson, E.: On the collision of imperfectly elastic bodies. Technical report, Report British Association for the Advancement of Science, 4th meeting (1835)
536. Hogan, N.: Stable execution of contact tasks using impedance control. Proc. IEEE Int. Conf. Robot. Autom. **4**, 1047–1054 (1987)
537. Hollandsworth, P.E., Busby, H.R.: Impact force identification using the general inverse technique. Int. J. Impact Eng. **8**(4), 315–322 (1989)
538. Holmes, P.J.: The dynamics of repeated impacts with a sinusoidally vibrating table. J. Sound Vib. **84**(2), 173–189 (1982)
539. Holtzman, R., Silin, D.B., Patzek, T.W.: Frictional granular mechanics: a variational approach. Int. J. Numer. Methods Eng. **81**(10), 1259–1280 (2010)
540. Hongler, M.O., Streit, L.: On the origin of chaos in gearbox models. Phys. D: Nonlinear Phenom. **29**(3), 402–408 (1988)
541. Horak, F.: Impact of a rough ball spinning round its vertical diameter onto a horizontal plane. Trans. Faculty Mech. Elec, Eng (1948)
542. Horvay, G., Veluswami, M.A.: Hertzian impact of two elastic spheres in the presence of surface damping. Acta Mech. **35**, 285–290 (1980)
543. Housner, G.W.: The behaviour or inverted pendulum structures during earthquakes. Bull. Seis. Soc. Am. **53**(2), 403–417 (1963)
544. Hsu, W.C., Shabana, A.A.: Finite element analysis of impact-induced transverse wawes in rotating beams. J. Sound Vib. **168**(2), 355–369 (1993)
545. Hu, S., Guo, X.: A dissipative contact force model for impact analysis in multibody dynamics. Multibody Syst. Dyn. **35**, 131–151 (2015). doi:10.1007/s11044-015-9453-z
546. Hu, S., Lakshmikantham, V., Leela, S.: Impulsive differential systems and the pulse phenomena. J. Math. Anal. Appl. **137**(2), 605–612 (1989)

547. Hua, D., Lancaster, P.: Linear matrix equations from an inverse problem of vibration theory. Linear Algebra Appl. **246**, 31–47 (1996)
548. Huang, H.P.: Constrained manipulators and contact force control of contour following problems. Ph.D. thesis, Department of Electrical Engineering and Computer Science, University of Michigan, (1986)
549. Huang, H.P., MacClamroch, N.H.: Time optimal control for a robotic contour following problem. IEEE J. Robot. Autom. (1988). doi:10.1109/56.2077
550. Huang, J., Ma, Z.X., Ren, L.S., Li, Y., Zhou, Z.X., Liu, S.: A new engineering model of debris cloud produced by hypervelocity impact. Int. J. Impact Eng. **56** (2013)
551. Huang, P., Hu, Z., Zhang, F.: Dynamic modelling and coordinated controller designing for the manoeuvrable tether-net space robot system. Multibody Syst. Dyn. (2015). doi:10.1007/s11044-015-9478-3
552. Huang, P., Xu, W., Liang, B., Xu, Y.: Configuration control of space robots forimpact minimization. In: Proceedings of IEEE International Conference on Robotics and Biomimetics, pp. 357–362. Kunning, China (2006)
553. Huber, O., Acary, V., Brogliato, B., Plestan, F.: Discrete-time twisting controller without numerical chattering: analysis and experimental results with an implicit method. In: Proceedings of the 53rd IEEE Conference on Decision and Control, pp. 4373–4378. Los Angeles, USA (2014). doi:10.1109/CDC.2014.7040071
554. Huber, O., Acary, V., Brogliato, B., Plestan, F.: Implicit discrete-time twisting controller without numerical chattering: analysis and experimental results. Control Eng. Pract. **46**(1), 125–141 (2016). doi:10.1016/j.conengprac.2015.10.013
555. Hunt, K.H., Crossley, F.R.E.: Coefficient of restitution interpreted as damping in vibroimpact. ASME J. Appl. Mech. **42**(2), 440–445 (1975). doi:10.1115/1.3423596
556. Hunter, S.C.: Energy absorbed by elastic waves during impacts. J. Mech. Phys. Solids **5**(3), 162–171 (1957)
557. Hurmuzlu, Y.: An energy based coefficient of restitution for planar impacts of slender bars with massive external surfaces. ASME J. Appl. Mech. **65**(4), 952–962 (1998). doi:10.1115/1.2791939
558. Hurmuzlu, Y., Ceanga, V.: Impulse correlation ratio in sloving multiple impact problems. In: Brogliato, B. (ed.) Impacts in Mechanical Systems, Lecture Notes in Physics, vol. 551, pp. 235–273. Springer (2000)
559. Hurmuzlu, Y., Chang, T.H.: Rigid body collisions of a special class of planar kinematic chains. IEEE Trans. Syst., Man Cybern. **22**(5), 964–971 (1992)
560. Hurmuzlu, Y., Génot, F., Brogliato, B.: Modelling, stability and control of biped robots-a general framework. Automatica **40**(10), 1647–1664 (2004)
561. Hurmuzlu, Y., Marghitu, D.B.: Rigid body collisions of planar kinematic chains with multiple contact points. Int. J. Robot. Res. **13**(1), 82–92 (1994)
562. Hürzeler, C.: Modeling and design of unmanned rotorcraft systems for contact based inspection. Ph.D. thesis, ETH Zürich (2013)
563. Hutchings, I.M.: Energy absorbed by elastic waves duinrg plastic impact. J. Phys. D: Appl. Phys. **12**, 1819–1824 (1979)
564. Hutchings, I.M., Millan, N.H.M., Rickerby, D.G.: Further studies of the oblique impact of a hard sphere against a ductile solid. Int. J. Mech. Sci. **23**(11), 639–646 (1981)
565. Huygens, C.: Christiaan Huygens Opuscula Posthuma, chap. De motu corporum ex percussione. Ostwalds Klassiker Bd, Leiden (1703)
566. Huygens, C.: Treatise on Light. MacMillan and Co, London (1912). Huygens wrote his Treatise in 1678
567. Hyde, J.M., Cutkosky, M.R.: Contact transition control: an experimental study. IEEE Control Syst. **14**(1), 25–31 (1994)
568. Ibort, A., de Leon, M., Lacomba, E.A., de Diego, D.M., Pitanga, P.: Mechanical systems subjected to impulsive constraints. J. Phys. A: Math. Gen. **30**, 5835–5854 (2015)
569. Ibort, A., de Leon, M., Lacomba, E.A., Marrero, J.C., de Diego, D.M., Pitanga, P.: Geometric formulation of Carnot's theorem. J. Phys. A: Math. Gen. **34**, 1691–1712 (2001)

570. Ibrahim, R.A., Sayad, M.A.: Simultaneous parametric and internal resonances in systems simulating liquid sloshing impact. In: Pfeiffer, F., Glocker, C. (eds.) Proceedings of IUTAM Symposium on Unilateral Multibody Dynamics, Solid Mechanics and its Applications, pp. 97–106. Kluwer Academic Publisher, Munich, Germany (1999)
571. Iltis, C.: The decline of Cartesianism in mechanics: the Leibnizian-Cartesian debat. Isis (1973). Published by the University of Chicago Press on behalf of The History of Science Society
572. Iltis, C.: The Leibnizian-Newtonian debates: natural philosophy and social psychology. Br. J. Hist. Sci. **6**(24), 343–377 (1973)
573. Imre, B., Räbsamen, S., Springman, S.M.: A coefficient of restitution of rock materials. Comput. Geosci. **34**, 339–350 (2008)
574. Imura, J., van der Schaft, A.J.: Characterization of well-posedness of piecewise linear systems. IEEE Trans. Autom. Control **45**(9), 1600–1619 (2000)
575. Ismail, K., Stronge, W.J.: Viscoplastic analysis for direct impact of sport balls. Int. J. Non-Linear Mech. **47**(1), 16–21 (2012)
576. Ismail, K.A., Stronge, W.J.: Impact of viscoplastic bodies: dissipation and restitution. ASME J. Appl. Mech. **75**(6), 061,011 (2008)
577. Isomaki, H.M., von Boehm, J., Raty, R.: Fractal basin boundaries of an impacting particle. Phys. Lett. A **126**(8–9), 484–490 (1988)
578. Ivanov, A.P.: Periodic motions of a heavy symmetrical rigid body with collisions against a horizontal plane. Izv. Akad. Nauk USSR **2**, 30–35 (1985)
579. Ivanov, A.P.: On the correctness of the basic problem of dynamics in systems with friction. J. Appl. Math. Mech. **50**(5), 547–550 (1986)
580. Ivanov, A.P.: A constructive model of impact with friction. J. Appl. Math. Mech. **52**(6), 700–704 (1988)
581. Ivanov, A.P.: Impacts in a system with certain unilateral couplings. J. Appl. Math. Mech. **51**(4), 436–442 (1988)
582. Ivanov, A.P.: The preservation of the stability of a mechanical system when a non-retaining constraint is weakened. J. Appl. Math. Mech. **53**(4), 417–424 (1989)
583. Ivanov, A.P.: Collision-free motion in systems with non-retaining constraints. J. Appl. Math. Mech. **56**(1), 1–12 (1992)
584. Ivanov, A.P.: Energetics of a collision with friction. J. Appl. Math. Mech. **56**(4), 527–534 (1992)
585. Ivanov, A.P.: Analytical methods in the theory of vibro-impact systems. J. Appl. Math. Mech. **57**(2), 221–236 (1993)
586. Ivanov, A.P.: Stabilization of an impact oscillator near grazing incidence owing to resonance. J. Sound Vib. **162**(3), 562–565 (1993)
587. Ivanov, A.P.: The dynamics of systems near to grazing collision. J. Appl. Math. Mech. **58**(3), 437–444 (1994)
588. Ivanov, A.P.: Impact oscillations: linear theory of stability and bifurcations. J. Sound Vib. **178**(3), 361–378 (1994)
589. Ivanov, A.P.: On multiple impacts. J. Appl. Math. Mech. **59**(6), 887–902 (1995)
590. Ivanov, A.P.: The problem of the center of percussion. J. Appl. Math. Mech. **59**(1), 151–153 (1995)
591. Ivanov, A.P.: Bifurcations in impact systems. Chaos, Solitons Fractals **7**(10), 1675–1634 (1996)
592. Ivanov, A.P.: A Kelvin theorem and partial work of impulsive forces. ASME J. Appl. Mech. **64**(2), 438–440 (1997)
593. Ivanov, A.P.: The stability of equilibrium in systems with friction. J. Appl. Math. Mech. **71**, 385–395 (2002)
594. Ivanov, A.P.: Singularities in the dynamics of systems with non-ideal constraints. J. Appl. Math. Mech. **67**(2), 185–192 (2003)
595. Ivanov, A.P.: The equilibrium of systems with dry friction. J. Appl. Math. Mech. Appeared. Prikl. Mat. Mekh. **79**(3), 317–333 (2015)

596. Ivanov, A.P., Markeev, A.: The dynamics of systems with unilateral constraints. J. Appl. Math. Mech. **48**(4), 448–451 (1984)
597. Iwatsubo, T., Kawamura, S., Miyamoto, K., Yamaguchi, T.: Analysis of golf impact phenomenon and ball trajectory. JSME Int. J. Ser. C, Mech. Syst., Mach. Elem. Manuf. **41**(4), 822–828 (1998)
598. Jackson, R.L., Chusoipin, I., Green, I.: A finite element study of the residual stress and deformation in hemispherical contact. ASME J. Tribol. **127**, 484–493 (2005)
599. Jackson, R.L., Chusoipin, I., Green, I.: A finite element study of the residual stress and strain formation in spherical contacts. J. Tribol. **60**(3), 217–229 (2010)
600. Jackson, R.L., Green, I.: A finite element study of elasto-plastic hemispherical contact against a rigid flat. ASME J. Tribol. **127**, 343–354 (2005)
601. Jackson, R.L., Green, I., Marghitu, D.B.: Predicting the coefficient of restitution of impacting elastic-perfectly plastic spheres. Nonlinear Dyn. **60**(3), 217–229 (2010)
602. Jacobs, D.A., Waldron, K.J.: Modeling inelastic collisions with the Hunt-Crossley model using the energetic coefficient of restitution. ASME J. Comput. Nonlinear Dyn. (2014). doi:10.1115/1.4028473
603. Jaeger, J.: Analytical solutions of contact impact problems. ASME Appl. Mech. Rev. **47**(2), 35–54 (1994). doi:10.1115/1.3111070
604. Jaeger, J.: Oblique impact of similar bodies with circular contact. Acta Mech. **107**(1–4), 101–115 (1994)
605. Jafari, R., Mathis, F.B., Mukherjee, R., Khalil, H.: Enlarging the region of attraction of equilibria of underactuated systems using impulsive inputs. IEEE Trans. Autom. Control (2015). doi:10.1109/TCST.2015.2424925
606. Jain, A.: Operational space inertia for closed-chain robotic systems. ASME J. Comput. Nonlinear Dyn. **9**(2), 021,015 (2014). doi:10.1115/1.4025893
607. Jamari, J., Schipper, D.J.: Experimental investigation of fully plastic contact of a sphere against a hard flat. ASME J. Tribol. **128**, 230–235 (2006)
608. James, G.: Nonlinear waves in Newton's cradle and the discrete p-Schrödinger equation. Math. Models Meth. Appl. Sci. **21**, 2335–2377 (2011)
609. James, G.: Periodic travelling waves and compactons in granular chains. J. Nonlinear Sci. **22**(5), 813–848 (2012)
610. James, G.: Breathers in oscillator chains with Hertzian interactions. Phys. D **251**, 39–59 (2013)
611. Janin, O., Lamarque, C.H.: Comparison of several numerical methods for mechanical systems with impacts. Int. J. Numer. Methods Eng. **51**(9), 1101–1132 (2001)
612. Jatav, K.S., Dhar, J.: Hybrid approach for pest control with impulsive releasing of natural enemies and chemical pesticides: a plant-pest-natural enemy model. Nonlinear Anal.: Hybrid Syst. **12**, 79–92 (2014)
613. Jayaprakash, K.R., Starsvetsky, Y., Vakakis, A.F.: New family of solitary waves in granular dimer chains with no precompression. Phys. Rev. E **83**, 036,606 (2011)
614. Jean, M.: Simulation numérique des problèmes de contact avec frottement. Matériaux et Techniques **81**(1–3), 22–32 (1993)
615. Jean, M.: The non-smooth contact dynamics method. Comput. Methods Appl. Mech. Eng. **177**(3–4), 235–257 (1999)
616. Jean, M., Acary, V., Monerie, Y.: Non-smooth contact dynamics approach of cohesive materials. Philos. Trans. Roy. Soc. London Ser. A. Math., Phys. Eng. Sci. (2001)
617. Jean, M., Moreau, J.J.: Dynamics in the presence of unilateral contacts and dry friction; a numerical approach. In: G.D. Piero, F. Maceri (eds.) Unilateral Problems in Structural Analysis 2, CISM Courses and Lectures, vol. 304, pp. 151–196. Springer (1987)
618. Jean, M., Pratt, E.: A system of rigid bodies with friction. Int. J. Eng. Sci. **23**(5), 497–513 (1985)
619. Jellet, J.H.: A treatise on the Theory of Friction. Hodges, Foster and Co, Dublin (1872). Also MacMillan and Co, London

620. Jenkins, J.T.: Boundary conditions for rapid granular flow: flat, frictional walls. ASME J. Appl. Mech. **59**(1), 120–127 (1992)
621. Jia, Y.B.: Three-dimensional impact: energy-based modeling of tangential compliance. Int. J. Robot. Res. **32**(1), 56–83 (2013). doi:10.1177/0278364912457832
622. Jia, Y.B., Mason, M., Erdmann, M.: A state transition diagram for simultaneous collisions with application in billiard shooting. In: Chirikjian, G., Choset, H., Morales, M., Murphey, T. (eds.) Algorithmic Foundations of Robotics, Springer Tracts in Advanced Robotics, vol. VIII, pp. 135–150. Springer, Berlin (2010)
623. Jia, Y.B., Mason, M., Erdmann, M.: Multiple impacts: A state transition diagram approach. Int. J. Robot. Res. **32**(1), 84–114 (2013). doi:10.1177/0278364912461539
624. Jin, H., Zackenhouse, M.: Yoyo dynamics: Sequence of collisions captured by a restitution effect. ASME J. Dyn. Syst., Meas. Control **124**, 390–397 (2002)
625. Job, S., Melo, F., Sokolow, A., Sen, S.: Solitary wave trains in granular chains: experiments, theory and simulations. Granular Matter **10**(1), 13–20 (2007). doi:10.1007/s10035-007-0054-2
626. Johnson, K.L.: The bounce of 'superball'. Int. J. Mech. Eng. Educ. **11**(1), 57–63 (1983)
627. Johnson, K.L.: Contact Mechanics. Cambridge University Press, Cambridge (1985)
628. Johnson, K.L.: Mechanics of adhesion. Triology. International **31**(8), 413–418 (1998)
629. Johnson, K.L., Greenwood, J.A.: An adhesion map for the contact of elastic spheres. J. Colloid Interf. Sci. **192**, 326–333 (1997)
630. Joukovsky, N.: Sur la percussion des corps. Journal de Mathématiques Pures et Appliquées **3**(4), 417–424 (1878)
631. Jourdain, P.E.B.: Note on an analogue of Gauss' principle of least constraint. Q. J. Pure Appl. Math. **40**, 153–197 (1909)
632. Jr., N.D.N.: Linear collisions with harmonic oscillator forces: The inverse scattering problem. Am. J. Phys. **47**(2), 161–165 (1979)
633. Kahng, J., Amirouche, F.M.L.: Impact force analysis in mechanical hand design. Proc. IEEE Int. Conf. Robot. Autom. **4**, 2061–2067 (1987)
634. Kahraman, A., Blakenship, G.W.: Interactions between commensurate parametric and forcing excitations in a system with clearance. J. Sound Vib. **194**(3), 317–336 (1996)
635. Kahraman, A., Singh, R.: Nonlinear dynamics of a spur gear pair. J. Sound Vib. **142**(1), 49–75 (1990)
636. Kahraman, A., Singh, R.: Nonlinear dynamics of a gear rotor system with multiple clearances. J. Sound Vib. **144**(3), 469–506 (1991)
637. Kahraman, A., Singh, R.: Dynamics of an oscillator with both clearance and continuous nonlinearities. J. Sound Vib. **153**(1), 180–185 (1992)
638. Kailath, T.: Linear Systems. Prentice-Hall (1980)
639. Kalagnanam, J.R.: Controlling chaos: The example of an impact oscillator. ASME J. Dyn. Syst. Meas. Control **116**(3), 557–564 (1994)
640. Kalmar, M.: Thomas Hariot's de reflexione corporum rotundorum: an early solution to the problem of impact. Arch. Hist. Exact Sci. **16**(3), 201–230 (1977). doi:10.1007/BF00328155
641. Kane, T.R.: A dynamics puzzle. Stanford mechanics Alumni club Newsletter (1984)
642. Kane, T.R., Levinson, D.: Dynamics: Theory and Applications. Mac Graw Hill, New York (1985)
643. Kanno, Y.: Nonsmooth Mechanics and Convex Optimization. CRC Press, Taylor and Francis Group (2011)
644. Kapitaniak, T.: Chaotic Oscillations in Mechanical Systems. Manchester University Press (1991)
645. Kapoulitsas, G.M.: On the collision of rigid bodies. ZAMP J. Appl. Math. Phys. **46**(5), 709–723 (1995)
646. Karagiannis, K., Pfeiffer, F.: Theoretical and experimental investigations of gear-rattling. Nonlinear Dyn. **2**(5), 367–387 (1991)
647. Karplus, M., Weaver, D.L.: Protein folding dynamics: The diffusion-collision model and experimental data. Protein Sci. **3**(4), 650–668 (1994)

648. Karyeaclis, M.P., Caughey, T.K.: Stability of a semi-active impact damper: part 1-global behaviour; part 2-periodic solutions. ASME J. Appl. Mech. **56**(4), 926–940 (1989)
649. Kastner-Maresch, A., Lempio, F.: Difference methods with selection strategies for differential inclusions. Numer. Funct. Anal. Optim. **14**(5–6), 555–572 (1993)
650. Kecskemethy, A., Lüder, J.: Rigid and elastic approaches for the modeling of collisions with friction in multibody systems. Zeitschrift für angewandte Mathematik und Mechanik **76**(5), 243–244 (1996). ICIAM / GAMM 95. Part V, Hamburg, Germany, 03–07-1995
651. Keller, J.B.: Impact with friction. ASME J. Appl. Mech. **53**(1), 1–4 (1986). doi:10.1115/1.3171712
652. Keller, J.B.: Impact with an impulsive frictional moment. ASME J. Appl. Mech. **54**(1), 239–240 (1987). doi:10.1115/1.3172971
653. Kelvin, W.T., Tait, P.G.: Treatise on Natural Philosophy, vol. 1. Clarendon Press, Oxford, UK (1895)
654. Kenaley, G.L., Cutkosky, M.R.: Electrorheological fluid-logical fluid-based robotic fingers with tactile sensing. In: Proceedings of IEEE International Conference Robotics and Automation, pp. 132–136. Scottsdale, Arizona, USA (1989)
655. Kerschen, G., Peeters, M., Golinval, J.C., Vakakis, A.F.: Nonlinear normal modes, Part I: a useful framework for the structural dynamicist. Mechanical Systems and Signal Processing **23**, 170–194 (2009)
656. Kharaz, A.H., Gorham, D.A.: A study of the restitution coefficient in elastic-plastic impacts. Philos. Mag. A-Phys. Condens. Matter Struct. Defects Mech. Prop. **80**, 549–559 (2000)
657. Kharaz, A.H., Gorham, D.A., Salman, A.D.: An experimental study of the elastic rebound of spheres. Powder Technol. **120**, 281–291 (2001)
658. Khatib, O., Burdick, J.: Motion and force control of robot manipulators. In: Proceedings of IEEE International Conference on Robotics and Automation, pp. 1381–1386. San-Fransisco, USA (1986)
659. Khulief, Y.A., Shabana, A.A.: Dynamic analysis of constrained system of rigid and flexible bodies with intermittent motion. ASME J. Mech., Transmissions Autom. Des. **108**(1), 38–45 (1986)
660. Khulief, Y.A., Shabana, A.A.: Dynamic analysis of constrained systems of rigid and flexible bodies with intermittent motions. ASME J. Mech., Transmission Autom. Des. **108**(1), 38–45 (1986). doi:10.1115/1.3260781
661. Khulief, Y.A., Shabana, A.A.: Dynamics of multibody systems with variable kinematic structure. ASME J. Mech., Transmissions Autom. Des. **108**(2), 167–175 (1986)
662. Khulief, Y.A., Shabana, A.A.: A continuous force model for the impact analysis of flexible multibody systems. Mech. Mach. Theory **22**(3), 213–224 (1987)
663. Kikuuwe, R., Takesue, N., Sano, A., Mochiyama, H., Fujimoto, H.: Admittance and impedance representations of friction based on implicit Euler integration. IEEE Trans. Robot. **22**(6), 1176–1188 (2006)
664. Kikuuwe, R., Yasukouchi, S., Fujimoto, H., Yamamoto, M.: Proxy-based sliding mode control: a safer extension of PID position control. IEEE Trans. Robot. **26**(4), 670–683 (2010)
665. Kim, J.O., Gertz, M.W., Khosla, P.K.: Exploiting redundancy to reduce impact force. J. Intell. Robot. Syst. **9**, 273–290 (1994)
666. King, H., White, R., Maxwell, I., Menon, N.: Inelastic impact of a sphere on a massive plane: Nonmonotonic velocity-dependence of the restitution coefficient. Europhys. Lett. **93**(1), 14,002 (2011)
667. Kirgetov, V.I.: On the purely elastic impact of material systems. Prikl. Matem. Mekhan. **24**(5), 781–789 (1960)
668. Kirgetov, V.I.: Analytical method of mechanics in the theory of a perfectly elastic impact of material systems. Prikl. Matem. Mekhan. **25**(3), 407–412 (1961)
669. Kirgetov, V.I.: On the theory of an absolutely elastic impact on material systems. Prikl. Matem. Mekhan. **25**(1), 3–8 (1961)
670. Kitagaki, K., Uchiyama, M.: Optimal approach velocity of end-effector to the environment. In: Proceedings of IEEE International Conference on Robotics and Automation, pp. 1928–1934. Nice, France (1992)

671. Klarbring, A.: A mathematical programming approach to three dimensional contact problems with friction. Comput. Methods Appl. Mech. Eng. **58**(2), 175–200 (1986)
672. Klarbring, A.: A mathematical programming approach to contact problems with friction and varying contact surface. Comput. Struct. **30**(5), 1185–1198 (1988)
673. Klarbring, A.: Examples of non-uniqueness and non-existence of solutions to quasistatic contacts. Ing. Archiv. **60**(8), 529–541 (1990). doi:10.1007/BF00541909
674. Klein, F.: Zu Painlevés kritik des Coulombschen reibungsgsetze. Zeitsch. Math. Phys. **58**, 186–191 (1909)
675. Kogut, I., Komvopoulos, K.: Analysis of the spherical indentation cycle for elastic-perfectly plastic solids. J. Mater. Res. **19**(12), 3641 (2002)
676. Kogut, L., Etsion, I.: Elastic-plastic contact analysis of a sphere and a rigid flat. ASME J. Appl. Mech. **69**, 657–662 (2002)
677. Kogut, L., Etsion, I.: A static friction model for elastic-plastic contacting rough surfaces. ASME J, Tribol (2004)
678. Konashenkova, T.D., Moshuck, H.K.: Stochastic mechanical systems with a non-retaining constraint. J. Appl. Math. Mech. **58**(3), 403–412 (1994)
679. Koshy, C.S., Flores, P., Lankarani, H.M.: Study of the effect of contact force model on the dynamic response of mechanical systems with dry clearance joints: computational and experimental approaches. Nonlinear Dyn. **73**, 325–338 (2013)
680. Kotera, T., Yamanashi, H.: Chaotic behaviour in an impact vibration system, 2nd report: Influence of damping coefficient and coefficient of restitution. Trans. Jpn. Soc. Mech. Eng. **29**, 1883–1886 (1986)
681. Kowalik, Z.J., Franaszek, M., Pieranski, P.: Self reanimating chaos in the bouncing-ball system. Phys. Rev. A **37**(10), 4016–4022 (1988)
682. Kozlov, V.V.: A constructive method of establishing the validity of the theory of systems with non-retaining constraints. J. Appl. Math. Mech. **52**(6), 691–699 (1988)
683. Kozlov, V.V., Treshchev, D.V.: Billiards. A Genetic Introduction to the Dynamics of Systems with Impacts. Amer. Math. Soc., Providence, RI (1991)
684. Kozol, J.E., Brach, R.M.: Two-dimensional vibratory impact with chaos. J. Sound Vib. **148**(2), 319–327 (1991)
685. Krinner, A., Thümmel, T.: Non-smooth behaviour of a linkage mechanism with revolute clearance joints. In: New Advances in Mechanisms, Transmissions and Applications, pp. 233–241. Springer (2014)
686. Kruger, A.Y., Minchenko, L., Outrata, J.V.: On relaxing the Mangasarian-Fromovitz constraint qualification. Positivity **18**, 171–189 (2014). doi:10.1007/s11117-013-0238-4
687. Ksendo, A.A., Nagaev, R.F.: Infinite-collision periodic states on a vibrating conveyor. Izv. AN SSSR Mekhanika Tverdogo Tela **6**(5), 29–35 (1971)
688. Kuninaka, H., Hayakawa, H.: Simulation of the oblique impact of a lattice system. J. Phys. Soc. Jpn. **72**, 1655–1663 (2003)
689. Kuninaka, H., Hayakawa, H.: Anomalous behaviour of the coefficient of normal restitution in oblique impact. Phys. Rev. Lett. **93**(15), 154,301 (2004)
690. Kurzweil, J.: Generalized ordinary differential equations. Czechosl. Math. J. **8**, 360–388 (1958)
691. Kuwabara, G., Kono, K.: Restitution in a collision between two spheres. Japan. J. Appl. Phys. **26**(8), 1230–1233 (1987)
692. Laghdir, M.: Solutions des équations régissant le mouvement des particules en contact avec frottement sec et recevant des impulsions. Ph.D. thesis, Université des sciences et techniques du Languedoc, Mathématiques fondamentales et appliquées, Montpellier, France (1987)
693. Laghdir, M., Monteiro-Marques, M.D.P.: Dynamics of a particle with damping, friction, and percussional effects. J. Math. Anal. Appl. **196**(3), 902–920 (1995)
694. Laghdir, M., Monteiro-Marques, M.D.P.: Motion of a particle submitted to dry friction and to normal percussions. Portugaliae Math. **52**(2), 227–239 (1995)
695. Lakmeche, A., Arino, O.: Nonlinear mathematical model of pulsed-therapy of heterogeneous tumors. Nonlinear Anal.: Real World Appl. **2**, 455–465 (2001)

696. Lakshmikantham, V., Liu, X.: Stability criteria for impulsive differential equations in terms of two measures. J. Math. Anal. Appl. **137**(2), 591–604 (1989)
697. Lamarque, C.H., Gendelman, O.V., Savadkoohi, A.T., Etcheverria, E.: Targeted energy transfer in mechanical systems by means of non-smooth nonlinear energy sink. Acta Mech. **221**, 175–200 (2011)
698. Lamarque, C.H., Savadkoohi, A.T., Dimitrijevic, Z.: Dynamics of a linear system with time-dependent mass and a coupled light mass with non-smooth potential. Meccanica **49**, 135–145 (2014)
699. Lamba, H., Budd, C.J.: Scaling of Lyapunov exponents of nonsmooth bifurcations. Phys. Rev. E **50**(1), 84–90 (1994)
700. Lancaster, P., Tismenestsky, M.: The Theory of Matrices, with Applications, second edn. Academic Press (1985)
701. Lancioni, G., Lenci, S., Galvanetto, U.: Non-linear dynamics of a mechanical system with a frictional unilateral constraint. Int. J. Non-Linear Mech. **44**, 658–674 (2009)
702. Lancioni, G., Lenci, S., Galvanetto, U.: Dynamics of windscreen wiper blades: Squeal noise, reversal noise and chattering. Int. J. Non-Linear Mech. (2015). doi:10.1016/j.ijnonlinmec.2015.10.003
703. Lanczos, C.: Variational Principles of Mechanics. Dover (1970). Fourth edition
704. Lankarani, H.M., Nikravesh, P.E.: A contact force model with hysteresis damping for impact analysis of multibody systems. ASME J. Mech. Des. **112**(3), 369–376 (1990). doi:10.1115/1.2912617
705. Lankarani, H.M., Nikravesh, P.E.: Continuous contact force models for impact analysis in multibody systems. Nonlinear Dyn. **5**(2), 193–207 (1994)
706. Laulusa, A., Bauchau, O.A.: Review of classical approaches for constraint enforcement in multibody systems. ASME J. Comput. Nonlinear Dyn. **3**(1), 011,004 (2008)
707. Laxalde, D., Legrand, M.: Nonlinear modal analysis of mechanical systems with frictionless contact interfaces. Comput. Mech. **47**(4), 469–478 (2011). doi:10.1007/s00466-010-0556-3
708. Le, x.A.: The Painlevé paradoxes and the law of motion of mechanical systems with Coulomb friction. J. Appl. Math. Mech. **54**(4), 430–438 (1990)
709. Le, x.A.: Dynamics of Mechanical Systems with Coulomb Friction. Foundations of Engineering Mechanics. Springer, Berlin (2003)
710. Lean, G.H.: Subharmonic motions of moored ships subjected to wave action. Trans. R. Naval Arch. **113**, 387–399 (1971)
711. Lebeau, G., Schatzman, M.: A wave problem in a half-space with a one-sided constraint at the boundary. J. Differ. Equ. **53**(3), 309–361 (1984)
712. Lecornu, L.: Sur la loi de Coulomb. Comptes-rendus Acad. Sci. Paris **140**, 847–848 (1905)
713. Lee, C.H., Byrne, K.P.: Calculating the time-histories of impacting systems described by their receptances. ASME J. Vib. Acoust. **120**(2), 491–495 (1998)
714. Lee, C.H., Masaki, S., Kobayashi, S.: Analysis of ball indentation. Int. J. Mech. Sci. **14**, 417–426 (1972)
715. Lee, E., Park, J., Loparo, K.A., Schrader, C.B., Chang, P.H.: Bang-bang impact control using hybrid impedance/time-delay control. IEEE/ASME Trans. Mech. **8**(2), 272–277 (2003)
716. Lee, T.W., Wang, A.C.: On the dynamics of intermittent motion mechanisms, Part 1: Dynamic model and response. ASME J. Mech., Trans. Autom. Des. **105**(3), 534–541 (1983)
717. Lee, Y.S., Nucera, F., Vakakis, A.F., McFarland, D.M., Bergman, L.A.: Periodic orbits, damped transitions and targeted energy transfers in oscillators with vibro-impact attachments. Phys. D **238**, 1868–1896 (2009)
718. Leela, S.: Asymptotically self invariant sets and perturbed systems. Annali di Matematica Pura ed Applicata XCI **I**(4), 85–93 (1972)
719. Leela, S.: Stability of measure differential equations. Pacific J. Math. **55**(2), 489–498 (1974)
720. Leenaerts, D.: On linear dynamic compementarity systems. IEEE Trans Circ. Syst. I **46**(8), 1022–1026 (1999)

721. Leibniz, G.W.: Reply to Malebranche. Nouvelles de la République des Lettres **9**, 744–753 (1687). Also Philos. Schriften, vol.III, p. 53. (2015)
722. Leibniz, G.W.: Letter to Bernoulli. Mathematische Schriften **III**, 544 (1688)
723. Leine, R.I.: Non-smooth stability analysis of the parametrically excited impact oscillator. Int. J. Non-Linear Mech. **47**, 1020–1032 (2012)
724. Leine, R.I., Aeberhard, U., Glocker, C.: Hamilton's principle as variational inequality for mechanical systems with impact. J. Nonlinear Sci. **19**(6), 633–664 (2009)
725. Leine, R.I., Brogliato, B., Nijmeijer, H.: Periodic motion and bifurcations induced by the Painlevé paradox. Eur. J. Mech. A/Solids **21**(5), 869–896 (2002)
726. Leine, R.I., Glocker, C.: A set-valued force law for spatial Coulomb-Contensou friction. Eur. J. Mech. A/Solids **22**, 193–216 (2003)
727. Leine, R.I., Heimsch, T.F.: Global uniform symptotic attractive stability of the non-autonomous bouncing ball system. Phys. D **241**, 2029–2041 (2012)
728. Leine, R.I., Nijmeijer, H.: Dynamics and Bifurcations in Non-Smooth Mechanical Systems. Lecture Notes in Applied and Computational Mechanics, vol. 18. Springer, Berlin (2004)
729. Leine, R.I., Schweizer, A., Christen, M., Glover, J., Bartelt, P., Gerber, W.: Simulation of rockfall trajectories with consideration of rock shape. Multibody Syst. Dyn. **32**, 241–271 (2014)
730. Leine, R.I., van de Wouw, N.: Stability and Convergence of Mechanical Systems with Unilateral Constraints. Lecture Notes in Applied and Computational Mechanics, vol. 36. Springer, Berlin (2008)
731. Leine, R.I., van de Wouw, N.: Stability properties of equilibrium sets of nonlinear mechanical systems with dry friction and impact. Nonlinear Dyn. **51**(4), 551–583 (2008)
732. Leine, R.I., van de Wouw, N.: Uniform convergence of monotone measure differential inclusions: with application to the control of mechanical systems with unilateral constraints. Int. J. Bifurcat. Chaos **18**(5), 1435–1457 (2008)
733. Leroy, B.: Collision between two balls accompanied by deformation: a qualitative approach to Hertz' theory. Am. J. Phys. **53**(4), 346,349 (1985)
734. Levant, A.: Sliding order and sliding accuracy in sliding mode control. Int. J. Control **58**, 1247–1263 (1993)
735. Levinson, D., Kane, T.R.: Docking of a spacecraft with an unrestained orbiting structure. J. Astronaut. Sci. **31**(1), 23–48 (1983)
736. Lewis, A.D., Rogers, R.J.: Experimental and numerical study of forces during oblique impacts. J. Sound Vib. **125**(3), 403–412 (1988)
737. Li, G.X., Rand, R.H., Moon, F.C.: Bifurcations and chaos in a forced zero-stiffness impact oscillator. Int. J. Non-linear Mech. **25**(4), 417–432 (1990)
738. Li, L.Y., Wu, C.Y., Thornton, C.: A theoretical model for the contact of elastoplastic bodies. Proc. Inst. Mech. Eng. **216**, 421–431 (2002)
739. Li, Z., Soh, C.B., Xu, X.: Stability of impulsive differential equations. J. Math. Anal. Appl. **216**(2), 644–653 (1997)
740. Liang, C.H., Bhasin, S., Dupree, K., Dixon, W.E.: A force limiting adaptive controller for a robotic system unergoing a noncontact-to-contact transition. IEEE Trans. Control Syst. Technol. **17**(6), 1330–1341 (2009)
741. Licht, C., Pratt, E., Raous, M.: Remarks on a numerical method for unilateral contact including friction. Unilateral Probl. Struct. Anal. IV. Int. Ser. Numer. Math. **101**, 129–144 (1991)
742. Lichtenberg, A.J., Lieberman, M.A.: Regular and Chaotic Dynamics, Applied Mathematics, vol. 38. Springer (1991). 2nd edition
743. Lieber, P., Jensen, D.P.: An acceleration damper: Development, design, and some applications. Trans. ASME **67**, 523–530 (1945)
744. Lieber, P., Trip, F.: Experimental results on the acceleration damper. Tech. Rep. TR AE 5401, Rensselaer Polytechnic Institute Aeronautical Laboratory, USA (1954)
745. Lin, C., Wang, Q.G.: On uniqueness ofsolutions to relay feedback systems. Automatica **38**, 177–180 (2002)

746. Lin, Z.C., Patel, R.V., Balafoutis, C.A.: Impact reduction for redundant manipulators using augmented impedance control. J. Robot. Syst. **12**(5), 301–313 (1995)
747. Lipscombe, P.R., Pellegrino, S.: Free rocking of prismatic blocks. J. Eng. Mech. **119**(7), 1378–1410 (1993)
748. Liu, C., Zhang, H., Zhao, Z., Brogliato, B.: Impact-contact dynamics in a disc-ball system. Proc. Roy. Soc. London A: Math., Phys. Eng. Sci. **469**(2152) (2013). doi:10.1098/rspa.2012.0741
749. Liu, C., Zhao, Z., Brogliato, B.: Energy dissipation and dispersion effects in a granular media. Phys. Rev. E **78**(3), 031,307 (2008)
750. Liu, C., Zhao, Z., Brogliato, B.: Frictionless multiple impacts in multibody systems: Part i. theoretical framework. Proc. Roy. Soc. A, Math., Phys. Eng. Sci. **464**(2100), 3193–3211 (2008)
751. Liu, C., Zhao, Z., Brogliato, B.: Theoretical analysis and numerical algorithm for frictionless multiple impacts in multibody systems. INRIA Research Report (2008). https://hal.inria.fr/inria-00204018
752. Liu, C., Zhao, Z., Brogliato, B.: Variable structure dynamics in a bouncing dimer (2008). INRIA Research Report RR-6718, https://hal.inria.fr/inria-00337482
753. Liu, C., Zhao, Z., Brogliato, B.: Frictionless multiple impacts in multibody systems: Part ii. numerical algorithm and simulation results. Proc. Roy. Soc. A, Math., Phys. Eng. Sci. **465**(2101), 1–23 (2009)
754. Liu, C.S., Zhang, K., Yang, R.: The FEM analysis and approximate model for cylindrical joints with clearances. Mech. Mach. Theory **42**, 183–197 (2007)
755. Liu, M.Z., Liang, H., Yang, Z.W.: Stability of Runge-Kutta methods in the numerical solution of linear impulsive differential equations. Appl. Math. Comput. **192**, 346–357 (2007)
756. Liu, X.: Stability theory for impulsive differential equations in terms of two different measures. In: Proceedings of Int. Conf.on Differential Equations: Theory and Applications in Stability and Control, vol. 127. Marcel Dekker, Colorado College in Colorado Springs (1989). Lecture Notes in Pure and Applied Mathematics, 1991
757. Loft, K., Price, M.C., Cole, M.J., Burchell, M.J.: Impacts into metals targets at velocities greater than 1 km s^{-1}: A new online resource for the hypervelocity impact community and an illustration of the geometric change of debris cloud impact patterns with impact velocity. Int. J. Impact Eng. **56**, 47–60 (2013)
758. Lokhorst, D.M., Mills, J.K.: Implementation of a discontinuous control law on a robot during collision with a stiff environment. In: Proceedings of IEEE Conference on Robotics and Automation, vol. 1, pp. 56–61. Cincinnatti, OH, USA (1990)
759. Lootsma, Y.J., van der Schaft, A.J., Çamlibel, M.K.: Uniqueness of solutions of relay systems. Automatica **35**(3), 467–478 (1999)
760. Lorenz, A., Tuozzolo, C., Louge, M.Y.: Measurements of impact properties of small, nearly spherical particles. Exp. Mech. **37**(3), 292–298 (1997)
761. Lötstedt, P.: Coulomb friction in two-dimensional rigid body systems. Zeitschrifts für Angewandte Mathematik und Mechanik **61**(12), 605–615 (1981)
762. Lötstedt, P.: Mechanical systems of rigid bodies subject to unilateral constraints. SIAM J. Appl. Math. **42**(2), 281–296 (1982)
763. Lötstedt, P.: Numerical simulation of time dependent contact and friction problems in rigid body mechanics. SIAM J. Sci. Stat. Comput. **5**(2), 370–393 (1984)
764. Love, A.E.H.: A Treatrise on the Mathematical Theory of Elasticity. Cambridge University Press (1892). Further editions in 1906, 1920, 1927, 1944, 2013
765. Love, A.E.H.: Theoretical Mechanics. Cambridge University Press (1897)
766. Lozano, R., Brogliato, B.: Adaptive control of robot manipulators with flexible joints. IEEE Trans. Autom. Control 37(2), 174–181 (1992); Correction in "Correction to "Adaptive control of robot manipulators with flexible joints" ". IEEE Trans. Autom. Control **41**(6), 920–922 (1996)
767. Lubarda, V.A.: The bounds on the coefficients of restitution for the frictional impact of rigid pendulum against a fixed surface. ASME J. Appl. Mech. **77**, 011,006 (2010)

768. Lüder, J., Kecskemethy, A., Hiller, M.: Modelling and experimental validation of the eccentric collision with friction of a planar bar on a rigid plane. Zeitschrift für Angewandte Mathematik und Mechanik **77**(S2), S611–S612 (1997)
769. Luding, S.: Collisions and contacts between two particles. In: H. Hermann, J. Hovi, S. Luding (eds.) Physics of Dry Granular media, Proc. of Dry Granular Materials, NATO-ASI Proceedings, vol. 350, pp. 285–304. Kluwer Academic Publishers (1998)
770. Luding, S.: Cohesive, frictional powders: contact models for tension. Granular Matter **10**, 235–246 (2008)
771. Luding, S., Clément, E., Blumen, A., Rajchenbach, J., Duran, J.: Anomalous energy dissipation in molecular-dynamics simulations of grains: the "detachment" effect. Phys. Rev. E **50**(5), 4113–4124 (1994)
772. Lumay, G., Dorbolo, S., Gerasymov, O., Vandewalle, N.: Experimental study of a vertical column of grains submitted to a series of impulses. Eur. Phys. J. E: Soft Matter Biolo. Phys. **36**, 16 (2013)
773. Lun, C.K.K.: Kinetic theory for granular flow of dense, slightly inelastic, slightly rough spheres. J. Fluid Mech. **233**, 539–559 (1991)
774. Lun, C.K.K., Bent, A.A.: Computer simulation of simple shear flow of inelastic, frictional spheres. In: Thornton, C. (ed.) Proceedings of Powders and Grains 93, pp. 301–306 (1993)
775. Lun, C.K.K., Savage, A.B.: A simple kinetic theory for granular flow of rough, inelastic, spherical particles. ASME J. Appl. Mech. **54**(1), 47–53 (1987). doi:10.1115/1.3172993
776. Lyapunov, A.M.: Lectures on Theoretic Mechanics. Naukova Dumka, Kiev (1982). Lectures given at the Kharkov Polytechnic; chapter "Dynamics of systems of particles", section "On the action of impulsive forces to systems of particles"
777. Lygeros, J., Johansson, K.H., Simic, S.N., Zhang, J., Sastry, S.S.: Dynamical properties of hybrid automata. IEEE Trans. Autom. Control **48**(1), 2–17 (2003)
778. Ma, D., Liu, C.: Contact law and coefficient of restitution in elastoplastic spheres. ASME J. Appl. Mech. (2015). doi:10.1115/1.4031483
779. Ma, J., Qian, L., Chen, G., Li, M.: Dynamic analysis of mechanical systems with planar revolute joints with clearance. Mech. Mach. Theory **94** (2015)
780. Mabrouk, M.: Liaisons unilatérales et chocs élastiques quelconques: un résultat d'existence. C.R. Acad. Sci. Paris, Série I **326**, 1353–1357 (1998)
781. Mabrouk, M.: A unified variational model for the dynamics of perfect unilateral constraints. Eur. J. Mech. A/Solids **17**(5), 819–842 (1998)
782. Machado, M., Flores, P., Ambrosio, J., Completo, A.: Influence of the contact model on the dynamic response of the human knee joint. Proc. Inst. Mech. Eng., Part K: J. Multi-body Dyn. **225**, 344–358 (2011)
783. Machado, M., Moreira, P., Flores, P., Lankarani, H.M.: Compliant contact force models in multibody dyanmics: evolution of the Hertz contact theory. Mech. Mach. Theory **53**, 99 (2012)
784. MacLaurin, C.: A Treatise on Fluxions. Ruddimans, Edimburgh (1742)
785. MacLaurin, C., Murdoch, P.: An account of Sir Isaac Newton's Philosophical Discoveries, in Four Books, third edition edn. J. Nourse et al, London (1775). Book 2, Chapter 4: On Collision of Bodies
786. Maggi, S., Rinaldi, S.: A second-order impact model for forest fire regimes. Theoret. Popul. Biol. **70**(2), 174–182 (2006)
787. Mahfouz, I.A., Badrakhan, F.: Chaotic behaviour of some piecewise linear systems. part 1: Systems with setup spring or with unsymmetric elasticity, pp. 289–328. part 2: systems with clearance. J. Sound Vib. **143**(2), 255–328 (1990)
788. Maio, F.P.D., Renzo, A.D.: Analytical solution for the problem of frictional-elastic collisions of spherical particles using the linear model. Chem. Eng. Sci. **59**, 3461–3475 (2004)
789. Makarenkov, O., Lamb, J.S.W.: Dynamics and bifurcations of nonsmooth systems: A survey. Phys. D **241**, 1826–1844 (2012)
790. Makarenkov, O., Lamb, J.S.W. (eds.): Physica D: Dynamics and Bifurcations of Nonsmooth Systems, vol. 241. Elsevier (2012). Special Issue

791. Malca, C., Ambrosio, J., Ramalho, A.: An enhanced cylindrical contact force model for multibody dynamics applications. In: J.B. Jonker, W. Schielen, J.P. Meijaard, R.G.K.M. Aarts (eds.) Proc. of Euromech Colloquium 524 Multibody System Modelling, Control and Simulation for Engineering Design. University of Twente, Enschede, NL (2012)
792. Mamaev, I.S., Ivanova, T.B.: The dynamics of a rigid body witha sharp edge in contact with an inclined surface in the presence of dry friction. Regular and Chaotic Dynamics **19**(1), 116–139 (2014)
793. Mandal, N., Payandeh, S.: Experimental evaluation of the importance of compliance for robotic impact control. In: Proceedings of the second IEEE Control Application Conference, pp. 511–516. Vancouver, BC, Canada (1993)
794. Mandal, N., Payandeh, S.: Control strategies for robotic tasks: An experimental study. J. Robot. Syst. **12**(1), 67–92 (1995)
795. Mangasarian, O.L.: Nonlinear Programming. McGraw-Hill, New York (1969)
796. Mangwandi, C., Cheong, Y.S., Adams, M.J., Hounslow, M.J., Salman, A.D.: The coefficient of restitution of different representative types of granules. Chem. Eng. Sci. **62**(1–2), 437–450 (2007)
797. Mansour, W.M., Filho, D.R.T.: Impact dampers with Coulomb friction. J. Sound Vib. **33**(3), 247–265 (1974)
798. Marci, J.M.: De Proportione Motus seu Regula Sphygmica (1639). Jan Marek Marci, 1595–1667
799. Marconi, L., Naldi, R., Gentili, L.: Modelling and control of a flying robot interacting with the environment. Automatica **47**, 2571–2583 (2011)
800. Marghitu, D.B.: The impact of flexible links with solid lubrication. J. Sound Vib. **205**(5), 712–720 (1997)
801. Marhefka, D.W., Orin, D.E.: Simulation of contact using a nonlinear damping model. In: Proceedings of IEEE International Conference on Robotics and Automation, pp. 1662–1668. Minneapolis, USA (1996)
802. Marhefka, D.W., Orin, D.E.: A compliant contact model with nonlinear damping for simulation of robotic systems. IEEE Trans. Syst., Man Cybern.-Part A: Syst. Humans **29**(6), 566–572 (1999)
803. Mariti, L., Belfiore, N.P., Pennestri, E., Valentini, P.P.: Comparison of solution strategies for multibody dynamics equations. Int. J. Numer. Methods Eng. **88**, 637–656 (2011)
804. Markeev, A.P.: Stability of motion of a rigid body colliding with a horizontal plane. Mech. Solids (Izvestiya AN. Mekhanika Tverdogo Tela) **32**(5), 27–34 (1997)
805. Markeyev, A.A.: The stability of the permanent rotation of a body with a non-retaining constraint. Vestik. Mosk. Univ. Mat. Mekh. **3**, 48–54 (1992)
806. Markeyev, A.P.: The stability of the rotation of a rigid body about vertical when there are collisions with a horizontal plane. J. Appl. Math. Mech. **48**(3), 260–265 (1984)
807. Markeyev, A.P.: The motion of a rigid body with an ideal non-restoring constraint. J. Appl. Math. Mech. **49**(5), 545–552 (1985)
808. Markeyev, A.P.: A qualitative analysis of systems with an ideal non-conservative constraint. J. Appl. Math Mech. **53**(6), 685–688 (1989)
809. Markeyev, A.P.: An investigation of the stability of the periodic motion of a rigid body when there are collisions with a horizontal plane. J. Appl. Math. Mech. **58**(3), 445–456 (1994)
810. Marth, G.T., Tarn, T.J., Bejczy, A.K.: Stable phase transition control for robot arm motion. In: Proceedings of IEEE International Conference on Robotics and Automation, vol. 1, pp. 355–362. Atlanta, USA (1993)
811. Martin, M.T., Doyle, J.F.: Impact force identification from wave propagation responses. Int. J. Impact Eng. **18**(1), 65–77 (1996)
812. Martinelli, F., Menini, L., Tornambé, A.: Observability, reconstructibility and observer design for linear mechanical systems unobservable in absence of impacts. J. Dyn. Syst., Measur. Control **125**(4), 549–562 (2004)
813. Maso, G.D.: An Introduction to Γ-Convergence, PNLDE, vol. 8. Birkhauser, Boston (1993)

814. Maso, G.D., Rampazzo, F.: On systems of ordinary differential equations with measures as controls. Differ. Integr. Equ. **4**, 739–765 (1991)
815. Mason, M., Wang, Y.: On the inconsistency of rigid-body frictional planar mechanics. In: Proceedings of IEEE International Conference on Robotics and Automation, vol. 1, pp. 524–528. Philadelphia, PA, USA (1988)
816. Masoudi, R., Birkett, S., McPhee, J.: A mechanistic multibody model for simulating the dynamics of a vertical piano action. ASME J. Comput. Nonlinear Dyn. **9**, 031,014 (2014)
817. Masoudi, R., McPhee, J.: A novel micromechanical model of nonlinear compression hysteresis in compliant interfaces of multibody systems. Multibody Syst. Dyn. (2015). doi:10.1007/s11044-015-9483-6
818. Masri, S.F.: Theory of the dynamic vibration neutralizer with motion limiting stops. ASME J. Appl. Mech. **39**(2), 563–568 (1972)
819. Masri, S.F., Caughey, T.K.: On the stability of the impact damper. ASME J. Appl. Mech. **33**(3), 586–592 (1966)
820. Massah, H., Shaffer, F., Sinclair, J., Shahman, M.: Measurements of specular and diffuse particel-wall collision properties. In: C. Laguérie, J. Large (eds.) Fluidization VIII: Proceedings of the 8th International Conference Fluidization, pp. 641–648. Engineering Foundation (1995)
821. Mata-Jimenez, M., Brogliato, B.: Analysis of PD and nonlinear control of mechanical systems with dynamic backlash. J. Vib. Control **9**(1), 119–156 (2003)
822. Mate, C.M.: Tribology on the Small Scale. Mesoscopic Physics and Nanotechnology. Oxford University Press, Great Clarendon Street, Oxford, UK (2008)
823. Matrosov, V.M., Finogenko, I.A.: The solvability of the equations of motion of mechanical systems with sliding friction. J. Appl. Math. Mech. **58**(6), 945–954 (1994)
824. Matrosov, V.M., Finogenko, I.A.: Right-hand solutions of the differential equations of dynamics for mechanical systems with sliding friction. J. Appl. Math. Mech. **59**(6), 837–844 (1995)
825. Maugis, D.: Adhesion of spheres: The JKR-DMT transition using a Dugdale model. J. Colloid Interf. Sci. **150**(1), 243–269 (1992)
826. Maugis, D.: Contact. Adhesion and Rupture of Elastic Solids. Solid-State Sciences. Springer, Heidelberg (2000)
827. Maury, B., Venel, J.: A discrete contact model for crowd motion. ESAIM Math. Modell. Numer. Anal. **45**, 145–168 (2011)
828. Maw, N., Barber, J.R., Fawcett, J.N.: The oblique impact of elastic spheres. Wear **38**(1), 101–114 (1976)
829. Maw, N., Barber, J.R., Fawcett, J.N.: The rebound of elastic bodies in oblique impact. Mech. Res. Commun. **4**(1), 17–22 (1977)
830. Maw, N., Barber, J.R., Fawcett, J.N.: The role of elastic tangential compliance in oblique impact. ASME J. Lubr. Technol. **103**(1), 74–80 (1981). doi:10.1115/1.3251617
831. May, H., Panagiatopoulos, P.: Clarke's generalized gradient and Fourier's principle. ZAMM-J. Appl. Math. Mech. **65**(2), 125–126 (1985)
832. May, H.O.: Variational principles and differential inclusions for unilateral constraints in analytical mechanics. Meccanica 315–319 (1984)
833. May, H.O.: Jourdain's principle for unilateral constraints. Acta Mech. **60**, 171–180 (1986)
834. Mazière, P.: Les lois du choc des corps à ressort parfait ou imparfait, déduites d'une explication probable de la cause physique du ressort. Recueil des Pièces, Paris I, 1–108 (1727)
835. McClamroch, N.H., Wang, D.: Feedback stabilization and tracking of constrained robots. IEEE Trans. Autom. Control **33**(5), 419–426 (1988)
836. Mekki, O., Frémond, M.: Collision of four balls aligned. Vietnam J. Mech. **32**(3), 145–156 (2010)
837. Mello, T., Tufillaro, N.: Strange attractors of a bouncing ball. Am. J. Phys. **55**(4), 316–320 (1987)
838. Melo, F., Job, S., Santibanez, F., Tapia, F.: Experimental evidence of shock mitigation in a hertzian tapered chain. Phys. Rev. E **73**(041305) (2006)

839. Menini, L., Tornambé, A.: Asymptotic tracking of periodic trajectories for a simple mechanical system subject to nonsmooth impacts. IEEE Trans. Autom. Control **46**(7), 1122–1126 (2001)
840. Menini, L., Tornambè, A.: Dynamic position feedback stabilisation of multidegree-of-freedom linear mechanical system subject to nonsmooth impacts. IEE Proc. Control Theory Appl. **148**(6), 488–496 (2001)
841. Menini, L., Tornambè, A.: Exponential and BIBS stabilisation of one degree of freedom mechanical system subject to single non-smooth impacts. IEE Proc. Control Theory Appl. **148**(2), 147–155 (2001)
842. Menini, L., Tornambé, A.: Velocity observers for linear mechanical systems subject to single non-smooth impacts. Syst. Control Lett. **43**, 193–202 (2001)
843. Menini, L., Tornambé, A.: State estimation of (otherwise unobservable) linear mechanical systems through the use of non-smooth impacts: the case of two mating gears. Automatica **38**(10), 1823–1826 (2002)
844. Menini, L., Tornambé, A.: Velocity observers for non-linear mechanical systems subject to non-smooth impacts. Automatica **38**, 2169–2175 (2002)
845. Merkin, D.: Introduction to the Theory of Stability, Texts in Applied Mathematics, vol. 24. Springer (1997)
846. Merlhiot, X.: On some industrial applications of time-stepping methods for nonsmooth mechanical systems: issues, successes and challenges. In: Proceedings Euromech Colloquium 516, Nonsmooth contact and impact laws in mechanics. Grenoble, France (2011)
847. Michel, A., Hou, L.: Modeling and qualitative theory for general hybrid dynamical and control systems. In: Proceedings of IFAC-IFIP-IMACS Conference on Control of Industrial Systems. Belfort, France (1997)
848. Michel, A.N., Hou, L., Liu, D.: Stability of Dynamical Systems. Birkhäuser Boston (2008)
849. Mills, J.: Stability of robotic manipulators during transition to and from compliant motion. Automatica **26**(5), 861–874 (1990)
850. Mills, J., Goldenberg, A.: Force and position control of manipulators during constrained motion tasks. IEEE Trans. Autom. Control **5**(1), 30–46 (1989)
851. Mills, J., Goldenberg, A.: Constrained motion task control of robotic manipulator. Mech. Mach. Theory **29**(1), 95–115 (1994)
852. Mills, J., Lokhorst, D.: Control of robotic manipulators during general task execution: a discontinuous control approach. Int. J. Robot. Res. **12**(2), 146–163 (1993)
853. Mills, J., Lokhorst, D.: Stability and control of robotic manipulators during contact/noncontact task transition. IEEE Trans. Robot. Autom. **9**(3), 335–345 (1993)
854. Mills, J., Nguyen, C.: Robotic manipulator collisions: modeling and simulation. ASME J. Dyn. Syst. Meas. Control **114**(4), 650–659 (1992)
855. Milman, Y., Chugunova, S.: Mechanical properties, indentation and dynamic yield stress of ceramic targets. Int. J. Impact Eng. **23**, 629–638 (1999)
856. Milman, Y., Galanov, B., Chugunova, S.: Plasticity characteristic obtained through hardness measurement. Acta Metall. Mater. **41**(9), 2523–2532 (1993)
857. Minamoto, H., Kawamura, S.: Effects of material strain rate sensitivity in low speed impact between two identical spheres. Int. J. Impact Eng. **36**(5), 680–686 (2009)
858. Minamoto, H., Kawamura, S.: Moderately high speed impact of two identical spheres. Int. J. Impact Eng. **38**(2–3), 123–129 (2011)
859. Minamoto, H., Seifried, R., Eberhard, P., Kawamura, S.: Analysis of repeated impacts on a steel rod with visco-plastic material behaviour. Eur. J. Mech. A/Solids **30**, 336–344 (2011)
860. Mindlin, R.: Compliance of elastic bodies in contact. J. Appl. Mech. **16**, 259–268 (1949)
861. Mindlin, R., Deresiewicz, H.: Elastic spheres in contact under varying oblique forces. ASME J. Appl. Mech. **20**, 327–344 (1953)
862. von Mises, R.: Zur kritik des reigbungsggesetze. Zeitsch. Math. Phys. **58**, 191–195 (1910)
863. Möller, M., Glocker, C.: Rigid body dynamics with a scalable body, quaternions and perfect constraints. Multibody Syst. Dyn. **27**(4), 437–454 (2012)

864. Mollon, G., Richefeu, V., Villard, P., Daudon, D.: Discrete modelling of rock avalanches: sensitivity to block and slope geometry. Granular Matter **17**, 645–666 (2015)
865. Monerie, Y., Acary, V.: Formulation dynamique d'un modèle de zone cohésive tridimensionel couplant endommagement et frottement. Revue Européenne des Eléments Finis **10**(02–03-04), 489–503 (2001)
866. Monteiro-Marques, M.D.P.: Chocs inélastiques standards: un résultat d'existence (1985). Exposé no 15, preprint no 85–3, Séminaire d'Analyse Convexe, université de Montpellier, France
867. Monteiro-Marques, M.D.P.: Differential Inclusions in Nonsmooth Mechanical Problems: Shocks and Dry Friction, Progress in Non Linear Differential Equations, vol. 9. Birkhauser, Boston (1993)
868. Monteiro-Marques, M.D.P.: An existence, uniqueness and regularity study of the dynamics of systems with one-dimensional friction. Eur. J. Mech. A/Solids **13**(2), 277–306 (1994)
869. Moon, F.C., Li, G.X.: Experimental study of chaotic vibrations in a pin jointed space truss structure. Am. Inst. Aeronaut. Astronaut. J. **28**(5), 915–921 (1990)
870. Moon, F.C., Shaw, S.W.: Chaotic vibrations of a beam with non-linear boundary conditions. Int. J. Non-Linear Mech. **18**(6), 465–477 (1983)
871. Moore, D.B., Shaw, S.W.: The experimental response of an impacting pendulum system. Int. J. Non-linear Mech. **25**(1), 1–16 (1990)
872. Moore, M., Wilhems, J.: Collision detection and response for computer animation. SIGGRAPH 88. Conference Proceedings, pp. 289–298. ACM, Atlanta, GA, USA (1988)
873. Morarescu, C.I., Brogliato, B.: Passivity-based switching control of flexible-joint complementarity mechanical systems. Automatica **46**(1), 160–166 (2010)
874. Morarescu, C.I., Brogliato, B.: Trajectory tracking control of multiconstraint complementarity lagrangian systems. IEEE Trans. Autom. Control **55**(6), 1300–1313 (2010)
875. Morarescu, C.I., Brogliato, B., Haad, S.: Passivity-based switching control of flexible-joint complementarity mechanical systems (2008). INRIA Research Report 6739, https://hal.inria.fr/inria-00342292
876. Moreau, J.J.: Décomposition orthogonale d'un espace hilbertien selon deux cônes mutuellement pôlaires. C.R. Acad. Sci. Paris **255**, 238 (1962)
877. Moreau, J.J.: Les liaisons unilatérales et le principe de Gauss. C.R. Acad. Sci. Paris **256**, 871–874 (1963)
878. Moreau, J.J.: Quadratic programming in mechanics: dynamics of one sided constraints. J. SIAM Control **4**(1), 153–158 (1966)
879. Moreau, J.J.: La notion de surpotentiel et les liaisons unilatérales en élastostatique. C.R. Acad. Sci. Paris Sér. A-B pp. A954–A957 (1968)
880. Moreau, J.J.: Rafle par un convexe variable (première partie): Exposé no 15. Université de Montpellier, France, Séminaire d'Analyse Convexe (1971)
881. Moreau, J.J.: Rafle par un convexe variable (deuxième partie): Exposé no 3. Université de Montpellier, France, Séminaire d'Analyse Convexe (1972)
882. Moreau, J.J.: Problème d'évolution associé à un convexe mobile d'un espace hilbertien. Comptes Rendus Acad. Sci. Paris Sér. A **276**, 791–794 (1973). 12 Mars
883. Moreau, J.J.: On unilateral constraints, friction and plasticity. In: Capriz, G., Stampacchia, G. (eds.) New Variational Techniques in Mathematical Physics, CIME II Ciclo, pp. 173–222. Ediz. Cremonese, Roma (1974)
884. Moreau, J.J.: Sur les mesures différentielles de fonctions vectorielles (1975). Séminaire d'Analyse Convexe, Montpellier, 5, exposé 17
885. Moreau, J.J.: Application of convex analysis to the treatment of elastoplastic systems. In: Germain, P., Nayroles, B. (eds.) Applications of Methods of Functional Analysis to Problems of Mechanics, Joint Symposium IUTAM/IMU. Lecture Notes in Mathematics, pp. 56–89. Springer, Marseille, France (1976)
886. Moreau, J.J.: Sur les mesures différentielles et certains problèmes d'évolution. C.R. Ac adémie des Sci., Paris **A-B**, 282, 837 (1976)

887. Moreau, J.J.: Evolution problem associated with a moving convex set in a Hilbert space. J. Differ. Equ. **26**(3), 347–374 (1977)
888. Moreau, J.J.: Approximation en graphe d'une évolution discontinue. RAIRO-Analyse Numérique **12**(1), 75–84 (1978)
889. Moreau, J.J.: Application of convex analysis to some problems of dry friction. In: Zorski, H. (ed.) Trends in Applications of Pure Mathematics to Mechanics, vol. 2, pp. 263–280. Pitman publishing Ltd, London (1979)
890. Moreau, J.J.: Liaisons unilatérales sans frottement et chocs inélastiques. C.R. Acad. Sci. Paris **296**, 1473–1476 (1983)
891. Moreau, J.J.: Standard inelastic shocks and the dynamics of unilateral constraints. In: CISM Courses and Lectures, vol. 288, pp. 173–221. Springer Verlag (1985). Preprint 84–2, February 1984, Laboratoire de Mécanique Générale des Milieux Continus, université des Sciences et Techniques du Languedoc, France
892. Moreau, J.J.: Dynamique de systèmes à liaisons unilatérales avec frottement sec éventuel; essais numériques. Tech. rep., Laboratoire de Mécanique et Génie Civil, Montpellier, France (1986). Technical note 85–1, Laboratoire de Mécanique Générale des Milieux Continus, universit des Sciences et Techniques du Languedoc, France
893. Moreau, J.J.: Bounded variation in time. In: Moreau, J.J., Panagiotopoulos, P., Starng, G. (eds.) Topics in Nonsmooth Dynamics, pp. 1–74. Birkhauser, Basel (1988)
894. Moreau, J.J.: Unilateral contact and dry friction in finite freedom dynamics. In: Moreau, J., Panagiotopoulos, P. (eds.) Nonsmooth Mechanics and Applications, CISM Courses and Lectures, vol. 302, pp. 1–82. Springer Verlag, International Center for Mechanical Sciences, Udine, Italy (1988)
895. Moreau, J.J.: An expression of classical dynamics. In: Ann. Inst. H. Poincaré, Anal. Non Linéaire, vol. 6, pp. 1–48 (1989). Also in Analyse non-linéaire, Gauthier-Villars, Paris, H. Attouch, J.P. Aubin, F. Clarke, I. Ekeland, Eds., pp. 1–48
896. Moreau, J.J.: Some numerical methods in multibody dynamics: application to granular materials. Eur. J. Mech. A/Solids **13**(4), 93–114 (1994)
897. Moreau, J.J.: Numerical aspects of the sweeping process. Comput. Methods Appl. Mech. Eng. **177**(3–4), 329–349 (1999)
898. Moreau, J.J.: Fonctionnelles Convexes. Istituto Poligrafico e Zecca dello Stato S.p.A., Roma, Italy, : Originally Séminaire sur les équations aux dérivées partielles, pp. 1966–1967. Collège de France, Paris (2003)
899. Moreau, J.J.: Indetermination due to dry friction in multibody dynamics. In: Neittaanmaki, P., Rossi, T., Korotov, S., Onate, E., Periaux, J., Knorzer, D. (eds.) European Congress on Computational Methods in Applied Sciences and Engineering. ECCOMAS. Jyväskylä, Finland (2004)
900. Moreau, J.J.: An introduction to unilateral dynamics. In: M.F. et al. (ed.) Novel Approaches in Civil Engineering. Springer, Berlin (2004)
901. Moreau, J.J., Panagiotopoulos, P. (eds.): Nonsmooth Mechanics and Applications, CISM Courses and Lectures, vol. 302. Springer, International Centre for Mechanical Sciences, Udine, Italy (1988)
902. Morgado, W.A.M., Oppenheim, I.: Energy dissipation for quasielastic granular particle collisions. Phys. Rev. E **55**(2), 1940–1945 (1997)
903. Morgensen, K.A., Pin, F.G.: Impact mitigation using kinematic constraints and the full space parameterization method. In: Proceedings of IEEE International Conference on Robotics and Automation, vol. 2, pp. 1897–1902. Minneapolis, USA (1996)
904. Morin, A.: Notions Fondamentales de Mécanique. Hachette, Paris (1855)
905. Mourya, R., Chatterjee, A.: Anomalous frictional behaviour in collisions of thin disks revisited. ASME J. Appl. Mech. **75**(2), 024,501 (2008)
906. Müller, P., Pöschel, T.: Collision of viscoelastic spheres: compact expressions for the coefficient of normal restitution. Phys. Rev. E **84**(2), 021,302 (2011)
907. Müller, P., Poschël, T.: Oblique impact of frictionless spheres: on the limitations of hard sphere models for granular dynamics. Granular Matter **14**, 115–120 (2012)

908. Müller, S., Kästner, M., Brummund, J., Ulbricht, V.: A nonlinear fractional viscoelastic material model for polymers. Comput. Mater. Sci. **50**, 2938–2949 (2011)
909. Murray, J.M.: Existence theorems for optimal control and calculus of variations problems where the states can jump. SIAM J. Control Optim. **24**(3), 412–438 (1986)
910. Myagchilov, S.V., Jenkins, J.T.: Analysis of the motion of a frictional elastic ball dropped on an inclined surface. ASME J. Appl. Mech. **64**(3), 707–709 (1997)
911. Nagaev, R.F., Yakimova, K.S.: Impact of a two-body elastic system on a fixed plane. Izv. AN SSSR, Mekhanika Tverdogo Tela **6**(6), 14–24 (1971)
912. Nagy, Z., Leine, R.I., Frutiger, D.R., Glocker, C., Nelson, B.J.: Modeling the motion of microrobots on surfaces using nonsmooth multibody dynamics. IEEE Trans. Robot. **28**(5), 1058–1068 (2012)
913. Nahon, M., Angeles, J.: Reducing the effects of shocks using redundant actuation. In: Proceedings of IEEE International Conference on Robotics and Automation, pp. 238–243. Sacramento, USA (1991)
914. Najafabadi, S.A.M., Kövecses, J., Angeles, J.: Generalization of the energetic coefficient of restitution for contacts in multibody systems. ASME J. Comput. Nonlinear Dyn. 3(4), 041,008 (2008)
915. Nakagawa, M., Agui, J.H., Wu, D.T., Extramiana, D.V.: Impulse dispersion in a tapered granular chain. Granular Matter **4**(167–174) (2003)
916. Naldi, R., Sanfelice, R.G.: Passivity-based control for hybrid systems with applications to mechanical systems exhibiting impacts. Automatica **9**(5), 1104–1116 (2013)
917. van Name, F.W.: Experiment for measuring the coefficient of restitution. Am. J. of Phys. **26**, 386–388 (1958)
918. Narabayashi, T., Shibaike, K., Ishizaka, A., Ozaki, K.: Effects of key parameters on energy distribution and kinetic characteristics in collision of bar and beam. J. Sound Vib. **308**, 548–562 (2007)
919. Natsavias, S., Babcock, C.D.: Behaviour of unanchored fluid filled tanks subjected to ground excitation. ASME J. Appl. Mech. **55**(3), 654–659 (1988)
920. Navier, C.L.M.H.: Résumé des Leçons Données sur l'Application de la Mécanique l'Etablissement des Constructions et des Machines, vol. 2. Carilian-Goeury, Paris (1838)
921. Neilson, R.D., Barr, A.D.S.: Dynamics of a rigid motor mounted on discontinuously nonlinear elastic supports. Proc. Inst. Mech. Eng., Part C. J. Mech. Eng. Sci. **202**(5), 369–376 (1988)
922. Neimark, Y.I., Fufaev, N.A.: The Painlevé paradoxes and the dynamics of a brake shoe. J. Appl. Math. Mech. **59**(3), 343–352 (1995)
923. Nenchev, D.N., Yoshida, K.: Impact analysis and post-impact motion control issues of a free-floating space robot subject to a force impulse. IEEE Trans. Robot. Autom. **15**(3), 548–557 (1999)
924. Nesterenko, V.F.: Propagation of nonlinear compression pulses in granular media. J. Appl. Mech. Tech. Phys. **24**(5), 733–743 (1983)
925. Newton, I.: Philosophia Naturalis Principia Mathematica. S. Pepys, Reg. Soc. PRAESES, London (1686)
926. Ngo, D., Griffiths, S., Khatri, D., Daraio, C.: Highly nonlinear solitary waves in chains of hollow spherical particles. Granular Matter **15**(2), 149–155 (2013)
927. Nguyen, D.T., Noah, S.T., Kettleborough, C.F.: Impact behaviour of an oscillator with limiting stops, part i: a parametric study. J. Sound Vib. **109**(2), 293–307 (1986)
928. Nguyen, N.S., Brogliato, B.: Shock dynamics in granular chains: numerical simulations and comparisons with experimental tests. Granular Matter **14**(3), 341–362 (2012)
929. Nguyen, N.S., Brogliato, B.: Multiple Impacts in Dissipative Granular Chains. Lecture Notes in Applied and Computational Mechanics, vol. 72. Springer, Berlin (2014)
930. Nijmeijer, H., van der Schaft, A.J.: Nonlinear Dynamical Control Systems. Springer (1990)
931. Nikol'skii, S.M. (ed.): Analysis III. Spaces of Differentiable Functions. Springer (1991)
932. Nordmark, A., Dankowicz, H., Champneys, A.: Discontinuity-induced bifurcations in systems with impacts and friction: Discontinuity in the impact law. Int. J. Non-Linear Mech. **44**, 1011–1023 (2009)

933. Nordmark, A., Dankowicz, H., Champneys, A.: Friction-induced reverse chatter in rigid-body mechanisms with impacts. IMA J. Appl. Math. **76**, 85–119 (2011)
934. Nordmark, A.B.: Non-periodic motion caused by grazing incidence in an impact oscillator. J. Sound Vib. **145**(2), 279–297 (1991)
935. Nordmark, A.B.: Effects due to low velocity impact in a mechanical oscillator. Int. J. Bifurcat. Chaos **2**(3), 597–605 (1992)
936. Nqi, F.Z.: Etude numérique de divers problèmes dynamiques avec impact et de leurs propriétés qualitatives. Ph.D. thesis, Laboratoire d'Analyse Numérique, Université Claude Bernard Lyon 1, France (1997)
937. Nqi, F.Z., Schatzman, M.: Computation of Lyapunov exponents for a dynamical system with impacts. Tech. rep., Laboratoire d'Analyse Numérique, Université Claude Bernard Lyon 1, France (1996). Internal Report 215
938. Nucera, F., Vakakis, A.F., McFarland, D.M., Bergman, L.A., Kerschen, G.: Targeted energy transfers in vibro- impact oscillators for seismic mitigation. Nonlinear Dyn. **50**, 651–677 (2007)
939. Nusse, H.E., Ott, E., Yorke, J.A.: Border-collision bifurcations: an explanation for observed bifurcation phenomena. Phys. Rev. E **49**(2), 1073–1076 (1994)
940. Olansen, J.B., Dunn, P.F.: Dispensing particles under atmospheric and vacuum conditions using an electrostatic device. J. Appl. Phys. **66**(12), 6098–6109 (1989)
941. Olyaei, A.A., Ghazavi, M.R.: Stabilizing slider-crank mechanism with clearance joints. Mech. Mach. Theory **53**, 17–29 (2012)
942. Or, Y.: Painlevé's paradox and dynamic jamming in simple models of passive dynamic walking. Regul. Chaotic Dyn. **19**(1), 64–80 (2014)
943. Or, Y., Ames, A.D.: Stability and completion of Zeno equilibria in Lagrangian hybrid systems. IEEE Trans. Autom. Control **56**(6), 1322–1336 (2011)
944. Or, Y., Rimon, E.: Investigation of Painlevé's paradox and dynamic jamming during mechanism sliding motion. Nonlinear Dyn. **67**(2), 1647–1668 (2012)
945. Or, Y., Teel, A.R.: Zeno stability of the set-valued bouncing ball. IEEE Trans. Automa. Control **56**(2), 447–452 (2011)
946. Orlov, Y.: Vibrocorrect differential equations with measures. Math. Notes Acad. Sci. USSR **38**(1), 574–580 (1985)
947. Orlov, Y.: Nonlinear control systems with impulsive inputs. In: Proceedings of 36th IEEE Conference Decision and Control, vol. 1, pp. 630–635. San Diego, USA (1997)
948. Orlov, Y.: Finite-time stability and robust control synthesis of uncertain switched systems. SIAM J. Control Optim. **43**(4), 1253–1271 (2005)
949. Ovcharenko, A., Halperin, G., Verberne, G., Etsion, I.: In situ investigation of the contact area in elastic-plastic spherical contact during loading-unloading. Tribol, Lett (2007)
950. Oza, H.B., Orlov, Y.V., Spurgeon, S.K.: Finite time stabilization of a perturbed double integrator with unilateral constraints. Math. Comput. Simul. **95**, 200–212 (2013)
951. Pagilla, P.R.: Control of contact problem in constrained Euler-Lagrange systems. IEEE Trans. Autom. Control **46**(10), 1595–1599 (2001)
952. Pagilla, P.R., Yu, B.: Experimental study of planar impact of a robot manipulator. IEEE/ASME Trans. Mech. **9**(1), 123–128 (2004)
953. Paidoussis, M.P., Li, G.X.: Cross-flow-induced chaotic vibrations of heat exchanger tubes impacting on loose supports. J. Sound Vib. **152**(2), 305–326 (1992)
954. Painlevé, P.: Leçons sur le Frottement. Hermann, Paris (1895)
955. Painlevé, P.: Sur les lois du frottement de glissement. C.R. Acad. Sci. Paris 121, 112–115 (1895). Note presentée par M. Appel. Also, vol. 141, pp. 401–405, pp. 546–552
956. Pal, R.K., Awasthi, A.P., Geubelle, P.H.: Wave propagation in elasto-plastic granular systems. Granular Matter **15**, 747–758 (2013)
957. Palas, H., Hsu, W.C., Shabana, A.A.: On the use of momentum balance method in transverse impact problems. ASME J. Vib. Acoust. **114**(3), 364–373 (1992)
958. Panagiotopoulos, P.D.: Ungleichungsprobleme und differentialinklusionen in der analytischen mechanik. In: Annual Proceedings of the School of Technology, Aristotle University, pp. 100–140 (1982). Vol. Θ'

959. Panagiotopoulos, P.D.: Variational principles for contact problems including impact phenomena. In: M. Raous, M. Jean, J. Moreau (eds.) Contact Mechanics, pp. 431–440. Plenum Press (1995)
960. Panagiotopoulos, P.D., Glocker, C.: Analytical mechanics. addendum i: Inequality constraints with elastic impacts. the convex case. ZAMM. Z. Angew. Math. Mech. **78**(4), 219–229 (1998)
961. Pandit, S.G., Deo, S.G.: Differential Systems Involving Impulses. Springer, Berlin (1982)
962. Pang, J.S., Shen, J.: Strongly regular differential variational systems. IEEE Trans. Autom. Control **52**(2), 242–255 (2007)
963. Pang, J.S., Trinkle, J.: Complementarity formulation and existence of solutions of dynamic rigid-body contact problems with Coulomb friction. Math. Program. **73**(2), 199–226 (1996)
964. Pang, J.S., Trinkle, J.: Stability characterizations of rigid body contact problems with Coulomb friction. ZAMM J. Appl. Math. Mech. Zeitschrift für Angewandte Mathematik und Mechanik **80**(10), 643–663 (2000)
965. Paola, M.D., Pirrotta, A.: Non-linear systems under impulsive parametric input. Int. J. Non-Linear Mech. **34**, 843–851 (1999)
966. Paoli, L.: Analyse numérique de vibrations avec contraintes unilatérales. Ph.D. thesis, Université Claude Bernard- Lyon 1, Laboratoire d'Analyse Numérique, Lyon, France (1993)
967. Paoli, L.: Continuous dependence on data for vibro-impact problems. Math. Models Methods Appl. Sci. (M3AS) **35**(1), 1–41 (2005)
968. Paoli, L.: A proximal-like method for a class of second order measure-differential inclusions describing vibro-impact problems. J. Differ. Equ. **250**, 476–514 (2011)
969. Paoli, L., Schatzman, M.: Mouvement à un nombre fini de degrés de liberté avec contraintes unilatérales: cas avec perte d'énergie. Math. Modell. Numer. Anal. (Modèlisation mathématique et analyse numérique) **27**(6), 673–717 (1993)
970. Paoli, L., Schatzman, M.: A numerical scheme for a dynamical impact problem with loss of energy in finite dimension. C.R. Acad. Sci. Paris 317, 211–215 (1993). Preprint A numerical scheme for a dynamical impact problem with loss of energy in finite dimension", Equipe d'analyse numérique Lyon-Saint Etienne, France, URA CNRS 740, Technical note 167, February
971. Paoli, L., Schatzman, M.: Theoretical and numerical study for a model of vibrations with unilateral constraints. In: Raous, M., Jean, M., Moreau, J. (eds.) Contact Mechanics, pp. 457–464. Plenum Press, New York (1995)
972. Paoli, L., Schatzman, M.: Theoretical and numerical study of vibrations with unilateral constraints: case of a nonconvex set of constraints. In: Proceedings of 4th World Congress on Computational Mechanics. IACM-International Association of Computational Mechanics, Buenos Aires, A (1998)
973. Paoli, L., Schatzman, M.: Penalty approximation for non-smooth constraints in vibroimpact. J. Differ. Equ. **177**(2), 375–418 (2001)
974. Paoli, L., Schatzman, M.: A numerical scheme for impact problems I: the one-dimensional case. II: the multidimensional case. SIAM J. Numer. Anal. **40**(2), 702–768 (2002)
975. Paoli, L., Schatzman, M.: Penalty approximation for dynamical systems submitted to multiple non-smooth constraints. Multibody Syst. Dyn. **8**, 347–366 (2002)
976. Papastavridis, J.G.: Impulsive motion of ideally constrained mechanical systems via analytical dynamics. Int. J. Eng. Sci. **27**(12), 1445–1461 (1989)
977. Parker, J.K., Paul, F.W.: Controlling the impact forces in pneumatic robot hand design. ASME J. Dyn. Syst. Meas. Control **109**(4), 328–334 (1987)
978. Parsa, K.: The Lagrangian derivation of Kane's equations. Transactions of the Canadian Society for Mechanical Engineering/de la Société Canadienne de Génie Mécanique **31**(4), 407–420 (2007)
979. Pasha, M., Dogbe, S., Hare, C., Hassanpour, A., Ghadiri, M.: A linear model of elasto-plastic and adhesive contact deformation. Granular Matter **16**, 151–162 (2014). doi:10.1007/s10035-013-0476-y

980. Pasquero, S.: Ideality criterion for unilateral constraints in time-dependent impulsive mechanics. AIP J. Math. Phys. **46**(11), 112,904 (2005)
981. Pasquero, S.: On the simultaneous presence of unilateral and kinetic constraints in time-dependent impulsive mechanics. AIP J. Math. Phys. **47**, 082,903 (2006)
982. Patricio, P.: The Hertz contact in chain of elastic collision. Am. J. Phys. **72**(12), 1488–1492 (2004)
983. Pauchard, L., Rica, S.: Contact and compression of elastic spherical shells: the physics of a ping-pong ball. Philos. Mag. B **78**(2), 225–233 (1998)
984. Payandeh, S.: A method for controlling robotic contact tasks. Robotica **14**(3), 281–288 (1996)
985. Payr, M.D.: An Experimental and Theoretical Study of Perfect Multiple Contact Collisions in Linear Chains of Bodies. Ph.D. thesis, ETH Zurich (2008). http://e-collection.library.ethz.ch/view/eth:30862
986. Pécol, P., Pont, S.D., Erlicher, S., Argoul, P.: Smooth/non-smooth contact modeling of human crowds movement: numerical aspects and application to emergency evacuations. Ann. Solid Struct. Mech. **2**, 69–85 (2011)
987. Pena, F., Lourenço, P.B., Campos-Costa, A.: Experimental dynamic behavior of free-standing multi-block structures under seismic loadings. J. Earthq. Eng. **12**, 953–979 (2008)
988. Pena, F., Prieto, F., Lourenço, P.B., Costa, A.C., Lemos, J.V.: On the dynamics of rocking motion of single rigid-block structures. Earthq. Eng. Struct. Dyn. **36**, 2383–2399 (2007)
989. Percivale, D.: Uniqueness in the elastic bounce problem. J. Differ. Equ. **56**(2), 206–215 (1985)
990. Percivale, D.: Uniqueness in the elastic bounce problem, ii. J. Differ. Equ. **90**(2), 304–315 (1991)
991. Pereira, C.M., Ramalho, A.L., Ambrosio, J.A.: A critical overview of internal and external cylinder contact force models. Nonlinear Dyn. **63**, 681–697 (2011)
992. Pereira, C.M., Ramalho, A.L., Ambrosio, J.A.: Applicability domain of internal cylindrical contact force models. Mech. Mach. Theory **78**, 141–157 (2014)
993. Pereira, F.L., Silva, G.N.: Lyapunov stability of measure driven impulsive systems. Differ. Equ. **40**(8), 1122–1130 (2004)
994. Pérès, J.: Choc en tenant compte du frottement. Nouvelles Annales de Math., 5$^{\text{ème}}$ série **2**, 98–107 (1923)
995. Pérès, J.: Mécanique Générale. Masson, Paris (1953)
996. Perret-Liaudet, J., Rigaud, E.: Experiments and numerical results on non-linear vibrations of an impacting Hertzian contact. Part 2: random excitation. J. Sound Vib. **265**, 309–327 (2003)
997. Persoz, B. (ed.): La Rhéologie: Recueil de Travaux des Sessions de Perfectionnement, Monographies du Centre d'Actualisation Scientifique et Technique, vol. 3. Masson, Institut National des Sciences Appliquées de Lyon (1969)
998. Peterka, F., Vacik, J.: Transition to chaotic motion in mechanical systems with impacts. J. Sound Vib. **154**(1), 95–115 (1992)
999. Peters, D.A.: Optimum spring-damper design for mass impact. SIAM Rev. **39**(1), 118–122 (1997)
1000. Pfeiffer, F.: On impacts with friction. Appl. Math. Comput. **217**, 1184–1192 (2010)
1001. Pfeiffer, F., Glocker, C.: Multibody Dynamics with Unilateral Contacts. Nonlinear Dynamics, Wiley interscience (1996)
1002. Phillips, E.: Liouville's Journal **14**, 312 (1849)
1003. Pierre, D.A.: Optimization Theory with Applications. Dover Publications, New York (1986)
1004. Pierrot, F., Jean, M., Dauchez, P.: Nonsmooth mechanics approach for robot simulations. In: Proceedings of IFAC Symposium on Robot Control SYROCO, pp. 577–582. Capri, Italy (1994)
1005. Pina, E.: Binary collisions in velocity space. Am. J. Phys. **46**, 528–529 (1978)
1006. Poinsot, L.: La percussion des corps. Journal de Mathématiques Pures et Appliquées **2**(3), 281–350 (1857)

1007. Poinsot, L.: Sur la quantité de mouvement qui est transmise à un corps par le choc d'un point massif qui vient le frapper dans une direction donnée. Journal de Mathématiques Pures et Appliquées **2**(4), 161–170 (1859)
1008. Poisson, S.D.: Traité de Mécanique. Bachelier, Paris (1833)
1009. Poliquin, R.A., Rockafellar, R.T., Thibault, L.: Local differentiability of distance functions. Trans. Amer. Math. Soc. **352**, 5231–5249 (2000)
1010. Pompei, A., Scalia, A., Sumbatyan, M.A.: Dynamics of rigid block due to horizontal ground motion. J. Eng. Mech. ASCE **124**(7), 713–717 (1998)
1011. Popplewell, N., Bapat, C.N., MacLachlan, K.: Stable periodic vibroimpacts of an oscillator. J. Sound Vib. **87**(1), 41–59 (1983)
1012. Porter, M.A., Daraio, C., Szelengowicz, I., Herbold, E.B., Kevrekidis, P.G.: Highly nonlinear solitary waves in heterogeneous periodic granular media. Phys. D **238**, 666–676 (2009)
1013. Posa, M., Tobenkin, M., Tedrake, R.: Stability analysis and control of rigid-body systems with impacts and friction. IEEE Trans. Autom. Control (2015). http://dx.doi.org/10.1109/TAC.2015.2459151
1014. Pouyet, J., Lataillade, J.L.: Dynamic investigation of hard viscoelastic materials by ball bouncing experiments. J. Mat. Sci. **10**, 2112–2116 (1975)
1015. Pozharitskii, G.K.: Extension of the principle of Gauss to systems with dry (Coulomb) friction. J. Appl. Math. Mech. **25**(3), 586–607 (1961)
1016. Prandtl, L.: Bemerkungen zu den aufsätzen der herren F. Klein, R.v. Mises und G. Hamel. Zeitsch. Math. Phys. **58**, 196–197 (1910)
1017. On the rocking behavior of rigid objects: Prieto, F., co, P.B.L. Meccanica **40**, 121–133 (2005)
1018. Prochazka, F., Valasek, M., Sika, Z.: Robust sliding mode control of redundantly actuated parallel mechanisms with respect to geometric imperfections. Multibody Syst. Dyn. (2015). doi:10.1007/s11044-015-9481-8
1019. Pustylnikov, L.D.: Existence of a set of positive measure of oscillating motions in a certain problem of dynamics. Dokl. Akad. Nauk SSSR, Soviet Math. Dokl. **202**(2) (1972)
1020. Pustylnikov, L.D.: Stable and oscillating motions in non-autonomous dynamical systems. Trans. Moscow Math. Soc. **14**, 1–101 (1978)
1021. Quinn, D.D.: The dynamics of two parametrically excited pendula with impacts. Int. J. Bifurcat. Chaos **15**(6), 1975–1988 (2005)
1022. Rabatel, M., Labbé, S., Weiss, J.: Dynamics of an assembly of rigid ice floes. J. Geophys. Res.: Oceans **120** (2015). doi:10.1002/2015JC010909
1023. Radjai, F., Jean, M., Moreau, J.J., Roux, S.: Force distributions in dense two-dimensional granular systems. Phys. Rev. Lett. **77**(2–8), 274–277 (1996)
1024. Radjai, F., Richefeu, V.: Contact dynamics as a nonsmooth discrete element method. Mech. Mater. **41**(6), 715–728 (2009). doi:10.1016/j.mechmat.2009.01.028
1025. Radjai, F., Wolf, D.E., Jean, M., Moreau, J.J.: Bimodal character of stress transmission in granular packings. Phys. Rev. Lett. **80**, 61–64 (1998). doi:10.1103/PhysRevLett.80.61
1026. Rakshit, S., Chatterjee, A.: Scalar generalization of Newtonian restitution for simultaneous impacts. Int. J. Mech. Sci. **103**, 141–157 (2015)
1027. Ramirez, R., Pöschel, T., Brilliantov, N.V., Schwager, T.: Coefficient of restitution of colliding viscoelastic spheres. Phys. Rev. E **60**(4), 4465–4472 (1999)
1028. Ramsey, G.P.: A simplified approach to collision processes. Am. J. Phys. **65**(5), 384–389 (1997)
1029. Ran, X.J., Liu, M.Z., Zhu, Q.Y.: Numerical methods for impulsive differential equation. Math. Comput. Modell. **48**, 46–55 (2008)
1030. Randelovic, B.M., Stefanovic, L.V., Dankovic, B.M.: Numerical solution of impulsive differential equations. Facta Universitatis (Nis), Ser. Math. Inform. **15**, 101–111 (2000)
1031. Rao, M.R.M., Rao, V.S.H.: Stability of impulsively perturbed systems. Bull. Austral. Math. Soc. **16**, 99–110 (1977)
1032. Raous, M.: Quasistatic Signorini problem with Coulomb friction and coupling to adhesion. In: Wriggers, P., Panagiotopoulos, P. (eds.) New developments in Contact Problems, CISM Courses and Lectures no 388, pp. 101–178. Springer Verlag, Wien (1999)

1033. Rayleigh, L.: XXII. On the production of vibrations by forces of relatively long duration, with application to the theory of collisions. Philos. Mag. Ser. 6 **11**(62), 283–291 (1906)
1034. Reed, J.: Energy losses due to elastic wave propagation during an elastic impact. J. Phys. D: Appl. Phys. **18**(12), 2329–2337 (1985)
1035. Reinsch, M.: Dispersion-free linear chains. Am. J. Phys. **62**(3), 271–278 (1994)
1036. Renzo, A.D., Maio, F.P.D.: Comparison of contact-force models for the simulation of collisions in DEM-based granular flow codes. Chem. Eng. Sci. **59**, 525–541 (2004)
1037. Renzo, A.D., Maio, F.P.D.: An improved integral non-linear model for the contact of particles in distinct element simulations. Chem. Eng. Sci. **60**, 1303–1312 (2005)
1038. Resal, H.: Sur la theorie des chocs. Comptes Rendus des Seances Hebdomadaires de l'Académie des Sciences, Paris LXXVII **I**(3), 153–157 (1874)
1039. Richefeu, V., Mollon, G., Daudon, D., Villard, P.: Dissipative contacts and realistic block shapes for modeling rock avalanches. Eng. Geol. **149–150**, 78–92 (2012)
1040. Rigaud, E., Perret-Liaudet, J.: Experiments and numerical results on non-linear vibrations of an impacting Hertzian contact. Part 1: harmonic excitation. J. Sound Vib. **265**, 289–307 (2003)
1041. Rismantab-Sany, J., Shabana, A.: On the use of momentum balance in the impact analysis of constrained of constrained elastic systems. ASME J. Vib., Acoust., Stress, Reliab. Des. **112**(1), 119–126 (1990)
1042. Rivadeneira, P.S., Moog, C.H.: Observability criteria for impulsive control systems with applications to biomedical engineering processes. Automatica **55**, 125–131 (2015)
1043. Rizzi, A.A., Koditschek, D.E.: Further progress in robot juggling: Solvable mirror laws. In: Proceedings of IEEE International Conference on Robotics and Automation, vol. 4, pp. 2935–2940. San Diego, USA (1994)
1044. Rizzi, A.A., Whitcomb, L.L., Koditschek, D.E.: Distributed real-time control of a spatial robot juggler. IEEE Comput. **25**(5), 12–24 (1992)
1045. Rockafellar, R.T.: Convex Analysis. Princeton University Press (1970)
1046. Rockafellar, R.T., Wets, R.J.B.: Variational Analysis, Comprehensive Studies in Mathematics, vol. 317. Springer, Berlin Heidelberg (1998)
1047. Rodriguez, A., Bowling, A.: Solution to indeterminate multipoint impact with frictional contact using constraints. Multibody Syst. Dyn. **28**(4), 313–330 (2012)
1048. Rodriguez, A., Bowling, A.: Study of Newton's cradle using a new discrete approach. Multibody Syst. Dyn. **33**(1), 61–92 (2015)
1049. Routh, E.J.: Dynamics of a System of Rigid Bodies, Part I. MacMillan, London,: Seventh edition. Dover publications, New York (1877). 1960
1050. Roux, S.: La philosophie mécanique 1630–1690. Ph.D. thesis, Centre Koyré, EHESS, Paris (1996)
1051. Rubin, M.B.: Physical restrictions on the impulse acting during three-dimensional impact of two "rigid" bodies. ASME J. Appl. Mech. **65**(2), 464–469 (1998)
1052. Rudin, W.: Principles of Mathematical Analysis, third, edition edn. Int. Series in Pure and Applied Mathematics, Mac Graw Hill (1964)
1053. Rudin, W.: Analyse Réelle et Complexe. Dunod, Paris (1998)
1054. Sadek, M.M.: Impact dampers for controlling vibration in machine tools. Machinery **120**, 152–161 (1972)
1055. Sadek, M.M., Mills, B.: The effect of gravity on the performance of an impact damper. i: Steady state motion, ii: Stability of vibration modes. J. Mech. Eng. Sci. **12**(4), 268–287 (1970)
1056. de Saint Venant, A.B.: Mémoire sur le choc longitudinal de deux barres élastiques de grosseurs et de matiéres semblables ou différentes, et sur la proportion de leur force vive qui est perdue pour la translation ultérieure; et généralement sur le mouvement longitudinal d'un systéme de deux ou plusieurs prismes élastiques. Journal de Mathématiques Pures et Appliquées (Journal de Liouville) série 2 **12**, 237–376 (1867)
1057. Sampei, M., Furuta, K.: Exact linearization with time scaling. IEEE Trans. Autom. Control **31**(5), 459–462 (1986)

1058. Sanders, A.P., Tibbits, I.B., Kakarla, D., Siskey, S., Ochoa, J.A., Oong, K.L., Brannon, R.M.: Contact-coupled impact of slender rods: analysis and experimental validation. Exp. Mech. **54**, 187–198 (2014)
1059. Santibanez, F., Munoz, R., Caussarieu, A., Job, S., Melo, F.: Experimental evidence of solitary wave interaction in hertzian chains. Phys. Rev. E **84**, 026,604 (2011). doi:10.1103/PhysRevE.84.026604
1060. Sato, K., Yamamoto, S., Kawakami, T.: Bifurcation sets and chaotic states of a gear system subjected to harmonic excitation. Comput. Mech. **7**(3), 173–182 (1991)
1061. Saux, C.L., Cevaer, F., Motro, R.: An event-driven algorithm in dynamics of multi-contact systems. In: M. Frémond, F. Maceri (eds.) Mechanics, Models and Methods in Civil Engineering, Lecture Notes in Applied and Computational Mechanics, vol. 61, pp. 395–408 (2012)
1062. de Saxcé, G., Feng, Z.Q.: The bipotential method: a constructive approach to design the complete contact law with friction and improved numerical algorithm. Math. Comput. Modell. **28**(4–8), 225–245 (1998)
1063. van der Schaft, A.J., Schumacher, J.M.: The complementary-slackness class of hybrid systems. Math. Control, Sig. Syst. **9**(3), 266–301 (1996)
1064. van der Schaft, A.J., Schumacher, J.M.: Complementarity modeling of hybrid systems. IEEE Trans. Autom. Control **43**(4), 483–490 (1998)
1065. van der Schaft, A.J., Schumacher, J.M.: An Introduction to Hybrid Dynamical Systems. Lecture Notes in Control and Information Sciences, vol. 251. Springer, London (2000)
1066. Schatzman, M.: A class of nonlinear differential equations of second order in time. Nonlinear Anal., Theory, Methods Appl. **2**(3), 355–373 (1978)
1067. Schatzman, M.: The isoenergetic change of time for convex irregular hamiltonian systems. Tech. rep., CEREMADE, Univ. Paris-Dauphine, France, Paris (1980)
1068. Schatzman, M.: Un problème hyperbolique du $2^{\text{ème}}$ ordre avec contrainte unilatérale: La corde vibrante avec obstacle ponctuel. J. Differ. Equ. **36**(2), 295–334 (1980)
1069. Schatzman, M.: Uniqueness and continuous dependence on data for one-dimensional impact problem. Math. Comput. Modell. **28**(4–8), 1–18 (1998)
1070. Schatzman, M.: Penalty method for impact in generalized coordinates. Philos. Trans. Roy. Soc. Math., Phys. Eng. Sci. **359**(1789), 2429–2446 (2001)
1071. Scheibe, F., Smith, M.C.: A behavioral approach to play in mechanical networks. SIAM J. Control Optim. **47**(6), 2967–2990 (2008)
1072. Schiehlen, W., Seifried, R.: Three approaches for elastodynamic contact in multibody systems. Multibody Syst. Dyn. **12**, 1–16 (2004)
1073. Schiehlen, W., Seifried, R., Eberhard, P.: Elastoplastic phenomena in multibody impact dynamics. Comput. Methods Appl. Mech. Engrg. **195**, 6874–6890 (2006)
1074. Schindler, T., Acary, V.: Timestepping schemes for nonsmooth dynamics based on discontinuous Galerking methods: Definition and outlook. Math. Comput. Simul. **95**, 180–199 (2013)
1075. Schindler, T., Rezaei, S., Kursawe, J., Acary, V.: Half-explicit timestepping schemes on velocity level based on time-discontinuous Galerkin methods. Comput. Methods Appl. Mech. Eng. **290**, 250–276 (2015)
1076. Schmaedeke, W.W.: Optimal control theory for nonlinear vector differential equations containing measures. SIAM J. Control **3**(2), 231–280 (1965)
1077. Schmidt, F., Lamarque, C.H.: Energy pumping for mechanical systems involving non-smooth Saint-Venant terms. Int. J. Non-Linear Mech. **45**(9), 866–875 (2010)
1078. Schmidt, R.A.: Motor Control and Learning: a Behaviour Emphasis, 2nd, edition edn. Human kinetics Publishers Inc, Champaign (1988)
1079. Schwager, T., Pöschel, T.: Coefficient of restitution and linear-dashpot model revisited. Granular Matter **9**(6), 465–469 (2007)
1080. Schwager, T., Pöschel, T.: Coefficient of restitution for viscoelastic spheres: The effect of delayed recovery. Phys. Rev. E **78**(5), 051,304 (2008)

1081. Schwartz, L.: Méthodes Mathématiques pour les Sciences Physiques. Enseignement des sciences. Hermann, Paris (1965)
1082. Schwartz, L.: Théorie des Distributions. Hermann, publications de l'institut de mathématique de l'université de Strasbourg, Paris (1966)
1083. Seifried, R., Schiehlen, W., Eberhard, P.: Numerical and experimental evaluation of the coefficient of restitution for repeated impacts. Int. J. Impact Eng. **32**, 508–524 (2005)
1084. Seifried, R., Schiehlen, W., Eberhard, P.: The role of the coefficient of restitution on impact problems in multi-body dynamics. Proc. Inst. Mech. Eng., Part K: J. Multi-body Dyn. **224**(3), 279–306 (2010)
1085. Sekhavat, P., Sepehri, N., Wu, Q.: Impact stabilizing controller for hydraulic actuators with friction: Theory and experiments. Control Eng. Pract. **14**, 1423–1433 (2006)
1086. Sekimoto, K.: Newton's cradle versus nonbinary collisions. Phys. Rev. Lett. **104**, 124,302 (2010)
1087. Sen, S., Hong, J., Bang, J., Avalos, E., Doney, R.: Solitary waves in the granular chain. Phys. Reports **462**, 21–66 (2008)
1088. Sessa, V., Iannelli, L., Vasca, F.: A complementarity model for closed-loop power converters. IEEE Trans. Power Electron. **29**(12), 6821–6835 (2014)
1089. 'sGravesand, W.: Essai d'une nouvelle théorie sur le choc des corps. Journal Littéraire de la Haye **xii**, 1–154 (1722). Also pages 190–197
1090. 'sGravesand, W.: Remarques sur la force des corps en mouvement et sur choc; précédées de quelques réflexions sur la manière d'écrire, de monsieur le docteur Samuel Clarke. Journal Littéraire de la Haye 189–197 (1729). Also pp. 407–430
1091. 'sGravesand, W.: Mathematical Elements of Natural Philosophy. trans. J.T. Desaguliers, London (1737). 5th Edition; First edition in 1721, London
1092. Shabana, A.A.: Euler parameters kinetic singularity. Proc. Inst. Mech. Eng. Part K: J. Multi-body Dyn. (2014). doi:10.1177/1464419314539301
1093. Shan, Y., Koren, Y.: Obstacle accomodation motion planning. IEEE Trans. Robot. Autom. **11**(1), 36–49 (1995)
1094. Sharif-Bakthiar, M., Shaw, S.W.: The dynamic response of a centrifugal pendulum vibration absorber with motion limiting stops. J. Sound Vib. **126**(2), 221–235 (1988)
1095. Shaw, J., Shaw, S.W.: The onset of chaos in a two-degree of freedom impacting system. ASME J. Appl. Mech. **56**(1), 168–174 (1989)
1096. Shaw, S.W.: The dynamics of a harmonically excited system having rigid amplitude constraints. part 1: Subharmonic motions and local bifurcations; part 2: Chaotic motions and global bifurcations. ASME J. Appl. Mech. **52**(2), 453–464 (1985)
1097. Shaw, S.W.: Forced vibrations of a beam with one sided amplitude constraint: theory and experiments. J. Sound Vib. **99**(2), 199–212 (1985)
1098. Shaw, S.W., Holmes, P.J.: A periodically forced impact oscillator with large dissipation. ASME J. Appl. Mech. **50**(4a), 849–857 (1983)
1099. Shaw, S.W., Holmes, P.J.: A periodically forced piecewise linear oscillator. J. Sound Vib. **90**(1), 129–155 (1983)
1100. Shaw, S.W., Rand, R.H.: The transition to chaos in a simple mechanical system. Int. J. Non-Linear Mech. **24**(1), 41–56 (1989)
1101. Shaw, S.W., Tung, P.C.: The dynamic response of a system with preloaded compliance. ASME J. Dyn. Syst. Meas. Control **110**(3), 273–283 (1988)
1102. Shen, J., Pang, J.S.: Linear complementarity systems: Zeno states. SIAM J. Control Optim. **44**(3), 1040–1066 (2005)
1103. Shen, Y.: Painlevé paradox and dynamic jam of a three-dimensional elastic rod. Arch. Appl. Mech. **85**(6), 805–816 (2015)
1104. Shen, Y., Stronge, W.J.: Painlevé paradox during oblique impact with friction. Eur. J. Mech. A/Solids **30**, 457–467 (2011)
1105. Sherikov, A., Dimitrov, D., Wieber, P.B.: Whole body motion controller with long-term balance constraints. In: 14th IEEE International Conference on Humanoids Robots, pp. 444–450. Madrid, Spain (2014)

1106. Shevitz, D., Paden, B.: Lyapunov stability theory of nonsmooth systems. IEEE Trans. Autom. Control **39**(9), 1910–1914 (1994)
1107. Shi, P.: The restitution coefficient for a linear elastic rod. Math. Comput. Modell. **28**(4–8), 427–435 (1998)
1108. Shi, X., Zhao, Y.: Comparison of various adhesion contact theories and the influence of dimensionless load parameter. J. Adhesion Sci. Technol. **18**(1), 55–68 (2004)
1109. Shimoga, K., Goldenberg, A.: Soft materials for robotic fingers. In: Proceedings of IEEE International Conference on Robotics and Automation, vol. 2, pp. 1300–1305. Nice, France (1992)
1110. Shimoga, K., Goldenberg, A.: Soft robotic fingertips, part i: a comparison of construction materials. Int. J. Robot. Res. **15**(4), 320–334 (1996)
1111. Shoji, Y., Inaba, M., Fukuda, T., Hosokai, H.: Stable contact force control of a link manipulator with collision phenomena. In: Proceedings of IEEE Int. Workshop in Intelligent Robots and Systems, vol. 2, pp. 501–507 (1990)
1112. Shorten, R., Wirth, F., Mason, O., Wulff, K., King, C.: Stability criteria for switched and hybrid systems. SIAM Rev. **49**(4), 545–592 (2007)
1113. Simon, R.: The development of a mathematical tool for evaluating golf club performance. In: Proceedings of ASME Design Engineering Conference. New York city, USA (1967)
1114. Sinai, Y.: Introduction to Ergodic Theory. Princeton University Press (1976)
1115. Sinitsyn, V.: The principle of least constraint for systems with non-restoring constraints. J. Appl. Math. Mech. **54**(6), 920–925 (1990)
1116. Sithig, G.P.M.: discussion on "swerve during three-dimensional impact of rough rigid bodies" by w.j. stronge (stronge, w. j., 1994, asme j. appl. mech., **61**, 605611). ASME J. Appl. Mech. **62**(2), 551–552 (1995)
1117. Sithig, G.P.M.: Rigid body impact with friction- various approaches compared. In: R. Batra, A. Mal, G.M. Sithig (eds.) in Impact, Waves and Fracture, vol. 205, pp. 307–317. ASME (1995)
1118. Skipor, E., Bain, L.: Application of impact damping to rotary printing equipment. ASME J. Mech. Des. **102**(2), 338–343 (1980)
1119. Slotine, J.J., Li, W.: Adaptive manipulator control: A case study. IEEE Trans. Autom. Control **33**, 995–1003 (1988)
1120. Smirnov, G.: Introduction to the Theory of Differential Inclusions, Graduate Studies in Mathematics, vol. 41. Amreican Mathematical Society (2001)
1121. Smith, C.: Predicting rebounds using rigid body dynamics. ASME J. Appl. Mech. **58**(3), 754–758 (1991)
1122. Smith, C.: P.P., L.: Coefficients of restitution. ASME J. Appl. Mech. **59**(4), 963–969 (1992). doi:10.1115/1.2894067
1123. Smith, D.: Gears and Vibrations-A Basic Approach to Understanding Gear Noise. McMillan Press Ltd (1983)
1124. Soderquist, B., Wernersson, A.: Information for assembly from impacts. In: Proceedings of IEEE International Conference on Robotics and Automation, vol. 3, pp. 2012–2017. Nice, France (1992)
1125. Soderquist, B., Zhong, Z.: Proposed mechatronics applications of impacts. Proceedings of JSME Conf. on Advanced Mechatronics, pp. 255–260. Tokyo, Japan (1993)
1126. Sondergaard, R., Chaney, K., Brennen, C.: Measurements of solid spheres bouncing off flat plates. ASME J. Appl. Mech. **57**(3), 694–699 (1990)
1127. Song, P., Kraus, P., Kumar, V., Dupont, P.: Analysis of rigid-body dynamic models for simulation of systems with frictional contacts. ASME J. Appl. Mech. **68**, 118–128 (2001)
1128. Song, P., Pang, J.S., Kumar, R.: A semi-implicit time-stepping model for frictional compliant contact problems. Int. J. Numer. Methods Eng. **60**(13), 2231–2261 (2004)
1129. Sontag, E.: Mathematical Control Theory. Springer Verlag, Deterministic Finite Dimensional Systems. Texts in Applied Mathematics (1990)
1130. Souchet, R.: Restitution and friction laws in rigid body collisions. Int. J. Eng. Sci. **32**(5), 863–876 (1994)

1131. Spanos, P., Koh, A.: Rocking of rigid blocks due to harmonic shaking. ASCE J. Eng. Mech. **110**(11), 1627–1642 (1984)
1132. Spasic, D., Atanackovic, T.: A model for three spheres in colinear impact. Arch. Appl. Mech. **71**, 327–340 (2001)
1133. Spong, M.: Modeling and control of elastic joint robots. ASME J. Dyn. Syst. Meas. Control **109**(4), 310–319 (1987)
1134. Spong, M., Ortega, R., Kelly, R.: Comments on "adaptive manipulator control: a case study", by J. Slotine and W. Li. IEEE Trans. Autom. Control **35**(6), 761–762 (1990)
1135. Staricek, I., Cvengros, J.: Elastic collision of hard spheres in the space. Acta Phys. Slov. **42**(4), 193–209 (1992)
1136. Staron, L., Radjai, F., Vilotte, J.P.: Multi-scale analysis of the stress state in a granular slope in transition to failure. Eur. Phys. J. E **18**, 311–320 (2005)
1137. Staron, L., Radjai, F., Vilotte, J.P.: Granular micro-structure and avalanche precursors. J. Stat. Mech.: Theory Exp. **2006**(07), P07,014 (2006)
1138. Stensson, A., Nordmark, A.: Chaotic vibrations of a spring, mass system with a unilateral displacement limitation- theory and experiments, : Preprint. Lulea University of Technology, Sweden (1992)
1139. Stepanenko, Y., Sankar, T.S.: Vibro-impact analysis of control systems with mechanical clearance and its application to robotic actuators. ASME J. Dyn. Syst. Meas. Contr. **108**, 9–16 (1986)
1140. Stevens, A.B., Hrenya, C.M.: Comparison of soft-sphere models to measurements of collision properties during normal impacts. Power Technol. **154**, 99–109 (2005)
1141. Stewart, D.E.: Existence of solutions to rigid body dynamics and the Painlevé paradoxes. C.R. Acad. Sci. Paris Série 1 **325**, 689–693 (1997)
1142. Stewart, D.E.: Convergence of a time-stepping scheme for rigid-body dynamics and resolution of Painlevé's problem. Arch. Rational Mech. Anal. **145**(3), 215–260 (1998)
1143. Stewart, D.E., Trinkle, J.C.: An implicit time-stepping scheme rigid body dynamics with inelastic collisions and Coulomb friction. Int. J. Numer. Methods Eng. **39**(15), 2673–2691 (1996)
1144. Stoianovici, D., Hurmuzlu, Y.: A critical study of the applicability of rigid body collision theory. ASME J. Appl. Mech. **63**, 307–316 (1996). (See also Discussion by A. Chatterjee and A. Ruina: "A Critical Study of the Applicability of Rigid-Body Collision Theory" (Stoianovici, D., and Hurmuzlu, Y., 1996, ASME J. Appl. Mech., **63**, pp. 307–316))
1145. Storakers, B., Larsson, J.: On inelastic impact and dynamic hardness. Arch. Mech. (Archiwum Mechaniki Stosowanej) **52**(4–5), 779–798 (2000)
1146. Stowe, L.G.: Using the graphics calculator-in collision problems. Phys. Teacher **33**(5), 318–319 (1995)
1147. Stronge, W.J.: The domino effect: A wave of destabilizing collisions in a periodic array. Proc. Roy. Soc. Lond. A **409**(1836), 199–208 (1987)
1148. Stronge, W.J.: Rigid body collision with friction. Proc. Roy. Soc. Lond. A **431**(1881), 169–181 (1990)
1149. Stronge, W.J.: Friction in collisions: resolution of a paradox. J. Appl. Phys. **69**(2), 610–612 (1991)
1150. Stronge, W.J.: Energy dissipated in planar collisions. ASME J. Appl. Mech. **59**(3), 681–682 (1992)
1151. Stronge, W.J.: Discussion: "two-dimensional rigid-body collisions with friction" (wang, y., and mason, m. t., 1992, asme j. appl mech., 59, pp. 536642). ASME J. Appl. Mech. **60**(2), 564–566 (1993). doi:10.1115/1.2900835
1152. Stronge, W.J.: Planar impact of rough compliant bodies. Int. J. Impact Eng. **15**(4), 435–450 (1994)
1153. Stronge, W.J.: Swerve during three-dimensional impact of rough rigid bodies. ASME J. Appl. Mech. **61**(3), 605–611 (1994). doi:10.1115/1.2901502
1154. Stronge, W.J.: Coupling of friction and internal dissipation in planar collisions of compliant bodies. In: Raous, M., Jean, M., Moreau, J. (eds.) Contact Mechanics, pp. 417–426. Plenum Press, New York (1995)

1155. Stronge, W.J.: Theoretical coefficient of restitution for planar impact of rough elasto-plastic bodies. In: R. Batra, A. Mal, G. MacSithigh (eds.) ASME AMD Impact, Waves and Fracture, Joint ASME Applied Mechanics and Materia, vol. 205, pp. 351–362. ASME (1995)
1156. Stronge, W.J.: Contact problems for elasto-plastic impact in multi-body systems. In: B. Brogliato (ed.) Impact in Multi-Body Systems Impacts in mechanical systems: Analysis and modelling, Lecture Notes in Physics, vol. 551, pp. 189–234. Springer Verlag (2000). Proceedings of the Euromech Colloquium Impacts in Mechanical Systems, Grenoble, June 1999
1157. Stronge, W.J.: Impact Mechanics. Cambridge University Press (2000)
1158. Stronge, W.J.: Comment: collision with friction; part B: Poissons and Stronges hypotheses. Multibody Syst. Dyn. **24**(1), 123–127 (2010)
1159. Stronge, W.J.: Smooth dynamics of oblique impact with friction. Int. J. Impact Eng. **51**, 36–49 (2013)
1160. Stronge, W.J.: Energetically consistent calculations for oblique impact in unbalanced systems with friction. ASME J. Appl. Mech. **82**(8), 081,003 (2015). doi:10.1115/1.4030459
1161. Stroock, D.W.: A Concise Introduction to the Theory of Integration, second edn. Birkhauser (1994)
1162. Studer, C.: Numerics of Unilateral Contacts and Friction. Lecture Notes in Applied and Computational Mechanics, vol. 47. Springer, Berlin (2009)
1163. Studer, C., Glocker, C.: Representation of normal cone inclusion problems in dynamics via non-linear equations. Arch. Appl. Mech. **76**(5–6), 327–348 (2006). doi:10.1007/s00419-006-0031-y
1164. Styler, E.E.: Determining the friction coefficient in impact with the aid of stroboscopic photography. Trans. VNIIP Tuglemash Institute 20 (1975)
1165. Sugiura, K., Maeno, N.: Wind(tunnel measureents of restitution coefficients and ejection number of snow particles in drifting snow: determination of splash functions. Boundary-Layer Meteorol. **95**, 123–143 (2000)
1166. Sundararajan, G., Shewmon, P.G.: The oblique impact of a hard ball against ductile, semi-infinite target materials-experiment and analysis. Int. J. Impact Eng. **6**(1), 3–22 (1987)
1167. Sung, C.K., Yu, W.S.: Dynamics of a harmonically excited impact damper: bifurcation and chaotic motion. J. Sound Vib. **158**(2), 317–329 (1992)
1168. Supulver, K.D., Bridges, F.G., Lin, D.N.C.: The coefficient of restitution of ice particles in glancing collisions: experimental results for unfrosted surfaces. Icarus **113**, 188–199 (1995)
1169. Sussmann, H.: On the gap between deterministic and stochastic ordinary differential equations. Ann. Probab. **6**(1), 19–41 (1978)
1170. Svahn, F., Dankowicz, H.: Controlled onset of low-velocity collisions in a vibro-impacting system with friction. Proc. Roy. Soc. London A: Math., Phys. Eng. Sci. **465**(2112), 3647–3665 (2009). doi:10.1098/rspa.2009.0207
1171. Swadener, J.G., George, E.P., Pharr, G.M.: The correlation of the indentation size effects measured with indenters of various shapes. J. Mech. Phys. **50**, 681–694 (2002)
1172. Szczgielski, W., Schweitzer, G.: Dynamics of a high-speed rotor touching a boundary. In: Bianchi, G., Schiehlen, W. (eds.) IUTAM/IFoMM Symposium Dynamics of Multibody Systems, pp. 287–298. Springer, Udine, Italy (1986)
1173. Thümmel, T., Funk, K.: Multibody modelling of linkage mechanisms including friction, clearance and impact. Proceedings of the 10th World Congress on the Theory of Machines and Mechanisms in Oulu. June 20 to 24, vol. 4, pp. 1387–1392. Oulu University Press, Finland (1999)
1174. Tabor, D.: A simple theory of static and dynaimc hardness. Proceedings of the Royal Society of London, Series A **192**, 247–274 (1948)
1175. Tabor, D.: The Hardness of Metals. Oxford University Press, Oxford Classics Texts in the Physical Sciences (1951)
1176. Tabor, D.: Surface forces and surface interactions. J. Colloid Interf. Sci. **58**(1), 2–13 (1977)
1177. Tabor, D.: Indentation hardness: Fifty years on a personal view. Philos. Mag. A **74**(5), 1207–1212 (1996)

1178. Talpaert, Y.: Mécanique analytique, tome II: Dynamique des systèmes matériels. Editions Marketing, coll. Ellipses, Paris (1982)
1179. Tang, Y., Chang, Z., Dong, X., Hu, Y., Yu, Z.: Nonlinear dynamics and analysis of a four-bar linkage with clearance. Front. Mech. Eng. **8**(2), 160–168 (2013)
1180. Tanwani, A., Brogliato, B., Prieur, C.: On output regulation in systems with differential variational inequalities (2014). https://hal.archives-ouvertes.fr/hal-01065090; extended version of 53rd IEEE Conference on Decision and Control, December 2014, Los Angeles
1181. Tanwani, A., Brogliato, B., Prieur, C.: Stability and observer design for lur'e systems with multivalued, non-monotone, time-varying nonlinearities and state jumps. SIAM J. Control Optim. **56**(2), 3639–3672 (2014). doi:10.1137/120902252
1182. Tanwani, A., Brogliato, B., Prieur, C.: Stability notions for a class of nonlinear systems with measure inputs. Math. Control, Sig. Syst. **27**(2), 245–275 (2015). doi:10.1007/s00498-015-0140-7
1183. Tanwani, A., Brogliato, B., Prieur, C.: Observer design for frictionless and unilaterally constrained mechanical systems: a passivity-based approach. IEEE Trans. Autom. Control (2016). doi:10.1109/TAC.2015.2492098
1184. Tasaki, H.: The coefficient of restitution does not exceed unity. J. Stat. Phys. **123**(6), 1361–1374 (2006)
1185. Tatara, Y.: Effects of external force on contacting times and coefficient of restitution in a periodic collision. ASME J. Appl. Mech. **44**(4), 773–774 (1977)
1186. Tatara, Y., Moriwaki, N.: Study on impact of equivalent two bodies: : Coefficients of restitution of spheres of brass, lead, glass, porcelain and agate, and the material properties. Jpn. Soc. Mech. Eng. **25**(202), 631–637 (1982)
1187. Tavakoli, A., Gharib, M., Hurmuzlu, Y.: Collision of two mass baton with massive external surfaces. ASME J. Appl. Mech. **79**, 051,019 (2012)
1188. Teel, A.R., Forni, F., Zaccarian, L.: Lyapunov-based sufficient conditions for exponential stability inhybrid systems. IEEE Trans. Autom. Control **58**(6), 1591–1596 (2013)
1189. Thompson, J.M.T., Bokaian, A.R., Ghaffari, R.: Subharmonic and chaotic motions of compliant offshore structures and articulated mooring towers. ASME J. Energy Resour. Technol. **106**(2), 191–198 (1984)
1190. Thompson, J.M.T., Ghaffari, R.: Chaos after period doubling bifurcations in the resonance of an impact oscillator. Phys. Lett. A **91**(1), 5–8 (1982)
1191. Thompson, J.M.T., Ghaffari, R.: Chaotic dynamics of an impact oscillator. Phys. Rev. A **27**(3), 1741–1743 (1983)
1192. Thomson, W., Tait, P.G.: Treatise on Natural Philosophy. Clarendon Press, Oxford (1867)
1193. Thorin, A., Boutillon, X., Lozada, J.: Modelling the dynamics of the piano action: Is apparent success real? Acta Acustica united with Acustica **100**(6), 1162–1171 (2014)
1194. Thornton, C.: Coefficient of restitution for collinear collisions of elastic-perfectly plastic spheres. ASME J. Appl. Mech. **64**(2), 383–386 (1997)
1195. Thornton, C., Cummins, S., Cleary, P.: An investigation of the comparative behaviour of alternative contact force models during inelastic collisions. Powder Technol. **233**(1), 30–46 (2013)
1196. Thornton, C., Cummins, S.J., Cleary, P.W.: An investigation of the comparative behaviour of alternative contact force models during elastic collisions. Powder Technol. **210**, 189–197 (2011)
1197. Thuan, L.Q., Camlibel, M.K.: On the existence, uniqueness and nature of Carathéodory and Filippov solutions for bimodal piecewise affine dynamical systems. Syst. Control Lett. 76–85 (2014)
1198. Thümmel, T.: Experimentelle mechanismendynamik: Messung, modellierung, simulation, verifikation, interpretation und beeinflussung typischer schwingungsphänomene an einem mechanismenprüfstand. Ph.D. thesis, München, Technische Universität München, Habil.-Schr., 2012 (2012)
1199. Thümmel, T., Ginzinger, L.: Measurements and simulations of a crank and rocker mechanism including friction, clearance and impacts. In. In Proceedings of the IX. International

Conference on the Theory of Machines and Mechanisms in Liberec/Czech Republic, Aug. 31-Sept. 2004, pp. 763–768. Technical University of Liberec, Department of Textile Machine Design (2004)
1200. Thümmel, T., Roßner, M.: Introduction to modelling and parameter identification methodology of linkages by measurements and simulation. In: Proceedings of the 13th World Congress in Mechanism and Machine Science, Guanajuato, Mexico, 19–25 June, vol. IMD-123 (2011)
1201. Thümmel, T., Rutzmoser, J.: M. Robner, H.: Friction modeling and parameter value estimation of mechanisms. The 2nd Joint International Conference on Multibody Systems Dynamics. May 29-June 1 2012, Stuttgart, Germany, pp. 302–312. University of Stuttgart, Institute of Engineering and Computational Mechanics (2012)
1202. Timoshenko, S.: Théorie de l'Elasticité. Béranger, Paris, Liège (1948)
1203. Timoshenko, S.P., Goodier, J.N.: Theory of Elasticity, 3rd edn. McGraw Hill, New York (1970)
1204. Tomei, P.: A simple PD controller for robots with elastic joints. IEEE Trans. Autom. Control **36**(10), 1208–1213 (1991)
1205. Tornambé, A.: Modeling and controlling two bodies before, after and during the period of a one-degree-of freedom impact. In: Proceedings of seventh International Conference on Advanced Robotics. San Feliu de Guixols, Spain (1995)
1206. Tornambé, A.: Global regulation of planar robot arm striking a surface. IEEE Trans. Autom. Control **41**(10), 1517–1521 (1996)
1207. Tornambé, A.: Modeling and controling two-degree-of freedom impacts. IEE Proc. Control Appl. **143**(1), 85–90 (1996)
1208. Tornambé, A.: Modeling and control of the impact in mechanical systems: Theory and experimental results. IEEE Trans. Autom. Control **44**(2), 294–309 (1999)
1209. Toulemonde, C., Gontier, C.: Multiple degree of freedom impact oscillator. Eur. J. Mech. A/Solids **16**(5), 879–904 (1997)
1210. Toulemonde, C., Gontier, C.: Sticking motions of impact oscillators. Eur. J. Mech. A/Solids **17**(2), 339–366 (1998)
1211. Towne, D.H., Hadlock, C.R.: One-dimensional collisions and chebyshev polynomials. Am. J. Phys. **45**(3), 225–259 (1977)
1212. Transeth, A.A., Leine, R.I., Glocker, C., Pettersen, K.Y.: 3-d snake robot motion: Nonsmooth modeling, simulations, and experiments. IEEE Trans. Robot. **24**(2), 361–376 (2008)
1213. Transeth, A.A., Leine, R.I., Glocker, C., Pettersen, K.Y., Liljebäck, P.: Snake robot obstacle-aided locomotion: Modeling, simulations, and experiments. IEEE Trans. Robot. **24**(1), 88–104 (2008)
1214. Trenn, S.: Solution concepts for linear DAEs: A survey. In: A. Ilchmann, T. Reis (eds.) Surveys in Differential-Algebraic Equations I, Differential-Algebraic Equations Forum, pp. 137–172. Springer, Berlin (2013). doi:10.1007/978-3-642-34928-7_4
1215. Trenn, S., Liberzon, D.: Switched nonlinear differential algebraic equations: Solution theory, Lyapunov functions, and stability. Automatica **48**, 954–963 (2012)
1216. Trinkle, J., Pang, J.S., Sudarsky, S., Lo, G.: On dynamic multi-rigid-body contact problems with Coulomb friction. ZAMM-Z. Angew. App. Math. Mech. **77**(4), 267–279 (1997)
1217. Trinkle, J.C., Tzitzouris, J.A., Pang, J.S.: Dynamic multi-rigid-body systems with concurrent distributed contacts. Phil. Trans. R. Soc. Lond. A **359**(1789), 2575–2593 (2001)
1218. Truesdell, C.: Essays on the History of Mechanics. Springer (1968)
1219. Tschoegl, N.W.: The Phenomenological Theory of Linear Viscoelastic Behavior. An Introduction. Springer, Berlin (1989)
1220. Tsuji, Y., Tanaka, T., Ishida, T.: Lagrangian numerical simulation of plug flow of cohesionless particles in a horizontal pipe. Powder Technol. **71**, 239–250 (1992)
1221. Tufillaro, N.B., Albano, A.M.: Chaotic dynamics of a bouncing ball. Am. J. Phys. **54**(10), 939–944 (1986)
1222. Tung, P.C., Shaw, S.W.: The dynamics of an impact print hammer. J. Vib. Acoust. Stress Reliab. Des. **110**(2), 193–200 (1988)

1223. Tzénoff, I.: Sur les percussions appliquées aux systèmes matériels. Mathematische Annalen 92(1–2), pages = 42–57, month =, (1924)
1224. Vahid-Araghi, O., Golnaraghi, F.: Friction-Induced Vibration in Lead Screw Drives. Springer (2011). doi:10.1007/978-1-4419-1752-2
1225. Valentine, F.A.: The problem of Lagrange with differential inequalities as added side conditions. In: Contributions to the Calculus of Variations, pp. 403–447. University of Chicago Press, Chicagon USA (1937)
1226. Varedi, S.M., Daniali, H.M., Dardel, M.: Dynamic synthesis of a planar slider-crank mechanism with clearances. Nonlinear Dyn. (2014). doi:10.1007/s11071-014-1762-x
1227. Vasca, F., Iannelli, L., Camlibel, M.K., Frasca, R.: A new perspective for modeling power electronics converters: complementarity framework. IEEE Trans. Power Electron. **24**, 456–468 (2009)
1228. Veluswami, M.A., Crossley, F.R.E.: Multiple impacts of a ball between two plates, part 1: some experimental observations, part 2: Mathematical modelling. ASME J. Eng. Ind. **97**(3), 820–835 (1975)
1229. Vidyasagar, M.: Nonlinear Systems Analysis. Prentice-Hall (1993)
1230. Vilain, C.: Huygens et le relatif. Ph.D. thesis, Science History and Epsitemology, University Paris 7 (1993)
1231. Villagio, P.: The rebound of an elastic sphere against a rigid wall. ASME J. Appl. Mech. **63**, 259–263 (1996)
1232. Vinogradov, V.N., Biryukov, V.I., Nazarov, S.I., Chervyakov, I.B.: Experimental study of the coefficient of friction during the impact of a sphere on a plane surface. Sov. J. Friction Wear (Trenie i Iznos) **2**(5), 107–109 (1981)
1233. van Vliet, J., Sharf, I., Ma, O.: Experimental validation of contact dynamics simulation of constrained robotic tasks. Int. J. Robot. Res. **19**(12), 1203–1217 (2000)
1234. Volpe, R., Khosla, P.: A theoretical and experimental investigation of impact control for manipulators. Int. J. Robot. Res. **12**(4), 351–365 (1993)
1235. Vol'pert, A.I., Hudjaev, S.I.: Analysis in Classes of Discontinuous Functions and Equations of Mathematical Physics. Martinus Nijhoff publisher, Dordrecht, NL (1985)
1236. Wagg, D.J.: A note on coefficient of restitution models including the effects of impact induced vibration. J. Sound Vib. **300**, 1071–1078 (2007)
1237. Wagg, D.J., Bihsop, S.R.: A note on modelling multi-degree-of-freedom vibro-impact systems using coefficient of restitution model. J. Sound Vib. **236**(1), 176–184 (2000)
1238. Wagg, D.J., Bishop, S.R.: Application of non-smooth modelling techniques to the dynamics of a flexible impacting beam. J. Sound Vib. **256**(5), 803–820 (2002)
1239. Wagg, D.J., Karpodinis, G., Bishop, S.R.: A experimental study of the impulse response of a vibro-impacting cantilever. J. Sound Vib. **228**(2), 243–264 (1999)
1240. Walker, I.D.: The use of kinematic redundancy in reducing impact and contact effects in manipulation. In: Proceedings of IEEE International Conference Robotics and Automation, vol. 1, pp. 434–439. Cincinnati, OH, USA (1990)
1241. Walker, J.S., Soule, T.: Chaos in a simple impact oscillator: the bender bouncer. Am. J. Phys. **64**(4), 397–409 (1996)
1242. Walton, O.R.: Numerical simulation of inelastic, frictional particle-particle interactions. In: M. Roco (ed.) Particulate Two-Phase Flow, chapter 25, pp. 884–911. Butterworth-Heinemann (1993)
1243. Walton, O.R., Braun, R.L.: Stress calculations for assemblies of inelastic speres in uniform shear. Acta Mech. **63**(1–4), 73–86 (1986)
1244. Walton, O.R., Braun, R.L.: Viscosity, granular-temperature, and stress calculations for shearing assemblies of inelastic, frictional disks. J. Rheol. **30**(5), 949–980 (1986)
1245. Wang, B., Brogliato, B., Acary, V., Boubakir, A., Plestan, F.: Experimental comparisons between implicit and explicit implementations of discrete-time sliding mode controllers: Toward input and output chattering suppression. IEEE Trans. Control Syst. Technol. **23**(5), 2071–2075 (2015). doi:10.1109/TCST.2015.2396473

1246. Wang, E., Geubelle, P., Lambros, J.: An experimental study of the dynamic elasto-plastic contact behavior of metallic granules. ASME J. Appl. Mech. **80**(2), 021,009 (2013)
1247. Wang, E., On, T., Lambros, J.: An experimental study of the dynamic elasto-plastic contact behavior of dimer metallic granules. Exp. Mech. **53**(5), 883–892 (2013)
1248. Wang, J., Liu, C., Ma, D.: Experimental study of transport of a dimer on a vertically oscillating plate. Proc. Roy. Soc. London A: Math., Phys. Eng. Sci. **470**(2171) (2014). doi:10.1098/rspa.2014.0439
1249. Wang, J., Liu, C., Zhao, Z.: Nonsmooth dynamics of a 3D rigid body on a vibrating plate. Multibody Syst. Dyn. **32**, 217–239 (2014)
1250. Wang, L., Chen, L., Nieto, J.J.: The dynamics of an epidemic model for pest control with impulsive effect. Nonlinear Anal.: Real World Appl. **11**, 1374–1386 (2010)
1251. Wang, Q.J.: Conformal-contact elements and systems. In: Q.J. Wang, Y. Chung (eds.) Encyclopedia of Tribology, pp. 434–440. Springer (2013). doi:10.1007/978-0-387-92897-5_22
1252. Wang, Y.: Dynamic modeling and stability analysis of mechanical systems with time-varying topologies. ASME J. Mech. Des. **115**(4), 808–816 (1993)
1253. Wang, Y.: Global analysis and simulation of mechanical systems with time-varying topologies. ASME J. Mech. Des. **115**(4), 817–821 (1993)
1254. Wang, Y., Mason, M.T.: Modelling impact dynamics for robotic operations. Proceedings of IEEE International Conference on Robotics and Automation **4**, 678–685 (1987)
1255. Wang, Y., Mason, M.T.: Two-dimensional rigid-body collisions with friction. ASME J. Appl. Mech. **59**(3), 635–642 (1992). Discussion by W.J. Stronge, same journal, pp. 564–566, June 1993
1256. Warburton, G.B.: Discussion of "on the theory of the acceleration damper". J. Appl. Mech. 24, 322–324: Discussion on Grubin's paper. ASME J, Applied Mechanics (1957). 1956
1257. Watanabe, T.: Steady impact vibrations of continuous elements (case of colliding once in a half cycle). Bull. Jpan Soc. Mech. Eng. **24**(187), 222–228 (1981)
1258. Wee, L.B., Walker, M.W.: On the dynamics of contact between space robots and configuration control of impact minimization. IEEE Trans. Robot. Autom. **9**(5), 581–591 (1993)
1259. Wehage, R.A., Haug, E.J.: Dynamic analysis of mechanical systems with intermittent motion. ASME J. Mech. Des. **104**(4), 778–784 (1982)
1260. Weir, G., Tallon, S.: The coefficient of restitution for normal incident, low velocity particle impacts. Chem. Eng. Sci. **60**(13), 3637–3647 (2005)
1261. Weng, S., Young, K.Y.: An impact control scheme inspired by human reflex. J. Robot. Syst. **13**(12), 837–855 (1996)
1262. Whiston, G.S.: Global dynamics of vibro-impacting linear oscillators. J. Sound Vib. **118**(3), 395–429 (1987)
1263. Whiston, G.S.: The vibro-impact response of a harmonically excited and preloaded one dimensional linear oscillator. J. Sound Vib. **115**(2), 303–319 (1987)
1264. Whiston, G.S.: Singularities in vibro-impact dynamics. J. Sound Vib. **152**(3), 427–460 (1992)
1265. Whittaker, E.T.: A Treatise on the Analytical Dynamics of Particles and Rigid Bodies. Cambridge Univ. Press, Cambridge, UK (1904)
1266. Wiesenfield, K., Tufillaro, N.B.: Suppression of period doubling in the dynamics of a bouncing ball. Physica D: Nonlinear Phenomena **26**(1–3), 321–335 (1987)
1267. Wilms, E.V., Cohen, H.: Displacement, velocity and acceleration dependent damping in a two-degree-of-freedom system. Zeitschrift für angewandte Mathematik und Physik ZAMP (J. of Applied Math. and Physics) **3**(3), 537–540 (1979)
1268. Wilms, E.V., Cohen, H.: A two-degree-of-freedom system with Coulomb bearing friction. ASME J. Appl. Mech. **46**(1), 217–218 (1979)
1269. Wilms, E.V., Cohen, H.: Planar motion of a rigid body with a friction rotor. ASME J. Appl. Mech. **48**(1), 205–206 (1981)
1270. Wilms, E.V., Cohen, H.: Limitations of the Coulomb friction model for two elementary dynamical systems. Int. J. Mech. Eng. Educ. **11**, 107–112 (1983)

1271. Wilms, E.V., Cohen, H.: The occurrence of Painlevé's paradox in the motion of a rotating shaft. ASME J. Appl. Mech. **64**(4), 1008–1010 (1997)
1272. Wilson, J.F.: Reconstruction of tractor semitrailer accidents using Gauss's principle of least constraint. Int. J. Impact Eng. **11**(2), 139–148 (1991)
1273. Windisch, B., Bray, D., Duke, T.: Balls and chains-a mesoscopic approach to tethered protein domains. Biophys. J. **91**(7), 2383–2392 (2006)
1274. Wojtkowski, M.P.: A system of one dimensional balls with gravity. Commun. Math. Phys. **126**(3), 507–533 (1990)
1275. Wojtyra, M.: Joint reactions in rigid body mechanisms with dependent constraints. Mech. Mach. Theory **44**(12), 2265–2278 (2009)
1276. Wong, C.X., Daniel, M.C., Rongong, J.A.: Energy dissipation prediction of particle dampers. J. Sound Vib. **319**(1–2), 91–118 (2009)
1277. Wood, L.A., Byrne, K.P.: Analysis of a random repeated impact process. J. Sound Vib. **82**(3), 329–345 (1981)
1278. van de Wouw, N., Leine, R.I.: Robust impulsive control of motion systems with uncertain friction. Int. J. Robust Nonlinear Control **22**, 369–397 (2012)
1279. Wu, C.Y., Li, L.Y., Thorton, C.: Rebound behaviour of spheres for plastic impacts. Int. J. Impact Eng. **28**(9), 929–946 (2003)
1280. Wu, C.Y., Li, L.Y., Thorton, C.: Energy dissipation during normal impact of elastic and elastic-plastic spheres. Int. J. Impact Eng. **32**, 593–604 (2005)
1281. Wu, S.C., Yang, S.M., Haug, E.J.: Dynamics and mechanical systems with Coulomb friction, stiction, impact and constraint addition-deletion-ii, planar systems-iii, spatial systems. Mech. Mach. Theory **21**(5), 401–425 (1986)
1282. Wu, Y., Tarn, T.J., Xi, N., Isidori, A.: On robust impact control via positive acceleration feedback for robot manipulators. In: Proceedings of IEEE International Conference on Robotics and Automation, vol. 2, pp. 1891–1896. Minneapolis, MN, USA (1996)
1283. Xie, G., Wang, L.: Controllability and observability of a class of linear impulsive systems. J. Math. Anal. Appl. **304**, 336–355 (2005)
1284. Xiong, X., Kikuuwe, R., Yamamoto, M.: A differential-algebraic multistate friction model. In: Noda, I., Ando, N., Brugali, D., Kuffner, J. (eds.) Simulation, Modeling, and Programming for Autonomous Robots, Third International Conference, SIMPAR. Lecture Notes in Computer Science, vol. 7628, pp. 77–88. Springer, Tsukuba, Japan (2012)
1285. Xiong, X., Kikuuwe, R., Yamamoto, M.: A differential algebraic method to approximate nonsmooth mechanical systems by ordinary differential equations. J. Appl. Math. (2013). doi:10.1155/2013/320276
1286. Xiong, X., Kikuuwe, R., Yamamoto, M.: A multiscale friction model described by continuous differential equations. Tribol. Lett. **51**, 513–523 (2013)
1287. Xiong, X., Kikuuwe, R., Yamamoto, M.: A contact force model with nonlinear compliance and residual indentation. ASME J. Appl. Mech. **81**(02), 021,003 (2014)
1288. Xu, S., Ruan, D., Lu, G., Yu, T.X.: Collision and rebounding of circular rings on rigid target. Int. J. Impact Eng. (2014). http://dx.doi.org/10.1016/j.ijimpeng.2014.07.005
1289. Xu, W.L., Han, J.D., Tso, S.K.: Experimental study of contact transition control incorporating joint acceleration feedback. IEEE/ASME Trans. Mech. **5**(3), 292–301 (2000)
1290. Yanabe, S., Kaneko, S., Kanemitsu, Y., Toumi, N., Sugiyama, K.: Rotor vibration due to collision with annular guard during passage through critical speed. ASME J. Vib. Acoust. **120**(2), 544–550 (1998)
1291. Yao, W., Chen, B., Liu, C.: Energetic coefficient of restitution for planar impact in multi-rigid-body systems with friction. Int. J. Impact Eng. **31**, 255–265 (2005)
1292. Ye, H., Michel, A.N., Hou, L.: Stability theory for hybrid dynamical systems. In: Proceedings 34th IEEE Conference on Decision and Control, pp. 2679–2684. New Orleans, USA (1995)
1293. Ye, H., Michel, A.N., Hou, L.: Stability theory for hybrid dynamical systems. IEEE Trans. Autom. Control **43**(4), 483–490 (1998)
1294. Ye, N., Komvopoulos, K.: Indentation analysis of elastic-plastic homogeneous and layered media: criteria for determining the real material hardness. J. Tribol. **125**(4), 685–691 (2003)

1295. Yigit, A.S.: On the use of an elastic-plastic contact law for the impact of a single flexible link. ASME J. Dyn. Syst., Meas. Control **117**(4), 527–533 (1995)
1296. Yigit, A.S., Christoforou, A.P.: On the impact of a spherical indenter and an elastic-plastic transversely isotropic half-space. Compos. Eng. **4**(11), 1143–1152 (1994)
1297. Yigit, A.S., Christoforou, A.P., Majeed, M.A.: A nonlinear visco-elastoplastic impact model and the coefficient of restitution. Nonlinear Dyn. **66**, 509–521 (2011)
1298. Yigit, A.S., Ulsoy, A.G., Scott, R.A.: Dynamics of radially rotating beam with impact, part 1: Theoretical and computational model, part 2: Experimental and simulation results. ASME J. Vib. Acoust. **112**(1), 65–77 (1990)
1299. Yigit, A.S., Ulsoy, A.G., Scott, R.A.: Spring-dashpot models for the dynamics of a radially rotating beam with impact. J. Sound Vib. **142**(3), 515–525 (1990)
1300. Yilmaz, C., Gharib, M., Hurmuzlu, Y.: Solving frictionless rocking block problem with multiple impacts. Proc. Roy. Soc. London A: Math., Phys. Eng. Sci. **465**(2111), 3323–3339 (2009)
1301. Yoshida, K.: Impact dynamics representation and control with extended-inversed inertia tensor for space manipulators. In: T. Kanade, R. Paul (eds.) Proceedings of the Sixth International Symposium on Robotics Research, pp. 453–463 (1994)
1302. Yoshida, K., Mavroidis, C., Dubowsky, S.: Impact dynamics of space long reach manipulators. In: Proceedings of IEEE International Conference on Robotics and Automation, vol. 2, pp. 1909–1916. Minneapolis, MN, USA (1996)
1303. Yoshikawa, K., Yamada, K.: Impact estimation of a space robot at capturing a target. In: Proceedings of IEEE/RSJ International Conference on Intelligent Robots and Systems, pp. 1570–1577. Munich, G (1994)
1304. Yoshikawa, T.: Foundations of Robotics. Analysis and Control. MIT Press, Cambridge, Massachusetts, London, England (1990)
1305. Youcef-Toumi, K., Gutz, D.A.: Impact and force control: modeling and experiments. ASME J. Dyn. Syst. Meas. Control **116**(1), 89–98 (1994)
1306. Young, L.C.: Lectures on the Calculus of Variations and Optimal Control Theory. Chelsea Publishing Company, New York (1980)
1307. Youssouf, D.I.: Un corps dur peut-il rebondir ? Matapli **49**, 31–40 (1997)
1308. Yu, X., Wang, B., Galias, Z., Chen, G.: Discretization effect on equivalent control-based multi-input sliding-mode control systems. IEEE Trans. Autom. Control **53**(6), 1563–1569 (2008)
1309. Yu, Y., Ding, X.: Safe landing analysis of a quadrarotor aircraft with two legs. J. Intell. Robot. Syst. (2014). doi:10.1007/s10846-014-0044-7
1310. Zavala-Rio, A., Brogliato, B.: Hybrid feedback strategies for the control of juggling robots. In: Astolfi, A., Limebeer, D., Vinter, R., Melchiorri, C., Tornambé, A. (eds.) Proc. Workshop on Modeling and Control of Mechanical Systems. World Scientific Publ, Imperial College, London (1997)
1311. Zavala-Rio, A., Brogliato, B.: On the control of a one degree-of-freedom juggling robot. Dyn. Control **9**, 67–90 (1999)
1312. Zavala-Rio, A., Brogliato, B.: Direct adaptive control of a one degree-of-freedom complementary-slackness juggler. Automatica **37**(7), 117–1123 (2001)
1313. Zbiciak, A., Kozyra, Z.: Dynamic analysis of a soft-contact problem using viscoelastic and fractional-elastic rheological models. Arc. Civil Mech. Eng. **15**, 286–291 (2015). http://dx.doi.org/10.1016/j.acme.2014.03.002
1314. Zener, C.: The intrinsic inelasticity of large plates. Phys. Rev. **59**(8), 669–673 (1941)
1315. Zener, C., Feshbach, H.: A method of calculating energy losses during impact. ASME J. Appl. Mech. **61**, 67–70 (1939)
1316. Zhang, D., Nagurney, A.: On the stability of projected dynamical systems. J. Optim. Theory Appl. **85**(1), 97–124 (1995)
1317. Zhang, D.G., Angeles, J.: Impact dynamics of flexible-joint robots. Comput. Struct. **83**(1), 25–33 (2005)

1318. Zhang, H., Brogliato, B., Liu, C.: Study of the planar rocking-block dynamics with Coulomb friction: Critical kinetic angles. ASME J. Comput. Nonlinear Dyn. **8**(2), 021,002 (2013). http://dx.doi.org/10.1115/1.4007056
1319. Zhang, H., Brogliato, B., Liu, C.: Dynamics of planar rocking-blocks with Coulomb friction and unilateral constraints: comparisons between experimental and numerical data. Multibody Syst. Dyn. **32**(1), 1–25 (2014). doi:10.1007/s11044-013-9356-9
1320. Zhang, H., Liu, C., Zhao, Z., Brogliato, B.: Energy evolution in complex impacts with friction. Sci. China Phys. Mech. Astron. **56**(5), 875–881 (2013)
1321. Zhang, H., Liu, C., Zhen, Z., Brogliato, B.: Energy evolution in complex impacts with friction. Sci. China: Phys., Mech. Astron. **56**(5), 875–881 (2013)
1322. Zhang, X., Vu-Quoc, L.: Modeling the dependence of the coefficient of restitution on the impact velocity in elasto-plastic collisions. Int. J. Impact Eng. **27**, 317–341 (2002)
1323. Zhang, Y., Sharf, I.: Compliant force modeling for impact analysis. In: Proceedings ASME Int. Design technical Conf. Salt Lake City, UT, USA (2004). Paper no DETC2004-57220
1324. Zhang, Y., Sharf, I.: Validation of nonlinear viscoelastic contact force models for low speed impact. ASME J. Appl. Mech. **76**(5), 051,002 (2009). doi:10.1115/1.3112739
1325. Zhao, S., Sun, J.: Controllability and observability for a class of time-varying impulsive systems. Nonlinear Anal.: Real World Appl. **10**, 1370–1380 (2009)
1326. Zhao, Y., Maietta, D., Chang, L.: An asperity microcontact model incorporating the transition from elastic deformation to fully plastic flow. ASME J. Tribol. **122**, 86–93 (2000)
1327. Zhao, Z., Liu, C., Brogliato, B.: Planar dynamics of a rigid body system with frictional impacts. ii. qualitative analysis and numerical simulations. Proc. Roy. Soc. A, Math., Phys. Eng. Sci. **465**(2107), 2267–2292 (2009)
1328. Zhao, Z., Liu, C., Chen, B.: The Painlevé paradox studied at a 3D slender rod. Multibody Syst. Dyn. **19**(4), 323–343 (2008)
1329. Zhao, Z., Liu, C., Chen, B., Brogliato, B.: Asymptotic analysis of Painlevé's paradox. Multibody Syst. Dyn. **35**(3), 299–319 (2015). doi:10.1007/s11044-014-9448-1
1330. Zhao, Z., Liu, C., Ma, D.: Pure rotation of a prism on a ramp. Proc. Roy. Soc. London A: Math., Phys. Eng. Sci. **470**(2169) (2014). doi:10.1098/rspa.2014.0007
1331. Zhao, Z., Liu, C., Ma, W., Chen, B.: Experimental investigation of the Painlevé paradox in a robotic system. ASME J. Appl. Mech. **75**, 041,006 (2008)
1332. Zhen, R.R.I., Goldenberg, A.A.: Variable structure hybrid control of manipulators in unconstrained and constrained motion. ASME J. Dyn. Syst. Meas. Contr. **118**(2), 327–332 (1996)
1333. Zheng, Y.F.: Collision effects on two coordinating robots in assembly and the effect minimization. IEEE Trans. Syst., Man, Cybern. **17**(1), 108–116 (1987)
1334. Zheng, Y.F., Hemami, H.: Mathematical modeling of a robot collision with its environment. J. Robot. Syst. **2**(3), 289–307 (1985)
1335. Zhong, Z.H., Mackerle, J.: Contact-impact problems: A review with bibliography. ASME Appl. Mech. Rev. **47**(2), 55–76 (1994). doi:10.1115/1.3111071
1336. Zhuravlev, V.F.: A method for analysing vibro-impact systems using by means of special functions. Izv. Akad. Nauk. SSSR., MTT (Mechanics of Solids) **2** (1976)
1337. Zhuravlev, V.F.: Investigation of some vibration-collision systems by the method of non-smooth transformations. Izv. Akad. Nauk USSR, MTT (Mechanics of Solids) **6**, 24–28 (1977)
1338. Zhuravlev, V.F.: Equations of motion of mechanical systems with ideal one-sided link. J. Appl. Math. Mech. **42**(5), 839–847 (1978)
1339. Zhuravlev, V.F., Privalov, Y.: Investigation of the forced oscillations of a gyroscope with a collision absorber by the averaging method. Izv. Akad. Nauk USSR, MTT (Mechanics of Solids) **3**, 18–22 (1976)
1340. Zmitrowicz, A.: Contact stresses: a short survey of models and methods of computations. Arch. Appl. Mech. **80**(12), 1407–1428 (2010)

Index

B. Brogliato, *Nonsmooth Mechanics*, Communications and Control Engineering,
DOI 10.1007/978-3-319-28664-8